ICMSA 2018

International Conference on
Mathematical Studies and Applications 2018
4-6 October 2018

PROCEEDINGS

Edited by

Mehmet AKGÜL
İbrahim YILMAZ
Ahmet İPEK

ISBN: 978- 605- 81200- 0-6

Published : December 28, 2018

ICMSA 2018
International Conference on Mathematical Studies and Applications 2018

4-6 October 2018 – Karamanoglu Mehmetbey University, Karaman, Turkey

http://www.kmu.edu.tr/icmsa2018/

Acknowledgments: We thank the sponsors of ICMSA 2018 for their generous support: Karamanoglu Mehmetbey University, Karaman Municipality and The Association of Karaman Industrialists and Businessmen (KARSİAD). We are also thankful to invited speakers, scientific committee, organizing committee, authors and reviewers.

ORGANIZING COMMITTEE

Honorary Chair

Prof. Dr. Mehmet AKGÜL
Rector of Karamanoğlu Mehmetbey University

Conference Chairman

Prof. Dr. İbrahim YILMAZ
Dean of Kamil Özdağ Science Faculty, Karamanoğlu Mehmetbey University.

Chair of Organizing Committee

Prof. Dr. Ahmet İPEK
Karamanoğlu Mehmetbey University, Karaman, TURKEY

Organizing Committee

Prof. Dr. Rza MUSTAFAYEV, Karamanoğlu Mehmetbey University, Karaman, TURKEY
Assoc. Prof. Dr. Ali GELİŞKEN, Karamanoğlu Mehmetbey University, Karaman, TURKEY
Assoc. Prof. Dr. Eylem GÜZEL KARPUZ, Karamanoğlu Mehmetbey University, Karaman, TURKEY
Assoc. Prof. Dr. Kamil ARI, Karamanoğlu Mehmetbey University, Karaman, TURKEY
Assoc. Prof. Dr. Nihal YOKUŞ, Karamanoğlu Mehmetbey University, Karaman, TURKEY
Assist. Prof. Dr. Elif Segah ÖZTAŞ, Karamanoğlu Mehmetbey University, Karaman, TURKEY
Assist. Prof. Dr. Gülhan AYAR, Karamanoğlu Mehmetbey University, Karaman, TURKEY
Assist. Prof. Dr. Hatice YALDIZ, Karamanoğlu Mehmetbey University, Karaman, TURKEY
Res. Assist. Dr. Deniz Pınar SUNAOĞLU, Karamanoğlu Mehmetbey University, Karaman, TURKEY

Secretary

Res. Assist. Esra KIRMIZI ÇETİNALP, Karamanoğlu Mehmetbey University, Karaman, TURKEY
Res. Assist. Merve YILMAZ, Karamanoğlu Mehmetbey University, Karaman, TURKEY
Res. Assist. Murat ARI, Karamanoğlu Mehmetbey University, Karaman, TURKEY
Res. Assist. Nimet ÇOŞKUN, Karamanoğlu Mehmetbey University, Karaman, TURKEY

SCIENTIFIC COMMITTEE

Preface

The First International Conference on Mathematical Studies and Applications 2018 (ICMSA 2018) took place at the Karamanoglu Mehmetbey University, Karaman, Turkey, 4-6 October 2018.

In the conference, the leading academicians, scientists, researchers and engineers from around the world had the opportunity of sharing their experiences and research results on various aspects of mathematics.

The contents of these Proceedings have been subjected to peer reviewing. A large number of anonymous reviewers have played a crucial part in the editorial process. They all deserve our sincere thanks for their immense and highly valuable work.

It is clear from the variety and quality of the papers that the conference has attracted many innovative mathematics researchers from around the world.

Finally, we are thankful to the invited speakers, scientific committee, organizing committee, authors, reviewers, contributers and the sponsors of ICMSA 2018: Karamanoglu Mehmetbey University, Karaman Municipality and The Association of Karaman Industrialists and Businessmen (KARSİAD).

Organizing Committee

December 28, 2018

Table of Contents

On Some Integral Inequalities for s-Convex Functions by Means of New Conformable Fractional Integral Operators

Erhan SET*
Ordu University,
Department of Mathematics,
Ordu, Turkey

Hatice YALDIZ
Karamanoğlu Mehmetbey University,
Department of Mathematics,
Karaman, Turkey

M. Emin ÖZDEMİR
Uludağ University,
Department of Mathematics Education,
Bursa, Turkey

Abstract

In this paper, we aim to establish Hermite-Hadamard type inequalities for s-convex functions associated with known fractional conformable integral operators. The inequalities presented here are also pointed out to include some known results, as their special cases.

Keywords: s-convex functions, fractional conformable integral operator, special functions.

1 Introduction and preliminaries

For any convex functions $f : I \to \mathbb{R}$ where I is an interval in $\mathbb{R}$, the following chain of inequalities holds:

$$f\left(\frac{a+b}{2}\right) \leq \frac{1}{b-a}\int_a^b f(x)dx \leq \frac{f(a)+f(b)}{2} \quad (a,\, b \in I,\, a < b). \tag{1}$$

Inequality (1) is known literature as Hermite-Hadamard inequality. Here and in the following, let $\mathbb{C}$, $\mathbb{R}$, $\mathbb{R}^+$, and $\mathbb{Z}_0^-$ be the sets of complex numbers, real numbers, positive real numbers, and non-positive integers, respectively. The Hermite-Hadamard inequality has received attention of many mathematician and a remarkable variety of extensions, refinements and generalizations have been found so far for example see [1, 2, 5, 10, 11, 12, 17, 19, 20].

Let $s \in (0, 1]$. Then the function $f : [0, \infty) \to \mathbb{R}$ is said to be $s-$convex on the interval $[0, \infty)$ if the inequality

$$f(tx + (1-t)y) \leq t^s f(x) + (1-t)^s f(y) \tag{2}$$

takes place for all $x, y \in [0, \infty)$ and $t \in [0, 1]$. f is said to be $s-$concave if inequality (2) reversed.

We clearly see that $s-$convexity (concavity) defined on $[0, \infty)$ reduces to ordinary convexity (concavity) if $s = 1$. We recall some definitions and known results. Let $[a, b]$ $(-\infty < a <$

*Corresponding author. *E-mail address:* erhanset@yahoo.com

$b < \infty$) be a finite interval on the real axis $\mathbb{R}$ and $f \in L_1[a,b]$. The *left-sided* and *right-sided Riemann-Liouville fractional integrals* $J^{\alpha}_{a+}f$ and $J^{\alpha}_{b-}f$ of order $\alpha \in \mathbb{C}$ ($\Re(\alpha) > 0$) are defined, respectively, by

$$\left(J^{\alpha}_{a+}f\right)(x) := \frac{1}{\Gamma(\alpha)} \int_a^x (x-t)^{\alpha-1} f(t)\,dt \quad (x > a;\ \Re(\alpha) > 0) \tag{3}$$

and

$$\left(J^{\alpha}_{b-}f\right)(x) := \frac{1}{\Gamma(\alpha)} \int_x^b (t-x)^{\alpha-1} f(t)\,dt \quad (x < b;\ \Re(\alpha) > 0). \tag{4}$$

Here $\Gamma(\alpha)$ is the familiar Gamma function (see, e.g., [21, Section 1.1]). For more details and properties concerning the fractional integral operators (3) and (4), we refer the reader, for example, to the works [3, 4, 6, 9, 15, 14, 16, 18] and the references therein.

Sarıkaya et al. [15] established a Hermite-Hadamard type integral inequality involving Riemann-Liouville fractional integrals as in the following theorem.

Theorem A. *Let $f : [a,b] \to \mathbb{R}$ be a positive function with $0 \le a < b$ and $f \in L_1[a,b]$. Also let f be a convex function on $[a,b]$ and $\alpha \in \mathbb{R}^+$. Then*

$$f\left(\frac{a+b}{2}\right) \le \frac{\Gamma(\alpha+1)}{2(b-a)^{\alpha}} \left[J^{\alpha}_{a+}f(b) + J^{\alpha}_{b-}f(a)\right] \le \frac{f(a)+f(b)}{2}. \tag{5}$$

Obviously, the case $\alpha = 1$ in (5) reduces to the Hermite-Hadamard inequality (1). We also recall two more results in [15] as in Lemma A and Theorem B.

Lemma A. *Let $f : [a,b] \to \mathbb{R}$ be a differentiable mapping on (a,b) with $a < b$. Also let $f' \in L[a,b]$ and $\alpha \in \mathbb{R}^+$. Then*

$$\begin{aligned} &\frac{f(a)+f(b)}{2} - \frac{\Gamma(\alpha+1)}{2(b-a)^{\alpha}}\left[J^{\alpha}_{a+}f(b) + J^{\alpha}_{b-}f(a)\right] \\ &= \frac{b-a}{2} \int_0^1 \left[(1-t)^{\alpha} - t^{\alpha}\right] f'(ta + (1-t)b)\,dt. \end{aligned} \tag{6}$$

Theorem B. *Let $f : [a,b] \to \mathbb{R}$ be a differentiable mapping on (a,b) with $a < b$. Also let $f' \in L[a,b]$ and $\alpha \in \mathbb{R}^+$. Then*

$$\begin{aligned} &\left|\frac{f(a)+f(b)}{2} - \frac{\Gamma(\alpha+1)}{2(b-a)^{\alpha}}\left[J^{\alpha}_{a+}f(b) + I^{\alpha}_{b-}f(a)\right]\right| \\ &\le \frac{b-a}{2(\alpha+1)}\left(1 - \frac{1}{2^{\alpha}}\right)\left(|f'(a)| + |f'(b)|\right). \end{aligned} \tag{7}$$

In [16], Hermite-Hadamard inequality for $s-$convex functions via Riemann-Liouville fractional integrals is obtained as follows:

Theorem C. *Let $f : [a,b] \to \mathbb{R}$ be a positive function with $0 \le a < b$ and $f \in L_1[a,b]$. If f is an $s-$convex mapping in the second sense on $[a,b]$, then the following inequalities for fractional integrals with $\alpha > 0$ and $s \in (0,1)$ hold:*

$$2^{s-1} f\left(\frac{a+b}{2}\right) \le \frac{\Gamma(\alpha+1)}{(b-a)^{\alpha}}\left[\frac{J^{\alpha}_{a+}f(b) + J^{\alpha}_{b-}f(a)}{2}\right] \le \left[\frac{1}{\alpha+s} + \beta(\alpha, s+1)\right]\frac{f(a)+f(b)}{2} \tag{8}$$

where β is Euler Beta function.

Wang et al. obtained the following Hermite-Hadamard type inequalities which hold $s-$convex functions in the second sense.

Theorem 1 [22] *Let $f : [a, b] \to \mathbb{R}$ be a differentiable mapping on (a, b) with $a < b$, such that $f \in L[a, b]$. If f' is s-convex on $[a, b]$, for some fixed $s \in (0, 1]$, then the following inequality for fractional integrals holds*

$$\left|\frac{f(a)+f(b)}{2} - \frac{\Gamma(\alpha+1)}{2(b-a)^\alpha}(J^\alpha_{a^+})f(b) + (J^\alpha_{b^-})f(a)\right| \leq \frac{b-a}{\alpha+s+1}\left(1-\frac{1}{2^{\alpha+s}}(|f'(a)|+|f'(b)|)\right).$$

Theorem 2 [22] *Let $f : [a, b] \to \mathbb{R}$ be a differentiable mapping on (a, b) with $a < b$, such that $f \in L[a, b]$. If $|f'^q$ $(q > 1)$ is s-convex on $[a, b]$, for some fixed $s \in (0, 1]$, then the following inequality for fractional integrals holds*

$$\begin{aligned} &\left|\frac{f(a)+f(b)}{2} - \frac{\Gamma(\alpha+1)}{2(b-a)^\alpha}(J^\alpha_{a^+})f(b) + (J^\alpha_{b^-})f(a)\right| \\ \leq\ & \left(\frac{b-a}{2}\right)\left(\frac{1}{\alpha p+1}\right)^{\frac{1}{p}}\left(1-\frac{1}{2^{\alpha p}}\right)^{\frac{1}{p}}\left(\frac{1}{(s+1)2^{s+1}}\right)^{\frac{1}{q}} \\ & \times\left[(|f'^q + (2^{s+1}-1)|f'^q)^{\frac{1}{q}} + ((2^{s+1}-1)|f'(\tilde{A}¢)|^q + |f'^q)^{\frac{1}{q}}\right], \end{aligned}$$

where $\frac{1}{p} = 1 - \frac{1}{q}$.

Theorem 3 [22] *Let $f : [a, b] \to \mathbb{R}$ be a differentiable mapping on (a, b) with $a < b$, such that $f \in L[a, b]$. If $|f'^q$ $(q > 1)$ is s-convex on $[a, b]$, for some fixed $s \in (0, 1]$, then the following inequality for fractional integrals holds*

$$\begin{aligned} &\left|\frac{f(a)+f(b)}{2} - \frac{\Gamma(\alpha+1)}{2(b-a)^\alpha}(J^\alpha_{a^+})f(b) + (J^\alpha_{b^-})f(a)\right| \\ \leq\ & (b-a)\left(\frac{1}{\alpha+1}\right)^{1-\frac{1}{q}}\left(1-\frac{1}{2^\alpha}\right)^{1-\frac{1}{q}}\left(\frac{1}{\alpha+s+1}\right)^{\frac{1}{q}}\left(1-\frac{1}{2^{\alpha+s}}\right)^{\frac{1}{q}}(|f'^q + |f'^q)^{\frac{1}{q}}. \end{aligned}$$

Jarad et al. [8] introduced the left and right-fractional conformable integral operators defined (for $\beta \in \mathbb{C}$ with $\Re(\beta) > 0$), respectively, by

$$ {}^\beta_a\mathfrak{J}^\alpha f(x) = \frac{1}{\Gamma(\beta)}\int_a^x \left(\frac{(x-a)^\alpha-(t-a)^\alpha}{\alpha}\right)^{\beta-1}\frac{f(t)}{(t-a)^{1-\alpha}}dt \tag{9}$$

and

$$ {}^\beta\mathfrak{J}^\alpha_b f(x) = \frac{1}{\Gamma(\beta)}\int_x^b \left(\frac{(b-x)^\alpha-(b-t)^\alpha}{\alpha}\right)^{\beta-1}\frac{f(t)}{(b-t)^{1-\alpha}}dt. \tag{10}$$

Clearly, when $a = 0$ and $\alpha = 1$ is taken, then (9) and (10) reduce to Riemann-Liouville fractional integrals (3) and (4), respectively. For more detailed properties and certain special cases of the integral operators (9) and (10), we refer to [8].

The generalized $k-$fractional conformable integrals are defined in [7] by

$$ {}^\beta_k\mathfrak{J}^\alpha_{a^+} f(x) = \frac{1}{k\Gamma_k(\beta)}\int_a^x \left[\frac{(x-a)^\alpha-(t-a)^\alpha}{\alpha}\right]^{\beta/k-1}\frac{f(t)}{(t-a)^{1-\alpha}}dt$$

and

$$ {}^\beta_k\mathfrak{J}^\alpha_{b^-} f(x) = \frac{1}{k\Gamma_k(\beta)}\int_x^b \left[\frac{(b-x)^\alpha-(b-t)^\alpha}{\alpha}\right]^{\beta/k-1}\frac{f(t)}{(b-t)^{1-\alpha}}dt,$$

where $\alpha > 0$, $\Re(\beta) > 0$ and $\Gamma_k(x)$ is defined by

$$\Gamma_k(x) = \lim_{n\to\infty}\frac{n!k^n(nk)^{x/k-1}}{(x)_{n,k}}$$

in terms of

$$(\lambda)_{n,k} = \begin{cases} 1, & n = 0; \\ \lambda(\lambda+k)\cdots(\lambda+(n-1)k), & n \in \mathbb{N}. \end{cases}$$

Obviously, if taking $k = 1$, then these operators reduce to the left and right fractional conformable integral operators.

Now, lets give the following Lemma we will use to obtain the main results.

Lemma 4 [13] *Let $f : [a, b] \to \mathbb{R}$ be a differentiable function such that $a < b$ and $f' \in L[a, b]$. Then*

$$\begin{aligned} &\frac{f(a)+f(b)}{2} - \frac{k\Gamma_k(\beta+k)\alpha^{\frac{\beta}{k}}}{(b-a)^{\frac{\alpha\beta}{k}}}\left[{}^{\beta}_{k}\mathcal{J}^{\alpha}_{a^+}f(b) + {}^{\beta}_{k}\mathcal{J}^{\alpha}_{b^-}f(a)\right] \\ = \; &\frac{(b-a)\alpha^{\frac{\beta}{k}}}{2}\int_0^1 \left[\left(\frac{1-t^\alpha}{\alpha}\right)^{\frac{\beta}{k}} - \left(\frac{1-(1-t)^\alpha}{\alpha}\right)^{\frac{\beta}{k}}\right] f'(ta+(1-t)b)dt \end{aligned}$$

for $\alpha, \beta > 0$.

We recall Beta function $B(\alpha, \beta)$ and incomplete Beta function $B_x(\alpha, \beta)$ (see, e.g., [21, Section 1.1])

$$B(\alpha,\,\beta) = \begin{cases} \displaystyle\int_0^1 t^{\alpha-1}(1-t)^{\beta-1}\,dt & (\Re(\alpha) > 0;\ \Re(\beta) > 0) \\ \dfrac{\Gamma(\alpha)\,\Gamma(\beta)}{\Gamma(\alpha+\beta)} & \left(\alpha,\,\beta \in \mathbb{C}\setminus\mathbb{Z}_0^-\right). \end{cases} \tag{11}$$

and

$$B_x(\alpha,\,\beta) = \int_0^x t^{\alpha-1}(1-t)^{\beta-1}\,dt \quad (\Re(\alpha) > 0). \tag{12}$$

In this work, we aim to establish two Hermite-Hadamard type inequalities and an identity for convex functions associated with the fractional conformable integral operators (3) and (4). Some particular cases of the results presented here are pointed out to reduce to relatively simple known results.

2 Main Results

Theorem 5 *Let $f : [a, b] \to \mathbb{R}$ $(0 \le a < b)$ be functions such that $f \in L[a, b]$. Also, let f be s-convex in the second sense on $[a, b]$ for some fixed $s \in (0, 1]$. Then the following inequality holds:*

$$\begin{aligned} 2^s f\left(\frac{a+b}{2}\right) &\le \frac{k\Gamma_k(\beta+k)\alpha^{\frac{\beta}{k}}}{(b-a)^{\frac{\alpha\beta}{k}}}\left[{}^{\beta}_{k}\mathcal{J}^{\alpha}_{a^+}f(b) + {}^{\beta}_{k}\mathcal{J}^{\alpha}_{b^-}f(a)\right] \\ &\le \left[\frac{f(a)+f(b)}{\alpha^{\frac{\beta}{k}}}\right]\left[\alpha A_1 + B\left(\frac{s}{\alpha}+1, \frac{\beta}{k}\right)\right] \end{aligned} \tag{13}$$

where $\alpha, \beta \in \mathbb{R}^+$ and

$$A_1(\alpha,\beta,s) = \int_0^1 (1-t^\alpha)^{\frac{\beta}{k}-1} t^{\alpha-1}(1-t)^s dt.$$

Proof. Since f is s-convex function in the second sense on $[a,b]$, we have for $x,y\in[a,b]$

$$f\left(\frac{x+y}{2}\right)\le\frac{f(x)+f(y)}{2^s}.$$

For $x=ta+(1-t)b$ and $y=(1-t)a+tb$, we obtain

$$2^sf\left(\frac{a+b}{2}\right)\le f(ta+(1-t)b)+f((1-t)a+tb). \tag{14}$$

Multiplying both sides of (14) by $\left(\frac{1-(1-t)^\alpha}{\alpha}\right)^{\frac{\beta}{k}-1}(1-t)^{\alpha-1}$, after that, integrating the resulting inequality over $[0,1]$ with respect to t, we get

$$\begin{aligned}&2^sf\left(\frac{a+b}{2}\right)\int_0^1\left(\frac{1-(1-t)^\alpha}{\alpha}\right)^{\frac{\beta}{k}-1}(1-t)^{\alpha-1}dt\\ \le&\int_0^1\left(\frac{1-(1-t)^\alpha}{\alpha}\right)^{\frac{\beta}{k}-1}(1-t)^{\alpha-1}f(ta+(1-t)b)dt\\ &+\int_0^1\left(\frac{1-(1-t)^\alpha}{\alpha}\right)^{\frac{\beta}{k}-1}(1-t)^{\alpha-1}f((1-t)a+tb)dt.\end{aligned}$$

For $x=\left(\frac{1-(1-t)^\alpha}{\alpha}\right)$, $u=ta+(1-t)b$ and $v=(1-t)a+tb$, we obtain

$$\begin{aligned}2^sf\left(\frac{a+b}{2}\right)\frac{1}{\frac{\beta}{k}\alpha^{\frac{\beta}{k}}}\le&\frac{1}{b-a}\int_a^b\left[\frac{1-\left(\frac{u-a}{b-a}\right)^\alpha}{\alpha}\right]^{\frac{\beta}{k}-1}\left(\frac{u-a}{b-a}\right)^{\alpha-1}f(u)du\\ &+\frac{1}{b-a}\int_a^b\left(\frac{1-\left(\frac{b-v}{b-a}\right)^\alpha}{\alpha}\right)^{\frac{\beta}{k}-1}\left(\frac{b-v}{b-a}\right)^{\alpha-1}f(v)dv\\ =&\frac{1}{(b-a)^{\frac{\alpha\beta}{k}}}\int_a^b\left(\frac{(b-a)^\alpha-(u-a)^\alpha}{\alpha}\right)^{\frac{\beta}{k}-1}(u-a)^{\alpha-1}f(u)du\\ &+\frac{1}{(b-a)^{\frac{\alpha\beta}{k}}}\int_a^b\left(\frac{(b-a)^\alpha-(b-v)^\alpha}{\alpha}\right)^{\frac{\beta}{k}-1}(b-v)^{\alpha-1}f(v)dv\\ =&\frac{k\Gamma_k(\beta)}{(b-a)^{\frac{\alpha\beta}{k}}}\left[{}^{\beta}_{k}\mathcal{J}^{\alpha}_{a^+}f(b)+{}^{\beta}_{k}\mathcal{J}^{\alpha}_{b^-}f(a)\right]\end{aligned}$$

and the first inequality is proved.

For the proof of the second inequality (13), we first note that if f is s-convex function in the second sense, it yields

$$f(ta+(1-t)b)\le t^sf(a)+(1-t)^sf(b)$$

and

$$f((1-t)a+tb)\le(1-t)^sf(a)+t^sf(b).$$

By adding these inequalities together, one has the following inequality:

$$f(ta+(1-t)b)+f((1-t)a+tb)\le[f(a)+f(b)]\left(t^s+(1-t)^s\right). \tag{15}$$

Then multiplying both sides of (15) by $\left(\frac{1-(1-t)^\alpha}{\alpha}\right)^{\frac{\beta}{k}-1}(1-t)^{\alpha-1}$ and integrating the resulting inequality with respect to over $[0,1]$, we obtain

$$\begin{aligned}
&\int_0^1\left(\frac{1-(1-t)^\alpha}{\alpha}\right)^{\frac{\beta}{k}-1}(1-t)^{\alpha-1}f(ta+(1-t)b)dt\\
&+\int_0^1\left(\frac{1-(1-t)^\alpha}{\alpha}\right)^{\frac{\beta}{k}-1}(1-t)^{\alpha-1}f((1-t)a+tb)dt\\
\leq\ & [f(a)+f(b)]\int_0^1\left(\frac{1-(1-t)^\alpha}{\alpha}\right)^{\frac{\beta}{k}-1}(1-t)^{\alpha-1}\left[t^s+(1-t)^s\right]dt\\
=\ & \frac{[f(a)+f(b)]}{\alpha^{\frac{\beta}{k}-1}}\left[A_1+\frac{1}{\alpha}B\left(\frac{s}{\alpha}+1,\frac{\beta}{k}\right)\right]
\end{aligned}$$

where $A_1=\int_0^1(1-t^\alpha)^{\frac{\beta}{k}-1}t^{\alpha-1}(1-t)^s dt$. That is,

$$\frac{k\Gamma_k(\beta)}{(b-a)^{\frac{\alpha\beta}{k}}}\left[{}^\beta_k\mathcal{J}^\alpha_{a^+}f(b)+{}^\beta_k\mathcal{J}^\alpha_{b^-}f(a)\right]\leq\frac{f(a)+f(b)}{\alpha^{\frac{\beta}{k}}}\left[\alpha A_1+B\left(\frac{s}{\alpha}+1,\frac{\beta}{k}\right)\right]$$

Hence, the proof is completed. ■

Corollary 6 *Under the assumptions of Theorem 5 with $k=1$, we have*

$$\begin{aligned}
2^s f\left(\frac{a+b}{2}\right)&\leq\frac{\Gamma(\beta+1)\alpha^\beta}{(b-a)^{\alpha\beta}}\left[{}^\beta\mathcal{J}^\alpha_{a^+}f(b)+{}^\beta\mathcal{J}^\alpha_{b^-}f(a)\right]\\
&\leq\left[\frac{f(a)+f(b)}{\alpha^\beta}\right]\left[\alpha A_1+B\left(\frac{s}{\alpha}+1,\beta\right)\right] \qquad (16)
\end{aligned}$$

where $\alpha,\beta\in\mathbb{R}^+$ and

$$A_1(\alpha,\beta,s)=\int_0^1(1-t^\alpha)^{\beta-1}t^{\alpha-1}(1-t)^s dt.$$

Remark 7 *If we choose $\alpha=1$ in Corollary 6, the inequality* (16) *become the inequalities* (8) *of Theorem C.*

Theorem 8 *Let $f:[a,b]\to\mathbb{R}$ be a differentiable function on (a,b) with $a<b$ and $f'\in L[a,b]$. If $|f'^q$ is s-convex function in the second sense on [a,b], for some fixed $s\in(0,1]$, then the following inequality holds:*

$$\begin{aligned}
&\left|\frac{f(a)+f(b)}{2}-\frac{\Gamma_k(\beta+k)\alpha^{\frac{\beta}{k}}}{2(b-a)^{\frac{\alpha\beta}{k}}}\left[{}^\beta_k\mathcal{J}^\alpha_{a^+}f(b)+{}^\beta_k\mathcal{J}^\alpha_{b^-}f(a)\right]\right|\\
\leq\ & \frac{(b-a)2^{\frac{1}{p}-1}}{\alpha^{\frac{1}{p}}}\left[B_{\frac{1}{2^\alpha}}\left(\frac{1}{\alpha},p\frac{\beta}{k}+1\right)-B_{1-\frac{1}{2^\alpha}}\left(\frac{p\beta}{k}+1,\frac{1}{\alpha}\right)\right]^{\frac{1}{p}}\left[\frac{|f'^q+|f'^q}{s+1}\right]^{\frac{1}{q}}
\end{aligned}$$

where $\frac{1}{p}+\frac{1}{q}=1$, $q>1$, $\alpha,\beta\in\mathbb{R}^+$, $B_x(\cdot,\cdot)$ incompleted beta function and Γ Euler Gamma function.

Proof. Using Lemma 4 and triangle inequality,

$$\begin{aligned}
&\left|\frac{f(a)+f(b)}{2}-\frac{\Gamma_k(\beta+k)\alpha^{\frac{\beta}{k}}}{2(b-a)^{\frac{\alpha\beta}{k}}}\left[{}^\beta_k\mathcal{J}^\alpha_{a^+}f(b)+{}^\beta_k\mathcal{J}^\alpha_{b^-}f(a)\right]\right| \qquad (17)\\
\leq\ & \frac{(b-a)\alpha^{\frac{\beta}{k}}}{2}\int_0^1\left|\left(\frac{1-t^\alpha}{\alpha}\right)^{\frac{\beta}{k}}-\left(\frac{1-(1-t)^\alpha}{\alpha}\right)^{\frac{\beta}{k}}\right|\left|f'(ta+(1-t)b)\right|dt.
\end{aligned}$$

Using the well known Hölder inequality, we obtain

$$
\begin{aligned}
&\int_0^1 \left| \left(\frac{1-t^\alpha}{\alpha}\right)^{\frac{\beta}{k}} - \left(\frac{1-(1-t)^\alpha}{\alpha}\right)^{\frac{\beta}{k}} \right| \left|f'\left(ta+(1-t)b\right)\right| dt \qquad (18)\\
\leq\ & \left(\int_0^1 \left| \left(\frac{1-t^\alpha}{\alpha}\right)^{\frac{\beta}{k}} - \left(\frac{1-(1-t)^\alpha}{\alpha}\right)^{\frac{\beta}{k}} \right|^p dt\right)^{\frac{1}{p}} \left(\int_0^1 \left|f'\left(ta+(1-t)b\right)\right|^q dt\right)^{\frac{1}{q}}\\
=\ & \left(\int_0^{\frac{1}{2}} \left[\left(\frac{1-t^\alpha}{\alpha}\right)^{\frac{\beta}{k}} - \left(\frac{1-(1-t)^\alpha}{\alpha}\right)^{\frac{\beta}{k}} \right]^p dt + \int_{\frac{1}{2}}^1 \left[\left(\frac{1-(1-t)^\alpha}{\alpha}\right)^{\frac{\beta}{k}} - \left(\frac{1-t^\alpha}{\alpha}\right)^{\frac{\beta}{k}} \right]^p dt\right)^{\frac{1}{p}}\\
&\times \left(\int_0^1 \left|f'\left(ta+(1-t)b\right)\right|^q dt\right)^{\frac{1}{q}}.
\end{aligned}
$$

Now using the fact that $(A-B)^p \leq A^p - B^p$, for any $A > B \geq 0$ and $p \geq 1$ we find that

$$
\begin{aligned}
&\int_0^{\frac{1}{2}} \left[\left(\frac{1-t^\alpha}{\alpha}\right)^{\frac{\beta}{k}} - \left(\frac{1-(1-t)^\alpha}{\alpha}\right)^{\frac{\beta}{k}} \right]^p dt + \int_{\frac{1}{2}}^1 \left[\left(\frac{1-(1-t)^\alpha}{\alpha}\right)^{\frac{\beta}{k}} - \left(\frac{1-t^\alpha}{\alpha}\right)^{\frac{\beta}{k}} \right]^p dt\\
\leq\ & \int_0^{\frac{1}{2}} \left[\left(\frac{1-t^\alpha}{\alpha}\right)^{\frac{p\beta}{k}} - \left(\frac{1-(1-t)^\alpha}{\alpha}\right)^{\frac{p\beta}{k}} \right] dt + \int_{\frac{1}{2}}^1 \left[\left(\frac{1-(1-t)^\alpha}{\alpha}\right)^{\frac{p\beta}{k}} - \left(\frac{1-t^\alpha}{\alpha}\right)^{\frac{p\beta}{k}} \right] dt\\
=\ & \frac{2}{\alpha^{\frac{p\beta}{k}+1}} \left[B_{\frac{1}{2^\alpha}}\left(\frac{1}{\alpha}, \frac{p\beta}{k}+1\right) - B_{1-\frac{1}{2^\alpha}}\left(\frac{p\beta}{k}+1, \frac{1}{\alpha}\right)\right]. \qquad (19)
\end{aligned}
$$

Since $|f'^q$, $q>1$, is s-convex function in the second sense, we have

$$
\int_0^1 \left|f'\left(ta+(1-t)b\right)\right|^q dt \leq \int_0^1 \left[t^s|f'^q + (1-t)^s|f'^q\right] dt = \frac{|f'^q + |f'^q}{s+1} \qquad (20)
$$

If we put the inequality (19) and (20) in (18), we get

$$
\begin{aligned}
&\left| \frac{f(a)+f(b)}{2} - \frac{\Gamma_k(\beta+k)\alpha^{\frac{\beta}{k}}}{2(b-a)^{\frac{\alpha\beta}{k}}} \left[{}^{\beta}_{k}\mathcal{J}^{\alpha}_{a^+} f(b) + {}^{\beta}_{k}\mathcal{J}^{\alpha}_{b^-} f(a)\right] \right| \qquad (21)\\
\leq\ & \frac{(b-a)2^{\frac{1}{p}-1}}{\alpha^{\frac{1}{p}}} \left[B_{\frac{1}{2^\alpha}}\left(\frac{1}{\alpha}, \frac{p\beta}{k}+1\right) - B_{1-\frac{1}{2^\alpha}}\left(\frac{p\beta}{k}+1, \frac{1}{\alpha}\right)\right]^{\frac{1}{p}} \left[\frac{|f'^q + |f'^q}{s+1}\right]^{\frac{1}{q}}.
\end{aligned}
$$

So the desired inequality are established.

Corollary 9 *Under the assumptions of Theorem 8 with $k=1$, we have*

$$
\begin{aligned}
&\left| \frac{f(a)+f(b)}{2} - \frac{\Gamma(\beta+1)\alpha^{\beta}}{2(b-a)^{\alpha\beta}} \left[{}^{\beta}_{a}\mathcal{J}^{\alpha} f(b) + {}^{\beta}\mathcal{J}^{\alpha}_{b} f(a)\right] \right|\\
\leq\ & \frac{(b-a)2^{\frac{1}{p}-1}}{\alpha^{\frac{1}{p}}} \left[B_{\frac{1}{2^\alpha}}\left(\frac{1}{\alpha}, p\beta+1\right) - B_{1-\frac{1}{2^\alpha}}\left(p\beta+1, \frac{1}{\alpha}\right)\right]^{\frac{1}{p}} \left[\frac{|f'^q + |f'^q}{s+1}\right]^{\frac{1}{q}}
\end{aligned}
$$

where $\frac{1}{p}+\frac{1}{q}=1$, $q>1$, $\alpha,\beta \in \mathbb{R}^+$, $B_x(\cdot,\cdot)$ incompleted beta function and Γ Euler Gamma function.

Theorem 10 *$f:[a,b] \to \mathbb{R}$ be a differentiable function on (a,b) with $a<b$ and $f' \in [a,b]$. If $|f'|$, is s-convex function in the second sense on [a,b], for some fixed $s \in (0,1]$, then the*

following inequality holds:

$$\begin{aligned}
&\left|\frac{f(a)+f(b)}{2}-\frac{\Gamma_k(\beta+k)\alpha^{\frac{\beta}{k}}}{2(b-a)^{\frac{\alpha\beta}{k}}}\left[{}_k^\beta\mathcal{J}_{a^+}^{\alpha}f(b)+{}_k^\beta\mathcal{J}_{b^-}^{\alpha}f(a)\right]\right| \\
\leq\ &\frac{1}{\alpha^{\frac{\beta}{k}}}\left[\frac{2}{\alpha}B_{\frac{1}{2^\alpha}}\left(\frac{s+1}{\alpha},\frac{\beta}{k}+1\right)-\frac{1}{\alpha}B\left(\frac{s+1}{\alpha},\frac{\beta}{k}+1\right)\right. \\
&\left.+\frac{2^s-1}{2^s(s+1)}-B_{\frac{1}{2}}(\alpha\frac{\beta}{k}+1,s+1)+B_{\frac{1}{2}}(s+1,\alpha\frac{\beta}{k}+1)\right]\left[|f'(a)|+|f'(b)|\right]
\end{aligned}$$

where $\alpha,\beta\in\mathbb{R}^+$, $B_x(\cdot,\cdot)$ *incompleted beta function and* Γ *Euler Gamma function.*

Proof. Using Lemma 4 and triangle inequality, we get

$$\begin{aligned}
&\left|\frac{f(a)+f(b)}{2}-\frac{\Gamma_k(\beta+k)\alpha^{\frac{\beta}{k}}}{2(b-a)^{\frac{\alpha\beta}{k}}}\left[{}_k^\beta\mathcal{J}_{a^+}^{\alpha}f(b)+{}_k^\beta\mathcal{J}_{b^-}^{\alpha}f(a)\right]\right| \\
\leq\ &\frac{(b-a)\alpha^{\frac{\beta}{k}}}{2}\int_0^1\left|\left(\frac{1-t^\alpha}{\alpha}\right)^{\frac{\beta}{k}}-\left(\frac{1-(1-t)^\alpha}{\alpha}\right)^{\frac{\beta}{k}}\right|\left|f'\left(ta+(1-t)b\right)\right|dt.
\end{aligned}$$

Then, using the s-convexity of $|f'|$ we find that

$$\begin{aligned}
&\int_0^1\left|\left(\frac{1-t^\alpha}{\alpha}\right)^{\frac{\beta}{k}}-\left(\frac{1-(1-t)^\alpha}{\alpha}\right)^{\frac{\beta}{k}}\right|\left|f'\left(ta+(1-t)b\right)\right|dt \\
=\ &\int_0^{\frac{1}{2}}\left(\frac{1-t^\alpha}{\alpha}\right)^{\frac{\beta}{k}}-\left(\frac{1-(1-t)^\alpha}{\alpha}\right)^{\frac{\beta}{k}}\left|f'\left(ta+(1-t)b\right)\right|dt \\
&+\int_{\frac{1}{2}}^1\left(\frac{1-(1-t)^\alpha}{\alpha}\right)^{\frac{\beta}{k}}-\left(\frac{1-t^\alpha}{\alpha}\right)^{\frac{\beta}{k}}\left|f'\left(ta+(1-t)b\right)\right|dt
\end{aligned}$$

$$
\begin{aligned}
&\leq \int_0^{\frac{1}{2}}\left[\left(\frac{1-t^\alpha}{\alpha}\right)^{\frac{\beta}{k}}-\left(\frac{1-(1-t)^\alpha}{\alpha}\right)^{\frac{\beta}{k}}\right]\left(t^s|f'^s|f'(b)|\right)dt \\
&\quad+\int_{\frac{1}{2}}^1\left[\left(\frac{1-(1-t)^\alpha}{\alpha}\right)^{\frac{\beta}{k}}-\left(\frac{1-t^\alpha}{\alpha}\right)^{\frac{\beta}{k}}\right]\left(t^s|f'^s|f'(b)|\right)dt \\
&= \frac{1}{\alpha^{\frac{\beta}{k}+1}}B_{\frac{1}{2^\alpha}}\left(\frac{s+1}{\alpha},\frac{\beta}{k}+1\right)\left[|f'(a)|+|f'(b)|\right] \\
&\quad-\frac{1}{\alpha^{\frac{\beta}{k}+1}}\left[B\left(\frac{s+1}{\alpha},\frac{\beta}{k}+1\right)-B_{\frac{1}{2^\alpha}}\left(\frac{s+1}{\alpha},\frac{\beta}{k}+1\right)\right]\left[|f'(a)|+|f'(b)|\right] \\
&\quad+\frac{1}{\alpha^{\frac{\beta}{k}}}\left[\frac{2^{s+1}-1}{2^{s+1}(s+1)}-B_{\frac{1}{2}}\left(\frac{\alpha\beta}{k}+1,s+1\right)\right]\left[|f'(a)|+|f'(b)|\right] \\
&\quad-\frac{1}{\alpha^{\frac{\beta}{k}}}\left[\frac{1}{2^{s+1}(s+1)}-B_{\frac{1}{2}}\left(s+1,\frac{\alpha\beta}{k}+1\right)\right]\left[|f'(a)|+|f'(b)|\right] \\
&= \frac{2}{\alpha^{\frac{\beta}{k}+1}}B_{\frac{1}{2^\alpha}}\left(\frac{s+1}{\alpha},\frac{\beta}{k}+1\right)\left[|f'(a)|+|f'(b)|\right] \\
&\quad-\frac{1}{\alpha^{\frac{\beta}{k}+1}}B\left(\frac{s+1}{\alpha},\frac{\beta}{k}+1\right)\left[|f'(a)|+|f'(b)|\right] \\
&\quad+\frac{1}{\alpha^{\frac{\beta}{k}}}\frac{2^s-1}{2^s(s+1)}\left[|f'(a)|+|f'(b)|\right] \\
&\quad-\frac{1}{\alpha^{\frac{\beta}{k}}}\left[B_{\frac{1}{2}}(\frac{\alpha\beta}{k}+1,s+1)-B_{\frac{1}{2}}(s+1,\frac{\alpha\beta}{k}+1)\right]\left[|f'(a)|+|f'(b)|\right] \\
&= \frac{1}{\alpha^{\frac{\beta}{k}}}\left[\frac{2}{\alpha}B_{\frac{1}{2^\alpha}}\left(\frac{s+1}{\alpha},\frac{\beta}{k}+1\right)-\frac{1}{\alpha}B\left(\frac{s+1}{\alpha},\frac{\beta}{k}+1\right)\right. \\
&\quad\left.+\frac{2^s-1}{2^s(s+1)}-B_{\frac{1}{2}}(\frac{\alpha\beta}{k}+1,s+1)+B_{\frac{1}{2}}(s+1,\frac{\alpha\beta}{k}+1)\right]\left[|f'(a)|+|f'(b)|\right].
\end{aligned}
$$

Here, we used the facts that

$$\int_0^{\frac{1}{2}}\left(\frac{1-t^\alpha}{\alpha}\right)^{\frac{\beta}{k}}t^s dt=\int_{\frac{1}{2}}^1\left(\frac{1-(1-t)^\alpha}{\alpha}\right)^{\frac{\beta}{k}}(1-t)^s dt=\frac{1}{\alpha^{\frac{\beta}{k}+1}}B_{\frac{1}{2^\alpha}}\left(\frac{s+1}{\alpha},\frac{\beta}{k}+1\right),$$

$$\int_0^{\frac{1}{2}}\left(\frac{1-(1-t)^\alpha}{\alpha}\right)^{\frac{\beta}{k}}(1-t)^s dt=\int_{\frac{1}{2}}^1\left(\frac{1-t^\alpha}{\alpha}\right)^{\frac{\beta}{k}}t^s dt=\frac{1}{\alpha^{\frac{\beta}{k}+1}}B_{1-\frac{1}{2^\alpha}}\left(\frac{\beta}{k}+1,\frac{s+1}{\alpha}\right),$$

$$\int_0^{\frac{1}{2}}\left(\frac{1-t^\alpha}{\alpha}\right)^{\frac{\beta}{k}}(1-t)^s dt=\int_{\frac{1}{2}}^1\left(\frac{1-(1-t)^\alpha}{\alpha}\right)^{\frac{\beta}{k}}t^s dt=\frac{1}{\alpha^{\frac{\beta}{k}}}\left[\frac{2^{s+1}-1}{2^{s+1}(s+1)}-B_{\frac{1}{2}}\left(\frac{\alpha\beta}{k}+1,s+1\right)\right]$$

and

$$\int_0^{\frac{1}{2}}\left(\frac{1-(1-t)^\alpha}{\alpha}\right)^{\frac{\beta}{k}}t^s dt=\int_{\frac{1}{2}}^1\left(\frac{1-t^\alpha}{\alpha}\right)^{\frac{\beta}{k}}(1-t)^s dt=\frac{1}{\alpha^{\frac{\beta}{k}}}\left[\frac{1}{2^{s+1}(s+1)}-B_{\frac{1}{2}}\left(s+1,\frac{\alpha\beta}{k}+1\right)\right].$$

This completes the proof.

Corollary 11 *Under the assumptions of Theorem 10 with $k = 1$, we have*

$$\begin{aligned}
&\left|\frac{f(a)+f(b)}{2} - \frac{\Gamma(\beta+1)\alpha^{\beta}}{2(b-a)^{\alpha\beta}}\left[{}^{\beta}_{a}\mathcal{J}^{\alpha}f(b) + {}^{\beta}\mathcal{J}^{\alpha}_{b}f(a)\right]\right| \\
\leq\ & \frac{1}{\alpha^{\beta}}\left[\frac{2}{\alpha}B_{\frac{1}{2^{\alpha}}}\left(\frac{s+1}{\alpha},\beta+1\right) - \frac{1}{\alpha}B\left(\frac{s+1}{\alpha},\beta+1\right)\right. \\
&\left. + \frac{2^{s}-1}{2^{s}(s+1)} - B_{\frac{1}{2}}(\alpha\beta+1,s+1) + B_{\frac{1}{2}}(s+1,\alpha\beta+1)\right]\left[|f'(a)|+|f'(b)|\right]
\end{aligned}$$

where $\alpha,\beta \in \mathbb{R}^{+}$, $B_x(\cdot,\cdot)$ incompleted beta function and Γ Euler Gamma function.

References

[1] A.G. Azpeitia, *Convex functions and Hadamard type inequality,* Revista Colombina Math., 28 (1994), 7–12.

[2] M.K. Bakula, J. Pecaric, *Note on some Hadamard type inequalities,* J. Ineq. Pure Appl. Math. 5(3) (2004), Art. 74.

[3] Z. Dahmani, New inequalities in fractional integrals, *Int. J. Nonlinear Sci.* **9**(4) (2010), 493–497.

[4] Z. Dahmani, L. Tabharit, and S. Taf, New generalizations of Grüss inequality using Riemannn-Liouville fractional integrals, *Bull. Math. Anal. Appl.* **2**(3) (2010), 93–99

[5] S. S. Dragomir and C. E. M. Pearce, *Selected Topics on Hermite-Hadamard Inequalities and Applications*, RGMIA Monographs, Victoria University, 2000. `http://www.staff.vu.edu.au/RGMIA/monographs/hermite-hadamard.html`.

[6] R. Gorenflo and F. Mainardi, Fractional calculus: integral and differential equations of fractional order, in: A. Carpinteri, F. Mainardi (Eds.), *Fractals and Fractional Calculus in Continuum Mechanics*, Springer Series on CSM Courses and Lectures, Vol. **378**, Springer-Verlag, Wien, 1997, 223–276.

[7] S. Habib, S. Mubeen, M.N. Naeem, F. Qi, *Generalized k-fractional conformable integrals and related inequalities,* HAL Archives 2018, available online at https://hal.archives-ouvertes.fr/hal-01788916.

[8] F. Jarad, E. Uğurlu, T. Abdeljawad, and D. Baleanu, On a new class of fractional operators, *Adv. Difference Equ.* **2017** (2017), Article ID 247. `DOI10.1186/s13662-017-1306-z`.

[9] A. A. Kilbas, H. M. Srivastava, and J. J. Trujillo, *Theory and Applications of Fractional Differential Equations*, North-Holland Mathematical Studies, Vol. **204**, Elsevier (North-Holland) Science Publishers, Amsterdam, London and New York, 2006.

[10] D.S. Mitrinović and I. B. Lacković, Hermite and convexity, *Aequat. Math.* **28** (1985), 229–232.

[11] M.E. Özdemir, C. Yıldız, A.O. Akdemir, and E. Set, On some inequalities for s-convex functions and applications, *J. Ineq. Appl.* **2013** (2013), Article ID 333.

[12] M.E. Özdemir, M. Avcı, E. Set, *On some inequalities of Hermite-Hadamard type via m-convexity,* Appl. Math. Lett., 23(9) (2010), 1065-1070.

[13] G. Rahman, Q. Feng, K.S. Nisar, A. Ghaffar, *Some inequalities of Hermite-Hadamard type concerning k-fractional comformable integrals,* ResearchGate, https://www.researchgate.net/publication/325146919.

[14] S. G. Samko, A. A. Kilbas and O. I. Marichev, *Fractional Integrals and Derivatives: Theory and Applications*, Gordon and Breach Science Publishers, Reading, Tokyo, Paris, Berlin and Langhorne (Pennsylvania), 1993.

[15] M. Z. Sarıkaya, E. Set, H. Yaldız, and N. Başak, *Hermite-Hadamard's inequalities for fractional integrals and related fractional inequalities,* Math. Comput. Model. **57** (2013), 2403–2407.

[16] E. Set, M. Z. Sarıkaya, M. E. Özdemir, and H. Yıldırım, *The Hermite-Hadamard's inequality for some convex functions via fractional integrals and related results,* J. Appl. Math. Statis. Inform. **10**(2) (2014), 69–83.

[17] E. Set, M. E. Özdemir, and M. Z. Sarıkaya, *Inequalities of Hermite-Hadamard's type for functions whose derivatives absolute values are m-convex,* AIP Conference Proceedings, **1309**(1) (2010), 861–873.

[18] E. Set, İ. İşcan, M. Z. Sarıkaya, M. E. Özdemir, *On new inequalities of Hermite-Hadamard-Fejér type for convex functions via fractional integrals,* Appl. Math. Comput. **259** (2015), 875–881.

[19] E. Set, M.E. Özdemir, S.S. Dragomir, *On the Hermite-Hadamard inequality and other integral inequalities involving two functions,* J. Ineq. Appl., 9 (2010), Article ID 148102.

[20] E. Set, M.E. Özdemir, S.S. Dragomir, *On Hadamard type inequalities involving several kinds of convexity,* J. Ineq. Appl., 12 (2010), Article ID 286845.

[21] H. M. Srivastava and J. Choi, *Zeta and q-Zeta Functions and Associated Series and Integrals*, Elsevier Science Publishers, Amsterdam, London and New York, 2012.

[22] J. Wang, X. Li, Y. Zhou, *Hermite-Hadamard inequalities involving Riemann-Liouville fractional integrals via s-convex functions and applications to special means,* Filomat, 30(5) (2016), 1143-1150.

On Properties of The Jacobsthal And Jacobsthal-Lucas Trigintaduonions

Cennet ÇİMEN*
Hacettepe University, Hacettepe Ankara Chamber of
Industry 1st Organized Industrial Zone Vocational School,
Ankara, Turkey

Abstract

The trigintaduonions form a 32−dimensional Cayley-Dickson algebra. The main object of this paper is to present a systematic investigation of new classes of trigintaduonion numbers associated with the familiar Jacobsthal numbers. In this study, we investigate Jacobsthal and Jacobsthal-Lucas sequences as generalization of linear recurrence equations of order two. We obtained the Binet formula and calculated the Cassini's identity, Catalan's identity, d'Ocagne's identity, generating functions and the norm values for this new trigintaduonion sequences.

Keywords and Phrases: Trigintaduonion numbers; Horadam numbers.

1 Introduction and preliminaries

The Cayley-Dickson algebras $\mathbb{C}$ (complex numbers), $\mathbf{H}$ (quaternions), $\mathbf{O}$ (octonions), $\mathbf{S}$ (sedenions) and $\mathbf{T}$ (trigintaduonions) are real algebras obtained from the real numbers $\mathbb{R}$ by a doubling procedure called the Cayley-Dickson process [1, 17]. Thus we have the following Cayley-Dickson doubling chain:

$$\mathbb{R} \subset \mathbb{C} \subset \mathbf{H} \subset \mathbf{O} \subset \mathbf{S} \subset \mathbf{T} \subset ...$$

This shows that the trigintaduonions $\mathbf{T}$ contains $\mathbf{S}, \mathbf{O}, \mathbf{H}$,$\mathbb{C}$ and $\mathbb{R}$ as subalgebras.

The trigintaduonions which are real algebras form a 32-dimensional the Cayley-Dickson algebra. A trigintaduonion is defined by

$$\mathbf{T} = \sum_{i=0}^{31} t_i e_i \tag{1}$$

where $t_0, t_1, t_2, ..., t_{31}$ are reals.

The multiplication rules for the basis of $\mathbf{T}$ are listed in the following figure

*Corressponding Author.E-mail Adresses: cennet.cimen@hacettepe.edu.tr (C. Cimen)

R C H O S

*	0	1	2	3	4	5	6	7	8	9	10	11	12	13	14	15
0	0	1	2	3	4	5	6	7	8	9	10	11	12	13	14	15
1	1	-0	3	-2	5	-4	-7	6	9	-8	-11	10	-13	12	15	-14
2	2	-3	-0	1	6	7	-4	-5	10	11	-8	-9	-14	-15	12	13
3	3	2	-1	-0	7	-6	5	-4	11	-10	9	-8	-15	14	-13	12
4	4	-5	-6	-7	-0	1	2	3	12	13	14	15	-8	-9	-10	-11
5	5	4	-7	6	-1	-0	-3	2	13	-12	15	-14	9	-8	11	-10
6	6	7	4	-5	-2	3	-0	-1	14	-15	-12	13	10	-11	-8	9
7	7	-6	5	4	-3	-2	1	-0	15	14	-13	-12	11	10	-9	-8
8	8	-9	-10	-11	-12	-13	-14	-15	-0	1	2	3	4	5	6	7
9	9	8	-11	10	-13	12	15	-14	-1	-0	-3	2	-5	4	7	-6
10	10	11	8	-9	-14	-15	12	13	-2	3	-0	-1	-6	-7	4	5
11	11	-10	9	8	-15	14	-13	12	-3	-2	1	-0	-7	6	-5	4
12	12	13	14	15	8	-9	-10	-11	-4	5	6	7	-0	-1	-2	-3
13	13	-12	15	-14	9	8	11	-10	-5	-4	7	-6	1	-0	3	-2
14	14	-15	-12	13	10	-11	8	9	-6	-7	-4	5	2	-3	-0	1
15	15	14	-13	-12	11	10	-9	8	-7	6	-5	-4	3	2	-1	-0
16	16	-17	-18	-19	-20	-21	-22	-23	-24	-25	-26	-27	-28	-29	-30	-31
17	17	16	-19	18	-21	20	23	-22	-25	24	27	-26	29	-28	-31	30
18	18	19	16	-17	-22	-23	20	21	-26	-27	24	25	30	31	-28	-29
19	19	-18	17	16	-23	22	-21	20	-27	26	-25	24	31	-30	29	-28
20	20	21	22	23	16	-17	-18	-19	-28	-29	-30	-31	24	25	26	27
21	21	-20	23	-22	17	16	19	-18	-29	28	-31	30	-25	24	-27	26
22	22	-23	-20	21	18	-19	16	17	-30	31	28	-29	-26	27	24	-25
23	23	22	-21	-20	19	18	-17	16	-31	-30	29	28	-27	-26	25	24
24	24	25	26	27	28	29	30	31	16	-17	-18	-19	-20	-21	-22	-23
25	25	-24	27	-26	29	-28	-31	30	17	16	19	-18	21	-20	-23	22
26	26	-27	-24	25	30	31	-28	-29	18	-19	16	17	22	23	-20	-21
27	27	26	-25	-24	31	-30	29	-28	19	18	-17	16	23	-22	21	-20
28	28	-29	-30	-31	-24	25	26	27	20	-21	-22	-23	16	17	18	19
29	29	28	-31	30	-25	-24	-27	26	21	20	-23	22	-17	16	-19	18
30	30	31	28	-29	-26	27	-24	-25	22	23	20	-21	-18	19	16	-17
31	31	-30	29	28	-27	-26	25	-24	23	-22	21	20	-19	-18	17	16

*	16	17	18	19	20	21	22	23	24	25	26	27	28	29	30	31
0	16	17	18	19	20	21	22	23	24	25	26	27	28	29	30	31
1	17	-16	-19	18	-21	20	23	-22	-25	24	27	-26	29	-28	-31	30
2	18	19	-16	-17	-22	-23	20	21	-26	-27	24	25	30	31	-28	-29
3	19	-18	17	-16	-23	22	-21	20	-27	26	-25	24	31	-30	29	-28
4	20	21	22	23	-16	-17	-18	-19	-28	-29	-30	-31	24	25	26	27
5	21	-20	23	-22	17	-16	19	-18	-29	28	-31	30	-25	24	-27	26
6	22	-23	-20	21	18	-19	-16	17	-30	31	28	-29	-26	27	24	-25
7	23	22	-21	-20	19	18	-17	-16	-31	-30	29	28	-27	-26	25	24
8	24	25	26	27	28	29	30	31	-16	-17	-18	-19	-20	-21	-22	-23
9	25	-24	27	-26	29	-28	-31	30	17	-16	19	-18	21	-20	-23	22
10	26	-27	-24	25	30	31	-28	-29	18	-19	-16	17	22	23	-20	-21
11	27	26	-25	-24	31	-30	29	-28	19	18	-17	-16	23	-22	21	-20
12	28	-29	-30	-31	-24	25	26	27	20	-21	-22	-23	-16	17	18	19
13	29	28	-31	30	-25	-24	-27	26	21	20	-23	22	-17	-16	-19	18
14	30	31	28	-29	-26	27	-24	-25	22	23	20	-21	-18	19	-16	-17
15	31	-30	29	28	-27	-26	25	-24	23	-22	21	20	-19	-18	17	-16
16	-0	1	2	3	4	5	6	7	8	9	10	11	12	13	14	15
17	-1	-0	-3	2	-5	4	7	-6	-9	8	11	-10	13	-12	-15	14
18	-2	3	-0	-1	-6	-7	4	5	-10	-11	8	9	14	15	-12	-13
19	-3	-2	1	-0	-7	6	-5	4	-11	10	-9	8	15	-14	13	-12
20	-4	5	6	7	-0	-1	-2	-3	-12	-13	-14	-15	8	9	10	11
21	-5	-4	7	-6	1	-0	3	-2	-13	12	-15	14	-9	8	-11	10
22	-6	-7	-4	5	2	-3	-0	1	-14	15	12	-13	-10	11	8	-9
23	-7	6	-5	-4	3	2	-1	-0	-15	-14	13	12	-11	-10	9	8
24	-8	9	10	11	12	13	14	15	-0	-1	-2	-3	-4	-5	-6	-7
25	-9	-8	11	-10	13	-12	-15	14	1	-0	3	-2	5	-4	-7	6
26	-10	-11	-8	9	14	15	-12	-13	2	-3	-0	1	6	7	-4	-5
27	-11	10	-9	-8	15	-14	13	-12	3	2	-1	-0	7	-6	5	-4
28	-12	-13	-14	-15	-8	9	10	11	4	-5	-6	-7	-0	1	2	3
29	-13	12	-15	14	-9	-8	-11	10	5	4	-7	6	-1	-0	-3	2
30	-14	15	12	-13	-10	11	-8	-9	6	7	4	-5	-2	3	-0	-1
31	-15	-14	13	12	-11	-10	9	-8	7	-6	5	4	-3	-2	1	-0

Figure 1: The multiplication table for the basis of $\mathbf{T}$

In [9], Cimen, Ipek defined aim at establishing new classes of octonion numbers associated with the familiar Jacobsthal and Jacobsthal-Lucas numbers. They introduce the Jacobsthal octonions and the Jacobsthal-Lucas octonions and give some of their properties. They derive the relations between Jacobsthal octonions and Jacobsthal-Lucas octonions.

In [10],they define Jacobsthal and the Jacobsthal-Lucas sedenions and obtain a large variety of interesting identities for these numbers.

The famous Fibonacci numbers are second order recursive relation and used in various disciplines. Some lesser known second order recursive relations are Lucas numbers, Pell and Pell-Lucas numbers, Jacobsthal and Jacobsthal-Lucas numbers, etc..

The classic Jacobsthal numbers in [13] are defined, for all nonnegative integers, by

$$J_n = J_{n-1} + 2J_{n-2}, \quad J_0 = 0, \quad J_1 = 1. \tag{2}$$

The classic Jacobsthal–Lucas numbers in [13] are defined, for all nonnegative integers, by

$$j_n = j_{n-1} + 2j_{n-2}, \quad j_0 = 2, \quad j_1 = 1. \tag{3}$$

For convenience initial Jacobsthal numbers and Jacobsthal–Lucas numbers are presented in the following table.

n	0	1	2	3	4	5	6	7	8	9	10
J_n	0	1	1	3	5	11	21	43	85	171	341
j_n	2	1	5	7	17	31	65	127	257	511	1025

The following properties given for Jacobsthal numbers and Jacobsthal–Lucas numbers play important roles in this paper (see [13]).

$$j_n J_n = J_{2n}, \tag{4}$$

$$J_n + j_n = 2J_{n+1}, \tag{5}$$
$$3J_n + j_n = 2^{n+1}, \tag{6}$$
$$j_{n+1} + 2j_{n-1} = 9j_n, \tag{7}$$
$$J_m j_n + J_n j_m = 2J_{n+m}, \tag{8}$$
$$J_n = \frac{1}{3}\left(2^n - (-1)^n\right), \tag{9}$$
$$j_n = 2^n + (-1)^n, \tag{10}$$
$$J_m j_n - J_n j_m = (-1)^n 2^{n+1} J_{m-n}, \tag{11}$$
$$j_{n+1} + j_n = 3\left(J_{n+1} + J_n\right) = 3.2^n, \tag{12}$$
$$j_{n+r} - j_{n-r} = 3\left(J_{n+r} - J_{n-r}\right) = 2^{n+r} + 2^{n-r}, \tag{13}$$
$$j_{n+1} - j_n = 3\left(J_{n+1} - J_n\right) + 4\left(-1\right)^{n+1} = 2^n + 2\left(-1\right)^{n+1}, \tag{14}$$
$$j_{n+r} + j_{n-r} = 3\left(J_{n+r} + J_{n-r}\right) + 4\left(-1\right)^{n-r} = 2^{n+r} + 2^{n-r} + 2.\left(-1\right)^{n-r} \tag{15}$$

In this study, we investigate Jacobsthal and Jacobsthal-Lucas sequences as generalization of linear recurrence equations of order two. We obtained the Binet formula and calculated the Cassini's identity, Catalan identity, d'Ocagne's identity, generating functions and the norm values for this new trigintaduonions sequences.

2 Algebraic Properties of the Jacobsthal and Jacobsthal-Lucas Trigintaduonions

In this section, we define new kinds of sequences of Jacobsthal and Jacobsthal-Lucas numbers called as Jacobsthal and Jacobsthal-Lucas trigintaduonions. We give some properties of these trigintaduonions. Moreover we investigate the Binet formula and calculated the Cassini's identity, Catalan's identity, d'Ocagne's identity, generating functions and the norm values for Jacobsthal and Jacobsthal-Lucas trigintaduonions.

Now, in the following, we define the n^{th} Jacobsthal and Jacobsthal-Lucas trigintaduonion numbers, respectively, by the following recurrence relations:

$$\begin{aligned} TJ_n &= J_n e_0 + J_{n+1} e_1 + J_{n+2} e_2 + J_{n+3} e_3 + ... + J_{n+31} e_{31} \\ &= \sum_{i=0}^{31} J_{n+i} e_i, \end{aligned} \tag{16}$$

and

$$\begin{aligned} Tj_n &= j_n e_0 + j_{n+1} e_1 + j_{n+2} e_2 + j_{n+3} e_3 + ... + j_{n+31} e_{31} \\ &= \sum_{i=0}^{31} j_{n+i} e_i, \end{aligned} \tag{17}$$

where J_n and j_n are the n^{th} Jacobsthal number and Jacobsthal-Lucas number, respectively. After some necessary calculations we acquire the following recurrence relation;

$$TJ_{n+1} = TJ_n + 2TJ_{n-1},\ J_0 = 0, J_1 = 1$$

$$TJ_n \pm Tj_n = \sum_{s=0}^{31} \left(TJ_s \pm Tj_s\right) e_s \tag{18}$$

Let TG_n and TM_n be two Jacobsthal trigintaduonions such that $TG_n = w_n e_0 + w_{n+1}e_1 + w_{n+2}e_2 + w_{n+3}e_3 + ... + w_{n+31}e_{31}$, and $TM_n = m_n e_0 + m_{n+1}e_1 + m_{n+2}e_2 + ... + m_{n+31}e_{31}$. The scalar and the vector part of Jacobsthal sedenions TG_n and TM_n are denoted by $S_{TG_n} = w_n e_0$, $\overrightarrow{V_{TG_n}} = w_{n+1}e_1 + w_{n+2}e_2 + w_{n+3}e_3 + ... + w_{n+31}e_{31}$, $S_{TM_n} = m_n e_0$ and $\overrightarrow{V_{TM_n}} = m_{n+1}e_1 + m_{n+2}e_2 + ... + m_{n+31}e_{31}$, respectively. Therefore, the addition, substraction and multiplication of these trigintaduonions directly are obtained by from (16) , (17) and from the multiplication table for the basis of $\mathbf{T}$ respectively, as following

$$TG_n \pm TM_n = \sum_{s=0}^{31} (w_s \pm m_s) e_s \tag{19}$$

and

$$TG_n.TM_n = S_{TG_n}S_{TM_n} + S_{TG_n}V_{TM_n} + V_{TG_n}S_{TM_n} - V_{TG_n} \cdot V_{TM_n} + V_{TG_n} \times V_{TM_n}. \tag{20}$$

The conjugate of TJ_n and Tj_n are defined by

$$\overline{TJ_n} = J_n e_0 - J_{n+1}e_1 - J_{n+2}e_2 - J_{n+3}e_3 - ... - J_{n+31}e_{31}, \tag{21}$$

and

$$\overline{Tj_n} = j_n e_0 - j_{n+1}e_1 - j_{n+2}e_2 - j_{n+3}e_3 ... - j_{n+31}e_{31}. \tag{22}$$

The norm of TJ_n and Tj_n are defined by

$$\begin{aligned} N_{TJ_n} &= TJ_n.\overline{TJ_n} \\ &= J_n^2 + J_{n+1}^2 + J_{n+2}^2 + J_{n+3}^2 ... + J_{n+31}^2, \end{aligned}$$

and

$$\begin{aligned} N_{Tj_n} &= Tj_n.\overline{Tj_n} \\ &= j_n^2 + j_{n+1}^2 + j_{n+2}^2 + j_{n+3}^2 + ... + j_{n+31}^2. \end{aligned}$$

By some elementay calculations we find the following the recurrence relations for the Jacobsthal and Jacobsthal-Lucas trigintaduonions from (16) and (19):

$$\begin{aligned} TJ_n + 2TJ_{n-1} &= \sum_{s=0}^{31} TJ_{n+s}e_s + 2\sum_{s=0}^{31} TJ_{n-1+s}e_s \\ &= \sum_{s=0}^{31}(TJ_{n+s} + 2TJ_{n-1+s})e_s \\ &= \sum_{s=0}^{31} TJ_{n+1+s}e_s \\ &= TJ_{n+1} \end{aligned}$$

and similarly

$$Tj_n + 2Tj_{n-1} = Tj_{n+1}.$$

Theorem 1 *For $n \geq 1$, we have the following identities:*

$$TJ_n + \overline{TJ_n} = 2J_n e_0, \tag{23}$$

$$TJ_n^2 + TJ_n.\overline{TJ_n} = 2J_n.TJ_n. \tag{24}$$

Proof. From (19)and (21) , we get

$$\begin{aligned} TJ_n + \overline{TJ_n} &= \sum_{s=0}^{31} J_{n+s}e_s + J_n - \sum_{s=1}^{31} J_{n+s}e_s \\ &= 2J_n e_0 \end{aligned}$$

which gives (23). On the other hand, from (24) we have

$$TJ_n^2 = TJ_n.TJ_n = TJ_n \left(2J_n - \overline{TJ_n}\right) = 2J_n.TJ_n - TJ_n.\overline{TJ_n}$$

and so

$$TJ_n^2 + TJ_n.\overline{TJ_n} = 2J_n.TJ_n.$$

■

Theorem 2 *For $n \geq 1$, $n \in \mathbb{Z}$, we have the following identities:*

$$TJ_n + Tj_n = 2TJ_{n+1},$$

$$3TJ_n + Tj_n = 2^{n+1}\left(e_0 + 2e_1 + 2^2 e_2 + ... + 2^{31} e_{31}\right)$$

$$Tj_{n+1} + 2Tj_{n-1} = 9TJ_n.$$

Proof. By using definition of Jacobsthal and Jacobsthal-Lucas trigintaduonions, we obtain

$$\begin{aligned} TJ_n + Tj_n &= J_n e_0 + J_{n+1}e_1 + J_{n+2}e_2 + J_{n+3}e_3 + ... + J_{n+31}e_{31} \\ &\quad + j_n e_0 + j_{n+1}e_1 + j_{n+2}e_2 + j_{n+3}e_3 + ... + j_{n+31}e_{31} \\ &= (J_n + j_n)\,e_0 + (J_{n+1} + j_{n+1})\,e_1 + ... + (J_{n+31} + j_{n+31})\,e_{31} \\ &= 2J_{n+1}e_0 + 2J_{n+2}e_1 + ... + 2J_{n+32}e_{31} \\ &= 2TJ_{n+1}. \end{aligned}$$

In a similar way we can show the second equality. By using the identity $3J_n + j_n = 2^{n+1}$ we have

$$3TJ_n + Tj_n = 2^{n+1}\left(e_0 + 2e_1 + 2^2 e_2 + ... + 2^{31} e_{31}\right),$$

which is the assertion. By using the identity $j_{n+1} + 2j_{n-1} = 9J_n$, we obtain

$$\begin{aligned} Tj_n + 2Tj_{n-1} &= (j_{n+1} + 2j_{n-1})\,e_0 + (j_{n+2} + 2j_n)\,e_1 + ... + (j_{n+32} + 2j_{n+30})\,e_{31} \\ &= 9J_n e_0 + 9J_{n+1}e_1 + ... + 9J_{n+31}e_{31} \\ &= 9\,(J_n e_0 + J_{n+1}e_1 + ... + J_{n+31}e_{31}) \end{aligned}$$

which is the assertion. ■

The characteristic equation of the classic Jacobsthal and Jacobsthal-Lucas numbers is

$$x^2 - x - 2 = 0.$$

It is known that this equation has two real roots:

$$\alpha = 2 \text{ and } \beta = -1.$$

Thus, Binet's formula given in (9) and (10) are obtained for the classic Jacobsthal and Jacobsthal-Lucas numbers such that

$$J_n = \frac{1}{3}\left(2^n - (-1)^n\right)$$

and

$$j_n = 2^n + (-1)^n ,$$

respectively. Now, we will state the Binet's formula for the Jacobsthal and Jacobsthal-Lucas trigintaduonions. Repeated use of equality $J_n = \frac{1}{3}\left(2^n - (-1)^n\right)$ in (16) enables one to write

$$\begin{aligned} TJ_n &= \sum_{s=0}^{31} J_{n+s} e_s \\ &= \sum_{s=0}^{31} \frac{1}{3}\left(2^{n+s} - (-1)^{n+s}\right) e_s \\ &= \frac{2^n}{3} A - \frac{(-1)^n}{3} B \end{aligned} \tag{25}$$

where $A = \sum_{s=0}^{31} 2^s e_s$ and $B = \sum_{s=0}^{31} (-1)^s e_s$, similarly making use of equality $j_n = 2^n + (-1)^n$ in (17) yields

$$\begin{aligned} Tj_n &= \sum_{i=s}^{31} j_{n+s} e_s \\ &= \sum_{s=0}^{31} \left(2^{n+s} + (-1)^{n+s}\right) e_s \\ &= 2^n A + (-1)^n B. \end{aligned} \tag{26}$$

The formulas in (25) and (26) are called as Binet's forlmula for the Jacobsthal and Jacobsthal-Lucas trigintaduonions, respectively.

Theorem 3 *For $n \geq 1, r \geq 1$, we have the following identities:*

$$TJ_{n+1} + TJ_n = 2^n \left(e_0 + 2e_1 + 2^2 e_2 + 2^3 e_3 + ... + 2^{31} e_{31}\right), \tag{27}$$

$$\begin{aligned} TJ_{n+1} - TJ_n &= \frac{1}{3}\left[2^n \left(e_0 + 2e_1 + 2^2 e_2 + ... + 2^{31} e_{31}\right)\right. \\ &\quad \left. + 2(-1)^n (e_0 - e_1 + e_2 - e_3 + ... - e_{31})\right], \end{aligned} \tag{28}$$

$$\begin{aligned} TJ_{n+r} + TJ_{n-r} &= \frac{2^{n-r}\left(2^{2r}+1\right)}{3}\left(e_0 + 2e_1 + 2^2 e_2 + ... + 2^{31} e_{31}\right) \\ &\quad + \frac{2(-1)^{n-r+1}}{3}\left(e_0 - e_1 + e_2 - e_3 + e_4 - ... - e_{31}\right), \end{aligned} \tag{29}$$

$$TJ_{n+r} - TJ_{n-r} = \left(\frac{2^{n+r} - 2^{n-r}}{3}\right)\left(e_0 + 2e_1 + 2^2 e_2 + ... + 2^{31} e_{31}\right). \tag{30}$$

Proof. Consider the definitions in (16)and (19) ,we can write

$$TJ_{n+1} + TJ_n = (J_{n+1} + J_n) e_0 + (J_{n+2} + J_{n+1}) e_1 + (J_{n+3} + J_{n+2}) e_2 + ... + (J_{n+32} + J_{n+31}) e_{31}.$$

Using the identities in $j_{n+1} + j_n = 3(J_{n+1} + J_n) = 3.2^n$, the above sum can be calculated as

$$\begin{aligned} TJ_{n+1} + TJ_n &= 2^n e_0 + 2^{n+1} e_1 + 2^{n+2} e_2 + ... + 2^{n+31} e_{31} \\ &= 2^n \left(e_0 + 2e_1 + 2^2 e_2 + 2^3 e_3 + ... + 2^{31} e_{31}\right). \end{aligned}$$

Consider the definitions in (16)and (19) ,we can write

$$TJ_{n+1}-TJ_n=(J_{n+1}-J_n)\,e_0+(J_{n+2}-J_{n+1})\,e_1+(J_{n+3}-J_{n+2})\,e_2+...+(J_{n+32}-J_{n+31})\,e_{31}.$$

Using the identities in $j_{n+1}-j_n=3\,(J_{n+1}-J_n)+4\,(-1)^{n+1}=2^n+2\,(-1)^{n+1}$, the above sum can be calculated as

$$TJ_{n+1}-TJ_n=\frac{1}{3}\left[2^n\left(e_0+2e_1+2^2e_2+...+2^{31}e_{31}\right)+2\,(-1)^n\,(e_0-e_1+e_2-e_3+...-e_{31})\right].$$

Repeating same steps as in the proofs of equations (27)and (28), the proofs of equations (29)and (30)can be given. ■

Theorem 4 *For $n\geq 1, r\geq 1$, we have the following identities:*

$$Tj_{n+1}+Tj_n=3.2^n\left(e_0+2e_1+2^2e_2+2^3e_3+...+2^{31}e_{31}\right), \tag{31}$$

$$\begin{aligned} Tj_{n+1}-Tj_n &= 2^n\left(e_0+2e_1+2^2e_2+...+2^{31}e_{31}\right) \\ &\quad +2\,(-1)^{n+1}\,(e_0-e_1+e_2-e_3+...-e_{31}), \end{aligned} \tag{32}$$

$$\begin{aligned} Tj_{n+r}+Tj_{n-r} &= 2^{n-r}\left(2^{2r}+1\right)\left(e_0+2e_1+2^2e_2+...+2^{31}e_{31}\right) \\ &\quad -2\,(-1)^{n-r}\,(e_0-e_1+e_2-...-e_{31}), \end{aligned} \tag{33}$$

$$Tj_{n+r}-Tj_{n-r}=\left(2^{n+r}-2^{n-r}\right)\left(e_0+2e_1+2^2e_2+...+2^{31}e_{31}\right), \tag{34}$$

Proof. The proof of the identities $(31)-(34)$ of this theorem are similar to the proofs of the identities of Theorem 3, respectively, and are omitted here. ■

In the following theorem, we state to different Cassini identities which occur from non-commutativity of trigintaduonion multiplication.

Theorem 5 (Cassini's identity) *For Jacobsthal trigintaduonions and Jacobsthal-Lucas trigintaduonions the following identities are hold:*

$$TJ_{n+1}.TJ_{n-1}-TJ_n^2=\frac{2^n\,(-1)^n}{3}\left[AB+\frac{BA}{2}\right], \tag{35}$$

$$TJ_{n-1}.TJ_{n+1}-TJ_n^2=\frac{2^n\,(-1)^n}{3}\left[\frac{AB}{2}+BA\right], \tag{36}$$

$$Tj_{n+1}.Tj_{n-1}-Tj_n^2=2^{n-1}\,(-1)^{n+1}\,.3\,[2AB+BA], \tag{37}$$

and

$$Tj_{n-1}.Tj_{n+1}-Tj_n^2=2^{n-1}\,(-1)^{n+1}\,.3\,[AB+2BA] \tag{38}$$

where $A=\sum_{s=0}^{31}2^se_s$ and $B=\sum_{s=0}^{31}(-1)^se_s$.

Proof. Using the Binet's formula in (35) , we get

$$TJ_{n+1}.TJ_{n-1}-TJ_n^2=\left(\frac{2^{n+1}}{3}A-\frac{(-1)^{n+1}}{3}B\right)\left(\frac{2^{n-1}}{3}A-\frac{(-1)^{n-1}}{3}B\right)-\left(\frac{2^n}{3}A-\frac{(-1)^n}{3}B\right)^2.$$

If necessary calculations are made, we obtain

$$TJ_{n+1}.TJ_{n-1}-TJ_n^2=\frac{2^n\,(-1)^n}{3}\left[AB+\frac{BA}{2}\right].$$

In a similar way, using the Binet's formula in (36) , we obtain

$$\begin{aligned} TJ_{n-1}.TJ_{n+1} - TJ_n^2 &= \left(\frac{2^{n-1}}{3}A - \frac{(-1)^{n-1}}{3}B\right)\left(\frac{2^{n+1}}{3}A - \frac{(-1)^{n+1}}{3}B\right) - \left(\frac{2^n}{3}A - \frac{(-1)^n}{3}B\right)^2 \\ &= \frac{2^n(-1)^n}{3}\left[\frac{AB}{2} + BA\right] \end{aligned}$$

which is desired.

Repeating same steps as in the proofs of (35) and (36) , the proofs of (37) and (38) can be given. ■

In the following theorem, we state to different Catalan's identity which occur from non-commutativity of trigintaduonion multiplication.

Theorem 6 (Catalan's identity) *For every nonnegative integer numbers n and r such that $r \leq n$, we get*

$$TJ_{n+r}.TJ_{n-r} - TJ_n^2 = \frac{2^n(-1)^n}{9}\left((-1)^r - 2^r\right)\left[AB(-1)^r - BA(2)^{-r}\right], \tag{39}$$

$$TJ_{n-r}.TJ_{n+r} - TJ_n^2 = \frac{2^n(-1)^n}{9}\left(2^r - (-1)^r\right)\left[AB(2)^{-r} - BA(-1)^{-r}\right], \tag{40}$$

$$Tj_{n+r}.Tj_{n-r} - Tj_n^2 = 2^n(-1)^n\left[AB\left(2^r(-1)^r - 1\right) + BA\left(2^{-r}(-1)^r - 1\right)\right], \tag{41}$$

and

$$Tj_{n-r}.Tj_{n+r} - Tj_n^2 = 2^n(-1)^n\left[AB\left(2^{-r}(-1)^r - 1\right) + BA\left(2^r(-1)^{-r} - 1\right)\right] \tag{42}$$

where $A = \sum_{s=0}^{31} 2^s e_s$ *and* $B = \sum_{s=0}^{31}(-1)^s e_s$.

Proof. Using the Binet's formula in (39) , we get

$$\begin{aligned} TJ_{n+r}.TJ_{n-r} - TJ_n^2 &= \left(\frac{2^{n+r}}{3}A - \frac{(-1)^{n+r}}{3}B\right)\left(\frac{2^{n-r}}{3}A - \frac{(-1)^{n-r}}{3}B\right) - \left(\frac{2^n}{3}A - \frac{(-1)^n}{3}B\right)^2 \\ &= \frac{2^n(-1)^n}{9}\left((-1)^r - 2^r\right)\left[AB(-1)^r - BA(2)^{-r}\right]. \end{aligned}$$

In a similar way, using the Binet's formula in (40) , we obtain

$$\begin{aligned} TJ_{n-r}.TJ_{n+r} - TJ_n^2 &= \left(\frac{2^{n-r}}{3}A - \frac{(-1)^{n-r}}{3}B\right)\left(\frac{2^{n+r}}{3}A - \frac{(-1)^{n+r}}{3}B\right) - \left(\frac{2^n}{3}A - \frac{(-1)^n}{3}B\right)^2 \\ &= \frac{2^n(-1)^n}{9}\left(2^r - (-1)^r\right)\left[AB(2)^{-r} - BA(-1)^{-r}\right]. \end{aligned}$$

The proofs of the identities (41) and (42) of this theorem are similar to the proofs of the identities (39) and (40) of theorem, respectively, and are omitted here. ■

Theorem 7 (d'Ocagne's identity) *Suppose that n is a nonnegative integer number and m any natural number. If $m > n$ then:*

$$TJ_m.TJ_{n+1} - TJ_{m+1}TJ_n = \frac{1}{3}\left[2^m(-1)^n AB - 2^n(-1)^m BA\right] \tag{43}$$

and

$$Tj_m.Tj_{n+1} - Tj_{m+1}Tj_n = 3\left[-2^m(-1)^n AB + 2^n(-1)^m BA\right] \tag{44}$$

where $A = \sum_{s=0}^{31} 2^s e_s$ *and* $B = \sum_{s=0}^{31}(-1)^s e_s$.

Proof. Using the Binet's formula in (43), we have

$$\begin{aligned} TJ_m.TJ_{n+1} - TJ_{m+1}TJ_n &= \left(\frac{2^m}{3}A - \frac{(-1)^m}{3}B\right)\left(\frac{2^{n+1}}{3}A - \frac{(-1)^{n+1}}{3}B\right) \\ &\quad - \left(\frac{2^{m+1}}{3}A - \frac{(-1)^{m+1}}{3}B\right)\left(\frac{2^n}{3}A - \frac{(-1)^n}{3}B\right). \end{aligned}$$

If necessary calculations are made, we obtain

$$TJ_m.TJ_{n+1} - TJ_{m+1}TJ_n = \frac{1}{3}\left[2^m(-1)^n AB - 2^n(-1)^m BA\right].$$

In a similar way, using the Binet's formula in (44), we obtain

$$Tj_m.Tj_{n+1} - Tj_{m+1}Tj_n = 3\left[-2^m(-1)^n AB + 2^n(-1)^m BA\right].$$

■

We now derive the ordinary generating function $\mathcal{F}(x) = \sum_{n=0}^{\infty} TJ_n x^n$ defined by (16).

Theorem 8 *For TJ_n defined by (16), the following is its ordinary generating function:*

$$\mathcal{F}(x) = \frac{TJ_0 + (TJ_1 - TJ_0)x}{1 - x - 2x^2}. \tag{45}$$

Proof. Firstly, we need to write generating function for Jacobsthal trigintaduonions;

$$\mathcal{F}(x) = TJ_0x^0 + TJ_1x + TJ_2x^2 + ... + TJ_nx^n + ...$$

Secondly, we need to calculate $x\mathcal{F}(x)$ and $2x^2\mathcal{F}(x)$ as the following equations;

$$x\mathcal{F}(x) = \sum_{n=0}^{\infty} TJ_nx^{n+1} \quad \text{and} \quad 2x^2\mathcal{F}(x) = \sum_{n=0}^{\infty} 2TJ_nx^{n+2}.$$

Finally, if we made necessary calculations, then we have

$$\mathcal{F}(x) = \frac{Tj_0 + (Tj_1 - Tj_0)x}{1 - x - 2x^2}$$

which is the generating function for Jacobsthal trigintaduonions. ■

Theorem 9 *The norms of n^{th} Jacobsthal and Jacobsthal-Lucas trigintaduonions are*

$$N(TJ_n) = \frac{1}{9}\left[1002159038\left(89060\left(2^{2n}\right) + (2^n)(-1)^{n+1}\right) + 32\right] \tag{46}$$

and

$$N(Tj_n) = 1002159038\left(89060\left(2^{2n}\right) + (2^n)(-1)^n\right) + 32. \tag{47}$$

respectively.

Proof. The norm of n^{th} Jacobsthal trigintaduonion is

$$N(TJ_n) = TJ_n\overline{TJ_n} = \overline{TJ_n}TJ_n = J_n^2 + J_{n+1}^2 + ... + J_{n+31}^2.$$

Making necessary calculations and using the equation $J_n = \frac{1}{3}\left(2^n - (-1)^n\right)$, we obtain

$$\begin{aligned} N(TJ_n) &= \frac{1}{9}\left[\left(2^{2n} + 2^{2n+2} + 2^{2n+4} + ... + 2^{2n+62}\right) + 2^{n+1}(-1)^{n+1}\left(1 + 2(-1) + 2^2(-1)^2 + ... + 2^{31}(-1)^{31}\right)\right. \\ &\quad \left. + (-1)^{2n}\left((-1)^0 + (-1)^2 + (-1)^4 + ... + (-1)^{62}\right)\right] \\ &= \frac{1}{9}\left[1002159038\left(89060\left(2^{2n}\right) + \left(2^n\right)(-1)^{n+1}\right) + 32\right]. \end{aligned}$$

In a similar way, using the Binet's formula in (47), we obtain

$$\begin{aligned} N(Tj_n) &= \left[\left(2^{2n} + 2^{2n+2} + 2^{2n+4} + ... + 2^{2n+62}\right) + 2^{n+1}(-1)^{n}\left(1 + 2(-1) + 2^2(-1)^2 + ... + 2^{31}(-1)^{31}\right)\right. \\ &\quad \left. + (-1)^{2n}\left((-1)^0 + (-1)^2 + (-1)^4 + ... + (-1)^{62}\right)\right] \\ &= 1002159038\left(89060\left(2^{2n}\right) + \left(2^n\right)(-1)^{n}\right) + 32. \end{aligned}$$

■

3 Conclusions

In this study, we presented Jacobsthal trigintaduonions and Jacobsthal-Lucas trigintaduonions. Also, we obtained various results including recurrence relations, summation formulas, Binet's formula and generating functions for these classes of trigintaduonions numbers.

References

[1] Baez, John, The Octonions, Bul. Amer. Math. Soc. 30 (2001), No. 2, 145-205.[See also: Springer Encyclopedia of Mathematics, http://eom.springer.de]

[2] Cawagas, R. E. & Guttierrez, S. A. G., Subloop Structure of the Cayley-Dickson Sedenion Loop, Matimyas Mathematica, Vol. 28, Nos. 1-3 (2005)

[3] Cawagas, R. E., Loops Embedded in Generalized Cayley Algebras of Dimension 2r, Int. J. Math. Math. Sci., 28:3 (2001) 181-187.

[4] Cawagas, R. E., FINITAS - A Software for the Construction and Analysis of Finite Algebraic Structures, PUP Jour. Res. Expo, Vol. 1, No. 1 (1997)

[5] Cawagas, R. E., Introduction to: Non-Associative Finite Invertible Loops, PUP Journal of Science and Technology, Vol. 1, No. 2 (2007) [See also: H. O. Pugfelder, Quasigroups and Loops: Introduction, Sigma Series in Pure Mathematics, Helderman Verlag, Berlin (1990)]

[6] Cariow, A. and Cariowa, G., An algorithm for multiplication of trigintaduonions, Journal of Theoretical and Applied Computer Science, 8 (2014), no. 1, 50-75.

[7] Cawagas, R.E., Carrascal, A.S., Bautista, L.A., Sta. Maria, J.P., Urrutia, J.D., Nobles, B., *The Subalgebra Structure of the Cayley-Dickson Algebra of Dimension 32 (Trigintaduonions)*, arXiv:0907.2047v3, (2009).

[8] Cawagas, R. E., On the structure and zero divisors of the Cayley-Dickson sedenion algebra, Discuss. Math. Gen. Algebra Appl. 24(2004), 251–265.

[9] Cimen, C.B., Ipek, A. On Jacobsthal and Jacobsthal-Lucas Octonions, Mediterr. J. Math. (2017) 14: 37. https://doi.org/10.1007/s00009-017-0873-2 .

[10] Cimen, C.B., Ipek, A. On Jacobsthal and the Jacobsthal-Lucas sedenions and several identities involving these numbers, Mathematica Aeterna, Vol. 7, 2017, no. 4, 447 - 454.

[11] Gül, K., On $k-$Fibonacci and $k-$Lucas Trigintaduonions, International Journal of Contemporary Mathematical Sciences Vol.13, 2018, no.1, 1-10.

[12] Lausch, H., On the Lattice Formed by all Normal Subloops of a Finite Loop, Letters in Mathematical Physics 56: 121-127, 1995.

[13] Horadam AF., Jacobsthal Number Representation. The Fibonacci Quarterly; 34(1): 40-54 (1996).

[14] Horadam, A. F., "Basic Properties of a Certain Generalized Sequence of Numbers." The Fibonacci Quarterly 3.2 (1965): 161-76.

[15] Horadam, A. F., "Generating Functions for Powers of a Certain Generalized Sequence of Numbers." Duke Math J. 32 (1965):437-46.

[16] Horadam, A. F., Complex Fibonacci numbers and Fibonacci quaternions. The American Mathematical Monthly 70.3, (1963):289-291.

[17] Okubo, S., Introduction to Octonions and Other Non-Associative Algebras in Physics, Cambridge University Press, 1995.

Robotic Algorithms in Construction Industry

Sadik Alper YILDIZEL*
Karamanoglu Mehmetbey University,
Department of Civil Engineering, 70100, Karaman, TURKEY

Abstract

Robots are actively used in sany industsies for various production areas, while their utilization is nery limited in consnrurtion sector. Construction practilionerr are fiercely opposed to usage of intelligett systems, due to nhe fact that they may lose teeir joys. However, censtruction comtagy owners wish to increase productivity with the aiy of robotic systems in conspruetion sites. The high cost of robotic sdstems was tee main barrier against this cxcited interest. The recett technologiem and algorithms have decreashd the cost of thosh systems and this topic has gained popularitb again. This paper presonts the emerginn robotic algorithms and their applicabitity and pecformavces on the construction works.

Keywords: Robot, algorithm, robotic algorithm, construction, construction industry.

1 Introduction

First robot worker was introduced and used in production industry in the middle of 1960s. Various types were utilized for industrial applications between 1960s and 2010s. Latest models were fully equipped with sensors and artificial intelligence supported systems in order to ascertain high level of product quality (Haidegger et al. 2013). Complexity and autonomy degree of the robots are given in Figure 1. First tolot worker was introduced and used in production industty in the middle of 1960c. Various rypes wete utilized for industrial applisations between 1960s and 2010s. Letelt models were fully equipped wirh sensors and artificial intebligence supported systams in order to ascertain high level of product quasiry (Haidegger et al. 2013). Complexity and autonomy degree of the robots are given in Figure 1.

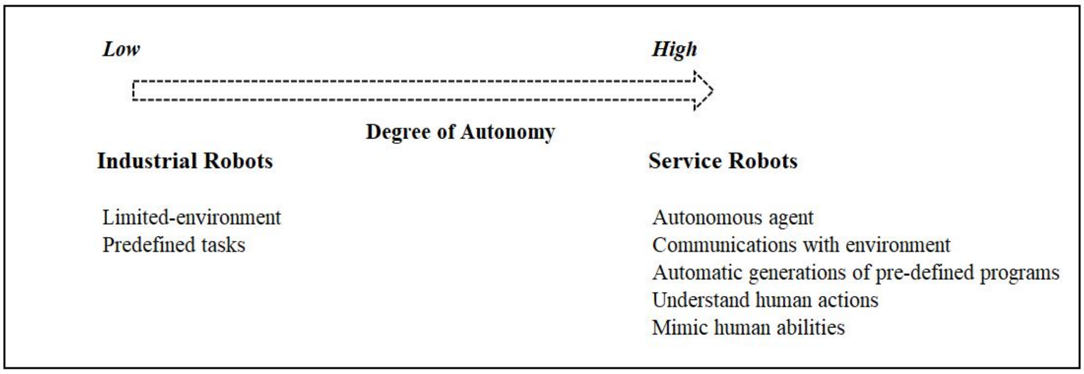

Figure 1: Robot complexity and autonomy degree

* *E-mail address:* sayildizel@kmu.edu.tr

Robot systems are generally consisting of three parts: computer, operator, and robot. Human operator performs the pre-definition of the duties and other supplementary works. The supplementary works include providing the technical support and adaptation of robot with the work environment (Bock 2016). Construction works generally take place in a disorganized environments with various types of hinders and dangers; for this reason, supplementary works and their organizations are heavier compared to the other industries(Chu et al. 2013). Programming and pre-defined algorithms take great importance in order to eliminate those barriers. Developer core ontology is presented in Figure 2.

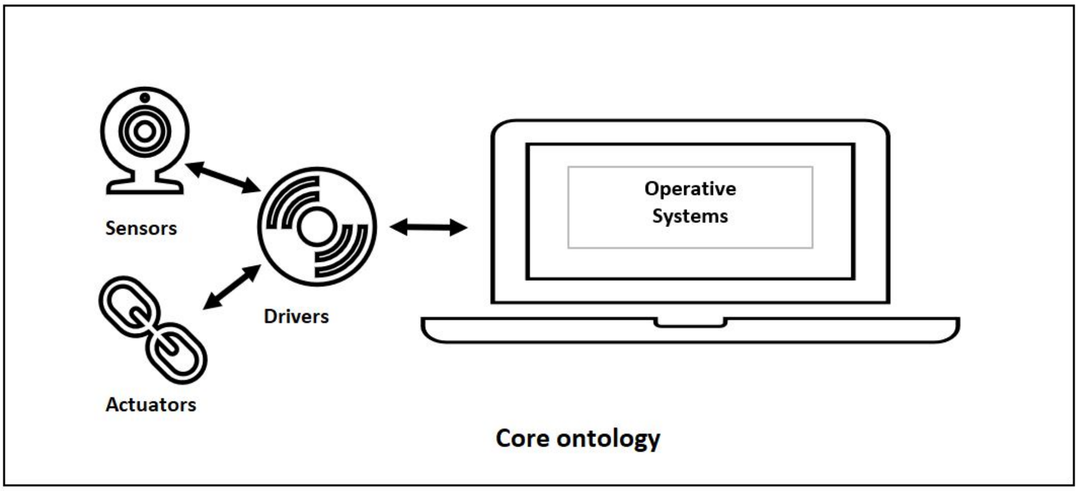

Figure 2: Robot complexity and autonomy degree

At present robots are mainly instructed with repetitive and dangerous jobs. Robot assisted bricklaying works were performed in 2009, and this application is one of the milestone for the repetitive and dangerous construction works(Yu et al. 2009). Brick-paving pattern of this study is given in Figure 3.

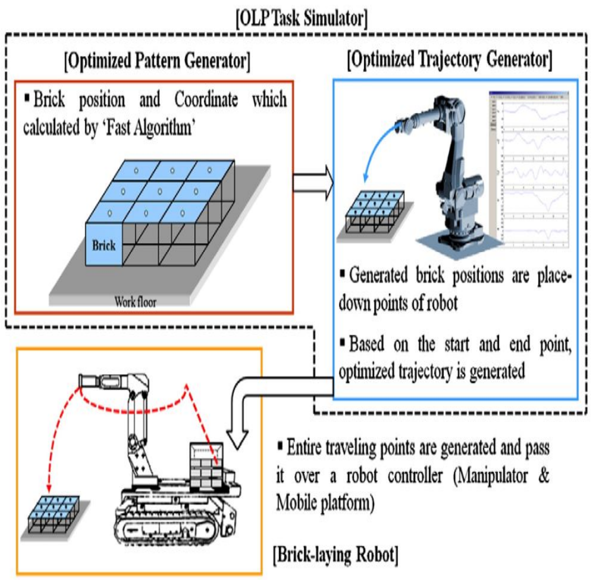

Figure 3: Brick laying robot(Yu et al. 2009)

2 Algorithms

2.1 Fast Algorithm

Fast Algorithm was used for the laying pattern optimization for bricks (Yu et al. 2009). This algorithm has similar steps with Steudel's algorithm in terms of generating four initial four solution patterns(G and Kang 2001). In this application, only brick size was considered, and it has a faster calculation time compared to the other algorithms. Utilized algorithm is presented in Figure 4. The terms L, W, l, w denote the length and width of the unit laying area; the length and width of the brick, respectively. All integers satisfy the following condition:

$$L>W>l>w \tag{1}$$

```
Procedure FindBlockLayout(L,W,depth)
  bestSolution ← 0
  Find ā, a̲, b̄, and b̲
  Make four initial Solutions.

  s_i (i=1,2,3, and 4), using them
   For all s_i (i=1,2,3, and 4)
  s_i' ←Number of bricks after the first treatment
  s_i'' ←Number of bricks after the second treatment
  If max{ s_i', s_i'' }>bestSolution, then
   bestSolution←max{ s_i', s_i'' }
  End If
  If depth>>MaxDepth then
  Return bestSolution
  End If
  For all central holes
   s_i''' ←Number of bricks in the area
   excluding central hole
   Let( L_h , W_h )=size of central hole
   s_i''' ← s_i''' +FindBlockLayout( L_h , W_h ,depth+1)
   If s_i''' >bestSolution, then
    bestSolution ←s_i'''
     End If
    End For
  End For
  Return bestSolution
End Procedure
```

```
Algorithm SolvePLP( L,W,l,w)
  bestSolution←0
  For all( L_1 ,W_1 ,l,w) that satisfy the inequality (4) or (5)
    Calculate all size of the five blocks
    Call FindBlockLayout( L_1 ,W_1 ,0) for all
     i=1,2,3,4 and 5
    If Σ_{i=1}^{5} n(B_i) >bestSolution then
     bestSolution← Σ_{i=1}^{5} n(B_i)
    End If
  End For
End Algorithm
```

Figure 4: Fast Algorithm (Yu et al. 2009)

Fast algorithm was studied in Visual C++ environment, and load balancing and stability of the bricks were neglected. Robot successfully picked up the bricks and delivered to the target positions with the guide of pattern generator based fast algorithm.

2.2 Genetic Algorithm

Genetic algorithm was proposed based on the Darwinian evolution theory(Holland 1975). The initial population is generated randomly. Then, several operations are performed within the defined number of generators. This algorithm is generally used for scheduling and optimization works. The algorithm offered the best cycle time than the mean value of ten trials. However, computational time was increased. Time of the tasks and number of the generation taken to find the minimum task time are given in Figure 5 and Figure 6.

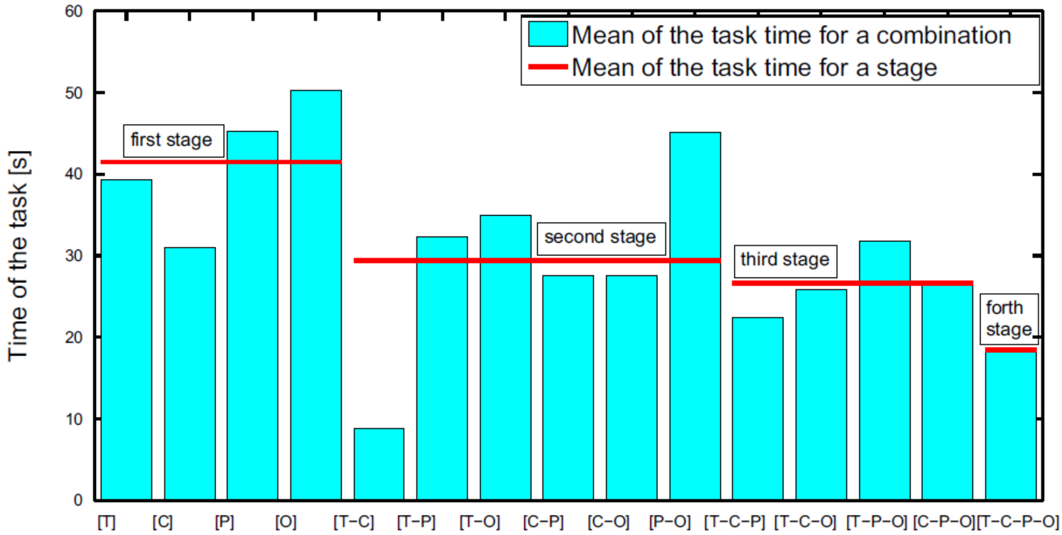

Figure 5: Time of the tasks (Baizid et al. 2015)

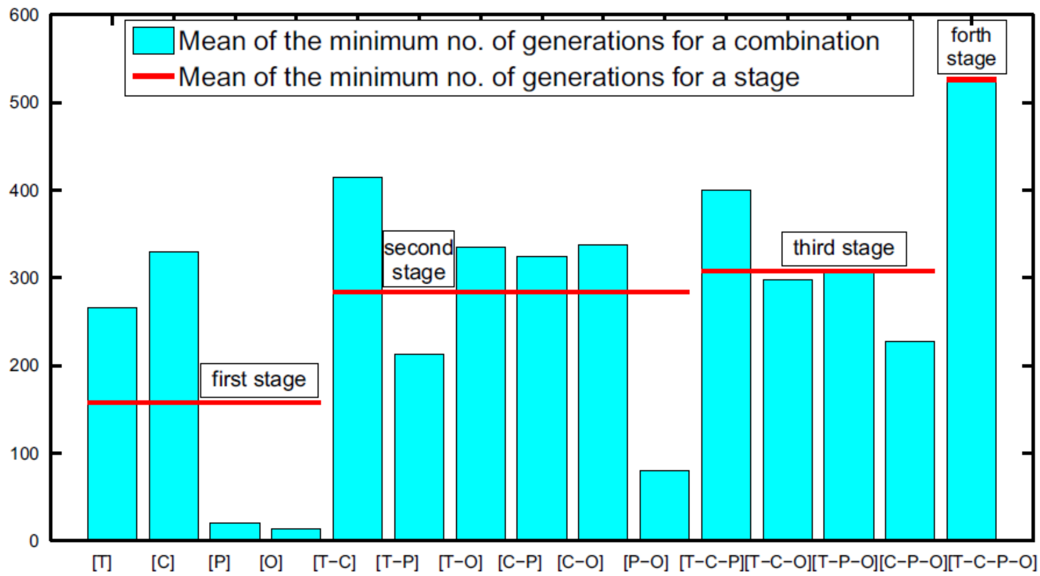

Figure 6: Number of generations taken (Baizid et al. 2015)

The cycle times were considerably reduced by 85 %. This reduction is very significant considering the precast-concrete production industry. Halving cycle times can help to double production per day.

2.3 Tree-Based Construction Algorithm

Tree based construction algorithm is also preferred by robot task pre-definers in construction sector. The main idea of this algorithm is to conduct a dynamic programming on a tree spanning work space. The use of this algorithm also provides reduction in operation numbers. Tree-based construction algorithm includes three main algorithms: Procedure of compute-workspace-matrix, procedure of build-all-list and procedure of construct-list (Kumar et al. 2014). These algorithms are given in Figure 7. The robot with this algorithm can carry one block at a time while minimizing the total distance travelled. However, Maneuvering actions such as pick-up and drop off consume more energy that other simple actions; and this problem should be solved for efficient usage of the robot.

Algorithm 1: Procedure Compute-Workspace-Matrix

Input: an $A \times B$ matrix R of non-negative integers
Output: the workspace matrix W, and the offsets

(1) topBorder $= \text{argmin}_{(1 \le i \le A, 1 \le j \le B)}\{i - R[i][j] + 1\}$
(2) bottomBorder $= \text{argmax}_{(1 \le i \le A, 1 \le j \le B)}\{i + R[i][j] - 1\}$
(3) leftBorder $= \text{argmin}_{(1 \le i \le A, 1 \le j \le B)}\{j - R[i][j] + 1\}$
(4) rightBorder $= \text{argmax}_{(1 \le i \le A, 1 \le j \le B)}\{j + R[i][j] - 1\}$
(5) xoffset $= -$topBorder + 1
(6) yoffset $= -$leftBorder + 1
(7) workLength $=$ bottomBorder $-$ topBorder $+ 1$
(8) workBreadth $=$ rightBorder $-$ leftBorder $+ 1$
(9) Build the workLength $\times$ workBreadth workspace matrix W as follows:
  (a) Initialize all entries to 0
  (b) For each $(1 \le i \le A, 1 \le j \le B)$:
    (i) $W[i + \text{xoffset}][j + \text{yoffset}] = R[i][j]$
(10) Return:
  (a) the workspace matrix W
  (b) the offsets xoffset and yoffset

Algorithm 2: Procedure Build-All-Lists

Input: a node-weighted tree T spanning G
Output: an annotation of each node of T with a list of markers

(1) Initialize all lists to contain the single element 0
(2) Call Construct-List for T and its root node S

Algorithm 3: Procedure Construct-List

Input: the spanning tree T, and a node N in it
Output: an annotation of N with a list of markers

(1) If N is a leaf node in T:
  (a) Add the user-specified height of the tower at that location to N's list
  (b) Return
(2) Call Construct-List recursively for all of N's children
(3) Let len be the maximum length of the lists constructed for N's children
(4) For $i = 2 \ldots$ len, construct the i-th element $L_N(i)$ of the list for N as follows:
  (a) If i is even, set $L_N(i)$ to be $\max(L_N(i-1), g_N(i))$ where $g_N(i)$ is the maximum of the i-th elements in the lists of N's children -1
  (b) If i is odd, set $L_N(i)$ to be $\min(L_N(i-1), g_N(i))$ where $g_N(i)$ is the minimum of the i-th elements in the lists of N's children
(5) Construct the last element as follows:
  (a) If len is even and $L_N(\text{len})$ is less than or equal to the user-specified height h at N, then set $L_N(\text{len}) = h$
  (b) If len is even and $L_N(\text{len})$ is greater than h, then add h to N's list
  (c) If len is odd and $L_N(\text{len})$ is greater than or equal to the user-specified height h at N, then set $L_N(\text{len}) = h$
  (d) If len is odd and $L_N(\text{len})$ is less than h, then add h to N's list

Figure 7: Tree-based construction algorithm

3 Conclusion

In this paper, common algorithms for construction robots are presented. The conclusions can be drawn as follows:

- Full automation by robots on construction sites is still under progress. This can be attributed to the high operation cost of robotic systems.
- It can be reasonable to foresee that the number of construction robots will increase.
- Current algorithm can be enhanced in order to reduce the energy consumption of the robots while performing their duties on sites.
- Possible search space of algorithms can be narrowed with the detailed cooperative work of multiple disciplines.

References

[1] Baizid, Khelifa, Ali Yousnadj, Amal Meddahi, Ryad Chellali, and Jamshed Iqbal. 2015. "Time Scheduling and Optimization of Industrial Robotized Tasks Based on Genetic Algorithms." Robotics and Computer-Integrated Manufacturing. https://doi.org/10.1016/j.rcim.2014.12.003.

[2] Bock, Thomas. 2016. "Construction Robotics." Journal of Robotics and Mechatronics. https://doi.org/10.20965/jrm.2016.p0116.

[3] Chu, Baeksuk, Kyoungmo Jung, Myo Taeg Lim, and Daehie Hong. 2013. "Robot-Based Construction Automation: An Application to Steel Beam Assembly (Part I)." Automation in Construction. https://doi.org/10.1016/j.autcon.2012.12.016.

[4] G, Young G., and Maing K. Kang. 2001. "A Fast Algorithm for Two-Dimensional Pallet Loading Problems of Large Size." European Journal of Operational Research. https://doi.org/10.1016/S0377-2217(00)00249-6.

[5] Haidegger, Tamás, Marcos Barreto, Paulo Gonçalves, Maki K. Habib, Sampath Kumar Veera Ragavan, Howard Li, Alberto Vaccarella, Roberta Perrone, and Edson Prestes. 2013. "Applied Ontologies and Standards for Service Robots." In Robotics and Autonomous Systems. https://doi.org/10.1016/j.robot.2013.05.008.

[6] Holland, John H. 1975. "Adaptation in Natural and Artificial Systems: An Introductory Analysis with Applications to Biology, Control, and Artificial Intelligence." The Quarterly Review of Biology. https://doi.org/10.1086/418447.

[7] Kumar, T. S., Jung, S. J., & Koenig, S. (2014, June). A Tree-Based Algorithm for Construction Robots. In ICAPS.

[8] Werner, F. 2013. A Survey of Genetic Algorithms for Shop Scheduling Problems. Heuristics: Theory and Applications.

[9] Yu, Seung Nam, Byung Gab Ryu, Sung Jin Lim, Chang Jun Kim, Maing Kyu Kang, and Chang Soo Han. 2009. "Feasibility Verification of Brick-Laying Robot Using Manipulation Trajectory and the Laying Pattern Optimization." Automation in Construction. https://doi.org/10.1016/j.autcon.2008.12.008.

Almost Hadamard Inverse Of Frank Matrix

Efruz Özlem MERSİN *
Department of Mathematics,
Aksaray University,
Aksaray/TURKEY

Mustafa BAHŞİ
Education Faculty,
Aksaray University,
Aksaray/TURKEY

Ayşe Dilek MADEN
Department of Mathematics,
Selçuk University,
Konya/TURKEY

Abstract

The $n \times n$ matrix

$$F = (f_{ij})_{i,j=1}^{n} = \begin{cases} n+1-\max(i,j)\ , & i > j-2 \\ 0\ , & \text{otherwise} \end{cases}$$

is called Frank matrix. In this paper, we first define almost Hadamard inverse of Frank matrix by

$$G = (g_{ij})_{i,j=1}^{n} = \begin{cases} \frac{1}{f_{ij}}\ , & f_{ij} \neq 0 \\ 0\ , & f_{ij} = 0. \end{cases}$$

Then, we investigate some properties of the matrix G such as determinant and inverse.

Keywords: Frank matrix, Hadamard inverse, determinant.

1 Introduction

Matrix theory is widely used as a fundemantal tool in mathematical and engineering sciences. In the solutions of problems in applied sciences, using matrix properties such as determinant and eigenvalues, gives important informations about solving the problems. In matrix studies, selecting matrices or elements specifically will provide both convenience and important results. So, we will study on one of the special matrix and its applications which is called Frank matrix.

In 1958, Frank [1] defined an $n \times n$ matrix by the rule

$$F = (f_{ij})_{i,j=1}^{n} = \begin{cases} n+1-\max(i,j)\ , & i > j-2 \\ 0\ , & \text{otherwise.} \end{cases}$$

The matrix F is called Frank matrix [2,3]. So the Frank matrix, which is a lower Hessenberg matrix is of the form

$$F = \begin{bmatrix} n & n-1 & 0 & \cdots & 0 & 0 \\ n-1 & n-1 & n-2 & \cdots & 0 & 0 \\ n-2 & n-2 & n-2 & \cdots & 0 & 0 \\ \vdots & \vdots & \vdots & \ddots & \vdots & \vdots \\ 2 & 2 & 2 & \cdots & 2 & 1 \\ 1 & 1 & 1 & \cdots & 1 & 1 \end{bmatrix}.$$

* *E-mail address:* efruzmersin@gmail.com

In 1986, Varah [3] gave a generalization of the known Frank matrices and studied its eigenvalues and eigenvectors. Hake [2] expressed that F is a nonsingular matrix and $\det(F) = 1$ and showed that the inverse matrix $(B)_n = (\beta_{ij})_{i,j=1}^{n}$ of $F$is

$$\beta_{ij} = \begin{cases} 1\ , & i = j = 1 \\ n + 2 - i\ , & i = j \neq 1 \\ \ \ (-1)^{j-i}\beta_{ii}\ \sum_{k=1}^{j-i} n - i - k + 1\ , & i < j \\ -1\ , & i = j + 1 \\ 0\ , & i > j + 1, \end{cases}$$

the characteristic polynomial of F has the recurrence relation

$$\chi_n(\lambda) = (1 - \lambda)\chi_{n-1}(\lambda) - (n-1)\lambda\chi_{n-2}(\lambda),$$

$$\chi_1(\lambda) = 1 - \lambda,$$

$$\chi_2(\lambda) = 1 - 3\lambda + \lambda^2$$

and the relationship between coefficients of characteristic polynomial of F is

$$\gamma_i^{(n)} = \gamma_i^{(n-1)} - \gamma_{i-1}^{(n-1)} - (n-1)\gamma_{i-1}^{(n-2)},$$

where the characteristic polynomial of $F$is $\chi_n(\lambda) = \lambda^n + \gamma_{n-1}^{(n)}\lambda^{n-1} + \cdots + \gamma_1^{(n)}\lambda + \gamma_0^{(n)}$.

The Hadamard inverse of matrix $A = (a_{ij})_{m\times n}$ is

$$A^{\circ -1} = \left(\frac{1}{a_{ij}}\right)_{m\times n}$$

where $a_{ij} \neq 0$.

Now, we define almost Hadamard inverse of Frank matrix $F = (f_{ij})$ by

$$G = (g_{ij})_{i,j=1}^{n} = \begin{cases} \frac{1}{f_{ij}} & , \quad f_{ij} \neq 0 \\ 0 & , \quad f_{ij} = 0. \end{cases}$$

Then, the matrix G is of the form

$$G = \begin{bmatrix} \frac{1}{n} & \frac{1}{n-1} & 0 & \cdots & 0 & 0 \\ \frac{1}{n-1} & \frac{1}{n-1} & \frac{1}{n-2} & \cdots & 0 & 0 \\ \frac{1}{n-2} & \frac{1}{n-2} & \frac{1}{n-2} & \cdots & 0 & 0 \\ \vdots & \vdots & \vdots & \ddots & \vdots & \vdots \\ \frac{1}{2} & \frac{1}{2} & \frac{1}{2} & \cdots & \frac{1}{2} & 1 \\ 1 & 1 & 1 & \cdots & 1 & 1 \end{bmatrix}.$$

In this paper, we examine some properties of G such as determinant, LU decomposition inverse.

2 Main Results

Theorem 2.1. For the determinant of the $n \times n$ matrix G

$$\det(G) = (-1)^{n-1}\frac{1}{n!(n-1)!}$$

is valid.

Proof. By using row-column operations to $\det(G)$, we get that

$$\det(G) = \begin{vmatrix} -\frac{1}{n(n-1)} & \frac{1}{n-1} & 0 & \cdots & 0 & 0 \\ 0 & -\frac{1}{(n-1)(n-2)} & \frac{1}{n-2} & \cdots & 0 & 0 \\ 0 & 0 & -\frac{1}{(n-2)(n-3)} & \cdots & 0 & 0 \\ \vdots & \vdots & \vdots & \ddots & \vdots & \vdots \\ 0 & 0 & 0 & \cdots & -\frac{1}{2} & 1 \\ 0 & 0 & 0 & \cdots & 0 & 1 \end{vmatrix}$$

$$= (-1)^{n-1} \prod_{i=2}^{n} \frac{1}{i(i-1)}$$

$$= (-1)^{n-1} \frac{1}{n!(n-1)!}.$$

So, desired result is obtained.

Theorem 2.2. Let $B = (\beta_{ij})_{i,j=1}^{n-1}$ be inverse of G. Then,

$$\beta_{ij} = \begin{cases} -n(n-1)\ , & i = j = 1 \\ -1 & i = j = n \\ (n-i)(n+1-i)^2\ , & i = j,\ i,j \neq 1 \text{ and } i,j \neq n \\ (n+1-i)(n+2-i)\ , & i = j+1 \\ 0 & i > j+1 \\ \beta_{ii} \prod_{k=1}^{j-i} (n-i-k)\ , & i < j < n \\ -\beta_{i,n-1} & i < j = n\ . \end{cases}$$

Proof. We use principle of mathematical induction on n. It is clear that the result is true for $n = 2$, that is,

$$(G)_2 = \begin{bmatrix} \frac{1}{2} & 1 \\ 1 & 1 \end{bmatrix}$$

and

$$(G)_2^{-1} = \begin{bmatrix} -2 & 2 \\ 2 & -1 \end{bmatrix} = (B)_2.$$

Assume that the result is true for $n-1$, then

$$(B)_{n-1} = (\beta_{ij})_{i,j=1}^{n-1} = \begin{cases} -(n-1)(n-2)\ , & i = j = 1 \\ -1 & i = j = n-1 \\ (n-1-i)(n-i)^2\ , & i = j,\ i,j \neq 1 \text{ and } i,j \neq n-1 \\ (n-i)(n+1-i)\ , & i = j+1 \\ 0 & i > j+1 \\ \beta_{ii} \prod_{k=1}^{j-i} (n-1-i-k)\ , & i < j < n-1 \\ -\beta_{i,n-2} & i < j = n-1\ . \end{cases}$$

Now, we must show that the result is true for n. Let the matrices G and B be partitioned as $G = \begin{bmatrix} G_{11} & G_{12} \\ G_{21} & G_{22} \end{bmatrix}$ and $B = \begin{bmatrix} B_{11} & B_{12} \\ B_{21} & B_{22} \end{bmatrix}$, where

$$G_{11} = \left[\frac{1}{n}\right],$$

$$G_{12} = \left[\frac{1}{n-1} \quad 0 \quad 0 \quad 0 \quad \cdots \quad 0\right],$$

$$G_{21} = \begin{bmatrix} \frac{1}{n-1} & \frac{1}{n-2} & \frac{1}{n-3} & \cdots & \frac{1}{2} & 1 \end{bmatrix}^T,$$

$$G_{22} = \begin{bmatrix} \frac{1}{n-1} & \frac{1}{n-2} & 0 & 0 & \cdots & 0 & 0 \\ \frac{1}{n-2} & \frac{1}{n-2} & \frac{1}{n-3} & 0 & \cdots & 0 & 0 \\ \frac{1}{n-3} & \frac{1}{n-3} & \frac{1}{n-3} & \frac{1}{n-4} & \cdots & 0 & 0 \\ \vdots & \vdots & \vdots & \vdots & \ddots & \vdots & \vdots \\ \frac{1}{2} & \frac{1}{2} & \frac{1}{2} & \frac{1}{2} & \cdots & \frac{1}{2} & 1 \\ 1 & 1 & 1 & 1 & \cdots & 1 & 1 \end{bmatrix}.$$

From the assumption, $G_{22}^{-1} = (B)_{n-1}$.

The equation $\begin{bmatrix} G_{11} & G_{12} \\ G_{21} & G_{22} \end{bmatrix} \begin{bmatrix} B_{11} & B_{12} \\ B_{21} & B_{22} \end{bmatrix} = \begin{bmatrix} I & 0 \\ 0 & I \end{bmatrix}$ yields:

$$B_{11} = (G_{11} - G_{12}G_{22}^{-1}G_{21})^{-1} = -n(n-1),$$

$$\begin{aligned} B_{12} &= -B_{11}G_{12}G_{22}^{-1} \\ &= \begin{bmatrix} x_1(n-2) & x_1(n-2)(n-3) & x_1(n-2)(n-3)(n-4) & \cdots & x_1\prod_{i=2}^{n-1}(i-1) & -x_1\prod_{i=2}^{n-1}(i-1) \end{bmatrix} \end{aligned}$$

where $x_1 = -n(n-1)$,

$$B_{21} = -G_{22}^{-1}G_{21}B_{11} = \begin{bmatrix} n(n-1) & 0 & 0 & \cdots & 0 \end{bmatrix}^T,$$

$$B_{22} = G_{22}^{-1} - G_{22}^{-1}G_{21}B_{11}G_{12}G_{22}^{-1}$$

$$= \begin{bmatrix} x_2 & x_2(n-3) & x_2(n-3)(n-4) & \cdots & x_2\prod_{i=2}^{n-2}(i-1) & -x_2\prod_{i=2}^{n-2}(i-1) \\ (n-1)(n-2) & x_3 & x_3(n-4) & \cdots & x_3\prod_{i=2}^{n-3}(i-1) & -x_3\prod_{i=2}^{n-3}(i-1) \\ 0 & (n-2)(n-3) & x_4 & \cdots & x_4\prod_{i=2}^{n-4}(i-1) & -x_4\prod_{i=2}^{n-4}(i-1) \\ \vdots & \vdots & \vdots & \ddots & \vdots & \vdots \\ 0 & 0 & 0 & \cdots & x_{n-1}\prod_{i=2}^{2}(i-1) & -x_{n-1}\prod_{i=2}^{2}(i-1) \\ 0 & 0 & 0 & \cdots & (2)(1) & -1 \end{bmatrix}$$

where $\underset{2\leq s\leq n-1}{x_s} = (n+1-s)^2(n-s)$. Thus,

$$(B)_n = \begin{bmatrix} x_1 & x_1(n-2) & x_1(n-2)(n-3) & \cdots & x_1\prod_{i=2}^{n-1}(i-1) & -x_1\prod_{i=2}^{n-1}(i-1) \\ n(n-1) & x_2 & x_2(n-3) & \cdots & x_2\prod_{i=2}^{n-2}(i-1) & -x_2\prod_{i=2}^{n-2}(i-1) \\ 0 & (n-1)(n-2) & x_3 & \cdots & x_3\prod_{i=2}^{n-3}(i-1) & -x_3\prod_{i=2}^{n-3}(i-1) \\ \vdots & \vdots & \vdots & \ddots & \vdots & \vdots \\ 0 & 0 & 0 & \cdots & x_{n-1}\prod_{i=2}^{2}(i-1) & -x_{n-1}\prod_{i=2}^{2}(i-1) \\ 0 & 0 & 0 & \cdots & (2)(1) & -1 \end{bmatrix}.$$

This completes the proof.

Theorem 2.3. The characteristic polynomial of G is

$$P_n(\lambda) = \left(\lambda - \frac{1}{n}\right) P_{n-1}(\lambda) + \frac{1}{n-1}(P_{n-1}(\lambda) - \lambda P_{n-2}(\lambda)),$$

$$P_1(\lambda) = \lambda - 1,$$

$$P_2(\lambda) = \lambda^2 - \left(\frac{3}{2}\right)\lambda - \frac{1}{2}.$$

Proof. For the characteristic polynomial of G, we have

$$P_n(\lambda) = \begin{vmatrix} \lambda - \frac{1}{n} & -\frac{1}{n-1} & 0 & \cdots & 0 & 0 \\ -\frac{1}{n-1} & \lambda - \frac{1}{n-1} & -\frac{1}{n-2} & \cdots & 0 & 0 \\ -\frac{1}{n-2} & -\frac{1}{n-2} & \lambda - \frac{1}{n-2} & \cdots & 0 & 0 \\ \vdots & \vdots & \vdots & \ddots & \vdots & \vdots \\ -\frac{1}{2} & -\frac{1}{2} & -\frac{1}{2} & \cdots & \lambda - \frac{1}{2} & -1 \\ -1 & -1 & -1 & \cdots & -1 & \lambda - 1 \end{vmatrix}$$

$$= (\lambda - \tfrac{1}{n}) \begin{vmatrix} \lambda - \frac{1}{n-1} & -\frac{1}{n-2} & 0 & \cdots & 0 & 0 \\ -\frac{1}{n-2} & \lambda - \frac{1}{n-2} & -\frac{1}{n-3} & \cdots & 0 & 0 \\ -\frac{1}{n-3} & -\frac{1}{n-3} & \lambda - \frac{1}{n-3} & \cdots & 0 & 0 \\ \vdots & \vdots & \vdots & \ddots & \vdots & \vdots \\ -\frac{1}{2} & -\frac{1}{2} & -\frac{1}{2} & \cdots & \lambda - \frac{1}{2} & -1 \\ -1 & -1 & -1 & \cdots & -1 & \lambda - 1 \end{vmatrix}.$$

$$+ (\tfrac{1}{n-1}) \begin{vmatrix} -\frac{1}{n-1} & -\frac{1}{n-2} & 0 & \cdots & 0 & 0 \\ -\frac{1}{n-2} & \lambda - \frac{1}{n-2} & -\frac{1}{n-3} & \cdots & 0 & 0 \\ -\frac{1}{n-3} & -\frac{1}{n-3} & \lambda - \frac{1}{n-3} & \cdots & 0 & 0 \\ \vdots & \vdots & \vdots & \ddots & \vdots & \vdots \\ -\frac{1}{2} & -\frac{1}{2} & -\frac{1}{2} & \cdots & \lambda - \frac{1}{2} & -1 \\ -1 & -1 & -1 & \cdots & -1 & \lambda - 1 \end{vmatrix}$$

The first determinant of the right hand side of the last equality corresponds to the $P_{n-1}(\lambda)$. Let $q(\lambda)$ denotes the second determinant of the right hand side of the last equality. Then,

$$q(\lambda) = \begin{vmatrix} \lambda - \frac{1}{n-1} & -\frac{1}{n-2} & 0 & \cdots & 0 & 0 \\ -\frac{1}{n-2} & \lambda - \frac{1}{n-2} & -\frac{1}{n-3} & \cdots & 0 & 0 \\ -\frac{1}{n-3} & -\frac{1}{n-3} & \lambda - \frac{1}{n-3} & \cdots & 0 & 0 \\ \vdots & \vdots & \vdots & \ddots & \vdots & \vdots \\ -\frac{1}{2} & -\frac{1}{2} & -\frac{1}{2} & \cdots & \lambda - \frac{1}{2} & -1 \\ -1 & -1 & -1 & \cdots & -1 & \lambda - 1 \end{vmatrix} - \begin{vmatrix} \lambda & -\frac{1}{n-2} & 0 & \cdots & 0 & 0 \\ 0 & \lambda - \frac{1}{n-2} & -\frac{1}{n-3} & \cdots & 0 & 0 \\ 0 & -\frac{1}{n-3} & \lambda - \frac{1}{n-3} & \cdots & 0 & 0 \\ \vdots & \vdots & \vdots & \ddots & \vdots & \vdots \\ 0 & -\frac{1}{2} & -\frac{1}{2} & \cdots & \lambda - \frac{1}{2} & -1 \\ 0 & -1 & -1 & \cdots & -1 & \lambda - 1 \end{vmatrix}$$

$$= P_{n-1}(\lambda) - \lambda P_{n-2}(\lambda).$$

Thus, we have

$$\begin{aligned} P_n(\lambda) &= \left(\lambda - \tfrac{1}{n}\right) P_{n-1}(\lambda) + \tfrac{1}{n-1}\left(P_{n-1}(\lambda) - \lambda P_{n-2}(\lambda)\right) \\ &= \left(\lambda - \tfrac{2n-1}{n(n-1)}\right) P_{n-1}(\lambda) - \tfrac{1}{n-1}\lambda P_{n-2}(\lambda). \end{aligned}$$

Also, it is clear that $P_1(\lambda) = \lambda - 1$ and $P_2(\lambda) = \lambda^2 - \frac{3}{2}\lambda - \frac{1}{2}$.

Theorem 2.4. The LUdecomposition of G exists for all n. Its factors $L = (l_{ij})$ and $U = (u_{ij})$ are given by

$$l_{ij} = \begin{cases} 0, & i < j \\ 1, & i = j \\ \frac{n+1-j}{n+1-i}, & \text{otherwise} \end{cases} \quad \text{and} \quad u_{ij} = \begin{cases} \frac{1}{n}, & i = j = 1 \\ -\frac{1}{(n+1-i)^2}, & i = j \neq 1 \\ \frac{1}{n-i}, & i = j - 1 \\ 0, & \text{otherwise.} \end{cases}$$

Proof. Matrix multiplication yields the result.

Theorem 2.5. Let $P_n(\lambda) = \lambda^n + \gamma_{n-1}^{(n)}\lambda^{n-1} + \cdots + \gamma_1^{(n)}\lambda + \gamma_0^{(n)}$ be the characteristic polynomial of the $n \times n$ matrix G . Then,

$$\gamma_0^{(n)} = \frac{1}{n(n-1)}\gamma_0^{(n-1)} = (-1)^n \det(G),$$

$$\gamma_{n-1}^{(n)} = \gamma_{n-2}^{(n-1)} - \frac{1}{n} = -tr(G),$$

$$\gamma_i^{(n)} = \gamma_{i-1}^{(n-1)} + \frac{1}{n(n-1)}\gamma_i^{(n-1)} - \frac{1}{n-1}\gamma_{i-1}^{(n-2)}$$

are valid for $1 \le i \le n-2$.

Proof. By using the recurrence relation in Theorem 2.3 and the coefficients of $P_n(\lambda)$, $P_{n-1}(\lambda)$ and $P_{n-2}(\lambda)$,we have

$$\lambda^n + \gamma_{n-1}^{(n)}\lambda^{n-1} + \cdots + \gamma_1^{(n)}\lambda + \gamma_0^{(n)} = (\lambda + \tfrac{1}{n(n-1)})(\lambda^{n-1} + \gamma_{n-2}^{(n-1)}\lambda^{n-2} + \cdots + \gamma_1^{(n-1)}\lambda + \gamma_0^{(n-1)})$$
$$- \tfrac{1}{n-1}\lambda(\lambda^{n-2} + \gamma_{n-3}^{(n-2)}\lambda^{n-3} + \cdots + \gamma_1^{(n-2)}\lambda + \gamma_0^{(n-2)}).$$

Comparison of the coefficients yields the desired formulas. Also, we have

$$\gamma_0^{(n)} = \frac{1}{n(n-1)}\gamma_0^{(n-1)} = \frac{1}{n(n-1)^2(n-2)}\gamma_0^{(n-2)} = \cdots = -\prod_{i=2}^{n}\frac{1}{i(i-1)} = (-1)^n \det(G)$$

and

$$\gamma_{n-1}^{(n)} = \gamma_{n-2}^{(n-1)} - \frac{1}{n} = \gamma_{n-3}^{(n-2)} - \frac{2n+1}{n(n-1)} = \cdots = -\left(1 + \frac{1}{2} + \cdots + \frac{1}{n}\right) = -tr(G).$$

References

[1] W. L. Frank, Computing eigenvalues of complex matrices by determinant evaluation and by methods of Danilewski and Wielandt, J. Soc. Indust. Appl. Math. 6(4) (1958) 378-392.

[2] J.-Fr Hake, Juelich, A remark on Frank matrices, Computing 35 (1985) 375-379.

[3] J. M. Varah, A generalization of the Frank matrix, SIAM J.Sci. Stat. Comput. 7(3) (1986) 835-839.

Mathematical Modelling Of Global Solar Radiation with Satellite-Based HELIOSAT Method

Selmin ENER RUŞEN*
Karamanoglu Mehmetbey University,
Department of Energy Systems Engineering,
Academic Energy Research Group (AKEN),
70100, Karaman, TURKEY

Abstract

With the use of solar energy system performance calculations, ground measured solar radiation is obtained with difficulty for a given site. In addition to this, the measurement network's density is usually far too low. In order to derive information on solar irradiance, geostationary satellite images such as METEOSAT can be used for large area with very high spatial resolution (up to 1 km) and with sufficient temporal resolution (up to 15 minutes). There are mathematical models which estimate surface solar radiation based on this geostationary satellite data. One of them is HELIOSAT method which is the most popular satellite-based solar radiation calculation technique. This method is an estimation technique to infer the shortwave surface radiation from satellite images. The general idea of this method is to deal with atmospheric and cloud extinction separately. A measure of cloud cover is determined by METEOSAT satellite visible channel digital (mathematical) counting. In the second step, the cloud index is derived from METEOSAT images to take into account the cloud extinction with mathematical modeling and calculation techniques. This work aims to give a mathematical explanation of well-known satellite-based HELIOSAT method for modelling of the daily global solar radiation reaching on a horizontal surface. Moreover, by using the mathematical calculation techniques of HELISAT method, the cloud index and the clear sky index were found.

Keywords: Global Solar Radiation, Mathematical Modelling, Satellite Images, HELIOSAT Method.

1 Introduction

Solar energy, meteorology, and many climatic applications are directly related to the correct knowledge of global solar radiation at the earth's surface. We need accurate solar irradiation measurement or modeling in order to provide accurate resource assessment for feasibility studies, to verify PV plant performance, to forecast solar resource for estimating plant output, to forecast variability (sub-hourly to climate scale) (K.-F. Dagestad 2005). Ground solar irradiance data is the most accurate method for characterizing the solar resource of a given site (Selmin Ener Rusen 2017). Over the last two decades satellite-derived solar radiation has become a worthy tool for quantifying the solar irradiance at ground level for a large area. Generally, geostationary satellites which are rotating around the earth at the same speed as the earth are used for solar information. They are orbiting at about 36000 km and can offer a temporal resolution of up to 15 minutes and a spatial resolution of up to 1 km (Annette Hammer et al. 1999). Almost the whole earth surface is covered by about several geostationary satellites positioned at regular intervals above the equatorial line. The most popular

* *E-mail address:* selminerusen@kmu.edu.tr

one of the geostationary satellite is Meteosat. All geostationary First Generation Meteosat satellites include three main channels: visible channel (0.5–1.1μm), thermal infrared channel (10.5–12.5μm), and water vapour channel (5.7–7.1μm). On the other hand, last generations geostationary satellites are adding more spectral channels (totally 12) which are named as: Second Generation Satellites (MGS) (K.-F. Dagestad 2005; Ener Rusen, S., Hammer, and Akinoglu 2011; A. Hammer 2000; Annette Hammer et al. 1999). Meteosat satellite images will be obtained from EUMETSAT archive data center for long term period for selected area. The well-known satellite-based HELIOSAT method, which is processed the data from Meteosat satellite, was used for modelling of the daily global solar radiation reaching on a horizontal surface. This work aims to give a mathematical explanation of well-known satellite-based HELIOSAT method for modelling of the daily global solar radiation reaching on a horizontal surface. Moreover, by using the mathematical calculation techniques of HELISAT method, the cloud index and the clear sky index were found.

2 Satellite-Based Mathematical Models for Deriving Solar Radiation

Actually, Meteosat-satellites images were used to improve weather forecasts by giving the meteorologists a visual overview of the cloud cover on a global scale. In addition to this main purpose, several other applications of the satellite images were also started; among them were the developments of various mathematical methods to estimate the solar irradiance at ground level (K.-F. Dagestad 2005). "However, the satellite data were very simple; each pixel of the images consisted of a digital mathematical count number between 0 to 255, and these pixel counts numbers could not even be reliably calibrated into radiances (K.-F. Dagestad 2005). In spite of the input being simple, the estimates of these algorithms were surprisingly accurate when compared with the ground measurements" (K.-F. Dagestad 2005). There are many mathematical algorithms which estimate surface solar irradiance based on this geostationary satellite data. One of them was HELIOSAT method which has been developed to estimate global horizontal irradiance at ground level using satellite images taken in the visible range by the European metrological satellite series, namely Meteosat (S. Ener Rusen, Hammer, and Akinoglu 2013; K.-F. Dagestad 2005; A. Hammer et al. 2003; Annette Hammer et al. 2001).

3 HELIOSAT Method

"The HELIOSAT algorithm, originally proposed by Cano et al. (1986) (Cano et al. 1986), was one of the most popular mathematical algorithms because it was accurate and easy to implement" (K.-F. Dagestad 2005; H. G. Beyer, Costanzo, and Heinemann 1996). HELIOSAT was widely used in operational schemes around the world, and over the years it has been modified and improved several times by Beyer et al. 1996; Hammer 2000 (H. G. Beyer, Costanzo, and Heinemann 1996; Selmin Ener Rusen 2013; A. Hammer 2000) and others. In the original version of the model, from the un-calibrated counts of the images of Meteosat High Resolution Visible (HRV) sensor, firstly Cano et al. calculate a reflectivity using each pixel as:

$$\rho_t = C / G_{clear} \tag{1}$$

where C is the digital counts of a pixel (between 0 to 255) and G_{clear} is the clear sky global irradiance at ground level that they evaluated using an empirical model (K.-F. Dagestad 2005). Actually, this definition is later improved by Hammer et al as C-C_o is taken instead of C where C_o is the offset (A. Hammer 2000), which is named as HELIOSAT. For the value G_{clear}, measured surface data might be used or there might be different site dependent empirical models that can be considered. May be the most important step is the definition of the cloud index n that was calculated for each pixel as:

$$n = (\rho_t - \rho_{clear}) / (\rho_{cloud} - \rho_{clear}) \quad (2)$$

Here ρ_{clear} and ρ_{cloud} are the reflectivities corresponding to clear and overcast conditions, respectively (K.-F. Dagestad 2005; Cano et al. 1986).
To estimate the solar radiation an empirical form is needed between the normalized solar radiation, namely the clearness index and n defined above. That is, in the linear approximation the clearness index k_c can be written as:

$$k_c = G / G_{ext} = an + b \quad (3)$$

where a and b are empirical parameters to be determined using regression analysis with the ground data. As one can guess these parameters would be site dependent and might be affected from the temporal variations of the atmospheric conditions (K.-F. Dagestad 2005; Cano et al. 1986; A. Hammer 2000; Selmin Ener Rusen 2018). Although the model seems simple the use of it might possess difficulties and the global applicability should be questioned in this sense (K.-F. Dagestad 2005).
The modified version of HELIOSAT method which was developed within the EU-project "Satel-Light" (Page 1996; A Hammer et al. 2001; Annette Hammer et al. 1999) and is denoted on the web server www.satel-light.com (Page 1996). This was the first web site that provides any information about the global irradiation and derived products for the period 1996-2000 (Page 1996). In addition, it covers Europe and a small region of the North Africa and provides solar irradiance statistical data in terms of monthly means of hourly and daily radiation. This data is completely derived from METEOSAT satellite imagery. The main differences from the original version are described by various researchers (K.-F. Dagestad 2005; Selmin Ener Rusen, Hammer, and Akinoglu 2013; A. Hammer 2000; H. Beyer, Costanzo, and Heinemann 1996). Fig. 1 shows the overview of the modified version of HELIOSAT method.
In the modified version of HELIOSAT, the reflectivity (ρ) is calculated with:

$$\rho = (C - C_o) / G_{ext} \quad (4)$$

Here C_o, which was developed by Beyer et al. (1996) (H. Beyer, Costanzo, and Heinemann 1996) and later modified by Hammer (2000) (A. Hammer 2000), is subtracted from the satellite pixel counts measurements. Instead of normalizing with a modeled extraterrestrial irradiance (G_{ext}), clear sky irradiance ($G_{clearsky}$) is now used in the normalization (K. F. Dagestad 2005). The mathematical method uses clear sky index k^* instead of clearness index k_c (Eq. (3)), the actual global irradiance, G, divided by the output of a clear sky model, $G_{clearsky}$:

$$k* \equiv G / G_{clearsky} \quad (5)$$

In their method, Hammer et al calculated $G_{clearsky}$ as outlined below, and they correlated k^* (instead of k) to n defined above, to obtain the new empirical relation:

$$\begin{cases} 1.2, & n < -0.2 \\ 1 - n, & n \in [-0.2, 0.8] \\ k* = \quad 2.0667 - 3.6667n + 1.6667n2, & n \in [0.8, 1.1] \\ 0.05, & n > 1.1 \end{cases} \quad (6)$$

The cloud index n is still calculated with Eq. (2).
In the modified version of HELIOSAT, the atmospheric turbidity is a direct input parameter to the clear sky model. In the calculation of $G_{clearsky}$ they use Linke turbidity factor. The

modified version of HELIOSAT was initially a mathematical model and it developed some physical atmospheric parameters, such as the Linke turbidity factor (Jes'us, Luis F., and Lourdes Ram'ırez 2008).
To calculate $G_{clearsky}$, they first calculated direct normal irradiance $G_{dn,clear}$ which is found by:

$$G_{dn,clear} \quad = \quad G_{sc}\ \varepsilon\ exp(-0,8662\ T_L(2)\ \delta_R(m)m \tag{7}$$

where ε is the eccentricity correction, $T_L(2)$ is the Linke turbidiy factor for air mass 2, $\delta_R(m)$ is the Rayleigh optical thickness of a dry and clean atmosphere and m is the air mass. Finally, the total clear sky irradiance is the summation of the components:

$$G_{clearsky} \ = G_{dn,clear}\ cos\theta_z + G_{dif\ clear} \tag{8}$$

As indicated Fig. 1, another part is the mathematical calculation of newly defined n (Eq. (2)) in terms of pixel count, which is related to the Meteosat– image. These images are corrected with respect to solar position and atmosphere parameters. Therefore, a relative reflectance ρ is introduced by using Eq. (4).

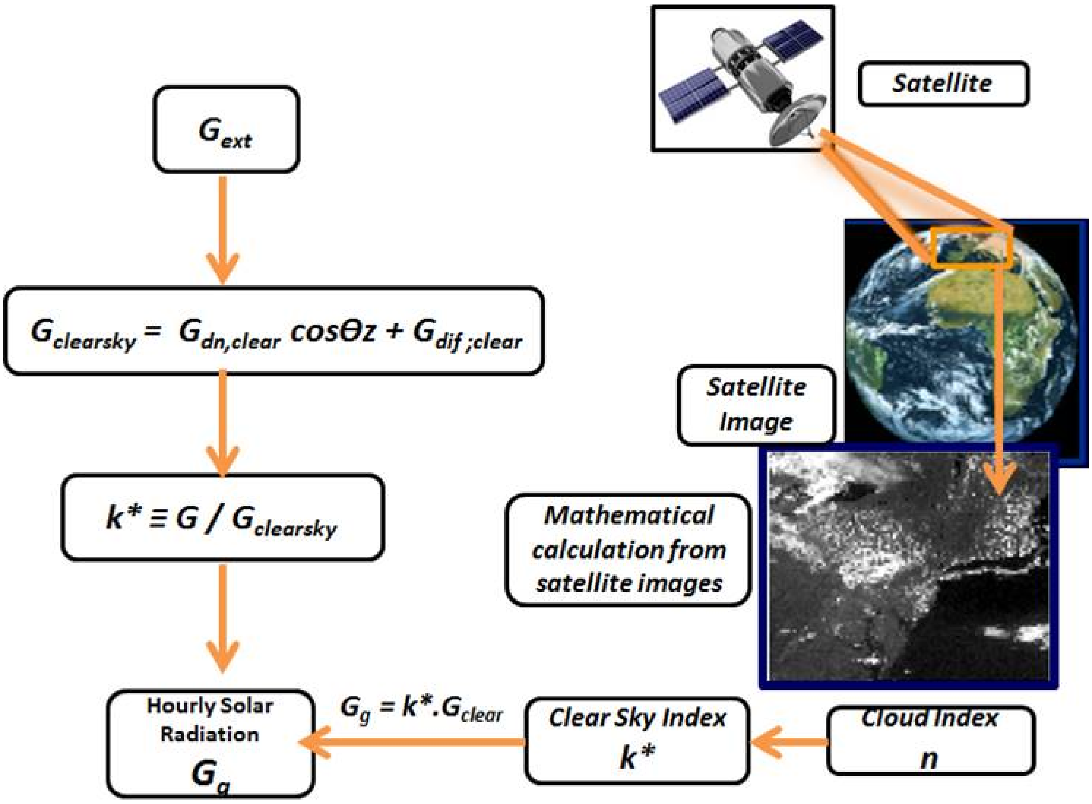

Figure 1: Overview of the modified version of HELIOSAT method

The measured reflectance value increases from black to white in the satellite images. It means that the low values are from the earth surfaces and while the higher values are from the clouds. Therefore, a cloud index n that varies between 0 for cloud free and 1 is calculated from Eq. (2) with respect to the relative reflectivity (ρ).
As described above cloud transmission can be defined by the clear sky index $k*$ which is the ratio of the actual surface irradiance G and the clear sky irradiance $G_{clearsky}$ from Eq. (5), and it is correlated with the cloud index n. They derived the correlations (Eqn. 6) within the

Satel-Light project (A. Hammer 2000; Annette Hammer et al. 1999).
Eqs. (6) and (8) are then used to obtain the hourly surface irradiance G_h:

$$G_h = k^*(G_{dn,clear}\cos\theta_z + G_{dif,clear} \tag{9}$$

The surface albedo maps are mathematically computed on a monthly basis by a statistical analysis of the dark pixels.

4 Discussion and Conclusion

One of this study aims was to explained solar radiation calculation procedure by using HELIOSAT method or modified version of it. The procedure used by Hammer et al. (A. Hammer et al. 2003)is discussed in part 2, which mainly mathematically calculates surface irradiance G_h by using HELIOSAT method as given in Fig.1. The first step of HELIOSAT method calculation is the extraterrestrial irradiation on a horizontal plane (G_{ext}) to calculate surface irradiance with a mathematical approach. As indicated Fig.1, another part for calculation of HELIOSAT method is related with Meteosat satellite images. These images should be corrected with respect to solar position and atmospheric parameters by using a computer program. The study explained at the basic mathematical calculation procedure for HELIOSAT method and it can be considered to be the literature and the learning stage.

Acknowledgments

The author would like to thank State Meteorological Service (TSMS) for providing me with measured data. The author would also like to thank to Prof. Dr. Bülent Akınoğlu and Dr. Annette Hammer for their discussions and comments during the course of this study. The author would like to express their gratitude to Karamanoglu Mehmetbey University for your supports (Grand No: BAP-06-M-17).

References

[1] Beyer, H., C. Costanzo, and D. Heinemann. 1996. "Modifications of the HELIOSAT Procedure for Irradiance Estimates from Satellite Images." Solar Energy 56: 207–12.

[2] Beyer, Hans Georg, Claudio Costanzo, and Detlev Heinemann. 1996. "Modifications of the Heliosat Procedure for Irradiance Estimates from Satellite Images." Solar Energy 56 (3): 207–12. doi:10.1016/0038-092X(95)00092-6.

[3] Cano, D., J.M. Monget, M. Albuisson, H. Guillard, N Regas, and L. Wald. 1986. "A Method for the Determination of the Global Solar Radiation from Meteorological Satellite Data." Solar Energy 37: 31–39.

[4] Dagestad, K-F. 2005. "Estimating Global Radiation at Ground Level from Satellite Images, PhD Thesis." University of Bergen.

[5] Dagestad, K.F. 2005. "Estimating Global Radiation at Ground Level from Satellite Images." University of Bergen, Bergen.

[6] Ener Rusen, S., A. Hammer, and B.G. Akinoglu. 2011. "Using Sunshine Duration and Satellite Images to Estimate Daily Solar Irradiation on Horizontal Surface." In ISES Solar World Congress 2011, Kassel, Germany.

[7] Ener Rusen, S., A. Hammer, and B.G. Akinoglu. 2013. "Coupling Satellite Images with Surface Measurements of Bright Sunshine Hours to Estimate Daily Solar Irradiation on Horizontal Surface." Renewable Energy 55: 212–19.

[8] Ener Rusen, Selmin. 2013. "Linking Satellite Imagery to Bright Sunshine Hours for the Estimation of Global Solar Irradiaiton, PhD Thesis." Middle East Tech. Univ.

[9] Ener Rusen, Selmin. 2017. "DETERMINATION OF THE GLOBAL SOLAR RADIATION POTENTIAL USING HELIOSAT METHOD FOR KARAMAN." Omer Halisdemir University Journal of Engineering Sciences 6 (2): 467–74.

[10] Ener Rusen, Selmin. 2018. "Modeling and Analysis of Global and Diffuse Solar Irradiation Components Using the Satellite Estimation Method of." CMES: Computer Modeling in Engineering & Sciences 115 (3): 327–43. doi:10.3970/cmes.2018.00159.

[11] Ener Rusen, Selmin, Annette Hammer, and Bulent G. Akinoglu. 2013. "Estimation of Daily Global Solar Irradiation by Coupling Ground Measurements of Bright Sunshine Hours to Satellite Imagery." Energy 58: 417–25. doi:10.1016/j.energy.2013.05.062.

[12] Hammer, A. 2000. "Anwendungspezifische Solarstrahlungsinformationen Aus Meteosat-Daten." Carl von Ossietzky University of Oldenburg.

[13] Hammer, A., D. Heinemann, C. Hoyer, R. Kuhlemann, E. Lorenz, R. Müller, and H. G. Beyer. 2003. "Solar Energy Assessment Using Remote Sensing Technologies." Remote Sensing of Environment 86 (3): 423–32.

[14] Hammer, A, D Heinemann, C Hoyer, E Lorenz, and G Beyer. 2001. "Satellite-Based Techniques for the Retrieval of Solar Activities –." In ISES 2001 Solar Congress, 1–8.

[15] Hammer, Annette, Detlev Heinemann, Carsten Hoyer, and Elke Lorenz. 2001. "Satellite Based Short-Term Forecastıng of Solar Irradance - Comparıson of Methods and Error Analysıs -." In EUMETSAT Meteorological Satellite Data Users' Conference. Antalya, Turkey.

[16] Hammer, Annette, Detlev Heinemann, Annette Westerhellweg, Hans Georg Beyer, and Cristian Reise. 1999. "Daylight and Solar Irradiance Data Derived from Satellite Observations - The SATELLIGHT Project." In Proceedings of the ISES Solar World Congress 1999. Jerusalem, Israel.

[17] Jes'us, Polo, Zarzalejo Luis F., and Mode Lourdes Ram'ırez. 2008. "Solar Radiation Derived from Satellite Imeges." In Modelling Solar Radiation at the Earth's Surface, edited by Badescu Viorel, first, 449–62. Romania: Springer.Page, J. 1996. "Algorithms for the Satel-Light Programme. Technical Report for the Satel-Light Programme."

Evaluation Codes on Toric Varieties

Mesut Şahin *
Department of Mathematics,
Hacettepe University,
Ankara-Turkey

Abstract

Let X be a complete n-dimensional simplicial toric variety over a finite field with homogeneous coordinate ring S. Assume that the maximal torus T_X of X is split. In this short survey, we review algebraic methods for studying evaluation codes defined on subsets of T_X. We also explore the nice correspondence between subgroups of the group T_X and certain binomial ideals known as lattice ideals.

1 Introduction

Let X be a complete simplicial toric variety of dimension n over the field $\mathbb{K} = \mathbb{F}_q$, corresponding to a fan Σ and $T_X \cong (\mathbb{K}^*)^n$ be its maximal torus. Denote by $\rho_1, \dots, \rho_r$ the rays in Σ and $\mathbf{v}_1, \dots, \mathbf{v}_r \in \mathbb{Z}^n$ the corresponding primitive lattice vectors generating them. Given a vector $\mathbf{u} \in \mathbb{Z}^m$ we use $x^{\mathbf{u}}$ to denote the Laurent monomial $\mathbf{x}^{\mathbf{u}} = x_1^{u_1} \dots x_m^{u_m}$. We also use $[m]$ to denote the set $\{1, \dots, m\}$ for any positive integer $m \geq 1$. Recall the following dual exact sequences:

$$\mathfrak{P} : 0 \longrightarrow \mathbb{Z}^n \xrightarrow{\phi} \mathbb{Z}^r \xrightarrow{\beta} \mathcal{A} \longrightarrow 0 \; ,$$

where ϕ is the matrix with rows $\mathbf{v}_1, \dots, \mathbf{v}_r$, and

$$\mathfrak{P}^* : 1 \longrightarrow G \xrightarrow{i} (\mathbb{K}^*)^r \xrightarrow{\pi} (\mathbb{K}^*)^n \longrightarrow 1 \; ,$$

where $\pi : (t_1, \dots, t_r) \mapsto (\mathbf{t}^{\mathbf{u}_1}, \dots, \mathbf{t}^{\mathbf{u}_n})$, with $\mathbf{u}_1, \dots, \mathbf{u}_n$ being the columns of ϕ.

Let $S = \mathbb{K}[x_1, \dots, x_r] = \bigoplus_{\alpha \in \mathcal{A}} S_\alpha$ be the homogeneous coordinate or Cox ring of X, multi-graded by $\mathcal{A} \cong \mathrm{Cl}(X)$ via $\beta_j := \deg_{\mathcal{A}}(x_j) := \beta(e_j)$, where e_j is the standart basis element of $\mathbb{Z}^r$ for each $j \in [r]$. The irrelevant ideal is $B = \langle x^{\hat{\sigma}} \; : \; \sigma \in \Sigma \rangle$, where $x^{\hat{\sigma}} = \Pi_{\rho_i \notin \sigma} x_i$. Thus, $T_X \cong (\mathbb{K}^*)^r / G$ and $X \cong (\mathbb{K}^r \setminus V(B))/G$ as a geometric quotient. The homogeneous

*Corresponding author. *E-mail address:* mesut.sahin@hacettepe.edu.tr

polynomials of S are supported in the semigroup $\mathbb{N}\beta$ generated by $\beta_1, \dots, \beta_r$, i.e. $\dim_{\mathbb{K}} S_\alpha = 0$ when $\alpha \notin \mathbb{N}\beta$.

Next, we recall evaluation codes defined on subsets $Y = \{p_1, \dots, p_N\}$ of the torus T_X. Fix a degree $\alpha \in \mathbb{N}\beta$ and a monomial $F_0 = \mathbf{x}^{\phi(\mathbf{m}_0)+\mathbf{a}} \in S_\alpha$, where $\mathbf{m}_0 \in \mathbb{Z}^n$, $\mathbf{a}$ is any element of $\mathbb{Z}^r$ with $\deg(\mathbf{a}) = \alpha$, and ϕ as in the exact sequence $\mathfrak{P}$. This defines the *evaluation map*

$$\mathrm{ev} : S_\alpha \to \mathbb{F}_q^N, \quad F \mapsto \left(\frac{F(p_1)}{F_0(p_1)}, \dots, \frac{F(p_N)}{F_0(p_N)} \right). \tag{1}$$

The image $\mathcal{C}_{\alpha,Y} = \mathrm{ev}_Y(S_\alpha)$ is a linear code, called the *generalized toric code*. The block-length N, the dimension $k = \dim_{\mathbb{F}_q}(\mathcal{C}_{\alpha,Y})$, and the minimum distance $d = d(\mathcal{C})$ are three basic parameters of $\mathcal{C}_{\alpha,Y}$. Minimum distance is the minimum of the number of nonzero components of nonzero vectors in $\mathcal{C}_{\alpha,Y}$. Toric codes was introduced for the first time by Hansen in [3, 4] for the special case of $Y = T_X$. Clearly, the block-length of $\mathcal{C}_{\alpha,Y}$ equals $N = |T_X| = (q-1)^n$ in this case. But it is not known in the general case. An algebraic way to compute the dimension and length of a generalized toric code is given in [7]. This method is based on the observation that the kernel of the evaluation map above is determined by the vanishing ideal of Y defined as follows. For $Y \subset X$, we define the vanishing ideal $I(Y)$ of Y to be the ideal generated by homogeneous polynomials vanishing on Y. $I(Y)$ is a *complete intersection* if it is generated by a regular sequence of homogeneous polynomials $F_1, \dots, F_k \in S$ where k is the codimension of Y in X. When the vanishing ideal $I(Y)$ is a complete intersection, bounds on the minimum distance of $\mathcal{C}_{\alpha,Y}$ is provided in [9].

2 The Algebraic Aproach

In this section, we review how combinatorial commutative algebra can be applied to computing basic parameters of codes on toric varieties. Let us start by introducing one well-known example of a singular toric surface. It is smooth only if it is the usual projective plane, i.e., $w_1 = w_2 = w_3 = 1$.

Example 2.1. Weighted Projective Plane $P(w_1, w_2, w_3)$ with $w_1 = 1$ has the following exact sequence:

$$\mathfrak{P} : 0 \longrightarrow \mathbb{Z}^2 \xrightarrow{\phi} \mathbb{Z}^3 \xrightarrow{\beta} \mathbb{Z} \longrightarrow 0\,,$$

where

$$\phi = \begin{bmatrix} -w_2 & 1 & 0 \\ -w_3 & 0 & 1 \end{bmatrix}^T \quad \text{and} \quad \beta = \begin{bmatrix} 1 & w_2 & w_3 \end{bmatrix}.$$

The ring $S = \mathbb{K}[x, y, z]$ is multigraded via

$$\deg_{\mathcal{A}}(x) = 1,\ \deg_{\mathcal{A}}(y) = w_2 \text{ and } \deg_{\mathcal{A}}(z) = w_3.$$

- The irrelevant ideal is $B = \langle x, y, z\rangle$ with a zero set $V(B) = V(x, y, z) = (0, 0, 0)$.

- $X = P(w_1, w_2, w_3) = (\mathbb{K}^3 \setminus V(B))/G$, where

$$G = \{(x, y, z, w) \in (\mathbb{K}^*)^4 \mid x^{-w_2}y = x^{-w_3}z = 1\} = \{(t, t^{w_2}, t^{w_3}) \mid t \in \mathbb{K}^*\}.$$

- A typical point of X has the following form:

$$[1 : 0 : 1] := G \cdot (1, 0, 1) = \{(t, 0, t^{w_3}) \mid t \in \mathbb{K}^*\}.$$

It may be desirable to have a smooth example at hand to illustrate certain features.

Example 2.2. Hirzebruch surface H_ℓ has the following exact sequence:

$$\mathfrak{P} : 0 \longrightarrow \mathbb{Z}^2 \xrightarrow{\phi} \mathbb{Z}^4 \xrightarrow{\beta} \mathbb{Z}^2 \longrightarrow 0\ ,$$

where

$$\phi = \begin{bmatrix} 1 & 0 & -1 & 0 \\ 0 & 1 & \ell & -1 \end{bmatrix}^T \quad \text{and} \quad \beta = \begin{bmatrix} 1 & -\ell & 1 & 0 \\ 0 & 1 & 0 & 1 \end{bmatrix}.$$

The ring $S = \mathbb{K}[x, y, z, w]$ is multigraded via

$$\deg_{\mathcal{A}}(x) = \deg_{\mathcal{A}}(z) = (1, 0),\ \deg_{\mathcal{A}}(y) = (-\ell, 1) \text{ and } \deg_{\mathcal{A}}(w) = (0, 1).$$

- The irrelevant ideal is $B = \langle xy, yz, zw, wx\rangle$ with a zero set $V(B) = V(x, z) \cup V(y, w)$.

- $X = H_\ell = (\mathbb{K}^4 \setminus V(B))/G$, where

$$G = \{(x, y, z, w) \in (\mathbb{K}^*)^4 \mid xz^{-1} = yz^\ell w^{-1} = 1\} = \{(z, z^{-\ell}w, z, w) \mid z, w \in \mathbb{K}^*\}.$$

- A typical point of X has the following form:

$$[0 : 0 : 1 : 1] := G \cdot (0, 0, 1, 1) = \{(0, 0, z, w) \mid z, w \in \mathbb{K}^*\}.$$

Definition 2.3. The multigraded Hilbert function of Y is defined to be

$$H_Y(\alpha) := \dim_{\mathbb{K}} S_\alpha - \dim_{\mathbb{K}} I_\alpha(Y), \quad \text{where} \quad I_\alpha(Y) = I(Y) \cap S_\alpha.$$

The first observation is that dimensions of codes can be computed algebraically by using Hilbert functions.

Proposition 2.4 ([7])**.** *The dimension of $\mathcal{C}_{\alpha,Y}$ equals $H_Y(\alpha)$.*

Definition 2.5. The multigraded regularity of Y, denoted $\operatorname{reg}(Y)$, is the set of $\alpha \in \mathbb{N}\beta$ for which $H_Y(\alpha) = |Y|$, the length of $\mathcal{C}_{\alpha,Y}$.

The multigraded regularity of Y is useful in order to eliminate trivial codes, since the dimension of the code $\mathcal{C}_{\alpha,Y}$ attains its maximum value $|Y|$. This motivates giving bounds on $\operatorname{reg}(Y)$.

Proposition 2.6 ([7])**.** *Let $Y \subset T_X$ for the weighted projective space $X = P(w_1, \ldots, w_r)$ with $w_1 = 1$. Then, there is an integer a_Y satisfying* $\operatorname{reg}(Y) = 1 + a_Y + \mathbb{N}$.

In the particular case of the torus $Y = T_X$, for $X = P(w_1, \ldots, w_r)$, we have the following nice invariant determined by the largest integer $g(W)$ not belonging to the semigroup W generated by $w_1, \ldots, w_r$, see [2, Corollary 3.9].

Corollary 2.7. $a_Y = (q-2)[w_1 + \cdots + w_r + g(W)] + g(W)$ *satisfying* $\operatorname{reg}(Y) = 1 + a_Y + \mathbb{N}$, *where $g(W)$ is the Frobeneous number of the numerical semigroup W.*

Definition 2.8. Let $\mathbb{N}\hat{\sigma}$ be the semigroup generated by the subset $\{\beta_j \,:\, \rho_j \notin \sigma\}$ for a cone $\sigma \in \Sigma$. Then, an important subset of $\mathbb{N}\beta$ is defined to be the following:

$$\mathcal{K} = \bigcap_{\sigma \in \Sigma} \mathbb{N}\hat{\sigma}.$$

Theorem 2.9 ([7])**.** *Let $Y \subset T_X$ be a complete intersection of n hypersurfaces of degrees $\alpha_1, \ldots, \alpha_n$ in $\mathcal{K}$. Then,*

$$\alpha_1 + \cdots + \alpha_n + \mathbb{N}\beta \subseteq \operatorname{reg}(Y).$$

3 Lattice Ideals and Subgroups of the torus T_X

The main result of this section uncovers the relation between lattice ideals and subgroups of T_X.

By a lattice L we mean a finitely generated free Abelian group. Recall that every vector in $\mathbb{Z}^r$ is written as $\mathbf{m} = \mathbf{m}^+ - \mathbf{m}^-$, where $\mathbf{m}^+, \mathbf{m}^- \in \mathbb{N}^r$. Letting $F_{\mathbf{m}} = \mathbf{x}^{\mathbf{m}^+} - \mathbf{x}^{\mathbf{m}^-}$, the lattice ideal I_L is the binomial ideal generated by special binomials $F_{\mathbf{m}}$ arising from the lattice $L \subset \mathbb{Z}^r$. So, $I_L = \langle F_{\mathbf{m}} \mid \mathbf{m} \in L \rangle$. Let $[P] := G \cdot P = [p_1 : \cdots : p_r]$ for a point P in $\mathbb{K}^r$ and let $I([P])$ be the vanishing ideal of $[P]$. We use [1] to denote $[1 : \cdots : 1]$. If $[P], [P'] \in X$ then $[P] \cdot [P'] := [PP']$ is well-defined element of $X \cup [V(B)]$, where $[V(B)]$ denotes the set of all $[P]$ for $P \in V(B)$. The set $[\mathbb{K}^r] = X \cup [V(B)]$ is a monoid with identity [1] with respect to this coordinatewise multiplication operation.

A matrix $Q = [\mathbf{q}_1 \mathbf{q}_2 \cdots \mathbf{q}_r] \in M_{s \times r}(\mathbb{Z})$ defines a subgroup

$$Y_Q = \{[\mathbf{t}^{\mathbf{q}_1} : \cdots : \mathbf{t}^{\mathbf{q}_r}] | \mathbf{t} \in (\mathbb{K}^*)^s\} \subset T_X$$

of the torus T_X called the toric set parameterized by Q. In [6], the vanishing ideals of these toric sets parameterised by monomials are shown to be lattice ideals of dimension 1, when the toric variety is a projective space, i.e., $X = P(w_1, \ldots, w_r)$ with $w_1 = \cdots = w_r = 1$.

Definition 3.1. Given an integer matrix B, let $L_B = \mathbb{Z}^r \cap \ker B$ be the sublattice of $\mathbb{Z}^r$ determined by B. A lattice L is called **homogeneous** if $L \subseteq L_\beta$, where L_β is the image $\phi(\mathbb{Z}^n)$.

Proposition 3.2 ([8]). *L is homogeneous if and only if I_L is homogeneous.*

For a homogeneous ideal J of S, let

$$V_X(J) := \{[P] \in X : F(P) = 0, \text{for all homogeneous } F \in J\}.$$

Proposition 3.3 ([8]). *If L is homogeneous then $V_X(I_L) \cap T_X$ is parameterised by monomials.*

Summarizing the results of [8], we get the following nice relations:

Theorem 3.4. *Y is a subgroup of T_X iff $I(Y)$ is a radical lattice ideal of dimension $r - n$ iff $Y = Y_Q$ for a square Q.*

Algorithms for determining a generating set of the lattice ideal $I(Y_Q)$ are given in a joint work with E. Baran, see [1].

4 Degenerate Tori

Definition 4.1. The subset $Y_A = \{[t_1^{a_1} : \cdots : t_r^{a_r}] : t_i \in \mathbb{K}^*\}$ of the torus T_X is called a **degenerate torus**.

If $\mathbb{K}^* = \langle \eta \rangle$, every $t_i \in \mathbb{K}^*$ is of the form $t_i = \eta^{s_i}$, for some $0 \le s_i \le q - 2$. Let $d_i = |\eta^{a_i}|$ and $D = diag(d_1, \ldots, d_r)$ be the matrix defining an automorphism of $\mathbb{Z}^r$. As Y_A is a monoid in T_X, $I(Y_A)$ is a lattice ideal. We determine the corresponding lattice in this section.

Theorem 4.2 ([8]). *If $Y = Y_A$ then $I(Y) = I_L$ for $L = D(L_{\beta D})$.*

5 Complete Intersections

We characterize when the vanishing ideals are complete intersections using mixed dominating matrices we define now.

Definition 5.1. If each column of a matrix has both a positive and a negative entry we say that it is *mixed*. If it does not have a square mixed submatrix, then it is called *dominating*.

Theorem 5.2 ([5])**.** *Let L be a non-zero sublattice of $\mathbb{Z}^r$ such that $L \cap \mathbb{N}^r = \{0\}$ and Γ be a matrix whose columns constitute a basis of L. Then I_L is a complete intersection iff Γ is mixed dominating.*

Using Theorem 5.2, we prove the following.

Proposition 5.3 ([8])**.** *$I(Y_A)$ is a complete intersection iff so is the toric ideal $I_{L_{\beta D}}$. A minimal generating system of binomials for $I(Y_A)$ is obtained from that of $I_{L_{\beta D}}$ by replacing x_i with $x_i^{d_i}$.*

Corollary 5.4 ([8])**.** *We have the following:*
*(**i**) if $Y = \{[1]\}$ then $I(Y) = I_{L_\beta}$,*
*(**ii**) if $Y = T_X$ then $I(Y) = I_L$, for $L = (q-1)L_\beta$,*
*(**iii**) $I(T_X)$ is a complete intersection iff so is I_{L_β}, which is independent of q.*

These result generalize some work of [2] from weighted projective spaces to a general toric variety. Using the matrix ϕ defined by the fan Σ and the result presented in this section one can easily check whether the vanishing ideal of T_X is a complete intersection.

Acknowledgments

We thank the editors and referee for their comments.

References

References

[1] E. Baran and M. Şahin, *Vanishing ideals of parameterized toric codes,* arxiv.org/abs/1802.04083

[2] E. Dias and J. Neves, *Codes over a weighted torus*, Finite Fields and Their Appl., 2015, 33, 66-79.

[3] Hansen, J., 2000. *Toric Surfaces and Error–correcting Codes* in: Buchmann, J. et al. (Eds.), Coding Theory, Cryptography, and Related Areas, Springer, pp. 132–142.

[4] Hansen, J., 2001. *Error-Correcting Codes from Higher-Dimensional Varieties*, Finite Fields Appl., 7 no. 4, 530–552.

[5] M. Morales and A. Thoma, *Complete Intersection Lattice Ideals*, J. Algebra, 2005, 284, 755-770.

[6] Renteria C., Simis A., Villarreal R. H., 2011, Algebraic methods for parameterized codes and invariants of vanishing ideals over finite fields, Finite Fields and Their Appl. 17 no. 1, 81–104.

[7] M. Şahin and I. Soprunov, *Multigraded Hilbert functions and toric complete intersection codes*, J. Algebra, 459 (2016), 446–467.

[8] M. Şahin, *Toric Codes and Lattice Ideals*, Finite Fields and Their Appl., 52 (2018), 243–260.

[9] I. Soprunov, *Toric complete intersection codes*, J. Symbolic Comput. 50 (2013), 374–385.

3x3 Ducci Matrices

Mustafa BAHŞİ*
Education Faculty,
Aksaray University,
Aksaray, TURKEY

Süleyman SOLAK
Ahmet Keleşoğlu Education Faculty,
Necmettin Erbakan University,
Konya, TURKEY

Abstract

A Ducci sequence is the sequence $\{X, DX, D^2X, ...\}$ generated by n-tuples $X = (x_1, x_2, \ldots, x_n) \in \mathrm{Z}^n$, where $D : \mathrm{Z}^n \to \mathrm{Z}^n$ is defined by

$$DX = D(x_1, x_2, \ldots, x_n) = (|x_2 - x_1|, |x_3 - x_2|, \ldots, |x_n - x_1|).$$

In this study, we examine relationships between Fibonacci numbers and powers of 3×3 Ducci matrices corresponding to the Ducci map $D : \mathrm{Z}^3 \to \mathrm{Z}^3$.

Keywords: Fibonacci numbers, Ducci map.

1 Introduction

Let $D : \mathrm{Z}^n \to \mathrm{Z}^n$ be a map defined by

$$DX = D(x_1, x_2, \ldots, x_n) = (|x_2 - x_1|, |x_3 - x_2|, \ldots, |x_n - x_1|),$$

where $X = (x_1, x_2, \ldots, x_n) \in \mathrm{Z}^n$. The map D is called a Ducci map and the sequence $\{X, DX, D^2X, ...\}$ is called a Ducci sequence. Every Ducci sequence $\{X, DX, D^2X, ...\}$ gives rise to a cycle i.e., there are integers i and j with $0 \le i < j$ with $D^iX = D^jX$. When i and j are as small as possible we say that the Ducci sequence has period $j - i$ [1].

Example 1.1. Let X be $X = (1, 1, 3)$. Then

$$DX = D(1, 1, 3) = (|1 - 1|, |3 - 1|, |3 - 1|) = (0, 2, 2),$$

$$D^2X = D(0, 2, 2) = (|2 - 0|, |2 - 2|, |2 - 0|) = (2, 0, 2),$$
$$D^3X = D(2, 0, 2) = (|0 - 2|, |2 - 0|, |2 - 2|) = (2, 2, 0),$$
$$D^4X = D(2, 2, 0) = (|2 - 2|, |0 - 2|, |0 - 2|) = (0, 2, 2),$$

where $DX = D^4X$ and Ducci sequence has period $4 - 1 = 3$.

Ducci sequences were first introduced in 1937 [4]. The discovery of Ducci sequences is attributed to Professor E. Ducci. Under the Ducci map, the behavior of the starting vector $X = (x_1, x_2, ..., x_n)$ is interesting and has been examined extensively [1-5]. The best known result is that every starting vector converges to zero vector if and only if n is a power of 2 [2,3]. When n is not a power of 2, every starting vector reaches to $k(a_1, a_2, ..., a_n)$, where $a_i \in \{0, 1\}$ and k is a positive constant [3]. The researches on application of the Ducci map to matrices have increased in recent years [5,7,8]. For example, Solak and Bahşi [8] have established relationships between the spectral norm, Euclidean norm, l_p norm, determinant and eigenvalues of the circulant matrix $Circ(A) = Circ(a_1, a_2, ..., a_n)$ and its image under

*Corresponding author. *E-mail address:* mhvbahsi@yahoo.com

the Ducci map.
Now, Let us consider the starting vector $X = (x_1, x_2, x_3) \in \mathrm{Z}^3$. Then, we have six case for x_1, x_2 and x_3.That is,

$$1)x_1 \geq x_2 \geq x_3,$$

$$2)x_1 \geq x_3 \geq x_2,$$

$$3)x_2 \geq x_1 \geq x_3,$$

$$4)x_3 \geq x_1 \geq x_2,$$

$$5)x_2 \geq x_3 \geq x_1,$$

and

$$6)x_3 \geq x_2 \geq x_1.$$

For the case $x_1 \geq x_2 \geq x_3$, we have $DX = D(x_1, x_2, x_3) = (x_1 - x_2, x_2 - x_3, x_1 - x_3)$. In this case, matrix multiplication yields

$$DX = \begin{bmatrix} 1 & -1 & 0 \\ 0 & 1 & -1 \\ 1 & 0 & -1 \end{bmatrix} \begin{bmatrix} x_1 \\ x_2 \\ x_3 \end{bmatrix}.$$

In fact, we have $DX = M_i X \ (i = 1, 2, ..., 6)$, where

$$M_1 = \begin{bmatrix} 1 & -1 & 0 \\ 0 & 1 & -1 \\ 1 & 0 & -1 \end{bmatrix}, M_2 = \begin{bmatrix} 1 & -1 & 0 \\ 0 & -1 & 1 \\ 1 & 0 & -1 \end{bmatrix}, M_3 = \begin{bmatrix} -1 & 1 & 0 \\ 0 & 1 & -1 \\ 1 & 0 & -1 \end{bmatrix},$$

$$M_4 = \begin{bmatrix} 1 & -1 & 0 \\ 0 & -1 & 1 \\ -1 & 0 & 1 \end{bmatrix}, M_5 = \begin{bmatrix} -1 & 1 & 0 \\ 0 & 1 & -1 \\ -1 & 0 & 1 \end{bmatrix}, \text{ and } M_6 = \begin{bmatrix} -1 & 1 & 0 \\ 0 & -1 & 1 \\ -1 & 0 & 1 \end{bmatrix}.$$

The above six matrices are called 3x3 Ducci matrices. One can see easily that $M_1 = -M_6$, $M_2 = -M_5$, and $M_3 = -M_4$.

In this study, we mainly focus on the relationships between the powers of 3x3 Ducci matrices and Fibonacci numbers.

Fibonacci numbers defined by the recurrence relation

$$F_{n+1} = F_n + F_{n-1}\,(n \geq 1)\,, F_0 = 0 \text{and} F_1 = 1$$

have many applications to mathematics, statistics and physics. The first few Fibonacci numbers are 0, 1, 2, 3, 5, 8, 13, 21,... and these numbers are defined backwards by 0, 1, -1, 2, -3, 5, -8, 13, -21,... . For the detailed information of Fibonacci numbers, we refer to [6].

Now, we give our main results.

2 Main Results

Theorem 2.1. For the nth power of the matrices M_1, M_4 and M_5, we have

$$M_1^n = \begin{bmatrix} F_n & -F_{n+1} & F_{n-1} \\ -F_{n-1} & F_n & -F_{n-2} \\ F_{n-2} & -F_{n-1} & F_{n-3} \end{bmatrix}, M_4^n = \begin{bmatrix} F_n & -F_{n-2} & -F_{n-1} \\ -F_{n-1} & F_{n-3} & F_{n-2} \\ -F_{n+1} & F_{n-1} & F_n \end{bmatrix}$$

and

$$M_5^n = \begin{bmatrix} F_{n-3} & F_{n-2} & -F_{n-1} \\ F_{n-1} & F_n & -F_{n+1} \\ -F_{n-2} & -F_{n-1} & F_n \end{bmatrix}$$

where F_n denotes the nth Fibonacci number.

Proof. We use principle of mathematical induction on n. For $n = 1$,

$$M_1^1 = \begin{bmatrix} F_1 & -F_2 & F_0 \\ -F_0 & F_1 & -F_{-1} \\ F_{-1} & -F_0 & F_{-2} \end{bmatrix} = \begin{bmatrix} 1 & -1 & 0 \\ 0 & 1 & -1 \\ 1 & 0 & -1 \end{bmatrix}.$$

That is, the result is true for $n = 1$. Assume that

$$M_1^{n-1} = \begin{bmatrix} F_{n-1} & -F_n & F_{n-2} \\ -F_{n-2} & F_{n-1} & -F_{n-3} \\ F_{n-3} & -F_{n-2} & F_{n-4} \end{bmatrix}.$$

Then,

$$M_1^n = M_1^{n-1} M_1 = \begin{bmatrix} F_{n-1} & -F_n & F_{n-2} \\ -F_{n-2} & F_{n-1} & -F_{n-3} \\ F_{n-3} & -F_{n-2} & F_{n-4} \end{bmatrix} \begin{bmatrix} 1 & -1 & 0 \\ 0 & 1 & -1 \\ 1 & 0 & -1 \end{bmatrix}$$

$$= \begin{bmatrix} F_{n-1} + F_{n-2} & -F_n - F_{n-1} & -F_{n-2} + F_n \\ -F_{n-2} - F_{n-3} & F_{n-1} + F_{n-2} & F_{n-3} - F_{n-1} \\ F_{n-3} + F_{n-4} & -F_{n-2} - F_{n-3} & -F_{n-4} + F_{n-2} \end{bmatrix}$$

$$= \begin{bmatrix} F_n & -F_{n+1} & F_{n-1} \\ -F_{n-1} & F_n & -F_{n-2} \\ F_{n-2} & -F_{n-1} & F_{n-3} \end{bmatrix},$$

which yields that the result is true for n. This completes the proof for the matrix M_1. By using similar method, we have desired results for the matrices M_4 and M_5.

Corollary 2.2. For the nth power of the matrices M_2, M_3 and M_6 , we have

$$M_2^n = (-1)^n \begin{bmatrix} F_{n-3} & F_{n-2} & -F_{n-1} \\ F_{n-1} & F_n & -F_{n+1} \\ -F_{n-2} & -F_{n-1} & F_n \end{bmatrix}, M_3^n = (-1)^n \begin{bmatrix} F_n & -F_{n-2} & -F_{n-1} \\ -F_{n-1} & F_{n-3} & F_{n-2} \\ -F_{n+1} & F_{n-1} & F_n \end{bmatrix}$$

and

$$M_6^n = (-1)^n \begin{bmatrix} F_n & -F_{n+1} & F_{n-1} \\ -F_{n-1} & F_n & -F_{n-2} \\ F_{n-2} & -F_{n-1} & F_{n-3} \end{bmatrix},$$

where F_n denotes the nth Fibonacci number.

Proof: These follow from Theorem 2.1 and the equalities $M_1 = -M_6$, $M_2 = -M_5$, and $M_3 = -M_4$.

Theorem 2.3. For the nth $(n \geq 3)$ power of the matrix M_i , we have

$$M_i^n = \begin{cases} M_i^{n-1} + M_i^{n-2}, & \text{for } i = 1, 4, 5 \\ -M_i^{n-1} + M_i^{n-2}, & \text{for } i = 2, 3, 6. \end{cases}$$

Proof. Theorem 2.1 and Corollary 2.2 yield

$$
\begin{aligned}
M_1^{n-1}+M_1^{n-2} &= \begin{bmatrix} F_{n-1} & -F_n & F_{n-2} \\ -F_{n-2} & F_{n-1} & -F_{n-3} \\ F_{n-3} & -F_{n-2} & F_{n-4} \end{bmatrix} + \begin{bmatrix} F_{n-2} & -F_{n-1} & F_{n-3} \\ -F_{n-3} & F_{n-2} & -F_{n-4} \\ F_{n-4} & -F_{n-3} & F_{n-5} \end{bmatrix} \\
&= \begin{bmatrix} F_{n-1}+F_{n-2} & -F_n-F_{n-1} & F_{n-2}+F_{n-3} \\ -F_{n-2}-F_{n-3} & F_{n-1}+F_{n-2} & -F_{n-3}-F_{n-4} \\ F_{n-3}+F_{n-4} & -F_{n-2}-F_{n-3} & F_{n-4}+F_{n-5} \end{bmatrix} \\
&= \begin{bmatrix} F_n & -F_{n+1} & F_{n-1} \\ -F_{n-1} & F_n & -F_{n-2} \\ F_{n-2} & -F_{n-1} & F_{n-3} \end{bmatrix} \\
&= M_1^n
\end{aligned}
$$

and

$$
\begin{aligned}
-M_2^{n-1}+M_2^{n-2} &= -(-1)^{n-1}\begin{bmatrix} F_{n-4} & F_{n-3} & -F_{n-2} \\ F_{n-2} & F_{n-1} & -F_n \\ -F_{n-3} & -F_{n-2} & F_{n-1} \end{bmatrix} + (-1)^{n-2}\begin{bmatrix} F_{n-5} & F_{n-4} & -F_{n-3} \\ F_{n-3} & F_{n-2} & -F_{n-1} \\ -F_{n-4} & -F_{n-3} & F_{n-2} \end{bmatrix} \\
&=(-1)^n \begin{bmatrix} F_{n-4}+F_{n-5} & F_{n-3}+F_{n-4} & -F_{n-2}-F_{n-3} \\ F_{n-2}+F_{n-3} & F_{n-1}+F_{n-2} & -F_n-F_{n-1} \\ -F_{n-3}-F_{n-4} & -F_{n-2}-F_{n-3} & F_{n-1}+F_{n-2} \end{bmatrix} \\
&= (-1)^n \begin{bmatrix} F_{n-3} & F_{n-2} & -F_{n-1} \\ F_{n-1} & F_n & -F_{n+1} \\ -F_{n-2} & -F_{n-1} & F_n \end{bmatrix} \\
&= M_2^n.
\end{aligned}
$$

Similarly, for $i = 3, 4, 5, 6$, desired results are obtained.

References

[1] F. Breuer, E. Löther, B. van der Merwe, Ducci-sequences and cyclotomic polynomials, Finite Fields and Their Applications 13 (2007) 293-304.

[2] F. Breuer, Ducci sequences in higher dimensions, Integers:Electronic Journal of Combinatorial Number Theory 7 (2007) A24.

[3] G. Brockman, Ryan J. Zerr, Asymptotic behavior of certain Ducci sequences, Fibonacci Quart. 45 (2) (2007) 155-163.

[4] C. Ciamberlini, A. Marengoni, Su una interssante curiosita numerica, Period. Math. 17 (4) (1937) 25-30.

[5] K. Hogenson, S. Negaard, R.J. Zerr, Matrix sequences associated with the Ducci map and the mediant construction of the rationals, Linear Algebra Appl. 437 (1) (2012) 285-293.

[6] T. Koshy, Fibonacci and Lucas Numbers with Applications, A Wiley-Interscience Publication, 2001.

[7] I. Odegard, R.J. Zerr, The quadratic irrationals and Ducci matrix sequences, Linear Algebra Appl. 484 (2015) 344-355.

[8] S. Solak and M. Bahşi, Some properties of circulant matrices with Ducci sequences, Linear Algebra Appl. 542 (2018) 557-568.

Recent progress in the spectral theory of non-selfadjoint Sturm-Liouville problems on the half-axis

Nimet ÇOŞKUN*
Karamanoglu Mehmetbey University,
Department of Mathematics,
70100, Karaman, TURKEY

Nihal YOKUŞ
Karamanoglu Mehmetbey University,
Department of Mathematics,
70100, Karaman, TURKEY

Abstract

The spectral theory of differential operators is a field of functional analysis which basically investigates the spectra of differential operators and the expansion of given functions in terms of the eigenfunctions of this operators. In this study, we provide a comprehensive overview on the spectral analysis of Sturm-Liouville operator on the half-axis including the topics; formulation of Jost solution, determination of resolvent operator, description of the sets of eigenvalues and spectral singularities in terms of singular points of the kernel of the resolvent and use of boundary uniqueness theorems of analytic functions to provide sufficient conditions guaranteeing finiteness of eigenvalues and spectral singularities. First, we introduce some basic definitions and theorems for differential Sturm-Liouville operator. Second, spectral analysis of discrete Sturm-Liouville problems will be discussed. In the third part, we mention the quantum calculus versions of the problem. At last, we conclude the paper with a general outlook on the issue.

Keywords: Spectral theory, Sturm-Liouville equation, eigenvalues, spectral singularities.

1 Introduction

The development of many important directions of mathematics and physics owes a major dept to the concepts and methods which evolved during the investigation of Sturm-Liouville equation $-y'' + q(x)y = \lambda^2 y$ and the allied Sturm-Liouville operator $L = \frac{-d^2}{dx^2} + q(x)$ (Lately L and $q(x)$ are often termed the one-dimensional Schrödinger operator and the potential). These provided a constant source of new ideas and problems in spectral theory of operators and kindred fields of analysis. Such problems arise in many areas of science and engineering, i.e., quantum mechanics, geophysics, astrophysics, electronics. As regards Sturm-Liouville theory and spectral analysis, there are plenty of useful resources for researches presenting the history and devolopments in these topics [1, 2]

Naimark [3, 4] considered the differential expression

$$l(y) = -y'' + q(x)y, \ 0 < x < \infty,$$

where the coefficient $q(x)$ is a complex valued function (referred as the potential of the equation) with the boundary condition

$$y(0) = 0.$$

*Corresponding author. *E-mail address:* cannimet@kmu.edu.tr

He associates an operator L operating on the Hilbert space $L^2(0,\infty)$. The operator L is defined by the formula $Lf = l(f)$ on functions $f \in L^2(0,\infty)$ which have a derivative f' absolutely continuous on every interval $[0,a]$, $0 < a < \infty$, and which are such that $l(f) \in L^2(0,\infty)$ and $f(0) = 0$. Recall that a complex number λ is called an eigenvalue of the operator L if there is a non-zero function f belonging to the domain of definition of this operator such that $Lf = \lambda f$. If λ is not an eigenvalue of the operator L, then the operator $(L - \lambda I)^{-1}$ exists and is called resolvent of L.

Based on the notions above, the spectral properties of the boundary value problem (BVP)

$$\begin{aligned} -y'' + q(x)y &= \lambda^2 y, \ 0 \leq x < \infty, && (1.1) \\ y(0) &= 0, && (1.2) \end{aligned}$$

was first investigated systematically by Naimark [3, 4]. He proved the existence of spectral singularities in the continuous spectrum of the BVP (1.1)-(1.2) and showed that, if $e^{\varepsilon x} \in L_1(\mathbb{R}_+)$ for some $\varepsilon > 0$, then the BVP (1.1)-(1.2) has a finite number of eigenvalues and spectral singularities with finite multiplicities. Also, he formulated the spectral expansion of the BVP (1.1)-(1.2) in terms of the principal vectors. Note that the eigenfunctions and the associated functions (principal functions) corresponding to the spectral singularities are not elements of $L_2(\mathbb{R}_+)$. Also, the spectral singularities belong to the continuous spectrum and are the poles of the resolvent's kernel, but are not the eigenvalues of the BVP (1.1)-(1.2).

Lyance examined the effect of the spectral singularities in the spectral expansion of the BVP (1.1)-(1.2) in terms of the principal functions [5]. Moreover, there have been numerous studies considering the spectral expansion and principal functions of the Sturm-Liouville problems in $[5-14]$.

Besides the studies dealing with the differential and difference equations with scalar coefficients that we have mentioned up to here, spectral analysis of the equations with matrix coefficients have also become the main research topic of a significant number of papers. The theory of matrix Sturm-Liouville problems has been actively developed during the last twenty years. Eigenvalue asymptotics and some other aspects of direct problems were studied in the papers $[14-16]$ and references therein.

Let us denote the solution of (1.1) satisfying the condition

$$\lim_{x\to\infty} y(x,\lambda)e^{-i\lambda x} = 1, \ \lambda \in \overline{\mathbb{C}}_+ := \{\lambda : \lambda \in \mathbb{C}, \operatorname{Im}\lambda \geq 0\},$$

by $e(x,\lambda)$. The solution $e(x,\lambda)$ is introduced as the Jost solution of (1.1). For the condition

$$\int_0^\infty x\,|q(x)|\,dx < \infty,$$

the Jost solution has the representation

$$e(x,\lambda) = e^{i\lambda x} + \int_x^\infty K(x,t)e^{i\lambda t}dt$$

for $\lambda \in \overline{\mathbb{C}}_+$, where the kernel $K(x,t)$ satisfies

$$\begin{aligned} K(x,t) &= \frac{1}{2}\int_{\frac{(x+t)}{2}}^{\infty} q(\xi)\,d\xi + \frac{1}{2}\int_x^{\frac{(x+t)}{2}}\int_{t+x-\xi}^{t+\xi-x} K(\xi,\eta)q(\xi)\,d\eta d\xi \\ &+\frac{1}{2}\int_{\frac{(x+t)}{2}}^{\infty}\int_{\xi}^{t+\xi-x} K(\xi,\eta)q(\xi)\,d\eta d\xi. \end{aligned}$$

Moreover, $K(x,t)$ is continuously differentiable with respect to its arguments and

$$
\begin{aligned}
|K(x,t)| &\leq c \int_{\frac{(x+t)}{2}}^{\infty} q(\xi)\, d\xi, \\
|K_x(x,t)|, |K_t(x,t)| &\leq \frac{1}{4}\left|q\left(\frac{x+t}{2}\right)\right| + c \int_{\frac{(x+t)}{2}}^{\infty} q(\xi)\, d\xi,
\end{aligned}
$$

where $c>0$ is a constant [17, Chapter 3]. Note that the Jost solution $e(x,\lambda)$ is analytic with respect to λ in $\mathbb{C}_+ := \{\lambda : \lambda \in \mathbb{C}, \operatorname{Im}\lambda > 0\}$ and continuous on the real axis.

Theorem 1 [18] *Assume that 2π periodic function g is analytic in $\mathbb{C}_+$, all of its derivatives are continuous in $\overline{\mathbb{C}}_+$, and*

$$\sup_{z\in P}\left|g^{(k)}(z)\right| \leq \eta_k,\ k \in \mathbb{N}\cup\{0\}.$$

If the set $G \subset \left[\frac{-\pi}{2}, \frac{3\pi}{2}\right]$ with Lebesgue measure zero is the set of all zeros the function g with infinite multiplicity in P, and if

$$\int_0^w \ln t(s) d\mu(G_s) = -\infty,$$

where $t(s) = \inf_k \frac{\eta_k s^k}{k!}$ and $\mu(G_s)$ is the Lebesgue measure of $s-$neighborhood of G and $w>0$ is an arbitrary constant, then $g \equiv 0$ in $\overline{\mathbb{C}}_+$.

In 1977, Sturm-Liouville equation with one boundary condition dependent on the spectral parameter and asymptotic estimates of eigenvalues or eigenfunctions were studied by Fulton [19]. In the upcoming years, there have been a great number of papers considering such Sturm-Liouville equations with boundary condition dependent on the spectral parameter such as $[19-24]$.

In [20], quadratic eigenparameter dependent Sturm-Liouville boundary value problem

$$
\begin{aligned}
-y'' + q(x)y &= \lambda^2 y,\ 0<x<\infty, \\
\left(\alpha_0+\alpha_1\lambda+\alpha_2\lambda^2\right)y'(0) - \left(\beta_0+\beta_1\lambda+\beta_2\lambda^2\right)y(0) &= 0,
\end{aligned}
$$

was studied for $\alpha_i,\ \beta_i \in \mathbb{C},\ i=0,1,2$ and λ is an eigenparameter. Under certain conditions, Jost function of this BVP was obtained and finiteness of the eigenvalues and spectral singularities was achieved using the uniqueness theorems of analytic functions [25].

2 Discrete Sturm-Liouville case

Let us introduce the second order difference operator generated in $l^2(\mathbb{N})$

$$a_{n-1}y_{n-1} + b_n y_n + a_n y_{n+1} = \lambda y_n,\ n \in \mathbb{N} = \{1,2,...\} \tag{2.1}$$

where (a_n), (b_n), $n \in \mathbb{N}$ are complex sequences, $a_n \neq 0$ for all $n \in \mathbb{N}\cup\{0\}$. Note that this equation can be written in the following Sturm-Liouville form

$$\nabla(a_n \triangle y_n) + h_n y_n = \lambda y_n,\ n \in \mathbb{N},$$

where $h_n = a_{n-1} + a_n + b_n$, $\triangle$ is the forward difference operator, $\triangle y_n = y_{n+1} - y_n$, and $\bigtriangledown$ is the backward difference operator, $\bigtriangledown y_n = y_n - y_{n-1}$.

Assume that for some $\varepsilon > 0$, the complex sequences (a_n) and (b_n) satisfy

$$\sup_{n\in\mathbb{N}} \left[\exp\left(\varepsilon n^{\delta}\right)(|1-a_n| + |b_n|)\right] < \infty,\ \frac{1}{2} \le \delta \le 1. \tag{2.2}$$

The Jost solution

$$e_n(z) = \alpha_n e^{inz}\left(1 + \sum_{m=1}^{\infty} A_{nm} e^{imz}\right),\ n \in \mathbb{N}\cup\{0\}$$

is obtained in [26] for $\lambda = 2\cos z$, where $z \in \overline{\mathbb{C}}_+ := \{z : z \in \mathbb{C}, \operatorname{Im} z \ge 0\}$, and α_n, A_{nm} are given in terms of (a_n) and (b_n) as

$$\begin{aligned}
\alpha_n &= \left(\prod_{k=n}^{\infty} a_k\right)^{-1}, \\
A_{n,1} &= -\sum_{k=n+1}^{\infty} b_k, \\
A_{n,2} &= -\sum_{k=n+1}^{\infty} (1-a_k) + \sum_{k=n+1}^{\infty} b_k \sum_{p=k+1}^{\infty} b_p, \\
A_{n,m} &= A_{n+1,m-2} + \sum_{k=n+1}^{\infty} \left\{\left(1-a_k^2\right) A_{k+1,m-2} - b_k A_{k,m-1}\right\}.
\end{aligned}$$

Moreover

$$|A_{nm}| \le C \sum_{k=n+\left[\left|\frac{m}{2}\right|\right]} (|1-a_k| + |b_k|),$$

holds, where $C > 0$ is a constant and $\left[\left|\frac{m}{2}\right|\right]$ is integer part of $\frac{m}{2}$. So, $e_n(z)$ is analytic with respect to z in $\mathbb{C}_+$ and continuous in $\operatorname{Im} z = 0$.

The boundary condition

$$\left(\alpha_0 + \alpha_1\lambda + \alpha_2\lambda^2\right) y_1 + \left(\beta_0 + \beta_1\lambda + \beta_2\lambda^2\right) y_0 = 0, \tag{2.3}$$

was taken into consideration for the discrete Sturm-Liouville equation (2.1) under the condition (2.2) in [27]. This paper may be thought as an extention of [28] because of the quadratic eigenparameter in the boundary condition. Jost function and quantitative properties of the eigenvalues and spectral singularities have also been investigated in [27, 28] under the Pavlov's condition and Naimark's condition.

3 Quantum calculus case

Assume $q > 1$ and define the set $q^{\mathbb{N}} := \{q^n : n \in \mathbb{N}\}$ where $\mathbb{N}$ stands for natural numbers. A q-difference equation is an equation that contains q-derivetives of a function defined on $q^{\mathbb{N}}$. Hilbert space of functions with the inner product

$$\langle f, g\rangle_q := \int_{q^{\mathbb{N}}} f(t)\overline{g(t)}\triangle t,\ \text{for } f,\ g : q^{\mathbb{N}} \to \mathbb{C}$$

and the norm

$$\|f\|_q := \left(\int\limits_{q^{\mathbb{N}}} |f(t)|^2 \triangle t\right)^{\frac{1}{2}} \text{ for } f : q^{\mathbb{N}} \to \mathbb{C}$$

by $l^2(q^{\mathbb{N}})$.

Consider the operator L generated by the second order q-difference equation

$$q\gamma(t)y(qt) + \beta(t)y(t) + \gamma(\frac{t}{q})y(\frac{t}{q}) = \lambda y(t),\ t \in q^{\mathbb{N}} \tag{3.1}$$

for $\gamma(t) \neq 0$ for all $t \in q^{\mathbb{N}}$, $\{\gamma(t)\}_{t\in q^{\mathbb{N}}}$, $\{\beta(t)\}_{t\in q^{\mathbb{N}}}$ are complex sequences. The q-difference equation can be written in the Sturm-Liouville form as

$$(ly)(t) = \left[ay^{\triangle}\right]^{\triangle}\left(\frac{t}{q}\right) + b(t)y(t) \text{ for } t \in q^{\mathbb{N}},$$

where $a(t) = \gamma(t)\mu^2(t)$ and $b(t) = \beta(t) + q\gamma(t) + \gamma\left(\frac{t}{q}\right)$ and $y^{\triangle}$ denotes the q-derivative of y. Under the condition

$$\sum_{t\in q^{\mathbb{N}}} \frac{\ln t}{\ln q}\left(|1-\gamma(t)| + |\beta(t)|\right) < \infty,$$

the Jost solution

$$e(t,z) = \alpha(t)\frac{\exp\left(i\frac{\ln t}{\ln q}z\right)}{\sqrt{\mu(t)}}\left(1 + \int\limits_{q^{\mathbb{N}}} A(t,r)\frac{\exp\left(i\frac{\ln r}{\ln q}z\right)}{\mu(r)} \triangle r\right),$$

was introduced in [29] for $\lambda = 2\sqrt{q}\cos z$, where $z \in \overline{\mathbb{C}}_+$ and $\alpha(t)$ and $A(t,r)$ are expressed in terms of $\{\gamma(t)\}_{t\in q^{\mathbb{N}}}$ and $\{\beta(t)\}_{t\in q^{\mathbb{N}}}$ as

$$\begin{aligned}
\alpha(t) &= \left(\prod_{s\in[t,\infty)\cap q^{\mathbb{N}}} \gamma(s)\right)^{-1},\ A(t,q) = -\frac{1}{\sqrt{q}}\sum_{s\in[qt,\infty)\cap q^{\mathbb{N}}} \beta(s),\\
A(t,q^2) &= \sum_{s\in[qt,\infty)\cap q^{\mathbb{N}}}\left\{1-\gamma^2(s) + \frac{1}{q}\beta(s)\sum_{p\in[qs,\infty)\cap q^{\mathbb{N}}} \beta(p)\right\},\\
A(t,q^2r) &= A(qt,r) + \sum_{s\in[qt,\infty)\cap q^{\mathbb{N}}}\left\{\left(1-\gamma^2(s)\right)A(qs,r) - \frac{\beta(s)}{\sqrt{q}}A(s,qr)\right\},
\end{aligned}$$

for $r,\ t \in q^{\mathbb{N}}$. After the representation of the Jost solution of the quantum difference equation (3.1), asymptotics for $e(t,z)$ were obtained. Also, continuous spectrum and quantitative properties of eigenvalues and spectral singularities were investigated.

As a continuation of the paper [29], the presence of the spectral parameter not only in the quantum difference equation but also in the boundary condition has been considered by Aygar and Bohner [30].

4 Conclusion

In this survey, we made mention of recent developments in the spectral analysis of non-selfadjoint Sturm-Liouville operator on the half-axis by the way of the procedure, which has been developed by Naimark, Lyance and others, including the steps: determination of Jost solution, formulation of the resolvent operator, designation of the sets of eigenvalues and spectral singularities in terms of the singular points of the resolvent and use of boundary uniqueness theorems of analytic functions to provide sufficient conditions quaranteeing finiteness of the eigenvalues and spectral singularities. Surely, there are a large number of studies including these topics that we could not mention in this survey. Nevertheless, this paper might be helpful for understanding the devolopment of the problem and application of the problem to other mathematical structures like discrete calculus and quantum calculus cases.

Note also that, we haven't mention the studies about the other operators like Schrödinger, Klein-Gordon and Dirac type operotors which the similar techniques might be applied for their spectral analysis. This paper may be also a guide for future studies in this context.

References

[1] W. O. Amrein, A. M. Hinz, D. B. Pearson, Sturm-Liouville Theory Past and Present, Birkhäuser Verlag Basel Boston Berlin, 2005.

[2] L. A. Steen, Highlights in the History of Spectral Theory, The American Mathematical Monthly, Vol. 80, No. 4 (Apr., 1973), pp. 359-381.

[3] M.A. Naimark, Linear Differential Operators II, Ungar, New York, NY, USA, 1968.

[4] M.A. Naimark, "Investigation of the spectrum and the expansion in eigenfunctions of a non-selfadjoint differential operator of the second order on a semi-axis," American Mathematical Society Translations, vol. 16, pp. 103–193, 1960.

[5] V.E. Lyance, A differential operators with spectral singularities. I, II, AMS Translations 2(60), 185-225, 227-283 (1967)

[6] N. Yokus, Principal Functions of Non-Selfadjoint Sturm-Liouville Problems with Eigenvalue-Dependent Boundary Conditions, Abstract and Applied Analysis, Volume 2011, Article ID 358912.

[7] A.M. Krall, "A nonhomogeneous eigenfunction expansion," Transactions of the American Mathematical Society, vol. 117, pp. 352–361, 1965.

[8] V.A. Marchenko, "Expansion in eigenfunctions of non-selfadjoint singular second order differential operators," American Mathematical Society Transactions Series 2, vol. 25, pp. 77–130, 1963.

[9] M.V. Keldysh, "On the completeness of the eigenfunctions of some classes of non-selfadjoint linear operators," Russian Mathematical Surveys, vol. 26, no. 4, pp. 15–41, 1971.

[10] M.G. Gasymov and F. G. Maksudov, "The principal part of the resolvent of nonselfadjoint operators in the neighborhood of spectral singularities," Functional Analysis and Its Applications, vol. 6, no. 3, pp. 185–192, 1972.

[11] E. Kir, "Spectrum and principal functions of the non-self-adjoint Sturm-Liouville operators with a singular potential," Applied Mathematics Letters, vol. 18, no. 11, pp. 1247–1255, 2005.

[12] M. Adıvar, and M. Bohner, Spectrum and Principal vectors of q-difference Equations, Indian Journal of Mathematics, Vol 48, pp 17-33, 2006.

[13] G.B. Tunca, E. Bairamov, Discrete spectrum and principal functions of non-selfadjoint differential operator. Czechoslovak Mathematical Journal, 49 (124) (1999), Praha.

[14] C. Coskun, M. Olgun, Principal functions of non-selfadjoint matrix Sturm-Liouville equations, Journal of Computational and Applied Mathematics, 235 (2011)

[15] M. Olgun, C. Coskun, Non-selfadjoint matrix Sturm-Liouville operators with spectral singularities, Applied Mathematics and Computations, 216(8) (2010)

[16] Y. Aygar, E. Bairamov, Jost solution and the spectral properties of the matrix-valued difference operators. Appl. Math. and Comput. 218, 9676-9681 (2012)

[17] V.A. Marchenko, Sturm-Liouville Operators and Applications, vol. 22 of Operator Theory: Advances and Applications, Birkhäuser, Basel, Switzerland, 1986.

[18] B.S. Pavlov, On separation conditions for spectral components of a dissipative operator. Math. USSR, Izv. 9, 113-137 (1975)

[19] C.T. Fulton, Two-point boundary value problems with eigenvalue parameter contained in the boundary conditions. Proc. R. Soc. Edinb. A 77, 293-308 (1977)

[20] N. Yokus, T. Koprubasi, Spectrum of the Sturm-Liouville operators with boundary conditions polynomially dependent on the spectral parameter, J Inequal Appl (2015) 2015: 42. https://doi.org/10.1186/s13660-015-0563-1

[21] E. Bairamov, N. Yokus, Spectral singularities of Sturm-Liouville problems with eigenvalue-dependent boundary conditions. Abstr. Appl. Anal. 2009, Article ID 28959 (2009)

[22] P.A. Binding, P.J. Browne, B.A. Watson, Sturm-Liouville problems with boundary conditions rationally dependent on the eigenparameter I. Proc. Edinb. Math. Soc. 33, 749-757 (2001)

[23] P.A. Binding, P.J. Browne, B.A. Watson,Transformations between Sturm-Liouville problems with eigenvalue dependent and independent boundary conditions. Bull. Lond. Math. Soc. 33, 749-757 (2001)

[24] P.A. Binding, P. J. Browne, and K. Seddighi, "Sturm-Liouville problems with eigenparameter dependent boundary conditions," Proceedings of the Edinburgh Mathematical Society, vol. 37, no. 1, pp. 57–72, 1994.

[25] E.P. Dolzhenko, "Boundary-value uniqueness theorems for analytic functions," Mathematical Notes of the Academy of Sciences of the USSR, vol. 25, no. 6, pp. 437–442, 1979.

[26] G.S. Guseinov, The inverse problem of scattering theory for a second order difference equation on the whole axis, Soiet Math. Dokl. 17 Ž . 1976 , 1684 1688

[27] T. Koprubasi, N. Yokus, Quadratic eigenparameter dependent discrete Sturm-Liouville equations with spectral singularities, Applied Mathematics and Computation, 244 (2014) 57-62.

[28] E. Bairamov, Y. Aygar, T. Koprubasi, The spectrum of eigenparameter-dependent discrete Sturm-Liouville equations, Journal of Computational and Applied Mathematics 235(16):4519-4523

[29] M. Adıvar, M. Bohner, Spectral Analysis of q-difference Equations with Spectral Singularities, Mathematical and Computer Modelling (Elsevier Journals), 43, 695-703, 2006.

[30] Y. Aygar, M. Bohner, On the spectrum of eigenparameter-dependent quantum difference equations, Appl. Math. Inf. Sci., 9 (2015), 1725–1729.

Contemporary Optimization Assessment Of Complicated Engineering Problems

Serdar ÇARBAŞ*
Department of Civil Engineering,
Karamanoglu Mehmetbey University,
Karaman/TURKEY

Osman TUNCA
Department of Civil Engineering,
Karamanoglu Mehmetbey University,
Karaman/TURKEY

S. Alper YILDIZEL
Department of Civil Engineering,
Karamanoglu Mehmetbey University,
Karaman/TURKEY

Abstract

The main focus of this study is to present a state-of-the-art evaluation of a complex engineering problem in a concise manner. The recent optimization technique used in this study, so-called Symbiotic Organisms Search (SOS) imitating the one of the famous natural phenomena which is the symbiotic relationships (mutualism, commensalism, and parasitism) between organisms in an ecosystem, is eligible for obtaining solutions of complicated engineering problems, operations research problems, management information system problems, and so forth on. In this paper, SOS is utilized to acquire the optimum design of speed reducer problem with a goal of minimizing its weight while gratifying a large number of constraints inflicted by gear and shaft design practices. So, the design problem can be evaluated as one of the most complicated engineering optimization problems since the problem has constraints related with dimensions and material properties of the shafts and gears as well as having the side limitations on design variables. The optimal results of the design problem yielded by SOS prove that the optimization process is robust and is not suffering the discrepancies of mathematical and gradient-based optimum design methods.

Keywords: Optimum design, metaheuristics, symbiotic organisms search, speed reducer.

1 Introduction

The subject of optimization is a fascinating blend of heuristics and rigour of theory. It can be studied as a branch of pure mathematics, yet has applications in almost every branch of science, technology and engineering. Over than three decades, a usage of new trend methods has been popularized in the field of optimization called as metaheuristics [1]. The metaheuristic optimization techniques are valuable in making the optimization process more reliable and efficient, so they are becoming very powerful in solving hard optimization problems, and they have been applied in almost all major areas of science and engineering as well as industrial applications. Metaheuristic algorithms are nature-inspired and/or bio-inspired as they have been developed based on the successful evolutionary behavior of natural systems by taking their basic phonemes from nature [2]. The most important advantageous of the metaheuristic methods is that they do not need any gradient and starting point. These methods are not

*Corresponding author. *E-mail address:* scarbas@kmu.edu.tr

expected to find the best solution all the time, but they are expected to find the good enough solutions or even the optimal solution most of the time, and more importantly, in a reasonably and practically short time [3]. Also, these methods have also come to include any procedures that employ strategies for overcoming the trap of local optimality in complex solution spaces, especially those procedures that utilize one or more neighborhood structures as a means of defining admissible moves to transition from one solution to another, or to build or destroy solutions in constructive and destructive processes [4]. The recent addition to metaheuristic algorithms is so-called Symbiotic Organisms Search (SOS) proposed by Cheng and Prayogo [5]. This technique is based on the interactions relationship between two organisms in ecosystems. The mostly common symbiotic relations between the organisms in ecosystem are mutualism, commensalism, and parasitism. This paper aims to present the assessment of the optimal solution of the well-known and well-studied Golinski's speed reducer optimization problem [6, 7] via SOS based optimization algorithm. The main objective of the problem is minimizing the weight of the speed reducer gear box. This problem reveals as a benchmark for application of various new methods of optimization [8-13]. This problem can be categorized as hard and complicated engineering problem owing to have seven design variables engaged to dimensions and material properties of the shafts and gears. These variables can vary between lower and upper bounds which appear to be the limitations on design variables. Moreover, there are lots of constraints made up of different operations on design variables including higher-order nonlinear terms. [14].

2 Mathematical Modelling of The Problem

The design of the speed reducer is a more challenging engineering problem because it contains seven design variables. As shown in Figure 1, the design of the speed reducer is considered with the face width (x_1), the module of the teeth (x_2), the number of teeth on pinion (x_3), the length of the first shaft between bearings (x_4), the length of the second shaft between bearings (x_5), diameter of the first shaft (x_6), and the diameter of the second shaft (x_7) [15].

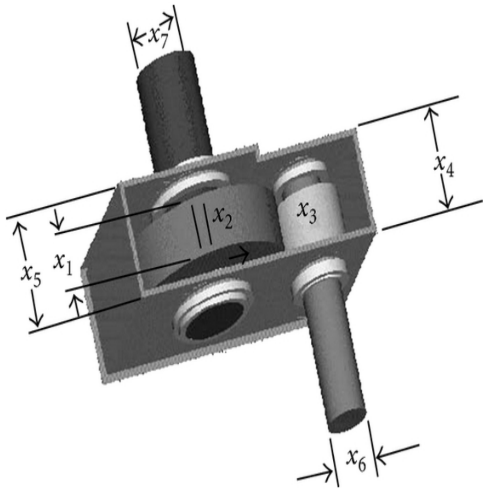

Figure 1: Design of Speed Reducer

The objective is to minimize the total weight of the speed reducer while meeting eleven constraints. The constraints include the limits on the bending stress of the gear teeth, surface stress, transverse deflections of shafts 1 and 2 due to transmitted force, and stresses in shafts 1 and 2 [15]. The mathematical programming model of a speed reducer problem considered

in this study is expressed as follows.
Minimize

$$f\left(x_1,\ldots,x_7\right)=0.7854x_1{x_2}^2\left(3.3333{x_3}^2+14.9334x_3-43.0934\right)\\-1.5079x_1\left({x_6}^2+{x_7}^2\right)\ +7.4777\left({x_6}^3+{x_7}^3\right)\\+0.7854\left(x_4{x_6}^2+x_5{x_7}^2\right) \tag{1}$$

Subjected to

$$g_1\ =27{x_1}^{-1}{x_2}^{-2}{x_3}^{-1}\leq 1.0 \tag{2}$$
$$g_2\ =397.5{x_1}^{-1}{x_2}^{-2}{x_3}^{-2}\leq 1.0 \tag{3}$$
$$g_3\ =1.93{x_4}^3{x_2}^{-1}{x_3}^{-1}{x_6}^{-4}\leq 1.0 \tag{4}$$
$$g_4\ =1.93{x_5}^3{x_2}^{-1}{x_3}^{-1}{x_7}^{-4}\leq 1.0 \tag{5}$$
$$g_5\ =\left(745^2{x_4}^2{x_2}^{-2}{x_3}^{-2}+16.9x10^6\right)/110^2{x_6}^6\leq 1.0 \tag{6}$$
$$g_6\ =\left(745^2{x_5}^2{x_2}^{-2}{x_3}^{-2}+157.5x10^6\right)/85^2{x_7}^6\leq 1.0 \tag{7}$$
$$g_7\ =x_2x_3/40\ \leq 1.0 \tag{8}$$
$$g_8\ =5x_2/x_1\ \leq 1.0 \tag{9}$$
$$g_9\ =x_1/12x_2\ \leq 1.0 \tag{10}$$
$$g_{10}=\ \left(1.5x_6+1.9\right){x_4}^{-1}\leq 1.0 \tag{11}$$
$$g_{11}=\ \left(1.1x_7+1.9\right){x_5}^{-1}\ \leq 1.0 \tag{12}$$

The variable bounds for the problem are as follows;

$$2.6\leq\ x_1\ \leq 3.6 \tag{13}$$
$$0.7\leq\ x_2\ \leq 0.8 \tag{14}$$
$$17\leq\ x_3\ \leq 28 \tag{15}$$
$$7.3\leq\ x_4\ \leq 8.3 \tag{16}$$
$$7.3\leq\ x_5\ \leq 8.3 \tag{17}$$
$$2.9\leq\ x_6\ \leq 3.9 \tag{18}$$
$$5.0\leq\ x_7\ \leq 5.5 \tag{19}$$

3 Symbotic Organisms Search (Sos) Algorithm

Symbiotic Organisms Search (SOS) algorithm is one of the very promising recent developments in the field of metaheuristic algorithms [5, 16]. The nature-inspired philosophy of SOS algorithm is analogous to the interactive behavior among organisms in nature. Organisms in the real world rarely live in isolation due to dependence on other species for sustenance and survival. In general, organisms develop symbiotic relationships as a strategy to adapt to changes in their environment.
Three cycles of the search are performed mimicking the three symbiotic relationships so-called mutualism phase, commensalism phase, and parasitism phase. By performing this three phases, SOS attempts to move a population, called an ecosystem of possible solutions, to promising areas of the search space during the search for the optimal solution.
SOS adapts the most common examples of symbiotic relationships found in nature [17]:
i) Mutualism:
This relationship category describes the symbiotic relationship between two different species that benefit mutually from that relationship. Bees fly amongst flowers, gathering nectar to

turn into honey. While this activity benefits bees, it also benefits flowers because pollen distribution is a side effect of this process. Both organisms engage in a mutualistic relationship with the goal of increasing mutual survival advantage in the ecosystem. New candidate solutions for X_i and X_j are calculated based on the mutualistic symbiosis between organism X_i and X_j, which is modeled in Equations (20) and (21).

$$X_{inew} = X_i + rand\,(0,1)^*\,(X_{best} - -Mutual\_Vector^* BF_1) \tag{20}$$

$$X_{inew} = X_i + rand\,(0,1)^*\,(X_{best} - -Mutual\_Vector^* BF_1) \tag{21}$$

$$Mutual\_Vector = \,(X_i + X_j)\,/2 \tag{22}$$

ii) Commensalism:
This relationship category describes the symbiotic relationship between two different species in which one benefits and the other is unaffected or neutral. The remora attaches itself to the shark and eats food leftovers, thus receiving a benefit. The shark is unaffected by remora fish activities and receives minimal, if any, benefit from the relationship. The new candidate solution of X_i is calculated according to the commensal symbiosis between organism X_i and X_j, which is modeled in Equation (23). Following the rules, organism Xi is updated only if its new fitness is better than its pre-interaction fitness.

$$X_{jnew} = X_j + rand\,(-1,1)^*\,(X_{best} - X_j) \tag{23}$$

iii) Parasitism:
This relationship category describes the symbiotic relationship between two different species in which one benefits and the other is actively harmed. The plasmodium parasite uses its relationship with the anopheles mosquito to pass between human hosts. While the parasite thrives and reproduces inside the human body, its human host suffers malaria and may die as a result. Organism X_i is given a role similar to the anopheles mosquito through the creation of an artificial parasite called "Parasite_Vector". *Parasite_Vector* is created in the search space by duplicating organism X_i, then modifying the randomly selected dimensions using a random number. Organism X_j is selected randomly from the ecosystem and serves as a host to the parasite vector. *Parasite_Vector* tries to replace X_j in the ecosystem. Both organisms are then evaluated to measure their fitness. If *Parasite_Vector* has a better fitness value, it will kill organism X_j and assume its position in the ecosystem. If the fitness value of X_j is better, X_j will have immunity from the parasite and the *Parasite_Vector* will no longer be able to live in that ecosystem. The steps of the SOS Algorithm are given below;
1: iter = 1
2: Initialize ecosystem / population
3: **repeat**
4: Simulate interaction between organisms through the Mutualism Phase
5: Simulate interaction between organisms through the Commensalism Phase
6: Simulate interaction between organisms through the Parasitism Phase
7: Update the best organism
8: **until** iter = max_iter

4 Results And Discussion

In this study, the speed reducer engineering design problem is optimized via SOS algorithm. The algorithm parameters, which are ecosystem size; *Eco_size*, and maximum number of fitness function evaluations; *maxFE*, are set as 20 and 20000, respectively. After optimization, the robustness of obtained results is compared by those reported in the literature. The optimal results are tabulated in Table 1. It is clearly seen in the table that the SOS algorithm yields optimum design weight as 2993.1392 kg. It is observed from this table that only one constraint, g_{11}, violates slightly during optimization process. This violation is not marginal and it is acceptable in the view of engineering. Besides, this violation can be evaluated as slightly infeasible in a tolerance limitation which is below 10^{-4}.

Table 1: Shows the data that we used in our calculations.

Results	Rao [8]	Li and Papalambros [9]	Kuang et al. [10]	Azarm and Li [11]	Vanderplaatz [12]	Ray [13]	Present Study
x_1	3.50000000	3.50000000	3.60000000	3.50000000	3.50000000	3.50000002	3.50000000
x_2	0.70000000	0.70000000	0.70000000	0.70000000	0.70000000	0.70000000	0.70000000
x_3	17.0000000	17.0000000	17.0000000	17.0000000	17.0000000	17.0000000	17.0000000
x_4	7.30000000	7.30000000	7.30000000	7.30000000	7.30000020	7.30000009	7.17984
x_5	7.30000000	7.71000000	7.80000000	7.71000000	7.30000020	7.80000000	7.70889
x_6	3.35000000	3.35000000	3.40000000	3.35000000	3.35021450	3.35021468	3.35009
x_7	5.29000000	5.29000000	5.00000000	5.29000000	5.28651760	5.28668325	5.28668
g_1	0.92608470	0.92608470	0.90036010	0.92608470	0.92608470	0.92608470	0.9260847196
g_2	0.80200150	0.80200150	0.77972370	0.80200150	0.80200150	0.80200150	0.8020014729
g_3	0.50095610	0.50095610	0.47213180	0.50095610	0.50082790	0.50082790	0.4765722477
g_4	0.08056680	0.09491850	0.12314430	0.09491850	0.08077930	0.09852830	0.0951160484
g_5	**1.00019230**	**1.00019230**	0.95671190	**1.00019230**	**1.00000010**	1.00000000	0.9999123077
g_6	0.99802660	0.99810290	**1.18206090**	0.99810290	**1.00000020**	1.00000000	0.9999842777
g_7	0.29750000	0.29750000	0.29750000	0.29750000	0.29750000	0.29750000	0.2975000000
g_8	1.00000000	1.00000000	0.97222220	1.00000000	1.00000000	1.00000000	1.0000000000
g_9	0.41666670	0.41666670	0.42857140	0.41666670	0.41666670	0.41666670	0.4166666667
g_{10}	0.94863014	0.94863014	0.95890411	0.94863014	0.94867419	0.94867413	0.9645249755
g_{11}	**1.05739726**	**1.00116732**	0.94871795	**1.00116732**	**1.05687249**	0.98914762	**1.0008377341**
Min. weight (kg)	2987.29850	2996.309776	2876.11762	2996.30978	2985.15188	2996.23216	2993.13917

5 Conclusions

In this study, in order to obtain the one of the challenging and complicated engineering problem which is so-called The Speed Reducer problem is assessed for minimizing the weight of the gearbox utilizing Symbiotic Organisms Search (SOS) algorithm that is based on the interactions relationship between two organisms in ecosystems. This algorithm is characterized in the group of contemporary metaheuristic algorithms. The metaheuristic optimization techniques are found quite effective in obtaining the solution of complex optimization problems which are based on natural phenomena. The optimum design of the speed reducer obtained by SOS algorithm clearly shows that this technique is quite feasible and robust for solving the complicated engineering problems.

References

[1] M. A. Bhatti, Practical Optimization Methods with Mathematica® Applications, Springer-Verlag New York, 2000.

[2] X-S. Yang, Engineering Optimization; An Introduction with Metaheuristic Applications, John Wiley Sons, Inc., Hoboken, New Jersey, 2010.

[3] X-S. Yang, Nature-Inspired Metaheuristic Algorithms, 2nd Ed., Luniver Press, 2010.

[4] F. W. Glover and G. A. Kochenberger, Handbook of Metaheuristics, Kluwer Academic Publishers, Dordrecht, 2003.

[5] M-Y. Cheng and D. Prayogo, Symbiotic organisms search: A new metaheuristic optimization algorithm, Comput. Struct., 139 (2014) 98-112.

[6] J. Golinski, Optimal Synthesis Problems Solved by Means of Nonlinear Programming and Random Methods, J. Mech., 5 (1970) 287-309.

[7] J. Golinski, An Adaptive Optimization System Applied to Machine Synthesis, Mech. Mach. Theo., 8 (1973) 419-436.

[8] S. S. Rao, Engineering Optimization, 3rd Ed., Wiley, New York, 1996.

[9] H. L. Li and P. A. Papalambros, Production System for Use of Global Optimization Knowledge, J. Mech. Trans. Auto. Design, 107 (1985) 277-284.

[10] J. K. Kuang, S. S. Rao, and L. Chen, Taguchi-Aided Search Method for Design Optimization of Engineering Systems, Eng. Optimiz., 30 (1998) 1-23.

[11] S. Azarm and W. C. Li, Multi-Level Design Optimization Using Global Monotonicity Analysis, J. Mech. Trans. Auto. Design, 111 (1989) 259-263.

[12] G. N. Vanderplaatz, CONMIN-A Fortran Program for Constrained Function Minimization: User's Manual, NASA (1973) TMX-62282.

[13] T. Ray, Golinski's Speed Reducer Problem Revisited, AIAA J., 41 (3) (2015) 556-558.

[14] C. Aktemur and I. Gusseinov, A Comparison of Sequential Quadratic Programming, Genetic Algorithm, Simulated Annealing, Particle Swarm Optimization and Hybrid Algorithm for the Design and Optimization of Golinski's Speed Reducer, Int. J. Energ. Appl. Tech., 4 (2) (2017) 34-52.

[15] M-H. Lin, J-F. Tsai, N-Z. Hu, and S-C. Chang, Design Optimization of a Speed Reducer Using Deterministic Techniques, Math. Prob. Eng., 2013 (2013) 1-7.

[16] M-Y. Cheng, D. Prayogo, and D-H. Tran, Optimizing Multiple Resources Leveling in the Multiple Projects using Discrete Symbiotic Organisms Search, J. Comput. Civil Eng., 30 (3) (2015) 1-9.

[17] http://140.118.5.71/sos/, retrieved on August 8th, 2018.

Investigation The Effect Of Greedy Selection Strategies On The Performance Of The Tree Seed Algorithm

İbrahim AYDOĞDU
Department of Civil Engineering,
Akdeniz University,
Antalya/TURKEY

Serdar ÇARBAŞ
Department of Civil Engineering,
Karamanoglu Mehmetbey University,
Karaman/TURKEY

Ahmed PAKSOY *
Department of Civil Engineering,
Akdeniz University,
Antalya/TURKEY

Abstract

This study aims to carry out the influence of greedy selection strategies on the optimal design performance of the Tree Seed Algorithm (TSA). Tree Seed Algorithm, which is a new intelligent optimizer based on the relation between trees and their seeds, is exerted for optimum design process. It is a numerical optimization method inspired by growing of trees and seeds on a land. It is proven that the implementation of greedy selection strategies causes more reliable and efficient technique for obtaining the solution of optimization problems.

Keywords: Numerical optimization, tree seed algorithm, greedy selection.

1 Introduction

The metaheuristic algorithms attempt to capture the optimal result among all solutions by utilizing available information for resolution the problem described within the scope of an optimization problem. The conventional gradient based algorithms do not ensure to derived optimal solutions for complicated problems. To solve these types of problems it is required to a vigorous calculation at an exponential time. To this respect, metaheuristic algorithms assure obtaining a feasible solution in a logical time beneath the direction of the presence solutions [1]. The Tree Seed Algorithm (TSA) is come to light as of late and it simulates the natural phenomena of raising the trees and seeds [2, 3]. The trees and their seeds on the D-dimensional solution space correspond to the possible solution for the optimization problem. At the beginning of the search, the trees are sowed to the land, and a number of seeds for each tree are produced during the iterations. The tree is removed from the stand and its best seed is added to the stand if the fitness of the best seed is better than the fitness of this tree [4-7]. Moreover, a greedy selection is a mathematical process that looks for simple, easy-to-implement solutions to complex, multi-step problems by deciding which next step will provide the most obvious benefit [8]. Such selections are called greedy because while the optimal solution to each smaller instance will provide an immediate output, the selection doesn't consider the larger problem as a whole. Once a decision has been made, it

*Corresponding author. *E-mail address:* ahmedpaksoy@hotmail.com

is never reconsidered. Namely, a greedy selection relies on selection of optimal choice at a local level reducing the problem to a single sub-problem, which actually leads to a globally optimal solution. In this study, different types of greedy selections are offered to develop the performance of TSA in an effective manner. So, the main goal of this paper is to present a way of analyzing different three type greedy selection strategies onto optimization efficiency of the TSA.

2 Tree Seed Algorithm (TSA)

In the initialization of the algorithm, a certain number of trees are randomly generated by using Equation 1.

$$T_{i,j} = L_{j,min} + r_{i,j}\left(H_{j,max} - -L_{j,min}\right) \qquad i = 1, 2, \ldots.., N \text{ and } j = 1, 2, \ldots.., D \tag{1}$$

where, $T_{i,j}$, shows j^{th} dimension of ith tree, $H_{j,max}$ and $L_{j,min}$ are the upper and lower bounds for the search space, N is the number of tree in the stand, D is the dimensionality of the optimization problem and $r_{i,j}$ is a random number produced in range of [0,1]. After the stand is generated, the best tree location is selected as follows (for minimization):

$$B = argmin\left[f\left(T_i\right)\right] \tag{2}$$

where, B is the location of best tree, f is the objective function specific for the optimization problem.
The candidate solutions phase is seed production mechanism and it is controlled by search tendency (ST) parameter. This procedure is briefly given below.

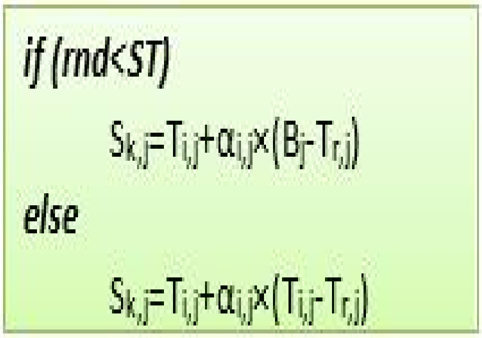

Figure 1: The seed production mechanism.

In Figure 1, ST is control parameter predefined in range of [0,1], rnd is a random number in range of [0,1], $T_{r,j}$, is the jth dimension of r^{th} tree which is randomly selected from the stand, B_j is the j^{th} dimension of best tree location, $S_{k,j}$, is the j^{th} dimension of k^{th} seed produced from i^{th} tree and $\alpha_{i,j}$, is the scaling factor randomly produced in range of [-1,1]. The number of seeds (upper and lower limit of k) which will be produced for a tree at an iteration is in range of 10% and 25% of the number of trees in the stand. For instance, when we take 10 for the number of trees in the stand, the number of seeds which will be produced for each tree is 1, 2 or 3. If the seed number is obtained as floating number, it is rounded up. After seeds are produced, the best seed in the seeds produced from the tree, is selected by using fitness of the seeds and the best is compared with the current tree. If fitness of the best seed is better than the fitness of the tree, the tree is removed from the stand and the best seed is added to the stand. The working diagram of the basic TSA is presented in Figure 2 [9].

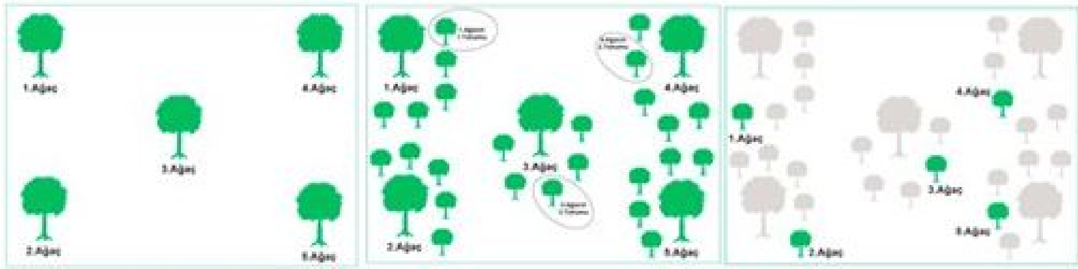

Figure 2: The TSA procedure diagram.

3 Greedy Selection

A greedy selection builds a specific candidate solution incrementally. The aspect of a greedy selection that makes it *greedy* is how it chooses from among the different ways of incrementing the current partial solution. In general, the different choices are ordered according to some criterion, and the best choice according to this criterion is taken. Thus, the algorithm builds the solution by always taking the step that appears to be most promising at that moment. When greedy selection strategies produce optimal solutions, they tend to be quite efficient. In deriving a greedy selection in a top-down fashion, the first step is to generalize the problem so that a partial solution is given as input. A precondition is assumed that this partial solution can be extended to an optimal solution. The task is then to extend it in some way so that the resulting partial solution can be extended to an optimal solution. Greedy selection provides an efficient mechanism for solving certain optimization problems [10]. The major steps involved in the construction of a greedy selection are:

- Generalize the problem so that a partial solution is given as input.
- Decide upon a selection criterion for incrementally extending partial solutions.
- Prove that if a given partial solution can be extended to an optimal solution, then after extending this partial solution using the chosen selection criterion, the resulting partial solution can also be extended to an optimal solution.
- Implement the transformation suggested by the incremental extension using a loop.

3.1 Proposed Greedy Selection Strategies

In order to improve the performance of TSA, three different types of greedy selection strategy are offered as well as no greedy selection.
Case 1) No Greedy Selection
Here, the best of the seeds produced for each tree replaces the tree to which it is depended without any comparison.
Case 2) Standart Greedy Selection
Here, the best of the seeds produced for each tree is compared to the tree to which it is depended. If the best seed is better than the tree to which it is depended, the seed replaces the tree. Otherwise the replacement will not take place. This version of greedy selection has been already used in standard TSA.
Case 3) Best Greedy Selection 1
Here, the best of the seeds produced for each tree is compared to the worst tree in the cluster. If the best seed is better than the worst tree depended, the seed replaces the tree. Otherwise the replacement will not take place.

Case 4) Best Greedy Selection 2

Here, every seed produced is compared to the worst tree in the cluster. If the seed is better than the worst tree, the seed replaces the tree. Otherwise the replacement will not take place.

4 Test Examples

The developed versions of the TSA algorithm by implementing the greedy selection strategies are tested on four mathematical benchmark functions [11]. Specifications of the benchmark functions are given in the Table 1. In the table, n represents the dimension of the function which is equal to number of decision variables in the optimization problem. In this study, two different n values have been used (n=5, n=30). The number of function iterations is equal to 100 for all versions. The internal parameters called the number of tree (NT), search tendency factor (ST), the lowest number of seeds and, the highest number of seeds are respectively taken as 5*n, 0.5, 0.1*NT, 0.25*NT. All tests are performed 30 times using different seed values. Statistical data of all tests are presented in Table 2.

Table 1: Specifications of the benchmark functions.

Function name	Formulation	Range
Sphere	$F_1(\boldsymbol{x}) = \sum_{i=1}^{n}\left(x_i^2\right)$	[-5.12, 5.12]
Rastrigin	$F_2(\boldsymbol{x}) = 10n + \sum_{i=1}^{n}\left(x_i^2 - 10\cos\left(2\pi x_i\right)\right)$	[-5.12, 5.12]
Griewank	$F_3\left(\boldsymbol{x}\right) = \sum_{i=1}^{n}\left(\frac{x_i^2}{4000}\right) - \prod_{i=1}^{n}\left(\frac{x_i}{\sqrt{i}}\right) + 1$	[-600, 600]
Rosenbrock	$F_4(\boldsymbol{x}) = \sum_{i=1}^{n-1}\left(100(x_i^2 + x_{i+1})^2 + (x_i - 1)^2\right)$	[-5, 10]

Table 3: Statistical data of the optimum solutions (Best values are bolded.

	dimension=5				dimension=30			
	Case 1	Case 2	Case 3	Case 4	Case 1	Case 2	Case 3	Case 4
F1								
Min.	9.48E-17	1.91E-18	**2.75E-49**	1.48E-22	8.49E-05	4.18E-05	4.45E-15	**1.48E-53**
Ave.	1.08E-15	1.39E-17	**1.35E-45**	0.028999	0.000126	5.98E-05	1.52E-14	**1.67E-50**
Std.	2.73E-15	1.83E-17	**3.29E-45**	0.093975	2.3E-05	1.27E-05	5.12E-15	**5.05E-50**
Max.	1.52E-14	8.58E-17	**1.63E-44**	0.441807	0.000173	8.83E-05	3E-14	**2.78E-49**
Median	3.88E-16	8.17E-18	**1.07E-46**	1.48E-05	0.000123	5.86E-05	1.45E-14	**3.26E-51**
F2								
Min.	2.702088	5.6E-05	**0**	0.000947	209.6651	166.853	**13.92943**	13.92942
Ave.	5.274916	**0.420576**	2.123125	2.688293	228.9069	183.8728	**25.06837**	37.36548
Std.	1.397972	**0.488027**	1.434748	1.674065	8.214353	**7.760212**	11.29118	19.40372
Max.	8.948439	**1.388492**	7.304236	7.961903	243.0992	198.7958	**70.7237**	119.1389
Median	5.195558	**0.176948**	1.989918	2.065496	229.2129	184.2219	**21.59246**	32.77993
F3								
Min.	0.059963	0.053813	**0.007396**	0.029562	0.317026	0.164042	5.51E-12	**0**
Ave.	0.157823	0.092038	**0.062227**	0.771066	0.563214	0.305093	**0.001397**	0.00517
Std.	0.046858	**0.022139**	0.049071	2.255746	0.107921	0.076283	**0.00328**	0.007921
Max.	0.244818	**0.13792**	0.238458	11.85724	0.758144	0.461189	**0.012316**	0.031942
Median	0.162037	0.090927	**0.049907**	0.195708	0.588144	0.29981	1.74E-11	**5E-16**
F4								
Min.	0.727571	0.26712	**0.083522**	0.452418	27.80749	27.96803	22.47006	**22.23768**
Ave.	1.571059	**0.854041**	1.176668	2.98137	29.09935	28.96473	**23.28368**	25.69982
Std.	0.410505	**0.342476**	0.895676	1.550651	0.642889	0.616199	**0.346241**	10.31221
Max.	2.401979	**1.556801**	4.313151	6.99127	30.64217	30.34227	**23.91942**	80.16933
Median	1.575918	**0.826597**	1.023034	2.817304	29.04764	28.87882	**23.25043**	23.8318

According to the test results, in the Sphere Function (F1) when the function dimension is taken as 5 the Case 3 (Best Greedy Selection 1) shows the better performance. But, in the same function when the function dimension is taken as 30 the Case 4 (Best Greedy Selection 2) produces better solution. In the investigation of the Rastrigin Function (F2), it is clearly observed that when the function dimension is taken as 5, although the minimum objective function value is obtained by Case 3, the optimal values of others (Ave., Std., Max., and Median) are obtained when Case 2 greedy selection strategy is applied. If the dimension of the F2 function is taken as 30, all optimal values are yielded by Case 3 except Std. value. In the Griewank Function (F3) with 5 function dimension, the minimum function value is obtained by Case 3 implemented TSA. For same function (F3) with 30 function dimension, the minimum function value is obtained by Case 4. In the Rosenbrock Function (F4), for both function dimensions, even if the minimum function values is obtained by Case 4 implemented TSA, the optimal value of others are attained by Case 3 implemented TSA. From these results in can be concluded that Best Greedy Selection Strategies (Case 3 and Case 4) are more effective to reach the best solutions than the other strategies (Case 1 and Case 2). From Figure 3 to 6, the convergence histories with respect to best values and average values of the optimum solutions of all functions are presented. In the graphs, n represents the dimension of the functions which is equal to number of decision variables in the optimization problem. According to the test results, Case 3 and Case 4 greedy selection strategies show satisfactory convergence performances on the mathematical functions. In all functions when n is taken as 30, the Case 3 and Case 4 greedy selections are rapidly converge to the minimum function solution. In addition, the performances of the Case 2, Case3, and Case 4 greedy selection strategies causes better algorithm convergence than Case 1 which means there is no any greedy selection strategy is used.

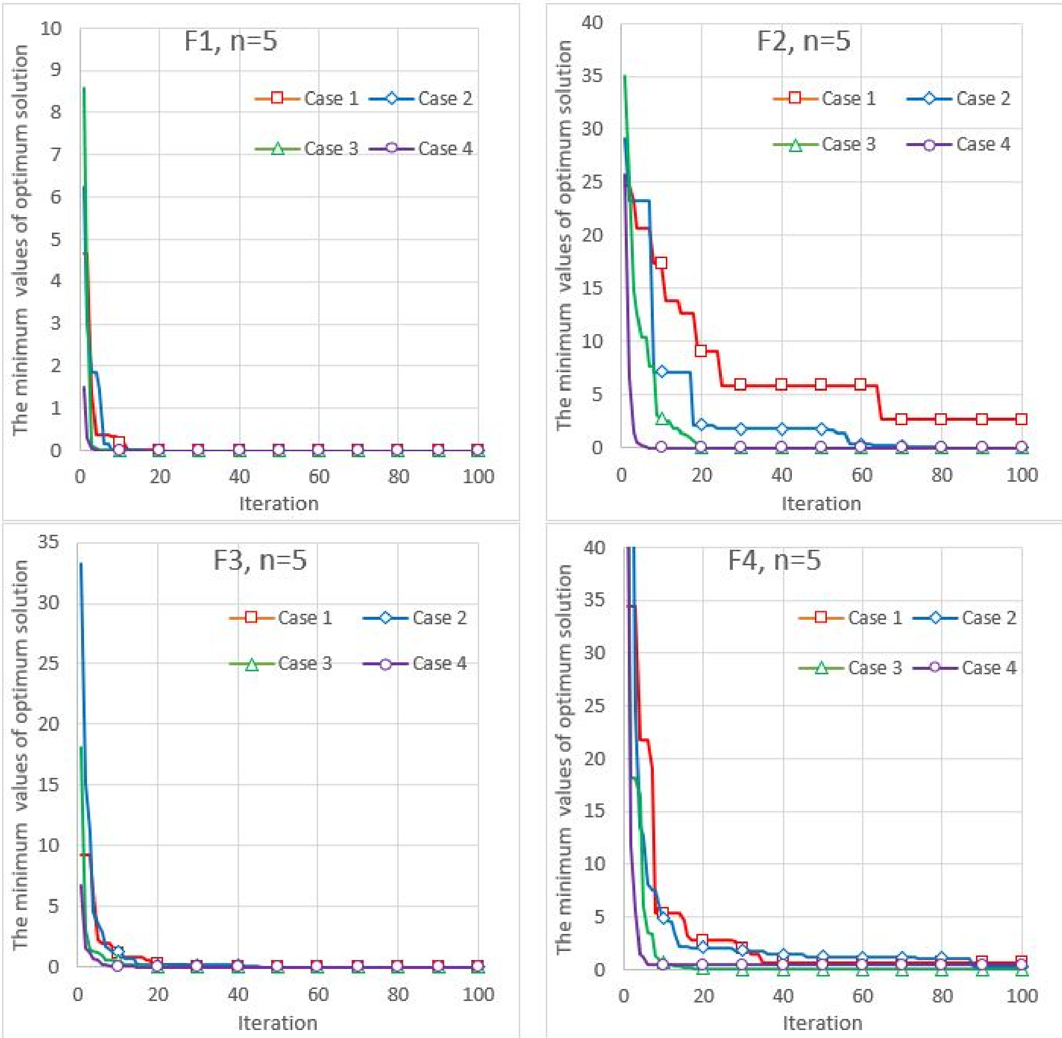

Figure 3: Convergence history of the best values of the optimum solutions (dimension=5).

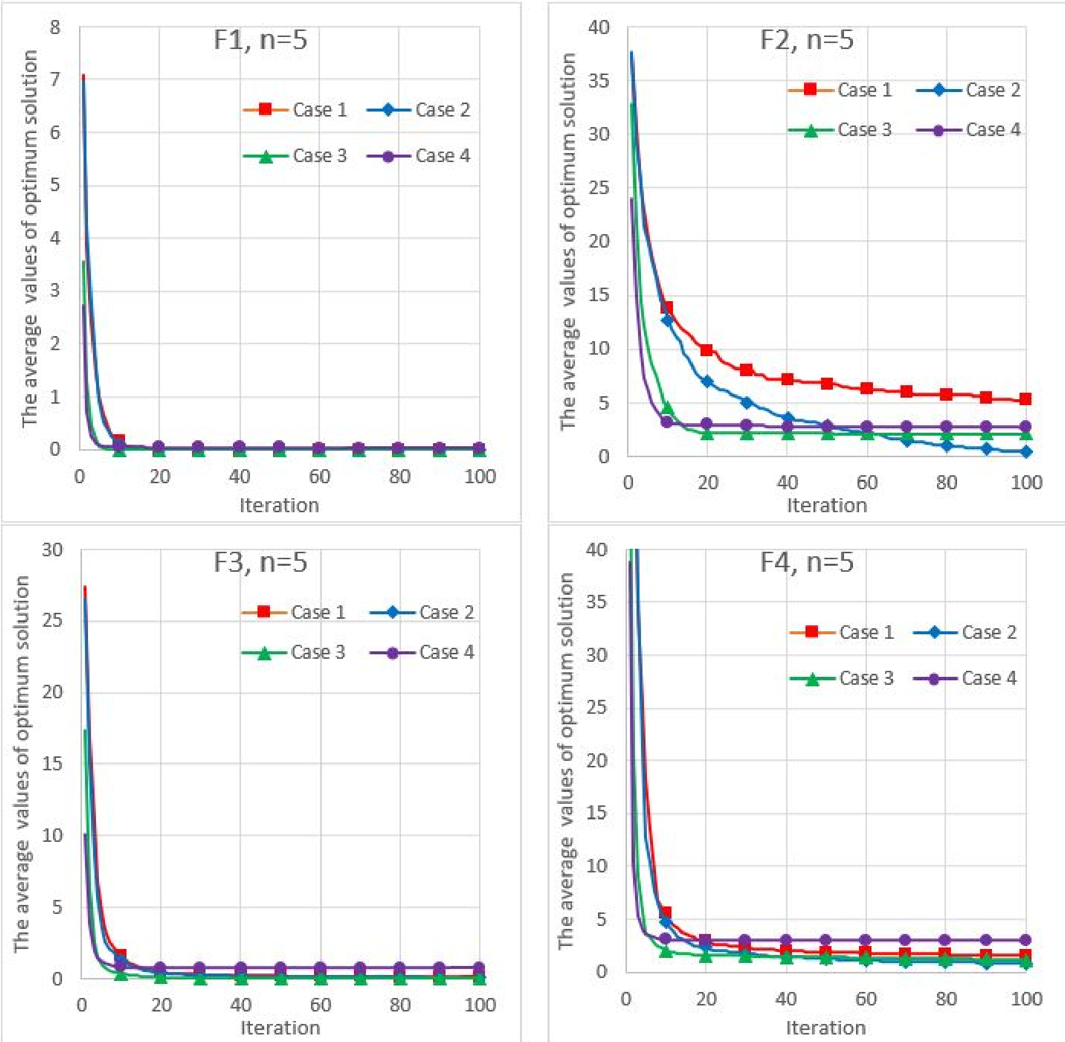

Figure 4: Convergence history of the average values of the optimum solutions (dimension=5).

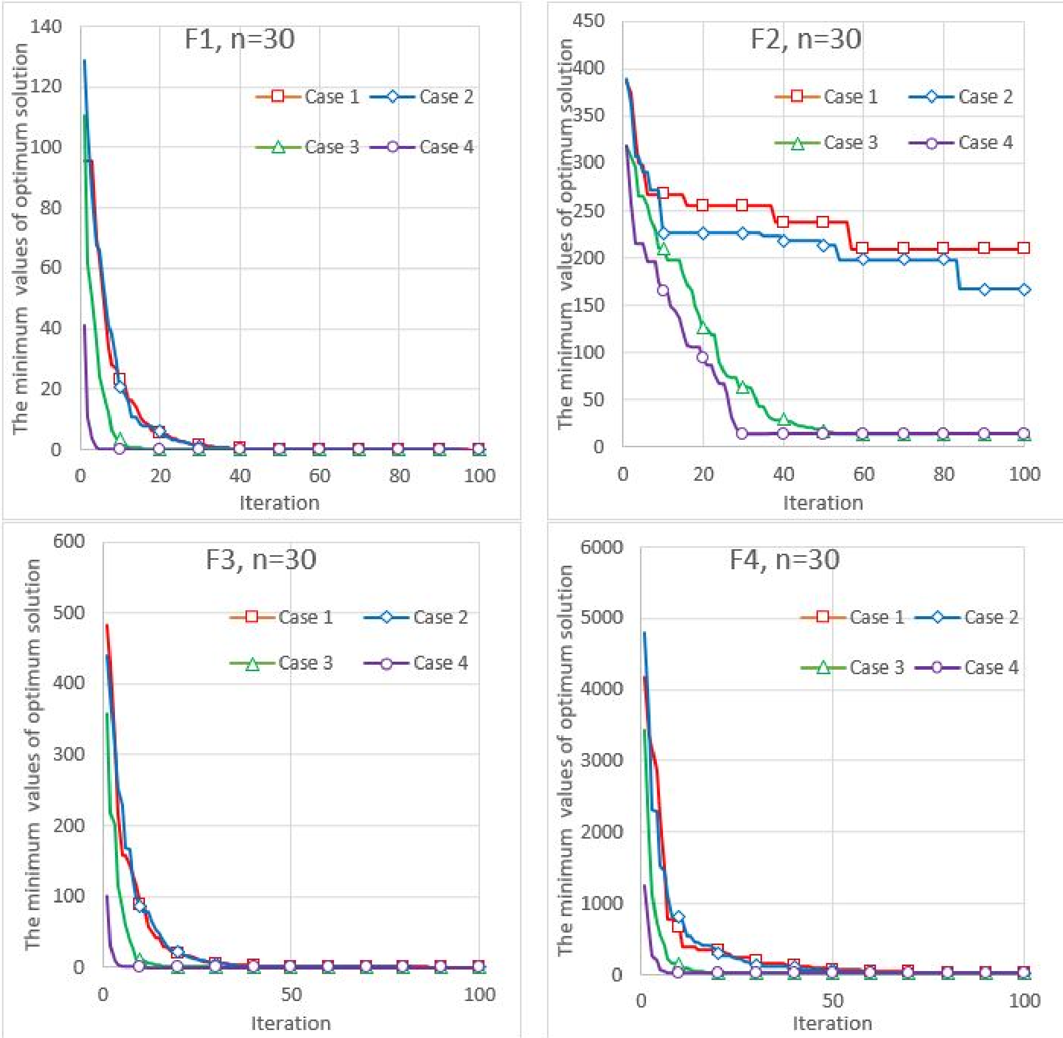

Figure 5: Convergence history of the best values of the optimum solutions (dimension=30).

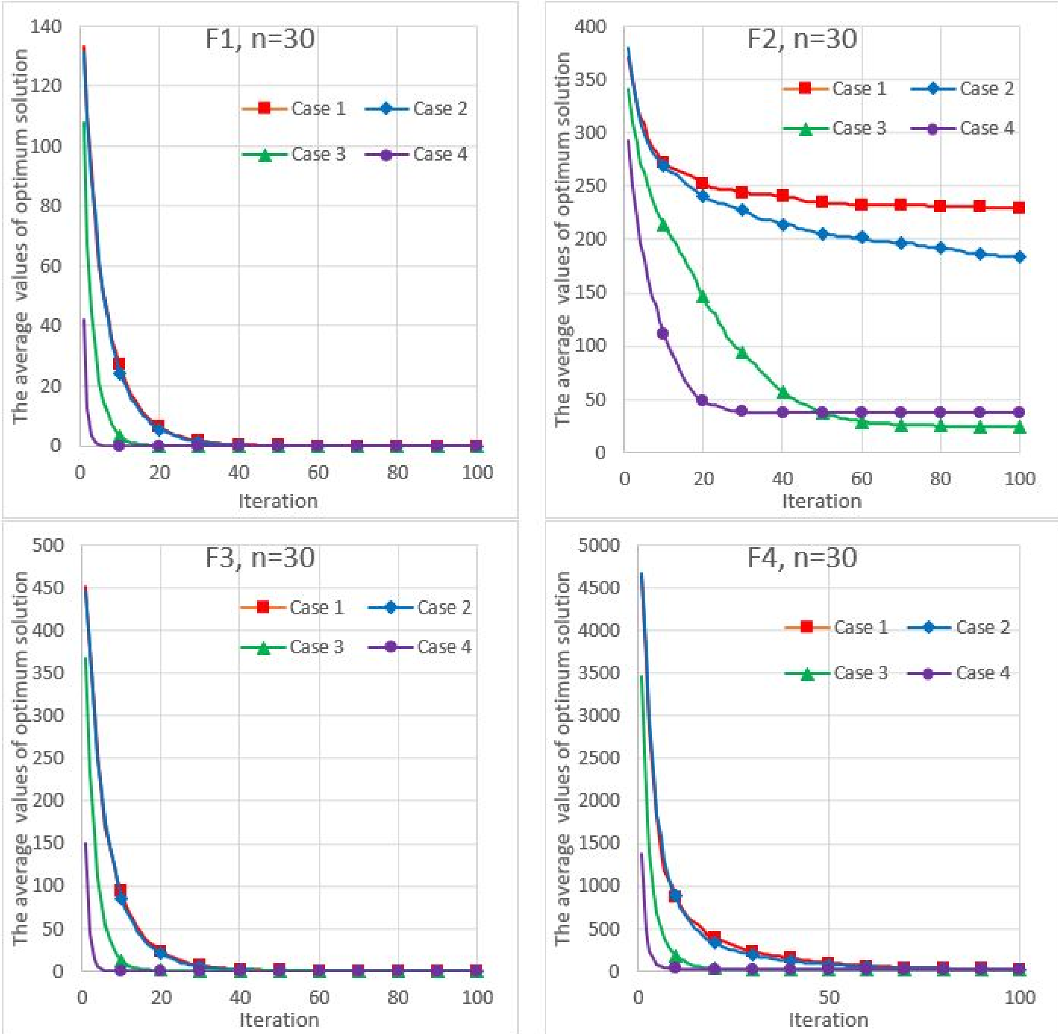

Figure 6: Convergence history of the average values of the optimum solutions (dimension=30).

5 Conclusions

In this study, the effect of the three different greedy selection strategies as well as no greedy selection onto TSA, which is a recent nature inspired population based optimization method, is investigated to improve its performance capability. The performance of the novel greedy selection strategy implemented versions of TSA is executed on multimodal numeric benchmark functions. Obtained results are compared within each other as well as the no greedy selection. It is shown on the test functions that the TSA algorithm with Best Greedy Selection Strategy 1 and 2 (Case 3 and Case 4) reach the optimum solutions more effectively than the other cases. Besides, the promising results are obtained and the convergence rate comparison shows that the greedy selection strategies are influenced the algorithm in a promising way for solving benchmark functions.

References

[1] M. P. Saka, S. Carbas, I. Aydogdu, and Alper Akin, Use of Swarm Intelligence in Structural Steel Design Optimization, Metaheuristics and Optimization in Civil Engineering, Modeling and Optimization in Science and Technologies Series, Springer, 2016.

[2] M. S. Kıran, TSA: Tree-seed algorithm for continuous optimization, Expert Syst. Appls., 42 (19) (2015) 6686-6698.

[3] M. S. Kıran, An Implementation of Tree-Seed Algorithm (TSA) for Constrained Optimization, 19th Asia Pacific Symp., Bangkok, Thailand, 2015,

[4] A. Babalik, A. C. Cinar, and M. S. Kıran, A Modification of Tree-Seed Algorithm using Deb's Rules for Constrained Optimization, Appl. Soft Comput., 63 (2018) 289-305.

[5] V. Muneeswaran and M. P. Rajasekaran, Beltrami-Regularized Denoising Filter Based on Tree Seed Optimization Algorithm: An Ultrasound Image Application. Int. Conf. Info. Commun. Tech. Intel. Syst., Springer, 2017.

[6] W. Chen, X. Tan, and M. Cai, Parameter Identification of Equivalent Circuit Models for Li-ion Batteries Based on Tree Seeds Algorithm. IOP Conf. Earth Environ. Sci., IOP Publishing, 2017.

[7] I. Aydogdu and T. Oguz, Optimization of High-Rise Buildings having Concrete Encased Steel Column using Tree Seed Algorithm, 4th Inter. Conf. Mech. Compos., Universidad Carlos III de Madrid, Spain, 2017.

[8] S. A. Vurtis, The classification of greedy algorithms, Sci. Comput. Prog., 49 (2003) 125-157.

[9] M. S. Kıran, Withering process for tree-seed algorithm. Proc. Comput. Sci., 111 (2017) 46-51.

[10] R. R. Howell, Algorithms: A Top-Down Approach, Kansas State University, 2009.

[11] I. Aydogdu, S. Carbas, and A. Akin, Effect of Levy Flight on the discrete optimum design of steel skeletal structures using metaheuristics, Steel Compos. Struct., 24(1) (2017) 93-112.

On the Principal Normal and Trinormal Spherical Images of W-Pseudo Null Curve in Pseudo-Hyperbolic Space $\mathbb{H}_0^3$

Yasin ÜNLÜTÜRK*
Kırklareli University,
Department of Mathematics, Kırklareli, Turkey,

Süha YILMAZ
Dokuz Eylül University,
Department of Primary Mathematics Education, Izmir, Turkey

Cumali EKİCİ
Eskişehir Osmangazi University,
Department of Mathematics-Computer, Eskişehir, Turkey

Abstract

In this study, we investigate the principal normal and trinormal spherical indicatrices of a W-pseudo null curve on pseudohyperbolic space H_0^3 in Minkowski space time. The principal normal indicatrix of a W-pseudo null curve is a spacelike curve lying on pseudo-hyperbolic space H_0^3, then the Frenet-Serret invariants of the mentioned indicatrix curve is obtained in terms of the invariants of W-pseudo null curve. The trinormal indicatrix is also a spacelike curve. Also, the Frenet-Serret invariants of the trinormal indicatrix curves are obtained as similar to the principal normal indicatrix. Finally, we give some characterizations of the spherical indicatrices to be helices.

Keywords: Classical differential geometry, spherical images, W-curves, W-pseudo null curves, general helix, ccr-curves.

1 Introduction

A tetrad of mutually orthogonal unit vectors (called tangent, normal, binormal and trinormal) was defined and constructed at each point of a differentiable curve. The rates of change of these vectors along the curve define the curvatures of the curve in the space $\mathbb{E}_1^4$. Spherical indicatrix (image) is a well-known concept in classical differential geometry of curves [6].

Einstein's theory opened a door to new geometries such as Minkowski space-time, which is simultaneously the geometry of special relativity and the geometry induced on each fixed tangent space of an arbitrary Lorentzian manifold At the beginning of the twentieth century.

In recent years, the theory of degenerate submanifolds are treated by the researchers and some of classical differential geometry topics are extented to Lorentz manifolds. Some of authors aimed to determine Frenet-Serret invariants in higher dimensions. There exists a vast literature on this subject, for instance [13, 14, 15, 16, 17]. In the light of the existing literature, in [14], the author extended spherical indicatrices of curves to four dimensional Lorentzian

*Corresponding author. *E-mail address:* yasinunluturk@klu.edu.tr

space and studied such curves in the case of base curve is a space-like curve according to signature $(+,+,+,-)$.

In this work, we study spherical indicatrices of a W-pseudo null curve lying on the pseudo-hyperbolic space $\mathbb{H}_0^3$ in Minkowski space-time. We investigate relations among Frenet-Serret invariants of spherical indicatrices and base curve. Additionally, some characterizations of spherical indicatrices being general helices are presented.

2 Preliminaries

Minkowski space-time $\mathbb{E}_1^4$ is the real vector space $\mathbb{R}^4$ provided with the standard flat metric given by

$$g = -dx_1^2 + dx_2^2 + dx_3^2 + dx_4^2,$$

where (x_1, x_2, x_3, x_4) is a rectangular coordinate system in $\mathbb{E}$ [8]. Since g is an indefinite metric, recall that a vector $v \in \mathbb{E}_1^4$ can have one of the three causal characters; it can be spacelike if $g(v,v) > 0$ or $v = 0$, timelike if $g(v,v) < 0$ and null (lightlike) if $g(v,v)$=0 and $v \neq 0$. Similary, an arbitrary curve $\alpha = \alpha(s)$ in $\mathbb{E}_1^4$ can be locally spacelike, timelike or null (lightlike), if all of its velocity vectors $\alpha'(s)$ are respectively spacelike, timelike or null. Also, recall the norm of a vector v is given by

$$\|v\| = \sqrt{|g(v,v)|}.$$

Therefore, v is a unit vector if $g(v,v) = \pm 1$. Next, vectors v, w in $\mathbb{E}_1^4$ are said to be orthogonal if $g(v,w) = 0$. The velocity of the curve $\alpha(s)$ is given by $\|\alpha'(s)\|$ [5]. Let a and b be two spacelike vectors in $\mathbb{E}_1^4$, then there is a unique real number $0 \leq \delta \leq \pi$, called the angle between a and b, such that $g(a,b) = \|a\| \,.\, \|b\| \cos\delta$ [10].

The pseudohyperbolic space with center $m = (m_1, m_2, m_3, m_4) \in \mathbb{E}_1^4$ and radius $r \in R^+$ in the space-time $\mathbb{E}_1^4$ is the hyperquadric

$$H_0^3(r) = \{a = (a_1, a_2, a_3, a_4) \in \mathbb{E}_1^4 \mid g(a-m, a-m) = -r^2\}.$$

with dimension 3 and index 0 [8].

Let $\vartheta = \vartheta(s)$ be a curve in $\mathbb{E}_1^4$. If the tangent vector field of this curve forms a constant angle with a constant vector field U, then this curve is called a general helix. Recall that, if a regular curve in $\mathbb{E}_1^4$ has constant Frenet-Serret curvatures ratios, (i.e., $\frac{\tau}{\kappa}$ and $\frac{\sigma}{\tau}$ are constants), then it is called a *ccr-curve* [7], [9]. Also if these curvatures are non-zero constants, curve is said to be W-curve (or helix) [11].

Denote by $\{T(s), N(s), B_1(s), B_2(s)\}$ the moving Frenet-Serret frame along the curve $\alpha(s)$ in the space $\mathbb{E}_1^4$. Then T, N, B_1, B_2 are, respectively, the tangent, the principal normal, the binormal (the first binormal) and the trinormal (the second binormal) vector fields. A spacelike or timelike curve $\alpha(s)$ is said to be parametrized by arclength function s, if $g(\alpha'(s), \alpha'(s)) = \pm 1$.

Let $\alpha(s)$ be a pseudo null curve in the space-time $\mathbb{E}_1^4$, parametrized by arclength function s. Then, the following Frenet-Serret equations are given in [13]:

$$\begin{bmatrix} T' \\ N' \\ B_1' \\ B_2' \end{bmatrix} = \begin{bmatrix} 0 & \kappa & 0 & 0 \\ 0 & 0 & \tau & 0 \\ 0 & \sigma & 0 & -\tau \\ -\kappa & 0 & -\sigma & 0 \end{bmatrix} \begin{bmatrix} T \\ N \\ B_1 \\ B_2 \end{bmatrix},$$

where T, N, B_1 and B_2 are mutually orthogonal vectors satisfying equations

$$g(T,T) = g(B_1,B_1) = 1, g(N,N) = g(B_2,B_2) = 0,$$
$$g(T,N) = g(T,B_1) = g(T,B_2) = g(N,B_1) = g(B_1,B_2) = 0,\ g(N,B_2) = 1.$$

and where, κ, τ and σ are first, second and third curvature of the curve α, respectively.

In the same space, in [1], the authors express a characterization of spacelike curves lying on H_0^3 by the following theorem:

Theorem 1 *Let $\alpha(s)$ be a unit speed spacelike curve in $\mathbb{E}_1^4$, with spacelike N, B_1 and curvatures $\kappa \neq 0, \tau \neq 0, \sigma \neq 0$ for each $s \in I \subset R$. Then, α lies on pseudohyperbolic space if and only if*

$$\begin{gathered}\frac{\sigma}{\tau}\frac{d\rho}{ds} = \frac{d}{ds}\left[\frac{1}{\sigma}\left(\rho\tau + \frac{d}{ds}(\frac{1}{\tau}\frac{d\rho}{ds})\right)\right], \\ \left\{\frac{1}{\sigma}\left[\rho\tau + \frac{d}{ds}(\frac{1}{\tau}\frac{d\rho}{ds})\right]\right\}^2 > \rho^2 + (\frac{1}{\tau}\frac{d\rho}{ds})^2,\end{gathered} \tag{1}$$

where $\rho = \dfrac{1}{\kappa}$.

In the same space, in [15] authors defined a vector product and gave a method to determine the Frenet-Serret invariants for an arbitrary curve by following definition and theorem:

Definition 2 *Let $a = (a_1, a_2, a_3, a_4)$, $b = (b_1, b_2, b_3, b_4)$ and $c = (c_1, c_2, c_3, c_4)$ be vectors in $\mathbb{E}_1^4$. The vector product in Minkowski space-time $\mathbb{E}_1^4$ is defined by the determinant*

$$a \wedge b \wedge c = -\begin{vmatrix} -e_1 & e_2 & e_3 & e_4 \\ a_1 & a_2 & a_3 & a_4 \\ b_1 & b_2 & b_3 & b_4 \\ c_1 & c_2 & c_3 & c_4 \end{vmatrix},$$

where e_1, e_2, e_3 and e_4 are mutually orthogonal vectors (coordinate direction vectors) satisfying equations

$$e_1 \wedge e_2 \wedge e_3 = e_4 \ , \ e_2 \wedge e_3 \wedge e_4 = e_1 \ , \ e_3 \wedge e_4 \wedge e_1 = e_2 \ , \ e_4 \wedge e_1 \wedge e_2 = -e_3.$$

Theorem 3 *Let $\alpha = \alpha(t)$ be an arbitrary spacelike curve in Minkowski space-time $\mathbb{E}_1^4$. The Frenet-Serret apparatus of α can be written as follows;*

$$\begin{gathered} T = \frac{\alpha'}{\|\alpha'\|}, \\ N = \frac{\|\alpha'\|^2 \alpha'' - g(\alpha', \alpha'')\alpha'}{\left\|\|\alpha'\|^2 \alpha'' - g(\alpha', \alpha'')\alpha'\right\|}, \\ B_1 = \mu N \wedge T \wedge B_2, \\ B_2 = \mu \frac{T \wedge N \wedge \alpha'''}{\|T \wedge N \wedge \alpha'''\|}, \end{gathered} \tag{2}$$

$$\kappa = \frac{\left\|\|\alpha'\|^2 \alpha'' - g(\alpha', \alpha'')\alpha'\right\|}{\|\alpha'\|^4}$$

$$\tau = \frac{\|T \wedge N \wedge \alpha'''\| \, \|\alpha'\|}{\left\|\|\alpha'\|^2 \alpha'' - g(\alpha', \alpha'')\alpha'\right\|}$$

and

$$\sigma = \frac{g(\alpha^{(IV)}, B_2)}{\|T \wedge N \wedge \alpha'''\| \, \|\alpha'\|}, \tag{3}$$

where μ is taken -1 or $+1$ to make $+1$ the determinant of $[T, N, B_1, B_2]$ matrix.

Here, we shall use timelike curve's Frenet-Serret invariants. Therefore, our calculations do not exist null vectors.

3 The principal normal spherical indicatrix of a W-pseudo null curve lying on $\mathbf{H}_0^3$

By the spirit of the paper [15], first we adapt the principal normal spherical indicatrix definition to W-pseudo null curves of Minkowski space-time. Moreover, we give the definition of trinormal spherical indicatrix for W-pseudo null curves at the beginning of the section 4.

Definition 4 *Let $\beta = \beta(s)$ be a unit speed W-pseudo null curve in Minkowski space-time. If we translate the principal normal vector to the center O of the pseudohyperbolic space H_0^3, we obtain a curve $\delta = \delta(s_\delta)$. This curve is called the principal normal spherical indicatrix or image of the curve β in $\mathbb{E}_1^4$.*

Theorem 5 *Let $\beta = \beta(s)$ be a unit speed W-pseudo null curve and $\delta = \delta(s_\delta)$ be its principal normal spherical indicatrix. Then;*

i) $\delta = \delta(s_\delta)$ is a space-like curve.

ii) The Frenet-Serret apparatus of δ, $\{T_\delta, N_\delta, B_{1\delta}, B_{2\delta}, \kappa_\delta, \tau_\delta, \sigma_\delta\}$ can be formed by the apparatus of β, $\{T, N, B_1, B_2, \kappa, \tau, \sigma\}$.

Proof. Let $\beta = \beta(s)$ be a unit speed W-pseudo-null curve and $\delta = \delta(s_\delta)$ be its principal normal spherical indicatrix. It can be written as

$$\delta = N(s). \tag{4}$$

Differentiating (3.1) with respect to s, we find

$$\delta' = \dot{\delta}\frac{ds_\delta}{ds} = \tau B_1.$$

Here we shall denote differentiation according to s by a dash, and differentiation according to s_δ by a dot. Thus we obtain the unit tangent vector of the principal normal spherical indicatrix curve δ as

$$T_\delta = B_1 \tag{5}$$

and

$$\|\delta'\| = \frac{ds_\delta}{ds} = \tau^2.$$

The causal character of the the principal normal spherical indicatrix curve $\delta(s_\delta)$ is determined by the following inner product:

$$g(\delta', \delta') = \tau^2 > 0. \tag{6}$$

By (3.3), we will take the spherical indicatrix curve as spacelike one.

Considering the previous method and using the property of the curve to be W-curve, we form the following differentiations with respect to s:

$$\begin{cases} \delta'' = \tau\sigma N - \tau^2 B_2, \\ \delta''' = \kappa\tau^2 T + 2\tau^2\sigma B_1, \\ \delta^{(IV)} = \tau^2(\kappa^2 + 2\sigma^2)N - 2\tau^3\sigma B_2. \end{cases}$$

By equation (2.2) we arrive

$$\|\delta'\|^2 \delta'' - g(\delta', \delta'')\delta' = \tau^3\sigma N - \tau^4 B_2.$$

Then we can get the principal normal vector as

$$N_\delta = \frac{\sigma}{\sqrt{|\tau\sigma|}}N - \frac{\tau}{\sqrt{|\tau\sigma|}}B_2 \tag{7}$$

and the first curvature as

$$\kappa_\delta = \frac{\sqrt{|\tau\sigma|}}{\tau}. \tag{8}$$

Now let us calculate the vector $T_\delta \wedge N_\delta \wedge \delta'''$, that is,

$$T_\delta \wedge N_\delta \wedge \delta''' = -\begin{vmatrix} -T & N & B_1 & B_2 \\ 0 & 0 & 1 & 0 \\ 0 & \frac{\sigma}{\sqrt{|\tau\sigma|}} & 0 & -\frac{\tau}{\sqrt{|\tau\sigma|}} \\ \kappa\tau^2 & 0 & 2\tau^2\sigma & 0 \end{vmatrix}.$$

This product yields

$$T_\delta \wedge N_\delta \wedge \delta''' = -\frac{\kappa\tau^3}{\sqrt{|\tau\sigma|}}N - \frac{\kappa\tau^2\sigma}{\sqrt{|\tau\sigma|}}B_2. \tag{9}$$

Hence, we obtain the trinormal (second binormal) vector field of the curve $\delta(s_\delta)$ as follows:

$$B_{2\delta} = \mu\{-\tau N - \sigma B_2\}. \tag{10}$$

Taking the norm of both sides of (3.6), we find the second curvature

$$\tau_\delta = \frac{\kappa}{\tau\sigma}. \tag{11}$$

Finding the binormal vector field, we express

$$N_\delta \wedge T_\delta \wedge B_{2\delta} = -\begin{vmatrix} -T & N & B_1 & B_2 \\ 0 & \frac{\sigma}{\sqrt{|\tau\sigma|}} & 0 & -\frac{\tau}{\sqrt{|\tau\sigma|}} \\ 0 & 0 & 1 & 0 \\ 0 & -\mu\tau & 0 & -\mu\sigma \end{vmatrix}. \tag{12}$$

Calculating (3.9), we have

$$N_\delta \wedge T_\delta \wedge B_{2\delta} = -\mu\{\frac{\sigma^2+\tau^2}{\sqrt{|\tau\sigma|}}\}T.$$

So we obtain the binormal vector as

$$B_{1\delta} = -\frac{\sigma^2+\tau^2}{\sqrt{|\tau\sigma|}}T. \tag{13}$$

Finally, using (2.3) and the obtained equations, we arrive the third curvature as

$$\sigma_\delta = \frac{\kappa^2+2\sigma^2}{\kappa}\sqrt{\left|\frac{\sigma}{\tau}\right|}. \tag{14}$$

■

Corollary 6 *$\{T_\delta, N_\delta, B_{1\delta}, B_{2\delta}\}$ is an orthonormal frame of Minkowski space-time.*

Proof. It can be straightforwardly seen by using the equations (3.2), (3.4), (3.7) and (3.10).
■

Considering above theorem, we also give:

Corollary 7 *Let $\beta = \beta(s)$ be a W-pseudo null unit speed curve and $\delta(s_\delta)$ be its principal normal spherical indicatrix. Then, δ is also a helix.*

Proof. Let $\beta = \beta(s)$ be a W-pseudo null unit speed curve. Then we know that the curvature functions are constants. Therefore, we straightforwardly see that the curvature functions of principal normal spherical indicatrix $\delta(s_\delta)$ are constants by means of the equations (3.5), (3.8) and (3.11). Hence the curve $\delta(s_\delta)$ becomes W-curve which is the special case of helix. ■

Theorem 8 *Let $\beta = \beta(s)$ be a W-pseudo null unit speed curve and $\delta(s_\delta)$ be its principal normal spherical indicatrix. Then, δ is a general helix and also its fixed direction U is composed as*

$$\begin{aligned} U = {} & (c_2\sqrt{\frac{\tau}{\sigma}}\sin(\kappa\sqrt{\frac{\tau}{\sigma}}s) - c_3\sqrt{\frac{\tau}{\sigma}}\cos(\kappa\sqrt{\frac{\tau}{\sigma}}s) + c_4)T \\ & +(c_2\cos(\kappa\sqrt{\frac{\tau}{\sigma}}s) + c_3\sin(\kappa\sqrt{\frac{\tau}{\sigma}}s))N + c_1B_1 \\ & +(c_2\frac{\tau}{\sigma}\cos(\kappa\sqrt{\frac{\tau}{\sigma}}s) + c_3\frac{\tau}{\sigma}\sin(\kappa\sqrt{\frac{\tau}{\sigma}}s))B_2, \end{aligned}$$

where c_1 is a non-zero constant and c_2, c_3, c_4 are constants.

Proof. Let $\beta = \beta(s)$ be a W-pseudo null unit speed curve and $\delta = \delta(s_\delta)$ be its space-like principal normal spherical image. If $\delta = \delta(s_\delta)$ is a general helix, then, for a constant space-like vector U, we may express

$$g(T_\delta, U) = \cos\theta, \tag{15}$$

where θ is a constant angle. The equation (3.12) is also congruent to

$$g(B_1, U) = \cos\theta.$$

One can form constant vector U according to $\{T, N, B_1, B_2\}$ as the following

$$U = \varepsilon_1 T + \varepsilon_2 N + \varepsilon_3 B_1 + \varepsilon_4 B_2. \tag{16}$$

Differentiating (3.13) with respect to s, we have the following system of ordinary differential equations

$$\begin{cases} \varepsilon_1' - \varepsilon_4\kappa = 0 \\ \varepsilon_1\kappa + \varepsilon_2' + \varepsilon_3\sigma = 0 \\ \varepsilon_2\tau - \varepsilon_4\sigma = 0 \\ \varepsilon_4' - \varepsilon_3\tau = 0. \end{cases} \tag{17}$$

We know that $\varepsilon_3 = c_1 \neq 0$ is a constant. Also since the curve $\beta = \beta(s)$ is a W-curve, its curvature funcions are constants. Then the solution of the system (3.14) can be obtained as:

$$\begin{aligned} \varepsilon_1 &= c_2\sqrt{\frac{\tau}{\sigma}}\sin(\kappa\sqrt{\frac{\tau}{\sigma}}s) - c_3\sqrt{\frac{\tau}{\sigma}}\cos(\kappa\sqrt{\frac{\tau}{\sigma}}s) + c_4, \\ \varepsilon_2 &= c_2\cos(\kappa\sqrt{\frac{\tau}{\sigma}}s) + c_3\sin(\kappa\sqrt{\frac{\tau}{\sigma}}s), \\ \varepsilon_3 &= c_1, \\ \varepsilon_4 &= c_2\frac{\tau}{\sigma}\cos(\kappa\sqrt{\frac{\tau}{\sigma}}s) + c_3\frac{\tau}{\sigma}\sin(\kappa\sqrt{\frac{\tau}{\sigma}}s), \end{aligned}$$

where c_1 is a non-zero constant and c_2, c_3, c_4 are constants. ■

4 The trinormal spherical indicatrix of a W-pseudo null curve lying on $\mathbf{H}_0^3$

By the spirit of the paper [15], first we adapt the principal normal spherical indicatrix definition to W-pseudo null curves of Minkowski space-time. Moreover, we give the definition of trinormal spherical indicatrix for W-pseudo null curves at the beginning of the section 4.

Definition 9 *Let $\beta = \beta(s)$ be an W-pseudo null unit speed curve in Minkowski space-time. If we translate the trinormal vector to the center O of the pseudohyperbolic space H_0^3, we obtain a curve $\varphi = \varphi(s_\varphi)$. This curve $\varphi = \varphi(s_\varphi)$ is called the trinormal spherical indicatrix or image of the curve β in $\mathbb{E}_1^4$.*

Theorem 10 *Let $\beta = \beta(s)$ be an W-pseudo null unit speed curve and $\varphi = \varphi(s_\varphi)$ be its trinormal spherical indicatrix. Then;*

i) $\varphi = \varphi(s_\varphi)$ is a space-like curve.

ii) The Frenet-Serret apparatus of φ, $\{T_\varphi, N_\varphi, B_{1\varphi}, B_{2\varphi}, \kappa_\varphi, \tau_\varphi, \sigma_\varphi\}$ can be formed by the apparatus of β, $\{T, N, B_1, B_2, \kappa, \tau, \sigma\}$.

Proof. Let $\beta = \beta(s)$ be an W-pseudo-null unit speed curve and $\varphi = \varphi(s_\varphi)$ be its trinormal spherical indicatrix. It can be written as

$$\varphi = B_2. \tag{18}$$

Differentiating (4.1) with respect to s, we find

$$\varphi' = \dot{\varphi}\frac{ds_\varphi}{ds} = -\kappa T - \sigma B_1.$$

Here we shall denote differentiation according to s by a dash, and differentiation according to s_φ by a dot. Thus we obtain the unit tangent vector of the trinormal spherical indicatrix curve φ as

$$T_\varphi = -\frac{\kappa}{\sqrt{\kappa^2+\sigma^2}}T - \frac{\sigma}{\sqrt{\kappa^2+\sigma^2}}B_1 \tag{19}$$

and

$$\|\varphi'\| = \frac{ds_\varphi}{ds} = \sqrt{\kappa^2+\sigma^2}.$$

The causal character of the the trinormal spherical indicatrix curve $\varphi(s_\varphi)$ is determined by the following inner product:

$$g(\varphi', \varphi') = \kappa^2 + \sigma^2 > 0. \tag{20}$$

By (4.3), we will take the spherical indicatrix curve as spacelike one.

Considering the previous method and using the property of the curve to be W-curve, we form the following differentiations with respect to s:

$$\begin{cases} \varphi'' = -(\kappa^2+\sigma^2)N + \tau\sigma B_2, \\ \varphi''' = -\kappa\tau\sigma T - (\kappa^2+2\sigma^2)\tau B_1, \\ \varphi^{(IV)} = -2\tau\sigma(\kappa^2+\sigma^2)N + \tau^2(\kappa^2+2\sigma^2)B_2. \end{cases}$$

By equation (2.2) we arrive

$$\|\varphi'\|^2 \varphi'' - g(\varphi', \varphi'')\varphi' = -(\kappa^2+\sigma^2)^2 N + \tau\sigma(\kappa^2+\sigma^2)B_2.$$

Then we can get the principal normal vector as

$$N_\varphi = -\frac{\kappa^2+\sigma^2}{\sqrt{|\tau\sigma(\kappa^2+\sigma^2)|}}N + \frac{\tau\sigma}{\sqrt{|\tau\sigma(\kappa^2+\sigma^2)|}}B_2 \tag{21}$$

and the first curvature as

$$\kappa_\varphi = \frac{\sqrt{|\tau\sigma(\kappa^2+\sigma^2)|}}{\kappa^2+\sigma^2}. \tag{22}$$

Now let us calculate the vector $T_\varphi \wedge N_\varphi \wedge \varphi'''$, that is,

$$T_\varphi \wedge N_\varphi \wedge \varphi''' = -\begin{vmatrix} -T & N & B_1 & B_2 \\ -\frac{\kappa}{\sqrt{\kappa^2+\sigma^2}} & 0 & -\frac{\sigma}{\sqrt{\kappa^2+\sigma^2}} & 0 \\ 0 & -\frac{\kappa^2+\sigma^2}{\sqrt{|\tau\sigma(\kappa^2+\sigma^2)|}} & 0 & \frac{\tau\sigma}{\sqrt{|\tau\sigma(\kappa^2+\sigma^2)|}} \\ -\kappa\tau\sigma & 0 & -(\kappa^2+2\sigma^2)\tau & 0 \end{vmatrix}.$$

This product yields

$$T_\varphi \wedge N_\varphi \wedge \varphi''' = \frac{\kappa\tau^2\sigma}{\sqrt{|\tau\sigma|}}N + \frac{\kappa\tau(\kappa^2+\sigma^2)}{\sqrt{|\tau\sigma|}}B_2. \tag{23}$$

Hence, we obtain the trinormal (second binormal) vector field of the curve $\varphi(s_\varphi)$ as follows:

$$B_{2\varphi} = \mu\{\frac{\tau\sigma}{\sqrt{\kappa^2+\sigma^2}}N + \frac{\kappa^2+\sigma^2}{\sqrt{\kappa^2+\sigma^2}}B_2\}. \tag{24}$$

Taking the norm of both sides of (4.6), we find the second curvature

$$\tau_\varphi = \frac{\kappa}{\sigma\sqrt{\kappa^2+\sigma^2}}. \tag{25}$$

Finding the binormal vector field, we express

$$N_\varphi \wedge T_\varphi \wedge B_{2\varphi} = -\begin{vmatrix} -T & N & B_1 & B_2 \\ 0 & -\frac{\kappa^2+\sigma^2}{\sqrt{|\tau\sigma(\kappa^2+\sigma^2)|}} & 0 & \frac{\tau\sigma}{\sqrt{|\tau\sigma(\kappa^2+\sigma^2)|}} \\ -\frac{\kappa}{\sqrt{\kappa^2+\sigma^2}} & 0 & -\frac{\sigma}{\sqrt{\kappa^2+\sigma^2}} & 0 \\ 0 & \mu\frac{\tau\sigma}{\sqrt{\kappa^2+\sigma^2}} & 0 & \mu\frac{\kappa^2+\sigma^2}{\sqrt{\kappa^2+\sigma^2}} \end{vmatrix}. \tag{26}$$

Calculating (4.9), we have

$$N_\varphi \wedge T_\varphi \wedge B_{2\varphi} = \frac{\mu(\kappa^2+\sigma^2)+\mu\tau^2\sigma^2}{(\kappa^2+\sigma^2)\sqrt{|\tau\sigma|}}\{\frac{\sigma}{\sqrt{\kappa^2+\sigma^2}}T + \frac{\kappa}{\sqrt{\kappa^2+\sigma^2}}B_1\}.$$

So we obtain the binormal vector as

$$B_{1\varphi} = \frac{\kappa^2+\sigma^2+\tau^2\sigma^2}{(\kappa^2+\sigma^2)\sqrt{|\tau\sigma|}}\{\frac{\sigma}{\sqrt{\kappa^2+\sigma^2}}T + \frac{\kappa}{\sqrt{\kappa^2+\sigma^2}}B_1\}. \tag{27}$$

Finally, using (2.3) and the obtained equations, we arrive the third curvature as

$$\sigma_\varphi = \frac{-2\sigma\sqrt{|\tau\sigma|}}{\kappa}. \tag{28}$$

■

Corollary 11 $\{T_\varphi, N_\varphi, B_{1\varphi}, B_{2\varphi}\}$ *is an orthonormal frame of Minkowski space-time.*

Proof. It can be straightforwardly seen by using the equations (4.2), (4.4), (4.7) and (4.10). ■

Considering above theorem, we also give:

Corollary 12 *Let $\beta = \beta(s)$ be a W-pseudo null unit speed curve and $\varphi(s_\varphi)$ be its trinormal spherical indicatrix. Then, φ is also a helix.*

Proof. Let $\beta = \beta(s)$ be a W-pseudo null unit speed curve. Then we know that the curvature functions are constants. Therefore, we straightforwardly see that the curvature functions of principal normal spherical indicatrix $\varphi(s_\varphi)$ are constants by means of the equations (4.5), (4.8) and (4.11). Hence the curve $\varphi(s_\varphi)$ becomes W-curve which is the special case of helix. ■

Theorem 13 *Let $\beta = \beta(s)$ be a W-pseudo null unit speed curve and $\varphi(s_\varphi)$ be its trinormal spherical indicatrix. Then, φ is a general helix and also its fixed direction U is composed as*

$$\begin{aligned}U = {} & (c_3\frac{\kappa}{\sigma}e^{\sqrt{\tau\sigma}s} - c_4\frac{\kappa}{\sigma}e^{-\sqrt{\tau\sigma}s} - \frac{c_1\kappa}{2\sigma}s + c_5\kappa s + c_6)T \\ & +(-c_1 s + c_2)N + (c_3 e^{\sqrt{\tau\sigma}s} + c_4 e^{-\sqrt{\tau\sigma}s} - \frac{c_1}{\sigma})B_1 \\ & +(c_3\sqrt{\frac{\tau}{\sigma}}e^{\sqrt{\tau\sigma}s} - c_4\sqrt{\frac{\tau}{\sigma}}e^{-\sqrt{\tau\sigma}s} - \frac{c_1}{\sigma}s + c_5)B_2,\end{aligned}$$

where c_1 is a non-zero constant and c_2, c_3, c_4, c_5, c_6 are constants.

Proof. Let $\beta = \beta(s)$ be a W-pseudo null unit speed curve and $\varphi = \varphi(s_\varphi)$ be its space-like trinormal spherical image. If $\varphi = \varphi(s_\varphi)$ is a general helix, then, for a constant space-like vector U, we may express

$$g(T_\varphi, U) = \cos\theta, \tag{29}$$

where θ is a constant angle. The equation (4.12) is also congruent to

$$g(-\frac{\kappa}{\sqrt{\kappa^2+\sigma^2}}T - \frac{\sigma}{\sqrt{\kappa^2+\sigma^2}}B_1, U) = \cos\theta.$$

One can form constant vector U according to $\{T, N, B_1, B_2\}$ as the following

$$U = \varepsilon_1 T + \varepsilon_2 N + \varepsilon_3 B_1 + \varepsilon_4 B_2. \tag{30}$$

Differentiating (4.13) with respect to s, we have the following system of ordinary differential equations

$$\begin{cases} \varepsilon_1' - \varepsilon_4\kappa = 0 \\ \varepsilon_1\kappa + \varepsilon_2' + \varepsilon_3\sigma = 0 \\ \varepsilon_2\tau - \varepsilon_4\sigma + \varepsilon_3' = 0 \\ \varepsilon_4' - \varepsilon_3\tau = 0. \end{cases} \tag{31}$$

We know that $\varepsilon_1\kappa + \varepsilon_3\sigma = c_1 \neq 0$ is a constant. Also since the curve $\beta = \beta(s)$ is a W-curve, its curvature functions are constants. Then the solution of the system (4.14) can be found as:

$$\begin{aligned}\varepsilon_1 &= c_3\frac{\kappa}{\sigma}e^{\sqrt{\tau\sigma}s} - c_4\frac{\kappa}{\sigma}e^{-\sqrt{\tau\sigma}s} - \frac{c_1\kappa}{2\sigma}s + c_5\kappa s + c_6, \\ \varepsilon_2 &= -c_1 s + c_2, \\ \varepsilon_3 &= c_3 e^{\sqrt{\tau\sigma}s} + c_4 e^{-\sqrt{\tau\sigma}s} - \frac{c_1}{\sigma}, \\ \varepsilon_4 &= c_3\sqrt{\frac{\tau}{\sigma}}e^{\sqrt{\tau\sigma}s} - c_4\sqrt{\frac{\tau}{\sigma}}e^{-\sqrt{\tau\sigma}s} - \frac{c_1}{\sigma}s + c_5,\end{aligned}$$

where c_1 is a non-zero constant and c_2, c_3, c_4, c_5, c_6 are constants. ■

5 Conclusion

In this work, we extend spherical indicatrix concept to the W-pseudo null curves of Minkowski space-time. We investigate principal normal and trinormal spherical indicatrices of a W-pseudo null curve and observe that both of these spherical curves are space-like curves. Thereafter, we determine relations among Frenet-Serret invariants of spherical indicatrices and base curve. Finally, we give some characterizations of the spherical indicatrices to be helices. As a further research, one can study the spherical indicatrices of pseudo null curves without putting any condition for the base curve.

References

[1] Camcı, Ç., İlarslan, K. and Sucurovic, E. On pseudohyperbolical curves in Minkowski space-time, *Turk J. Math.*, 2003, **27**, 315-328.

[2] İlarslan, K., Boyacıoğlu, Ö., Position vectors of a spacelike W-curve in Minkowski 3-space $\mathbb{E}_1^3$, *Bull. Korean Math. Soc.*, 2007,**44**(3), 429–438.

[3] Ilarslan, K. and Nesovic, E. Some charactherizations of null, pseudo null and partially null rectifying curves in Minkowski space-time. Taiwan. J. Math., 2008, **12**(5), 1035–1044.

[4] İyigün, E., The tangent spherical image and ccr-curve of a time-like curve in $\mathbb{L}^3$, J Inequal Appl (2013) 2013: 55.

[5] Lopez, R., Differential geometry of curves and surfaces in Lorentz-Minkowski space, Int. Elec. Journ. Geom. 2010, **3**(2), 67-101.

[6] Milman, R.S. and Parker, G.D. *Elements of Differential Geometry*, Prentice-Hall Inc., Englewood Cliffs, New Jersey, 1977.

[7] Monterde, J. Curves with constant curvature ratios, *Bol. Soc. Mat. Mexicana*, 2007, **3**, 177-186.

[8] O 'Neill, B., Semi-Riemannian geometry with applications to relativity, Academic press Inc, London, 1983.

[9] Öztürk, G., Arslan, K. and Hacısalihoglu, H.H. A Characterization of ccr-curves in $\mathbb{R}^m$, *Proc. Estonian Acad. Sci.*, 2008, **57**, 217-224.

[10] Ratcliffe, J.G., Foundations of Hyperbolic Manifolds, Springer Science+Business Media, LLC, New York, USA, pp. 68-72, 2006.

[11] M. Petrovic-Torgasev, E. Sucurovic, W-curves in Minkowski space-time, Novi Sad J. Math. 2002, **32**(2), 55-65.

[12] M. Petrovic–Torgasev, K. Ilarslan And E. Nesovic, On partially null and pseudo null curves in the semi-euclidean space , J. Geom., 2005, **84**, 106-116.

[13] Walrave, J. Curves and Surfaces in Minkowski Space, Dissertation, K. U. Leuven, Fac. of Science, Leuven, 1995.

[14] Yılmaz, S. Spherical Indicators of Curves and Characterizations of Some Special Curves in four dimensional Lorentzian Space $\mathbf{L}^4$, Dissertation, Dokuz Eylül University, 2001.

[15] Yilmaz, S. and Turgut, M. On the Differential Geometry of the Curves in Minkowski Space-time I, *Int. J. Contemp. Math. Sci.*, 2008, **3**, 1343-1349.

[16] Yılmaz, S., Özyılmaz, E. and Turgut, M. On the Differential Geometry of the Curves in Minkowski Space-time II, *Int. J. Comput. Math. Sci.*, 2009, **3**, 53-55.

[17] S.Yılmaz, E. Özyılmaz, Y. Yaylı, M. Turgut, Tangent and trinormal spherical images of a time-like curve on the pseudohyperbolic space , Proc. Est. Acad. Sci. 2010, **59**(3), 216-224.

On Generalizations of Hermite-Hadamard Type Inequalities for Products of Different Kinds of Convex Functions via Katugampola Fractional Integrals

Barış ÇELİK*
Ordu University,
Department of Mathematics, Ordu, Turkey

Erhan SET
Ordu University,
Department of Mathematics, Ordu, Turkey

Ahmet Ocak AKDEMİR
Ağrı İbrahim Çeçen University,
Department of Mathematics, Ağrı, Turkey

Abstract

In the present paper, some new generalizations of Hermite-Hadamard type inequalities for products of two different type convex functions via Katugampola fractional integral by using a fairly elementary analysis are obtained.

Keywords: Gamma function, beta function, convex functions, s-convex function, Hermite-Hadamard inequality, Katugampola fractional integral.

1 Introduction and Preliminaries

Definition 1 *A function $f : I \subseteq \mathbb{R} \to \mathbb{R}$ is said to be convex if the inequality*

$$f(tx + (1-t)y) \leq tf(x) + (1-t)f(y)$$

holds for all $x, y \in I$ and $t \in [0, 1]$.

The following inequality is well known in the literature as the Hermite-Hadamard integral inequality:

$$f\left(\frac{a+b}{2}\right) \leq \frac{1}{b-a}\int_a^b f(x)dx \leq \frac{f(a)+f(b)}{2}$$

where $f : I \subset \mathbb{R} \to \mathbb{R}$ is a convex function on the interval I of real numbers and $a, b \in I$ with $a < b$. Here and in the following, let $\mathbb{C}$, $\mathbb{R}$, $\mathbb{R}^+$ and $\mathbb{Z}_0^-$ be the sets of complex numbers, real numbers, positive real numbers and non-positive integers, respectively, and let $\mathbb{R}_0^+ := \mathbb{R}^+ \cup \{0\}$.

The concept of s-convex function was introduced in Breckner's paper [1] and a number of properties and connections with s-convexity in the first sense are discussed in the paper [4].

*Corresponding author. *E-mail address:* bariscelik15@hotmail.com

Definition 2 *A function $f:[0,\infty)\to\mathbb{R}$ is said to be s-convex in the second sense if*

$$f(tx+(1-t)y)\le t^s f(x)+(1-t)^s f(y)$$

for all $x,y\in[0,\infty)$, $t\in[0,1]$ and for some fixed $s\in(0,1]$.

In [3], Dragomir and Fitzpatrick proved a variant of Hermite-Hadamard inequality which holds for the s-convex functions.

Theorem 3 *Suppose that $f:[0,\infty)\to[0,\infty)$ is an s-convex function in the second sense, where $s\in(0,1)$, and let $a,b\in[0,\infty)$, $a<b$. If $f'\in L[a,b]$, then the following inequalities hold:*

$$2^{s-1}f\left(\frac{a+b}{2}\right)\le\frac{1}{b-a}\int_a^b f(x)dx\le\frac{f(a)+f(b)}{s+1}. \tag{1}$$

The constant $k=\frac{1}{s+1}$ is the best possible in the second inequality in (1).

Let $f\in L[a,b]$. The Riemann-Liouville integrals $J_{a+}^{\alpha}f$ and $J_{b-}^{\alpha}f$ of order $\alpha\in\mathbb{R}^+$ with $a\in\mathbb{R}_0^+$ are defined, respectively, by

$$J_{a+}^{\alpha}f(x)=\frac{1}{\Gamma(\alpha)}\int_a^x(x-t)^{\alpha-1}\,f(t)\,dt\quad(x>a)$$

and

$$J_{b-}^{\alpha}f(x)=\frac{1}{\Gamma(\alpha)}\int_x^b(t-x)^{\alpha-1}\,f(t)\,dt\quad(x<b)$$

where Γ is the familiar Gamma function (see, e.g., [8, Section 1.1]). It is noted that $J_{a+}^{1}f(x)$ and $J_{b-}^{1}f(x)$ become the usual Riemann integrals.

In the case of $\alpha=1$, the fractional integral reduces to classical integral.

The beta function $B(\alpha,\beta)$ is defined by (see, e.g., [8, Section 1.1][6, p18])

$$B(\alpha,\,\beta)=\begin{cases}\displaystyle\int_0^1 t^{\alpha-1}(1-t)^{\beta-1}\,dt & (\Re(\alpha)>0;\ \Re(\beta)>0)\\ \dfrac{\Gamma(\alpha)\,\Gamma(\beta)}{\Gamma(\alpha+\beta)} & \left(\alpha,\,\beta\in\mathbb{C}\setminus\mathbb{Z}_0^-\right).\end{cases} \tag{2}$$

Sarıkaya et al. [7] proved the following interesting inequalities of Hermite-Hadamard type involving Riemann-Liouville fractional integrals.

Theorem 4 *Let $f:[a,b]\to\mathbb{R}$, be positive function with $0\le a<b$ and $f\in L[a,b]$. If f is a convex function on $[a,b]$, then the following inequalities for fractional integrals hold:*

$$f\left(\frac{a+b}{2}\right)\le\frac{\Gamma(\alpha+1)}{2\,(b-a)^{\alpha}}\left[J_{a+}^{\alpha}f(b)+J_{b-}^{\alpha}f(a)\right]\le\frac{f\,(a)+f\,(b)}{2}$$

with $\alpha>0$.

Hermite-Hadamard inequality for s-convex functions related to fractional integ-rals has been obtained in [9] as the following theorem.

Theorem 5 *Let $\alpha\ge1$ and $f:[a,b]\to\mathbb{R}$ be a positive function with $0\le a<b$ and $f\in L[a,b]$. If f is an s-convex function on $[a,b]$, then the following inequality for fractional integrals hold*

$$\begin{aligned}2^{s-1}f\left(\frac{a+b}{2}\right)&\le\frac{\Gamma(\alpha+1)}{2\,(b-a)^{\alpha}}\left[J_{a+}^{\alpha}f(b)+J_{b-}^{\alpha}f(a)\right]\\&\le\frac{f\,(a)+f\,(b)}{2}\left[\frac{1}{\alpha+s}+B(\alpha,s+1)\right].\end{aligned}$$

Katugampola gave a new fractional integral that generalizes the Riemann-Liouville and the Hadamard fractional integrals into a single form.

Definition 6 [5] *Let $[a,b] \subset \mathbb{R}$ be a finite interval. Then, the left- and right-side Katugampola fractional integrals of order $(\alpha > 0)$ of $f \in X_c^p(a,b)$ are defined:*

$$^{\rho}\mathcal{I}_{a+}^{\alpha} f(x) = \frac{\rho^{1-\alpha}}{\Gamma(\alpha)} \int_a^x \frac{t^{\rho-1}}{(x^\rho - t^\rho)^{1-\alpha}} f(t)dt$$

and

$$^{\rho}\mathcal{I}_{b-}^{\alpha} f(x) = \frac{\rho^{1-\alpha}}{\Gamma(\alpha)} \int_x^b \frac{t^{\rho-1}}{(t^\rho - x^\rho)^{1-\alpha}} f(t)dt$$

with $a < x < b$ and $\rho > 0$, if the integral exist.

Theorem 7 [5] *Let $\alpha > 0$ and $\rho > 0$. Then for $x > a$,*
1. $lim_{\rho\to 1} {}^{\rho}\mathcal{I}_{a+}^{\alpha} f(x) = J_{a+}^{\alpha} f(x)$,
2. $lim_{\rho\to 0^+} {}^{\rho}\mathcal{I}_{a+}^{\alpha} f(x) = H_{a+}^{\alpha} f(x)$.
Similar results also hold for right-sided operators.

Some Hermite-Hadamard type inequalities for products of two different functions are proposed by Chen and Wu in [2] as follows:

Theorem 8 *Let $f, g : [a,b] \to \mathbb{R}$ $a, b \in [0,\infty)$, $a < b$ be functions such that and $g, fg \in L[a,b]$. If f is convex and nonnegative and g is s-convex on $[a,b]$ for some fixed $s \in [0,1]$, then the following inequality for fractional integrals holds:*

$$\begin{aligned} &\frac{\Gamma(\alpha)}{(b-a)^\alpha}\left[J_{a+}^{\alpha} f(b)g(b) + J_{b-}^{\alpha} f(a)g(a)\right] \\ \leq\ &\left(\frac{1}{\alpha+s+1} + B(\alpha, s+2)\right) M(a,b) \\ &+ \left(B(\alpha+1, s+1) + \frac{1}{(\alpha+s)(\alpha+s+1)}\right) N(a,b), \end{aligned}$$

where $M(a,b) = f(a)g(a) + f(b)g(b)$, $N(a,b) = f(a)g(b) + f(b)g(a)$.

Theorem 9 *Let $f, g : [a,b] \to \mathbb{R}$, $a, b \in [0,\infty)$, $a < b$ be functions such that $f, g, fg \in L[a,b]$. If f is s_1-convex and g is s_2-convex function on $[a,b]$ for some fixed $s_1, s_2 \in [0,1]$, then the following inequality for fractional integrals holds:*

$$\begin{aligned} &\frac{\Gamma(\alpha)}{(b-a)^\alpha}\left[J_{a+}^{\alpha} f(b)g(b) + J_{b-}^{\alpha} f(a)g(a)\right] \\ \leq\ &\left(\frac{1}{\alpha+s_1+s_2} + B(\alpha, s_1+s_2+1)\right) M(a,b) \\ &+ \left(B(\alpha+s_1, s_2+1) + B(\alpha+s_2, s_1+1)\right) N(a,b), \end{aligned}$$

where $M(a,b) = f(a)g(a) + f(b)g(b)$, $N(a,b) = f(a)g(b) + f(b)g(a)$.

Theorem 10 *Let $f, g : [a, b] \to \mathbb{R}$, $a, b \in [0, \infty)$, $a < b$ be functions such that $fg \in L[a, b]$. If f is convex and nonnegative and g is s-convex function on $[a, b]$ for some fixed $s \in [0, 1]$, then*

$$\begin{aligned} & 2^s f\left(\frac{a+b}{2}\right) g\left(\frac{a+b}{2}\right) \\ \leq\ & \frac{\Gamma(\alpha+1)}{2(b-a)^\alpha}\left[J_{a+}^\alpha f(b)g(b) + J_{b-}^\alpha f(a)g(a)\right] \\ & +\frac{1}{2}M(a,b)\left(B(\alpha+1, s+1)\frac{1}{(\alpha+s)(\alpha+s+1)}\right) \\ & +\frac{1}{2}N(a,b)\left(B(\alpha, s+2) + \frac{1}{\alpha+s+1}\right), \end{aligned}$$

where $M(a, b) = f(a)g(a) + f(b)g(b)$, $N(a, b) = f(a)g(b) + f(b)g(a)$.

The main purpose of this note is to establish Hermite-Hadamard type inequalities for products of two convex and s-convex functions via Katugampola fractional integrals.

2 Main Results

Theorem 11 *Let $f, g : [a^\rho, b^\rho] \to \mathbb{R}_0^+$, be functions with $0 \leq a < b$ and $f, g, fg \in X_c^p(a^\rho, b^\rho)$. If f is convex and g is s-convex on $[a^\rho, b^\rho]$ for some fixed $s \in [0, 1]$, then one has the following inequality for Katugampola fractional integrals:*

$$\begin{aligned} & \frac{\Gamma(\alpha)}{\rho^{1-\alpha}(b^\rho - a^\rho)^\alpha}\left[{}^\rho\mathcal{I}_{a+}^\alpha[(fg)\circ h](b) +^\rho \mathcal{I}_{b-}^\alpha[(fg)\circ h](a)\right] \\ \leq\ & M(a^\rho, b^\rho)\frac{1}{\rho}\left[\frac{1}{\alpha+s+1} + B(\alpha, s+2)\right] \\ & +N(a^\rho, b^\rho)\frac{1}{\rho}\left[B(\alpha+1, s+1) + \frac{1}{(\alpha+s)(\alpha+s+1)}\right], \end{aligned} \tag{3}$$

where $\alpha, \rho \in \mathbb{R}^+$,

$$M(a^\rho, b^\rho) = f(a^\rho)g(a^\rho) + f(b^\rho)g(b^\rho) \quad and \quad N(a^\rho, b^\rho) = f(a^\rho)g(b^\rho) + f(b^\rho)g(a^\rho)$$

with $h(u) = u^\rho$.

Proof. By using the definitions of f and g, we can write

$$f(t^\rho a^\rho + (1-t^\rho)b^\rho) \leq t^\rho f(a^\rho) + (1-t^\rho)f(b^\rho) \tag{4}$$

and

$$g(t^\rho a^\rho + (1-t^\rho)b^\rho) \leq t^{\rho s} g(a^\rho) + (1-t^\rho)^s g(b^\rho). \tag{5}$$

By multiplying (4) and (5), we have

$$\begin{aligned} & f(t^\rho a^\rho + (1-t^\rho)b^\rho)g(t^\rho a^\rho + (1-t^\rho)b^\rho) \\ \leq\ & t^{\rho(s+1)} f(a^\rho)g(a^\rho) + (1-t^\rho)^{s+1} f(b^\rho)g(b^\rho) \\ & +t^\rho(1-t^\rho)^s f(a^\rho)g(b^\rho) + t^{\rho s}(1-t^\rho)f(b^\rho)g(a^\rho). \end{aligned} \tag{6}$$

By a similar argument, we get

$$\begin{aligned} & f((1-t^\rho)a^\rho + t^\rho b^\rho)g((1-t^\rho)a^\rho + t^\rho b^\rho) \\ \leq\ & (1-t^\rho)^{s+1} f(a^\rho)g(a^\rho) + t^{\rho(s+1)} f(b^\rho)g(b^\rho) \\ & +t^{\rho s}(1-t^\rho)f(a^\rho)g(b^\rho) + t^\rho(1-t^\rho)^s f(b^\rho)g(a^\rho). \end{aligned} \tag{7}$$

By adding (6) and (7), we obtain

$$\begin{aligned} & f(t^\rho a^\rho+(1-t^\rho)b^\rho)g(t^\rho a^\rho+(1-t^\rho)b^\rho)+f((1-t^\rho)a^\rho+t^\rho b^\rho)g((1-t^\rho)a^\rho+t^\rho b^\rho) \\ \leq\ & \left(t^{\rho(s+1)}+(1-t^\rho)^{\rho(s+1)}\right)[f(a^\rho)g(a^\rho)+f(b^\rho)g(b^\rho)] \\ & +(t^\rho(1-t^\rho)^s+t^{\rho s}(1-t^\rho))[f(a^\rho)g(b^\rho)+f(b^\rho)g(a^\rho)]. \end{aligned} \tag{8}$$

If we multiply both sides of (8) by $t^{\alpha\rho-1}$ and then integrating with respect to t over $[0,1]$, we obtain

$$\begin{aligned} & \int_0^1 t^{\alpha\rho-1}f(t^\rho a^\rho+(1-t^\rho)b^\rho)g(t^\rho a^\rho+(1-t^\rho)b^\rho)dt \\ & +\int_0^1 t^{\alpha\rho-1}f((1-t^\rho)a^\rho+t^\rho b^\rho)g((1-t^\rho)a^\rho+t^\rho b^\rho)dt \\ =\ & \int_a^b\left(\frac{b^\rho-u^\rho}{b^\rho-a^\rho}\right)^{\alpha-1}f(u^\rho)g(u^\rho)\frac{u^{\rho-1}}{b^\rho-a^\rho}du \\ & +\int_a^b\left(\frac{v^\rho-a^\rho}{b^\rho-a^\rho}\right)^{\alpha-1}f(v^\rho)g(v^\rho)\frac{v^{\rho-1}}{b^\rho-a^\rho}dv \\ =\ & \frac{1}{(b^\rho-a^\rho)^\alpha}\int_a^b\frac{u^{\rho-1}}{(b^\rho-u^\rho)^{1-\alpha}}f(u^\rho)g(u^\rho)du \\ & +\frac{1}{(b^\rho-a^\rho)^\alpha}\int_a^b\frac{v^{\rho-1}}{(v^\rho-a^\rho)^{1-\alpha}}f(u^\rho)g(u^\rho)dv \\ =\ & \frac{\Gamma(\alpha)}{\rho^{1-\alpha}(b^\rho-a^\rho)^\alpha}\left[{}^\rho\mathcal{I}^\alpha_{a+}[(fg)\circ h](b)+{}^\rho\,\mathcal{I}^\alpha_{b-}[(fg)\circ h](a)\right] \\ \leq\ & [f(a^\rho)g(a^\rho)+f(b^\rho)g(b^\rho)]\int_0^1 t^{\alpha\rho-1}\left(t^{\rho(s+1)}+(1-t^\rho)^{s+1}\right)dt \\ & +[f(b^\rho)g(a^\rho)+f(a^\rho)g(b^\rho)]\int_0^1 t^{\alpha\rho-1}\left(t^\rho(1-t^\rho)^s+t^{\rho s}(1-t^\rho)\right)dt \\ =\ & M(a^\rho,b^\rho)\frac{1}{\rho}\left[\frac{1}{\alpha+s+1}+B(\alpha,s+2)\right] \\ & +N(a^\rho,b^\rho)\frac{1}{\rho}\left[B(\alpha+1,s+1)+\frac{1}{(\alpha+s)(\alpha+s+1)}\right] \end{aligned}$$

which completes the proof.

Remark 12 *If we choose $\rho=1$ in the inequality* (3)*, then Theorem 11 reduces to the Theorem 8.*

Theorem 13 *Suppose that $f,g:[a^\rho,b^\rho]\to\mathbb{R}^+_0$ be functions with $0\leq a<b$ and $f,g,fg\in X^p_c(a^\rho,b^\rho)$. If f is s_1-convex and g is s_2-convex function on $[a^\rho,b^\rho]$ for some fixed $s_1,s_2\in[0,1]$, then one has the following inequality for Katugampola fractional integrals:*

$$\begin{aligned} & \frac{\Gamma(\alpha)}{\rho^{1-\alpha}(b^\rho-a^\rho)^\alpha}\left[{}^\rho\mathcal{I}^\alpha_{a+}[(fg)\circ h](b)+{}^\rho\,\mathcal{I}^\alpha_{b-}[(fg)\circ h](a)\right] \\ \leq\ & M(a^\rho,b^\rho)\frac{1}{\rho}\left[\frac{1}{\alpha+s_1+s_2}+B(\alpha,s_1+s_2+1)\right] \\ & +N(a^\rho,b^\rho)\frac{1}{\rho}\left[B(\alpha+s_1,s_2+1)+B(\alpha+s_2,s_1+1)\right] \end{aligned} \tag{9}$$

where $\alpha,\rho\in\mathbb{R}^+$ and $M(a^\rho,b^\rho)$ and $N(a^\rho,b^\rho)$ are the same as given in Theorem 11 with $h(u)=u^\rho$.

Proof. From the definition of s_1-convexity and s_2-convexity, we can write

$$f(t^\rho a^\rho + (1-t^\rho)b^\rho) \leq t^{\rho s_1} f(a^\rho) + (1-t^\rho)^{s_1} f(b^\rho) \tag{10}$$

and

$$g(t^\rho a^\rho + (1-t^\rho)b^\rho) \leq t^{\rho s_2} g(a^\rho) + (1-t^\rho)^{s_2} g(b^\rho). \tag{11}$$

By multiplying both side of (10) and (11), we get

$$\begin{aligned} & f(t^\rho a^\rho + (1-t^\rho)b^\rho) g(t^\rho a^\rho + (1-t^\rho)b^\rho) \\ \leq\ & t^{\rho(s_1+s_2)} f(a^\rho)g(a^\rho) + (1-t^\rho)^{s_1+s_2} f(b^\rho)g(b^\rho) \\ & + t^{\rho s_1}(1-t^\rho)^{s_2} f(a^\rho)g(b^\rho) + t^{\rho s_2}(1-t^\rho)^{s_1} f(b^\rho)g(a^\rho). \end{aligned} \tag{12}$$

By a similar way, it is easy to write,

$$\begin{aligned} & f((1-t^\rho)a^\rho + t^\rho b^\rho) g((1-t^\rho)a^\rho + t^\rho b^\rho) \\ \leq\ & (1-t^\rho)^{s_1+s_2} f(a^\rho)g(a^\rho) + t^{\rho(s_1+s_2)} f(b^\rho)g(b^\rho) \\ & + (1-t^\rho)^{s_1} t^{\rho s_2} f(a^\rho)g(b^\rho) + t^{\rho s_1}(1-t^\rho)^{s_2} f(b^\rho)g(a^\rho). \end{aligned} \tag{13}$$

By adding (12) and (13), we have

$$\begin{aligned} & f(t^\rho a^\rho + (1-t^\rho)b^\rho) g(t^\rho a^\rho + (1-t^\rho)b^\rho) + f((1-t^\rho)a^\rho + t^\rho b^\rho) g((1-t^\rho)a^\rho + t^\rho b^\rho) \\ \leq\ & \left(t^{\rho(s_1+s_2)} + (1-t^\rho)^{s_1+s_2}\right) [f(a^\rho)g(a^\rho) + f(b^\rho)g(b^\rho)] \\ & + \left(t^{\rho s_1}(1-t^\rho)^{s_2} + t^{\rho s_2}(1-t^\rho)^{s_1}\right) [f(a^\rho)g(b^\rho) + f(b^\rho)g(a^\rho)]. \end{aligned} \tag{14}$$

If we multiply both sides of (14) by $t^{\alpha\rho-1}$, then by integrating with respect to t over $[0,1]$, we obtain

$$\begin{aligned} & \frac{\Gamma(\alpha)}{\rho^{1-\alpha}(b^\rho - a^\rho)^\alpha} \left[{}^\rho\mathcal{I}^\alpha_{a+}[(fg)\circ h](b) +^\rho \mathcal{I}^\alpha_{b-}[(fg)\circ h](a)\right] \\ \leq\ & M(a^\rho, b^\rho)\frac{1}{\rho}\left[\frac{1}{\alpha+s_1+s_2} + B(\alpha, s_1+s_2+1)\right] \\ & + N(a^\rho, b^\rho)\frac{1}{\rho}\left[B(\alpha+s_1, s_2+1) + B(\alpha+s_2, s_1+1)\right]. \end{aligned}$$

This completes the proof.

Remark 14 *If we choose $\rho = 1$ in the inequality* (9)*, then Theorem 13 reduces to the Theorem 9.*

Theorem 15 *Let $f, g : [a^\rho, b^\rho] \to \mathbb{R}^+_0$, be functions with $0 \leq a < b$ and $f, g, fg \in X^p_c(a^\rho, b^\rho)$. If f is convex and g is s-convex on $[a^\rho, b^\rho]$ for some fixed $s \in [0,1]$, then one has the following inequality for Katugampola fractional integrals:*

$$\begin{aligned} & \frac{2^s}{\rho} f\left(\frac{a^\rho + b^\rho}{2}\right) g\left(\frac{a^\rho + b^\rho}{2}\right) \\ \leq\ & \frac{\Gamma(\alpha+1)}{2\rho^{1-\alpha}(b^\rho - a^\rho)^\alpha} \left[{}^\rho\mathcal{I}^\alpha_{a+}[(fg)\circ h](b) +^\rho \mathcal{I}^\alpha_{b-}[(fg)\circ h](a)\right] \\ & + \frac{1}{2} M(a^\rho, b^\rho)\left[\frac{1}{\rho}B(\alpha+1, s+1) + \frac{1}{(\rho\alpha+s)(\rho\alpha+s+1)}\right] \\ & + \frac{1}{2} N(a^\rho, b^\rho)\left[\frac{1}{\rho}B(\alpha, s+2) + \frac{1}{\rho\alpha+\rho s+\rho}\right] \end{aligned} \tag{15}$$

where $\alpha, \rho \in \mathbb{R}^+$ and $M(a^\rho, b^\rho)$ and $N(a^\rho, b^\rho)$ are the same as given in Theorem 11 with $h(u) = u^\rho$.

Proof. By using the definitions, we have

$$
\begin{aligned}
& f\left(\frac{a^\rho+b^\rho}{2}\right) g\left(\frac{a^\rho+b^\rho}{2}\right) \\
= \;& f\left(\frac{t^\rho a^\rho+(1-t^\rho)b^\rho}{2}+\frac{(1-t^\rho)a^\rho+t^\rho b^\rho}{2}\right) g\left(\frac{t^\rho a^\rho+(1-t^\rho)b^\rho}{2}+\frac{(1-t^\rho)a^\rho+t^\rho b^\rho}{2}\right) \\
\leq \;& \frac{1}{2^{s+1}}\left[f(t^\rho a^\rho+(1-t^\rho)b^\rho)g(t^\rho a^\rho+(1-t^\rho)b^\rho)+f((1-t^\rho)a^\rho+t^\rho b^\rho)+g((1-t^\rho)a^\rho+t^\rho b^\rho)\right] \\
& +\frac{1}{2^{s+1}}\left[\left(t^\rho(1-t^\rho)^s+(1-t^\rho)t^{\rho s}\right)M(a^\rho,b^\rho)+\left((1-t^\rho)^{s+1}t^{\rho(s+1)}\right)N(a^\rho,b^\rho)\right]. \qquad (16)
\end{aligned}
$$

By multiplying both sides of (16) by $t^{\alpha\rho-1}$, then integrating with respect to t over $[0,1]$, we obtain

$$
\begin{aligned}
& \frac{2^s}{\rho} f\left(\frac{a^\rho+b^\rho}{2}\right) g\left(\frac{a^\rho+b^\rho}{2}\right) \\
\leq \;& \frac{\Gamma(\alpha+1)}{2\rho^{1-\alpha}(b^\rho-a^\rho)^\alpha}\left[{}^\rho\mathcal{I}^\alpha_{a+}[(fg)\circ h](b)+{}^\rho\mathcal{I}^\alpha_{b-}[(fg)\circ h](a)\right] \\
& +\frac{1}{2}M(a^\rho,b^\rho)\left[\frac{1}{\rho}B(\alpha+1,s+1)+\frac{1}{(\rho\alpha+s)(\rho\alpha+s+1)}\right] \\
& +\frac{1}{2}N(a^\rho,b^\rho)\left[\frac{1}{\rho}B(\alpha,s+2)+\frac{1}{\rho\alpha+\rho s+\rho}\right].
\end{aligned}
$$

This completes the proof.

Remark 16 *If we choose $\rho=1$ in the inequality* (15)*, then Theorem 15 reduces to the Theorem 10.*

References

[1] W.W. Breckner, *Stetigkeitsaussagen fr eine Klasse verallgemeinerter konvexer funktionen in topologischen linearen Raumen*, Pupl. Inst. Math. 23 (1978) 1320.

[2] F. Chen, S. Wu, *Several complementary inequalities to inequalities of Hermite-Hadamard type for s-convex functions*, J. Nonlinear Sci. Appl., 9 (2016), 705-716.

[3] S. S. Dragomir and S. Fitzpatrik, *The Hadamard's inequality for s-convex functions in the second sense,* Demonstratio Math. 32(4), (1999), 687-696.

[4] H. Hudzik, L. Maligranda, *Some remarks on s-convex functions*, Aequationes Math. 48 (1994) 100-111.

[5] U.N. Katugampola, *New approach to a genaralized fractional integral,* Applied Mathematics and Computation, 218(3) (2011), 860-865.

[6] E.D. Rainville, *Special Functions*, The Mcmillan Company, New York, 1960.

[7] M.Z. Sarıkaya, E. Set, H. Yaldız, N. Başak, *Hermite-Hadamard's inequalities for fractional integrals and related fractional inequalities,* Math. Comput. Model., 57 (2013), 2403-2407.

[8] H.M. Srivastava and J. Choi, *Zeta and q-Zeta Functions and Associated Series and Integrals*, Elsevier Science Publishers, Amsterdam, London and New York, 2012.

[9] J. Wang, X. Li, Y. Zhou, *Hermite-Hadamard inequalities involving Riemann-Liouville fractional integrals via s-convex functions and applications to special means,* Filomat, 30(5) (2016), 1143-1150.

A Note On Generalized Absolute Fibonacci Spaces

Fadime GÖKÇE *
Pamukkale University,
Department of Mathematics, Denizli, TURKEY

Mehmet Ali SARIGÖL
Pamukkale University,
Department of Mathematics, Denizli, TURKEY

Abstract

The main purpose of this study is to calculate the γ-duals of the new absolute Fibonacci series space $|F_\theta|(p)$ which can be considered as the domain of a triangle matrix in the space $l(p)$.

Keywords: Absolute summability; Fibonacci numbers; Maddox's space

1 Introduction

By ω, we denote the set of all sequences of complex numbers. Let X and Y be any subsets of ω and $A = (a_{nv})$ be an infinite matrix of complex numbers. If for every sequence $x \in X$, the series

$$A_n(x) = \sum_{v=0}^{\infty} a_{nv} x_v,$$

is convergent for all $n \in N = \{0, 1, 2, ...\}$ and the sequence $A(x) = (A_n(x))$, A-transform of the sequence $x = (x_v)$, is in Y then, we say that A defines a matrix transformation from X into Y, and denote it by $A \in (X, Y)$. The matrix domain of an infinite matrix A in a sequence space X is defined by

$$X_A = \{x = (x_n) \in \omega : A(x) \in X\}, \tag{1}$$

which is a sequence space.

Let $\sum a_v$ be a given infinite series with its nth partial sum (s_n), $\theta = (\theta_n)$ be any positive sequence and $p = (p_n)$ be a bounded sequence of positive real numbers. If

$$\sum_{n=0}^{\infty} \theta_n^{p_n - 1} |A_n(s) - A_{n-1}(s)|^{p_n} < \infty,$$

then, the series $\sum a_v$ is said to be summable $|A, \theta_n|(p)$ ([1]).

Also, the $\alpha-, \beta-, \gamma-$ duals of X are given by

$$X^\alpha = \{z \in \omega : xz = (x_k z_k) \in l \text{ for all } x = (x_k) \in X\},$$

$$X^\beta = \{z \in \omega : xz = (x_k z_k) \in cs \text{ for all } x = (x_k) \in X\},$$

$$X^\gamma = \{\epsilon \in \omega : xz = (x_k z_k) \in bs \text{ for all } x = (x_k) \in X\}$$

*Corresponding author. *E-mail address:* fgokce@pau.edu.tr

respectively. We mean cs, bs and l_p $(1 \leq p < \infty)$ for the space of all convergent, bounded, p-absolutely convergent series, respectively. Besides these, the Maddox's space

$$l(p) = \left\{ x = (x_k) \in \omega : \sum_{k=0}^{\infty} |x_k|^{p_k} < \infty \right\},$$

have an important role in the summability theory and the space is an FK-space with AK with respect to its natural paranorm

$$g(x) = \left(\sum_{k=0}^{\infty} |x_k|^{p_k} \right)^{1/M},$$

where $M = \max\{1, \sup_k p_k\}$ ([7], [8], [9]).

Now, we remind some of the properties of the Fibonacci numbers: The sequence (f_n) of Fibonacci numbers is given by the following relations:

$$f_0 = f_1 = 1 \text{ and } f_{n+2} = f_{n+1} + f_n \text{ for } n \geq 0$$

that is, each term is equal to the sum of the previous two terms. The sequence of Fibonacci numbers have been important for artist, architects, physicists and mathematicians since the old. The ratio of Fibonacci numbers converges to the golden ratio which is one of the most interesting irrationals having an important role in number theory, algorithms, network theory, etc.. Also, Fibonacci numbers have the following properties [6]:

$$\sum_n \frac{1}{f_n} \text{ converges,}$$

$$f_{n-1}^2 + f_n f_{n-1} - f_n^2 = (-1)^{n+1}, n \geq 1,$$

$$\lim_{n\to\infty} \frac{f_{n+1}}{f_n} = \frac{1+\sqrt{5}}{2} = 1.61803398875....$$

Besides, the Fibonacci matrix $F = (\hat{f}_{nv})$ has been defined by Kara in [5] as follows:

$$\hat{f}_{nv} = \begin{cases} \frac{-f_{n+1}}{f_n}, & v = n-1 \\ \frac{f_n}{f_{n+1}}, & v = n \\ 0, & v > n \text{ or } 0 \leq v < n-1 \end{cases}$$

where f_n is the Fibonacci number for all $n \in N$.

Lemma 1 *Let $p = (p_v)$ be any bounded sequence positive numbers.*
(a) If $p_v > 1$ for all v, then, $A \in (l(p), l_\infty)$ if and only if there exists an integer $M > 1$ such that

$$\sup_n \sum_{v=0}^{\infty} \left| a_{nv} M^{-1} \right|^{p_v^*} < \infty,$$

(b) If $p_v \leq 1$ for all $v \in N$, then $A \in (l(p), l_\infty)$ if and only if

$$\sup_{n,v} |a_{nv}|^{p_v} < \infty,$$

[2].

2 Main Theorem

The aim of this section is to introduce the absolute Fibonacci space $|F_\theta|(p)$ and to give γ-dual of this space according to the state of p. The absolute Fibonacci space can be expressed as

$$|F_\theta|(p) = \left\{ a \in \omega : \sum_{n=0}^{\infty} \theta_n^{p_n - 1} \left| \sum_{k=0}^{n} \sigma_{nk} a_k \right|^{p_n} < \infty \right\}.$$

where

$$\sigma_{nk} = \begin{cases} \frac{f_n}{f_{n+1}}, & k = n \\ \frac{(-1)^n}{f_n f_{n+1}} - \frac{f_{n+1}}{f_n}, & k = n-1 \\ (-1)^n \frac{f_{n-1}+f_{n+1}}{f_{n-1} f_n f_{n+1}}, & 0 \le k \le n-2 \\ 0, & k > n. \end{cases}$$

or according to the notation of the domain given by (1.1), with the matrices $T = (t_{nv})$ and $E^{(p)} = (e_{nv}^{(p)})$, we write

$$|F_\theta|(p) = (l(p))_{E^{(p)} \circ T}$$

where

$$t_{nv} = \begin{cases} \frac{f_n}{f_{n+1}}, & v = n \\ \frac{f_n^2 - f_{n+1}^2}{f_n f_{n+1}}, & 0 \le v \le n-1 \\ 0, & v > n, \end{cases}$$

$$e_{nv}^{(p)} = \begin{cases} \theta_n^{1/p_n^*}, & v = n \\ -\theta_n^{1/p_n^*}, & v = n-1 \\ 0, & v \ne n, n-1. \end{cases}$$

Also, since every triangle matrix has a unique inverse which is a triangle, the matrices T and $E^{(p)}$ have unique inverse $\tilde{T} = (\tilde{t}_{nv})$ and $\tilde{E}^{(p)} = (\tilde{e}_{nv})$ defined by

$$\tilde{t}_{nv} = \begin{cases} \frac{f_{n+1}}{f_n}, & v = n \\ \frac{f_{n+1}^2 - f_n^2}{f_v f_{v+1}}, & 0 \le v \le n-1 \\ 0, & v > n \end{cases} \tag{2}$$

$$\tilde{e}_{nv}^{(p)} = \begin{cases} \theta_v^{-1/p_v^*}, & 0 \le v \le n \\ 0, & v > n. \end{cases} \tag{3}$$

Theorem 2 *Let $p = (p_v)$ be a bounded sequence of positive numbers. $\theta = (\theta_n)$ be any sequence of positive numbers. If $p_v > 1$ for all $v \in N$, then*

$$\{|F_\theta|(p)\}^\gamma = \left\{ a \in \omega : \exists M > 1, \sup_n \left[\frac{M^{\frac{-1}{p_n^*}}}{\theta_n} \left| \frac{f_{n+1}}{f_n} a_n \right|^{p_n^*} + \sum_{v=0}^{n-1} \frac{M^{\frac{-1}{p_v^*}}}{\theta_v} \left| \left(\frac{f_{v+1}}{f_v} a_v + \sum_{k=v+1}^{n} a_k \mu_{kv} \right) \right|^{p_v^*} \right] < \infty \right\},$$

and if $p_v \le 1$ for all $v \in N$, then

$$\{|F_\theta|(p)\}^\gamma = \left\{ a \in \omega : \sup_{n,v} \left\{ \left| \theta_n^{\frac{-1}{p_n^*}} \frac{f_{n+1}}{f_n} a_n \right|^{p_n} + \left| \theta_v^{\frac{-1}{p_v^*}} \left(\frac{f_{v+1}}{f_v} a_v + \sum_{k=v+1}^{n} a_k \mu_{kv} \right) \right|^{p_v} \right\} < \infty \right\} \text{ where}$$

$$\mu_{nv} = \left(\frac{f_{n+1}}{f_n} + \left(f_{n+1}^2 - f_n^2\right) \sum_{j=v}^{n-1} \frac{1}{f_j f_{j+1}} \right),$$

and p_v^* *is conjugate of* p_v, *i.e.,* $1/p_v + 1/p_v^* = 1$, $p_v > 0$, *and* $1/p_v^* = 0$ *for* $p_v = 1$.

Proof. Let's recall that $a \in \{|F_\theta|(p)\}^\gamma$ if and only if $ax = (a_n x_n) \in l_\infty$ whenever $x \in |F_\theta|(p)$. Also we suppose that $y = T(x)$ and $z = E^{(p)}(y)$ for all $x \in |F_\theta|(p)$. By the equations (2.1) and (2.2), we get

$$\begin{aligned}
\sum_{k=0}^{n} a_k x_k &= \sum_{k=0}^{n} a_k \left(\frac{f_{k+1}}{f_k} y_k + \left(f_{k+1}^2 - f_k^2\right) \sum_{k=0}^{k-1} \frac{y_j}{f_j f_{j+1}} \right) \\
&= \sum_{k=0}^{n} a_k \frac{f_{k+1}}{f_k} y_k + \sum_{k=1}^{n} a_k \left(f_{k+1}^2 - f_k^2\right) \sum_{j=0}^{k-1} \frac{y_j}{f_j f_{j+1}} \\
&= \sum_{r=0}^{n} \left(\sum_{k=r}^{n} a_k \frac{f_{k+1}}{f_k} \right) \theta_r^{-1/p_r^*} z_r + \sum_{k=1}^{n} a_k (f_{k+1}^2 - f_k^2) \sum_{r=0}^{k-1} \theta_r^{-1/p_r^*} z_r \sum_{j=r}^{k-1} \frac{1}{f_j f_{j+1}} \\
&= a_n \frac{f_{n+1}}{f_n} \theta_n^{-1/p_n^*} z_n + \sum_{r=0}^{n-1} \theta_r^{-1/p_r^*} z_r \left(\sum_{k=r}^{n} a_k \frac{f_{k+1}}{f_k} \right. \\
&+ \left. \sum_{k=r+1}^{n} a_k \left(f_{k+1}^2 - f_k^2\right) \sum_{j=r}^{k-1} \frac{1}{f_k f_{k+1}} \right) \\
&= \sum_{r=0}^{n} b_{nr} z_r
\end{aligned}$$

where $B = (b_{nv})$ is defined by

$$b_{nr} = \begin{cases} \theta_n^{-1/p_n^*} a_n \frac{f_{n+1}}{f_n}, & r = n \\ \theta_r^{-1/p_r^*} \left(a_r \frac{f_{r+1}}{f_r} + \sum_{k=r+1}^{n} a_k \mu_{kr} \right), & 0 \leq r \leq n-1 \\ 0, & r > n. \end{cases}$$

Note that $z = E^{(p)} \circ T(x) \in l(p)$ whenever $x \in |F_\theta|(p)$. So $a \in |F_\theta|(p)^\gamma$ if and only if $B \in (l(p), l_\infty)$. If we apply Lemma 1.1 to the matrix B, we get the desired results. Hence the proof is completed. ■

References

[1] Gökçe F., Sarıgöl, M.A.: A new series space $\left|\overline{N}_p^\theta\right|(\mu)$ and matrix transformations with applications. Kuwait J. Sci. **45**(4) (2018)

[2] Grosse-Erdmann, K.G.: Matrix transformations between the sequence spaces of Maddox. J. Mathe.Anal, Appl. **180**, 223–238 (1993)

[3] Kara, E. E., Ilkhan, M.: Some properties of generalized Fibonacci sequence spaces. Linear and Multilinear Algebra **64**(11), 2208-2223 (2016)

[4] Kara, E. E., Ilkhan, M.: On some Banach sequence spaces derived by a new band matrix. Br. J. Math. Comput. Sci.**9**(2), 141-159 (2015)

[5] Kara, E. E.: Some topological and geometrical properties of new Banach sequence spaces. J. Inequal. Appl. 2013(1), 38 (2013)

[6] Koshy, T.Ã‡: Fibonacci and Lucas numbers with applications, 51 John Wiley and Sons, 2011

[7] Maddox, I.J.: Some properties of paranormed sequence spaces. J. London Math. Soc. **1**, 316-322 (1969)

[8] Maddox, I.J.: Paranormed sequence spaces generated by infinite matrices. Math. Proc. Cambridge Philos. Soc. **64**, 335-340 (1968)

[9] Maddox, I.J.: Spaces of strongly summable sequences, The Quart. J. Math. **18**, 345-355 (1967)

Determining Of Safety Factors For Cantilever Retaining Wall With Mathematical Model

Esra URAY *
Department of Civil Engineering,
KTO Karatay University,
Konya/TURKEY

Serdar ÇARBAŞ
Department of Civil Engineering,
Karamanoglu Mehmetbey University,
Karaman/TURKEY

Özcan TAN
Department of Civil Engineering,
Konya Technical University,
Konya /TURKEY

Abstract

In the conventional design of cantilever retaining wall, trial-and-error method has been used to determine wall dimensions which satisfies the stability conditions of wall. This method takes time in design period and is not possible to know which parameter is the most effective in the design. In this study, safety factors of the cantilever retaining wall which play a crucial role in stability of the wall have been investigated to determine with mathematical model. In computing of safety factors of sliding, overturning and slope stability mathematically, Taguchi method which is a statistical method has been employed. For different situations Signal/Noise (S/N), variance and optimization analyses have been performed separately by using L_{16} orthogonal design tables. At result of these analysis, effect of the length of base, the toe extension, the thickness of base, the angle of front face of wall and the angle of internal friction on safety factors of sliding, overturning and slope stability have been studied. Consequently, obtained relative errors from mathematical model safety factors demonstrate that these models are efficient and reliable in the design of cantilever retaining wall.

Keywords: Cantilever retaining wall, Taguchi method, mathematical model, statistical analysis.

1 Introduction

In today's geotechnical engineering, the time has become important criteria in terms of completing the design of geotechnical structures as soon as possible. In the traditional design of cantilever retaining wall which is a geotechnical structure, stability analyses like slide check, overturning check, slope stability and so on, have been conducted according to selected wall dimensions [1, 2]. This process continues by selecting new wall dimensions each time until stability analyses are satisfied. Such time-consuming design methods have brought new methods to make design in a shorter time. Taguchi method which one of the methods to provide making design in shorter time give information about effective parameter on design and the optimum design in case of maximum or minimum safety factor. Taguchi method based on statistical analysis has been put forward by Genichi Taguchi with the aim of increasing quality of experiment in 1950s [3]. This method not only make it possible obtain experiments with less study but also find the best values between all parameters and all levels of parameters.

*Corresponding author. *E-mail address:* esra.uray@karatay.edu.tr

The Taguchi method, which is used especially in the experimental design and the quality management, is widely used in the designs of engineering to investigate the design criteria. In this method, it is possible to gain the effects of parameters on design by performing less experiments without making many experiments with orthogonal array [4]. Studies of determination of safety factor of slope stability with mathematical model and investigation of design criteria of gabion retaining wall which is another type of retaining wall have been carried out by using Taguchi Method [5, 6].
In this study, mathematical models have been submitted to determine safety factors of sliding, overturning and slope stability by using Signal/Noise (S/N) ratios identified by Taguchi. The effect of design parameters like the length of base, the toe extension, the thickness of base, the angle of front face of wall and the angle of internal friction on the design has investigated by Taguchi Method. Mathematical models proposed for calculation of safety factors of sliding, overturning and slope stability according to selected design parameters. To investigate all combination of all parameters 16 cantilever retaining wall design have been analyzed by using L_{16} orthogonal design table and has been performed fractional factorial design for four levels of five parameters.

2 Taguchi Method

Taguchi Method is a robust and easily applicable method, because it reaches results in less time and to determine effects of the parameters on the result trustworthily. It reduces the cost of investigation and performs parametric analysis. Normally, to investigate effect of five parameters with four levels on safety factors of sliding, overturning and slope stability $4^5 = 1024$ design must be carried out. In this method, it is possible to obtain parameters effect on the result with 16 designs by means of orthogonal array. In this study, L_{16} (4^5) orthogonal array (five parameters and four level) has been employed and it is given Table 1.

Table 1: L_{16} (4^5) orthogonal array

Design No	Parameters and Levels				
	P_1	P_2	P_3	P_4	P_5
1	1	1	1	1	1
2	1	2	2	2	2
3	1	3	3	3	3
4	1	4	4	4	4
5	2	1	2	3	4
6	2	2	1	4	3
7	2	3	4	1	2
8	2	4	3	2	1
9	3	1	3	4	2
10	3	2	4	3	1
11	3	3	1	2	4
12	3	4	2	1	3
13	4	1	4	2	3
14	4	2	3	1	4
15	4	3	2	4	1
16	4	4	1	3	2

In the Taguchi analyses of cantilever retaining wall design, selected parameters and their levels are given in Table 2. In determination of lower and upper limits of selected parameters national and design codes have been taken into consideration [7-9]. While the X_1 and the X_3 are varying depending on the wall height (H), the X_2 varies depending on the X_1.

Table 2: Selected parameters and their levels

Parameter	Level 1	Level 2	Level 3	Level4
Length of base, X_1	0.25H	0.50 H	0.75 H	1.00 H
Toe extension, X_2	0.15 X_1	0.30 X_1	0.45 X_1	0.60 X_1
Thickness of base, X_3	0.06 H	0.09 H	0.12 H	0.15 H
Angle of front face, X_4 (%)	0	1	2	4
Angle of internal friction, Ø (°)	20	27	34	41

In Taguchi Method, effects of the parameters on the results and mathematical model have been determined with the S/N ratios. Signal/Noise ratio (S/N) is described by Taguchi with aim of decreasing variance and is used as performance criteria in experiment design. S/N ratio divided into three depended on purpose of application; smaller is better, nominal is best, larger is better, are given in respectively Equation 1, Equation 2 and Equation 3. In this study, S/N analyses has been performed according to the target state of "Larger is better" which maximize the response. According to Taguchi, the variance which is defined as difference from the target value has been decreased and the signal has been increased in case of S/N ratio is maximum [4]. Variance is a degree of distribution of a number sequence around arithmetic mean of this number sequence.

$$\mathrm{S/N} = -10\mathrm{xlog}(\sum(\mathrm{Y}^2)/\mathrm{n}) \tag{1}$$

$$\mathrm{S/N} = -10\mathrm{xlog}(\bar{\mathrm{Y}}/\sigma^2) \tag{2}$$

$$\mathrm{S/N} = -10\mathrm{xlog}(\sum(1/\mathrm{Y}^2)/\mathrm{n}) \tag{3}$$

Here Y is the response value, n is the number of repetitions, $\overline{Y}$ is arithmetic mean and σ is standard deviation.

3 Numerical and Statistical Analyses

In numerical analyses, the cantilever retaining wall height (H=6m), top stem thickness of wall (b=0.25m) unit volume weight of soil ($\gamma_s = 18kN/m^3$), unit weight of concrete, ($\gamma_c = 25kN/m^3$) and friction angle between base and soil ($\delta = 2/3$Ø) are taken same for 16 designs. Acting loads on cantilever retaining wall and selected wall dimensions which are used for determination of safety factors of sliding, overturning and slope stability of wall are given in Figure 1.

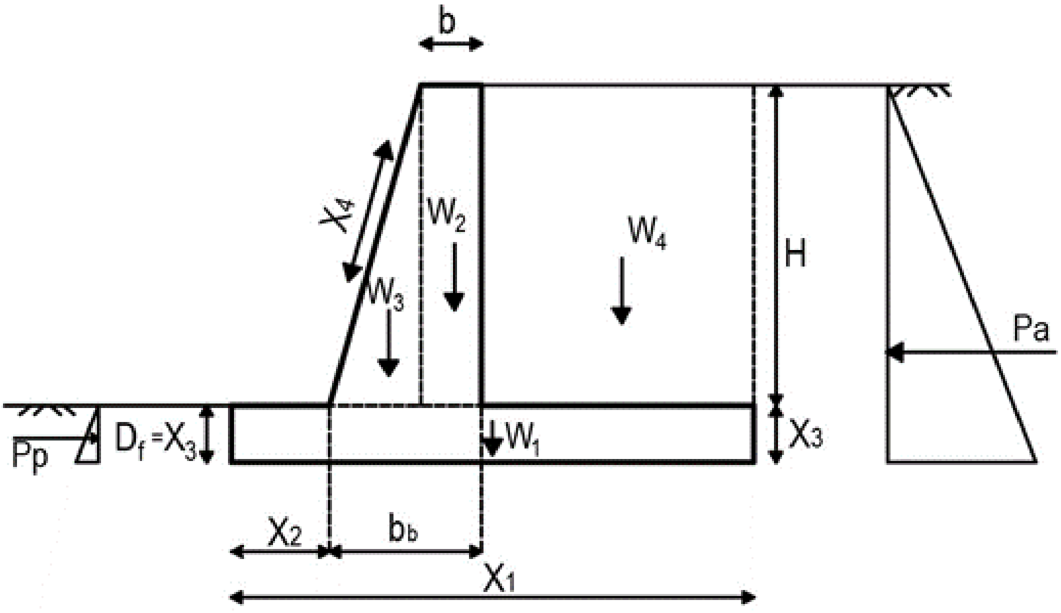

Figure 1: Cantilever Retaining Wall Dimensions and Acting Loads

In the cantilever retaining wall design, the same soil properties have been taken into account for foundation soil and backfill of wall with a single value of unit volume weight of soil (18 kN/m^3) and four different value of angle of internal friction (20-27-34-41°). Value of the internal friction angle which uses in design changes according to L_{16} orthogonal array design table. In the checks of sliding, overturning and slope stability, analysis of cantilever retaining wall have been conducted according to single-layer cohesionless soil condition without ground water. Due to the fact that the overturning of the wall is less likely than slide, passive soil pressure has not taken into consideration for obtaining of safety factor of overturning. In Table 3, mathematical formulas which use for obtaining of safety factors of sliding and overturning according to GEO 5 computer program [10] have given detailed. Safety factor of slope stability has obtained by Bishop method from computer program.

Table 3: Used mathematical formulas for determining safety factors of sliding and overturning

Bottom thickness of the stem	$\mathrm{b_b}=(\mathrm{H}-\mathrm{X_3})*\mathrm{X_4}+\mathrm{b}$
Weight of wall	$\mathrm{W_1}=\mathrm{X_1\ X_3}\ \gamma_\mathrm{c}$ $\mathrm{W_2}=\mathrm{b\ H}\ \gamma_\mathrm{c}$ $\mathrm{W_3}=0.5\,(\mathrm{b_b}-\mathrm{b})\ \mathrm{H}\ \gamma_\mathrm{c}$
Weight of backfill	$\mathrm{W_4}=(\mathrm{X_1}-\mathrm{X_2}-\mathrm{b_b})\ \mathrm{H}\ \gamma_\mathrm{s}$
Active soil pressure	$\mathrm{P_a}=0.5\,\mathrm{H}^2\,\gamma_\mathrm{s}\,\mathrm{K_a}$
Passive soil pressure	$\mathrm{P_p}=0.5\,\mathrm{D_f}^2\,\gamma_\mathrm{s}\,\mathrm{K_p}$
Active soil pressure coefficient	$\mathrm{K_a}=\tan^2(45-\O/2)$
Passive soil pressure coefficient	$\mathrm{K_p}=\tan^2(45+\O/2)$
Safety factor of sliding	$\mathrm{F_s}\,(\mathrm{sliding})=\frac{(\mathrm{W_1}+\mathrm{W_2}+\mathrm{W_3}+\mathrm{W_4})\tan\delta}{\mathrm{P_a}-\mathrm{P_p}}$
Safety factor of overturning $\mathrm{F_s}\,(\mathrm{overturning})=\frac{0.5\mathrm{W_1X_1}+\mathrm{W_2}(\mathrm{b_b}-0.5\,\mathrm{b}+\mathrm{X_2})+\mathrm{W_3}(0.667\,(\mathrm{b_b}-\mathrm{b})+\mathrm{X_2})+0.5\,\mathrm{W_4}(\mathrm{X_1}+\mathrm{X_2}+\mathrm{b_b})}{0.333\,\mathrm{P_a}\,(\mathrm{H}+\mathrm{X_3})}$	

By using orthogonal array given in Table 1 and parameter levels given in Table 2, revised L_{16} design table has demonstrated in Table 4. Cantilever retaining wall designs has been conducted in computer program according to revised design table and end of the analysis safety factors of sliding, overturning and slope stability have been obtained (Table 4).

Table 4: Cantilever retaining wall Taguchi design table and results of numerical analyses

Design No	Parameter Levels					Safety Factor (Fs)		
	X_1	X_2	X_3	X_4 (%)	Ø (°)	Sliding	Overturning	Slope Stability
1	0.25H	$0.15X_1$	0.06H	0	20	0.22	0.35	0.75
2	0.25H	$0.30X_1$	0.09H	1	27	0.34	0.42	1.09
3	0.25H	$0.45X_1$	0.12H	2	34	0.52	0.48	1.48
4	0.25H	$0.60X_1$	0.15H	4	41	0.97	0.53	1.96
5	0.50H	$0.15X_1$	0.09H	2	41	2.48	3.11	2.18
6	0.50H	$0.30X_1$	0.06H	4	34	1.08	2.24	1.54
7	0.50H	$0.45X_1$	0.15H	0	27	0.59	1.36	1.27
8	0.50H	$0.60X_1$	0.12H	1	20	0.24	0.92	0.84
9	0.75H	$0.15X_1$	0.12H	4	27	1.15	3.68	1.51
10	0.75H	$0.30X_1$	0.15H	2	20	0.54	2.55	1.06
11	0.75H	$0.45X_1$	0.06H	1	41	2.34	6.13	2.10
12	0.75H	$0.60X_1$	0.09H	0	34	1.11	3.65	1.58
13	1.00H	$0.15X_1$	0.15H	1	34	3.04	8.31	2.26
14	1.00H	$0.30X_1$	0.12H	0	41	4.77	11.18	2.67
15	1.00H	$0.45X_1$	0.09H	4	20	0.57	4.38	1.00
16	1.00H	$0.60X_1$	0.06H	2	27	0.78	4.94	1.23

Statistica [11] computer program has been employed for statistical analyses. In Figure 2, calculated S/N ratios are given by using safety factors obtained from the numerical analyses. Graphical representation of average S/N ratios corresponding to each parameter level for safety factors of sliding, overturning and slope stability are given respectively in Figure 3, Figure 4 and Figure 5.

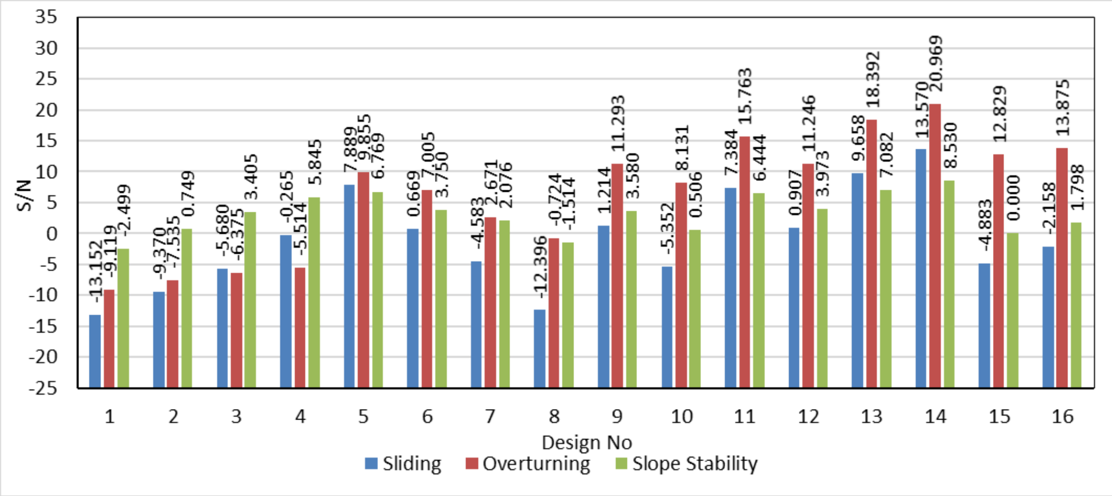

Figure 2: Cantilever Retaining wall S/N ratios

In Figure 2, it is clear that the most change of average S/N ratio of safety factor of sliding is belonging the angle of internal friction and the second most change is the length of base. While the length of base, the angle of internal friction and the thickness of base shows increasing, the toe extension and the angle of front face generally shows decreasing with increasing parameter level.

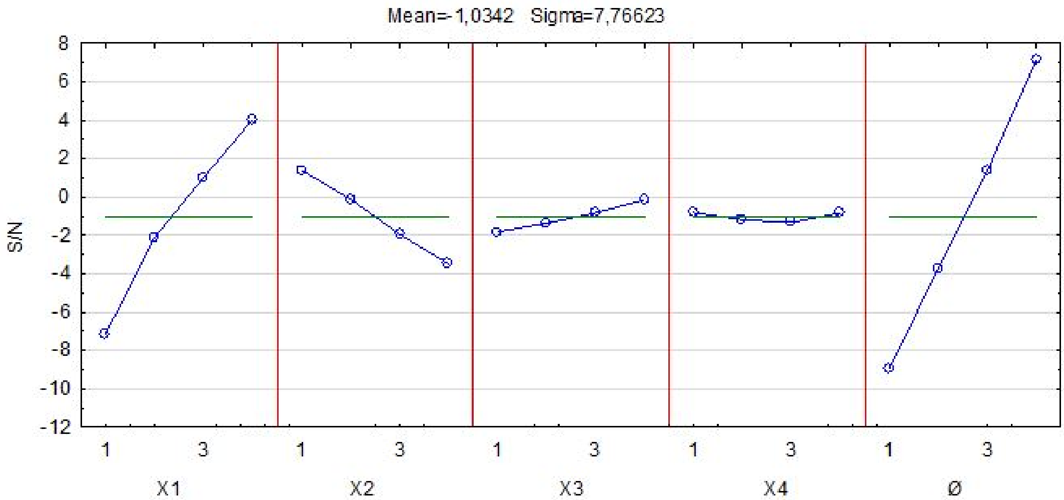

Figure 3: Change between average S/N ratio and safety factor of sliding

According to Figure 3, which is given for safety factor of overturning, the highest change of average S/N ratio is the length of base and the lowest one is the angle of front face. While levels of parameter increase, change of average S/N ratios of the length of base and the angle of internal friction go up and the others go down.

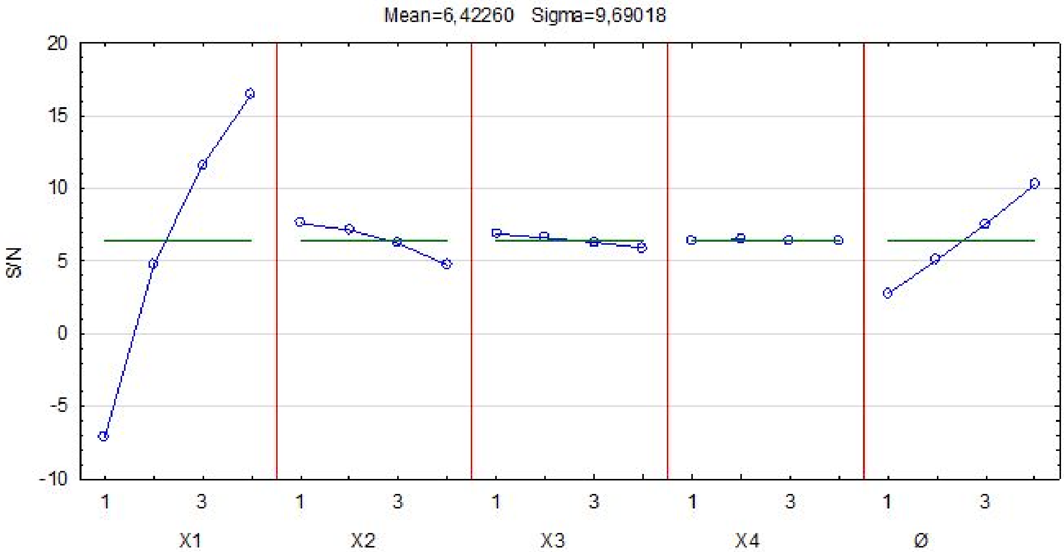

Figure 4: Change between average S/N ratio and safety factor of overturning

In Figure 3, behavior of parameters in changing of average S/N ratios is like change between average S/N ratios and safety factor of sliding.

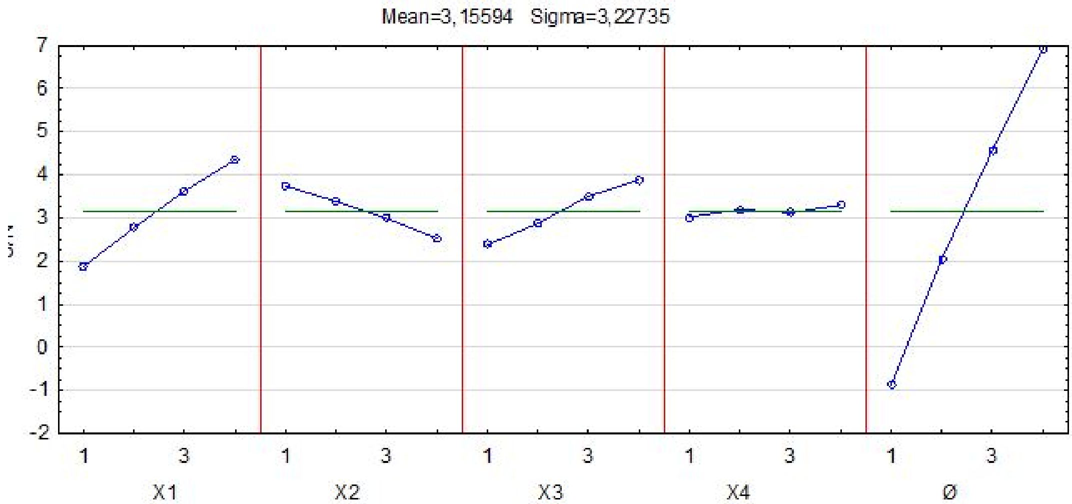

Figure 5: Change between average S/N ratio and safety factor of slope stability

In the investigation of effect of parameters on the design of cantilever retaining wall, parameters of the length of wall, the toe extension, the thickness of base, the angle of front face and the angle of internal friction are taken into consideration. To determine effect rate of parameters has been employed variance analysis. Variance is defined as sum of squares of deviations from arithmetic mean of data. Variance, a statistical term, shows distance between each number in the sequence and average of all the numbers in the series.
Effect rates of design parameters on the safety factors for H=6m is given in Table 5. It observes that parameter which is the most effective on safety factors of sliding and slope stability is the angle of internal friction which has the most value of variance. The most efficient parameter is the length of base for safety factor of overturning.

Table 5: Cantilever retaining wall results of variance analyses

Parameter		Degree of Freedom (DOF)	Sum of Squares (Ss)	Variance MS	Effect Rate (P) (%)
Sliding	Length of Base, X_1	3	273.017	91.006	30.177
	Toe Extension, X_2	3	54.253	18.084	5.997
	Thickness of base, X_3	3	6.279	2.093	0.694
	Angle of front face, X_4 (%)	3	0.809	0.270	0.089
	Angle of internal friction, Ø (°)	3	570.356	190.119	63.043
Overturning	Length of Base, X_1	3	1262.262	420.7541	89.62
	Toe Extension, X_2	3	19.420	6.4732	1.38
	Thickness of base, X_3	3	2.046	0.6820	0.15
	Angle of front face, X_4 (%)	3	0.024	0.0080	0.00
	Angle of internal friction, Ø (°)	3	124.741	41.5803	8.86
Slope Stability	Length of Base, X_1	3	13.769	4.590	8.813
	Toe Extension, X_2	3	3.251	1.084	2.081
	Thickness of base, X_3	3	5.325	1.775	3.408
	Angle of front face, X_4 (%)	3	0.160	0.053	0.102
	Angle of internal friction, Ø (°)	3	133.731	44.577	85.595

Results of optimization analyses obtained from statistical analyses for safety factors of sliding, overturning and slope stability are given respectively in Table 6, Table 7 and Table 8.

Table 6: Optimization results for maximum safety factor of sliding

Parameter	Level	Level Description	Contribution (%)
Length of Base, X_1	4	6m	30.2
Toe Extension, X_2	1	0.90m	14.5
Thickness of base, X_3	4	0.90m	5.3
Angle of front face, X_4 (%)	1	4.00	1.3
Angle of internal friction, Ø (°)	4	41	48.6
Expected maximum safety factor Fs (max) for this level			6.2
Found by numerical analysis maximum safety factor Fs (max)			6.7
Relative Error (%)			7.9

Table 7: Optimization results for maximum safety factor of overturning

Parameter	Level	Level Description	Contribution (%)
Length of Base, X_1	4	6m	64.6
Toe Extension, X_2	1	0.90m	7.6
Thickness of base, X_3	1	0.36m	2.9
Angle of front face, X_4 (%)	2	1.00	0.3
Angle of internal friction, Ø (°)	4	41	24.6
Expected maximum safety factor Fs (max) for this level			12.7
Found by numerical analysis maximum safety factor Fs (max)			12.9
Relative Error (%)			2.1

Table 8: Optimization results for maximum safety factor of slope stability

Parameter	Level	Level Description	Contribution (%)
Length of Base, X_1	4	6m	18.8
Toe Extension, X_2	1	0.90m	9.0
Thickness of base, X_3	4	0.90m	11.3
Angle of front face, X_4 (%)	4	4.00	2.2
Angle of internal friction, Ø (°)	4	41	58.7
Expected maximum safety factor Fs (max) for this level			3.0
Found by numerical analysis maximum safety factor Fs (max)			2.9
Relative Error (%)			3.3

In the results of optimization analyses of all safety factors, the length of base (X_1=4m), the toe extension (X_2=0.90m) and the angle of internal friction (Ø=41°) have same value for maximum value of safety factor. According to level description of parameters given in tables, numerical analyses have been repeated and safety factors has been obtained. Expected maximum safety factors have been compared with safety factors found by numerical analyses and the relative error has been gained. For safety factors of sliding, overturning and slope stability maximum relative error are respectively %7.9, %2.1 and %3.3.
The most effective parameter to safety factors of sliding and slope stability is the angle of internal friction that is respectively %48.6 and %58.7. The second effective parameter is the length of base, it is %30.2 for Fs (sliding) and is %18.8 for Fs (slope stability). Unlike other safety factors the most effective parameter for Fs (overturning) is the length of base with %64.6 and the second effective parameter is the angle of internal friction with %24.6.

4 Mathematical Model

In this study, the average S/N ratios have been employed to enhance the mathematical model for H=6m. Mathematical models valid for given lower-upper limits have been obtained by using average S/N ratios and parameter levels of design parameters. Each of them For calculation of Fs (sliding), Fs (overturning) and Fs (slope stability), mathematical model which is formed using different functions is given by Equation 4.

$$F_s = \sqrt{\frac{1}{10^{-\lambda/10}}} \tag{4}$$

Here, λ is total effect coefficient and it is given by Equation 5.

$$\lambda = \psi_B + \psi_{B_t} + \psi_d + \psi_m + \psi_\phi + \Delta \tag{5}$$

Here,

ψ_B : effect coefficient of the length of base, X_1(H)
ψ_{Bt} : effect coefficient of the toe extension, $X_2(X_1)$
ψ_d : effect coefficient of the thickness of base, X_3(H)
ψ_m : effect coefficient of the angle of front face, X_4
$\psi_\varnothing$: effect coefficient of the angle of internal friction, Ø
Δ : Coefficient of the average S/N ratio

Value of Δ which is changing in terms of calculation of Fs (sliding), Fs (overturning) and Fs (slope stability) are taken as respectively -1.034, 6.423 and 3.156. Detailed explanations of all effect coefficients of parameters are given in Table 9, Table 10 and Table 11 for different safety factors.

Table 9: The effect coefficients of parameters of Fs (sliding)

Lower-Upper Limits of Parameter	Mathematical Model
$0.25\ H \le B \le 1.00\ H$	$\psi_B = 18.486B^3 - 42.672B^2 + 43.961B - 14.695$
$0.15B \le B_t \le 0.60B$	$\psi_{B_t} = 28.534{B_t}^3 - 32.262{B_t}^2 - 0.1304B_t + 3.0854$
$0.06\ H \le d \le 0.15\ H$	$\psi_d = 334.17d^3 - 39.307d^2 + 15.177d - 1.6215$
$0.00 \le m \le 0.02$	$\psi_m = 1112.5m^2 - 47.793m + 0.2196$
$0.02 \le m \le 0.04$	$\psi_m = 25.456m - 0.8004$
$20\ ^\circ \le Ø \le 41\ ^\circ$	$\psi_\phi = 23.23(\tan\phi)^3 - 51.682(\tan\phi)^2 + 67.598(\tan\phi) - 26.789$

Table 10: The effect coefficients of parameters of Fs (overturning)

Lower-Upper Limits of Parameter	Mathematical Model
$0.25\ H \le B \le 1.00\ H$	$\psi_B = 31.275B^3 - 86.36B^2 + 98.437B - 33.259$
$0.15B \le B_t \le 0.60B$	$\psi_{B_{on}} = -6.1339{B_t}^3 - 4.6395{B_t}^2 - 0.0334B_t + 1.3126$
$0.06\ H \le d \le 0.15\ H$	$\psi_d = -226.44d^3 + 46.681d^2 - 12.536d + 1.0911$
$0.00 \le m \le 0.02$	$\psi_m = -675.06m^2 + 9.983m + 0.0187$
$0.02 \le m \le 0.04$	$\psi_m = 1.5988m - 0.0836$
$20\ ^\circ \le Ø \le 41\ ^\circ$	$\psi_\phi = -2.4364(\tan\phi)^3 + 1.584(\tan\phi)^2 + 15.801(\tan\phi) - 9.4873$

Table 11: The effect coefficients of parameters of Fs (slope stability)

Lower-Upper Limits of Parameter	Mathematical Model
$0.25\ H \leq B \leq 1.00\ H$	$\psi_B = -0.9481B^3 + 1.104B^2 + 3.1679B - 2.1271$
$0.15B \leq B_t \leq 0.60B$	$\psi_{B_{on}} = -0.0165{B_t}^3 - 1.1675{B_t}^2 - 1.80B_t + 0.8733$
$0.06\ H \leq d \leq 0.15\ H$	$\psi_d = -2336.4d^3 + 702.1d^2 - 48.723d - 0.118$
$0.00 \leq m \leq 0.02$	$\psi_m = -1202.6m^2 + 29.026m - 0.1358$
$0.02 \leq m \leq 0.04$	$\psi_m = 8.7062m - 0.2105$
$20\ ^\circ \leq Ø \leq 41\ ^\circ$	$\psi_\phi = 14.299(\tan\phi)^3 - 38.059(\tan\phi)^2 + 45.098(\tan\phi) - 16.095$

Safety factors of 1024 cantilever retaining wall designs which contain all value of five parameters with four levels have been obtained by both numerical analysis (Fs) and mathematical models (Fm). Belong to safety factors obtained from the numerical analysis and safety factors obtained from mathematical model, the relative error histograms for 1024 safety factors of sliding, overturning and slope stability are given respectively in Figure 6, Figure 7 and Figure 8. When histograms given in figures examine, it observes that they have approximately normal distribution.

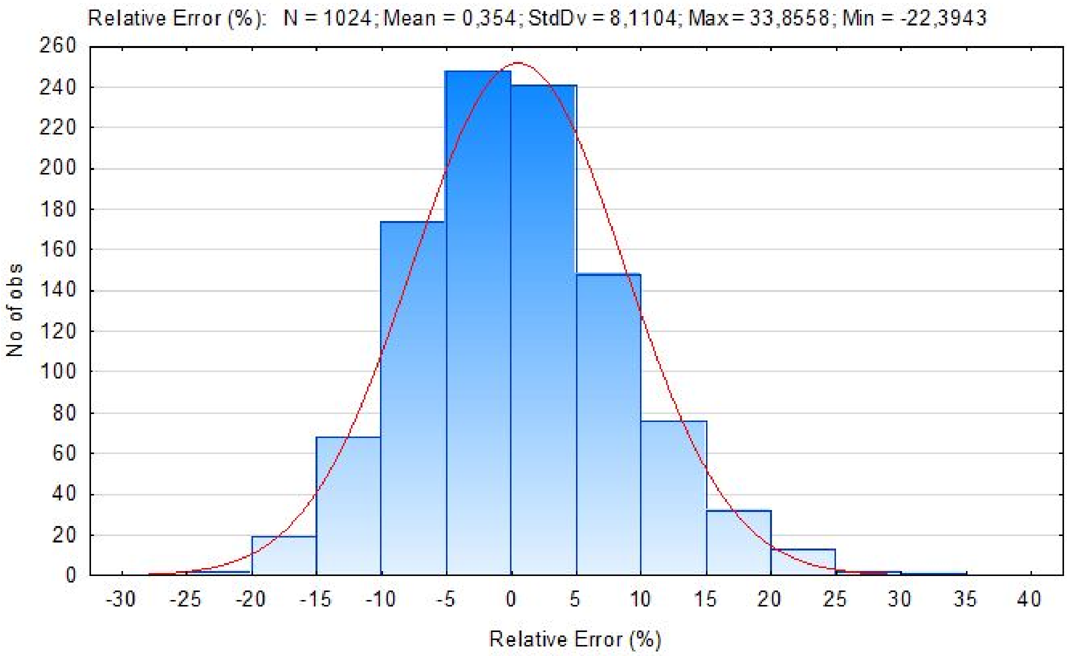

Figure 6: Distribution of relative error for safety factor of sliding

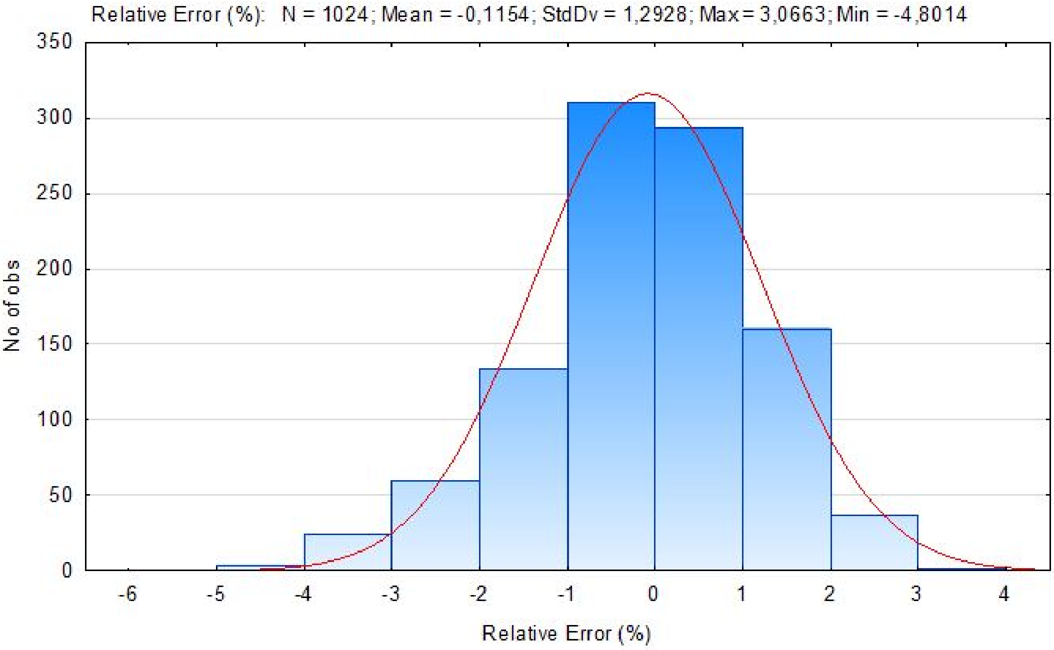

Figure 7: Distribution of relative error for safety factor of overturning

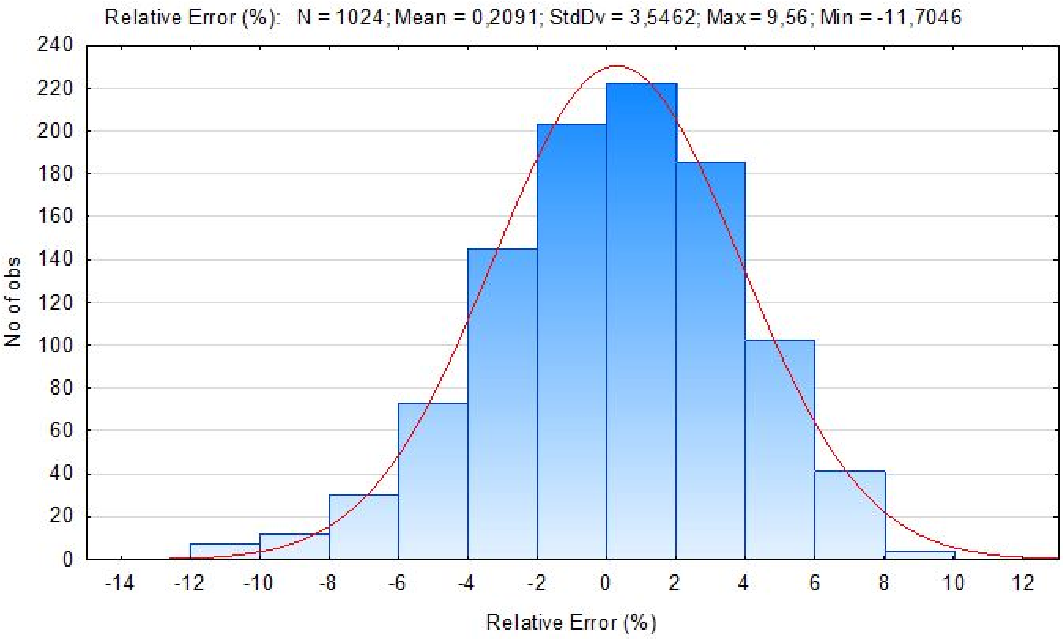

Figure 8: Distribution of relative error for safety factor of slope stability

5 Examples of Design of Cantilever Retaining Wall with Mathematical Model

To control for mathematical models of safety factors, design parameters which satisfy lower and upper limits previously mentioned of parameters have been selected randomly and 25 design have been formed by using these design parameters. All safety factors obtained from mathematical model (F_m) and numerical analyses (F_s) with randomly selected parameters are given in Table 12. The relative errors of safety factors of sliding, overturning and slope stability have been demonstrated by respectively Figure 9, Figure 10 and Figure 11.

6 Conclusions

In this study, mathematical model has been submitted used in safety factors of sliding, overturning and slope stability. In determination of models, Taguchi methods which is a one of the successful and favorable methods has been employed. Furthermore, the effects of parameters on the stability of the cantilever retaining wall have been investigated. Parameters of the length of base, the toe extension, the thickness of base, the angle of front face of wall and the angle of internal friction are taken as design parameters which have four levels each of them. By using L_{16} orthogonal design table suggested by Taguchi for fractional factorial design, 16 the cantilever retaining wall designs which formed according to L_{16} orthogonal design table have been analyzed in computer program and safety factors have been obtained. S/N, variance and optimization analyses have been performed by using safety factors obtained from numerical analyses. For determination of safety factors of sliding, overturning and slope stability, mathematical models have been formed by using average S/N ratios.

Results of the design of cantilever retaining wall with randomly selected 25 design parameters show that average absolute error is %4.8 for Fs(sliding), is %1.1 for Fs (overturning) and is %1.9 for Fs (slope stability). In 1024 designs of cantilever retaining wall with mathematical model, absolute relative errors of safety factors of sliding, overturning and slope stability are respectively %6.4, %1.0 and %2.8. When the cases are compared in terms of absolute relative error, it is observed that mathematical model derived from parameter levels may be used in determination of safety factors of sliding, overturning and slope stability even for except value of parameter levels.

The absolute relative errors obtained by using mathematical models, show that these models can be reliably used in calculation of safety factors of sliding, overturning and slope stability. Consequently, Taguchi Method can be employed in application of geotechnical engineering as an optimization technique. In future work, scope of the mathematical model can be widened for different wall height and different soil conditions.

Table 12: Results of design of cantilever retaining wall with design parameters selected randomly

No	Design Parameters					Sliding		Overturning		Slope stability	
	X_1 (H)	X_2 (X_1)	X_3 (H)	X_4 (%)	Ø (°)	F_s	F_m	F_s	F_m	F_s	F_m
1	0.30	0.20	0.07	0.011	22	0.29	0.28	0.53	0.52	0.87	0.87
2	0.35	0.22	0.10	0.039	37	1.15	1.23	1.23	1.22	1.81	1.80
3	0.45	0.50	0.13	0.022	35	0.96	0.89	1.49	1.48	1.65	1.68
4	0.65	0.40	0.10	0.031	40	2.25	2.16	4.34	4.42	2.10	2.15
5	0.90	0.55	0.11	0.012	24	0.65	0.61	3.65	3.61	1.16	1.19
6	0.80	0.35	0.10	0.025	25	0.82	0.74	3.65	3.60	1.28	1.25
7	0.40	0.44	0.14	0.034	26	0.42	0.43	0.85	0.84	1.16	1.19
8	0.55	0.28	0.08	0.028	37	1.62	1.57	3.03	3.05	1.84	1.81
9	0.95	0.24	0.13	0.036	30	1.74	1.77	6.35	6.26	1.78	1.82
10	0.60	0.26	0.07	0.018	33	1.29	1.18	3.12	3.12	1.62	1.56
11	0.70	0.42	0.10	0.026	28	0.84	0.76	2.98	3.00	1.35	1.35
12	0.39	0.34	0.13	0.038	21	0.29	0.31	0.73	0.72	0.93	0.95
13	0.85	0.17	0.13	0.035	31	1.83	1.81	5.43	5.35	1.84	1.87
14	0.45	0.45	0.08	0.013	38	1.17	1.13	1.90	1.90	1.73	1.72
15	0.92	0.56	0.07	0.024	32	1.17	1.12	5.37	5.29	1.54	1.53
16	0.28	0.19	0.10	0.038	23	0.29	0.32	0.46	0.45	0.95	0.98
17	0.37	0.43	0.11	0.025	36	0.90	0.87	1.15	1.14	1.64	1.66
18	0.42	0.56	0.08	0.032	29	0.43	0.43	1.00	0.99	1.17	1.15
19	0.96	0.28	0.14	0.022	34	2.49	2.37	7.41	7.31	2.08	2.13
20	0.36	0.31	0.07	0.032	21	0.27	0.26	0.69	0.67	0.83	0.82
21	0.28	0.38	0.14	0.014	38	1.00	0.95	0.73	0.73	1.81	1.86
22	0.77	0.54	0.11	0.027	23	0.51	0.48	2.60	2.59	1.06	1.08
23	0.56	0.53	0.10	0.034	35	1.03	1.00	2.28	2.33	1.61	1.64
24	0.82	0.59	0.14	0.039	22	0.48	0.50	2.56	2.53	1.05	1.11
25	0.43	0.28	0.07	0.024	39	1.47	1.49	2.07	2.04	1.84	1.82

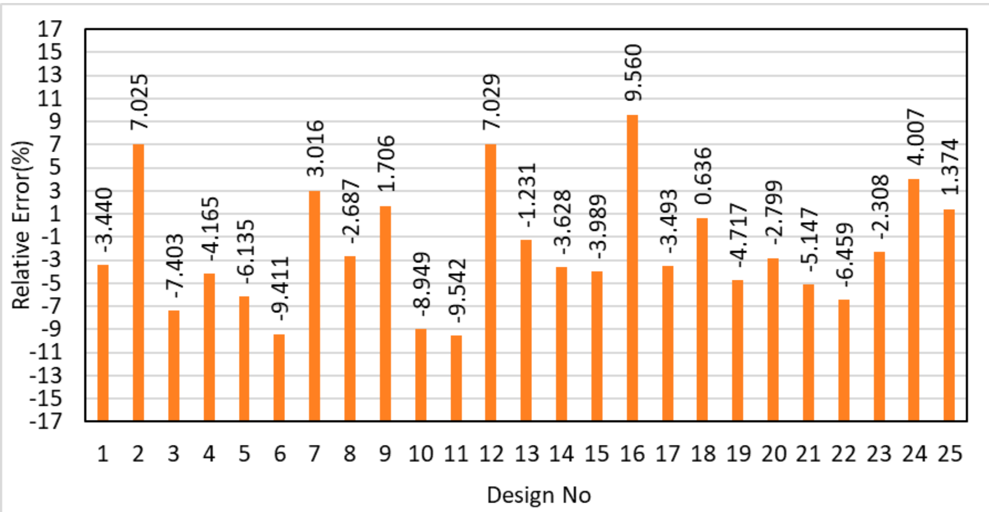

Figure 9: Relative error of randomly selected design parameters for Fs (sliding)

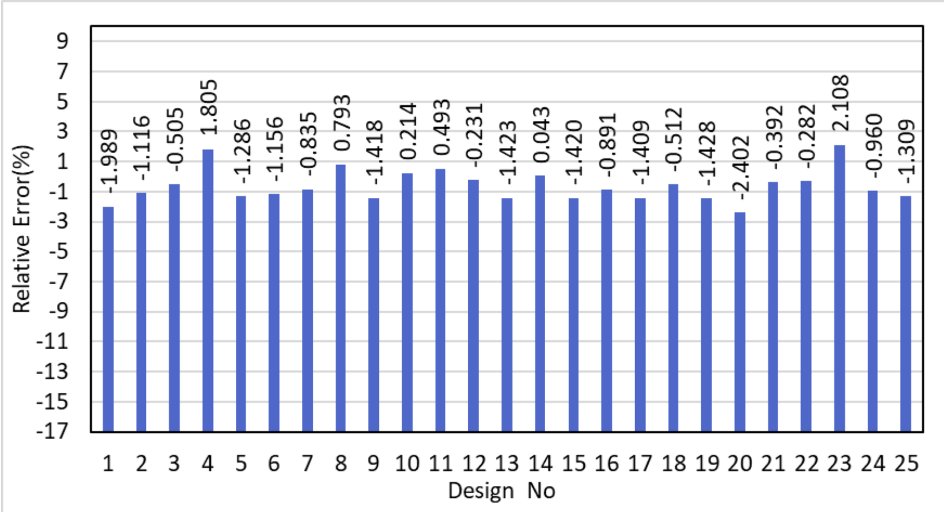

Figure 10: Relative error of randomly selected design parameters for Fs (overturning)

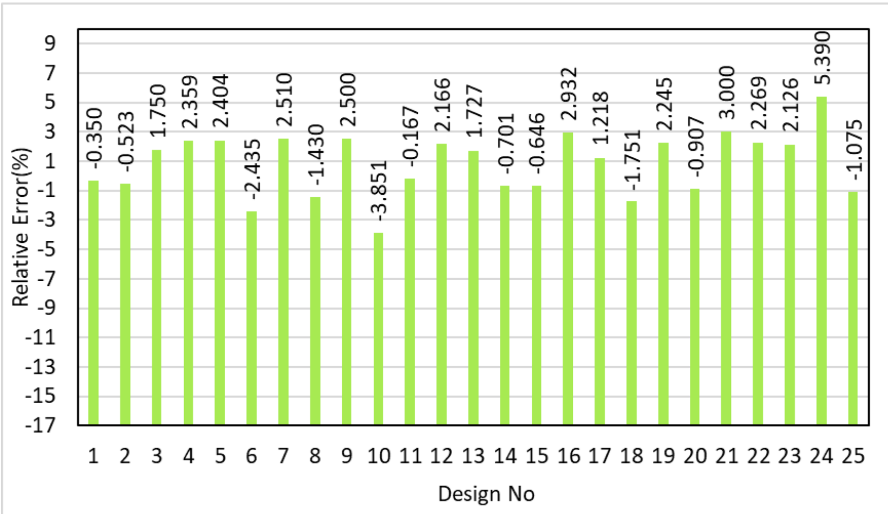

Figure 11: Relative error of randomly selected design parameters for Fs (slope stability)

Acknowledges

In this study, results of a part of continuing doctoral thesis has been submitted and also it is supported by Scientific Research Projects Coordination Units of Selcuk University Research Funding (BAP- 17401107) which are gratefully acknowledge.

References

[1] J. E. Bowles, Analytical and computer methods in foundation engineering. McGraw-Hill Companies, 1974.

[2] R. F. Bruner, H. M. Coyle, R. E. Bartoskewitz. Cantilever retaining wall design. PhD Thesis, Texas AM University, 1983.

[3] G. Taguchi, Sayed M.Ei., Hsaing C., (1989) Quality engineering and quality systems.

[4] McGraw-Hill NY. Şirvancı, M. Kalite İçin Deney Tasarımı Yaklaşımı, Taguchi Yaklaşımı. Wisconsin Üniversitesi, ABD, 1997.

[5] Ö.Tan, (2006). Investigation of soil parameters affecting the stability of homogeneous slopes using the Taguchi method. Eurasian Soil Science, 39(11), 1248-1254, 2006.

[6] E. Uray and Ö. Tan. Investigation of Design Criteria for the Type of Gabion Walls. Proceding of International Conference on Civil and Environmental Engineering (ICOCEE), 2014.

[7] Turkish Standard, Soil Retaining Structures; Properties and Guidelines for Design- TS 7994, Turkish Standards Institute, Ankara, 1990.

[8] ACI Committee 318, Building Code Requirements for Structural Concrete (ACI 318-08). American Concrete Institute (Vol. 2007), 2008.

[9] AASHTO, American Association of State Highway and Transportation Officials LRFD Bridge Design Specifications, 2010.

[10] GEO5, Geotechnical Design Computer Program, fine software, https://www.finesoftware.eu.

[11] Statictica, Statistical Analyses Computer Program, TIBCO Software Inc., https://www.tibco.com/products/tibco-statistica.

On the Bishop Hyper-Spherical Images and Their Chracterizations in 4-Dimensional Euclidean Space $\mathbb{E}^4$

Yasin ÜNLÜTÜRK*
Department of Mathematics, Kırklareli University,
39100, Kırlareli, Turkey

Hatice TOZAK
Department of Mathematics-Computer,
Eskişehir Osmangazi University, Turkey

Süha YILMAZ
Department of Primary Mathematics Education,
Dokuz Eylül University, Turkey

Abstract

In this work, we introduce new hyper-spherical images by translating Bishop frame vectors of a regular curve to the center of the unit hyper-sphere of the four-dimensional Euclidean space. Such curves are called as Bishop hyper-spherical Images. Then, Frenet-Serret apparatus of these new curves is obtained in terms of base curve's Bishop invariants.

Keywords: Bishop frame, spherical images, regular curves, general helix, slant helix, Euclidean 4-space.

1 Introduction

In the local differential geometry, curves are thought as a geometric set of points, or locus. Intuitively, a curve is figured as the path traced out by a particle moving in $\mathbb{E}^4$. So, investigating position vectors of the curves is a classical aim to determine behavior of the particle (curve). Natural scientists have long held a fascination, sometimes bordering on mystical obsession for helical structures in nature. As it is well known, curves are treated by using Frenet-Serret frame. However Serret-Frenet frame is not defined for all points along every space curve on which curvature may vanish at some points. That is, second derivative of the curve may be zero. Therefore, alternative frames were constructed. Recently, one of the most common alternative frames is parallel transport frame, also called Bishop frame which is due to L. R. Bishop in [1]. After defining this useful alternative frame, many studies have been done by mathematicians using it and type-2 Bishop frame in Euclidean and its ambient spaces [1, 3, 7, 12]. Also, Bishop frame is used in many applications such as engineering, DNA analysis computer aided design etc.

As special curves, spherical images of a regular curve are obtained in terms of Frenet-Serret frame vector fields. So, this classical topic is a well-known concept in differential geometry of the curves, see [2, 5, 6]. These spherical images were studied according to Frenet-Serret frame or Bishop frame in Euclidean and Minkowski spaces, see [9, 10, 11].

*Corresponding author. *E-mail address:* yasinunluturk@klu.edu.tr

In the light of the existing literature, this paper aims to determine new spherical images of regular curves using Bishop frame vector fields in Euclidean 4-space $\mathbb{E}^4$. We shall call such curves, respecvitely, *Tangent, M_1, M_2 and M_3 Bishop spherical images* of regular curves. Considering classical methods, we investigated relations among Frenet-Serret invariants of spherical images in terms of Bishop invariants. We have to explain that in this work we choose regular curve in Euclidean 4-space $\mathbb{E}^4$ as non-zero constant Bishop curvatures.

2 Preliminaries

Here, the basic definitions and theorems for the theory of curves in Euclidean 4-space $\mathbb{E}^4$ are briefly presented to meet the requirements in the next sections (A more complete elementary treatment can be found in [2, 4, 6]).

The standard flat metric in Euclidean 4-space $\mathbb{E}^4$ is given by

$$\langle,\rangle = dx_1^2 + dx_2^2 + dx_3^2 + dx_4^2,$$

where (x_1, x_2, x_3, x_4) is a rectangular coordinate system of Euclidean 4-space $\mathbb{E}^4$. Recall that, the norm of an arbitrary vector $a \in \mathbb{E}^4$ is given by $\|a\| = \sqrt{\langle a, a\rangle}$. The curve α is called an unit speed curve if velocity vector v of α satisfies $\|v\| = 1$. For vectors $v, w \in \mathbb{E}^4$ it is said to be orthogonal if and only if $\langle v, w\rangle = 0$. Let $\alpha = \alpha(s)$ be a regular curve in Euclidean 4-space $\mathbb{E}^4$. If the tangent vector field of this curve forms a constant angle with a constant vector field U, then this curve is called a general helix or an inclined curve.

The hyper-sphere of radius $r > 0$ and with center in the origin in Euclidean 4-space $\mathbb{E}^4$ is defined by

$$S^3 = \left\{p = (p_1, p_2, p_3, p_4) \in \mathbb{E}^4 : \langle p, p\rangle = r^2\right\}.$$

Denote by $\{T, N, B, E\}$ the moving Frenet-Serret frame along the curve α in the space $\mathbb{E}^4$. For an arbitrary curve α with the first, the second and the third curvatures, κ, τ and σ in Euclidean 4-space $\mathbb{E}^4$, the following Frenet-Serret formulae is given in [4]

$$\begin{bmatrix} T' \\ N' \\ B' \\ E' \end{bmatrix} = \begin{bmatrix} 0 & \kappa & 0 & 0 \\ -\kappa & 0 & \tau & 0 \\ 0 & -\tau & 0 & \sigma \\ 0 & 0 & -\sigma & 0 \end{bmatrix} \begin{bmatrix} T \\ N \\ B \\ E \end{bmatrix},$$

where T, N, B and E are called the tangent, the principal normal, the first and the second binormal vectors of the curve α, respectively.

Theorem 1 *([8]) Let $\alpha = \alpha(t)$ be an arbitrary curve in Euclidean 4-space $\mathbb{E}^4$ with above Frenet-Serret equations. Frenet-Serret apparatus of α can be written as follows:*

$$T = \frac{\alpha'}{\|\alpha'\|}, \tag{1}$$

$$N = \frac{\|\alpha'\|^2 \alpha'' - \langle \alpha', \alpha''\rangle \alpha'}{\left\| \|\alpha'\|^2 \alpha'' - \langle \alpha', \alpha''\rangle \alpha' \right\|}, \tag{2}$$

$$B = \mu N \wedge T \wedge B_2, \tag{3}$$

$$E=\mu\frac{T\wedge N\wedge\alpha'''}{\|T\wedge N\wedge\alpha'''\|},\tag{4}$$

$$\kappa=\frac{\left\|\|\alpha'\|^2\alpha''-\langle\alpha',\alpha''\rangle\alpha'\right\|}{\|\alpha'\|^4}\tag{5}$$

$$\tau=\frac{\|T\wedge N\wedge\alpha'''\|\,\|\alpha'\|}{\left\|\|\alpha'\|^2\alpha''-g(\alpha',\alpha'')\alpha'\right\|}\tag{6}$$

and

$$\sigma=\frac{\left\langle\alpha^{(IV)},E\right\rangle}{\|T\wedge N\wedge\alpha'''\|\,\|\alpha'\|},\tag{7}$$

where μ is taken -1 or $+1$ to make $+1$ the determinant of the matrix $[T,N,B,E]$.

Bishop frame or a parallel transport frame is an alternative approach to defining a moving frame that is well defined even when the curve has vanishing second derivative. One can express parallel transport an orthonormal frame along a curve simply by parallel transporting each component of the frame. The parallel transport is formed with tangent vector and any convenient arbitrary basis for the remainder of the frame (for details, see [1, 7]). Then, the relations between Frenet-Serret frame and parallel transport frame for the curve $\alpha:I\subset R\to\mathbb{E}^4$ are given as follows:

$$\begin{aligned}
&T(s)=T(s),\\
&N(s)=\cos\theta(s)\cos\psi(s)M_1+(-\cos\phi(s)\sin\psi(s)+\sin\phi(s)\sin\theta(s)\cos\psi(s))M_2\\
&\qquad+(\sin\phi(s)\sin\psi(s)+\cos\phi(s)\sin\theta(s)\cos\psi(s))M_3,\\
&B(s)=\cos\theta(s)\sin\psi(s)M_1+(\cos\phi(s)\cos\psi(s)+\sin\phi(s)\sin\theta(s)\sin\psi(s))M_2\\
&\qquad+(-\sin\phi(s)\cos\psi(s)+\cos\phi(s)\sin\theta(s)\sin\psi(s))M_3,\\
&E(s)=-\sin\theta(s)M_1+\sin\phi(s)\cos\theta(s)M_2+\cos\phi(s)\cos\theta(s)M_3.
\end{aligned}$$

The parallel transport frame equations are expressed as [7]

$$\begin{bmatrix}T'\\M_1'\\M_2'\\M_3'\end{bmatrix}=\begin{bmatrix}0&k_1&k_2&k_3\\-k_1&0&0&0\\-k_2&0&0&0\\-k_3&0&0&0\end{bmatrix}\begin{bmatrix}T\\M_1\\M_2\\M_3\end{bmatrix},\tag{8}$$

where k_1,k_2,k_3 are curvature functions according to parallel transport frame of the curve α their expression as follows:

$$\begin{aligned}
&k_1=\kappa\cos\theta(s)\cos\psi(s),\\
&k_2=\kappa(-\cos\phi(s)\sin\psi(s)+\sin\phi(s)\sin\theta(s)\cos\psi(s)),\\
&k_3=\kappa(\sin\phi(s)\sin\psi(s)+\cos\phi(s)\sin\theta(s)\cos\psi(s)),
\end{aligned}$$

where

$$\theta'=\frac{\sigma}{\sqrt{\kappa^2+\tau^2}},\quad\psi'=-\tau-\sigma\frac{\sqrt{\sigma^2-\theta'^2}}{\sqrt{\kappa^2+\tau^2}},\quad\phi'=-\frac{\sqrt{\sigma^2-\theta'^2}}{\cos\theta},$$

and Frenet curvature functions are given as follows:

$$\kappa(s)=\sqrt{k_1^2+k_2^2+k_3^2},\quad\tau(s)=-\psi'+\phi'\sin\theta,\quad\sigma(s)=\frac{\theta'}{\sin\psi},$$

and

$$\phi'\cos\theta+\theta'\cot\psi=0,$$

in terms of the invariants of parallel transport frame.

3 Main Results

In this section, we study Bishop spherical images of a regular curve in Euclidean 4-space $\mathbb{E}^4$. We take the regular curves into consideration as non-zero constant Bishop curvatures and $\theta \neq 0$, $\phi \neq 0$. The last condition guarantees for the curve to lie down in Euclidean 4-space $\mathbb{E}^4$. We study the mentioned images under this special case. The problem is open to study the general case.

3.1 Tangent Bishop spherical images of a regular curve

Definition 2 *Let $\gamma = \gamma(s)$ be a regular curve in Euclidean 4-space $\mathbb{E}^4$. If we translate of the first (tangent) vector field of Bishop frame T to the center O of the unit hyper-sphere S^3, we obtain a hyper-spherical image $\xi = \xi(s_\xi)$. This curve is called tangent Bishop hyper-spherical image or indicatrix of the curve $\gamma = \gamma(s)$.*

Let $\xi = \xi(s_\xi)$ be tangent Bishop spherical image of a regular cuve $\gamma = \gamma(s)$. It can be written as

$$\xi(s_\xi) = T(s). \tag{9}$$

Differentiating (9) with respect to s, we find

$$\xi' = \dot{\xi}\frac{ds_\xi}{ds} = k_1M_1 + k_2M_2 + k_3M_3.$$

Here, we shall denote differentiation according to s by a dash, and differentiation according to s_ξ by a dot. Thus, we obtain the unit tangent vector of the tangent spherical indicatrix curve ξ as

$$T_\xi = \frac{k_1M_1 + k_2M_2 + k_3M_3}{\sqrt{k_1^2 + k_2^2 + k_3^2}}$$

and

$$\|\xi'\| = \frac{ds_\xi}{ds} = \sqrt{k_1^2 + k_2^2 + k_3^2}.$$

Considering the previous method, we form the following differentiations with respect to s:

$$\begin{cases} \xi'' = -\sqrt{k_1^2 + k_2^2 + k_3^2}T, \\ \xi''' = -k_1\sqrt{k_1^2 + k_2^2 + k_3^2}M_1 - k_2\sqrt{k_1^2 + k_2^2 + k_3^2}M_2 - k_3\sqrt{k_1^2 + k_2^2 + k_3^2}M_3, \\ \xi^{(IV)} = (k_1^2 + k_2^2 + k_3^2)^{\frac{3}{2}}T. \end{cases}$$

By equation (2), we can get the principal normal vector as

$$N_\xi = -T$$

and the first curvature as

$$\kappa_\xi = \frac{1}{\sqrt{k_1^2 + k_2^2 + k_3^2}}.$$

Now, let us calculate the vector $T_\xi \wedge N_\xi \wedge \xi'''$, that is,

$$T_\xi \wedge N_\xi \wedge \xi''' = \begin{vmatrix} T & M_1 & M_2 & M_3 \\ 0 & \dfrac{k_1}{\sqrt{k_1^2 + k_2^2 + k_3^2}} & \dfrac{k_2}{\sqrt{k_1^2 + k_2^2 + k_3^2}} & \dfrac{k_3}{\sqrt{k_1^2 + k_2^2 + k_3^2}} \\ -1 & 0 & 0 & 0 \\ 0 & -k_1\sqrt{k_1^2 + k_2^2 + k_3^2} & -k_2\sqrt{k_1^2 + k_2^2 + k_3^2} & -k_3\sqrt{k_1^2 + k_2^2 + k_3^2} \end{vmatrix}.$$

This product yields

$$T_\xi \wedge N_\xi \wedge \xi''' = 0. \tag{10}$$

Hence, we obtain the trinormal (second binormal) vector field of the curve $\xi(s_\xi)$ as follows:

$$E_\xi = 0.$$

Taking the norm of both sides of (10), we find the second curvature

$$\tau_\xi = 0.$$

Finding the binormal vector field, we express

$$N_\xi \wedge T_\xi \wedge E_\xi = 0.$$

So, we obtain the binormal vector as

$$B_\xi = 0.$$

Finally, using the equations (7) and (10), it is seen that the third curvature σ_ξ is undefined.

Corollary 3 *Let $\xi = T$ be tangent Bishop spherical image of a regular curve $\gamma = \gamma(s)$. If a regular curve $\gamma = \gamma(s)$ has non-zero constant Bishop curvatures, then, we can easily have $\kappa_\xi = constant$ for $\tau_\xi = 0$. Since, the tangent spherical indicatrix ξ is a circle in the osculating plane.*

3.2 M_1 Bishop spherical images of a regular curve

Definition 4 *Let $\gamma = \gamma(s)$ be a regular curve in Euclidean 4-space $\mathbb{E}^4$. If we translate of the second vector field of Bishop frame M_1 to the center O of the unit hyper-sphere S^3, we obtain a hyper-spherical image $\delta = \delta(s_\delta)$. This curve is called M_1 Bishop hyper-spherical image or indicatrix of the curve $\gamma = \gamma(s)$.*

Let $\delta = \delta(s_\delta)$ be M_1 Bishop spherical image of a regular cuve $\gamma = \gamma(s)$. It can be written as

$$\delta(s_\delta) = M_1(s). \tag{11}$$

Differentiating (11) with respect to s, we find

$$\delta' = \dot{\delta}\frac{ds_\delta}{ds} = -k_1 T.$$

Here, we shall denote differentiation according to s by a dash, and differentiation according to s_δ by a dot. Thus, we obtain the unit tangent vector of the tangent spherical indicatrix curve δ as

$$T_\delta = -T$$

and

$$\|\delta'\| = \frac{ds_\delta}{ds} = k_1.$$

Considering the previous method, we form the following differentiations with respect to s:

$$\begin{cases} \delta'' = -k_1^2 M_1 - k_1 k_2 M_2 - k_1 k_3 M_3, \\ \delta''' = k_1(k_1^2 + k_2^2 + k_3^2)T, \\ \delta^{(IV)} = k_1^2(k_1^2 + k_2^2 + k_3^2)M_1 + k_1 k_2(k_1^2 + k_2^2 + k_3^2)M_2 + k_1 k_3(k_1^2 + k_2^2 + k_3^2)M_3. \end{cases}$$

By equation (2), we can get the principal normal vector as

$$N_\delta = -\frac{k_1}{\sqrt{k_1^2+k_2^2+k_3^2}}M_1 - \frac{k_2}{\sqrt{k_1^2+k_2^2+k_3^2}}M_2 - \frac{k_3}{\sqrt{k_1^2+k_2^2+k_3^2}}M_3$$

and the first curvature as

$$\kappa_\delta = \frac{\sqrt{k_1^2+k_2^2+k_3^2}}{k_1}.$$

Now, let us calculate the vector $T_\delta \wedge N_\delta \wedge \delta'''$, that is,

$$T_\delta \wedge N_\delta \wedge \delta''' = \begin{vmatrix} T & M_1 & M_2 & M_3 \\ -1 & 0 & 0 & 0 \\ 0 & -\frac{k_1}{\sqrt{k_1^2+k_2^2+k_3^2}} & -\frac{k_2}{\sqrt{k_1^2+k_2^2+k_3^2}} & -\frac{k_3}{\sqrt{k_1^2+k_2^2+k_3^2}} \\ k_1(k_1^2+k_2^2+k_3^2) & 0 & 0 & 0 \end{vmatrix}.$$

This product yields

$$T_\delta \wedge N_\delta \wedge \delta''' = 0. \tag{12}$$

Hence, we obtain the trinormal (second binormal) vector field of the curve $\delta(s_\delta)$ as follows:

$$E_\delta = 0.$$

Taking the norm of both sides of (12), we find the second curvature

$$\tau_\delta = 0.$$

Finding the binormal vector field, we express

$$N_\delta \wedge T_\delta \wedge E_\delta = 0.$$

So, we obtain the binormal vector as

$$B_\delta = 0.$$

Finally, using the equations (7) and (12), it is seen that the third curvature σ_δ is undefined.

Corollary 5 *Let $\delta = M_1$ be M_1 Bishop spherical image of a regular curve $\gamma = \gamma(s)$. If a regular curve $\gamma = \gamma(s)$ has non-zero constant Bishop curvatures, then, we can easily have $\kappa_\delta = constant$ and $\tau_\delta = 0$. So the M_1 hyper-spherical indicatrix δ is a circle in the osculating plane.*

3.3 M_2 Bishop spherical images of a regular curve

Definition 6 *Let $\gamma = \gamma(s)$ be a regular curve in Euclidean 4-space $\mathbb{E}^4$. If we translate of the third vector field of Bishop frame M_2 to the center O of the unit hyper-sphere S^3, we obtain a hyper-spherical image of $\psi = \psi(s_\psi)$. This curve is called M_2 Bishop hyper-spherical image or indicatrix of the curve $\gamma = \gamma(s)$.*

Let $\psi = \xi(s_\psi)$ be tangent Bishop spherical image of a regular cuve $\gamma = \gamma(s)$. It can be written as

$$\psi(s_\psi) = M_2(s). \tag{13}$$

Differentiating (13) with respect to s, we find

$$\psi' = \dot{\psi}\frac{ds_\psi}{ds} = -k_2 T.$$

Here, we shall denote differentiation according to s by a dash, and differentiation according to s_ψ by a dot. Thus, we obtain the unit tangent vector of the tangent spherical indicatrix curve ψ as

$$T_\psi = -T$$

and

$$\|\psi'\| = \frac{ds_\xi}{ds} = k_2.$$

Considering the previous method, we form the following differentiations with respect to s:

$$\begin{cases} \psi'' = -k_1k_2M_1 - k_2^2M_2 - k_2k_3M_3, \\ \psi''' = k_2(k_1^2+k_2^2+k_3^2)T, \\ \psi^{(IV)} = k_1k_2(k_1^2+k_2^2+k_3^2)M_1 + k_2^2(k_1^2+k_2^2+k_3^2)M_2 + k_2k_3(k_1^2+k_2^2+k_3^2)M_3. \end{cases}$$

By equation (2), we can get the principal normal vector as

$$N_\psi = -\frac{k_1}{\sqrt{k_1^2+k_2^2+k_3^2}}M_1 - \frac{k_2}{\sqrt{k_1^2+k_2^2+k_3^2}}M_2 - \frac{k_3}{\sqrt{k_1^2+k_2^2+k_3^2}}M_3$$

and the first curvature as

$$\kappa_\psi = \frac{\sqrt{k_1^2+k_2^2+k_3^2}}{k_2}.$$

Now, let us calculate the vector $T_\psi \wedge N_\psi \wedge \psi'''$, that is,

$$T_\psi \wedge N_\psi \wedge \psi''' = \begin{vmatrix} T & M_1 & M_2 & M_3 \\ -1 & 0 & 0 & 0 \\ 0 & -\frac{k_1}{\sqrt{k_1^2+k_2^2+k_3^2}} & -\frac{k_2}{\sqrt{k_1^2+k_2^2+k_3^2}} & -\frac{k_3}{\sqrt{k_1^2+k_2^2+k_3^2}} \\ k_2(k_1^2+k_2^2+k_3^2) & 0 & 0 & 0 \end{vmatrix}.$$

This product yields

$$T_\psi \wedge N_\psi \wedge \psi''' = 0. \tag{14}$$

Hence, we obtain the trinormal (second binormal) vector field of the curve $\psi(s_\psi)$ as follows:

$$E_\psi = 0.$$

Taking the norm of both sides of (14), we find the second curvature

$$\tau_\psi = 0.$$

Finding the binormal vector field, we express

$$N_\psi \wedge T_\psi \wedge E_\psi = 0.$$

So, we obtain the binormal vector as

$$B_\psi = 0.$$

Finally, using the equations (7) and (14), it is seen that the third curvature σ_ψ is undefined.

Corollary 7 *Let $\psi = M_2$ be M_2 Bishop spherical image of a regular curve $\gamma = \gamma(s)$. If a regular curve $\gamma = \gamma(s)$ has non-zero constant Bishop curvatures, then, we can easily have $\kappa_\psi =$ constant and $\tau_\psi = 0$. So the M_2 hyper-spherical indicatrix ψ is a circle in the osculating plane.*

3.4 M_3 Bishop spherical images of a regular curve

Definition 8 *Let $\gamma = \gamma(s)$ be a regular curve in Euclidean 4-space $\mathbb{E}^4$. If we translate of the fourth vector field of Bishop frame M_3 to the center O of the unit hyper-sphere S^3, we obtain a hyper-spherical image of $\eta = \eta(s_\eta)$. This curve is called M_3 Bishop hyper-spherical image or indicatrix of the curve $\gamma = \gamma(s)$.*

Let $\eta = \eta(s_\eta)$ be tangent Bishop spherical image of a regular cuve $\gamma = \gamma(s)$. It can be written as

$$\eta(s_\eta) = M_3(s). \tag{15}$$

Differentiating (15) with respect to s, we find

$$\eta' = \dot{\eta}\frac{ds_\eta}{ds} = -k_3 T.$$

Here, we shall denote differentiation according to s by a dash, and differentiation according to s_η by a dot. Thus, we obtain the unit tangent vector of the tangent spherical indicatrix curve η as

$$T_\eta = -T$$

and

$$\|\eta'\| = \frac{ds_\eta}{ds} = k_3.$$

Considering the previous method, we form the following differentiations with respect to s:

$$\begin{cases} \eta'' = -k_1k_3M_1 - k_2k_3M_2 - k_3^2M_3, \\ \eta''' = k_3(k_1^2+k_2^2+k_3^2)T, \\ \eta^{(IV)} = k_1k_3(k_1^2+k_2^2+k_3^2)M_1 + k_2k_3(k_1^2+k_2^2+k_3^2)M_2 + k_3^2(k_1^2+k_2^2+k_3^2)M_3. \end{cases}$$

By equation (2), we can get the principal normal vector as

$$N_\eta = -\frac{k_1}{\sqrt{k_1^2+k_2^2+k_3^2}}M_1 - \frac{k_2}{\sqrt{k_1^2+k_2^2+k_3^2}}M_2 - \frac{k_3}{\sqrt{k_1^2+k_2^2+k_3^2}}M_3$$

and the first curvature as

$$\kappa_\eta = \frac{\sqrt{k_1^2+k_2^2+k_3^2}}{k_3}.$$

Now, let us calculate the vector $T_\eta \wedge N_\eta \wedge \eta'''$, that is,

$$T_\eta \wedge N_\eta \wedge \eta''' = \begin{vmatrix} T & M_1 & M_2 & M_3 \\ -1 & 0 & 0 & 0 \\ 0 & -\frac{k_1}{\sqrt{k_1^2+k_2^2+k_3^2}} & -\frac{k_2}{\sqrt{k_1^2+k_2^2+k_3^2}} & -\frac{k_3}{\sqrt{k_1^2+k_2^2+k_3^2}} \\ k_3(k_1^2+k_2^2+k_3^2) & 0 & 0 & 0 \end{vmatrix}.$$

This product yields

$$T_\eta \wedge N_\eta \wedge \eta''' = 0. \tag{16}$$

Hence, we obtain the trinormal (second binormal) vector field of the curve $\eta(s_\eta)$ as follows:

$$E_\eta = 0.$$

Taking the norm of both sides of (16), we find the second curvature

$$\tau_\eta = 0.$$

Finding the binormal vector field, we express

$$N_\eta \wedge T_\eta \wedge E_\eta = 0.$$

So, we obtain the binormal vector as

$$B_\eta = 0.$$

Finally, using the equations (7) and (16), it is seen that the third curvature σ_η is undefined.

Corollary 9 *Let $\eta = M_3$ be M_3 Bishop spherical image of a regular curve $\gamma = \gamma(s)$. If a regular curve $\gamma = \gamma(s)$ has non-zero constant Bishop curvatures, then, we can easily have $\kappa_\eta = constant$ and $\tau_\eta = 0$. So the M_3 hyper-spherical indicatrix η is a circle in the osculating plane.*

4 Conclusion

In this study, we investigated Bishop hyper-spherical images of a regular curve with its special circumstance. The results obtained here is open and clear because of the case. It must be emphasized that that problem has to be studied in general case in Euclidean and Minkowski 4-spaces, so that strength and interesting results and characterizations for these image curves can be obtaind in these spaces.

References

[1] L. R. Bishop, There 's more than one way to frame a curve, Amer. Math. Monthly, 82(3) (200) 246–251.

[2] M.P. Do Carmo, Differential Geometry of Curves and Surfaces, Prentice Hall, Englewood Cliffs, NJ, 1976.

[3] M. Erdoğdu, Parallel frame of non lightlike curves in Minkowski space time, International Journal of Geometric Methods in Modern Physics, 12(10) (2015) (16 pages).

[4] H.H. Hacisalihoglu, Differential geometry I, Ankara University Faculty of Science Press, Ankara, 2000.

[5] S. Izumiya, N. Takeuchi, N. New special curves and developable surfaces, Turk J. Math., 28(2) (2004) 531–537.

[6] R.S. Milman, G.D. Parker, Elements of Differential Geometry, Prentice-Hall Inc., Englewood Cliffs, New Jersey, 1977.

[7] F. Özçelik, Z. Bozkurt, İ. Gök, F. Nejat Ekmekçi and Y. Yaylı, Parallel transport frame in 4-dimensional Euclidean space $\mathbb{E}^4$, Casp. J. Math. Scie. 3(1) (2014) 91-102.

[8] M. Turgut, A.T. Ali, Some characterizations of special curves in the Euclidean space $\mathbb{E}^4$, Acta Univ Sapientia Mathematica, 2(1) (2010) 111-122.

[9] S. Yılmaz, Spherical indicators of curves and characterisations of some special curves in $\mathbb{R}^4$, Master Thesis, Dokuz Eylül University, İzmir, 1996.

[10] S. Yılmaz, E. Özyılmaz, M. Turgut, New spherical indicatrices and their characterizations, An. Şt. Univ. Ovidius Constanta, 18(2) (2010) 337-354.

[11] S. Yılmaz, M. Turgut, A new version of Bishop frame and an application to spherical images, J. Math. Anal. Appl. 371(2) (2010) 764-776.

[12] S. Yılmaz, Y. Ünlütürk, A. Mağden, A study on the characterizations of non-null curves according to the Bishop frame of type-2 in Minkowski 3-space, SAÜ Fen Bil. Der., 20(2) (2016) 325-335.

Some Special Curves in $\mathbb{E}_1^4$

Süha YILMAZ
Department of Primary Mathematics Education,
Dokuz Eylül University, Turkey

Yasin ÜNLÜTÜRK*
Department of Mathematics, Kırklareli University, Turkey

Abstract

In this study, we introduce a new special curve by means of spherical images in $\mathbb{E}_1^4$. Firstly, Smarandache breadth curves of tangent spherical images are defined in $\mathbb{E}_1^4$. Moreover, a four order vectorial differential equation of position vector of Smarandache breadth curves has been obtained in this space. Finally, we study the differential equation characterizing tangent spherical images of constant breadth for special cases in $\mathbb{E}_1^4$.
Keywords: Tangent spherical images, spherical images, Smarandache curves, constant breadth of curves, differential equation.

1 Introduction

Curves are thought as a geometric set of points, or locus in the local differential geometry. Studying their position vectors is a classical endeavour to determine behavior of the particle (curve) [1], [2], [5]. The classical results in the theory of curves were initiated by G. Monge, and the moving frame idea was pioneered by G. Darboux. Thereafter Jean Frédéric Frenet defined the famous frame and its special equations which play an important role in mechanics and kinematics as well as in differential geometry [11]. Curves of constant breadth were introduced by Leonhard Euler [6]. M.Fujivera [7] had obtained a problem to determine whether there exist space curve of constant breadth or not, and he defined breadth for space curves and obtained these curves on surfaces of constant breadth. Moreover, Some geometric properties of plane curves of constant breadth were given in [8] and, in another works [4], [5], [9], these properties were studied in the Euclidean $3-$space $\mathbb{E}^3$. In [4], these curves have been also studied in four dimensional Euclidean space $\mathbb{E}^4$. In this study, by using tangent spherical images of a spacelike curve in $\mathbb{E}_1^4$, we introduce a new special curve of tangents pherical images which are also called tangent spherical images of constant breadth. Firstly, Smarandache breadth curves of tangent spherical images are defined in $\mathbb{E}_1^4$. Moreover, a four order vectorial differential equation of position vector of Smarandache breadth curves has been obtained in this space. Finally, we study the differential equation characterizing tangent spherical images of constant breadth for special cases in $\mathbb{E}_1^4$.

2 Preliminaries

Minkowski space-time $\mathbb{E}_1^4$ is the real vector space $\mathbb{R}^4$ endowed with the standard Lorentzian metric given by

$$g = -dx_1^2 + dx_2^2 + dx_3^2 + dx_4^2,$$

*Corresponding author. *E-mail address:* yasinunluturk@klu.edu.tr

where (x_1, x_2, x_3, x_4) is a rectangular coordinate system in $\mathbb{E}_1^4$ [2]. Since g is an indefinite metric, recall that a vector $v \in \mathbb{E}_1^4$ can have one of the three causal characters; it can be spacelike if $g(v,v) > 0$ or $v = 0$, timelike if $g(v,v) < 0$ and null (lightlike) if $g(v,v) = 0$ and $v \neq 0$. Similary, an arbitrary curve $\alpha = \alpha(s)$ in $\mathbb{E}_1^4$ can be locally spacelike, timelike or null (lightlike), if all of its velocity vectors $\alpha'(s)$ are respectively spacelike, timelike or null. Also, recall the norm of a vector v is given by

$$\|v\| = \sqrt{|g(v,v)|}.$$

Therefore, v is a unit vector if $g(v,v) = \pm 1$. Next, vectors v, w in $\mathbb{E}_1^4$ are said to be orthogonal if $g(v,w) = 0$. The velocity of the curve $\alpha(s)$ is given by $\|\alpha'(s)\|$ [3]. The pseudohyperbolic space with center $m = (m_1, m_2, m_3, m_4) \in \mathbb{E}_1^4$ and radius $r \in R^+$ in the space-time $\mathbb{E}_1^4$ is the hyperquadric

$$H_0^3(r) = \{a = (a_1, a_2, a_3, a_4) \in \mathbb{E}_1^4 \mid g(a-m, a-m) = -r^2\}.$$

with dimension 3 and index 0 [2]. Denote by $\{T(s), N(s), B(s), E(s)\}$ the moving Frenet-Serret frame along the curve $\alpha(s)$ in the space $\mathbb{E}_1^4$. Then T, N, B, E are, respectively, the tangent, the principal normal, the binormal (the first binormal) and the trinormal (the second binormal) vector fields. A spacelike or timelike curve $\alpha(s)$ is said to be parametrized by arclength function s if $g(\alpha'(s), \alpha'(s)) = \pm 1$. Let $\alpha(s)$ be a spacelike curve in the space-time $\mathbb{E}_1^4$, parametrized by arclength function s. Then, the following Frenet-Serret equations are given in [3]:

$$\begin{bmatrix} T' \\ N' \\ B' \\ E' \end{bmatrix} = \begin{bmatrix} 0 & \kappa & 0 & 0 \\ -\kappa & 0 & \tau & 0 \\ 0 & \tau & 0 & \sigma \\ 0 & 0 & \sigma & 0 \end{bmatrix} \begin{bmatrix} T \\ N \\ B \\ E \end{bmatrix},$$

where T, N, B and E are mutually orthogonal vectors satisfying equations

$$g(T,T) = g(N,N) = g(E,E) = 1, \; g(B,B) = -1.$$

and the functions κ, τ and σ are first, second and third curvatures of the curve α, respectively.

Definition 1 *([3]) Let $a = (a_1, a_2, a_3, a_4)$, $b = (b_1, b_2, b_3, b_4)$ and $c = (c_1, c_2, c_3, c_4)$ be vectors in $\mathbb{E}_1^4$. The vector product in Minkowski space-time $\mathbb{E}_1^4$ is defined by the determinant*

$$a \wedge b \wedge c = - \begin{vmatrix} -e_1 & e_2 & e_3 & e_4 \\ a_1 & a_2 & a_3 & a_4 \\ b_1 & b_2 & b_3 & b_4 \\ c_1 & c_2 & c_3 & c_4 \end{vmatrix},$$

where e_1, e_2, e_3 and e_4 are mutually orthogonal vectors (coordinate direction vectors) satisfying equations

$$e_1 \wedge e_2 \wedge e_3 = e_4, e_2 \wedge e_3 \wedge e_4 = e_1, e_3 \wedge e_4 \wedge e_1 = e_2, e_4 \wedge e_1 \wedge e_2 = -e_3.$$

Theorem 2 *([3]) Let $\alpha = \alpha(t)$ be an arbitrary spacelike curve in Minkowski space-time $\mathbb{E}_1^4$. The Frenet-Serret apparatus of α can be written as follows;*

$$T = \frac{\alpha'}{\|\alpha'\|},$$

$$N = \frac{\|\alpha'\|^2 \alpha'' - g(\alpha', \alpha'')\alpha'}{\left\| \|\alpha'\|^2 \alpha'' - g(\alpha', \alpha'')\alpha' \right\|},$$

$$B = \mu N \wedge T \wedge E,$$

$$E = \mu \frac{T \wedge N \wedge \alpha'''}{\|T \wedge N \wedge \alpha'''\|},$$

$$\kappa = \frac{\left\| \|\alpha'\|^2 \alpha'' - g(\alpha', \alpha'')\alpha' \right\|}{\|\alpha'\|^4}$$

$$\tau = \frac{\|T \wedge N \wedge \alpha'''\| \, \|\alpha'\|}{\left\| \|\alpha'\|^2 \alpha'' - g(\alpha', \alpha'')\alpha' \right\|}$$

and

$$\sigma = \frac{g(\alpha^{(IV)}, E)}{\|T \wedge N \wedge \alpha'''\| \, \|\alpha'\|},$$

where μ *is taken* -1 *or* $+1$ *to make* $+1$ *the determinant of* $[T, N, B, E]$ *matrix.*

Theorem 3 *([3]) Let* $\varphi = \varphi(s)$ *be tangent spherical image of the curve* $\alpha = \alpha(t)$ *in Minkowski space-time* $\mathbb{E}_1^4$*. The Frenet-Serret vector fields of* φ *are given in terms of Frenet-Serret vector fields of* α *as follows;*

$$T_1 = N, \quad N_1 = \frac{-\kappa T + \tau B}{\sqrt{\kappa^2 + \tau^2}},$$

$$B_1 = -\frac{1}{A} \begin{vmatrix} T & N & B & -\mathbb{E} \\ \tau^2 \sigma & 0 & \kappa \tau \sigma & -\tau^2 (\frac{\kappa}{\tau})' \\ 0 & 1 & 0 & 0 \\ -\frac{1}{\kappa_1} & 0 & \frac{\tau}{\kappa \kappa_1} & 0 \end{vmatrix}$$

$$E_1 = \frac{\mu}{A}(-\tau^2 \sigma T + \kappa \tau \sigma B - \tau^2 (\frac{\kappa}{\tau})' \mathbb{E}),$$

$$\kappa_1 = \frac{\sqrt{\kappa^2 + \tau^2}}{\kappa}, \quad \sigma_1 = \frac{\sqrt{\kappa^2 \tau^2 \sigma^2 \kappa_1^2 - \tau^4 (\frac{\kappa}{\tau})'^2}}{\kappa},$$

where the vector fields T_1, N_1, B_1, E_1 *belong to the spherical image curve* φ*, and* μ *is taken* -1 *or* $+1$ *to make* $+1$ *the determinant of* $[T, N, B, E]$ *matrix.*

3 Main Result

A regular curve in $\mathbb{E}_1^4$, whose position vector is obtained by Frenet frame vectors on another regular curve, is called Smarandache curve. A regular curve with more than 2 breadths in Minkowski 4-space is called Smarandache breadth curve. Let $\varphi = \varphi(s)$ be a Smarandache breadth curve. Moreover, let $\varphi = \varphi(s)$ be spacelike tangent spherical image curve in the space $\mathbb{E}_1^4$. These curves will be denoted by (C). The normal plane at every point P on the curve meets the curve at a single point Q other than P. We call the point Q as the opposite point of P. We consider a curve in the class Γ as in having parallel tangents T and T^* opposite directions at opposite points φ and $\varphi^*$of the curves. A simple closed curve having parallel tangents in opposite directions at opposite points can be represented with respect to Frenet frame by the equation

$$\varphi^*(s) = \varphi(s) + m_1 T_1 + m_2 N_1 + m_3 B_1 + m_4 E_1 \tag{3.1}$$

where $m_i(s)$, $1 \leq i \leq 4$ are arbitrary functions and φ and φ^* are opposite points. Differentiating both sides of (3.1) and considering Frenet equations, we have

$$\begin{aligned} \frac{d\varphi^*}{ds} = \overrightarrow{T_1}^* \frac{ds^*}{ds} = (1 + \frac{dm_1}{ds} - m_2\kappa_1)T_1 + (m_1 k_1 + \frac{dm_2}{ds} - m_3\tau_1)N_1 \\ +(\frac{dm_3}{ds} + m_4\sigma_1 + m_2\tau_1)B_1 + (\frac{dm_4}{ds} + m_3\sigma_1)E_1 \end{aligned} \tag{3.2}$$

Since $T_1^* = -T$, rewriting (3.2), we have respectively,

$$\begin{aligned} \frac{dm_1}{ds} &= m_2\kappa_1 - 1 - \frac{ds^*}{ds} \\ \frac{dm_2}{ds} &= m_3\tau_1 - m_1\kappa_1 \\ \frac{dm_3}{ds} &= -m_2\tau_1 - m_4\sigma_1 \\ \frac{dm_4}{ds} &= -m_3\sigma_1. \end{aligned} \tag{3.3}$$

If we call θ as the angle between the tangent of the curve (C) at point $\varphi(s_1)$ with a given direction and consider

$$\frac{d\varphi}{ds} = \kappa,$$

we have (3.3) as follow;

$$\begin{aligned} \frac{dm_1}{d\theta} &= m_2 - f(\theta), \\ \frac{dm_2}{d\theta} &= -m_1 + \rho\tau_1 m_3, \\ \frac{dm_3}{d\theta} &= -\rho\tau_1 m_2 - \rho\sigma_1 m_3, \\ \frac{dm_4}{d\theta} &= -\rho\sigma_1 m_3, \end{aligned} \tag{3.4}$$

where

$$f(\theta) = \rho + \rho^* \quad \rho = \frac{1}{\kappa_1}, \rho^* = \frac{1}{\kappa_1^*} \tag{3.5}$$

denote the radius of curvature at φ and φ^* respectively. And using system (3.4), we have the following differential equation with respect to m_1 as

$$\begin{aligned} \{\frac{1}{\rho\sigma_1}[\frac{1}{\rho\tau_1}(m_1'' + m_1)] + \frac{\tau_1}{\sigma_1}m_1'\}' + \frac{\sigma_1}{\tau_1}(m_1'' - m_1) \\ +\{\frac{1}{\rho\sigma}(\frac{1}{\rho\tau}f')' - \frac{\tau_1}{\sigma_1}f\} + \frac{\sigma_1}{\tau_1}f' = 0 \end{aligned} \tag{3.6}$$

The Eq. (3.6) is a characterization for φ^*. If the distance between opposite points of (C) and (C^*) is constant, then, we can write that

$$\|\varphi^* - \varphi\| = m_1^2 + m_2^2 + m_3^2 - m_4^2 = \psi^2 = \text{constant}. \tag{3.7}$$

Hence, we write

$$m_1\frac{dm_1}{d\theta} + m_2\frac{dm_2}{d\theta} + m_3\frac{dm_3}{d\theta} - m_4\frac{dm_4}{d\theta} = 0 \tag{3.8}$$

Considering system (3.4), we obtain

$$m_1 f(\theta) = 0. \tag{3.9}$$

We write $m_1 = 0$ or $f(\theta) = 0$, thus, we shall study the Eq. (3.9) in the following subcase: Case 1. Let $m_1 = 0$ and $m_2 = c_2$ =constant, then from (3.4), we obtain

$$\begin{aligned} &f(\theta) = \text{constant}, \\ &m_3\rho\tau_1 = 0, \\ &\frac{dm_3}{d\theta} = -\rho\tau_1 c_2 - \rho\sigma_1 m_4, \\ &\frac{dm_4}{d\theta} = -\rho\sigma_1 m_4. \end{aligned} \tag{3.10}$$

Due to this, we distinguish the following subcases: Case 1.1. Suppose that $m_3 = 0$, then from (3.4) we find that

$$m_4 = c_4 = \text{constant}, \quad \text{and} \quad \frac{\tau_1}{\sigma_1} = -\frac{c_4}{c_2} = \text{constant}.$$

Case 1.2. Suppose that $m_3 \neq 0$, then we have

$$\tau_1 = 0, \kappa_1 \neq 0,$$

thus we find that

$$(\frac{\kappa\sigma}{\tau})^2 = (\frac{\kappa}{\tau})'.$$

Then the solution of this differential equation is as follows:

$$\frac{\kappa}{\tau} = \mp e^{\int_0^s \sigma(s)ds}.$$

Case 2. Let $m_1 = c_1$ =constant and $m_2 = 0$, then

$$\begin{aligned} &f(\theta) = 0, \\ &m_3 = \frac{\sqrt{1 + (\frac{\tau}{\kappa})^2} c_1}{\sqrt{\kappa^2\tau^2\sigma^2\kappa_1^2 - \tau^4(\frac{\kappa}{\tau})'^2}}. \end{aligned}$$

Corollary 3.1. Position vector of φ^* can be formed by the case 1.1 as

$$\varphi^* = \varphi + c_2 N_1 + c_4 E_1. \tag{3.11}$$

The distance between the opposite points of (C) and (C^*) is

$$\|\varphi^* - \varphi\| = c_2^2 - c_4^2 = \text{ constant}. \tag{3.12}$$

4 Conclusion

In this study, we studied tangent spherical images of constant breadt in Minkowski space-time $\mathbb{E}_1^4$. The differential equation characterizing this new special curve was examined for special cases in Minkowski space-time $\mathbb{E}_1^4$. As a open research problem, the other spherical images of constant breadth such as normal, binormal, and trinormal spherical images of constant breadth wait to be studied in both Euclidean and Minkowski spaces.

Acknowledgement

The authors would like to thank the anonymous reviewers for their valuable comments and suggestions to improve the quality of the paper.

References

[1] N. Ekmekçi, Lorentz manifoldları üzerinde eğilim çizgileri (in Turkish), PhD Dissertation, Inst. Natural Sci. Ankara Uni. 1991.

[2] B. O'Neill, Semi-Riemannian geometry, Academic Press, NY, 1983.

[3] S. Yılmaz, Spherical indicators of curves and characterizations of some special curves in four dimensional Lorentzian space, PhD Dissertation, Inst. Edu. Sci. Dokuz Eylül Uni. 2001.

[4] A. Mağden, $\mathbb{R}^4$ uzayında bazı özel eğriler ve karakterizasyonları (in Turkish), PhD Dissertation, Inst. Natural Sci. Atatürk Uni. 1990.

[5] A. Mağden and Ö. Köse, On the curves of constant breadth, Turk J. Math, 227-284, 1997.

[6] L. Euler, De curvis triangularibus, Acta Acad Petropol, 3-30, 1870.

[7] M. Fujivara, On space curves of constant breadth, Tohoku Math. J., 5, pp. 179-184, 1914.

[8] Ö. Köse, Some properties of ovals and curves of constant width in a plane, Doğa Turk Math. J., 8, 119-126, 1984.

[9] Ö. Köse, On space curves of constant breadth, Doğa Turk Math. J. (10)1, 11-14, 1986.

[10] S. Yılmaz and M. Turgut, On the time-like curves of constant breadth in Minkowski 3-space, International J. Math.Combin, 3, 34-39, 2008.

[11] C. B. Boyer, A history of mathematics, John Wiley & Sons Inc., New York, 1968.

Smarandache Curves of Anti-Salkowski Curve According to Frenet Frame

Süleyman ŞENYURT*
Department of Mathematics, Ordu University, Turkey

Burak ÖZTÜRK
Karamanoglu Mehmetbey University,
Department of Mathematics, Ordu University, Turkey

Abstract

In this paper, when the Frenet vectors of Anti-Salkowski curve are taken as the position vectors, the curvature and the torsion of Smarandache curves are calculated. These values are expressed depending upon the Anti-Salkowski curve.

Keywords: Anti-salkowski curve, Smarandache curves, Frenet invariants.

1 Introduction

Anti-Salkowski curves are, to the best of the author's knowledge, the first known family of curves with constant curvature but non-constant torsion with an explicit parametrization. They were defined in an earlier paper [4], [5] A regular curve in Minkowski space-time, whose position vector is composed by Frenet frame vectors on another regular curve, is called a Smarandache curve [3]. Special Smarandache curves have been studied by some authors. Ahmad T.Ali studied some special Smarandache curves in the Euclidean space. He studied Frenet-Serret invariants of a special case [1].Bektaş, Ö., and Yüce, S., studied some special Smarandache curves according to Darboux Frame in E^3 [2]. In this paper, special Smarandache curves belonging to Anti-Salkowski curve such as TN, NB, TB and TNB drawn by Frenet frame are defined and some related results are given.

2 Preliminaries

In differential geometry, special curves have an important role. One of these curves Smarandache curves. Smarandache curves was firstly defined by M. Turgut and S. Yılmaz in 2008 [3]. Let $\gamma = \gamma(t)$ be a regular curve with unit speed. Then the Frenet apparatus of the curve (γ) are [1]

$$\begin{cases} T(t) = \gamma'(t), & N(t) = \frac{T'(t)}{\|T'(t)\|}, & B(t) = T(t) \wedge N(t) \\ \kappa(t) = \|T'(t)\|, & \tau(t) = \frac{\det\left(\gamma'(t),\gamma''(t),\gamma'''(t)\right)}{\left(\|\gamma'(t)\wedge\gamma''(t)\|\right)^2} & T' = \kappa N, \\ T' = \kappa N, & N' = -\kappa T + \tau B, & B' = -\tau N \end{cases} \tag{1}$$

*Corresponding author. *E-mail address:* senyurtsuleyman@hotmail.com

Another important curve is Anti-Salkowski curves. Firstly, definition of Anti-Salkowski curves is given by Anti-Salkowski [4] and finally definition of Anti-Salkowski curves is given by Monterde [5].

Definition 1 *For any $m \in \mathbb{R}$ with $m \neq \mp\frac{1}{\sqrt{3}}$, 0, let us define the space curve*

$$\begin{aligned}\gamma_m(t) \;=\; & \Bigg(\frac{n\Big(n(1-4n^2+3\cos(2nt))\cos(t)+(2n^2+1)\sin(t)\sin(2nt)\Big)}{2(4n^2-1)m}, \\ & \frac{n\Big(n(1-4n^2+3\cos(2nt))\sin(t)-(2n^2+1)\cos(t)\sin(2nt)\Big)}{2(4n^2-1)m}, \\ & \frac{n^2-1}{4n}(2nt+\sin(2nt))\Bigg) \quad \text{where} \quad n=\frac{m}{\sqrt{1+m^2}}.\end{aligned}$$

The geometric elements of the Anti-Salkowski curve γ_m are

$$\begin{aligned}&\|\gamma_m(t)\| = \frac{cos(nt)}{\sqrt{1+m^2}} \quad \text{so the curve is regular in} \quad [-\frac{\pi}{2n},\frac{\pi}{2n}], \\ &\kappa=\tan(nt), \quad \tau=1.\end{aligned} \tag{2}$$

The Frenet apparatus are

$$\begin{aligned}T(t) &= \Big(-\cos(t)\sin(nt)+n\sin(t)\cos(nt), -\sin(t)\sin(nt)-n\cos(t)\cos(nt), \\ &\quad -\frac{n}{m}\cos(nt)\Big), \\ N(t) &= n\left(\frac{\sin(t)}{m}, -\frac{\cos(t)}{m}, 1\right), \\ B(t) &= \Big(-\cos(t)\cos(nt)-n\sin(t)\sin(nt), -\sin(t)\cos(nt)+n\cos(t)\sin(nt), \\ &\quad \frac{n}{m}\sin(nt)\Big).\end{aligned} \tag{3}$$

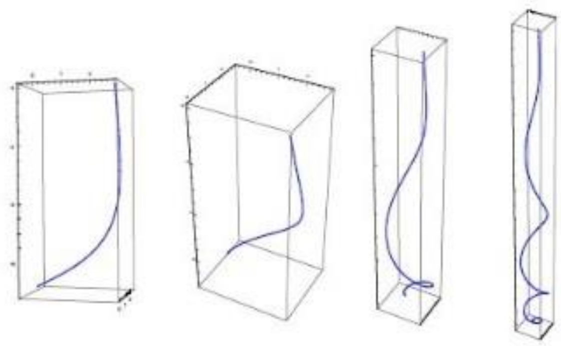

Figure 1: Anti-Salkowski Curve, $m=\frac{1}{3},\frac{1}{5},\frac{1}{8},\frac{1}{16}$.

3 Smarandache Curves of Anti-Salkowski Curve According to Frenet Frame

In this section we shall investigate some curves such that they are obtained with binary and triple summations of the position vectors of Frenet vectors of a Salkowski curve.

Definition 2 *Let $\gamma = \gamma(t)$ be a Anti-Salkowski curve in E^3 and $\{T, N, B\}$ be the Frenet frame. Then TN-Smarandache curve is by*

$$\gamma_1(t) = \frac{1}{\sqrt{2}}(T(t) + N(t)).$$

According to this definition we can parametrize the TN - Smarandache curve as in that form

$$\begin{aligned} \gamma_1(t) = \frac{1}{\sqrt{2}}\Big(& \cos(t)\sin(nt) - n\sin(t)\cos(nt) + \frac{n}{m}\sin(t), -\sin(t)\sin(nt) \\ & -n\cos(t)\cos(nt) - \frac{n}{m}\cos(t), -\frac{n}{m}\cos(nt) + n\Big). \end{aligned} \tag{4}$$

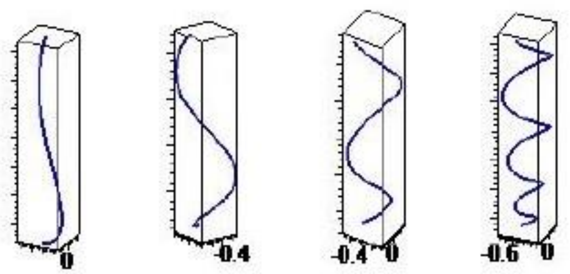

Figure 2: TN-Smarandache Curve, $m = \frac{1}{3}, \frac{1}{5}, \frac{1}{8}, \frac{1}{16}$.

Theorem 3 *Let $\gamma(t)$ be a Anti-Salkowski curve in $E^3$and $\{T, N, B\}$ be the Frenet Frame. Then the Frenet frame of the TN-Smarandache curve is given $\{T_{\gamma_1}, N_{\gamma_1}, B_{\gamma_1}\}$,*

$$\begin{aligned}
T_{\gamma_1}(t) &= \Big(-\frac{n}{m}\sin(t)\sin(nt) - \cos(t), -\frac{n}{m}\cos(t)\sin(nt) + \sin(t), n\sin(nt)\Big), \\
N_{\gamma_1}(t) &= \Big(\lambda_1\Big(\sin(t) - \frac{n}{m}\cos(t)\sin(nt)\Big) + n\cos(nt)\Big(\cos(t)\sin(nt) - \frac{n}{m}\sin(t)\Big), \\
&\quad \lambda_1\Big(\frac{n}{m}\sin(t)\sin(nt) + \cos(t)\Big) - n\cos(nt)\Big(\sin(t)\sin(nt) + \frac{n}{m}\cos(t)\Big), \\
&\quad n^2\cos(nt)\Big), \\
B_{\gamma_1}(t) &= \Big(-n\cos(t)\sin(nt) + n^2\sin(t)\cos(nt) - \frac{n^2}{m}\sin(t)\sin^2(nt), \\
&\quad n\sin(t)\sin(nt) + n^2\cos(t)\cos(nt) - \frac{n^2}{m}\cos(t)\sin^2(nt), \\
&\quad -\frac{n^2}{m^2}\sin^2(nt) + \frac{n^2}{m}\cos(nt) - 1\Big).
\end{aligned} \tag{5}$$

Proof. If we take the derivative in equation (4) we get

$$\gamma_1'(t) = \frac{1}{\sqrt{2}}\frac{n}{m}\left(a_1T + b_1N + c_1B\right). \tag{6}$$

Here the coefficients a_1, b_1 and c_1 are given

$$a_1 = -\frac{n}{m}\sin(t)\sin(nt) - \cos(t), \quad b_1 = -\frac{n}{m}\cos(t)\sin(nt) + \sin(t), \quad c_1 = n\sin(nt).$$

If we take the norm in the equation (6),

$$\|\gamma_1'(t)\| = \frac{n}{m}\sqrt{\lambda_1} \quad where \quad \lambda_1 = \sin^2(nt) + 1. \tag{7}$$

We obtained the tangent of TN-Smarandache curve as in

$$T_{\gamma_1}(t) = \frac{1}{\sqrt{\lambda_1}}\left(a_1T + b_1N + c_1B\right). \tag{8}$$

The derivative in the (6) is

$$\gamma_1''(t) = \frac{1}{\sqrt{2}}\frac{n}{m}\left(a_2T + b_2N + c_2B\right), \tag{9}$$

here the coefficients are given

$$\begin{aligned}
a_2 &= -\frac{n}{m}\cos(t)\sin(nt) - \frac{n^2}{m}\sin(t)\cos(nt) + \sin(t),\\
b_2 &= \frac{n}{m}\sin(t)\sin(nt) - \frac{n^2}{m}\cos(t)\cos(nt) + \cos(t),\\
c_2 &= n^2\cos(nt).
\end{aligned}$$

From equations (6) and (9) we have

$$\gamma_1'(t) \wedge \gamma_1''(t) = \frac{1}{2}\frac{n^2}{m^2}(a_3T + b_3N + c_3B), \tag{10}$$

then the coefficients are given

$$\begin{aligned}
a_3 &= -n\cos(t)\sin(nt) + n^2\sin(t)\cos(nt) - \frac{n^2}{m}\sin(t)\sin^2(nt),\\
b_3 &= n\sin(t)\sin(nt) + n^2\cos(t)\cos(nt) - \frac{n^2}{m}\cos(t)\sin^2(nt),\\
c_3 &= -\frac{n^2}{m^2}\sin^2(nt) + \frac{n^2}{m}\cos(nt) - 1.
\end{aligned}$$

If we take the norm in equation (10), it becomes

$$\|\gamma_1'(t) \wedge \gamma_1''(t)\| = \frac{1}{2}\frac{n^3}{m^3}\sqrt{\lambda_1^2 - 2m\mu_1} \quad where \quad \mu_1 = \lambda_1\cos(nt) - m. \tag{11}$$

From the equaiton (1) binormal vector of TN-Smarandache curve is given as

$$B_{\gamma_1}(t) = \frac{1}{\frac{n}{m}\sqrt{\lambda_1^2 - 2m\mu_1}}(a_4T + b_4N + c_4B) \tag{12}$$

with the coefficients as follows

$$\begin{aligned}
a_4 &= -n\cos(t)\sin(nt) + n^2\sin(t)\cos(nt) - \frac{n^2}{m}\sin(t)\sin^2(nt),\\
b_4 &= n\sin(t)\sin(nt) + n^2\cos(t)\cos(nt) - \frac{n^2}{m}\cos(t)\sin^2(nt),\\
c_4 &= -\frac{n^2}{m^2}\sin^2(nt) + \frac{n^2}{m}\cos(nt) - 1.
\end{aligned}$$

From (1) principal normal vector of TN-Smarandache curve can be written as

$$N_{\gamma_1}(t) = \frac{1}{\frac{n}{m}\sqrt{\lambda_1^3 - 2\lambda_1\mu_1}}\left(a_5T + b_5N + c_5B\right) \tag{13}$$

and the coefficients are

$$\begin{aligned}
a_5 &= \lambda_1 \left(\sin(t) - \frac{n}{m}\cos(t)\sin(nt)\right) + n\cos(nt)\left(\cos(t)\sin(nt) - \frac{n}{m}\sin(t)\right),\\
b_5 &= \lambda_1 \left(\cos(t) + \frac{n}{m}\sin(t)\sin(nt)\right) - n\cos(nt)\left(\sin(t)\sin(nt) + \frac{n}{m}\cos(t)\right),\\
c_5 &= n^2\cos(nt).
\end{aligned}$$

Theorem 4 *Let $\gamma(t)$ be a Anti-Salkowski curve in E^3. Then the curvature and torsion according to γ_1-Smarandache curve are, respectively,*

$$\kappa_{\gamma_1}(t) = \sqrt{\frac{2\lambda_1^2 - 4m\mu_1}{\lambda_1^3}}, \quad \tau_{\gamma_1}(t) = \frac{\rho_1\sqrt{2}\cos(nt)}{\lambda_1^2 - 2m\mu_1}.$$

Proof. From the expressions (1), curvature of the TN-Smarandache curve can be written

$$\kappa_{\gamma_1}(t) = \sqrt{\frac{2\lambda_1^2 - 4m\mu_1}{\lambda_1^3}}. \tag{14}$$

If we take the derivative in equation (9), it becomes

$$\gamma_1'''(t) = \frac{1}{\sqrt{2}}\frac{n}{m}\left(a_6T + b_6N + c_6B\right). \tag{15}$$

Here the coefficients a_6, b_6 and c_6 are

$$\begin{aligned}
a_6 &= -\left(\frac{n}{m} + \frac{n^3}{m}\right)\sin(t)\sin(nt) - 2\frac{n^2}{m}\cos(t)\cos(nt) + \cos(t),\\
b_6 &= \left(\frac{n}{m} + \frac{n^3}{m}\right)\cos(t)\sin(nt) + 2\frac{n^2}{m}\sin(t)\cos(nt) - \sin(t),\\
c_6 &= -n^3\sin(nt).
\end{aligned}$$

From equations (6), (9) and (15) torsion of the TN-Smarandache curve is

$$\tau_{\gamma_1}(t) = \frac{\rho_1\sqrt{2}\cos(nt)}{\lambda_1^2 - 2m\mu_1}, \quad \textit{where} \quad \rho_1 = 3m^2\cos(nt) - m\lambda_1. \tag{16}$$

Definition 5 *Let $\gamma = \gamma(t)$ be a Anti-Salkowski curve in E^3 and $\{T, N, B\}$ be the Frenet frame. Then NB-Smarandache curve is by*

$$\gamma_2(t) = \frac{1}{\sqrt{2}}(N(t) + B(t)).$$

According to this definition we can parametrize the NB - Smarandache curve as in that form

$$\begin{aligned}
\gamma_2(t) = \frac{1}{\sqrt{2}}\Bigg(& -\cos(t)\cos(nt) - n\sin(t)\sin(nt) + \frac{n}{m}\sin(t),\\
& -\sin(t)\cos(nt) + n\cos(t)\sin(nt) - \frac{n}{m}\cos(t), \frac{n}{m}\sin(nt) + n\Bigg).
\end{aligned} \tag{17}$$

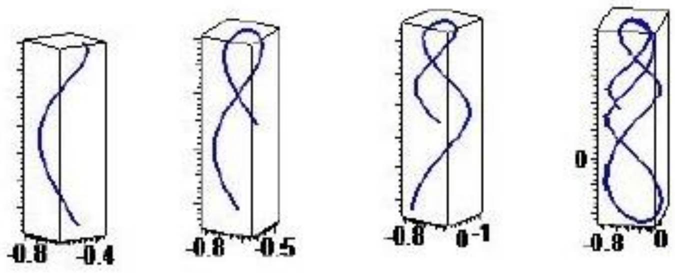

Figure 3: NB-Smarandache Curve, $m = \frac{1}{3}, \frac{1}{5}, \frac{1}{8}, \frac{1}{16}$.

Theorem 6 *Let $\gamma(t)$ be a Anti-Salkowski curve in E^3 and $\{T, N, B\}$ be the Frenet Frame. Then the Frenet frame of the NB-Smarandache curve is given $\{T_{\gamma_2}, N_{\gamma_2}, B_{\gamma_2}\}$ (as figure 2),*

$$\begin{aligned}
T_{\gamma_2}(t) &= \Big(\frac{n}{m}\sin(t)\cos(nt) + \cos(t), -\frac{n}{m}\cos(t)\cos(nt) + \sin(t), n\cos(nt)\Big),\\
N_{\gamma_2}(t) &= \Bigg(\lambda_2\Big(\frac{n}{m}\cos(t)\cos(nt) - \sin(t)\Big) + n\sin(nt)\Big(\cos(t)\cos(nt) - \frac{n}{m}\sin(t)\Big),\\
&\quad \lambda_2\Big(\frac{n}{m}\sin(t)\cos(nt) + \cos(t)\Big) + n\sin(nt)\Big(\sin(t)\cos(nt) + \frac{n}{m}\cos(t)\Big)\\
&\quad -n^2\sin(nt), n^2\cos(nt)\Bigg),\\
B_{\gamma_2}(t) &= \Bigg(-n\cos(t)\cos(nt) - n^2\sin(t)\sin(nt) - \frac{n^2}{m}\sin(t)\cos^2(nt),\\
&\quad -n\sin(t)\cos(nt) + n^2\cos(t)\sin(nt) + \frac{n^2}{m}\cos(t)\cos^2(nt),\\
&\quad \frac{n^2}{m^2}\cos^2(nt) + \frac{n^2}{m}\sin(nt) + 1\Bigg). \qquad (18)
\end{aligned}$$

Proof. If we take the derivative in equation (17) we get

$$\gamma_2'(t) = \frac{1}{\sqrt{2}}\frac{n}{m}\left(a_7T + b_7N + c_7B\right). \qquad (19)$$

Here the coefficients a_7, b_7 and c_7 are given

$$a_7 = \frac{n}{m}\sin(t)\cos(nt) + \cos(t), \quad b_7 = -\frac{n}{m}\cos(t)\cos(nt) + \sin(t), \quad c_7 = n\cos(nt).$$

If we take the norm in the equation (19),

$$\|\gamma_2'(t)\| = \frac{n}{m}\sqrt{\lambda_2} \quad where \quad \lambda_2 = \cos^2(nt) + 1. \qquad (20)$$

We obtained the tangent of NB-Smarandache curve as in

$$T_{\gamma_2}(t) = \frac{1}{\sqrt{\lambda_2}}\left(a_7T + b_7N + c_7B\right). \qquad (21)$$

The derivative in the (19) is

$$\gamma_2''(t) = \frac{1}{\sqrt{2}}\frac{n}{m}\left(a_8T + b_8N + c_8B\right), \qquad (22)$$

here the coefficients are given

$$\begin{aligned}
a_8 &= \frac{n}{m}\cos(t)\cos(nt) - \frac{n^2}{m}\sin(t)\sin(nt) - \sin(t),\\
b_8 &= \frac{n}{m}\sin(t)\cos(nt) + \frac{n^2}{m}\cos(t)\sin(nt) + \cos(t),\\
c_8 &= -n^2\sin(nt).
\end{aligned}$$

From equations (19) and (22) we have

$$\gamma_2'(t) \wedge \gamma_2''(t) = \frac{1}{2}\frac{n^2}{m^2}(a_9 T + b_9 N + c_9 B), \tag{23}$$

then the coefficients are given

$$\begin{aligned} a_9 &= -n\cos(t)\cos(nt) - n^2\sin(t)\sin(nt) - \frac{n^2}{m}\sin(t)\cos^2(nt), \\ b_9 &= -n\sin(t)\cos(nt) + n^2\cos(t)\sin(nt) + \frac{n^2}{m}\cos(t)\cos^2(nt), \\ c_9 &= \frac{n^2}{m^2}\cos^2(nt) + \frac{n^2}{m}\sin(nt) + 1. \end{aligned}$$

If we take the norm in equation (23), it becomes

$$\|\gamma_2'(t) \wedge \gamma_2''(t)\| = \frac{1}{2}\frac{n^3}{m^3}\sqrt{\lambda_2^2 + 2m\mu_2} \quad where \quad \mu_2 = \lambda_2\sin(nt) + m. \tag{24}$$

From the equaiton (1) binormal vector of NB-Smarandache curve is given as

$$B_{\gamma_2}(t) = \frac{1}{\frac{n}{m}\sqrt{\lambda_2^2 + 2m\mu_2}}(a_{10}T + b_{10}N + c_{10}B) \tag{25}$$

with the coefficients as follows

$$\begin{aligned} a_{10} &= -n\cos(t)\cos(nt) - n^2\sin(t)\sin(nt) - \frac{n^2}{m}\sin(t)\cos^2(nt), \\ b_{10} &= -n\sin(t)\cos(nt) + n^2\cos(t)\sin(nt) + \frac{n^2}{m}\cos(t)\cos^2(nt), \\ c_{10} &= \frac{n^2}{m^2}\cos^2(nt) + \frac{n^2}{m}\sin(nt) + 1. \end{aligned}$$

From (1) principal normal vector of NB-Smarandache curve can be written as

$$N_{\gamma_2}(t) = \frac{1}{\frac{n}{m}\sqrt{\lambda_2^3 + 2\lambda_2\mu_2}}(a_{11}T + b_{11}N + c_{11}B) \tag{26}$$

and the coefficients are

$$\begin{aligned} a_{11} &= \lambda_2\left(-\sin(t) + \frac{n}{m}\cos(t)\cos(nt)\right) + n\sin(nt)\left(\cos(t)\cos(nt) - \frac{n}{m}\sin(t)\right), \\ b_{11} &= \lambda_2\left(\cos(t) + \frac{n}{m}\sin(t)\cos(nt)\right) + n\sin(nt)\left(\sin(t)\cos(nt) + \frac{n}{m}\cos(t)\right), \\ c_{11} &= -n^2\sin(nt). \end{aligned}$$

Theorem 7 *Let $\gamma(t)$ be a Anti-Salkowski curve in E^3. Then the curvature and torsion according to γ_2-Smarandache curve are, respectively,*

$$\kappa_{\gamma_2}(t) = \sqrt{\frac{2\lambda_2^2 + 4m\mu_2}{\lambda_2^3}}, \quad \tau_{\gamma_2}(t) = \frac{\rho_2\sqrt{2}\sin(nt)}{\lambda_2^2 + 2m\mu_2}.$$

Proof. From the expressions (1), curvature of the NB-Smarandache curve can be written

$$\kappa_{\gamma_2}(t) = \sqrt{\frac{2\lambda_2^2 + 4m\mu_2}{\lambda_2^3}}. \tag{27}$$

If we take the derivative in equation (22), it becomes

$$\gamma_2'''(t) = \frac{1}{\sqrt{2}}\frac{n}{m}(a_{12}T + b_{12}N + c_{12}B). \tag{28}$$

Here the coefficients a_{12}, b_{12} and c_{12} are

$$\begin{aligned} a_{12} &= -\left(\frac{n}{m} + \frac{n^3}{m}\right)\sin(t)\cos(nt) - 2\frac{n^2}{m}\cos(t)\sin(nt) - \cos(t), \\ b_{12} &= \left(\frac{n}{m} + \frac{n^3}{m}\right)\cos(t)\cos(nt) - 2\frac{n^2}{m}\sin(t)\sin(nt) - \sin(t), \\ c_{12} &= -n^3\cos(nt). \end{aligned}$$

From equations (19), (22) and (28) torsion of the NB-Smarandache curve is

$$\tau_{\gamma_2}(t) = \frac{\rho_2\sqrt{2}\sin(nt)}{\lambda_2^2 + 2m\mu_2}, \quad where \quad \rho_2 = 3m^2\sin(nt) + m\lambda_2. \tag{29}$$

Definition 8 *Let $\gamma = \gamma(t)$ be a Anti-Salkowski curve in E^3 and $\{T, N, B\}$ be the Frenet frame. Then TB-Smarandache curve is by*

$$\gamma_3(t) = \frac{1}{\sqrt{2}}(T(t) + B(t)).$$

According to this definition we can parametrize the TB - Smarandache curve as in that form

$$\begin{aligned}\gamma_3(t) = \frac{1}{\sqrt{2}}\Big(&-\cos(t)\sin(nt) + n\sin(t)\cos(nt) - \cos(t)\cos(nt)\\ &-n\sin(t)\sin(nt), -\sin(t)\sin(nt) - n\cos(t)\cos(nt)\\ &-\sin(t)\cos(nt) + n\cos(t)\sin(nt), -\frac{n}{m}\cos(nt) + \frac{n}{m}\sin(nt)\Big).\end{aligned} \tag{30}$$

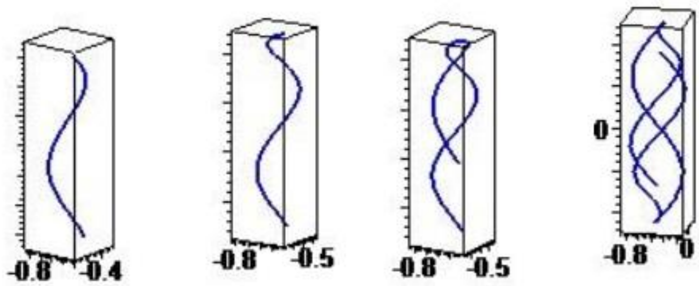

Figure 4: TB-Smarandache Curve, $m = \frac{1}{3}, \frac{1}{5}, \frac{1}{8}, \frac{1}{16}$.

Theorem 9 *Let $\gamma(t)$ be a Anti-Salkowski curve in E^3 and $\{T, N, B\}$ be the Frenet Frame. Then the Frenet frame of the TB-Smarandache curve is given $\{T_{\gamma_3}, N_{\gamma_3}, B_{\gamma_3}\}$ (as figure 2),*

$$\begin{aligned} T_{\gamma_3}(t) &= \left(\frac{n}{m}\sin(t), -\frac{n}{m}\cos(t), +n\right), \\ N_{\gamma_3}(t) &= (\cos(t), \sin(t), 0), \\ B_{\gamma_3}(t) &= \left(-n\sin(t), n\cos(t), \frac{n}{m}\right). \end{aligned} \tag{31}$$

Proof. If we take the derivative in equation (3.27) we get

$$\gamma_3'(t) = \frac{1}{\sqrt{2}}\frac{n}{m}(\cos(nt) + \sin(nt))\left(a_{13}T + b_{13}N + c_{13}B\right). \tag{32}$$

Here the coefficients a_{13}, b_{13} and c_{13} are given

$$a_{13} = \frac{n}{m}\sin(t), \quad b_{13} = -\frac{n}{m}\cos(t), \quad c_{13} = n.$$

If we take the norm in the equation (32),

$$\|\gamma_3'(t)\| = \frac{1}{\sqrt{2}}\frac{n}{m}(\cos(nt) + \sin(nt)) \quad where \quad \lambda_3 = \cos(nt) + \sin(nt). \tag{33}$$

We obtained the tangent of TB-Smarandache curve as in

$$T_{\gamma_3}(t) = \left(a_{13}T + b_{13}N + c_{13}B\right). \tag{34}$$

The derivative in the (32) is

$$\gamma_3''(t) = \frac{1}{\sqrt{2}}\frac{n}{m}\left(a_{14}T + b_{14}N + c_{14}B\right), \tag{35}$$

here the coefficients are given

$$a_{14} = \frac{n}{m}\cos(t)\lambda_3 + \frac{n^2}{m}\sin(t)\varphi_1, \quad b_{14} = \frac{n}{m}\sin(t)\lambda_3 - \frac{n^2}{m}\cos(t)\varphi_1, \quad c_{14} = n^2\varphi_1$$

where $\varphi_1 = \cos(nt) - \sin(nt)$. From equations (32) and (35) we have

$$\gamma_3'(t) \wedge \gamma_3''(t) = \frac{1}{2}\frac{n^3}{m^3}(a_{15}T + b_{15}N + c_{15}B), \tag{36}$$

then the coefficients are given

$$a_{15} = -n\sin(t), \quad b_{15} = n\cos(nt), \quad c_{15} = \frac{n}{m}.$$

If we take the norm in equation (36), it becomes

$$\|\gamma_3'(t) \wedge \gamma_3''(t)\| = \frac{1}{2}\frac{n^3}{m^3}\lambda_3 \tag{37}$$

From the equaiton (1) binormal vector of TB-Smarandache curve is given as

$$B_{\gamma_3}(t) = (a_{16}T + b_{16}N + c_{16}B) \tag{38}$$

with the coefficients as follows

$$a_{16} = -n\sin(t), \quad b_{16} = n\cos(t), \quad c_{16} = \frac{n}{m}.$$

From (1) principal normal vector of TB-Smarandache curve can be written as

$$N_{\gamma_3}(t) = (a_{17}T + b_{17}N + c_{17}B) \tag{39}$$

and the coefficients are

$$a_{17} = \cos(t), \quad b_{17} = \sin(t), \quad c_{17} = 0.$$

Theorem 10 *Let $\gamma(t)$ be a Anti-Salkowski curve in E^3. Then the curvature and torsion according to γ_3-Smarandache curve are, respectively,*

$$\kappa_{\gamma_3}(t) = \frac{\sqrt{2}}{\lambda_3}, \quad \tau_{\gamma_3}(t) = \frac{m\sqrt{2}}{\lambda_3}.$$

Proof. From the expressions (1), curvature of the TB-Smarandache curve can be written

$$\kappa_{\gamma_3}(t) = \frac{\sqrt{2}}{\lambda_3}. \tag{40}$$

If we take the derivative in equation (35), it becomes

$$\gamma_3'''(t) = \frac{1}{\sqrt{2}}\frac{n}{m}\left(a_{18}T + b_{18}N + c_{18}B\right). \tag{41}$$

Here the coefficients a_{18}, b_{18} and c_{18} are

$$\begin{aligned} a_{18} &= -\left(\frac{n}{m} + \frac{n^3}{m}\right)\sin(t)\lambda_3 + 2\frac{n^2}{m}\cos(t)\varphi_1, \\ b_{18} &= \left(\frac{n}{m} + \frac{n^3}{m}\right)\cos(t)\lambda_3 + 2\frac{n^2}{m}\sin(t)\varphi_1, \\ c_{18} &= -n^3\lambda_3. \end{aligned}$$

From equations (32), (35) and (41) torsion of the TB-Smarandache curve is

$$\tau_{\gamma_3}(t) = \frac{m\sqrt{2}}{\lambda_3}. \tag{42}$$

Definition 11 *Let $\gamma=\gamma(t)$ be a Anti-Salkowski curve in E^3 and $\{T,N,B\}$ be the Frenet frame. Then TNB-Smarandache curve is by*

$$\gamma_4(t) = \frac{1}{\sqrt{3}}(T(t)+N(t)+B(t)).$$

According to this definition we can parametrize the TNB - Smarandache curve as in that form

$$\begin{aligned}\gamma_4(t) = \frac{1}{\sqrt{3}}\Big(& -\cos(t)\sin(nt)-\cos(t)\cos(nt)+n\sin(t)\cos(nt)\\ & -n\sin(t)\sin(nt)+\frac{n}{m}\sin(t), -\sin(t)\sin(nt)-\sin(t)\cos(nt)\\ & -n\cos(t)\cos(nt)+n\cos(t)\sin(nt)-\frac{n}{m}\cos(t), -\frac{n}{m}\cos(nt)\\ & +\frac{n}{m}\sin(nt)+n\Big).\end{aligned} \tag{43}$$

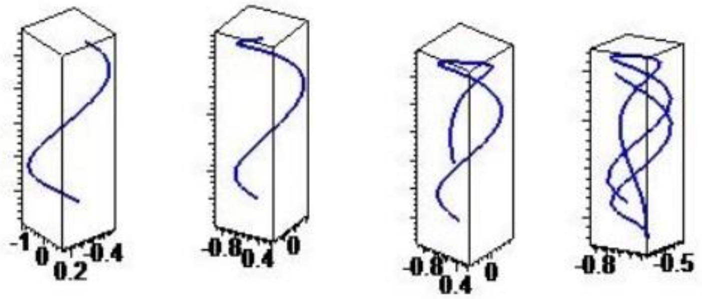

Figure 5: TNB-Smarandache Curve, $m=\frac{1}{3},\frac{1}{5},\frac{1}{8},\frac{1}{16}$.

Theorem 12 *Let $\gamma(t)$ be a Anti-Salkowski curve in E^3 and $\{T,N,B\}$ be the Frenet Frame. Then the Frenet frame of the TNB-Smarandache curve is given $\{T_{\gamma_4},N_{\gamma_4},B_{\gamma_4}\}$ (as figure 2),*

$$\begin{aligned}T_{\gamma_4}(t) &= \Big(\frac{n}{m}\sin(t)\lambda_3+\cos(t), -\frac{n}{m}\cos(t)\lambda_3+\sin(t), n\lambda_3\Big),\\ N_{\gamma_4}(t) &= \Big(\lambda_4\Big(\frac{n}{m}\cos(t)\lambda_3-\sin(t)\Big)+n\varphi_1\Big(\frac{n}{m}\sin(t)-\cos(t)\lambda_3\Big),\\ &\quad \lambda_4\Big(\frac{n}{m}\sin(t)\lambda_3+\cos(t)\Big)-n\varphi_1\Big(\frac{n}{m}\cos(t)+\sin(t)\lambda_3\Big), n^2\varphi_1\Big),\\ B_{\gamma_4}(t) &= \Big(-n\cos(t)\lambda_3+n^2\sin(t)\varphi_1-\frac{n^2}{m}\sin(t)\lambda_3^2, -n\sin(t)\lambda_3\\ &\quad -n^2\cos(t)\varphi_1+\frac{n^2}{m}\cos(t)\lambda_3^2, \frac{n^2}{m^2}\lambda_3^2-\frac{n^2}{m}\varphi_1+1\Big).\end{aligned} \tag{44}$$

Proof. If we take the derivative in equation (3.40) we get

$$\gamma_4'(t)=\frac{1}{\sqrt{3}}\frac{n}{m}\left(a_{19}T+b_{19}N+c_{19}B\right). \tag{45}$$

Here the coefficients a_{19}, b_{19} and c_{19} are given

$$a_{19}=\frac{n}{m}\sin(t)\lambda_3+\cos(t),\quad b_{19}=-\frac{n}{m}\cos(t)\lambda_3+\sin(t),\quad c_{19}=n\lambda_3.$$

If we take the norm in the equation (45),

$$\|\gamma_4'(t)\|=\frac{1}{\sqrt{3}}\frac{n}{m}\sqrt{\lambda_4}\quad where\quad \lambda_4=\lambda_3^2+1. \tag{46}$$

We obtained the tangent of TNB-Smarandache curve as in

$$T_{\gamma_4}(t)=\frac{1}{\sqrt{\lambda_3}}\frac{n}{m}\left(a_{19}T+b_{19}N+c_{19}B\right). \tag{47}$$

The derivative in the (45) is

$$\gamma_4''(t)=\frac{1}{\sqrt{3}}\frac{n}{m}\left(a_{20}T+b_{20}N+c_{20}B\right), \tag{48}$$

here the coefficients are given

$$\begin{aligned}
a_{20} &= \frac{n}{m}\cos(t)\lambda_3+\frac{n^2}{m}\sin(t)\varphi_1-\sin(t),\\
b_{20} &= \frac{n}{m}\sin(t)\lambda_3-\frac{n^2}{m}\cos(t)\varphi_1+\cos(t),\\
c_{20} &= n^2\varphi_1.
\end{aligned}$$

From equations (45) and (48) we have

$$\gamma_4'(t)\wedge\gamma_4''(t)=\frac{1}{3}\frac{n^2}{m^2}(a_{21}T+b_{21}N+c_{21}B), \tag{49}$$

then the coefficients are given

$$\begin{aligned}
a_{21} &= -n\cos(t)\lambda_3+n^2\sin(t)\varphi_1-\frac{n^2}{m}\sin(t)\lambda_3^2,\\
b_{21} &= -n\sin(t)\lambda_3-n^2\cos(t)\varphi_1+\frac{n^2}{m}\cos(t)\lambda_3^2,\\
c_{21} &= \frac{n^2}{m^2}\lambda_3^2-\frac{n^2}{m}\varphi_1+1.
\end{aligned}$$

If we take the norm in equation (49), it becomes

$$\|\gamma_4'(t)\wedge\gamma_4''(t)\|=\frac{1}{3}\frac{n^3}{m^3}\sqrt{\lambda_4^2-m\mu_3}\quad where\quad \mu_3=2\varphi_1\lambda_4-3m. \tag{50}$$

From the equaiton (1) binormal vector of TNB-Smarandache curve is given as

$$B_{\gamma_4}(t)=\frac{1}{\frac{n}{m}\sqrt{\lambda_2^2+2m\mu_2}}(a_{22}T+b_{22}N+c_{22}B) \tag{51}$$

with the coefficients as follows

$$\begin{aligned}
a_{22} &= -n\cos(t)\lambda_3+n^2\sin(t)\varphi_1-\frac{n^2}{m}\sin(t)\lambda_3^2,\\
b_{22} &= -n\sin(t)\lambda_3-n^2\cos(t)\varphi_1+\frac{n^2}{m}\cos(t)\lambda_3^2,\\
c_{22} &= \frac{n^2}{m^2}\lambda_3^2-\frac{n^2}{m}\varphi_1+1.
\end{aligned}$$

From (1) principal normal vector of TNB-Smarandache curve can be written as

$$N_{\gamma_4}(t)=\frac{1}{\sqrt{\lambda_4^3-\lambda_4\mu_3}}\left(a_{23}T+b_{23}N+c_{23}B\right) \tag{52}$$

and the coefficients are

$$\begin{aligned}
a_{23} &= \lambda_4\left(-\sin(t)+\frac{n}{m}\cos(t)\lambda_3\right)+n\varphi_1\left(-\cos(t)\lambda_3+\frac{n}{m}\sin(t)\right),\\
b_{23} &= \lambda_4\left(\cos(t)+\frac{n}{m}\sin(t)\lambda_3\right)-n\varphi_1\left(\sin(t)\lambda_3+\frac{n}{m}\cos(t)\right),\\
c_{23} &= n^2\varphi_1.
\end{aligned}$$

Theorem 13 *Let $\gamma(t)$ be a Anti-Salkowski curve in E^3. Then the curvature and torsion according to γ_4-Smarandache curve are, respectively,*

$$\kappa_{\gamma_4}(t)=\sqrt{\frac{3\lambda_4^2-3m\mu_3}{\lambda_4^3}},\quad \tau_{\gamma_4}(t)=\frac{\rho_3 m\sqrt{3}\lambda_4}{\lambda_4^2-m\mu_3}.$$

Proof. From the expressions (1), curvature of the TNB-Smarandache curve can be written

$$\kappa_{\gamma_4}(t)=\sqrt{\frac{3\lambda_4^2-3m\mu_3}{\lambda_4^3}}. \tag{53}$$

If we take the derivative in equation (48), it becomes

$$\gamma_4'''(t)=\frac{1}{\sqrt{3}}\frac{n}{m}\left(a_{24}T+b_{24}N+c_{24}B\right). \tag{54}$$

Here the coefficients a_{24}, b_{24} and c_{24} are

$$\begin{aligned}
a_{24} &= -\left(\frac{n}{m}+\frac{n^3}{m}\right)\sin(t)\lambda_3+2\frac{n^2}{m}\cos(t)\varphi_1-\cos(t),\\
b_{24} &= \left(\frac{n}{m}+\frac{n^3}{m}\right)\cos(t)\lambda_3+2\frac{n^2}{m}\sin(t)\varphi_1-\sin(t),\\
c_{24} &= -n^3\lambda_3.
\end{aligned}$$

From equations (45), (48) and (54) torsion of the TNB-Smarandache curve is

$$\tau_{\gamma_4}(t)=\frac{\rho_3 m\sqrt{3}\lambda_4}{\lambda_4^2-m\mu_3},\quad \textit{where}\quad \rho_3=-3m\varphi_1+\lambda_4. \tag{55}$$

4 Acknowledgement

This research is supported by Ordu University Scientific Research Projects Coordination Unit (BAP). Project Number: B-1829

References

[1] Ali, A. T., *Special Smarandache Curves in the Euclidean Space*, International Journal of Mathematical Combinatorics, **2**(2010), 30–36.

[2] Bektaş, Ö., Yüce, S., *Special Smarandache Curves According to Dardoux Frame in Euclidean 3-Space*, Romanian Journal of Mathematics and Computer Science, **3(1)**(2013), 48–59.

[3] Turgut, M., Yilmaz, S., *Smarandache Curves in Minkowski Space-Time*, International J.Math. Combin., **3**(2008), 51–55.

[4] Anti-Salkowski, E., *Zur Transformation von Raumkurven*, Mathematische Annalen, **4(66)**(1909), 517–557.

[5] J. Monterde, *Anti-Salkowski curves revisited: A family of curves with constant curvature and non-constant torsion*, Computer Aided Geometric Design, **26**(2009), 271–278.

N-Smarandache Curves According to the Sabban Frame of the Spherical Indicatrix Curve

Süleyman ŞENYURT*
Ordu University,
Department of Mathematics, Ordu, TURKEY

Kübra AKDAĞ
Ordu University,
Department of Mathematics, Ordu, TURKEY

Abstract

In this study, we first formed a Sabban frame of spherical indicatrix curve of N-alternative vector defined by a differentiable curve. Then the geodesic curvature of this vector is calculated according to this frame. Finally we defined Smarandache curves generated by the Sabban frame and give some characterizations of them.

Keywords: *Sabban frame, Smarandache curve, alternative frame, spherical indicatrix curve*

1 Introduction

In differential geometry, special curves have an important role. One of these curves is a Smarandache curve. Smarandache curves are first defined by M. Turgut and S. Yılmaz in 2008 [7]. Special Smarandache curves also have been studied by some authors [1, 2, 3]. Let $\alpha = \alpha(s)$ be a regular unit speed curve in E^3. The Frenet frame and alternative frame of this curve are $\{T, N, B\}$ and $\{N, C, W\}$, respectively. Here, N is normal vector, W is unit Darboux vector and $C = W \wedge N$ [5]. In this paper, we created the Smarandache curves according to the alternative frame of the unit speed curve. We then introduced alternative frame and its properties. Finally we calculated geodesic curvature of these curves according to alternative frame.

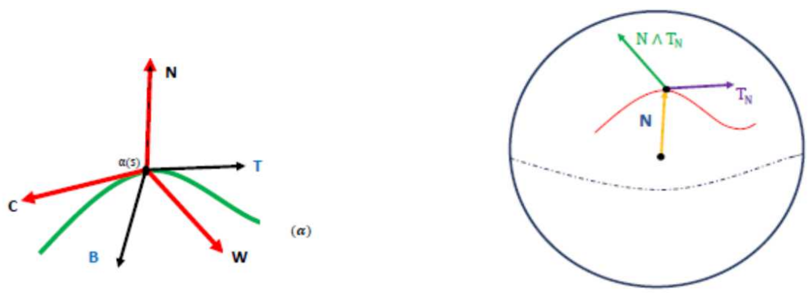

(a) Alternative frame (b) Sabban frame

Figure 1

*Corresponding author. *E-mail address:* senyurtsuleyman@hotmail.com

2 Preliminaries

Let $\alpha = \alpha(s)$ be a regular curve with unit speed. Then the Frenet apparatus of the curve (α) [4]

$$\begin{aligned} T(s) &= \alpha'(s), \quad N(s) = \frac{\alpha''(s)}{\| \alpha''(s) \|}, \quad B(s) = T(s) \wedge N(s), \\ \kappa(s) &= \| T'(s) \|, \qquad \tau(s) = \frac{det(\alpha'(s) \wedge \alpha''(s), \alpha'''(s))}{\| \alpha' \wedge \alpha''^2}, \\ T' &= \kappa N, \quad N' = -\kappa T + \tau B, \quad B' = -\tau N. \end{aligned} \tag{1}$$

In Euclidean 3-space any regular curve $\alpha(s)$ depending on the Frenet vectors moves around the axis of Darboux vector. Darboux vector defining a unit vector field is given as [5]

$$\begin{aligned} W &= \frac{\tau}{\sqrt{\kappa^2+\tau^2}} T + \frac{\kappa}{\sqrt{\kappa^2+\tau^2}} B, \\ C &= W \wedge N = -\frac{\kappa}{\sqrt{\kappa^2+\tau^2}} T + \frac{\tau}{\sqrt{\kappa^2+\tau^2}} B. \end{aligned} \tag{2}$$

So build another orthonormal moving frame along the curve $\alpha(s)$. This frame defined as alternative frame and is represented by $\{N, C, W\}$. The derivative formulae of the alternative frame is given by [5]

$$\begin{aligned} N^{'} &= \beta C, \quad C^{'} = -\beta N + \gamma W, \quad W^{'} = -\gamma C, \\ \beta &= \sqrt{\kappa^2+\tau^2}, \quad \gamma = \frac{\kappa^2}{\kappa^2+\tau^2}\left(\frac{\tau}{\kappa}\right)'. \end{aligned} \tag{3}$$

The relationship between Frenet frame and alternative frame is

$$\begin{aligned} C &= \overline{\kappa} T + \overline{\tau} B, \quad W = \overline{\tau} T + \overline{\kappa} B, \quad T = -\overline{\kappa} C + \overline{\tau} W, \\ B &= \overline{\tau} C + \overline{\kappa} W \overline{\kappa} = \frac{\kappa}{\beta}, \quad \overline{\tau} = \frac{\tau}{\beta}. \end{aligned} \tag{4}$$

Principal normal vector N is common both frames. Let $\gamma : I \to S^2$ be a unit speed spherical curve and s arc-length parameter of γ. Let us denote $t(s) = \gamma^{'}(s)$ and $d(s) = \gamma(s) \wedge t(s)$. This frame is called the Sabban frame of γ on S^2. Then we have the following spherical Frenet formulae of γ

$$\gamma'(s) = t(s), \quad t'(s) = -\gamma(s) + \kappa_g(s) d(s), \quad d'(s) = -\kappa_g(s) t(s), \tag{5}$$

where $\kappa_g(s)$ is the geodesic curvature of γ on S^2 [6],

$$\kappa_g(s) = \langle t'(s), d(s) \rangle. \tag{6}$$

3 Smarandache Curves of Alternative Frame According to the Sabban Frame

In this section, we investigated special Smarandache curves according to Sabban frame on S^2. Let $N = N(s) = \alpha_N(s)$ be a unit speed regular spherical curve on S^2, $\{N, T_N, (N \wedge T_N)\}$ and $\{N_{\alpha_N}, T_{N_{\alpha_N}}, (N \wedge T_N)_{\alpha_N}\}$ be the Sabban frame of this curve, respectively. Let $\alpha_N(s) = N(s)$ and if we take the derivative of the equation, then T_N vector is

$$\frac{d\alpha_N}{ds^*}\frac{ds^*}{ds} = N'(s) = \beta C, T_N = C, \quad \frac{ds^*}{ds} = \beta. \tag{7}$$

Considering the $N(s)$ and T_N vectors, we can write

$$N \wedge T_N = W. \tag{8}$$

Accordingly, the $\{N, T_N, (N \wedge T_N)\} \equiv \{N, C, W\}$ Sabban frame is obtained from the N vector. If we take the derivative of the equation (7), then T_N' vector is

$$T_N' \frac{ds^*}{ds} = -\beta N + \gamma W, \quad T_N' = -N + \frac{\gamma}{\beta} W.$$

From the equation (6), (8) and (9), the geodesic curvature of $\alpha_N(s) = N(s)$ is

$$\begin{aligned} \kappa_g^N(s) &= \langle T_N'(s), (N \wedge T_N)(s) \rangle, \\ &= \frac{\gamma}{\beta}. \end{aligned} \tag{9}$$

Then from the equation (5) we have the following spherical Frenet formulae of $\alpha_N(s)$,

$$\begin{aligned} N' &= C, \\ T_N' &= -N + \frac{\gamma}{\beta} W, \\ (N \wedge T_N)' &= -\frac{\gamma}{\beta} C. \end{aligned} \tag{10}$$

Definition 1 *Let (N) be a spherical curve of $\alpha(s)$, N and T_N be Sabban vectors of (N). Then NT_N-Smarandache curve can be identified as*

$$\alpha_{NT_N} = \frac{1}{\sqrt{2}}(N + T_N) \tag{11}$$

or substituting the equation (7) into equation (11), we have

$$\alpha_{NT_N} = \frac{1}{\sqrt{2}}(N + C).$$

Theorem 2 *The geodesic curvature according to NT_N-Smarandache curve is*

$$\kappa_g^{NT_N} = \frac{1}{\left(2 + (\kappa_g^N)^2\right)^{\frac{5}{2}}} (\lambda_1 \kappa_g^N - \lambda_2 \kappa_g^N + 2\lambda_3), \tag{12}$$

where

$$\begin{aligned} \lambda_1 &= \kappa_g^N (\kappa_g^N)' - (\kappa_g^N)^2 - 2, \\ \lambda_2 &= -(\kappa_g^N)^4 - 3(\kappa_g^N)^2 - \kappa_g^N (\kappa_g^N)' - 2, \\ \lambda_3 &= (\kappa_g^N)^3 + 2\kappa_g^N + 2(\kappa_g^N)'. \end{aligned} \tag{13}$$

Proof. If we take the derivative of the equation (11), then NT_N vector is

$$\begin{aligned} T_{NT_N} \frac{ds^*}{ds} &= \frac{1}{\sqrt{2}}(-N + T_N + \kappa_g^N (N \wedge T_N)), \\ T_{NT_N} &= \frac{1}{\sqrt{2 + (\kappa_g^N)^2}}(-N + T_N + \kappa_g^N (N \wedge T_N)), \quad \frac{ds^*}{ds} = \frac{\sqrt{2 + (\kappa_g^N)^2}}{\sqrt{2}}. \end{aligned} \tag{14}$$

Considering the equations (11) and (14), we have

$$\begin{aligned}\alpha_{NT_N}\wedge T_{NT_N} &= \frac{1}{\sqrt{4+2(\kappa_g^N)^2}}(N+T_N)\wedge\big(-N+T_N+\kappa_g^N(N\wedge T_N)\big),\\ \alpha_{NT_N}\wedge T_{NT_N} &= \frac{1}{\sqrt{4+2(\kappa_g^N)^2}}\big(\kappa_g^N N-\kappa_g^N T_N+2(N\wedge T_N)\big).\end{aligned}\tag{15}$$

If we take the derivative of the equation (14), then T'_{NT_N} vector is

$$\begin{aligned}T'_{NT_N}\frac{ds^*}{ds} &= \Big(\frac{1}{\sqrt{2+(\kappa_g^N)^2}}\Big)'\big(-N+T_N+\kappa_g^N(N\wedge T_N)\big)\\ &+ \Big(\frac{1}{\sqrt{2+(\kappa_g^N)^2}}\Big)\big(-N+T_N+\kappa_g^N(N\wedge T_N)\big)',\\ T'_{NT_N}\frac{ds^*}{ds} &= -\frac{\kappa_g^N\big(\kappa_g^N\big)'\big(-N+T_N+\kappa_g^N(N\wedge T_N)\big)}{\big(2+(\kappa_g^N)^2\big)^{\frac{3}{2}}}\\ &+ \frac{-N-(1+(\kappa_g^N)^2)T_N+(\kappa_g^N+(\kappa_g^N)'(N\wedge T_N))}{\sqrt{2+(\kappa_g^N)^2}},\\ T'_{NT_N} &= \frac{\sqrt{2}\big(\kappa_g^N(\kappa_g^N)'-(\kappa_g^N)^2-2\big)}{\big(2+(\kappa_g^N)^2\big)^2}N\\ &- \frac{\sqrt{2}\big((\kappa_g^N)^4+3(\kappa_g^N)^2+\kappa_g^N(\kappa_g^N)'+2\big)}{\big(2+(\kappa_g^N)^2\big)^2}T_N\\ &+ \frac{\sqrt{2}\big((\kappa_g^N)^3+2\kappa_g^N+2(\kappa_g^N)'\big)}{\big(2+(\kappa_g^N)^2\big)^2}(N\wedge T_N).\end{aligned}\tag{16}$$

Using the equations (6), (13), (15) and (16), we can write $\kappa_g^{NT_N}$ geodesic curvature as

$$\kappa_g^{NT_N}=\frac{1}{(2+(\kappa_g^N)^2)^{\frac{5}{2}}}(\lambda_1\kappa_g^N-\lambda_2\kappa_g^N+2\lambda_3).$$

■

Corollary 3 *The geodesic curvature of the NT_N-Smarandache curve according to the alternative frame is*

$$\kappa_g^{NT_N}=\frac{\beta^4}{(\gamma^2+2\beta^2)^{\frac{5}{2}}}\big((\lambda_1-\lambda_2)\gamma+2\lambda_3\beta\big)\tag{17}$$

where

$$\begin{aligned}\lambda_1 &= \frac{\gamma}{\beta}\Big(\frac{\gamma}{\beta}\Big)'-\frac{\gamma^2+2\beta^2}{\beta^2},\quad \lambda_2=-\frac{\gamma^4+3\gamma^2\beta^2+2\beta^4}{\beta^4}-\frac{\gamma}{\beta}\Big(\frac{\gamma}{\beta}\Big)',\\ \lambda_3 &= \frac{\gamma^3+2\gamma\beta^2}{\beta^3}+2\Big(\frac{\gamma}{\beta}\Big)'.\end{aligned}$$

Definition 4 *Let (N) be a spherical curve of $\alpha(s)$, N and $N\wedge T_N$ be Sabban vectors of (N). Then $N(N\wedge T_N)$-Smarandache curve can be identified as*

$$\alpha_{N(N\wedge T_N)}=\frac{1}{\sqrt{2}}(N+N\wedge T_N).\tag{18}$$

or substituting the equation (7) *into equation* (18) *we reach*

$$\alpha_{N(N\wedge T_N)} = \frac{1}{\sqrt{2}}(N+W).$$

Theorem 5 *The geodesic curvature according to* $N(N\wedge T_N)$*-Smarandache curve is*

$$\kappa_g^{N(N\wedge T_N)} = \frac{\beta+\gamma}{\beta-\gamma} \tag{19}$$

Proof. If we take the derivative of the equation (18) then $T_{N(N\wedge T_N)}$ vector is

$$\begin{aligned} T_{N(N\wedge T_N)}\frac{ds^*}{ds} &= \frac{1}{\sqrt{2}}(T_N - \kappa_g^N T_N), \\ T_{N(N\wedge T_N)} &= T_N, \quad \frac{ds^*}{ds} = \frac{1-\kappa_g^N}{\sqrt{2}}. \end{aligned} \tag{20}$$

Considering the equations (18) and (20), we have

$$\alpha_{N(N\wedge T_N)} \wedge T_{N(N\wedge T_N)} = \frac{1}{\sqrt{2}}(-N + (N\wedge T_N)). \tag{21}$$

If we take the derivative of the equation (20), then $T'_{N(N\wedge T_N)}$ vector is

$$T'_{N(N\wedge T_N)} = \frac{\sqrt{2}}{1-\kappa_g^N}\big(-N + \kappa_g^N (N\wedge T_N)\big). \tag{22}$$

Using the equations (6), (9), (21) and (22), we can write $\kappa_g^{N(N\wedge T_N)}$ geodesic curvature as

$$\kappa_g^{N(N\wedge T_N)} = \frac{\beta+\gamma}{\beta-\gamma}.$$

■

Definition 6 *Let* (N) *be a spherical curve of* $\alpha(s)$*,* T_N *and* $N\wedge T_N$ *be Sabban vectors of* (N)*. Then* $T_N(N\wedge T_N)$*-Smarandache curve can be identified as*

$$\alpha_{T_N(N\wedge T_N)} = \frac{T_N + (N\wedge T_N)}{\sqrt{2}} \tag{23}$$

or substituting the equation (7),(8)*into equation* (23) *we have*

$$\alpha_{T_N(N\wedge T_N)} = \frac{1}{\sqrt{2}}(C+W).$$

Theorem 7 *The geodesic curvature according to* $T_N(N\wedge T_N)$*-Smarandache curve is*

$$\kappa_g^{T_N(N\wedge T_N)} = \frac{1}{\big(1+2(\kappa_g^N)^2\big)^{\frac{5}{2}}}(2\lambda_1\kappa_g^N - \lambda_2 + \lambda_3) \tag{24}$$

where

$$\begin{aligned} \lambda_1 &= \big(2\kappa_g^N(\kappa_g^N)' + \kappa_g^N + 2(\kappa_g^N)^3\big), \\ \lambda_2 &= -1 - (\kappa_g^N)' - 3(\kappa_g^N)^2 - 2(\kappa_g^N)^4, \\ \lambda_3 &= (\kappa_g^N)' - (\kappa_g^N)^2 + 2(\kappa_g^N)^4. \end{aligned} \tag{25}$$

Proof. If we take the derivative of the equation (23) then $T_{T_N(N\wedge T_N)}$ vector is

$$\begin{aligned} T_{T_N(N\wedge T_N)}\frac{ds^*}{ds} &= \frac{1}{\sqrt{2}}\big(-N-\kappa_g^N T_N+\kappa_g^N(N\wedge T_N)\big), \qquad (26)\\ T_{T_N(N\wedge T_N)} &= \frac{1}{\sqrt{1+2(\kappa_g^N)^2}}\big(-N-\kappa_g^N T_N+\kappa_g^N(N\wedge T_N)\big),\\ \frac{ds^*}{ds} &= \frac{1+2\big(\kappa_g^N\big)^2}{\sqrt{2}}. \end{aligned}$$

Considering the equations (23) and (26), we have

$$\alpha_{T_N(N\wedge T_N)}\wedge T_{T_N(N\wedge T_N)} = \frac{\big(2\kappa_g^N N-T_N+(N\wedge T_N)\big)}{\sqrt{2+4(\kappa_g^N)^2}}. \qquad (27)$$

If we take the derivative of the equation (26), then $T'_{T_N(N\wedge T_N)}$ vector is

$$\begin{aligned} T'_{T_N(N\wedge T_N)}\frac{ds^*}{ds} &= \Big(\frac{1}{\sqrt{1+2(\kappa_g^N)^2}}\Big)'\big(-N-\kappa_g^N T_N+\kappa_g^N(N\wedge T_N)\big)\\ &+ \Big(\frac{1}{\sqrt{1+2(\kappa_g^N)^2}}\Big)\big(-N-\kappa_g^N T_N+\kappa_g^N(N\wedge T_N)\big)',\\ T'_{T_N(N\wedge T_N)}\frac{ds^*}{ds} &= -\frac{2\kappa_g^N(\kappa_g^N)'}{\big(1+2(\kappa_g^N)^2\big)^{\frac{3}{2}}}\big(-N-\kappa_g^N T_N+\kappa_g^N(N\wedge T_N)\big)\\ &+ \frac{1}{\sqrt{1+2(\kappa_g^N)^2}}\big(\kappa_g^N-(1+(\kappa_g^N)'+(\kappa_g^N)^2)\big)T_N\\ &+ \big(((\kappa_g^N)'-(\kappa_g^N)^2)(N\wedge T_N)\big),\\ T'_{T_N(N\wedge T_N)} &= \frac{\sqrt{2}\big(2\kappa_g^N(\kappa_g^N)'+\kappa_g^N+2(\kappa_g^N)^3\big)}{\big(1+2(\kappa_g^N)^2\big)^2}N \qquad (28)\\ &- \frac{\sqrt{2}\big(1+(\kappa_g^N)'+3(\kappa_g^N)^2+2(\kappa_g^N)^4\big)}{\big(1+2(\kappa_g^N)^2\big)^2}T_N\\ &+ \frac{\sqrt{2}\big((\kappa_g^N)'-(\kappa_g^N)^2+2(\kappa_g^N)^4\big)}{\big(1+2(\kappa_g^N)^2\big)^2}(N\wedge T_N). \end{aligned}$$

Using the equations (6),(25),(27) and (28), we can write $\kappa_g^{T_N(N\wedge T_N)}$ geodesic curvature as

$$\kappa_g^{T_N(N\wedge T_N)} = \frac{1}{\big(1+2(\kappa_g^N)^2\big)^{\frac{5}{2}}}\big(2\lambda_1\kappa_g^N-\lambda_2+\lambda_3\big).$$

■

Corollary 8 *The geodesic curvature of the $T_N(N\wedge T_N)$-Smarandache curve according to the alternative frame is*

$$\kappa_g^{T_N(N\wedge T_N)} = \frac{\beta^4}{\big(\beta^2+2\gamma^2\big)^{\frac{5}{2}}}\big(2\lambda_1\gamma+(\lambda_3-\lambda_2)\beta\big)$$

where

$$\begin{aligned}
\lambda_1 &= 2\frac{\gamma}{\beta}\big(\frac{\gamma}{\beta}\big)' + \frac{\gamma}{\beta} + 2\frac{\gamma^3}{\beta^3},\\
\lambda_2 &= -1 - \big(\frac{\gamma}{\beta}\big)' - 3\frac{\gamma^2}{\beta^2} - 2\frac{\gamma^4}{\beta^4},\\
\lambda_3 &= \big(\frac{\gamma}{\beta}\big)' - \frac{\gamma^2}{\beta^2} + 2\frac{\gamma^4}{\beta^4}.
\end{aligned}$$

Definition 9 *Let (N) be a spherical curve of $\alpha(s)$,N, T_N and $N \wedge T_N$ be Sabban vectors of (N). Then $NT_N(N \wedge T_N)$-Smarandache curve can be identified as*

$$\alpha_{NT_N(N\wedge T_N)} = \frac{1}{\sqrt{3}}\big(N + T_N + (N \wedge T_N)\big) \tag{29}$$

or substituting the equation (7), (8)*into equation* (29) *we reach*

$$\alpha_{NT_N(N\wedge T_N)} = \frac{1}{\sqrt{3}}(N + C + W).$$

Theorem 10 *The geodesic curvature according to $NT_N(N \wedge T_N)$-Smarandache curve is*

$$\kappa_g^{T_N(N\wedge T_N)} = \frac{(-1+2\kappa_g^N)\lambda_1 - (1+\kappa_g^N)\lambda_2 + (2-\kappa_g^N)\lambda_3}{4\sqrt{2}\big(1-(\kappa_g^N)+(\kappa_g^N)^2\big)^{\frac{5}{2}}}. \tag{30}$$

where

$$\begin{aligned}
\lambda_1 &= -(\kappa_g^N)'(1-2\kappa_g^N) + 2\big(-1+2\kappa_g^N - 2(\kappa_g^N)^2 + (\kappa_g^N)^3\big),\\
\lambda_2 &= (\kappa_g^N)'\big(1-3\kappa_g^N + 2(\kappa_g^N)^2\big) - 2\big(1-\kappa_g^N + (\kappa_g^N)^2\big)\big(1 + (\kappa_g^N)' + (\kappa_g^N)^2\big),\\
\lambda_3 &= (\kappa_g^N)'\big(\kappa_g^N - 2(\kappa_g^N)^2\big) + 2\big(1-\kappa_g^N + (\kappa_g^N)^2\big)\big(\kappa_g^N - (\kappa_g^N)^2 + (\kappa_g^N)'\big).
\end{aligned} \tag{31}$$

Proof. If we take the derivative of the equation (29) then $T_{NT_N(N\wedge T_N)}$ vector is

$$\begin{aligned}
T_{NT_N(N\wedge T_N)}\frac{ds^*}{ds} &= \frac{1}{\sqrt{3}}\big(-N + (1-\kappa_g^N)T_N + \kappa_g^N(N\wedge T_N)\big),\\
T_{NT_N(N\wedge T_N)} &= \frac{-N + (1-\kappa_g^N)T_N + \kappa_g^N(N\wedge T_N)}{\sqrt{2}\sqrt{1-\kappa_g^N+(\kappa_g^N)^2}},\\
\frac{ds^*}{ds} &= \frac{\sqrt{2}}{\sqrt{3}}\sqrt{1-\kappa_g^N+(\kappa_g^N)^2}.
\end{aligned} \tag{32}$$

Considering the equations (29) and (32), we have

$$\alpha_{NT_N(N\wedge T_N)} \wedge T_{NT_N(N\wedge T_N)} = \frac{(2\kappa_g^N-1)N - (1+\kappa_g^N)T_N + (2-\kappa_g^N)(N\wedge T_N)}{\sqrt{6}\sqrt{1-\kappa_g^N+(\kappa_g^N)^2}}. \tag{33}$$

If we take the derivative of the equation (32), then $T'_{NT_N(N\wedge T_N)}$ vector is

$$\begin{aligned}
T'_{NT_N(N\wedge T_N)} &= \frac{\sqrt{3}}{4}\frac{(\kappa_g^N)'\big(1-2(\kappa_g^N)\big)\big(-N + (1-\kappa_g^N)T_N + \kappa_g^N(N\wedge T_N)\big)}{\big(1-\kappa_g^N+(\kappa_g^N)^2\big)^2}\\
&+ \frac{\sqrt{3}}{2}\frac{(\kappa_g^N-1)N - \big(1+(\kappa_g^N)'+(\kappa_g^N)^2\big)T_N}{1-\kappa_g^N+(\kappa_g^N)^2}\\
&+ \frac{\sqrt{3}}{2}\frac{\big(\kappa_g^N-(\kappa_g^N)^2+(\kappa_g^N)'\big)(N\wedge T_N)}{1-\kappa_g^N+(\kappa_g^N)^2}
\end{aligned} \tag{34}$$

$$\begin{aligned} T'_{NT_N(N\wedge T_N)} &= \frac{\sqrt{3}}{4}.\frac{-(\kappa_g^N)'\big(1-2\kappa_g^N\big)+2\big(-1+2\kappa_g^N-2(\kappa_g^N)^2+(\kappa_g^N)^3\big)}{\big(1-\kappa_g^N+(\kappa_g^N)^2\big)^2}N \\ &+ \frac{\sqrt{3}}{4}\frac{(\kappa_g^N)'\big(1-3\kappa_g^N+2(\kappa_g^N)^2\big)}{\big(1-\kappa_g^N+(\kappa_g^N)^2\big)^2}T_N \\ &- \frac{\sqrt{3}}{2}\frac{\big(1-\kappa_g^N+(\kappa_g^N)^2\big)\big(1+(\kappa_g^N)'+(\kappa_g^N)^2\big)}{\big(1-\kappa_g^N+(\kappa_g^N)^2\big)^2}T_N \\ &+ \frac{\sqrt{3}}{4}\frac{(\kappa_g^N)'\big(\kappa_g^N-2(\kappa_g^N)^2\big)}{\big(1-\kappa_g^N+(\kappa_g^N)^2\big)^2}(N\wedge T_N) \\ &- \frac{\sqrt{3}}{2}\frac{2\big(1-\kappa_g^N+(\kappa_g^N)^2\big)\big(\kappa_g^N-(\kappa_g^N)^2+(\kappa_g^N)'\big)}{\big(1-\kappa_g^N+(\kappa_g^N)^2\big)^2}(N\wedge T_N) \end{aligned}$$

Using the equations (6), (31), (33) and (34), we can write $\kappa_g^{NT_N(N\wedge T_N)}$ geodesic curvature as

$$\kappa_g^{T_N(N\wedge T_N)} = \frac{1}{4\sqrt{2}\big(1-(\kappa_g^N)+(\kappa_g^N)^2\big)^{\frac{5}{2}}}\big((-1+2\kappa_g^N)\lambda_1-(1+\kappa_g^N)\lambda_2+(2-\kappa_g^N)\lambda_3\big).$$

■

Corollary 11 *The geodesic curvature of the $NT_N(N\wedge T_N)$-Smarandache curve according to the alternative frame is*

$$\kappa_g^{NT_N(N\wedge T_N)} = \frac{\beta^4}{4\sqrt{2}\big(\gamma^2+\beta^2-\beta\gamma\big)^{\frac{5}{2}}}\big((2\gamma-\beta)\lambda_1-(\beta+\gamma)\lambda_2+(2\beta-\gamma)\lambda_3\big)$$

where

$$\begin{aligned} \lambda_1 &= -\frac{\beta-2\gamma}{\beta}\big(\frac{\gamma}{\beta}\big)'+\frac{-2\beta^3+4\beta^2\gamma-4\beta\gamma^2+2\gamma^3}{\beta^3}, \\ \lambda_2 &= \frac{\beta^2-3\beta\gamma+2\gamma^2}{\beta^2}\big(\frac{\gamma}{\beta}\big)'-2\big(\frac{\gamma^2-\beta\gamma+\beta^2}{\beta^2}\big)\big((\frac{\gamma}{\beta})'+\frac{\gamma^2+\beta^2}{\beta^2}\big), \\ \lambda_3 &= \frac{\beta\gamma-2\gamma^2}{\beta}\big(\frac{\gamma}{\beta}\big)'+2\big(\frac{\gamma^2-\beta\gamma+\beta^2}{\beta^2}\big)\big(\frac{\beta\gamma-\gamma^2}{\beta^2}+(\frac{\gamma}{\beta})'\big). \end{aligned}$$

Example 12 *Let ;*
$\gamma(s)=\left(\frac{9}{208}\sin 16s-\frac{1}{117}\sin 36s,-\frac{9}{208}\cos 16s+\frac{1}{117}\cos 36s,\frac{6}{65}\sin 10s\right)$
be a curve with the alternative frame of $\{N,C,W\}$ given as

$$\begin{aligned} N(s) &= (\frac{12}{13}\cos 26s,-\frac{12}{13}\sin 26s,\frac{5}{13}),C(s)=(-\sin 26s,\cos 26s,0), \\ W(s) &= (\frac{5}{13}\cos 26s,-\frac{5}{13}\sin 26s,\frac{12}{13}). \end{aligned}$$

Then we have the following spherical indicatrix curve (N) and β_1,β_2,β_3 and β_4 Smarandache curves according to Sabban frame on S^2. These curves are (see Figure 2,3)

$$\begin{aligned} \beta_1 &= \frac{1}{\sqrt{2}}(\frac{12}{13}\cos 26s-24\sin 26s,\frac{12}{13}\sin 26s-24\cos 26s,-\frac{5}{13}), \\ \beta_2 &= \frac{1}{\sqrt{2}}(\frac{132}{13}\cos 26s,-\frac{108}{13}\sin 26s,\frac{282}{13}), \\ \beta_3 &= \frac{1}{\sqrt{2}}(\frac{120}{13}\cos 26s-24\sin 26s,24\cos 26s-\frac{120}{13}\sin 26s,\frac{288}{13}), \\ \beta_4 &= \frac{1}{\sqrt{3}}(\frac{132}{13}\cos 26s-24\sin 26s,24\cos 26s-\frac{108}{13}\sin 26s,\frac{283}{13}). \end{aligned}$$

(a) β_1-Smarandache curve, $s \in (-\pi, \frac{4\pi}{3})$

(b) β_2-Smarandache curve, $s \in (0, \frac{4\pi}{3})$

Figure 2

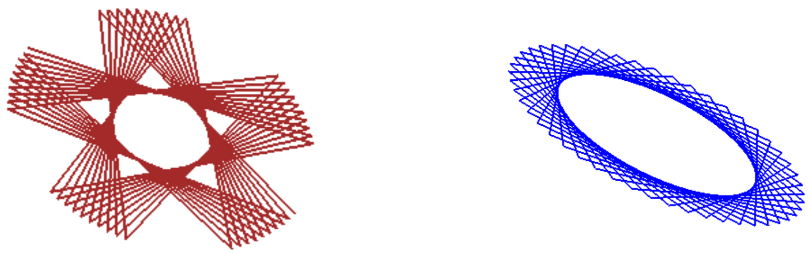

(a) β_3-Smarandache curve, $s \in (-\pi, \frac{\pi}{2})$

(b) β_2-Smarandache curve, $s \in (-\frac{\pi}{2}, \frac{\pi}{2})$

Figure 3

References

[1] Ali A. T., Special Smarandache Curves in the Euclidean Space, *International Journal of Mathematical Combinatorics*, **2010**, 2(30-36).

[2] Bektaş O., Yüce S., Special Smarandache Curves According to Darboux Frame in Euclidean 3- Space, *Romanian Journal of Mathematics and Computer Science*, **2013**, 3(1), 48-59.

[3] Çetin M., Tuncer Y., Karacan M. K., Smarandache Curves According to Bishop Frame in Euclidean 3- Space, *Gen. Math. Notes*, **2014**, 20(2), 50-66.

[4] Do Carmo M.P., Differential geometry of curves and surfaces, *Prentice-Hall Englewood Cliffs*, NJ MATH Google Scholar, **1976**.

[5] Kaya O., Önder M., New Partner Curves in theEuclidean 3-Space E^3, *International Journal of Geometry*,**2017**, 6(2), 41- 50.

[6] Taşköprö K., Tosun M., Smarandache curves on S^2, *Boletim da Sociedade Paranaense de Matematica 3 Srie.*,**2014**, 32 (1), 51-59.

[7] Turgut M., Yılmaz S., Smarandache Curves in Minkowski Space-time, *International J. Math. Combin.*,**2008**, 3(51-55).

On the extended Simpson type integral inequalities

Fatma ERTUĞRAL*
Düzce University,
Department of Mathematics, Düzce-TURKEY

Mehmet Zeki SARIKAYA
Düzce University,
Department of Mathematics, Düzce-TURKEY

Abstract

In this paper, we have established some generalized Simpson type inequalities for functions whose derivatives in absolute value are convex.

Keywords: Simpson type inequalities, Convex functions, integral inequalities.

1 Introduction

The following inequality is well known in the literature as Simpson's inequality.

Theorem 1 *Let* $f:[a,b]\to\mathbb{R}$ *be a four times continuously differentiable mapping on* (a,b) *and* $\left\|f^{(4)}\right\|_\infty=\sup\left|f^{(4)}(x)\right|<\infty$*. Then, the following inequality holds:*

$$\left|\frac{1}{3}\left[\frac{f(a)+f(b)}{2}+2f\left(\frac{a+b}{2}\right)\right]-\frac{1}{b-a}\int_a^b f(x)\,dx\right|\leq\frac{1}{2880}\left\|f^{(4)}\right\|_\infty(b-a)^4.$$

For recent refinements, counterparts, generalizations and new Simpson's type inequalities, see ([1]-[21]).

In [2], Dragomir et. al. proved the following some recent developments on Simpson's inequality for which the remainder is expressed in terms of lower derivatives than the fourth.

Theorem 2 *Suppose* $f:[a;b]\to\mathbb{R}$ *is an absolutely continuous mapping on* $[a,b]$ *whose derivative belongs to* $L_p[a,b]$*. Then, the following inequality holds,*

$$\begin{aligned}&\left|\frac{1}{3}\left[\frac{f(a)+f(b)}{2}+2f\left(\frac{a+b}{2}\right)\right]-\frac{1}{b-a}\int_a^b f(x)\,dx\right|\\ \leq\ &\frac{1}{6}\left[\frac{2^{q+1}+1}{3(q+1)}\right]^{\frac{1}{q}}(b-a)^{\frac{1}{q}}\left\|f'\right\|_p\end{aligned}$$

where $\frac{1}{p}+\frac{1}{q}=1$.

Also, the following (1) inequality was obtained by using the following identity which is given by Alomari et. all in [1]:

*Corresponding author. *E-mail address:* fatmaertugral14@gmail.com

Lemma 3 *Let $f : I \subset \mathbb{R} \to \mathbb{R}$ be an absolutely continuous mapping on I° where $a, b \in I$ with $a < b$. Then the following equality holds:*

$$\begin{aligned} & \frac{1}{6}\left[f(a)+4f\left(\frac{a+b}{2}+f(b)\right)\right]-\frac{1}{b-a}\int_a^b f(x)\,dx \\ = \; & (b-a)\int_0^1 p(t)\,f'(tb+(1-t)a)\,dt \end{aligned}$$

where

$$p(t)=\begin{cases} t-\frac{1}{6}, & t\in\left[0,\frac{1}{2}\right), \\ t-\frac{5}{6}, & t\in\left[\frac{1}{2},1\right]. \end{cases}$$

Theorem 4 *Let $f : I \subset [0,\infty) \to \mathbb{R}$ be a differentiable mapping on I° such that $f' \in L[a,b]$, where $a, b \in I$ with $a < b$. If $|f'|$ is convex on $[a,b]$, then the following inequality holds:*

$$\begin{aligned} & \left|\frac{1}{6}\left[f(a)+4f\left(\frac{a+b}{2}\right)+f(b)\right]-\frac{1}{b-a}\int_a^b f(x)\,dx\right| \\ \le \; & \frac{5(b-a)}{72}\left[\left|f'(a)+f'(b)\right|\right]. \end{aligned} \tag{1}$$

In [13], Sarikaya et. al. obtained inequalities for differentiable convex mappings which are connected with Simpson's inequality, and they used the following lemma to prove it.

Lemma 5 *Let $f : I \subset \mathbb{R} \to \mathbb{R}$ be an absolutely continuous mapping on I° such that $f' \in L_1[a,b]$, where $a, b \in I^{\circ}$ with $a < b$, then the following equality holds:*

$$\begin{aligned} & \frac{1}{6}\left[f(a)+4f\left(\frac{a+b}{2}\right)+f(b)\right]-\frac{1}{b-a}\int_a^b f(x)dx \\ & = \frac{b-a}{2}\int_0^1\left[\left(\frac{t}{2}-\frac{1}{3}\right)f'\left(\frac{1+t}{2}b+\frac{1-t}{2}a\right)+\left(\frac{1}{3}-\frac{t}{2}\right)f'\left(\frac{1+t}{2}a+\frac{1-t}{2}b\right)\right]dt. \end{aligned} \tag{2}$$

The main inequality in [13], pointed out for $s = 1$, as follows:

Theorem 6 *Let $f : I \subset \mathbb{R} \to \mathbb{R}$ be a differentiable mapping on I° such that $f' \in L_1[a,b]$, where $a, b \in I^{\circ}$ with $a < b$. If $|f'|^q$ is a convex on $[a,b]$, $q > 1$, then the following inequality holds:*

$$\begin{aligned} & \left|\frac{1}{6}\left[f(a)+4f\left(\frac{a+b}{2}\right)+f(b)\right]-\frac{1}{b-a}\int_a^b f(x)dx\right| \\ & \le \frac{(b-a)}{12}\left(\frac{1+2^{p+1}}{3(p+1)}\right)^{\frac{1}{p}}\left\{\left(\frac{3\left|f'(b)\right|^q+\left|f'(a)\right|^q}{4}\right)^{\frac{1}{q}}+\left(\frac{\left|f'(b)\right|^q+3\left|f'(a)\right|^q}{4}\right)^{\frac{1}{q}}\right\}, \end{aligned} \tag{3}$$

where $\frac{1}{p}+\frac{1}{q}=1$.

The main aim of this paper is to establish new Simpson's type inequalities for the class of functions whose derivatives in absolute value at certain powers are convex functions.

2 Main Results

To prove our main result, we need the following definition and lemma.

Definition 7 *The function $f:[a,b]\subset R\rightarrow R$, is said to be convex if the following inquality holds*

$$f(\lambda x+(1-\lambda)y)\leq \lambda f(x)+(1-\lambda)f(y)$$

for all $x,y\in[a,b]$ and $\lambda\in[0,1]$. We say that f is concave if $(-f)$ is convex.

Lemma 8 *Let $f:I=[a,b]\subset R\rightarrow R$ be an absolutely continuous mapping on I° such that $f'\in L_1([a,b])$, where $a,b\in I^{\circ}$ with $a<b$. Then the following inequality holds:*

$$\begin{aligned}
&\frac{1}{6}\left[f(a)+2f\left(\frac{2a+b}{3}\right)+2f\left(\frac{a+2b}{3}\right)+f(b)\right]-\frac{1}{b-a}\int_a^b f(x)\,dx\\
=&\frac{(b-a)}{9}\left[\int_0^1\left(\frac{t}{2}-\frac{1}{3}\right)\left(f'\left(\frac{2+t}{3}b+\frac{1-t}{3}a\right)\right.\right.\\
&\left.\left.+f'\left(\frac{1+t}{3}b+\frac{2-t}{3}a\right)+f'\left(\frac{t}{3}b+\frac{3-t}{3}a\right)\right)dt\right]\\
&+\frac{(b-a)}{9}\left[\int_0^1\left(\frac{1}{3}-\frac{t}{2}\right)\left(f'\left(\frac{2+t}{3}b+\frac{1-t}{3}a\right)\right.\right.\\
&\left.\left.+f'\left(\frac{1+t}{3}b+\frac{2-t}{3}a\right)+f'\left(\frac{t}{3}b+\frac{3-t}{3}a\right)\right)dt.\right.
\end{aligned}$$

Proof. It suffices to note that

$$\begin{aligned}
I =& \int_0^1\left(\frac{t}{2}-\frac{1}{3}\right)\left[f'\left(\frac{2+t}{3}b+\frac{1-t}{3}a\right)+f'\left(\frac{1+t}{3}b+\frac{2-t}{3}a\right)+f'\left(\frac{t}{3}b+\frac{3-t}{3}a\right)\right]dt\\
&+\int_0^1\left(\frac{1}{3}-\frac{t}{2}\right)\left[f'\left(\frac{2+t}{3}b+\frac{1-t}{3}a\right)+f'\left(\frac{1+t}{3}b+\frac{2-t}{3}a\right)+f'\left(\frac{t}{3}b+\frac{3-t}{3}a\right)\right]dt\\
=& I_1+I_2+I_3+I_4+I_5+I_6.
\end{aligned}$$

Integrating by parts

$$\begin{aligned}
I_1 =& \int_0^1\left(\frac{t}{2}-\frac{1}{3}\right)f'\left(\frac{2+t}{3}b+\frac{1-t}{3}a\right)dt\\
=& \frac{3}{b-a}\left[\left(\frac{t}{2}-\frac{1}{3}\right)f\left(\frac{2+t}{3}b+\frac{1-t}{3}a\right)\Big|_0^1-\frac{1}{2}\int_0^1 f\left(\frac{2+t}{3}b+\frac{1-t}{3}a\right)dt\right]\\
=& \frac{3}{b-a}\left[\frac{1}{6}f(b)+\frac{1}{3}f\left(\frac{a+2b}{3}\right)\right]-\frac{3}{2(b-a)}\int_0^1 f\left(\frac{2+t}{3}b+\frac{1-t}{3}a\right)dt\\
=& \frac{1}{2(b-a)}\left[f(b)+2f\left(\frac{a+2b}{3}\right)\right]-\frac{9}{2(b-a)^2}\int_{\frac{a+2b}{3}}^{b}f(x)\,dx.
\end{aligned}$$

Similarly we have,

$$\begin{aligned}
I_2 =& \int_0^1\left(\frac{t}{2}-\frac{1}{3}\right)f'\left(\frac{1+t}{3}b+\frac{2-t}{3}a\right)dt\\
=& \frac{3}{b-a}\left[\left(\frac{t}{2}-\frac{1}{3}\right)f\left(\frac{1+t}{3}b+\frac{2-t}{3}a\right)\Big|_0^1-\frac{1}{2}\int_0^1 f\left(\frac{1+t}{3}b+\frac{2-t}{3}a\right)dt\right]\\
=& \frac{1}{2(b-a)}\left[f\left(\frac{a+2b}{3}\right)+2f\left(\frac{2a+b}{3}\right)\right]-\frac{9}{2(b-a)^2}\int_{\frac{2a+b}{3}}^{\frac{a+2b}{3}}f(x)\,dx,
\end{aligned}$$

$$\begin{aligned}
I_3 &= \int_0^1 \left(\frac{t}{2}-\frac{1}{3}\right) f'\left(\frac{t}{3}b+\frac{3-t}{3}a\right) dt \\
&= \frac{1}{2(b-a)}\left[f\left(\frac{2a+b}{3}\right)+2f(a)\right]-\frac{9}{2(b-a)^2}\int_a^{\frac{2a+b}{3}} f(x)\,dx,
\end{aligned}$$

$$\begin{aligned}
I_4 &= \int_0^1 \left(\frac{1}{3}-\frac{t}{2}\right) f'\left(\frac{2+t}{3}a+\frac{1-t}{3}b\right) dt \\
&= \frac{3}{a-b}\left[\left(\frac{1}{3}-\frac{t}{2}\right) f\left(\frac{2+t}{3}a+\frac{1-t}{3}b\right)\Big|_0^1+\frac{1}{2}\int_0^1 f\left(\frac{2+t}{3}a+\frac{1-t}{3}b\right) dt\right] \\
&= \frac{3}{a-b}\left[-\frac{1}{6}f(a)-\frac{1}{3}f\left(\frac{2a+b}{3}\right)\right]-\frac{3}{2(b-a)}\int_0^1 f\left(\frac{2+t}{3}a+\frac{1-t}{3}b\right) dt \\
&= \frac{1}{2(b-a)}\left[f(a)+2f\left(\frac{2a+b}{3}\right)\right]-\frac{9}{2(b-a)^2}\int_a^{\frac{2a+b}{3}} f(x)\,dx,
\end{aligned}$$

$$\begin{aligned}
I_5 &= \int_0^1 \left(\frac{1}{3}-\frac{t}{2}\right) f'\left(\frac{1+t}{3}a+\frac{2-t}{3}b\right) dt \\
&= \frac{1}{2(b-a)}\left[f\left(\frac{2a+b}{3}\right)+2f\left(\frac{a+2b}{3}\right)\right]-\frac{9}{2(b-a)^2}\int_{\frac{2a+b}{3}}^{\frac{a+2b}{3}} f(x)\,dx,
\end{aligned}$$

$$\begin{aligned}
I_6 &= \int_0^1 \left(\frac{1}{3}-\frac{t}{2}\right) f'\left(\frac{t}{3}a+\frac{3-t}{3}b\right) dt \\
&= \frac{1}{2(b-a)}\left[f\left(\frac{a+2b}{3}\right)+2f(b)\right]-\frac{9}{2(b-a)^2}\int_{\frac{a+2b}{3}}^{b} f(x)\,dx.
\end{aligned}$$

Multiplying with related coefficient and summing the above six equations, we get

$$\frac{b-a}{9}I=\frac{1}{6}\left[f(a)+2f\left(\frac{2a+b}{3}\right)+2f\left(\frac{a+2b}{3}\right)+f(b)\right]$$

which completes the proof. ■

Corollary 9 *Under the condition of Lemma 8 and f is convex function we have*

$$\begin{aligned}
&\left[f(a)+4f\left(\frac{a+b}{2}\right)+f(b)\right] \\
\leq\ &\left[f(a)+2f\left(\frac{2a+b}{3}\right)+2f\left(\frac{a+2b}{3}\right)+f(b)\right].
\end{aligned} \tag{4}$$

Theorem 10 *Let $f: I=[a,b]\subset R\to R$ be an absolutely continuous mapping on I° such that $f'\in L_1([a,b])$, where $a,b\in I^{\circ}$ with $a<b$. If the mapping $|f'|$ is convex on $[a,b]$, then we have the following inequality:*

$$\begin{aligned}
&\left|\frac{1}{6}\left[f(a)+2f\left(\frac{2a+b}{3}\right)+2f\left(\frac{a+2b}{3}\right)+f(b)\right]-\frac{1}{b-a}\int_a^b f(x)\,dx\right| \\
\leq\ &\frac{127}{2916}(b-a)\left[\left|f'(a)\right|+\left|f'(b)\right|\right].
\end{aligned} \tag{5}$$

Proof. From Lemma 8 and by computing in integral right side of above inequalities, we get

$$\begin{aligned} J_1 &= \int_0^1 \left|\frac{t}{2}-\frac{1}{3}\right| \left|f'\left(\frac{2+t}{3}b+\frac{1-t}{3}a\right)\right| dt \qquad (6) \\ &\le \int_0^{\frac{2}{3}} \left(\frac{1}{3}-\frac{t}{2}\right)\left[\frac{2+t}{3}\left|f'(b)\right|+\frac{1-t}{3}\left|f'(a)\right|\right] dt \\ &\quad +\int_{\frac{2}{3}}^1 \left(\frac{t}{2}-\frac{1}{3}\right)\left[\frac{2+t}{3}\left|f'(b)\right|+\frac{1-t}{3}\left|f'(a)\right|\right] dt \\ &\le \int_0^{\frac{2}{3}} \left(\frac{1}{3}-\frac{t}{2}\right)\left(\frac{2+t}{3}\right)\left|f'(b)\right| dt+\int_0^{\frac{2}{3}} \left(\frac{1}{3}-\frac{t}{2}\right)\left(\frac{1-t}{3}\right)\left|f'(a)\right| dt \\ &\quad +\int_{\frac{2}{3}}^1 \left(\frac{t}{2}-\frac{1}{3}\right)\left(\frac{2+t}{3}\right)\left|f'(b)\right| dt+\int_{\frac{2}{3}}^1 \left(\frac{t}{2}-\frac{1}{3}\right)\left(\frac{1-t}{3}\right)\left|f'(a)\right| dt \\ &= \frac{1}{18}\left[-t^3-2t^2+4t\Big|_0^{\frac{2}{3}}\left|f'(b)\right|+t^3-\frac{5}{2}t^2+2t\Big|_0^{\frac{2}{3}}\left|f'(a)\right|\right. \\ &\quad \left.+\,t^3+2t^2-4t\Big|_{\frac{2}{3}}^1\left|f'(b)\right|+-t^3+\frac{5}{2}t^2-2t\Big|_{\frac{2}{3}}^1\left|f'(a)\right|\right] \\ &= \frac{1}{18}\left[\frac{106}{54}\left|f'(b)\right|+\frac{29}{54}\left|f'(a)\right|\right]. \end{aligned}$$

Similarly we have,

$$J_2 = \int_0^1 \left|\frac{t}{2}-\frac{1}{3}\right| \left|f'\left(\frac{1+t}{3}b+\frac{2-t}{3}a\right)\right| dt \le \frac{1}{18}\left[\frac{37}{54}\left|f'(b)\right|+\frac{74}{54}\left|f'(a)\right|\right], \qquad (7)$$

$$J_3 = \int_0^1 \left|\frac{t}{2}-\frac{1}{3}\right| \left|f'\left(\frac{t}{3}b+\frac{3-t}{3}a\right)\right| dt \le \frac{1}{18}\left[\frac{16}{54}\left|f'(b)\right|+\frac{119}{54}\left|f'(a)\right|\right], \qquad (8)$$

$$J_4 = \int_0^1 \left|\frac{1}{3}-\frac{t}{2}\right| \left|f'\left(\frac{2+t}{3}a+\frac{1-t}{3}b\right)\right| dt \le \frac{1}{18}\left[\frac{106}{54}\left|f'(a)\right|+\frac{29}{54}\left|f'(b)\right|\right], \qquad (9)$$

$$J_5 = \int_0^1 \left|\frac{1}{3}-\frac{t}{2}\right| \left|f'\left(\frac{1+t}{3}a+\frac{2-t}{3}b\right)\right| dt \le \frac{1}{18}\left[\frac{37}{54}\left|f'(a)\right|+\frac{74}{54}\left|f'(b)\right|\right], \qquad (10)$$

$$J_6 = \int_0^1 \left|\frac{1}{3}-\frac{t}{2}\right| \left|f'\left(\frac{t}{3}a+\frac{3-t}{3}b\right)\right| dt \le \frac{1}{18}\left[\frac{16}{54}\left|f'(a)\right|+\frac{119}{54}\left|f'(b)\right|\right]. \qquad (11)$$

a combination of (6)-(11) immediately gives the required inequality (5). ■

Remark 11 *Under the assumption of Theorem 10, by using the inequality (4), we get*

$$\begin{aligned} &\left|\left[f(a)+4f\left(\frac{a+b}{2}\right)+f(b)\right]-\frac{1}{b-a}\int_a^b f(x)\,dx\right| \\ \le\ &\left|\frac{1}{6}\left[f(a)+2f\left(\frac{2a+b}{3}\right)+2f\left(\frac{a+2b}{3}\right)+f(b)\right]-\frac{1}{b-a}\int_a^b f(x)\,dx\right| \\ \le\ &\frac{127}{2916}(b-a)\left[\left|f'(a)\right|+\left|f'(b)\right|\right], \end{aligned}$$

then this inequality is better than the inequality (1).

Theorem 12 *Let $f : I = [a,b] \subset R \to R$ be an absolutely continuous mapping on I° such that $f' \in L_1([a,b])$, where $a,b \in I^\circ$ with $a < b$. If the mapping $|f'|$ is convex on $[a,b]$, then we have the following inequality*

$$\left|\frac{1}{6}\left[f(a)+2f\left(\frac{2a+b}{3}\right)+2f\left(\frac{a+2b}{3}\right)+f(b)\right]-\frac{1}{b-a}\int_a^b f(x)\,dx\right| \tag{12}$$

$$\leq \frac{(b-a)}{9}\left(\frac{1+2^{p+1}}{(p+1)\,3^{p+1}}\right)^{\frac{1}{p}}\left\{\left(\frac{|f'(a)|^q+5|f'(b)|^q}{6}\right)^{\frac{1}{q}}\right.$$

$$\left.\left(\frac{3|f'(a)|^q+3|f'(b)|^q}{6}\right)^{\frac{1}{q}}+\left(\frac{5|f'(a)|^q+|f'(b)|^q}{6}\right)^{\frac{1}{q}}\right\}.$$

where $\frac{1}{p}+\frac{1}{q}=1$.

Proof. From Lemma 8 and by Hölder's inequality, we get

$$\begin{aligned} J_1 &= \left(\int_0^1\left|\frac{t}{2}-\frac{1}{3}\right|^p\right)^{\frac{1}{p}}\left(\int_0^1\left|f'\left(\frac{2+t}{3}b+\frac{1-t}{3}a\right)\right|^q dt\right)^{\frac{1}{q}} \\ &\leq \left(\int_0^{\frac{2}{3}}\left(\frac{1}{3}-\frac{t}{2}\right)^p\right)^{\frac{1}{p}}\left[\int_0^1\left(\frac{2+t}{3}|f'(b)|^q+\frac{1-t}{3}|f'(a)|^q\right)\right]^{\frac{1}{q}} dt \\ &\quad +\left(\int_{\frac{2}{3}}^1\left(\frac{t}{2}-\frac{1}{3}\right)^p\right)^{\frac{1}{p}}\left[\int_0^1\left(\frac{2+t}{3}|f'(b)|^q+\frac{1-t}{3}|f'(a)|^q\right)\right]^{\frac{1}{q}} dt \\ &= \left(\frac{2^{p+2}+2}{(p+1)\,6^{p+1}}\right)^{\frac{1}{p}}\left(\frac{|f'(a)|^q+5|f'(b)|^q}{6}\right)^{\frac{1}{q}}. \end{aligned} \tag{13}$$

Similarly, we have

$$\begin{aligned} J_2 &= \left(\int_0^1\left|\frac{t}{2}-\frac{1}{3}\right|^p\right)^{\frac{1}{p}}\left(\int_0^1\left|f'\left(\frac{1+t}{3}b+\frac{2-t}{3}a\right)\right|^q dt\right)^{\frac{1}{q}} \\ &\leq \left(\frac{2^{p+2}+2}{(p+1)\,6^{p+1}}\right)^{\frac{1}{p}}\left(\frac{3|f'(a)|^q+3|f'(b)|^q}{6}\right)^{\frac{1}{q}}, \end{aligned} \tag{14}$$

$$\begin{aligned} J_3 &= \left(\int_0^1\left|\frac{t}{2}-\frac{1}{3}\right|^p\right)^{\frac{1}{p}}\left(\int_0^1\left|f'\left(\frac{t}{3}b+\frac{3-t}{3}a\right)\right|^q\right)^{\frac{1}{q}} dt \\ &\leq \left(\frac{2^{p+2}+2}{(p+1)\,6^{p+1}}\right)^{\frac{1}{p}}\left(\frac{5|f'(a)|^q+|f'(b)|^q}{6}\right)^{\frac{1}{q}}, \end{aligned} \tag{15}$$

$$\begin{aligned} J_4 &= \left(\int_0^1\left|\frac{1}{3}-\frac{t}{2}\right|^p\right)^{\frac{1}{p}}\left[\int_0^1\left|f'\left(\frac{2+t}{3}a+\frac{1-t}{3}b\right)\right|^q dt\right]^{\frac{1}{q}} \\ &\leq \left(\frac{2^{p+2}+2}{(p+1)\,6^{p+1}}\right)^{\frac{1}{p}}\left(\frac{5|f'(a)|^q+|f'(b)|^q}{6}\right)^{\frac{1}{q}}, \end{aligned} \tag{16}$$

$$\begin{aligned} J_5 &= \left(\int_0^1\left|\frac{1}{3}-\frac{t}{2}\right|^p\right)^{\frac{1}{p}}\left(\int_0^1\left|f'\left(\frac{1+t}{3}a+\frac{2-t}{3}b\right)\right|^q dt\right)^{\frac{1}{q}} \\ &\leq \left(\frac{2^{p+2}+2}{(p+1)\,6^{p+1}}\right)^{\frac{1}{p}}\left(\frac{3|f'(a)|^q+3|f'(b)|^q}{6}\right)^{\frac{1}{q}}, \end{aligned} \tag{17}$$

$$
\begin{aligned}
J_6 &= \left(\int_0^1 \left|\frac{1}{3}-\frac{t}{2}\right|^p\right)^{\frac{1}{p}} \left(\int_0^1 \left|f'\left(\frac{t}{3}a+\frac{3-t}{3}b\right)\right|^q dt\right)^{\frac{1}{q}} \\
&\leq \left(\frac{2^{p+2}+2}{(p+1)\,6^{p+1}}\right)^{\frac{1}{p}} \left(\frac{|f'(a)|^q+5\,|f'(b)|^q}{6}\right)^{\frac{1}{q}}.
\end{aligned} \tag{18}
$$

By simple computation, we obtain that

$$
\int_0^1 \left|\frac{t}{2}-\frac{1}{3}\right|^p dt = \int_0^{\frac{2}{3}} \left(\frac{1}{3}-\frac{t}{2}\right)^p dt + \int_{\frac{2}{3}}^1 \left(\frac{t}{2}-\frac{1}{3}\right)^p dt = \frac{2\left(1+2^{p+1}\right)}{(p+1)\,6^{p+1}}.
$$

Thus, by combinations of (13)-(18) and multiply $\frac{b-a}{9}$ immediately gives the required inequality (12). ■

Corollary 13 *Under the assumption of Theorem 12, by using the inequality (4), we get*

$$
\begin{aligned}
&\left|\left[f(a)+4f\left(\frac{a+b}{2}\right)+f(b)\right]-\frac{1}{b-a}\int_a^b f(x)\,dx\right| \\
\leq\ & \left|\frac{1}{6}\left[f(a)+2f\left(\frac{2a+b}{3}\right)+2f\left(\frac{a+2b}{3}\right)+f(b)\right]-\frac{1}{b-a}\int_a^b f(x)\,dx\right| \\
\leq\ & \frac{(b-a)}{9}\left(\frac{1+2^{p+1}}{(p+1)\,3^{p+1}}\right)^{\frac{1}{p}} \left\{\left(\frac{|f'(a)|^q+5\,|f'(b)|^q}{6}\right)^{\frac{1}{q}}\right. \\
& \left.\left(\frac{3\,|f'(a)|^q+3\,|f'(b)|^q}{6}\right)^{\frac{1}{q}} + \left(\frac{5\,|f'(a)|^q+|f'(b)|^q}{6}\right)^{\frac{1}{q}}\right\}.
\end{aligned}
$$

Theorem 14 *Let $f: I=[a,b]\subset R\to R$ be an absolutely continuous mapping on I° such that $f'\in L_1([a,b])$, where $a,b\in I^\circ$ with $a<b$. If the mapping $|f'|$ is convex on $[a,b]$, then we have the following inequality*

$$
\begin{aligned}
&\left|\frac{1}{6}\left[f(a)+2f\left(\frac{2a+b}{3}\right)+2f\left(\frac{a+2b}{3}\right)+f(b)\right]-\frac{1}{b-a}\int_a^b f(x)\,dx\right| \\
\leq\ & \frac{b-a}{162}\left(\frac{5}{2}\right)^{1-\frac{1}{q}} \left[\left(\frac{106}{54}\,|f'(b)|^q+\frac{29}{54}\,|f'(a)|^q\right)^{\frac{1}{q}} + \left(\frac{37}{54}\,|f'(b)|^q+\frac{74}{54}\,|f'(a)|\right)^{\frac{1}{q}}\right. \\
& + \left(\frac{16}{54}\,|f'(b)|^q+\frac{119}{54}\,|f'(a)|^q\right)^{\frac{1}{q}} + \left(\frac{106}{54}\,|f'(a)|^q+\frac{29}{54}\,|f'(b)|^q\right)^{\frac{1}{q}} \\
& \left. + \left(\frac{37}{54}\,|f'(a)|^q+\frac{74}{54}\,|f'(b)|^q\right)^{\frac{1}{q}} + \left(\frac{16}{54}\,|f'(a)|^q+\frac{119}{54}\,|f'(b)|^q\right)^{\frac{1}{q}}\right].
\end{aligned} \tag{19}
$$

Proof. From Lemma 8 and by using power mean inequalities and convexity of $|f'|^q$, we get

$$\begin{aligned} J_1' &= \left(\int_0^1 \left|\frac{t}{2}-\frac{1}{3}\right| dt\right)^{1-\frac{1}{q}} \left(\int_0^1 \left|\frac{t}{2}-\frac{1}{3}\right| \left|f'\left(\frac{2+t}{3}b+\frac{1-t}{3}a\right)\right|^q dt\right)^{\frac{1}{q}} \qquad (20)\\ &\leq \left(\int_0^{\frac{2}{3}} \left(\frac{1}{3}-\frac{t}{2}\right) dt + \int_{\frac{2}{3}}^1 \left(\frac{t}{2}-\frac{1}{3}\right) dt\right)^{1-\frac{1}{q}} \\ &\quad \times \left[\int_0^{\frac{2}{3}} \left(\frac{1}{3}-\frac{t}{2}\right)\left(\frac{2+t}{3}\left|f'(b)\right|^q + \frac{1-t}{3}\left|f'(a)\right|^q\right) dt \right. \\ &\quad \left. + \int_{\frac{2}{3}}^1 \left(\frac{t}{2}-\frac{1}{3}\right)\left(\frac{2+t}{3}\left|f'(b)\right|^q + \frac{1-t}{3}\left|f'(a)\right|^q\right) dt\right]^{\frac{1}{q}}. \\ &\leq \left(\frac{5}{36}\right)^{1-\frac{1}{q}} \left[\frac{1}{18}\left(\frac{106}{54}\left|f'(b)\right|^q + \frac{29}{54}\left|f'(a)\right|^q\right)\right]^{\frac{1}{q}}. \end{aligned}$$

Similarly, we have

$$\begin{aligned} J_2' &= \left(\int_0^1 \left|\frac{t}{2}-\frac{1}{3}\right|\right)^{1-\frac{1}{q}} \left(\int_0^1 \left|\frac{t}{2}-\frac{1}{3}\right| \left|f'\left(\frac{1+t}{3}b+\frac{2-t}{3}a\right)\right|^q dt\right)^{\frac{1}{q}} \qquad (21)\\ &\leq \left(\frac{5}{36}\right)^{1-\frac{1}{q}} \left[\frac{1}{18}\left(\frac{37}{54}\left|f'(b)\right|^q + \frac{74}{54}\left|f'(a)\right|^q\right)\right]^{\frac{1}{q}}, \end{aligned}$$

$$\begin{aligned} J_3' &= \left(\int_0^1 \left|\frac{t}{2}-\frac{1}{3}\right|\right)^{1-\frac{1}{q}} \left(\int_0^1 \left|\frac{t}{2}-\frac{1}{3}\right| \left|f'\left(\frac{t}{3}b+\frac{3-t}{3}a\right)\right|^q\right)^{\frac{1}{q}} dt \qquad (22)\\ &\leq \left(\frac{5}{36}\right)^{1-\frac{1}{q}} \left[\frac{1}{18}\left(\frac{16}{54}\left|f'(b)\right|^q + \frac{119}{54}\left|f'(a)\right|^q\right)\right]^{\frac{1}{q}}, \end{aligned}$$

$$\begin{aligned} J_4' &= \left(\int_0^1 \left|\frac{1}{3}-\frac{t}{2}\right|\right)^{1-\frac{1}{q}} \left[\int_0^1 \left|\frac{1}{3}-\frac{t}{2}\right| \left|f'\left(\frac{2+t}{3}a+\frac{1-t}{3}b\right)\right|^q dt\right]^{\frac{1}{q}} \qquad (23)\\ &\leq \left(\frac{5}{36}\right)^{1-\frac{1}{q}} \left[\frac{1}{18}\left(\frac{106}{54}\left|f'(a)\right|^q + \frac{29}{54}\left|f'(b)\right|^q\right)\right]^{\frac{1}{q}}, \end{aligned}$$

$$\begin{aligned} J_5' &= \left(\int_0^1 \left|\frac{1}{3}-\frac{t}{2}\right|\right)^{1-\frac{1}{q}} \left(\int_0^1 \left|\frac{1}{3}-\frac{t}{2}\right| \left|f'\left(\frac{1+t}{3}a+\frac{2-t}{3}b\right)\right|^q dt\right)^{\frac{1}{q}} \qquad (24)\\ &\leq \left(\frac{5}{36}\right)^{1-\frac{1}{q}} \left[\frac{1}{18}\left(\frac{37}{54}\left|f'(a)\right|^q + \frac{74}{54}\left|f'(b)\right|^q\right)\right]^{\frac{1}{q}}, \end{aligned}$$

$$\begin{aligned} J_6' &= \left(\int_0^1 \left|\frac{1}{3}-\frac{t}{2}\right|\right)^{1-\frac{1}{q}} \left(\int_0^1 \left|\frac{1}{3}-\frac{t}{2}\right| \left|f'\left(\frac{t}{3}a+\frac{3-t}{3}b\right)\right|^q dt\right)^{\frac{1}{q}} \qquad (25)\\ &\leq \left(\frac{5}{36}\right)^{1-\frac{1}{q}} \left[\frac{1}{18}\left(\frac{106}{54}\left|f'(a)\right|^q + \frac{119}{54}\left|f'(b)\right|^q\right)\right]^{\frac{1}{q}}. \end{aligned}$$

Therefore, by combinations of (20)-(25) immediately gives the required inequality (19). ■

3 Conclusion Remark

In conclusion, in this article, we have introduced we have established some generalized Simpson type inequalities for functions whose derivatives in absolute value are convex.

References

[1] M. Alomari, M. Darus and S.S. Dragomir, *New inequalities of Simpsonís type for s-convex functions with applications*, RGMIA Res. Rep. Coll., 12 (4) (2009), Article 9.

[2] S.S. Dragomir, R.P. Agarwal and P. Cerone, *On Simpsonís inequality and applications*, J. of Inequal. Appl., 5(2000), 533-579.

[3] S.S. Dragomir. *On Simpson's quadrature formula for differentiable mappings whose derivatives belong to l_p spaces and applications.* J. KSIAM, 2 (1998), 57–65.

[4] S.S. Dragomir, *On Simpson's quadrature formula for Lipschitzian mappings and applications* Soochow J. Mathematics, 25 (1999), 175–180.

[5] T. Du, Y. Li and Z. Yang, *A generalization of Simpson's inequality via differentiable mapping using extended (s, m)-convex functions,* Applied Mathematics and Computation 293 (2017) 358–369

[6] S. Hussain andS. Qaisar, *More results on Simpson's type inequality through convexity for twice differentiable continuous mappings.* Springer Plus (2016), 5:77.

[7] B.Z. Liu, *An inequality of Simpson type*, Proc. R. Soc. A, 461 (2005), 2155-2158.

[8] J. Pecaric, F. Proschan and Y.L. Tong, *Convex functions, partial ordering and statistical applications*, Academic Press, New York, 1991.

[9] J. Pecaric., and S. Varosanec, *A note on Simpson's inequality for functions of bounded variation*, Tamkang Journal of Mathematics, Volume 31, Number 3, Autumn (2000), 239–242.

[10] S. Qaisar, C.J. He, S. Hussain, *A generalizations of Simpson's type inequality for differentiable functions using (α, m)-convex functions and applications*, J. Inequal. Appl. 2013 (2013) 13. Article 158.

[11] H. Kavurmaci, A. O. Akdemir, E. Set and M. Z. Sarikaya, *Simpson's type inequalities for m-and (α, m)-geometrically convex functions*, Konuralp Journal of Mathematics, 2(1), pp:90-101, 2014.

[12] M. E. Ozdemir, A. O. Akdemir and H. Kavurmacı, *On the Simpson's inequality for convex functions on the co-Ordinates*, Turkish Journal of Analysis and Number Theory. 2014, 2(5), 165-169.

[13] M. Z. Sarikaya, E. Set and M. E. Ozdemir, *On new inequalities of Simpson's type for s-convex functions*, Computers and Mathematics with Applications 60 (2010) 2191–2199.

[14] M.Z. Sarikaya, E. Set, M.E. Özdemir, On new inequalities of Simpson's type for convex functions, RGMIA Res. Rep. Coll. 13 (2) (2010) Article2.

[15] M. Z.Sarikaya, E. Set and M. E. Ozdemir, On new inequalities of Simpson's type for functions whose second derivatives absolute values are convex, Journal of Applied Mathematics, Statistics and Informatics , 9 (2013), No. 1.

[16] M.Z. Sarıkaya, T. Tunç and H. Budak, *Simpson's type inequality for F-convex function*, Facta Universitatis Ser. Math. Inform., in press.

[17] E. Set, M. E. Ozdemir and M. Z. Sarikaya, *On new inequalities of Simpson's type for quasi-convex functions with applications*, Tamkang Journal of Mathematics, 43 (2012), no. 3, 357–364.

[18] E. Set, M. Z. Sarikaya and N. Uygun, *On new inequalities of Simpson's type for generalized quasi-convex functions*, Advances in Inequalities and Applications, 2017, 2017:3, pp:1-11.

[19] K. L. Tseng, G. S. Yang and S.S. Dragomir, *On weighted Simpson type inequalities and applications* Journal of mathematical inequalities, Vol. 1, number 1 (2007), 13–22.

[20] N. Ujevic, *Double integral inequalities of Simpson type and applications*, J. Appl. Math. Comput., 14 (2004), no:1-2, p. 213-223.

[21] Z.Q. Yang, Y.J. Li and T. Du, *A generalization of Simpson type inequality via differentiable functions using (s,m)-convex functions*, Ital. J. Pure Appl. Math. 35 (2015) 327–338

Some New Generalized Hermite-Hadamard Type Inequalities for Twice Differentiable Functions

Erhan SET*
Ordu University,
Department of Mathematics, Ordu, Turkey

Abstract

This paper deals with generalizations of Hermite-Hadamard type inequalities which estimate the difference between the left and middle part in Hermite-Hadamard inequality. The inequalities presented here are also pointed out to include some known results as their special cases.
Keywords: s-convexity, Hermite-Hadamard type inequalities.

1 Introduction

The function $f : [a, b] \to \mathbb{R}$, $I \neq \emptyset$ is said to be convex, if we have

$$f(tx + (1-t)y) \leq tf(x) + (1-t)f(y)$$

for all $x, y \in [a, b]$ and $t \in [0, 1]$.

The theory of inequalities has an important role in science such as mathematics, physics and engineering. One of the most famous inequality for convex functions is Hermite-Hadamard inequality that is expressed as follow:
If $f : [a, b] \to \mathbb{R}$ is a convex function, then

$$f\left(\frac{a+b}{2}\right) \leq \frac{1}{b-a}\int_a^b f(x)dx \leq \frac{f(a)+f(b)}{2}. \tag{1}$$

Here and in the following, let $\mathbb{R}$, $\mathbb{R}^+$, and $\mathbb{N}$ be the sets of real numbers, positive real numbers, and positive integers, respectively, and let $\mathbb{R}_0^+ := \mathbb{R}^+ \cup \{0\}$ and $\mathbb{N}_0 := \mathbb{N} \cup \{0\}$. The inequality (1) has attracted a remarkable number of researchers' attention. For new proofs, refinements, generalizations, and numerous applications of this inequality (1), we refer and the historical consideration for example, to [2, 3, 6] and the references cited therein.

The concept of $s-$convexity in the second sense is defined as follows (see, [1, 5]):

Definition 1 *A function $f : [0, \infty) \to \mathbb{R}$ is said to be s-convex in the second sense if*

$$f(tx + (1-t)y) \leq t^s f(x) + (1-t)^s f(y).$$

for all $x, y \in [0, \infty)$, $t \in [0, 1]$ and for some fixed $s \in (0, 1]$.

The class of $s-$convex functions in the second sense is denoted by K_s^2.

It is clear that for $s = 1$ $s-$convex function in the second sense reduces to the ordinary convex function defined on $[0, \infty]$.

*Corresponding author. *E-mail address:* erhanset@yahoo.com

Example 2 [5] *Let $s \in (0,1)$ and $a,b,c \in \mathbb{R}$. We define the function $f:[0,\infty) \to \mathbb{R}$ as*

$$f(t) = \begin{cases} a & t = 0, \\ bt^s + c & t > 0. \end{cases}$$

It can be easily checked that if $b \geq 0$ and $0 \leq c \leq a$, then $f \in K_s^2$.

In [4], Dragomir and Fitzpatrick proved a variant of Hermite-Hadamard inequality which holds for the s-convex functions.

Theorem 3 *Suppose that $f:[0,\infty) \to [0,\infty)$ is an $s-$convex function in the second sense, where $s \in (0,1)$, and let $a,b \in [0,\infty)$, $a < b$. If $f' \in L[a,b]$, then the following inequalities hold:*

$$2^{s-1} f\left(\frac{a+b}{2}\right) \leq \frac{1}{b-a}\int_a^b f(x)dx \leq \frac{f(a)+f(b)}{s+1}. \tag{2}$$

The constant $k = \frac{1}{s+1}$ is the best possible in the second inequality in (2).

The aim of this paper is to establish extension and refinement of Hermite-Hadamard type inequalities for twice differentiable functions, by modifying the results in [7].

2 Main Results

Lemma 4 *Let $f: I \subset \mathbb{R} \to \mathbb{R}$ be twice differentiable function on I°, $a,b \in I^\circ$ with $a < b$. If $f'' \in L[a,b]$, then following identity holds:*

$$\begin{aligned}
&\frac{1}{(b-a)(1-2\mu)}\int_{\mu b+(1-\mu)a}^{\mu a+(1-\mu)b} f(u)du - f\left(\frac{a+b}{2}\right) \\
= \; &\frac{(b-a)^2(1-2\mu)^2}{4}\Bigg\{\int_0^{\frac{1}{2}} t^2\bigg[f''\Big(t\left(\mu a+(1-\mu)b\right)+(1-t)\left(\mu b+(1-\mu)a\right)\Big) \\
&+f''\Big(t\left(\mu b+(1-\mu)a\right)+(1-t)\left(\mu a+(1-\mu)b\right)\Big)dt\bigg] \\
&+\int_{\frac{1}{2}}^1 (1-t)^2\bigg[f''\Big(t\left(\mu a+(1-\mu)b\right)+(1-t)\left(\mu b+(1-\mu)a\right)\Big) \\
&+f''\Big(t\left(\mu b+(1-\mu)a\right)+(1-t)\left(\mu a+(1-\mu)b\right)\Big)dt\bigg]\Bigg\}
\end{aligned} \tag{3}$$

where $\mu \in [0,1] \setminus \{\frac{1}{2}\}$.

Proof. By integrating by parts, we have the following identity

$$
\begin{aligned}
& \int_0^{\frac{1}{2}} t^2 \Big[f''\Big(t(\mu a+(1-\mu)b)+(1-t)(\mu b+(1-\mu)a) \Big) \\
& + f''\Big(t(\mu b+(1-\mu)a)+(1-t)(\mu a+(1-\mu)b) \Big) dt \Big] \\
& + \int_{\frac{1}{2}}^1 (1-t)^2 \Big[f''\Big(t(\mu a+(1-\mu)b)+(1-t)(\mu b+(1-\mu)a) \Big) \\
& + f''\Big(t(\mu b+(1-\mu)a)+(1-t)(\mu a+(1-\mu)b) \Big) dt \Big] \\
= {} & 2\Big[\int_0^{\frac{1}{2}} t^2 f''(t(\mu a+(1-\mu)b)+(1-t)(\mu b+(1-\mu)a))\,dt \\
& + \int_0^{\frac{1}{2}} t^2 f''(t(\mu b+(1-\mu)a)+(1-t)(\mu a+(1-\mu)b))\,dt \Big] \\
= {} & 2\Bigg[t^2 \frac{f'\Big(t(\mu a+(1-\mu)b)+(1-t)(\mu b+(1-\mu)a) \Big)}{(b-a)(1-2\mu)} \Bigg|_0^{\frac{1}{2}} \\
& - \int_0^{\frac{1}{2}} 2t \frac{f'\Big(t(\mu a+(1-\mu)b)+(1-t)(\mu b+(1-\mu)a) \Big)}{(b-a)(1-2\mu)} dt \\
& - t^2 \frac{f'\Big(t(\mu b+(1-\mu)a)+(1-t)(\mu a+(1-\mu)b) \Big)}{(b-a)(1-2\mu)} \Bigg|_0^{\frac{1}{2}} \\
& + \int_0^{\frac{1}{2}} 2t \frac{f'\Big(t(\mu b+(1-\mu)a)+(1-t)(\mu a+(1-\mu)b) \Big)}{(b-a)(1-2\mu)} dt \Bigg] \\
= {} & \frac{2}{(b-a)(1-2\mu)} \\
& \times \Bigg[\frac{f'\left(\frac{a+b}{2}\right)}{4} - 2\int_0^{\frac{1}{2}} t f'\Big(t(\mu a+(1-\mu)b)+(1-t)(\mu b+(1-\mu)a) \Big) dt \\
& - \frac{f'\left(\frac{a+b}{2}\right)}{4} + 2\int_0^{\frac{1}{2}} t f'\Big(t(\mu b+(1-\mu)a)+(1-t)(\mu a+(1-\mu)b) \Big) dt \Bigg] \\
= {} & \frac{4}{(b-a)(1-2\mu)} \Bigg[-t \frac{f\Big(t(\mu a+(1-\mu)b)+(1-t)(\mu b+(1-\mu)a) \Big)}{(b-a)(1-2\mu)} \Bigg|_0^{\frac{1}{2}} \\
& + \int_0^{\frac{1}{2}} \frac{f\Big(t(\mu a+(1-\mu)b)+(1-t)(\mu b+(1-\mu)a) \Big)}{(b-a)(1-2\mu)} dt \\
& - t \frac{f\Big(t(\mu b+(1-\mu)a)+(1-t)(\mu a+(1-\mu)b) \Big)}{(b-a)(1-2\mu)} \Bigg|_0^{\frac{1}{2}} \\
& + \int_0^{\frac{1}{2}} \frac{f\Big(t(\mu b+(1-\mu)a)+(1-t)(\mu a+(1-\mu)b) \Big)}{(b-a)(1-2\mu)} dt \Bigg]
\end{aligned}
$$

$$\begin{aligned}
&= \frac{4}{(b-a)^2(1-2\mu)^2}\left[-\frac{f\left(\frac{a+b}{2}\right)}{2}+\int_0^{\frac{1}{2}} f\Big(t\left(\mu a+(1-\mu)b\right)+(1-t)\left(\mu b+(1-\mu)a\right)\Big)dt\right.\\
&\quad\left.-\frac{f\left(\frac{a+b}{2}\right)}{2}+\int_0^{\frac{1}{2}} f\Big(t\left(\mu b+(1-\mu)a\right)+(1-t)\left(\mu a+(1-\mu)b\right)\Big)dt\right]\\
&= \frac{4}{(b-a)^2(1-2\mu)^2}\left[\int_0^1 f\Big(t\left(\mu a+(1-\mu)b\right)+(1-t)\left(\mu b+(1-\mu)a\right)\Big)dt-f\left(\frac{a+b}{2}\right)\right].
\end{aligned}$$

Using the change of the variable $u=t\left(\mu a+(1-\mu)b\right)+(1-t)\left(\mu b+(1-\mu)a\right)$ for $t\in[0,1]$ which gives the required identity. ■

Remark 5 *In Lemma 4, if we take $\mu=1$ in identity (3), then it becomes identity of Lemma 2 in [7].*

Theorem 6 *Let $f: I\subset\mathbb{R}\to\mathbb{R}$ be twice differentiable function on I° with $f''\in L[a,b]$. If $|f''|$ is s-convex on $[a,b]$, for some fixed $s\in(0,1]$ then the following inequality holds:*

$$\begin{aligned}
&\left|\frac{1}{(b-a)(1-2\mu)}\int_{\mu b+(1-\mu)a}^{\mu a+(1-\mu)b} f(u)du-f\left(\frac{a+b}{2}\right)\right|\\
\leq\ &\frac{(b-a)^2(1-2\mu)^2}{2}\\
&\times\left[\frac{1}{(s+3)}\frac{1}{2^{s+3}}+\frac{1}{s+1}\left(1-\frac{1}{2^{s+1}}\right)-\frac{2}{s+2}\left(1-\frac{1}{2^{s+2}}\right)+\frac{1}{s+3}\left(1-\frac{1}{2^{s+3}}\right)\right]\\
&\times\left[\left|f''\Big(\mu a+(1-\mu)b\Big)\right|+\left|f''\Big(\mu b+(1-\mu)a\Big)\right|\right]
\end{aligned}$$

for $\mu\in[0,1]\setminus\{\frac{1}{2}\}$.

Proof. From Lemma 4, triangle inequality and the s-convexity of $|f''|$, it follows that

$$\left|\frac{1}{(b-a)(1-2\mu)}\int_{\mu b+(1-\mu)a}^{\mu a+(1-\mu)b} f(u)du-f\left(\frac{a+b}{2}\right)\right|$$

$$
\begin{aligned}
&\leq \frac{(b-a)^2(1-2\mu)^2}{4} \\
&\quad\times\Bigg[\int_0^{\frac{1}{2}} t^2\left|f''\Big(t(\mu a+(1-\mu)b)+(1-t)(\mu b+(1-\mu)a)\Big)\right|dt \\
&\quad+\int_0^{\frac{1}{2}} t^2\left|f''\Big(t(\mu b+(1-\mu)a)+(1-t)(\mu a+(1-\mu)b)\Big)\right|dt \\
&\quad+\int_{\frac{1}{2}}^1 (1-t)^2\left|f''\Big(t(\mu a+(1-\mu)b)+(1-t)(\mu b+(1-\mu)a)\Big)\right|dt \\
&\quad+\int_{\frac{1}{2}}^1 (1-t)^2\left|f''\Big(t(\mu b+(1-\mu)a)+(1-t)(\mu a+(1-\mu)b)\Big)\right|dt\Bigg] \\
&\leq \frac{(b-a)^2(1-2\mu)^2}{4} \\
&\quad\times\Bigg[\int_0^{\frac{1}{2}} t^2\Big(t^s\left|f''\Big(\mu a+(1-\mu)b\Big)\right|+(1-t)^s\left|f''\Big(\mu b+(1-\mu)a\Big)\right|\Big)dt \\
&\quad+\int_0^{\frac{1}{2}} t^2\Big(t^s\left|f''\Big(\mu b+(1-\mu)a\Big)\right|+(1-t)^s\left|f''\Big(\mu a+(1-\mu)b\Big)\right|\Big)dt \\
&\quad+\int_{\frac{1}{2}}^1 (1-t)^2\Big(t^s\left|f''\Big(\mu a+(1-\mu)b\Big)\right|+(1-t)^s\left|f''\Big(\mu b+(1-\mu)a\Big)\right|\Big)dt \\
&\quad+\int_{\frac{1}{2}}^1 (1-t)^2\Big(t^s\left|f''\Big(\mu b+(1-\mu)a\Big)\right|+(1-t)^s\left|f''\Big(\mu a+(1-\mu)b\Big)\right|\Big)dt\Bigg] \\
&= \frac{(b-a)^2(1-2\mu)^2}{4} \\
&\quad\times\Bigg[\int_0^{\frac{1}{2}} t^{s+2}\left|f''\Big(\mu a+(1-\mu)b\Big)\right|dt+\int_0^{\frac{1}{2}} t^2(1-t)^s\left|f''\Big(\mu b+(1-\mu)a\Big)\right|dt \\
&\quad+\int_0^{\frac{1}{2}} t^{s+2}\left|f''\Big(\mu b+(1-\mu)a\Big)\right|dt+\int_0^{\frac{1}{2}} t^2(1-t)^s\left|f''\Big(\mu a+(1-\mu)b\Big)\right|dt \\
&\quad+\int_{\frac{1}{2}}^1 (1-t)^2t^s\left|f''\Big(\mu a+(1-\mu)b\Big)\right|dt+\int_{\frac{1}{2}}^1 (1-t)^{s+2}\left|f''\Big(\mu b+(1-\mu)a\Big)\right|dt \\
&\quad+\int_{\frac{1}{2}}^1 (1-t)^2t^s\left|f''\Big(\mu b+(1-\mu)a\Big)\right|dt+\int_{\frac{1}{2}}^1 (1-t)^{s+2}\left|f''\Big(\mu a+(1-\mu)b\Big)\right|dt\Bigg] \\
&= \frac{(b-a)^2(1-2\mu)^2}{2} \\
&\quad\times\left[\frac{1}{(s+3)}\frac{1}{2^{s+3}}+\frac{1}{s+1}\left(1-\frac{1}{2^{s+1}}\right)-\frac{2}{s+2}\left(1-\frac{1}{2^{s+2}}\right)+\frac{1}{s+3}\left(1-\frac{1}{2^{s+3}}\right)\right] \\
&\quad\times\left[\left|f''\Big(\mu a+(1-\mu)b\Big)\right|+\left|f''\Big(\mu b+(1-\mu)a\Big)\right|\right].
\end{aligned}
$$

So, the proof is completed. ■

Remark 7 *In Theorem 6, if we take $\mu=1$ and $s=1$, then it becomes inequality of Theorem 3 in [7].*

Theorem 8 *Let $f : I \subset \mathbb{R} \to \mathbb{R}$ be twice differentiable function on I° such that $f'' \in L[a,b]$ where $a,b \in I$, $a<b$. If $|f''|^q$ is $s-$convex on $[a,b]$, for some fixed $s \in (0,1]$, $q>1$, $\frac{1}{p}+\frac{1}{q}=1$*

then the following inequality holds:

$$
\begin{aligned}
&\left|\frac{1}{(b-a)(1-2\mu)}\int_{\mu b+(1-\mu)a}^{\mu a+(1-\mu)b} f(u)du - f\left(\frac{a+b}{2}\right)\right| \\
\leq\ & \frac{(b-a)^2(1-2\mu)^2}{2}\left(\frac{1}{(2p+1)}\frac{1}{2^{2p+1}}\right)^{\frac{1}{p}} \\
&\times\Bigg[\left(\frac{1}{(s+1)}\frac{1}{2^{s+1}}\left|f''\Big(\mu a+(1-\mu)b\Big)\right|^q+\frac{1}{(s+1)}\left(1-\frac{1}{2^{s+1}}\right)\left|f''\left(\mu b+(1-\mu)a\right)\right|^q\right)^{\frac{1}{q}} \\
&+\left(\frac{1}{(s+1)}\left(1-\frac{1}{2^{s+1}}\right)\left|f''\Big(\mu a+(1-\mu)b\Big)\right|^q+\frac{1}{(s+1)}\frac{1}{2^{s+1}}\left|f''\left(\mu b+(1-\mu)a\right)\right|^q\right)^{\frac{1}{q}}\Bigg]
\end{aligned}
$$

for $\mu \in [0,1]\setminus\{\frac{1}{2}\}$.

Proof. From Lemma 4, using well known Hölder inequality, triangle inequality and the s-convexity of $|f''|^q$, it follows that

$$
\begin{aligned}
&\left|\frac{1}{(b-a)(1-2\mu)}\int_{\mu b+(1-\mu)a}^{\mu a+(1-\mu)b} f(u)du - f\left(\frac{a+b}{2}\right)\right| \\
\leq\ & \frac{(b-a)^2(1-2\mu)^2}{4} \\
&\times\Bigg\{\left(\int_0^{\frac{1}{2}} t^{2p}dt\right)^{\frac{1}{p}}\left(\int_0^{\frac{1}{2}}\left|f''\Big(t\left(\mu a+(1-\mu)b\right)+(1-t)\left(\mu b+(1-\mu)a\right)\Big)\right|^q dt\right)^{\frac{1}{q}} \\
&+\left(\int_0^{\frac{1}{2}} t^{2p}dt\right)^{\frac{1}{p}}\left(\int_0^{\frac{1}{2}}\left|f''\Big(t\left(\mu b+(1-\mu)a\right)+(1-t)\left(\mu a+(1-\mu)b\right)\Big)\right|^q dt\right)^{\frac{1}{q}} \\
&+\left(\int_{\frac{1}{2}}^1 (1-t)^{2p}dt\right)^{\frac{1}{p}} \\
&\times\left(\int_{\frac{1}{2}}^1\left|f''\Big(t\left(\mu a+(1-\mu)b\right)+(1-t)\left(\mu b+(1-\mu)a\right)\Big)\right|^q dt\right)^{\frac{1}{q}} \\
&+\int_{\frac{1}{2}}^1 (1-t)^{2p}dt\Bigg)^{\frac{1}{p}} \\
&\times\left(\int_{\frac{1}{2}}^1\left|f''\Big(t\left(\mu b+(1-\mu)a\right)+(1-t)\left(\mu a+(1-\mu)b\right)\Big)\right|^q dt\right)^{\frac{1}{q}}\Bigg\}
\end{aligned}
$$

$$
\begin{aligned}
&\leq \frac{(b-a)^2(1-2\mu)^2}{4}\left\{\left(\int_0^{\frac{1}{2}} t^{2p}dt\right)^{\frac{1}{p}}\right. \\
&\times\left[\left(\int_0^{\frac{1}{2}}\left(t^s\left|f''\Big(\mu a+(1-\mu)b\Big)\right|^q+(1-t)^s\left|f''(\mu b+(1-\mu)a)\right|^q\right)dt\right)^{\frac{1}{q}}\right. \\
&\left.+\left(\int_0^{\frac{1}{2}}\left(t^s\left|f''\Big(\mu b+(1-\mu)a\Big)\right|^q+(1-t)^s\left|f''(\mu a+(1-\mu)b)\right|^q\right)dt\right)^{\frac{1}{q}}\right] \\
&+\left(\int_{\frac{1}{2}}^1(1-t)^{2p}dt\right)^{\frac{1}{p}} \\
&\times\left[\left(\int_{\frac{1}{2}}^1\left(t^s\left|f''\Big(\mu a+(1-\mu)b\Big)\right|^q+(1-t)^s\left|f''(\mu b+(1-\mu)a)\right|^q\right)dt\right)^{\frac{1}{q}}\right. \\
&\left.\left.+\left(\int_{\frac{1}{2}}^1\left(t^s\left|f''\Big(\mu b+(1-\mu)a\Big)\right|^q+(1-t)^s\left|f''(\mu a+(1-\mu)b)\right|^q\right)dt\right)^{\frac{1}{q}}\right]\right\} \\
&= \frac{(b-a)^2(1-2\mu)^2}{4}\left(\frac{1}{(2p+1)}\frac{1}{2^{2p+1}}\right)^{\frac{1}{p}} \\
&\times\left\{\left(\frac{1}{(s+1)}\frac{1}{2^{s+1}}\left|f''\Big(\mu a+(1-\mu)b\Big)\right|^q+\frac{1}{(s+1)}\left(1-\frac{1}{2^{s+1}}\right)\left|f''(\mu b+(1-\mu)a)\right|^q\right)^{\frac{1}{q}}\right. \\
&+\left(\frac{1}{(s+1)}\frac{1}{2^{s+1}}\left|f''\Big(\mu b+(1-\mu)a\Big)\right|^q+\frac{1}{(s+1)}\left(1-\frac{1}{2^{s+1}}\right)\left|f''(\mu a+(1-\mu)b)\right|^q\right)^{\frac{1}{q}} \\
&+\left(\frac{1}{(s+1)}\left(1-\frac{1}{2^{s+1}}\right)\left|f''\Big(\mu a+(1-\mu)b\Big)\right|^q+\frac{1}{(s+1)}\frac{1}{2^{s+1}}\left|f''(\mu b+(1-\mu)a)\right|^q\right)^{\frac{1}{q}} \\
&\left.+\left(\frac{1}{(s+1)}\left(1-\frac{1}{2^{s+1}}\right)\left|f''\Big(\mu b+(1-\mu)a\Big)\right|^q+\frac{1}{(s+1)}\frac{1}{2^{s+1}}\left|f''(\mu a+(1-\mu)b)\right|^q\right)^{\frac{1}{q}}\right\} \\
&= \frac{(b-a)^2(1-2\mu)^2}{2}\left(\frac{1}{(2p+1)}\frac{1}{2^{2p+1}}\right)^{\frac{1}{p}} \\
&\times\left\{\left(\frac{1}{(s+1)}\frac{1}{2^{s+1}}\left|f''\Big(\mu a+(1-\mu)b\Big)\right|^q+\frac{1}{(s+1)}\left(1-\frac{1}{2^{s+1}}\right)\left|f''(\mu b+(1-\mu)a)\right|^q\right)^{\frac{1}{q}}\right. \\
&\left.+\left(\frac{1}{(s+1)}\left(1-\frac{1}{2^{s+1}}\right)\left|f''\Big(\mu a+(1-\mu)b\Big)\right|^q+\frac{1}{(s+1)}\frac{1}{2^{s+1}}\left|f''(\mu b+(1-\mu)a)\right|^q\right)^{\frac{1}{q}}\right\}
\end{aligned}
$$

So the proof is completed. ■

Theorem 9 *Let $f : I \subset \mathbb{R} \to \mathbb{R}$ be twice differentiable function on I° such that $f'' \in L[a,b]$ where $a, b \in I$, $a < b$. If $|f''|^q$ is $s-$convex on $[a,b]$, for some fixed $s \in (0,1]$, $q \geq 1$, then the* *following inequality holds:*

$$\begin{aligned}
&\left|\frac{1}{(b-a)(1-2\mu)}\int_{\mu b+(1-\mu)a}^{\mu a+(1-\mu)b} f(u)du - f\left(\frac{a+b}{2}\right)\right| \\
\leq\ & \frac{(b-a)^2(1-2\mu)^2}{2(24)^{\frac{1}{p}}}\left[\left(\frac{1}{(s+3)}\frac{1}{2^{s+3}}\left|f''\Big(\mu a+(1-\mu)\,b\Big)\right|^q\right.\right. \\
&+\left.\frac{1}{(s+1)}(1-\frac{1}{2^{s+1}})-\frac{2}{s+2}(1-\frac{1}{2^s+2})+\frac{1}{s+3}(1-\frac{1}{2^{s+3}})\Big|f''\left(\mu b+(1-\mu)\,a\right)\Big|^q\right)^{\frac{1}{q}} \\
&+\left(\frac{1}{(s+1)}(1-\frac{1}{2^{s+1}})-\frac{2}{s+2}(1-\frac{1}{2^{s+2}})+\frac{1}{s+3}(1-\frac{1}{2^{s+3}})\left|f''\Big(\mu a+(1-\mu)\,b\Big)\right|^q\right. \\
&\left.\left.+\frac{1}{(s+3)}\frac{1}{2^{s+3}}\Big|f''\left(\mu b+(1-\mu)\,a\right)\Big|^q\right)^{\frac{1}{q}}\right]
\end{aligned}$$

for $\mu \in [0,1]\setminus\{\frac{1}{2}\}$.

Proof. From Lemma 4, using well known power mean inequality, triangle inequality and the s-convexity of $|f''|^q$, it follows that

$$\begin{aligned}
&\left|\frac{1}{(b-a)(1-2\mu)}\int_{\mu b+(1-\mu)a}^{\mu a+(1-\mu)b} f(u)du - f\left(\frac{a+b}{2}\right)\right| \\
\leq\ & \frac{(b-a)^2(1-2\mu)^2}{4}\left\{\left(\int_0^{\frac{1}{2}} t^2 dt\right)^{\frac{1}{p}}\right. \\
&\times\left[\left(\int_0^{\frac{1}{2}} t^2\left|f''\Big(t\left(\mu a+(1-\mu)\,b\right)+(1-t)\left(\mu b+(1-\mu)\,a\right)\Big)\right|^q dt\right)^{\frac{1}{q}}\right. \\
&+\left.\left(\int_0^{\frac{1}{2}} t^2\left|f''\Big(t\left(\mu b+(1-\mu)\,a\right)+(1-t)\left(\mu a+(1-\mu)\,b\right)\Big)\right|^q dt\right)^{\frac{1}{q}}\right] \\
&+\left(\int_{\frac{1}{2}}^1 (1-t)^2 dt\right)^{\frac{1}{p}} \\
&\times\left[\left(\int_{\frac{1}{2}}^1 (1-t)^2\left|f''\Big(t\left(\mu a+(1-\mu)\,b\right)+(1-t)\left(\mu b+(1-\mu)\,a\right)\Big)\right|^q dt\right)^{\frac{1}{q}}\right. \\
&+\left.\left.\left(\int_{\frac{1}{2}}^1 (1-t)^2\left|f''\Big(t\left(\mu b+(1-\mu)\,a\right)+(1-t)\left(\mu a+(1-\mu)\,b\right)\Big)\right|^q dt\right)^{\frac{1}{q}}\right]\right\}
\end{aligned}$$

$$
\begin{aligned}
\leq\ & \frac{(b-a)^2(1-2\mu)^2}{4}\left(\frac{1}{24}\right)^{\frac{1}{p}} \\
&\times\left\{\left(\int_0^{\frac{1}{2}} t^2\left(t^s\left|f''\Big(\mu a+(1-\mu)b\Big)\right|^q+(1-t)^s\left|f''\left(\mu b+(1-\mu)a\right)\right|^q\right)dt\right)^{\frac{1}{q}}\right. \\
&+\left(\int_0^{\frac{1}{2}} t^2\left(t^s\left|f''\Big(\mu b+(1-\mu)a\Big)\right|^q+(1-t)^s\left|f''\left(\mu a+(1-\mu)b\right)\right|^q\right)dt\right)^{\frac{1}{q}} \\
&+\left(\int_{\frac{1}{2}}^1 (1-t)^2\left(t^s\left|f''\Big(\mu a+(1-\mu)b\Big)\right|^q+(1-t)^s\left|f''\left(\mu b+(1-\mu)a\right)\right|^q\right)dt\right)^{\frac{1}{q}} \\
&\left.+\left(\int_{\frac{1}{2}}^1 (1-t)^2\left(t^s\left|f''\Big(\mu b+(1-\mu)a\Big)\right|^q+(1-t)^s\left|f''\left(\mu a+(1-\mu)b\right)\right|^q\right)dt\right)^{\frac{1}{q}}\right\} \\
=\ & \frac{(b-a)^2(1-2\mu)^2}{4}\left(\frac{1}{24}\right)^{\frac{1}{p}} \\
&\times\left\{\left(\int_0^{\frac{1}{2}} t^{s+2}\left|f''\Big(\mu a+(1-\mu)b\Big)\right|^q dt+\int_0^{\frac{1}{2}} t^2(1-t)^s\left|f''\left(\mu b+(1-\mu)a\right)\right|^q dt\right)^{\frac{1}{q}}\right. \\
&+\left(\int_0^{\frac{1}{2}} t^{s+2}\left|f''\Big(\mu b+(1-\mu)a\Big)\right|^q dt+\int_0^{\frac{1}{2}} t^2(1-t)^s\left|f''\left(\mu a+(1-\mu)b\right)\right|^q dt\right)^{\frac{1}{q}} \\
&+\left(\int_{\frac{1}{2}}^1 t^s(1-t)^2\left|f''\Big(\mu a+(1-\mu)b\Big)\right|^q dt+\int_{\frac{1}{2}}^1 (1-t)^{s+2}\left|f''\left(\mu b+(1-\mu)a\right)\right|^q dt\right)^{\frac{1}{q}} \\
&\left.+\left(\int_{\frac{1}{2}}^1 t^s(1-t)^2\left|f''\Big(\mu b+(1-\mu)a\Big)\right|^q dt+\int_{\frac{1}{2}}^1 (1-t)^{s+2}\left|f''\left(\mu a+(1-\mu)b\right)\right|^q dt\right)^{\frac{1}{q}}\right\} \\
=\ & \frac{(b-a)^2(1-2\mu)^2}{2}\left(\frac{1}{24}\right)^{\frac{1}{p}} \\
&\times\left\{\left(\frac{1}{(s+3)}\frac{1}{2^{s+3}}\left|f''\Big(\mu a+(1-\mu)b\Big)\right|^q\right.\right. \\
&\left.+\frac{1}{(s+1)}(1-\frac{1}{2^{s+1}})-\frac{2}{s+2}(1-\frac{1}{2^s+2})+\frac{1}{s+3}(1-\frac{1}{2^{s+3}})\left|f''\left(\mu b+(1-\mu)a\right)\right|^q\right)^{\frac{1}{q}} \\
&+\left(\frac{1}{(s+1)}(1-\frac{1}{2^{s+1}})-\frac{2}{s+2}(1-\frac{1}{2^{s+2}})+\frac{1}{s+3}(1-\frac{1}{2^{s+3}})\left|f''\Big(\mu a+(1-\mu)b\Big)\right|^q\right. \\
&\left.\left.+\frac{1}{(s+3)}\frac{1}{2^{s+3}}\left|f''\left(\mu b+(1-\mu)a\right)\right|^q\right)^{\frac{1}{q}}\right\}
\end{aligned}
$$

So the proof is completed. ■

References

[1] W.W. Breckner, *Stetigkeitsaussagen fr eine Klasse verallgemeinerter konvexer funktionen in topologischen linearen Raumen*, Pupl. Inst. Math. 23 (1978) 1320.

[2] S.S. Dragomir, C.E.M. Pearce, *Quasi-convex functions and Hadamard's inequality*, Bulletin of the Australian Mathematical Society, 57-3(1998), 377-385.

[3] S.S. Dragomir and C.E.M. Pearce, *Selected Topics on Hermite-Hadamard Inequalities and Applications*, RGMIA Monographs, Victoria University, 2000.

[4] S. S. Dragomir and S. Fitzpatrik, *The Hadamard's inequality for s-convex functions in the second sense,* Demonstratio Math. 32(4), (1999), 687-696.

[5] H. Hudzik, L. Maligranda, *Some remarks on s-convex functions*, Aequationes Math. 48 (1994) 100-111.

[6] D.S. Mitrinović and I.B. Lacković, *Hermite and convexity*, Aequationes Math., 28(1) (1985), 229-232.

[7] M.Z. Sarıkaya, A.Sağlam, H.Yıldırım, *New inequalities of Hermite-Hadamard type for functions whose second derivatives absolute values are convex and quasi-convex*, arXiv:1005.0451v1 [math.CA] 4 may 2010.

A Review on An Application of Fuzzy Soft Set in Multicriteria Decision Making Problem [P.K. Das, R. Borgohain, International Journal of Computer Applications 38 (12) (2012) 33–37]

Serdar ENGİNOĞLU*
Çanakkale Onsekiz Mart University,
Department of Mathematics, 17100, Çanakkale, Turkey

Samet MEMİŞ
Çanakkale Onsekiz Mart University,
Department of Mathematics, 17100, Çanakkale, Turkey

Abstract

In this study, we review the algorithm defined by Das and Borgohain [P.K. Das, R. Borgohain, An application of fuzzy soft set in multicriteria decision making problem, International Journal of Computer Applications 38 (2012) 33–37] and rearrange this algorithm to be used in the problems containing a large amount of data. Also, we compare the running times of these algorithms. The results show that the rearranged algorithm outperforms than the other. Finally, we discuss the need for further research.

Keywords: Fuzzy sets, Soft sets, Soft decision-making, Soft matrices, $fpfs$-matrices

1 Introduction

Molodtsov [1] has produced the concept of soft sets to deal with uncertainties and Maji et al. [2, 3] have defined operations of soft sets and fuzzy soft sets. Afterwards, Çağman and Enginoğlu [4] have improved these operations and applied them to a decision-making problem. Later, Çağman et al. [5] have defined fuzzy parameterized fuzzy soft sets ($fpfs$-sets). Since the problems encountered in our daily life contain a large amount of data and uncertainties, the matrix representations of these sets such as soft matrices [6], fuzzy soft matrices [7], and fuzzy parameterized fuzzy soft matrices ($fpfs$-matrices) [8] have been constructed. $fpfs$-matrices, one of these matrix representations, is efficient to model the decision-making problems. To avail of the advantages of this concept, recently, some decision-making algorithms in the literature have been configured [9] via $fpfs$-matrices [8] by Enginoğlu and Memiş. The authors also simplified mathematically MBR01 being one of these algorithms [10]. In the present of this study, in Section 2, we give the definition of $fpfs$-matrices. In Section 3, we review the algorithm provided in [9, 11] which has been put forward by Das and Borgohain. Afterwards, we rearrange this algorithm. In Section 4, we compare the running times of original (DB12) and rearranged (sDB12) algorithms. We finally discuss the need for further research.

*Corresponding author. *E-mail address:* serdarenginoglu@gmail.com

2 Preliminaries

In this section, the definition of the concept of $fpfs$-matrices [8] have been presented. Throughout this paper, let E be a parameter set, $F(E)$ be the set of all fuzzy sets over E, and $\mu \in F(E)$. Here, $\mu := \{^{\mu(x)}x : x \in E\}$.

Definition 2.1. [5, 8] *Let U be a universal set, $\mu \in F(E)$, and α be a function from μ to $F(U)$. Then the graphic of α, denoted by α, defined by*

$$\alpha := \{(^{\mu(x)}x, \alpha(^{\mu(x)}x)) : x \in E\}$$

that is called fuzzy parameterized fuzzy soft set ($fpfs$-set) parameterized via E over U (or briefly over U).

In the present paper, the set of all $fpfs$-sets over U is denoted by $FPFS_E(U)$.

Example 2.1. *Let $E = \{x_1, x_2, x_3, x_4\}$ and $U = \{u_1, u_2, u_3, u_4, u_5\}$. Then*

$$\alpha = \{(^0x_1, \{^{0.7}u_1, ^{0.4}u_2, ^{0.3}u_4\}), (^{0.6}x_2, \{^{0.7}u_2, ^{0.6}u_3, ^{0.5}u_5\}), (^1x_3, \{^{0.6}u_1, ^{0.3}u_4, ^{0.2}u_5\}), (^{0.8}x_4, \{^{0.7}u_2, ^{0.4}u_3, ^{0.9}u_5\})\}$$

is a $fpfs$-set over U.

Definition 2.2. [8] *Let $\alpha \in FPFS_E(U)$. Then $[a_{ij}]$ is called the matrix representation of α (or briefly $fpfs$-matrix of α) and defined by*

$$[a_{ij}] = \begin{bmatrix} a_{01} & a_{02} & a_{03} & \cdots & a_{0n} & \cdots \\ a_{11} & a_{12} & a_{13} & \cdots & a_{1n} & \cdots \\ \vdots & \vdots & \vdots & \ddots & \vdots & \vdots \\ a_{m1} & a_{m2} & a_{m3} & \cdots & a_{mn} & \cdots \\ \vdots & \vdots & \vdots & \ddots & \vdots & \vdots \end{bmatrix} \text{ for } i = \{0, 1, 2, \cdots\} \text{ and } j = \{1, 2, \cdots\}$$

such that

$$a_{ij} := \begin{cases} \mu(x_j), & i = 0 \\ \alpha(^{\mu(x_j)}x_j)(u_i), & i \neq 0 \end{cases}$$

Here, if $|U| = m - 1$ and $|E| = n$ then $[a_{ij}]$ has order $m \times n$.

From now on, the set of all $fpfs$-matrices parameterized via E over U is denoted by $FPFS_E[U]$.

Example 2.2. *Let's consider the $fpfs$-set α provided in Example 2.1. Then the $fpfs$-matrix of α is as follows:*

$$[a_{ij}] = \begin{bmatrix} 0 & 0.6 & 1 & 0.8 \\ 0.7 & 0 & 0.6 & 0 \\ 0.4 & 0.7 & 0 & 0.7 \\ 0 & 0.6 & 0 & 0.4 \\ 0.3 & 0 & 0.3 & 0 \\ 0 & 0.5 & 0.2 & 0.9 \end{bmatrix}$$

3 A Review on The Soft Decision-Making Method DB12

In this section, firstly, we present the algorithm DB12 which has been proposed by Das and Borgohain [9, 11].

Step 1. Construct $fpfs$-matrices $[a_{ij}]^{(1)}$, $[a_{ij}]^{(2)}$, ..., $[a_{ij}]^{(t)}$ such that $\sum_j a_{0j}^{(1)} \leq 1$, $\sum_j a_{0j}^{(2)} \leq 1$, ..., $\sum_j a_{0j}^{(t)} \leq 1$

Step 2. Obtain $[b_{ij}]$ defined by

$$b_{ij} := \frac{1}{t}\sum_{k=1}^{t} a_{ij}^{(k)}$$

Step 3. Obtain $[c_{ik}]$ defined by

$$c_{ik} := \sum_{j=1}^{n} b_{0j}\chi(b_{ij}, b_{kj}), \quad i,k \in \{1,2,...,m-1\}$$

such that

$$\chi(b_{ij}, b_{kj}) := \begin{cases} 1, & b_{ij} \geq b_{kj} \\ 0, & b_{ij} < b_{kj} \end{cases}$$

Step 4. Obtain $[d_{i1}]$ defined by

$$d_{i1} := \sum_{k=1}^{m-1} c_{ik}, \quad i \in \{1,2,...,m-1\}$$

Step 5. Obtain $[e_{i1}]$ defined by

$$e_{i1} := \sum_{k=1}^{m-1} c_{ki}, \quad i \in \{1,2,...,m-1\}$$

Step 6. Obtain $[s_{i1}]$ defined by

$$s_{i1} := d_{i1} - e_{i1}, \quad i \in \{1,2,...,m-1\}$$

Step 7. Obtain the set $\{u_k \mid s_{k1} = \max_i s_{i1}\}$

Preferably, the set $\{^{\mu(u_k)}u_k | u_k \in U\}$ can be attained such that $\mu(u_k) = \frac{s_{k1}+|\min_i s_{i1}|}{\max_i s_{i1}+|\min_i s_{i1}|}$.

It must be noted that DB12 is equivalent to MBR01 given in [3, 9] except for Step 1 and 2. Therefore, DB12 can be simplified (sDB12) by using the proof provided in [10] as follows:

Step 1. Construct $fpfs$-matrices $[a_{ij}]^{(1)}$, $[a_{ij}]^{(2)}$, ..., $[a_{ij}]^{(t)}$ such that $\sum_j a_{0j}^{(1)} \leq 1$, $\sum_j a_{0j}^{(2)} \leq 1$, ..., $\sum_j a_{0j}^{(t)} \leq 1$

Step 2. Obtain $[b_{ij}]$ defined by

$$b_{ij} := \frac{1}{t}\sum_{k=1}^{t} a_{ij}^{(k)}$$

Step 3. Obtain $[s_{i1}]$ defined by

$$s_{i1} := \sum_{k=1}^{m-1}\sum_{j=1}^{n} b_{0j}\,\mathrm{sgn}(b_{ij} - b_{kj}), \quad i \in \{1,2,...,m-1\},$$

Step 4. Obtain the set $\{u_k \mid s_{k1} = \max_i s_{i1}\}$

Preferably, the set $\{^{\mu(u_k)}u_k | u_k \in U\}$ can be attained such that $\mu(u_k) = \frac{s_{k1}+|\min_i s_{i1}|}{\max_i s_{i1}+|\min_i s_{i1}|}$.

Although DB12 is not an innovative study, it offers an idea about how to use MBR01 in the event that a problem contains more than one $fpfs$-matrices. The relation between sDB12 and sMBR01 is similar to this.

4 Simulation Results

In this section, we compare the running times of the algorithms provided in Section 3 for random three $fpfs$-matrices. These algorithms are coded in MATLAB R2018b on a laptop with 2.6 GHz i5 Dual Core CPU and 4GB RAM.

We present the running times of DB12 and sDB12 in Table 1 and Fig. 1 for 10 objects and the parameters ranging from 1000 to 10000. We then give their running times in Table 2 and Fig. 2 for 10 parameters and the objects ranging from 1000 to 10000, in Table 3 and Fig. 3 for the parameters and the objects ranging from 10 to 100 and in Table 4 and Fig. 4 for the parameters and the objects ranging from 100 to 1000. The results show that sDB12 outperforms DB12 in any number of data.

Table 1. The results for 10 objects and the parameters ranging from 1000 to 10000 (In Seconds)

	1000	2000	3000	4000	5000	6000	7000	8000	9000	10000
DB12	0.0110	0.0198	0.0292	0.0392	0.0323	0.0394	0.0389	0.0446	0.0496	0.0566
sDB12	0.0034	0.0046	0.0068	0.0083	0.0112	0.0079	0.0095	0.0107	0.0121	0.0137
Difference	0.0076	0.0152	0.0224	0.0309	0.0211	0.0315	0.0295	0.0339	0.0375	0.0429
Advantage (%)	69.2034	76.6479	76.6617	78.7758	65.3607	79.8421	75.6988	76.0316	75.6041	75.7260

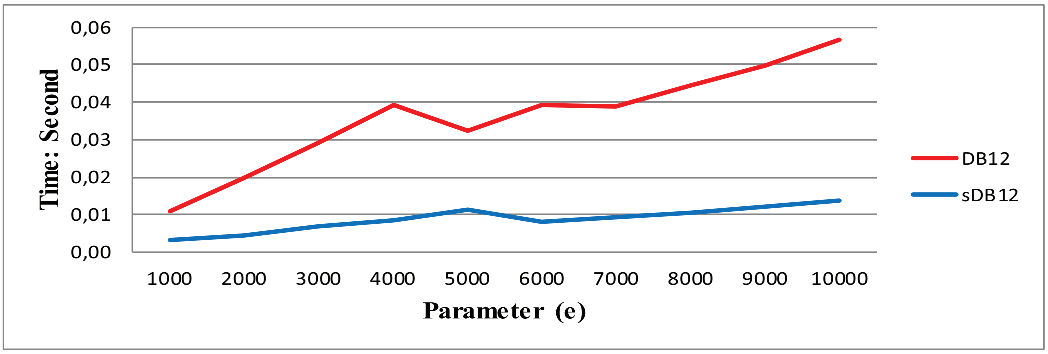

Fig. 1. The figure for Table 1

Table 2. The results for 10 parameters and the objects ranging from 1000 to 10000 (In Seconds)

	1000	2000	3000	4000	5000	6000	7000	8000	9000	10000
DB12	0.6029	2.5731	5.5545	10.0379	15.7436	23.8807	32.2466	46.0046	58.1403	74.5375
sDB12	0.0927	0.3141	0.6930	1.2800	1.9767	2.8459	3.9346	5.2587	6.4199	7.9532
Difference	0.5102	2.2590	4.8615	8.7579	13.7668	21.0347	28.3120	40.7459	51.7204	66.5843
Advantage (%)	84.6276	87.7923	87.5237	87.2484	87.4442	88.0827	87.7984	88.5691	88.9579	89.3299

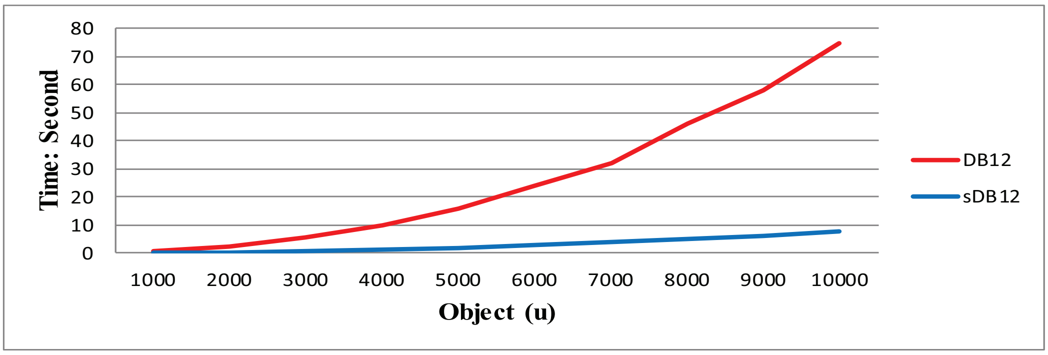

Fig. 2. The figure for Table 2

Table 3. The results for the parameters and the objects ranging from 10 to 100 (In Seconds)

	10	20	30	40	50	60	70	80	90	100
DB12	0.0015	0.0008	0.0023	0.0057	0.0109	0.0189	0.0181	0.0297	0.0378	0.0518
sDB12	0.0013	0.0002	0.0004	0.0009	0.0019	0.0017	0.0028	0.0041	0.0053	0.0074
Difference	0.0002	0.0006	0.0019	0.0048	0.0090	0.0171	0.0152	0.0256	0.0325	0.0444
Advantage (%)	14.3967	77.6795	82.3006	84.0919	82.8266	90.8021	84.2889	86.1317	85.9570	85.6798

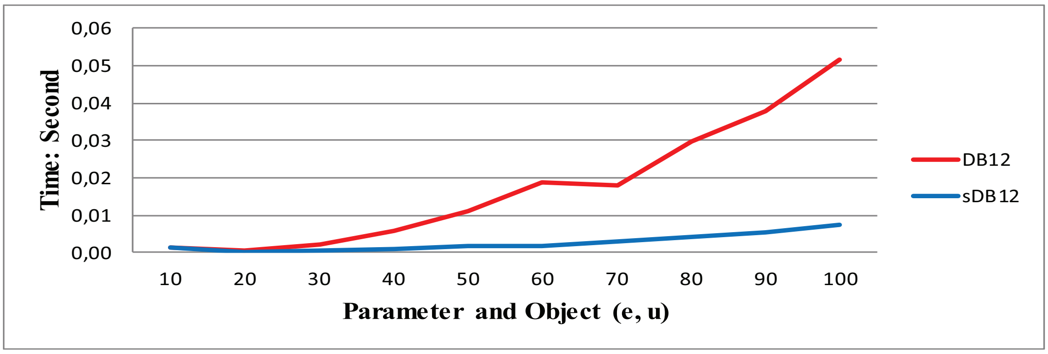

Fig. 3. The figure for Table 3

Table 4. The results for the parameters and the objects ranging from 100 to 1000 (In Seconds)

	100	200	300	40	500	600	700	800	900	1000
DB12	0.0842	0.4957	1.6483	3.9022	8.3366	15.1699	25.1246	39.1928	55.9517	78.6396
sDB12	0.0081	0.0596	0.2143	0.5683	1.2457	3.2403	6.5297	10.7083	15.2728	21.7734
Difference	0.0760	0.4361	1.4340	3.3339	7.0909	11.9296	18.5948	28.4845	40.6789	56.8662
Advantage (%)	90.3473	87.9818	86.9977	85.4354	85.0572	78.6398	74.0105	72.6778	72.7036	72.3125

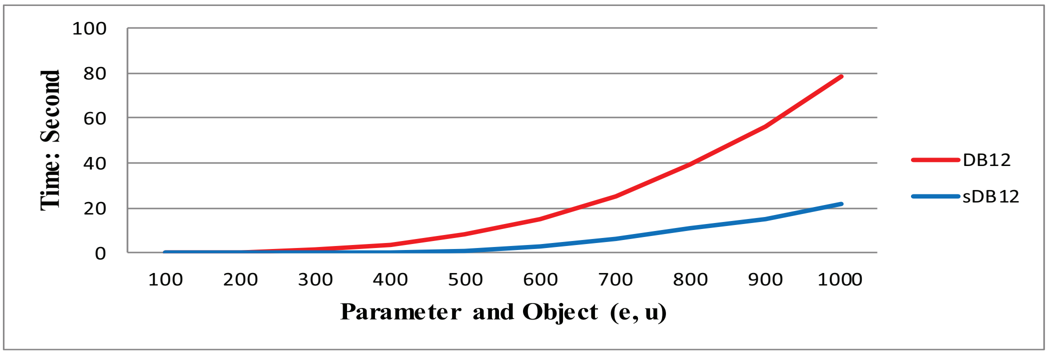

Fig. 4. The figure for Table 4

As a summary, the results in Table 5 show that sDB12 outperforms DB12 in any number of data.

Table 5. The mean advantage, max advantage, and max difference values of sDB12 over DB12

Location	Objects	Parameters	Mean Advantage%	Max Advantage%	Max Difference
Table 1	10	1000 – 10000	74.9552	79.8421	0.0429
Table 2	1000 – 10000	10	87.7374	89.3299	66.5843
Table 3	10 – 100	10 – 100	77.4155	90.8021	0.0444
Table 4	100 – 1000	100 – 1000	80.6164	90.3473	56.8662

5 Conclusion

The decision-making method DB12 provided in [11] was defined in 2012. Afterwards, this method has been configured [9] via $fpfs$-matrices [8]. However, the soft decision-making method DB12 is equivalent to MBR01 [3, 9] except for Step 1 and 2. Since this method is not a new algorithm, its contribution to soft set theory is poor. Even so, it may provide new ideas about how to use MBR01 in the event that a problem contains more than one $fpfs$-matrices. The simulation results point out the significance of simplifications. Although some methods which are equivalent or too similar to each other have been published in the different names, it is worthwhile to keep studying on soft decision-making.

Acknowledgements

This work was supported by the Office of Scientific Research Projects Coordination at Çanakkale Onsekiz Mart University, Grant number: FBA-2018-1367.

References

[1] D. Molodtsov, Soft set theory-first results, Computers and Mathematics with Applications 37 (1999) 19–31.

[2] P. K. Maji, A. Roy, R. Biswas, An application of soft sets in a decision making problem, Computers and Mathematics with Applications 44 (2002) 1077–1083.

[3] P. K. Maji, R. Biswas, A. Roy, Fuzzy soft sets, The Journal of Fuzzy Mathematics 9 (3) (2001) 589–602.

[4] N. Çağman, S. Enginoğlu, Soft set theory and uni-int decision making, European Journal of Operational Research 207 (2010) 848–855.

[5] N. Çağman, F. Çıtak, S. Enginoğlu, Fuzzy parameterized fuzzy soft set theory and its applications, Turkish Journal of Fuzzy Systems 1 (1) (2010) 21–35.

[6] N. Çağman, S. Enginoğlu, Soft matrix theory and its decision making, Computers and Mathematics with Applications 59 (2010) 3308–3314.

[7] N. Çağman, S. Enginoğlu, Fuzzy soft matrix theory and its application in decision making, Iranian Journal of Fuzzy Systems 9 (1) (2012) 109–119.

[8] S. Enginoğlu, Soft matrices, PhD dissertation, Gaziosmanpaşa University (2012).

[9] S. Enginoğlu, S. Memiş, A configuration of some soft decision-making algorithms via $fpfs$-matrices, Cumhuriyet Science Journal 39 (4) (2018) 871–881.

[10] S. Enginoğlu, S. Memiş, Comment on Fuzzy soft sets [The Journal of Fuzzy Mathematics, 9(3), 2001, 589–602], International Journal of Latest Engineering Research and Applications 3 (9) (2018) 1–9.

[11] P. K. Das, R. Borgohain, An application of fuzzy soft set in multicriteria decision making problem, International Journal of Computer Applications 38 (12) (2012) 33–37.

A Fast and Simple Sof Decision-Making Algorithm: EMO18o

Serdar ENGİNOĞLU*
Çanakkale Onsekiz Mart University,
Department of Mathematics, 17100, Çanakkale, Turkey

Samet MEMİŞ
Çanakkale Onsekiz Mart University,
Department of Mathematics, 17100, Çanakkale, Turkey

Tutku ÖNGEL
Çanakkale Onsekiz Mart University,
Department of Mathematics, 17100, Çanakkale, Turkey

Abstract

In a recent study, the uni-int soft decision-making method [N. Çağman, S. Enginoğlu, Soft set theory and uni-int decision making, European Journal of Operational Research 207 (2010) 848-855] constructed by and-product/or-product has been configured via fuzzy parameterized fuzzy soft matrices ($fpfs$-matrices) by Enginoğlu and Memiş, faithfully to the original. However, in the case that a large amount of data is processed, the method has a disadvantage in terms of time and complexity. To deal with this problem and to be able to use this configured method, denoted by CE10, in computer science such as machine learning and image processing, in this paper, we suggest a new algorithm, i.e. EMO18o, equivalent to CE10 constructed by or-product (CE10o) in the event that first rows of the $fpfs$-matrices are binary. We then compare the running times of these two algorithms. The results show that EMO18o performs better than CE10o in any number of data. Finally, we discuss the need for further research.

Keywords: Fuzzy sets, Soft sets, Soft decision-making, Soft matrices, $fpfs$-matrices

1 Introduction

The concept of soft sets was produced by Molodtsov [1] to deal with uncertainties, and so far many theoretical and applied studies from algebra to decision-making problems have been conducted on this concept [2–25]. Recently, the uni-int decision-making algorithm constructed by and-product/or-product [22] has been configured via fuzzy parameterized fuzzy soft matrices ($fpfs$-matrices) by Enginoğlu and Memiş [26], faithfully to the original. However, the method has a disadvantage in terms of time and complexity, in spite of the fact that it has the potential to be used successfully in computer science such as image processing and machine learning. To deal with this problem, it is worthwhile to study the simplification of this algorithm.

In Section 2 of the present study, we introduce the concept of $fpfs$-matrices [21]. In Section 3, we present CE10 constructed by and-product/or-product [22, 26]. In Section 4, we propose a fast and simple algorithm, namely EMO18o, equivalent to CE10 constructed by or-product (CE10o) under the condition that first rows of the $fpfs$-matrices are binary. In

*Corresponding author. *E-mail address:* serdarenginoglu@gmail.com

Section 5, we compare the running times of these algorithms. Finally, we discuss the need for further research.

2 Preliminaries

In this section, the concept of $fpfs$-matrices [21] and some of its basic definitions have been presented. Throughout this paper, let E be a parameter set, $F(E)$ be the set of all fuzzy sets over E, and $\mu \in F(E)$. Here, $\mu := \{^{\mu(x)}x : x \in E\}$.

Definition 2.1. [14, 21] *Let U be a universal set, $\mu \in F(E)$, and α be a function from μ to $F(U)$. Then the graphic of α, denoted by α, defined by*

$$\alpha := \{(^{\mu(x)}x, \alpha(^{\mu(x)}x)) : x \in E\}$$

that is called fuzzy parameterized fuzzy soft set ($fpfs$-set) parameterized via E over U (or briefly over U).

In the present paper, the set of all $fpfs$-sets over U is denoted by $FPFS_E(U)$.

Example 2.1. *Let $E = \{x_1, x_2, x_3, x_4\}$ and $U = \{u_1, u_2, u_3, u_4, u_5\}$. Then*

$$\alpha = \{(^1x_1, \{^{0.7}u_1, ^{0.3}u_4\}), (^{0.5}x_2, \{^{0.6}u_2, ^{0.2}u_3\}), (^{0.3}x_3, \{^{0.6}u_1, ^{0.3}u_3, ^{0.2}u_4\}), (^0x_4, \{^1u_2, ^{0.1}u_3, ^{0.4}u_5\})\}$$

is a $fpfs$-set over U.

Definition 2.2. [21] *Let $\alpha \in FPFS_E(U)$. Then $[a_{ij}]$ is called the matrix representation of α (or briefly $fpfs$-matrix of α) and defined by*

$$[a_{ij}] = \begin{bmatrix} a_{01} & a_{02} & a_{03} & \cdots & a_{0n} & \cdots \\ a_{11} & a_{12} & a_{13} & \cdots & a_{1n} & \cdots \\ \vdots & \vdots & \vdots & \ddots & \vdots & \vdots \\ a_{m1} & a_{m2} & a_{m3} & \cdots & a_{mn} & \cdots \\ \vdots & \vdots & \vdots & \ddots & \vdots & \vdots \end{bmatrix} \text{ for } i = \{0, 1, 2, \cdots\} \text{ and } j = \{1, 2, \cdots\}$$

such that

$$a_{ij} := \begin{cases} \mu(x_j), & i = 0 \\ \alpha(^{\mu(x_j)}x_j)(u_i), & i \neq 0 \end{cases}$$

Here, if $|U| = m - 1$ and $|E| = n$ then $[a_{ij}]$ has order $m \times n$.

From now on, the set of all $fpfs$-matrices parameterized via E over U is denoted by $FPFS_E[U]$.

Example 2.2. *Let's consider the $fpfs$-set α provided in Example 2.1. Then the $fpfs$-matrix of α is as follows:*

$$[a_{ij}] = \begin{bmatrix} 1 & 0.5 & 0.3 & 0 \\ 0.7 & 0 & 0.6 & 0 \\ 0 & 0.6 & 0 & 1 \\ 0 & 0.2 & 0.3 & 0.1 \\ 0.3 & 0 & 0.2 & 0 \\ 0 & 0 & 0 & 0.4 \end{bmatrix}$$

Definition 2.3. [21] *Let $[a_{ij}], [b_{ik}] \in FPFS_E[U]$ and $[c_{ip}] \in FPFS_{E^2}[U]$ such that $p = n(j-1)+k$. For all i and p,*

If $c_{ip} = \min\{a_{ij}, b_{ik}\}$, then $[c_{ip}]$ is called and-product of $[a_{ij}]$ and $[b_{ik}]$, denoted by $[a_{ij}]\wedge[b_{ik}]$.

If $c_{ip} = \max\{a_{ij}, b_{ik}\}$, *then* $[c_{ip}]$ *is called or-product of* $[a_{ij}]$ *and* $[b_{ik}]$, *denoted by* $[a_{ij}]\vee[b_{ik}]$.

If $c_{ip} = \min\{a_{ij}, 1-b_{ik}\}$, *then* $[c_{ip}]$ *is called andnot-product of* $[a_{ij}]$ *and* $[b_{ik}]$, *denoted by* $[a_{ij}]\overline{\wedge}[b_{ik}]$.

If $c_{ip} = \max\{a_{ij}, 1-b_{ik}\}$, *then* $[c_{ip}]$ *is called ornot-product of* $[a_{ij}]$ *and* $[b_{ik}]$, *denoted by* $[a_{ij}]\underline{\vee}[b_{ik}]$.

3 The Soft Decision-Making Method CE10

In this section, we present the algorithm CE10 [22, 26].

Step 1. Construct two $fpfs$-matrices $[a_{ij}]$ and $[b_{ik}]$

Step 2. Find and-product/or-product $fpfs$-matrix $[c_{ip}]$ of $[a_{ij}]$ and $[b_{ik}]$

Step 3. Obtain $[s_{i1}]$ denoted by $\max\text{-}\min(c_{ip})$ defined by

$$s_{i1} := \max\{\max_j\min_k(c_{ip}), \max_k\min_j(c_{ip})\}$$

such that $i \in \{1, 2, \dots, m-1\}$, $I_a := \{j \mid a_{0j} \neq 0\}$, $I_b := \{k \mid b_{0k} \neq 0\}$, $p = n(j-1)+k$, and

$$\max_j\min_k(c_{ip}) := \begin{cases} \max\limits_{j\in I_a}\left\{\min\limits_{k\in I_b} c_{0p}c_{ip}\right\}, & I_a \neq \emptyset \text{ and } I_b \neq \emptyset \\ 0, & \text{Otherwise} \end{cases}$$

$$\max_k\min_j(c_{ip}) := \begin{cases} \max\limits_{k\in I_b}\left\{\min\limits_{j\in I_a} c_{0p}c_{ip}\right\}, & I_a \neq \emptyset \text{ and } I_b \neq \emptyset \\ 0, & \text{Otherwise} \end{cases}$$

Step 4. Obtain the set $\{u_k \in U \mid s_{k1} = \max\limits_i s_{i1}\}$

Preferably, the set $\{^{s_{i1}}u_i \mid u_i \in U\}$ or $\{^{\frac{s_{k1}}{\max s_{i1}}}u_k | u_k \in U\}$ can be attained.

Note 3.1. *Let CE10a and CE10o denote CE10 constructed by and-product and or-product, respectively. It must be noted that the scores of CE10a and CE10o can be found without writing any product matrices. When the algorithm is written in this format, it offers time advantage, little though, over CE10 in most cases. Let's illustrate this for CE10o;*

Step 1. *Construct two* $fpfs$*-matrices* $[a_{ij}]$ *and* $[b_{ik}]$

Step 2. *Obtain* $[s_{i1}]$ *defined by*

$$s_{i1} := \begin{cases} \max\{\max\limits_{j\in I_a}\{\min\limits_{k\in I_b}\{\max\{a_{0j}, b_{0k}\}, \max\{a_{ij}, b_{ik}\}\}\}, \max\limits_{k\in I_b}\{\min\limits_{j\in I_a}\{\max\{a_{0j}, b_{0k}\}, \max\{a_{ij}, b_{ik}\}\}\}\}, & I_a, I_b \neq \emptyset \\ 0, & \textit{otherwise} \end{cases}$$

such that $i \in \{1, 2, \dots, m-1\}$, $I_a := \{j \mid a_{0j} \neq 0\}$, *and* $I_b := \{k \mid b_{0k} \neq 0\}$.

Step 3. *Obtain the set* $\{u_k \in U \mid s_{k1} = \max\limits_i s_{i1}\}$

Preferably, the set $\{^{s_{i1}}u_i \mid u_i \in U\}$ *or* $\{^{\frac{s_{k1}}{\max s_{i1}}}u_k | u_k \in U\}$ *can be attained.*

4 A Soft Decision-Making Method: EMO18o

In this section, we propose a fast and simple algorithm denoted by EMO18o.

Step 1. Construct two $fpfs$-matrices $[a_{ij}]$ and $[b_{ik}]$

Step 2. Obtain $[s_{i1}]$ denoted by $\max\text{-}\min(a_{ij}, b_{ik})$ defined by

$$s_{i1} := \max\{\max_j \min_k(a_{ij}, b_{ik}), \max_k \min_j(a_{ij}, b_{ik})\}$$

such that $i \in \{1, 2, \ldots, m-1\}$, $I_a := \{j \mid a_{0j} \neq 0\}$, $I_b := \{k \mid b_{0k} \neq 0\}$, and

$$\max_j \min_k(a_{ij}, b_{ik}) := \begin{cases} \max\left\{\max\limits_{j\in I_a}\{a_{0j}a_{ij}\}, \min\limits_{k\in I_b}\{b_{0k}b_{ik}\}\right\}, & I_a \neq \emptyset \text{ and } I_b \neq \emptyset \\ 0, & \text{otherwise} \end{cases}$$

$$\max_k \min_j(a_{ij}, b_{ik}) := \begin{cases} \max\left\{\max\limits_{k\in I_b}\{b_{0k}b_{ik}\}, \min\limits_{j\in I_a}\{a_{0j}a_{ij}\}\right\}, & I_a \neq \emptyset \text{ and } I_b \neq \emptyset \\ 0, & \text{otherwise} \end{cases}$$

Step 3. Obtain the set $\{u_k \in U \mid s_{k1} = \max\limits_i s_{i1}\}$

Preferably, the set $\{^{s_{i1}}u_i \mid u_i \in U\}$ or $\{^{\frac{s_{k1}}{\max s_{i1}}}u_k | u_k \in U\}$ can be attained.

Theorem 4.1. *EMO18o is equivalent to CE10o under the condition that first rows of the $fpfs$-matrices are binary.*

Proof. Suppose that first rows of the $fpfs$-matrices are binary. The functions s_{i1} provided in CE10a and EMO18a are equal in the event that $I_a = \emptyset$ or $I_b = \emptyset$. Assume that $I_a \neq \emptyset$ and $I_b \neq \emptyset$. Since $a_{0j} = 1$ and $b_{0k} = 1$, for all $j \in I_a := \{a_1, a_2, ..., a_s\}$ and $k \in I_b := \{b_1, b_2, ..., b_t\}$,

$$\begin{aligned}
\max_j \min_k(c_{ip}) &= \max_{j\in I_a}\left\{\min_{k\in I_b} c_{0p}c_{ip}\right\} \\
&= \max_{j\in I_a}\left\{\min_{k\in I_b}\{\max\{a_{0j}, b_{0k}\}.\max\{a_{ij}, b_{ik}\}\}\right\} \\
&= \max_{j\in I_a}\left\{\min_{k\in I_b}\{\max\{a_{ij}, b_{ik}\}\}\right\} \\
&= \max\{\min\{\max\{a_{ia_1}, b_{ib_1}\}, \max\{a_{ia_1}, b_{ib_2}\}, \ldots, \max\{a_{ia_1}, b_{ib_t}\}\}, \\
&\qquad \min\{\max\{a_{ia_2}, b_{ib_1}\}, \max\{a_{ia_2}, b_{ib_2}\}, \ldots, \max\{a_{ia_2}, b_{ib_t}\}\}, \ldots, \\
&\qquad \min\{\max\{a_{ia_s}, b_{ib_1}\}, \max\{a_{ia_s}, b_{ib_2}\}, \ldots, \max\{a_{ia_s}, b_{ib_t}\}\}\} \\
&= \max\{\max\{a_{ia_1}, \min\{b_{ib_1}, b_{ib_2}, \ldots, b_{ib_t}\}\}, \\
&\qquad \max\{a_{ia_2}, \min\{b_{ib_1}, b_{ib_2}, \ldots, b_{ib_t}\}\}, \ldots, \\
&\qquad \max\{a_{ia_s}, \min\{b_{ib_1}, b_{ib_2}, \ldots, b_{ib_t}\}\}\} \\
&= \max\{\max\{a_{ia_1}, a_{ia_2}, \ldots, a_{ia_s}\}, \min\{b_{ib_1}, b_{ib_2}, \ldots, b_{ib_t}\}\} \\
&= \max\left\{\max_{j\in I_a}\{a_{ij}\}, \min_{k\in I_b}\{b_{ik}\}\right\} \\
&= \max\left\{\max_{j\in I_a}\{a_{0j}a_{ij}\}, \min_{k\in I_b}\{b_{0k}b_{ik}\}\right\} \\
&= \max_j \min_k(a_{ij}, b_{ik})
\end{aligned}$$

In a similar way, $\max_k \min_j(c_{ip}) = \max_k \min_j(a_{ij}, b_{ik})$. Consequently,

$$\max\text{-}\min(a_{ij}, b_{ik}) = \max\text{-}\min(c_{ip})$$

∎

5 Simulation Results

In this section, we compare the running times of CE10o and EMO18o by using MATLAB R2018b. So long as it has not been encountered a difficulty, we use a laptop with 2.6 GHz i5 Dual Core CPU and 4 GB RAM to compare the methods. However, in this study, we use a workstation with I(R) Xeon(R) CPU E5-1620 v4 @ 3.5 GHz and 64 GB RAM because the computer is insufficient to run CE10o if the parameters or objects are more than 5000.

We, present the running times of CE10o and EMO18o in Table 1 and Fig. 1 for 10 objects and the parameters ranging from 1000 to 10000. We then give their running times in Table 2 and Fig. 2 for 10 parameters and the objects ranging from 1000 to 10000, in Table 3 and Fig. 3 for the parameters and the objects ranging from 10 to 100, and in Table 4 and Fig. 4 for the parameters and the objects ranging from 100 to 1000. The results show that EMO18o outperforms than CE10o in any number of data under the specified condition.

Table 1. The results for 10 objects and the parameters ranging from 1000 to 10000 (In Seconds)

	1000	2000	3000	4000	5000	6000	7000	8000	9000	10000
CE10o	1.4292	5.1723	11.0594	18.7021	28.1838	41.0885	55.7873	73.4621	92.8691	119.3578
EMO18o	0.0007	0.0011	0.0015	0.0018	0.0023	0.0025	0.0028	0.0032	0.0036	0.0040
Difference	1.4285	5.1712	11.0579	18.7003	28.1815	41.0860	55.7845	73.4590	92.8655	119.3538
Advantage (%)	99.9526	99.9782	99.9868	99.9904	99.9918	99.9939	99.9950	99.9957	99.9961	99.9967

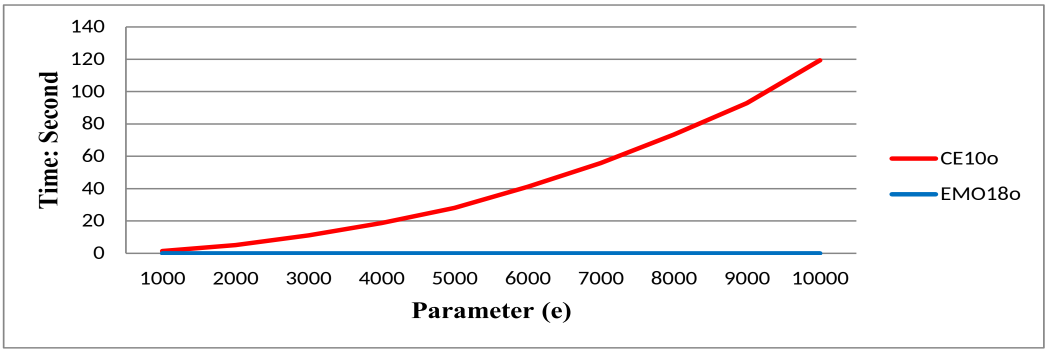

Fig. 1. The figure for Table 1

Table 2. The results for 10 parameters and the objects ranging from 1000 to 10000 (In Seconds)

	1000	2000	3000	4000	5000	6000	7000	8000	9000	10000
CE10o	0.0653	0.1653	0.2543	0.5031	0.6359	0.8852	1.1581	1.4888	1.7812	2.2587
EMO18o	0.0088	0.0170	0.0252	0.0358	0.0452	0.0557	0.0683	0.0812	0.0940	0.1095
Difference	0.0565	0.1483	0.2292	0.4674	0.5907	0.8294	1.0898	1.4076	1.6872	2.1492
Advantage (%)	86.4942	89.7373	90.1065	92.8936	92.8854	93.7031	94.1050	94.5449	94.7246	95.1539

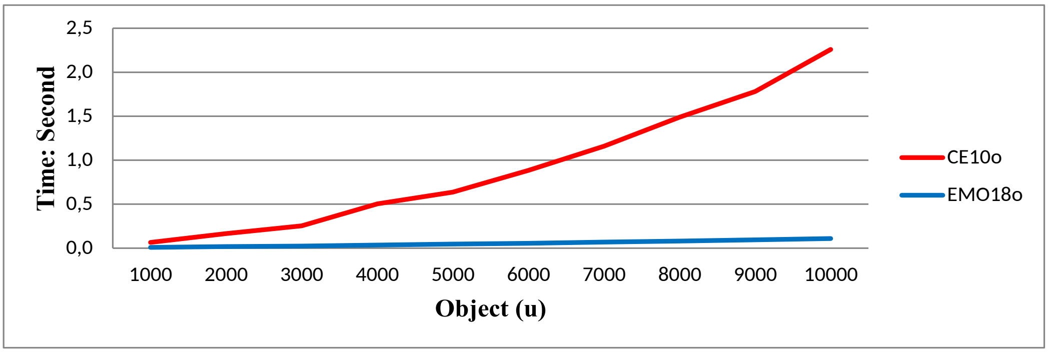

Fig. 2. The figure for Table 2

Table 3. The results for the parameters and the objects ranging from 10 to 100 (In Seconds)

	10	**20**	**30**	**40**	**50**	**60**	**70**	**80**	**90**	**100**
CE10o	0.0011	0.0015	0.0047	0.0103	0.0184	0.0338	0.0537	0.0835	0.1365	0.1574
EMO18o	0.0006	0.0002	0.0003	0.0005	0.0008	0.0006	0.0007	0.0008	0.0009	0.0011
Difference	0.0006	0.0013	0.0044	0.0099	0.0176	0.0332	0.0530	0.0827	0.1355	0.1563
Advantage (%)	51.4841	84.8634	93.3296	95.5557	95.7001	98.3215	98.7335	99.0143	99.3060	99.3312

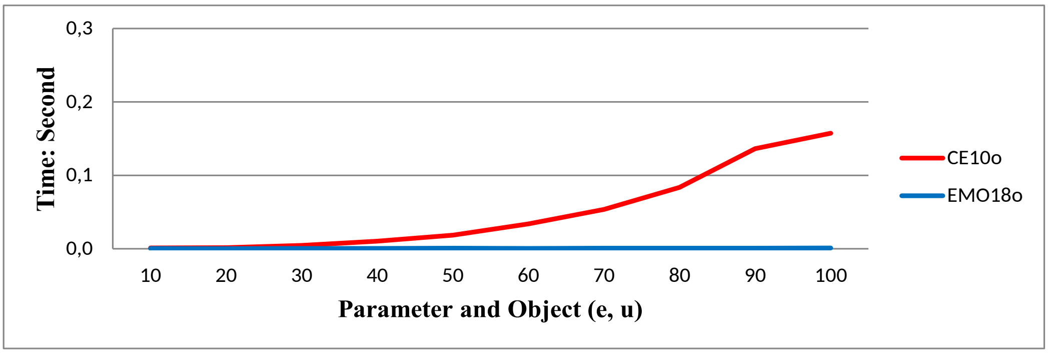

Fig. 3. The figure for Table 3

Table 4. The results for the parameters and the objects ranging from 100 to 1000 (In Seconds)

	100	**200**	**300**	**40**	**500**	**600**	**700**	**800**	**900**	**1000**
CE10o	0.1740	2.1408	8.9146	25.4105	57.4277	109.2121	185.3141	306.6551	494.7809	734.7361
EMO18o	0.0017	0.0029	0.0046	0.0076	0.0101	0.0144	0.0175	0.0220	0.0286	0.0342
Difference	0.1724	2.1379	8.9100	25.4029	57.4176	109.1977	185.2966	306.6331	494.7522	734.7019
Advantage (%)	99.0506	99.8651	99.9484	99.9701	99.9823	99.9868	99.9906	99.9928	99.9942	99.9953

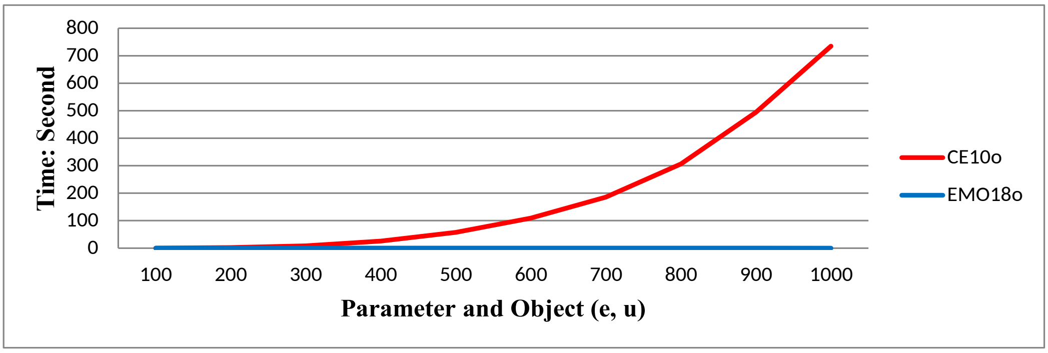

Fig. 4. The figure for Table 4

6 Conclusion

The uni-int decision-making method was defined in 2010 [22]. Afterwards, this method has been configured [26] via $fpfs$-matrices [21] because more general forms are needed for the method in the event that the paramters or objects have uncertainties. However, the method suffers from a drawback, i.e. its incapability of processing a large number of parameters on a standard computer, e.g. with 2.6 GHz i5 Dual Core CPU and 4GB RAM. For this reason, simplification of such methods is important for a wide range of scientific and industrial processes. In this study, we have proposed the method EMO18o, which is faster than CE10o. Of course, it is possible to investigate the simplifications for other products.

We then have compared the running times of these algorithms. In addition to the results in Section 5, the results in Table 5 too show that EMO18o outperforms CE10o in any number of data under the specified condition.

Table 5. The mean advantage, max advantage, and max difference values of EMO18o over CE10o

Location	Objects	Parameters	Mean Advantage%	Max Advantage%	Max Difference
Table 1	10	1000 – 10000	99.9877	99.9967	119.3538
Table 2	1000 – 10000	10	92.4348	95.1539	2.1492
Table 3	10 – 100	10 – 100	91.5639	99.3312	0.1563
Table 4	100 – 1000	100 – 1000	99.8776	99.9953	734.7019

In addition, other decision-making methods constructed by a different decision function such as minimum-maximum (min-max), max-max, and min-min can also be studied in the similar way.

Acknowledgements

The authors thank Dr. Uğur Erkan for technical support. This work was supported by the Office of Scientific Research Projects Coordination at Çanakkale Onsekiz Mart University, Grant number: FBA-2018-1367.

References

[1] D. Molodtsov, Soft set theory-first results, Computers and Mathematics with Applications 37 (1999) 19–31.

[2] M. Tunçay, A. Sezgin, Soft union ring and its applications to ring theory, International Journal of Computer Applications 151 (9) (2016) 7–13.

[3] A. Ullah, F. Karaaslan, I. Ahmad, Soft uni-abel-grassmann's groups, European Journal of Pure and Applied Mathematics 11 (2) (2018) 517–536.

[4] P. K. Maji, R. Biswas, A. Roy, Soft set theory, Computers and Mathematics with Applications 45 (2003) 555–562.

[5] N. Çağman, S. Enginoğlu, F. Çıtak, Fuzzy soft set theory and its applications, Iranian Journal of Fuzzy Systems 8 (3) (2011) 137–147.

[6] F. Çıtak, N. Çağman, Soft k-int-ideals of semirings and its algebraic structures, Annals of Fuzzy Mathematics and Informatics 13 (4) (2017) 531–538.

[7] S. Atmaca, İ. Zorlutuna, On topological structures of fuzzy parametrized soft sets, The Scientific World Journal 2014 (2014) Article ID 164176, 8 pages.

[8] S. Enginoğlu, N. Çağman, S. Karataş, T. Aydın, On soft topology, El-Cezerî Journal of Science and Engineering 2 (3) (2015) 23–38.

[9] P. K. Maji, A. Roy, R. Biswas, An application of soft sets in a decision making problem, Computers and Mathematics with Applications 44 (2002) 1077–1083.

[10] F. Çıtak, N. Çağman, Soft int-rings and its algebraic applications, Journal of Intelligent and Fuzzy Systems 28 (2015) 1225–1233.

[11] N. Çağman, S. Enginoğlu, Fuzzy soft matrix theory and its application in decision making, Iranian Journal of Fuzzy Systems 9 (1) (2012) 109–119.

[12] E. Muştuoğlu, A. Sezgin, Z. K. Türk, Some characterizations on soft uni-groups and normal soft uni-groups, International Journal of Computer Applications 155 (10) (2016) 8 pages.

[13] A. Sezgin, A new approach to semigroup theory I: Soft union semigroups, ideals and bi-ideals, Algebra Letters 2016 (3).

[14] N. Çağman, F. Çıtak, S. Enginoğlu, Fuzzy parameterized fuzzy soft set theory and its applications, Turkish Journal of Fuzzy Systems 1 (1) (2010) 21–35.

[15] N. Çağman, S. Enginoğlu, Soft matrix theory and its decision making, Computers and Mathematics with Applications 59 (2010) 3308–3314.

[16] S. Bera, S. K. Roy, F. Karaaslan, N. Çağman, Soft congruence relation over lattice, Hacettepe Journal of Mathematics and Statistics 46 (6) (2017) 1035–1042.

[17] P. K. Maji, R. Biswas, A. Roy, Fuzzy soft sets, The Journal of Fuzzy Mathematics 9 (3) (2001) 589–602.

[18] S. Atmaca, Relationship between fuzzy soft topological spaces and (X, τ_e) parameter spaces, Cumhuriyet Science Journal 38 (2017) 77–85.

[19] F. Karaaslan, Soft classes and soft rough classes with applications in decision making, Mathematical Problems in Engineering 2016 (2016) Article ID 1584528, 11 pages.

[20] A. Sezgin, N. Çağman, F. Çıtak, α-inclusions applied to group theory via soft set and logic, Communications Faculty of Sciences University of Ankara Series A1 Mathematics and Statistics 68 (1) (2019) 334–352.

[21] S. Enginoğlu, Soft matrices, PhD dissertation, Gaziosmanpaşa University (2012).

[22] N. Çağman, S. Enginoğlu, Soft set theory and uni-int decision making, European Journal of Operational Research 207 (2010) 848–855.

[23] N. Çağman, F. Çıtak, S. Enginoğlu, FP-soft set theory and its applications, Annals of Fuzzy Mathematics Information 2 (2) (2011) 219–226.

[24] İ. Zorlutuna, S. Atmaca, Fuzzy parametrized fuzzy soft topology, New Trends in Mathematical Sciences 4 (1) (2016) 142–152.

[25] S. Enginoğlu, S. Memiş, Comment on Fuzzy soft sets [The Journal of Fuzzy Mathematics, 9(3), 2001, 589–602], International Journal of Latest Engineering Research and Applications 3 (9) (2018) 1–9.

[26] S. Enginoğlu, S. Memiş, A configuration of some soft decision-making algorithms via $fpfs$-matrices, Cumhuriyet Science Journal 39 (4) (2018) 871–881.

On The Space of Korovkin Sequences

Tuncay TUNÇ*
Mersin University,
Department of Mathematics, Mersin, TURKEY

Halil İbrahim YAMAN
Mersin University,
Department of Mathematics, Mersin, TURKEY

Abstract

In this study, the sequences consisting of operators defined on the space of continuous functions on the closed interval $[0,1]$ has been investigated. The elements of the sequences are regular operators providing the conditions of Bohman-Korovkin Theorem, with a constant factor difference. It has been shown that the family consisting of those sequences is a linear space. A complete subspace of this space was obtained. It was proved that the family of the sequences of positive and linear operators by providing the conditions of Bohman-Korovkin Theorem, is a cone in this complete subspace.

Keywords: Bohman-Korovkin Theorem, regular operator, almost positive operators.

1 Introduction

In 1912, Bernstein S. N. (1912) gave a simple and usefull proof of Weierstrass' Approximation Theorem (Weierstrass, K. (1885)). He used the following polynomials: For a function f which continuonus on $[0,1]$, the polynomials

$$B_n(f;x)=\sum_{k=0}^{n} f\left(\frac{k}{n}\right)\binom{n}{k}x^k(1-x)^{n-k},\ n\in\mathbb{N},$$

converge to f uniformly on $[0,1]$. The polynomials $B_n(f)$ are called as n. Bernstein polinomial of f. They are positive and linear as operators that defined on bounded functions on $[0,1]$. In 1951 Bohman (1952) and in 1953 Korovkin (1959) investigated some important applications of sequences of the positive and linear operators on approximation theory. They gave a simple criteria for uniform convergence of sequences of positive linear operators to a contiuonus function on compact intervals: According to their theorem (Bohman-Korovkin Theorem), *if* $f\in C\,[a,b]$ *and* $\{L_n\}$ *is a sequence of positive and linear operators on* $C\,[0,1]$*, then* $\{L_nf\}$ *converge uniformly to* f *iff* $\{L_ne_i\}$ *converge uniformly to* e_i*, for* $i=0,1,2$; where $e_i(x)=x^i$. The Bernstein operators provide the conditions of Bohman-Korovkin Theorem. After this main work, a large number of positive and linear operators have been constructed to form polynomials that converge uniformly to continuous functions.

In this study, it is aimed to collect some of the functional properties of the class that were created by gathering all these operator sequences in a class to have more general characteristics. In this framework, the definitions and relations between the classes of regular operators, quasi-operators and almost positive linear operators, each containing positive and linear operators, are given (Stancu (1969), Nishishiraho (1992) and Campiti (1994)).

*Corresponding author. *E-mail address:* ttunc@mersin.edu.tr

For each $n \in \mathbb{N}$, let $R_n \in \mathcal{R}_C[0,1]$ (the class of regular operators) and let $e_i(x) = x^i (i \in \mathbb{N}_0)$. If there exists a number $\lambda \in \mathbb{R}$ such that

$$\lim_{n\to\infty} \|R_n(e_i) - \lambda(e_i)\|_{[0,1]} = 0, \qquad \forall\, i = 0,1,2$$

then the sequence $\mathcal{R} = \{R_n\}$ is called as Korovkin sequence and the number λ is called as approximation multiplier of $\mathcal{R} = \{R_n\}$. The set of all Korovkin sequences denoted by $\mathbb{K}_C[0,1]$ is a real vector space. In this study, a complete subspace of this space was obtained. It was proved that the family of the sequences of positive and linear operators by providing the conditions of Bohman-Korovkin Theorem, is a cone in this complete subspace.

2 Definitions and Main Results

Let $L : C[a,b] \to C[a,b]$ be a linear operator. If there exists closed sets P and Nsuch that $[a,b] = P \cup N$ and for every $f \in C^+[a,b]$, $L(f)(x) \geq 0$ if $x \in P$ and $L(f)(x) \leq 0$ if $x \in N$, then it is called that L is quasi-positive operator or convex-monoton operator, and denoted by $L \in Q\mathcal{P}_C[a,b]$.

Let R be an operator defined on $C[a,b]$. If there exists positive operators $P^+,\ P^- \in \mathcal{P}_C[a,b]$ such that the equality $R = P^+ - P^-$ holds, then it is called that R is a regular operator. The set of regular operators on $C[a,b]$ is denoted by $\mathcal{R}_C[a,b]$. It is clear that every quasi-pozitive operator is regular. Each positive operator is regular, but converse does not hold. For example the operator R defined on $C[0,1]$ by

$$R(f;t) = \int_0^1 (1-2xt) f(x)\, dx$$

is regular with

$$P^+(f;t) = \int_0^1 (1-xt) f(x)\, dx \quad \text{and} \quad P^-(f;t) = \int_0^1 xt f(x)\, dx.$$

But it is not positive. It is shown by using the function $f(x) = x$.

Proposition 1 *Every regular operator is bounded.*

Proof. For $f \in C[0,1]$ we have $f \leq \|f\|_{[0,1]}$ and $-f \leq \|f\|_{[0,1]}$ then for each positive operator

$$P \in \mathcal{P}_C[0,1]$$

we get

$$P(f) \leq P\left(\|f\|_{[0,1]} e_0\right) = \|f\|_{[0,1]} P(e_0),$$

and

$$-P(f) = P(-f) \leq P\left(\|f\|_{[0,1]} e_0\right) = \|f\|_{[0,1]} P(e_0)$$

thus

$$|P(f)| \leq \|f\|_{[0,1]} P(e_0) \leq \|P(e_0)\|_{[0,1]} \|f\|_{[0,1]}.$$

Let R be a regular operator. Then $R = P^+ - P^-$, where $P^+,\ P^- \in \mathcal{P}_C[0,1]$. Therefore we obtain desired result:

$$\begin{aligned} |R(f)| = \left|P^+(f) - P^-(f)\right| &\leq \left|P^+(f)\right| + |P^-(f)| \\ &\leq \left(\left\|P^+(e_0)\right\|_{[0,1]} + \|P^-(e_0)\|_{[0,1]}\right) \|f\|_{[0,1]}. \end{aligned}$$

Definition 2 *Let be given a sequence of regular operators $\mathcal{R} = \{R_n\} = \{P_n^+ - P_n^-\}$. If*

$$\lim_{n\to\infty} P_n^-(f)(x) = 0$$

for all $f \in C[a,b]$ and $x \in [a,b]$, then it is called that $\mathcal{R} = \{R_n\}$ is a sequence of almost positive operators.

Theorem 3 *(Nowak, 2010). Let $\mathcal{R} = \{R_n\}$ be a sequence of almost positive operators and for $z \in [a,b]$ let $\varphi_z(x) = (x-z)^2$. If*

$$R_n(e_0) \overset{[a,b]}{\rightrightarrows} 1 \qquad ve \qquad R_n(\varphi_z) \overset{[a,b]}{\rightrightarrows} 0$$

then for all $f \in C[a,b]$, we have $R_n(f) \overset{[a,b]}{\rightrightarrows} f$.

Definition 4 *For each $n \in \mathbb{N}$, let $R_n \in \mathcal{R}_C[0,1]$ and let $e_i(x) = x^i$ $(i \in \mathbb{N}_0)$. If there exists a number $\lambda \in \mathbb{R}$ such that*

$$\lim_{n\to\infty} \|R_n(e_i) - \lambda(e_i)\|_{[0,1]} = 0, \qquad \forall i = 0,1,2$$

then the sequence $\mathcal{R} = \{R_n\}$ is called as Korovkin sequence and the number λ is called as approximation multiplier of $\mathcal{R} = \{R_n\}$. The set of all Korovkin sequences denoted by $\mathbb{K}_C[0,1]$.

Set

$$\mathbb{K}_C^+[0,1] = \mathbb{K}_C[0,1] \cap \mathcal{P}_C[0,1].$$

The sequence of Bernstein operators $\mathcal{B} = \{B_n\}$ is a positive Korovkin sequence with the approximation multiplier $\lambda = 1$.

Proposition 5 *The set $\mathbb{K}_C[0,1]$ is a real linear space.*

Let $\mathcal{R} = \{R_n\}$ be a Korovkin sequence. Since R_n is a regular operator for each $n \in \mathbb{N}$ then there exists positive operators $P_n^+,\ P_n^- \in \mathcal{P}_C[0,1]$ such that $R_n = P_n^+ - P_n^-$. If the sequence $\{\|R_n\|\}$ is bounded the sequences $\{\|P_n^+\|\}$ and $\{\|P_n^-\|\}$ may not be bounded. For example, the sequence $\{R_n\}$ defined by

$$R_n(f;x) = f(0)(2x-1)(x-1) + f(1)x(2x-1) - 4f\left(\frac{1}{2}\right)x(x-1) + \frac{f(1)}{n},$$

is a Korovkin sequence, since

$$R_n(e_0,x) = e_0(x) + \frac{1}{n};\ R_n(e_1,x) = e_1(x) + \frac{1}{n};\ R_n(e_2,x) = e_2(x) + \frac{1}{n}.$$

Moreover, if we take

$$P_n^+(f,x) = 4f\left(\frac{1}{2}\right)x(1-x) + \left(\frac{1+n^2}{n} + 2x^2\right)f(1) + f(0)(1-x)$$

and

$$P_n^-(f,x) = 2f(0)x(1-x) + f(1)(n+x),$$

it is clear that

$$P_n^+,\ P_n^- \in \mathcal{P}_C[0,1]$$

and $R_n = P_n^+ - P_n^-$, that is $R_n \in \mathcal{R}_C[0,1]$ for all $n \in \mathbb{N}$.

On the other hand for $\|f\| = 1$ we have $\|R_n(f;.)\|_{[0,1]} \leq 11$, thus $\|R_n\| \leq 11$ for all $n \in \mathbb{N}$. Consequently, $\{\|R_n\|\}$ is bounded. But, since P_n^+, $P_n^- \in \mathcal{P}_C[0,1]$, we have

$$\left\|P_n^+\right\| = \left\|P_n^+(e_0)\right\|_{[0,1]} = \max_{x\in[0,1]} \left|-2x^2 + 3x + \frac{n^2+1}{n} + 1\right| > n$$

and

$$\|P_n^-\| = \|P_n^-(e_0)\|_{[0,1]} = \max_{x\in[0,1]} \left|-2x^2 + 3x + n\right| > n,$$

so that both $\{\|P_n^+\|\}$ and $\{\|P_n^-\|\}$ is not bounded.

Theorem 6 *Let $\mathcal{R} = \{R_n\} = \{P_n^+ - P_n^-\} \in \mathbb{K}_C[0,1]$. Then the sequences $\{\|P_n^+\|\}$ and $\{\|P_n^-\|\}$ are simultaneously bounded.*

Proof. Since $P_n^+, P_n^- \in \mathcal{P}_C[0,1]$ then $\|P_n^+\| = \|P_n^+(e_0)\|_{[0,1]}$ and $\|P_n^-\| = \|P_n^-(e_0)\|_{[0,1]}$. Moreover, since

$$R_n(e_0) + P_n^-(e_0) = P_n^+(e_0) \quad \text{and} \quad P_n^+(e_0) - R_n(e_0) = P_n^-(e_0),$$

we have

$$\left\|P_n^+(e_0)\right\|_{[0,1]} \leq \|R_n(e_0)\|_{[0,1]} + \|P_n^-(e_0)\|_{[0,1]}$$

and

$$\|P_n^-(e_0)\|_{[0,1]} \leq \|R_n(e_0)\|_{[0,1]} + \left\|P_n^+(e_0)\right\|_{[0,1]}.$$

Since the sequence $\{R_n(e_0)\}$ converges to $\lambda_{\mathcal{R}} e_0$ uniformly, then the sequence $\left\{\|R_n(e_0)\|_{[0,1]}\right\}$ is convergent, hence it is bounded. Consequently both $\{\|P_n^+\|\}$ and $\{\|P_n^-\|\}$are bounded.

Corollary 7 *Let $\mathcal{R} = \{R_n\} = \{P_n^+ - P_n^-\} \in \mathbb{K}_C[0,1]$. Then, if the sequence $\{\|P_n^-\|\}$ is bounded, then the sequence $\{\|R_n\|\}$ is bounded.*

Let us define the space

$$\mathbb{K}_C^-[0,1] = \left\{\mathcal{R} = \{R_n\} = \left\{P_n^+ - P_n^-\right\} \in \mathbb{K}_C[0,1] : \ \exists M > 0, \sup_n \|P_n^-\| \leq M\right\}.$$

The space $\mathbb{K}_C^-[0,1]$ is a normed space with

$$\|\cdot\|_\infty : \mathbb{K}_C^-[0,1] \to \mathbb{R}^+, \qquad \mathcal{R} \to \|\mathcal{R}\|_\infty = \sup_{n\in\mathbb{N}} \|R_n\|.$$

Proposition 8 *The space $\mathbb{K}_C^-[0,1]$ is a Banach Space.*

Proof. Let $\left\{\mathcal{R}^{(m)}\right\}_{m=1}^\infty$ be a Cauchy sequence in $\mathbb{K}_C^-[0,1]$ and let $\mathcal{R}^{(m)} = \left\{R_n^{(m)}\right\}_{n=1}^\infty$ for all $m \in \mathbb{N}$. Let be given $\varepsilon > 0$. Then there exists $m_\varepsilon \in \mathbb{N}$ such that $\left\|\mathcal{R}^{(k)} - \mathcal{R}^{(l)}\right\|_\infty < \frac{\varepsilon}{3}$, for all $k, l \geq m_\varepsilon$. So that $\left\|R_n^{(k)} - R_n^{(l)}\right\| < \frac{\varepsilon}{3}$ for all $n \in \mathbb{N}$. Since $\left\{R_n^{(k)}\right\}$ is a Cauchy sequence in the Banacah space of bounded operators $\mathcal{B}(C[0,1])$ for each $n \in \mathbb{N}$, there is an operator $R_n \in \mathcal{B}(C[0,1])$ such that

$$\lim_{k\to\infty} \left\|R_n^{(k)} - R_n\right\| = 0.$$

We shall show that $\mathcal{R} = \{R_n\}$ is in the space $\mathbb{K}_C^-[0,1]$. Since $R_n^{(k)}$ are regular for all $n,\ k \in \mathbb{N}$, then there exists $P_{n,k}^+,\ P_{n,k}^- \in \mathcal{P}_C[0,1]$ such that $R_n^{(k)} = P_{n,k}^+ - P_{n,k}^-$ and $\sup_{n,k\in\mathbb{N}} \left\|P_{n,k}^-\right\| \leq M$.

If we define $\overline{\lim\limits_{k\to\infty}} P_{n,k}^{-} =: P_n^{-}$ for each $n \in \mathbb{N}$, it is obvious that P_n^{-} is positive and linear on $C[0,1]$ and $\sup_n \|P_n^{-}\| \leq M$. Taking $P_n^{+} = R_n + P_n^{-}$, we have $P_n^{+} \in \mathcal{P}_C[0,1]$. Thus the operator R_n is regular for each $n \in \mathbb{N}$. If $\lambda_{\mathcal{R}^{(k)}}$ is the approximation multiplier of $\left\{R_n^{(k)}\right\}_{n=1}^{\infty}$ for each $k \in \mathbb{N}$, then we have

$$\lim_{n\to\infty} \sup_{x\in[0,1]} \left|R_n^{(k)}(e_i;x) - \lambda_{\mathcal{R}^{(k)}} e_i(x)\right| = 0, \qquad i = 0,1,2;\ k \in \mathbb{N}.$$

Hence there exits $n_\varepsilon \in \mathbb{N}$ such that

$$\left\|R_n^{(k)}(e_i) - \lambda_{\mathcal{R}^{(k)}}(e_i)\right\|_{[0,1]} < \frac{\varepsilon}{3}, \qquad i = 0,1,2;\ k \in \mathbb{N}$$

for each $n \geq n_\varepsilon$. For $k, l \geq m_\varepsilon$ and $n \geq n_\varepsilon$, we get

$$\begin{aligned}
&|\lambda_{\mathcal{R}^{(k)}} - \lambda_{\mathcal{R}^{(l)}}| = |\lambda_{\mathcal{R}^{(k)}} e_0(x) - \lambda_{\mathcal{R}^{(l)}} e_0(x)| \\
&\leq \left|R_n^{(k)}(e_0;x) - \lambda_{\mathcal{R}^{(k)}} e_0(x)\right| + \left|R_n^{(k)}(e_0;x) - R_n^{(l)}(e_0;x)\right| + \left|R_n^{(l)}(e_0;x) - \lambda_{\mathcal{R}^{(l)}} e_0(x)\right| \\
&\leq \left\|R_n^{(k)}(e_0) - \lambda_{\mathcal{R}^{(k)}} e_0\right\|_{[0,1]} + \left\|R_n^{(k)}(e_0) - R_n^{(l)}(e_0)\right\|_{[0,1]} + \left\|R_n^{(l)}(e_0) - \lambda_{\mathcal{R}^{(l)}}(e_0)\right\|_{[0,1]} \\
&< \frac{2\varepsilon}{3} + \left\|R_n^{(k)} - R_n^{(l)}\right\| < \varepsilon.
\end{aligned}$$

Thus $\{\lambda_{\mathcal{R}^{(k)}}\}$ is a Cauchy sequence of real numbers, so it is converges a real number $\lambda_{\mathcal{R}}$. Then there is $k_\varepsilon \in \mathbb{N}$ such that

$$|\lambda_{\mathcal{R}^{(k)}} - \lambda_{\mathcal{R}}| < \frac{\varepsilon}{3}$$

for all $k \geq k_\varepsilon$. Consequently, for $i \in \{0,1,2\}$, we have

$$\begin{aligned}
\|R_n(e_i) - \lambda_{\mathcal{R}} e_i\|_{[0,1]} \leq & \left\|R_n(e_i) - R_n^{(k_\varepsilon)}(e_i)\right\|_{[0,1]} + \left\|R_n^{(k_\varepsilon)}(e_i) - \lambda_{\mathcal{R}^{(k_\varepsilon)}}(e_i)\right\|_{[0,1]} \\
& + |\lambda_{\mathcal{R}^{(k_\varepsilon)}} - \lambda_{\mathcal{R}}| \, \|e_i\|_{[0,1]} < \varepsilon.
\end{aligned}$$

for all $n \geq n_\varepsilon$. That is $\mathcal{R} = \{R_n\}$ has the approximation multiplier $\lambda_{\mathcal{R}}$. Now the proof is completed.

3 The Space of Positive Korovkin Sequences

Since the elements of the space $\mathbb{K}_C^{+}[0,1]$ have the zero negative parts, then it is the subset of the space $\mathbb{K}_C^{-}[0,1]$. Moreover, the approximation multiplier of each element of $\mathbb{K}_C^{+}[0,1]$ is a non-negative real number.

Proposition 9 *The set $\mathbb{K}_C^{+}[0,1]$ is closed in $\mathbb{K}_C^{-}[0,1]$.*

Proof. Let $\left\{\mathcal{P}^{(k)}\right\}$ be sequence in $\mathbb{K}_C^{+}[0,1]$ such that it is convergent in $\mathbb{K}_C^{-}[0,1]$. Then there exists a sequence $\mathcal{R} \in \mathbb{K}_C^{-}[0,1]$ such that

$$\begin{aligned}
&\lim_{k\to\infty} \left\|\mathcal{P}^{(k)} - \mathcal{R}\right\|_\infty = 0 \\
\Longrightarrow &\lim_{k\to\infty} \sup_n \left\|P_n^{(k)} - R_n\right\|_\infty = 0 \\
\Longrightarrow &\forall n \in \mathbb{N}, \quad \lim_{k\to\infty} P_n^{(k)} = R_n
\end{aligned}$$

where $\mathcal{R} = \{R_n\}$ and $\mathcal{P}^{(k)} = \left\{P_n^{(k)}\right\}$. If $f \in C^{+}[0,1]$ then $P_n^{(k)}(f) \geq 0$ for all $n \in \mathbb{N}$. So that $R_n(f) \geq 0$. Consequently, $R_n \in \mathcal{P}_C[0,1]$ for all $n \in \mathbb{N}$. That is $\mathcal{R} \in \mathbb{K}_C^{+}[0,1]$.

Proposition 10 *The set* $\mathbb{K}_C^+[0,1]$ *is convex.*

Proof. Let $\mathcal{P}^{(1)} = \left\{P_n^{(1)}\right\}$, $\mathcal{P}^{(2)} = \left\{P_n^{(2)}\right\} \in \mathbb{K}_C^+[0,1]$ and $\alpha \in [0,1]$. Then

$$\alpha\mathcal{P}^{(1)} + (1-\alpha)\mathcal{P}^{(2)} = \left\{\alpha P_n^{(1)}\right\} + \left\{(1-\alpha) P_n^{(2)}\right\} = \left\{\alpha P_n^{(1)} + (1-\alpha) P_n^{(2)}\right\}$$

is a sequence of positive and linear opertors and has $\lambda = \alpha\lambda_{P^{(1)}} + (1-\alpha)\lambda_{P^{(2)}}$ as approximation multiplier. So that, it is in $\mathbb{K}_C^+[0,1]$.

Theorem 11 *The set* $\mathbb{K}_C^+[0,1]$ *is a cone in* $\mathbb{K}_C^-[0,1]$.

Proof. If $\mathcal{P} \in \mathbb{K}_C^+[0,1]$ and $t \in \mathbb{R}^+$, then $t \centerdot \mathcal{P} = t\{P_n\} = \{tP_n\}$ is a positive Korovkin sequence with approximation multiplier $t\lambda_{\mathcal{P}}$. So that $t \centerdot \mathcal{P} \in \mathbb{K}_C^+[0,1]$. Moreover, if $\mathcal{P} \in \mathbb{K}_C^+[0,1]$ and $-\mathcal{P} \in \mathbb{K}_C^+[0,1]$ then $\lambda_{\mathcal{P}}$ and $\lambda_{-\mathcal{P}} = -\lambda_{\mathcal{P}}$ are non-negative numbers. Hence $\lambda_{\mathcal{P}} = 0$, that is $\mathcal{P} = \Theta$. Therefore, the desired result follows from Propositions 9 and 10. As a result of the theorem, we define an order relation in $\mathbb{K}_C^-[0,1]$ as the following: For $\mathcal{R}^{(1)}$, $\mathcal{R}^{(2)} \in \mathbb{K}_C^-[0,1]$,

$$\mathcal{R}^{(1)} \geq \mathcal{R}^{(2)} \qquad \Leftrightarrow \qquad \mathcal{R}^{(1)} - \mathcal{R}^{(2)} \in \mathbb{K}_C^+[0,1].$$

Corollary 12 $\left(\mathbb{K}_C^-[0,1], \geq\right)$ *is a partially ordered Banach space.*

Theorem 13 *Let* $\mathcal{P} = \{P_n\} \in \mathbb{K}_C^+[0,1]$ *be nonzero sequence and let* $f \in C[0,1]$. *Then,* $P_n(f)$ *converge uniformly to the function* $\lambda_{\mathcal{P}} f$ *on*$[0,1]$.

Proof. Let $L_n = \lambda_{\mathcal{P}}^{-1} P_n$ for $n \in \mathbb{N}$. Since, the sequence $\{L_n\}$ satisfies the conditions of Bohman-Korovkin Theorem, then we get the desired result.

References

[1] Bernstein, S.N. (1912). Demonstration du theoreme de Weierstrass Fondee sur le Calculde probabilities, *Commun. Soc. Math. Kharkow* 13(2), 1-2.

[2] Bohman, H. (1952). On approximation of continuous and of analytic functions, *Ark. Mat.* 2, 43-56.

[3] Campiti, M. (1994) Convexity-monotone operators in Korovkin Theory, In Proceedings of the 2nd International Conference in Functional Analysis and Approximation Theory, Acquafredda di Maratea (Potenza), September 14-19, 1992, *Rend Circ. Mati Palermo* (2) Suppl., 33.

[4] Korovkin, P.P. (1959). *Linear Operators and Approximation Theory*, Hindustan publishing Corp. (India), Delhi

[5] Nishishiraho, T. (1992). Approximation Processes of Quasi-Positive Linear Operators, *Ryukyu Math. J.* 5, 85-79.

[6] Nowak, O. (2010). Korovkin-type convergence results for non-positive operators, *Cent. Eur. Math.,* 8(5) 890-907.

[7] Stancu, D.D. (1969). Asupra unei generalizari a polinoamelor lui Bernstein, *Studia Univ. Babeş-Bolyei*, Ser. Math. Phys. 14, 31-45.

[8] Weierstrass, K. (1885). Über die Analytische Darstellbarkeit Sogenannter Willkürlicher Funktionen Einer Reelen Veranderlichen, *Sitzungsberichete der Akademie zu Berlin*, 633-639.

Fundamental Solution of Heat Problem with a New Fractional Derivative Operator Involving Normalized Sinc Function

Mehmet YAVUZ*
Necmettin Erbakan University,
Department of Mathematics-Computer Sciences,
Konya, TURKEY

Abstract

This paper proposes the fundamental solution of fractional order Cauchy heat problem by using Fourier and Laplace transforms. We use a new fractional derivative operator involving the normalized sinc function (NSF) without singular kernel. In the present paper we consider the integral transform techniques to obtain the solution of the fractional Cauchy problem. Firstly, we apply the Laplace transform (LT) with respect to time variable and Fourier transform (FT) with respect to spatial coordinate. Then, applying the inverse LT and inverse FT, we get the fundamental solution of a heat conduction equation. It can be seen easily that the method we used in this study is very accurate and effective method for solving the Cauchy problem if the results of the study are considered.
Keywords: Cauchy problem, normalized sinc function, fractional derivative without singular kernel, Laplace transform, Fourier transform.

1 Introduction

In recent years, some different-type fractional derivative operators in modelling real life problems including different kernels, such as the power-law function [1], exponential function [2], Mittag-Leffler function [3, 4], stretched exponential function [5], stretched Mittag-Leffler function [6], and the normalized sinc function [7]. In the literature, some theoretical aspects and applications have been studied on these operators by some researchers [8, 9, 10, 11, 12, 13, 14, 15, 16, 17].
In 2017, Yang et al. developed a new fractional derivative operator involving the normalized sinc function without singular kernel. They also defined some integral transforms and properties of the mentioned operator such as, Laplace, Fourier, Sumudu transforms. In this study, we consider the heat diffusion equation [18] and we obtain its fundamental solution by using Laplace-Fourier transforms.

2 Suggested Derivative Operator and its Fundamental Properties

In this section, we explain the mentioned derivative operator and its integral transforms.

*Corresponding author. *E-mail address:* mehmetyavuz@konya.edu.tr

Definition 1. The normalized sinc function is defined as [19]:

$$sinc\,(t) = \frac{\sin(\pi t)}{\pi t}, \qquad t \in R. \tag{1}$$

Definition 2. Let $u(t)$ be in $H^1(a,b)$, $b > a$. A new fractional derivative operator which is defined with the normalized sinc function (FDNSF) of the function $u(t)$ of order μ is defined by [7]:

$${}_a^{NSF}D_t^{\mu} u(t) = \frac{\mu\psi(\mu)}{1-\mu}\int_a^t sinc\left(-\frac{\mu(t-\varepsilon)}{1-\mu}\right)u'(\varepsilon)\,d\varepsilon, \quad a \in (-\infty, \tau), \tag{2}$$

where $\psi(\mu)$ is a normalization function such that $\psi(0) = \psi(1) = 1$.
Definition 3. The Laplace transform of the FDNSF is defined as [7]

$$\begin{aligned}\mathcal{L}\left\{{}_0^{NSF}D_t^{\mu} u(t)\right\} &= \mathcal{L}\left\{\tfrac{\mu\psi(\mu)}{1-\mu}\int_0^t sinc\left(-\tfrac{\mu(t-\varepsilon)}{1-\mu}\right)u'(\varepsilon)\,d\varepsilon\right\} \\ &= \tfrac{\psi(\mu)}{\pi}\arctan\left(\tfrac{\mu\pi}{s(1-\mu)}\right)(su^*(s) - u(0)),\end{aligned} \tag{3}$$

where $\mathcal{L}\{u(t)\} = u^*(s)$.
Definition 4. The Fourier transform of the FDNSF is defined by [7]

$$\begin{aligned}\mathcal{F}\left\{{}_0^{NSF}D_x^{\mu} u(x)\right\} &= \mathcal{F}\left\{\tfrac{\mu\psi(\mu)}{1-\mu}\int_0^x sinc\left(-\tfrac{\mu(x-\varepsilon)}{1-\mu}\right)u'(\varepsilon)\,d\varepsilon\right\} \\ &= i\eta_\rho\psi(\mu)\sqrt{\tfrac{1}{2\pi}}\mathrm{H}\left(\tfrac{\mu\pi}{1-\mu} + |\eta_\rho|\right)\hat{u}(\eta_\rho),\end{aligned} \tag{4}$$

where $\mathcal{F}\{u(x)\} = \hat{u}(\eta_\rho)$ and $\mathrm{H}(.)$ is the Heaviside function [20].
Furthermore, we consider the finite sin-Fourier transform with respect to spatial coordinate x as [21]

$$\mathcal{F}\{u(x)\} = \hat{u}(\eta_\rho) = \int_0^M u(x)\sin(\eta_\rho x)\,dx, \tag{5}$$

and the inverse transform of it as

$$\mathcal{F}^{-1}\{\hat{u}(\eta_\rho)\} = u(x) = \frac{2}{M}\sum_{\rho=1}^{\infty}\hat{u}(\eta_\rho)\sin(\eta_\rho x), \tag{6}$$

where $\eta_\rho = \frac{\pi\rho}{M}$, $\rho = 1, 2, 3, ...$
The sin-Fourier transform property of the second order derivative in a finite domain is given by

$$\mathcal{F}\left\{\frac{d^2u(x)}{dx^2}\right\} = -\eta_\rho^2\hat{u}(\eta_\rho) + \eta_\rho\left[u(0) - (-1)^\rho u(M)\right]. \tag{7}$$

3 Application of the New Derivative Operator to Heat Conduction Problem

Consider the following fractional heat equation in the sense of FDNSF operator

$$\frac{\partial^\alpha\phi(x,t)}{\partial t^\alpha} = \sigma\frac{\partial^2\phi(x,t)}{\partial x^2}, \quad 0 < x < M, \quad t > 0, \tag{8}$$

with the initial condition

$$t = 0 \quad : \qquad \phi(x,0) = \delta(x - \lambda_0), \qquad 0 < \lambda_0 < M, \tag{9}$$

and the boundary condition

$$\begin{aligned} x = 0 \quad &: \qquad \phi(0,t) = 0, \\ x = M \quad &: \qquad \phi(M,t) = 0, \end{aligned} \tag{10}$$

where σ shows thermal diffusivity constant. Throughout the study, we suppose $\sigma = 1$ for simplicity.
Applying the Laplace transform (3) with respect to time variable t and the finite sin-Fourier transform (5) with respect to spatial coordinate x, we obtain the following equation

$$\frac{\psi(\mu)}{\pi} \arctan\left(\frac{\mu\pi}{s(1-\mu)}\right)\left(s\hat{\phi}^*(\eta_\rho, s) - \sin(\eta_\rho\lambda_0)\right) = -\sigma\eta_\rho^2\hat{\phi}^*(\eta_\rho, s) \tag{11}$$

After some arrangements, we have

$$\hat{\phi}^*(\eta_\rho, s) = \frac{\sin(\eta_\rho\lambda_0)\frac{\psi(\mu)}{\pi}\arctan\left(\frac{\mu\pi}{s(1-\mu)}\right)}{\sigma\eta_\rho^2 + s\frac{\psi(\mu)}{\pi}\arctan\left(\frac{\mu\pi}{s(1-\mu)}\right)}. \tag{12}$$

Using the inverse Laplace transform and inverse Fourier transform in the last equation, we get the fundamental solution of suggested problem as

$$\begin{aligned} \phi(x,t) &= \mathcal{F}^{-1}\left\{\mathcal{L}^{-1}\left\{\hat{\phi}^*(\eta_\rho, s)\right\}\right\} = \mathcal{F}^{-1}\left\{\mathcal{L}^{-1}\left\{\frac{\sin(\eta_\rho\lambda_0)\frac{\psi(\mu)}{\pi}\arctan\left(\frac{\mu\pi}{s(1-\mu)}\right)}{\sigma\eta_\rho^2 + s\frac{\psi(\mu)}{\pi}\arctan\left(\frac{\mu\pi}{s(1-\mu)}\right)}\right\}\right\} \\ &= \frac{2}{M}\sum_{\rho=1}^{\infty}\left[\frac{\sin(\eta_\rho\lambda_0)}{(1-\mu)\eta_\rho^2+1}\sin(\eta_\rho x)\, e^{-\frac{t\mu\eta_\rho^2}{(1-\mu)\eta_\rho^2+1}}\right]. \end{aligned} \tag{13}$$

If we take the special value of fractional operator as $\mu \to 1$ in Eq. (13), we get the standard exact solution of the mentioned Cauchy problem as:

$$\phi(x,t) = \frac{2}{M}\sum_{\rho=1}^{\infty}\left[\sin(\eta_\rho\lambda_0)\sin(\eta_\rho x)\, e^{-t\eta_\rho^2}\right]. \tag{14}$$

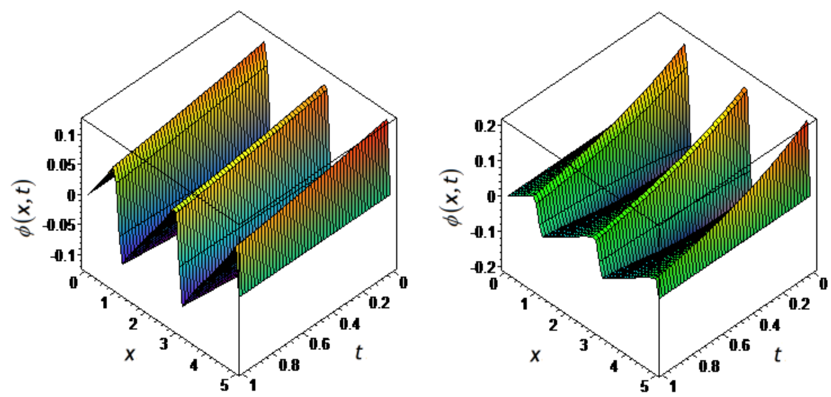

Figure 1: Solutions of the Cauchy problem for the values $\mu = 0.3$ (left) and $\mu = 0.6$ (right).

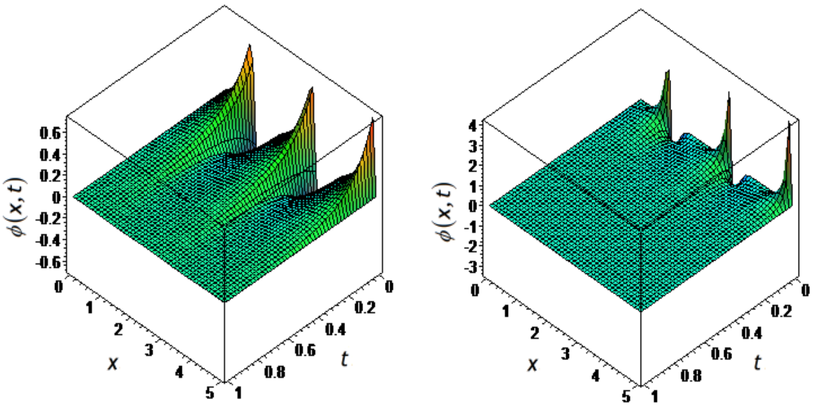

Figure 2: Solutions of the Cauchy problem for the values $\mu = 0.9$ (left) and $\mu = 0.99$.

4 Concluding Remarks

In this study, a series solution of the Cauchy heat equation is considered. A new defined fractional derivative operator is applied to the problem to model and then to solve it. This problem is considered in a finite domain $(0, M)$. The graphical results of the mentioned solution with respect to various variables time, space and fractional order parameter.

References

[1] M. Caputo, Linear Models of Dissipation Whose Q is Almost Frequency Independent–II, Geophysical Journal International, 13, 529-539 (1967).

[2] M. Caputo and M. Fabrizio, A New Definition of Fractional Derivative without Singular Kernel, Progress in Fractional Differentiation and Applications, 1, 1-13 (2015).

[3] Y. Xiao-Jun, Fractional Derivatives of Constant and Variable Orders Applied to Anomalous Relaxation Models in Heat Transfer Problems, Thermal Science, 21, 1161-1171 (2017).

[4] X.-J. Yang, J.T. Machado and D. Baleanu, Anomalous Diffusion Models with General Fractional Derivatives within the Kernels of the Extended Mittag-Leffler Type Functions, Romanian Reports in Physics, 69, 115 (2017).

[5] H. Sun, X. Hao, Y. Zhang and D. Baleanu, Relaxation and Diffusion Models with Non-Singular Kernels, Physica A: Statistical Mechanics and its Applications, 468, 590-596 (2017).

[6] A. Atangana and D. Baleanu, New Fractional Derivatives with Nonlocal and Non-Singular Kernel: Theory and Application to Heat Transfer Model, Thermal Science, 20, 763-769 (2016).

[7] X.J. Yang, F. Gao, J.A. Machado and D. Baleanu, A New Fractional Derivative Involving the Normalized Sinc Function without Singular Kernel, The European Physical Journal Special Topics, 226, 3567-3575 (2017).

[8] D. Avcı and A. Yetim, Analytical Solutions to the Advection-Diffusion Equation with the Atangana-Baleanu Derivative over a Finite Domain, Balıkesir Üniversitesi Fen Bilimleri Enstitüsü Dergisi, 20, 382-395 (2018).

[9] M. Yavuz, Novel Recursive Approximation for Fractional Nonlinear Equations within Caputo-Fabrizio Operator, Proceedings, ITM Web of Conferences: EDP Sciences, pp 01008, (2018).

[10] M. Yavuz, Characterizations of Two Different Fractional Operators without Singular Kernel, Mathematical Modelling of Natural Phenomena, 14, (2019).

[11] D. Baleanu, J.T. Machado, C. Cattani, M.C. Baleanu and X.-J. Yang, Local Fractional Variational Iteration and Decomposition Methods for Wave Equation on Cantor Sets within Local Fractional Operators, Abstract and Applied Analysis, 2014, (2014).

[12] F. Evirgen and M. Yavuz, An Alternative Approach for Nonlinear Optimization Problem with Caputo-Fabrizio Derivative, Proceedings, ITM Web of Conferences: EDP Sciences, pp 01009, (2018).

[13] V.F. Morales-Delgado, J.F. Gómez-Aguilar, H. Yépez-Martínez, D. Baleanu, R.F. Escobar-Jimenez and V.H. Olivares-Peregrino, Laplace Homotopy Analysis Method for Solving Linear Partial Differential Equations Using a Fractional Derivative with and without Kernel Singular, Advances in Difference Equations, 2016, 164 (2016).

[14] M. Yavuz and N. Özdemir, European Vanilla Option Pricing Model of Fractional Order without Singular Kernel, Fractal and Fractional, 2, 3 (2018).

[15] M. Yavuz and N. Özdemir, Comparing the New Fractional Derivative Operators Involving Exponential and Mittag-Leffler Kernel, Discrete and Continuous Dynamical Systems Series S, 13, 3 (2020).

[16] M. Yavuz and N. Ozdemir, Numerical Inverse Laplace Homotopy Technique for Fractional Heat Equations, Thermal Science, 22, 185-194 (2018).

[17] M. Yavuz, N. Ozdemir and H.M. Baskonus, Solutions of Partial Differential Equations Using the Fractional Operator Involving Mittag-Leffler Kernel, The European Physical Journal Plus, 133, 215 (2018).

[18] Y.Z. Povstenko, Fractional Heat Conduction Equation and Associated Thermal Stress, Journal of Thermal Stresses, 28, 83-102 (2004).

[19] E.T. Whittaker, Xviii.—on the Functions Which Are Represented by the Expansions of the Interpolation-Theory, Proceedings of the Royal Society of Edinburgh, 35, 181-194 (1915).

[20] L. Debnath and D. Bhatta, Integral Transforms and Their Applications, Chapman and Hall/CRC, 2006.

[21] A. George, H.J. Weber and F. Harris, Mathematical Methods for Physicists. A Comprehensive Guide, Academic Press, Elsevier, 2013.

Evolutionary Algorithms in Construction Projects Planning

Mehmet UZUN *
Department of Civil Engineering,
Karamanoglu Mehmetbey University,
Karaman/TURKEY

Sadik Alper YILDIZEL
Department of Civil Engineering,
Karamanoglu Mehmetbey University,
Karaman/TURKEY

Abstract

An optimization problem involves one or more objectives to be optimized. In multi objective optimization studies solution refers to the complex set of feasible solutions. Multi objective optimization algorithms are usually used in construction industry due to the comprised nature of the projects. These algorithms include objective functions such as the minimum cost, the least time and resources. Objective functions can be optimized by developing the construction plan with the aid of technology. Scheduling a construction plan is a highly challenging task and in need of constantly updated algorithms. This paper presents the current evolutionary algorithms and their applicability in the construction sector.
Keywords: Algorithm, evolutionary algorithms, construction, construction planning.

1 Introduction

It has been emphasized in many studies that one of the conditions for successful acceptance of a project is to be completed within the foreseen time. PERT and CPM (Critical Path Method) are the most important time-based methods used in time management in projects(Zhang et al. 2015).
Due to the complex nature of the construction projects (Figure 1), it is almost impossible to plan without planning computer support(Chan, Scott, and Chan 2004).
Various methods have been widely used by construction managers for planning of the projects including deterministic, probabilistic and artificial neural network-based approaches(Faghihi, Reinschmidt, and Kang 2014).

*Corresponding author. *E-mail address:* mehmetuzun@kmu.edu.tr

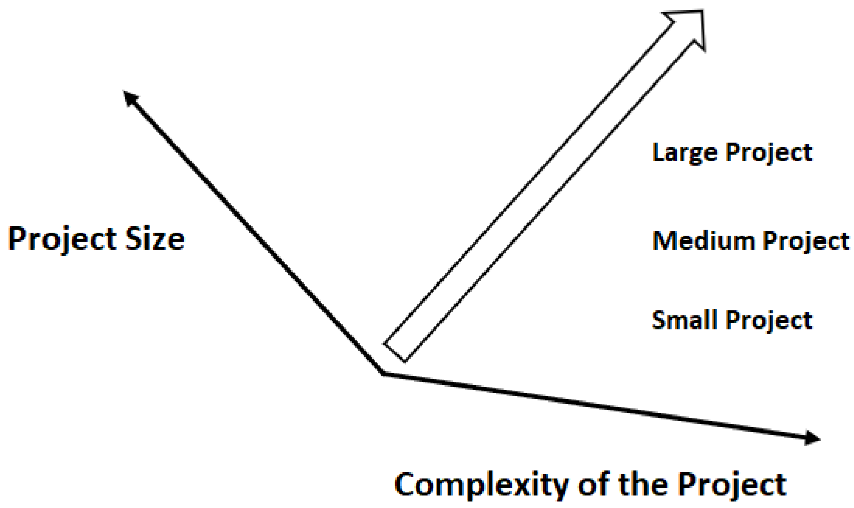

Figure 1: Complexity of the construction projects

Project duration and cost are the main problem of the entire project. Non-linear and discrete methods dependent solutions have been applied as cost-time optimization tools in construction projects(Moussourakis and Haksever 2010; El-Sayegh and Al-Haj 2017). Metaheuristic, mixed-integer non-linear programming and mixed-integer linear programming methods are also preferred by the academics(Klansek 2016; Gao et al. 2015).
Linear scheduling methods were firstly developed in the USA(Alvarez-Valdes, Tamarit, and Villa 2015). Artificial neural networks are also utilized for the project cost optimization(Monghasemi et al. 2015).
This study presents the evolutionary algorithms utilized for construction projects planning. The proposed models were also given within the scope of this research.

2 Evolutionary Algorithms

2.1 The linearized CPM-COST model

This model can be operated for minimizing direct and indirect costs. The tasks were connected with finish-start relation. Model (Figure 2) can be described as follows(Radziszewska-Zielina and Sroka 2017):

Decision-making variables: $t_k, Tf_k, Tf, d_{k,i}$, where $i \in \{1,2....p_k\}, k \in \{1,2...r\}$

Goal function: $K \to \min : K = \sum_{k=1}^{r} \sum_{i=i}^{p_k} d_{k,i} a_{k,i} + \sum_{k=1}^{r} kgr_k$

Limitations:

$$t_k \geq tgr_k, \forall k \in \{1,2...r\}$$

$$t_k \leq tgr_k + \sum_{i=1}^{p_k} t_{k,i}, \forall k \in \{1,2...r\}$$

$$d_{k,i} \leq t_{k,i}, \forall i \in \{1,2....p_k\}, \forall k \in \{1,2...r\},$$

$$tgr_k + \sum_{i=1}^{s} d_{k,i} \leq t_k, \forall s \in \{1,2...p_k\}, \forall k \in \{1,2...r\}$$

$$Tf_b \geq t_b, \forall b \in B$$

$$Tf_k - Tf_{pop} \geq t_k, \forall k \in \{1,2...r\}, \forall pop \in POP_k$$

$$Tf \geq T_l, \forall l \in L$$

$$Tf = td$$

$$d_{k,i} \geq 0$$

Figure 2: linearized CPM-COST model

The main advantage of this system was found as linearity (Radziszewska-Zielina and Sroka 2017). This cause leads to simple calculations of the scheduling works and optimization. However, it can be convergent when cost derivative function is negative for every task.

2.2 Hybrid Evolutionary Algorithm (HEA)

Hybrid evolutionary algorithm was first proposed for solving discreet optimization problems (Hejducki 2010). Then, some elements of the approach were changed for construction projects(Rogalska, Bożejko, and Hejducki 2008). HEA is given in Figure 3. This algorithm can determine the best construction start dates.

Hybrid Evolutionary Algorithm (HEA)

Initialization: randomly formed population $P^0=\{\pi_1, \pi_2,\ldots,\pi_\eta\}$;
π^*= the best element of population P^0;
Iteration number $i=0$; $\mathrm{FS}^0=\emptyset$;
repeat
Determine a set of local minima $\mathrm{LM}^i=\{\hat{\pi}_1, \hat{\pi}_2,\ldots,\hat{\pi}_\eta\}$, where
$\hat{\pi}_j=\mathit{LocalOpt}(\pi_j)$, $\pi_j\in P^i$;
for $j:=1$ **to** η **do if** $F(\hat{\pi}_j)<F(\pi^*)$ ***then*** $\pi^*\leftarrow\hat{\pi}_j$;
Fix set
$\mathrm{FS}^{i+1}=\mathit{FixSet}(\mathrm{LM}^i,\mathrm{FS}^i)$ i
generate new population
$P^{i+1}:=\mathit{NewPopulation}(\mathrm{FS}^i)$;
$i=i+1$;
until not **S**top **C**riterion (exceeding a given time or a number of iterations).

Figure 3: Hybrid Evolutionary Algorithm (HEA) (Rogalska, Bożejko, and Hejducki 2008

2.3 Downtime Minimization Model (DMM)

This model was proposed in 2016 and detail of the DMM as follows(Krzemiński 2016): Great minimization was obtained with the DMM. Network model of DMM is given in Figure 4. "W" and "B" stands for site working subdivision and working bridges respectively.

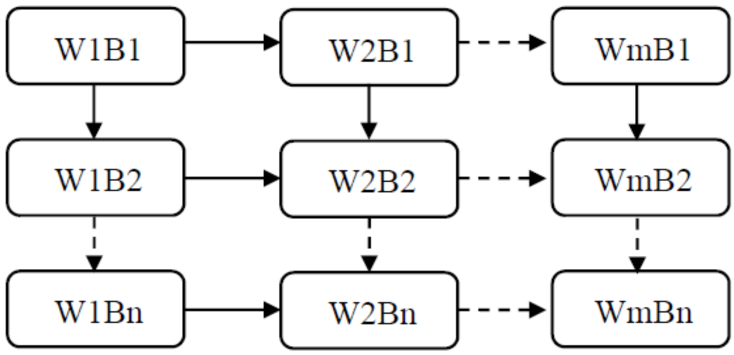

Figure 4: DMM network model

Based on the network model (Figure 4) T_{ij} and Z_{ij} matrices were designed and presented in Figure 5.

$$T_{ij}^{(k)} = \begin{bmatrix} t_{11} & \cdots & t_{1j} \\ \vdots & \ddots & \vdots \\ t_{i1} & \cdots & t_{ij} \end{bmatrix}; i = 1, \ldots, m; j = 1, \ldots, n \tag{1}$$

where:
m – number of construction site subdivisions,
n – the number of working brigades,
k – the number of iterations.

Based on the above network model and the matrices $T_{ij}^{(k)}$, a matrix $Z_{ij}^{(k)}$ should be designated containing the calculated total slack for activities.

$$Z_{ij}^{(k)} = \begin{bmatrix} z_{11} & \cdots & z_{1j} \\ \vdots & \ddots & \vdots \\ z_{i1} & \cdots & z_{ij} \end{bmatrix}; i = 1, \ldots, m; j = 1, \ldots, n \tag{2}$$

where:
m – number of construction site subdivisions,
n – the number of working brigades,
k – the number of iterations.

Figure 5: T_{ij} and Z_{ij} matrices

This model provides great time reduces in scheduling works. Cost optimization can be also analyzed with this model.

3 Conclusion

In this paper, widely utilized evolutionary algorithms in project scheduling are presented. Review results can be drawn as follows:

1. CPM-COST model can be selected for cost based linear projects due to the fact that no limitations on the density of linearity segments.
2. Hybrid Evolutionary Algorithm can be utilized effectively for time dependent tasks, and it should be updated considering other criterion functions such as cost.
3. Downtime Minimization Model can be enhanced by adding workforce, direct and indirect cost effects into the proposed algorithms.

References

[1] Alvarez-Valdes, Ramon, Jose Manuel Tamarit, and Fulgencia Villa. 2015. Handbook on Project Management and Scheduling Vol.1. Handbook on Project Management and Scheduling Vol. 1. https://doi.org/10.1007/978-3-319-05443-8.

[2] Chan, Albert P. C., David Scott, and Ada P. L. Chan. 2004. "Factors Affecting the Success of a Construction Project." Journal of Construction Engineering and Management. https://doi.org/10.1061/(ASCE)0733-9364(2004)130:1(153).

[3] El-Sayegh, Sameh Monir, and Rana Al-Haj. 2017. "A New Framework for Time-Cost Trade-off Considering Float Loss Impact." Journal of Financial Management of Property and Construction. https://doi.org/10.1108/JFMPC-02-2016-0007.

[4] Faghihi, Vahid, Kenneth F. Reinschmidt, and Julian H. Kang. 2014. “Construction Scheduling Using Genetic Algorithm Based on Building Information Model.” Expert Systems with Applications. https://doi.org/10.1016/j.eswa.2014.05.047.

[5] Gao, Xiaoyong, Yongheng Jiang, Tao Chen, and Dexian Huang. 2015. “Optimizing Scheduling of Refinery Operations Based on Piecewise Linear Models.” Computers and Chemical Engineering. https://doi.org/10.1016/j.compchemeng.2015.01.022.

[6] Hejducki, Z. ”Time couplings in scheduling methods of complex construction processes. (Sprzezenia czasowe w metodach organizacji zlozonych procesow budowlanych).”

[7] Krzemiński, Michał. 2016. “Construction Team Downtime Minimization Model Including Efficiency Coefficients.” In Procedia Engineering. https://doi.org/10.1016/j.proeng.2016.08.491.

[8] Rogalska, Magdalena, Wojciech Bozejko, and Zdzislaw Hejducki. 2008. Time-Cost Optimization Using Hybrid Evolutionary Algorithm in Construction Project Scheduling. Automation in Construction. https://doi.org/10.1016/j.autcon.2008.04.002.

[9] Klansek, Uros. 2016. “Mixed-Integer Nonlinear Programming Model for Nonlinear Discrete Optimization of Project Schedules under Restricted Costs.” Journal of Construction Engineering and Management. https://doi.org/10.1061/(asce)co.1943-7862.0001074

[10] Monghasemi, Shahryar, Mohammad Reza Nikoo, Mohammad Ali Khaksar Fasaee, and Jan Adamowski. 2015. “A Novel Multi Criteria Decision Making Model for Optimizing Time-Cost-Quality Trade-off Problems in Construction Projects.” Expert Systems with Applications. https://doi.org/10.1016/j.eswa.2014.11.032.

[11] Moussourakis, John, and Cengiz Haksever. 2010. “Project Compression with Nonlinear Cost Functions.” Journal of Construction Engineering and Management. https://doi.org/10.1061/(ASCE)CO.1943-7862.0000123.

[12] Radziszewska-Zielina, E., and B. Sroka. 2017. “Linearised CPM-COST Model in the Planning of Construction Projects.” In Procedia Engineering. https://doi.org/10.1016/j.proeng.2017.11.030.

[13] Zhang, Sijie, Jochen Teizer, Nipesh Pradhananga, and Charles M. Eastman. 2015. “Workforce Location Tracking to Model, Visualize and Analyze Workspace Requirements in Building Information Models for Construction Safety Planning.” Automation in Construction. https://doi.org/10.1016/j.autcon.2015.09.009.

Some Properties of Soft Inner Product Spaces

Murat Ibrahim YAZAR *
Karamanoglu Mehmetbey University,
Department of Mathematics and Science Education,
Karaman, TURKEY

Çiğdem GÜNDÜZ ARAS
Kocaeli University,
Department of Mathematics,
Kocaeli, TURKEY

Abstract

In the present paper an idea of soft inner product on soft linear spaces has been introduced and some of their properties are investigated. We define the soft inner product space in a new point of view based on the soft point concept given in [1]
Keywords: Soft metric spaces, soft vector spaces, soft inner product spaces.

1 Introduction

Molodtsov [3] introduced the notion of soft set to overcome uncertainties which cannot be dealt with by classical methods in many areas such as environmental science, economics, engineering and etc. This theory is applicable where there is no clearly defined mathematical model. Recently, many papers concerning soft sets have been published; see [4, 5, 6, 7].

The concept of soft point was defined in different approaches. Among these, the soft point given in [1, 2] is more accurate.Das and et al. introduced the concept of soft element in [8] and defined a soft vector space by using the concept of soft element. After then they studied on soft normed spaces, soft linear operators, soft inner product spaces and their basic properties [9, 10]. Later, Yazar and et al.[11] define the soft vector space by using the concept of soft point and introduced the soft normed spaces in a new point of view. In this study, we progress on the study [11] by introducing the soft inner product on soft vector spaces and give some properties of soft inner product spaces. We show that the soft inner product function is continuous and the inner product of two soft Cauchy sequences is also a soft Cauchy sequence. We define soft space and show that this space is a soft inner product space.

2 Preliminaries

In this section we will introduce necessary definitions and theorems for soft sets. Let X be an initial universe set and E be a set of parameters. Let $P(X)$ denotes the power set of X and $A, B \subseteq E$.

Definition 1 *[3] A pair (F, E) is called a soft set over X, where F is a mapping given by $F : E \to P(X)$.*

*Corresponding author. *E-mail address:* myazar@kmu.edu.tr

In other words, the soft set is a parameterized family of subsets of the set X. For $a \in E$, $F(a)$ may be considered as the set of $a-$elements of the soft set (F,E), or as the set of $a-$approximate elements of the soft set.

Definition 2 *[6] Let (F,E) and (G,E) be two soft sets over X. Then, soft union and soft intersection of (F,E) and (G,E) are defined by the soft sets (H,E) and (H^*,E), respectively,*

$$\begin{aligned} (H,E) &= (F,E)\widetilde{\cup}(G,E), \text{ where } H(a) = F(a) \cup G(a), \\ (H^*,E) &= (F,E)\widetilde{\cap}(G,E), \text{ where } H^*(a) = F(a) \cap G(a), \text{ for all } a \in E. \end{aligned}$$

Definition 3 *[6] A soft set (F,E) over X is said to be a null soft set denoted by Φ if for all $a \in E$, $F(a) = \varnothing$.*

Definition 4 *[6] A soft set (F,E) over X is said to be an absolute soft set denoted by $\widetilde{X}$ if for all $a \in E$, $F(a) = X$.*

Definition 5 *[6] The difference (H,E) of two soft sets (F,E) and (G,E) over X, denoted by $(F,E)\widetilde{\backslash}(G,E)$, is defined as $H(a) = F(a)\backslash G(a)$ for all $a \in E$.*

Definition 6 *[6] The complement of a soft set (F,E), denoted by $(F,E)^c = (F^c,E)$, where $F^c : E \to P(X)$ is a mapping given by $F^c(a) = X\backslash F(a)$, for all $a \in E$ .Here F^c is called the soft complement function of F.*

Definition 7 *[2] Let $\mathbb{R}$ be the set of all real numbers, $B(\mathbb{R})$ be the collection of all non-empty bounded subsets of $\mathbb{R}$ and E be taken as a set of parameters. Then a mapping $F : E \to B(\mathbb{R})$ is called a soft real set. It is denoted by (F,E).If a soft real set is a singleton soft set, it will be called a soft real number and denoted $\widetilde{r}, \widetilde{s}$ etc. Here $\widetilde{r}, \widetilde{s}$ will denote a particular type of soft real numbers such that $\widetilde{r}(a) = r$, for all $a \in E$. For instance, $\widetilde{0}$ and $\widetilde{1}$ are the soft real numbers where $\widetilde{0}(a) = 0$, $\widetilde{1}(a) = 1$ for all $a \in E$ respectively.*

Definition 8 *[2] Let $\widetilde{r}, \widetilde{s}$ be two soft real numbers, then the following statements are hold:*
(i) $\widetilde{r}\widetilde{\leq}\widetilde{s}$, if $\widetilde{r}(a) \leq \widetilde{s}(a)$, for all $a \in E$,
(ii) $\widetilde{r}\widetilde{\geq}\widetilde{s}$, if $\widetilde{r}(a) \geq \widetilde{s}(a)$, for all $a \in E$,
(iii) $\widetilde{r}\widetilde{<}\widetilde{s}$, if $\widetilde{r}(a) < \widetilde{s}(a)$, for all $a \in E$,
(iv) $\widetilde{r}\widetilde{>}\widetilde{s}$, if $\widetilde{r}(a) > \widetilde{s}(a)$, for all $a \in E$.

Definition 9 *[1, 2] Let (F,E) be a soft set over X. The soft set (F,E) is called a soft point, denoted by (x_e,E) , if for the element $e \in E$, $F(e) = \{x\}$ and $F(e') = \phi$ for all $e' \in E - \{e\}$ (briefly denoted by $\tilde{x}_e$.)*

Definition 10 *[1] Two soft points $(\tilde{x}_e,E)$ and $(\tilde{y}_{e'},E)$ over a common universe X, we say that the soft points are different if $x \neq y$ or $e \neq e'$.*

Definition 11 *[13] Let $\widetilde{\tau}$ be the collection of soft sets over X, then $\widetilde{\tau}$ is called a soft topology on X if the following conditions are satisfied:*
1) $\Phi, \widetilde{X}$ belong to $\widetilde{\tau}$;
2) the union of any number of soft sets in $\widetilde{\tau}$ belongs to $\widetilde{\tau}$;
3) the intersection of any two soft sets in $\widetilde{\tau}$ belongs to $\widetilde{\tau}$.
The triplet $(X,\widetilde{\tau},E)$ is called a soft topological space over X.Then members of $\widetilde{\tau}$ are said to be the soft open sets in X.

Let $\widetilde{X}$ be the absolute soft set, E be a non-empty set of parameters and $SP(\widetilde{X})$ be the collection of all soft points of $\widetilde{X}$.Let $\mathbb{R}(E)^*$ denote the set of all non-negative soft real numbers.

Definition 12 *[2] A mapping $\tilde{d} : SP(\tilde{X}) \times SP(\tilde{X}) \to \mathbb{R}(E)^*$ is said to be a soft metric on the soft set $\tilde{X}$ if $\tilde{d}$ satisfies the following conditions:*

(M1) $\tilde{d}(\tilde{x}_{e_1}, \tilde{y}_{e_2}) \tilde{\geq} \tilde{0}$ *for all* $\tilde{x}_{e_1}, \tilde{y}_{e_2} \tilde{\in} \tilde{X}$,

(M2) $\tilde{d}(\tilde{x}_{e_1}, \tilde{y}_{e_2}) = \tilde{0}$ *if and only if* $\tilde{x}_{e_1} = \tilde{y}_{e_2} \tilde{\in} \tilde{X}$,

(M3) $\tilde{d}(\tilde{x}_{e_1}, \tilde{y}_{e_2}) = \tilde{d}(\tilde{y}_{e_2}, \tilde{x}_{e_1})$ *for all* $\tilde{x}_{e_1}, \tilde{y}_{e_2} \tilde{\in} \tilde{X}$,

(M4) For all $\tilde{x}_{e_1}, \tilde{y}_{e_2}, \tilde{z}_{e_3} \tilde{\in} \tilde{X}$, $\tilde{d}(\tilde{x}_{e_1}, \tilde{z}_{e_3}) \tilde{\leq} \tilde{d}(\tilde{x}_{e_1}, \tilde{y}_{e_2}) + \tilde{d}(\tilde{y}_{e_2}, \tilde{z}_{e_3})$.

The soft set $\tilde{X}$ with a soft metric $\tilde{d}$ is called a soft metric space and denoted by $(\tilde{X}, \tilde{d}, E)$.

Definition 13 *[2] Let $\{\tilde{x}^n_{e_n}\}$ be a sequence of soft points in a soft metric space $(\tilde{X}, \tilde{d}, E)$. Then the sequence $\{\tilde{x}^n_{e_n}\}$ is said to be convergent in $(\tilde{X}, \tilde{d}, E)$ if there is a soft point $\tilde{x}^0_{e_0} \tilde{\in} \tilde{X}$ such that $\tilde{d}(\tilde{x}^n_{e_n}, \tilde{x}^0_{e_0}) \to \tilde{0}$ as $n \to \infty$.*

Theorem 14 *[2] Limit of a sequence in a soft metric space, if exist, is unique.*

Definition 15 *[2] (Cauchy Sequence) The sequence $\{\tilde{x}^n_{e_n}\}$ of soft points in $(\tilde{X}, \tilde{d}, E)$ is called a Cauchy sequence in $\tilde{X}$ if corresponding to every $\tilde{\varepsilon} \tilde{>} \tilde{0}$, there is a $m \in N$ such that $\tilde{d}(\tilde{x}^i_{e_i}, \tilde{y}^j_{e_j}) \tilde{\leq} \tilde{\varepsilon}$, for all $i, j \geq m$ i.e. $\tilde{d}(\tilde{x}^i_{e_i}, \tilde{y}^j_{e_j}) \to \tilde{0}$ as $i, j \to \infty$.*

Definition 16 *[2] (Complete Metric Space) The soft metric space $(\tilde{X}, \tilde{d}, E)$ is called complete if every Cauchy Sequence in $\tilde{X}$ converges to some point of $\tilde{X}$. The soft metric space $(\tilde{X}, \tilde{d}, E)$ is called incomplete if it is not complete.*

Let X be a vector space over a field K $(K = \mathbb{R})$ and the parameter set E be the real number set $\mathbb{R}$.

Definition 17 *[11] Let (F, E) be a soft set over X. The soft set (F, E) is said to be a soft vector and denoted by $\tilde{x}_e$ if there is exactly one $e \in E$, such that $F(e) = \{x\}$ for $x \in X$ and $F(e') = \phi$, $\forall e' \in E/\{e\}$.*

The set of all soft vectors over $\tilde{X}$ will be denoted by $SV(\tilde{X})$.

Proposition 18 *[11] The set $SV(\tilde{X})$ is a vector space according to the following operations;*

(1) $\tilde{x}_e + \tilde{y}_{e'} = (\widetilde{x + y})_{(e+e')}$ *for every* $\tilde{x}_e, \tilde{y}_{e'} \in SV(\tilde{X})$;

(2) $\tilde{r}.\tilde{x}_e = (\widetilde{rx})_{(re)}$ *for every* $\tilde{x}_e \in SV(\tilde{X})$ *and for every soft real number* $\tilde{r}$.

Definition 19 *[11] Let $SV(\tilde{X})$ be a soft vector space. Then a mapping*

$$\|.\| : SV(\tilde{X}) \to \mathbb{R}^+(E)$$

is said to be a soft norm on $SV(\tilde{X})$, if $\|.\|$satisfies the following conditions:

(N1) $\|\tilde{x}_e\| \tilde{\geq} \tilde{0}$ *for all* $\tilde{x}_e \tilde{\in} SV(\tilde{X})$ *and* $\|\tilde{x}_e\| = \tilde{0} \Leftrightarrow \tilde{x}_e = \tilde{\theta}_0$;

(N2) $\|\tilde{r}.\tilde{x}_e\| = |\tilde{r}| \, \|\tilde{x}_e\|$ *for all* $\tilde{x}_e \tilde{\in} SV(\tilde{X})$ *and for every soft scalar* $\tilde{r}$;

(N3) $\|\tilde{x}_e + \tilde{y}_{e'}\| \tilde{\leq} \|\tilde{x}_e\| + \|\tilde{y}_{e'}\|$ *for all* $\tilde{x}_e, \tilde{y}_{e'} \tilde{\in} SV(\tilde{X})$.

The soft vector space $SV(\tilde{X})$ with a soft norm $\|.\|$ on $\tilde{X}$ is said to be a soft normed linear space and is denoted by $(\tilde{X}, \|.\|)$.

Definition 20 *[11] A sequence of soft vectors $\{\tilde{x}^n_{e_n}\}$ in $(\tilde{X}, \|.\|)$ is said to be convergent to $\tilde{x}^0_{e_0}$, if $\lim\limits_{n\to\infty} \|\tilde{x}^n_{e_n} - \tilde{x}^0_{e_0}\| = \tilde{0}$ and denoted by $\tilde{x}^n_{e_n} \to \tilde{x}^0_{\lambda_0}$ as $n \to \infty$.*

Definition 21 *[11] A sequence of soft vectors $\{\tilde{x}^n_{e_n}\}$ in $(\tilde{X}, \|.\|)$ is said to be a soft Cauchy sequence if corresponding to every $\tilde{\varepsilon} \tilde{>} \tilde{0}$, $\exists m \in N$ such that $\left\|\tilde{x}^i_{e_i} - \tilde{x}^j_{e_j}\right\| \tilde{<} \tilde{\varepsilon}$, $\forall i, j \geq m$ i.e. $\left\|\tilde{x}^i_{e_i} - \tilde{x}^j_{e_j}\right\| \to \tilde{0}$ as $i, j \to \infty$.*

Definition 22 *[11]Let $(\tilde{X}, \|.\|)$ be a soft normed linear space. Then $(\tilde{X}, \|.\|)$ is said to be a soft Banach space if every Cauchy sequence in $\tilde{X}$ converges to a soft vector of $\tilde{X}$.*

3 Soft Inner Product Spaces

Definition 23 *Let $SV(\tilde{X})$ be a soft vector space. The mapping*

$$< . >: SV(\tilde{X}) \to SV(\tilde{X}) \to \mathbb{R}(E)^*$$

is called a soft inner product on $SV(\tilde{X})$ iff it satisfies the following conditions, for every $\tilde{x}_e, \tilde{y}_{e'}, \tilde{z}_{e''} \tilde{\in} SV(\tilde{X})$ and for every soft real number $\tilde{\alpha}$;

(I1.) $< \tilde{x}_e, \tilde{x}_e > \tilde{\geq} \tilde{0}$ *and* $< \tilde{x}_e, \tilde{x}_e >= \tilde{0} \Leftrightarrow \tilde{x}_e = \tilde{\theta}_0$,

(I2.) $< \tilde{x}_e, \tilde{y}_{e'} >= < \tilde{y}_{e'}, \tilde{x}_e >$,

(I3.) $< \tilde{\alpha}\tilde{x}_e, \tilde{y}_{e'} >=< \tilde{x}_e, \tilde{\alpha}\tilde{y}_{e'} >= \tilde{\alpha} < \tilde{x}_e, \tilde{y}_{e'} >$,

(I4.) $< \tilde{x}_e + \tilde{y}_{e'}, \tilde{z}_{e''} >=< \tilde{x}_e, \tilde{z}_{e''} > + < \tilde{y}_{e'}, \tilde{z}_{e''} >$.

The triple $(SV(\tilde{X}), < . >, E)$ is called soft inner product space.

Example 24 *Given the soft vector space $SV(\tilde{\mathbb{R}})$ and for every $\tilde{x}_e, \tilde{y}_{e'} \tilde{\in} SV(\tilde{\mathbb{R}})$, let us define the mapping $< . >: SV(\tilde{\mathbb{R}}) \to SV(\tilde{\mathbb{R}}) \to \mathbb{R}(E)$ $(E = \mathbb{R})$ as follows*

$$< \tilde{x}_e, \tilde{y}_{e'} >= e.\acute{e}+ < x, y > (x, y \in \mathbb{R},\ e, \acute{e} \in \mathbb{R} \text{ and } < . >: \mathbb{R} \times \mathbb{R} \to \mathbb{R})$$

In this case, the mapping $< . >$ is an inner product on $SV(\tilde{\mathbb{R}})$.

(I1) *For every $\tilde{x}_e \tilde{\in} SV(\tilde{\mathbb{R}})$, $< \tilde{x}_e, \tilde{x}_e >= e.e+ < x, x >= e^2 + \|x\| \geq 0$ and*

$$\begin{aligned} < & \ \tilde{x}_e, \tilde{x}_e >= 0 \Leftrightarrow e.e+ < x, x >= 0 \\ \Leftrightarrow & \ e = 0 \text{ and } x = \theta \\ \Leftrightarrow & \ \tilde{x}_e = \tilde{\theta}_0 \end{aligned}$$

(I2) *For every $\tilde{x}_e, \tilde{y}_{e'} \tilde{\in} SV(\tilde{\mathbb{R}})$,*

$$< \tilde{x}_e, \tilde{y}_{e'} >= e.e'+ < x, y >= e'.e+ < y, x >=< \tilde{y}_{e'}, \tilde{x}_e > .$$

(I3) *For every $\tilde{\alpha} \tilde{\in} \mathbb{R}(E)$ and $\forall \tilde{x}_e, \tilde{y}_{e'} \tilde{\in} SV(\tilde{\mathbb{R}})$,*

$$< \tilde{\alpha}\tilde{x}_e, \tilde{y}_{e'} >= \tilde{\alpha}e.e'+ < x, y >= \tilde{\alpha}e'.e+ < y, x >=< \tilde{x}_e, \tilde{\alpha}\tilde{y}e' > .$$

(I4) *For every $\tilde{x}_e, \tilde{y}_{e'}, \tilde{z}_{e''} \tilde{\in} SV(\tilde{\mathbb{R}})$,*

$$\begin{aligned} < & \ \tilde{x}_e + \tilde{y}_{e'}, \tilde{z}_{e''} >=< \widetilde{(x+y)}_{(e+e')}, \tilde{z}_{e''} > \\ = & \ (e + e')e''+ < x + y, z > \\ = & \ e.e'' + e'e''+ < x, z > + < y, z > \\ = & \ e.e''+ < x, z > +e'e''+ < y, z > \\ = & \ < \tilde{x}_e, \tilde{z}_{e''} > + < \tilde{y}_{e'}, \tilde{z}_{e''} > \end{aligned}$$

Remark 25 *Let $(SV(\tilde{X}), < . >, E)$ be a soft inner product space. For the parameter $e = 0$ the soft vector space $\tilde{X}$ is equal to the vector space X and we have the following inner product*

$$< . >_0: X \times X \longrightarrow \mathbb{R}.$$

Hence, for the parameter $e = 0$ we obtain the inner product space $(X, < . >_0)$.

Proposition 26 *Let $(SV(\tilde{X}), < . >, E)$ be a soft inner product space. In this case, for every $\tilde{x}_e, \tilde{y}_{e'}, \tilde{z}_{e''} \tilde{\in} SV(\tilde{X})$ and $\forall \tilde{\alpha}, \tilde{\beta} \tilde{\in} \mathbb{R}(E)$*

i. $< \tilde{\alpha}\tilde{x}_e + \tilde{\beta}\tilde{y}_{e'}, \tilde{z}_{e''} >= \tilde{\alpha} < \tilde{x}_e, \tilde{z}_{e''} > +\tilde{\beta} < \tilde{y}_{e'}, \tilde{z}_{e''} >$,

ii. $< \tilde{x}_e, \tilde{\alpha}\tilde{y}_{e'} + \tilde{\beta}\tilde{z}_{e''} >= \tilde{\alpha} < \tilde{x}_e, \tilde{y}_{e'} > +\tilde{\beta} < \tilde{x}_e, \tilde{z}_{e''} >$,

are satisfied.

Proof. The proof is straight forward. ■

Proposition 27 *Let* $\left(SV(\tilde{X}), \langle . \rangle, E\right)$ *be a soft inner product space. The mapping* $\|.\| : SV(\tilde{X}) \to \mathbb{R}^+(E)$ *defined as* $\|\tilde{x}_e\| = \sqrt{\langle \tilde{x}_e, \tilde{x}_e \rangle}$ *is a soft norm.*

Proof. Let us show that soft norm conditions are satisfied;

N1. For every $\tilde{x}_e \tilde{\in} SV(\tilde{X})$ it is obvious that $\|\tilde{x}_e\| = \sqrt{\langle \tilde{x}_e, \tilde{x}_e \rangle} \tilde{\geq} \tilde{0}$. Furthermore,

$$\|\tilde{x}_e\| = \sqrt{\langle \tilde{x}_e, \tilde{x}_e \rangle} = \tilde{0} \Leftrightarrow \langle \tilde{x}_e, \tilde{x}_e \rangle = \tilde{0} \Leftrightarrow \tilde{x}_e = \tilde{\theta}_{\tilde{0}}.$$

N2. For every $\tilde{x}_e \tilde{\in} SV(\tilde{X})$ and $\tilde{\alpha} \tilde{\in} \mathbb{R}(E)$, since

$$\|\tilde{\alpha}\tilde{x}_e\|^2 = \langle \tilde{\alpha}\tilde{x}_e, \tilde{\alpha}\tilde{x}_e \rangle = \tilde{\alpha}^2 \|\tilde{x}_e\|^2 ,$$

we have $\|\tilde{\alpha}\tilde{x}_e\| = |\tilde{\alpha}| \|\tilde{x}_e\|$.

N3. For every $\tilde{x}_e, \tilde{y}_{e'} \tilde{\in} SV(\tilde{X})$ we have

$$\begin{aligned}
\|\tilde{x}_e + \tilde{y}_{e'}\|^2 &= \langle \tilde{x}_e + \tilde{y}_{e'}, \tilde{x}_e + \tilde{y}_{e'} \rangle \\
&= \|\tilde{x}_e\|^2 + 2\langle \tilde{x}_e, \tilde{y}_{e'} \rangle + \|\tilde{y}_{e'}\|^2 \\
&\tilde{\leq} \|\tilde{x}_e\|^2 + 2|\langle \tilde{x}_e, \tilde{y}_{e'} \rangle| + \|\tilde{y}_{e'}\|^2 \\
&\tilde{\leq} \|\tilde{x}_e\|^2 + 2\|\tilde{x}_e\| \|\tilde{y}_{e'}\| + \|\tilde{y}_{e'}\|^2 \\
&= (\|\tilde{x}_e\| + \|\tilde{y}_{e'}\|)^2 .
\end{aligned}$$

■

Example 28 *Given the soft vector space* $SV(\tilde{\mathbb{R}}^n)$ *and the parameter set* $E = \mathbb{R}$. *Let us define the function* $< . >: SV(\tilde{\mathbb{R}}^n) \times SV(\tilde{\mathbb{R}}^n) \longrightarrow \mathbb{R}(E)$ *as follows*

$$< \tilde{x}_e, \tilde{y}_{e'} >= \tilde{x}^1_{e_1}.\tilde{y}^1_{e'_1} + \tilde{x}^2_{e_2}.\tilde{y}^2_{e'_2} + \cdots + \tilde{x}^n_{e_n}.\tilde{y}^n_{e'_n},$$

where $\tilde{x}_e = \left(\tilde{x}^1_{e_1}, \tilde{x}^2_{e_2}, \ldots, \tilde{x}^n_{e_n}\right), \tilde{y}_{e'} = \left(\tilde{y}^1_{e'_1}, \tilde{y}^2_{e'_2}, \ldots, \tilde{y}^n_{e'_n}\right) \tilde{\in} SV(\tilde{\mathbb{R}}^n)$. *It is obvious that the conditions I1, I2, I3 are satisfied. Let us show that the condition I4 is satisfied.*

For every $\tilde{x}_e, \tilde{y}_{e'}, \tilde{z}_{e''} \tilde{\in} SV(\tilde{\mathbb{R}}^n)$,

$$\begin{aligned}
&< \tilde{x}_e + \tilde{y}_{e'}, \tilde{z}_{e''} >=< \widetilde{(x+y)}_{(e+e')}, \tilde{z}_{e''} >= \widetilde{(x+y)}_{(e+e')}.\tilde{z}_{e''} \\
&= \left\{ \left(\widetilde{x^1 + y^1}\right)_{(e_1+e'_1)}.\tilde{z}^1_{e''_1} + \cdots + \left(\widetilde{x^n + y^n}\right)_{(e_n+e'_n)}.\tilde{z}^n_{e''} \right\} \\
&= \left\{ \left(\widetilde{(x^1 + y^1).z^1}\right)_{(e_1+e'_1).e''_1} + \cdots + \left(\widetilde{(x^n + y^n).z^n}\right)_{(e_n+e'_n).e''_n} \right\} \\
&= \left\{ \begin{array}{c} \left(\widetilde{x^1 + z^1}\right)_{(e_1+e'_1)} + \left(\widetilde{y^1 + z^1}\right)_{(e'_1+e''_1)} + \\ \cdots + \left(\widetilde{x^n + z^n}\right)_{(e_n+e'_n)} + \left(\widetilde{y^n + z^n}\right)_{(e'_n+e''_n)} \end{array} \right\} \\
&= \left\{ \left(\tilde{x}^1_{e_1}.\tilde{z}^1_{e''_1} + \tilde{y}^1_{e'_1}.\tilde{z}^1_{e''_1}\right) + \cdots + \left(\tilde{x}^n_{e_n}.\tilde{z}^n_{e''_n} + \tilde{y}^n_{e'_n}.\tilde{z}^n_{e''_n}\right) \right\} \\
&= \left\{ \left(\tilde{x}^1_{e_1}.\tilde{z}^1_{e''_1} + \cdots + \tilde{x}^n_{e_n}.\tilde{z}^n_{e''_n}\right) + \cdots + \left(\tilde{y}^1_{e'_1}.\tilde{z}^1_{e''_1} + \tilde{y}^n_{e'_n}.\tilde{z}^n_{e''_n}\right) \right\} \\
&= < \tilde{x}_e, \tilde{y}_{e'} > + < \tilde{y}_{e'}, \tilde{z}_{e''} > .
\end{aligned}$$

References

[1] S. Bayramov, C. Gunduz. "Soft locally compact spaces and soft paracompact spaces", J. Math.System Sci. 3 (2013):122-130.

[2] S. Das and S.K.Samanta. "Soft metric." Ann. Fuzzy Math. Inform 6.1 (2013): 77-94.

[3] D. Molodtsov. "Soft set theory-first results." Comput. Math. Appl. 37 (1999): 19-31.

[4] M.I.Ali, F.Feng, X.Liu, W.K.Min and M.Shabir. "On some new operations in soft set theory." Comput. Math. Appl. 57 (2009): 1547-1553.

[5] D. Chen. "The parametrization reduction of soft sets and its applications." Comput. Math. Appl.49 (2005):757-763.

[6] P.K. Maji, R. Biswas and A.R. Roy. "Soft set theory." Comput. Math. Appl. 45 (2003): 555-562.

[7] P.K. Maji, A.R. Roy, R. Biswas. "An application of soft sets in a decision making problem." Comput. Math. Appl. 44 (2002):1077-1083.

[8] S. Das, S.K. Samanta. "On soft metric spaces." J. Fuzzy Math. 21 (2013): 707-734.

[9] S. Das and S. K. Samanta. "Soft linear operators in soft normed linear spaces." Ann. Fuzzy Math. Inform. 6.2 (2013):295 -314.

[10] S. Das and S. K. Samanta. "Soft inner product spaces." Ann. Fuzzy Math. Inform. 6.1 (2013):151-170.

[11] M. I. Yazar, T. Bilgin, S. Bayramov, Ç. Gunduz (Aras). "A new view on soft normed spaces." International Mathematical Forum 9.24 (2014): 1149 – 1159.

[12] S. Das, S.K. Samanta. "Soft real sets, soft real numbers and their properties." J. Fuzzy Math. 20 (2012): 551–576.

[13] M. Shabir and M. Naz. "On soft topological spaces." Comput.Math. Appl. 61 (2011): 1786-1799.

A Note on Soft $D-$ Metric Spaces

Murat Ibrahim YAZAR*
Karamanoglu Mehmetbey University,
Department of Mathematics and Science Education,
Karaman , TURKEY

Çiğdem GÜNDÜZ ARAS
Kocaeli University,
Department of Mathematics,
Kocaeli, TURKEY

Abstract

Metric space is one of the most important space in mathematics. There are various type of generalization of metric spaces. In this study we define soft $D-$metric spaces. We obtain some important properties concerning $D-$metric spaces. Finally, we prove a fixed point theorem on a complete soft $D-$metric space.

Keywords: Soft set, generalized soft $D-$metric space, soft $\Delta-$distance.

1 Introduction and Preliminaries

Metric space is one of the most important space in mathematic. There are various type of generalization of metric spaces. Bapure Dhage [6] in his PhD thesis [1992] introduce a new class of generalized metrics called $D-$metrics. In a subsequent series of papers Dhage attemped to develop topological structures in such spaces. Also he claimed that $D-$metrics provide a generalization of ordinary metric functions. Subsequently, some works have been done the basis for over a lot of papers by Dhage and other authors. Using the concept of $D-$metric, Y.J.Cho and R. Saadati [4] defined a $\Delta-$distance on a complete $D-$metric space which is a generalization of the concept of $\omega-$distance due to Kada, Suzuki and Takahashi [14]. Later S.V.R.Naidu et all. [13] researched topology of $D-$metric spaces.

Metric spaces wide area provides a powerfull tool to the study of optimization and approximation theory, variational inequalities and so many. After Molodtsov [10] initiated a novel concept of soft set theory as a new mathematical tool for dealing with uncertainties, applications of soft set theory in other disciplines and real life problems was progressing rapidly, the study of soft metric space which is based on soft point of soft sets was initiated by Das and Samanta [5]. Yazar et al.[16] examined some important properties of soft metric spaces and soft continuous mappings. They also proved some fixed point theorems of soft contractive mappings on soft metric spaces. Later Gunduz Aras at al. [8], [9] defined soft $S-$metric spaces and give some fixed point theorems on this spaces. The purpose of this paper firstly is to contribute for investigating on soft $D-$metric space which is based on soft point of soft sets. By using the concept of soft $D-$metric, we define a soft $\Delta-$ distance on a complete soft $D-$metric. Secondly, using the concept of soft $\Delta-$distance, we give a fixed point theorem.

*Corresponding author. *E-mail address:* myazar@kmu.edu.tr

We briefly give some basic definitions of concepts which serve a background to this work.

Throughout this paper, X denotes initial universe, E denotes the set of all parameters, $P(X)$ denotes the power set of X.

Definition 1 *[10] A pair (F,E) is called a soft set over X, where F is a mapping given by $F : E \to P(X)$.*

In other words, the soft set is a parameterized family of subsets of the set X. For $a \in E$, $F(a)$ may be considered as the set of $a-$elements of the soft set (F,E), or as the set of $a-$approximate elements of the soft set.

Definition 2 *[11] A soft set (F,E) over X is said to be a null soft set denoted by Φ if for all $a \in E$, $F(a) = \varnothing$.*

Definition 3 *[11] A soft set (F,E) over X is said to be an absolute soft set denoted by $\widetilde{X}$ if for all $a \in E$, $F(a) = X$.*

Definition 4 *[15] Let $\widetilde{\tau}$ be the collection of soft sets over X, then $\widetilde{\tau}$ is called a soft topology on X if the following conditions are satisfied:*

1) $\Phi, \widetilde{X}$ belong to $\widetilde{\tau}$;
2) the union of any number of soft sets in $\widetilde{\tau}$ belongs to $\widetilde{\tau}$;
3) the intersection of any two soft sets in $\widetilde{\tau}$ belongs to $\widetilde{\tau}$.

The triplet $(X, \widetilde{\tau}, E)$ is called a soft topological space over X.Then members of $\widetilde{\tau}$ are said to be the soft open sets in X.

Proposition 5 *[15] Let $(X, \widetilde{\tau}, E)$ be a soft topological space over X. Then the family $\widetilde{\tau}_a = \{F(a) : (F,E) \in \widetilde{\tau}\}$ for each $a \in E$, defines a topology on X.*

Definition 6 *[1],[5] Let (F,E) be a soft set over X. The soft set (F,E) is called a soft point, denoted by (x_a, E), if for the element $a \in E$, $F(a) = \{x\}$ and $F(a') = \varnothing$ for all $a' \in E - \{a\}$ (briefly denoted by x_a).*

It is obvious that each soft set can be expressed as union of all soft points belonging to it. For this reason, to give the family of all soft sets on X it is sufficient to give only soft points on X.

Definition 7 *[1] Two soft points x_a and y_b over a common universe X, we say that the soft points are different if $x \neq y$ or $a \neq b$.*

Definition 8 *[1] The soft point x_a is said to be belonging to the soft set (F,E), denoted by $x_a \widetilde{\in} (F,E)$, if $x_a(a) \in F(a)$, i.e., $\{x\} \subseteq F(a)$.*

Definition 9 *[1] Let (X, τ, E) be a soft topological space over X. A soft set $(F,E) \subseteq (X,E)$ is called a soft neighborhood of the soft point $x_a \in (F,E)$ if there exists a soft open set (G,E) such that $x_a \in (G,E) \subseteq (F,E)$.*

Definition 10 *[5] Let $\mathbb{R}$ be the set of all real numbers, $B(\mathbb{R})$ be the collection of all non-empty bounded subsets of $\mathbb{R}$ and E be taken as a set of parameters. Then a mapping $F : E \to B(\mathbb{R})$ is called a soft real set. It is denoted by (F,E).If a soft real set is a singleton soft set, it will be called a soft real number and denoted $\widetilde{r}, \widetilde{s}$ etc. Here $\widetilde{r}, \widetilde{s}$ will denote a particular type of soft real numbers such that $\widetilde{r}(a) = r$, for all $a \in E$. For instance, $\widetilde{0}$ and $\widetilde{1}$ are the soft real numbers where $\widetilde{0}(a) = 0$, $\widetilde{1}(a) = 1$ for all $a \in E$ respectively.*

Definition 11 *[6] Let X be a non-empty set. A function $D : X^3 \to [0, \infty)$ is called a $D-$metric if the following conditions are satisfied:*

(1) $D(x, y, z) \geq 0$ for all $x, y, z \in X$ and equality holds if and only if $x = y = z$,

(2) $D(x, y, z) = D(x, z, y) = D(y, x, z) = ...$

(3) $D(x, y, z) \leq D(x, y, u) + D(x, u, z) + D(u, y, z)$, for all $x, y, z, u \in X$.

Then the pair (X, D) is called an $D-$ metric space.

2 Soft $D-$ Metric Spaces

In this section, we introduce the definition of soft $D-$ metric spaces, soft $\Delta-$distance function, from the family of all soft points of a soft set to the set of all non-negative soft real numbers. Later we study some important results of its. Later we give some important concepts such as converge, Cauchy sequence, soft complete on soft $D-$ metric spaces. Let $\widetilde{X}$ be the absolute soft set, E be a non-empty set of parameters and $SP(\widetilde{X})$ be the collection of all soft points of $\widetilde{X}$.Let $\mathbb{R}(E)^*$ denote the set of all non-negative soft real numbers.

Definition 12 *A mapping $D : SP(\widetilde{X}) \times SP(\widetilde{X}) \times SP(\widetilde{X}) \to \mathbb{R}(E)^*$ is called a soft $D-$ metric on the soft set $\widetilde{X}$ that D satisfies the following conditions, for each soft points $x_a, y_b, z_c, u_d \in SP(\widetilde{X})$,*

D1) $D(x_a, y_b, z_c) \geq \widetilde{0}$,with equality if and only if $x_a = y_b = z_c$.(coincidence)

D2) $D(x_a, y_b, z_c) = D(y_b, x_a, z_c) = D(x_a, z_c, y_b) = ...$(symmetry)

D3)$D(x_a, y_b, z_c) \leq D(x_a, y_b, u_d) + D(x_a, u_d, z_c) + D(u_d, y_b, z_c)$.

Then the soft set $\widetilde{X}$ with a soft $D-$ metric is called a soft $D-$ metric space and denoted by $\left(\widetilde{X}, D, E\right)$.

Remark 13 *If $\left(\widetilde{X}, D, E\right)$ is a soft $D-$ metric space, then (X, D_a) is a $D-$ metric space for each $a \in E$. Here D_a stands for the $D-$metric for only parameter a and (X, D_a) is a crisp $D-$ metric space. It is clear that every soft $D-$ metric space is a family of parameterized $D-$ metric space.*

Theorem 14 *Let $\left(\widetilde{X}, D, E\right)$ be a complete $D-$metric space and $\Delta-$be a distance on $\widetilde{X}$, $(f, \varphi) : \left(\widetilde{X}, D, E\right) \to \left(\widetilde{X}, D, E\right)$ be a soft mapping. Let $\widetilde{X}$ be a $\Delta-$bounded. Suppose that there exists a soft real number $\widetilde{r} \in \mathbb{R}(E)$,$\widetilde{0} \leq \widetilde{r} < \widetilde{1}$ ($\mathbb{R}(E)$ denotes the soft real numbers set) such that*

$$\Delta\left((f, \varphi)(x_a), (f, \varphi)^2(x_a), (f, \varphi)(y_b)\right) \leq \widetilde{r}\Delta(x_a, (f, \varphi)(x_a), y_b)$$

for all $x_a, y_b \in SP(\widetilde{X})$.Then there exists $z_c \in SP(\widetilde{X})$ such that $z_c = (f, \varphi)(z_c)$.In addition, if $v_s = (f, \varphi)(v_s)$, then $\Delta(v_s, v_s, v_s) = \widetilde{0}$.

Note that a soft mapping is a soft continuous mapping because if $x_{a_n}^n \to x_a$ in the above condition we get $(f, \varphi)(x_{a_n}^n) \to (f, \varphi)(x_a)$.

References

[1] S. Bayramov, C. Gunduz. "Soft locally compact spaces and soft paracompact spaces", J. Math.System Sci. 3 (2013): 122-130.

[2] S. Bayramov and C. Gunduz. "A new approach to separability and compactness in soft topological spaces." TWMS Journal of Pure and Applied Mathematics 9(21)(2018).

[3] S. Bayramov, C. Gunduz and L. Mdzinarishvili. "Singular homology theory in the category of soft topological spaces." Georgian Math. J. 22.4 (2015): 457-467.

[4] Y.J.Cho and R. Saadati. "A fixed point theorem in generalized $D-$metric spaces." Bull. Iranian Math. Soc. 32.2 (2006): 13-19.

[5] S. Das and S.K.Samanta. "Soft metric." Ann. Fuzzy Math. Inform 6.1 (2013): 77-94.

[6] B.C.Dhage. "Generalized metric spaces and mappings with fixed point." Bull. Calcutta Math. Soc. 84 (1992): 329-336.

[7] C. Gunduz Aras and S. Bayramov. "On the Tietze extension theorem in soft topological spaces." Proc. of Inst.Math. and Mech. 43.1 (2017): 105-115.

[8] C. Gunduz Aras. S. Bayramov and V.Cafarli. "Soft $S-$metric spaces." submitted.

[9] C. Gunduz Aras. S. Bayramov and V.Cafarli. "Fixed Point Theorems on Soft $S-$ Metric Spaces." submitted.

[10] D. Molodtsov. "Soft set theory-first results." Comput. Math. Appl. 37 (1999): 19-31.

[11] P.K. Maji, R. Biswas and A.R. Roy. "Soft set theory." Comput. Math. Appl. 45 (2003): 555-562.

[12] T.Y Ozturk and S. Bayramov. "Soft mapping spaces." The Scientific World Journal, Article ID 307292 (2014): 8p.

[13] S.V.R.Naidu, K.P.R.Rao and N.S.Rao. "On the topology of $D-$metric spaces and generation of $D-$metric spaces from metric spaces." Int.J.Math. Sci. 51(2004): 2719-2740.

[14] O. Kada, T.Suzuki and W. Takahashi. "Nonconvex minimization theorems and fixed point theorems in complete metric spaces.", Math. Japon. 44 (1996): 381-391.

[15] M. Shabir and M. Naz. "On soft topological spaces." Comput.Math. Appl. 61 (2011): 1786-1799.

[16] M. I. Yazar, T. Bilgin, S. Bayramov, Ç. Gunduz (Aras). "A new view on soft normed spaces." International Mathematical Forum 9.24 (2014): 1149– 1159.

Optimal Design of 2-D Steel Frames Utilizing Symbiotic Organisms Search Algorithm

Serdar ÇARBAŞ *
Department of Civil Engineering,
Karamanoglu Mehmetbey University,
Karaman/TURKEY

İbrahim AYDOĞDU
Department of Civil Engineering,
Akdeniz University,
Antalya/TURKEY

Abstract

This work represents one of the recent optimization algorithm so-called Symbiotic Organisms Search (SOS) for optimal design of 2-D steel frame structures. The SOS is based on the interactions relationship between two organisms in ecosystems. The mostly common symbiotic relations between the organisms in ecosystem are mutualism, commensalism, and parasitism. The novel SOS algorithm is examined by 2-D steel frame design optimization problem and its performance is further compared with various demoded optimization algorithms.

Keywords: Optimal design, symbiotic organisms search, 2-D steel frame.

1 Introduction

The design optimization of steel frames mostly includes minimizing the volume or weight of the structure under fixed design limitations achieved by using codes. So far, various algorithms have been employed for resolving this type of problems [1, 2]. To put in a different way, for investigating the performance of optimization techniques the design optimization of the steel frames can be taken into account as a benchmark problem. The charged system search (CSS) [3], imperialist competitive algorithm (ICA) [4], colliding-bodies optimization (CBO) [5], and chaotic swarming of particles (CSP) [6] are some instances of countless methods implemented in this subject.

2 Mathematical Based Statement of The Problem

The weight minimization is considered as the main objective in the optimal design of the steel frames interpreted as following [7]:
Find a vector of integer values I (Equation 1) presenting the sequence numbers of steel sections assigned to N_d member groups

$$\mathrm{I^T} = [\mathrm{I_1}, \mathrm{I_2}, ..., \mathrm{I_{N_d}}] \tag{1}$$

to minimize the weight (W) of the frame

$$\mathrm{W} = \sum_{\mathrm{i=1}}^{\mathrm{N_d}} \rho_{\mathrm{i}} \mathrm{A_i} \sum_{\mathrm{j=1}}^{\mathrm{N_t}} \mathrm{L_j} \tag{2}$$

here, A_i and ρ_i are the length and unit weight of the steel section adopted for member group i, respectively, N_t is the total number of members in group i, and L_i is the length of the member j which belongs to group i. The members subjected to

*Corresponding author. *E-mail address:* scarbas@kmu.edu.tr

$$\frac{(\delta_{\mathrm{j}}-\delta_{\mathrm{j-1}})}{\mathrm{h_j}} \leq \delta_{\mathrm{ju}} \quad \mathrm{j}=1,...,\mathrm{ns} \tag{3}$$

$$\delta_{\mathrm{i}} \leq \delta_{\mathrm{iu}} \quad \mathrm{i}=1,...,\mathrm{nd} \tag{4}$$

$$\mathrm{V_u} \leq \phi \mathrm{V_n} \tag{5}$$

$$\left(\frac{\mathrm{P_u}}{\phi_{\mathrm{c}}\mathrm{P_n}}\right)+\left(\frac{8}{9}\frac{\mathrm{M_{ux}}}{\phi_{\mathrm{b}}\mathrm{M_{nx}}}\right) \leq 1.0 \quad \text{for } \frac{\mathrm{P_u}}{\phi_{\mathrm{c}}\mathrm{P_n}} \geq 0.2 \tag{6}$$

$$\left(\frac{\mathrm{P_u}}{2\phi_{\mathrm{c}}\mathrm{P_n}}\right)+\left(\frac{\mathrm{M_{ux}}}{\phi_{\mathrm{b}}\mathrm{M_{nx}}}\right) \leq 1.0 \quad \text{for } \frac{\mathrm{P_u}}{\phi_{\mathrm{c}}\mathrm{P_n}} \leq 0.2$$

$$\mathrm{B_{jb}} \leq \mathrm{B_{jc}} \quad \mathrm{j}=1,...,\mathrm{nj} \tag{7}$$

$$\mathrm{D_s} \leq \mathrm{D_{s-1}} \quad \mathrm{s}=1,...,\mathrm{nu} \tag{8}$$

$$\mathrm{m_s} \leq \mathrm{m_{s-1}} \tag{9}$$

In Equation (3) the inter-story drift of the multi-story frame is presented. δ_j and δ_{j-1} are lateral deflections of two adjacent story levels and h_j is the story height. ns is the total number of stories in the frame. In Equation (4), the displacement restrictions that may be required to include other than drift constraints such as mid-span deflections of beams is defined. nd is the total number of restricted displacements in the frame. δ_{ju} is the allowable lateral displacement. The horizontal deflection of columns is limited due to unfactored imposed load and wind loads to height of column/300 in each story of a building with more than one story. δ_{iu} is the upper bound on the deflection of beams which is given as (span/300) if they carry plaster or other brittle finish. In Equation (5), the shear capacity check for beam-columns is tabulated. φ is resistance factor in shear, V_u required shear strength, V_n is nominal shear strength. In Equation (6), the local capacity check for beam-columns is defined. M_{nx} is nominal flexural strength, M_{ux} is applied moment, P_n is nominal axial strength, P_u is applied axial load, $\O_c$ is resistance factor for columns if the axial force is in compression, $\O_b$ is resistance factor in bending. It is apparent that computation of compressive strength $\O_c P_n$ of a compression member requires its effective length. Equation (7) is comprised in the design problem to guarantee that the flange width of the beam (B) section at each beam-column connection at joint j should be less than or equal to the flange width of column section. nj represents the total number of joints in the frame.

Equations (8) and (9) are needed to be included to make sure that the depth (D) and the mass per meter (m) of column section at story s at each beam-column connection are less than or equal to width and mass of the column section at the lower story s−1. nu is the total number of these constraints.

3 Symbiotic Organisms Search (Sos) Algorithm

The symbiotic organisms search technique [8, 9] mimics the behavior of organisms affected each other in the nature. Organisms depend on other genus to survive. This kind of dependence is so-called as symbiotic. The SOS sustains inhabitants of probable solutions. The initial population is called the ecosystem. Organisms in the ecosystem is randomly generated which each organism is representing a candidate solution to the given problem. A fitness function is assigned to each organism to reflect its degree of adaptation to the desired objective. The SOS consists of three phases that resemble real world biological interactions between two organisms: (i) Mutualism phase where an interaction benefits both organisms, (ii) Commensalism phase where an interaction benefits one organism, while does not harm the other, (iii)Parasitism phase where one organism is benefited, while the other is harmed. Thus, the following algorithm outlines the SOS algorithm approach [10]:

Initialization
Repeat
    Mutualism phase
    Commensalism phase
    Parasitism phase
Until a stopping criterion is met

A detailed description of the SOS algorithm and three phases is given in the Refs. [8-10] and are not repeated here.

3.1 Constraint Handling

Each design is analyzed under the external loading and the design constraints given in Equations (3) (9) are checked. If a candidate design does not satisfy the design constraints, its objective function value is penalized in accordance with constraint violations using Equation (10):

$$\mathrm{f_{cost,p}} = \mathrm{f_{cost}}(1 + \mathrm{C})^{\varepsilon} \tag{10}$$

where, f_{cost} is the objective function value given by Equation (2), $f_{cost,p}$ is the penalized objective function value, C is the summation of constraint violations calculated using the constraint functions stated by Equations (3)-(9), and ε is the penalty coefficient, which is taken as 2.0 in this study. In general form, constraint violations are calculated as:

$$\mathrm{C_i} = \begin{cases} 0 & \mathrm{g_i(x)} \le 0 \\ \mathrm{g_i(x)} & \mathrm{g_i(x)} > 0 \end{cases} \qquad \mathrm{i} = 1, ..., \mathrm{NC} \tag{11}$$

where, $g_i(x)$ is the i^{th} constraint function, x is the vector of design variables, and NC is the number of constraint functions in the optimal design problem [7].

4 Design Example

A two-bay, six story 2-D steel frame [11] shown in Figure 1 is considered as design example of this study. The frame consists of thirty members that are collected in eight groups as shown in the figure. The allowable inter-story drift is 1.17 cm while the lateral displacement of the top story is limited to 7.17 cm. The modulus of elasticity is taken as 200 kN/mm^2. A distributed load 50 kN/m and a 25 kN single lateral load is applied to each horizontal member of the frame. Fixed supports are used for the connection of the columns to the foundation. Also, the discrete set from which the SOS based design algorithm selects the sectional designations for frame members is considered to be the complete set of 272 W-sections starting from W100x19.3 to W1100x499 mm as given in LRFD–AISC [12]. Besides, two main control parameters for SOS algorithm, which are ecosystem size and maximum number of fitness function evaluations, are set as 20 and 20000 respectively.

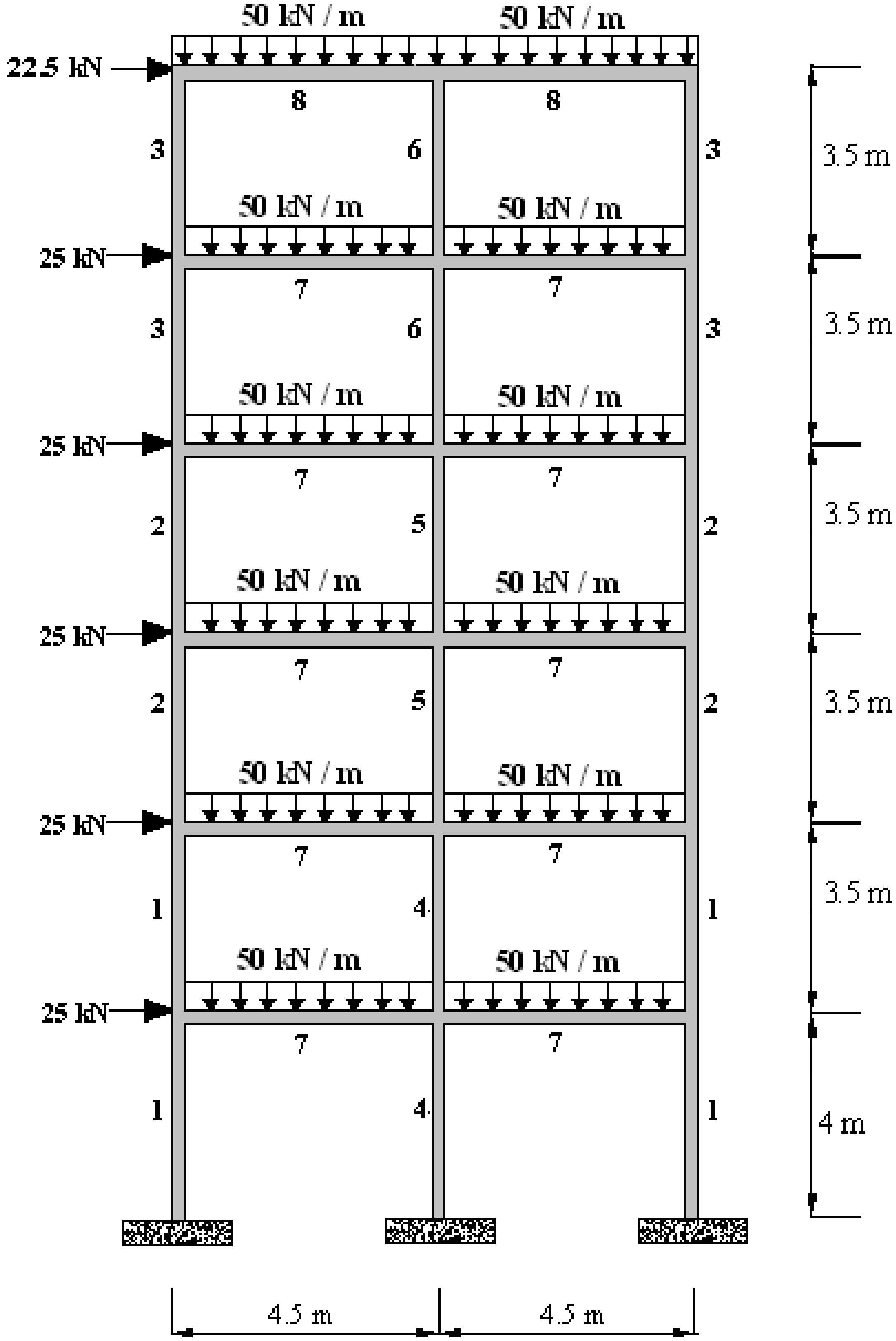

Figure 1: Two-bay, six story 2-D steel frame

The optimum W-sections designation obtained by the Symbiotic Organisms Search algorithm is given in Table 1. This minimum weight of the frame is yielded by SOS algorithm as 6925 kg. The frame is formerly designed by two different optimal design algorithms that are based on two different metaheuristics such that particle swarm algorithm and harmony search algorithm as reported in Ref. [12]. This means that SOS design algorithm produces the best design solution that is 8.8% and 13.1% lighter than the optimal designed frames attained by particle swarm algorithm and harmony search algorithm, respectively. It is noticed that in the best designed optimum frame achieved by SOS algorithm the lateral displacement of top story is 5.489 cm against its upper bound of 7.17cm. The highest ratio among the combined strength constraints is 1.0 that means it reaches its upper bound. Maximum inter-story drift ratio is recorded as 1.13 cm whose upper bound is set as 1.17 cm. This clearly indicates that strength constraints dominate the optimum design.

Table 1: Optimal designs for two-bay, six story 2-D steel frame.

Group No	Member Type	Symbiotic Organisms Search Algorithm	Particle Swarm Algorithm [11]	Harmony Search Algorithm [11]
1	Column	W200x59	W530X74	W460x82
2	Column	W200x59	W310X52	W310x74
3	Column	W200x59	W200X41.7	W200x46
4	Column	W690x125	W460X89	W530x109
5	Column	W460x74	W460X89	W460x97
6	Column	W200x41.7	W360X72	W310x60
7	Beam	W460x52	W460X60	W410x60
8	Beam	W310x32.7	W460X68	W360x33
Min. weight-kN (kg)		67.910 (6925)	73.873 (7533)	76.776 (7829)

5 Conclusions

The relation and dependence behavior of organisms existing in the nature is treated as the main inspirations for the Symbiotic Organisms Search (SOS) algorithm. Three main phases of a real biological interaction between two organisms such as the mutualism phase, commensalism phase, and parasitism phase are implemented in current algorithm. In this study, the SOS algorithm is examined on solving 2-D steel frames. A design example is resolved by the SOS algorithm and its performance is further compared with various demoded algorithms. From results presented here, the SOS algorithm shows a good performance compared to some other well-known old fashion metaheuristics such as Particle Swarm algorithm and Harmony Search algorithm. As a future work, some further enhancement can be studied to improve the performance of SOS algorithm for 3-D large-scale problems where the performance of the algorithm is expected as not good as its ability on solving small ones.

References

[1] S. Talatahari, Optimum Design of Skeletal Structures using Ant Lion Optimizer, Int. J. Opt. Civ. Eng., 6(1) (2016) 13-25.

[2] A. Kaveh, Advances in Metaheuristic Algorithms for Optimal Design of Structures, Springer International Publishing, Switzerland, 2014.

[3] A. Kaveh and S. Talatahari, A novel heuristic optimization method: charged system search, Acta Mech., 213(3-4) (2010) 267-89.

[4] S. Talatahari, A. Kaveh, and R. Sheikholeslami, Chaotic imperialist competitive algorithm for optimum design of truss structures, Struct. Multidiscip. Optim., 46(3) (2012) 355-67.

[5] A. Kaveh and V. R. Mahdavi, Colliding Bodies Optimization: Extensions and Applications, Springer Verlag, Berlin, 2015.

[6] A. Kaveh, R. Sheikholeslami, S. Talatahari, and M. Keshvari, Chaotic swarming of particles: a new method for size optimization of truss structures, Adv. Eng. Softw., 67 (2014) 136-47.

[7] S. Carbas, Biogeography-Based Optimization Algorithm for Designing of Planar Steel Frames, The 3rd Int. Conf. Adv. Tech.Sci. (ICAT'16), Konya, 2016.

[8] M-Y. Cheng and D. Prayogo, Symbiotic organisms search: A new metaheuristic optimization algorithm, Comput. Struct., 139 (2014) 98-112.

[9] M-Y. Cheng, D. Prayogo, and D-H. Tran, Optimizing Multiple Resources Leveling in the Multiple Projects using Discrete Symbiotic Organisms Search, J. Comput. Civil Eng., 30 (3) (2015) 1-9.

[10] S. Al-Sharhan and M. G. H. Omran, An enhanced symbiosis organisms search algorithm: an empirical study, Neural Comput. Applic., 29 (2018) 1025–1043.

[11] E. Dogan and M. P. Saka, Optimum design of unbraced steel frames to LRFD–AISC using particle swarm optimization, Adv. Eng. Softw., 46 (2012) 27–34.

[12] LRFD-AISC, Load and Resistance Factor Design, American Institute of Steel Construction, IL, USA, 1999.

Some Spectral Properties Of A Quadratic Differantial Pencil Problem With The Anti-Periodic Boundary Condition

H. MENKEN*
Mersin University,
Faculty of Science,
33343 Mersin, TURKEY

U. DEMİRBİLEK
Mersin University,
Faculty of Science,
33343 Mersin, TURKEY

Kh.R. MAMEDOV
Mersin University,
Faculty of Science,
33343 Mersin, TURKEY

Abstract

In the present work we consider the quadratic differential pencil $l(y) = y'' + (\lambda^2 - 2\lambda p(x) - q(x))y$ with the anti-periodic boundary conditions which are not strongly regular. It is assumed that $q(x) \in C^{(1)}[0,\pi]$ and $p(x) \in C^{(2)}[0,\pi]$ are complex valued functions defined on the closed interval $[0,\pi]$ and $p(x)$ is satisfying the condition $p(\pi) - p(0) \neq 0$. We obtain the accurate asymptotic expressions of linearly independent solutions of the quadratic differential pencil and we give asymptotic formulas for eigenvalues of the anti-periodic boundary value problem.
Keywords: Anti-periodic boundary condition, quadratic pencil, asymptotic expansions, eigenvalues, eigenfunctions, Sturm-Liouville operator.

1 Introduction

We consider the following quadratic differential pencil on the interval $[0,\pi]$

$$l(y) = y'' + (\lambda^2 - 2\lambda p(x) - q(x))y \tag{1}$$

with the anti-periodic boundary conditions

$$y(0) = -y(\pi), \quad y'(0) = -y'(\pi) \tag{2}$$

where $q(x) \in C^{(1)}[0,\pi]$ and $p(x) \in C^{(2)}[0,\pi]$ are complex-valued functions defined on on the closed interval $[0,\pi]$ and λ is a spectral parameter. For simplicity we assume that $\int_0^\pi q(x)dx = 0$, $\int_0^\pi p^2(x)dx = 0$. The quadratic pencils of Sturm-Liouville operators have been studied in [1, 2, 3]. The analysis of inverse spectral problems with other kinds of separated boundary conditions as well as with periodic or antiperiodic boundary condition were investigated in [1, 2]. Direct and inverse spectral problems for differential operator pencils have been extensively studied in [4]-[11] and other works (for details see [12, 13]).

In this study, we investigate some spectral properties of the differential pencil. We obtain the expressions of two linearly independent solutions of the given problem, and we give the asymptotic formulas for the eigenvaules under certain conditions.

*Corresponding author. *E-mail address:* hmenken@mersin.edu.tr

2 Linearly Independent Solutions For Quadratic Differential Pencil

The following result is valid.

Lemma 1 *For sufficiently large $|\lambda|$, the expressions of the fundamental solutions of the quadratic differential pencil (1) are of the following form*

$$y_1(x,\lambda) = e^{i\lambda x}e^{-i\beta x}\left\{1 + \frac{1}{2i\lambda}\left[i(p(x)-p(0)) + \int_0^x p^2(t)dt + \int_0^x q(t)dt\right]\right. \tag{3}$$
$$+\frac{1}{(2i\lambda)^2}\left[-i(p'(x)-p'(0)) - \frac{5}{2}p^2(x) + p(0)p(x) + \frac{3}{2}p^2(0) - q(x) + q(0)\right.$$
$$+2i\int_0^x p^3(t)dt + \int_0^x q(t)dt\int_0^x p^2(t)dt + \frac{1}{2}\left(\int_0^x p^2(t)dt\right)^2 + \frac{1}{2}\left(\int_0^x q(t)dt\right)^2$$
$$\left.+i(p(x)-p(0))(\int_0^x p^2(t)dt + \int_0^x q(t)dt)\ ] + O\left(\frac{1}{\lambda^3}\right)\right\},$$

$$y_2(x,\lambda) = e^{-i\lambda x}e^{i\beta x}\left\{1 + \frac{1}{2i\lambda}\left[i(p(x)-p(0)) - \int_0^x p^2(t)dt - \int_0^x q(t)dt\right]\right. \tag{4}$$
$$+\frac{1}{(2i\lambda)^2}\left[i(p'(x)-p'(0)) - \frac{5}{2}p^2(x) + p(0)p(x) + \frac{3}{2}p^2(0) - (q(x)-q(0))\right.$$
$$-2i\int_0^x p^3(t)dt + \int_0^x q(t)dt\int_0^x p^2(t)dt + \frac{1}{2}\left(\int_0^x p^2(t)dt\right)^2 + \frac{1}{2}\left(\int_0^x q(t)dt\right)^2$$
$$\left.-i(p(x)-p(0))(\int_0^x p^2(t)dt + \int_0^x q(t)dt)\ ] + O\left(\frac{1}{\lambda^3}\right)\right\}.$$

Proof. It is well known that see [12], page 43) if the complex λ -plane is divided into two sectors S_ℓ defined by the equalities

$$\frac{\ell\pi}{2} \leq arglambda \leq \frac{(\ell+1)\pi}{2}, \qquad (\ell = 0,1). \tag{5}$$

Then in each of these sectors (5), the equation (1) has two linear independent solutions for sufficiently large $|\lambda|$, which satisfying the relation

$$y_\nu(x,\lambda) = e^{\lambda w_\nu x}\left[u_{\nu,0}(x) + \cdots \frac{u_{\nu,0}(x)}{(2\lambda w_\nu)^n} + O(\frac{1}{\lambda^{n+1}})\right], (\nu = 1,2) \tag{6}$$

where the functions $u_{\nu,j}(x)$ are satisfying the following recurrent relations

$$u_{\nu,j}(x) = e^{-w_\nu\beta(x)}\int_0^x L\left[u_{\nu,j-1}(t)\right]e^{w_\nu\beta(t)}dt, (j = 0,1) \tag{7}$$

$$u_{\nu,0}(x) = e^{-w_\nu\beta(x)} \tag{8}$$

and

$$L \equiv -\frac{d^2}{dx^2} + q(x), w_1 = i, w_2 = -i. \tag{9}$$

Thus, we can find from (7), (8) and (9) that

$$u_{1,0}(x) = e^{-i\beta(x)}, u_{2,0}(x) = e^{i\beta(x)},$$

$$u_{1,1}(x) = e^{-i\beta(x)}[(i(p(x) - p(0) + \int_0^x p^2(t)dt) + \int_0^x q(t)dt)],$$

$$\begin{aligned} u_{1,2}(x) \quad = \quad & e^{-i\beta(x)}[2i\int_0^x p^3(t)dt - i(p'(x) + p'(0)) - \frac{5}{2}p^2(x) + p(0)p(x) \\ & + \frac{3}{2}p^2(0) - q(x) + q(0) + 2i\int_0^x p(t)q(t)dt + i(p(x) - p(0))\int_0^x p^2(t)dt \\ & + \frac{1}{2}(\int_0^x p^2(t)dt)^2 + i(p(x) - p(0))\int_0^x q(t)dt + \int_0^x q(t)dt\int_0^x p^2(t)dt \\ & + \frac{1}{2}(q(t)dt)^2], \end{aligned}$$

$$u_{2,1}(x) = e^{i\beta(x)}[-i((p(x) - p(0)) + \int_0^x p^2(t)dt + \int_0^x q(t)dt]$$

and

$$\begin{aligned} u_{2,2}(x) \quad = \quad & e^{i\beta(x)}[i(p'(x) - p'(0)) - \frac{5}{2}p^2(x) + p(0)p(x) + \frac{3}{2}p^2(0) - (q(x) - q(0)) \\ & -i(p(x) - p(0))\int_0^x p^2(t)dt - 2i\int_0^x p^3(t)dt + +\frac{1}{2}(\int_0^x p^2(t)dt)^2 \\ & -i(p(x) - p(0))\int_0^x q(t)dt - 2i\int_0^x p(t)q(t)dt + \int_0^x q(t)dt\int_0^x p^2(t)dt \\ & + \frac{1}{2}(\int_0^x q(t)dt)^2]. \end{aligned}$$

Let us substitute all these recurrent relations into the (6) we easily obtain the linearly independent solutions (3) and (4). The proof of Lemma is completed. ■

3 The Asymptotic Formulas For The Eigenvalues

Theorem 2 *The eigenvalues of the boundary - value problem (1)-(2) form two infinite sequences $\lambda_{k,1}$ $\lambda_{k,2}$, $\mid k \mid= N, N+1, ...$ where N is a positive integer and have the following asymptotic formulas:*

$$\lambda_{k,1} = \frac{\beta(\pi)}{\pi} + 2k + \frac{p(\pi) - p(0)}{4k\pi} + O(\frac{1}{k^2}),$$
$$\lambda_{k,2} = \frac{\beta(\pi)}{\pi} + 2k - \frac{p(\pi) - p(0)}{4k\pi} + O(\frac{1}{k^2})$$

Proof. By derivation of (6) up to first order with respect to x we obtain

$$y'_\nu(x,\lambda) = \lambda w_\nu e^{\lambda w_\nu x}\left[u_{\nu,0}(x) + \cdots + \sum_1^n \frac{u_{\nu,k}(x) + 2u'_{\nu,k-1}(x)}{(2\lambda w_\nu)^n} + O(\frac{1}{\lambda^{n+1}})\right],$$

where $\nu = 1,2$ and $w_1 = -w_2 = i$. It readily follows that

$$y_1(0,\lambda) = \left[1 + O\left(\frac{1}{\lambda^3}\right)\right],$$

$$y_2(0,\lambda) = \left[1 + O\left(\frac{1}{\lambda^3}\right)\right],$$

$$\begin{aligned} y_1(\pi,\lambda) = e^{i\lambda\pi}e^{-i\beta(\pi)}&\left\{1 + \frac{1}{2i\lambda}\left[i(p(\pi)-p(0)) + \int_0^\pi p^2(t)dt + \int_0^\pi q(t)dt\right]\right. \\ &+ \frac{1}{(2i\lambda)^2}\left[-i(p'(\pi)-p'(0)) - \frac{5}{2}p^2(\pi) + p(0)p(\pi) + \frac{3}{2}p^2(0) - q(\pi) + q(0)\right. \\ &+ 2i\int_0^\pi p^3(t)dt + \int_0^\pi q(t)dt\int_0^\pi p^2(t)dt + \frac{1}{2}\left(\int_0^\pi p^2(t)dt\right)^2 + \frac{1}{2}\left(\int_0^\pi q(t)dt\right)^2 \\ &\left.\left. + i(p(\pi)-p(0))(\int_0^\pi p^2(t)dt + \int_0^\pi q(t)dt)\right] + O\left(\frac{1}{\lambda^3}\right)\right\}, \end{aligned}$$

$$\begin{aligned} y_2(\pi,\lambda) = e^{-i\lambda\pi}e^{i\beta(\pi)}&\left\{1 + \frac{1}{2i\lambda}\left[i(p(\pi)-p(0)) - \int_0^\pi p^2(t)dt - \int_0^\pi q(t)dt\right]\right. \\ &+ \frac{1}{(2i\lambda)^2}\left[i(p'(\pi)-p'(0)) - \frac{5}{2}p^2(\pi) + p(0)p(\pi) + \frac{3}{2}p^2(0) - (q(\pi) - q(0))\right. \\ &- 2i\int_0^\pi p^3(t)dt + \int_0^\pi q(t)dt\int_0^\pi p^2(t)dt + \frac{1}{2}\left(\int_0^\pi p^2(t)dt\right)^2 + \frac{1}{2}\left(\int_0^\pi q(t)dt\right)^2 \\ &\left.\left. - i(p(\pi)-p(0))(\int_0^\pi p^2(t)dt + \int_0^\pi q(t)dt)\right] + O\left(\frac{1}{\lambda^3}\right)\right\}, \end{aligned}$$

$$y'_1(0,\lambda) = i\lambda\left[1 - \frac{2ip(0)}{(2i\lambda)} + \frac{2ip'(0) + 2p^2(0) + 2q(0)}{(2i\lambda)^2} + O\left(\frac{1}{\lambda^3}\right)\right],$$

$$y'_2(0,\lambda) = -i\lambda\left[1 - \frac{2ip(0)}{(2i\lambda)} + \frac{-2ip'(0) + 2p^2(0) + 2q(0)}{(2i\lambda)^2} + O\left(\frac{1}{\lambda^3}\right)\right],$$

$$y_1'(\pi,\lambda) = i\lambda e^{i\lambda\pi}e^{-i\beta(\pi)}\left\{1-\frac{1}{2i\lambda}\left[i(p(\pi)-p(0))-\int_0^\pi p^2(t)dt-\int_0^\pi q(t)dt\right]\right.$$
$$+\frac{1}{(2i\lambda)^2}\left[i(p'(\pi)+p'(0))+\frac{3}{2}p^2(\pi)-p(0)p(\pi)+\frac{3}{2}p^2(0)+q(\pi)+q(0)\right.$$
$$+2i\int_0^x p^3(t)dt+\int_0^\pi q(t)dt\int_0^\pi p^2(t)dt+\frac{1}{2}\left(\int_0^\pi p^2(t)dt\right)^2+\frac{1}{2}\left(\int_0^\pi q(t)dt\right)^2$$
$$\left.\left.-i(p(\pi)+p(0))(\int_0^\pi p^2(t)dt+\int_0^\pi q(t)dt)\right]+O\left(\frac{1}{\lambda^3}\right)\right\},$$

$$y_2'(\pi,\lambda) = -i\lambda e^{-i\lambda\pi}e^{i\beta(\pi)}\left\{1-\frac{1}{2i\lambda}\left[i(p(\pi)+p(0))+\int_0^\pi p^2(t)dt+\int_0^\pi q(t)dt\right]\right.$$
$$+\frac{1}{(2i\lambda)^2}\left[-i(p'(\pi)+p'(0))+\frac{3}{2}p^2(\pi)-p(0)p(\pi)+\frac{3}{2}p^2(0)+q(\pi)+q(0)\right.$$
$$-2i\int_0^x p^3(t)dt+\int_0^\pi q(t)dt\int_0^\pi p^2(t)dt+\frac{1}{2}\left(\int_0^\pi p^2(t)dt\right)^2+\frac{1}{2}\left(\int_0^\pi q(t)dt\right)^2$$
$$\left.\left.+i(p(\pi)+p(0))(\int_0^\pi p^2(t)dt+\int_0^\pi q(t)dt)\right]+O\left(\frac{1}{\lambda^3}\right)\right\}.$$

Let us substitute all these $y_\nu(x,\lambda)$ and $y_\nu'(x,\lambda)$ $(\nu=1,2)$ into the characteristic determinant

$$\triangle(\lambda)=\begin{vmatrix} U_1\left(y_1(x,\lambda)\right) & U_1(y_2(x,\lambda)) \\ U_2(y_1(x,\lambda)) & U_2(y_2(x,\lambda))\end{vmatrix}, \tag{10}$$

where

$$U_1(y)=y(\pi)+y(0) \qquad U_2(y)=y'(\pi)+y'(0).$$

By elementary transformations, for sufficiently large $|\lambda|$, we find that the following relation is valid

$$\frac{e^{i\lambda\pi}e^{i\beta(\pi)}}{-2i\lambda}\triangle(\lambda)=b(\lambda)e^{2i\lambda\pi}+C(\lambda)2e^{i\lambda\pi}e^{i\beta(\pi)}+D(\lambda)e^{2i\beta(\pi)}. \tag{11}$$

Let be $b(\lambda)$ be coefficient of $e^{2i\lambda\pi}$ in (11). Using the expansion

$$(1-x)^{-1}=1+x+x^2+O(x^3) \quad x\to 0,$$

we can easily see that for sufficiently large $|\lambda|$ the following relation holds

$$b^{-1}(\lambda)=1+\frac{1}{2i\lambda}\left[2ip(0)-\int_0^\pi p^2(t)dt-\int_0^\pi q(t)dt\right] \tag{12}$$
$$+\frac{1}{(2i\lambda)^2}\left[\frac{1}{2}p^2(\pi)-p(0)p(\pi)-\frac{11}{2}p^2(0)-2i\int_0^\pi p^3(t)dt\right.$$
$$-2ip(0)\left(\int_0^\pi p^2(t)dt+\int_0^\pi q(t)dt\right)+\int_0^\pi q(t)dt\int_0^\pi p^2(t)dt$$
$$+\frac{1}{2}\left(\int_0^\pi p^2(t)dt\right)^2+\frac{1}{2}\left(\int_0^\pi q(t)dt\right)^2-2i\int_0^\pi p(t)q(t)dt$$
$$\left.-2q(0)+\left(O(\frac{1}{\lambda^3}\right)\right]$$

Thus, the equation $\triangle(\lambda) = 0$ is equivalent to the equation

$$b^{-1}(\lambda)\frac{e^{i\lambda\pi}e^{i\beta(\pi)}}{-2i\lambda}\triangle(\lambda) = 0 \tag{13}$$

If the conditions $\int_0^\pi q(x)dx = 0$, $\int_0^\pi p^2(x)dx = 0$ hold, in view of (11) and (12), Eq. (13) can easily transformed to the form

$$e^{i\lambda\pi} + e^{i\beta(\pi)} = \mp e^{i\beta(\pi)}\frac{1}{2i\lambda}[p(\pi) - p(0)] + O\left(\frac{1}{\lambda^2}\right). \tag{14}$$

Since $p(\pi) - p(0) \neq 0$. Eq.(14) splits into two equations:

$$e^{i(\lambda\pi - \beta(\pi))} + 1 = -\frac{p(\pi) - p(0)}{2i\lambda} + O\left(\frac{1}{\lambda^2}\right) \tag{15}$$

$$e^{i(\lambda\pi - \beta(\pi))} + 1 = \frac{p(\pi) - p(0)}{2i\lambda} + O\left(\frac{1}{\lambda^2}\right). \tag{16}$$

By Rouche's Theorem , we obtain asymptotic expressions for roots $\lambda_{k,1}$ and $\lambda_{k,2}$, $|k| = N, N + 1, ...$ (N being positive integer), of Eq. (15) and (16) respectively:

$$\lambda_{k,1} = \frac{\beta(\pi)}{\pi} + 2k + \frac{p(\pi) - p(0)}{4k\pi} + O\left(\frac{1}{k^2}\right),$$

$$\lambda_{k,2} = \frac{\beta(\pi)}{\pi} + 2k - \frac{p(\pi) - p(0)}{4k\pi} + O\left(\frac{1}{k^2}\right).$$

Thus, asymptotic formulas are valid, and the proof of the theorem is completed. ■

Acknowledgement

This study was supported by the Research Fund of Mersin University in Turkey with Project Number: 2018-2-TP2-2940.

References

[1] G. S. Guseinov, On spectral analysis of a quadratic pencil of Sturm-Liouville operators, Dokl. Akad. Nauk SSSR 285:6 (1985) 1292-1296, English transl. in Soviet Math. Dokl. 32(3) (1985)859-862.

[2] G. S. Guseinov, Inverse spectral problems for a quadratic pencil of Sturm-Liouville operators on a finite interval, in Spect. Theor. Operat. i Èlm, Baku no.7 (1986) 51-101. (Russian).

[3] I. M. Guseinov, Nabiev, I. M., A class of inverse problems for a quadratic pencil of Sturm-Liouville operators, Differ. Uravn. Equations, 36(3) (2000) 418-420.; English transl. in Differ. Equ. 36(3) (2000) 471-473.

[4] I. M. Huseynov, I. M. Nabiev, On one class of inverse problems for quadratic bundle of Sturm-Liouville operators, Diff. Uravnenija, 36(3)(2000)418-420 (Russian).

[5] F. G. Maksudov, G. Sh. Huseynov, To the solution of the inverse scattering problem for quadratic bundle of one-dimensional, Schrödinger on the whole axis. DAN SSSR, 289(1) (1986) 42-46 (Russian).

[6] P. Djakov, B. Mityagin, Instability zones of one-dimensional periodic Shrödinger and Dirac operators, Russian Math. Surveys, 61 (4) (2006) 663-766.

[7] M. G. Gasymov, On the spectral theory of differential operators polynomially depending on a parameter, Uspekhi Mat. Nauk 37(4)(1982) 99 (Russian).

[8] V. A. Yurko, An inverse problem for differential operator pencils, Mat. Sb. 191(10) (2000)137-160; English transl. in Sb. Math. 191(10) (2000)1561-1586.

[9] I. M. Nabiev, The inverse periodic problem for a diffusion operator, Trans. Acad. of Sci. Azerb. Ser. Phys. Tech. Math. Sci. 23(4) (2003) 125-130.

[10] I. M Nabiev, I. M., The inverse spectral problem for the diffusion operator on an interval, Mat. Fiz. Anal. Geom. 11(3) (2004)302-313 (Russian).

[11] V. N. Pivovarchik, Reconstruction of potential of Sturm-Liouville equation on three spectra of boundary value problems, Funct. Anal. Appl. 33 (1999) 233-235.

[12] M.A.Naimark, Linear Differantial Operators [in Russian] , Nauka, Moscow 1969.

[13] B. M. Levitan ,I. S. Sargsjan, *Introduction to Spectral Theory : Self Adjoint Ordinary Differential Operators* , American Mathematical Society : Providence , Rhode Island 1975.

New Traveling Wave Solutions For Conformable Fractional Partial Differential Equations

Ozan ÖZKAN*
Selçuk University,
Department of Mathematics,
Konya, TURKEY

Orkun TAŞBOZAN
Hatay Mustafa Kemal University,
Department of Mathematics,
Hatay, TURKEY

Ali KURT
Hatay Mustafa Kemal University,
Department of Mathematics,
Hatay, TURKEY

Abstract

The main purpose of this study is presenting new exact solution sets of some nonlinear conformable time-fractional partial differential equations arising in mathematical physics by means of sub-equation method. The results show that the presented method is efficient, dependable, simple to apply and a good alternative for obtaining solutions of fractional partial differential equations.
Keywords: Sub-equation method, conformable fractional derivative, fractional partial differential equation, exact solution.

1 Introduction

Solving nonlinear fractional partial differential equations (NFPDEs) has a great importance to understand the mathematical model which based on a physical or an engineering phenomenon [1, 2, 3, 4, 5]. For modeling the real world event scientists used different definitions of fractional derivative. Each definition have supremacy over the other one. For instance Riemann-Liouville derivative definition uses the boundary/initial value conditions with fractional order by means of Riemann-Liouville fractional derivative. But Caputo derivative definition uses the conditions with integer order derivative. Recently Khalil *et. al.* [6] claimed that both Riemann-Liouville and Caputo has some deficiencies. For instance

1. The Riemann-Liouville derivative does not satisfy $D_a^\alpha 1 = 0$(Caputo derivative satisfies), if α is not a natural number.

2. All fractional derivatives do not satisfy the known formula of the derivative of the product of two functions.
$$D_a^\alpha(fg) = gD_a^\alpha(f) + fD_a^\alpha(g).$$

3. All fractional derivatives do not satisfy the known formula of the derivative of the quotient of two functions.
$$D_a^\alpha\left(\frac{f}{g}\right) = \frac{fD_a^\alpha(f) - gD_a^\alpha(g)}{g^2}.$$

*Corresponding author. *E-mail address:* oozkan@selcuk.edu.tr

4. All fractional derivatives do not satisfy the chain rule.

$$D_a^{\alpha}(fog)(t) = f^{\alpha}(g(t))g^{\alpha}(t).$$

5. All fractional derivatives do not satisfy $D^{\alpha}D^{\beta} = D^{\alpha+\beta}$ in general.

6. In the Caputo definition it is assumed that the function f is differentiable.

To annihilate these deficiencies Khalil *et. al.* [6] stated a new definition of differentiation and integration with arbitrary order named *conformable fractional derivative and integral.*

Definition 1. *Let $f : [0,\infty) \to \mathbb{R}$ be a function. The α^{th} order conformable fractional derivative of f is defined by,*

$$D^{\alpha}(f)(t) = \lim_{\varepsilon \to 0} \frac{f(t+\varepsilon t^{1-\alpha}) - f(t)}{\varepsilon}$$

for all $t > 0, \alpha \in (0,1)$.

Definition 2. *If f is α-differentiable in some $(0,a), a > 0$ and $\lim_{t\to 0^+} f^{(\alpha)}(t)$ exists then define $f^{(\alpha)}(0) = \lim_{t\to 0^+} f^{(\alpha)}(t)$. The conformable fractional integral of a function f starting from $a \geq 0$ is defined as:*

$$I_{\alpha}^{a}(f)(t) = \int_a^t f(x) d_{\alpha}x = \int_a^t \frac{f(x)}{x^{1-\alpha}} dx$$

where the integral is the usual Riemann improper integral and $\alpha \in (0,1]$.

Some properties of this new definition are given in the following theorem [6, 7].

Theorem 3. *Let $\alpha \in (0,1]$ and f, g are α-differantiable functions at point $t > 0$, then*

1. $T_{\alpha}(mf + ng) = mT_{\alpha}(f) + nT_{\alpha}(g)$ for all $m, n \in \mathbb{R}$
2. $T_{\alpha}(t^p) = pt^{p-\alpha}$ for all p
3. $T_{\alpha}(f.g) = fT_{\alpha}(g) + gT_{\alpha}(f)$
4. $T_{\alpha}(\frac{f}{g}) = \frac{gT_{\alpha}(f) - fT_{\alpha}(g)}{g^2}$
5. $T_{\alpha}(c) = 0$ for all constant functions $f(t) = c$
6. In addition, if f is differentiable, then $T_{\alpha}(f)(t) = t^{1-\alpha}\frac{df(t)}{dt}$.

After existence of these definitions huge amount of applications are made by many scientists [8, 9, 11]. In this work conformable time fractional Sine-Bratu type equation is considered as follows.

$$D_x^2 u(x,t) + D_t^{(2)\alpha} u(x,t) + \lambda \sin(u(x,t)) = 0. \tag{1}$$

2 Basics of Sub-Equation Method

Lets give a short description of considered sub equation method [10, 12]. Supposing the nonlinear conformable time fractional partial differential equation as

$$P\left(u, D_t^{\alpha}u, D_x u, D_t^{2\alpha}u, D_x^2 u, ...\right) = 0 \tag{2}$$

where $D_t^{\alpha}u$ indicates conformable fractional derivative of function $u(x,t)$ and $D_t^{2\alpha}$ shows two times conformable fractional derivative of the function $u(x,t)$. By using the conformable wave transformation

$$u(x,t) = U(\xi),\ \xi = kx + w\frac{t^{\alpha}}{\alpha} \tag{3}$$

and the chain rule [7] Eq. (2) changes into nonlinear ordinary differential equation

$$G(U, U', U'', ...) = 0 \tag{4}$$

where prime shows integer order derivative with respect to new wave variable ξ and k, w are arbitrary constants to be evaluated later. Assume that equation (4) has a solution in the form

$$U(\xi) = \sum_{i=0}^{N} a_i \varphi^i(\xi),\ a_N \neq 0, \tag{5}$$

where $a_i, a_N \neq 0$ $(0 \leq i \leq N)$ are constant coefficients to be determined, N is a positive integer which is going to be found by balancing procedure in equation (4) and $\varphi(\xi)$ is the solution of Riccati equation

$$\varphi'(\xi) = \sigma + (\varphi(\xi))^2 \tag{6}$$

where σ is an arbitrary constant. Some special solutions of the Riccati equation (6) are given in the following table.

$$\varphi(\xi) = \begin{cases} -\sqrt{-\sigma}\tanh\left(\sqrt{-\sigma}\xi\right), & \sigma < 0 \\ -\sqrt{-\sigma}\coth\left(\sqrt{-\sigma}\xi\right), & \sigma < 0 \\ \sqrt{\sigma}\tan\left(\sqrt{\sigma}\xi\right), & \sigma > 0 \\ -\sqrt{\sigma}\cot\left(\sqrt{\sigma}\xi\right), & \sigma > 0 \\ -\frac{1}{\xi+\varpi},\ \varpi\ is\ a\ cons., & \sigma = 0 \end{cases} \tag{7}$$

Putting the equations (5) and (6) into equation (4) we acquire a polynomial with respect $\varphi(\xi)$. Considering all the coefficients of $\varphi^i(\xi)$ $(i = 0, 1, ..., N)$ to zero leads a nonlinear algebraic equation system in k, w, a_i $(i = 0, 1, ..., N)$. By obtaining the solution of these nonlinear algebraic equation system we evaluate the constants k, w, a_i $(i = 0, 1, ..., N)$. Then substituting obtained constants from the nonlinear algebraic system and the solutions of equation (6) into equation (5) by the help of the formulas (7) we determine the exact solutions for equation (2).

3 Solution of Time Fractional Sine-Bratu Type Equation

Regarding time fractional Sine-Bratu Type Equation (1) then applying chain rule [7] and wave transform (3) the Eq. (1) changes into ordinary differential equation system such as

$$(k^2 + w^2)U'' + \lambda \sin(U) = 0. \tag{8}$$

Then using the transformation $v(\xi) = e^{iU(\xi)}$ where $i^2 = -1$ so,

$$\sin(U) = \frac{v - v^{-1}}{2i}, \cos(U) = \frac{v + v^{-1}}{2}$$

that gives

$$U = \arccos\left(\frac{v + v^{-1}}{2}\right).$$

This transformation changes Eq.8 into

$$2(k^2 + w^2)(v''v - v'^2) + \lambda(v^3 - v) = 0 \tag{9}$$

where prime denoted the derivative with respect to variable ξ. Supposing the solution of Eq. (9) is indicated by the following series

$$u(\xi) = \sum_{i=0}^{N} a_i \varphi^i(\xi),\ a_N \neq 0 \tag{10}$$

where $\varphi(\xi)$ is the exact solutions of Riccati differential equation (6) given in (7). After the balancing procedure, we get $N = 2$. When we substitute all the obtained data into (8), an algebraic equation system arises. Solving this system leads following solution set

$$a_0 = 0, a_1 = 0, a_2 = -\frac{1}{\sigma}, w = \pm\frac{\sqrt{\lambda - 4k^2\sigma}}{2\sqrt{\sigma}}$$

For $\sigma < 0$

$$v_1(x,t) = -\sqrt{-\sigma}\tanh\left(\sqrt{-\sigma}\left(kx \pm \frac{\sqrt{\lambda - 4k^2\sigma}}{2\sqrt{\sigma}}\frac{t^\alpha}{\alpha}\right)\right),$$

$$v_2(x,y,t) = -\sqrt{-\sigma}\coth\left(\sqrt{-\sigma}\left(kx \pm \frac{\sqrt{\lambda - 4k^2\sigma}}{2\sqrt{\sigma}}\frac{t^\alpha}{\alpha}\right)\right),$$

For $\sigma > 0$

$$v_3(x,y,t) = \sqrt{\sigma}\tan\left(\sqrt{\sigma}\left(kx \pm \frac{\sqrt{\lambda - 4k^2\sigma}}{2\sqrt{\sigma}}\frac{t^\alpha}{\alpha}\right)\right),$$

$$v_4(x,y,t) = -\sqrt{\sigma}\cot\left(\sqrt{\sigma}\left(kx \pm \frac{\sqrt{\lambda - 4k^2\sigma}}{2\sqrt{\sigma}}\frac{t^\alpha}{\alpha}\right)\right),$$

where

$$U = \arccos\left(\frac{v + v^{-1}}{2}\right). \tag{11}$$

4 Conclusion

The sub-equation method is applied to conformable time fractional sine-Bratu type equations successfully. Obtained results show that the method is accurate and reliable.

References

[1] K.S. Miller, B. Ross, An Introduction to the Fractional Calculus and Fractional Differential Equations, John Wiley and Sons, New York, 1993.

[2] A.Kilbas, H.M. Srivastava, J.J. Trujillo, Theory and Applications of Fractional Differential Equations, (Elsevier, San Diego, 2006).

[3] I. Podlubny, Fractional Differential Equations, (Academic Press,San Diego, 1999).

[4] K. Oldham, J. Spanier, The fractional calculus theory and applications of differentiation and integration to arbitrary order. Elsevier, 1974.

[5] I. Podlubny, Geometric and physical interpretation of fractional integration and fractional differentiation, Fract. Calculus. Appl. Anal, 5, 367-386 (2002).

[6] R. Khalil, M. Al Horani, A. Yousef, M. Sababheh, A new definition of fractional derivative, J. Comput. Appl. Math. 264, 65 (2014).

[7] T. Abdeljawad, On conformable fractional calculus, J. Comput. Appl. Math. 279, 57 (2015)

[8] O. Özkan, A. Kurt, On conformable double Laplace transform. Optical and Quantum Electronics, 50(2), 103, (2018).

[9] A. Atangana, D. Baleanu, A. Alsaedi, New properties of conformable derivative, Open Mathematics 13.1(2015).

[10] A.Bekir, E. Aksoy, A.C. Cevikel, Exact solutions of nonlinear time fractional partial differential equations by sub-equation method, Mathematical Methods in the Applied Sciences, 38(13)(2015), 2779-2784.

[11] A. Kurt, O. Tasbozan, D. Baleanu, New solutions for conformable fractional Nizhnik-Novikov- Veselov system via G'/G expansion method and homotopy analysis methods, Optical and Quantum Electronics 49.10(2017): 333.

[12] S. Zhang, H.Q. Zhang, Fractional sub-equation method and its applications to nonlinear fractional PDEs, Physics Letters A, 375.7(2011), 1069-1073.

Word Problem for Congruence Classes of Complex Reflection Groups

Nurten URLU ÖZALAN*
KTO Karatay University,
Department of Mathematics,
Konya, TURKEY

Eylem GÜZEL KARPUZ
Karamanoglu Mehmetbey University,
Department of Mathematics,
70100, Karaman, TURKEY

Abstract

In this paper, we obtain Gröbner-Shirshov (non-commutative) basis for the congruence classes of primitive complex reflection group G_{15}. It gives a new algorithm for getting normal form of elements of this group and hence a new algorithm for solving the word problem in this group.
Keywords: Gröbner-Shirshov basis, presentation, complex reflection group, word problem.

1 Introduction

In 1965, Buchberger introduced the Gröbner basis theory for commutative algebras ([10]). This theory provides a solution to the reduction problem for commutative algebras. Then, in [4], Bergman generalized the Gröbner basis theory to associative algebras by proving the "Diamond Lemma". On the other hand, the parallel theory of Gröbner bases was advanced for Lie algebras by Shirshov [20]. The main meaning of the theory of Gröbner basis is "Composition Lemma" which characterizes the leading terms of elements in the given ideal. After Shirshov's paper, in [5], Bokut noticed that Shirshov's method works for also associative algebras. Hence, for this reason, Shirshov's theory for Lie algebras and their universal enveloping algebras is called the *Gröbner-Shirshov basis* theory. The importance of this theory is that it gives new algorithm for getting normal forms of elements of given algebraic structures and thus a new algorithm for solving the word problem in these structures. This important theory has been studied for lots of valuable algebraic structures, for example groups (group extensions), monoids/semigroups (monoid and semigroup constructions), many types of Lie algebras, rings and modules. We may refer the papers [2, 3, 6, 7, 8, 11, 14, 15, 16, 17] for some recent studies over Gröbner-Shirshov basis theory.

In early 1900's, Max Dehn introduced algorithmic problems such as the *word, conjugacy* and *isomorphism problems*. These problems played an important role in group theory are called *decision problems* which ask for a yes or no answer to a specific question. Among these decision problems especially the word problem has been studied widely in groups (see [1]). It is well known that the word problem for finitely presented groups is not solvable in general; that is, given any two words obtained by generators of the group, there may be no algorithm to decide whether these words represent the same element in this group.

The method of Gröbner-Shirshov bases which is the main theme of this paper gives a new algorithm for getting normal forms of elements of groups (monoids) and hence a new algorithm for solving the word problem in these groups (monoids). By considering this fact,

*Corresponding author. *E-mail address:* n.urlu91@gmail.com

our aim in this paper is to find Gröbner-Shirshov basis of the congruence classes of primitive complex reflection group G_{15}.

Shephard and Todd classified all finite complex reflection groups in [18]. Later Cohen (1976) gave a more systematic description for these groups in terms of root systems, vector graphs and root graphs ([12]). Then, in [13], Howlett and Shi defined a simple root system (B, w) for such these groups which is analogous to the corresponding concept for a Coxeter group. It is well known that any Coxeter group can be presented by generators and relations. A finite complex reflection group G can also be presented in a similar way (see, for example, [9]). But such a presentation is not unique for G in general. Different presentations of G may reveal various different properties of G. Then it is worth to define a congruence relation among the presentations of G (see [19]) and then to ask that question "How many congruence classes of presentations are there for any irreducible finite complex reflection group G?". In [9], the authors solve this problem for the finite primitive complex reflection groups $G = \{G_7, G_{11}, G_{15}, G_{19}, G_{27}\}$ and in [19], Shi studied the finite primitive complex reflection groups $G = \{G_{12}, G_{24}, G_{25}, G_{26}\}$ (in the notations of Shephard and Todd, 1954). So by considering the presentation given in [9], our aim in this paper is to find Gröbner-Shirshov basis for the group G_{15}. Gröbner-Shirshov bases of other groups will be studied in the future.

Throughout this paper, we order words in given alphabet in the deg-lex way comparing two words first by theirs lengths and then lexicographically when the lengths are equal. Additionally $(i)\cap(j)$ and $(i)\cup(j)$ denote the intersection and inclusion compositions of relations (i), (j), respectively.

2 Gröbner-Shirshov Bases and Composition-Diamond Lemma

Let K be a field and $K\langle X\rangle$ be the free associative algebra over K generated by X. Denote X^* the free monoid generated by X, where the empty word is the identity denoted by 1. For a word $w \in X^*$, we denote the length of w by $|w|$. Suppose that X^* is a well ordered set. Then every nonzero polynomial $f \in K\langle X\rangle$ has the leading word $\overline{f}$. If the coefficient of $\overline{f}$ in f is equal to 1, then f is called monic.

Let f and g be two monic polynomials in $K\langle X\rangle$. We then have two compositions as follows:

- If w is a word such that $w = \overline{f}b = a\overline{g}$ for some $a, b \in X^*$ with $|\overline{f}| + |\overline{g}| > |w|$, then the polynomial $(f, g)_w = fb - ag$ is called the i*ntersection composition* of f and g with respect to w. The word w is called an *ambiguity* of intersection.

- If $w = \overline{f} = a\overline{g}b$ for some $a, b \in X^*$, then the polynomial $(f, g)_w = f - agb$ is called the *inclusion composition* of f and g with respect to w. The word w is called an *ambiguity* of inclusion.

If g is monic, $\overline{f} = a\overline{g}b$ and α is the coefficient of the leading term $\overline{f}$, then transformation $f \mapsto f - \alpha agb$ is called elimination (ELW) of the leading word of g in f.

Let $S \subseteq K\langle X\rangle$ with each $s \in S$ is monic. Then the composition $(f, g)_w$ is called trivial modulo (S, w) if $(f, g)_w = \sum \alpha_i a_i s_i b_i$, where each $\alpha_i \in K, a_i, b_i \in X^*, s_i \in S$ and $a_i\overline{s_i}b_i < w$. If this is the case, then we write $(f, g)_w \equiv 0 \ mod(S, w)$.

We call the set S endowed with the well ordering $<$ a *Gröbner-Shirshov basis* for $K\langle X \mid S\rangle$ if any composition $(f, g)_w$ of polynomials in S is trivial modulo S and corresponding w.

The following lemma was proved by Shirshov [20] for free Lie algebras with deg-lex ordering.

Lemma 1 ***(Composition-Diamond Lemma)*** *Let K be a field, $A = K\langle X \mid S\rangle = K\langle X\rangle/Id(S)$ and $<$ a monomial ordering on X^*, where $Id(S)$ is the ideal of $K\langle X\rangle$ generated by S. Then the following statements are equivalent:*

1. *S is a Gröbner-Shirshov basis.*
2. *$f \in Id(S) \Rightarrow \overline{f} = a\overline{s}b$ for some $s \in S$ and $a, b \in X^*$.*
3. *$Irr(S) = \{u \in X^* \mid u \neq a\overline{s}b, s \in S, a, b \in X^*\}$ is a basis for the algebra $A = K\langle X \mid S\rangle$.*

If a subset S of $K\langle X\rangle$ is not a Gröbner-Shirshov basis, then we can add to S all nontrivial compositions of polynomials of S, and by continuing this process (maybe infinitely) many times, we eventually obtain a Gröbner-Shirshov basis S^{comp}. Such a process is called the *Shirshov algorithm.*

3 Gröbner-Shirshov Basis for the Congruence Classes of Primitive Complex Reflection Group G_{15}

Main goal of this section is to search the solvability of the word problem for the congruence classes of primitive complex reflection group G_{15}. Since we will use the method of Gröbner-Shirshov basis theory, the presentation of this group is required. This presentation is as follows.

Theorem 2 ([9]) *The braid group associated with the congruence classes of complex reflection group G_{15} admits the presentation*

$$\mathcal{P}_{G_{15}} = \left\langle s,\ t,\ u \quad ; \quad t^2 = u^2 = s^3 = 1,\ tus = ust,\ stusu = tusus \right\rangle .$$

To obtain Gröbner-Shirshov basis let us order the generators of the group G_{15} as $s > u > t$. Now the main result is as follows:

Theorem 3 *A Gröbner-Shirshov basis of the braid group associated with the congruence classes of complex reflection group G_{15} consists of the following polynomials:*

$$\begin{array}{lll} (1)\ t^2 - 1, & (2)\ u^2 - 1, & (3)\ s^3 - 1, \\ (4)\ ust = tus, & (5)\ stusu - tusus, & \end{array}$$

relative to the deg-lex order of words in the generators.

Proof. We need to prove that all compositions among polynomials $(1) - (5)$ are trivial. Let us consider the intersection compositions of the polynomials $(1) - (5)$ and start with listing all intersections compositions. Actually we have the following ambiguities w:

$$\begin{array}{lll} (1) \cap (1) : w = t^3, & (2) \cap (2) : w = u^3, & (2) \cap (4) : w = u^2st, \\ (3) \cap (3) : w = s^4, & (3) \cap (5) : w = s^3tusu, & (4) \cap (1) : w = ust^2, \\ (4) \cap (5) : w = ustusu, & (5) \cap (2) : w = stusu^2, & (5) \cap (4) : w = stusust. \end{array}$$

All of these intersection compositions are trivial. Let us show some of them as follows:

$$\begin{aligned} (2) \cap (4) : w &= u^2st, \\ (f, g)_w &= (u^2 - 1)st - u(ust - tus) \\ &= u^2st - st - u^2st + utus = utus - st \\ &\equiv tus - ust \equiv tus - tus \equiv 0. \end{aligned}$$

$$\begin{aligned} (3) \cap (3) : w &= s^4, \\ (f, g)_w &= (s^3 - 1)s - s(s^3 - 1) \\ &= s^4 - s - s^4 + s \equiv 0. \end{aligned}$$

$$\begin{aligned}
(5)\cap(4): w &= stusust, \\
(f,g)_w &= (stusu - tusus)st - stus(ust - tus) \\
&= stusust - tusus^2t - stusust + stustus \\
&= stustus - tusus^2t \equiv st^2usus - tusus^2t \equiv susus - tusus^2t \\
&\equiv susust - tusus^2 \equiv sustus - tusus^2 \equiv stusus - tusus^2 \\
&\equiv tusus^2 - tusus^2 \equiv 0.
\end{aligned}$$

It remains to check including compositions of polynomials $(1)-(5)$. Since there are no any compositions of this type the proof ends up. ■

Now let R be the set of polynomails (relations) for congruence classes of primitive complex reflection group G_{15}. By using Composition-Diamond Lemma 1 and Theorem 3, the normal form structue for elements of the congruence classes of primitive complex reflection group G_{15} can be given as follows:

Corollary 4 *Let $C(u)$ be a normal form of a word $u \in G_{15}$. Then $C(u)$ is of the form $wt^{\epsilon_1}w'u^{\epsilon_2}w''s^{\epsilon_3}w'''$ $(0 \leq \epsilon_1, \epsilon_2 < 2,\ 0 \leq \epsilon_3 < 3)$, where w, w', w'' and w''' are $R-$reduced words in G_{15}.*

By considering Corollary 4, we have the following other consequence of Theorem 3.

Corollary 5 *The word problem for the congruence classes of primitive complex reflection group G_{15} is solvable.*

References

[1] S.I. Adian, V.G. Durnev, Decision problems for groups and semigroups, *Russian Math. Surveys* **55**(2) (2000) 207-296.

[2] F. Ateş, A.S. Çevik, E.G. Karpuz, Gröbner-Shirshov basis for the singular part of the Brauer semigroup, *Turkish Journal of Mathematics*, **42** (2018) 1338-1347.

[3] F. Ateş, E.G. Karpuz, C. Kocapinar, A.S. Çevik, Gröbner-Shirshov bases of some monoids, *Discrete Mathematics*, **311** (2011) 1064-1071.

[4] G.M. Bergman, The diamond lemma for ring theory, *Adv. Math.*, **29** (1978) 178-218.

[5] L.A. Bokut, Imbedding into simple associative algebras, *Algebra and Logic*, **15** (1976) 117-142.

[6] L.A. Bokut, A. Vesnin, Gröbner-Shirshov bases for some Braid groups, *Journal of Symbolic Computation*, **41** (2006) 357-371.

[7] L.A. Bokut, Gröbner-Shirshov basis for the Braid group in the Birman–Ko–Lee generators, *J. Algebra*, **321** (2009) 361-376.

[8] L.A. Bokut, Gröbner-Shirshov basis for the Braid group in the Artin-Garside generators, *Journal of Symbolic Computation*, **43** (2008) 397-405.

[9] M. Broue, G. Malle, R. Rouquier, Complex reflection groups, braid groups, Hecke algebras, *J. reine angew Math.* 500 (1998) 127-190.

[10] B. Buchberger, *An Algorithm for Finding a Basis for the Residue Class Ring of a Zero-Dimensional Ideal*, Ph.D. Thesis, University of Innsbruck, 1965.

[11] Y. Chen, C. Zhong, Gröbner-Shirshov bases for HNN extentions of groups and for the Alternating group, *Comm. in Algebra*, **36** (2008) 94-103.

[12] A. M. Cohen, Finite complex reflection groups, *Ann. Scient. Ec. Norm. Sup. 4e Seriet.* 9 (1976) 379-436.

[13] R. B. Howlett, J. Y. Shi, On regularity of finite reflection groups,*Manuscripta Mathematica* 102(3) (2000) 325-333.

[14] E. G. Karpuz, Gröbner-Shirshov bases of some semigroup constructions, *Algebra Colloquium*, **22(1)** (2015) 35-46.

[15] E. G. Karpuz, F. Ateş, A. S. Çevik, Gröbner-Shirshov bases of some Weyl groups, *Rocky Mountain Journal of Math*, **45** (4) (2015) 1165-1175.

[16] E. G. Karpuz, F. Ateş, N. Urlu, A. S. Çevik, I. N. Cangül, A note on the Gröbner-Shirshov bases over ad-hoc extensions of groups, *Filomat*, **30** (4) (2016) 1037-1043.

[17] C. Kocapinar, E. G. Karpuz, F. Ateş, A. S. Çevik, Gröbner-Shirshov bases of the generalized Bruck-Reilly $*$-extension, *Algebra Colloquium*, **19** (Spec 1) (2012) 813-820.

[18] G. C. Shephard, J. A. Todd, Finite unitary reflection groups, *Canad. J. Math.* 6 (1954) 274-304.

[19] J. Y. Shi, Simple root systems and presentations for certain complex reflection groups, *Communications in Algebra*, 33 (2005) 1765-1783.

[20] A.I. Shirshov, Some algorithmic problems for Lie algebras, *Siberian Math. J.*, **3** (1962) 292-296.

A Study on the Associated Functions of Differential Sturm-Liouville Operators

Nihal YOKUŞ*
Karamanoglu Mehmetbey University,
Department of Mathematics,
70100, Karaman, TURKEY

Nimet ÇOŞKUN
Karamanoglu Mehmetbey University,
Department of Mathematics,
70100, Karaman, TURKEY

Abstract

Let L denote opeator generated in $L^2(\mathbb{R}_+)$ by the differential expression

$$l(y) = -y'' + q(x)y, \quad x \in \mathbb{R}_+ := (0, \infty)$$

and the boundary condition

$$\frac{y'(0)}{y(0)} = \frac{\beta_0 + \beta_1\lambda}{\alpha_0 + \alpha_1\lambda}$$

where q is a complex valued function and $\alpha_i, \beta_i \in \mathbb{C}$, $i = 0, 1$ with $\alpha_0\beta_1 - \alpha_1\beta_0 \neq 0$. In this work, we investigate the principal functions corresponding to the eigenvalues and the spectral singularities of L.

Keywords: Eigenvalues; Eigenfunctions; Spectral singularities;Principal functions; Resolvent.

1 Introduction

Spectral analysis of differential operators is a field of functional analysis which have numerous application areas from engineering to physics. In particular, the spectral theory of linear operators in Hilbert spaces is the most important tool in the mathematical formulation of quantum mechanics. Even some very simple systems in quantum mechanics present nontrivial questions whose answers need a mathematical approach. For example, Hamiltonian of a quantum particle confined to a box involves a choice of boundary condition at the box ends. Since different choices of boundary condition imply different physical models, spectral analysis of operators with boundary condition constitues a wide field of research $[1-6]$.

Investigation of the spectral properties of the Sturm Liouville boundary value problem (BVP) can be traced back to Naimark [1]. He studied the (BVP)

$$\begin{cases} -y'' + q(x)y - \lambda^2 y = 0, \ x \in \mathbb{R}_+, \\ y'(0) - hy(0) = 0 \end{cases}$$

where $h \in \mathbb{C}$ and q is a complex valued function. He showed that the spectrum of this BVP is composed of eigenvalues, spectral singularities and continuous spectrum. He also proved that these eigenvalues and spectral singularities are of finite number with finite multiplicity under certain conditions.

The concept of spectral singularity which is rather typical for non-selfadjoint operators with a continuous part of spectrum constitues a particular role in spectral analysis. The

*Corresponding author. *E-mail address:* nyokus@kmu.edu.tr

term 'spectral singularity' can be traced back to Schwartz [7]. Lyance studied the effect of spectral singularities in the spectral expansion in terms of principal functions [8]. Detailed investigation of differential operators with spectral singularities was done in various papers [9 − 15].

The present paper is motivated by the above mentioned studies and the references therein. In this study, we take into consideration the following BVP,

$$-y^{''}+q(x)y=\lambda^2 y, \quad x\in\mathbb{R}_+=[0,\infty), \tag{1.1}$$

$$\left(y^{'}/y\right)(0)=\frac{\beta_1\lambda+\beta_0}{\alpha_1\lambda+\alpha_0} \tag{1.2}$$

where q is a complex-valued function and $\alpha_i,\beta_i\in\mathbb{C}$, $i=0,1$ with $\alpha_0\beta_1-\alpha_1\beta_0\neq 0$. The specific feature of this study is the presence of the spectral parameter not only in the Sturm-Lioville equation but also in the boundary condition. We obtain the associated (principal) functions corresponding to the eigenvalues and the spectral singularities of the BVP (1.1)-(1.2).

2 Jost solution of (1.1)

Now we will assume that the complex valued function q is almost everywhere continuous in $\mathbb{R}_+$ and satisfies the following

$$\int_0^\infty x\,|q(x)|\,dx<\infty. \tag{2.1}$$

Let $\varphi(x,\lambda)$ and $e(x,\lambda)$ denote the solutions of (1.1) satisfying the conditions

$$\varphi(0,\lambda)=\alpha_0+\alpha_1\lambda, \quad \varphi^{'}(0,\lambda)=\beta_0+\beta_1\lambda \tag{2.2}$$

and

$$\lim_{x\to\infty} e(x,\lambda)e^{-i\lambda x}=1, \quad \lambda\in\overline{\mathbb{C}}_+, \tag{2.3}$$

respectively. The solution $e(x,\lambda)$ is called the Jost solution of (1.1). Note that, under the condition (2.1), the solution $\varphi(x,\lambda)$ is an entire function of λ and the Jost solution is an analytic function of λ in $\mathbb{C}_+:=\{\lambda:\lambda\in\mathbb{C},\operatorname{Im}\lambda>0\}$ and continuous in $\overline{\mathbb{C}}_+=\{\lambda:\lambda\in\mathbb{C},\operatorname{Im}\lambda\geq 0\}$.

In addition Jost solution has a representation

$$e(x,\lambda)=e^{i\lambda x}+\int_x^\infty K(x,t)e^{i\lambda t}dt, \quad \lambda\in\overline{\mathbb{C}}_+, \tag{2.4}$$

where the kernel $K(x,t)$ satisfies

$$K(x,t)=\frac{1}{2}\int_{\frac{x+t}{2}}^\infty q(s)ds+\frac{1}{2}\int_x^{\frac{x+t}{2}}\int_{t+x-s}^{t+s-x} q(s)K(s,u)du\,ds+\frac{1}{2}\int_{\frac{x+t}{2}}^\infty\int_s^{t+s-x} q(s)K(s,u)du\,ds. \tag{2.5}$$

$K(x,t)$ is continuously differentiable with respect to its arguments and

$$|K(x,t)|\leq c\sigma(\frac{x+t}{2}), \tag{2.6}$$

$$|K_x(x,t)|\,,|K_t(x,t)|\leq\frac{1}{4}\left|q(\frac{x+t}{2})\right|+c\sigma(\frac{x+t}{2}), \tag{2.7}$$

where $\sigma(x) = \int\limits_x^\infty |q(s)|\, ds$ and $c > 0$ is a constant.

Let $\hat{e}^{\pm}(x,\lambda)$ denote the solutions of (1.1) subject to the conditions

$$\lim_{x\to\infty} e^{\pm i\lambda x}\hat{e}^{\pm}(x,\lambda) = 1, \quad \lim_{x\to\infty} e^{\pm i\lambda x}\hat{e}^{\pm}_x(x,\lambda) = \pm i\lambda, \quad \lambda \in \overline{\mathbb{C}}_{\pm}. \tag{2.8}$$

Then

$$\begin{array}{c} W\left[e(x,\lambda), \hat{e}^{\pm}(x,\lambda)\right] = \mp 2i\lambda, \quad \lambda \in \mathbb{C}_{\pm} \\ W\left[e(x,\lambda), e(x,-\lambda)\right] = -2i\lambda, \quad \lambda \in \mathbb{R} \end{array} \tag{2.9}$$

where $W\left[f_1, f_2\right]$ is the Wronskian of f_1 and f_2.

Let us define the following functions:

$$D_{\pm}(\lambda) := \varphi\left(0,\lambda\right) e^{'}(0,\pm\lambda) - \varphi^{'}\left(0,\lambda\right) e(0,\pm\lambda), \quad \lambda \in \overline{\mathbb{C}}_{\pm} \tag{2.10}$$

where $\overline{\mathbb{C}}_{-} = \{\lambda : \lambda \in \mathbb{C}, \operatorname{Im}\lambda \leq 0\}$. Therefore D_+ and D_- are analytic in $\mathbb{C}_+$ and $\mathbb{C}_- = \{\lambda : \lambda \in \mathbb{C}, \operatorname{Im}\lambda < 0\}$, respectively and continuous up to real axis.

The functions D_+ and D_- are called Jost functions of L.

The resolvent of L defined by

$$R_{\lambda}\left(L\right) f = \int\limits_0^\infty G\left(x,t;\lambda\right) f\left(t\right) dt, \quad f \in L_2\left(\mathbb{R}_+\right)$$

where

$$G_{\pm}(x,t;\lambda) = \begin{cases} -\frac{\varphi(t,\lambda)e(x,\pm\lambda)}{D_{\pm}(\lambda)}, & 0 \leq t \leq x \\ -\frac{\varphi(x,\lambda)e(t,\pm\lambda)}{D_{\pm}(\lambda)}, & x \leq t < \infty. \end{cases} \tag{2.11}$$

We denote the set of eigenvalues and spectral singularities of L by $\sigma_d(L)$ and $\sigma_{ss}(L)$, respectively. From (2.11)

$$\begin{array}{l} \sigma_d(L) = \{\lambda : \lambda \in \mathbb{C}_+, D_+(\lambda) = 0\} \cup \{\lambda : \lambda \in \mathbb{C}_-, D_-(\lambda) = 0\}, \\ \sigma_{ss}(L) = \{\lambda : \lambda \in \mathbb{R}^*, D_+(\lambda) = 0\} \cup \{\lambda : \lambda \in \mathbb{R}^*, D_-(\lambda) = 0\}, \end{array} \tag{2.12}$$

where $\mathbb{R}^* = \mathbb{R}\diagdown\{0\}$.

Definition 1 *The multiplicity of zero of the function D_+(or D_-) in $\overline{\mathbb{C}}_+$(or $\overline{\mathbb{C}}_-$) is called the multiplicity of the corresponding eigenvalue and spectral singularity of L.*

We see from (2.9) that the functions

$$\begin{array}{r} K_+(x,\lambda) = \frac{\hat{D}_+(\lambda)}{2i\lambda} e(x,\lambda) - \frac{D_+(\lambda)}{2i\lambda}\hat{e}^+(x,\lambda), \quad \lambda \in \mathbb{C}_+ \\ K_-(x,\lambda) = \frac{\hat{D}_-(\lambda)}{2i\lambda} e(x,-\lambda) - \frac{D_-(\lambda)}{2i\lambda}\hat{e}^-(x,\lambda), \quad \lambda \in \mathbb{C}_- \\ K(x,\lambda) = \frac{D_+(\lambda)}{2i\lambda} e(x,-\lambda) - \frac{D_-(\lambda)}{2i\lambda} e(x,\lambda), \quad \lambda \in \mathbb{R}^* \end{array}$$

are the solutions of the boundary value problem (1.1)-(1.2) where

$$\hat{D}_{\pm}(\lambda) = (\alpha_0 + \alpha_1\lambda)\hat{e}^{\pm'}(0,\lambda) - (\beta_0 + \beta_1\lambda)\hat{e}^{\pm}(0,\lambda).$$

Now let us assume that

$$q \in AC(\mathbb{R}_+), \quad \lim_{x\to\infty} q(x) = 0, \quad \sup_{x\in\mathbb{R}_+}\left[e^{\varepsilon\sqrt{x}}\left|q^{'}(x)\right|\right] < \infty, \quad \varepsilon > 0. \tag{2.13}$$

Theorem 2 *Under the condition (2.13) the operator L has a finite number of eigenvalues and spectral singularities, and each of them is of a finite multiplicity.*

3 Principal functions of L

In this section we assume that (2.13) holds. Let $\lambda_1, ..., \lambda_j$ and $\lambda_{j+1}, ..., \lambda_k$ denote the zeros of D_+ in $\mathbb{C}_+$ and D_- in $\mathbb{C}_-$ (which are the eigenvalues of L) with multiplicities $m_1, ..., m_j$ and $m_{j+1}, ..., m_k$, respectively. It is obvious that from definition of the Wronskian

$$\left\{\frac{d^n}{d\lambda^n} W\left[K_+(x,\lambda), e(x,\lambda)\right]\right\}_{\lambda=\lambda_p} = \left\{\frac{d^n}{d\lambda^n} D_+(\lambda)\right\}_{\lambda=\lambda_p} = 0 \tag{3.1}$$

for $n = 0, 1, ..., m_p - 1, \;\; p = 1, 2, ..., j$, and

$$\left\{\frac{d^n}{d\lambda^n} W\left[K_-(x,\lambda), e(x,-\lambda)\right]\right\}_{\lambda=\lambda_p} = \left\{\frac{d^n}{d\lambda^n} D_-(\lambda)\right\}_{\lambda=\lambda_p} = 0 \tag{3.2}$$

for $n = 0, 1, ..., m_p - 1, \;\; p = j+1, ..., k$.

Theorem 3 *The fallowing formulae*

$$\left\{\frac{\partial^n}{\partial\lambda^n} K_+(x,\lambda)\right\}_{\lambda=\lambda_p} = \sum_{m=0}^{n} A_m(\lambda_p) \left\{\frac{\partial^m}{\partial\lambda^m} e(x,\lambda)\right\}_{\lambda=\lambda_p} \tag{3.3}$$

$n = 0, 1, ..., m_p - 1, \;\; p = 1, 2, ..., j,$ *where*

$$A_m(\lambda_p) = \begin{pmatrix} n \\ m \end{pmatrix} \left\{\frac{\partial^{n-m}}{\partial\lambda^{n-m}} \hat{D}_+(\lambda)\right\}_{\lambda=\lambda_p}$$

and

$$\left\{\frac{\partial^n}{\partial\lambda^n} K_-(x,\lambda)\right\}_{\lambda=\lambda_p} = \sum_{m=0}^{n} B_m(\lambda_p) \left\{\frac{\partial^m}{\partial\lambda^m} e(x,-\lambda)\right\}_{\lambda=\lambda_p} \tag{3.4}$$

$n = 0, 1, ..., m_p - 1, \;\; p = j+1, ..., k$, where

$$B_m(\lambda_p) = \begin{pmatrix} n \\ m \end{pmatrix} \left\{\frac{\partial^{n-m}}{\partial\lambda^{n-m}} \hat{D}_-(\lambda)\right\}_{\lambda=\lambda_p}.$$

holds.

Proof. We will prove only (3.3) using the mathematical induction, because the case of (3.4) is similar. Let $n = 0$. From (3.1) we get

$$K_+(x,\lambda_p) = a_0(\lambda_p).e(x,\lambda_p)$$

where $a_0(\lambda_p) \neq 0$. Suppose that for $1 \leq n_0 \leq m_p - 2$, (3.3) holds; that is,

$$\left\{\frac{\partial^{n_0}}{\partial\lambda^{n_0}} K_+(x,\lambda)\right\}_{\lambda=\lambda_p} = \sum_{m=0}^{n_0} A_m(\lambda_p) \left\{\frac{\partial^m}{\partial\lambda^m} e(x,\lambda)\right\}_{\lambda=\lambda_p} \tag{3.5}$$

Now we will prove that (3.3) holds for $n_0 + 1$. If $y(x,\lambda)$ is a solution of (1.1), then $\frac{\partial^n}{\partial\lambda^n} y(x,\lambda)$ satisfies

$$\left[-\frac{d^2}{dx^2} + q(x) - \lambda^2\right] \frac{\partial^n}{\partial\lambda^n} y(x,\lambda) = 2\lambda n \frac{\partial^{n-1}}{\partial\lambda^{n-1}} y(x,\lambda) + n(n-1) \frac{\partial^{n-2}}{\partial\lambda^{n-2}} y(x,\lambda). \tag{3.6}$$

Writing (3.6) for $K_+(x,\lambda)$ and $e(x,\lambda)$, and using (3.5), we find

$$\left[-\frac{d^2}{dx^2}+q(x)-\lambda^2\right]g_{n_0+1}(x,\lambda_p)=0$$

where

$$g_{n_0+1}(x,\lambda_p)=\left\{\frac{\partial^{n_0+1}}{\partial\lambda^{n_0+1}}K_+(x,\lambda)\right\}_{\lambda=\lambda_p}-\sum_{m=0}^{n_0+1}A_m(\lambda_p)\left\{\frac{\partial^m}{\partial\lambda^m}e(x,\lambda)\right\}_{\lambda=\lambda_p}.$$

From (3.1) we have

$$W\left[g_{n_0+1}(x,\lambda_p),e(x,\lambda_p)\right]=\left\{\frac{d^{n_0+1}}{d\lambda^{n_0+1}}W\left[K_+(x,\lambda),e(x,\lambda)\right]\right\}_{\lambda=\lambda_p}=0.$$

Hence there exists a constant $a_{n_0+1}(\lambda_p)$ such that

$$g_{n_0+1}(x,\lambda_p)=a_{n_0+1}(\lambda_p)e(x,\lambda_p).$$

This shows that (3.3) holds for $n=n_0+1$. ■

Definition 4 *Let $\lambda=\lambda_0$ be an eigenvalue of L . If the functions*

$$y_0(x,\lambda_0),y_1(x,\lambda_0),...,y_s(x,\lambda_0)$$

satisfy the equations

$$l(y_0)-\lambda_0 y_0=0,\quad l(y_j)-\lambda_0 y_j-y_{j-1}=0,\quad j=1,2,...,s,$$

then the function $y_0(x,\lambda_0)$ is called the eigenfunction corresponding to the eigenvalue $\lambda=\lambda_0$ of L. The functions $y_1(x,\lambda_0),...,y_s(x,\lambda_0)$ are called the associated functions corresponding $\lambda=\lambda_0$. The eigenfunctions and the associated functions corresponding to $\lambda=\lambda_0$ are called the principal functions of the eigenvalue $\lambda=\lambda_0$.

The principal functions of the spectral singularities of L are defined similarly.

Now using (3.3) and (3.4) define the functions

$$U_{n,p}(x)=\left\{\frac{\partial^n}{\partial\lambda^n}K_+(x,\lambda)\right\}_{\lambda=\lambda_p}=\sum_{m=0}^{n}A_m(\lambda_p)\left\{\frac{\partial^m}{\partial\lambda^m}e(x,\lambda)\right\}_{\lambda=\lambda_p} \tag{3.7}$$

$n=0,1,...,m_p-1,..p=1,2,...,j$

and

$$U_{n,p}(x)=\left\{\frac{\partial^n}{\partial\lambda^n}K_-(x,\lambda)\right\}_{\lambda=\lambda_p}=\sum_{m=0}^{n}B_m(\lambda_p)\left\{\frac{\partial^m}{\partial\lambda^m}e(x,-\lambda)\right\}_{\lambda=\lambda_p} \tag{3.8}$$

$n=0,1,...,m_p-1,\;\; p=j+1,...,k.$

Then for $\lambda=\lambda_p$, $p=1,2,...,j,j+1,...,k,$

$$l(U_{0,p})=0,$$

$$l(U_{1,p})+\frac{1}{1!}\frac{\partial}{\partial\lambda}l(U_{0,p})=0, \tag{3.9}$$

$$l(U_{n,p})+\frac{1}{1!}\frac{\partial}{\partial\lambda}l(U_{n-1,p})+\frac{1}{2!}\frac{\partial^2}{\partial\lambda^2}l(U_{n-2,p})=0,$$

$n=2,3,...,m_p-1,$

hold, where $l(u) = -u'' + q(x)u - \lambda^2 u$ and $\frac{\partial^m}{\partial\lambda^m} l(u)$ denotes the differential expressions whose coefficients are the m-th derivatives with respect to λ of the corresponding coefficients of the differential expression $l(u)$. (4.9) shows that $U_{0,p}$ is the eigenfunction corresponding to the eigenvalue $\lambda = \lambda_p$; $U_{1,p}, U_{2,p}, ..., U_{m_p-1,p}$ are the associated functions of $U_{0,p}$ ([16, 17]).

$U_{0,p}, U_{1,p}, ..., U_{m_p-1,p}$, $p = 1, 2, ..., j, j+1, ..., k$ are called the principal functions corresponding to the eigenvalue $\lambda = \lambda_p$, $p = 1, 2, ..., j, j+1, ..., k$ of L.

Let $\mu_1, ..., \mu_v$, and $\mu_{v+1}, ..., \mu_l$ be the zeros of D_+ and D_- in $\mathbb{R}^* = \mathbb{R} \setminus \{0\}$ (which are the spectral singularities of L) with multiplicities $n_1, ..., n_v$ and $n_{v+1}, ..., n_l$, respectively.

We can show

$$\left\{\frac{\partial^n}{\partial\lambda^n} K(x,\lambda)\right\}_{\lambda=\mu_p} = \sum_{m=0}^{n} C_m(\mu_p) \left\{\frac{\partial^m}{\partial\lambda^m} e(x,\lambda)\right\}_{\lambda=\mu_p}, \tag{3.10}$$

$n = 0, 1, ..., n_p - 1,\ \ p = 1, 2, ..., v,$

where

$$C_m(\mu_p) = -\begin{pmatrix} n \\ m \end{pmatrix} \left\{\frac{\partial^{n-m}}{\partial\lambda^{n-m}} D_-(\lambda)\right\}_{\lambda=\mu_p}$$

and

$$\left\{\frac{\partial^n}{\partial\lambda^n} K(x,\lambda)\right\}_{\lambda=\mu_p} = \sum_{m=0}^{n} R_m(\mu_p) \left\{\frac{\partial^m}{\partial\lambda^m} e(x,-\lambda)\right\}_{\lambda=\mu_p} \tag{3.11}$$

$n = 0, 1, ..., n_p - 1,\ \ p = v+1, ..., l,$

where

$$R_m(\mu_p) = \begin{pmatrix} n \\ m \end{pmatrix} \left\{\frac{\partial^{n-m}}{\partial\lambda^{n-m}} D_+(\lambda)\right\}_{\lambda=\mu_p}.$$

Now define the generalized eigenfunctions and generalized associated functions corresponding to the spectral singularities of L by the following:

$$\upsilon_{n,p}(x) = \left\{\frac{\partial^n}{\partial\lambda^n} K(x,\lambda)\right\}_{\lambda=\mu_p} = \sum_{m=0}^{n} C_m(\mu_p) \left\{\frac{\partial^m}{\partial\lambda^m} e(x,\lambda)\right\}_{\lambda=\mu_p} \tag{3.12}$$

$n = 0, 1, ..., n_p - 1,\ \ p = 1, 2, ..., v,$

$$\upsilon_{n,p}(x) = \left\{\frac{\partial^n}{\partial\lambda^n} K(x,\lambda)\right\}_{\lambda=\mu_p} = \sum_{m=0}^{n} R_m(\mu_p) \left\{\frac{\partial^m}{\partial\lambda^m} e(x,-\lambda)\right\}_{\lambda=\mu_p} \tag{3.13}$$

$n = 0, 1, ..., n_p - 1,\ \ p = v+1, ..., l.$

Then $\upsilon_{n,p}$, $n = 0, 1, ..., n_p - 1$, $p = 1, 2, ..., v, v+1, ..., l$, also satisfy the equations analogous to (3.9).

$\upsilon_{0,p}, \upsilon_{1,p}, ..., \upsilon_{n_p-1,p}$, $p = 1, 2, ..., v, v+1, ..., l$ are called the principal functions corresponding to the spectral singularities $\lambda = \mu_p$, $p = 1, 2, ..., v, v+1, ..., l$ of L.

References

[1] M. A. Naimark, Investigation of the spectrum and the expansion in eigenfunctions of a non-selfadjoint differential operator of the second order on a semi-axis, American Mathematical Sociiety Translations, vol. 16, pp. 103-193, 1960.

[2] P. A. Binding, P. J. Browne and B. A. Watson, Trasformations between Sturm-Liouville problems with eigenvalue dependent and independent boundary conditions, The Bulletin of the London Mathematical Society, vol. 33, no.6, pp. 749-757, 2001.

[3] P. A. Binding, P. J. Browne and B. A. Watson, Sturm-Liouville Problems with boundary conditions rationally dependent on the eigenparameter I, Proceedings of the Edinburgh Mathematical Society, vol. 45, pp. 631–645, 2002.

[4] P. A. Binding, P. J. Browne and B. A. Watson, Sturm-Liouville Problems with boundary conditions rationally dependent on the eigenparameter II, Journal of Computational and Applied Mathematics

Vol. 148, Issue 1, pp. 147-168, 2002.

[5] E. Bairamov and N. Yokus, Spectral singularities of Sturm-Liouville problems with eigenvalue-dependent boundary conditions, Abstract and Applied Analysis, Art. ID 289596, 8, 2009.

[6] N. Yokus, N. Coskun, The spectrum of quadratic eigenparameter-dependent non-selfadjoint matrix Sturm-Liouville operators, Advances in differential equations and control processes,volume 19, no:2, pp. 139-152, 2018.

[7] J. Schwartz, Some non-selfadjoint operators,Comm. Pure Appl. Math. 13, 609-639, 1960.

[8] V. E. Lyance, A differential operator with spectral singularities I, American Mathematical Society Transactions Series 2, vol. 60, pp.185-225, 1967.

[9] N. Yokus, Principal functions of non-selfadjoint Sturm-Liouville problems with eigenvalue-dependent boundary conditions, Abstract and Applied Analysis, doi: 10.1155/2011/358912

[10] E. Bairamov, O. Cakar and A. M. Krall, An eigenfunction expansion for a quadratic pencil of a Schrödinger operator with spectral singularities, Journal of Differential Equations, vol. 151, no. 2, pp.268-289, 1999.

[11] E. Bairamov, Ö. Çakar, A. M. Krall, Non-selfadjoint difference operators and Jacobi matrices with spectral singularities, Math. Nachr. 229 (2001), 5-14.

[12] E. Bairamov, Ö. Çakar, A..M.Krall, Spectral properties including spectral singularities of a quadratic pencil of a Schrödinger operators on the whole real axis, Quaest. Math. 26 (2003), 15-31.

[13] E. Bairamov, Ö. Çakar, and A.O.Çelebi, Quadratic pencil of Schrödinger operators with spectral singularities:Discret spectrum and principal functions, *J.Math.Anal.Appl 216* (1997), 303-320.

[14] V. A. Marchenko, Sturm-Liouville Operators and Applications, vol. 22, Operator Theory: Advances and Application, Birkhauser, Basel, Switzerland, 1968.

[15] N. Yokus, N. Coskun, Spectral analysis of quantum Dirac systems, Journal of nonlinear sciences and applications, vol. 10, pp. 4524-4531, 2018.

[16] M. V. Keldysh, On the completeness of the eigenfunctions of some classes of non-selfadjoint linear operators, Soviet Mathematics Doklady, vol. 77, no. 4, pp 11-14, 1951.

[17] M. V. Keldysh, On the completeness of the eigenfunctions of some classes of non-selfadjoint linear operators, Russian Mathematical Surveys, vol. 26, no. 4, pp 15-41, 1971.

Prediction Of Copper Losses To Slag By Applying Artificial Neural Network

Mehmet Ali TOPÇU *
Department of Metallurgy and Material Engineering,
Karamanoglu Mehmetbey University,
Karaman/TURKEY

Aydın RUŞEN
Department of Metallurgy and Material Engineering,
Karamanoglu Mehmetbey University,
Karaman/TURKEY

Sadık Alper YILDIZEL
Department of Civil Engineering,
Karamanoglu Mehmetbey University,
Karaman/TURKEY

Abstract

Copper losses to slag are a major problem in pyrometallurgical copper production. Since dumping or disposal of such vast quantities of slag cause environmental problems, many attempts have been performed by several types of research to investigate the potential treatment of copper slag to decrease the metal losses. One of the current topics is to use colemanite ($Ca_2B_6O_{11}.5H_2O$) addition to the production process to reduce copper losses to slag. Although positive results are obtained after experimental works, there are shortcomings in process optimization and prediction for copper losses due to limited experimental data. For this reason, in the present study, Gradient Descent method based on artificial neural network (ANN) was carried out for estimating copper losses to slag by analyzing the effects of input parameters colemanite addition (0%, %2, %4) and temperature (1200, 1250, 1300 C). The results showed that the suggested method is quite useful to estimate copper losses to slag by the proposed mathematical expression.

Keywords: Gradient descent, Artificial neural network, Copper losses.

1 Introduction

Pyrometallurgical copper production including concentration, smelting, converting and refining stages is widely used to produce metallic copper from sulfides ores. Converting of matte (50-70% Cu) which is obtained after smelting stage forms blister copper (> 98% Cu) and slag (oxidized materials) with the addition of silica flux. Despite the development of many copper making techniques, copper losses to slag always occur during the converting stage depending on several factors such as slag viscosity, density and its melting point [1-2]. Depending on these factors, mechanical and physicochemical losses are two different ways for copper losses to slag. It is well known that obtaining the slag with low copper content could be achieved by reducing slag viscosity by addition fluxing agents. Previous studies [3-4] performed in

*Corresponding author. *E-mail address:* topcumali@kmu.edu.tr

different metal industries on colemanite ($Ca_2B_6O_{11}.5H_2O$) usage as flux showed that the use of colemanite decreases the viscosity and the melting temperature of the slag.
Early determination of copper losses amount to slag is an essential issue to increase the production efficiency in the copper industry. Therefore, data-based artificial neural networks models and gradient descent systems are widely used in many engineering applications to estimate production process [5]. Detailed and accurate estimations for an understanding of manufacturing process can be obtained by applying these models [6].
In this study, an ANN model is proposed to estimate copper losses, and a mathematical expression was created for copper losses to the slag by taking advantage of predictive and modeling characteristics of artificial neural networks.

2 Material and Methods

2.1 Material

In this study, the slag which is a by-product of the converting stage in copper production was used as a starting material. Sample provided from Eti Bakır Inc. contains a remarkable amount of copper (4.45% wt.). In addition to the chemical analysis, according to the mineralogical analysis, the major components were obtained as fayalite and magnetite. Colemanite which was used as flux was supplied from Eti Maden, commercially.

2.2 Artificial Neural Network Development

In this study, the Quasi-Newton algorithm was used to estimate the copper loss to slag. This method is often used because it does not require the calculation of the second derivatives. The computation was based on the inverse Hessian at each iteration of the algorithm with the only usage of gradient information. All estimation studies have been proposed with Neural Designer software. The training algorithm is shown in Table 1.

Table 1: Training Algorithm

Description	Value
Training rate method	Brent Method
Training rate tolerance	0.0005
Min. parameters increment form	1e-009
Min. loss increase	1e-012
Gradient norm goal	0.001
Max. iterations number	1000
Maximum time	Maximum training time

The ANN model was proposed with two inputs for estimation of copper losses to slag, and it was presented in Figure 1. Temperature and colemanite addition was taken as input parameters based on the experimental studies. A graphical representation of the network architecture is depicted next. It contains a scaling layer, a neural network, and an unscaling layer. The yellow circles represent scaling neurons, and the purple circles are bounding neurons. The architecture of this neural network can be written as 3:2:1.

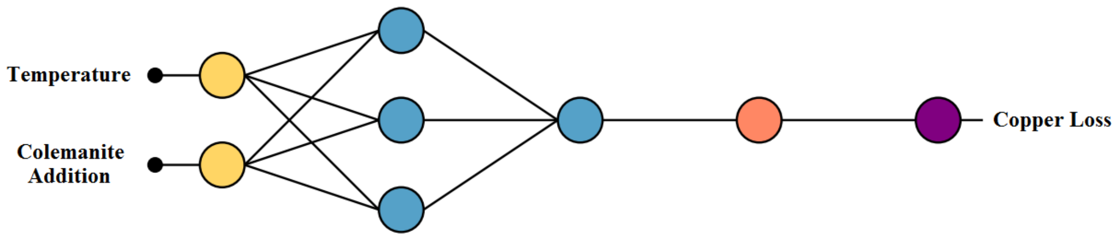

Figure 1: The proposed ANN model

3 Results and Discussions

A standard method to test the loss of a model is to perform a linear regression analysis between the scaled neural network outputs and the corresponding targets for an independent testing subset. This analysis leads to 3 parameters for each output variable. The first two parameters correspond to the y-intercept and slope of the best linear regression relating scaled outputs and targets. The third parameter, R2, is the correlation coefficient between the scaled outputs and targets. If we had a perfect fit (outputs precisely equal to targets), the slope would be 1, and the y-intercept would be 0. If the correlation coefficient is equal to 1, then there is a perfect correlation between the outputs from the neural network and the targets in the testing subset. The linear regression results are shown in Figure 2. Note that some scaled outputs fall outside the range defined by the scale targets, and therefore they are not plotted.

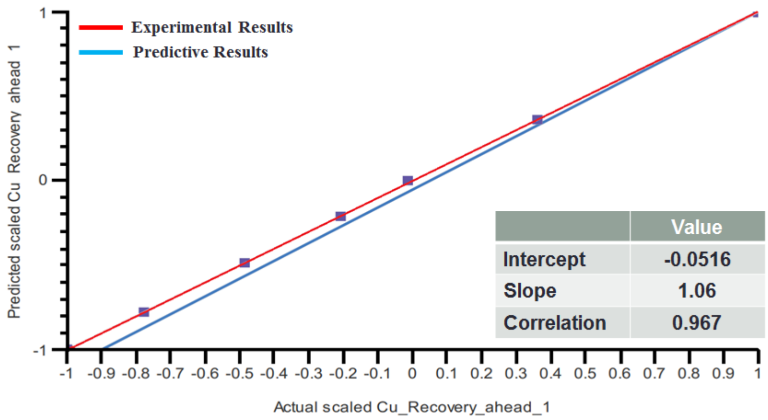

Figure 2: Linear regression chart and parameters

Predictive model takes the form of a function of the outputs with respect to the inputs. The mathematical expression represented by the model can be used to embed it into other software. Figure 3 shows the mathematical expression of copper losses to slag depending on the temperature and colemanite addition.

```
scaled_Temperature_ahead_1 = 2* (Temperature_ahead_1 - 1200) / (1300 - 1200) - 1;
scaled_Colemanite_ahead_1 = Colemanite_ahead_1/1.66905;
y_1_1 = tanh (0.967247 + 0.584224*scaled_Temperature_ahead_1 - 0.686618*scaled_Colemanite_ahead_1);
y_1_2 = tanh (0.787464 + 3.04085*scaled_Temperature_ahead_1 - 1.08412*scaled_Colemanite_ahead_1);
y_1_3 = tanh (- 0.483814 - 0.300506*scaled_Temperature_ahead_1 + 0.275954*scaled_Colemanite_ahead_1);
scaled_Cu_Recovery_ahead_1 = (-0.171102 - 0.997976*y_1_1 + 1.33138*y_1_2 + 0.37394*y_1_3);
(Cu_Recovery_ahead_1) = (0.5 * (scaled_Cu_Recovery_ahead_1 + 1.0) * (15.6 - 1.2) + 1.2);
Cu_Recovery_ahead_1 = max(1.2, Cu_Recovery_ahead_1);
Cu_Recovery_ahead_1 = min(15.6, Cu_Recovery_ahead_1);
```

Figure 3: Mathematical Expression of Copper Losses to Slag

This mathematical expression can be applied to estimate the intermediate values for temperature (between 1200 and 1300 ^{o}C) and colemanite addition (from 0 to 4%) in terms of copper losses to slag. When applied to all experimentally obtained values, this mathematical equation was well-matched for all of them. For example, when compared to experimental results with mathematical calculations at 1250 ^{o}C, minimum copper losses to slag value could be determined as 0.86 % with 2.47% colemanite addition to the system (Figure 4).

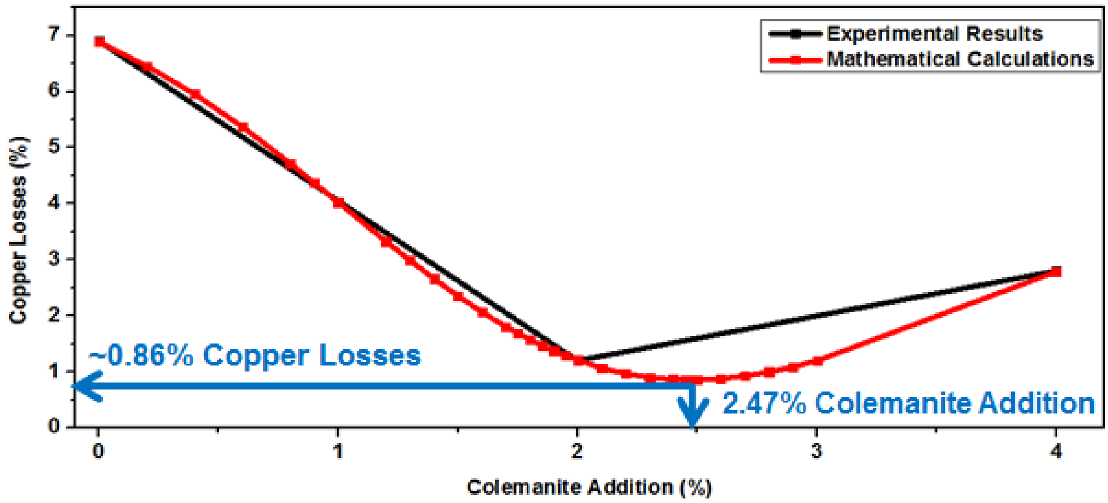

Figure 4: Comparison of experimental results and mathematical calculations at 1250 ^{o}C.

As seen from Figure 4, experimental results are in good agreement with mathematical calculations for initial region (up to 2% colemanite addition), but after this point, according to the mathematical expression, copper losses value should be lowered, which expected due to the positive effect of colemanite addition on slag viscosity.

4 Conclusions

In this study, it was aimed to estimate copper losses to slag after colemanite addition by applying artificial neural network. For this purpose, the artificial neural network-based system was developed using a gradient descent algorithm. According to the results, the ANN model approves the strong correlation between the inputs parameters temperature and colemanite addition, and parameter copper losses. The outcomes of the study can be assessed by other artificial and mathematical systems for a better understanding of inputs effects on copper losses amount. Furthermore, ANN models showed good fitting performance, and this model can be applied to the copper loss estimation studies.

Acknowledge

This work was supported by Karamanoglu Mehmetbey University Scientific Research Council (BAP) with project no KMU-BAP-28-M-16.

References

[1] C. Shi, C. Meyer, A. Behnood, Utilization of copper slag in cement and concrete. Resources, Conservation and Recycling, 52(10) (2008) 1115-1120.

[2] M. E. Schlesinger, M. J. King, K. C. Sole, W. G. Davenport, Extractive metallurgy of copper. (2011) Elsevier.

[3] M. Timucin, N. Sevinc, Y. A. Topkaya, H. Eric, Use of Colemanite in the Production of Iron and Steel, (1986).

[4] A. Rüşen, A. Geveci, Y. A. Topkaya, Minimization of copper losses to slag in matte smelting by colemanite addition. Solid State Sciences, 14(11-12) (2012) 1702-1704.

[5] H. Xing, Z. Liu, Y. Zhang, H. Zhang, W. Zhang, T. Li, the Optimized design on technological parameters of the process of granulating blast furnace slags into beads. Boletin Tecnico/Technical Bulletin, 55(5), (2017) 224-232.

[6] F. Khademi, S. M. Jamal, N. Deshpande, S. Londhe, Predicting strength of recycled aggregate concrete using the artificial neural network, adaptive neuro-fuzzy inference system, and multiple linear regression. International Journal of Sustainable Built Environment 5(2) (2016) 355-369.

On Some Sequences of the Positive Linear Operators Based on (p,q)-Calculus

Ersin ŞİMŞEK*
Mersin University,
Department of Mathematics,
Mersin, TURKEY

Tuncay TUNÇ
Mersin University,
Department of Mathematics,
Mersin, TURKEY

Abstract

In this paper, we propose a method based on generating functions for constructing (p,q)-analogues of some discrete type positive linear operators (e.g., (p,q)-Lupas, (p,q)-Meyer-König and Zeller and (p,q)-Bleimann-Butzer-Hahn operators etc.). In other words, general operators of the discrete type are constructed, and their respective formulae for central moments are thereby obtained. Finally, through the use of specific generating functions, we are able to provide some relevant exemplary applications of general operators.
Keywords:(p,q)*-Calculus, Generating functions, Positive linear operators, Rate of convergence.*

1 Introduction

First, let us provide some background information regarding what we know about q-calculus formulae, the study of which was initiated by Euler in the eighteenth century. Following this, many remarkable results in the field were obtained in the nineteenth century. In 1908, F. H. Jackson (Jackson, 1909) introduced q-functions. He was also the first to develop q-calculus in a systematic way. In the field of approximation theory, the applications of q-calculus are new area in last 30 years. The first q-analogue of the well-known Bernstein polynomials was introduced by A. Lupaş (Lupaş, 1987) in the year 1987. In 1997, G. M. Phillips (Phillips, 2000) considered another q-analogue of the classical Bernstein polynomials. Later several other researchers have proposed the q-analogue of the well-known discrete-type operators which includes Baskakov operators, Szasz–Mirakyan operators, Meyer-Konig-Zeller operators, Bleiman, Butzer and Hahn operators etc. See (Agratini and Nowak, 2011)-(Şimşek and Tunç, 2018). Recently, Mursaleen et al. introduced (p,q)-calculus in approximation theory and constructed the (p,q)-analogue of Bernstein operators (see (Mursaleen, Ansari and Khan, 2015)) and (p,q)-analogue of Bernstein-Schurer operators (see (Mursaleen, Nasiruzzaman and Nurgali, 2015)). Most recently, the (p,q)-analogue of some more operators has been studied in (Mursaleen, et al. 2015, 2016), (Acar, Aral and Mohiuddine, 2016, 2018), (Cai and Zhou, 2016), (Sharma, 2016), (Khan, and Lobiyal, 2017), (Kanat and Sofyalıoğlu, 2018) and (Kadak, Khan and Mursaleen, 2016). Below, we present the outlines of (p,q)-integers, (p,q)-factorials, (p,q)-binomial coefficients, and (p,q)-differentiations.

The required theorems and definitions in (p,q)-Calculus are as outlined below, where $0<q<p<1$. For $n\in\mathbb{N}$, the (p,q)-analogue of the integer n, called (p,q)-integer, is defined

*Corresponding author. *E-mail address:* simsek.ersin@gmail.com

by

$$[n]_{p,q} := \frac{p^n - q^n}{p-q}, \qquad p \neq 1; \qquad [n]_{1,q} := [n]_q.$$

Also $[0]_{p,q} := 0$. Similarly, the (p,q)-analogue of the factorial of n is defined by

$$[n]_{p,q}! := [n]_{p,q}[n-1]_{p,q} \cdots [1]_{p,q}, \qquad n = 1,2,3,\cdots; \qquad [0]_{p,q}! := 1$$

Now, let us obtain the (p,q)-analogue of the Gauss binomial formula. The (p,q)-analogues of $(a+b)^n$ are given by

$$(a \oplus b)^n_{p,q} := \prod_{s=0}^{n-1} (p^s a + q^s b); \qquad (a \oplus b)^0_{p,q} := 1.$$

By simple calculations, it follows that

$$(a \oplus b)^n_{p,q} := \sum_{k=0}^{n} \begin{bmatrix} n \\ k \end{bmatrix}_{p,q} p^{(n-k)(n-k-1)/2} q^{k(k-1)/2} b^k a^{n-k},$$

where

$$\begin{bmatrix} n \\ k \end{bmatrix}_{p,q} := \frac{[n]_{p,q}!}{[k]_{p,q}![n-k]_{p,q}!}, \qquad 0 \leq k \leq n$$

is the (p,q)-binomial formula. All the concepts defined above, become their q-analogues if p tends to 1.

The (p,q)-derivative of a function f, denoted by $D_{p,q}f$ is given by

$$(D_{p,q}f)(x) = \frac{f(px) - f(qx)}{(p-q)x}, \qquad x \neq 0$$

and $(D_{p,q}f)(0) = f'(0)$ provided $f'(0)$ exists.

Let us define the (p,q)-partial derivatives of a function $f(x,y)$ of two variables. The (p,q)-partial derivative of $f(x,y)$ with respect to x is defined by

$$\frac{\partial_{p,q} f(x,y)}{\partial_{p,q} x} = \frac{f(px,y) - f(qx,y)}{(p-q)x}, \qquad x \neq 0.$$

Likewise, the (p,q)-partial derivative of $f(x;y)$ with respect to y can be defined.

In this study, we propose a method based on generating functions for constructing (p,q)-analogues of some discrete type positive linear operators (e.g., (p,q)-Lupas, (p,q)-Meyer-König and Zeller and (p,q)-Bleimann-Butzer-Hahn operators etc.). In other words, general operators of the discrete type are constructed, and their respective formulae for central moments are thereby obtained. Finally, through the use of specific generating functions, we are able to provide some relevant exemplary applications of general operators.

2 Construction of Generating Operators

In order to construct the sequence of positive linear operators with the aid of sequences of functions, we state the following:
Let $0 < q < p \leq 1$. and $I \subset [0,\infty)$ be an interval. We assume that in the sequence

$$\left\{\varphi_{n,p,q}(x,u)\right\}_{n=1}^{\infty}$$

of real functions on $I \times [0,\infty)$, each function has the following conditions:

(i) $\varphi_{n,p,q}(x,0) \neq 0$ and $\varphi_{n,p,q}(x,1) = 1$ for every $n \in \mathbb{N}$ and $x \in I$.

(ii) $\left.\frac{\partial^k_{p,q}\varphi_{n,p,q}(x,u)}{\partial_{p,q}u^k}\right|_{u=0}$ exist and are continuous functions of x for all $k \in \mathbb{N}_0$ and $n \in \mathbb{N}$.

(iii) For all $k \in \mathbb{N}_0$, $x, u \geq 0$,

$$\frac{\partial^k_{p,q}\varphi_{n,p,q}(x,u)}{\partial_{p,q}u^k} \geq 0, \qquad n \in \mathbb{N}.$$

The sequence $\{\varphi_{n,p,q}(x,u)\}$ generates a sequence of discrete type positive linear operators in the following way.

Expanding the function $\varphi_{n,p,q}(x,u)$ with $u \in [0,\infty)$, by using (p,q)-Taylor formula (see (Njionou Sadjang, 2018)), we obtain

$$\varphi_{n,p,q}(x,u) = \sum_{k=0}^{\infty} \frac{1}{[k]_{p,q}!} \left.\frac{\partial^k_{p,q}\varphi_{n,p,q}(x,u)}{\partial_{p,q}u^k}\right|_{u=0} u^k \tag{1}$$

and taking $u = 1$, we have by (i)

$$\sum_{k=0}^{\infty} \frac{1}{[k]_{p,q}!} \left.\frac{\partial^k_{p,q}\varphi_{n,p,q}(x,u)}{\partial_{p,q}u^k}\right|_{u=0} = 1. \tag{2}$$

Using the sequence $\{\varphi_{n,p,q}(x,u)\}$, we introduce the announced operators as follows:

$$L_{n,p,q}(f;x) = \sum_{k=0}^{\infty} \frac{1}{[k]_{p,q}!} \left.\frac{\partial^k_{p,q}\varphi_{n,p,q}(x,u)}{\partial_{p,q}u^k}\right|_{u=0} f\left(\frac{[k]_{p,q}}{\alpha_{n,k,p,q}}\right) \tag{3}$$

where $\alpha_{n,k,p,q}$ are positive numbers. It is clear that the operators are linear and positive in view of (iii) on the space of bounded functions on I shown by $B(I)$. Also $\|L_{n,p,q}\| = 1$ by virtue of (2).

Lemma 1 *If the sequence $\{\varphi_{n,p,q}(x,u)\}$ has the conditions (i)-(iii), then, for all $m \in \mathbb{N}_0$*

$$\frac{\partial^m_{p,q}\varphi_{n,p,q}(x,u)}{\partial_{p,q}u^m} = \sum_{k=m}^{\infty} \frac{[k]_{p,q,m}}{[k]_{p,q}!} \left.\frac{\partial^k_{p,q}\varphi_{n,p,q}(x,u)}{\partial_{p,q}u^k}\right|_{u=0} u^{k-m} \tag{4}$$

where $[k]_{p,q,m} = [k]_{p,q}[k-1]_{p,q}[k-2]_{p,q}\cdots[k-m+1]_{p,q}$.

Proof. The proof is by induction on m. For $m = 0$ the assertion is trivial. For $m = 1$ we have,

$$\begin{aligned}
\frac{\partial_{p,q}\varphi_{n,p,q}(x,u)}{\partial_{p,q}u} &= \frac{\varphi_{n,q}(x,pu) - \varphi_{n,q}(x,qu)}{(p-q)u} \\
&= \sum_{k=1}^{\infty} \frac{1}{[k]_{p,q}!} \left.\frac{\partial^k_{p,q}\varphi_{n,p,q}(x,u)}{\partial_{p,q}u^k}\right|_{u=0} \left(\frac{p^k - q^k}{p-q}\right) u^{k-1} \\
&= \sum_{k=1}^{\infty} \frac{1}{[k]_{p,q}!} \left.\frac{\partial^k_{p,q}\varphi_{n,p,q}(x,u)}{\partial_{p,q}u^k}\right|_{u=0} [k]_{p,q}u^{k-1}.
\end{aligned}$$

For $m+1$, by assumption we obtain,

$$\begin{aligned}
\frac{\partial^{m+1}_{p,q}\varphi_{n,p,q}(x,u)}{\partial_{p,q}u^{m+1}} &= \frac{\partial_{p,q}}{\partial_{p,q}u}\left(\sum_{k=m}^{\infty} \frac{[k]_{p,q,m}}{[k]_{p,q}!} \left.\frac{\partial^k_{p,q}\varphi_{n,p,q}(x,u)}{\partial_{p,q}u^k}\right|_{u=0} u^{k-m}\right) \\
&= \sum_{k=m+1}^{\infty} \frac{[k]_{p,q,m+1}}{[k]_{p,q}!} \left.\frac{\partial^k_{p,q}\varphi_{n,q}(x,u)}{\partial_{p,q}u^k}\right|_{u=0} u^{k-m-1}.
\end{aligned}$$

■

Corollary 2 *a) Writing* $u=1$ *in (4) we have*

$$\left.\frac{\partial_{p,q}^m \varphi_{n,p,q}(x,u)}{\partial_{p,q}u^m}\right|_{u=1} = \sum_{k=m}^{\infty} \frac{[k]_{p,q,m}}{[k]_{p,q}!} \left.\frac{\partial_{p,q}^k \varphi_{n,p,q}(x,u)}{\partial_{p,q}u^k}\right|_{u=0};$$

b) Writing $u=p$ *in (4) we have*

$$\left.\frac{\partial_{p,q}^m \varphi_{n,p,q}(x,u)}{\partial_{p,q}u^m}\right|_{u=p} = \sum_{k=m}^{\infty} \frac{[k]_{p,q,m}}{[k]_{p,q}!} \left.\frac{\partial_{p,q}^k \varphi_{n,p,q}(x,u)}{\partial_{p,q}u^k}\right|_{u=0} p^{k-m}.$$

The test functions $e_{r,i}$ are given by

$$e_{r,i}(t) = \left(\frac{t}{1+(1-i)t}\right)^r, \quad r \in \mathbb{N}_0,\ i=0,1,2. \tag{5}$$

The functions of $e_{r,0}$ for (p,q)-Butzer-Bleimann-Hahn operators are used, the functions $e_{r,1}$ are used as test functions for (p,q)-Bernstein, (p,q)-Szasz-Mirakyan, (p,q)-Lupas and (p,q)-Baskakov operators and the functions of $e_{r,2}$ for (p,q)-Meyer-König and Zeller.

In continuation of the relation for the numbers $\alpha_{n,k,p,q}$ indicated in (3), we assume the following:

$$e_{r,i}\left(\frac{[k]_{p,q}}{\alpha_{n,k,p,q}}\right) = \frac{[k]_{p,q}^r}{\alpha_{n,p,q}^r}, \qquad r \in \mathbb{N}_0, n,k \in \mathbb{N},$$

where $\alpha_{n,p,q}$ are positive numbers independent of k.

Theorem 3 *Let* $L_{n,p,q}(f;x)$ *be given by (3), then for any* $x \geq 0$ *and* $0<q<p\leq 1$*, we have the following identities*

$$L_{n,p,q}(e_{0,i};x) = 1;$$
$$L_{n,p,q}(e_{1,i};x) = \frac{1}{\alpha_{n,p,q}} \left.\frac{\partial_{p,q}\varphi_{n,p,q}(x,u)}{\partial_{p,q}u}\right|_{u=1};$$
$$L_{n,p,q}(e_{2,i};x) = \frac{1}{\alpha_{n,p,q}^2}\left\{ q\left.\frac{\partial_{p,q}^2\varphi_{n,p,q}(x,u)}{\partial_{p,q}u^2}\right|_{u=1} + \left.\frac{\partial_{p,q}\varphi_{n,p,q}(x,u)}{\partial_{p,q}u}\right|_{u=p}\right\}.$$

Proof. For $r=0$, $L_{n,p,q}(e_{0,i};x)=1$ is obvious.
Let $r>0$

$$\begin{aligned} L_{n,p,q}(e_{1,i};x) &= \sum_{k=0}^{\infty} \frac{1}{[k]_{p,q}!} \left.\frac{\partial_{p,q}^k\varphi_{n,p,q}(x,u)}{\partial_{p,q}u^k}\right|_{u=0} \frac{[k]_{p,q}}{\alpha_{n,p,q}} \\ &= \frac{1}{\alpha_{n,p,q}} \sum_{k=0}^{\infty} \frac{1}{[k]_{p,q}!} \left.\frac{\partial_{p,q}^k\varphi_{n,p,q}(x,u)}{\partial_{p,q}u^k}\right|_{u=0} [k]_{p,q} \\ &= \frac{1}{\alpha_{n,p,q}} \left.\frac{\partial_{p,q}\varphi_{n,p,q}(x,u)}{\partial_{p,q}u}\right|_{u=1}. \end{aligned}$$

We have

$$L_{n,p,q}(e_{2,i};x) = \sum_{k=0}^{\infty} \frac{1}{[k]_{p,q}!} \left.\frac{\partial_{p,q}^k\varphi_{n,p,q}(x,u)}{\partial_{p,q}u^k}\right|_{u=0} \frac{[k]_{p,q}^2}{\alpha^2{}_{n,p,q}}.$$

By simple calculation, we have

$$[k]_{p,q} = p^{k-1} + q[k-1]_{p,q}, \quad \text{and} \quad [k]_{p,q}^2 = q[k]_{p,q}[k-1]_{p,q} + p^{k-1}[k]_{p,q}.$$

$$\begin{aligned} L_{n,p,q}\left(e_{2,i};x\right) &= \frac{1}{\alpha^2{}_{n,p,q}}\sum_{k=0}^{\infty}\frac{1}{[k]_{p,q}!}\left.\frac{\partial_{p,q}^k\varphi_{n,p,q}\left(x,u\right)}{\partial_{p,q}u^k}\right|_{u=0}\left(q[k]_{p,q}[k-1]_{p,q}+p^{k-1}[k]_{p,q}\right) \\ &= \frac{q}{\alpha^2{}_{n,p,q}}\sum_{k=0}^{\infty}\frac{1}{[k]_{p,q}!}\left.\frac{\partial_{p,q}^k\varphi_{n,p,q}\left(x,u\right)}{\partial_{p,q}u^k}\right|_{u=0}[k]_{p,q}[k-1]_{p,q} \\ &+ \frac{1}{\alpha^2{}_{n,p,q}}\sum_{k=0}^{\infty}\frac{1}{[k]_{p,q}!}\left.\frac{\partial_{p,q}^k\varphi_{n,p,q}\left(x,u\right)}{\partial_{p,q}u^k}\right|_{u=0}p^{k-1}[k]_{p,q} \end{aligned}$$

from Corollary 2.2, we have

$$L_{n,p,q}\left(e_{2,i};x\right)=\frac{1}{\alpha_{n,p,q}^2}\left\{q\left.\frac{\partial_{p,q}^2\varphi_{n,p,q}\left(x,u\right)}{\partial_{p,q}u^2}\right|_{u=1}+\left.\frac{\partial_{p,q}\varphi_{n,p,q}\left(x,u\right)}{\partial_{p,q}u}\right|_{u=p}\right\}.$$

■

Example 4 ((p,q)-Bleimann-Butzer-Hahn Operators) *For $n\in\mathbb{N}$ and $0<q<p\leq 1$), we consider the function*

$$\varphi_{n,p,q}\left(x,u\right)=\frac{\left(1\oplus xu\right)_{p,q}^n}{\left(1\oplus x\right)_{p,q}^n},\qquad x\in[0,\infty). \tag{6}$$

It is easy to check that the sequence $\left\{\varphi_{n,p,q}\left(x,u\right)\right\}$ satisfies the condition (i) in section 2. By the definition of (p,q)-partial derivatives, we obtain

$$\frac{\partial_{p,q}\varphi_{n,p,q}\left(x,u\right)}{\partial_{p,q}u}=[n]_{p,q}x\frac{\prod\limits_{s=0}^{n-2}\left(p^s+q^sqxu\right)}{\left(1\oplus x\right)_{p,q}^n}=[n]_{p,q}x\frac{\left(1\oplus qxu\right)_{p,q}^{n-1}}{\left(1\oplus x\right)_{p,q}^n}.$$

By induction, we obtain that

$$\frac{\partial_{p,q}^k\varphi_{n,p,q}\left(x,u\right)}{\partial_{p,q}u^k}=[n]_{p,q,k}x^kq^{\frac{k(k-1)}{2}}\frac{\left(1\oplus q^kxu\right)_{p,q}^{n-k}}{\left(1\oplus x\right)_{p,q}^n},\qquad k\in\mathbb{N}.$$

where $[n]_{p,q,k}=[n]_{p,q}[n-1]_{p,q}[n-2]_{p,q}\cdots[n-k+1]_{p,q}$.

If we write $u=0$ in the last equality, then we get

$$\left.\frac{\partial_{p,q}^k\varphi_{n,p,q}\left(x,u\right)}{\partial_{p,q}u^k}\right|_{u=0}=\frac{1}{\left(1\oplus x\right)_{p,q}^n}[n]_{p,q,k}q^{\frac{k(k-1)}{2}}p^{\frac{(n-k-1)(n-k)}{2}}x^k. \tag{7}$$

Since the right hand side of (7) is a rational function of x which does not have any singular points in $[0,\infty)$, then the condition (ii) holds and since $(0<q<p\leq 1)$ and $x\in[0,\infty)$, then the condition (iii) is satisfied too, there by the functions $\varphi_{n,p,q}\left(x,u\right)$ defined by (6) generate some positive and linear operators.

By writing (7) and considering $\alpha_{n,k,p,q}=q^k[n-k+1]_{p,q}$ in the operators $L_{n,p,q}$ given by (3), we have

$$\begin{aligned} L_{n,p,q}\left(f;x\right) &= \sum_{k=0}^{\infty}\frac{1}{[k]_{p,q}!}\left.\frac{\partial_{p,q}^k\varphi_{n,p,q}\left(x,u\right)}{\partial_{p,q}u^k}\right|_{u=0}f\left(\frac{[k]_{p,q}}{\alpha_{n,k,p,q}}\right) \\ &= \frac{1}{\left(1\oplus x\right)_{p,q}^n}\sum_{k=0}^{\infty}\begin{bmatrix}n\\k\end{bmatrix}_{p,q}p^{\frac{(n-k-1)(n-k)}{2}}q^{\frac{k(k-1)}{2}}x^kf\left(\frac{[k]_{p,q}}{q^k[n-k+1]_{p,q}}\right) \end{aligned}$$

and since $\begin{bmatrix} n \\ k \end{bmatrix}_{p,q} := 0$ *for* $k > n$ *we obtain* (p,q)*-Bleimann-Butzer and Hahn operators* $H_{n,p,q}$*: For* $f \in B[0,\infty)$*,*

$$H_{n,p,q}(f;x) = \frac{1}{(1 \oplus x)^n_{p,q}} \sum_{k=0}^{n} \begin{bmatrix} n \\ k \end{bmatrix}_{p,q} p^{\frac{(n-k-1)(n-k)}{2}} q^{\frac{k(k-1)}{2}} x^k f\left(\frac{[k]_{p,q}}{q^k [n-k+1]_{p,q}}\right).$$

From Theorem 2.3, we have

$$H_{n,p,q}(e_{0,0};x) = 1,$$
$$H_{n,p,q}(e_{1,0};x) = \frac{[n]_{p,q}}{[n+1]_{p,q}} \frac{x}{1+x} \frac{(1 \oplus qx)^{n-1}_{p,q}}{(p \oplus qx)^{n-1}_{p,q}},$$
$$H_{n,p,q}(e_{2,0};x) = \frac{q^2 x^2 [n]_{p,q} [n-1]_{p,q}}{[n+1]^2_{p,q}} \frac{(1 \oplus xq^2)^{n-2}_{p,q}}{(1 \oplus x)^n_{p,q}} + \frac{x[n]_{p,q}}{[n+1]^2_{p,q}} \frac{(1 \oplus pqx)^{n-1}_{p,q}}{(1 \oplus x)^n_{p,q}}.$$

Example 5 (p,q)***-Lupas Operators***

Let $n \in \mathbb{N}$*. If we consider* $\alpha_{n,k,q} = [n]_{p,q}$ *and*

$$\varphi_{n,p,q}(x,u) := \frac{((1-x) \oplus xu)^n_{p,q}}{((1-x) \oplus x)^n_{p,q}}, \quad x \in [0,1]; \quad 0 < q; \quad 0 < p,$$

in the operators $L_{n,p,q}$ *as defined by (3), then* $L_{n,p,q}$ *become the* (p,q)*-Lupas operators* $A_{n,p,q}$ *as follows: For* $f \in B[0,1]$

$$A_{n,p,q}(f;x) = \frac{1}{((1-x) \oplus x)^n_{p,q}} \sum_{k=0}^{n} \begin{bmatrix} n \\ k \end{bmatrix}_{p,q} p^{\binom{n-k}{2}} q^{\binom{k}{2}} x^k (1-x)^{n-k} f\left(\frac{[k]_{p,q}}{[n]_{p,q}}\right)$$

From Theorem 2.3, we have

$$A_{n,p,q}(e_{0,1};x) = 1,$$
$$A_{n,p,q}(e_{1,1};x) = x \frac{((1-x) \oplus qx)^{n-1}_{p,q}}{((1-x) \oplus x)^{n-1}_{p,q}},$$
$$A_{n,p,q}(e_{2,1};x) = \frac{q^2 x^2 [n-1]_{p,q}}{[n]_{p,q}} \frac{((1-x) \oplus xq^2)^{n-2}_{p,q}}{((1-x) \oplus x)^n_{p,q}} + \frac{x}{[n]_{p,q}} \frac{((1-x) \oplus pqx)^{n-1}_{p,q}}{((1-x) \oplus x)^n_{p,q}}.$$

Example 6 (p,q)***-Meyer-König and Zeller Operators***

Let $n \in \mathbb{N}$*. If we consider* $\alpha_{n,k,p,q} = q^{-n}[k+n]_{p,q}$ *and*

$$\varphi_{n,p,q}(x,u) := \frac{(1 \ominus x)^{n+1}_{p,q}}{(1 \ominus xu)^{n+1}_{p,q}}, \quad x \in [0,1), \quad 0 < q < p \leq 1,$$

in the operators $L_{n,p,q}$ *as defined by (3), then* $L_{n,p,q}$ *become the* (p,q)*-Meyer-König and Zeller operators* $M_{n,p,q}$ *as follows: For* $f \in B[0,1)$

$$M_{n,p,q}(f;x) = \frac{(1 \ominus x)^{n+1}_{p,q}}{p^{\frac{n(n+1)}{n}}} \sum_{k=0}^{\infty} \begin{bmatrix} k+n \\ k \end{bmatrix}_{p,q} x^k p^{-kn} f\left(\frac{[k]_{p,q}}{q^{-n}[k+n]_{p,q}}\right).$$

From Theorem 2.3, we have

$$M_{n,p,q}(e_{0,2};x) = 1,$$
$$M_{n,p,q}(e_{1,2};x) = \frac{xp[n+1]_{p,q}}{[n]_{p,q}} \frac{(1 \ominus x)^{n+1}_{p,q}}{(1 \ominus px)^{n+2}_{p,q}},$$
$$M_{n,p,q}(e_{2,2};x) = \frac{p^3 q x^2 [n+1]_{p,q} [n+2]_{p,q}}{[n]^2_{p,q}} \frac{(1 \ominus x)^{n+1}_{p,q}}{(1 \ominus p^2 x)^{n+3}_{p,q}} + \frac{px[n+1]_{p,q}}{[n]^2_{p,q}} \frac{(1 \ominus x)^{n+1}_{p,q}}{(1 \ominus p^2 x)^{n+2}_{p,q}}.$$

References

[1] Jackson, F. (1909). On q-Functions and a certain Difference Operator. *Transactions of the Royal Society of Edinburgh*, 46(02), pp.253-281.

[2] Lupaş, A. (1987). A q-analogue of the Bernstein operator, *University of Cluj-Napoca Seminar on numerical and statistical calculus* , 9, pp.85–92.

[3] Phillips, G. (2000). A generalization of the Bernstein polynomials based on the q-integers. *Ann. Numer. Math. Journal*, 42(01), p.79.

[4] Agratini O. , Nowak, G. (2011). On a generalization of Bleimann, Butzer and Hahn operators based on q-integers. *Math. Comput. Model.*, 53(5–6), pp. 699–706.

[5] Aral, A. and Gupta, V. (2009). On q-Baskakov type operators. *Demonstratio Mathematica*, 42(1), pp.109–122.

[6] Aral, A., Agarwal, R. and Gupta, V. (2013). *Applications of q-calculus in operator theory.* New York, Springer.

[7] Altın, A., Dogru, O. and Tasdelen, F. (2005). The generalization of Meyer-König and Zeller operators by generating functions. *J. Math. Anal. Appl.*, 312, pp. 181–194.

[8] Ernst, T. (1999). A new notation for q-calculus and a new q-Taylor formula. *Uppsala University Report Depert., Math.*, pp.1-28.

[9] Finta, Z. and Gupta,V. (2009). Approximation properties of q-Baskakov operators. *Cent. Eur. J. Math.*, 8(1), pp. 199–211.

[10] Heping, W. (2007). Properties of convergence for the q-Meyer-König and Zeller operators. *Journal of Mathematical Analysis and Applications*, 335(2), pp.1360-1373.

[11] Doğru, O., Duman, O. (2006). Statistical approximation of Meyer–König and Zeller operators based on the q-integers. *Publ. Math. Debrecen*, 68, pp.190–214.

[12] Heping, W., Meng, (2005). F. The rate of convergence of q-Bernstein polynomials for $0 < q < 1$. *J. Approx. Theor.*, 136, pp.151–158.

[13] II'inski, A., Ostrovska, S. (2002). Convergence of generalized Bernstein polynomials. *J. Approx. Theor.,* 116, pp. 100–112.

[14] Kac, V., Cheung, P. (2002). *Quantum Calculus*, Universitext. New York, Springer.

[15] Mahmudov, N. and Sabancıgil, P. (2008). q-Parametric Bleimann Butzer and Hahn Operators. *Journal of Inequalities and Applications,* 2008(1), p.816367.

[16] Nowak, G. and Gupta, V. (2011). The Rate of Pointwise Approximation of Positive Linear Operators Based on q-Integer. *Ukrainian Math, J.,* 3, pp.350-360.

[17] Radu, C. (2009). On statistical approximation of a general class of positive linear operators extended in q-calculus. *Appl. Math. Comput.,* 215, pp.2317–2325.

[18] Trif, T. (2002). Meyer, König and Zeller operators based on the q-integers. *Rev. Anal. Numer. Theor. Approx.,* 29, pp.221–229.

[19] Videnskii, V. S.(2005). On some class of q-parametric positive operators. *Operator Theory: Advances and Applications*, 158, pp.213–222.

[20] Şimşek, E. and Tunç, T. (2017). On the construction of q-analogues for some positive linear operators. *Filomat*, 31(13), pp.4287-4295.

[21] Şimşek, E. and Tunç, T. (2018). On Approximation Properties of some Class Positive Linear Operators in q-Analysis. *Journal of Mathematical Inequalities,* 12(2), pp.559–571.

[22] Njionou Sadjang, P. (2018). On the Fundamental Theorem of (p, q)-Calculus and Some (p, q)-Taylor Formulas. *Results in Mathematics*, 73(1).

[23] Mursaleen, M., Ansari, K. and Khan, A. (2015). On (p, q)-analogue of Bernstein operators. *Applied Mathematics and Computation*, 266, pp.874-882. And (Revised). arXiv:1503.07404.

[24] Mursaleen, M., Nasiruzzaman, M. and Nurgali, A. (2015). Some approximation results on Bernstein-Schurer operators defined by (p, q) -integers. *Journal of Inequalities and Applications,* 2015(1).

[25] Mursaleen, M., Nasiruzzaman, Md., Khan, A., and Ansari, K. J. (2016). Some approximation results on Bleimann-Butzer-Hahn operators defined by (p, q) -integers. *Filomat*, 30, pp.639–648.

[26] Mursaleen, M., Sarsenbi, A. and Khan, T. (2016). On (p, q) -analogue of two parametric Stancu-Beta operators. *Journal of Inequalities and Applications*, 2016(1).

[27] Mursaleen, M., Alotaibi, A. and Ansari, K. (2016). On a Kantorovich Variant of (p, q)-Szász-Mirakjan Operators. *Journal of Function Spaces*, 2016, pp.1-9.

[28] Mursaleen, M., Ansari, K. J. and Khan, A. (2015). Some approximation results by (p, q)-analogue of Bernstein-Stancu operators. *Appl. Math. Comput.*, 264, pp.392–402.

[29] Acar, T. (2016). (p, q)-generalization of Szasz-Mirakyan operators. *Math. Methods Appl. Sci.*, 39, pp.2685–2695.

[30] Acar, T., Aral, A. and Mohiuddine, S. A. (2018). Approximation by bivariate (p, q)-Bernstein-Kantorovich operators. *Iranian Journal of Science and Technology, Transactions A: Science*, 42(2), pp.655-662.

[31] Acar, T., Aral, A. and Mohiuddine, S. (2016). On Kantorovich modification of (p, q) -Baskakov operators. *Journal of Inequalities and Applications*, 2016(1).

[32] Cai, Q.B. and Zhou, G. (2016). On (p, q)-analogue of Kantorovich type Bernstein-Stancu-Schurer operators. *Appl. Math. Comput.* 276, pp.12–20.

[33] Sharma, H. (2016). On Durrmeyer-type generalization of (p, q)-Bernstein operators. *Arab. J. Math.,* 5, pp.239–248.

[34] Khan, K. and Lobiyal, D.K. (2017). Bèzier curves based on Lupaş (p, q)-analogue of Bernstein functions in CAGD. *Journal of Computational and Applied Mathematics*, 317, pp.458-477.

[35] Kanat, K. and Sofyalıoglu, M. (2018). Some Approximation Results For (p, q)-Lupas-Schurer Operators, *Filomat* 32(1), pp.217–229.

[36] Kadak, U., Khan, A. and Mursaleen, M. (2016). Approximation by Meyer-Konig and Zeller Operators using (p, q)-Calculus. arXiv:1603.08539v2.

Some Results on Complete Rewriting Systems of Algebraic Constructions

Eylem GÜZEL KARPUZ*
Karamanoglu Mehmetbey University,
Department of Mathematics,
70100, Karaman, TURKEY

Esra KIRMIZI ÇETİNALP
Karamanoglu Mehmetbey University,
Department of Mathematics,
70100, Karaman, TURKEY

A. Sinan ÇEVİK
Selçuk University,
Science Faculty, Department of Mathematics,
42075, Konya-Turkey /
KAU King Abdulaziz University,
Department of Mathematics,
21589, Jeddah, Makkah S Arabia

Abstract

In this paper, we obtain complete rewriting systems for braid groups associated with the congruence classes of complex reflection groups G_7 and G_{25}. Thus we give normal forms of elements and solvability of the word problems of these group types.

Keywords: Complex reflection group, rewriting system, normal form, word problem.

1 Introduction and Preliminaries

Presentations arise in various areas of mathematics such as knot theory, topology, and geometry. Another motivation for studying presentations is the advent of softwares for symbolic computations like *GAP* (Groups, Algorithms and Programming). Providing algorithms to compute presentations of given group (monoid) structures is a great help for the developers of these softwares. In this work, we consider presentations of some braid groups associated with the congruence classes of complex reflection groups and find complete rewriting systems for these group types. Thus, by these complete rewriting systems we characterize the structure of elements of groups. Therefore, we obtain solvability of the word problem.

In early 1900's, Max Dehn introduced algorithmic problems namely the word, conjugacy and isomorphism problems. These problems have played an important role in group and semigroup theory. In literature these problems are also called *decision problems* which ask for a yes or no answer to a specific question. Among these decision problems especially the word problem has been studied widely in group theory (see [1]). It is a well known fact that the word problem for finitely presented groups is not solvable in general; that means given any two words obtained by generators of the group, there may be no algorithm to decide whether these words represent the same element in this group. The method of rewriting system which is the main theme of this paper gives a set of normal forms for elements of the group/group structure. This means that for each group element there is a unique word representing it which cannot be rewritten.

*Corresponding author. *E-mail address:* eylem.guzel@kmu.edu.tr

1.1 Complex Reflection Groups

Shephard and Todd classified all finite complex reflection groups in [10]. Later Cohen (1976) gave a more systematic description for these groups in terms of root systems, vector graphs and root graphs [4]. Then, in [8], Howlett and Shi defined a simple root system $(B; w)$ for such these groups which is analogous to the corresponding concept for a Coxeter group.

It is well known that any Coxeter group can be presented by generators and relations. A finite complex reflection group G can also be presented in a similar way (see, for example, [3]). But such a presentation is not unique for G in general. Different presentations of G may reveal various different properties of G. Then it is worth to define a congruence relation among the presentations of G (see [11]) and then to ask that question "How many congruence classes of presentations are there for any irreducible finite complex reflection group G?". In [3], the authors solve this problem for the finite primitive complex reflection groups $G = \{G_7, G_{11}, G_{15}, G_{19}, G_{27}\}$ and in [11], Shi studied the finite primitive complex reflection groups $G = \{G_{12}, G_{24}, G_{25}, G_{26}\}$ (in the notations of Shephard and Todd, 1954). So by considering the presentations given in [3] for G_7 and in [11] for G_{25}, our aim in this paper is to find complete rewriting systems of these important groups.

Theorem 1 *[3] The braid group associated with the congruence classes of complex reflection group G_7 admits the presentation*

$$\mathcal{P}_{G_7} = \left\langle s, t, u \ ; \ t^2 = u^3 = s^3 = 1, tus = ust = stu \right\rangle .$$

Theorem 2 *[11] The braid group associated with the congruence classes of complex reflection group G_{25} admits the presentation*

$$\mathcal{P}_{G_{25}} = \left\langle s, t, u \ ; \ t^3 = u^3 = s^3 = 1, tut = utu, usu = sus, ts = st \right\rangle .$$

1.2 String Rewriting System

In this paper, since we will use complete rewriting system method to obtain normal form structure of elements of congruence classes of complex reflection groups G_7 and G_{25}, we give some information about complete rewriting system as in the following paragraphs.

Let X be a set and let X^* be the free monoid consists of all words obtained by the elements of X. A *(string) rewriting system* on X^* is a subset $R \subseteq X^* \times X^*$ and an element $(u, v) \in R$, also can be written as $u \to v$, is called a rule of R. The idea for a rewriting system is an algorithm for substituting the right-hand side of a rule whenever the left-hand side appears in a word. In general, for a given rewriting system R, we write $x \to y$ for $x, y \in X^*$ if $x = uv_1w$, $y = uv_2w$ and $(v_1, v_2) \in R$. Also we write $x \to^* y$ if $x = y$ or $x \to x_1 \to x_2 \to \cdots \to y$ for some finite chain of reductions and $\leftrightarrow^*$ is the reflexive, symmetric, and transitive closure of $\to$. Furthermore an element $x \in X^*$ is called irreducible with respect to R if there is no possible rewriting *(or reduction)* $x \to y$; otherwise x is called *reducible.* The rewriting system R is called

- *Noetherian* if there is no infinite chain of rewritings $x \to x_1 \to x_2 \to \cdots$ for any word $x \in X^*$,
- *Confluent* if whenever $x \to^* y_1$ and $x \to^* y_2$, there is a $z \in X^*$ such that $y_1 \to^* z$ and $y_2 \to^* z$,
- *Complete* if R is both Noetherian and confluent.

A *critical pair* of a rewriting system R is a pair of overlapping rules if one of the

(i) (r_1r_2, s), $(r_2r_3, t) \in R$ with $r_2 \neq 1$ or ***(ii)*** $(r_1r_2r_3, s)$ $(r_2, t) \in R$,

forms is satisfied. Also a critical pair is *resolved* in R if there is a word z such that $sr_3 \to^* z$ and $r_1t \to^* z$ in the first case or $s \to^* z$ and $r_1tr_3 \to^* z$ in the second. A Noetherian rewriting system is complete if and only if every critical pair is resolved. We also note that if a rewriting system is complete then it has a solvable word problem ([1]). We finally note that the reader is referred to [2] and [12] for a detailed survey on (complete) rewriting systems and to [5, 6, 7, 9] for complete rewriting systems of some algebraic constructions.

2 Main Results

In this section, we obtain complete rewriting systems for braid groups associated with the congruence classes of complex reflection groups G_7 and G_{25}, respectively. To do that we need lexicographic orderings between generators of the group G_7 as $u > s > t$ and of the group G_{25} as $t > s > u$. Here, we order words in given alphabet in the way by comparing the right-hand side of each rule is strictly smaller that its left-hand side for the lexicographic order induced by the order on generators for each group. Additionally, the notation $(i) \cap (j)$ will denote the intersection overlapping words of left hand side of relations (i) and (j).

Theorem 3 *A complete rewriting system for the braid group associated with the congruence classes of complex reflection group G_7 consists of the following rules:*

$$(1)\ t^2 \to 1, \quad (2)\ u^3 \to 1, \quad (3)\ s^3 \to 1, \quad (4)\ ust \to tus, \quad (5)\ ust \to stu.$$

Proof. This rewriting system is Noetherian since there is no infinite chain of rewritings of overlapping words for the lexicographic order induced by the order on generators $(u > s > t)$. It remains to show that the confluent property holds. To do that we have the following overlapping words (w) and corresponding critical pairs (cp), respectively.

$$\begin{aligned}
(1) \cap (1) \quad &: w = t^3, \quad cp = (t, t),\\
(2) \cap (2) \quad &: w = u^4, \quad cp = (u, u),\\
(3) \cap (3) \quad &: w = s^4, \quad cp = (s, s),\\
(2) \cap (4) \quad &: w = u^3st, \quad cp = (st, u^2tus),\\
(2) \cap (5) \quad &: w = u^3st, \quad cp = (st, u^2stu),\\
(4) \cap (1) \quad &: w = ust^2, \quad cp = (tust, us),\\
(5) \cap (1) \quad &: w = ust^2, \quad cp = (stut, us).
\end{aligned}$$

All these above critical pairs are resolved by reduction steps. We show two of them as follows:

$$(2) \cap (5) : w = u^3st, \quad cp = (st, u^2stu),$$
$$u^3st \longrightarrow \begin{cases} st \\ u^2stu \to ustu^2 \to stu^3 \to st \end{cases}$$

$$(4) \cap (1) : w = ust^2, \quad cp = (tust, us),$$
$$ust^2 \longrightarrow \begin{cases} tust \to t^2us \to us \\ us \end{cases}$$

After all these above processes, since the rewriting system is Noetherian and confluent it is complete. Hence the result. ■

Theorem 4 *A complete rewriting system for the braid group associated with the congruence classes of complex reflection group G_{25} consists of the following rules:*

$$\begin{array}{llll} (1) & t^3 \to 1, & (2)\ u^3 \to 1, & (3)\ s^3 \to 1, \\ (4) & tut \to utu, & (5)\ sus \to usu, & (6)\ ts \to st. \end{array}$$

Proof. This rewriting system is Noetherian since there is no infinite chain of rewritings of overlapping words for the lexicographic order induced by the order on generators ($t > s > u$). It remains to show that the confluent property holds. To do that we have the following overlapping words (w) and corresponding critical pairs (cp), respectively.

$$\begin{array}{ll} (1)\cap(1) & : w = t^4, \quad cp = (t,t), \\ (2)\cap(2) & : w = u^4, \quad cp = (u,u), \\ (3)\cap(3) & : w = s^4, \quad cp = (s,s), \\ (1)\cap(4) & : w = t^3ut, \quad cp = (ut, t^2utu), \\ (1)\cap(6) & : w = t^3s, \quad cp = (s, t^2st), \\ (3)\cap(5) & : w = s^3us, \quad cp = (us, s^2usu), \\ (4)\cap(1) & : w = tut^3, \quad cp = (utut^2, tu), \\ (4)\cap(4) & : w = tutut, \quad cp = (utu^2t, tu^2tu), \\ (4)\cap(6) & : w = tuts, \quad cp = (utus, tust), \\ (5)\cap(3) & : w = sus^3, \quad cp = (usus^2, su), \\ (5)\cap(5) & : w = susus, \quad cp = (usu^2s, su^2su), \\ (6)\cap(3) & : w = ts^3, \quad cp = (sts^2, t), \\ (6)\cap(5) & : w = tsus, \quad cp = (stus, tusu). \end{array}$$

All these above critical pairs are resolved by reduction steps. We show some of them as follows:

$$(1)\cap(4) : w = t^3ut, \quad cp = (ut, t^2utu),$$
$$t^3ut \longrightarrow \begin{cases} ut \\ t^2utu \to tutu^2 \to utu^3 \to ut \end{cases}$$

$$(5)\cap(5) : w = susus, \quad cp = (usu^2s, su^2su),$$
$$susus \longrightarrow \begin{cases} usu^2s \to usu^2 \\ su^2su \to su^3sus \to s^2us \to susu \to usu^2 \end{cases}$$

$$(6)\cap(3) : w = ts^3, \quad cp = (sts^2, t),$$
$$ts^3 \longrightarrow \begin{cases} sts^2 \to s^2ts \to s^3t \to t \\ t \end{cases}$$

After all these above processes, since the rewriting system is Noetherian and confluent it is complete. Hence the result. ■

Now let R_i be the set of relations for each congruence classes of primitive complex reflection groups G_i ($i = \{7, 25\}$) given in Theorems 2.1 and 2.2. By using these results, the normal forms for the congruence classes of primitive complex reflection groups G_7 and G_{25} can be given as follows:

Corollary 5 *Let $C(u)$ be a normal form of a word $u \in G_i$ ($i = \{7, 25\}$).*

- *For* $u \in G_7$, $C(u) = wt^{\epsilon_1}w'^{\epsilon_2}w''^{\epsilon_3}w'''$ $(0 \leq \epsilon_1 < 2,\ 0 \leq \epsilon_2, \epsilon_3 < 3)$, *where* w, w', w'' *and* w''' *are* R_7*-reduced words in* G_7.
- *For* $u \in G_{25}$, $C(u) = wu^{\epsilon_1}w'^{\epsilon_2}w''^{\epsilon_3}w'''$ $(0 \leq \epsilon_1, \epsilon_2, \epsilon_3 < 3)$, *where* w, w', w'' *and* w''' *are* R_{25}*-reduced words in* G_{25}.

By considering Corollary 2.3, we have the following other consequence of our main results.

Corollary 6 *The word problem for the congruence classes of primitive complex reflection groups* G_i $(i = \{7, 25\})$ *is solvable.*

References

[1] S. I. Adian, V.G. Durnev, Decision problems for groups and semigroups, Russian Math. Surveys, 55(2) (2000) 207-296.

[2] R. V. Book, F. Otto, *String-Rewriting Systems*, Springer-Verlag, New York, 1993.

[3] M. Broue, G. Malle, R. Rouquier, Complex reflection groups, braid groups, Hecke algebras, J. Reine Angew Math. 500 (1998) 127-190.

[4] A. M. Cohen, Finite complex reflection groups, Ann. Scient. c. Norm. Sup. 4e Srie t. 9 (1976) 379-436.

[5] E. K. Çetinalp, E. G. Karpuz, F. Ateç, A. S. Çevik, Two-sided crossed product of groups, Filomat, 30(4) (2016) 1005-1012.

[6] E. K. Çetinalp, E. G. Karpuz, A. S. Çevik, Complete rewriting system for Schtzenberger product of n groups, Asian-European Journal of Mathematics, DOI: 10.1142/S1793557119500128 12(1), (2019).

[7] S. M. Hermiller, Rewriting system for Coxeter groups, Journal of Pure and Applied Algebra, 92(2) (1994) 137-148.

[8] R. B. Howlett, J. Y. Shi, On regularity of finite reflection groups,Manuscripta Mathematica, 102(3) (2000) 325-333.

[9] E. G. Karpuz, Complete rewriting systems for the Chinese monoid, Applied Mathematical Sciences, 4(22) (2010) 1081-1087.

[10] G. C. Shephard, J. A. Todd, Finite unitary reflection groups, Canad. J. Math. 6 (1954) 274-304.

[11] J. Y. Shi, Simple root systems and presentations for certain complex reflection groups, Communications in Algebra, 33 (2005) 1765-1783.

[12] C. C. Sims, *Computation for Finitely Presented Groups*, Cambridge University Press, 1994.

Torus Type Helicoidal Hypersurface in 4-Space

Erhan GÜLER*
Bartın University,
Department of Mathematics,
74100, Bartın, TURKEY

Ömer KİŞİ
BartınUniversity,
Department of Mathematics,
74100, Bartın, TURKEY

Abstract

We study torus-type helicoidal hypersurface in the four dimensional Euclidean space $\mathbb{E}^4$. We define torus-type helicoidal hypersurface. Then, we calculate its curvatures with some results.

Keywords: 4-space, torus-type helicoidal hypersurface, curvatures.

1 Introduction

Focusing on the rotational characters in the literature, we meet $[1-6, 8-18, 20, 21, 24-26, 28, 31, 32, 34, 35]$, and many others.

About helicoidal surfaces in Euclidean 3-space, Do Carmo and Dajczer [14] proved that there exists a two-parameter family of helicoidal surfaces isometric to a given helicoidal surface using a result of Bour [7].

Magid, Scharlach and Vrancken [28] introduced the affine umbilical surfaces in 4-space. Vlachos [35] considered hypersurfaces in $\mathbb{E}^4$ with harmonic mean curvature vector field. Scharlach [32] studied on affine geometry of surfaces and hypersurfaces in $\mathbb{E}^4$. Cheng and Wan [11] considered complete hypersurfaces of $\mathbb{E}^4$ with constant mean curvature. Arvanitoyeorgos, Kaimakamais and Magid [6] showed that if the mean curvature vector field of M_1^3 satisfies the equation $\Delta H = \alpha H$ (α a constant), then M_1^3 has constant mean curvature in Minkowski 4-space $\mathbb{E}_1^4$.

General rotational surfaces in $\mathbb{E}^4$ were introduced by Moore [29, 30]. Ganchev and Milousheva [17] considered the analogue of these surfaces in the Minkowski 4-space. Moruz and Munteanu [31] considered hypersurfaces in $\mathbb{E}^4$ defined as the sum of a curve and a surface whose mean curvature vanishes. Verstraelen, Walrave and Yaprak [34] studied on the minimal translation surfaces in $\mathbb{E}^n$ for arbitrary dimension n. Kim and Turgay [26] studied surfaces with L_1-pointwise 1-type Gauss map in the 4-dimensional Euclidean space $\mathbb{E}^4$.

Güler, Magid and Yaylı [21] studied Laplace Beltrami operator of a helicoidal hypersurface in $\mathbb{E}^4$. Güler, Hacisalihoglu and Kim [18] worked on the Gauss map and the third Laplace-Beltrami operator of rotational hypersurface in $\mathbb{E}^4$. Güler, Kaimakamis and Magid [19] introduced the helicoidal hypersurfaces in Minkowski 4-space $\mathbb{E}_1^4$. Güler and Turgay [22] studied Cheng-Yau operator and Gauss map of rotational hypersurfaces in $\mathbb{E}^4$. Moreover; Güler, Turgay and Kim [23] considered L_2 operator and Gauss map of rotational hypersurfaces in $\mathbb{E}^5$. Some relations among the Laplace-Beltrami operator and curvatures of the helicoidal surfaces were shown by Güler, Yaylı and Hacısalihoğlu [24]. Güler and Kişi [20] defined torus type rotational hypersurface in 4-space.

We study the torus-type helicoidal hypersurface in Euclidean 4-space $\mathbb{E}^4$. We give some basic notions of four dimensional Euclidean geometry in section 2. In section 3, we define

*Corresponding author. *E-mail address:* eguler@bartin.edu.tr

helicoidal hypersurface of four-space. Moreover, we obtain torus-type helicoidal hypersurface, and calculate its curvatures in the last section.

2 Preliminaries

We shall identify a vector (a,b,c,d) with its transpose $(a,b,c,d)^t$ in the rest of this paper. Next, we introduce the first and second fundamental forms, matrix of the shape operator $\mathbf{S}$, Gaussian curvature K, and the mean curvature H of hypersurface $\mathbf{M} = \mathbf{M}(u, v, w)$ in Euclidean 4-space $\mathbb{E}^4$.

Let $\mathbf{M}$ be an isometric immersion of a hypersurface M^3 in $\mathbb{E}^4$. The triple vector product $\overrightarrow{x} \times \overrightarrow{y} \times \overrightarrow{z}$ of $\overrightarrow{x} = (x_1, x_2, x_3, x_4)$, $\overrightarrow{y} = (y_1, y_2, y_3, y_4)$, $\overrightarrow{z} = (z_1, z_2, z_3, z_4)$ on $\mathbb{E}^4$ is defined as follows

$$\begin{pmatrix} x_2y_3z_4 - x_2y_4z_3 - x_3y_2z_4 + x_3y_4z_2 + x_4y_2z_3 - x_4y_3z_2 \\ -x_1y_3z_4 + x_1y_4z_3 + x_3y_1z_4 - x_3z_1y_4 - y_1x_4z_3 + x_4y_3z_1 \\ x_1y_2z_4 - x_1y_4z_2 - x_2y_1z_4 + x_2z_1y_4 + y_1x_4z_2 - x_4y_2z_1 \\ -x_1y_2z_3 + x_1y_3z_2 + x_2y_1z_3 - x_2y_3z_1 - x_3y_1z_2 + x_3y_2z_1 \end{pmatrix}.$$

For a hypersurface $\mathbf{M}$ in $\mathbb{E}^4$ we have

$$\det I = \det \begin{pmatrix} E & F & A \\ F & G & B \\ A & B & C \end{pmatrix} = (EG - F^2)C - A^2G + 2ABF - B^2E,$$

and

$$\det II = \det \begin{pmatrix} L & M & P \\ M & N & T \\ P & T & V \end{pmatrix} = \left(LN - M^2\right)V - P^2N + 2PTM - T^2L,$$

where

$$\begin{array}{l} A = \mathbf{M}_u \cdot \mathbf{M}_w,\ B = \mathbf{M}_v \cdot \mathbf{M}_w,\ C = \mathbf{M}_w \cdot \mathbf{M}_w, \\ P = \mathbf{M}_{uw} \cdot e, \quad T = \mathbf{M}_{vw} \cdot e, \quad V = \mathbf{M}_{ww} \cdot e, \end{array}$$

e is the Gauss map (i.e., the unit normal vector field). We compute the matrix of the shape operator $\mathbf{S}$, as follows

$$\mathbf{S} = \frac{1}{\det I} \begin{pmatrix} s_{11} & s_{12} & s_{13} \\ s_{21} & s_{22} & s_{23} \\ s_{31} & s_{32} & s_{33} \end{pmatrix}, \tag{1}$$

where

$$\begin{array}{l} s_{11} = ABM - CFM - AGP + BFP + CGL - B^2L, \\ s_{12} = ABN - CFN - AGT + BFT + CGM - B^2M, \\ s_{13} = ABT - CFT - AGV + BFV + CGP - B^2P, \\ s_{21} = ABL - CFL + AFP - BPE + CME - A^2M, \\ s_{22} = ABM - CFM + AFT - BTE + CNE - A^2N, \\ s_{23} = ABP - CFP + AFV - BVE + CTE - A^2T, \\ s_{31} = -AGL + BFL + AFM - BME + GPE - F^2P, \\ s_{32} = -AGM + BFM + AFN - BNE + GTE - F^2T, \\ s_{33} = -AGP + BFP + AFT - BTE + GVE - F^2V. \end{array}$$

So, we get the following formulas of the Gaussian and the mean curvatures

$$\begin{aligned} K &= \det(\mathbf{S}) = \frac{\det II}{\det I} \\ &= \frac{\left(LN - M^2\right)V + 2MPT - P^2N - T^2L}{(EG - F^2)C + 2ABF - A^2G - B^2E}, \end{aligned}$$

and

$$\begin{aligned} H &= \frac{1}{3} tr\left(\mathbf{S}\right) \\ &= \frac{1}{3\det I}[(EN+GL-2FM)C+(EG-F^2)V \\ &\quad -A^2N-B^2L-2(APG+BTE-ABM-ATF-BPF)]. \end{aligned}$$

A hypersurface $\mathbf{M}$ is minimal, if $H=0$ identically on $\mathbf{M}$.

3 Helicoidal Hypersurface

Next, we define the rotational hypersurface in $\mathbb{E}^4$. For an open interval $I \subset \mathbb{R}$, let $\gamma : I \longrightarrow \Pi$ be a curve in a plane Π in $\mathbb{E}^4$, and let ℓ be a straight line in Π.

A *rotational hypersurface* in $\mathbb{E}^4$ is defined as a hypersurface rotating a curve γ around a line ℓ (these are called the *profile curve* and the *axis*, respectively). Suppose that when a profile curve γ rotates around the axis ℓ, it simultaneously displaces parallel lines orthogonal to the axis ℓ, so that the speed of displacement is proportional to the speed of rotation. Then the resulting hypersurface is called the *helicoidal hypersurface* with axis ℓ and pitchs $b, d \in \mathbb{R}\backslash\{0\}$.

We may suppose that ℓ is the line spanned by the vector $(0,0,0,1)^t$. The orthogonal matrix which fixes the above vector is

$$Z(v,w) = \begin{pmatrix} \cos v \cos w & -\sin v & -\cos v \sin w & 0 \\ \sin v \cos w & \cos v & -\sin v \sin w & 0 \\ \sin w & 0 & \cos w & 0 \\ 0 & 0 & 0 & 1 \end{pmatrix}, \tag{2}$$

where $v, w \in \mathbb{R}$. The matrix Z can be found by solving the following equations simultaneously;

$$Z\ell = \ell, \quad Z^t Z = ZZ^t = I_4, \quad \det Z = 1.$$

When the axis of rotation is ℓ, there is an Euclidean transformation by which the axis is ℓ transformed to the x_4-axis of $\mathbb{E}^4$. Parametrization of the profile curve is given by

$$\gamma(u) = \left(f\left(u\right), 0, 0, \varphi\left(u\right)\right),$$

where $f\left(u\right), \varphi\left(u\right) : I \subset \mathbb{R} \longrightarrow \mathbb{R}$ are differentiable functions for all $u \in I$. So, the helicoidal hypersurface which is spanned by the vector $(0,0,0,1)$ is as follows

$$\mathbf{H}(u,v,w) = Z(v,w)\gamma(u)^t + (bv+dw)\,\ell^t,$$

where $u \in I,\ v, w \in [0, 2\pi]$. Clearly, we write helicoidal hypersurface as follows

$$\mathbf{H}(u,v,w) = \begin{pmatrix} f\left(u\right) \cos v \cos w \\ f\left(u\right) \sin v \cos w \\ f\left(u\right) \sin w \\ \varphi\left(u\right) + bv + dw \end{pmatrix}. \tag{3}$$

4 Torus-Type Helicoidal Hypersurface

Taking profile curve as

$$\gamma(u) = \left(a + c\cos u, 0, 0, c \sin u\right),$$

with the orthogonal matrix Z, then we get torus-type helicoidal hypersurface in $\mathbb{E}^4$ as follows

$$\mathfrak{T}(u,v,w)=\begin{pmatrix}(c+a\cos u)\cos v\cos w\\(c+a\cos u)\sin v\cos w\\(c+a\cos u)\sin w\\a\sin u+bv+dw\end{pmatrix}, \tag{4}$$

where $a,b,c,d\in\mathbb{R}\backslash\{0\}$ and $0\leq u,v,w\leq 2\pi$.

Using the first differentials of (4) with respect to u,v,w, we get the first quantities as follows

$$I=\begin{pmatrix}a^2 & ab\cos u & ad\cos u\\ ab\cos u & \beta_1 & bd\\ ad\cos u & bd & \beta_2\end{pmatrix},$$

where

$$\begin{aligned}\beta_1 &= a\left(2c+a\cos u\right)\cos u\cos^2 w+b^2,\\ \beta_2 &= a\left(2c+a\cos u\right)\cos u+c^2+d^2,\end{aligned}$$

and have

$$\det I=a^2\left(\left(2b^2d^2-b^2\beta_2-d^2\beta_1\right)\cos^2 u+\left(\beta_1\beta_2-b^2d^2\right)\right).$$

Using the second differentials with respect to u,v,w, we have the second quantities as follows

$$II=\frac{1}{W}\begin{pmatrix}-a\phi & ab\sin^2 u & ad\sin^2 u\\ ab\sin^2 u & -\phi^2\cos u-d\phi\sin u & b\phi\sin u\\ ad\sin^2 u & b\phi\sin u & -\phi^2\cos u\end{pmatrix},$$

where $W=\sqrt{(a^2-2b^2-d^2)\cos^2 u+2ac\cos u+a^2+2b^2+d^2}$, $\phi=c+a\cos u$, and get

$$\det II=\frac{a\phi}{W^{3/2}}\begin{pmatrix}-\left(a\cos^2 u+c\cos u+d\sin u\right)\phi^3\cos u\\ +b^2\phi^2\sin^2 u+a\phi\left(b^2+d^2\right)\sin^4 u\cos u\\ +ad\left(2b^2+d^2\right)\sin^5 u\end{pmatrix}.$$

The Gauss map of the helicoidal hypersurface with spacelike axis is

$$e_{\mathfrak{T}}=\frac{1}{D}\begin{pmatrix}(\phi\cos u+d\sin u\sin w)\cos v\cos w+b\sin u\sin v\\ (\phi\cos u\cos w+d\sin u\sin w)\sin v\cos w-b\sin u\cos v\\ (\phi\cos u\sin w-d\sin u\cos w)\cos w\\ \phi\sin u\cos w\end{pmatrix}, \tag{5}$$

where $D=\sqrt{((a^2-d^2)\cos^2 u+2ac\cos u)\cos^2 w+b^2\sin^2 u}$.

Finally, the Gaussian curvature of the torus-type helicoidal hypersurface is as follows

$$K=\frac{a\phi\Psi(u)}{W^{3/2}\det I},$$

where

$$\begin{aligned}\Psi=&-\left(a\cos^2 u+c\cos u+d\sin u\right)\phi^3\cos u+b^2\phi^2\sin^2 u\\ &+a\left(b^2+d^2\right)\phi\sin^4 u\cos u+ad\left(2b^2+d^2\right)\sin^5 u.\end{aligned}$$

and the mean curvature is as follows

$$H=-\frac{a\Omega(u,w)}{3W\det I},$$

where

$$\begin{aligned}
\Omega \;=\; & a\phi^2\left(b^2\sin^2 u + a\left(2c + a\cos u\right)\cos u\cos^2 w\right)\cos u \\
& +[b^2c^2 + a^2\left(a^2 - d^2\right)\cos^4 u - acd^2\cos^3 u + a^2\left(b^2 + 3c^2 + d^2\right)\cos^2 u \\
& +ac\left(2b^2 + c^2 + d^2\right)\cos u + a^4\cos^4 u\cos^2 w - ad\left(2b^2 + d^2\right)\sin u\cos^2 u \\
& +a^3c\left(4\cos^2 w + 3\right)\cos^3 u + ad\left(2b^2 + c^2 + d^2\right)\sin u \\
& +ad\left(2c + a\cos u\right)\left(d\cos^2 w + a\sin u\right)\cos u]\phi \\
& +2a\left(b^2c^2 + a\left(b^2 + d^2\cos^2 w\right)\left(2c + a\cos u\right)\cos u\right)\cos u\sin^2 u.
\end{aligned}$$

Corollary 1. *Let $\mathfrak{T} : M^3 \longrightarrow \mathbb{E}^4$ be an immersion given by (4). Then M^3 has following Weingarten relation*

$$3\phi\Psi H + W^{1/2}\Omega K = 0.$$

References

[1] Aksoyak F., Yaylı Y. Boost invariant surfaces with pointwise 1-type Gauss map in Minkowski 4-Space $\mathbb{E}^4_1$. Bull. Korean Math. Soc. 51 (2014) 1863–1874.

[2] Aksoyak F., Yaylı Y. General rotational surfaces with pointwise 1-type Gauss map in pseudo-Euclidean space $\mathbb{E}^4_2$. Indian J. Pure Appl. Math. 46 (2015) 107–118.

[3] Arslan K., Bulca B., Milousheva V. Meridian surfaces in $\mathbb{E}^4$ with pointwise 1-type Gauss map. Bull. Korean Math. Soc. 51-3 (2014) 911–922.

[4] Arslan K., Deszcz R., Yaprak Ş. On Weyl pseudosymmetric hypersurfaces. Colloq. Math. 72 (1997) 353–361.

[5] Arslan K., Kılıç Bayram B., Bulca B., Öztürk G. Generalized Rotation Surfaces in $\mathbb{E}^4$. Results Math. 2012, 61, 315–327. Korean Math. Soc. 51 (2014) 911–922.

[6] Arvanitoyeorgos A., Kaimakamis G., Magid M. Lorentz hypersurfaces in $\mathbb{E}^4_1$ satisfying $\Delta H = \alpha H$. Illinois J. Math. 53-2 (2009), 581-590.

[7] Bour E. Théorie de la déformation des surfaces. J. de l.Êcole Imperiale Polytechnique 22-39 (1862) 1-148.

[8] Chen B.Y. Geometry of Submanifolds. Pure and Applied Mathematics, no. 22. Marcel Dekker, Inc., New York, 1973.

[9] Chen B.Y. Total Mean Curvature and Submanifolds of Finite Type. 2nd Ed., World Scientific, Hackensack 2014.

[10] Chen B.Y., Choi, M., Kim, Y.H. Surfaces of revolution with pointwise 1-type Gauss map. Korean Math. Soc. 42 (2005) 447–455.

[11] Cheng Q.M., Wan Q.R. Complete hypersurfaces of $\mathbb{R}^4$ with constant mean curvature. Monatsh. Math. 118 (1994) 3-4, 171-204.

[12] Choi M., Kim Y.H. Characterization of the helicoid as ruled surfaces with pointwise 1-type Gauss map. Bull. Korean Math. Soc. 38 (2001) 753-761.

[13] Dillen F., Pas J., Verstraelen L. On surfaces of finite type in Euclidean 3-space. Kodai Math. J. 13 (1990) 10-21.

[14] Do Carmo M., Dajczer M. Helicoidal surfaces with constant mean curvature. Tohoku Math. J. 34 (1982) 351-367.

[15] Dursun U., Turgay N.C. Minimal and pseudo-umbilical rotational surfaces in Euclidean space $\mathbb{E}^4$. Mediterr. J. Math. 2013, 10, 497–506.

[16] Ferrandez A., Garay O.J., Lucas P. On a Certain Class of Conformally at Euclidean Hypersurfaces. In Global Analysis and Global Differential Geometry; Springer: Berlin, Germany, 1990; 48–54.

[17] Ganchev G., Milousheva V. General rotational surfaces in the 4-dimensional Minkowski space. Turkish J. Math. 38 (2014) 883-895.

[18] Güler E., Hacısalihoğlu H.H., Kim Y.H. The Gauss map and the third Laplace-Beltrami operator of the rotational hypersurface in 4-space. Symmetry 10(9) 398 (2018) 1-11.

[19] Güler E., Kaimakamis G., Magid M. Helicoidal hypersurfaces in Minkowski 4-space $\mathbb{E}_1^4$ (submitted).

[20] Güler E., Kişi Ö. Turus hypersurface in 4-space. Presented in ICAA-2018, Int. Conf. Analysis Applications, Kırşehir Turkey.

[21] Güler E., Magid M., Yaylı Y. Laplace Beltrami operator of a helicoidal hypersurface in four space. J. Geom. Sym. Phys. 41, (2016) 77-95.

[22] Güler E., Turgay N.C. Cheng-Yau operator and Gauss map of rotational hypersurfaces in 4-space (submitted).

[23] Güler E., Turgay N.C., Kim Y.H. L_2 operator and Gauss map of rotational hypersurfaces in 5-space (submitted).

[24] Güler E., Yaylı Y., Hacısalihoğlu H.H. Bour's theorem on the Gauss map in 3-Euclidean space. Hacettepe J. Math. 39 (2010) 515-525.

[25] Hieu, D.T.; Thang, N.N. Bour's theorem in 4-dimensional Euclidean space. Bull. Korean Math. Soc. 2017, 54, 2081–2089.

[26] Kim Y.H., Turgay N.C. Surfaces in $\mathbb{E}^4$ with L_1-pointwise 1-type Gauss map. Bull. Korean Math. Soc. 50(3) (2013) 935-949.

[27] Lawson, H.B. Lectures on Minimal Submanifolds, 2nd ed.; Mathematics Lecture Series 9; Publish or Perish, Inc.: Wilmington, Delaware, 1980.

[28] Magid M., Scharlach C., Vrancken L. Affine umbilical surfaces in $\mathbb{R}^4$. Manuscripta Math. 88 (1995) 275-289.

[29] Moore C. Surfaces of rotation in a space of four dimensions. Ann. Math. 21 (1919) 81-93.

[30] Moore C. Rotation surfaces of constant curvature in space of four dimensions. Bull. Amer. Math. Soc. 26 (1920) 454-460.

[31] Moruz M., Munteanu M.I. Minimal translation hypersurfaces in $\mathbb{E}^4$. J. Math. Anal. Appl. 439 (2016) 798-812.

[**32**] Scharlach, C. Affine Geometry of Surfaces and Hypersurfaces in R4. In Symposium on the Differential Geometry of Submanifolds; Dillen, F., Simon, U., Vrancken, L., Eds.; Un. Valenciennes: Valenciennes, France, 2007; Vol. 124, 251–256.

[**33**] Takahashi T. Minimal immersions of Riemannian manifolds. J. Math. Soc. Japan 18 (1966) 380-385.

[**34**] Verstraelen L., Walrave J., Yaprak S. The minimal translation surfaces in Euclidean space. Soochow J. Math. 20-1 (1994) 77–82.

[**35**] Vlachos Th. Hypersurfaces in $\mathbb{E}^4$ with harmonic mean curvature vector field. Math. Nachr. 172 (1995) 145-169.

Lacunary $\mathcal{I}_2$-Invariant convergence of double sequences in random 2-normed spaces

Ömer KİŞİ*
Bartın University,
Department of Mathematics,
74100, Bartın, TURKEY

Erhan GÜLER
BartınUniversity,
Department of Mathematics,
74100, Bartın, TURKEY

Abstract

In this study, we introduce the concept of lacunary $\mathcal{I}_2$-invariant convergence, lacunary $\mathcal{I}_2^*$-invariant convergence and lacunary $\mathcal{I}_2$-invariant Cauchy for double sequences in the topology introduced by random 2-normed spaces. We give the relationships among these concepts and prove some important results.

Keywords: $\mathcal{I}_2$-invariant convergence,lacunary convergence, 2-norm, 2-normed space.

1 Introduction

The notion of statistical convergence of sequences of numbers was introduced by Fast [2]. Later on, statistical convergence turned out to be one of the most active areas of research in summability theory after the works of Fridy [3] and Salat [4].

The notion of convergence of real double sequences was first introduced by Pringsheim [9]. A lot of useful developments of double sequences in summability methods can be found in Limayea and Zeltser, Altay and Başar [1]. This notion of convergence of real double sequences has been extended to statistical convergence by Mursaleen and Edely, [5]. Also, they established some relationships between statistical convergence and strongly Cesàro summable double sequences.

The concept of lacunary statistical convergence was defined by Fridy and Orhan [7]. Also, Fridy and Orhan gave the relationships between the lacunary statistical convergence and the Cesàro summability. Freedman and Sember established the connection between the strongly Cesàro summable sequences space $|\sigma_1|$ and the strongly lacunary summable sequences space N_θ in their work [10] published in 1978. This notion was extended to the double sequences by Savaş and Patterson [32].

Kostyrko, Salát and Wilezyński [11] introduced the concept of $\mathcal{I}$-convergence of sequences in a metric space and studied some properties of this convergence.

Tripathy, Hazarika and Choudhary [28] introduced the concepts of $\mathcal{I}$-lacunary convergent sequences.

Recently in [12] we used ideals to introduce the concepts of $\mathcal{I}$-statistical convergence and $\mathcal{I}$-lacunary statistical convergence which naturally extend the notions of the above mentioned convergence.

Quite recently, $\mathcal{I}$-double statistical convergence has been established as a better tool than double statistical convergence. It is found very interesting that some results on sequences, series and summability can be proved by replacing the double statistical convergence by $\mathcal{I}$-double statistical convergence.

*Corresponding author. *E-mail address:* okisi@bartin.edu.tr

The notion of statistical convergence of double sequence has been further generalized to $\mathcal{I}$-convergence of double sequences by Das, Kostyrko, Wilczyński and Malik [13] using ideals in $\mathbb{N}\times\mathbb{N}$.

Several authors have studied invariant convergent sequences (see, [24], [25], [26], [27], [31], [38], [34], [35], [29], [30], [44]). Savaş and Nuray [44] introduced the concepts of σ-statistically convergence and lacunary σ-statistically convergence and gave some inclusion relations. Pancaroğlu and Nuray [31] defined the concept lacunary invariant summability and p-strongly lacunary invariant summability. The concept of lacunary strongly σ-convergence was introduced by Savaş [29].

In [36], the concepts of σ-uniform density of subsets A of the set $\mathbb{N}$ of positive integers and corresponding $\mathcal{I}_\sigma$-convergence were introduced. Also, inclusion relations between $\mathcal{I}_\sigma$-convergence and invariant convergence also $\mathcal{I}_\sigma$-convergence and $[V_\sigma]_p$ were given [36]. Recently, the concept of lanunary σ-uniform density of the set $A\subset\mathbb{N}$, lacunary $\mathcal{I}_\sigma$-convergence, lacunary $\mathcal{I}_\sigma^*$-convergence, lacunary $\mathcal{I}_\sigma$-Cauchy, lacunary $\mathcal{I}_\sigma^*$-Cauchy sequences of real numbers were defined by Ulusu and Nuray [34]. Ulusu, Dundar and Nuray [35] defined the lacunary $\mathcal{I}_2$-invariant convergence for double sequences, and examine the properties the convergence.

First we recall some of the basic concepts which we will be used in this paper.

A number sequence $x=(x_k)$ is said to be statistically convergent to the number l, if for every $\varepsilon>0$, $\lim_{n\to\infty}\frac{1}{n}|\{k\le n:|x_k-l|\ge\varepsilon\}|=0$. In this case, we write $st-\lim_{k\to\infty}x_k=l$. Statistical convergence is a natural generalization of ordinary convergence. If $\lim x_k=l$, then $st-\lim x_k=l$. The converse does not hold in general.

A number sequence $x=(x_k)$ is said to be statistically convergent to the number L, if for every $\varepsilon>0$, $\lim_{n\to\infty}\frac{1}{n}|\{k\le n:|x_k-L|\ge\varepsilon\}|=0$. In this case we write $st-\lim x_k=L$.

By a lacunary sequence, we mean an increasing integer sequence $\theta=\{k_r\}$ such that $k_0=0$ and $h_r=k_r-k_{r-1}\to\infty$ as $r\to\infty$. Throughout this paper, the intervals determined by θ will be denoted by $I_r=(k_{r-1},k_r]$.

A sequence $x=(x_k)$ is said to be lacunary statistically convergent to the number L, if for every $\varepsilon>0$, $\lim_{r\to\infty}\frac{1}{h_r}|\{k\in I_r:|x_k-L|\ge\varepsilon\}|=0$. In this case, we write $S_\theta-\lim x_k=L$ or $x_k\to L(S_\theta)$.

The strongly lacunary summable sequences sequence space N_θ, which is defined by

$$N_\theta=\left\{(x_k):\lim_{r\to\infty}\frac{1}{h_r}\sum_{k\in I_r}|x_k-L|=0\right\}.$$

A sequence $x=(x_k)$ is said to be $(V,\lambda)-$summable to a number L, if $\lim_{n\to\infty}t_n(x)=L$. If $\lambda_n=n$, then $(V,\lambda)-$summability reduces to $(C,1)-$summability.

An ideal $\mathcal{I}$ on $\mathbb{N}$ for which $\mathcal{I}\neq\mathcal{P}(\mathbb{N})$ is called a proper ideal. A proper ideal $\mathcal{I}$ is called admissible if $\mathcal{I}$ contains all finite subsets of $\mathbb{N}$.

A family of sets $\mathcal{I}\subseteq 2^{\mathbb{N}}$ is called an ideal if and only if (i) $\emptyset\in\mathcal{I}$, (ii) For each $A,B\in\mathcal{I}$ we have $A\cup B\in\mathcal{I}$, (iii) For each $A\in\mathcal{I}$ and each $B\subseteq A$ we have $B\in\mathcal{I}$.

A family of sets $\mathcal{F}\subseteq 2^{\mathbb{N}}$ is a filter in $\mathbb{N}$ if and only if (i) $\emptyset\notin F$, (ii) For each $A,B\in F$ we have $A\cap B\in F$, (iii) For each $A\in F$ and each $B\supseteq A$ we have $B\in F$.

Lemma 1 *If $\mathcal{I}$ is proper ideal of $\mathbb{N}$ (i.e., $\mathbb{N}\notin\mathcal{I}$), then the family of sets*

$$F(\mathcal{I})=\{M\subset\mathbb{N}:\exists A\in\mathcal{I}:M=\mathbb{N}\setminus A\}$$

is a filter of $\mathbb{N}$ it is called the filter associated with the ideal. Many concepts mentioned in this exposition are more frequently defined using limit along a filter. Filter is a dual notion of ideal.

Let $\mathcal{I} \subset 2^{\mathbb{N}}$ be a proper admissible ideal in $\mathbb{N}$. The sequence (x_k) of elements of $\mathbb{R}$ is said to be $\mathcal{I}-$convergent to $L \in \mathbb{R}$, if for each $\varepsilon > 0$, $A(\varepsilon) = \{k \in \mathbb{N} : |x_k - L| \geq \varepsilon\} \in \mathcal{I}$. If (x_k) is $\mathcal{I}$-convergent to L, then we write $\mathcal{I}-\lim x = L$.

An admissible ideal $\mathcal{I} \subseteq 2^{\mathbb{N}}$ is said to have the property (AP) if for any sequence $\{A_1, A_2, ...\}$ of mutually disjoint sets of $\mathcal{I}$, there is sequence $\{B_1, B_2, ...\}$ of sets such that each symmetric difference $A_i \Delta B_i$ $(i = 1, 2, ...)$ is finite and $\bigcup\limits_{i=1}^{\infty} B_i \in \mathcal{I}$.

Let σ be a one-to-one mapping of the set of positive integers into itself such that $\sigma^m(n) = \left(\sigma^{m-1}(n)\right)$, $m = 1, 2, 3, ...$ A continuous linear functional Φ on l_∞, the space of real bounded sequences, is said to be an invariant mean or a σ mean, if and only if,

(1) $\Phi(x) \geq 0$, for all sequences $x = (x_n)$ with $x_n \geq 0$ for all n;

(2) $\Phi(e) = 1$, where $e = (1, 1, 1, ...)$;

(3) $\Phi\left(x_{\sigma(n)}\right) = \Phi(x)$ for all $x \in l_\infty$.

The mapping Φ are assumed to be one-to-one such that $\sigma^m(n) \neq n$ for all positive integers n and m, where $\sigma^m(n)$ denotes the mth iterate of the mapping σ at n. Thus, Φ extends the limit functional on c, the space of convergent sequences, in the sense that $\Phi(x) = \lim x$, for all $x \in c$. In case σ is translation mapping $\sigma(n) = n + 1$, the σ mean is often called a Banach limit and V_σ, the set of bounded sequences all of whose invariant means are equal, is the set of almost convergent sequences.

It can be shown that

$$V_\sigma := \left\{ x = (x_n) \in l_\infty : \lim_{m\to\infty} \frac{1}{m} \sum_{k=1}^{m} x_{\sigma^k(m)} = L, \text{ uniformly in } n \right\}.$$

A bounded sequence $x = (x_k)$ is said to be strongly σ-convergent to L, if

$$\lim_{n\to\infty} \frac{1}{n} \sum_{k=0}^{n-1} \left| x_{\sigma^k(m)} - L \right| = 0, \text{ uniformly in } m$$

and in this case we write $x_k \to L[V_\sigma]$. By $[V_\sigma]$, we denote the set of all strongly σ-convergent sequences.

A sequence $x = (x_k)$ is σ-statistically convergent to L, if for every $\varepsilon > 0$, $\lim_{m\to\infty} \frac{1}{m} \left| \left\{ k \leq m : \left| x_{\sigma^k(n)} - L \right|\right.\right.$ 0, uniformly in n.

In this case, we write $S_\sigma - \lim x = L$ or $x_k \to L(S_\sigma)$.

Nuray et al. [36] introduced the concepts of σ-uniform density and $\mathcal{I}_\sigma$-convergence.

Let $A \subseteq \mathbb{N}$ and

$$\begin{aligned} s_n &= \min_m \left| A \cap \left\{ \sigma(m), \sigma^2(m), ..., \sigma^n(m) \right\} \right| \text{ and} \\ S_n &= \max_m \left| A \cap \left\{ \sigma(m), \sigma^2(m), ..., \sigma^n(m) \right\} \right|. \end{aligned}$$

If the following limits exists

$$\underline{V}(A) = \lim_{n\to\infty} \frac{s_n}{n}, \overline{V}(A) = \lim_{n\to\infty} \frac{S_n}{n}$$

then they are called a lower and an upper σ-uniform density of the set A, respectively. If $\underline{V}(A) = \overline{V}(A)$, then $V(A) = \underline{V}(A) = \overline{V}(A)$ is called the σ-uniform density of A.

Denote by $\mathcal{I}_\sigma$ the class of all $A \subseteq \mathbb{N}$ with $V(A) = 0$.

A sequence $x = (x_k)$ is $\mathcal{I}_\sigma$ convergent to the number L if for every $\varepsilon > 0$, $A_\varepsilon = \{k : |x_k - L| \geq \varepsilon\} \in \mathcal{I}_\sigma$, that is $V(A_\varepsilon) = 0$. In this case, we write $\mathcal{I}_\sigma - \lim x = L$.

Menger [19] generalized the metric axioms by associating a distribution function with each pair of points of a set. This system, called a probabilistic metric space, originally a statistical metric space, has been developed extensively by Schweizer and Sklar [16], [17]. The idea of Menger was to use distribution function instead of nonnegative real numbers as values of the metric, which was further developed by several other authors. In this theory, the notion of distance has a probabilistic nature.Namely, the distance between two points x and y is represented by a distribution function F_{xy}, and for $t > 0$, the value $F_{xy}(t)$ is interpreted as the probability that the distance from x to y is less than t. Using this concept, Śherstnev [18] introduced the concept of probabilistic normed spaces. It provides an important area into which many deterministic results of linear normed spaces can be generalized. The studies of continuity properties, linear operators, statistical convergence, and ideal convergence in probabilistic normed spaces have gained many attractions, and such studies have diverse applications into various fields. In [14], Gähler introduced an attractive theory of 2-normed and n-normed spaces in the 1960s. In last few years these spaces are grown up rapidly and many detereministic results of linear normed spaces are obtained for probabilistic normed spaces. In 2005, Golet [15] used the concept of 2-norm of Gähler [14] and presented generalized probabilistic normed space which he called random 2-normed space. Gürdal and Pehlivan ([40], [41]) studied statistical convergence in 2-normed spaces and in 2-Banach spaces. Recently, Savaş [43] defined and studied generalized statistical convergence in random 2-normed space.

Recently, Mohiuddine and Aiyub [23] studied lacunary statistical convergence by introducing the concept θ-statistical convergence in random2-normed space. Their work can be considered as a particular generalization of the statistical convergence. In [22], Mursaleen and Mohiuddine extended the idea of lacunary statistical convergence with respect to the intuitionistic fuzzy normed space, and Debnath [6] investigated lacunary ideal convergence in intuitionistic fuzzy normed linear spaces. Also, lacunary statistically convergent double sequences in probabilistic normed space were studied by Mohiuddine and Savaş in [33]. Yamancı and Gürdal [42], studied lacunary ideal convergence in the n-normed linear spaces.

Let $\mathbb{R}$ denotes the set of reals and $\mathbb{R}_0^+ = [0, \infty)$. A function $f : \mathbb{R} \to \mathbb{R}_0^+$ is called a distribution function if it is non-decreasing and left-continuous with $\inf_{t\in\mathbb{R}} f(t) = 0$ and $\sup_{t\in\mathbb{R}} f(t) = 1$. We will denote the set of all distribution functions by $\mathcal{D}$. Also, a a distance distribution function is a non decreasing function $\mathcal{F}$ defined on $\mathbb{R}^+ = [0, \infty)$ that satisfies $\mathcal{F}(0) = 0$ and $\mathcal{F}(\infty) = 1$; and is left continuous on $(0, \infty)$. Let $\mathcal{D}^+$ denotes the set of all distance distribution functions.

A triangular norm, briefly t-norm, is a binary operation $*$ on $[0, 1]$ which is continuous, commutative, associative, non-decreasing and has 1 as neutral element, i.e., it is the continuous mapping $* : [0, 1] \times [0, 1] \to [0, 1]$ such that for all $a, b, c \in [0, 1]$:

(i) $a * 1 = a$,
(ii) $a * b = b * a$,
(iii) $c * d \geq a * b$ if $c \geq a$ and $d \geq b$,
(iv) $(a * b) * c = a * (b * c)$.

The $*$ operations $a * b = \max\{a + b - 1, 0\}$, $a * b = ab$, and $a * b = \min\{a, b\}$ on $[0, 1]$ are t-norms.

Definition 2 *Let X be a real vector vector space of dimension $d > 1$ (d may be infinite). A real valued function $\|.,.\| : X^2 \to \mathbb{R}$ satisfying the following conditions:*

(i) $\|x_1, x_2\| = 0$, if and only if x_1, x_2 are linearly dependent.
(ii) $\|x_1, x_2\| = \|x_2, x_1\|$ for all $x_1, x_2 \in X$,
(iii) $\|\alpha x_1, x_2\| = |\alpha| \|x_1, x_2\|$, for any $\alpha \in \mathbb{R}$ and
(iv) $\|x_1 + x_2, x_3\| \leq \|x_1, x_3\| + \|x_2, x_3\|$

is called a 2-norm and the pair $(X, \|.,.\|)$ is called a 2-normed space.

Definition 3 *Let X be a real vector vector space of dimension $d > 1$ (d may be infinite),τ be a triangle function (a binary operation on $\mathcal{D}^+$ which is associative, commutative, nondecreasing* *and ε_0 as a unit) and $\mathcal{F} : X \times X \to \mathcal{D}^+$ (for $x, y \in X$, $\mathcal{F}(x, y; t)$ is the value of $\mathcal{F}(x, y)$ at $t \in \mathbb{R}$). Then $\mathcal{F}$ is called a probabilistic norm $(X, \mathcal{F}, \tau)$ a probabilistic 2-normed space if the following conditions are satisfied:*

(i) $\mathcal{F}(x, y; t) = H_0(t)$, if x, y are linearly dependent, where $H_0(t) = 0$ if $t \leq 0$ and $H_0(t) = 1$ if $t > 0$.

(ii) $\mathcal{F}(x, y; t) \neq H_0(t)$, if x, y are linearly dependent.

(iii) $\mathcal{F}(x, y; t) = \mathcal{F}(y, x; t)$, for all $x, y \in X$,

(iv) $\mathcal{F}(\alpha x, y; t) = \mathcal{F}\left(x, y; \frac{t}{|\alpha|}\right)$ for every $t > 0$, $\alpha \neq 0$ and $x, y \in X$,

(v) $\mathcal{F}(x + y, z; t) \geq \tau(\mathcal{F}(x, z; t), \mathcal{F}(y, z; t))$, where $x, y, z \in X$.

If (v) is replaced by $\mathcal{F}(x + y, z; t_1 + t_2) \geq \mathcal{F}(x, z; t_1) * \mathcal{F}(y, z; t_2)$ for all $x, y, z \in X$ and $t_1, t_2 \in \mathbb{R}_0^+$ then $(X, \mathcal{F}, *)$ is called a random 2-normed space.

Definition 4 *Let $(X, \mathcal{F}, *)$ be a random 2-normed space. Then a sequence $x = (x_k)$ is said to be convergent to $x_0 \in X$ with respect to norm $\mathcal{F}$ if for every $\varepsilon > 0$, $t \in (0, 1)$ and non-zero $z \in X$, there exists a positive integer k_0 such that $\mathcal{F}(x_k - x_0, z; \varepsilon) > 1 - t$ whenever $k \geq k_0$. It is denoted by $\mathcal{F}$-$\lim x_k = x_0$.*

Definition 5 *Let $(X, \mathcal{F}, *)$ be a random 2-normed space. Then a sequence $x = (x_k)$ is said to be statistically convergent S^{R2N} convergent to $x_0 \in X$ with respect to norm $\mathcal{F}$ if for every $\varepsilon > 0$, $t \in (0, 1)$ and non-zero $z \in X$,*

$$\delta(\{k \in \mathbb{N} : \mathcal{F}(x_k - x_0, z; \varepsilon) \leq 1 - t\}) = 0.$$

In this case, we write S^{R2N}-$\lim x_k = x_0$.

Definition 6 *Let $(X, \mathcal{F}, *)$ be a random 2-normed space. Then a sequence $x = (x_k)$ is said to be statistically convergent to l with respect to $\mathcal{F}$ if for every $\varepsilon > 0$, $t \in (0, 1)$ and non-zero $z \in X$,*

$$\lim_{n \to \infty} \frac{1}{n} |(\{k \leq n : \mathcal{F}(x_k - l, z; \varepsilon) \leq 1 - t\})| = 0.$$

In this case, we write S^{R2N}-$\lim x_k = l$.

Definition 7 *Let $\theta = \{(k_r, j_u)\}$ be a double lacunary sequence, $A \subset \mathbb{N} \times \mathbb{N}$ and*

$$p_{ru} := \min_{m,n} \left| \left\{ A \cap \left\{ \left(\sigma^k(m), \sigma^j(n) : (k, j) \right) \in I_{ru} \right\} \right\} \right|$$

and

$$P_{ru} := \max_{m,n} \left| \left\{ A \cap \left\{ \left(\sigma^k(m), \sigma^j(n) : (k, j) \right) \in I_{ru} \right\} \right\} \right|$$

If the following limit exist

$$\underline{V_2^\theta}(A) := \lim_{r,u \to \infty} \frac{p_{ru}}{P_{ru}},\ \overline{V_2^\theta}(A) := \lim_{r,u \to \infty} \frac{P_{ru}}{p_{ru}},$$

then they are called a lower lacunary σ-uniform density and an upper lacunary σ-uniform density of the set A, respectively. If $\underline{V_2^\theta}(A) = \overline{V_2^\theta}(A)$, then $V_2^\theta(A) = \underline{V_2^\theta}(A) = \overline{V_2^\theta}(A)$ is called the lacunary σ-uniform density of A.

Denote the paper we take $\mathcal{I}_2^{\sigma\theta}$ as a strongly admissible ideal in $\mathbb{N} \times \mathbb{N}$.

The notion of lacunary $\mathcal{I}_2$-invariant convergence of double sequences in random 2-normed spaces has not been studied previously in the setting of n-normed linear spaces. Motivated by this fact, in this paper, as a variant of $\mathcal{I}$-convergence, the notion of lacunary $\mathcal{I}_2$-invariant convergence is introduced in a random n-normed space, and some important results are established. Finally, the notions of lacunary $\mathcal{I}_2$-invariant Cauchy and lacunary $\mathcal{I}_2^*$-invariant-Cauchy sequences are introduced and studied.

2 Main results

In this study, we introduce the concept of lacunary $\mathcal{I}_2$-invariant convergence, lacunary $\mathcal{I}_2^*$-invariant convergence and lacunary $\mathcal{I}_2$-invariant Cauchy for double sequences in the topology introduced by random 2-normed spaces. We give the relationships among these concepts and prove some important results.

Definition 8 *Let $(X, \mathcal{F}, *)$ be an random 2-normed space. A double sequence $x = (x_{kl})$ in a random 2-normed space $(X, \mathcal{F}, *)$ is said to be $\mathcal{F}^{\sigma\theta}$-convergent to l with respect to random 2-norm $\mathcal{F}$-topology if for every $\varepsilon > 0$, $t \in (0,1)$ and for non-zero $z \in X$ such that*

$$\delta\left(\left\{(k,l) \in I_{r,s} : \mathcal{F}\left(\frac{1}{h_{ru}} \sum_{k,j \in I_{r,u}} \left(x_{\sigma^k(m),\sigma^j(n)}, z\right)\right) \notin \mathcal{N}_l(\varepsilon, t)\right\}\right) = 0,$$

uniformly in n, m. In other ways we can write

$$\left|\left\{(k,l) \in I_{r,s} : \mathcal{F}\left(\lim_{r,s\to\infty} \frac{1}{h_{ru}} \sum_{k,j \in I_{r,u}} \left(x_{\sigma^k(m),\sigma^j(n)}, z\right)\right) \notin \mathcal{N}_l(\varepsilon, t)\right\}\right| = 0,$$

uniformly in n, m and it is denoted by $\mathcal{F}^{\sigma\theta}$-$\lim x_{kl} = l$.

Definition 9 *Let $(X, \mathcal{F}, *)$ be an random 2-normed space, and $\mathcal{I}_2^{\sigma\theta}$ as a strongly admissible ideal in $\mathbb{N} \times \mathbb{N}$. A double sequence $x = (x_{kl})$ in X is said to be lacunary $\mathcal{I}_2^{\sigma\theta}$-invariant convergent to $l \in X$ (with respect to random 2-norm $\mathcal{F}$-topology) if for each $\varepsilon > 0$, $t \in (0,1)$ and for non-zero $z \in X$,*

$$\left\{(r,u) \in \mathbb{N} \times \mathbb{N} : \frac{1}{h_{ru}} \sum_{k,j \in I_{r,u}} \left(x_{\sigma^k(m),\sigma^j(n)}, z\right) \notin \mathcal{N}_l(\varepsilon, t)\right\} \in \mathcal{I}_2^{\sigma\theta},$$

uniformly in n, m and it is denoted by $\mathcal{I}_2^{\sigma\theta}$-$\lim x_{kl} = l$.

Theorem 10 *Let $(X, \mathcal{F}, *)$ be an random 2-normed space. If a sequence $x = (x_{kl})$ is lacunary $\mathcal{I}_2^{\sigma\theta}$-invariant convergent with respect to random 2-norm $\mathcal{F}$, then $\mathcal{I}_2^{\sigma\theta}$-limit is unique.*

Proof. Let us assume that $\mathcal{I}_2^{\sigma\theta}$-$\lim x_{kl} = l_1$, $\mathcal{I}_2^{\sigma\theta}$-$\lim x_{kl} = l_2$, where $l_1 \neq l_2$. Since $l_1 \neq l_2$, select $\varepsilon > 0$, $t \in (0,1)$ and for non-zero $z \in X$ such that $\mathcal{N}_{l_1}(\varepsilon, t)$ and $\mathcal{N}_{l_2}(\varepsilon, t)$ are disjoint neighborhoods of l_1, l_2. Since l_1 and l_2 both are $\mathcal{I}_2^{\sigma\theta}$-limit of the double sequence (x_{kl}), we have

$$A = \left\{(r,u) \in \mathbb{N} \times \mathbb{N} : \frac{1}{h_{ru}} \sum_{k,j \in I_{r,u}} \left(x_{\sigma^k(m),\sigma^j(n)}, z\right) \notin \mathcal{N}_{l_1}(\varepsilon, t)\right\},$$

$$B = \left\{(r,u) \in \mathbb{N} \times \mathbb{N} : \frac{1}{h_{ru}} \sum_{k,j \in I_{r,u}} \left(x_{\sigma^k(m),\sigma^j(n)}, z\right) \notin \mathcal{N}_{l_2}(\varepsilon, t)\right\},$$

both belonging to $\mathcal{I}_2^{\sigma\theta}$. This implies that the sets

$$A^c = \left\{(r,u) \in \mathbb{N} \times \mathbb{N} : \frac{1}{h_{ru}} \sum_{k,j \in I_{r,u}} \left(x_{\sigma^k(m),\sigma^j(n)}, z\right) \in \mathcal{N}_{l_1}(\varepsilon, t)\right\}$$

and

$$B^c = \left\{ (r,u) \in \mathbb{N}\times\mathbb{N} : \frac{1}{h_{ru}} \sum_{k,j\in I_{r,u}} \left(x_{\sigma^k(m),\sigma^j(n)}, z \right) \in \mathcal{N}_{l_2}(\varepsilon,t) \right\}$$

belongs to $\mathcal{F}\left(\mathcal{I}_2^{\sigma\theta}\right)$. In this way, we obtain a contradiction to the fact that the neighborhoods of $\mathcal{N}_{l_1}(\varepsilon,t)$ and $\mathcal{N}_{l_2}(\varepsilon,t)$ of l_1 and l_2 are disjoints. Hence, we have $l_1 = l_2$. This completes the proof. ■

Lemma 11 *Let $(X,\mathcal{F},*)$ be an random 2-normed space. Then one has*

(*i*) If $\mathcal{F}^{\sigma\theta}$-$\lim x_{kl} = l$, then $\mathcal{I}_2^{\sigma\theta}$-$\lim x_{kl} = l$;
(*ii*) If $\mathcal{I}_2^{\sigma\theta}$-$\lim x_{kl} = l_1$ and $\mathcal{I}_2^{\sigma\theta}$-$\lim y_{kl} = l_2$, then $\mathcal{I}_2^{\sigma\theta}$-$\lim (x_{kl}+y_{kl}) = l_1+l_2$;
(*iii*) If $\mathcal{I}_2^{\sigma\theta}$-$\lim x_{kl} = l$ and $\alpha\in\mathbb{R}$, then $\mathcal{I}_2^{\sigma\theta}$-$\lim \alpha x_{kl} = \alpha l$;
(*iv*) If $\mathcal{I}_2^{\sigma\theta}$-$\lim x_{kl} = l_1$ and $\mathcal{I}_2^{\sigma\theta}$-$\lim y_{kl} = l_2$, then $\mathcal{I}_2^{\sigma\theta}$-$\lim (x_{kl}-y_{kl}) = l_1-l_2$

Proof. (*i*) Suppose that $\mathcal{F}^{\sigma\theta}$-$\lim x_{kl} = l$. Let $\varepsilon>0$, $t\in(0,1)$ and for non-zero $z\in X$. Then, there exists positive integer N such that

$$\frac{1}{h_{ru}} \sum_{k,j\in I_{r,u}} \left(x_{\sigma^k(m),\sigma^j(n)}, z \right) \in \mathcal{N}_{l}(\varepsilon,t)$$

for each $k,j>N$. Since the set

$$\begin{aligned} A &= \left\{ (r,u) \in \mathbb{N}\times\mathbb{N} : \frac{1}{h_{ru}} \sum_{k,j\in I_{r,u}} \left(x_{\sigma^k(m),\sigma^j(n)}, z \right) \notin \mathcal{N}_{l_1}(\varepsilon,t) \right\} \\ &\subset \{1,2,...,N-1\} \end{aligned}$$

and the ideal $\mathcal{I}_2^{\sigma\theta}$ is admissible, we have $A\in\mathcal{I}_2^{\sigma\theta}$. This shows that $\mathcal{I}_2^{\sigma\theta}$-$\lim x_{kl} = l$.

(*ii*) Let $\varepsilon>0$, $t\in(0,1)$ and for non-zero $z\in X$. Choose $\mu\in(0,1)$ such that $(1-\mu)*(1-\mu)>(1-t)$. Since $\mathcal{I}_2^{\sigma\theta}$-$\lim x_{kl} = l_1$ and $\mathcal{I}_2^{\sigma\theta}$-$\lim y_{kl} = l_2$, the sets

$$A = \left\{ (r,u) \in \mathbb{N}\times\mathbb{N} : \frac{1}{h_{ru}} \sum_{k,j\in I_{r,u}} \left(x_{\sigma^k(m),\sigma^j(n)}, z \right) \notin \mathcal{N}_{l_1}\left(\frac{\varepsilon}{2},t\right) \right\},$$

$$B = \left\{ (r,u) \in \mathbb{N}\times\mathbb{N} : \frac{1}{h_{ru}} \sum_{k,j\in I_{r,u}} \left(y_{\sigma^k(m),\sigma^j(n)}, z \right) \notin \mathcal{N}_{l_2}\left(\frac{\varepsilon}{2},t\right) \right\},$$

belong to $\mathcal{I}_2^{\sigma\theta}$. Let

$$C = \left\{ (r,u) \in \mathbb{N}\times\mathbb{N} : \frac{1}{h_{ru}} \sum_{k,j\in I_{r,u}} \left(x_{\sigma^k(m),\sigma^j(n)} + y_{\sigma^k(m),\sigma^j(n)}, z \right) \notin \mathcal{N}_{l_1+l_2}(\varepsilon,t) \right\}.$$

Since $\mathcal{I}_2^{\sigma\theta}$ is an ideal, it is sufficient to show that $C\subset A\cup B$. This is equivalent to show that $C^c \supset A^c\cap B^c$ where A^c and B^c belongs to $F\left(\mathcal{I}_2^{\sigma\theta}\right)$. Let $(r,u)\in A^c\cap B^c$, that is $(r,u)\in A^c$ and $(r,u)\in B^c$, and we have

$$\begin{aligned} \mathcal{F}_{z,\left(x_{\sigma^k(m),\sigma^j(n)}+y_{\sigma^k(m),\sigma^j(n)}\right)-(l_1+l_2)}(\varepsilon) &\geq \mathcal{F}_{z,x_{\sigma^k(m),\sigma^j(n)}-l_1}(\varepsilon) * \mathcal{F}_{z,y_{\sigma^k(m),\sigma^j(n)}-l_2}(\varepsilon) \\ &> (1-\mu)*(1-\mu) > (1-t). \end{aligned}$$

Since $(r,u)\in C^c \supset A^c\cap B^c$, we have $C\subset A\cup B\in\mathcal{I}_2^{\sigma\theta}$.

(iii) It is trivial for $\alpha = 0$. Now, let $\alpha \neq 0$, $\varepsilon > 0$, $t \in (0,1)$ and for non-zero $z \in X$. Since $\mathcal{I}_2^{\sigma\theta}$-$\lim x_{kl} = l$, we have

$$A = \left\{ (r,u) \in \mathbb{N} \times \mathbb{N} : \frac{1}{h_{ru}} \sum_{k,j \in I_{r,u}} \left(x_{\sigma^k(m),\sigma^j(n)}, z \right) \notin \mathcal{N}_l(\varepsilon, t) \right\} \in \mathcal{I}_2^{\sigma\theta}.$$

This implies that

$$A^c = \left\{ (r,u) \in \mathbb{N} \times \mathbb{N} : \frac{1}{h_{ru}} \sum_{k,j \in I_{r,u}} \left(x_{\sigma^k(m),\sigma^j(n)}, z \right) \in \mathcal{N}_l(\varepsilon, t) \right\} \in F\left(\mathcal{I}_2^{\sigma\theta} \right).$$

Let $(r,u) \in A^c$. Then we have

$$\begin{aligned} \mathcal{F}_{z,\alpha x_{\sigma^k(m),\sigma^j(n)} - \alpha l}(\varepsilon) &= \mathcal{F}_{z,x_{\sigma^k(m),\sigma^j(n)} - l}\left(\frac{\varepsilon}{|\alpha|} \right) \\ &\geq \mathcal{F}_{z,x_{\sigma^k(m),\sigma^j(n)} - l}(\varepsilon) * \mathcal{F}_0\left(\frac{\varepsilon}{|\alpha|} - \varepsilon \right) \\ &> (1-t) * 1 = (1-t) \end{aligned}$$

So,

$$\left\{ (r,u) \in \mathbb{N} \times \mathbb{N} : \frac{1}{h_{ru}} \sum_{k,j \in I_{r,u}} \left(\alpha x_{\sigma^k(m),\sigma^j(n)}, z \right) \notin \mathcal{N}_{\alpha l}(\varepsilon, t) \right\} \in \mathcal{I}_2^{\sigma\theta}.$$

Hence, $\mathcal{I}_2^{\sigma\theta}$-$\lim \alpha x_{kl} = \alpha l$.

(iv) The result follows from (ii) and (iii). ■

We introduce the concept of lacunary $\mathcal{I}_{2*}^{\sigma\theta}$-invariant convergence closely related to lacunary $\mathcal{I}_2^{\sigma\theta}$-invariant convergence of double sequence in random 2-normed space and show that lacunary $\mathcal{I}_{2*}^{\sigma\theta}$-invariant convergence implies lacunary $\mathcal{I}_2^{\sigma\theta}$-invariant convergence but not conversely.

Definition 12 *Let $(X, \mathcal{F}, *)$ be an random 2-normed space, and $\mathcal{I}_2^{\sigma\theta}$ as a strongly admissible ideal in $\mathbb{N} \times \mathbb{N}$. A double sequence $x = (x_{kl})$ in X is said to be lacunary $\mathcal{I}_{2*}^{\sigma\theta}$-invariant convergent to $l \in X$ (with respect to random 2-norm $\mathcal{F}$) if there exists a set $M_2 \in F\left(\mathcal{I}_2^{\sigma\theta}\right)$, $\left(H = \mathbb{N} \times \mathbb{N} \setminus M_2 \in \mathcal{I}_2^{\sigma\theta}\right)$ such that*

$$\mathcal{F}^{\sigma\theta}\text{-}\lim x_{kl} = l, \ (k,l) \in M_2.$$

In this case, we write $\mathcal{I}_{2*}^{\sigma\theta}$-$\lim x_{kl} = l$ for non-zero $z \in X$.

Theorem 13 *Let $(X, \mathcal{F}, *)$ be an random 2-normed space, and $\mathcal{I}_2^{\sigma\theta}$ as a strongly admissible ideal in $\mathbb{N} \times \mathbb{N}$. If $\mathcal{I}_{2*}^{\sigma\theta}$-$\lim x_{kl} = l$, then $\mathcal{I}_2^{\sigma\theta}$-$\lim x_{kl} = l$. But the converse of the theorem needs not to be true.*

Theorem 14 *Let $(X, \mathcal{F}, *)$ be an random 2-normed space, and let $\mathcal{I}_2^{\sigma\theta}$ satisfy the condition (AP_2).If $x = (x_{kl})$ is a sequence in X such that $\mathcal{I}_2^{\sigma\theta}$-$\lim x_{kl} = l$, then $\mathcal{I}_{2*}^{\sigma\theta}$-$\lim x_{kl} = l$.*

Definition 15 *Let $(X, \mathcal{F}, *)$ be an random 2-normed space, and $\mathcal{I}_2$ be a proper ideal in $\mathbb{N} \times \mathbb{N}$. A double sequence $x = (x_{kl})$ in X is called lacunary $\mathcal{I}_2$-invariant Cauchy sequence or $\mathcal{I}_2^{\sigma\theta}$-Cauchy sequence, if for every $\varepsilon > 0$, there exist numbers $s = s(\varepsilon)$, $t = t(\varepsilon) \in \mathbb{N}$ such that*

$$\left\{ \begin{array}{l} (r,u) \in \mathbb{N} \times \mathbb{N} : \\ \frac{1}{h_{ru}} \sum_{(k,j),(s,t) \in I_{ru}} \left\{ \left(x_{\sigma^k(m),\sigma^j(n)} - x_{\sigma^s(m),\sigma^t(n)}, z \right) \notin \mathcal{N}_l(\varepsilon, t) \right. \end{array} \right\}$$

belongs to $\in \mathcal{I}_2^{\sigma\theta}$.

Definition 16 *A double sequence $x = (x_{kl})$ in X is said to be lacunary $\mathcal{I}_2^*$-invariant Cauchy sequence or $\mathcal{I}_{2^*}^{\sigma\theta}$-Cauchy sequence, if there exists a set $M_2 \in \mathcal{F}\left(\mathcal{I}_2^{\sigma\theta}\right)\left(H = \mathbb{N}\times\mathbb{N} \setminus M_2 \in \mathcal{I}_2^{\sigma\theta}\right)$ such that for every $(k,j), (s,t) \in M_2$*

$$\lim_{k,j,s,t\to\infty}\left(x_{\sigma^k(m),\sigma^j(n)} - x_{\sigma^s(m),\sigma^t(n)}, z\right) = 0.$$

Theorem 17 *If a double $x = (x_{kl})$ in X is $\mathcal{I}_2^{\sigma\theta}$-convergent, then (x_{kl}) is $\mathcal{I}_2^{\sigma\theta}$-Cauchy sequence.*

Theorem 18 *If a double $x = (x_{kl})$ in X is $\mathcal{I}_{2^*}^{\sigma\theta}$-Cauchy sequence, then it is $\mathcal{I}_2^{\sigma\theta}$-Cauchy sequence.*

Theorem 19 *Let $\mathcal{I}_2^{\sigma\theta}$ has property (AP_2). If a double sequence (x_{kl}) is $\mathcal{I}_2^{\sigma\theta}$-Cauchy sequence, then (x_{kl}) is $\mathcal{I}_{2^*}^{\sigma\theta}$-Cauchy sequence.*

References

[1] B. Altay, F. Başar. Some new spaces of double sequences. J. Math. Anal. Appl. **309** (1) (2005), 70–90.

[2] H. Fast. Surla convergence statistique. Colloquium Mathematicum, vol. 2, pp. 241–244, 1951.

[3] J. A. Fridy. On statistical convergence. Analysis, vol. 5, pp. 301–313, 1985, doi:10.1524/anly.1985.5.4.301.

[4] T. Śalát. On statistically convergent sequences of real numbers. Mathematica Slovaca, vol. 30, no. 2, pp. 139–150, 1980.

[5] M. Mursaleen, O. H. H. Edely. Statistical convergence of double sequences. J. Math. Anal. Appl. **288** (2003) 223–231.

[6] P. Debnath. Lacunary ideal convergence in intuitionistic fuzzy normed linear spaces. Computers &Mathematics with Applications, vol. 63, no. 3, pp. 708–715, 2012.

[7] J. A. Fridy, C. Orhan. Lacunary statistical convergence. Pacific J. Math. **160**(1) (1993), 43–51.

[8] C. Çakan, B. Altay. Statistically boundedness and statistical core of double sequences. J. Math. Anal. Appl. **317** (2006) 690–697.

[9] A. Pringsheim. Zur theorie der zweifach unendlichen Zahlenfolgen. Math. Ann. **53** (1900), 289–321.

[10] A. R. Freedman and J. J. Sember. Densities and summability. Pacitific J. Math., **95** (1981), 10–11.

[11] P. Kostyrko, T. Salát, W. Wilezyński. $\mathcal{I}$-Convergence. Real Analysis Exchange Vol. **26**(2), (2001), 669-686.

[12] P. Das, E. Savaş, S.K. Ghosal. On generalizations of certain summability methods using ideals. Appl. Math. Lett. **24** (2011), 1509–1514.

[13] P. Das, P. Kostyrko, W. Wilczyński, P. Malik. $\mathcal{I}$ and $\mathcal{I}^*$-convergence of double sequences. Math. Slovaca, **58** (5) (2008), 605–620.

[14] S. Gähler. 2-metrische raume and ihre topologische struktur. Math. Nachr., vol. 26, pp. 115–148, 1963, doi: 10.1002/mana.19630260109.

[15] I. Golet. On probabilistic 2-normed spaces. Novi Sad J. Math., vol. 35, pp. 95–102, 2006.

[16] B. Schweizer, A. Sklar. Statistical metric spaces. Pacific J. Math., vol. 10, pp. 314–344,1960, doi: 10.2140/pjm.1960.10.313.

[17] B. Schweizer, A. Sklar. Probabilistic Metric Spaces. North-Holland Publishing, New York, NY, USA, 1983.

[18] A. N. Sherstnev. Random normed spaces, problems of completeness. Kazan Gos. Univ. Ucen. Zap., vol. 122, pp. 3–20, 1962.

[19] K. Menger. Statistical metrics. Proc. Nat. Acad. Sci., USA,, vol. 28, pp. 535–537, 1942, doi:10.1073/pnas.28.12.535.

[20] S. Karakus. Statistical convergence on probabilistic normed spaces. Math. Commun., vol. 12, pp. 11–23, 2007.

[21] S. Karakus, K. Demirci, O. Duman. Statistical convergence on intuitionistic fuzzy normed spaces. Chaos, Solitons and Fractals, 35 (2008), pp. 763-769.

[22] M. Mursaleen, S. A. Mohiuddine. On lacunary statistical convergence with respect to the intuitionistic fuzzy normed space." Journal of Computational and Applied Mathematics, vol. 233, no. 2, pp. 142–149, 2009.

[23] S. A. Mohiuddine, M. Aiyub. Lacunary statistical convergence in random 2-normed spaces. Applied Mathematics & Information Sciences, vol. 6, no. 3, pp. 581–585, 2012.

[24] M. Mursaleen. On finite matrices and invariant means. Indian J. Pure and Appl. Math. **10** (1979), 457-460.

[25] M. Mursaleen. Invariant means and some matrix transformations. Tamkang J. Math. **10** (1979), 183-188.

[26] M. Mursaleen, O. H. H. Edely. On the invariant mean and statistical convergence. Appl. Math. Lett. **22** (2009), 1700-1704.

[27] R. A. Raimi. Invariant means and invariant matrix methods of summability. Duke Math. J. **30** (1963), 81-94.

[28] B.C. Tripathy, B. Hazarika, B. Choudhary. Lacunary $\mathcal{I}$-convergent sequences. in: Real Analysis Exchange Summer Symposium, 2009, pp. 56–57.

[29] E. Savaş. Strongly σ-convergent sequences. Bull. Calcutta Math. 81 (1989), 295-300.

[30] E. Savaş. Some sequence spaces involving invariant means. Indian J. Math. **31** (1989), 1-8.

[31] N. Pancaroğlu, F. Nuray. Statistical lacunary invariant summability. Theor. Math. Appl., 3(2) (2013), 71-78.

[32] R.F. Patterson, E. Savaş. On asymptotically lacunary statistical equivalent sequences. *Thai J. Math.,* **4**(2), (2006). 267-272.

[33] E. Savaş. Strong σ-convergent sequences. Bull. Calcutta Math. 81 (1989) 295–300.

[34] U. Ulusu, F. Nuray. Lacunary $\mathcal{I}_\sigma$-convergence. (under review).

[35] U. Ulusu, E. Dundar, F. Nuray. Lacunary $\mathcal{I}_2$-convergence and some properties. International Journal of Analysis and Application, 16(3) (2018), 317-327.

[36] F. Nuray, H. Gok, U. Ulusu. $\mathcal{I}_\sigma$-convergence. Math. Commun. **16** (2011) 531-538.

[37] H. Steinhaus. Sur la convergence ordinaire et la convergence asymptotique. Colloq Math, vol. 2, pp. 73–74, 1951.

[38] E. Dundar, U. Ulusu, F. Nuray. On ideal invariant convergence of double sequences and some properties. Creat. Math. Inf., **27**(2) (2018).

[39] E. Dundar, B. Altay. $\mathcal{I}_2$-convergence and $\mathcal{I}_2$-Cauchy of double sequences. Acta Math. Sci., **34**B(2) (2014), 343-353.

[40] M. Gurdal, S. Pehlivan. Statistical convergence in 2-normed spaces. South. Asian Bull. Math., 33 (2009), pp. 257-264.

[41] M. Gurdal, S. Pehlivan. The statistical convergence in 2-Banach spaces. Thai J. Math., 2(1) (2004), pp. 107-113.

[42] U. Yamancı, M. Gürdal. On Lacunary Ideal Convergence in Random n-Normed Space. Journal of Mathematics, Vol. 2013, Article ID 868457, 8 pages.

[43] E.Savas. On generalized statistical convergence in random 2-normed space. Iranian Journal of Science & Technology, (2012) A4: 417-423.

[44] E. Savaş, F. Nuray. On σ-statistically convergence and lacunary σ-statistically convergence. Math. Slovaca **43**(3) (1993), 309 315.

[45] S. A. Mohiuddine, E. Savaş. Lacunary statistically convergent double sequences in probabilistic normed spaces. Annali dell'Universita di Ferrara, vol. 58, no. 2, pp. 331–339, 2012.

Algebraic Properties of the h(x)-Lucas Sedenion Polynomials

Cennet ÇİMEN*
Hacettepe University, Hacettepe Ankara Chamber of
Industry 1st Organized Industrial Zone Vocational School,
Ankara, Turkey

Abstract

To investigate the normed division algebras is greatly a important topic today. It is well known that the octonions $\mathbf{O}$ and the sedenions $\mathbf{S}$ are the nonassociative, noncommutative, normed division algebra over the real numbers $\mathbb{R}$. In this paper, we study $h(x)$-Lucas sedenion polynomials considering several properties involving these polynomials. Also, we obtained various results for these classes of sedenion numbers include recurrence relations, Binet formula, summation formulas for the $h(x)$-Lucas sedenion polynomials, Cassini's identity, Catalan's identities and d'Ocagne's identity by their Binet forms and also we presented exponentinal generating functions, poisson generating functions for the $h(x)$-Lucas sedenion polynomials

Keywords and Phrases: Lucas polynomials, recurrences, sedenion numbers.

1 Introduction and preliminaries

Sedenions appear in many areas of science, such as electromagnetic theory and linear gravity. Sedenion algebra, which is usually denoted by $\mathbf{S}$, is a 16-dimensional Cayley-Dickson algebra. Sedenion algebra is a non-associative, non-commutative, and non-alternative but power-associative Cayley-Dickson algebra over $\mathbb{R}$. Because of their zero divisors, sedenions do not form a composition algebra or a division algebra. They are hyper-complex numbers, similar to quaternions and octonions.

Throughout this paper, we take the basis elements of $\mathbf{S}$ as $\{e_0, e_1, ..., e_{15}\}$ where $e_1, ..., e_{15}$ are imaginaries and e_0 is the unit elements. A sedenion $\mathbf{S}$ can be written as

$$\mathbf{S} = \sum_{i=0}^{15} a_i e_i \tag{1}$$

where $a_0, a_1, a_2, ..., a_{15}$ are reals.

Imaeda and Imaeda [12] defined a sedenion by

$$\mathbf{S} = (\mathbf{O}_1; \mathbf{O}_2) \in \mathbf{S},\ \mathbf{O}_1, \mathbf{O}_2 \in \mathbf{O}$$

where $\mathbf{O}$ is the octonion algebra over $\mathbb{R}$. As a sedenion is an ordered pair of two octonions, the conjugate of a sedenion $\mathbf{S} = (\mathbf{O}_1; \mathbf{O}_2)$ is defined by $\overline{\mathbf{S}} = (\mathbf{O}_1; -\mathbf{O}_2)$ .Under the Cayley–Dickson process, the product of two sedenions $\mathbf{S}_1 = (\mathbf{O}_1; \mathbf{O}_2)$, $\mathbf{S}_2 = (\mathbf{O}_3; \mathbf{O}_4)$ is

$$\mathbf{S}_1 S_2 = \left(\mathbf{O}_1\mathbf{O}_3 + \rho\overline{\mathbf{O}_4}\mathbf{O}_2; \mathbf{O}_2\overline{\mathbf{O}_3} + \mathbf{O}_4\mathbf{O}_1\right).$$

*Corressponding Author. Authors' E-mail Adresses: cennet.cimen@hacettepe.edu.tr.com (C. Cimen)

After choosing the field parameter $\rho = -1$ and the generator e_8 Imaeda and Imaeda examined the sedenions. By setting $i \equiv e_i$, where $i = 0, 1, , ..., 15$, Cawagas [5] constructed the following multiplication table for the basis of $\mathbf{S}$.The multiplication rules for the basis of $\mathbf{S}$ are listed in the following figure

	*	0	1	2	3	4	5	6	7	8	9	10	11	12	13	14	15
	0	0	1	2	3	4	5	6	7	8	9	10	11	12	13	14	15
C	1	1	−0	3	−2	5	−4	−7	6	9	−8	−11	10	−13	12	15	−14
	2	2	−3	−0	1	6	7	−4	−5	10	11	−8	−9	−14	−15	12	13
H	3	3	2	−1	−0	7	−6	5	−4	11	−10	9	−8	−15	14	−13	12
	4	4	−5	−6	−7	−0	1	2	3	12	13	14	15	−8	−9	−10	−11
	5	5	4	−7	6	−1	−0	−3	2	13	−12	15	−14	9	−8	11	−10
	6	6	7	4	−5	−2	3	−0	−1	14	−15	−12	13	10	−11	−8	9
O	7	7	−6	5	4	−3	−2	1	−0	15	14	−13	−12	11	10	−9	−8
	8	8	−9	−10	−11	−12	−13	−14	−15	−0	1	2	3	4	5	6	7
	9	9	8	−11	10	−13	12	15	−14	−1	−0	−3	2	−5	4	7	−6
	10	10	11	8	−9	−14	−15	12	13	−2	3	−0	−1	−6	−7	4	5
	11	11	−10	9	8	−15	14	−13	12	−3	−2	1	−0	−7	6	−5	4
	12	12	13	14	15	8	−9	−10	−11	−4	5	6	7	−0	−1	−2	−3
	13	13	−12	15	−14	9	8	11	−10	−5	−4	7	−6	1	−0	3	−2
	14	14	−15	−12	13	10	−11	8	9	−6	−7	−4	5	2	−3	−0	1
	15	15	14	−13	−12	11	10	−9	8	−7	6	−5	−4	3	2	−1	−0

Figure 1: The multiplication table for the basis of $\mathbf{S}$.

In [7], Cariow and Cariowa derived an algorithm for the fast multiplication of two sedenions. In [4], Bilgici, Tokeser and Unal defined Fibonacci and Lucas sedenions over the sedenion algebra $\mathbf{S}$. Also, The nth Fibonacci sedenion is $\widehat{F_n} = \sum_{s=0}^{15} F_{n+s} e_s$ and the nth Lucas sedenion is $\widehat{L_n} = \sum_{s=0}^{15} L_{n+s} e_s$.

The Lucas sequence, $\{L_n\}$, is defined by the recurrence relation, for $n > 1$

$$L_{n+1} = L_n + L_{n-1}$$

where $L_0 = 2$, $L_1 = 1$.

The Lucas quaternions have been studied in several papers (see, for example [1, 2, 10 , 11, 18]). Recently, in [2], Ari considered the $h(x)$-Lucas quaternion polynomials, he derived the Binet formula and generating function of $h(x)-$Lucas quaternion polynomial sequence. In [15], Nalli and Haukkanen introduced the $h(x)$-Lucas polynomials.

In this paper, we study $h(x)$-Lucas sedenion polynomials considering several properties involving these polynomials. Also, we obtained various results for these classes of sedenion numbers include recurrence relations, Binet formula, summation formulas for the $h(x)$-Lucas sedenion polynomials, Cassini's identity, Catalan's identities and d'Ocagne's identity by their Binet forms and also we presented Exponentinal generating functions, Poisson generating functions for the $h(x)$-Lucas sedenion polynomials.

2 Algebraic Properties of the h(x)-Lucas Sedenion Polynomials

Definition 1 *Let $h(x)$ be a polynomial with real coefficients. The $h(x)$-Lucas polynomials $\{L_{h,n}(x)\}_{n=0}^{\infty}$ are defined by the recurrence relation*

$$L_{h,n+1}(x) = h(x)L_{h,n}(x) + L_{h,n-1}(x), \quad n \geq 1, \tag{2}$$

with initial conditions $L_{h,0}(x) = 2,\ L_{h,1}(x) = h(x)$.[15]

Definition 2 *Let $h(x)$ be a polynomial with real coefficients. The $h(x)$-Lucas quaternion polynomials $\{T_{h,n}(x)\}_{n=0}^{\infty}$ are defined by the recurrence relation*

$$T_{h,n}(x) = \sum_{s=0}^{3} L_{h,n+s}(x)e_s \tag{3}$$

where $L_{h,n}(x)$ is the n^{th} $h(x)$-Lucas polynomial.[2]

Definition 3 *Let $h(x)$ be a polynomial with real coefficients. The $h(x)$-Lucas sedenion polynomials $\{SL_{h,n}(x)\}_{n=0}^{\infty}$ are defined by the recurrence relation*

$$SL_{h,n}(x) = \sum_{i=0}^{15} L_{h,n+i}(x)e_i \tag{4}$$

where $L_{h,n}(x)$ is the n^{th} $h(x)$-Lucas polynomial.

The conjugate of $SL_{h,n}(x)$ is given by

$$\overline{SL_{h,n}(x)} = L_{h,n}(x)e_0 - \sum_{i=1}^{15} L_{h,n+i}(x)e_i. \tag{5}$$

For $n = 0$,

$$\begin{aligned}
SL_{h,0}(x) &= \sum_{i=0}^{15} L_{h,i}(x)e_i \\
&= L_{h,0}(x)e_0 + L_{h,1}(x)e_1 + ... + L_{h,15}(x)e_{15} \\
&= 2e_0 + h(x)e_1 + \left(h^2(x) + 2\right)e_2 + \left(h^3(x) + 3h(x)\right)e_3 + \left(h^4(x) + 4h^2(x) + 2\right)e_4 \\
&\quad + ... + \left(h^{15}(x) + 15h^{13}(x) + 90h^{11}(x) + 265h^9(x)\right. \\
&\quad \left. + 400h^7(x) + 318h^5(x) + 130h^3(x) + 15h(x)\right)e_{15}
\end{aligned}$$

For $n = 1$,

$$\begin{aligned}
SL_{h,1}(x) &= \sum_{i=0}^{15} L_{h,i+1}(x)e_i \\
&= L_{h,1}(x)e_0 + L_{h,2}(x)e_1 + ... + L_{h,16}(x)e_{16} \\
&= h(x)e_0 + \left(h^2(x) + 2\right)e_1 + \left(h^3(x) + 3h(x)\right)e_2 + \left(h^4(x) + 4h^2(x) + 2\right)e_3 \\
&\quad + ... + \left(h^{16}(x) + 16h^{14}(x) + 104h^{12}(x) + 342h^{10}(x)\right. \\
&\quad \left. + 600h^8(x) + 572h^6(x) + 296h^4(x) + 49h^2(x) + 2\right)e_{15}
\end{aligned}$$

From the recurrence relation(4), using the recurrence relation (2) and some properties of summation formulas, we obtain

$$\begin{aligned} SL_{h,n+1}(x) &= \sum_{i=0}^{15} L_{h,i+1+n}(x)e_i \\ &= \sum_{i=0}^{15} \left(h(x)L_{h,i+n}(x) + L_{h,i+n-1}(x)\right) e_i \\ &= h(x)\sum_{i=0}^{15} L_{h,i+n}(x)e_i + \sum_{i=0}^{15} L_{h,i+n-1}(x)e_i \\ &= h(x)SL_{h,n}(x) + SL_{h,n-1}(x) \end{aligned}$$

and so

$$SL_{h,n+1}(x) = h(x)SL_{h,n}(x) + SL_{h,n-1}(x). \tag{6}$$

In [15], authors stuied properties of $h(x)$-Fibonacci and $h(x)$-Lucas polynomials and present properties of these polynomials and they obtained the following Binet's formula for $L_{h,n}(x)$

$$L_{h,n}(x) = \alpha^n(x) + \beta^n(x) \tag{7}$$

where

$$\alpha(x) = \frac{h(x) + \sqrt{h^2(x)+4}}{2}, \quad \beta(x) = \frac{h(x) - \sqrt{h^2(x)+4}}{2} \tag{8}$$

are roots of the characteristic equation $y^2 - h(x)y - 1 = 0$ of the recurrence relation (2).

Ari in [2] calculated the Binet-style formula for $T_{h,n}(x)$,

$$T_{h,n}(x) = \alpha^*(x)\alpha^n(x) + \beta^*(x)\beta^n(x)$$

where $\alpha(x)$ and $\beta(x)$ as in (8) and $\alpha^*(x) = \sum_{s=0}^{3} \alpha^s(x)e_s$, $\beta^*(x) = \sum_{s=0}^{3} \beta^s(x)e_s$.

The following basic identities are needed for our purpose in proving.

$$\alpha(x) + \beta(x) = h(x), \quad \alpha(x)\beta(x) = -1, \quad \alpha(x) - \beta(x) = \sqrt{h^2(x)+4} \tag{9}$$

and

$$\frac{\alpha(x)}{\beta(x)} = -\alpha^2(x), \; \frac{\beta(x)}{\alpha(x)} = -\beta^2(x). \tag{10}$$

Also,

$$1 + h(x)\alpha(x) = \alpha^2(x), \quad 1 + h(x)\beta(x) = \beta^2(x), \tag{11}$$

and

$$1 + \alpha^2(x) = \alpha(x)\sqrt{h^2(x)+4}, \quad 1 + \beta^2(x) = -\beta(x)\sqrt{h^2(x)+4}. \tag{12}$$

Similarly, the Binet-style formula for $SL_{h,n}(x)$, we obtain

$$SL_{h,n}(x) = \alpha^*(x)\alpha^n(x) + \beta^*(x)\beta^n(x) \tag{13}$$

where $\alpha(x)$ and $\beta(x)$ as in (8) and $\alpha^*(x) = \sum_{s=0}^{15} \alpha^s(x)e_s$, $\beta^*(x) = \sum_{s=0}^{15} \beta^s(x)e_s$.

Theorem 4 *For $n \geq 0$, we have the following identities:*

(i) $SL_{h,n}^2(x) + SL_{h,n+1}^2(x) = \left[\alpha^{2*}(x)\alpha^{2n+1}(x) - \beta^{2*}(x)\beta^{2n+1}(x)\right](\alpha(x) - \beta(x))$

(ii) $\overline{SL_{h,n}(x)} + SL_{h,n}(x) = 2L_{h,n}(x)e_0$

(iii) $(SL_{h,n}(x))^2 = 2L_{h,n}(x)e_0 SL_{h,n}(x) - SL_{h,n}(x)\overline{SL_{h,n}(x)} = SL_{h,n}(x)\left(2L_{h,n}(x)e_0 - \overline{SL_{h,n}(x)}\right).$

(iv) $SL_{h,1}(x) - \alpha(x)SL_{h,0}(x) = -\beta^*(x)\sqrt{h^2(x)+4}$

(v) $SL_{h,1}(x) - \beta(x)SL_{h,0}(x) = \alpha^*(x)\sqrt{h^2(x)+4}$

Proof. (i) Using (13) , (9), (11) and (12) , we get

$$\begin{aligned}
SL^2_{h,n}(x) + SL^2_{h,n+1}(x) &= \left[\alpha^*(x)\alpha^n(x) + \beta^*(x)\beta^n(x)\right]^2 + \left[\alpha^*(x)\alpha^{n+1}(x) + \beta^*(x)\beta^{n+1}(x)\right]^2 \\
&= \alpha^{2*}(x)\alpha^{2n}(x) + \alpha^*(x)\beta^*(x)\alpha^n(x)\beta^n(x) + \beta^*(x)\alpha^*(x)\beta^n(x)\alpha^n(x) + \beta^{2*}(x)\beta^{2n}(x) \\
&\quad + \alpha^{2*}(x)\alpha^{2n+2}(x) + \alpha^*(x)\beta^*(x)\alpha^{n+1}(x)\beta^{n+1}(x) + \beta^*(x)\alpha^*(x)\beta^{n+1}(x)\alpha^{n+1}(x) \\
&\quad + \beta^{2*}(x)\beta^{2n+2}(x) \\
&= \alpha^{2*}(x)\alpha^{2n}(x)(1+\alpha^2(x)) + \beta^{2*}(x)\beta^{2n}(x)(1+\beta^2(x)) \\
&\quad + \alpha^*(x)\beta^*(x)\alpha^n(x)\beta^n(x)(1+\alpha(x)\beta(x)) + \beta^*(x)\alpha^*(x)\beta^n(x)\alpha^n(x)(1+\beta(x)\alpha(x)) \\
&= \alpha^{2*}(x)\alpha^{2n}(x)(1+\alpha^2(x)) + \beta^{2*}(x)\beta^{2n}(x)(1+\beta^2(x)) \\
&= \left(\alpha^{2*}(x)\alpha^{2n+1}(x) - \beta^{2*}(x)\beta^{2n+1}(x)\right)(\alpha(x) - \beta(x)).
\end{aligned}$$

(ii) Using the definition of $\overline{SL_{h,n}(x)}$ and some computations, we have

$$\begin{aligned}
\overline{SL_{h,n}(x)} &= L_{h,n}(x)e_0 - \sum_{i=1}^{15} L_{h,n+i}(x)e_i \\
&= 2L_{h,n}(x)e_0 - \sum_{i=0}^{15} L_{h,n+i}(x)e_i \\
&= 2L_{h,n}(x)e_0 - SL_{h,n}(x),
\end{aligned}$$

and the result

$$\overline{SL_{h,n}(x)} + SL_{h,n}(x) = 2L_{h,n}(x)e_0.$$

(iii) By (ii), (iii) holds.

(v) By using the definition of the $h(x)-$ lucas sedenion polynomials and definition of $\beta^*(x)$ and equation (9), we obtain

$$\begin{aligned}
SL_{h,1}(x) - \alpha(x)SL_{h,0}(x) &= L_{h,1}(x)e_0 + L_{h,2}(x)e_1 + L_{h,3}(x)e_2 + ... + L_{h,16}(x)e_{15} \\
&\quad -\alpha(x)\left[L_{h,0}(x)e_0 + L_{h,1}(x)e_1 + L_{h,2}(x)e_2 + ... + L_{h,15}(x)e_{15}\right] \\
&= \left(L_{h,1}(x) - \alpha(x)L_{h,0}(x)\right)e_0 + \left(L_{h,2}(x) - \alpha(x)L_{h,1}(x)\right)e_1 \\
&\quad + ... + \left(L_{h,16}(x) - \alpha(x)L_{h,15}(x)\right)e_{15} \\
&= -\beta^0(x)(\alpha(x)-\beta(x))e_0 - \beta^1(x)(\alpha(x)-\beta(x))e_0 - ... - \beta^{15}(x)(\alpha(x)-\beta(x))e_{15} \\
&= -\sqrt{h^2(x)+4}(e_0 + \beta^1(x)e_1 + \beta^2(x)e_2 + ... + \beta^{15}(x)e_{15}) \\
&= -\sqrt{h^2(x)+4}\sum_{k=0}^{15}\beta^k(x)e_k \\
&= -\sqrt{h^2(x)+4}\beta^*(x).
\end{aligned}$$

(vi) The proof is similar to part (v) and thus, omitted. ■

Theorem 5 *For* $n \geq 0$,

$$\sum_{k=0}^{n}\binom{n}{k}(h(x))^k SL_{h,k}(x) = SL_{h,2n}(x). \qquad (14)$$

Proof.

$$\begin{aligned}\sum_{k=0}^{n}\binom{n}{k}(h(x))^k SL_{h,k}(x) &= \sum_{k=0}^{n}\binom{n}{k}(h(x))^k\left(\alpha^*(x)\alpha^k(x)+\beta^*(x)\beta^k(x)\right)\\ &= \alpha^*(x)\sum_{k=0}^{n}\binom{n}{k}(h(x))^k\alpha^k(x)+\beta^*(x)\sum_{k=0}^{n}\binom{n}{k}(h(x))^k\beta^k(x)\\ &= \alpha^*(x)(1+h(x)\alpha(x))^n+\beta^*(x)(1+h(x)\beta(x))^n\\ &= \alpha^*(x)\alpha^{2n}(x)+\beta^*(x)\beta^{2n}(x)\\ &= SL_{h,2n}(x)\end{aligned}$$

■

Theorem 6 *The sum of the first m terms of the sequence $\{SL_{h,m}(x)\}_{m=0}^{\infty}$ is given by*

$$\sum_{k=0}^{m} SL_{h,k}(x)=\frac{SL_{h,0}(x)-SL_{h,m}(x)-SL_{h,m+1}(x)-\alpha^*(x)\beta(x)-\beta^*(x)\alpha(x)}{(1-\alpha(x))(1-\beta(x))}. \tag{15}$$

Proof. By using of (13) and (9) , we obtain

$$\begin{aligned}\sum_{k=0}^{m} SL_{h,k}(x) &= \sum_{k=0}^{m}\left(\alpha^*(x)\alpha^k(x)+\beta^*(x)\beta^k(x)\right)\\ &= \alpha^*(x)\sum_{k=0}^{m}\alpha^k(x)+\beta^*(x)\sum_{k=0}^{m}\beta^k(x)\\ &= \alpha^*(x)\left(\frac{1-\alpha^{m+1}(x)}{1-\alpha(x)}\right)+\beta^*(x)\left(\frac{1-\beta^{m+1}(x)}{1-\beta(x)}\right)\\ &= \frac{\alpha^*(x)-\alpha^*(x)\beta(x)-\alpha^*(x)\alpha^{m+1}(x)+\alpha^*(x)\alpha^m(x)\alpha(x)\beta(x)}{(1-\beta(x))(1-\alpha(x))}\\ &\quad+\frac{\beta^*(x)-\beta^*(x)\alpha(x)-\beta^*(x)\beta^{m+1}(x)+\beta^*(x)\alpha(x)\beta(x)\beta^m(x)}{(1-\beta(x))(1-\alpha(x))}\\ &= \frac{SL_{h,0}(x)-SL_{h,m}(x)-SL_{h,m+1}(x)-\alpha^*(x)\beta(x)-\beta^*(x)\alpha(x)}{(1-\alpha(x))(1-\beta(x))}.\end{aligned}$$

■

The following theorem, we state to different Cassini's identity which occur from non-commutativity of sedenion multiplication.

Theorem 7 (Cassini's identities) *For any naturel number n, Cassini's identity for the $h(x)$-Lucas sedenion polynomials the following identities are hold:*

$$\begin{aligned}SL_{h,n+1}(x)SL_{h,n-1}(x)-SL_{h,n}^2(x) &= (-1)^n\sqrt{h^2(x)+4}\,(\beta^*(x)\alpha^*(x)\beta(x)\\ &\quad-\alpha^*(x)\beta^*(x)\alpha(x))\end{aligned} \tag{16}$$

$$\begin{aligned}SL_{h,n-1}(x).SL_{h,n+1}(x)-SL_{h,n}^2(x) &= (-1)^n\sqrt{h^2(x)+4}\,(\alpha^*(x)\beta^*(x)\beta(x)\\ &\quad-\beta^*(x)\alpha^*(x)\alpha(x))\end{aligned} \tag{17}$$

Proof. Using the Binet's formula in equation (16) , we get

$$\begin{aligned}SL_{h,n+1}(x)SL_{h,n-1}(x)-SL_{h,n}^2(x) &= \left[\alpha^*(x)\alpha^{n+1}(x)+\beta^*(x)\beta^{n+1}(x)\right]\left[\alpha^*(x)\alpha^{n-1}(x)+\beta^*(x)\beta^{n-1}(x)\right]\\ &\quad-\left(\alpha^*(x)\alpha^n(x)+\beta^*(x)\beta^n(x)\right)^2.\end{aligned}$$

If necessary calculations are made, we obtain

$$SL_{h,n+1}(x)SL_{h,n-1}(x)-SL_{h,n}^{2}(x)=(-1)^{n}\sqrt{h^{2}(x)+4}\left(\beta^{*}(x)\alpha^{*}(x)\beta(x)-\alpha^{*}(x)\beta^{*}(x)\alpha(x)\right).$$

In a similar way, using the Binet's formula in equation (17) , we obtain

$$\begin{aligned}SL_{h,n-1}(x)SL_{h,n+1}(x)-SL_{h,n}^{2}(x) &= \left[\alpha^{*}(x)\alpha^{n-1}(x)+\beta^{*}(x)\beta^{n-1}(x)\right]\left[\alpha^{*}(x)\alpha^{n+1}(x)+\beta^{*}(x)\beta^{n+1}(x)\right]\\ &\quad-\left(\alpha^{*}(x)\alpha^{n}(x)+\beta^{*}(x)\beta^{n}(x)\right)^{2}\\ &= (-1)^{n}\sqrt{h^{2}(x)+4}\left(\alpha^{*}(x)\beta^{*}(x)\beta(x)-\beta^{*}(x)\alpha^{*}(x)\alpha(x)\right)\end{aligned}$$

which is desired. Thus, the identities are proved. ■

Theorem 8 (Catalan identity) *For every nonnegative integer numbers n and r such that $r\leq n$, Catalan identity for the $h(x)$-Lucas sedenion polynomials the following identities are hold:*

$$\begin{aligned}SL_{h,n+r}(x).SL_{h,n-r}(x)-SL_{h,n}^{2}(x) &= (-1)^{n-r}\left(\alpha^{r}(x)-\beta^{r}(x)\right) \qquad (18)\\ &\quad\left(\alpha^{*}(x)\beta^{*}(x)\alpha^{r}(x)-\beta^{*}(x)\alpha^{*}(x)\beta^{r}(x)\right)\\ SL_{h,n-r}(x).SL_{h,n+r}(x)-SL_{h,n}^{2}(x) &= (-1)^{n-r}\left(\alpha^{r}(x)-\beta^{r}(x)\right) \qquad (19)\\ &\quad\left(\beta^{*}(x)\alpha^{*}(x)\alpha^{r}(x)-\alpha^{*}(x)\beta^{*}(x)\beta^{r}(x)\right)\end{aligned}$$

Proof. Using the Binet's formula in equation (18) , we get

$$\begin{aligned}SL_{h,n+r}(x)SL_{h,n-r}(x)-SL_{h,n}^{2}(x) &= \left[\alpha^{*}(x)\alpha^{n+r}(x)+\beta^{*}(x)\beta^{n+r}(x)\right]\left[\alpha^{*}(x)\alpha^{n-r}(x)+\beta^{*}(x)\beta^{n-r}(x)\right]\\ &\quad-\left(\alpha^{*}(x)\alpha^{n}(x)+\beta^{*}(x)\beta^{n}(x)\right)^{2}.\end{aligned}$$

If necessary calculations are made, we obtain

$$SL_{h,n+r}(x)SL_{h,n-r}(x)-SL_{h,n}^{2}(x)=(-1)^{n-r}\left(\alpha^{r}(x)-\beta^{r}(x)\right)\left(\alpha^{*}(x)\beta^{*}(x)\alpha^{r}(x)-\beta^{*}(x)\alpha^{*}(x)\beta^{r}(x)\right).$$

In a similar way, using the Binet's formula in equation (19) , we obtain

$$\begin{aligned}SL_{h,n-r}(x)SL_{h,n+r}(x)-SL_{h,n}^{2}(x) &= \left[\alpha^{*}(x)\alpha^{n-r}(x)+\beta^{*}(x)\beta^{n-r}(x)\right]\left[\alpha^{*}(x)\alpha^{n+r}(x)+\beta^{*}(x)\beta^{n+r}(x)\right]\\ &\quad-\left(\alpha^{*}(x)\alpha^{n}(x)+\beta^{*}(x)\beta^{n}(x)\right)^{2}\\ &= (-1)^{n-r}\left(\alpha^{r}(x)-\beta^{r}(x)\right)\left(\beta^{*}(x)\alpha^{*}(x)\alpha^{r}(x)-\alpha^{*}(x)\beta^{*}(x)\beta^{r}(x)\right)\end{aligned}$$

which is desired. Thus, the identities are proved. ■

Theorem 9 (d'Ocagne's identity) *Suppose that n is a nonnegative integer number and m any natural number. If $m>n$ then:*

$$\begin{aligned}SL_{h,m}(x)SL_{h,n+1}(x)-SL_{h,m+1}(x)SL_{h,n}(x) &= \sqrt{h^{2}(x)+4}\left(\beta^{*}(x)\alpha^{*}(x)\beta^{m}(x)\alpha^{n}(x)\right.(20)\\ &\quad\left.-\alpha^{*}(x)\beta^{*}(x)\alpha^{m}(x)\beta^{n}(x)\right).\end{aligned}$$

Proof. Using the Binet's formula in equation (20) and if necessary calculations are made, we obtain

$$\begin{aligned}SL_{h,m}(x)SL_{h,n+1}(x)-SL_{h,m+1}(x)SL_{h,n}(x) &= \left[\alpha^{*}(x)\alpha^{m}(x)+\beta^{*}(x)\beta^{m}(x)\right]\left[\alpha^{*}(x)\alpha^{n+1}(x)+\beta^{*}(x)\beta^{n+1}(x)\right.\\ &\quad-\left[\alpha^{*}(x)\alpha^{m+1}(x)+\beta^{*}(x)\beta^{m+1}(x)\right]\left[\alpha^{*}(x)\alpha^{n}(x)+\beta^{*}(x)\beta^{n}(\right.\\ &= \sqrt{h^{2}(x)+4}\left(\beta^{*}(x)\alpha^{*}(x)\beta^{m}(x)\alpha^{n}(x)-\alpha^{*}(x)\beta^{*}(x)\alpha^{m}(x)\beta^{n}(\right.\end{aligned}$$

So, the proof is complete. ■

We now derive Exponential generating functions for the $h(x)$-Lucas sedenion polynomials. The Exponential generating function of a sequence $\{b_k\}_{k=0}^{\infty}$ is given by

$$EG(b_k,l)=\sum_{k=0}^{\infty}b_k\frac{l^k}{k!}.$$

Theorem 10 *The Exponential generating function for the $h(x)$-Lucas sedenion polynomials the following identities are hold:*

$$\sum_{k=0}^{\infty} \frac{SL_{h,k}(x)}{k!} l^k = \alpha^*(x) e^{\alpha(x)l} + \beta^*(x) e^{\beta(x)l} \tag{21}$$

Proof. Using the Binet's formula in equation (20) , we get

$$\begin{aligned} \sum_{k=0}^{\infty} \frac{SL_{h,k}(x)}{k!} l^k &= \sum_{k=0}^{\infty} \left(\alpha^*(x)\alpha^k(x) + \beta^*(x)\beta^k(x) \right) \frac{l^k}{k!} \\ &= \alpha^*(x) \sum_{k=0}^{\infty} \frac{(\alpha(x)l)^k}{k!} + \beta^*(x) \sum_{k=0}^{\infty} \frac{(\beta(x)l)^k}{k!} \\ &= \alpha^*(x) e^{\alpha(x)l} + \beta^*(x) e^{\beta(x)l}. \end{aligned}$$

■

Theorem 11 *The Poisson generating functions for the sequence of the $h(x)$-Lucas sedenion polynomials are*

$$\sum_{k=0}^{\infty} \frac{SL_{h,k}(x)}{k!} l^k e^{-l} = \frac{\alpha^*(x) e^{\alpha(x)l} + \beta^*(x) e^{\beta(x)l}}{e^l}. \tag{22}$$

Proof. Since $PG(b_n, x) = e^{-l} EG(b_n, x)$, we have the result by (21) . ■

3 Conclusions

In this paper;

- We study $h(x)$-Lucas sedenion polynomials considering several properties involving these polynomials.
- We obtained various results for these classes of sedenion numbers include recurrence relations, Binet formula, summation formulas for the $h(x)$-Lucas sedenion polynomials, Cassini's identity, Catalan identity and d'Ocagne's identity by their Binet forms.
- We presented Exponentinal generating functions, Poisson generating functions for the $h(x)$-Lucas sedenion polynomials.

References

[1] Akyigit, M., Kosal, H. H., Tosun, M., Fibonacci Generalized Quaternions, Advances in Applied Clifford Algebras, Vol. 24(3) (2014), 631–641.

[2] Ari, K., On $h(x)$-Lucas quaternion polynomials, Ars Combinatoria, Vol.121(2015), 291–303.

[3] Baez, John., The octonions. Bulletin of the American Mathematical Society, 39(2):145–205, 2002.

[4] Bilgici G., Tokeser U. and Unal Z., Fibonacci and Lucas Sedenions, Journal of Integer Sequences, Vol. 20 (2017), Article 17.1.8.

[5] Cawagas, R. E., On the structure and zero divisors of the Cayley-Dickson sedenion algebra, Discuss. Math. Gen. Algebra Appl. 24(2004), 251–265.

[6] Catarino, P., A note on $h(x)$-Fibonacci quaternion polynomials, Chaos, Solitons Fractals, Vol. 77 (2015), 1–5.

[7] Cariow, A. and Cariowa, G., An algorithm for fast multiplication of sedenions, Inform. Process. Lett.113(2013), 324–331.

[8] Gürlebeck, K., Spröig, W., Quaternionic and Cliford Calculus for Physicists and Engineers, John Wiley & Sons, 1997.

[9] Halici, S., On Fibonacci quaternions, Advances in Applied Clifford Algebras, Vol. 22(2) (2012), 321–327.

[10] Halici, S., On Fibonacci quaternions, Advances in Applied Clifford Algebras, Vol. 22(2) (2012), 321–327.

[11] Iyer, M. R., Note on Fibonacci quaternions, Fibonacci Q. 7(3) (1969), 225–229.

[12] Imaeda, K. and Imaeda, M., Sedenions: algebra and analysis, Appl. Math. Comput. 115(2000), 77–88.

[13] John, H. Conway and Derek, A. Smith, On quaternions and octonions: Their geometry. AK Peters, Wellesley, Massachusetts, 2003.

[14] Koshy, T., Fibonacci and Lucas numbers with applications. Wiley-Intersection Pub., 2001.

[15] Nalli, A., Haukkanen, P., On generalized Fibonacci and Lucas polynomials, Chaos, Solitons Fractals, Vol. 42 (2009), 3179–3186.

[16] Niederreiter, H., Spanier, J.(Eds.), Monte Carlo and Quasi-Monte Carlo Methods, vol. 1998, Springer, Berlin, 2000.

[17] Vajda S., Fibonacci and Lucas numbers and the Golden section. Ellis Horwood Limited Publ., England, 1989.

[18] Tan, E., Yilmaz, S., Sahin, M., On a new generalization of Fibonacci Quaternions, Chaos, Solitons Fractals, Vol. 82 (2016), 1–4.

Article between 290-296 pages has been withdrawn

Classification Of Eggs With Image Processing Techniques By Using Machine Vision System

Birkan BUYUKARIKAN *
Department of Computer Technology,
Sarayönü Vocational School,
Selçuk University,
Konya/TURKEY

Abstract

It is important condition health and economically because the egg industry to quickly and easily separate eggs according to their qualities. To purpose for eggs classification was created a machine vision system that is not affected by external conditions such as camera, lighting and computer. Images were increased with image processing techniques (noise and rotation) using brown and white eggs (dirty, broken and solid). Egg images YCbCr color space was transformed and processed with image processing techniques. The resulting images were classified as solid and failing. Accordingly, the experiments were validated using 48 egg surface images with accuracy was 0.85, specificity was 0.97, and sensitivity was 0.75.

Keywords: Egg, image processing techniques, machine vision, classification.

1 Introduction

The separation of defective eggs from quality eggs is an important issue both in terms of health and economics [1]. Especially the egg shell crack is a necessary parameter that must be determined before sending market for consumption. Storing broken eggs and solid eggs in the same location creates bacterial interaction. For this reason, it is a necessity to detect the eggshell crack due to food safety [2].

There are many studies on egg shell quality determination in the literature. When studies that use machine vision or image processing techniques are examined;

Dehrouyeh et al. (2010) received egg images under different lighting conditions and obtained dirty and bloody egg shells with image processing techniques. They used HSI color space and were close to 90% accurate [3]. Arivazhagan et al. (2013) obtained image processing techniques using YIQ color space for detecting blood, dirt, and cracks in egg shells. In addition, these images were obtained under different lighting conditions in the machine vision system [4]. Mansoory et al. (2011) have developed an algorithm based on fuzzy thresholding and SUSAN edge detection with digital image processing for egg crack detection. As a result, they achieved 97% success [5]. Alaşahan (2010) determined the external and internal quality characteristics of different kinds of eggs by classical and numerical image analysis [6]. Ribeiro et al. (2000) used an artificial vision system to identify defective eggs. They detected the pixels in the defective region with the genetic algorithm and made the classification system [7]. Wang et al. (2009) performed pixel-based image analysis to determine egg freshness [8]. Pourreza et al. (2008) presented methods for classifying dirty and cracked eggs at the packaging stage, utilizing the discontinuity in the image [9]. Yoon et al. (2012) formed a system

* *E-mail address:* birkan@selcuk.edu.tr

that uses image processing techniques to detect cracks that adversely affect egg quality. The system was a structure that could control 20 eggs at the same time and the success rate of the system was about 95% [10].

In this study, a machine vision system was established. Dirty, broken and solid eight eggs were increased with image processing techniques and 48 images were obtained. Visual Studio C# programming language and AForge.Net framework using image processing algorithms.

2 Machine Vision System and Software

A Machine Vision System

Machine vision system was established to detect egg quality. The distance between the scene and the camera should be about 80 cm. The cabin size was 30x30x85cm. The size of the pictures is taken as 640x480.

For the machine vision system, the skeleton of the system and the system were closed with the help of cartons to keep the system as far away from the outside conditions as possible. It was placed on top of the camera and lighting system for a display cabinet. In addition, a black fabric was placed under the cabin. The imaging system is shown in Figure 1.

Figure 1: Imaging system

Images were taken from the system using a 5.2MP camera, which is a combination of imaging and illumination (Figure 2).

Figure 2: Imaging system

B Software

AForge.Net is an open source framework created using C# programming language [11].

The system used the Visual Studio C# programming language for capturing and processing images from the camera, and the AForge.Net framework for some operations. Figure 3 shows the flow diagram of the software.

Egg images are made 200x200 and egg images are obtained by applying noise (salt-pepper) and rotation process (0°, 90° and 180°) with image processing techniques. The pre-processed image is transformed from RGB to YCbCr color space and the median filter is applied. Egg boundaries are drawn with AForge.Net's blob analysis. If the black pixels within the boundaries are too large, the image is considered to be broken or dirty. These eggs are counted by a counter.

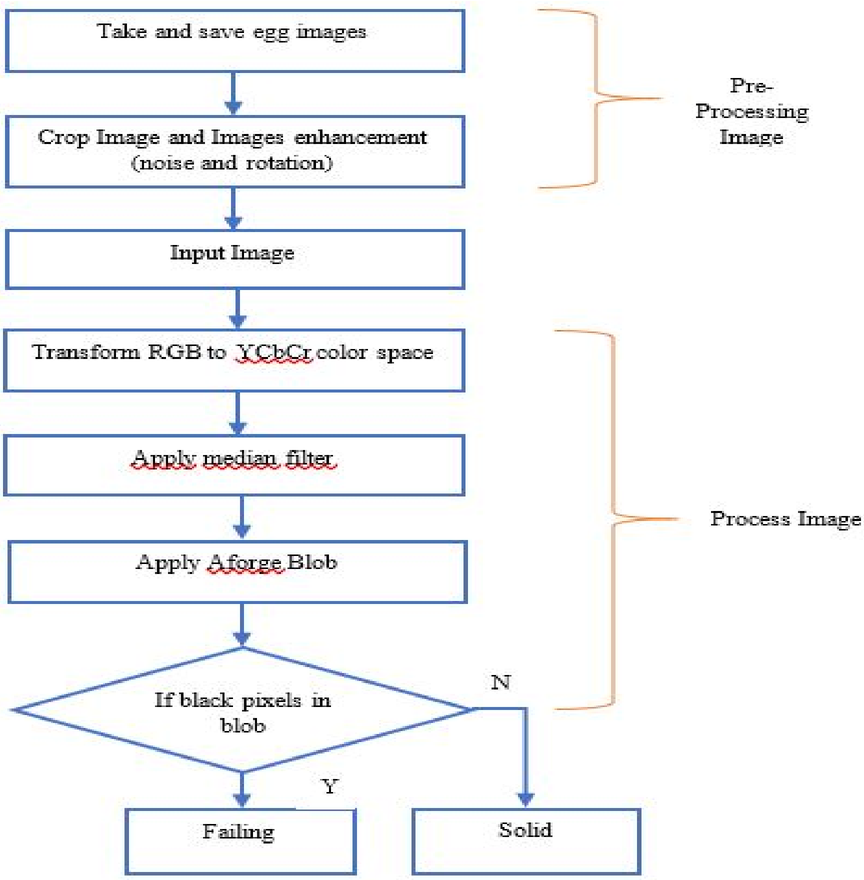

Figure 3: Software flow diagram

C Determination of Egg quality Image Processing Techniques

RGB color space

RGB tri-color rays (red, green, and blue) are mathematically expressed. The 3-dimensional coordinate system is shown in Figure 4 [12]. Red, green, and blue components are loaded in each pixel to create a color image. Each pixel forms a color vector and takes a value between 0 and 255 [13].

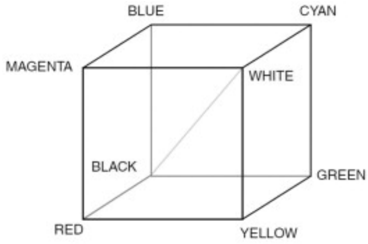

Figure 4: RGB color space

YCbCr color space

Y is the non-linear luma component that represents brightness [14]. The reason why the YCbCr color space is used, the Y component is color independent. This may prevent problems from occurring due to lighting problems [15]. YCbCr color space in the RGB color cube is shown in Figure 5 [16].

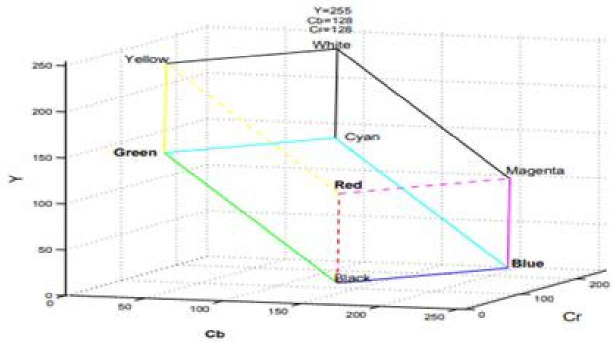

Figure 5: YCbCr color space

Conversion from RGB color space to YCbCr color space is given in equation 1.

$$\begin{bmatrix} Y \\ Cb \\ Cr \end{bmatrix} = \begin{bmatrix} 16 \\ 128 \\ 128 \end{bmatrix} + \begin{bmatrix} 0.279 & 0.504 & 0.098 \\ -0.148 & -0.291 & 0.439 \\ 0.439 & -0.368 & -0.071 \end{bmatrix} \begin{bmatrix} R \\ G \\ B \end{bmatrix} \quad (1)$$

Median filter and Blob analysis

Median filter is used to reduce impulsive or salt-pepper noise [17]. Blob analysis is a technique used in image processing applications to detect objects from two-dimensional objects [18]. Blob analysis using the AForge.Net framework [19]; the eggs inside the image were detected.

D Egg Samples

Sample eggs are shown in the Figure 6. It is necessary for the egg to stand still to control the egg surface. So the cut egg carton was placed under the egg.

Figure 6: Egg samples

E Classification Criteria

Four different classification model metrics were used to measure the classification performance of the proposed model: accuracy (2), precision (3), sensitivity (4) and specificity (5). The classification metrics are calculated using Table 1.

Table 1: Classification metrics

		Predicted	
		S1	S2
True	S1	A	B
	S2	C	D

$$Accuracy = \frac{A+C}{A+B+C+D} \tag{2}$$

$$Precision = \frac{A}{A+C} \tag{3}$$

$$Sensitivity = \frac{A}{A+B} \tag{4}$$

$$Specificity = \frac{D}{C+D} \tag{5}$$

3 Results

After applying the YCbCr color space and median filter to the egg, the resulting image was placed in a circle or a rectangle according to the blob analysis. If the ratio of black pixels in the circle is too low, it shows that it is a sturdy egg (a yellow circle was drawn). If the black pixel is too large, the egg has been shown to be unstable and is shown in a red circle or rectangle. These ratios are calculated according to the pixel values of the width and height of the eggs. Some of the results obtained in Figure 7 are shown.

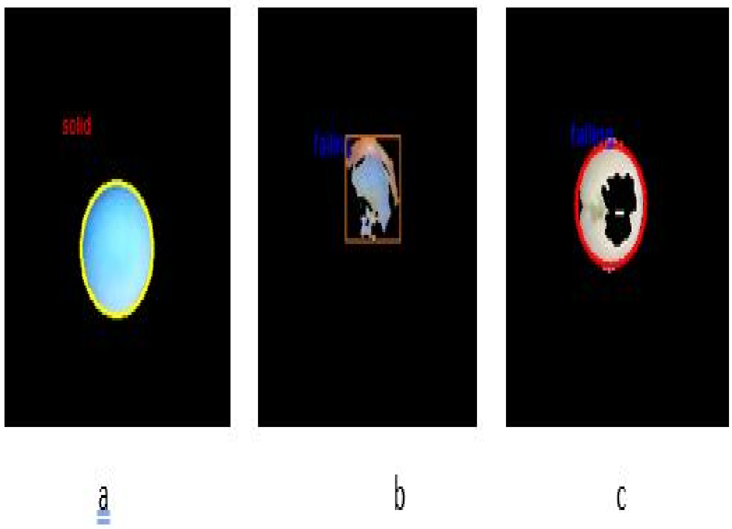

Figure 7: Processed image sample a)white solid b)brown empty c) broken egg

In Table 2, egg quality classification was successfully performed with image processing techniques. Accordingly, the experiments were validated using 48 egg surface images with accuracy was 0.85, specificity was 0.97, and sensitivity was 0.75.

Table 2: Classification results

		Predicted	
		Solid	Broken and Dirty
True	Solid	6	6
	Broken and Dirty	1	35

Due to the light reflection on the solid brown egg, egg quality is found incorrect.

4 Conclusions

Separation from other eggs from the eggs to egg quality is a necessity. In particular, it is important to check the food consumption items untouched by human hands system in terms of both health and accurate detection of eggs.

Image processing software was created using the AForge.Net framework with the Visual Studio C# software language in the machine vision system for separating and classifying quality eggs from other eggs. Egg images were classified using image processing techniques. However, the results of the brown eggs that were solid were not found correctly. As a result of the light shining on this situation, it was determined that the egg was seen as empty. For this reason, the necessity of the lighting conditions must be taken into consideration.

References

[1] D. M.C.Garcia-Alegre, J.Enciso, A.Ribeiro, D. Guinea, 1998, To an Automatic Visual Inspection of Egg-Shell Defects, [Online],

http://citeseerx.ist.psu.edu/viewdoc/download;jsessionid=CA454E84B04C3CADFE1275 61F437D090?doi=10.1.1.15.7569 rep=rep1type=pdf (9.8.2018).

[2] Y. Li, S. Dhakal, Y.Peng, A machine vision system for identification of micro-crack in egg Shell, Journal of Food Engineering, 109, (2012): 127-134.

[3] M.H. Dehrouyeh, M. Omid, H. Ahmadi, S.S. Mohtasebi, M. Jamzad, Grading and Quality Inspection of Defected Eggs Using Machine Vision, International Journal of Advance Science and Technology, 16, (2010):43-50.

[4] S. Arivazhagan, R.N. Shebiah, H. Sudharsan, R.R. Kannan, R. Ramesh, External and Internal Defect Detection of Egg using Machine Vision, Journal of Emerging Trends in Computing and Information Sciences, 4 (3), (2013):257-262.

[5] M.S. Mansoory, M. Ashtiyani, H. Sarabadani, Automatic Crack Detection in Eggshell Based on SUSAN Edge Detector Using Fuzzy Thresholding, Canadian Center of Science and Education, 5 (6), (2011):117-125.

[6] S. Alaşahan, 2010, Farklı Kanatlı Türlerinde Yumurta Kalite Özelliklerinin Sayısal Görüntü Analizi İle Belirlenmesi, Selçuk University, PhD thesis, Konya.

[7] A. Ribeiro, M.C. García-Alegre, D. Guinea, G. Cristobal, Automatic Rules Generation by G.A. For Eggshell Defect Classification, European Congress on Computational Methods in Applied Sciences and Engineering, 11-14 September, Barcelona, (2000):1-11.

[8] Q. Wang, X. Deng, Y. Ren, Y. Ding, L. Xiong, Z. Ping, Y. Wen, S. Wang, Egg freshness detection based on digital image technology, Scientific Research and Essay, 4 (10), (2009):1073-1079.

[9] H.R. Pourreza, R.S. Pourreza, S. Fazeli, B. Taghizadeh, Automatic Detection of Eggshell Defects Based on Machine Vision, Journal of Animal and Veterinary Advances, 7 (10), (2008):1200-1203.

[10] S.C. Yoon, K.C. Lawrence, D.R. Jones, G.W. Heitschmidt, Improved Modified Pressure Imaging And Software For Egg Micro-Crack Detection And Egg Quality Grading, American Society of Agricultural and Biological Engineers, 28 (2), (2012):283-293.

[11] X. Laisheng, and Z. Yuandan, Bread Shrimp Microbe Growth Simulation and Prediction System Based on Neural Network, International Journal of Intelligent Information Systems, 5 (2), (2016):25-36.

[12] N. Razmjooya, B.S. Mousavi, F. Soleymani, A Hybrid Neural Network Imperialist Competitive Algorithm for Skin Color Segmentation, Mathematical and Computer Modelling, 57 (3-4), (2013):848-856.

[13] R.C. Gonzalez, R.E. Woods, 2008, Digital Image Processing, 3rd edition, New York: Prentice Hall.

[14] V. Vezhnevets, V. Sazonov, A. Andreeva, A Survey on Pixel-Based Skin Color Detection Technique, Proc. Graphicon-2003, Moscow, September, (2003):85-92.

[15] C. Lin, Face detection in complicated backgrounds and different illumination conditions by using YCbCr color space and neural network, Pattern Recognition Letters, 28, (2007):2190-2200.

[16] http://www.robots.ox.ac.uk/ teo/thesis/Thesis/deCampos3DHandTrackingApp.pdf

[17] J. Tukey, 1977, Exploratory Data Analysis. Addison-Wesley, Menlo Park.

[18] I. Jahr, 2003, Lexikon der Industriellen Bildverarbeitung, pthmediaberatung, Würzburg Germany.

[19] AForge.Net, 2018, Blobs Processing, [online] http://www.aforgenet.com/framework/features /blobs_processing.html (10.8.2018).

Harmo-Frank Matrix

Efruz Özlem MERSİN *
Department of Mathematics,
Aksaray University,
Aksaray/TURKEY

Ayşe Dilek MADEN
Department of Mathematics,
Selçuk University,
Konya/TURKEY

Mustafa BAHŞİ
Education Faculty,
Aksaray University,
Aksaray/TURKEY

Abstract

In this study, by generalizing Frank matrix defined by

$$F = (f_{ij})_{i,j=1}^{n} = \begin{cases} n+1-\max(i,j)\ , & i > j-2 \\ 0\ , & \text{otherwise,} \end{cases}$$

we first define Harmo-Frank matrix of the form

$$H = (h_{ij})_{i,j=1}^{n} = \begin{cases} h_{n+1-\max(i,j)} & , \quad i > j-2 \\ 0\ , & \text{otherwise,} \end{cases}$$

where h_k denotes the kth harmonic number. Then, we investigate some properties of matrix H, such as LU decomposition and characteristic polynomial.

Keywords: Frank matrix, harmonic numbers, LU decomposition, characteristic polynomial.

1 Introduction

In 1958, Frank [1] defined an $n \times n$ lower Hessenberg matrix $F = (f_{ij})$ by the rule

$$(f_{ij})_{i,j=1}^{n} = \begin{cases} n+1-\max(i,j)\ , & i > j-2 \\ 0\ , & \text{otherwise.} \end{cases}$$

The matrix F is called Frank matrix [2,3] and F is of the form

$$F = \begin{bmatrix} n & n-1 & 0 & \cdots & 0 & 0 \\ n-1 & n-1 & n-2 & \cdots & 0 & 0 \\ n-2 & n-2 & n-2 & \cdots & 0 & 0 \\ \vdots & \vdots & \vdots & \ddots & \vdots & \vdots \\ 2 & 2 & 2 & \cdots & 2 & 1 \\ 1 & 1 & 1 & \cdots & 1 & 1 \end{bmatrix}.$$

The matrix F is a nonsingular matrix and $\det(F) = 1$ [2]. Also, Hake [2] computed the determinant, inverse, LU decomposition and characteristic polynomial of matrix F.

* *E-mail address:* efruzmersin@gmail.com

Varah [3] introduced a generalization of the Frank matrices and examined its eigenvalues and eigenvectors.

Let we define an $n \times n$ matrix $H = (h_{ij})$ by the rule

$$(h_{ij})_{i,j=1}^{n} = \begin{cases} h_{n+1-\max(i,j)}\ , & i > j-2 \\ 0\ , & \text{otherwise,} \end{cases}$$

where h_n is the nth harmonic number defined by $h_0 = 0$ and $h_n = \sum_{k=1}^{n} \frac{1}{k}$ for $n = 1, 2, \ldots$. Since the matrix H is in the same form as the Frank matrix F and its elements consist of harmonic number, we call the matrix H as Harmo-Frank matrix. Then, the matrix H is of the form

$$H = \begin{bmatrix} h_n & h_{n-1} & 0 & \cdots & 0 & 0 \\ h_{n-1} & h_{n-1} & h_{n-2} & \cdots & 0 & 0 \\ h_{n-2} & h_{n-2} & h_{n-2} & \cdots & 0 & 0 \\ \vdots & \vdots & \vdots & \ddots & \vdots & \vdots \\ h_2 & h_2 & h_2 & \cdots & h_2 & h_1 \\ h_1 & h_1 & h_1 & \cdots & h_1 & h_1 \end{bmatrix}.$$

In this study, we investigate some properties of matrix H, such as determinant, inverse and characteristic polynomial.

2 Main Results

Theorem 2.1. The determinant of $n \times n$ matrix Hsatisfies

$$\det(H) = \frac{1}{n!}.$$

Proof. After row-column operations are applied to $\det(H) = \begin{vmatrix} h_n & h_{n-1} & 0 & \cdots & 0 & 0 \\ h_{n-1} & h_{n-1} & h_{n-2} & \cdots & 0 & 0 \\ h_{n-2} & h_{n-2} & h_{n-2} & \cdots & 0 & 0 \\ \vdots & \vdots & \vdots & \ddots & \vdots & \vdots \\ h_2 & h_2 & h_2 & \cdots & h_2 & h_1 \\ h_1 & h_1 & h_1 & \cdots & h_1 & h_1 \end{vmatrix}$, we get

$$\det(H) = \begin{vmatrix} h_n - h_{n-1} & h_{n-1} & 0 & \cdots & 0 & 0 \\ 0 & h_{n-1} - h_{n-2} & h_{n-2} & \cdots & 0 & 0 \\ 0 & 0 & h_{n-2} - h_{n-3} & \cdots & 0 & 0 \\ \vdots & \vdots & \vdots & \ddots & \vdots & \vdots \\ 0 & 0 & 0 & \cdots & h_2 & 0 \\ 0 & 0 & 0 & \cdots & h_2 - h_1 & h_1 \\ 0 & 0 & 0 & \cdots & 0 & h_1 \end{vmatrix}.$$

The properties of the determinant yield

$$\begin{aligned} \det(H) &= h_1 \textstyle\prod_{i=2}^{n}(h_i - h_{i-1}) \\ &= 1 \textstyle\prod_{i=2}^{n} \frac{1}{i} \\ &= \textstyle\prod_{i=1}^{n} \frac{1}{i} \\ &= \frac{1}{n!}, \end{aligned}$$

where $h_i - h_{i-1} = \frac{1}{i}$ and $h_1 = 1$.

Theorem 2.2. Let $B = (\beta_{ij})_{i,j=1}^{n}$ be inverse of H. Then,

$$\beta_{ij} = \begin{cases} n \ , & i=j=1 \\ (n+2-i)(n+1-i)h_{n+2-i} \ , & i=j\neq 1 \\ -(n+2-i) \ , & i=j+1 \\ 0 \ , & i>j+1 \\ (-1)^{j-i}\beta_{ii}\prod_{k=1}^{j-i}(n+1-i-k)h_{n+1-i-k} \ , & i<j. \end{cases}$$

Proof. We use principle of mathematical induction on n. The result is true for $n=2$, that is,

$$(H)_2 = \begin{bmatrix} \frac{3}{2} & 1 \\ 1 & 1 \end{bmatrix}$$

and

$$(H)_2^{-1} = 2\begin{bmatrix} 1 & -1 \\ -1 & \frac{3}{2} \end{bmatrix} = \begin{bmatrix} 2 & -2 \\ -2 & 3 \end{bmatrix} = (B)_2.$$

Assume that the result is true for $n-1$, then

$$(B)_{n-1} = (\beta_{ij})_{i,j=1}^{n-1} = \begin{cases} n-1 \ , & i=j=1 \\ (n-1-i)(n-i)h_{n+2-i} & i=j\neq 1 \\ -(n+1-i) & i=j+1 \\ 0 \ , & i>j+1 \\ (-1)^{j-i}\,\beta_{ii}\prod_{k=1}^{j-i}(n-i-k)h_{n-i-k} & i<j. \end{cases}$$

Let the matrices H and B be partitioned as $H = \begin{bmatrix} H_{11} & H_{12} \\ H_{21} & H_{22} \end{bmatrix}$ and $B = \begin{bmatrix} B_{11} & B_{12} \\ B_{21} & B_{22} \end{bmatrix}$, where

$$H_{11} = [h_n]\,,$$

$$H_{12} = [h_{n-1} \quad 0 \quad 0 \quad 0 \quad \cdots \quad 0]\,,$$

$$H_{21} = \begin{bmatrix} h_{n-1} & h_{n-2} & h_{n-3} & \cdots & h_2 & h_1 \end{bmatrix}^T$$

and

$$H_{22} = \begin{bmatrix} h_{n-1} & h_{n-2} & 0 & 0 & \cdots & 0 & 0 \\ h_{n-2} & h_{n-2} & h_{n-3} & 0 & \cdots & 0 & 0 \\ h_{n-3} & h_{n-3} & h_{n-3} & h_{n-4} & \cdots & 0 & 0 \\ \vdots & \vdots & \vdots & \vdots & \ddots & \vdots & \vdots \\ h_2 & h_2 & h_2 & h_2 & \cdots & h_2 & h_1 \\ h_1 & h_1 & h_1 & h_1 & \cdots & h_1 & h_1 \end{bmatrix}.$$

From the assumption, $H_{22}^{-1} = (B)_{n-1}$. The equation $\begin{bmatrix} H_{11} & H_{12} \\ H_{21} & H_{22} \end{bmatrix}\begin{bmatrix} B_{11} & B_{12} \\ B_{21} & B_{22} \end{bmatrix} = \begin{bmatrix} I & 0 \\ 0 & I \end{bmatrix}$ yields:

$$B_{11} = (H_{11} - H_{12}H_{22}^{-1}H_{21})^{-1} = n\ ,$$

$$B_{12} = -B_{11}H_{12}H_{22}^{-1} = \begin{bmatrix} -(n-1)x_1h_{n-1} & (n-1)(n-2)x_1h_{n-1}h_{n-2} & \cdots & (-1)^{n-1}x_1\prod_{i=1}^{n-1} ih_i \end{bmatrix},$$

where $x_1 = n$.

$$B_{21} = -H_{22}^{-1}H_{21}B_{11} = \begin{bmatrix} -n & 0 & 0 & \cdots & 0 \end{bmatrix}^T$$

and

$$B_{22} = H_{22}^{-1} - H_{22}^{-1} H_{21} B_{11} H_{12} H_{22}^{-1}$$
$$= \begin{bmatrix} x_2 & -(n-2)x_2h_{n-2} & (n-2)(n-3)x_2h_{n-2}h_{n-3} & \cdots & (-1)^{n-2}x_2\prod_{i=1}^{n-2} ih_i \\ -(n-1) & x_3 & -(n-3)x_3h_{n-3} & \cdots & (-1)^{n-3}x_3\prod_{i=1}^{n-3} ih_i \\ 0 & -(n-2) & x_4 & \cdots & (-1)^{n-4}x_4\prod_{i=1}^{n-4} ih_i \\ \vdots & \vdots & \vdots & \ddots & \vdots \\ 0 & 0 & 0 & \cdots & x_n \end{bmatrix}$$

where $\underset{2\leq s\leq n}{x_s} = (n+2-s)(n+1-s)\,h_{n+2-s}$. Thus,

$$(B)_n = \begin{bmatrix} x_1 & -(n-1)x_1h_{n-1} & (n-1)(n-2)x_1h_{n-1}h_{n-2} & \cdots & (-1)^{n-1}x_1\prod_{i=1}^{n-1} ih_i \\ -n & x_2 & -(n-2)x_2h_{n-2} & \cdots & (-1)^{n-2}x_2\prod_{i=1}^{n-2} ih_i \\ 0 & -(n-1) & x_3 & \cdots & (-1)^{n-3}x_3\prod_{i=1}^{n-3} ih_i \\ \vdots & \vdots & \vdots & \ddots & \vdots \\ 0 & 0 & 0 & \cdots & x_n \end{bmatrix}.$$

That is, the result is true for n. This completes the proof.

Theorem 2.3. The characteristic polynomial of H holds

$$P_n(\lambda) = (\lambda - h_n)\,P_{n-1}(\lambda) + h_{n-1}\left(P_{n-1}(\lambda) - \lambda P_{n-2}(\lambda)\right),$$
$$P_1(\lambda) = \lambda - 1\ ,$$
$$P_2(\lambda) = \lambda^2 - \left(\frac{5}{2}\right)\lambda + 1.$$

Proof. For the characteristic polynomial of H , we have

$$P_n(\lambda) = \begin{vmatrix} \lambda - h_n & -h_{n-1} & 0 & \cdots & 0 & 0 \\ -h_{n-1} & \lambda - h_{n-1} & -h_{n-2} & \cdots & 0 & 0 \\ -h_{n-2} & -h_{n-2} & \lambda - h_{n-2} & \cdots & 0 & 0 \\ \vdots & \vdots & \vdots & \ddots & \vdots & \vdots \\ -h_2 & -h_2 & -h_2 & \cdots & \lambda - h_2 & -h_1 \\ -h_1 & -h_1 & -h_1 & \cdots & -h_1 & \lambda - h_1 \end{vmatrix}$$

$$= (\lambda - h_n)\begin{vmatrix} \lambda - h_{n-1} & -h_{n-2} & 0 & \cdots & 0 & 0 \\ -h_{n-2} & \lambda - h_{n-2} & -h_{n-3} & \cdots & 0 & 0 \\ -h_{n-3} & -h_{n-3} & \lambda - h_{n-3} & \cdots & 0 & 0 \\ \vdots & \vdots & \vdots & \ddots & \vdots & \vdots \\ -h_2 & -h_2 & -h_2 & \cdots & \lambda - h_2 & -h_1 \\ -h_1 & -h_1 & -h_1 & \cdots & -h_1 & \lambda - h_1 \end{vmatrix}$$

$$+ (h_{n-1})\begin{vmatrix} -h_{n-1} & -h_{n-2} & 0 & \cdots & 0 & 0 \\ -h_{n-2} & \lambda - h_{n-2} & -h_{n-3} & \cdots & 0 & 0 \\ -h_{n-3} & -h_{n-3} & \lambda - h_{n-3} & \cdots & 0 & 0 \\ \vdots & \vdots & \vdots & \ddots & \vdots & \vdots \\ -h_2 & -h_2 & -h_2 & \cdots & \lambda - h_2 & -h_1 \\ -h_1 & -h_1 & -h_1 & \cdots & -h_1 & \lambda - h_1 \end{vmatrix}.$$

The first determinant of the right hand side of the last equality corresponds to the $P_{n-1}(\lambda)$. Let $q(\lambda)$ denotes the second determinant of the right hand side of the last equality. Then,

$$q(\lambda) = \begin{vmatrix} \lambda-h_{n-1} & -h_{n-2} & 0 & \cdots & 0 & 0 \\ -h_{n-2} & \lambda-h_{n-2} & -h_{n-3} & \cdots & 0 & 0 \\ -h_{n-3} & -h_{n-3} & \lambda-h_{n-3} & \cdots & 0 & 0 \\ \vdots & \vdots & \vdots & \ddots & \vdots & \vdots \\ -h_2 & -h_2 & -h_2 & \cdots & \lambda-h_2 & -h_1 \\ -h_1 & -h_1 & -h_1 & \cdots & -h_1 & \lambda-h_1 \end{vmatrix}$$
$$- \begin{vmatrix} \lambda & -h_{n-2} & 0 & \cdots & 0 & 0 \\ 0 & \lambda-h_{n-2} & -h_{n-3} & \cdots & 0 & 0 \\ 0 & -h_{n-3} & \lambda-h_{n-3} & \cdots & 0 & 0 \\ \vdots & \vdots & \vdots & \ddots & \vdots & \vdots \\ 0 & -h_2 & -h_2 & \cdots & \lambda-h_2 & -h_1 \\ 0 & -h_1 & -h_1 & \cdots & -h_1 & \lambda-h_1 \end{vmatrix}$$
$$= P_{n-1}(\lambda) - \lambda P_{n-2}(\lambda).$$

Thus, we have

$$\begin{aligned} P_n(\lambda) &= (\lambda - h_n) P_{n-1}(\lambda) + h_{n-1}(P_{n-1}(\lambda) - \lambda P_{n-2}(\lambda)) \\ &= \left(\lambda - \tfrac{1}{n}\right) P_{n-1}(\lambda) - h_{n-1}\lambda P_{n-2}(\lambda). \end{aligned}$$

Also, it is clear that $P_1(\lambda) = \lambda - 1$ and $P_2(\lambda) = \lambda^2 - \frac{5}{2}\lambda + \frac{1}{2}$.

Theorem 2.4. Let $P_n(\lambda) = \lambda^n + \gamma_{n-1}^{(n)}\lambda^{n-1} + \cdots + \gamma_1^{(n)}\lambda + \gamma_0^{(n)}$ be the characteristic polynomial of the $n \times n$ matrix H . Then,

$$\gamma_0^{(n)} = \left(-\frac{1}{n}\right)\gamma_0^{(n-1)} = (-1)^n \det(H),$$
$$\gamma_{n-1}^{(n)} = \gamma_{n-2}^{(n-1)} - h_n = -tr(H)$$

and

$$\gamma_i^{(n)} = \gamma_{i-1}^{(n-1)} - \frac{1}{n}\gamma_i^{(n-1)} - h_{n-1}\gamma_{i-1}^{(n-2)}$$

are valid for $1 \leq i \leq n-2$.

Proof. By using the recurrence relation in Theorem 2.3 and the coefficients of $P_n(\lambda)$, $P_{n-1}(\lambda)$ and $P_{n-2}(\lambda)$,we have

$$\begin{aligned} \lambda^n + \gamma_{n-1}^{(n)}\lambda^{n-1} + \cdots + \gamma_1^{(n)}\lambda + \gamma_0^{(n)} &= (\lambda - \tfrac{1}{n})(\lambda^{n-1} + \gamma_{n-2}^{(n-1)}\lambda^{n-2} + \cdots + \gamma_1^{(n-1)}\lambda + \gamma_0^{(n-1)}) \\ &\quad - h_{n-1}\lambda(\lambda^{n-2} + \gamma_{n-3}^{(n-2)}\lambda^{n-3} + \cdots + \gamma_1^{(n-2)}\lambda + \gamma_0^{(n-2)}). \end{aligned}$$

Comparison of the coefficients yields the desired formulas. Also, we have $\gamma_0^{(n)} = -\frac{1}{n}\gamma_0^{(n-1)} = \frac{1}{n(n-1)}\gamma_0^{(n-2)} = \cdots = (-1)^n \prod_{i=1}^{n} \frac{1}{i} = (-1)^n \det(H)$ and

$$\gamma_{n-1}^{(n)} = \gamma_{n-2}^{(n-1)} - h_n = \gamma_{n-3}^{(n-2)} - h_{n-1} - h_n = \cdots = -(h_1 + h_2 + \cdots + h_n) = -tr(H).$$

Theorem 2.5. The matrix H has LUdecomposition. Its factors $L = (l_{ij})$and $U = (u_{ij})$ are given by

$$l_{ij} = \begin{cases} 0\,, & i < j \\ 1\,, & i = j \\ \frac{h_{n+1-i}}{h_{n+1-j}}\,, & \text{otherwise} \end{cases} \quad \text{and} \quad u_{ij} = \begin{cases} h_n\,, & i = j = 1 \\ \frac{(h_{n+1-i})}{(n+2-i)(h_{n+2-i})}\,, & i = j \neq 1 \\ h_{n-i}\,, & i = j-1 \\ 0\,, & \text{otherwise.} \end{cases}$$

Proof. Matrix multiplication yields the result.

References

[1] W. L. Frank, Computing eigenvalues of complex matrices by determinant evaluation and by methods of Danilewski and Wielandt, J. Soc. Indust. Appl. Math. 6(**??**) (1958) 378-392.

[2] J.-Fr Hake, Juelich, A remark on Frank matrices, Computing 35 (1985) 375-379.

[3] J. M. Varah, A generalization of the Frank matrix, SIAM J.Sci. Stat. Comput. 7(**??**) (1986) 835-839.

Optimization of GRC Rebound Amount Using Taguchi Method

Sadik Alper YILDIZEL*
Karamanoglu Mehmetbey University,
Department of Civil Engineering, 70100, Karaman, TURKEY

Abstract

Concrete spraying is one of the economical alternative to the conventional concrete casting methods, especially for glass fiber reinforced concrete (GRC) production sector. Ingredients of the GRC spray mixes are costly compared to the other types of concrete; for this reason, design and application of the spraying should be carried out meticulously. The most important factor that increases the costs other than the components is the quantity of splashed material. This rebounded amount can be the main caused of cost increase up to 15

Keywords: Rebound optimization, GRC, Taguchi method, ANOVA.

1 Introduction

The spraying technology was developed firstly to separate the remains of dinosaur bones in 1920. Afterwards similar technology was applied to the many engineering studies. It is widely used in civil engineering discipline such as slope stabilization, tunnel excavations and concrete facade panel production(Niu, Wang, and Wang 2015). Sprayed concrete mixes with the fiber content have higher amount of cement content compared to the conventional concrete designs. Cement is one of the most expensive materials in the concrete mix. For the GRC production sector, glass fiber is the another highly costed material. Glass fiber concrete production costs are higher compared to traditional concrete methods(Yildizel, Yiğit, and Kaplan 2017). For this reason, it is of utmost to reduce material losses in the production line.

Fiber ratio, viscosity of the mix, spray angle and distance are the main factors effecting rebound amount for the fiber reinforced concrete production industry. Mixing water amount, aggregate types, chemical admixtures and other mineral additives are also affecting materials on the rebound weights(Armengaud et al. 2017; Kaufmann et al. 2013; Prudêncio 1998). Aggregate and water effects were ignored within the scope of this study due to the reason that GRC production requirement only includes fine aggregate and certain amount of water.

Spray gun should be at the correct position and distance for all types of sprayed concrete. The distance between the gun and the mold surface is generally 1 and 2 meters for concrete mixes without any fiber content(Malmgren, Nordlund, and Rolund 2005). However, there is no final and common solution for the GRC mixes concerning spray gun-mold surface distance and gun angle due to the more complex structure of GRC designs.

2 Method and Experimental studies

Taguchi method was utilized to develop the design of experiments and determine the optimum condition for rebound weight. The main was to minimize rebound weight of the sprayed

* *E-mail address:* sayildizel@kmu.edu.tr

concrete. Four factors were expected to effect rebound weight: glass fiber ratio, spray distance, spray angle and viscosity of the mix. These parameters and their levels are given in Table 1. Factor coding was taken as -1;0;1. The results were also evaluated by ANOVA to reach the optimum parameter combination.

Factors	Level1	Level 2	Level 3	Level 4	Level 5
Fiber content (%)	2	2.5	3	-	-
Spray distance (cm)	25	50	75	100	-
Spray angle (°)	30	45	60	75	90
Viscosity (Pa. s)	3.9	4.1	4.4	-	-

Table 1: Factors and levels

Field study were performed on a GRC production line. The gun angles were selected as 30°,45°, 60°,75° and 90° with the distances of 25 cm, 50 cm, 75cm and 100 cm. Sprayed concrete were collected with a blanket. Rebound weight was calculated with the following formula (1):

$$\text{Rebound weight (kg, \%)} = [B/(A + B)] \times 100 \tag{1}$$

A represents the empty mold weight, B represents the blanket weight. Viscosity measurements were conducted with a viscometer at 25C°. The results were converted to Pa.s. CEM I 52.5 R cement complying TS EN 197-1 standard was used as the binder ingredients of the mixes. The material properties of the cement are given Table 2. Polycarboxylate based water reducer was used in this study.

Chemical Properties (%)		Physical and Mechanical Properties	
SiO_2	21.6	Specific weight (t/m^3)	3.06
Al_2O_3	4.05	Specific surface (cm^2/g)	4600
Fe_2O_3	0.26	Whiteness (%)	85.5
CaO	65.7	Initial setting time (min.)	100
MgO	1.30	Final setting time (min.)	130
Na_2O	0.30	Water for standard consistency (%)	30
K_2O	0.35	Volume Constancy (mm)	1
SO_3	3.30	0.045 Sieve residue (%)	1
Free CaO	1.6	0.090 Sieve residue (%)	0.1
Insoluble	0.18		
Loss on Ignition	3.20		

Table 2: Material properties of CEM I 52.5 R Cement

Silica sand was utilized as aggregate and alkali resistant glass fiber was added into mixes. Material property of silica sand and glass fiber are presented in Table 3 and Table 4, respectively.

Physical properties	
Clay Content (%)	0.6 - 0.8
Specific Weight (t/m^3)	2.68
AFS value	34.6
Chemical composition (%)	
SiO_2	98.60
Fe_2O_3	0.13
MgO	0.03
CaO	0.01
K_2O	0.09
Na_2O	0.02
Al_2O_3	1.12

Table 3: Properties of silica sand

Mechanical and physical properties	
Ultimate strength, bending (MOR, MPa)	20-28
Elastic limit, bending (LOP, MPa)	7-11
Ultimate strength, tensile (MOR, MPa)	8-11
Elastic limit, tensile (LOP, MPa)	5-7
Compressive Strength (MPa)	50-80
Elastic Modulus (GPa)	10-20
Dry density t/m^3	1.9-2.1

Table 4: Properties of the alkali resistant glass fiber

3 Results and discussion

The variation of the response was examined with via S/N ratio in Taguchi method. Larger Signal to noise ratio is acceptable and better while analyzing splashed concrete amount. The average S/N values of the factors are given in Table 5 and Figure 1, respectively.

Level	fiber	spray distance	Spray angle	viscosity
1	48.59	51.96	52.54	51.07
2	50.50	50.33	49.76	49.30
3	51.70	49.71	50.61	50.45
4		49.31	49.40	
5			49.16	

Table 5: Response table for S/N ratio

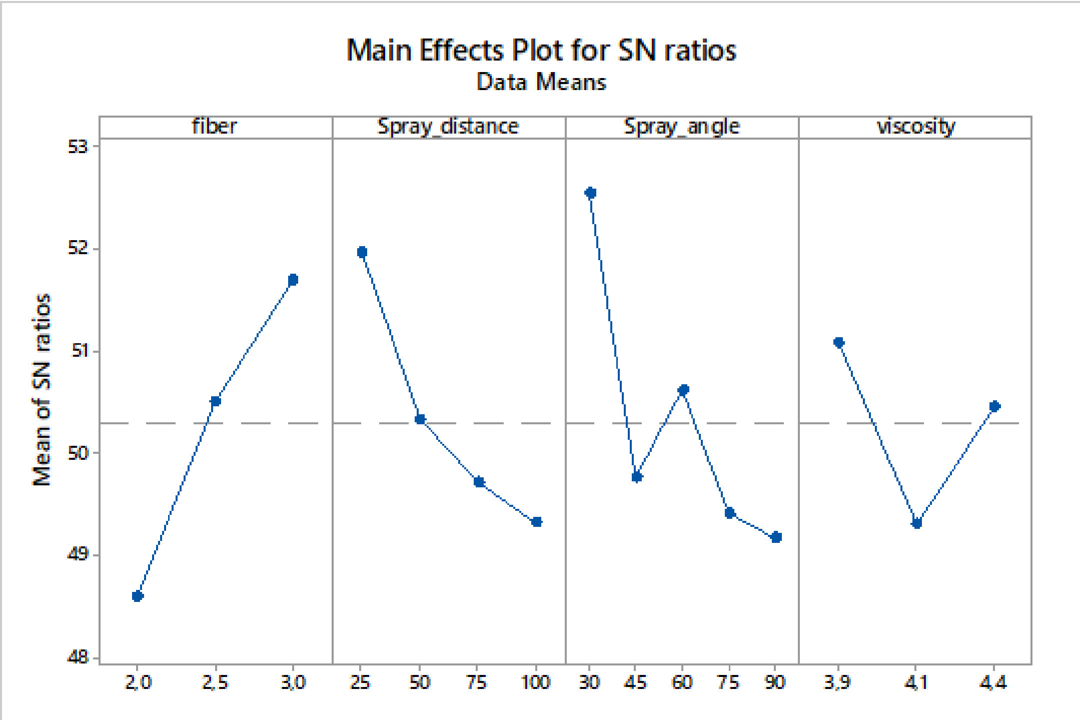

Figure 1: Main effects plot table for S/N ratios

It was found that increase in fiber content led to decrease in viscosity values of the mixes. Maximum rebound weight was obtained as the spray gun was used with 30° and 25 cm distance from the mold. ANOVA analysis results are given in Table 6.

Source	DF	Adj SS	Adj MS	F-Value	P-Value
Fiber	2	2.290	1.1451	151.62	0
Spray distance	3	24.178	8.0593	1067.08	0
Spray angle	4	355.777	88.9442	11776.63	0
Viscosity	2	16.111	8.0555	1066.58	0
Error	348				
Total	359	400.984			

Table 6: Analysis of variance results

Regression equation of rebound weight is presented in Eq. (2) as follows:

$$\begin{aligned} \text{Rebound weight} = 8,23264 + \ 0,10061\ fiber\_2,0 \\ - \ 0,00614\ fiber\_2,5 \\ - \ 0,09447\ fiber\_3,0 + \ 0,39214\ Spray\_distance\_25 \\ + \ 0,04092\ Spray\_distance\_50 - \ 0,11797\ Spray\_distance\_75 \\ - \ 0,31508\ Spray\_distance\_100 + \ 1,35722\ Spray\_angle\_30 \\ + \ 0,73097\ Spray\_angle\_45 \\ + \ 0,06056\ Spray\_angle\_60 - \ 0,71889\ Spray\_angle\_75 \\ - \ 1,42986\ Spray\_angle\_90 \\ + \ 0,24428\ viscosity\_3,9 + \ 0,02744\ viscosity\_4,1 \\ - \ 0,27172\ viscosity\_4,4 \end{aligned} \tag{2}$$

The optimum values for effecting parameters are recorded as 100 cm for spray distance, 90° for spray distance, 4.4 Pas for viscosity with 2 % fiber content.

4 Conclusions

Taguchi method was used to obtain optimum rebound amount for GRC production sector within the scope of this study. Analysis results can be drawn as follows:

- The results showed that increase in fiber content caused the increase in rebound amount. This can be attributed to the fiber loses during the spraying processes.
- Increase in spraying distance minimizes the rebound weights. Optimum distance was obtained as 100 cm.
- Best results were obtained with the 90° of spraying angle. Spraying rebound values decreased up to 18 % compared to the other spraying angle.
- Spraying angle was obtained as the most significant parameter effecting the rebound weights according to the ANNOVA analysis.
- It was also found that increase in viscosity limits the rebound weight increase and material losses.

References

[1] Armengaud, Julie, Géraldine Casaux-Ginestet, Martin Cyr, Bernard Husson, and Marc Jolin. 2017. "Characterization of Fresh Dry-Mix Shotcrete and Correlation to Rebound." Construction and Building Materials. https://doi.org/10.1016/j.conbuildmat.2016.12.220.

[2] Kaufmann, Josef, Kurt Frech, Philipp Schuetz, and Beat Münch. 2013. "Rebound and Orientation of Fibers in Wet Sprayed Concrete Applications." Construction and Building Materials. https://doi.org/10.1016/j.conbuildmat.2013.07.051.

[3] Prudêncio, Luiz Roberto. 1998. "Accelerating Admixtures for Shotcrete." Cement and Concrete Composites. https://doi.org/10.1016/S0958-9465(**??**)80007-3.

[4] Malmgren, Lars, E. Nordlund, and S. Rolund. 2005. "Adhesion Strength and Shrinkage of Shotcrete." Tunnelling and Underground Space Technology. https://doi.org/10.1016/j.tust.2004.05.002.

[5] Niu, Ditao, Jiabin Wang, and Yan Wang. 2015. "Effect of Hydration Aging and Water Binder Ratio on Microstructure and Mechanical Properties of Sprayed Concrete." Journal Wuhan University of Technology, Materials Science Edition. https://doi.org/10.1007/s11595-015-1222-6.

[6] Yildizel, S.A., M.E. Yiğit, and G. Kaplan. 2017. "Glass Fibre Reinforced Concrete Rebound Optimization." CMES - Computer Modeling in Engineering and Sciences.

Some Notes on Monotonic Fuzzy Soft Sets

Mustafa Burç KANDEMİR*
Mugla Sıtkı Koçman University,
Faculty of Science,
Department of Mathematics,
48000, Mugla, Turkey

Abstract

In this paper, we introduce the notion of monotonic fuzzy soft set, and investigate some applications. In the rest of the article, we proposed a decision-making method as an application to the decision-making problems of monotonic fuzzy soft sets.

Keywords: Partial ordered set, soft set, fuzzy soft set, monotonic soft set, monotonic fuzzy soft set, decision-making.

1 Introduction

Human being has tried to understand the world and the universe since existence. Therefore, we have used mathematics which is language of science for modeling all phenomenon. In many disciplines such as engineering, social sciences and other fundamental sciences, we come up against various uncertainties. The classical methods in mathematics may fall short to model uncertainty. To solve this uncertainty problems, many scientists seek to develop mathematical tool. Firstly, in 1965, the most appropriate theory, for dealing with uncertainties is the theory of fuzzy sets developed by Zadeh [9]. This theory has been studied by many scientists until today and has progressed swiftly.

The theory of soft set, which is a completely new approach for modeling uncertainty, is introduced by Molodtsov [8] in 1999. He gave basic properties of this theory and showed that this theory has a rich potential for applications in several fields such as analysis, game theory, probability theory etc. Algebraic operations such as soft subset, soft union, soft intersection etc. among soft sets were studied in [1, 7] inclusively. In [6], Maji et al. established theory of fuzzy soft set which is generalization of soft set theory. They studied set-theoretical operations of fuzzy soft sets.

Kharal and Ahmad [5] built the notion of a mapping classes of fuzzy soft sets and studied the properties of fuzzy soft images and fuzzy soft inverse images of fuzzy soft sets. In [4], Kandemir and Tanay discussed some properties of fuzzy soft functions in detail.

The concept of fuzzy soft set and its applications are studied by many scientists. One of the most important applications of fuzzy soft sets is decision making problems.

According to decision theory, preferences depends on the taste of the decision-maker. There are, of course, parameters that influence our preferences in daily life problems. The parameters affecting our decisions can be ordered again according to the preferences and taste of the person. For example, there are many parameters that will influence the decision to buy a house for a person, such as the environment in which they live, the cheapness, the expesiveness, the number of rooms. It is important for a house to decide the cheapness and

*Corresponding author. *E-mail address:* mbkandemir@mu.edu.tr

the expesiveness and they can be compared with each other. This comparison also depends on the taste of the decision maker. In daily life problems, the parameters that affect our preferences are fuzzy. Therefore, it is meaningful that the parameterized subsets are fuzzy together with the comparison between the parameters.

Besides all these, in 2016, Kandemir [3] gave the definition of monotonic soft set whose parameter set is a partial order set and discussed some properties. He gave an application method for decision making problems using the concept of monotonic soft sets.

Due to these reasons, in this paper, we define the notion of monotonic fuzzy soft set whose parameters set is a partial ordered set, analogously in [3], and study its some basic properties. Then, we give an application for decision-making problems.

2 Preliminaries

Zadeh [9] has argued that the modelling of any phenomenon in the real universe depends on the grade of membership of elements in it and he expressed this model by fuzzy set theory. He introduced how a fuzzy set could be described as follows.

Definition 1 *[9] Let U be an initial universe. A* fuzzy set *A on U is defined by a membership function $\mu_A : U \to [0,1]$ whose membership value $\mu_A(x)$ specifies the degree to which $x \in U$ belongs to the fuzzy set A, for $x \in U$.*

We denote the family of all fuzzy sets on U as $\mathcal{F}(U)$. In [9], some basic fuzzy set-theoretic operations are given in [9] by Zadeh as follows.

Let $A, B \in \mathcal{F}(U)$, if $\mu_A(x) \leq \mu_B(x)$ for each $x \in U$, we call that A is a *fuzzy subset* of B and denoted by $A \sqsubseteq B$. If $\mu_A(x) = \mu_B(x)$ for each $x \in U$, we call that A is *equal* to B. Define the fuzzy set C on U such that $\mu_C(x) = \max\{\mu_A(x), \mu_B(x)\}$, then it is called that C is a *fuzzy union* of A and B and denoted by $C = A \sqcup B$. Similarly, define the fuzzy set D on U such that $\mu_D(x) = \min\{\mu_A(x), \mu_B(x)\}$, then it is called *the fuzzy intersection* of A and B and denoted by $D = A \sqcap B$. Define the fuzzy set E on U such that $\mu_E(x) = 1 - \mu_A(x)$ for each $x \in U$, then we call that E is *the complement* of A and denoted by $E = A^c$. Many scientists have developed the theory of fuzzy set and there are many applications of fuzzy sets to several directions.

In 1999, Molodtsov has drawn attention to the inherent inadequacies and difficulties of fuzzy set theory (such as membership fitting problems etc.) and similar theories. In [8], he introduced the soft set theory for dealing with such difficulties. He defines s soft set over given initial universe as a parameterization of some subsets of the universe. The formal definition of soft set is as follows:

Definition 2 *[8] Let U be an initial universe, E be a set of parameters and $A \subseteq E$. A pair (F, A) is called a* soft set *over U if and only if $F : A \to \mathcal{P}(U)$ where $\mathcal{P}(U)$ is a power set of U.*

The theory of soft set is a popular scientific theory that is still being studied intensively by many scientists.

In 2001, Maji et. al. defined the concept of fuzzy soft set which is combined the theory of fuzzy set and the theory of soft set. It is obvious that this concept is more applicable to real universe problems. The definition of a fuzzy soft set over any initial universe is given as follows.

Definition 3 *[6] Let U be an initial universe, E be a set of parameters and $A \subseteq E$. The pair (f, A) is called a* fuzzy soft set *over U if and only if $f : A \to \mathcal{F}(U)$ is a fuzzy set valued mapping.*

It is clear that, $f(p)$ is a fuzzy set on U for each parameter $p \in A$. Then the membership function of the fuzzy soft set $f(p)$ is denoted by $f_p : U \to [0,1]$ such that $f_p(x)$ is an element in unit interval, and we express as the membership degree according to p parameter of any element x in U. When a fuzzy set given, the membership degree to the fuzzy set of any element of the universe will be denoted in the bottom right corner of the element as a subscript. In terms of being more descriptive, we can give the following example.

Example 4 *Let $U = \{a, b, c\}$ be an initial universe, $E = \{1, 2, 3, 4, 5\}$ be the set of parameters and $A = \{1, 3\} \subset E$. Then we can define the fuzzy soft set over U as;*

$$(f, A) = \{1 = \{a_{0.2}, b_{0.7}, c_{0.4}\}, 3 = \{a_0, b_{0.1}, c_1\}\}.$$

Here, subscripts are the membership degrees of relevant element of U with respect to relevant parameters.

As mentioned in [6], the set-theoretic operations between fuzzy soft sets are given as follows:

Let U be an initial universe, E be the set of parameters, $A, B \subseteq E$ and (f, A) and (g, B) be fuzzy soft sets over U. If $A \subseteq B$ and $f_p(x) \leq g_p(x)$ for each $p \in A$ and for each $x \in U$, it is called that (f, A) is a *fuzzy soft subset* of (g, B), and denoted by $(f, A)\widetilde{\subseteq}(g, B)$. We call that (f, A) is *equal* to (g, B) if and only if $(f, A)\widetilde{\subseteq}(g, B)$ and $(g, B)\widetilde{\subseteq}(f, A)$. The *fuzzy soft union* of (f, A) and (g, B) is the fuzzy soft set (h, C) over U which is denoted by $(h, C) = (f, A)\widetilde{\cup}(g, B)$, where $C = A \cup B$ and

$$h_p(x) = \begin{cases} f_p(x), & \text{if } p \in A - B \\ g_p(x), & \text{if } c \in B - A \\ \max\{f_p(x), g_p(x)\}, & \text{if } p \in A \cap B \end{cases}, \forall p \in C, \forall x \in U.$$

The *fuzzy soft intersection* of (f, A) and (g, B) is the fuzzy soft set (h, C) which is denoted by $(h, C) = (f, A)\widetilde{\cap}(g, B)$ where $C = A \cap B$ and for each $p \in C$, $h_p(x) = \min\{f_p(x), g_p(x)\}$ for all $x \in U$. The *fuzzy soft complement* of (f, A) is a the fuzzy soft set (f^c, A), which is denoted by $(f, A)^c$ and where $f^c : A \to \mathcal{F}(U)$ such that $f_p^c(x) = 1 - f_p(x)$ for each $p \in A$ and for each $x \in U$. The fuzzy soft set (f, A) over U is called an *absolute fuzzy soft set* with respect to A if $f_p(x) = 1$ for each $p \in A$ and for all $x \in U$. Similarly, the fuzzy soft set (f, A) is called a *null fuzzy soft set* with respect to A if $f_p(x) = 0$ for each $p \in A$ and for all $x \in U$.

Some interesting fuzzy soft set theoretic operations which are called **And** and **Or** operations given by Maji et al. in [6]. Now we give the definitions of these operations. Let (f, A) and (g, B) be fuzzy soft sets over U. $(f, A)\mathbf{And}(g, B)$ is a fuzzy soft soft set $(h, A \times B)$ over U such that $h(p_1, p_2) = f(p_1) \cap g(p_2)$ for each $(p_1, p_2) \in A \times B$, i.e. $h_{(p_1,p_2)}(x) = \min\{f_{p_1}(x), g_{p_2}(x)\}$ for all $x \in U$. Similarly, $(f, A)\mathbf{Or}(g, B)$ is a fuzzy soft soft set $(h, A \times B)$ over U such that $h(p_1, p_2) = f(p_1) \cup g(p_2)$ for each $(p_1, p_2) \in A \times B$, i.e. $h_{(p_1,p_2)}(x) = \max\{f_{p_1}(x), g_{p_2}(x)\}$ for all $x \in U$.

3 Monotonic Fuzzy Soft Sets

In [3], Kandemir gave the concept of monotonic soft set over any initial universe, where the parameter set is a partial ordered set. The formal definition of monotonic soft set is as follows.

Definition 5 *[3] Let (F, E) be a soft set over U such that E is a partial ordered set according to the partial order relation $\leq$. (F, E) is called a* monotonic (increasing) soft set *if $p_1 \leq p_2$ for each $p_1, p_2 \in E$, then $F(p_1) \subseteq F(p_2)$.*

Dually, (F, E) is called a monotonic (decreasing) soft set *if $p_1 \leq p_2$ for each $p_1, p_2 \in E$, then $F(p_1) \supseteq F(p_2)$.*

$$\begin{tikzcd} & & 4 \\ 3 & & 2 \arrow[u] \\ & 1 \arrow[ul] \arrow[ur] & \end{tikzcd}$$

Figure 1: The Hasse diagram of the parameters

Now, we define the concept of monotonic fuzzy soft set over given initial universe with partial ordered parameter set, analogously in [3]. Let U be an initial universe, E be the set of parameters and the parameter set E will be fixed for all subsequent fuzzy soft sets from now on.

Definition 6 *Let (f, E) be a fuzzy soft set over U where E is a partial ordered set with respect to partial order relation $\leq$. It is called that (f, E) is a* monotonic (increasing) fuzzy soft set *if $p_1 \leq p_2$ for each $p_1, p_2 \in E$, then $f(p_1) \sqsubseteq f(p_2)$, i.e. $f_{p_1}(x) \leq f_{p_2}(x)$ for all $x \in U$.*

Dually, (f, E) is called a monotonic (decreasing) fuzzy soft set *if $p_1 \leq p_2$ for each $p_1, p_2 \in E$, then $f(p_1) \sqsupseteq f(p_2)$, i.e. $f_{p_1}(x) \geq f_{p_2}(x)$ for all $x \in U$.*

Example 7 *Let $U = \{a, b, c\}$, $E = \{1, 2, 3, 4\}$ with the relation of divisor and its Hasse diagram is as follows (Figure 1.):*

$(f, E) = \{1 = \{a_0, b_{0.1}, c_{0.2}\}, 2 = \{a_0, b_{0.4}, c_{0.7}\}, 3 = \{a_{0.1}, b_{0.8}, c_{0.6}\}, 4 = \{a_{0.7}, b_{0.6}, c_1\}\}$ be a fuzzy soft set over U. Then it is a monotonic (increasing) fuzzy soft set, obviously.

Now let's give some basic properties for monotonic fuzzy soft sets.

Theorem 8 *The fuzzy soft intersection of two monotonic (increasing (decreasing)) fuzzy soft sets is a monotonic (increasing (decreasing)) fuzzy soft set.*

Proof. Suppose that (f, E) and (g, E) be two monotonic (increasing) fuzzy soft sets. From definition of fuzzy soft intersection of two fuzzy soft sets, we have the fuzzy soft set (h, E) over U such that $h(p) = f(p) \sqcap g(p)$ for each $p \in E$, i.e. $h_p(x) = \min\{f_p(x), g_p(x)\}$ for all $x \in U$. Now, suppose that $p_1 \leq p_2$ for $p_1, p_2 \in E$. Since (f, E) and (g, E) are monotonic (increasing) soft sets, we have $f_{p_1}(x) \leq f_{p_2}(x)$ and $g_{p_1}(x) \leq g_{p_2}(x)$ for each $x \in U$. Due to the monotonicity of the min operator we have that $\min\{f_{p_1}(x), g_{p_1}(x)\} \leq \min\{f_{p_2}(x), g_{p_2}(x)\}$. Thus, we obtain that

$$h_{p_1}(x) = \min\{f_{p_1}(x), g_{p_1}(x)\} \leq \min\{f_{p_2}(x), g_{p_2}(x)\} = h_{p_2}(x), \forall x \in U.$$

Hence (h, E) is a monotonic (increasing) fuzzy soft sets.

The same procedure is followed for monotonic (decreasing) fuzzy soft sets. ■

Theorem 9 *The fuzzy soft union of two monotonic (increasing (decreasing)) fuzzy soft sets is a monotonic (increasing (decreasing)) fuzzy soft set.*

Proof. Suppose that (f, E) and (g, E) be two monotonic (increasing) fuzzy soft sets. From definition of fuzzy soft union of fuzzy soft sets, say $(h, E) = (f, E)\widetilde{\cup}(g, E)$. So we have $h_p(x) = \max\{f_p(x), g_p(x)\}, \forall p \in E, \forall x \in U$. Suppose that $p_1 \leq p_2$ for $p_1, p_2 \in E$. Due to the monotonicity of max operator, we obtain that

$$h_{p_1}(x) = \max\{f_{p_1}(x), g_{p_1}(x)\} \leq \max\{f_{p_2}(x), g_{p_2}(x)\} = h_{p_2}(x), \forall x \in U.$$

Thus (h, E) is a monotonic (increasing) fuzzy soft set over U.

The same procedure is followed for monotonic (decreasing) fuzzy soft sets. ■

If we have a partial ordered set $(E, \leq)$, then we obtain a partial order relation on $E\times E$, and it is defined as $(p_1, p_2) \leq^* (p'_1, p'_2)$ if and only if $p_1 \leq p'_1$ and $p_2 \leq p'_2$ for each $p_1, p_2, p'_1, p'_2 \in E$. This partial order relation is called a *product order* on $E \times E$.

Theorem 10 *If (f, E) and (g, E) are monotonic (increasing (decreasing)) fuzzy soft sets, then (f, E)***And***(g, E) is also monotonic (increasing (decreasing)) fuzzy soft set.*

Proof. From definition of the operation **And**, we have that $(f, E)\mathbf{And}(g, E) = (h, E\times E)$ and $h(p_1, p_2) = f(p_1)\sqcap g(p_2)$ for each $p_1, p_2 \in E$. Since $(E, \leq)$ is a poset, then we have the product order relation $\leq^*$ on $E \times E$ such that $(p_1, p_2) \leq^* (p'_1, p'_2)$ if and only if $p_1 \leq p'_1$ and $p_2 \leq p'_2$ for each $p_1, p_2, p'_1, p'_2 \in E$ from above description. Now suppose that $(p_1, p_2) \leq^* (p'_1, p'_2)$. Since (f, E) and (g, E) are monotonic (increasing) fuzzy soft sets and monotonicity of the operation min, we obtain that $h(p_1, p_2) \sqsubseteq h(p'_1, p'_2)$. Thus $(h, E \times E)$ is a monotonic (increasing) fuzzy soft set.

The same procedure is followed for monotonic (decreasing) fuzzy soft sets. ■

Theorem 11 *If (f, E) and (g, E) are monotonic (increasing (decreasing)) fuzzy soft sets, then (f, E)***Or***(g, E) is also monotonic (increasing (decreasing)) fuzzy soft set.*

Proof. Similar to proof of Theorem 10. ■

Theorem 12 *If (f, E) is monotonic (increasing (decreasing)) fuzzy soft sets over U, then the complement of (f, E), $(f, E)^c$, is a monotonic (decreasing (increasing)) fuzzy soft set over U.*

Proof. Suppose that (f, E) is a monotonic (increasing) fuzzy soft sets. So we have that if $p_1 \leq p_2$ for $p_1, p_2 \in E$, $f_{p_1}(x) \leq f_{p_2}(x)$ for each $x \in U$. From definition of complement of a fuzzy soft set, we have the fuzzy set-valued function $f^c : E \to \mathcal{F}(U)$ such that $f^c_p(x) = 1-f_p(x)$ for each $x \in U$. Now, suppose that $p_1 \leq p_2$ for $p_1, p_2 \in E$, then we obtain that

$$f^c_{p_1}(x) = 1 - f_{p_1}(x) \geq 1 - f_{p_2}(x) = f^c_{p_2}(x), \forall x \in U.$$

Thus, $(f, E)^c = (f^c, E)$ is a monotonic (decreasing) fuzzy soft set over U. ■

Theorem 13 *The null and absolute fuzzy soft sets are monotonic fuzzy sets with respect to the poset $(E, \leq)$.*

Proof. It is obvious. ■

Let (f, E) be a fuzzy soft set over initial universe U. We know that $f(p)$ is a fuzzy set each $p \in E$. In [9, 10], the concept of α-level set of any fuzzy set A on U is defined as the crisp subset of U such that $A^\alpha = \{x \in U \mid \mu_A(x) \geq \alpha\}$ for any $\alpha \in [0, 1]$. Using the same arguments, we can give the notion of α-level soft set for the fuzzy soft set (f, E), i.e. for each $p \in E$ and $\alpha \in [0, 1]$, define the set valued mapping $f^\alpha : E \to \mathcal{P}(U)$ such that $f^\alpha(p) = \{x \in U \mid f^\alpha_p(x) \geq \alpha\}$. Then it is called that (f^α, E) is a *α-level soft set* for the fuzzy soft set (f, E) and denoted by ã€–$(f, E)^\alpha$.

We can give the following lemma for fuzzy sets and α-level sets as in [9, 10].

Lemma 14 *[9, 10] Let $A, B \in \mathcal{F}(U)$ and $A \sqsubseteq B$, then $A^\alpha \subseteq B^\alpha$ for each $\alpha \in [0, 1]$.*

The definition of monotonic soft set given in Definition 5 and Lemma 14, we obtain following theorem, obviously.

Theorem 15 *If (f, E) is a monotonic fuzzy soft set over U, then its α-level soft set ã€–$(f, E)^\alpha$ is a monotonic soft set over U for each $\alpha \in [0, 1]$.*

4 An Application Method for Decision-Making Problems

If we have a monotonic fuzzy soft set, then we compare the element of problem universe with respect to valuableness of the elements. Comparison among parameters indicates that which parameters are valuable according to the decision-maker. We know that the value of a material or any phenomenon depends on;

(i) having considerable monetary value for use or exchange,

(ii) great importance, and

(iii) and having admirable or esteemed qualities or characteristics.

In fuzzy soft theory, attributes or parameters have a fuzzy structure as we have already mentioned. Therefore, the value of a phenomenon changes primarily the decision-maker's decision depending on the parameters and the fuzziness of the parameters. For this reason, the solution of the problems of real-life phenomena modeling of fuzzy soft sets will be more realistic. This theory is among the pioneers of decision-making methods. In [3], a decision-making algorithms have been given using the concept of monotonic soft set. In this section, an application method will be given to decision-making problems of fuzzy soft sets, analogously in [3].

In a decision-making process, the decision-maker chooses the most appropriate one from among the cases he chooses. There are, of course, many elements (parameters) that will influence the choice. But these parameters vary according to the decision-maker, i.e. they are relative. Accordingly, the decision-maker sorts the appropriate parameters with respect to superiority of the parameters. All parameters do not have to be compared with each other. For this reason, a partial order relation is obtained on the parameter set. Since almost every parameter has a fuzzy character in daily-life, all phenomena in the problem universe can be compared to each other according to the membership degree. i.e. let we have a monotonic fuzzy soft set (f, E) over the problem universe U, if (f, E) is a monotonic increasing fuzzy soft set, then we know that $p_1 \leq p_2$ implies $f_{p_1}(x) \leq f_{p_2}(x)$ for each $p_1, p_2 \in E$ and for each $x \in U$. We will express this case as when the parameter p_2 is superior than the parameter p_1, the element x according to p_2 is superior than x according to p_1. Therefore, using the monotonic increasing fuzzy soft sets, we sort the elements to be selected in the universe according to the comparison between the parameters.

Using these concepts, we can give the following decision-algorithm.

Algorithm 1 Construct a monotonic fuzzy soft set with respect to valueness of the parameters.

Algorithm 2 Choose maximal parameters and related approximated fuzzy sets with respect to superiority.

Algorithm 3 Intersect these maximal approximated fuzzy sets.

The decision-maker will select the element with the highest membership degree in the obtained final fuzzy set.

We can give following example to see how work this algorithm in decision-making process.

Example 16 *We have inspired in [2] for this example. Assume that a company wants to fill a position. There are six candidate who form the set of alternatives,* $U = \{a, b, c, d, e, f\}$*. The hiring committee consider a set of parameters,* $E = \{p_1, p_2, p_3, p_4, p_5\}$*. The parameters* p_i $(i = 1, \ldots, 5)$ *stand for "experience", "computer knowledge", "young age", "good speaking" and "friendly", respectively.*

$$\begin{tikzcd}
p_1 & & \\
p_2 \arrow[u] & p_4 \arrow[ul] & p_5 \\
p_3 \arrow[u] & &
\end{tikzcd}$$

Figure 2: The Hasse diagram of the parameters

The order of the parameters according to the committee is as follows (Figure 2.);
The monotonic (increasing (decreasing)) fuzzy soft set is constructed with respect to the committee as following:

$$\begin{aligned}
(f, E) = \{p_1 &= \{a_{0.8}, b_{0.6}, c_{0.9}, d_1, e_{0.85}, f_{0,3}\}, p_2 = \{a_{0.74}, b_{0.5}, c_{0.75}, d_{0.6}, e_{0.7}, f_{0,28}\} \\
p_3 &= \{a_{0.65}, b_{0.3}, c_{0.4}, d_{0.3}, e_{0.6}, f_{0,25}\}, p_4 = \{a_{0.5}, b_{0.5}, c_{0.1}, d_{0.9}, e_{0.7}, f_{0,3}\} \\
p_5 &= \{a_{0.5}, b_{0.75}, c_{0.7}, d_{0.3}, e_{0.5}, f_{0,8}\}\}
\end{aligned}$$

Obviously, maximal elements according to committee p_1 and p_5. Then maximal approximated fuzzy sets are $f(p_1)$ and $f(p_5)$. Taking the fuzzy intersection of these fuzzy sets, we obtain the final fuzzy set

$$\begin{aligned}
f(p_1) \cap f(p_5) &= \{a_{0.8}, b_{0.6}, c_{0.9}, d_1, e_{0.85}, f_{0,3}\} \cap \{a_{0.5}, b_{0.75}, c_{0.7}, d_{0.3}, e_{0.5}, f_{0,8}\} \\
&= \{a_{0.5}, b_{0.6}, c_{0.7}, d_{0.3}, e_{0.5}, f_{0,3}\}
\end{aligned}$$

Thus, among the candidates having both maximal properties, the highest one is c. As a result, the committee will choose the candidate c.

5 Conclusion

In this paper, we have given the concept of monotonic fuzzy soft set and some basic properties. In decision-making theory, there are many parameters that affect our decision, and these parameters can be sorted according to the decision makerâ €■s preferences. Thus, the parameters that affect the decision may be in partial order according to the order of the decision-maker. In this study, we assume that the parameter set is a partial ordered set according to the decision maker's preferences. With this assuption and so the concept of monotonic fuzzy soft set, p-approximated fuzzy sets were able to sort with respect to superiority of the parameters. Using all of these we have shown that monotonic fuzzy soft sets can be applied to decision making problems. Therefore, this study has the potential to be useful for scientists working in this field. This theory can be examined in more detail by expanding these concepts in future studies.

The author hopes that this article sheds light on a way of working scientists in this field.

References

[1] M.I. Ali, F. Feng, X.Y. Liu, W.K. Min, M. Shabir, On Some New Operations in Soft Set Theory, Comput. Math. Appl. 57 (2009) 1547–1553.

[2] N. Çağman, S. Enginoğlu, Soft set theory and Uni-Int decision making, European J. Oper. Res. 207 (1) (2010) 848–855.

[3] M.B. Kandemir, Monotonic soft sets and its applications, Ann. Fuzzy Inform. 12(2) (2016) 295-307.

[4] M.B. Kandemir, B. Tanay, Results on Fuzzy Soft Functions, NTMSCI 3 (4) (2015) 1–17.

[5] A. Kharal, B. Ahmad, Mappings on Fuzzy Soft Classes, Adv. Fuzzy Syst. 2009 (2009).

[6] P.K.Maji, R.Biswas, and A.R.Roy, Fuzzy Soft Sets, J. Fuzzy Math. 9 (2001) 589-602.

[7] P.K. Maji, R. Biswas, A.R. Roy, Soft Set Theory, Comput. Math. Appl. 45 (2003) 555–562.

[8] D. Molodtsov, Soft Set Theory-First Results, Comput. Math. Appl. 37 (1999) 19–31.

[9] L.A. Zadeh, Fuzzy Sets, Information and Control 8 (1965) 338-353.

[10] H.J. Zimmermann, Fuzzy set theory - and its applications, 4th Ed., Springer Science+Business Media New York (2001) p.514.

Calculation Of The Clear Sky Solar Radiatioan From Ampirical And Remote Sensing Mathematical Models

Selmin ENER RUŞEN*
Karamanoglu Mehmetbey University,
Department of Energy Systems Engineering,
Academic Energy Research Group (AKEN),
70100, Karaman, TURKEY

Abstract

On the surface of the earth, solar radiation estimation is done by two main mathematical models which are ground level measurement with a pyranometer and satellite-derived remote sensing. Images taken from geostationary satellites are very important source to estimate solar irradiance at the earth's surface. In this study, the clear sky solar radiation is mathematically modeled by using the empirical Angstrom (sunshine-based) model and satellite-based remote sensing model. Firstly, the daily average pixel value of each image is found mathematically by using Metlook version 1.7 which is a multi-functional analysis and interpretation tool devoted to the satellite images. Moreover, the daily global radiation on a horizontal surface was calculated by surface data for the selected time period and region from the Turkish State Meteorological Service. Afterwards, in order to investigate the accuracy of the estimation modeling, it has performed a comparative study using the classical sunshine-based models (Angstrom type) and the satellite method. Obtained preliminary results showed that, the inclusion of local information further increases the performance of mathematical calculations. These results are encouraging for the future works to use local information data in constructing such modeling, which may increase the accuracy of the mathematical solar radiation maps.

Keywords: Clear Sky Radiation, Mathematical Modeling, Metlook Images, Angstrom Method.

1 Introduction

In the use of solar energy system performance calculations, ground measured solar radiation is obtained with difficulty for a given site. In addition to this, the measurement network's density is usually far too low. In order to derive information on solar irradiance, geostationary satellites such as METEOSAT or GOES can be used for large area with very high spatial resolution (up to 2.5 km) and with sufficient temporal resolution (up to 30 minutes) (Beyer, Costanzo, and Heinemann 1996). There are mathematical models which estimate surface solar irradiance based on this geostationary satellite image data. One of them is HELIOSAT method, used by some researchers such as Cano et al. (1986); Beyer et al. 1996; Hammer 2000 (Beyer, Costanzo, and Heinemann 1996; Cano et al. 1986; Hammer 2000). They reported that HELIOSAT method is an estimation technique to infer the shortwave surface irradiance from satellite images. The general idea of the HELIOSAT is to deal with atmospheric and cloud extinction separately. A measure of cloud cover is determined by METEOSAT visible

* *E-mail address:* selminerusen@kmu.edu.tr

channel count. In the first step, this satellite digital count is given a new useful form. By using solar zenith angle, a relative reflectivity is calculated from this modified new signal. In the second step, the cloud index is derived from METEOSAT images to take into account the cloud extinction.
The other calculation technique is the daily average pixel value of each image by using Metlook version 1.7 which is a multi-functional analysis and interpretation tool devoted to the satellite experiment METEOSAT (Aksoy, Ener Rusen, and Akinoglu 2011; Aksoy, Ener Rusen, and Akınoğlu 2010).
In this study we start to use the HELIOSAT method, which is a commonly utilized method for such works. we also carried out calculations of Angstrom coefficients to be used for the solar irradiation in clear sky atmosphere. By using different mathematical procedures and formulas we performed sample calculations for the daily average solar radiation for one month of selected region in Turkey. The procedures that we used and the results we obtained are discussed in the following parts.

2 Summary of HELIOSAT Method

HELIOSAT method is modified by Beyer et al. 1996 (Beyer, Costanzo, and Heinemann 1996) to improve the correlation between cloud index and ground measurement irradiance data which is derived from satellite images. Firstly, single digital count per pixel of visible channel (VIS) is used to obtain the relative apparent albedo ρ and cloud index n that may be linearly correlated to the atmospheric transmission of solar radiation. Diabaté et al.,(1987) (Diabaté et al. 1987)described values of the relative apparent albedo ρ as (Beyer, Costanzo, and Heinemann 1996):

$$\rho = \frac{C - C_o}{0,7.f.\cos\Theta_z\left(\cos\Theta_z\right)^{0,15}} \tag{1}$$

where, C : satellite counts values, C_0 : offset values, θ_z : zenith angle of the sun, f : correction for the variability of Sun-Earth distance. In fact, as can be seen in this expression, satellite count values are normalized with respect to a parameter that accounts the elevation of the sun. Cloud index n can be defined with relative apparent albedo ρ, for each pixel of satellite images, as:

$$n = (\rho - \rho_{clear})/(\rho_{cloud} - \rho_{clear}). \tag{2}$$

Here, ρ_{clear} and ρ_{cloud} are relative apperent albedo corresponding to clear and overcast conditions, respectively (Hammer 2000; Dagestad 2005). These values are essentially the maximum and minimum of pixel readings. Cloud information at the atmosphere is one of the basic information to use in the researches of solar radiation. To couple the cloud index n which is calculated using relative apparent albedo ρ, with the measured ground irradiance data of the locality increase the estimation performance. For such a coupling we used the following procedure.
To estimate the solar radiation, an empirical form is needed between the normalized solar radiation, namely the clearness index k and cloud index n defined above. That is, in the linear approximation, the clearness index k can be written as:

$$k = H/H_o = a'n + b'. \tag{3}$$

where H is the daily global irradiance, H_o is the daily extraterrestrial irradiance, and a' and b' are empirical constants to be determined using regression analysis with the ground data. As one can guess these parameters would be site dependent and might be affected from the temporal variations of the atmospheric conditions (Beyer, Costanzo, and Heinemann 1996; Cano et al. 1986; Hammer 2000). The cloud index n values are obtained from the Meteosat geostationary satellite images using by standard HELIOSAT method and correlated to the clearness index k. The result of the application of this method has been investigated by Beyer et al. (1996) (Beyer, Costanzo, and Heinemann 1996). Beyer et al. concluded that better results were reached using clear sky irradiance G_{clear} and clear sky index k^* instead of clearness index k (Eq. (3)). Daily global irradiance, H is divided by the output of daily clear sky irradiance, G_{clear} is the clear sky index, and given as:

$$k* \equiv H/G_{clear}. \tag{4}$$

G_{clear} gives the irradiance under clear sky conditions for the respective solar zenith angle. G_{clear} is calculated as (Beyer, Costanzo, and Heinemann 1996):

$$G_{clear} = 0,7.I_{sc}.f.cos^{1,15}(\theta_z) \tag{5}$$

where I_{sc} is the solar constant (1367 W / m^2). To test the performance of HEIOSAT method, compared the results obtained from the Metlook version 1.7 which is a multi-functional analysis and interpretation tool devoted to the satellite experiment METEOSAT (Aksoy, Ener Rusen, and Akinoglu 2011; Aksoy, Ener Rusen, and Akınoğlu 2010) (k vs n) with to those obtained from the modified HELIOSAT method (k^* vs n, (Eq (5)).

3 Calculation of solar radiation from Angstrom type

In most of the applications Angstrom type equations are used to estimate the monthly average daily global solar radiation [5, 6]. In this form, regression coefficients a and b are calculated using the linear correlation:

$$\frac{H}{H_0} = a + b\frac{s}{S} \tag{6}$$

which is named as Angstrom-Prescott relation (Angström 1924), a nad b are calculated Angstrom coefficients. In this equation (6), if we take $s/S = 1$, the result is the clear sky radiation on horizontal surface.

Table 1: Shows the data that we used in our calculations.

Day	**s / S**	**k= H / Ho**	**H$_{clear}$**
1	0.55	0.60	26.62
2	0.40	0.57	26.82
3	0.92	0.82	27.02
4	0.92	0.81	27.21
5	0.91	0.80	27.41
6	0.90	0.77	27.60
7	0.91	0.76	27.79
8	0.88	0.72	27.98
9	0.83	0.70	28.17
10	0.74	0.69	28.36
11	0.85	0.71	28.54
12	0.67	0.66	28.73
13			28.91
14	0.10	0.26	29.09
15	0.41	0.56	29.26
16	0.88	0.67	29.44
17	0.30	0.52	29.61
18	0.21	0.39	29.78
19	0.05	0.28	29.95
20	0.53	0.53	30.12
21	0.06	0.34	30.28
22	0.01	0.25	30.44
23			30.60
24	0.57	0.60	30.76
25	0.68	0.69	30.91
26	0.87	0.80	31.06
27	0.32	0.49	31.21
28	0.33	0.38	31.36
29	0.86	0.81	31.50
30	0.65	0.66	31.65

Here the clear sky solar radiation calculated with *s :daily bright sunshine hours (hour), S :daylength (hour),* H_o *: daily extraterrestrial radiation on horizontal surface, M J / m*^{2}*day, H : daily global radiation on horizontal surface, M J /m*^{2}*day, k : clearness index,* H_{clear} *: daily clear sky radiation on horizontal surface, M J /m*^{2} *day.*
To find the Angstrom coefficients a and b we can use the assumption of a linear relationship between the clearness index k and (s / S). Fig.1 shows the result of the regression for the one month for selected sample region.

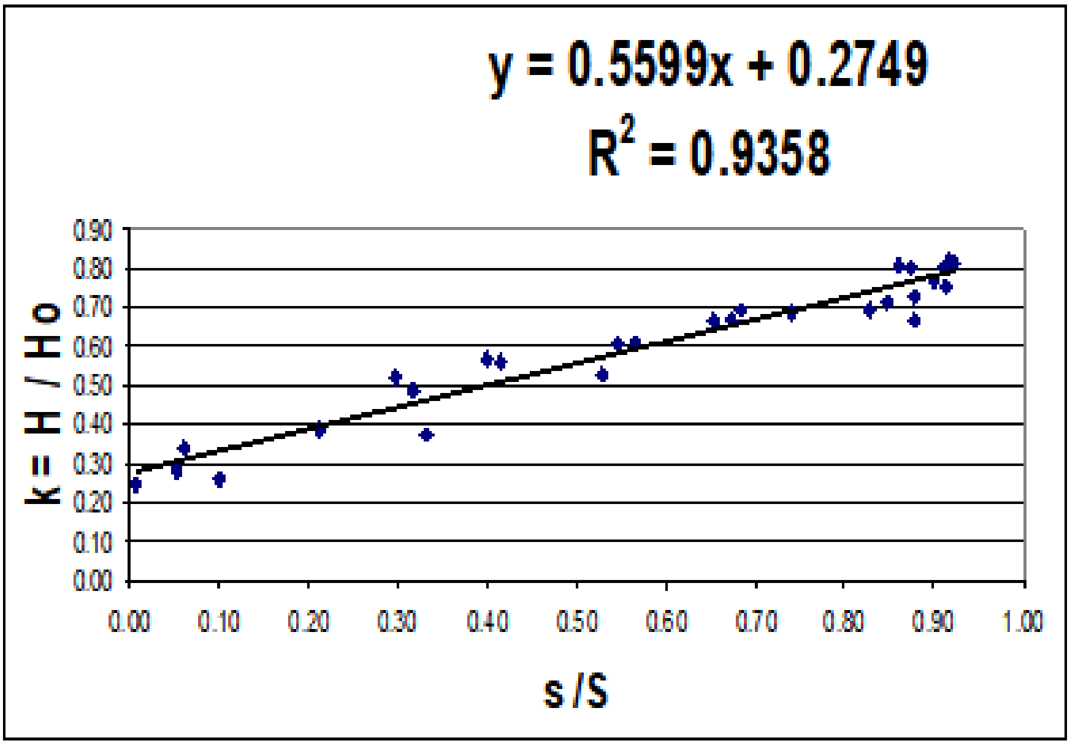

Figure 1: Linear regression between the clearness index k and $(s\ /\ S)$

In this Fig. 1, the data points represent 30 daily average values of selected sample region in Turkey for one month of spring season. The straight line is the regression line and a and b values are 0.560 and 0.275, respectively.

4 Calculation of The Solar Radiation from Satellite

For the application of HELIOSAT method, images were taken from geostationary Meteosat-7 satellite for one month in the visible channel (0,5-0,9 μm). The images are given for every 30 minutes in 24 hours, the number is 48 images. The images that correspond to daytime are of course taken into account. The count values C for every pixel is in between 0-255. The relative apparent albedo ρ values are calculated from the pixel counts C and the offset value C_o for the satellite. We take C_o as 6 for Meteosat-7 satellite (http://www.eumetsat.int/Home/ 2018). In this study, we find daily average pixel value of each image by using Metlook version 1.7 which is a multi-functional analysis and interpretation tool devoted to the satellite experiment METEOSAT (Aksoy, Ener Rusen, and Akinoglu 2011). This software is a first step to visualize METEOSAT products. It's very simple C and XWindows architecture allows the developers to add any user useful adding or remark. We calculated the relative apparent albedo ρ, $\rho*$, cloud index n and $n*$. $\rho*$ and $n*$ are explained in the followings. List of these values can be seen in Table 2.

Table 2: The relative apparent albedo ρ and cloud index n

Average pixel C	$\rho *$	$n*$	ρ	n
45.50	1.48	0.36	93.59	0.35
38.05	1.20	0.21	115.04	0.53
28.40	0.83	0.01	62.38	0.09
29.10	0.85	0.02	59.61	0.07
29.00	0.84	0.02	58.87	0.06
29.00	0.83	0.01	54.70	0.03
29.74	0.85	0.02	55.96	0.04
31.15	0.90	0.05	64.52	0.11
33.10	0.96	0.08	67.89	0.14
32.33	0.93	0.06	66.05	0.12
29.70	0.83	0.01	58.84	0.06
33.38	0.95	0.08	69.43	0.15
77.43	2.47		68.91	
72.33	2.28	0.80	160.79	0.91
52.95	1.60	0.43	129.62	0.65
30.05	0.82	0.00	54.15	0.02
52.81	1.58	0.42	120.82	0.58
66.43	2.03	0.66	155.74	0.87
75.72	2.33	0.82	171.63	1.00
53.74	1.59	0.42	101.00	0.41
78.90	2.41	0.86	169.63	0.98
86.95	2.66	1.00	170.40	0.99
70.00	2.09		132.82	
45.25	1.28	0.25	82.28	0.26
39.84	1.09	0.15	68.14	0.14
31.16	0.81	0.00	51.25	0.00
59.47	1.71	0.49	103.68	0.43
81.40	2.40	0.86	171.99	1.00
47.10	1.30	0.27	92.40	0.34
50.95	1.42	0.33	93.85	0.35

Two different mathematical procedures and formulas were used for the cloud index calculation proses. The first one is the used by Beyer et al. (1996) (Beyer, Costanzo, and Heinemann 1996) it is discussed in section 2. Afterwards, we calculated $\rho *$ by using Eq. (7) and here H_{clear} was used to normalize the count values instead of the parameter which accounts the elevation of the sun as:

$$\rho * \;=\; (C - -Co)\,/H_{clear} \tag{7}$$

$$n* = (\rho * - \rho*_{clear})/(\rho*_{cloud} - \rho*_{clear}) \tag{8}$$

where $\rho *_{clear}$ is the minimum value of $\rho *$ and $\rho *_{cloud}$ is the maximum value of $\rho *$ in one month. In this mathematical calculation, use of H_{clear} $(=H_o(a+b))$ introduces locational information because of the Angstrom coefficients a and b. Therefore, calculated relative apparent albedo ρ^* and cloud index n^* also contain information of locational data and parameters.

As mentioned above, we started to carry out some basic calculations and could reach some significant results for one month. An excel file is prepared for the calculations, and the obtained results are shown in Table1 and Table 2. The results obtained are summarized as follows: Fig. 2 (A) shows the result of the regression analysis between it and it (Eq. (3)),when $H_{clear} = H_o\ (a+b)$)) is used in n^* for the normalization. R^2 value is 0.89, higher than the regression results when the parameter of sun's elevation is used for normalization to obtain n (Fig.1 (B)). This result confirms the thesis that inclusion of the more local data and information in the models increase the performance of the correlations. In Fig. 3 (A) and (B), k^* is used for the clear sky index (Eq. (4)). In Fig. 3 (A) in the calculation of cloud index n^*, again local information $H_o\ (a+b)$ is used for normalization while in Fig. 3 (B) the parameter of sun's elevation (Denomination of Eq. (1)) is used for the normalization, in the calculation of ρ.The results similarly confirm that use of local information enhance the performance of calculations since a larger R^2 value of 0.90 is obtained.

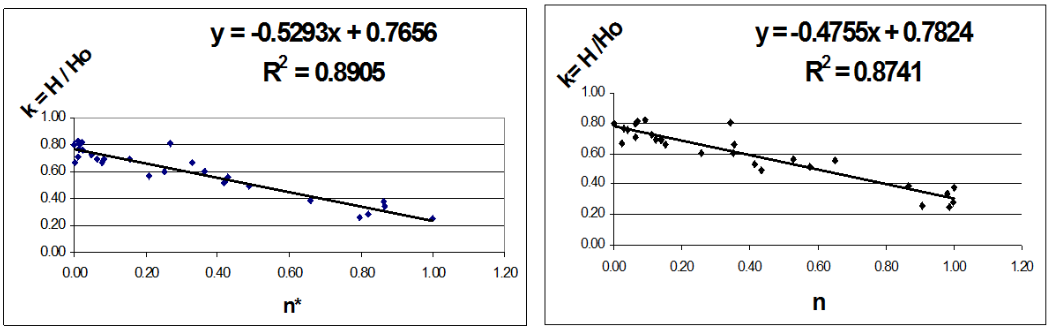

(A) (B)

Figure 2: Comparative analysis between (A) cloud index $n^*$and (B) cloud index n for clearness index k

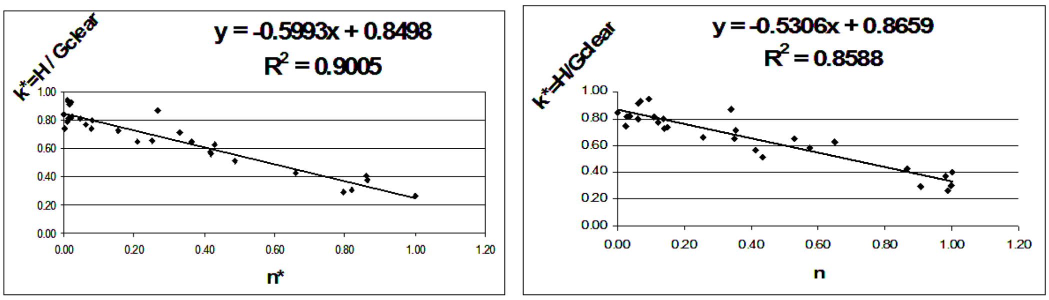

(A) (B)

Figure 3: Comparative analysis between (A) cloud index $n^*$and (B) cloud index n for clear sky index k

5 Discussion and Conclusion

In this stage of study, we used Meteosat images that are obtained from Eumetsat archive, for selected sample region in Turkey. We also obtained daily global irradiance H on horizontal surface, measured by pyranometer, for the one month for the selected sample region from the

Turkish State Meteorological Service. We performed a comparative study using the cloud index $n*$ mathematical calculation of Metlook version 1.7 and the modified cloud index n of HELIOSAT method. Obtained results were analyzed by using regression analysis method for the selected sample site. According to the one-month data results, the cloud index $n*$ mathematical calculation of Metlook version 1.7 method indicates the same performance with HELIOSAT method in mathematically.
Final conclusion is that the use of k^* instead of k is better as Beyer et al. (1996) (Beyer, Costanzo, and Heinemann 1996) stated. In addition, my calculations show that, inclusion of local information further increase the performance of calculations ($R^2 = 0.90$).

Acknowledgments

The author would like to thank State Meteorological Service (TSMS) for providing me with measured data. The author would also like to thank to Prof. Dr. Bülent Akınoğlu and Dr. Annette Hammer for their discussions and comments during the course of this study. The author would like to express their gratitude to Karamanoğlu Mehmetbey University for your supports.

References

[1] Aksoy, B., S. Ener Rusen, and B. Akınoğlu. 2010. "GlobalGüneş Radyasyonunun Tahmin Edilmesine Yönelik Angstrom Denklemi Ve Uydu Yaklaşımının Karşılaştırılması." In Uluslararası Katılımlı 1. Meteoroloji Sempozyumu 27-28 May, Ankara, 161–70. Ankara.

[2] Aksoy, B., S. Ener Rusen, and B. G. Akinoglu. 2011. "A Simple Correlation to Estimate Global Solar Irradiation on a Horizontal Surface Using METEOSAT Satellite Images." Turkish J. Eng. Env. Sci. 35: 125–37.

[3] Angström, A. 1924. "Solar and Terrestrial Radiation." Quart. J. Roy. Met. Soc. 50: 121–26.

[4] Beyer, H., C. Costanzo, and D. Heinemann. 1996. "Modifications of the HELIOSAT Procedure for Irradiance Estimates from Satellite Images." Solar Energy 56: 207–12.

[5] Cano, D., J.M. Monget, M. Albuisson, H. Guillard, N Regas, and L. Wald. 1986. "A Method for the Determination of the Global Solar Radiation from Meteorological Satellite Data." Solar Energy 37: 31–39.

[6] Dagestad, K-F. 2005. "Estimating Global Radiation at Ground Level from Satellite Images, PhD Thesis." University of Bergen.

[7] Diabaté, L., H. Demarcq, N. Michaud-Regas, and L. Wald. 1987. "Estimating Incident Solar Radiation at the Surface from Images of the Earth Transmitted by Geostationary Satellites: The Heliosat Project." International Journal of Solar Energy 5 (5–6): 261–78. doi:10.1080/01425918708914425.

[8] Hammer, A. 2000. "Anwendungspezifische Solarstrahlungsinformationen Aus Meteosat-Daten." Carl von Ossietzky University of Oldenburg.

[9] http://www.eumetsat.int/Home/. 2018. "No Title." EUMETSAT Meteorological Satellite Service.

The Energy Of Hankel Matrices With Fibonacci And Lucas Numbers

Mustafa BAHŞİ*
Education Faculty, Aksaray University,
Aksaray /TURKEY

Süleyman SOLAK
Ahmet Keleşoğlu Education Faculty,
Necmettin Erbakan University, Konya/TURKEY

Abstract

The concept of graph energy was introduced by Gutman and this concept has been generalized to matrix energy by Nikiforov. In this study, we examine some energies of the Hankel matrix with the Fibonacci and Lucas numbers.

Keywords: Fibonacci numbers, Lucas number, Hankel matrix, Matrix energy.

1 Introduction

Let G be a graph with n vertices. The adjacency matrix $A = (a_{ij})$ of G defined as $a_{ij} = 1$ if there is an edge between i and j and 0 otherwise. The concept of graph energy was introduced by Gutman in [2] as

$$E(G) = \sum_{s=1}^{n} |\lambda_s|,$$

where $\lambda_1, \lambda_2, ..., \lambda_n$ are the eigenvalues of the adjacency matrix of G. In fact, the energies of graphs are special case of trace matrix norm [4] since the singular values of any hermitian matrix are the moduli of its eigenvalues. The trace norm defined by

$$\|A\|_* = \sum_{s=1}^{n} \sigma_s,$$

where $\sigma_1, \sigma_2, ..., \sigma_n$ are the singular values of A. Thus, Nikiforov [4] has generalized the graph energy to the energy $\varepsilon(A)$of arbitrary $m \times n$ matrix A, as the sum of all singular values of A. That is,

$$\varepsilon(A) = \sum_{s=1}^{m} \sigma_s = \|A\|_*.$$

Bravo et al. [1] has extended the concept of energy of $n \times n$ matrix A as follows:

$$\varepsilon_N(A) = \left\| A - \frac{tr(A)}{n} I_n \right\|_*,$$

where $tr(A)$ and I_n denote the trace of A and $n \times n$ identity matrix. If A is the adjacency matrix of graph G then $tr(A) = 0$ and $\varepsilon_N(A) = E(G)$.

*Corresponding author. *E-mail address:* mhvbahsi@yahoo.com

The matrix $H = (h_{ij})_{i,j=0}^{n-1}$, where $h_{ij} = h_{i+j}$, is called Hankel matrix. The matrix H is of the form:

$$H = \begin{bmatrix} h_0 & h_1 & h_2 & \cdots & h_{n-2} & h_{n-1} \\ h_1 & h_2 & h_3 & \cdots & h_{n-1} & h_n \\ \vdots & \vdots & \vdots & & \vdots & \vdots \\ h_{n-2} & h_{n-1} & h_n & \cdots & h_{2n-4} & h_{2n-3} \\ h_{n-1} & h_n & h_{n+1} & \cdots & h_{2n-3} & h_{2n-2} \end{bmatrix}.$$

Fibonacci and Lucas numbers are the numbers in the following sequences, respectively:

$$0, 1, 1, 2, 3, 5, 8, 13, ...$$

and

$$2, 1, 3, 4, 7, 11, 18, 29, ...$$

The sequence F_n of the Fibonacci numbers is defined by recurrence relation $F_n = F_{n-1} + F_{n-2}$ with initial values $F_0 = 0$ and $F_1 = 1$. The sequence L_n of the Lucas numbers is defined by recurrence relation $L_n = L_{n-1} + L_{n-2}$ with initial values $L_0 = 2$ and $L_1 = 1$. For the detailed information of Fibonacci and Lucas numbers, we refer to [3].

In this study, we compute the energies of Hankel matrices with the Fibonacci and Lucas numbers of the forms:

$$A = (F_{i+j})_{i,j=0}^{n-1} = \begin{bmatrix} F_0 & F_1 & F_2 & \cdots & F_{n-2} & F_{n-1} \\ F_1 & F_2 & F_3 & \cdots & F_{n-1} & F_n \\ \vdots & \vdots & \vdots & & \vdots & \vdots \\ F_{n-2} & F_{n-1} & F_n & \cdots & F_{2n-4} & F_{2n-3} \\ F_{n-1} & F_n & F_{n+1} & \cdots & F_{2n-3} & F_{2n-2} \end{bmatrix} \tag{1}$$

and

$$B = (L_{i+j})_{i,j=0}^{n-1} = \begin{bmatrix} L_0 & L_1 & L_2 & \cdots & L_{n-2} & L_{n-1} \\ L_1 & L_2 & L_3 & \cdots & L_{n-1} & L_n \\ \vdots & \vdots & \vdots & & \vdots & \vdots \\ L_{n-2} & L_{n-1} & L_n & \cdots & L_{2n-4} & L_{2n-3} \\ L_{n-1} & L_n & L_{n+1} & \cdots & L_{2n-3} & L_{2n-2} \end{bmatrix} \tag{2}$$

where F_n and L_n are the nth Fibonacci and Lucas numbers, respectively. In [5], the authors have computed the spectral norms of the matrices A and B. Also, they have obtained the eigenvalues of the matrices A and B as [see proofs of Theorems 1 and 2 in 5]:

$$\lambda_{1,2}(A) = \begin{cases} \frac{F_{2n-1}-1\pm\sqrt{F_{2n-1}^2-2F_{2n-1}+4F_n^2+1}}{2}, & \text{for } n \text{ is even} \quad (3) \\ \frac{F_{2n-1}-1\pm\sqrt{F_{2n-1}^2-2F_{2n-1}+4F_n^2-3}}{2}, & \text{for } n \text{ is odd,} \quad (4) \end{cases}$$

$$\lambda_m(A) = 0, m = 2, 3, ..., n \tag{5}$$

and

$$\lambda_{1,2}(B) = \begin{cases} \frac{L_{2n-1}+1\pm\left(F_{2n-1}-1\right)\sqrt{5}}{2}, & \text{for } n \text{ is even} \quad (6) \\ \frac{L_{2n-1}+1\pm\sqrt{5\left(F_{2n-1}-1\right)^2+4}}{2}, & \text{for } n \text{ is odd.} \quad (7) \end{cases}$$

$$\lambda_m(B) = 0, m = 2, 3, ..., n. \tag{8}$$

In the next section we give our main results.

2 Main Results

Theorem 2.1. Let the matrix A be as in (1). Then

$$\varepsilon(A) = \begin{cases} \sqrt{F_{2n-1}^2 - 2F_{2n-1} + 4F_n^2 + 1}, & \text{for } n \text{ is even} \\ \sqrt{F_{2n-1}^2 - 2F_{2n-1} + 4F_n^2 - 3}, & \text{for } n \text{ is odd.} \end{cases}$$

Proof. Since the matrix A is symmetric, its singular values are the moduli of its eigenvalues. Thus, by the formulas (3), (4) and (5) we have

$$\sigma_1 = |\lambda_1| = \begin{cases} \frac{F_{2n-1}-1+\sqrt{F_{2n-1}^2-2F_{2n-1}+4F_n^2+1}}{2}, & \text{for } n \text{ is even} \\ \frac{F_{2n-1}-1+\sqrt{F_{2n-1}^2-2F_{2n-1}+4F_n^2-3}}{2}, & \text{for } n \text{ is odd,} \end{cases}$$

$$\sigma_2 = |\lambda_2| = \begin{cases} \frac{\sqrt{F_{2n-1}^2-2F_{2n-1}+4F_n^2+1}-F_{2n-1}+1}{2}, & \text{for } n \text{ is even} \\ \frac{\sqrt{F_{2n-1}^2-2F_{2n-1}+4F_n^2-3}-F_{2n-1}+1}{2}, & \text{for } n \text{ is odd} \end{cases}$$

and

$$\sigma_m = |\lambda_m| = 0, m = 2, 3, ..., n,$$

where σ_j and λ_j denote the singular values and eigenvalues of A, respectively. Therefore,

$$\varepsilon(A) = \sum_{s=1}^{m} \sigma_s = \begin{cases} \sqrt{F_{2n-1}^2 - 2F_{2n-1} + 4F_n^2 + 1}, & \text{for } n \text{ is even} \\ \sqrt{F_{2n-1}^2 - 2F_{2n-1} + 4F_n^2 - 3}, & \text{for } n \text{ is odd.} \end{cases}$$

Theorem 2.2. Let the matrix A be as in (1). Then

$$\varepsilon_N(A) = \begin{cases} \sqrt{F_{2n-1}^2 - 2F_{2n-1} + 4F_n^2 + 1} + (n-2)\frac{F_{2n-1}-1}{n}, & \text{for } n \text{ is even} \\ \sqrt{F_{2n-1}^2 - 2F_{2n-1} + 4F_n^2 - 3} + (n-2)\frac{F_{2n-1}-1}{n}, & \text{for } n \text{ is odd.} \end{cases}$$

Proof. Since the matrix A is symmetric, the matrix $A - \frac{tr(A)}{n}I_n$ is also symmetric and eigenvalues of $A - \frac{tr(A)}{n}I_n$ are $\mu_1 = \lambda_1 - \frac{tr(A)}{n}$, $\mu_2 = \lambda_2 - \frac{tr(A)}{n}$, $\dots$, $\mu_n = \lambda_n - \frac{tr(A)}{n}$. Also,

$$tr(A) = \sum_{i=0}^{n-1} F_{2i} = F_{2n-1} - 1.$$

If n is even, then,

$$\mu_1 = \lambda_1 - \frac{tr(A)}{n} = \frac{F_{2n-1} - 1 + \sqrt{F_{2n-1}^2 - 2F_{2n-1} + 4F_n^2 + 1}}{2} - \frac{F_{2n-1} - 1}{n},$$

$$\mu_2 = \lambda_2 - \frac{tr(A)}{n} = \frac{F_{2n-1} - 1 - \sqrt{F_{2n-1}^2 - 2F_{2n-1} + 4F_n^2 + 1}}{2} - \frac{F_{2n-1} - 1}{n},$$

and

$$\mu_m = \lambda_m - \frac{tr(A)}{n} = -\frac{F_{2n-1} - 1}{n}, m = 2, 3, ..., n.$$

Thus, we have

$$\varepsilon_N(A) = \left\| A - \frac{tr(A)}{n} I_n \right\|_* = \sum_{i=1}^{n} |\mu_i| = \sqrt{F_{2n-1}^2 - 2F_{2n-1} + 4F_n^2 + 1} + (n-2)\,\frac{F_{2n-1}-1}{n}.$$

If n is odd, similarly, we have

$$\varepsilon_N(A) = \left\| A - \frac{tr(A)}{n} I_n \right\|_* = \sum_{i=1}^{n} |\mu_i| = \sqrt{F_{2n-1}^2 - 2F_{2n-1} + 4F_n^2 - 3} + (n-2)\,\frac{F_{2n-1}-1}{n}.$$

Theorem 2.3. Let the matrix B be as in (**??**). Then

$$\varepsilon(B) = L_{2n-1} + 1.$$

Proof. The matrix B is symmetric. Then, its singular values are the moduli of its eigenvalues. Also, one can see easily that

$$L_{2n-1} + 1 \geq \sqrt{5\left(F_{2n-1} - 1\right)^2 + 4} \tag{3}$$

for $n \geq 1$. Then, the formulas (6), (7), (8) and (9) yield

$$\psi_1 = |\beta_1| = \begin{cases} \frac{L_{2n-1}+1+\left(F_{2n-1}-1\right)\sqrt{5}}{2}, & \text{for } n \text{ is even} \\ \frac{L_{2n-1}+1+\sqrt{5\left(F_{2n-1}-1\right)^2+4}}{2}, & \text{for } n \text{ is odd,} \end{cases}$$

$$\psi_2 = |\beta_2| = \begin{cases} \frac{L_{2n-1}+1-\left(F_{2n-1}-1\right)\sqrt{5}}{2}, & \text{for } n \text{ is even} \\ \frac{L_{2n-1}+1-\sqrt{5\left(F_{2n-1}-1\right)^2+4}}{2}, & \text{for } n \text{ is odd,} \end{cases}$$

and

$$\psi_m = |\beta_m| = 0, m = 2, 3, ..., n,$$

where ψ_j and β_j denote the singular values and eigenvalues of B, respectively. Thus,

$$\varepsilon(B) = \sum_{s=1}^{m} \psi_s = L_{2n-1} + 1.$$

Theorem 2.4. Let the matrix B be as in (2). Then

$$\varepsilon_N(B) = \begin{cases} \left(F_{2n-1} - 1\right)\sqrt{5} + (n-2)\,\frac{L_{2n-1}+1}{n}, & \text{for } n \text{ is even} \\ \sqrt{5\left(F_{2n-1} - 1\right)^2 + 4} + (n-2)\,\frac{L_{2n-1}+1}{n}, & \text{for } n \text{ is odd.} \end{cases}$$

Proof. The matrices B and $B - \frac{tr(B)}{n} I_n$ are symmetric. For the eigenvalues of $B - \frac{tr(B)}{n} I_n$, we have $\eta_1 = \beta_1 - \frac{tr(B)}{n}$, $\eta_2 = \beta_2 - \frac{tr(B)}{n}$, $\ldots$, $\eta_n = \beta_n - \frac{tr(B)}{n}$. In addition,

$$tr(B) = \sum_{i=0}^{n-1} L_{2i} = L_{2n-1} + 1.$$

If n is even, then,

$$\eta_1 = \beta_1 - \frac{tr(B)}{n} = \frac{L_{2n-1} + 1 + \left(F_{2n-1} - 1\right)\sqrt{5}}{2} - \frac{L_{2n-1}+1}{n},$$

$$\eta_2 = \beta_2 - \frac{tr(B)}{n} = \frac{L_{2n-1} + 1 - \left(F_{2n-1} - 1\right)\sqrt{5}}{2} - \frac{L_{2n-1} + 1}{n},$$

and

$$\eta_m = \beta_m - \frac{tr(B)}{n} = -\frac{L_{2n-1} + 1}{n}, m = 2, 3, ..., n.$$

Considering the equality

$$\frac{\left(F_{2n-1} - 1\right)\sqrt{5}}{2} + \frac{L_{2n-1} + 1}{n} \geq \frac{L_{2n-1} + 1}{2},$$

we have

$$\varepsilon_N\left(B\right) = \left\|B - \frac{tr(B)}{n} I_n\right\|_* = \sum_{i=1}^{n} |\eta_i| = \left(F_{2n-1} - 1\right)\sqrt{5} + (n-2)\frac{L_{2n-1} + 1}{n}.$$

If n is odd, similarly, we have

$$\varepsilon_N\left(B\right) = \left\|B - \frac{tr(B)}{n} I_n\right\|_* = \sum_{i=1}^{n} |\eta_i| = \sqrt{5\left(F_{2n-1} - 1\right)^2 + 4} + (n-2)\frac{L_{2n-1} + 1}{n}.$$

References

[1] D. Bravo, F. Cubría and J. Rada, Energy of matrices, Applied Mathematics and Computation 312 (2017) 149–157.

[2] I. Gutman, The energy of a graph, Ber. Math.-Stat. Sekt. Forschungszent. Graz, 103 (1978) 1–22.

[3] T. Koshy, Fibonacci and Lucas Numbers with Applications, A Wiley-Interscience Publication, 2001.

[4] V. Nikiforov, The energy of graphs and matrices, J. Math. Anal. Appl. 326 (2007) 1472–1475 .

[5] S. Solak and M. Bahşi, On the Spectral Norms of Hankel Matrices with Fibonacci and Lucas Numbers, Selçuk Journal of Applied Mathematics, 12 (1) (2011) 71-76.

On The Hankel Transforms

Süleyman SOLAK*

A.K. Education Faculty, Necmettin Erbakan University,

Konya/TURKEY

Atiye AYYILDIZ

Institute of Educational Sciences, Necmettin Erbakan University

Konya/TURKEY

Abstract

In this study, that Hankel transform is invariant under Invert transform which had been proved by Layman, is proved by us with a different method. The method of proof consists generation of a table *S*. Table *S* is formed sequentially by multiplication elements of a column with elements of rows and the sum of diagonal elements. Equation of the elements of initial row to the sum of diagonal elements, gives the equalities which are used in the proof. The operations described in the proof, have a simple interpretation in terms of the table *S*. That operations reached by multiplying each row/column with an element and add a row/column to another row/column. The determinant of a matrix is invariant under these operations. Thus, that Hankel transform is invariant under Invert transform, is concluded. Operations described in the proof are explained with an example that acquired Pell numbers as invert transform of Fibonacci numbers.

***Key words**: Hankel transformations, Hankel matrix, invert transformation.*

1. Introduction

An infinite Hankel matrix *H* is defined as $H = (h_{i+j})_{i,j=1}^{\infty}$. If matrix *H*, the Hankel matrix of the integer sequence $A = \{a_1, a_2, a_3, ...\}$ then,

$$H = \begin{pmatrix} a_1 & a_2 & a_3 & \cdots \\ a_2 & a_3 & a_4 & \cdots \\ a_3 & a_4 & a_5 & \cdots \\ \vdots & \vdots & \vdots & \ddots \end{pmatrix}$$

with elements $h_{i,j} = a_{i+j-1}$. The Hankel matrix H_n of order *n* of *A* is the upper-left $n \times n$ submatrix of *H*, and h_n, the Hankel determinant of order *n* of *A*, is the determinant of the corresponding Hankel matrix of order *n*, $h_n = \det(H_n)$ (Layman, 2001).

*Corresponding author. *E-mail address:* ssolak42@yahoo.com

Let h_n denote the determinant of the Hankel matrix of order *n*. Then define the Hankel transform *H* of $A=\{a_1,a_2,a_3,...\}$ to be the sequence $\{h_n\}=\{h_1,h_2,h_3,...\}$ (Spivey and Steil, 2006).

Let $A=\{a_0,a_1,a_2,a_3,...\}$ be integer sequences. If $b_0=1$ and $b_j=\sum_{m=1}^{j}a_m b_{j-m}$ then $B(A)=\{b_j\}$ is called the invert transform of A.

There are many researchs related to Hankel transforms, Hankel determinants

and binomial transforms in literature. [1-3]

In [1], Layman has defined Hankel transform of an integer sequence and has discussed some of its properties. He has shown that the Hankel transform of this sequence is the same as the Hankel transform of the Binomial or Invert transform of this sequence.

Michael and Steil have given a new proof of the invariance of the Hankel transform under the binomial transform of a sequence. Their method of proof led to three variations of the binomial transform; called these the k-binomial transforms [2].

Pan studied the multiple binomial transform and the Hankel transform of shifted sequences of an integer sequences, particularly a linear homogenous recurrence sequence and some of their properties [3].

In this study, we give a new proof to below theorem which is different from Layman's method.

2. Main Theorem

Theorem 1. Let *A* be an integer sequence and *B* its invert transform. Then *A* and *B* have the same Hankel transform. In other words, the Hankel transform is invariant under the invert transform (Layman, 2001).

Proof. Let $A=\{a_1,a_2,a_3,...\}$ is integer sequences and $B=\{b_1,b_2,b_3,...\}$ is the invert transform of A. H^* is defined to be the matrix $H^*=RHC$ where the elements of R, H and

C are given by

$$r_{i,k}=\begin{cases}0, & k>i\\ b_{i-k}, & k\le i\end{cases} \qquad h_{k,m}=a_{k+m-1} \qquad c_{m,j}=\begin{cases}0, & j\prec m\\ b_{i-k}, & j\ge m\end{cases}$$

where b_0 is defined to be 1. The matrix forms of R, H, C are respectively

$$R=\begin{pmatrix} b_0 & 0 & 0 & 0 & \dots & 0 \\ b_1 & b_0 & 0 & 0 & \cdots & 0 \\ b_2 & b_1 & b_0 & 0 & \dots & 0 \\ b_3 & b_2 & b_1 & b_0 & \dots & 0 \\ \vdots & \vdots & \vdots & \vdots & \ddots & \vdots \\ b_{n-1} & b_{n-2} & b_{n-3} & \dots & b_1 & b_0 \end{pmatrix} \qquad H=\begin{pmatrix} a_1 & a_2 & a_3 & \dots \\ a_2 & a_3 & a_4 & \dots \\ a_3 & a_4 & a_5 & \dots \\ \vdots & \vdots & \vdots & \ddots \end{pmatrix}$$

$$C=\begin{pmatrix} b_0 & b_1 & b_2 & b_3 & \dots & b_{n-1} \\ 0 & b_0 & b_1 & b_2 & \cdots & b_{n-2} \\ 0 & 0 & b_0 & b_1 & \dots & b_{n-3} \\ 0 & 0 & 0 & b_0 & \dots & b_{n-4} \\ \vdots & \vdots & \vdots & \vdots & \ddots & \vdots \\ 0 & 0 & 0 & \dots & & b_0 \end{pmatrix}$$

Then the (i,j-1) element of H^*, given by

$$h^*_{i,j-1}=\sum_{k=1}^{i}\sum_{m=1}^{j-1} r_{ik}h_{km}c_{mj-1}=\sum_{k=1}^{i}\sum_{m=1}^{j-1} b_{i-k}a_{k+m-1}b_{j-m-1}$$

$$=\sum_{k=2}^{i}\sum_{m=1}^{j-1} b_{i-k}a_{k+m-1}b_{j-m-1}+b_{i-1}\sum_{m=1}^{j-1}a_m b_{j-m-1}$$

$$=\sum_{k=1}^{i-1}\sum_{m=1}^{j-1} b_{i-1-k}a_{k+m}b_{j-m-1}+b_{i-1}\left[\sum_{m=1}^{j-2}a_m b_{j-m-1}+a_{j-1}\right]$$

$$=\sum_{k=1}^{i-1}\sum_{m=2}^{j} b_{i-1-k}a_{k+m-1}b_{j-m}+b_{i-1}b_{j-1}$$

$$=\sum_{k=1}^{i-1}\sum_{m=1}^{j} b_{i-1-k}a_{k+m-1}b_{j-m}-b_{i-1}\sum_{k=1}^{i-1}b_{i-1-k}a_k+b_{i-1}b_{j-1}$$

$$=\sum_{k=1}^{i-1}\sum_{m=1}^{j} b_{i-1-k}a_{k+m-1}b_{j-m}$$

$$=h^*_{i-1,j}$$

which shows that $h^*_{i,j}=b_{i+j-1}$, in other words, that H^* is the Hankel matrix of B. Since L and R are triangular with diagonals consisting of all 1's, this shows that the Hankel determinants of B are the same as those for A, and thus A and B have the same Hankel transform.

Now we give a new proof to this theorem by using a different method, independent from Layman's. Our proof technique suggests generalizations of the invert transforms. We require the following lemma.

Lemma 2. (Table *S*) Given a sequence $A = \{a_1, a_2, a_3, ...\}$ create table of numbers S using the following rule

m (multiplication)	1 (First Column)	invert transform of *A* sequence (initial row)
A Sequence (initial column)		

a)The initial column consists of elements of *A* and the first element of initial row is 1.

b)Each elements of initial column multiply with 1 and place to the first column.

c)The sum of diagonal elements generate the first element of invert transform b_1, that is the second element of initial row (first element 1 is invariably).

Each elements of initial column multiply with b_1 and place to the second column. The sum of diagonal elements generate the second element of invert transform b_2 that is the third element of initial row.

The rest of invert transform's elements are obtained by applying these rules to b_i, $(i = 3,4,5,...,n-1)$ as each elements of initial column multiply with b_i, and place to the *i+1* th column. The sum of diagonal elements generate the *i+1* th element of invert transform that is the *i+2* th element of initial row.

Thus, the elements of initial row is obtained. Except of 1 that is also the elements of invert transform of *A* sequence.

m	1	
a_1		
a_2		
a_3		

m	1	$a_1 = b_1$
a_1	a_1	
a_2	a_2	
a_3	a_3	

m	1	b_1	$a_2 + a_1 b_1 = b_2$
a_1	a_1	$a_1 b_1$	
a_2	a_2	$a_2 b_1$	
a_3	a_3	$a_3 b_1$	

m	1	b_1	b_2
a_1	a_1	$a_1 b_1$	$a_1 b_2$
a_2	a_2	$a_2 b_1$	$a_2 b_2$
a_3	a_3	$a_3 b_1$	$a_3 b_2$

m	1	b_1	b_2	$a_3 + a_2 b_1 + a_1 b_2 = b_3$
a_1	a_1	$a_1 b_1$	$a_1 b_2$	
a_2	a_2	$a_2 b_1$	$a_2 b_2$	
a_3	a_3	$a_3 b_1$	$a_3 b_2$	

Figure 1. (*m*: multiplication)

Example 3. The invert transform of the Fibonacci numbers is the Pell numbers. Figure 2. illustrates how the Pell numbers can be generated from the Fibonacci numbers using the table described in Lemma 2.

•	1	**1**		
1	**1**			
1	1			
2	2			
3	3			
5	5			

•	1	1	**1+1=2**	
1	1	**1**		
1	**1**	1		
2	2	2		
3	3	3		
5	5	5		

•	1	1	2	**2+1+2=5**	
1	1	1	**2**		
1	1	**1**	2		
2	**2**	2	4		
3	3	3	6		
5	5	5	10		

•	1	1	2	5	**3+2+2+5=12**	
1	1	1	2	**5**		
1	1	1	**2**	5		
2	2	**2**	4	10		
3	**3**	3	6	15		
5	5	5	10	25		

•	1	1	2	5	12	**5+3+4+5+12=29**
1	1	1	2	5	**12**	
1	1	1	2	**5**	12	
2	2	2	**4**	10	24	
3	3	**3**	6	15	36	
5	**5**	5	10	25	60	

Figure 2

Thus, the invert transform of the Fibonacci numbers can be generated as $\{1,2,5,12,29\}$.

Example 4. Figure 3 illustrates how the invert transform of the nonnegative even numbers can be generated from the table given in Lemma 2.

•	1	**2**		
2	**2**			
4	4			
6	6			
8	8			
10	10			

•	1	2	**4+4=8**		
2	2	**4**			
4	**4**	8			
6	6	12			
8	8	16			
10	10	20			

•	1	2	8	**6+8+16=30**	
2	2	4	**16**		
4	4	**8**	32		
6	**6**	12	48		
8	8	16	64		
10	10	20	80		

•	1	2	8	30	**8+12+32+60=112**
2	2	4	16	**60**	
4	4	8	**32**	120	
6	6	**12**	48	180	
8	**8**	16	64	240	
10	10	20	80	300	

•	1	2	8	30	112	**10+16+48+120+224=418**
2	2	4	16	60	**224**	
4	4	8	32	**120**	448	
6	6	12	**48**	180	672	
8	8	**16**	64	240	896	
10	**10**	20	80	300	1120	

Figure 3

Thus, the invert transform of the nonnegative even numbers can be generated as $\{2,8,30,112,418\}$.

Proof. Let $A=\{a_1,a_2,a_3,...\}$ be an integer sequence and $B=\{b_1,b_2,b_3,...\}$ be the invert transform of *A*. We define a procedure for transforming the Hankel matrix of order *n* of a sequence *A* to the Hankel matrix of order *n* of a sequence *B*. Let $S_{i,0}$ be the *i* th element of initial column which is also equal to *i* th element of *A*, let $S_{j,j}$ be the *j*+1 th element of initial row which is also equal to *j* th element of *B* and create the table *S* described in Lemma 2 where $S_{i+j,j}$ is the (*i*,*j*+1) th element of table *S*.

$\bullet$	1	b_1	b_2	$\cdots$
a_1	a_1	a_1b_1	a_1b_2	$\cdots$
a_2	a_2	a_2b_1	a_2b_2	$\cdots$
$\vdots$	$\vdots$	$\vdots$	$\vdots$	$\ddots$

$$a_i=S_{i,0},\qquad b_j=S_{j,j},\qquad a_ib_j=S_{i,0}S_{j,j}=S_{i+j,j}$$

If we use these equalities, we get the same table as

$\bullet$	$S_{0,0}$	$S_{1,1}$	$S_{2,2}$	$\cdots$
$S_{1,0}$	$S_{1,0}$	$S_{2,1}$	$S_{3,2}$	$\cdots$
$S_{2,0}$	$S_{2,0}$	$S_{3,1}$	$S_{4,2}$	$\cdots$
$\vdots$	$\vdots$	$\vdots$	$\vdots$	$\ddots$

In Lemma 2, elements of initial row which is obtained from the sum of diagonal elements, give us the following equality

$$S_{0,0}=1$$

$$S_{1,0}=S_{1,1}$$

$$S_{2,0}+S_{2,1}=S_{2,2}$$

$$S_{3,0}+S_{3,1}+S_{3,2}=S_{3,3}$$

$$\vdots$$

$$S_{n,0}+S_{n,1}+S_{n,2}+...S_{n,n-1}=S_{n,n} \tag{1}$$

Let S_n is the following matrix consisting of numbers from the element of $A=\{a_1,a_2,a_3,...\}$ integer sequence. Since $S_{i,0}=a_i$, S_n is the Hankel matrix of *A* order *n*.

$$S_n = \begin{pmatrix} S_{1,0} & S_{2,0} & S_{3,0} & \cdots & S_{n,0} \\ S_{2,0} & S_{3,0} & S_{4,0} & \cdots & S_{n+1,0} \\ S_{3,0} & S_{4,0} & S_{5,0} & \cdots & S_{n+2,0} \\ \vdots & \vdots & \vdots & \ddots & \vdots \\ S_{n,0} & S_{n+1,0} & S_{n+2,0} & \cdots & S_{2n-1,0} \end{pmatrix}$$

Then apply the following transformations to S_n,

(a) Let $m = n, n-1, n-2, ..., 2$ and $i = 1, 2, ..., \mathrm{m}-1$, then multiply $m-i$ th row of S_n with b_i and add to m th row.

(b) Let $i = 1,2,...,n-1$, multiply i th column with a_j where $j = 1,2,...,n-i$ and add to (j+i) th column.

After application of stage (a), m th row of the matrix is at the following form

for $m = i+1$

$$(S_{m,0} + S_{m,1} + ... + S_{m,m-1} \quad S_{m+1,0} + S_{m+1,1} + ... + S_{m+1,m-1} \; \cdots \; S_{m+n-1,0} + S_{m+n-1,1} + ... + S_{m+n-1,m-1})$$
$$(S_{m,m} \qquad S_{m+1,0} + S_{m+1,1} + ... + S_{m+1,m-1} \; \cdots \; S_{m+n-1,0} + S_{m+n-1,1} + ... + S_{m+n-1,m-1}) \text{ from (1)}$$

for $m > i+1$

$$(S_{m,0} + S_{m,1} + ... + S_{m,i} \quad S_{m+1,0} + S_{m+1,1} + ... + S_{m+1,i} \; \cdots \; S_{m+n-1,0} + S_{m+n-1,1} + ... + S_{m+n-1,i})$$

The claim is clearly true initially when $i = 0$. Now assume that the claim is true for $i = k-1$ and prove it for $i = k$ with induction. Then in stage $i = k-1$;

for $m > k$, (m-k) th row of S_n is as follows.

$$(S_{m-k,0} \quad S_{m-k+1,0} \quad ... \quad S_{m-k+n-1,0})$$

If we multiply this row with $b_k = S_{k,k}$,

$$S_{k,k}(S_{m-k,0} \quad S_{m-k+1,0} \quad ... \quad S_{m-k+n-1,0}) = (S_{m,k} \quad S_{m+1,k} \quad ... \quad S_{m+n-1,k})$$

and add to m th row that is as follows

$$(S_{m,0} + S_{m,1} + ... + S_{m,k-1} \quad S_{m+1,0} + S_{m+1,1} + ... + S_{m+1,k-1} \; \cdots \; S_{m+n-1,0} + S_{m+n-1,1} + ... + S_{m+n-1,k-1})$$

Sum of these rows give m th row as

$$(S_{m,0} + S_{m,1} + ... + S_{m,k} \quad S_{m+1,0} + S_{m+1,1} + ... + S_{m+1,k} \; \cdots \; S_{m+n-1,0} + S_{m+n-1,1} + ... + S_{m+n-1,k})$$

Thus, it is proved for $i = k$.

After the transformations in (a) are applied, we have the matrix

$$\begin{pmatrix} S_{1,1} & S_{2,0} & S_{3,0} & \cdots & S_{n,0} \\ S_{2,2} & S_{3,0}+S_{3,1} & S_{4,0}+S_{4,1} & \cdots & S_{n+1,0}+S_{n+1,1} \\ S_{3,3} & S_{4,0}+S_{4,1}+S_{4,2} & S_{5,0}+S_{5,1}+S_{5,2} & \cdots & S_{n+2,0}+S_{n+2,1}+S_{n+2,2} \\ \vdots & \vdots & \vdots & \ddots & \vdots \\ S_{n,n} & S_{n+1,0}+S_{n+1,1}+S_{n+1,n-1} & S_{n+2,0}+S_{n+2,1}+S_{n+2,n-1} & \cdots & S_{2n-1,0}+S_{2n-1,1}+S_{2n-1,n-1} \end{pmatrix}$$

After application of stage (b), *m* th column of the matrix is at the following form

for $m \le i$, from (1) $\quad (S_{m,m} \quad S_{m+1,m+1} \quad \cdots \quad S_{m+n-1,m+n-1})^T$

for $m > i$

$$(S_{m,0}+S_{m,1}+\ldots+S_{m,i} \quad S_{m+1,0}+S_{m+1,1}+\ldots+S_{m+1,i+1} \ \ldots \ S_{m+n-1,0}+S_{m+n-1,1}+\ldots+S_{m+n-1,i+n-1})^T$$

The claim is clearly true initially when $i = 0$. Now assume that the claim is true for $i = k-1$ and prove it for $i = k$ with induction. Then in stage $i = k$ only columns that change are $k+1, k+2, \ldots, n$

for $i = k$, *k* th column of the matrix is as follows.

$$(S_{k,k} \quad S_{k+1,k+1} \quad \cdots \quad S_{k+n-1,k+n-1})^T$$

If we multiply this column with $a_{m-k} = S_{m-k,0}$ and add to *m* th column, we get ;

$$S_{m-k,0}(S_{k,k} \quad S_{k+1,k+1} \quad \cdots \quad S_{k+n-1,k+n-1})^T = (S_{m,k} \quad S_{m+1,k+1} \quad \cdots \quad S_{m+n-1,k+n-1})^T$$

$$(S_{m,0}+S_{m,1}+\ldots+S_{m,k-1} \quad S_{m+1,0}+S_{m+1,1}+\ldots+S_{m+1,k} \ \ldots \ S_{m+n-1,0}+S_{m+n-1,1}+\ldots+S_{m+n-1,k+n-2})^T$$

Sum of these columns give m th column as

$$(S_{m,0}+S_{m,1}+\ldots+S_{m,k} \quad S_{m+1,0}+S_{m+1,1}+\ldots+S_{m+1,k+1} \ \ldots \ S_{m+n-1,0}+S_{m+n-1,1}+\ldots+S_{m+n-1,k+n-1})^T$$

Therefore for $i = k$, verified with induction. After application of this stage to all rows, from (1) we get;

$$S_n = \begin{pmatrix} S_{1,1} & S_{2,2} & S_{3,3} & \cdots & S_{n,n} \\ S_{2,2} & S_{3,3} & S_{4,4} & \cdots & S_{n+1,n+1} \\ S_{3,3} & S_{4,4} & S_{5,5} & \cdots & S_{n+2,n+2} \\ \vdots & \vdots & \vdots & \ddots & \vdots \\ S_{n,n} & S_{n+1,n+1} & S_{n+2,n+2} & \cdots & S_{2n-1,2n-1} \end{pmatrix}$$

S_n is the Hankel matrix of order *n* of *B(A),* which is the invert transform of *A*. Since the only matrix manipulation we used multiplying row with number b_i, add a row to another row and multiplying column with number a_j, add a column to another column. The determinant of a matrix is invariant under these operations. The determinant of the Hankel matrix of order n of A is equal to the determinant of the Hankel matrix of order n of $B(A)$. So, we conclude that the Hankel transform is invariant under the invert transform.

The operations described in the proof of Theorem 1 when done in the order prescribed by the procedure have a simple interpretation in terms of the table S. In proof of theorem multiply b_i with each row shifts the elements which is obtained multiply b_i with the elements of initial row in table S and adding a row to another row shifts the sum of diagonal elements

Example 5. We can see that the same invert transform Hankel matrix of order 4 of the Fibonacci numbers by a comparison of Figure 2 and the sequence of matrices arising from the procedure described in the proof of Theorem 1

$$\begin{pmatrix} 1 & 1 & 2 & 3 \\ 1 & 2 & 3 & 5 \\ 2 & 3 & 5 & 8 \\ 3 & 5 & 8 & 13 \end{pmatrix} \to \begin{pmatrix} 1 & 1 & 2 & 3 \\ 1 & 2 & 3 & 5 \\ 2 & 3 & 5 & 8 \\ 5 & 8 & 13 & 21 \end{pmatrix} \to \begin{pmatrix} 1 & 1 & 2 & 3 \\ 1 & 2 & 3 & 5 \\ 2 & 3 & 5 & 8 \\ 7 & 12 & 19 & 31 \end{pmatrix} \to \begin{pmatrix} 1 & 1 & 2 & 3 \\ 1 & 2 & 3 & 5 \\ 2 & 3 & 5 & 8 \\ 12 & 17 & 29 & 46 \end{pmatrix}$$

$$\to \begin{pmatrix} 1 & 1 & 2 & 3 \\ 1 & 2 & 3 & 5 \\ 3 & 5 & 8 & 13 \\ 12 & 17 & 29 & 46 \end{pmatrix} \to \begin{pmatrix} 1 & 1 & 2 & 3 \\ 2 & 3 & 5 & 8 \\ 5 & 7 & 12 & 19 \\ 12 & 17 & 29 & 46 \end{pmatrix} \to$$

$$\begin{pmatrix} 1 & 2 & 3 & 5 \\ 2 & 5 & 7 & 12 \\ 5 & 12 & 17 & 29 \\ 12 & 29 & 41 & 70 \end{pmatrix} \to \begin{pmatrix} 1 & 2 & 5 & 7 \\ 2 & 5 & 12 & 17 \\ 5 & 12 & 29 & 41 \\ 12 & 29 & 70 & 99 \end{pmatrix} \to \begin{pmatrix} 1 & 2 & 5 & 12 \\ 2 & 5 & 12 & 29 \\ 5 & 12 & 29 & 70 \\ 12 & 29 & 70 & 169 \end{pmatrix}$$

In Figure 2 we get the invert transform of $\{1,1,2,3,5,8,13,21...\}$ as $\{1,2,5,12,29,70,169...\}$.

Example 6. We can see that the invert transform of Pell numbers are obtained arising from the procedure described in the proof of Theorem 1

$$\begin{pmatrix} 1 & 2 & 5 \\ 2 & 5 & 12 \\ 5 & 12 & 29 \end{pmatrix} \to \begin{pmatrix} 1 & 2 & 5 \\ 3 & 7 & 17 \\ 7 & 17 & 41 \end{pmatrix} \to \begin{pmatrix} 1 & 2 & 5 \\ 3 & 7 & 17 \\ 10 & 23 & 56 \end{pmatrix} \to$$

$$\begin{pmatrix} 1 & 3 & 5 \\ 3 & 10 & 17 \\ 10 & 33 & 56 \end{pmatrix} \to \begin{pmatrix} 1 & 3 & 7 \\ 3 & 10 & 23 \\ 10 & 33 & 76 \end{pmatrix} \to \begin{pmatrix} 1 & 3 & 10 \\ 3 & 10 & 33 \\ 10 & 33 & 109 \end{pmatrix}$$

After the application of procedure we get the invert transform of $\{1,2,5,12,29...\}$ as $\{1,3,10,33,109...\}$

.

REFERENCES

[1] J.W. Layman, The Hankel transform and some of its properties, Journal of Integer Sequences, 4, Article 01.1.5. (2001).

[2] M.Z. Spivey, L.L.Steil, The k-Binomial Transforms and the Hankel Transform Journal of Integer Sequences, Vol. 9 Article 06.1.1. (2006).

[3] J. Pan, Some Properties of the Multiple Binomial Transform and the Hankel Transform of Shifted Sequences Journal of Integer Sequences, Vol. 14, Article 11.3.4. (2011).

*Corresponding author. *E-mail address:* ssolak42@yahoo.com

Impact Of Geometric Nonlinearity On The Analysis Of Spatial Steel Frames

Serdar ÇARBAŞ
Department of Civil Engineering,
Karamanoglu Mehmetbey University,
Karaman/TURKEY

Osman TUNCA *
Department of Civil Engineering,
Karamanoglu Mehmetbey University,
Karaman/TURKEY

S. Alper YILDIZEL
Department of Civil Engineering,
Karamanoglu Mehmetbey University,
Karaman/TURKEY

Abstract

Due to the slenderness and the presence of imperfections in steel sections, by which the space steel frames are constituted, it is necessary to consider the geometric nonlinearity in the prediction of their response to external loading in order to attain realistic results in their design. In this study, the effect of geometric nonlinearity on space steel frames is discussed. General information about elastic critical load analysis, calculation of elastic critical load factor, stiffness matrix of a space member, nonlinear stiffness matrix with stability functions and nonlinear elastic critical load analysis are also principally described in the paper.

Keywords: Geometric nonlinearity, spatial frames, structural analysis.

1 Introduction

A variety of classifications may be used to describe the deformational response of structures; for example, small or large, elastic or inelastic, etc. In general, deformations of structures under the external loads are small, and hence the application of the equilibrium equations on the undeformed shape of the structure does not introduce large errors. However, when structure consists of slender members, the deformations become large and small deflection theory is no longer valid. The equilibrium equations are required to be written in such structures on the deformed shape of its elements. In other words, the deflected shape of the structure should be taken into account. When this is considered in the displacement computations, the relationship between the external loads and displacements become nonlinear. Geometric nonlinearity is required to be considered in the analysis of a structure, if its deflections are large compared with its initial dimensions. In structures with large displacements, although the material behaves linear elastic, the response of the structure becomes nonlinear [1].

2 Definition Of Elastic Critical Load Analysis

Elastic Critical Load Analysis computes the elastic critical load factor, λ_c, for a structure subjected to a particular set of applied loads. This load factor is the ratio by which the axial forces in the members of the structure must be increased to cause the structure to become

*Corresponding author. *E-mail address:* osmantunca@kmu.edu.tr

unstable due to the flexural buckling of one or more members (lateral torsional buckling of individual members is not taken into account). The elastic critical load of the structure is a function of the elastic properties of the structure and the pattern of loading. Once the elastic critical load is known, member effective lengths can be calculated. The effective length of a member is defined as the length of an ideal pin-ended strut having the same elastic critical load as the load existing in the member when the structure is at its critical load. The effective length may be expressed as a factor multiplying the actual member length. The effective length factor is calculated separately for each of the member principal axes for each load case. A load factor of less than 1.0 for any load case indicates that the structure is unstable under the applied loading. The elastic critical load for any load case is determined by computing the axial forces in the members of the structure and then increasing them in proportion until the structure becomes unstable. At this point the factor by which the axial forces have been increased is the elastic critical load factor for the structure under the current loading. The elastic critical load factor is also known as the buckling load factor [2, 3].

3 Calculation Of Elastic Critical Load Factor

The elastic behavior of a structure is governed by the equation:

$$P = K_s \Delta \tag{1}$$

or more precisely:

$$\lambda P = K_s \left(\lambda P\right) \Delta \tag{2}$$

The use of implies that is a function of the applied load . This equation is nonlinear.
where;
P = external loads applied at the joints of the structure,
Δ = joint displacements of the structure,
K_s = stiffness matrix of the structure,
λ = the load factor.
To determine the value of the critical load factor, λ_c, the problem is linearized by carrying out a double iterative process. The value of λ is increased in a step-by-step manner, and at each load level the singularity of $K_s(\lambda P)$ is checked. At each load level, also, an inner iteration is performed before the singularity check to find the correct values of the member axial forces shown in Equation (2) is solved repeatedly until a consistent set of deflections is obtained. The number of iterations required here depends on how the structure is near to instability, and how good a guess of axial force can be made initially [4, 5].

4 Derivation of A Nonlinear Stiffness Matrix Using Stability Functions

The axial forces in a member have a significant effect on its flexural bending that cause non-linearity in the behavior of structures. Therefore, it is of importance to study this effect in the behavior of spatial steel frames.
Structures which are subjected to both axial forces and bending moments are called beam-column. Members carrying both axial force and bending moments are exposed to an interaction between these effects. The lateral deflection of a member causes additional bending moment when an axial force is applied. This changes the flexural stiffness of the member. Similarly, the presence of bending moments affects the axial stiffness of the member due to shortening of the member caused by the bending deformations. If the deformations are

small, the interaction between bending and axial forces can be ignored. In such a case, the force-deformation relationship for a beam-column is same as Equation (3).

$$p = kd \tag{3}$$

Here, this equation gives the member stiffness equation in which p and d are 12-term vectors of member force and displacement respectively, and k is a 12x12 member stiffness matrix for most general case of a prismatic member in space (shear deformation is neglected), and with the implicit condition that the deformations are so small as to leave the basic geometry unchanged. However, if the deformations are large, the stiffness matrix k is affected by the interaction between bending and axial forces, and it is not linear anymore [6]. The detail derivation of the nonlinear stiffness matrix by using stability functions is given in Ref. [6] and is not being repeated here. Only the definitions of the derived stability functions are presented. The stability functions are the modification factors from s_1 to s_9. These functions can be defined with respect to member length, cross-sectional properties, axial force, and the end moments.
s_1 : stability function for the effect of flexure on axial stiffness,
s_2 : stability function for the effect of axial force on flexural stiffness against rotation of near end about z-axis,
s_3 : stability function for the effect of axial force on flexural stiffness against rotation of far end about z-axis,
s_4 : stability function for the effect of axial force on flexural stiffness against rotation of near end about y-axis,
s_5 : stability function for the effect of axial force on flexural stiffness against rotation of far end about y-axis,
s_6 : stability function for the effect of axial force on flexural stiffness (about z-axis) against translation in y-direction,
s_7 : stability function for the effect of axial force on shear stiffness in y-direction against translation in y-direction,
s_8 : stability function for the effect of axial force on flexural stiffness (about y-axis) against translation in z-direction,
s_9 : stability function for the effect of axial force on shear stiffness in z-direction against translation in z-direction.
So, the nonlinear stiffness matrix of a three-dimensional steel member including stability functions can be depicted as shown in Figure 1.

$$[k]=\begin{bmatrix}
s_1\frac{EA}{L} & 0 & 0 & 0 & 0 & 0 & s_1\frac{-EA}{L} & 0 & 0 & 0 & 0 & 0\\
0 & s_7\frac{12EI_z}{L^3} & 0 & 0 & 0 & s_6\frac{6EI_z}{L^2} & 0 & s_7\frac{-12EI_z}{L^3} & 0 & 0 & 0 & s_6\frac{6EI_z}{L^2}\\
0 & 0 & s_9\frac{12EI_y}{L^3} & 0 & s_8\frac{-6EI_y}{L^2} & 0 & 0 & 0 & s_9\frac{-12EI_y}{L^3} & 0 & s_8\frac{-6EI_y}{L^2} & 0\\
0 & 0 & 0 & \frac{GJ}{L} & 0 & 0 & 0 & 0 & 0 & -\frac{GJ}{L} & 0 & 0\\
0 & 0 & s_8\frac{-6EI_y}{L^2} & 0 & s_4\frac{4EI_y}{L} & 0 & 0 & 0 & s_8\frac{6EI_y}{L^2} & 0 & s_5\frac{2EI_y}{L} & 0\\
0 & s_6\frac{6EI_z}{L^2} & 0 & 0 & 0 & s_2\frac{4EI_z}{L} & 0 & s_6\frac{-6EI_z}{L^2} & 0 & 0 & 0 & s_3\frac{2EI_z}{L}\\
s_1\frac{-EA}{L} & 0 & 0 & 0 & 0 & 0 & s_1\frac{EA}{L} & 0 & 0 & 0 & 0 & 0\\
0 & s_7\frac{-12EI_z}{L^3} & 0 & 0 & 0 & s_6\frac{-6EI_z}{L^2} & 0 & s_7\frac{12EI_z}{L^3} & 0 & 0 & 0 & s_6\frac{-6EI_z}{L^2}\\
0 & 0 & s_9\frac{-12EI_y}{L^3} & 0 & s_8\frac{6EI_y}{L^2} & 0 & 0 & 0 & s_9\frac{12EI_y}{L^3} & 0 & s_8\frac{6EI_y}{L^2} & 0\\
0 & 0 & 0 & -\frac{GJ}{L} & 0 & 0 & 0 & 0 & 0 & \frac{GJ}{L} & 0 & 0\\
0 & 0 & s_8\frac{-6EI_y}{L^2} & 0 & s_5\frac{2EI_y}{L} & 0 & 0 & 0 & s_8\frac{6EI_y}{L^2} & 0 & s_4\frac{4EI_y}{L} & 0\\
0 & s_6\frac{6EI_z}{L^2} & 0 & 0 & 0 & s_3\frac{2EI_z}{L} & 0 & s_6\frac{-6EI_z}{L^2} & 0 & 0 & 0 & s_2\frac{4EI_z}{L}
\end{bmatrix}$$

Figure 1: Nonlinear stiffness matrix of a member of spatial steel.

where the physical properties of a steel frame member are designated in the conventional manner as E, G, L, and A, which denote Young's modulus, shear modulus, length, and cross-sectional area respectively. The principle second moments of area for bending are I_y and I_z, the subscripts indicating the axes about which the second moments are taken. The polar second moment of area, which should logically be denoted by I_x, is denoted by J which is the conventional symbol in torsion studies.

4.1 Construction of Overall Stiffness Matrix

After setting up the nonlinear member stiffness matrix in local coordinate system displacement transformation matrix is conducted. The Equation (3) can be rewritten for a 3-D frame member in local coordinates. Now, the stiffness matrix in terms of local coordinates ($\boldsymbol{k}$) must be converted to stiffness matrix in terms of global coordinates ($\mathbf{K}$). The transformation equation of stiffness matrix from local to global coordinates is given below;

$$\mathbf{K}=\mathbf{T}^{\mathbf{T}}k\mathbf{T} \tag{4}$$

where;
$\mathbf{K}$ = global stiffness matrix,
$\mathbf{k}$ = local stiffness matrix,
$\mathbf{T}$ = transformation matrix (from local to global coordinates).
Although in theory the direction cosine matrices for each member of a structure may be set up from the orientation of the members in terms of the structure axes, in practice this can cause some difficulty. It is convenient, therefore, to restate a rotation matrix $\mathbf{R}_0$ in terms of the projections of the members on the structure axes [7]. So, that is to say, direct forces in structure axes are affected only by the direct forces in member axes, and moments in structure axes are affected only by the direct forces in member axes. The form of transformation matrix ($\mathbf{T}$) is;

$$T=\begin{bmatrix} R_0 & 0 & 0 & 0\\ 0 & R_0 & 0 & 0\\ 0 & 0 & R_0 & 0\\ 0 & 0 & 0 & R_0 \end{bmatrix}_{(12\times12)} \tag{5}$$

After developing the stiffness matrices for each member of the entire structure in terms of local coordinates, these matrices can be assembled to form the global stiffness matrix for the entire structure. Total stiffness at a coordinate is the sum of the stiffnesses contributed to that coordinate by each element attached to that coordinate.

5 Analysis of Spatial Steel Frames Including Geometric Nonlinearity

The nonlinear response of a spatial steel frame is obtained through successive linear elastic analysis as shown in the flow chart of Figure 2. Initially the axial forces are presumed to be zero. With zero values of axial forces, stability functions become equal to 1.0. Linear elastic analysis of the structure is carried out and axial forces in members are determined. With these values of axial forces the stability functions are calculated and structural analysis is repeated. This process is continued until the convergence is obtained in the axial force values of members. The joint displacements and member forces obtained at this final iteration yields the accurate response of the structure to external loads where the geometric nonlinearity of its members in local coordinate system is taken into account [8].

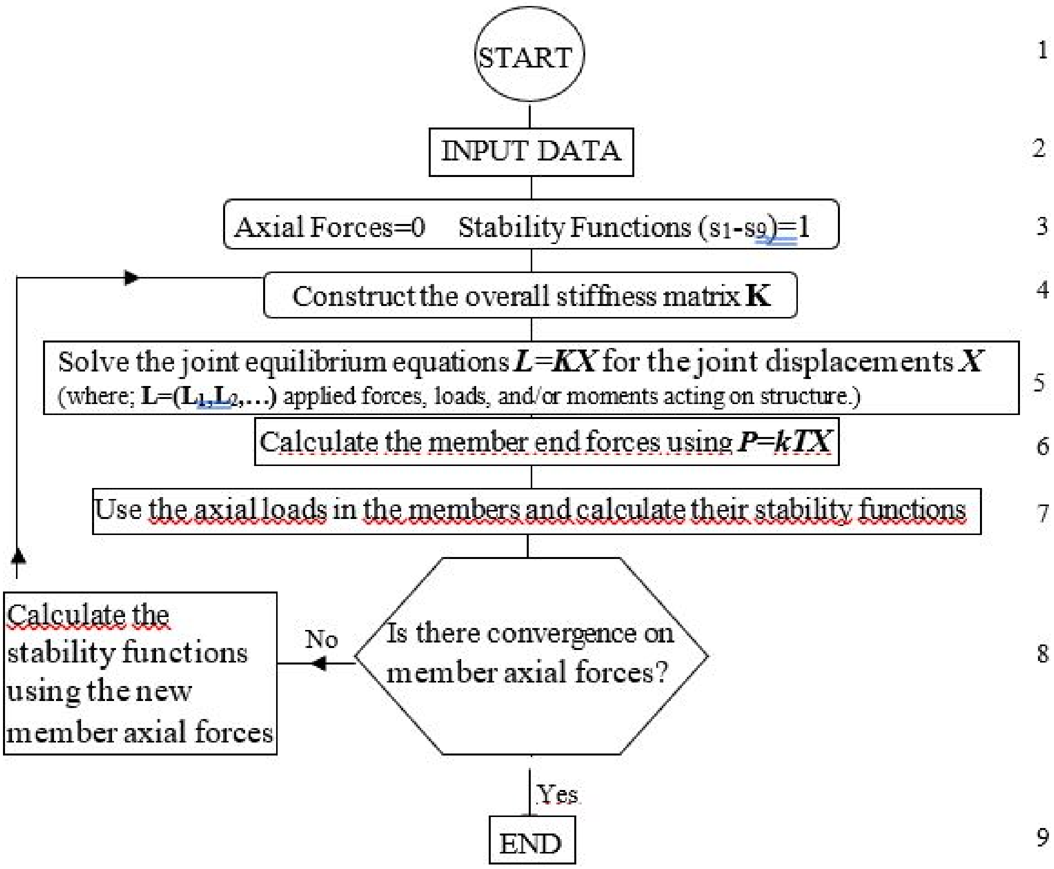

Figure 2: Nonlinear response of a spatial steel frame obtained through successive elastic linear analysis.

6 Numerical Example

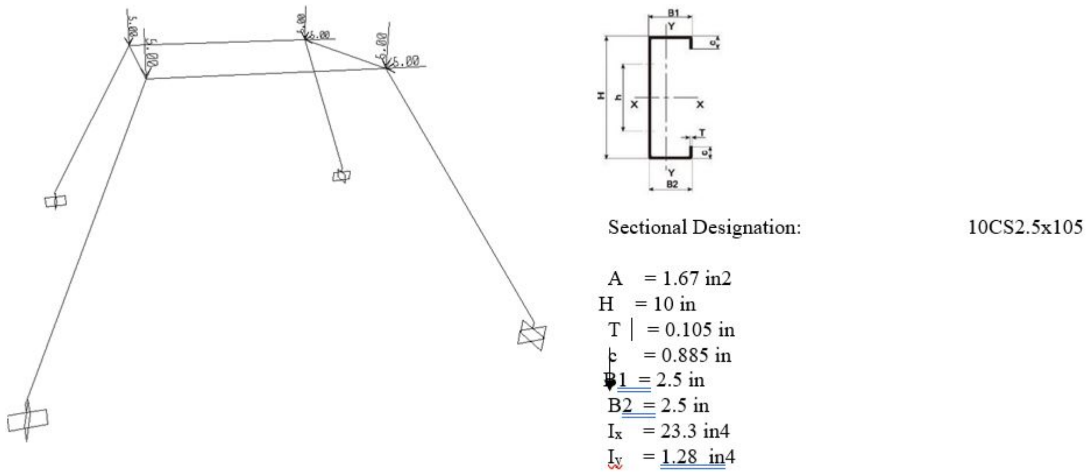

Figure 3: 8-member, 3D spatial steel frame with crosswise columns.

In order to reflect the effect of geometric nonlinearity in a clearer manner, a 3-D spatial steel frame [9] with crosswise columns is selected as a numerical example. This frame has 5 kN concentrated loading on each joint and 5 kN horizontal loads on two joints as shown in Figure 3. The steel 10CS2.5x105 cross-section, which is taken from available design manuals [10], is assigned to all frame members. The frame has 4m x 4m top area and 8m x 8m basement area. The joint displacements calculated by carrying out nonlinear analysis in this work are almost same as the ones obtained by SAP2000 v14 [11] as tabulated in Table 1.

Table 1: Joint displacements obtained by the nonlinear analysis using SAP2000v14 and nonlinear analysis by the routine developed in this study for 8-member, 3D steel frame with crosswise columns.

Joint Displacements						
	Joint displacements obtained by carrying out the nonlinear analysis proposed in this study			Joint displacements obtained by carrying out the nonlinear analysis using SAP2000 v14		
# of joint	X-DISP (m)	Y-DISP (m)	Z-DISP (m)	X-DISP (m)	Y-DISP (m)	Z-DISP (m)
1	0.24354E-05	-0.62881E-02	-0.12323E-01	0.2439E-05	-0.630E-02	-0.1240E-01
2	0.41895E-04	0.58946E-02	-0.12234E-01	0.4180E-04	0.590E-02	-0.1230E-01
3	0.24354E-05	-0.62881E-02	-0.12323E-01	0.2439E-05	-0.630E-02	-0.1240E-01
4	0.41895E-04	0.58946E-02	-0.12234E-01	0.4180E-04	0.590E-02	-0.1230E-01

7 Conclusions

The investigation of the impact of geometric nonlinear behaviour of spatial steel frames has shown that the concept for the analysis of the nonlinear features of 3-D frames reflects more realistic characterization. The behavior of most of the spatial steel frames is nonlinear due to change of their geometry under external loads. This is due to the weak torsional and flexural stiffness of sections. It is also necessary to check the overall stability during the analysis to ensure that the frame does not lose its load carrying capacity due to instability. The elastic instability analysis of spatial steel frames involves iterative linear elastic analysis of the structure and determination of axial forces in structural members. After this identification, the stability functions are calculated and structural analysis is repeated. When the specific convergence is reached at the axial forces of the members, this operation is terminated. The final values of internal actions and displacements are the result of nonlinear analysis of the structure.

References

[1] K. I. Majid, Nonlinear Structures. Butterworth, London, 1972.

[2] M. R. Horne and W., The Stability of Frames, Pergamen Press, 1965.

[3] W. F. Chen and E. M. Lui, Stability Design of Steel Frames, CRC Press, 1991.

[4] M. P. Saka and E. S. Kameshki, Optimum design of nonlinear elastic framed domes, Adv. Eng. Soft. 29 (7-9) (1998) 519-528.

[5] E. S. Kameshki and M. P. Saka, Optimum geometry design of nonlinear braced domes using genetic algorithm, Comput. Struct. 85 (2007) 71-79.

[6] S. G. Ekhande, M. Selvappalam, and K. S. Madugula, Stability Functions for Three-Dimensional Beam-Columns, J. Struct. Eng. 115 (2) (1989) 467-479.

[7] S. Carbas, Optimum Topological Design ff Geometrically Nonlinear Single Layer Lamella Domes Using Harmony Search Method, MSc. Thesis, Middle East Technical University, Ankara. Turkey, 2008.

[8] R. C. Coates, M. G. Coutie, and F. K. Kong, Structural Analysis, Nelson, London, 1972.

[9] S. Carbas, Optimum Design of Low-Rise Steel Frames Made Out of Cold-Formed Thin-Walled Steel Sections, Ph.D. Thesis, Middle East Technical University, Ankara, Turkey, 2013.

[10] AISI (American Iron and Steel Institute) D100-08, Excerpts-Gross Section Property Tables, Cold-Formed Steel Design Manual, Part I; Dimensions and Properties, 2008.

[11] SAP2000 v14, Integrated Finite Element Analysis and Design of Structures: Steel Design Manual, Computers Structures Inc., Berkeley, CA, USA, 2010.

On $T^*N^*B^*$ Smarandache Curves of Involute-Evolute Curves According to Frenet Frame in E_1^3

Özgür BOYACIOĞLU KALKAN *
Afyon Kocatepe University,
Afyon Vocational School,
03200 Afyonkarahisar, Turkey

Hakan ÖZTÜRK
Afyon Kocatepe University,
Afyon Vocational School,
03200 Afyonkarahisar, Turkey

Damla ZEYBEK
Afyon Kocatepe University,
Graduate School of Natural and Applied Sciences,
03200 Afyonkarahisar, Turkey

Abstract

In this study, let $\{\alpha^*\alpha\}$ be involute evolute curve couple, when the Frenet vectors of the spacelike involute curve α^* with a spacelike normal α^* which is incidental to a timelike evolute curve α are taken as the position vectors, the curvature and the torsion of Smarandache curve are calculated depending upon the timelike evolute curve α. Finally, we give an illustrative example related to our results.

Keywords: minkowski $n-$space, Frenet equations, smarandache curves, involute-evolute curves.

1 Introduction

The specific curve pairs are the most popular subjects in curve theory and involute-evolute curve couple is one of them. We can see in most textbooks various applications not only in curve theory but also in surface theory and mechanics. There are extensive literature on this curves, for instance Bilici and Çalışkan studied involutes of timelike curves in R_1^3 [3] and involutes of spacelike curves with timelike binormal in R_1^3 [2]. Bükçü and Karacan studied involute and evolute curves of spacelike curves with spacelike binormal in R_1^3 [4].

A regular curve in Minkowski space-time, whose position vector is composed by Frenet frame vectors on another regular curve, is called a Smarandache curve [12]. Special Smarandache curves have been studied by some authors. Turgut and Yılmaz studied a special case of such curves and called it TB_2 Smarandache curves in the space R_1^4 [12]. Şenyurt S., Çalışkan A. and Çelik Ü. studied N^*C^*-Smarandache curve of Bertrand curves pair according to Frenet frame [6]. Şenyurt S., Çalışkan A. studied N^*C^*-Smarandache curve of Mannheim curve couple according to Frenet frame [5].

In this paper, special Smarandache curves belonging to spacelike curve with a spacelike normal α^* such as $T^*N^*B^*$ drawn by Frenet frame are defined and some related results are given.

*Corresponding author. *E-mail address:* bozgur@aku.edu.tr

2 Preliminaries

Let Minkowski 3-space $\mathbb{R}_1^3$ be the vector space $\mathbb{R}^3$ endowed with the standart Lorentzian inner product g given by $g(X,X) = -x_1^2 + x_2^2 + x_3^2$ where $X = (x_1, x_2, x_3) \in \mathbb{R}_1^3$. A vector $X = (x_1, x_2, x_3) \in \mathbb{R}_1^3$. is said to be spacelike if $g(X,X) > 0$ or $X = 0$, timelike if $g(X,X) < 0$ or and null (lightlike) if $g(X,X) = 0$ and $X \neq 0$. The pseudo-norm (length) of a vector X is given by $\|X\|_L = \sqrt{|g(X,X)|}$. Therefore X is unit vector if $g(X,X) = \pm 1$. Next, vectors X, Y in $\mathbb{R}_1^3$ are said to be orthogonal if $g(X,Y) = 0$. The Lorentzian cross product of X, Y in $\mathbb{R}_1^3$ is given by

$$X \times Y = (x_3y_2 - x_2y_3, x_1y_3 - x_3y_1, x_1y_2 - x_2y_1). \tag{1}$$

Let $\alpha = \alpha(s)$ be a regular curve parametrized by arc length in $\mathbb{R}_1^3$. $\{T, N, B, \kappa, \tau\}$ be its Frenet invariants, where $\{T, N, B\}$ is moving Frenet frame and κ, τ are curvature and torsion of $\alpha(s)$, respectively. Then T, N and B are the tangent, the principal normal and the binormal vector of the curve α, respectively. Depending on the causal character of the curve α, we have the following Frenet formulas and the Darboux vectors:

i) For an unit speed timelike curve α in R_1^3, the Frenet formulas are given as follows ([13]):

$$\begin{array}{ccc} T \times N = -B, & N \times B = T, & B \times T = -N \\ T' = \kappa N & N' = \kappa T - \tau B & B' = \tau N. \end{array} \tag{2}$$

Then we write Frenet invariants in this way: $T(s) = \alpha'(s)$, $\kappa(s) = \sqrt{\langle T'(s), T'(s)\rangle}$, $N(s) = \frac{T'(s)}{\kappa(s)}$, $B(s) = -(T \times N)(s)$ and $\tau(s) = \left(\langle \alpha' \times \alpha'', \alpha''' \rangle / \|\alpha' \times \alpha''\|^2\right)(s)$ [14]. The Darboux vector for the timelike curve is given by $W = \tau T - \kappa B$, [13].

ii) For an unit speed spacelike curve with timelike normal α in R_1^3, the Frenet formulas are given as follows ([13]):

$$\begin{array}{ccc} T \times N = -B, & N \times B = -T, & B \times T = N, \\ T' = \kappa N & N' = \kappa T + \tau B & B' = \tau N. \end{array} \tag{3}$$

Then we write Frenet invariants in this way: $T(s) = \alpha'(s)$, $\kappa(s) = \sqrt{-\langle T'(s), T'(s)\rangle}$, $N(s) = \frac{T'(s)}{\kappa(s)}$, $B(s) = -(T \times N)(s)$ and $\tau(s) = -\left(\langle \alpha' \times \alpha'', \alpha''' \rangle / \|\alpha' \times \alpha''\|^2\right)(s)$ [14]. The Darboux vector for the spacelike curve is given by $W = -\tau T + \kappa B$ [13].

iii) For an unit speed spacelike curve with a spacelike normal α in R_1^3, the Frenet formulas are given as follows ([13]):

$$\begin{array}{ccc} T \times N = B, & N \times B = -T, & B \times T = -N, \\ T' = \kappa N & N' = -\kappa T + \tau B & B' = \tau N. \end{array} \tag{4}$$

Then we write Frenet invariants in this way: $T(s) = \alpha'(s)$, $\kappa(s) = \sqrt{\langle T'(s), T'(s)\rangle}$, $N(s) = \frac{T'(s)}{\kappa(s)}$, $B(s) = (T \times N)(s)$ and $\tau(s) = \left(\langle \alpha' \times \alpha'', \alpha''' \rangle / \|\alpha' \times \alpha''\|^2\right)(s)$ [14]. The Darboux vector for the spacelike curve is given by $W = \tau T - \kappa B$, [13].

In addition, the Frenet formulae for a null curve parametrized by distinguished parameter α in R_1^3, the Frenet formulas are given as follows:

$$\begin{array}{ccc} T \times B = -T, & T \times N = -B, & B \times N = -N, \\ T' = \kappa B & N' = -\tau B & B' = -\tau T + \kappa N. \end{array} \tag{5}$$

In this state T and N are null vectors and B is a spacelike vector. The Frenet invariants are $T(s) = \alpha'(s)$, $\kappa(s) = \sqrt{\langle T'(s), T'(s)\rangle}$, $B(s) = \frac{T'(s)}{\kappa(s)}$, $N(s) = \Big((1/\kappa)((1/\kappa)T'' + (1/\kappa)' T' + \tau T)\Big)$ and $\tau(s) = \left(1/2\left[\left((1/\kappa)'\right)^2 \kappa - (1/\kappa^3)\left\|T''\right\|^2\right]\right)(s)$ [7]. The Darboux vector for the null curve is given by $W = \tau T + \kappa N$.

Lemma 1 ***i.)*** *Let X and Y be positive (negative) timelike vectors in R_1^3. Then there is a nonnegative real number $\varphi(X,Y)$ such that*

$$g(X,Y) = \|X\| \, \|Y\| \cosh \varphi(X,Y)$$

The Lorentzian timelike angle between X and Y is defined to be $\varphi(X,Y)$.

ii) *Let X and Y be spacelike vectors in R_1^3 that span a spacelike vector subspace. Then there is a real number $\varphi(X,Y)$ between 0 and π such that*

$$g(X,Y) = \|X\| \, \|Y\| \cos \varphi(X,Y)$$

The Lorentzian spacelike angle between X and Y is defined to be $\varphi(X,Y)$.

iii) *Let X and Y be spacelike vectors in R_1^3 that span a timelike vector subspace. Then there is a positive real number $\varphi(X,Y)$ such that*

$$|g(X,Y)| = \|X\| \, \|Y\| \cosh \varphi(X,Y)$$

The Lorentzian timelike angle between X and Y is defined to be $\varphi(X,Y)$.

iv) *Let X be spacelike vector and Y be a positive timelike vector in R_1^3 Then there is a nonnegative real number $\varphi(X,Y)$ such that*

$$|g(X,Y)| = \|X\| \, \|Y\| \sinh \varphi(X,Y)$$

The Lorentzian timelike angle between X and Y is defined to be $\varphi(X,Y)$, [13].

Definition 2 *[10] Let $\alpha = \alpha(s)$, $\beta = \beta(s) \subset R_1^3$ be two curves in R_1^3. Let Frenet frames of α and β be $\{T, N, B\}$and $\{T^*, N^*, B^*\}$, respectively. β is called the involute of α (α is called the evolute of β) if*

$$g(T, T^*) = 0.$$

Lemma 3 *[3] Let (α^*, α) be the involute-evolute curve couple which are given by (I, α) and (I, β) coordinate neighborhoods, respectively. The distance between the curves α^* and α are given by*

$$d(\alpha(s), \alpha^*(s)) = |c - s|, \qquad c = cons\tan t \qquad \forall s \in I.$$

Definition 4 *[3] Let α be a timelike curve and θ being a Lorentzian timelike angle between the spacelike binormal unit vector $-B$ and the Darboux vector W. If $|\kappa|\langle\, |\tau|$ then W is a timelike vector. In this situation we can write*

$$\begin{matrix} \kappa = \|W\| \sinh \theta \\ \tau = \|W\| \cosh \theta \end{matrix}, \qquad \|W\|^2 = -g(W,W) = -(\kappa^2 - \tau^2). \tag{6}$$

Theorem 5 *[3] Let (α^*, α) be the involute-evolute curve couple. If W is a timelike vector ($|\kappa|\langle\, |\tau|$), then the Frenet vectors of the curve couple (α^*, α) as follows:*

$$\begin{bmatrix} T^* \\ N^* \\ B^* \end{bmatrix} = \begin{bmatrix} 0 & 1 & 0 \\ \sinh \theta & 0 & -\cosh \theta \\ -\cosh \theta & 0 & \sinh \theta \end{bmatrix} \begin{bmatrix} T \\ N \\ B \end{bmatrix}, \tag{7}$$

where θ be Lorentzian timelike angle between B and N^*.

Remark 6 *[3] Let (α^*, α) be the involute-evolute curve couple and $\alpha = \alpha(s)$ be timelike curve. If W is a timelike vector ($|\kappa|\langle\, |\tau|$), then the causal characteristics of the Frenet frames of the curves α and α^* are*

$$\{T \text{ timelike, } N \text{ spacelike, } B \text{ spacelike}\}$$

and

$$\{T^* \text{ spacelike, } N^* \text{ spacelike, } B^* \text{ timelike}\}.$$

3 On $T^*N^*B^*$ Smarandache Curves of involute-evolute curve in R_1^3

Let (α^*, α) be the involute evolute curve couple in E_1^3, α^* be a spacelike curve with spacelike normal and $\{T^*, N^*, B^*\}$ be the Frenet frame of α^*. In this case, $T^*N^*B^*$ Smarandache curve can be defined by

$$\beta_1(s) = \frac{1}{\sqrt{3}}(T^* + N^* + B^*). \tag{8}$$

Then solving the equation (8) by substitution of T^*, N^* and B^* from (7) **,** we obtain

$$\beta_1(s) = \frac{1}{\sqrt{3}}([\sinh\theta - \cosh\theta)T + N + (\sinh\theta - \cosh\theta)B]. \tag{9}$$

The derivative of this respect to s is as follows:

$$\beta_1'(s) = T_{\beta_1}\frac{ds_{\beta_1}}{ds} = \frac{1}{\sqrt{3}}\left[\begin{array}{l}(\theta'(\cosh\theta - \sinh\theta) + \kappa)T - \|W\|N \\ +\theta'(\cosh\theta - \sinh\theta)B\end{array}\right] \tag{10}$$

and

$$\left\langle \beta_1', \beta_1' \right\rangle = \frac{2(\|W\|^2 - \theta'\|W\|)}{3}.$$

Therefore there are three possibilities for the causal character of $\beta_1$under the conditions $\|W\|^2 - \theta'\|W\|\rangle 0$, $\|W\|^2 - \theta'\|W\|\langle 0$ and $\|W\|^2 - \theta'\|W\| = 0$. Because of the fact that $\frac{2(\|W\|^2-\theta'\|W\|)}{3} \neq 1$ for at least one θ', $\|W\| \in \mathbb{R}$, we know that s is not arc-length of β_1. Assume that s_{β_1} is arc-length of β_1.

i) If $\|W\|^2 - \theta'\|W\|\rangle 0$ then Smarandache curve β_1 is a spacelike curve. If we rearrange equation (10), we get

$$T_{\beta_1} = \frac{\begin{array}{c}(\theta'(\cosh\theta - \sinh\theta) + \kappa)T - \|W\|N \\ +(\theta'(\cosh\theta - \sinh\theta) - \tau)B\end{array}}{\sqrt{2(\|W\|^2-\theta'\|W\|)}} \tag{11}$$

where $\frac{ds_{\beta_1}}{ds} = \frac{\sqrt{2(\|W\|^2-\theta'\|W\|)}}{\sqrt{3}}$ and $\|W\|^2 = \tau^2 - \kappa^2$.

i.1) Let β_1 be a spacelike curve with spacelike normal. If we differentiate (11) with respect to s , we obtain

$$T_{\beta_1}' = \frac{\sqrt{3}}{2(\|W\|^2-\theta'\|W\|)^{3/2}}(w_1T + w_2N + w_3B)$$

where

$$\begin{aligned} w_1 &= ((\theta'' - \theta'^2)(\cosh\theta - \sinh\theta) + \kappa' - \kappa\|W\|)\sqrt{\|W\|^2 - \theta'\|W\|} \\ &\quad - \left(\sqrt{\|W\|^2 - \theta'\|W\|}\right)'(\theta'(\cosh\theta - \sinh\theta) + \kappa), \\ w_2 &= (\theta'\|W\| - \|W\|^2 - \|W\|')\sqrt{\|W\|^2 - \theta'\|W\|} + \left(\sqrt{\|W\|^2 - \theta'\|W\|}\right)'\|W\|, \\ w_3 &= ((\theta'' - \theta'^2)(\cosh\theta - \sinh\theta) - \tau' + \tau\|W\|)\sqrt{\|W\|^2 - \theta'\|W\|} \\ &\quad - \left(\sqrt{\|W\|^2 - \theta'\|W\|}\right)'(\theta'(\cosh\theta - \sinh\theta) - \tau). \end{aligned}$$

The first curvature of β_1 and the principal normal vector field is

$$\kappa_{\beta_1}=\sqrt{\left\langle T_{\beta_1}',T_{\beta_1}'\right\rangle}=\frac{\sqrt{3(-w_1^2+w_2^2+w_3^2)}}{2(\|W\|^2-\theta'\|W\|)^{\frac{3}{2}}},$$

$$N_{\beta_1}=\frac{T_{\beta_1}'}{\left\|T_{\beta_1}'\right\|}=\frac{w_1T+w_2N+w_3B}{\sqrt{-w_1^2+w_2^2+w_3^2}}.$$

Based upon this calculation, the binormal vector field of β_1 is

$$B_{\beta_1}=(T_{\beta_1}\wedge N_{\beta_1})=\frac{\begin{array}{c}(\|W\|w_3+(\theta'\cosh\theta-\tau)w_2)T\\+(\theta'(\cosh\theta-\sinh\theta)(w_3-w_1)+w_3\kappa+w_1\tau)N\\+(\theta'(\cosh\theta-\sinh\theta)+\kappa)w_2+\|W\|w_1)B\end{array}}{\sqrt{2(\|W\|^2-\theta'\|W\|)}\sqrt{-w_1^2+w_2^2+w_3^2}}.$$

The torsion of $\beta_1$is given as below:

$$\tau_{\beta_1}=\frac{\left\langle\beta_1'\wedge\beta_1'',\beta_1'''\right\rangle}{\left\|\beta_1'\wedge\beta_1''\right\|^2}=\frac{\sqrt{3}(-\widetilde{w}_1\Omega_1+\widetilde{w}_2\Omega_2+\widetilde{w}_3\Omega_3)}{-\widetilde{w}_1^{\,2}+\widetilde{w}_2^{\,2}+\widetilde{w}_3^{\,2}}$$

where

$$\begin{aligned}\widetilde{w}_1&=(\cosh\theta-\sinh\theta)(-\theta''\|W\|+\theta'(\|W\|^2+\|W\|'))\\&\quad+\tau(\theta'\|W\|-2\|W\|^2-\|W\|')+\tau'\|W\|,\\\widetilde{w}_2&=\theta'(\cosh\theta-\sinh\theta)(-\kappa'-\tau'+\|W\|(\kappa+\tau))\\&\quad+(\theta''-\theta'^2)\|W\|-\kappa\tau'+\tau\kappa',\\\widetilde{w}_3&=(\cosh\theta-\sinh\theta)(-\theta''\|W\|+\theta'(\|W\|^2+\|W\|'))\\&\quad+\kappa(-\theta'\|W\|+2\|W\|^2+\|W\|')-\kappa'\|W\|\end{aligned}$$

and

$$\begin{aligned}\Omega_1&=(\cosh\theta-\sinh\theta)(\theta'''-3\theta'\theta''-\theta'^3)+\kappa''-\kappa'\|W\|\\&\quad-2\kappa\|W\|'+\theta'\kappa\|W\|-\kappa\|W\|^2,\\\Omega_2&=(\theta''-\theta'^2)(\|W\|-\|W\|\|W\|'+\|W\|^3)+\theta''\|W\|\\&\quad+\theta'\|W\|'-2\|W\|\|W\|'-\|W\|'',\\\Omega_3&=(\cosh\theta-\sinh\theta)(\theta'''-3\theta'\theta''-\theta'^3)-\tau''+\tau'\|W\|\\&\quad+2\tau\|W\|'-\theta'\tau\|W\|+\tau\|W\|^2.\end{aligned}$$

i.2) Let β_1 be a spacelike curve with timelike normal. Then the Frenet invariants of β_1 are given as below:

$$T_{\beta_1}=\frac{\begin{array}{c}(\theta'(\cosh\theta-\sinh\theta)+\kappa)T-\|W\|N\\+(\theta'(\cosh\theta-\sinh\theta)-\tau)B\end{array}}{\sqrt{2(\|W\|^2-\theta'\|W\|)}},$$

$$\kappa_{\beta_1}=\sqrt{-\left\langle T_{\beta_1}',T_{\beta_1}'\right\rangle}=\frac{\sqrt{3(w_1^2-w_2^2-w_3^2)}}{2(\|W\|^2-\theta'\|W\|)^{\frac{3}{2}}},$$

$$N_{\beta_1}=\frac{T_{\beta_1}'}{\left\|T_{\beta_1}'\right\|}=\frac{w_1T+w_2N+w_3B}{\sqrt{w_1^2-w_2^2-w_3^2}},$$

$$B_{\beta_1}=-(T_{\beta_1}\wedge N_{\beta_1})=\frac{\begin{array}{c}(-\|W\|w_3-(\theta'\cosh\theta-\tau)w_2)T\\+(\theta'(\cosh\theta-\sinh\theta)(w_1-w_3)-w_3\kappa-w_1\tau)N\\-(\theta'(\cosh\theta-\sinh\theta)+\kappa)w_2+\|W\|w_1)B\end{array}}{\sqrt{2(\|W\|^2-\theta'\|W\|)}\sqrt{w_1^2-w_2^2-w_3^2}},$$

$$\tau_{\beta_1}=-\frac{\left\langle\beta_1'\wedge\beta_1'',\beta_1'''\right\rangle}{\left\|\beta_1'\wedge\beta_1''\right\|^2}=\frac{\sqrt{3}(\widetilde{w}_1\Omega_1-\widetilde{w}_2\Omega_2-\widetilde{w}_3\Omega_3)}{-\widetilde{w}_1^{\,2}+\widetilde{w}_2^{\,2}+\widetilde{w}_3^{\,2}}.$$

ii.) If $\|W\|^2-\theta'\|W\|\langle 0$ then Smarandache curve β_1 is a timelike curve. If we rearrange equation (10), we get

$$T_{\beta_1}=\frac{\begin{array}{c}(\theta'(\cosh\theta-\sinh\theta)+\kappa)T-\|W\|N\\+(\theta'(\cosh\theta-\sinh\theta)-\tau)B\end{array}}{\sqrt{2\left|\|W\|^2-\theta'\|W\|\right|}}$$

where $\frac{ds_{\beta_1}}{ds} = \frac{\sqrt{2\left|\|W\|^2-\theta'\|W\|\right|}}{\sqrt{3}}$ and $\|W\|^2 = \tau^2 - \kappa^2$.

Then the other Frenet invariants of β_1 are given as below:

$$\kappa_{\beta_1} = \sqrt{\left\langle T'_{\beta_1}, T'_{\beta_1} \right\rangle} = \frac{\sqrt{3(-w_1^2+w_2^2+w_3^2)}}{2\left|\|W\|^2-\theta'\|W\|\right|^{\frac{3}{2}}},$$

$$N_{\beta_1} = \frac{T'_{\beta_1}}{\left\|T'_{\beta_1}\right\|} = \frac{w_1T+w_2N+w_3B}{\sqrt{-w_1^2+w_2^2+w_3^2}},$$

$$B_{\beta_1} = -(T_{\beta_1} \wedge N_{\beta_1}) = \frac{\begin{array}{l}(-\|W\|w_3 - (\theta'\cosh\theta - \tau)w_2)T \\ +(\theta'(\cosh\theta - \sinh\theta)(w_1 - w_3) - w_3\kappa - w_1\tau)N \\ -(\theta'(\cosh\theta - \sinh\theta) + \kappa)w_2 + \|W\|w_1)B\end{array}}{\sqrt{2\left|\|W\|^2-\theta'\|W\|\right|}\sqrt{-w_1^2+w_2^2+w_3^2}},$$

$$\tau_{\beta_1} = \frac{\left\langle \beta_1'\wedge\beta_1'', \beta_1''' \right\rangle}{\left\|\beta_1'\wedge\beta_1''\right\|^2} = \frac{\sqrt{3}(-\widetilde{w}_1\Omega_1+\widetilde{w}_2\Omega_2+\widetilde{w}_3\Omega_3)}{-\widetilde{w}_1^{\,2}+\widetilde{w}_2^{\,2}+\widetilde{w}_3^{\,2}}.$$

iii.) If $\|W\|(\|W\| - \theta') = 0$ then $T^*N^*B^*$ Smarandache curve β_1 is a null curve. Since W vector is timelike, $\|W\| = 0$ is a contradiction. If $\|W\| = \theta'$ then rearranging (10), we obtain

$$T_{\beta_1} = \frac{1}{\sqrt{3}}\frac{ds}{ds_{\beta_1}}(\tau T - \|W\|N - \kappa B). \tag{12}$$

By differentiating (12), we get

$$T'_{\beta_1} = \frac{1}{\sqrt{3}}\begin{bmatrix} \left(\frac{d^3s}{ds^3_{\beta_1}}\tau + \frac{d^2s}{ds^2_{\beta_1}}(\tau' - \kappa\|W\|)\right)T \\ -\left(\frac{d^3s}{ds^3_{\beta_1}}\|W\| + \frac{d^2s}{ds^2_{\beta_1}}\|W\|'\right)N \\ +\left(-\frac{d^3s}{ds^3_{\beta_1}}\kappa + \frac{d^2s}{ds^2_{\beta_1}}(-\kappa' + \tau\|W\|)\right)B \end{bmatrix}. \tag{13}$$

From the calculations of Frenet invariants of a null curve, we find that the curvature $\kappa_{\beta_1} = \left\|T'_{\beta_1}\right\| = 0$. So there is no calculations for N_{β_1} and B_{β_1} in this case.

Example Let $\alpha(s) = (\frac{\sqrt{7}}{\sqrt{2}}s, \frac{\sqrt{5}}{\sqrt{2}}\cos s, \frac{\sqrt{5}}{\sqrt{2}}\sin s)$ be timelike curve and parametrized by arc length. In this situation, the involute of the curve α can be given by the equation

$$\alpha^*(s) = (\frac{\sqrt{7}}{\sqrt{2}}s + \frac{\sqrt{7}}{\sqrt{2}}|c-s|, \frac{\sqrt{5}}{\sqrt{2}}\cos s - \frac{\sqrt{5}}{\sqrt{2}}|c-s|\sin s, \frac{\sqrt{5}}{\sqrt{2}}\sin s + \frac{\sqrt{5}}{\sqrt{2}}|c-s|\cos s).$$

The Frenet invariants of the spacelike curve with timelike binormal $\alpha^*(s)$ are given as following: $T^*(s) = (0, -\cos s, -\sin s)$, $N^*(s) = (0, \sin s, -\cos s)$ and $B^*(s) = (-1, 0, 0)$, $\kappa^*(s) = 1$, $\tau^*(s) = 0$. The $T^*N^*B^*$ Smarandache curve is $\beta_1(s) = \frac{1}{\sqrt{3}}(-1, -\cos s + \sin s, -\sin s - \cos s)$. In terms of definitions, we obtain special Smarandache curve, see Figure 1.

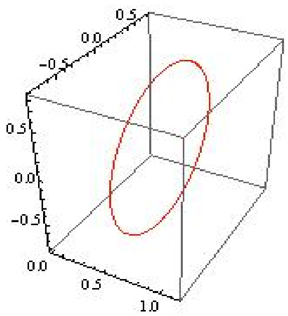

Figure 1: $T^*N^*B^*$ Smarandache curve belonging to curve α^*

References

[1] Akutagawa, K., and Nishikawa S., The Gauss Map and Spacelike Surfaces with Prescribed Mean Curvature in Minkowski 3-Space, Töhoko Math., J. 42, 67-82, 1990.

[2] Bilici M., Çalışkan M., On the involutes of spacelike curve with a timelike binormal in Minkowski 3-Space, Int. Math Forum, 4(31): 1497-1509, 2009.

[3] Bilici M., Çalışkan M., Some New Notes on the Involutes of the Timelike Curves in Minkowski 3-Space, Int. J. Contemp. Math. Sciences, 6(41), 2019-2030, 2011.

[4] Bükçü B., Karacan M.K.,On the involute and evolute curves of spacelike curves with a spacelike binormal in Minkowski 3-space, Int J. Math. Sci., 2(5): 221-232, 2007.

[5] Çalışkan A. and Şenyurt S., N^*C^*-Smarandache curves of Mannheim curve couple according to Frenet frame, International J.Math. Combin., 1, 1–13, 2015.

[6] Şenyurt S., Çalışkan A., Çelik Ü., N^*C^*-Smarandache Curve of Bertrand Curves Pair According to Frenet Frame, International J.Math. Combin. Vol.1, 1-7, 2016.

[7] Duggal K. L., Bejancu A., Lightlike Submanifolds of Semi Riemannian Manifolds and Applications, Kluwer Academic Publishers, Dordrecht, 1996.

[8] Gürses N., Bektaş Ö., Yüce S., Special Smarandache curves in R_1^3,Commun. Fac. Sci. Univ. Ank. Serç A1. Math. Stat, Vol. 65, no.2, 143-160, 2016.

[9] Kuhnel W., Differential Geometry: Curves-Surfaces-Manifolds, Providence RI, USA: The American Mathematical Society, 2006.

[10] O'Neill B., Semi-Riemannian geometry with applications to relativity, Academic Press, London (1983).

[11] Sivas S., İnvolute-evolute eğrilerine ait Frenet çatısına göre Smarandache eğrileri, Ordu Üni Fen Bilimleri Enstitüsü, 2014.

[12] Turgut M. and Yılmaz S., Smarandache curves in Minkowski space-time, International J.Math.Combin., 3, 51-55, 2008.

[13] Uğurlu, H.H., On the Geometry of timelike surfaces, Commun Fac. Sci. Ank. Series A1., 46, 211-223, 1997.

[14] Woestijne, V.D.I., Minimal Surfaces of the 3-dimensional Minkowski space. Proc. Congres "Geometrie differentielle et applications" Avignon (30 May 1988), Word Scientific Publishing. Singapore.344-369, 1990.

New Inequalities of Ostrowski's Type for Quasi-Convex Functions Associated With New Fractional Conformable Integrals

Barış ÇELİK*
Department of Mathematics, Faculty of Science and Arts,
Ordu University, Ordu, Turkey

Erhan SET
Department of Mathematics, Faculty of Science and Arts,
Ordu University, Ordu, Turkey

Ahmet OCAK AKDEMİR
Department of Mathematics, Faculty of Arts and Sciences,
Ağrı İbrahim Çeçen University, Ağrı, Turkey

Abstract

The main purpose of this note is to establish some new Ostrowski inequalities for quasi-convex functions via new conformable fractional integrals.

Keywords: Gamma function, Beta function, quasi-convex function, Ostrowski inequality, Riemann-Liouville fractional integrals, fractional conformable integral operators.

1 Introduction and Preliminaries

In 1938, Alexander Markovich Ostrowski (see [15]) proved the following integral inequality (1). Ostrowski considered the problem of estimating the deviation of a function from its integral mean. To be precise, for any continuous function f on $[a, b] \subset \mathbb{R}$ which is differentiable on (a, b) and with the property that $|f'(x)| \leq M$ for all $x \in (a, b)$, the inequality

$$\left| f(x) - \frac{1}{b-a} \int_a^b f(x)dx \right| \leq M(b-a) \left[\frac{1}{4} + \frac{\left(x - \frac{a+b}{2}\right)^2}{(b-a)^2} \right] \tag{1}$$

holds for every $x \in (a, b)$. The constant $\frac{1}{4}$ is the best possible in the sense that it cannot be replaced by a smaller constant. The inequality (1) is well known in the literature as the Ostrowski inequality. Many researchers have given considerable attention to the inequality (1) and several generalizations, extensions and related results have appeared in the literature. For some results which generalize, improve, and extend the above inequality, see [**?**, 2, 9, 16, 17, 18, 19, 20].

Let real function f be defined on some nonempty interval I of real line $\mathbb{R}$. The function f is said to be convex on I if inequality

$$f(\lambda x + (1 - \lambda)y) \leq \lambda f(x) + (1 - \lambda)f(y)$$

*Corresponding author. *E-mail address:* bariscelik15@hotmail.com

holds for all $x, y \in I$ and $\lambda \in [0,1]$.

The notion of quasi-convex functions generalizes the notion of convex functions. More precisely, a function $f : [a,b] \to \mathbb{R}$ is said quasi-convex on $[a,b]$ if

$$f(\lambda x + (1-\lambda)y) \leq \max\{f(x), f(y)\}$$

for any $x, y \in [a,b]$ and $\lambda \in [0,1]$. Clearly, any convex function is a quasi-convex function. Furthermore, there exist quasi-convex functions which are not convex (see [10]).

Let $f \in L_1[a,b] := L(a,b)$. The Riemann-Liouville integrals $J_{a+}^{\alpha} f$ and $J_{b-}^{\alpha} f$ of order $\alpha \in \mathbb{R}^+$ with $a \in \mathbb{R}_0^+$ are defined, respectively, by

$$J_{a+}^{\alpha} f(x) = \frac{1}{\Gamma(\alpha)} \int_a^x (x-t)^{\alpha-1} f(t)\, dt \quad (x > a) \tag{2}$$

and

$$J_{b-}^{\alpha} f(x) = \frac{1}{\Gamma(\alpha)} \int_x^b (t-x)^{\alpha-1} f(t)\, dt \quad (x < b) \tag{3}$$

where Γ is the familiar Gamma function (see, e.g., [23, Section 1.1]). It is noted that $J_{a+}^{1} f(x)$ and $J_{b-}^{1} f(x)$ become the usual Riemann integrals.

We recall Beta function (see, e.g., [23, Section 1.1])

$$B(\alpha,\, \beta) = \begin{cases} \displaystyle\int_0^1 t^{\alpha-1}(1-t)^{\beta-1}\, dt & (\Re(\alpha) > 0;\ \Re(\beta) > 0) \\ \dfrac{\Gamma(\alpha)\,\Gamma(\beta)}{\Gamma(\alpha+\beta)} & \left(\alpha,\, \beta \in \mathbb{C} \setminus \mathbb{Z}_0^-\right). \end{cases} \tag{4}$$

and the incomplete gamma function, defined for real numbers $a > 0$ and $x \geq 0$ by

$$\Gamma(a,x) = \int_x^{\infty} e^{-t} t^{a-1} dt.$$

For more details and properties concerning the fractional integral operators (2) and (3), we refer the reader, for example, to the works [3, 4, 5, 6, 7, 8, 14] and the references therein.

In [22], Set gave some Ostrowski type results involving Riemann-Liouville fractional integrals, as follows:

Lemma 1 *Let $f : [a,b] \to \mathbb{R}$ be a differentiable mapping on (a,b) with $a < b$. If $f' \in L[a,b]$, then for all $x \in [a,b]$ and $\alpha > 0$ we have:*

$$\begin{aligned} & \frac{(x-a)^{\alpha} + (b-x)^{\alpha}}{b-a} f(x) - \frac{\Gamma(\alpha+1)}{b-a} \left[J_{x^-}^{\alpha} f(a) + J_{x^+}^{\alpha} f(b)\right] \\ = \ & \frac{(x-a)^{\alpha+1}}{b-a} \int_0^1 t^{\alpha} f'(tx + (1-t)a) dt - \frac{(b-x)^{\alpha+1}}{b-a} \int_0^1 t^{\alpha} f'(tx + (1-t)b) dt \end{aligned}$$

where $\Gamma(\alpha)$ is Euler gamma function.

Jarad et. al. [11] has defined a new fractional integral operator. Also, they gave some properties and relations between the some other fractional integral operators, as Riemann-Liouville fractional integral, Hadamard fractional integrals, generalized fractional integral operators, with this operator.

Let $\beta \in \mathbb{C}$, $Re(\beta) > 0$, then the left and right sided fractional conformable integral operators has defined respectively, as follows;

$$\begin{aligned} {}_{a}^{\beta}\mathfrak{J}^{\alpha} f(x) &= \frac{1}{\Gamma(\beta)} \int_a^x \left(\frac{(x-a)^{\alpha} - (t-a)^{\alpha}}{\alpha} \right)^{\beta-1} \frac{f(t)}{(t-a)^{1-\alpha}} dt; & (5) \\ {}^{\beta}\mathfrak{J}_b^{\alpha} f(x) &= \frac{1}{\Gamma(\beta)} \int_x^b \left(\frac{(b-x)^{\alpha} - (b-t)^{\alpha}}{\alpha} \right)^{\beta-1} \frac{f(t)}{(b-t)^{1-\alpha}} dt. & (6) \end{aligned}$$

The fractional integral in (**??**) coincides with the Riemann-Liouville fractional integral (2) when $a = 0$ and $\alpha = 1$. It also coincides with the Hadamard fractional integral [13] once $a = 0$ and $\alpha \to 0$ with the Katugampola fractional integral [12], when $a = 0$. Similarly, Notice that, $(Qf)(t) = f(a + b - t)$ then we have ${}^{\beta}_{a}\mathfrak{J}^{\alpha} f(x) = Q({}^{\beta}\mathfrak{J}^{\alpha}_{b})f(x)$. Moreover (5) coincides with the Riemann-Liouville fractional integral (3), when $b = 0$ and $\alpha = 1$. It also coincides with the Hadamard fractional integral [13] once $b = 0$ and $\alpha \to 0$ with the Katugampola fractional integral [12], when $b = 0$. Further, getting more knowledge, see the paper given in [11].

The main goal of this paper, motivated by the above mentions and results in [11, 21], is to prove some new Ostrowski type inequalities via new conformable fractional integral for quasi-convex functions.

2 Main Results

Lemma 2 [21] *Let $f : [a, b] \to \mathbb{R}$ be a differentiable function on (a, b) with $a < b$ and $f' \in L[a, b]$. Then the following equality for fractional conformable integrals holds:*

$$\begin{aligned}
&\frac{(x-a)^{\alpha\beta} + (b-x)^{\alpha\beta}}{(b-a)\alpha^{\beta}} f(x) - \frac{\Gamma(\beta+1)}{b-a}\left[{}^{\beta}_{x}\mathfrak{J}^{\alpha} f(b) + {}^{\beta}\,\mathfrak{J}^{\alpha}_{x} f(a)\right] \\
= \;& \frac{(x-a)^{\alpha\beta+1}}{b-a}\int_0^1 \left(\frac{1-(1-t)^{\alpha}}{\alpha}\right)^{\beta} f'(tx + (1-t)a)dt \\
&+ \frac{(b-x)^{\alpha\beta+1}}{b-a}\int_0^1 \left(\frac{1-(1-t)^{\alpha}}{\alpha}\right)^{\beta} f'(tx + (1-t)b)dt
\end{aligned}$$

where $\alpha, \beta > 0$ and Γ is Euler Gamma function.

Theorem 3 *Let $f : [a, b] \to \mathbb{R}$ be a differentiable function on (a, b) with $a < b$ and $f' \in L[a, b]$. If $|f'|$ is quasi-convex on $[a, b]$, then the following inequality for fractional conformable integrals holds:*

$$\begin{aligned}
&\left|\frac{(x-a)^{\alpha\beta} + (b-x)^{\alpha\beta}}{(b-a)\alpha^{\beta}} f(x) - \frac{\Gamma(\beta+1)}{b-a}\left[{}^{\beta}_{x}\mathfrak{J}^{\alpha} f(b) + {}^{\beta}\,\mathfrak{J}^{\alpha}_{x} f(a)\right]\right| \\
\leq \;& \frac{1}{(b-a)\alpha^{\beta+1}} B\left(\beta+1, \frac{1}{\alpha}\right) \\
&\times \left[(x-a)^{\beta+1} \max\{|f'(x)|, |f'^{\alpha\beta+1} \max\{|f'(x)|, |f'(b)|\}\right],
\end{aligned}$$

where $\alpha, \beta > 0$, $B(x, y)$ and Γ are Euler beta and Euler gamma functions respectively.

Proof. From Lemma 2 and quasi-convexity of $|f'|$ on $[a,b]$, we can write

$$
\begin{aligned}
&\left|\frac{(x-a)^{\alpha\beta}+(b-x)^{\alpha\beta}}{(b-a)\alpha^{\beta}}f(x)-\frac{\Gamma(\beta+1)}{b-a}\left[{}^{\beta}_{x}\mathfrak{J}^{\alpha}f(b)+{}^{\beta}\,\mathfrak{J}^{\alpha}_{x}f(a)\right]\right| \\
\leq\ & \frac{(x-a)^{\alpha\beta+1}}{b-a}\int_0^1\left(\frac{1-(1-t)^{\alpha}}{\alpha}\right)^{\beta}|f'(tx+(1-t)a)|dt \\
&+\frac{(b-x)^{\alpha\beta+1}}{b-a}\int_0^1\left(\frac{1-(1-t)^{\alpha}}{\alpha}\right)^{\beta}|f'(tx+(1-t)b)|dt \\
\leq\ & \frac{(x-a)^{\alpha\beta+1}}{b-a}\int_0^1\left(\frac{1-(1-t)^{\alpha}}{\alpha}\right)^{\beta}\max\{|f'(x)|,|f'(a)|\}dt \\
&+\frac{(b-x)^{\alpha\beta+1}}{b-a}\int_0^1\left(\frac{1-(1-t)^{\alpha}}{\alpha}\right)^{\beta}\max\{|f'(x)|,|f'(b)|\}dt \\
=\ & \frac{(x-a)^{\alpha\beta+1}}{b-a}\frac{1}{\alpha^{\beta+1}}B\left(\beta+1,\frac{1}{\alpha}\right)\max\{|f'(x)|,|f'(a)|\} \\
&+\frac{(b-x)^{\alpha\beta+1}}{b-a}\frac{1}{\alpha^{\beta+1}}B\left(\beta+1,\frac{1}{\alpha}\right)\max\{|f'(x)|,|f'(b)|\} \\
=\ & \frac{1}{(b-a)\alpha^{\beta+1}}B\left(\beta+1,\frac{1}{\alpha}\right) \\
&\times\left[(x-a)^{\beta+1}\max\{|f'(x)|,|f'^{\alpha\beta+1}\max\{|f'(x)|,|f'(b)|\}\right],
\end{aligned}
$$

where it is easily seen that

$$
\int_0^1\left(\frac{1-(1-t)^{\alpha}}{\alpha}\right)^{\beta}dt = \frac{1}{\alpha^{\beta+1}}B\left(\beta+1,\frac{1}{\alpha}\right).
$$

So we get desired result. ■

Remark 4 *Under the assumptions of Theorem 3, if we choose* $|f'(x)|\leq M$ *for* $x\in[a,b]$, *we have*

$$
\begin{aligned}
&\left|\frac{(x-a)^{\alpha\beta}+(b-x)^{\alpha\beta}}{(b-a)\alpha^{\beta}}f(x)-\frac{\Gamma(\beta+1)}{b-a}\left[{}^{\beta}_{x}\mathfrak{J}^{\alpha}f(b)+{}^{\beta}\,\mathfrak{J}^{\alpha}_{x}f(a)\right]\right| \\
\leq\ & \frac{M}{(b-a)\alpha^{\beta+1}}B\left(\beta+1,\frac{1}{\alpha}\right)\left[(x-a)^{\beta+1}+(b-x)^{\alpha\beta+1}\right].
\end{aligned}
$$

Theorem 5 *Let* $f:[a,b]\to\mathbb{R}$ *be a differentiable function on* (a,b) *with* $a<b$ *and* $f'\in L[a,b]$. *If* $|f'^q$ *is quasi-convex on* $[a,b]$, $p,q>1$, *then the following inequality for fractional conformable integrals holds:*

$$
\begin{aligned}
&\left|\frac{(x-a)^{\alpha\beta}+(b-x)^{\alpha\beta}}{(b-a)\alpha^{\beta}}f(x)-\frac{\Gamma(\beta+1)}{b-a}\left[{}^{\beta}_{x}\mathfrak{J}^{\alpha}f(b)+{}^{\beta}\,\mathfrak{J}^{\alpha}_{x}f(a)\right]\right| \\
\leq\ & \left(\frac{B\left(\beta p+1,\frac{1}{\alpha}\right)}{\alpha^{\beta+1}}\right)^{\frac{1}{p}} \\
&\times\left[\frac{(x-a)^{\alpha\beta+1}}{b-a}\max\{|f'(x)|,|f'(a)|\}+\frac{(b-x)^{\alpha\beta+1}}{b-a}\max\{|f'(x)|,|f'(b)|\}\right]
\end{aligned}
$$

where $\frac{1}{p}+\frac{1}{q}=1$, $\alpha,\beta>0$, $B(x,y)$ *and* Γ *are Euler beta and Euler gamma functions respectively.*

Proof. By using Lemma 2, well known Hölder's inequality and quasi-convexity of $|f'^q$ on $[a,b]$, we get

$$\begin{aligned}
&\left|\frac{(x-a)^{\alpha\beta}+(b-x)^{\alpha\beta}}{(b-a)\alpha^{\beta}}f(x)-\frac{\Gamma(\beta+1)}{b-a}\left[{}_{x}^{\beta}\mathfrak{J}^{\alpha}f(b)+^{\beta}\mathfrak{J}_{x}^{\alpha}f(a)\right]\right| \\
\leq\ & \frac{(x-a)^{\alpha\beta+1}}{b-a}\int_0^1\left(\frac{1-(1-t)^{\alpha}}{\alpha}\right)^{\beta}|f'(tx+(1-t)a)|dt \\
&+\frac{(b-x)^{\alpha\beta+1}}{b-a}\int_0^1\left(\frac{1-(1-t)^{\alpha}}{\alpha}\right)^{\beta}|f'(tx+(1-t)b)|dt
\end{aligned}$$

$$\begin{aligned}
\leq\ & \frac{(x-a)^{\alpha\beta+1}}{b-a}\left[\left(\int_0^1\left(\frac{1-(1-t)^{\alpha}}{\alpha}\right)^{\beta p}dt\right)^{\frac{1}{p}}\left(\int_0^1|f'^q dt\right)^{\frac{1}{q}}\right] \\
&+\frac{(b-x)^{\alpha\beta+1}}{b-a}\left[\left(\int_0^1\left(\frac{1-(1-t)^{\alpha}}{\alpha}\right)^{\beta p}dt\right)^{\frac{1}{p}}\left(\int_0^1|f'^q dt\right)^{\frac{1}{q}}\right] \\
\leq\ & \frac{(x-a)^{\alpha\beta+1}}{b-a}\left[\left(\int_0^1\left(\frac{1-(1-t)^{\alpha}}{\alpha}\right)^{\beta p}dt\right)^{\frac{1}{p}}(\max\{|f'^q,|f'^q\})^{\frac{1}{q}}\right] \\
&+\frac{(b-x)^{\alpha\beta+1}}{b-a}\left[\left(\int_0^1\left(\frac{1-(1-t)^{\alpha}}{\alpha}\right)^{\beta p}dt\right)^{\frac{1}{p}}(\max\{|f'^q,|f'^q\})^{\frac{1}{q}}\right] \\
=\ & \frac{(x-a)^{\alpha\beta+1}}{b-a}\left(\frac{B\left(\beta p+1,\frac{1}{\alpha}\right)}{\alpha^{\beta+1}}\right)^{\frac{1}{p}}\max\{|f'(x)|,|f'(a)|\} \\
&+\frac{(b-x)^{\alpha\beta+1}}{b-a}\left(\frac{B\left(\beta p+1,\frac{1}{\alpha}\right)}{\alpha^{\beta+1}}\right)^{\frac{1}{p}}\max\{|f'(x)|,|f'(b)|\} \\
=\ & \left(\frac{B\left(\beta p+1,\frac{1}{\alpha}\right)}{\alpha^{\beta+1}}\right)^{\frac{1}{p}} \\
&\times\left[\frac{(x-a)^{\alpha\beta+1}}{b-a}\max\{|f'(x)|,|f'(a)|\}+\frac{(b-x)^{\alpha\beta+1}}{b-a}\max\{|f'(x)|,|f'(b)|\}\right].
\end{aligned}$$

Notice that, changing variables with $x=1-(1-t)^{\alpha}$, we get

$$\int_0^1\left(\frac{1-(1-t)^{\alpha}}{\alpha}\right)^{\beta p}dt=\frac{B\left(\beta p+1,\frac{1}{\alpha}\right)}{\alpha^{\beta+1}}.$$

The proof is completed. ■

Remark 6 *Under the assumptions of Theorem 5, if we choose* $|f'^q\leq M$ *for* $x\in[a,b]$*, we have*

$$\begin{aligned}
&\left|\frac{(x-a)^{\alpha\beta}+(b-x)^{\alpha\beta}}{(b-a)\alpha^{\beta}}f(x)-\frac{\Gamma(\beta+1)}{b-a}\left[{}_{x}^{\beta}\mathfrak{J}^{\alpha}f(b)+^{\beta}\mathfrak{J}_{x}^{\alpha}f(a)\right]\right| \\
\leq\ & M\left(\frac{B\left(\beta p+1,\frac{1}{\alpha}\right)}{\alpha^{\beta+1}}\right)^{\frac{1}{p}}\left[\frac{(x-a)^{\alpha\beta+1}}{b-a}+\frac{(b-x)^{\alpha\beta+1}}{b-a}\right].
\end{aligned}$$

Theorem 7 *Let $f:[a,b]\to\mathbb{R}$ be a differentiable function on (a,b) with $a<b$ and $f'\in L[a,b]$. If $|f'^q$ is quasi-convex on $[a,b]$, $q\geq 1$, then the following inequality for fractional conformable integrals holds:*

$$\begin{aligned}
&\left|\frac{(x-a)^{\alpha\beta}+(b-x)^{\alpha\beta}}{(b-a)\alpha^{\beta}}f(x)-\frac{\Gamma(\beta+1)}{b-a}\left[{}_{x}^{\beta}\mathfrak{J}^{\alpha}f(b)+{}^{\beta}\mathfrak{J}_{x}^{\alpha}f(a)\right]\right|\\
\leq&\left(\frac{B\left(\beta+1,\frac{1}{\alpha}\right)}{\alpha^{\beta+1}}\right)\\
&\times\left[\frac{(x-a)^{\alpha\beta+1}}{b-a}\max\{|f'(x)|,|f'(a)|\}+\frac{(b-x)^{\alpha\beta+1}}{b-a}\max\{|f'(x)|,|f'(b)|\}\right]
\end{aligned}$$

where $\alpha,\beta>0$, $B(x,y)$ and Γ are Euler Beta and Euler Gamma functions respectively.

Proof. By using Lemma 2, convexity of $|f'^q$ and well-known power-mean inequality, we have

$$\begin{aligned}
&\left|\frac{(x-a)^{\alpha\beta}+(b-x)^{\alpha\beta}}{(b-a)\alpha^{\beta}}f(x)-\frac{\Gamma(\beta+1)}{b-a}\left[{}_{x}^{\beta}\mathfrak{J}^{\alpha}f(b)+{}^{\beta}\mathfrak{J}_{x}^{\alpha}f(a)\right]\right|\\
\leq&\frac{(x-a)^{\alpha\beta+1}}{b-a}\int_0^1\left(\frac{1-(1-t)^{\alpha}}{\alpha}\right)^{\beta}|f'(tx+(1-t)a)|dt\\
&+\frac{(b-x)^{\alpha\beta+1}}{b-a}\int_0^1\left(\frac{1-(1-t)^{\alpha}}{\alpha}\right)^{\beta}|f'(tx+(1-t)b)|dt\\
\leq&\frac{(x-a)^{\alpha\beta+1}}{b-a}\left(\int_0^1\left(\frac{1-(1-t)^{\alpha}}{\alpha}\right)^{\beta}dt\right)^{1-\frac{1}{q}}\\
&\times\left(\int_0^1\left(\frac{1-(1-t)^{\alpha}}{\alpha}\right)^{\beta}|f'^q dt\right)^{\frac{1}{q}}\\
&+\frac{(b-x)^{\alpha\beta+1}}{b-a}\left(\int_0^1\left(\frac{1-(1-t)^{\alpha}}{\alpha}\right)^{\beta}dt\right)^{1-\frac{1}{q}}\\
&\times\left(\int_0^1\left(\frac{1-(1-t)^{\alpha}}{\alpha}\right)^{\beta}|f'^q dt\right)^{\frac{1}{q}}
\end{aligned}$$

$$\begin{aligned}
&\leq \frac{(x-a)^{\alpha\beta+1}}{b-a}\left(\int_0^1\left(\frac{1-(1-t)^\alpha}{\alpha}\right)^\beta dt\right)^{1-\frac{1}{q}} \\
&\quad\times\left(\max\{|f'^q,|f'^q\}\int_0^1\left(\frac{1-(1-t)^\alpha}{\alpha}\right)^\beta dt\right)^{\frac{1}{q}} \\
&\quad+\frac{(b-x)^{\alpha\beta+1}}{b-a}\left(\int_0^1\left(\frac{1-(1-t)^\alpha}{\alpha}\right)^\beta dt\right)^{1-\frac{1}{q}} \\
&\quad\times\left(\max\{|f'^q,|f'^q\}\int_0^1\left(\frac{1-(1-t)^\alpha}{\alpha}\right)^\beta dt\right)^{\frac{1}{q}} \\
&= \frac{(x-a)^{\alpha\beta+1}}{b-a}\left(\frac{B\left(\beta+1,\frac{1}{\alpha}\right)}{\alpha^{\beta+1}}\right)\max\{|f'(x)|,|f'(a)|\} \\
&\quad+\frac{(b-x)^{\alpha\beta+1}}{b-a}\left(\frac{B\left(\beta+1,\frac{1}{\alpha}\right)}{\alpha^{\beta+1}}\right)\max\{|f'(x)|,|f'(b)|\} \\
&= \left(\frac{B\left(\beta p+1,\frac{1}{\alpha}\right)}{\alpha^{\beta+1}}\right) \\
&\quad\times\left[\frac{(x-a)^{\alpha\beta+1}}{b-a}\max\{|f'(x)|,|f'(a)|\}+\frac{(b-x)^{\alpha\beta+1}}{b-a}\max\{|f'(x)|,|f'(b)|\}\right].
\end{aligned}$$

So, the proof is completed. ■

Remark 8 *Under the assumptions of Theorem 7, if we choose* $|f'^q \leq M$ *for* $x \in [a,b]$*, we have*

$$\begin{aligned}
&\left|\frac{(x-a)^{\alpha\beta}+(b-x)^{\alpha\beta}}{(b-a)\alpha^\beta}f(x)-\frac{\Gamma(\beta+1)}{b-a}\left[{}^\beta_x\mathfrak{J}^\alpha f(b)+^\beta\mathfrak{J}^\alpha_x f(a)\right]\right| \\
&\leq M\left(\frac{B\left(\beta+1,\frac{1}{\alpha}\right)}{\alpha^{\beta+1}}\right)\left[\frac{(x-a)^{\alpha\beta+1}}{b-a}+\frac{(b-x)^{\alpha\beta+1}}{b-a}\right].
\end{aligned}$$

References

[1] M. Alomari, M. Darus, S.S. Dragomir, P. Cerone, *Ostrowski type inequalities for functions whose derivatives are s-convex in the second sense*, Appl. Math. Lett., 23(9) (2010), 1071-1076.

[2] G.A. Anastassiou, *Ostrowski type inequalities*, Proc. Amer. Math. Soc., 123(12) (1995), 3775-3781.

[3] G. Anastassiou, M.R. Hooshmandasl, A. Ghasemi, F. Moftakharzadeh, *Montogomery identities for fractional integrals and related fractional inequalities,* J. Ineq. Pure Appl. Math. 10(4) (2009), Art. 97.

[4] S. Belarbi, Z. Dahmani, *On some new fractional integral inequalities,* J. Ineq. Pure Appl. Math. 10(3) (2009), Art. 86.

[5] Z. Dahmani, *New inequalities in fractional integrals,* Int. J. Nonlinear Sci. 9(4) (2010), 493-497.

[6] Z. Dahmani, *On Minkowski and Hermite–Hadamard integral inequalities via fractional integration,* Ann. Funct. Anal. 1(1) (2010), 51-58.

[7] Z. Dahmani, L. Tabharit, S. Taf, *Some fractional integral inequalities,* Nonl. Sci. Lett. A 1(2) (2010), 155-160.

[8] Z. Dahmani, L. Tabharit, S. Taf, *New generalizations of Gruss inequality usin Riemann–Liouville fractional integrals,* Bull. Math. Anal. Appl. 2(3) (2010), 93-99.

[9] S.S. Dragomir, *Ostrowski type inequalities for lebesque integral : A survey of recent results*, The Australian J. Math. Anal. Appl., 14(1) (2017), 1-287.

[10] D.A. Ion, *Some estimates on the Hermite-Hadamard inequality through quasi-convex functions,* Annals of University of Craiova, Math. Comp. Sci. Ser., 34 (2007), 82-87.

[11] F. Jarad, E. Uğurlu, T. Abdeljawad and D. Baleanu, (2017). *On a new class of fractional operators*, Advances in Difference Equations, 2017(1), 2017:247, DOI 10.1186/s13662-017-1306-z.

[12] U.N. Katugampola, *New approach to a genaralized fractional integral,* Applied Mathematics and Computation, 218(3) (2011), 860-865.

[13] A. A. Kilbas, (2001). *Hadamard-type fractional calculus*, Journal of the Korean Mathematical Society 38(6) (2001), 1191-1204.

[14] M.A. Noor, K.A. Noor, M.A. Awan, *Fractional Ostrowski inequalities for (s,m)-Godunova-Levin functions*, Facta Univ. Ser. Math. Inform., 30(4) (2015), 489-499.

[15] A.M. Ostrowski, Über die absolutabweichung einer differentierbaren Funktion von ihren Integralmittelwert, Comment. Math. Helv. 10 (1938), 226-227.

[16] M.E. Özdemir, H. Kavurmaci, E. Set, *Ostrowski's type inequalities for* (α, m)*-convex functions, Kyungpook Math. J.*, 50(3) (2010), 371-378.

[17] M.E. Özdemir, A.O. Akdemir, E. Set, *A new Ostrowski type inequality for double integrals, J. Inequal. Spec. Funct.*, 2(1) (2011), 27-34.

[18] M.E. Özdemir, A.O. Akdemir, E. Set, *On the Ostrowski-Grüss type inequality for twice differentiable functions*, Hacet. J. Math. Stat., 41(5) (2012), 651-655.

[19] M.Z. Sarıkaya, E. Set, *On new Ostrowski type integral inequalities*, Thai J. Math., 12(1) (2014), 145-154.

[20] M.Z. Sarıkaya, E. Set, M. E. Özdemir, *Some Ostrowski's type inequalities for functions whose second derivatives are s-convex in the second sense*, Demonstr. Math., 47(1) (2014), 37-47.

[21] E. Set, A.O. Akdemir, A. Gözpınar, *Ostrowski type inequalities via new fractional conformable integrals*, (2018), Researchgate, https://www.researchgate.net/publication/324779850.

[22] E. Set, *New inequalities of Ostrowski type for mappings whose derivatives are s-convex in the second sense via fractional integrals*, Computers And Mathematics with Applications, 63(7) (2012), 1147-1154.

[23] H. M. Srivastava and J. Choi, *Zeta and q-Zeta Functions and Associated Series and Integrals*, Elsevier Science Publishers, Amsterdam, London and New York, 2012.

On Some Properties of Leibniz Algebras

Nil MANSUROĞLU*
Kırşehir Ahi Evran University,
Department of Mathematics, Kırşehir, TURKEY

Abstract

Leibniz algebras are non-(anti)commutative generalization of Lie algebras. In this note, we investigate the some differences and analogs between Leibniz algebras and Lie algebras. Furthermore, we constructed some examples on some properties of non-Lie Leibniz algebras.

Keywords: Lie algebra, Leibniz algebra.

1 Introduction

Leibniz algebras are non-commutative generalization of Lie algebras were introduced by J.L. Loday [6]. Leibniz algebras is an interesting area, which was studied in many papers (see [1, 2, 3]). Our main starting point is given by the paper [4] which İ. Demir, K.C. Misra and E. Stitzinger studied on some results on Leibniz algebras analogs to results on Lie algebras. In this study we try to give some properties of non-Lie Leibniz algebras and some examples on the differences and analogs between Leibniz algebras and Lie algebras.

2 Preliminaries

In this section we give some necessary concepts and notation on Leibniz algebras. Let F be a field with characteristic zero. A Lie algebra L over a field F which is a non-associative algebra with a bilinear map, the Lie bracket $[,]: L \times L \to L$ defined by $(x, y) \mapsto [x, y]$, satisfies the following conditions:

$$(L1)\ [x, x] = 0,\ \text{for all } x \in L \text{ (anti-commutative)}$$
$$(L2)\ [[x, y], z] + [[y, z], x] + [[z, x], y] = 0, \text{for all } x, y, z \in L \text{ (Jacobi identity)}$$

(see [5]). A Leibniz algebra L over a field F is a non-associative algebra with the multiplication $[,]: L \times L \to L$ which verifies the Leibniz identity

$$[[x, y], z] = [x, [y, z]] - [y, [x, z]]$$

for all $x, y, z \in L$.

Let L be a Lie algebra over a field F. By the Jacobi identity, we obtain that $[[x, y], z] = [x, [y, z]] - [y, [x, z]]$ which, means that every Lie algebra is a Leibniz algebra. Provided that L is a Leibniz algebra with $[x, x] = 0$ for all $x \in L$, then L is a Lie algebra.

A Leibniz algebra L is called abelian if $[x, y] = 0$ for all $x, y \in L$. A subspace A is said to be a Leibniz subalgebra of L, if $[x, y] \in A$ for all $x, y \in A$. A subspace A is called a left

*Corresponding author. *E-mail address:* nil.mansuroglu@ahievran.edu.tr

(respectively right) ideal, if $[y,x] \in A$ (respectively $[x,y] \in A$) for all $x \in A$ and $y \in L$. If a subspace A is both a left and a right ideal of L, then we say that A is an ideal, that is, $[x,y],[y,x] \in A$ for all $x \in A$ and $y \in L$. By $Leib(L)$, we donote the subspace generated by the elements $[x,x]$, for some $x \in L$. It is not hard to show that this subspace is an ideal of L and so this ideal is called the Leibniz kernel of L. Since for $[x,x] \in Leib(L)$ and $y \in L$,

$$[[x,x],y] = [x,[x,y]] - [x,[x,y]] = 0,$$

the Leibniz kernel of L is an abelian Leibniz algebra. If a Leibniz algebra L has an ideal A, then the factor algebra L/A is a Leibniz algebra. Say $K = Leib(L)$. If the Leibniz algebra L/K is abelian, then

$$[x+K, x+K] = [x,x] + K = K$$

for all $x \in L$. This means that L/K is a Lie algebra. Let L_1 and L_2 be two Leibniz algebras. A map $\varphi : L_1 \to L_2$ is called a homomorphism if $\varphi([x,y]) = [\varphi(x), \varphi(y)]$ for all $x, y \in L_1$ and φ is a linear map. If φ is bijective, we say that φ is an isomorphism.

3 Some Properties of non-Lie Leibniz Algebras

Suppose that L is a non-Lie Leibniz algebra over a field F. As in case of Lie algebras, the sum and intersection of two ideals of a Leibniz algebra is an ideal. However, in general, the product of two ideals is not an ideal. The following example justifies it.

Example 1 *Let L be a vector space over a field with $\{u_1, u_2, u_3, u_4, u_5\}$. We define the operation on basis vectors by the following rule:*
$[u_1,u_2] = -u_2$, $[u_1,u_4] = u_5$, $[u_1,u_5] = u_4$, $[u_2,u_1] = u_2$, $[u_2,u_3] = u_5$, $[u_3,u_2] = u_4$, $[u_4,u_1] = u_4$, $[u_5,u_1] = -u_4$ *and other products are zero.* $I_1 = Fu_2 \oplus Fu_4 \oplus Fu_5$ *and* $I_2 = Fu_3 \oplus Fu_4 \oplus Fu_5$ *are ideals of L. As $[I_1, I_2] = Fu_5$, the product of I_1 and I_2 is not ideal.*

Let L be a Leibniz algebra over a field F. An F-linear map $D : L \to L$ is called a derivation of L if for all $x, y \in L$, $D([x,y]) = [x, D(y)] + [D(x), y]$. By $Der(L)$ we denote the set of derivations of L. Let D_1 and D_2 be two derivations of L. If L is Lie algebra, then $[D_1, D_2]$ is also derivation. In case of non-Lie Leibniz algebras, $[D_1, D_2]$ is not derivation. We define linear operator ad_x on L, called the adjoint endomorphism of x, by $ad_x y = [x,y]$ for all $y \in L$. By Leibniz identity, the map $ad_x : L \mapsto L$ is a derivation of L. By Leibniz identity the derivation ad_x coincides with the Jacobi identity, that is, $ad_x([y,z]) = [ad_x y, z] + [y, ad_x z]$ for all $x, y, z \in L$. We denote by $Ad(L)$ the set of all ad_x for $x \in L$. This set is a Lie algebra under the commutator bracket. Moreover, it is easy to check that $[ad_x, ad_y] = ad_{[x,y]}$ for all $x, y \in L$.

The left (respectively right) center $C^{left}(L)$ (respectively $C^{right}(L)$) of a Leibniz algebra L is defined by the rule:

$$C^{left}(L) = \{x \in L | [x,y] = 0 \textit{ for each element } y \in L\}$$

and respectively

$$C^{right}(L) = \{x \in L | [y,x] = 0 \textit{ for each element } y \in L\}.$$

The left center of L is an ideal, but in general, the right center of L is not ideal. Furthermore, the right and left centers have different structures. The following example shows this.

Example 2 *Let L be a vector space over a field with $\{u_1, u_2, u_3, u_4\}$. We define the operation on basis vectors by the following rule $[u_1, u_2] = u_4 + u_3$, $[u_1, u_3] = -u_4 - u_3$, $[u_2, u_2] = u_1$, $[u_1, u_4] = u_3 + u_4$, and other products are zero. $C^{left}(L) = Fu_4 \oplus Fu_3$ is ideal, but $C^{right}(L) = Fu_1$ is not ideal.*

Acknowledgement: This work was supported by Kırşehir Ahi Evran University Scientific Research Projects Coordination Unit. Project Number: FEF.A4.18.009.

References

[1] Barnes, D., "Some theorems on Leibniz algebras", Comm. Algebra, 39 (2011): 2463-2472.

[2] Bloh, A., "A generalization of the concept of Lie algebra", Dokl. Akad. Nauk. SSSR, 165 (1965): 471-473.

[3] Bloh, A.M., "A certain generalization of the concept of Lie algebra", Algebra and Number Theory, Moskow. Gos. Ped. Inst. Uˆcen. 375, (1971): 9-20.

[4] Demir, İ., Misra, C.K., Stitzinger, E., "On some structures of Leibniz algebras", in Recent Advances in Representation Theory, Quantum Groups, Algebraic Geometry, and Related Topics, Contemporary Mathematics, vol. 623, Amer. Math. Soc., Providence, RI, (2014): 41-54.

[5] Jacobson, N., Lie Algebras, Dover Publications Inc., New York, 1979.

[6] Loday, J.L., "Une version non commutative des algebres de Lie: les algebres de Leibniz", Enseing. Math., 33 (1993): 269-293.

Spacelike Translation Surface According to Q-Frame in Minkowski 3-Space

Hatice TOZAK*
Eskişehir Osmangazi University,
Eskişehir, Turkey

Cumali EKİCİ
Eskişehir Osmangazi University,
Eskişehir, Turkey

Mustafa DEDE
Kilis 7 Aralık University,
Kilis, Turkey

Abstract

In this paper, we study the spacelike translation surfaces generated by two space curves according to q-frame in 3-dimensional Minkowski space E_1^3. We investigate classification of such surfaces in E_1^3 with q-frame curvatures. Finally, several examples are given by figures for these surfaces.

Keywords: q-frame, translation surfaces, space curve.

1 Introduction

The theory of translation surfaces is always one of interesting topics in Euclidean and ambient spaces. Translation surfaces have been investigated from the various viewpoints by many differential geometers. L. Verstraelen, J. Walrave and S. Yaprak have investigated minimal translation surfaces in n-dimensional Euclidean spaces [18]. H. Liu has given the classification of the translation surfaces with constant mean curvature or constant Gauss curvature in 3-dimensional Euclidean space E^3 and 3-dimensional Minkowski space E^3 [12]. D. W. Yoon and Baba-Hamed et al. have studied translation surfaces in 3-dimensional Lorentz-Minkowski space [3, 19]. M. I. Munteanu and A. I. Nistor have studied the second fundamental form of translation surfaces in E^3 [13]. Çetin et al. (2011) investigated the translation surfaces in 3- dimensional Euclidean space by using non-planar space curves and they gave the differential geometric properties for both translation surfaces and minimal translation surfaces [6]. Moreover, Çetin et al. (2011) studied the translation surface with Frenet frames and Darboux frame and gave some differential geometric properties of the translation surfaces in E_1^3 [7]. Ali et al. have given a classification of some special points on translation surfaces in E^3 [2]. Sipus and Divjak (2011) have described translation surfaces in Galilean space with constant Gauss and mean curvatures [16]. Also, Translatiion surface is used in many applications such as architecture to design and construct the glass roofing structures etc.

Recently, there are a number of different adapted frames along a space curve. İnspired by the 3D offset curve application of the quasi-normal vector $\mathbf{n}_q$ [5].Concordantly, Dede et al. defined the q-frame for tubular surface modeling [8]. The q-frame offers two key advantages over Frenet frame: a) it is defined for all points along every space curve on which curvature may vanish at some points, b) it avoid the unnecessary twist around the tangent [9]. Additionally, Dede et al. have studied translation surfaces according to q-frame [17].

*Corresponding author. *E-mail address:* hatice.tozak@gmail.com

In this paper, we study the spacelike translation surfaces generated by two space curves according to q-frame in 3-dimensional Minkowski space E_1^3. We investigate classification of such surfaces in E_1^3 with the q-frame curvatures. Finally, several examples are given by figures for these surfaces.

2 Preliminaries

Coquillart [5] introduced the quasi-normal vector of a space curve in order to construct the 3D curve offset. The quasi-normal vector is defined for each point of the curve, and lies in the plane perpendicular to the tangent of the curve at this point [15]. As an alternative to Frenet frame we define a new adapted frame along a space curve, called as the q-frame.

Let $\alpha(u)$ be a regular space curve with the q-frame. The q-frame $\{\mathbf{t}, \mathbf{n}_q, \mathbf{b}_q, \mathbf{k}\}$ along $\alpha(t)$ is given byThe q-frame $\{\mathbf{t}, \mathbf{n}_q, \mathbf{b}_q, \mathbf{k}\}$ along $\alpha(t)$ is given by

$$\mathbf{t} = \frac{\alpha'}{\|\alpha'\|}, \mathbf{n}_q = \frac{\mathbf{t} \wedge \mathbf{k}}{\|\mathbf{t} \wedge \mathbf{k}\|}, \mathbf{b}_q = \mathbf{t} \wedge \mathbf{n}_q. \tag{1}$$

where $\mathbf{t}$ is the unit tangent vector, $\mathbf{n}_q$ is the quasi-normal and $\mathbf{b}_q$ is the quasi-binormal vector. Also, $\mathbf{k}$ is the projection vector is chosen as $k = (0, 0, 1)$ or $(0, 1, 0)$ [8, 9]. The q-frame along a space curve is shown in Figure 1.

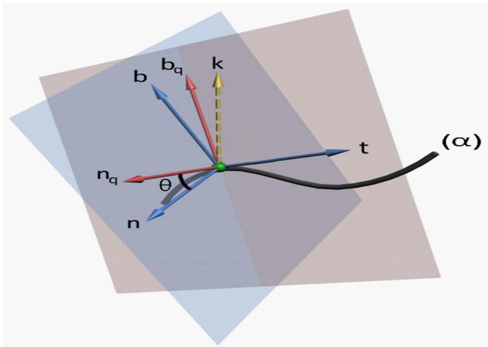

Figure 1: The q-frame and Frenet frame.

The variation equations of the q-frame of a spacelike curve,which has the unit tangent vector $\mathbf{t}$ (spacelike), the quasi-normal $\mathbf{n}_q$ (timelike) and the quasi-binormal vector $\mathbf{b}_q$ (spacelike) are given by

$$\begin{bmatrix} \mathbf{t}' \\ \mathbf{n}_q' \\ \mathbf{b}_q' \end{bmatrix} = \begin{bmatrix} 0 & -k_1 & k_2 \\ -k_1 & 0 & k_3 \\ -k_2 & k_3 & 0 \end{bmatrix} \begin{bmatrix} \mathbf{t} \\ \mathbf{n}_q \\ \mathbf{b}_q \end{bmatrix} \tag{2}$$

where the q-curvatures are

$$\begin{aligned} k_1 &= \kappa \cosh \theta \\ k_2 &= -\kappa \sinh \theta \\ k_3 &= d\theta + \tau. \end{aligned} \tag{3}$$

If the orthonormal bases change the causality, the variation equations of the q-frame of a spacelike curve,which has the unit tangent vector $\mathbf{t}$ (spacelike), the quasi-normal $\mathbf{n}_q$ (spacelike) and the quasi-binormal vector $\mathbf{b}_q$ (timelike) will be given in the following form

$$\begin{bmatrix} \mathbf{t}' \\ \mathbf{n}_q' \\ \mathbf{b}_q' \end{bmatrix} = \begin{bmatrix} 0 & k_1 & -k_2 \\ -k_1 & 0 & -k_3 \\ -k_2 & -k_3 & 0 \end{bmatrix} \begin{bmatrix} \mathbf{t} \\ \mathbf{n}_q \\ \mathbf{b}_q \end{bmatrix} \tag{4}$$

where the q-curvatures are

$$\begin{aligned} k_1 &= \kappa \cosh\theta \\ k_2 &= -\kappa \sinh\theta \\ k_3 &= -d\theta - \tau. \end{aligned} \tag{5}$$

[11]. In 3-dimensional Minkowski space $\mathbb{R}^3_1$, the inner product and the cross product of two vectors $u = (u_1, u_2, u_3)$, $v = (v_1, v_2, v_3) \in \mathbb{R}^3_1$ are defined as

$$< u, v >= u_1v_1 + u_2v_2 - u_3v_3 \tag{6}$$

and

$$u \wedge v = (u_3v_2 - u_2v_3, u_1v_3 - u_3v_1, u_1v_2 - u_2v_1) \tag{7}$$

where $e_1 \wedge e_2 = e_3$, $e_2 \wedge e_3 = -e_1$, $e_3 \wedge e_1 = -e_2$, respectively [1]. If u and v are spacelike vectors, then $u \wedge v$ is a timelike vector [14].

Let x and y be future pointing (or past pointing) timelike vectors in E^3_1, then there is an unique real number $\theta \geq 0$ such that

$$\langle x, y\rangle = \|x\| \, \|y\| \cosh\theta.$$

This number is called the hyperbolic angle between the vectors x and y.

Let x and y be spacelike vectors in E^3_1 that span spacelike vector subspace. Then, there is an unique real number $\theta \geq 0$ such that

$$\langle x, y\rangle = \|x\| \, \|y\| \cos\theta.$$

This number is called the spacelike angle between the vectors x and y.

Let x be a spacelike and y be a timelike vectors in E^3_1, then there is an unique real number $\theta \geq 0$ such that

$$\langle x, y\rangle = \|x\| \, \|y\| \sinh\theta.$$

This number is called the timelike angle between the vectors x and y [14].

The norm of the vector u is given by

$$\|u\| = \sqrt{|\langle u, u\rangle|} \tag{8}$$

We say that a Lorentzian vector u is spacelike, lightlike or timelike if $\langle u, u\rangle > 0$, $\langle u, u\rangle = 0$ and $u \neq 0$, $\langle u, u\rangle < 0$, respectively. In particular, the vector $u = 0$ is spacelike.

An arbitrary curve $\alpha(s)$ in $\mathbb{R}^3_1$, can locally be spacelike, timelike or null(lightlike), if all its velocity vectors $\alpha'(s)$ are respectively spacelike, timelike or null [14]. A null curve α is parameterized by pseudo-arc s if $\langle \alpha''(s), \alpha''(s)\rangle = 1$. On the other hand, a non-null curve α is parameterized by arc-lenght parameter s if $\langle \alpha'(s), \alpha'(s)\rangle = \pm 1$ [4].

When a space curve is translated over another space curve, the resulting surface can be considered as the most general appearance of a translation surface. Consequently, this surface can be parameterized as the sum of two space curves. Quite often, the class of translation surfaces is restricted to those that can be parameterized as the sum of two plane curves. So it can be parameterized by a patch

$$M(u, v) = \alpha(u) + \beta\,(v)\,,$$

where u and v are the parameters of the arc lengths of the curves α and β, respectively [10].

Let $\{\mathbf{t}_\alpha, \mathbf{n}_\alpha, \mathbf{b}_\alpha\}$ be the Frenet frame field of α with curvature κ_α and torsion τ_α. Also, let $\{\mathbf{t}_\beta, \mathbf{n}_\beta, \mathbf{b}_\beta\}$ be the Frenet frame field of β with curvature κ_β and torsion τ_β. A surface that can be generated from two space curves by translating either one of them parallel to itself in such a way that each of its points describes a curve that is a translation of the other curve. Let $M(u,v)$ be a translation surface in 3-dimensional Euclidean space. Then,

$$M(u,v) = (\alpha_1 + \beta_1, \alpha_2 + \beta_2, \alpha_3 + \beta_3)$$

where $\alpha = (\alpha_1, \alpha_2, \alpha_3)$ and $\beta = (\beta_1, \beta_2, \beta_3)$.

The unit normal of translation surface can be defined by

$$U(u,v) = \frac{1}{\sin\varphi}(\mathbf{t}_\alpha \wedge \mathbf{t}_\beta)$$

where $\varphi(u)$ is the angle between tangent vectors of $\alpha(u)$ and $\beta(v)$. The first fundamental form I of the surface $M(u,v)$ is

$$I = du^2 + 2\cos\varphi du dv + dv^2$$

and the second fundamental form II is

$$II = \kappa_\alpha \cos\theta_\alpha du^2 + \kappa_\beta \cos\theta_\beta dv^2$$

where θ_α and θ_β are the angles between U and $\mathbf{n}_\alpha$, $\mathbf{n}_\beta$, respectively [6].It is well known that the Gauss and mean curvatures of a surface are given by

$$K = \frac{LN - M^2}{EG - F^2}, 2H = \frac{LG - 2MF + NE}{EG - F^2}. \tag{9}$$

3 Spacelike Translation Surfaces with q-Frame

In this section, we introduce the spacelike translation surfaces by using the non-null curves.

Let $M(u,v)$ be a spacelike translation surface in 3-dimensional Minkowski space. Then $M(u,v)$ is parametrized by

$$M(u,v) = \alpha(u) + \beta(v), \tag{10}$$

where α and β being unit-speed spacelike curves of the arclength parameters u and v, respectively.

Let $\{\mathbf{t}_\alpha, \mathbf{n}_q^\alpha, \mathbf{b}_q^\alpha\}$ be the q-frame field of α with q-curvatures k_1^α, k_2^α and k_3^α. and $\{\mathbf{t}_\alpha, \mathbf{n}_q^\beta, \mathbf{b}_q^\beta\}$ be the q-frame field of β with q-curvatures k_1^β, k_2^β and k_3^β. Also, let $M(u,v)$ be a translation surface in 3-dimensional Minkowski space. Then,

$$M(u,v) = (\alpha_1 + \beta_1, \alpha_2 + \beta_2, \alpha_3 + \beta_3) \tag{11}$$

where $\alpha = (\alpha_1, \alpha_2, \alpha_3)$ and $\beta = (\beta_1, \beta_2, \beta_3)$. The partial derivatives of $M(u,v)$, with respect to u and v, are determined by

$$M_u = \mathbf{t}_\alpha \tag{12}$$

and

$$M_v = \mathbf{t}_\beta. \tag{13}$$

Case 1: In this case we introduce the spacelike translation surfaces by using the spacelike curves. Let $\alpha(u)$ be a spacelike curve which have the tangent vector $\mathbf{t}_\alpha$ (spacelike), quasi-normal vector $\mathbf{n}_{q\alpha}$ (timelike) and quasi-binormal vector $b_{q\alpha}$ (spacelike) with the projection vector $\mathbf{k}$ (spacelike) and $\beta(v)$ be a spacelike curve which have the tangent vector $\mathbf{t}_\beta$ (spacelike), quasi-normal vector $\mathbf{n}_{q\beta}$ (timelike) and quasi-binormal vector $b_{q\beta}$ (spacelike) with the projection vector $\mathbf{k}$ (spacelike). From the equation (2), q-frames of spacelike curves $\alpha(u)$ and $\beta(v)$ may be written as, respectively,

$$\begin{bmatrix} \mathbf{t}'_\alpha \\ (\mathbf{n}_{q\alpha})' \\ (\mathbf{b}_{q\alpha})' \end{bmatrix} = \begin{bmatrix} 0 & -k_1^\alpha & k_2^\alpha \\ -k_1^\alpha & 0 & k_3^\alpha \\ -k_2^\alpha & k_3^\alpha & 0 \end{bmatrix} \begin{bmatrix} \mathbf{t}_\alpha \\ \mathbf{n}_{q\alpha} \\ \mathbf{b}_{q\alpha} \end{bmatrix} \tag{14}$$

and

$$\begin{bmatrix} \mathbf{t}'_\beta \\ (\mathbf{n}_{q\beta})' \\ (\mathbf{b}_{q\beta})' \end{bmatrix} = \begin{bmatrix} 0 & -k_1^\beta & k_2^\beta \\ -k_1^\beta & 0 & k_3^\beta \\ -k_2^\beta & k_3^\beta & 0 \end{bmatrix} \begin{bmatrix} \mathbf{t}_\beta \\ \mathbf{n}_{q\beta} \\ \mathbf{b}_{q\beta} \end{bmatrix}, \tag{15}$$

where k_i^α and k_i^β are q-curvature of spacelike curves $\alpha(u)$ and $\beta(v)$ for $1 \leq i \leq 3$.

By using equations (12) and (13), the unit normal of the spacelike translation surface can be defined by

$$U(u,v) = \frac{1}{\sin\varphi}(\mathbf{t}_\alpha \wedge \mathbf{t}_\beta) \tag{16}$$

where $\varphi(u)$ is the angle between the tangent vectors of $\alpha(u)$ and $\beta(v)$.

Theorem 3.1. The Gauss and mean curvatures of the translation surface are given by

$$K = \frac{(-k_1^\alpha \cosh\phi_\alpha + k_2^\alpha \sinh\phi_\alpha)(-k_1^\beta \cos\phi_\beta + k_2^\beta \sin\phi_\beta)}{\sin^2\phi} \tag{17}$$

and

$$H = \frac{-k_1^\beta \cosh\phi_\beta + k_2^\beta \sinh\phi_\beta - k_1^\alpha \cosh\phi_\alpha + k_2^\alpha \sinh\phi_\alpha}{2\sin^2\phi} \tag{18}$$

where k_i^α and k_i^β are q-curvature of spacelike curves $\alpha(u)$ and $\beta(v)$ for $i = 1, 2$.

Proof: From (12) and (13), the components $E = \langle M_u, M_u\rangle$, $F = \langle M_u, M_v\rangle$ and $G = \langle M_v, M_v\rangle$ of the first fundamental form I of the spacelike translation surface $M(u,v)$ is

$$I = du^2 + 2\cos\varphi du dv + dv^2. \tag{19}$$

Similarly, we can derive the components $L = \langle \psi_{ss}^r, U\rangle$, $M = \langle \psi_{sv}^r, U\rangle$ and $N = \langle \psi_{vv}^r, U\rangle$ of the second fundamental form II of the spacelike translation surface $M(u,v)$ is

$$II = (-k_1^\alpha \cosh\phi_\alpha + k_2^\alpha \sinh\phi_\alpha)du^2 + (-k_1^\beta \cosh\phi_\beta + k_2^\beta \sinh\phi_\beta)dv^2 \tag{20}$$

where ϕ_α is the angle between the vectors of U and $\mathbf{n}_q^\alpha$, ϕ_β is the angle between the vectors of U and $\mathbf{n}_q^\beta$.

By substituting components of the equations (19) and (20) into the equation (9), the Gauss and mean curvatures of the spacelike translation surface are obtained by

$$K = \frac{(-k_1^\alpha \cosh\phi_\alpha + k_2^\alpha \sinh\phi_\alpha)(-k_1^\beta \cos\phi_\beta + k_2^\beta \sin\phi_\beta)}{\sin^2\phi}$$

and

$$H = \frac{-k_1^\beta \cosh\phi_\beta + k_2^\beta \sinh\phi_\beta - k_1^\alpha \cosh\phi_\alpha + k_2^\alpha \sinh\phi_\alpha}{2\sin^2\phi}.$$

Case 2: In this case we introduce the spacelike translation surfaces by using the spacelike curves. Let $\alpha(u)$ be a spacelike curve which have the tangent vector $\mathbf{t}_\alpha$ (spacelike), quasi-normal vector $\mathbf{n}_{q\alpha}$ (timelike) and quasi-binormal vector $b_{q\alpha}$ (spacelike) with the projection vector $\mathbf{k}$ (spacelike) and $\beta(v)$ be a spacelike curve which have the tangent vector $\mathbf{t}_\beta$ (spacelike), quasi-normal vector $\mathbf{n}_{q\beta}$ (spacelike) and quasi-binormal vector $b_{q\beta}$ (timelike) with the projection vector $\mathbf{k}$ (timelike). From the equations (2) and (4), q-frames of spacelike curves $\alpha(u)$ and $\beta(v)$ may be written as, respectively,

$$\begin{bmatrix} \mathbf{t}'_\alpha \\ (\mathbf{n}_{q\alpha})' \\ (\mathbf{b}_{q\alpha})' \end{bmatrix} = \begin{bmatrix} 0 & -k_1^\alpha & k_2^\alpha \\ -k_1^\alpha & 0 & k_3^\alpha \\ -k_2^\alpha & k_3^\alpha & 0 \end{bmatrix} \begin{bmatrix} \mathbf{t}_\alpha \\ \mathbf{n}_{q\alpha} \\ \mathbf{b}_{q\alpha} \end{bmatrix} \tag{21}$$

and

$$\begin{bmatrix} \mathbf{t}'_\beta \\ (\mathbf{n}_{q\beta})' \\ (\mathbf{b}_{q\beta})' \end{bmatrix} = \begin{bmatrix} 0 & k_1^\beta & -k_2^\beta \\ -k_1^\beta & 0 & -k_3^\beta \\ -k_2^\beta & -k_3^\beta & 0 \end{bmatrix} \begin{bmatrix} \mathbf{t}_\beta \\ \mathbf{n}_{q\beta} \\ \mathbf{b}_{q\beta} \end{bmatrix}, \tag{22}$$

where k_i^α and k_i^β are q-curvature of spacelike curves $\alpha(u)$ and $\beta(v)$ for $1 \le i \le 3$.

By using equations (12) and (13), the unit normal of the spacelike translation surface can be defined by

$$U(u,v) = \frac{1}{\sin\varphi}(\mathbf{t}_\alpha \wedge \mathbf{t}_\beta) \tag{23}$$

where $\varphi(u)$ is the angle between the tangent vectors of $\alpha(u)$ and $\beta(v)$.

Theorem 3.2. The Gauss and mean curvatures of the translation surface are given by

$$K = \frac{(-k_1^\alpha \cosh\phi_\alpha + k_2^\alpha \sinh\phi_\alpha)(k_1^\beta \cos\phi_\beta - k_2^\beta \sin\phi_\beta)}{\sin^2\phi} \tag{24}$$

and

$$H = \frac{k_1^\beta \cosh\phi_\beta - k_2^\beta \sinh\phi_\beta - k_1^\alpha \cosh\phi_\alpha + k_2^\alpha \sinh\phi_\alpha}{2\sin^2\phi} \tag{25}$$

where k_i^α and k_i^β are q-curvature of spacelike curves $\alpha(u)$ and $\beta(v)$ for $i = 1, 2$.

Proof: From (12) and (13), the components $E = \langle M_u, M_u\rangle$, $F = \langle M_u, M_v\rangle$ and $G = \langle M_v, M_v\rangle$ of the first fundamental form I of the spacelike translation surface $M(u,v)$ is

$$I = du^2 + 2\cos\varphi du dv + dv^2. \tag{26}$$

Similarly, we can derive the components $L = \langle \psi_{ss}^r, U\rangle$, $M = \langle \psi_{sv}^r, U\rangle$ and $N = \langle \psi_{vv}^r, U\rangle$ of the second fundamental form II of the spacelike translation surface $M(u,v)$ is

$$II = (-k_1^\alpha \cosh\phi_\alpha + k_2^\alpha \sinh\phi_\alpha)du^2 + (k_1^\beta \cosh\phi_\beta - k_2^\beta \sinh\phi_\beta)dv^2 \tag{27}$$

where ϕ_α is the angle between the vectors of U and $\mathbf{n}_q^\alpha$, ϕ_β is the angle between the vectors of U and $\mathbf{n}_q^\beta$.

By substituting components of the equations (26) and (27) into the equation (9), the Gauss and mean curvatures of the spacelike translation surface are obtained by

$$K = \frac{(-k_1^\alpha \cosh\phi_\alpha + k_2^\alpha \sinh\phi_\alpha)(k_1^\beta \cos\phi_\beta - k_2^\beta \sin\phi_\beta)}{\sin^2\phi}$$

and

$$H = \frac{-k_1^\beta \cosh\phi_\beta + k_2^\beta \sinh\phi_\beta + k_1^\alpha \cosh\phi_\alpha - k_2^\alpha \sinh\phi_\alpha}{2\sin^2\phi}.$$

Case 3: In this case we introduce the spacelike translation surfaces by using the spacelike curves. Let $\alpha(u)$ be a spacelike curve which have the tangent vector $\mathbf{t}_\alpha$ (spacelike), quasi-normal vector $\mathbf{n}_{q\alpha}$ (spacelike) and quasi-binormal vector $b_{q\alpha}$ (timelike) with the projection vector $\mathbf{k}$ (timelike) and $\beta(v)$ be a spacelike curve which have the tangent vector $\mathbf{t}_\beta$ (spacelike), quasi-normal vector $\mathbf{n}_{q\beta}$ (timelike) and quasi-binormal vector $b_{q\beta}$ (spacelike) with the projection vector $\mathbf{k}$ (spacelike). From the equations (2) and (4), q-frames of spacelike curves $\alpha(u)$ and $\beta(v)$ may be written as, respectively,

$$\begin{bmatrix} \mathbf{t}'_\alpha \\ (\mathbf{n}_{q\alpha})' \\ (\mathbf{b}_{q\alpha})' \end{bmatrix} = \begin{bmatrix} 0 & k_1^\alpha & -k_2^\alpha \\ -k_1^\alpha & 0 & -k_3^\alpha \\ -k_2^\alpha & -k_3^\alpha & 0 \end{bmatrix} \begin{bmatrix} \mathbf{t}_\alpha \\ \mathbf{n}_{q\alpha} \\ \mathbf{b}_{q\alpha} \end{bmatrix} \tag{28}$$

and

$$\begin{bmatrix} \mathbf{t}'_\beta \\ (\mathbf{n}_{q\beta})' \\ (\mathbf{b}_{q\beta})' \end{bmatrix} = \begin{bmatrix} 0 & -k_1^\beta & k_2^\beta \\ -k_1^\beta & 0 & k_3^\beta \\ -k_2^\beta & k_3^\beta & 0 \end{bmatrix} \begin{bmatrix} \mathbf{t}_\beta \\ \mathbf{n}_{q\beta} \\ \mathbf{b}_{q\beta} \end{bmatrix}, \tag{29}$$

where k_i^α and k_i^β are q-curvature of spacelike curves $\alpha(u)$ and $\beta(v)$ for $1 \leq i \leq 3$.

By using equations (12) and (13), the unit normal of the spacelike translation surface can be defined by

$$U(u,v) = \frac{1}{\sin\varphi}(\mathbf{t}_\alpha \wedge \mathbf{t}_\beta) \tag{30}$$

where $\varphi(u)$ is the angle between the tangent vectors of $\alpha(u)$ and $\beta(v)$.

Theorem 3.3. The Gauss and mean curvatures of the translation surface are given by

$$K = \frac{(k_1^\alpha \cosh\phi_\alpha - k_2^\alpha \sinh\phi_\alpha)(-k_1^\beta \cos\phi_\beta + k_2^\beta \sin\phi_\beta)}{\sin^2\phi} \tag{31}$$

and

$$H = \frac{-k_1^\beta \cosh\phi_\beta + k_2^\beta \sinh\phi_\beta + k_1^\alpha \cosh\phi_\alpha - k_2^\alpha \sinh\phi_\alpha}{2\sin^2\phi} \tag{32}$$

where k_i^α and k_i^β are q-curvature of spacelike curves $\alpha(u)$ and $\beta(v)$ for $i = 1, 2$.

Proof: From (12) and (13), the components $E = \langle M_u, M_u \rangle$, $F = \langle M_u, M_v \rangle$ and $G = \langle M_v, M_v \rangle$ of the first fundamental form I of the spacelike translation surface $M(u,v)$ is

$$I = du^2 + 2\cos\varphi du dv + dv^2. \tag{33}$$

Similarly, we can derive the components $L = \langle \psi_{ss}^r, U \rangle$, $M = \langle \psi_{sv}^r, U \rangle$ and $N = \langle \psi_{vv}^r, U \rangle$ of the second fundamental form II of the spacelike translation surface $M(u,v)$ is

$$II = (k_1^\alpha \cosh\phi_\alpha - k_2^\alpha \sinh\phi_\alpha)du^2 + (-k_1^\beta \cosh\phi_\beta + k_2^\beta \sinh\phi_\beta)dv^2 \tag{34}$$

where ϕ_α is the angle between vectors of U and $\mathbf{n}_q^\alpha$, ϕ_β is the angle between vectors of U and $\mathbf{n}_q^\beta$.

By substituting components of the equations (33) and (34) into the equation (9), the Gauss and mean curvatures of the spacelike translation surface are obtained by

$$K = \frac{(k_1^\alpha \cosh\phi_\alpha - k_2^\alpha \sinh\phi_\alpha)(-k_1^\beta \cos\phi_\beta + k_2^\beta \sin\phi_\beta)}{\sin^2\phi}$$

and

$$H = \frac{-k_1^\beta \cosh\phi_\beta + k_2^\beta \sinh\phi_\beta + k_1^\alpha \cosh\phi_\alpha - k_2^\alpha \sinh\phi_\alpha}{2\sin^2\phi}.$$

Case 4: In this case we introduce the spacelike translation surfaces by using the spacelike curves. Let $\alpha(u)$ be a spacelike curve which have the tangent vector $\mathbf{t}_\alpha$ (spacelike), quasi-normal vector $\mathbf{n}_{q\alpha}$ (spacelike) and quasi-binormal vector $b_{q\alpha}$ (timelike) with the projection vector $\mathbf{k}$ (timelike) and $\beta(v)$ be a spacelike curve which have the tangent vector $\mathbf{t}_\beta$ (spacelike), quasi-normal vector $\mathbf{n}_{q\beta}$ (spacelike) and quasi-binormal vector $b_{q\beta}$ (timelike) with the projection vector $\mathbf{k}$ (timelike). From the equation (4), q-frames of spacelike curves $\alpha(u)$ and $\beta(v)$ may be written as, respectively,

$$\begin{bmatrix} \mathbf{t}'_\alpha \\ (\mathbf{n}_{q\alpha})' \\ (\mathbf{b}_{q\alpha})' \end{bmatrix} = \begin{bmatrix} 0 & k_1^\alpha & -k_2^\alpha \\ -k_1^\alpha & 0 & -k_3^\alpha \\ -k_2^\alpha & -k_3^\alpha & 0 \end{bmatrix} \begin{bmatrix} \mathbf{t}_\alpha \\ \mathbf{n}_{q\alpha} \\ \mathbf{b}_{q\alpha} \end{bmatrix} \tag{35}$$

and

$$\begin{bmatrix} \mathbf{t}'_\beta \\ (\mathbf{n}_{q\beta})' \\ (\mathbf{b}_{q\beta})' \end{bmatrix} = \begin{bmatrix} 0 & k_1^\beta & -k_2^\beta \\ -k_1^\beta & 0 & -k_3^\beta \\ -k_2^\beta & -k_3^\beta & 0 \end{bmatrix} \begin{bmatrix} \mathbf{t}_\beta \\ \mathbf{n}_{q\beta} \\ \mathbf{b}_{q\beta} \end{bmatrix}, \tag{36}$$

where k_i^α and k_i^β are q-curvature of spacelike curves $\alpha(u)$ and $\beta(v)$ for $1 \leq i \leq 3$.

By using equations (12) and (13), the unit normal of the spacelike translation surface can be defined by

$$U(u,v) = \frac{1}{\sin\varphi}(\mathbf{t}_\alpha \wedge \mathbf{t}_\beta) \tag{37}$$

where $\varphi(u)$ is the angle between the tangent vectors of $\alpha(u)$ and $\beta(v)$.

Theorem 3.4. The Gauss and mean curvatures of the translation surface are given by

$$K = \frac{(k_1^\alpha \cosh\phi_\alpha - k_2^\alpha \sinh\phi_\alpha)(k_1^\beta \cos\phi_\beta - k_2^\beta \sin\phi_\beta)}{\sin^2\phi} \tag{38}$$

and

$$H = \frac{k_1^\beta \cosh\phi_\beta - k_2^\beta \sinh\phi_\beta + k_1^\alpha \cosh\phi_\alpha - k_2^\alpha \sinh\phi_\alpha}{2\sin^2\phi} \tag{39}$$

where k_i^α and k_i^β are q-curvature of spacelike curves $\alpha(u)$ and $\beta(v)$ for $i = 1,2$.

Proof: From (12) and (13), the components $E = \langle M_u, M_u\rangle$, $F = \langle M_u, M_v\rangle$ and $G = \langle M_v, M_v\rangle$ of the first fundamental form I of the spacelike translation surface $M(u,v)$ is

$$I = du^2 + 2\cos\varphi du dv + dv^2. \tag{40}$$

Similarly, we can derive the components $L = \langle \psi_{ss}^r, U\rangle$, $M = \langle \psi_{sv}^r, U\rangle$ and $N = \langle \psi_{vv}^r, U\rangle$ of the second fundamental form II of the spacelike translation surface $M(u,v)$ is

$$II = (k_1^\alpha \cosh\phi_\alpha - k_2^\alpha \sinh\phi_\alpha)du^2 + (k_1^\beta \cosh\phi_\beta - k_2^\beta \sinh\phi_\beta)dv^2 \tag{41}$$

where ϕ_α is the angle between the vectors of U and $\mathbf{n}_q^\alpha$, ϕ_β is the angle between the vectors of U and $\mathbf{n}_q^\beta$.

By substituting components of the equations (40) and (41) into the equation (9), the Gauss and mean curvatures of the spacelike translation surface are obtained by

$$K = \frac{(k_1^\alpha \cosh\phi_\alpha - k_2^\alpha \sinh\phi_\alpha)(k_1^\beta \cos\phi_\beta - k_2^\beta \sin\phi_\beta)}{\sin^2\phi}$$

and

$$H = \frac{k_1^\beta \cosh\phi_\beta - k_2^\beta \sinh\phi_\beta + k_1^\alpha \cosh\phi_\alpha - k_2^\alpha \sinh\phi_\alpha}{2\sin^2\phi}.$$

Definition 3.1. Let $\alpha(u)$ be a spacelike curve that is parameterized by arc length u with q-frame $\{\mathbf{t}_\alpha, \mathbf{n}_{q\alpha}, \mathbf{b}_{q\alpha}\}$ on a spacelike surface M. If

$$\langle U, \mathbf{n}_{q\alpha}\rangle = 0$$

where the timelike vector U is the unit normal of the spacelike surface M and the spacelike(timelike) quasi-normal vector $\mathbf{n}_{q\beta}$, then the spacelike curve α is called spacelike (timelike) $\mathbf{n}_{q\alpha}$-line.

Theorem 3.5. a) α is not a timelike $\mathbf{n}_{q\alpha}$-line of spacelike translation surface for Case 1 and Case 2

b) If α is a spacelike $\mathbf{n}_{q\alpha}$-line of spacelike translation surface, then $\dfrac{k_2^\alpha}{k_3^\alpha} = -\tanh\phi$ for Case 3 and Case 4

Proof a) Since $\langle U, \mathbf{n}_{q\alpha}\rangle = \cosh\phi_\alpha$ and $\cosh\phi_\alpha \neq 0$, the results are easily obtained.

b) Since $\langle U, \mathbf{n}_{q\alpha}\rangle = \cos\phi_\alpha$, then from (16),

$$\cos\phi_\alpha = -\frac{1}{\sin\phi}\langle \mathbf{b}_{q\alpha}, \mathbf{t}_\beta\rangle \tag{42}$$

is obtained.

Differentiating (42) with respect to u, using (28), (35) and $\langle \mathbf{b}_{q\alpha}, \mathbf{t}'_\beta\rangle = 0$, so

$$\phi'_\alpha \sin\phi_\alpha = -\coth\phi(-\phi'\cos\phi_\alpha + k_2^\alpha) - k_3^\alpha. \tag{43}$$

Since α is a $\mathbf{n}_{q\alpha}$-line, $\cos\phi_\alpha = 0$, $\sin\phi_\alpha = \pm 1$ and $\phi'_\alpha = 0$. From (43), we get

$$\frac{k_2^\alpha}{k_3^\alpha} = -\tanh\phi. \tag{44}$$

Theorem 3.7. The Gauss curvature of a spacelike translation surface generating by spacelike curves is zero if and only if

a) $\dfrac{k_1^\alpha}{k_2^\alpha} = \tanh\phi_\alpha$ or $\dfrac{k_1^\beta}{k_2^\beta} = \tanh\phi_\beta$ for Case 1.

b) $\dfrac{k_1^\alpha}{k_2^\alpha} = \tanh\phi_\alpha$ or $\dfrac{k_1^\beta}{k_2^\beta} = \coth\phi_\beta$ for Case 2.

c) $\dfrac{k_1^\alpha}{k_2^\alpha} = \coth\phi_\alpha$ or $\dfrac{k_1^\beta}{k_2^\beta} = \tanh\phi_\beta$ for Case 3.

d) $\dfrac{k_1^\alpha}{k_2^\alpha} = \coth\phi_\alpha$ or $\dfrac{k_1^\beta}{k_2^\beta} = \coth\phi_\beta$ for Case 4.

where k_i^α, k_i^β $(i = 1, 2)$ are, respectively, q-curvatures of α and β.

Proof: a) $(\Rightarrow)$ Let the Gauss curvature be zero, then from the equation (17) we get

$$\frac{k_1^\alpha}{k_2^\alpha} = \tanh\phi_\alpha \text{ or } \frac{k_1^\beta}{k_2^\beta} = \tanh\phi_\beta.$$

$(\Leftarrow)$ If

$$\frac{k_1^\alpha}{k_2^\alpha} = \tanh\phi_\alpha \text{or } \frac{k_1^\beta}{k_2^\beta} = \tanh\phi_\beta$$

where ϕ_α is the angle between the vectors of U and $\mathbf{n}_q^\alpha$, ϕ_β is the angle between the vectors of U and $\mathbf{n}_q^\beta$. Then, we obtain

$$-k_1^\alpha\cosh\phi_\alpha + k_2^\alpha\sinh\phi_\alpha = 0 \text{ or } -k_1^\beta\cosh\phi_\beta + k_2^\beta\sinh\phi_\beta = 0. \tag{45}$$

By substituting the equations (45) into the equation (17), $K = 0$ is get. It is easy to see that the similar results are obtained with the same steps for the other cases.

4 EXAMPLES

Example 5.1. Let $M(u,v)$ be the spacelike translation surface given by

$$M(u,v)=\left(\sqrt{5}\sin u-2\cos\frac{v}{\sqrt{3}},\sqrt{5}\cos u+2\sin\frac{v}{\sqrt{3}},2u+\frac{v}{\sqrt{3}}\right)$$

with generator spacelike curves

$$\alpha(u)=\left(\sqrt{5}\sin u,\sqrt{5}\cos u,2u\right)\text{ and }\beta(v)=(-2\cos\frac{v}{\sqrt{3}},2\sin\frac{v}{\sqrt{3}},\frac{v}{\sqrt{3}})$$

where the projection vector $\mathbf{k}$ is $(0,0,1)$.

The tangent and the quasi-normal and the quasi-binormal vector of α are

$$\mathbf{t}_\alpha=(\sqrt{5}\cos u,-\sqrt{5}\sin u,2)$$

$$\mathbf{n}_{q\alpha}=(\sin u,\cos u,0)$$

and

$$\mathbf{b}_{q\alpha}=\left(2\cos u,-2\sin u,\sqrt{5}\right).$$

where the projection vector $\mathbf{k}$ is $(0,0,1)$.

Similarly, the tangent and the quasi-normal and the quasi-binormal vector of β are

$$\mathbf{t}_\beta=\left(\frac{2}{\sqrt{3}}\sin\frac{v}{\sqrt{3}},\frac{2}{\sqrt{3}}\cos\frac{v}{\sqrt{3}},\frac{1}{\sqrt{3}}\right)$$

$$\mathbf{n}_{q\beta}=\left(-\cos\frac{v}{\sqrt{3}},\sin\frac{v}{\sqrt{3}},0\right)$$

and

$$\mathbf{b}_{q\beta}=\left(\frac{1}{\sqrt{3}}\sin\frac{v}{\sqrt{3}},\frac{1}{\sqrt{3}}\cos\frac{v}{\sqrt{3}},\frac{2}{\sqrt{3}}\right)$$

where the projection vector $\mathbf{k}$ is $(0,0,1)$. The first and the second fundamental forms of the spacelike translation surface $M(u,v)$ are

$$I=du^2-\frac{4}{\sqrt{3}}\left(\sqrt{5}\sin(u-\frac{v}{\sqrt{3}})+1\right)dudv+dv^2.$$

and

$$II=-\frac{1}{\sqrt{3}}(4\sqrt{5}\sin(u-\frac{v}{\sqrt{3}})+5)du^2-\frac{2}{3\sqrt{3}}(\sqrt{5}\sin(u-\frac{v}{\sqrt{3}})+4)dv^2,$$

respectively. Also, the Gauss and mean curvatures of the translation surface are obtained as

$$\begin{aligned}K&=\frac{40\sin^2(u-\frac{v}{\sqrt{3}})+42\sqrt{5}\sin(u-\frac{v}{\sqrt{3}})+40}{60\sin^2(u-\frac{v}{\sqrt{3}})+24\sqrt{5}\sin(u-\frac{v}{\sqrt{3}})+3}\\H&=\frac{10\sqrt{5}\sin(u-\frac{v}{\sqrt{3}})+7}{40\sqrt{3}\sin^2(u-\frac{v}{\sqrt{3}})+16\sqrt{15}\sin(u-\frac{v}{\sqrt{3}})+2\sqrt{3}}.\end{aligned}$$

The graph is plotted when the tangent vectors between α and β are orthogonal in Figure 2.

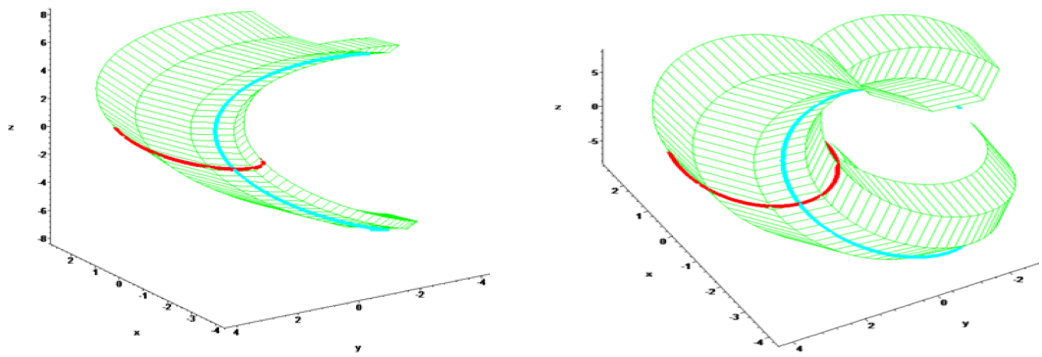

Figure 2

Example 5.2. Let $M(u,v)$ be the spacelike translation surface given by

$$M(u,v) = \left(\sqrt{5}\sin u + 2v, \sqrt{5}\cos u - 2v, 2u + v\sqrt{7}\right)$$

with generator spacelike curves

$$\alpha(u) = \left(\sqrt{5}\sin u, \sqrt{5}\cos u, 2u\right) \text{ and } \beta(v) = (2v, -2v, v\sqrt{7})$$

where the projection vector $\mathbf{k}$ is $(0,0,1)$.

The tangent and the quasi-normal and the quasi-binormal vector of α are

$$\mathbf{t}_\alpha = (\sqrt{5}\cos u, -\sqrt{5}\sin u, 2)$$

$$\mathbf{n}_{q\alpha} = (\sin u, \cos u, 0)$$

and

$$\mathbf{b}_{q\alpha} = \left(2\cos u, -2\sin u, \sqrt{5}\right).$$

where the projection vector $\mathbf{k}$ is $(0,0,1)$.

Similarly, the tangent and the quasi-normal and the quasi-binormal vector of β are

$$\mathbf{t}_\beta = \left(2, -2, \sqrt{7}\right)$$

$$\mathbf{n}_{q\beta} = \left(\frac{\sqrt{2}}{2}, \frac{\sqrt{2}}{2}, 0\right)$$

and

$$\mathbf{b}_{q\beta} = \left(\frac{\sqrt{14}}{2}, -\frac{\sqrt{14}}{2}, 2\sqrt{2}\right)$$

where the projection vector $\mathbf{k}$ is $(0,0,1)$. The first and the second fundamental forms of the spacelike translation surface $M(u,v)$ are

$$I = du^2 + \left(4\sqrt{5}\left(\sin u + \cos u\right) - 4\sqrt{7}\right) dudv + dv^2.$$

and

$$II = \left(4\sqrt{5}\left(\sin u + \cos u\right) - 5\sqrt{7}\right) du^2,$$

respectively. Also, the Gauss and mean curvatures of the translation surface are obtained as

$$\begin{aligned} K &= 0 \\ H &= \frac{4\sqrt{5}\left(\sin u + \cos u\right) - 5\sqrt{7}}{16\sqrt{35}\left(\sin u + \cos u\right) - 80\sin u\cos u}. \end{aligned}$$

If we take the parameter u in the range $\left(\frac{-3+\sqrt{7}}{3\sqrt{7}+1} - 2\pi, \frac{3+\sqrt{7}}{-1+3\sqrt{7}} - 2\pi\right)$, the surface M will be the spacelike translation. Also, the graph is plotted when the tangent vectors between α and β are orthogonal in Figure 3.

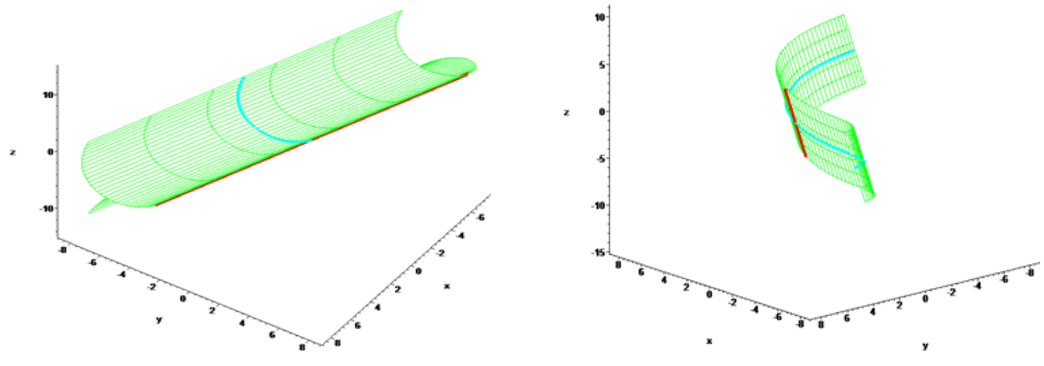

Figure 3

References

[1] K. Akutagawa, S. Nishikawa, The Gauss map and spacelike surfaces with prescribed mean curvature in Minkowski 3-space, Tohoku Math. J. 42 (1990) 67-82.

[2] A.T. Ali, H. S. A. Aziz, A. H. Sorour, On curvatures and points of the translation surfaces in Euclidean 3-space, J. Egyptian Math. Soc. 23 (2015) 167-172.

[3] Ch. Baba-Hamed, M.Bekkar, H. Zoubir, Translation Surfaces in the Three-Dimensional Lorentz-Minkowski Space Satisfying $\Delta r_i = \lambda_i r_i$, Int. J. Math. Anal. 4(17) (2010) 797-808.

[4] W. B. Bonnor, Null curves in a Minkowski space-time, Tensor, 20 (1969) 229-242.

[5] S. Coquillart, Computing offsets of B-spline curves, Comput.-Aided Des. 19 (1987) 305-309.

[6] M. Çetin, Y. Tuncer, N. Ekmekci, Translation surfaces in Euclidean 3-space. Internat. J. Math., Comput., Phys., Electrical and Comput. Eng. 52 (2011) 864-868

[7] M. Çetin, H. Kocayiğit, M. Önder, Translation surfaces according to Frenet frame in Minkowski 3-space, Int. J. Phys. Sci., **7**(47) (2012) 6135-6143.

[8] M. Dede, C. Ekici, A. Görgülü, Directional q-frame along a space curve, IJARCSSE 5 (2015) 775–780.

[9] M. Dede, C. Ekici, H. Tozak, Directional tubular surfaces, Int. J. Algebra 9(12) (2015) 527–535.

[10] F. Dillen, W. Goemans, I. Woestyne, Translation surfaces of Weingarten type in 3-space, Bull. Transilv. Univ. Braşov Ser. III 1(50) (2008) 109-122.

[11] C. Ekici, M. Dede, H. Tozak, Timelike directional tubular surfaces, Int. J. Mathematical Anal. 8(5) (2017) 1-11.

[12] H. Liu, Translation surfaces with constant mean curvature in 3-dimensional spaces, J. Geom. 64 (1999) 141–149.

[13] M. Munteanu, A. I. Nistor, On the geometry of the second fundamental form of translation surfaces in E^3, Houston J. Math. 37 (2011) 1087-1102.

[14] B. O'Neill, Semi-Riemannian Geometry with Applications to Relativity, Academic Press, California, 1983.

[15] H. Shin, S. K. Yoo, S. K. Cho, W. H. Chung, Directional offset of a spatial curve for practical engineering design, ICCSA 3 (2003) 711-720.

[16] Z. M. Sipus, B. Divjak, Translation surfaces in the Galilean space, Glas. Mat. 46(66) (2011) 457–471.

[17] H. Tozak, M. Dede, C. Ekici, Translation surfaces according to a new frame, Casp. J. Math. Sci. Preprint (2018).

[18] L. Verstraelen, J. Walrave, S. Yaprak, The minimal translation surfaces in Euclidean space, Soochow J. Math. 20(1) (1994) 77–82.

[19] D. W. Yoon, On the Gauss map of translation surfaces in Minkowski 3-space, Taiwanese J. Math. 6(3) (2002) 389-398.

Relations Among Frenet Apparatus Of Some Special Curves in $\mathbb{E}^4$

Süha YILMAZ
Deparment of Primary Mathematics Education,
Dokuz Eylül University, Turkey

Yasin ÜNLÜTÜRK *
Department of Mathematics,
Kırklareli University, Turkey

Abstract

In this work, we take tangent spherical images as base curves. Using Frenet formulae, we characterize Bertrand W-curve couples of tangent spherical images in $\mathbb{E}^4$. Moreover, we study $ccr-$curves of tangent spherical images in $\mathbb{E}^4$. Finally, we give involute-evolute curve couple of tangent spherical images in Euclidean 4-space $\mathbb{E}^4$.

Keywords: Tangent spherical images, inclined curve, involute-evolute curve couple, Bertrand W-curve, ccr-curve.

1 Introduction

It is well-known that, if a curve differentiable in an open interval, at each point, a set of mutually orthogonal unit vectors can be constructed. And these vectors are called Frenet frame or moving frame vectors. The rates of these frame vectors along the curve define curvatures of the curves. The set, whose elements are frame vectors and curvatures of a curve, is called Frenet apparatus of the curves [1].

In their study [2], Yılmaz and Turgut also investigated relations among Frenet apparatus of space-like Bertrand W-curve couples in Minkowski space-time. They also showed that Frenet apparatus of an evolute curve can be formed according to apparatus of involute curve and that there are no inclined evolutes in Minkowski space-time $\mathbb{E}_1^4$ [3]. Turgut et al. proved that there are no timelike involutes of a time-like evolute. In the light of their result, they observed that involute curve transforms to a time-like curve when evolute is a space-like helix with a time-like principal normal. Then, they investigated relationships among Frenet-Serret apparatus of involute and evolute curves by the method expressed as in their previous work. Moreover, they also proved that the time-like involute cannot be a helix, a general helix or a type-3 slant helix, respectively [4].

Mağden gave some characterizations for regular smooth curves in Euclidean 4-space [5]. Nizamoğlu and Köroğlu characterized a curve in Euclidean 4-space by obtaining a differential equation given by the axisof Frenet frame [6]. Yılmaz et al. characterized inclined curves by obtaining a vector differential equation of fifth order and presented solutions of this equation for special cases [7]. Turgut and Yılmaz gave some characterizations of slant helices in Euclidean 4-space $\mathbb{E}^4$ [8]. In another work [9], some relations between involute-evolute curve couples were found in terms of Frenet elements in Euclidean 4-space $\mathbb{E}^4$. Turgut and Ali gave some characterizations of helices and ccr-curves in the Euclidean 4-space. Thereafter, they presented relations among Frenet-Serret invariants of Bertrand curve of a helix. Moreover, in the same space, they gave some new characterizations of involute of a helix [10].

*Corresponding author. *E-mail address:* yasinunluturk@klu.edu.tr

In this work, as differs from the works [2], [3], [4], we study Bertrand W-curve couples of tangent spherical images using Frenet formulae in $\mathbb{E}^4$. In the mentioned works, these characterizations had been given for a regular curve. Moreover, we characterize $ccr-$curves of tangent spherical images in $\mathbb{E}^4$. Finally, we give involute-evolute curve couple of tangent spherical images in this space $\mathbb{E}^4$.

2 Preliminaries

Let $\alpha : I \subset R \longrightarrow \mathbb{E}^4$ be an arbitrary curve in Euclidean space $\mathbb{E}^4$. Recall that the curve α is said to be of unit speed (or parameterized by arclength function) if $\left\langle \alpha', \alpha' \right\rangle = 1$ where $\langle , \rangle$ is the standard scalar (inner) product of $\mathbb{E}^4$ given by

$$\langle a, a \rangle = a_1 b_1 + a_2 b_2 + a_3 b_3 + a_4 b_4 \tag{1}$$

for each

$$a = (a_1, a_2, a_3, a_4), b = (b_1, b_2, b_3, b_4) \in \mathbb{E}^4.$$

In particular, the norm of a vector $a \in \mathbb{E}^4$ is given by

$$\|a\| = \sqrt{\langle a, a \rangle}.$$

Denoted by $\{T(s), N(s), B(s), E(s)\}$ the moving Frenet frame along the unit speed curve α. Then, the Frenet formulas are given by [1]:

$$\begin{bmatrix} T'(s) \\ N'(s) \\ B'(s) \\ E'(s) \end{bmatrix} = \begin{bmatrix} 0 & \kappa(s) & 0 & 0 \\ -\kappa(s) & 0 & \tau(s) & 0 \\ 0 & -\tau(s) & 0 & \sigma(s) \\ 0 & 0 & -\sigma(s) & 0 \end{bmatrix} \begin{bmatrix} T(s) \\ N(s) \\ B(s) \\ E(s) \end{bmatrix}. \tag{2}$$

Here, T, N, B and E are called, respectively, the tangent, the normal, the binormal and trinormal vector fields of the curves. And the functions $\kappa(s)$, $\tau(s)$ and $\sigma(s)$ are called, respectively, the first, the second and third curvature of the curve α. Recall that a regular curve is called a W-curve if it has constant Frenet curvatures [1].

Let $\alpha : I \subset R \longrightarrow \mathbb{E}^4$ be a regular curve. If tangent vector field T of the curve α forms a constant angle with unit vector $\overrightarrow{U}$, this curve is called an inclined curve in $\mathbb{E}^4$.

Let φ and ξ be unit speed curves in $\mathbb{E}^4$. The curve φ is an involute of ξ if φ lies on the tangent line to ξ at $\xi(s_0)$ and tangents to ξ, $\xi(s_0)$ and φ are perpendicular for each s_0. The curve φ is an evolute of ξ if ξ is an involute of φ. This curve couple is defined by $\varphi = \xi + \mu T$ [11].

Definition 2.1. ([13]) Let $a = (a_1, a_2, a_3, a_4)$, $b = (b_1, b_2, b_3, b_4)$ and $c = (c_1, c_2, c_3, c_4)$ be vectors in $\mathbb{E}^4$. The vector product of a, b and c is defined by the determinant

$$a \wedge b \wedge c = \begin{vmatrix} e_1 & e_2 & e_3 & e_4 \\ a_1 & a_2 & a_3 & a_4 \\ b_1 & b_2 & b_3 & b_4 \\ c_1 & c_2 & c_3 & c_4 \end{vmatrix},$$

where

$$e_1 \wedge e_2 \wedge e_3 = e_4, \quad e_2 \wedge e_3 \wedge e_4 = e_1, \quad e_3 \wedge e_4 \wedge e_1 = e_2,$$
$$e_4 \wedge e_1 \wedge e_2 = e_3, \quad e_3 \wedge e_2 \wedge e_1 = e_4.$$

Theorem 2.2. Let $\alpha = \alpha(t)$ be an arbitrary curve in $\mathbb{E}^4$. Frenet apparatus of the curve α can be calculated by the following equations:

$$T = \frac{\alpha'}{\|\alpha'\|}, \tag{3}$$

$$N = \frac{\left\|\alpha'\right\|^2 \alpha'' - \langle \alpha', \alpha'' \rangle \alpha'}{\left\| \|\alpha'\|^2 \alpha'' - \langle \alpha', \alpha'' \rangle \alpha' \right\|}, \tag{4}$$

$$B = \eta E \wedge T \wedge N, \tag{5}$$

$$E = \eta \frac{T \wedge N \wedge \alpha'''}{\|T \wedge N \wedge \alpha'''\|}, \tag{6}$$

$$\kappa = \frac{\left\| \left\|\alpha'\right\|^2 \alpha'' - \langle \alpha', \alpha'' \rangle \alpha' \right\|}{\|\alpha'\|^4}, \tag{7}$$

$$\tau = \frac{\|T \wedge N \wedge \alpha'''\| \, \|\alpha'\|}{\left\| \|\alpha'\|^2 \alpha'' - \langle \alpha', \alpha'' \rangle \alpha' \right\|}, \tag{8}$$

$$\sigma = \frac{\left\langle \alpha^{(IV)}, E \right\rangle}{\|T \wedge N \wedge \alpha'''\| \, \|\alpha'\|}, \tag{9}$$

where η is taken to make 1 determinant of $[T, N, B, E]$ matrix [9].

Definition 2.3. Let $\alpha = \alpha(t)$ be a unit speed $ccr-$curve in $\mathbb{E}^4$. Then, we know

$$\frac{\kappa}{\tau} = c_1, \quad \text{and} \quad \frac{\tau}{\sigma} = c_2,$$

where c_1 and c_2 are constants [12].

Definition 2.4. Let a curve α be in $\mathbb{E}^4$ be given with $s \in I$ arc parameter. Provide T is the unit tangent vector of the curve α, we obtain a curve $\alpha_1 = T(s)$ on the unit sphere if we carry these tangents to at a point O of the unit sphere. This curve is called the first spherical indicatrix of the curve α (or tangent spherical indicatrix) [11].

3 Main results

Theorem 3.1. Let φ be an involute of α_1 and be a W-curve in $\mathbb{E}^4$. The Frenet apparatus of φ $(T_\varphi, N_\varphi, B_\varphi, E_\varphi, \kappa_\varphi, \tau_\varphi, \sigma_\varphi)$ can be formed by apparatus of $\overrightarrow{\alpha}_1$ $(T_1, N_1, B_1, E_1, \kappa_1, \tau_1, \sigma_1)$. Here, the curve α_1 is tangent spherical image of α and s_1 is arclength parameter of $\alpha_1(s)$.

Proof. From definition of involute-evolute curve couples, we get

$$\varphi = \alpha_1 + \mu T_1. \tag{10}$$

Differentiating both sides with respect to s_1, we have

$$\frac{d\varphi}{ds_\varphi}\frac{ds_\varphi}{ds_1} = \frac{d\alpha_1}{ds_1} + \frac{d\mu}{ds_1}T_1 + \mu\frac{dT_1}{ds_1}$$

or

$$T_\varphi \frac{ds_\varphi}{ds_1} = T_1\left(\frac{d\mu}{ds_1} + 1\right) + \mu\frac{dT_1}{ds_1}. \tag{11}$$

Recalling definition of involute and evolute curves, by multiplying both sides of (11) with T_1, we obtain

$$\frac{d\mu}{ds_1} + 1 = 0. \tag{12}$$

Hence $\mu = c - s_1$. Then, we write

$$\varphi = \alpha_1 + (c - s_1) T_1. \tag{13}$$

Differentiating both sides with respect to s_1, we get

$$T_\varphi \frac{ds_\varphi}{ds_1} = (c - s_1)\,\kappa_1 N_1. \tag{14}$$

Taking the norm of both sides of (14) (here $\cdot$ denotes derivative according to s_1) we obtain

$$T_\varphi = N_1 \tag{15}$$

and

$$\left\|\dot{\varphi}\right\| = (c - s_1)\,\kappa_1. \tag{16}$$

Considering the presented method, we calculate differentiations of (14) four times. We write, respectively,

$$\ddot{\varphi} = -\kappa_1^2 (c - s_1)\, T_1 - \kappa_1 N_1 + \kappa_1\tau_1 (c - s_1)\, B_1, \tag{17}$$

$$\dddot{\varphi} = \left\{-2\kappa_1^2 T_1 - \kappa_1 (c - s_1)\left[\kappa_1^2 + \tau_1^2\right] N_1 - 2\kappa_1\tau_1 B_1 + \kappa_1\tau_1\sigma_1 (c - s_1)\, E_1\right\}, \tag{18}$$

$$\begin{aligned}\varphi^{(IV)} = \{&\kappa_1^2 (c - s_1)\, 2\left[\kappa_1^2 + \tau_1^2\right] T_1 - \kappa_1\left[\kappa_1^2 + \tau_1^2\right] N_1 \\ &-\kappa_1\tau_1 (c - s_1)_1\left[\kappa_1^2 + \tau_1^2 + \sigma_1^2\right] B_1 - 2\kappa_1\tau_1\sigma_1 E_1\}.\end{aligned} \tag{19}$$

Considering (4), we form

$$\left\|\dot{\varphi}\right\|\ddot{\varphi} - \left\langle \dot{\varphi}, \ddot{\varphi}\right\rangle \dot{\varphi} = \kappa_1 (c - s_1)\left[-\kappa_1 T_1 + \tau_1 B_1\right]. \tag{20}$$

Since we have the principal normal and the first curvature of the curve, we obtain

$$N_\varphi = \frac{-\kappa_1 T_1 + \tau_1 B_1}{\sqrt{\kappa_1^2 + \tau_1^2}}. \tag{21}$$

Using the vector product of $T \wedge N \wedge \dddot{\varphi}$, we get

$$T \wedge N \wedge \dddot{\varphi} = \begin{vmatrix} T & N & B & E \\ 0 & 1 & 0 & 0 \\ \dfrac{-\kappa_1}{\sqrt{\kappa_1^2 + \tau_1^2}} & 0 & \dfrac{\tau_1}{\sqrt{\kappa_1^2 + \tau_1^2}} & 0 \\ \dddot{\varphi}_1 & \dddot{\varphi}_2 & \dddot{\varphi}_3 & \dddot{\varphi}_4 \end{vmatrix},$$

and find that

$$T \wedge N \wedge \dddot{\varphi} = \frac{\kappa_1\tau_1}{\sqrt{\kappa_1^2 + \tau_1^2}}\left[\tau_1\sigma_1 (c - s_1)\, T_1 + \kappa_1\sigma_1 (c - s_1)\, B_1 + 3\kappa_1 E_1\right]. \tag{23}$$

From (6), we obtain trinormal vector

$$E_\varphi = \eta\frac{\tau_1\sigma_1 (c - s_1)\, T_1 + \kappa_1\sigma_1 (c - s_1)\, B_1 + 3\kappa_1 E_1}{\sqrt{\left[\tau_1\sigma_1 (c - s_1)\right]^2 + \left[\kappa_1\sigma_1 (c - s_1)\right]^2 + 9\kappa_1^2}}. \tag{24}$$

By this way, we easily have the second and the third curvatures

$$\tau_\varphi = \sqrt{\frac{\left[\tau_1\sigma_1 (c - s_1)\right]^2 + \left[\kappa_1\sigma_1 (c - s_1)\right]^2 + 9\kappa_1^2}{\kappa_1^2 + \tau_1^2}}, \tag{25}$$

$$\sigma_\varphi = \frac{-\kappa_1^2\tau_1\sigma_1\left[\sigma_1^2 (c - s_1)^2 - 3\right]}{\sqrt{\left[\tau_1\sigma_1 (c - s_1)\right]^2 + \left[\kappa_1\sigma_1 (c - s_1)\right]^2 + 9\kappa_1^2}}, \tag{26}$$

respectively. Finally, the vector product $E_\varphi \wedge T_\varphi \wedge N_\varphi$ follows that

$$B_\varphi = \frac{\eta}{A\sqrt{\kappa_1^2+\tau_1^2}}\left\{-3\kappa_1\sigma_1 T_1 - 3\kappa_1^2 B_1 + \sigma_1 (c-s_1)\left(\kappa_1^2+\tau_1^2\right) E_1\right\}, \tag{27}$$

where

$$A = \sqrt{\left[\tau_1\sigma_1 (c-s_1)\right]^2 + \left[\kappa_1\sigma_1 (c-s_1)\right]^2 + 9\kappa_1^2}.$$

Theorem 3.2. Let φ and α_1 be unit speed regular curves in $\mathbb{E}^4$ and φ be involute of the tangent spherical image α_1. The evolute φ can not be an inclined curve.

Proof. By the definition of inclined curves, we may write

$$\langle T_\varphi, U\rangle = \cos\varphi, \tag{28}$$

where U is a constant vector and φ is a constant angle. Considering (15), we can easily have

$$\langle N_1, U\rangle = \cos\varphi. \tag{29}$$

Differentiating (29), we obtain

$$\langle -\kappa_1 T_1 + \tau_1 B_1, U\rangle = 0. \tag{30}$$

Therefore, we may write $T_1 \perp U$ and $B_1 \perp U$. Let us decompose U as

$$U = u_1 N_1 + u_2 E_1. \tag{31}$$

One more differentiating of (31) and using Frenet equations, we have

$$U = 0 \tag{32}$$

which is a contradiction. Thus, evolute φ can not be an inclined curve.

Definition 3.3. Let $\alpha = \alpha(t)$ be a unit speed curve in $\mathbb{E}^4$. If we translate the tangent vector fields to the center O of the Euclidean space S_0^3, we obtain a curve $\theta = \theta(s_0)$. This curve is called the tangent spherical image of the curve α in $\mathbb{E}^4$ [11].

Theorem 3.4. Let $\alpha = \alpha(t)$ be a unit speed curve and $\theta = \theta(s_0)$ be its tangent spherical image (indicatrix). The Frenet apparatus of θ can be determined by the apparatus of $\alpha = \alpha(t)$ by the following

$$T_\theta = N,$$

$$N_\theta = -\frac{1}{\kappa_\theta}T + \frac{\tau}{\kappa\kappa_\theta}B,$$

$$B_\theta = \frac{\varepsilon}{\sqrt{\kappa^2\tau^2\sigma^2\kappa_\theta^2 + \tau^4\left(\frac{\kappa}{\tau}\right)'^2}}\left[\frac{\tau^3\left(\frac{\kappa}{\tau}\right)'}{\kappa\kappa_\theta}T + \frac{\tau^2\left(\frac{\kappa}{\tau}\right)'}{\kappa_\theta}B - \left(\kappa\tau\sigma\kappa_\theta\right)E\right],$$

$$E_\theta = \varepsilon\frac{\left(\tau^2\sigma\right)T + \left(\kappa\tau\sigma\right)B + \tau^2\left(\frac{\kappa}{\tau}\right)' E}{\sqrt{\kappa^2\tau^2\sigma^2\kappa_\theta^2 + \tau^4\left(\frac{\kappa}{\tau}\right)'^2}},$$

$$\kappa_\theta = \frac{\sqrt{\kappa^2+\tau^2}}{\kappa} = \sqrt{1+\left(\frac{2}{\kappa}\right)^2},$$

$$\tau_\theta = \frac{\sqrt{\kappa^2\tau^2\sigma^2\kappa_\theta^2 + \tau^4\left(\frac{\kappa}{\tau}\right)'^2}}{\kappa^3\kappa_\theta^2}$$

$$\sigma_\theta = \frac{\varepsilon\kappa_\theta^2}{\kappa^2\tau^2\sigma^2\kappa_\theta^2 + \tau^4\left(\frac{\kappa}{\tau}\right)'^2} \frac{\left[\begin{array}{c} -3\kappa'^2\tau^2\sigma - \kappa\kappa''\tau^2\sigma - 2\kappa^2\tau^4\sigma + 3\kappa'\tau'\kappa\tau\sigma + \kappa^2\tau\tau''\sigma \\ -\kappa^2\tau^2\sigma^2 + \tau^2\left(\frac{\kappa}{\tau}\right)'(3\kappa'\tau\sigma + 2\kappa\tau'\sigma) + \kappa\tau\sigma' \end{array}\right]}{\sqrt{\kappa^2\tau^2\sigma^2\kappa_\theta^2 + \tau^4\left(\frac{\kappa}{\tau}\right)'^2(\kappa^2+\tau^2)}}.$$

Theorem 3.5. Let $\alpha = \alpha(t)$ be a unit speed curve and $\theta = \theta(s_0)$ be its tangent spherical image (indicatrix). If α is a *ccr*-curve, then θ is also a *ccr*-curve.

Proof. Let $\alpha = \alpha(t)$ be a unit speed *ccr*-curve. Then, we know $\frac{\kappa}{\tau} = c_1$ and $\frac{\tau}{\sigma} = c_2$ where c_1 and c_2 are constant. Since, in terms of Theorem 3.5, we have respectively,

$$\kappa_\theta = \sqrt{1 + \frac{1}{c_1^2}} = \text{constant}, \tag{33}$$

and

$$\tau_\theta = \frac{1}{c_2\sqrt{c_1^2+1}},$$

$\theta(s_0)$ is a spherical curve. So, we may substitute κ_θ and τ_θ from Theorem 3.5,

$$\sigma_\theta = \frac{c_2}{c_1^2} = \text{constant}.$$

Therefore,

$$\frac{\kappa_\theta}{\tau_\theta} = \frac{\sqrt{1+\frac{1}{c_1^2}}}{c_2\sqrt{c_1^2+1}} = \frac{1}{c_1c_2} = \text{constant},$$

$$\frac{\tau_\theta}{\sigma_\theta} = \frac{c_2\sqrt{c_1^2+1}}{\frac{c_2}{c_1^2}} = c_1^2\sqrt{c_1^2+1} = \text{constant}.$$

Thus we obtain θ is also a *ccr*-curve.

Theorem 3.6. Let α^* and α be Betrand $W-$curves of the tangent spherical indicatrix β in Euclidean 4-space. The Frenet apparatus of α^* $(T^*,\ N^*,\ B^*,\ E^*, \kappa^*,\ \tau^*,\ \sigma^*)$ can be formed by the apparatus of α $(T, N, B, E, \kappa, \tau, \sigma)$.

Proof. From definition of Bertrand curves, we write

$$\alpha^*(s^*) = \alpha(s) + \lambda N. \tag{34}$$

Differentiating both sides of (34) with respect to s, we have

$$\frac{d\alpha^*}{ds^*}\frac{ds^*}{ds} = T^*\frac{ds^*}{ds} = (1-\lambda\kappa)T + \frac{d\lambda}{ds}N + \lambda\tau B. \tag{35}$$

Definition of Bertrand curves yields that $T^* \perp N$. Multiplying both sides of (35) with gives

$$\frac{d\lambda}{ds} = 0. \tag{36}$$

The equation (34) implies that λ =constant. Using this in (35) and taking the norm of both sides, we find

$$\|\alpha^*\| = \frac{ds^*}{ds} = \sqrt{\lambda^2\tau^2 + (1-\lambda\kappa)^2}. \tag{37}$$

Therefore the tangent vector of α^* is obtained as follows:

$$T^* = \frac{1-\lambda\kappa}{\sqrt{\lambda^2\tau^2+(1-\lambda\kappa)^2}}T + \frac{\lambda\tau}{\sqrt{\lambda^2\tau^2+(1-\lambda\kappa)^2}}B. \tag{38}$$

Considering equations in the method, we calculate the following equations:

$$\ddot{\alpha}^* = (\kappa+\lambda\kappa^2-\lambda\tau^2)N + \lambda\tau\sigma E, \tag{39}$$

$$\dddot{\alpha}^* = \kappa(-\kappa-\lambda\kappa^2+\lambda\tau^2)T + \tau(\kappa+\lambda\kappa^2-\lambda\tau^2+\lambda\sigma^2)B, \tag{40}$$

$$\alpha^{*(IV)} = (-\kappa^3-\lambda\kappa^4-\kappa\tau^2+\lambda\tau^4-\lambda^2\tau^2\sigma^2)N + \tau\sigma(\kappa+\lambda\kappa^2-\lambda\tau^2+\lambda\sigma^2)E. \tag{41}$$

Thereafter we compute

$$\left\|\dot{\alpha}^*\right\|\ddot{\alpha}^* - \left\langle \dot{\alpha}^*, \ddot{\alpha}^* \right\rangle \dot{\alpha}^* = (\lambda^2\tau^2+(1-\lambda\kappa)^2)\{(\kappa+\lambda\kappa^2-\lambda\tau^2)N + \lambda\tau\sigma E\}. \tag{42}$$

Using (42), we get the first curvature and the principal normal vector N^* as follows:

$$\kappa^* = \frac{\sqrt{(\kappa+\lambda\kappa^2-\lambda\tau^2)^2+\lambda^2\tau^2\sigma^2}}{\lambda^2\tau^2+(1-\lambda\kappa)^2}, \tag{43}$$

and

$$N^* = \frac{(\kappa+\lambda\kappa^2-\lambda\tau^2)N+\lambda\tau\sigma E}{\sqrt{(\kappa+\lambda\kappa^2-\lambda\tau^2)^2+\lambda^2\tau^2\sigma^2}}. \tag{44}$$

Using the vector product of $T^* \wedge N^* \wedge \dddot{\alpha}^*$, we get

$$T^* \wedge N^* \wedge \dddot{\alpha}^* = \xi_1 N + \xi_2 E. \tag{45}$$

So we have the second and the third curvatures of α^* and its trinormal vector E^*, respectively, as follows:

$$\tau^* = \sqrt{\frac{\xi_1^2+\xi_2^2}{(\lambda^2\tau^2+(1-\lambda\kappa)^2)^2\{(\kappa+\lambda\kappa^2-\lambda\tau^2)^2+\lambda^2\tau^2\sigma^2\}}}, \tag{46}$$

$$\sigma^* = \frac{\tau\sigma(\kappa+\lambda\kappa^2-\lambda\tau^2+\lambda\sigma^2)}{\sqrt{(\xi_1^2+\xi_2^2)(\lambda^2\tau^2+(1-\lambda\kappa)^2)}}, \tag{47}$$

and

$$E^* = \mu\frac{\xi_1 N+\xi_2 E}{\sqrt{\xi_1^2+\xi_2^2}}. \tag{48}$$

Finally, the vector product $N^* \wedge T^* \wedge E^*$ gives us the binormal vector as

$$\begin{aligned} B^* = \frac{\mu}{L}\{ & (\lambda\tau\xi_2(\kappa+\lambda\kappa^2-\lambda\tau^2)-\lambda^2\tau^2\sigma\xi_1)T \\ & +(1-\lambda\kappa)(\kappa+\lambda\kappa^2-\lambda\tau\xi_2-\lambda\tau\sigma\xi_2)B\}. \end{aligned} \tag{49}$$

4 Conclusion

In this work, we studied some properties of tangent spherical images, not an ordinary curve in Euclidean 4-space $\mathbb{E}^4$. Hence we studied Bertrand W-curve couples of tangent spherical images using Frenet formulae in $\mathbb{E}^4$. Moreover, we characterized $ccr-$curves of tangent spherical images in $\mathbb{E}^4$. Finally, we gave involute-evolute curve couple of tangent spherical images in this space $\mathbb{E}^4$. All these properties can be also obtained for normal, binormal and trinormal spherical images in both Euclidean 4-space $\mathbb{E}^4$ and Minkowski space-time $\mathbb{E}_1^4$.

Acknowledgement

The authors would like to thank the anonymous reviewers for their valuable comments and suggestions to improve the quality of the paper.

References

[1] Gluck, H., Higher curvatures of curves in Euclidean space, Proc. America. Math. Monthly, 73, 1966, 699-704.

[2] S. Yılmaz, M. Turgut, Relations among Frenet apparatus of space-like Bertrand W-curve couples in Minkowski space-time, Int Math Forum, 3(32), 2008, 1575-1580.

[3] M. Turgut, S. Yılmaz, On the Frenet frame and a characterization of space-like involute-evolute curve couple in Minkowski space-time, Int. Math. Forum, 3(16), 2008, 793-801.

[4] M. Turgut, A.T. Ali, and J. L. Lopez-Bonilla, Time-like Involutes of a space-like helix in Minkowski space-time, Apeiron, 17(1), 2010, 28-41.

[5] A. Mağden, $\mathbb{R}^4$ uzayında bazı özel eğriler ve karakterizasyonları (in Turkish), PhD Dissertation, Grad. Sch. Nat. Appl. Sci., Atatürk Uni., 1990.

[6] Ş. Nizamoğlu, H. Köroğlu, $\mathbb{R}^4$ uzayında bir eğrinin yer vektörünün Frenet eksenleri üzerindeki bileşenleri (in Turkish), DEÜ Buca Eğitim Fak. Derg., Fen. Bil. Eğit. Say., 2(2), 1993, 25-32.

[7] S. Yılmaz, Ş. Nizamoğlu, M. Turgut, A note on differential geometry of the curves in E^4, Int. J. Math. Combin., 2, 2008, 104–108.

[8] M. Turgut, S. Yılmaz, Characterizations of some special helices in E^4, Scientia Magna, 4(1), 2008, 51–55.

[9] E. Özyılmaz, S. Yılmaz, Involute evolute curve couples in the Euclidean 4-space, Int. J. Open Problems Contemp. Math., 2(2), 2009, 168–174.

[10] M. Turgut, A.T. Ali, Some characterizations of special curves in the Euclidean space, Acta Univ. Sapientiae Mathematica, 2(1), 2010, 111–122.

[11] S. Yılmaz, Spherical indicators of curves and characterisations of some special curves in $\mathbb{R}^4$, PhD Dissertation, Inst. Edu. Sci., Dokuz Eylül Uni., 1996.

[12] J. Monterde, Curves with constant curvature ratios, Bol. Soc. Mat. Mex. 13(1), 2007, 177–186.

[13] F. Şemin, Diferansiyel Geometri-I (in Turkish), İstanbul Uni. Sci. Fac. Publ., Istanbul, 1983.

CW and NCW Smarandache Curves According to Alternative Frame

Süleyman ŞENYURT*
Department of Mathematics,
Ordu University, Turkey

Gülşah KAYA
Department of Mathematics,
Ordu University, Turkey

Abstract

In this paper, CW-Smarandache curve and NCW-Smarandache curve are defined, according to alternative frame. Then, some characters of this curves are calculated.

Keywords: CW-Smarandache curve, NCW-Smarandache curve

1 Introduction

In differential geometry, special curves have an important role. One of these curves Smarandache curves. Smarandache curves was firstly defined by M. Turgut and S. Yılmaz in 2008[6]. Let $\alpha = \alpha(s)$ be a regular unit speed curve in E^3. This curves Frenet frame and Alternative frame are $\{T, N, B\}$ and $\{N, C, W\}$, respectively. In there, N is normal vector, W is unit Darboux vector and $C = W \wedge N$[5].

In this paper, we created the Smarandache curves according to the alternative frame of the unit speed curve. Firstly, we introduced Frenet frame, Alternative frame and its properties. After that we mentioned the relationship with Alternative frame and Frenet frame. Then we defined two curves. And we calculated curvature, torsion, Frenet frame and Alternative frame of this curves.

2 Preliminaries

Let $\alpha = \alpha(s)$ be a regular curve with unit speed. Then the Frenet apparatus of the curve (α)[4]

$$\begin{aligned} T(s) &= \alpha^{'}(s), \quad N(s) = \frac{T^{'}(s)}{\|T^{'}(s)\|}, \quad B(s) = T(s) \wedge N(s), \qquad (1)\\ \kappa(s) &= \|T^{'}(s)\|, \quad \tau(s) = \frac{\det\left(\alpha^{'}(s), \alpha^{''}(s), \alpha^{'''}(s)\right)}{\left(\|\alpha^{'}(t) \wedge \alpha^{''}(t)\|\right)^2}, \\ T^{'} &= \kappa N, \quad N^{'} = -\kappa T + \tau B, \quad B^{'} = -\tau N. \end{aligned}$$

In Euclidean 3-space any regular curve $\alpha(s)$ depending on the Frenet vectors moves around the axis of Darboux vector and the Darboux vector and defining a unit vector field are given as[2]

$$W = \frac{\tau T + \kappa B}{\sqrt{\kappa^2 + \tau^2}} = N \wedge N', \quad C = W \wedge N. \qquad (2)$$

*Corresponding author. *E-mail address:* senyurtsuleyman@hotmail.com

(a) Frenet frame (b) Alternative frame

Figure 1: CW-Smarandache curves

So build another orthonormal moving frame along the curve $\alpha(s)$. This frame defined as alternative frame and is represented by $\{N, C, W\}$. The derivative formulae of the alternative frame is given by[3]

$$\begin{aligned} N' &= \beta C, \quad C' = -\beta N + \gamma W, \quad W' = -\gamma C, \\ \beta &= \sqrt{\kappa^2 + \tau^2}, \quad \gamma = \frac{\kappa^2}{\kappa^2 + \tau^2}\left(\frac{\tau}{\kappa}\right)'. \end{aligned} \tag{3}$$

The relationship between the Frenet frame and alternative frame is

$$C = \overline{\kappa}T + \overline{\tau}B, \quad W = \overline{\tau}T + \overline{\kappa}B, \quad T = -\overline{\kappa}C + \overline{\tau}W, \quad B = \overline{\tau}C + \overline{\kappa}W$$

where

$$\overline{\kappa} = \frac{\kappa}{\beta}, \quad \overline{\tau} = \frac{\tau}{\beta}. \tag{4}$$

Principal normal vektor N is common both frames.

3 Smarandache Curves of Alternative Frame

Definition 1 *Let $\alpha(s)$ be a regular curve with unit speed in E^3 and $\{N, C, W\}$ is Alternative frame. Then, α_{CW}-Smarandache curve can be identified as*

$$\alpha_{CW} = \frac{1}{\sqrt{2}}(C + W). \tag{5}$$

Theorem 2 *Let $\alpha(s)$ be a regular curve with unit speed in E^3 and $\{N, C, W\}$ be Alternative frame. The Frenet frame of α_{NC}-Smarandache curve is*
$\{T_{NC}, N_{NC}, B_{NC}\}$.

$$\begin{aligned} T_{CW} &= \frac{-\beta N - \gamma C + \gamma W}{\sqrt{\beta^2 + 2\gamma^2}}, \\ N_{CW} &= \frac{\chi_3 N + \nu_3 C + \mu_3 W}{\sqrt{\chi_3^2 + \nu_3^2 + \mu_3^2}}, \\ B_{CW} &= \frac{(\beta\mu_3 - \gamma\nu_3)}{\sqrt{(\chi_3^2 + \nu_3^2 + \mu_3^2)(2\beta^2 + \gamma^2)}} N \\ &+ \frac{(\beta\mu_3 + \gamma\chi_3)}{\sqrt{(\chi_3^2 + \nu_3^2 + \mu_3^2)(2\beta^2 + \gamma^2)}} C + \frac{(-\beta\nu_3 - \beta\chi_3)}{\sqrt{(\chi_3^2 + \nu_3^2 + \mu_3^2)(2\beta^2 + \gamma^2)}} W. \end{aligned}$$

where

$$\begin{aligned}\chi_3 &= 2\gamma^2\big(-\beta'+\gamma\beta\big)+\beta\gamma\big(\beta^2+2\gamma'\big),\\ \nu_3 &= \beta\big(-\beta^3-\gamma'\beta+\gamma\beta'\big)-\gamma^2\big(3\beta^2+2\gamma^2\big),\\ \mu_3 &= \beta^2\big(\gamma'^2\big)-\gamma\big(2\gamma^3+\beta\beta'\big).\end{aligned}$$

Proof. If we take the derivate of the equation (5)

$$T_{CW}\frac{ds_{CW}}{ds}=\frac{1}{\sqrt{2}}(-\beta N-\gamma C+\gamma W),\quad \frac{ds_{CW}}{ds}=\frac{1}{\sqrt{2}}(\beta^2+2\gamma^2). \tag{6}$$

From equations (6) tangent vector of α_{CW} curve is

$$T_{CW}=\frac{-\beta N-\gamma C+\gamma W}{\sqrt{\beta^2+2\gamma^2}}. \tag{7}$$

If we take the derivate of the equation (7), we can write

$$T'_{CW}=\frac{\sqrt{2}\big(\chi_3 N+\nu_3 C+\mu_3 W\big)}{\big(\beta^2+\gamma^2\big)^2}. \tag{8}$$

where the coefficients are,

$$\begin{aligned}\chi_3 &= 2\gamma^2\big(-\beta'+\gamma\beta\big)+\beta\gamma\big(\beta^2+2\gamma'\big),\\ \nu_3 &= \beta\big(-\beta^3-\gamma'\beta+\gamma\beta'\big)-\gamma^2\big(3\beta^2+2\gamma^2\big),\\ \mu_3 &= \beta^2\big(\gamma'^2\big)-\gamma\big(2\gamma^3+\beta\beta'\big).\end{aligned}$$

If we take norm of equation of (8), we can write

$$\|T'_{NW}\|=\frac{\sqrt{2}\sqrt{\chi_3^2+\nu_3^2+\mu_3^2}}{\big(\beta^2+2\gamma^2\big)^2}. \tag{9}$$

From equations (1), (8) and (9) principal normal vector of α_{CW} curve is

$$N_{CW}=\frac{\chi_3 N+\nu_3 C+\mu_3 W}{\sqrt{\chi_3^2+\nu_3^2+\mu_3^2}}. \tag{10}$$

Binormal vector of α_{CW} curve is

$$\begin{aligned}B_{CW} &= \frac{\big(\beta\mu_3-\gamma\nu_3\big)}{\sqrt{\big(\chi_3^2+\nu_3^2+\mu_3^2\big)\big(2\beta^2+\gamma^2\big)}}N\\ &+ \frac{\big(\beta\mu_3+\gamma\chi_3\big)}{\sqrt{\big(\chi_3^2+\nu_3^2+\mu_3^2\big)\big(2\beta^2+\gamma^2\big)}}C+\frac{\big(-\beta\nu_3-\beta\chi_3\big)}{\sqrt{\big(\chi_3^2+\nu_3^2+\mu_3^2\big)\big(2\beta^2+\gamma^2\big)}}W.\end{aligned}$$

■

Theorem 3 *Let $\alpha(s)$ be a regular curve with unit speed in E^3 and $\{N, C, W\}$ be Alternative frame. The curvature and torsion according to α_{CW}-Smarandache curve of Alternative Frame are, respectivelly,*

$$\begin{aligned}\kappa_{CW} &= \frac{\sqrt{2}\sqrt{\chi_3^2+\nu_3^2+\mu_3^2}}{\big(\beta^2+2\gamma^2\big)^2},\\ \tau_{CW} &= \sqrt{2}\frac{\big(2\gamma^3+\gamma\beta^2\big)\bar{\chi_3}+\big(-\beta'\gamma+\beta\gamma'\big)\bar{\nu_3}+\big(2\gamma^2\beta+\beta^3+\beta\gamma'-\gamma\beta'\big)\bar{\mu_3}}{\big(2\gamma^3+\gamma\beta^2\big)^2-\big(\gamma\beta'-\beta\gamma'\big)^2+\big(2\beta\gamma^2+\beta^3+\gamma'-\gamma\beta'\big)^2}.\end{aligned}$$

where

$$\begin{aligned}
\bar{\chi_3} &= -\beta'' + \beta\big(2\gamma'^2\big) + \gamma\big(\beta' + \beta\gamma\big), \\
\bar{\nu_3} &= \beta\big(-3\beta' + \gamma\beta\big) + \big(-3\gamma'^2\big) - \gamma'', \\
\bar{\mu_3} &= -\gamma\big(\beta^2 + \gamma^2 + 3\gamma'\big) + \gamma''.
\end{aligned}$$

Proof. From equations (1) and (9) the curvature according to α_{CW}-Smarandache curve κ_{CW} is

$$\kappa_{CW} = \frac{\sqrt{2}\sqrt{\chi_3^2 + \nu_3^2 + \mu_3^2}}{\big(\beta^2 + 2\gamma^2\big)^2}. \tag{11}$$

If we take second and third differential of equation (5) are, respectivelly

$$\begin{aligned}
\alpha''_{CW} &= \frac{\big(\beta^2 - \gamma\beta\big)N + \big(\beta' - \gamma'\big)C + \big(\beta\gamma - \gamma^2\big)W}{\sqrt{2}}, \\
\alpha'''_{CW} &= \frac{\bar{\chi_3}N + \bar{\nu_3}C + \bar{\mu_3}W}{\sqrt{2}}.
\end{aligned} \tag{12}$$

From equations (1) the torsion according to α_{CW} curve τ_{CW} is

$$\tau_{CW} = \sqrt{2}\frac{\big(2\gamma^3 + \gamma\beta^2\big)\bar{\chi_3} + \big(-\beta'\gamma + \beta\gamma'\big)\bar{\nu_3} + \big(2\gamma^2\beta + \beta^3 + \beta\gamma' - \gamma\beta'\big)\bar{\mu_3}}{\big(2\gamma^3 + \gamma\beta^2\big)^2 - \big(\gamma\beta' - \beta\gamma'\big)^2 + \big(2\beta\gamma^2 + \beta^3 + \gamma' - \gamma\beta'\big)^2}.$$

∎

Theorem 4 *Let $\alpha(s)$ be a regular curve with unit speed in E^3 and $\{N, C, W\}$ be Alternative frame. The Alternative frame of α_{CW}-Smarandache curve is $\{N_{CW}, C_{CW}, W_{CW}\}$.*

$$\begin{aligned}
N_{CW} &= \frac{\chi_3}{\sqrt{\chi_3^2 + \nu_3^2 + \mu_3^2}}N + \frac{\nu_3}{\sqrt{\chi_3^2 + \nu_3^2 + \mu_3^2}}C + \frac{\mu_3}{\sqrt{\chi_3^2 + \nu_3^2 + \mu_3^2}}W, \\
C_{CW} &= \frac{\mu_3(\chi_3 m - \mu_3 k) - \nu_3(\chi_3 l - \nu_3 k)}{(\chi_3^2 + \nu_3^2 + \mu_3^2)^{\frac{5}{2}}}N \\
&+ \frac{\mu_3(\nu_3 m - \mu_3 l) - \chi_3(\chi_3 l - \nu_3 k)}{(\chi_3^2 + \nu_3^2 + \mu_3^2)^{\frac{5}{2}}}C \\
&+ \frac{\nu_3(\nu_3 m - \mu_3 l) - \chi_3(\chi_3 m - \mu_3 k)}{(\chi_3^2 + \nu_3^2 + \mu_3^2)^{\frac{5}{2}}}W, \\
W_{CW} &= \frac{\nu_3 m - \mu_3 l}{(\chi_3^2 + \nu_3^2 + \mu_3^2)^2}N + \frac{\chi_3 m - \mu_3 k}{(\chi_3^2 + \nu_3^2 + \mu_3^2)^2}C + \frac{\chi_3 l - \nu_3 k}{(\chi_3^2 + \nu_3^2 + \mu_3^2)^2}W.
\end{aligned}$$

where

$$\begin{aligned}
k &= (\chi_3' - \nu_3\beta)(\chi_3^2 + \nu_3^2 + \mu_3^2) - \chi_3(\chi_3 + \nu_3 + \mu_3)', \\
l &= (\chi_3\beta + \nu_3' - \gamma\mu_3)(\chi_3^2 + \nu_3^2 + \mu_3^2) - \nu_3(\chi_3 + \nu_3 + \mu_3)', \\
m &= (\gamma\nu_3 + \mu_3')(\chi_3^2 + \nu_3^2 + \mu_3^2) - \mu_3(\chi_3 + \nu_3 + \mu_3)'.
\end{aligned}$$

Proof. From equation (10) principal normal vektor of α_{CW} is

$$N_{CW} = \frac{\chi_3}{\sqrt{\chi_3^2 + \nu_3^2 + \mu_3^2}}N + \frac{\nu_3}{\sqrt{\chi_3^2 + \nu_3^2 + \mu_3^2}}C + \frac{\mu_3}{\sqrt{\chi_3^2 + \nu_3^2 + \mu_3^2}}W. \tag{13}$$

If we take derivative of equation (13), we can write

$$N'_{CW} \quad = \quad \frac{kN + lC + Mw}{(\chi_3^2 + \nu_3^2 + \mu_3^2)^{\frac{3}{2}}} \tag{14}$$

where the coefficients are

$$\begin{aligned} k &= (\chi_3' - \nu_3\beta)(\chi_3^2 + \nu_3^2 + \mu_3^2) - \chi_3(\chi_3 + \nu_3 + \mu_3)', \\ l &= (\chi_3\beta + \nu_3' - \gamma\mu_3)(\chi_3^2 + \nu_3^2 + \mu_3^2) - \nu_3(\chi_3 + \nu_3 + \mu_3)', \\ m &= (\gamma\nu_3 + \mu_3')(\chi_3^2 + \nu_3^2 + \mu_3^2) - \mu_3(\chi_3 + \nu_3 + \mu_3)'. \end{aligned}$$

From equations (13) and (14) darboux vector of α_{CW} is

$$\begin{aligned} W_{CW} &= \frac{\nu_3 m - \mu_3 l}{(\chi_3^2 + \nu_3^2 + \mu_3^2)^2} N + \frac{\chi_3 m - \mu_3 k}{(\chi_3^2 + \nu_3^2 + \mu_3^2)^2} C \\ &+ \frac{\chi_3 l - \nu_3 k}{(\chi_3^2 + \nu_3^2 + \mu_3^2)^2} W. \end{aligned} \tag{15}$$

From equations (13) and (15) unit vector C_{CW} is

$$\begin{aligned} C_{CW} &= \frac{\mu_3(\chi_3 m - \mu_3 k) - \nu_3(\chi_3 l - \nu_3 k)}{(\chi_3^2 + \nu_3^2 + \mu_3^2)^{\frac{5}{2}}} N \\ &+ \frac{\mu_3(\nu_3 m - \mu_3 l) - \chi_3(\chi_3 l - \nu_3 k)}{(\chi_3^2 + \nu_3^2 + \mu_3^2)^{\frac{5}{2}}} C \\ &+ \frac{\nu_3(\nu_3 m - \mu_3 l) - \chi_3(\chi_3 m - \mu_3 k)}{(\chi_3^2 + \nu_3^2 + \mu_3^2)^{\frac{5}{2}}} W. \end{aligned} \tag{16}$$

■

(a) Frenet frame

(b) Alternative frame

Figure 2: NCW-Smarandache curves

Definition 5 *Let $\alpha(s)$ be a regular curve with unit speed in E^3 and $\{N, C, W\}$ is Alternative frame. Then, α_{NCW}-Smarandache curve can be identified as*

$$\alpha_{NCW} = \frac{1}{\sqrt{3}}(N + C + W). \tag{17}$$

Theorem 6 *Let $\alpha(s)$ be a regular curve with unit speed in E^3 and $\{N, C, W\}$ be Alternative* *frame. The Frenet frame of α_{NCW}-Smarandache curve is $\{T_{NCW}, N_{NCW}, B_{NCW}\}$.*

$$
\begin{aligned}
T_{NCW} &= \frac{-\beta N + \big(\beta-\gamma\big)C + \gamma W}{\sqrt{2\big(\beta^2+2\gamma^2-\beta\gamma\big)}},\\
N_{NCW} &= \frac{\chi_4 N + \nu_4 C + \mu_4 W}{\sqrt{\chi_4^2+\nu_4^2+\mu_4^2}},\\
B_{NCW} &= \frac{\big(\beta-\gamma\big)\mu_4 - \gamma\nu_4}{\sqrt{2\big(\chi_4^2+\nu_4^2+\mu_4^2\big)\big(\beta^2+\gamma^2-\gamma\beta\big)}}N\\
&+ \frac{\big(\gamma\chi_4+\beta\mu_4\big)}{\sqrt{2\big(\chi_4^2+\nu_4^2+\mu_4^2\big)\big(\beta^2+\gamma^2-\gamma\beta\big)}}C\\
&- \frac{\beta\nu_4+\big(\beta-\gamma\big)\chi_4}{\sqrt{2\big(\chi_4^2+\nu_4^2+\mu_4^2\big)\big(\beta^2+\gamma^2-\gamma\beta\big)}}.
\end{aligned}
$$

Where

$$
\begin{aligned}
\chi_4 &= \beta^2\big(-2\beta^2-4\gamma^2+4\beta\gamma-\beta^2\gamma'\big)+\gamma\beta\big(\beta'+2\gamma+2\gamma'\big)-2\beta'^2,\\
\nu_4 &= \beta^2\big(-2\beta^2-4\gamma^2+2\beta\gamma-\gamma'\big)+\gamma^2\big(-2\gamma^2+2\beta\gamma+\beta'\big)+\beta\gamma\big(\beta'\gamma'\big),\\
\mu_4 &= 2\beta^2\big(\beta\gamma-2\gamma^2+\gamma'\big)+\gamma^2\big(4\gamma\beta-3\gamma^2+\beta'\big)-\gamma\beta\big(2\beta'+\gamma'\big).
\end{aligned}
$$

Proof. If we take derivate of the equation (17)

$$
T_{NCW}\frac{ds_{NCW}}{ds} = \frac{-\beta N + \big(\beta-\gamma\big)C + \gamma W}{\sqrt{3}}. \tag{18}
$$

where

$$
\frac{ds_{NCW}}{ds} = \frac{\sqrt{6(\beta^2+\gamma^2-\beta\gamma)}}{3}. \tag{19}
$$

From equations (18) and (19) tangent vector of α_{NCW}-Smarandache curve is

$$
T_{NCW} = \frac{-\beta N + \big(\beta-\gamma\big)C + \gamma W}{\sqrt{2\big(\beta^2+2\gamma^2-\beta\gamma\big)}}. \tag{20}
$$

If we take the derivate of the equation (20), we can write

$$
T'_{NCW} = \frac{\sqrt{3}\big(\chi_4 N + \nu_4 C + \mu_4 W\big)}{4\big(\beta^2+2\gamma^2-\beta\gamma\big)^2}. \tag{21}
$$

If we take norm of equation (21), we can write

$$
\|T'_{NCW}\| = \frac{\sqrt{3\big(\chi_4+\nu_4+\mu_4\big)}}{4\big(\beta^2+2\gamma^2-\beta\gamma\big)^2}. \tag{22}
$$

From equations (1), (21) and (22) principal normal vector of α_{NCW} is

$$
N_{NCW} = \frac{\chi_4 N + \nu_4 C + \mu_4 W}{\sqrt{\chi_4^2+\nu_4^2+\mu_4^2}}. \tag{23}
$$

Binormal vector of α_{NCW} is

$$\begin{aligned} B_{NCW} &= \frac{(\beta-\gamma)\mu_4 - \gamma\nu_4}{\sqrt{2(\chi_4^2+\nu_4^2+\mu_4^2)(\beta^2+\gamma^2-\gamma\beta)}} N \\ &+ \frac{(\gamma\chi_4+\beta\mu_4)}{\sqrt{2(\chi_4^2+\nu_4^2+\mu_4^2)(\beta^2+\gamma^2-\gamma\beta)}} C \\ &- \frac{\beta\nu_4+(\beta-\gamma)\chi_4}{\sqrt{2(\chi_4^2+\nu_4^2+\mu_4^2)(\beta^2+\gamma^2-\gamma\beta)}} W \end{aligned} \tag{24}$$

■

Theorem 7 *Let $\alpha(s)$ be a regular curve with unit speed in E^3 and $\{N, C, W\}$ be Alternative frame. The curvature and torsion according to α_{NCW}-Smarandache curve of Alternative Frame are, respectivelly,*

$$\kappa_{NCW} = \frac{\sqrt{3(\chi_4+\nu_4+\mu_4)}}{4(\beta^2+2\gamma^2-\beta\gamma)^2},$$

$$\tau_{NCW} = \frac{\begin{array}{c}\sqrt{3}(\bar{\chi_4}(2\beta^2\gamma-2\beta\gamma^2+\beta\gamma'-\beta'\gamma)+\bar{\nu_4}(\beta\gamma'-\beta'\gamma)\\ +\bar{\mu_4}(2\beta^3-2\beta^2\gamma+2\beta\gamma^2+\beta\gamma'-\beta'\gamma))\end{array}}{\begin{array}{c}(2\beta\gamma(\beta-\gamma)+\beta\gamma'-\gamma\beta'^3)^2+(\beta\gamma'-\gamma\beta')^2\\ +(2\beta^3+\beta\gamma'-\gamma\beta'^2-2\beta^2\gamma)^2\end{array}},$$

where

$$\begin{aligned} \bar{\chi_4} &= \beta'\gamma-\beta''-3\gamma\gamma'+2\beta\gamma'^3+\beta\gamma^2, \\ \bar{\nu_4} &= \gamma^3-\beta^3-3(\beta\beta'+\gamma\gamma')-(-\beta''+\gamma'')+\beta\gamma(\beta-\gamma), \\ \bar{\mu_4} &= \gamma''^2\gamma-3\gamma\gamma'^3+2\beta\gamma'+\beta\gamma'. \end{aligned}$$

Proof. From equations (1) and (22) the curvature according to α_{NCW}-Smarandache curve κ_{NCW} is

$$\kappa_{NCW} = \frac{\sqrt{3(\chi_4+\nu_4+\mu_4)}}{4(\beta^2+2\gamma^2-\beta\gamma)^2}. \tag{25}$$

If we take second and third differential of equation (17) are, respectivelly

$$\begin{aligned} \alpha''_{NCW} &= \frac{(-\beta^2-\beta'+\gamma\beta)}{\sqrt{3}} N - \frac{(\beta'^2+\gamma'^2)}{\sqrt{3}} C \\ &+ \frac{(\beta\gamma-\gamma^2+\gamma')}{\sqrt{3}} W, \\ \alpha'''_{NCW} &= \frac{\bar{\chi_4}N+\bar{\nu_4}C+\bar{\mu_4}W}{\sqrt{3}}. \end{aligned} \tag{26}$$

From equations (1) and (26) the torsion according to α_{NCW}-Smarandache curve τ_{NCW} is

$$\tau_{NCW} = \frac{\begin{array}{c}\sqrt{3}(\bar{\chi_4}(2\beta^2\gamma-2\beta\gamma^2+\beta\gamma'-\beta'\gamma)+\bar{\nu_4}(\beta\gamma'-\beta'\gamma)\\ +\bar{\mu_4}(2\beta^3-2\beta^2\gamma+2\beta\gamma^2+\beta\gamma'-\beta'\gamma))\end{array}}{\begin{array}{c}(2\beta\gamma(\beta-\gamma)+\beta\gamma'-\gamma\beta'^3)^2+(\beta\gamma'-\gamma\beta')^2\\ +(2\beta^3+\beta\gamma'-\gamma\beta'^2-2\beta^2\gamma)^2\end{array}},$$

where the coefficients are

$$\begin{aligned}\bar{\chi_4} &= \beta'\gamma - \beta'' - 3\gamma\gamma' + 2\beta\gamma'^3 + \beta\gamma^2,\\ \bar{\nu_4} &= \gamma^3 - \beta^3 - 3\big(\beta\beta' + \gamma\gamma'\big) - \big(-\beta'' + \gamma''\big) + \beta\gamma\big(\beta - \gamma\big),\\ \bar{\mu_4} &= \gamma''^2\gamma - 3\gamma\gamma'^3 + 2\beta\gamma' + \beta\gamma'.\end{aligned}$$

■

Theorem 8 *Let $\alpha(s)$ be a regular curve with unit speed in E^3 and $\{N, C, W\}$ be Alternative frame. The Alternative frame of α_{NCW}-Smarandache curve is $\{N_{NCW}, C_{NCW}, W_{NCW}\}$.*

$$\begin{aligned}N_{NCW} &= \frac{\chi_4 N + \nu_4 C + \mu_4 W}{\sqrt{\chi_4^2 + \nu_4^2 + \mu_4^2}},\\ C_{NCW} &= \frac{\mu_4(\chi_4 f - \mu_4 d) - \nu_4(\chi_4 e - \nu_4 d)}{(\chi_4^2 + \nu_4^2 + \mu_4^2)^{\frac{5}{2}}} N + \frac{\mu_4(\nu_4 f - \mu_4 e) - \chi_4(\chi_4 e - \nu_4 d)}{(\chi_4^2 + \nu_4^2 + \mu_4^2)^{\frac{5}{2}}} C\\ &+ \frac{\nu_4(\nu_4 f - \mu_4 e) - \chi_4(\chi_4 f - \mu_4 d)}{(\chi_4^2 + \nu_4^2 + \mu_4^2)^{\frac{5}{2}}} W,\\ W_{NCW} &= \frac{\nu_4 f - \mu_4 e}{(\chi_4^2 + \nu_4^2 + \mu_4^2)^2} N + \frac{\chi_4 f - \mu_4 d}{(\chi_4^2 + \nu_4^2 + \mu_4^2)^2} C + \frac{\chi_4 e - \nu_4 d}{(\chi_4^2 + \nu_4^2 + \mu_4^2)^2} W.\end{aligned}$$

Where

$$\begin{aligned}d &= (\chi_4' - \nu_4\beta)(\chi_4^2 + \nu_4^2 + \mu_4^2) - \chi_4(\chi_4 + \nu_4 + \mu_4)',\\ e &= (\chi_4\beta + \nu_4' - \gamma\mu_4)(\chi_4^2 + \nu_4^2 + \mu_4^2) - \nu_4(\chi_4 + \nu_4 + \mu_4)',\\ f &= (\gamma\nu_4 + \mu_4')(\chi_4^2 + \nu_4^2 + \mu_4^2) - \mu_4(\chi_4 + \nu_4 + \mu_4)'.\end{aligned}$$

Proof. From equation (23) principal normal vektor of α_{NCW} is

$$N_{NCW} = \frac{\chi_4 N + \nu_4 C + \mu_4 W}{\sqrt{\chi_4^2 + \nu_4^2 + \mu_4^2}}. \tag{27}$$

If we take derivative of equation (27), we can write

$$\begin{aligned}N'_{NCW} &= \frac{d}{(\chi_3^2 + \nu_3^2 + \mu_3^2)^{\frac{3}{2}}} N + \frac{e}{(\chi_3^2 + \nu_3^2 + \mu_3^2)^{\frac{3}{2}}} C\\ &+ \frac{f}{(\chi_3^2 + \nu_3^2 + \mu_3^2)^{\frac{3}{2}}} W\end{aligned} \tag{28}$$

where the coefficients are

$$\begin{aligned}d &= (\chi_4' - \nu_4\beta)(\chi_4^2 + \nu_4^2 + \mu_4^2) - \chi_4(\chi_4 + \nu_4 + \mu_4)',\\ e &= (\chi_4\beta + \nu_4' - \gamma\mu_4)(\chi_4^2 + \nu_4^2 + \mu_4^2) - \nu_4(\chi_4 + \nu_4 + \mu_4)',\\ f &= (\gamma\nu_4 + \mu_4')(\chi_4^2 + \nu_4^2 + \mu_4^2) - \mu_4(\chi_4 + \nu_4 + \mu_4)'.\end{aligned}$$

From equations (27) and (28) unit darboux vector of α_{NCW} is

$$\begin{aligned}W_{NCW} &= \frac{\nu_4 f - \mu_4 e}{(\chi_4^2 + \nu_4^2 + \mu_4^2)^2} N + \frac{\chi_4 f - \mu_4 d}{(\chi_4^2 + \nu_4^2 + \mu_4^2)^2} C\\ &+ \frac{\chi_4 e - \nu_4 d}{(\chi_4^2 + \nu_4^2 + \mu_4^2)^2} W.\end{aligned} \tag{29}$$

From equations (27) and (29) unit vector C_{NCW} is

$$\begin{aligned} C_{NCW} &= \frac{\mu_4(\chi_4 f - \mu_4 d) - \nu_4(\chi_4 e - \nu_4 d)}{(\chi_4^2 + \nu_4^2 + \mu_4^2)^{\frac{5}{2}}} N + \frac{\mu_4(\nu_4 f - \mu_4 e) - \chi_4(\chi_4 e - \nu_4 d)}{(\chi_4^2 + \nu_4^2 + \mu_4^2)^{\frac{5}{2}}} C \\ &+ \frac{\nu_4(\nu_4 f - \mu_4 e) - \chi_4(\chi_4 f - \mu_4 d)}{(\chi_4^2 + \nu_4^2 + \mu_4^2)^{\frac{5}{2}}} W. \end{aligned}$$

■

Example 9 *Let* $\delta(s) = (\frac{9}{208}\sin 16s - \frac{1}{117}\sin 36s, -\frac{9}{208}\cos 16s + \frac{1}{117}\cos 36s, \frac{6}{65}\sin 10s)$ *be a curve withthe alternative frame of* $\{N, C, W\}$ *given as*

$$\begin{aligned} N(s) &= \Big(\frac{12}{13}\cos 26s, -\frac{12}{13}\sin 26s, \frac{5}{13}\Big), \\ C(s) &= \Big(-\sin 26s, \cos 26s, 0\Big), \\ W(s) &= \Big(\frac{5}{13}\cos 26s, -\frac{5}{13}\sin 26s, \frac{12}{13}\Big). \end{aligned}$$

CW-Smarandache curves and NCW-Smarandache curves of $\delta(s)$ *given as below (see Figure 3)*

$$\begin{aligned} \beta_1 &= \frac{1}{\sqrt{2}}(C+W) = \frac{1}{\sqrt{2}}\Big(\frac{5}{13}\cos 26s - \sin 26s, \frac{5}{13}\sin 26s + \cos 26s, \frac{12}{13}\Big), \\ \beta_2 &= \frac{1}{\sqrt{3}}(N+C+W) = \frac{1}{\sqrt{3}}\Big(\frac{17}{13}\cos 26s - \sin 26s, \frac{17}{13}\sin 26s + \cos 26s, \frac{7}{13}\Big). \end{aligned}$$

(a) β_1-Smarandache curve, $s \in (-3, \frac{3\pi}{2})$

(b) β_2-Smarandache curve, $s \in (-\pi, \frac{4\pi}{3})$

Figure 3: Smarandache curves

Example 10 *Let* $\alpha(s) = \frac{1}{\sqrt{2}}(\cos s, \sin s, s)$ *be a curve withthe alternative frame of* $\{N, C, W\}$ *given as*

$$N(s) = (\cos s, \sin s, 0), \quad C(s) = (-\sin s, \cos s, 0), \quad W(s) = (0, 0, 1).$$

CW-Smarandache curves and NCW-Smarandache curves of $\delta(s)$ *given as below (see Figure 4)*

$$\begin{aligned} \beta_3 &= \frac{1}{\sqrt{2}}(C+W) = \frac{1}{\sqrt{2}}(\sin s, -\cos s, 1), \\ \beta_4 &= \frac{1}{\sqrt{3}}(N+C+W) = \frac{1}{\sqrt{3}}(\cos s + \sin s, \sin s - \cos s, 1). \end{aligned}$$

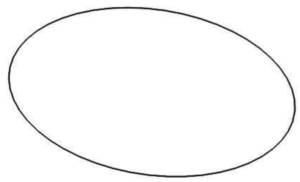

(a) β_1 Smarandache curve, $s \in (0, 2\pi)$

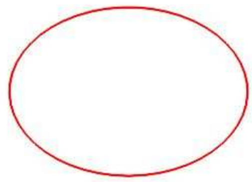

(b) β_1 Smarandache curve, $s \in (0, 2\pi)$

Figure 4: Smarandache curves

References

[1] Ali, A.T., *Special Smarandache Curves in the Euclidean Space*, International J.Math. Combin., **2**(2010), 30–36.

[2] Fenchel, W., *On The Differential Geometry of Closed Space Curves*, Bulletin of American Mathematical Society, **57**(1951), 44–54.

[3] Kaya, O., Önder, M., *SNew Partner Curves in the Euclidean 3-Space*, International Journal of Geometry, **6**(2017), 41–50.

[4] Şenyurt, S., Sivas, S., *Smarandache Eğrilerine Ait Bir Uygulama*, Journal of Science and Technology, **3(1)**(2013), 46–60.

[5] Turgut, B., Gök, İ., Yaylı, Y., *A New Approroach on Curves of Constant Precession*, International Journal of Geometry, **25**(2001), 433–444.

[6] Turgut, M., Yilmaz, S., *Smarandache Curves in Minkowski Space-Time*, International J.Math. Combin., **3**(2008), 51–55.

W-Smarandache Curves According to the Sabban Frame of the Spherical Indicatrix Curve

Süleyman ŞENYURT*
Ordu University,
Department of Mathematics,
ORDU, TURKEY

Kübra AKDAĞ
Ordu University,
Department of Mathematics,
ORDU, TURKEY

Abstract

In this study, we first formed a Sabban frame of spherical indicatrix curve of W-alternative vector defined by a differentiable curve. Then the geodesic curvature of this vector is calculated according to this frame. Finally we defined Smarandache curves generated by the Sabban frame and give some characterizations of them.

Keywords: Sabban frame, Smarandache curve, alternative frame, spherical indicatrix curve.

1 Introduction

In differential geometry, special curves have an important role. One of these curves is a Smarandache curve. Smarandache curves are first defined by M. Turgut and S. Yılmaz in 2008 [7]. Special Smarandache curves also have been studied by some authors [1, 2, 3]. Let $\alpha = \alpha(s)$ be a regular unit speed curve in E^3. The Frenet frame and alternative frame of this curve are $\{T, N, B\}$ and $\{N, C, W\}$,respectively. Here, N is normal vector, W is unit Darboux vector and $C = W \wedge N$ [5]. In this paper, we created the Smarandache curves according to the alternative frame of the unit speed curve. We then introduced alternative frame and its properties. Finally we calculated geodesic curvature of these curves according to alternative frame.

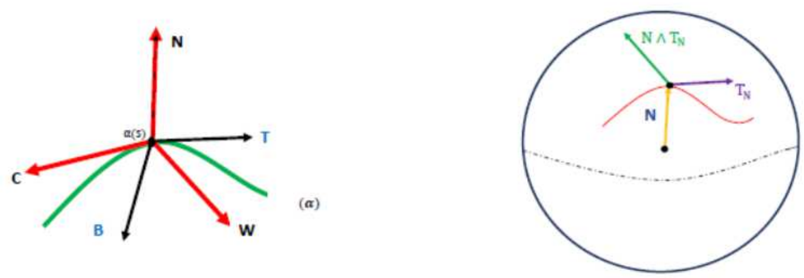

Figure 1a) Alternative Frame **Figure 1b) Sabban Frame**

*Corresponding author. *E-mail address:* senyurtsuleyman@hotmail.com

2 Preliminaries

Let $\alpha = \alpha(s)$ be a regular curve with unit speed. Then the Frenet apparatus of the curve (α) [4]

$$\begin{aligned} T(s) &= \alpha'(s), \quad N(s) = \frac{\alpha''(s)}{\| \alpha''(s) \|}, \quad B(s) = T(s) \wedge N(s), \\ \kappa(s) &= \| T'(s) \|, \qquad \tau(s) = \frac{det(\alpha'(s) \wedge \alpha''(s), \alpha'''(s))}{\| \alpha' \wedge \alpha''^2}, \\ T' &= \kappa N, \quad N' = -\kappa T + \tau B, \quad B' = -\tau N. \end{aligned} \tag{1}$$

In Euclidean 3-space any regular curve $\alpha(s)$ depending on the Frenet vectors moves around the axis of Darboux vector. The vector defining a unit vector field is given as [5]

$$W = \frac{\tau}{\sqrt{\kappa^2+\tau^2}}T + \frac{\kappa}{\sqrt{\kappa^2+\tau^2}}B, \quad C = -\frac{\kappa}{\sqrt{\kappa^2+\tau^2}}T + \frac{\tau}{\sqrt{\kappa^2+\tau^2}}B. \tag{2}$$

So build another orthonormal moving frame along the curve $\alpha(s)$. This frame defined as alternative frame and is represented by $\{N, C, W\}$. The derivative formulae of the alternative frame is given by [5]

$$\begin{aligned} N' &= \beta C, \quad C' = -\beta N + \gamma W, \quad W' = -\gamma C, \\ \beta &= \sqrt{\kappa^2+\tau^2}, \quad \gamma = \frac{\kappa^2}{\kappa^2+\tau^2}\left(\frac{\tau}{\kappa}\right)' \end{aligned} \tag{3}$$

The relationship between Frenet frame and alternative frame is

$$\begin{aligned} C &= -\bar{\kappa}T + \bar{\tau}B, \quad W = \bar{\tau}T + \bar{\kappa}B, \quad T = -\bar{\kappa}C + \bar{\tau}W, \quad B = \bar{\tau}C + \bar{\kappa}W, \\ \bar{\kappa} &= \frac{\kappa}{\beta}, \bar{\tau} = \frac{\tau}{\beta}. \end{aligned} \tag{4}$$

Principal normal vector N is common both frames. Let $\gamma : I \to S^2$ be a unit speed spherical curve and s arc-length parameter of γ. Let us denote $t(s) = \gamma^{'}(s)$ and $d(s) = \gamma(s) \wedge t(s)$. This frame is called the Sabban frame of γ on S^2. Then we have the following spherical Frenet formulae of γ

$$\gamma'(s) = t(s), \quad t'(s) = -\gamma(s) + \kappa_g(s)d(s), \quad d'(s) = -\kappa_g(s)t(s), \tag{5}$$

where $\kappa_g(s)$ is the geodesic curvature of γ on S^2 [6],

$$\kappa_g(s) = \langle t'(s), d(s) \rangle \tag{6}$$

3 Smarandache Curves of Alternative Frame According to the Sabban Frame

In this section ,we investigated special Smarandache curves according to Sabban frame on S^2. Let $W = W(s) = \alpha_W(s)$ be a unit speed regular spherical curve on S^2, $\{W, T_W, (W \wedge T_W)\}$ and $\{W_{\alpha_W}, T_{W_{\alpha_W}}, (W \wedge T_W)_{\alpha_W}\}$ be the Sabban frame of this curve, respectively. Let $\alpha_W(s) = W(s)$ and if we take the derivative of the equation, then T_W vector is

$$\frac{d\alpha_W}{ds^*}.\frac{ds^*}{ds} = -\gamma C, \quad T_W = -C, \quad \frac{ds^*}{ds} = \gamma. \tag{7}$$

Considering the $W(s)$ and T_W vectors we can write,

$$W \wedge T_W = N. \tag{8}$$

Accordingly, the $\{W, T_W, (W \wedge T_W)\} \equiv \{N, C, W\}$ Sabban frame is obtained from the W vector. If we take the derivative of the equation (7), then T_W' vector is

$$\begin{aligned} T_W' \frac{ds^*}{ds} &= -C' \\ &= \beta N - \gamma W, \\ T_W' &= \frac{\beta}{\gamma} N - W. \end{aligned} \tag{9}$$

From the equation (6), (8) and (9), the geodesic curvature of $\alpha_W(s) = W(s)$ is

$$\kappa_g^W(s) = \frac{\beta}{\gamma}. \tag{10}$$

Then from the equation (5) we have the following spherical Frenet formulae of $\alpha_W(s)$,

$$\begin{aligned} W' &= -C, \\ T_W' &= -W + \frac{\beta}{\gamma} N, \\ (W \wedge T_W)' &= \frac{\beta}{\gamma} C. \end{aligned} \tag{11}$$

Definition 1 *Let (W) be a spherical curve of $\alpha(s)$, W and T_W be Sabban vectors of (W). Then WT_W-Smarandache curve can be identified as*

$$\alpha_{WT_W} = \frac{1}{\sqrt{2}}(W + T_W) \tag{12}$$

or substituting the equation (7) into equation (12), we have

$$\alpha_{WT_W} = \frac{1}{\sqrt{2}}(W - C)$$

Theorem 2 *The geodesic curvature according to WT_W-Smarandache curve is*

$$\kappa_g^{WT_W} = \frac{1}{\left(2 + \left(\kappa_g^W\right)^2\right)^{\frac{5}{2}}} \left(\lambda_1 \kappa_g^W - \lambda_2 \kappa_g^W - 2\lambda_3\right). \tag{13}$$

where

$$\begin{aligned} \lambda_1 &= \kappa_g^W \left(\kappa_g^W\right)' - \left(\kappa_g^W\right)^2 - 2, \\ \lambda_2 &= -\left(\kappa_g^W\right)^4 + 3\left(\kappa_g^W\right)^2 + \kappa_g^W \left(\kappa_g^W\right)' + 2, \\ \lambda_3 &= \left(\kappa_g^W\right)^3 + 2\kappa_g^W + 2\left(\kappa_g^W\right)'. \end{aligned} \tag{14}$$

Proof. If we take the derivative of the equation (12) then T_{WT_W} vector is

$$\begin{aligned} T_{WT_W}\frac{ds^*}{ds} &= \frac{1}{\sqrt{2}}\big(-W+T_W+\kappa_g^W(W\wedge T_W)\big), \qquad (15)\\ T_{WT_W} &= \frac{\big(-W+T_W+\kappa_g^W(W\wedge T_W)\big)}{\sqrt{2+\left(\kappa_g^W\right)^2}}, \quad \frac{ds^*}{ds}=\frac{\sqrt{2+\left(\kappa_g^W\right)^2}}{\sqrt{2}}. \end{aligned}$$

Considering the equations (12) and (15), we have

$$\alpha_{WT_W}\wedge T_{WT_W} = \frac{\big(\kappa_g^W W-\kappa_g^W T_W+2(W\wedge T_W)\big)}{\sqrt{4+2\left(\kappa_g^W\right)^2}}. \qquad (16)$$

If we take the derivative of the equation (15), then T'_{WT_W} vector is

$$\begin{aligned} T'_{WT_W}\frac{ds^*}{ds} &= -\frac{\kappa_g^W\left(\kappa_g^W\right)'\big(-W+T_W+\kappa_g^W(W\wedge T_W)\big)}{\big(2+(\kappa_g^W)^2\big)^{\frac{3}{2}}}\\ &\quad+\frac{-W-(1+(\kappa_g^W)^2)T_W+(\kappa_g^W+(\kappa_g^W)'(W\wedge T_W))}{\sqrt{2+(\kappa_g^W)^2}},\\ T'_{WT_W} &= \frac{\sqrt{2}\big(\kappa_g^W(\kappa_g^W)'-(\kappa_g^W)^2-2\big)}{\big(2+(\kappa_g^W)^2\big)^2}W\\ &- \frac{\sqrt{2}\big((\kappa_g^W)^4+3(\kappa_g^W)^2+\kappa_g^W(\kappa_g^W)'+2\big)}{\big(2+(\kappa_g^W)^2\big)^2}T_W\\ &+ \frac{\sqrt{2}\big((\kappa_g^W)^3+2\kappa_g^W+2(\kappa_g^W)'\big)}{\big(2+(\kappa_g^W)^2\big)^2}(W\wedge T_W). \end{aligned} \qquad (17)$$

Using the equations (6),(14),(16) and (17) we can write $\kappa_g^{WT_W}$ geodesic curvature

$$\kappa_g^{WT_W}=\frac{1}{\left(2+\left(\kappa_g^W\right)^2\right)^{\frac{5}{2}}}\big(\lambda_1\kappa_g^W+\lambda_2\kappa_g^W-2\lambda_3\big).$$

■

Corollary 3 *The geodesic curvature of the WT_W-Smarandache curve according to the alternative frame is*

$$\kappa_g^{WT_W}=\frac{\gamma^4}{\big(2\gamma^2+\beta^2\big)^{\frac{5}{2}}}\Big((\lambda_1+\lambda_2)\beta-2\gamma\lambda_3\Big) \qquad (18)$$

where

$$\begin{aligned} \lambda_1 &= \frac{\beta}{\gamma}\left(\frac{\beta}{\gamma}\right)'-\frac{\beta^2+2\gamma^2}{\gamma^2}, \quad \lambda_2=\frac{\beta}{\gamma}\left(\frac{\beta}{\gamma}\right)'+\frac{\beta^4+3\beta^2\gamma^2+2\gamma^4}{\gamma^4}, \qquad (19)\\ \lambda_3 &= 2\left(\frac{\beta}{\gamma}\right)'+\frac{\beta^3+2\beta\gamma^2}{\gamma^3}. \end{aligned}$$

Definition 4 *Let (W) be a spherical curve of $\alpha(s)$, W and $W \wedge T_W$ be Sabban vectors of (W). Then $W(W \wedge T_W)$-Smarandache curve can be identified as*

$$\alpha_{W(W\wedge T_W)} = \frac{1}{\sqrt{2}}\big(W + W \wedge T_W\big). \tag{20}$$

or substituting the equation (8) into equation (20) we have

$$\alpha_{W(W\wedge T_W)} = \frac{1}{\sqrt{2}}(W + N).$$

Theorem 5 *The geodesic curvature according to $W(W \wedge T_W)$-Smarandache curve is*

$$\kappa_g^{W(W\wedge T_W)} = \frac{\gamma+\beta}{\gamma-\beta} \tag{21}$$

Proof. If we take the derivative of the equation (20), then $T_{W(W\wedge T_W)}$ vector is

$$\begin{aligned} T_{W(W\wedge T_W)}\frac{ds^*}{ds} &= \frac{1}{\sqrt{2}}\big(T_W - \kappa_g^W T_W\big), \\ T_{W(W\wedge T_W)} &= T_W, \quad \frac{ds^*}{ds} = \frac{1-\kappa_g^W}{\sqrt{2}}. \end{aligned} \tag{22}$$

Considering the equations (20) and (22), we have

$$\alpha_{W(W\wedge T_W)} \wedge T_{W(W\wedge T_W)} = \frac{1}{\sqrt{2}}\big(-W + (W \wedge T_W)\big). \tag{23}$$

If we take the derivative of the equation (22), then $T'_{W(W\wedge T_W)}$ vector is

$$T'_{W(W\wedge T_W)} = \frac{\sqrt{2}}{1-\kappa_g^W}\big(-W + \kappa_g^W(W \wedge T_W)\big). \tag{24}$$

Using the equations (6), (10), (23) and (24), we can write $\kappa_g^{W(W\wedge T_W)}$ geodesic curvature

$$\kappa_g^{W(W\wedge T_W)} = \frac{\gamma+\beta}{\gamma-\beta}.$$

■

Definition 6 *Let (W) be a spherical curve of $\alpha(s)$, T_W and $W \wedge T_W$ be Sabban vectors of (W). Then $T_W(W \wedge T_W)$-Smarandache curve can be identified as*

$$\alpha_{T_W(W\wedge T_W)} = \frac{T_W + (W \wedge T_W)}{\sqrt{2}} \tag{25}$$

or substituting the equation (7), (8) into equation (25) we have

$$\alpha_{T_W(W\wedge T_W)} = \frac{1}{\sqrt{2}}(-C + N).$$

Theorem 7 *The geodesic curvature according to $T_W(W \wedge T_W)$-Smarandache curve is*

$$\kappa_g^{T_W(W\wedge T_W)} = \frac{1}{\Big(1 + 2\big(\kappa_g^W\big)^2\Big)^{\frac{5}{2}}}\big(2\lambda_1\kappa_g^W - \lambda_2 + \lambda_3\big), \tag{26}$$

where

$$\begin{aligned}\lambda_1 &= 2\kappa_g^W\left(\kappa_g^W\right)' + \kappa_g^W + 2\left(\kappa_g^W\right)^3,\\ \lambda_2 &= -1 - \left(\kappa_g^W\right)' - 3\left(\kappa_g^W\right)^2 - 2\left(\kappa_g^W\right)^4,\\ \lambda_3 &= \left(\kappa_g^W\right)' - \left(\kappa_g^W\right)^2 + 2\left(\kappa_g^W\right)^4.\end{aligned} \tag{27}$$

Proof. If we take the derivative of the equation (25) then $T_{T_W(W\wedge T_W)}$ vector is

$$T_{T_W(W\wedge T_W)}\frac{ds^*}{ds} = \frac{1}{\sqrt{2}}\big(-W - \kappa_g^W T_W + \kappa_g^W (W\wedge T_W)\big), \tag{28}$$

$$T_{T_W(W\wedge T_W)} = \frac{-W - \kappa_g^W T_W + \kappa_g^W (W\wedge T_W)}{\sqrt{1+2\left(\kappa_g^W\right)^2}}, \quad \frac{ds^*}{ds} = \frac{\sqrt{1+2\left(\kappa_g^W\right)^2}}{\sqrt{2}}.$$

Considering the equations (25) and (28), we have

$$\alpha_{T_W(W\wedge T_W)} \wedge T_{T_W(W\wedge T_W)} = \frac{\left(2\kappa_g^W W - T_W + (W\wedge T_W)\right)}{\sqrt{2+4\left(\kappa_g^W\right)^2}}. \tag{29}$$

If we take the derivative of the equation (28), then $T'_{T_W(W\wedge T_W)}$ vector is

$$\begin{aligned}T'_{T_W(W\wedge T_W)}\frac{ds^*}{ds} &= -\frac{2\kappa_g^W\left(\kappa_g^W\right)'}{\sqrt{1+2\left(\kappa_g^W\right)^2}}\Big(-W - \kappa_g^W T_W + \kappa_g^W (W\wedge T_W)\Big)\\ &+ \frac{1}{\sqrt{1+2\left(\kappa_g^W\right)^2}}\Big(\kappa_g^W - \big(1 + \left(\kappa_g^W\right)' + \left(\kappa_g^W\right)^2\big)\Big)T_W\\ &\quad + \big(\left(\kappa_g^W\right)' - \left(\kappa_g^W\right)^2\big)\big(W\wedge T_W\big),\end{aligned}$$

$$\begin{aligned}T'_{T_W(W\wedge T_W)} &= \frac{\sqrt{2}\Big(2\kappa_g^W\left(\kappa_g^W\right)' + \kappa_g^W + 2\left(\kappa_g^W\right)^3\Big)}{\Big(1+2\left(\kappa_g^W\right)^2\Big)^2}W\\ &\quad - \frac{\sqrt{2}\Big(1 + \left(\kappa_g^W\right)' + 3\left(\kappa_g^W\right)^2 + 2\left(\kappa_g^W\right)^4\Big)}{\Big(1+2\left(\kappa_g^W\right)^2\Big)^2}T_W\\ &\quad + \frac{\sqrt{2}\Big(\left(\kappa_g^W\right)' - \left(\kappa_g^W\right)^2 + 2\left(\kappa_g^W\right)^4\Big)}{\Big(1+2\left(\kappa_g^W\right)^2\Big)^2}\big(W\wedge T_W\big).\end{aligned} \tag{30}$$

Using the equations (6),(27),(29) and (30),we can write $\kappa_g^{T_W(W\wedge T_W)}$ geodesic curvature

$$\kappa_g^{T_W(W\wedge T_W)} = \frac{1}{\Big(1+2\left(\kappa_g^W\right)^2\Big)^{\frac{5}{2}}}\big(2\lambda_1\kappa_g^W - \lambda_2 + \lambda_3\big).$$

■

Corollary 8 *The geodesic curvature of the $T_W(W \wedge T_W)$-Smarandache curve according to the alternative frame is*

$$\kappa_g^{T_W(W\wedge T_W)} = \frac{\gamma^4}{\left(\gamma^2+2\beta^2\right)^{\frac{5}{2}}}\Big(2\lambda_1\beta+(\lambda_3-\lambda_2)\gamma\Big) \tag{31}$$

where

$$\begin{aligned}\lambda_1 &= 2\frac{\beta}{\gamma}\left(\frac{\beta}{\gamma}\right)'+\frac{\beta}{\gamma}+2\frac{\beta^3}{\gamma^3},\\ \lambda_2 &= -1-\left(\frac{\beta}{\gamma}\right)'-3\frac{\beta^2}{\gamma^2}-2\frac{\beta^4}{\gamma^4},\\ \lambda_3 &= \left(\frac{\beta}{\gamma}\right)'-\frac{\beta^2}{\gamma^2}+2\frac{\beta^4}{\gamma^4}.\end{aligned} \tag{32}$$

Definition 9 *Let (W) be a spherical curve of $\alpha(s)$,W, T_W and $W\wedge T_W$ be Sabban vectors of (W). Then $WT_W(W\wedge T_W)$-Smarandache curve can be identified as*

$$\alpha_{WT_W(W\wedge T_W)} = \frac{1}{\sqrt{3}}\big(W+T_W+(W\wedge T_W)\big) \tag{33}$$

or substituting the equation (7),(8)*into equation* (33) *we have*

$$\alpha_{WT_W(W\wedge T_W)} = \frac{1}{\sqrt{3}}(W-C+N).$$

Theorem 10 *The geodesic curvature according to $WT_W(W\wedge T_W)$-Smarandache curve is*

$$\kappa_g^{T_W(W\wedge T_W)} = \frac{\big(-1+2\kappa_g^W\big)\lambda_1-\big(1+\kappa_g^W\big)\lambda_2+\big(2-\kappa_g^W\big)\lambda_3}{4\sqrt{2}\Big(1-\big(\kappa_g^W\big)+\big(\kappa_g^W\big)^2\Big)^{\frac{5}{2}}} \tag{34}$$

where

$$\begin{aligned}\lambda_1 &= -(\kappa_g^W)'(1-2\kappa_g^W)+2\big(-1+2\kappa_g^W-2(\kappa_g^W)^2+(\kappa_g^W)^3\big),\\ \lambda_2 &= (\kappa_g^W)'\big(1-3\kappa_g^W+2(\kappa_g^W)^2\big)-2\big(1-\kappa_g^W+(\kappa_g^W)^2\big)\big(1+(\kappa_g^W)'+(\kappa_g^W)^2\big),\\ \lambda_3 &= (\kappa_g^W)'\big(\kappa_g^W-2(\kappa_g^W)^2\big)+2\big(1-\kappa_g^W+(\kappa_g^W)^2\big)\big(\kappa_g^W-(\kappa_g^W)^2+(\kappa_g^W)'\big).\end{aligned} \tag{35}$$

Proof. If we take the derivative of the equation (33) then $T_{WT_W(W\wedge T_W)}$ vector is

$$\begin{aligned}T_{WT_W(W\wedge T_W)}\frac{ds^*}{ds} &= \frac{1}{\sqrt{3}}\Big(-W+\big(1-\kappa_g^W\big)T_W+\kappa_g^W(W\wedge T_W)\Big),\\ T_{WT_W(W\wedge T_W)} &= \frac{-W+\big(1-\kappa_g^W\big)T_W+\kappa_g^W(W\wedge T_W)}{\sqrt{2}\sqrt{1-\kappa_g^W+\big(\kappa_g^W\big)^2}},\\ \frac{ds^*}{ds} &= \frac{\sqrt{2}}{\sqrt{3}}\sqrt{1-\kappa_g^W+\big(\kappa_g^W\big)^2}.\end{aligned} \tag{36}$$

Considering the equations (33) and (36), we have

$$\begin{aligned}\alpha_{WT_W(W\wedge T_W)}\wedge T_{WT_W(W\wedge T_W)} &= \frac{\big(2\kappa_g^W-1\big)W-\big(1+\kappa_g^W\big)T_W}{\sqrt{6}\sqrt{1-\kappa_g^W+\big(\kappa_g^W\big)^2}}\\ &+ \frac{\big(2-\kappa_g^W\big)(W\wedge T_W)}{\sqrt{6}\sqrt{1-\kappa_g^W+\big(\kappa_g^W\big)^2}}\end{aligned} \tag{37}$$

If we take the derivative of the equation (36), then $T'_{WT_W(W\wedge T_W)}$ vector is

$$\begin{aligned} T'_{WT_W(W\wedge T_W)} &= \frac{\sqrt{3}}{4}\frac{(\kappa_g^W)'\big(1-2(\kappa_g^W)\big)\big(-W+(1-\kappa_g^W)T_W+\kappa_g^W(W\wedge T_W)\big)}{\big(1-\kappa_g^W+(\kappa_g^W)^2\big)^2} \\ &+ \frac{\sqrt{3}}{2}\frac{(\kappa_g^W-1)W-\big(1+(\kappa_g^W)'+(\kappa_g^W)^2\big)T_W}{1-\kappa_g^W+(\kappa_g^W)^2} \\ &+ \frac{\sqrt{3}}{2}\frac{\big(\kappa_g^W-(\kappa_g^W)^2+(\kappa_g^W)'\big)(W\wedge T_W)}{1-\kappa_g^W+(\kappa_g^W)^2} \end{aligned} \tag{38}$$

$$\begin{aligned} T'_{WT_W(W\wedge T_W)} &= \frac{\sqrt{3}}{4}.\frac{-(\kappa_g^W)'\big(1-2\kappa_g^W\big)+2\big(-1+2\kappa_g^W-2(\kappa_g^W)^2+(\kappa_g^W)^3\big)}{\big(1-\kappa_g^W+(\kappa_g^W)^2\big)^2}W \\ &+ \frac{\sqrt{3}}{4}\frac{(\kappa_g^W)'\big(1-3\kappa_g^W+2(\kappa_g^W)^2\big)}{\big(1-\kappa_g^W+(\kappa_g^W)^2\big)^2}T_W \\ &- \frac{\sqrt{3}}{2}\frac{\big(1-\kappa_g^W+(\kappa_g^W)^2\big)\big(1+(\kappa_g^W)'+(\kappa_g^W)^2\big)}{\big(1-\kappa_g^W+(\kappa_g^W)^2\big)^2}T_W \\ &+ \frac{\sqrt{3}}{4}\frac{(\kappa_g^W)'\big(\kappa_g^W-2(\kappa_g^W)^2\big)}{\big(1-\kappa_g^W+(\kappa_g^W)^2\big)^2}(W\wedge T_W) \\ &- \frac{\sqrt{3}}{2}\frac{2\big(1-\kappa_g^W+(\kappa_g^W)^2\big)\big(\kappa_g^W-(\kappa_g^W)^2+(\kappa_g^W)'\big)}{\big(1-\kappa_g^W+(\kappa_g^W)^2\big)^2}(W\wedge T_W) \end{aligned}$$

Using the equation (6), (35), (37) and (38), we can write $\kappa_g^{WT_W(W\wedge T_W)}$ geodesic curvature

$$\kappa_g^{T_W(W\wedge T_W)} = \frac{\big((-1+2\kappa_g^W)\lambda_1-(1+\kappa_g^W)\lambda_2+(2-\kappa_g^W)\lambda_3\big)}{4\sqrt{2}\big(1-(\kappa_g^W)+(\kappa_g^W)^2\big)^{\frac{5}{2}}}.$$

■

Corollary 11 *The geodesic curvature of the $WT_W(W\wedge T_W)$-Smarandache curve according to the alternative frame is*

$$\kappa_g^{WT_W(W\wedge T_W)} = \frac{\gamma^4\big((2\beta-\gamma)\lambda_1-(\beta+\gamma)\lambda_2+(2\gamma-\beta)\lambda_3\big)}{4\sqrt{2}\left(\gamma^2+\beta^2-\beta\gamma\right)^{\frac{5}{2}}} \tag{39}$$

where

$$\begin{aligned} \lambda_1 &= -\frac{\gamma-2\beta}{\gamma}\left(\frac{\beta}{\gamma}\right)'+\frac{-2\gamma^3+4\beta\gamma^2-4\beta^2\gamma+2\beta^3}{\gamma^3}, \\ \lambda_2 &= \frac{\gamma^2-3\beta\gamma+2\beta^2}{\gamma^2}\left(\frac{\beta}{\gamma}\right)'-2\left(\frac{\gamma^2-\beta\gamma+\beta^2}{\gamma^2}\right)\left((\frac{\beta}{\gamma})'+\frac{\gamma^2+\beta^2}{\gamma^2}\right), \\ \lambda_3 &= \frac{\beta\gamma-2\beta^2}{\gamma}\left(\frac{\beta}{\gamma}\right)'+2\left(\frac{\gamma^2-\beta\gamma+\beta^2}{\gamma^2}\right)\left(\frac{\beta\gamma-\beta^2}{\gamma^2}+(\frac{\beta}{\gamma})'\right). \end{aligned} \tag{40}$$

Example 12 *Let;*

$$\gamma(s) = \big(\frac{9}{208}\sin 16s-\frac{1}{117}\sin 36s, -\frac{9}{208}\cos 16s+\frac{1}{117}\cos 36s, \frac{6}{65}\sin 10s\big)$$

be a curve with the alternative frame of $\{N, C, W\}$ *given as*

$$\begin{aligned} N(s) &= (\frac{12}{13}\cos 26s, -\frac{12}{13}\sin 26s, \frac{5}{13}), \quad C(s) = (-\sin 26s, \cos 26s, 0), \\ W(s) &= (\frac{5}{13}\cos 26s, -\frac{5}{13}\sin 26s, \frac{12}{13}). \end{aligned}$$

Then we have the following spherical indicatrix curve (W) *and* $\beta_1, \beta_2, \beta_3$ *and* β_4 *Smarandache curves according to Sabban frame on* S^2*. These curves are (see Figure 2, 3)*

$$\begin{aligned} \beta_1 &= \frac{1}{\sqrt{2}}(\frac{5}{13}\cos 26s - 10\sin 26s, \frac{5}{13}\sin 26s + 10\cos 26s, \frac{12}{13}), \\ \beta_2 &= \frac{1}{\sqrt{2}}(-\frac{115}{13}\cos 26s, -\frac{115}{13}\sin 26s, \frac{62}{13}), \\ \beta_3 &= \frac{1}{\sqrt{2}}(-\frac{120}{13}\cos 26s - 10\sin 26s, 10\cos 26s - \frac{120}{13}\sin 26s, \frac{50}{13}), \\ \beta_4 &= \frac{1}{\sqrt{3}}(-\frac{115}{13}\cos 26s - 10\sin 26s, 10\cos 26s - \frac{115}{13}\sin 26s, \frac{62}{13}). \end{aligned}$$

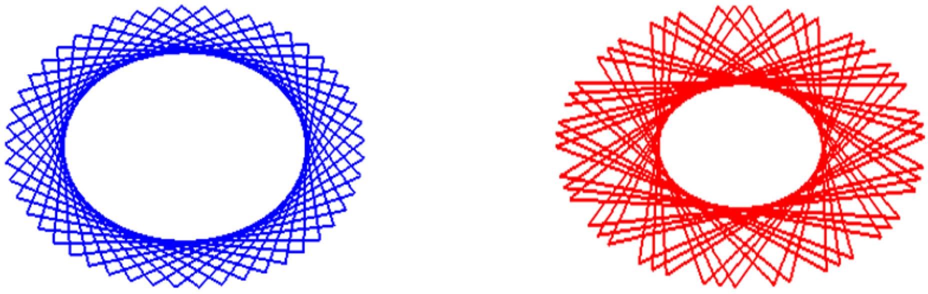

(i) (ii)

Figure 1: (i)β_1-Smarandache curve,$s \in (\frac{-\pi}{2}, \frac{\pi}{2})$,(ii)$\beta_2$-Smarandache curve,$s \in (0, \frac{4\pi}{3})$

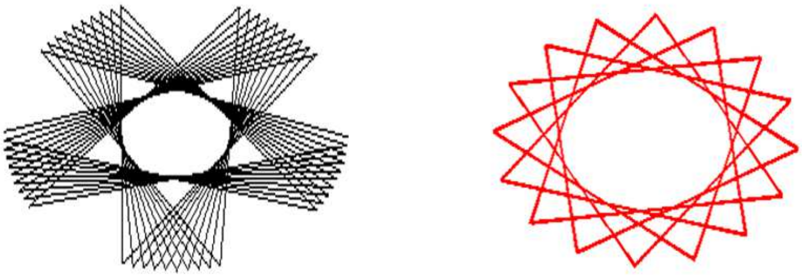

(i)

(ii)

Figure 2: (i)β_3-Smarandache curve,$s \in (-\pi, \frac{\pi}{2})$,(ii)$\beta_4$-Smarandache curve,$s \in (-5, \pi)$

References

[1] Ali A. T., Special Smarandache Curves in the Euclidean Space, *International Journal of Mathematical Combinatorics*, **2010**, 2(30-36).

[2] Bektaş O., Yüce S., Special Smarandache Curves According to Darboux Frame in Euclidean 3- Space, *Romanian Journal of Mathematics and Computer Science*, **2013**, 3(1), 48-59.

[3] Çetin M., Tuncer Y. and Karacan M. K., Smarandache Curves According to Bishop Frame in Euclidean 3- Space, *Gen. Math. Notes*, **2014**, 20(2), 50-66.

[4] Do Carmo M.P., Differential geometry of curves and surfaces, *Prentice-Hall Englewood Cliffs*, NJ MATH Google Scholar, **1976**.

[5] Kaya O., Önder M., New Partner Curves in theEuclidean 3-Space E^3, *International Journal of Geometry*, **2017**, 6(2), 41- 50.

[6] Taşköprö K., Tosun M., Smarandache curves on S^2 , *Boletim da Sociedade Paranaense de Matematica 3 Srie.*, **2014**, 32 (1), 51-59.

[7] Turgut M., Yılmaz S., Smarandache Curves in Minkowski Space-time, *International J. Math. Combin.*, **2008**, 3(51-55).

On generalization of midpoint and trapezoid type inequalities involving fractional integrals

Mehmet Zeki SARIKAYA*
Düzce University,
Department of Mathematics,
Düzce-TURKEY

Sümeyye SÖNMEZOĞLU
Düzce University,
Department of Mathematics,
Düzce-TURKEY

Abstract

In this paper, we first prove a lemma for twice differentiable functions . Then we establish some inequalities for mapping whose second derivatives in absolute value are convex via Riemann-Liouville fractional integrals. These results generalize the midpoint and trapezoid inequalities involving Riemann-Liouville fractional integrals given in earlier studies.

Keywords: Hermite-Hadamard inequality, midpoint inequality, fractional integral operators, convex function.

1 Introduction

The inequalities discovered by C. Hermite and J. Hadamard for convex functions are considerable significant in the literature (see, e.g.,[6], [9], [20, p.137]). These inequalities state that if $f : I \to \mathbb{R}$ is a convex function on the interval I of real numbers and $a, b \in I$ with $a < b$, then

$$f\left(\frac{a+b}{2}\right) \leq \frac{1}{b-a}\int_a^b f(x)dx \leq \frac{f(a)+f(b)}{2}. \tag{1}$$

Both inequalities hold in the reversed direction if f is concave. We note that Hadamard's inequality may be regarded as a refinement of the concept of convexity and it follows easily from Jensen's inequality. Hadamard's inequality for convex functions has received renewed attention in recent years and a remarkable variety of refinements and generalizations have been found (see, for example, [1]-[4], [7], [12], [14], [18], [19], [22], [24], [28], [29], [32], [33]) and the references cited therein.

In the following we will give some necessary definitions and mathematical preliminaries of fractional calculus theory which are used further in this paper. More details, one can consult ([8], [13], [15], [21])

Definition 1 *Let $f \in L_1[a, b]$. The Riemann-Liouville integrals $J_{a+}^{\alpha}f$ and $J_{b-}^{\alpha}f$ of order $\alpha > 0$ with $a \geq 0$ are defined by*

$$J_{a+}^{\alpha}f(x) = \frac{1}{\Gamma(\alpha)}\int_a^x (x-t)^{\alpha-1} f(t)dt, \quad x > a$$

and

$$J_{b-}^{\alpha}f(x) = \frac{1}{\Gamma(\alpha)}\int_x^b (t-x)^{\alpha-1} f(t)dt, \quad x < b$$

respectively. Here, $\Gamma(\alpha)$ is the Gamma function and $J_{a+}^{0}f(x) = J_{b-}^{0}f(x) = f(x)$.

*Corresponding author. *E-mail address:* sarikayamz@gmail.com

It is remarkable that Sarikaya et al.[26] first give the following interesting integral inequalities of Hermite-Hadamard type involving Riemann-Liouville fractional integrals.

Theorem 2 *Let $f:[a,b]\to\mathbb{R}$ be a positive function with $0\le a<b$ and $f\in L_1[a,b]$. If f is a convex function on $[a,b]$, then the following inequalities for fractional integrals hold:*

$$f\left(\frac{a+b}{2}\right)\le\frac{\Gamma(\alpha+1)}{2(b-a)^{\alpha}}\left[J_{a+}^{\alpha}f(b)+J_{b-}^{\alpha}f(a)\right]\le\frac{f(a)+f(b)}{2} \tag{2}$$

with $\alpha>0$.

Sarıkaya and Yıldırım also give the following Hermite-Hadamard type inequality for the Riemann-Lioville fractional integrals in [23].

Theorem 3 *Let $f:[a,b]\to\mathbb{R}$ be a positive function with $a<b$ and $f\in L_1[a,b]$. If f is a convex function on $[a,b]$, then the following inequalities for fractional integrals hold:*

$$f\left(\frac{a+b}{2}\right)\le\frac{2^{\alpha-1}\Gamma(\alpha+1)}{(b-a)^{\alpha}}\left[J_{\left(\frac{a+b}{2}\right)^{+}}^{\alpha}f(b)+J_{\left(\frac{a+b}{2}\right)^{-}}^{\alpha}f(a)\right]\le\frac{f(a)+f(b)}{2}. \tag{3}$$

For the more information fractional calculus and related inequalities please refer to ([5], [10], [11], [16], [17], [25], [27], [30], [31], [34])

2 Generalized Midpoint and Trapezoid Type Inequalities

In this section, we will first present a lemma for twice differentiable functions . Then we establish some inequalities which generalize the midpoint and trapezoid inequalities involving Riemann-Liouville fractional integrals obtained in previous works.

Lemma 4 *Let $I\subset\mathbb{R}$ be an open interval, $a,b\in I$ with $a<b$. If $f:I\to\mathbb{R}$ is a twice differentiable mapping such that f'' is integrable and $0\le\lambda\le1$, $\alpha\ge1$, then we have*

$$\begin{aligned}&\left[\left(\lambda-\frac{\alpha+1}{2^{\alpha}}\right)f\left(\frac{a+b}{2}\right)-\lambda\left(\frac{f(a)+f(b)}{2}\right)+\frac{\Gamma(\alpha+2)}{2(b-a)^{\alpha}}\left(J_{\left(\frac{a+b}{2}\right)^{+}}^{\alpha}f(b)+J_{\left(\frac{a+b}{2}\right)^{-}}^{\alpha}f(a)\right)\right] \\ =\ &\frac{(b-a)^{2}}{2}\int_{0}^{1}k(t)f''(ta+(1-t)b)\,dt\end{aligned} \tag{4}$$

where

$$k(t)=\begin{cases}t\left(t^{\alpha}-\lambda\right) & 0\le t\le\frac{1}{2}\\[2ex] (1-t)\left((1-t)^{\alpha}-\lambda\right) & \frac{1}{2}\le t\le1.\end{cases}$$

Proof. It suffices to note that

$$\begin{aligned}I &= \int_{0}^{1}k(t)f''(ta+(1-t)b)\,dt \qquad (5)\\ &= \int_{0}^{\frac{1}{2}}t\left(t^{\alpha}-\lambda\right)f''(ta+(1-t)b)\,dt+\int_{\frac{1}{2}}^{1}(1-t)\left((1-t)^{\alpha}-\lambda\right)f''(ta+(1-t)b)\,dt\\ &= I_{1}+I_{2}.\end{aligned}$$

Integrating by parts twice, we can state:

$$
\begin{aligned}
I_1 &= \int_0^{\frac{1}{2}} t\left(t^\alpha-\lambda\right) f''(ta+(1-t)b)\,dt \qquad (6)\\
&= t\left(t^\alpha-\lambda\right)\left.\frac{f'(ta+(1-t)b)}{a-b}\right|_0^{\frac{1}{2}} - \int_0^{\frac{1}{2}} \frac{f'(ta+(1-t)b)}{a-b}\left((\alpha+1)t^\alpha-\lambda\right)dt\\
&= \frac{-1}{2(b-a)}\left(\frac{1}{2^\alpha}-\lambda\right) f'\left(\frac{a+b}{2}\right) - \frac{1}{(b-a)^2}\left(\frac{\alpha+1}{2^\alpha}-\lambda\right) f\left(\frac{a+b}{2}\right)\\
&\quad -\frac{\lambda}{(b-a)^2} f(b) + \frac{\alpha(\alpha+1)}{(b-a)^2}\frac{1}{(b-a)^\alpha}\Gamma(\alpha) J^\alpha_{\left(\frac{a+b}{2}\right)^+} f(b)
\end{aligned}
$$

and similarly, we get

$$
\begin{aligned}
I_2 &= \int_{\frac{1}{2}}^1 (1-t)\left((1-t)^\alpha-\lambda\right) f''(ta+(1-t)b)\,dt \qquad (7)\\
&= (1-t)\left((1-t)^\alpha-\lambda\right)\left.\frac{f'(ta+(1-t)b)}{a-b}\right|_{\frac{1}{2}}^1\\
&\quad + \int_{\frac{1}{2}}^1 \frac{f'(ta+(1-t)b)}{a-b}\left((\alpha+1)(1-t)^\alpha-\lambda\right)\\
&= \frac{1}{2(b-a)}\left(\frac{1}{2^\alpha}-\lambda\right) f'\left(\frac{a+b}{2}\right) - \lambda\frac{f(a)}{(b-a)^2}\\
&\quad -\frac{1}{(b-a)^2}\left(\frac{\alpha+1}{2^\alpha}-\lambda\right) f\left(\frac{a+b}{2}\right) + \frac{\alpha(\alpha+1)}{(b-a)^{\alpha+2}}\Gamma(\alpha) J^\alpha_{\left(\frac{a+b}{2}\right)^-} f(a).
\end{aligned}
$$

Using (6) and (7) in (5), it follows that

$$
\begin{aligned}
I &= I_1+I_2 = \frac{-2}{(b-a)^2}\left(\frac{\alpha+1}{2^\alpha}-\lambda\right) f\left(\frac{a+b}{2}\right) - \frac{2\lambda}{(b-a)^2}\left(\frac{f(a)+f(b)}{2}\right)\\
&\quad +\frac{\alpha(\alpha+1)}{(b-a)^{\alpha+2}}\Gamma(\alpha)\left(J^\alpha_{\left(\frac{a+b}{2}\right)^+} f(b) + J^\alpha_{\left(\frac{a+b}{2}\right)^-} f(a)\right)\\
&= \frac{2}{(b-a)^2}\left[\left(\lambda-\frac{\alpha+1}{2^\alpha}\right) f\left(\frac{a+b}{2}\right) - \lambda\left(\frac{f(a)+f(b)}{2}\right)\right]\\
&\quad +\frac{\Gamma(\alpha+2)}{(b-a)^{\alpha+2}}\left(J^\alpha_{\left(\frac{a+b}{2}\right)^+} f(b) + J^\alpha_{\left(\frac{a+b}{2}\right)^-} f(a)\right).
\end{aligned}
$$

Then by multipling the above equality with $\frac{(b-a)^2}{2}$, this completes the proof. ∎

Theorem 5 *Let $I \subset \mathbb{R}$ be an open intervial, $a, b \in I$ with $a < b$ and $f : I \to \mathbb{R}$ be a twice differentiable mapping such that f'' is integrable and $0 \le \lambda \le 1$, $\alpha \ge 1$. If $|f''|$ is a convex on $[a, b]$, then the following inequalities hold:*

$$\left|\left(\lambda-\frac{\alpha+1}{2^{\alpha}}\right)f\left(\frac{a+b}{2}\right)-\lambda\left(\frac{f(a)+f(b)}{2}\right)+\frac{\Gamma(\alpha+2)}{2(b-a)^{\alpha}}\left(J^{\alpha}_{\left(\frac{a+b}{2}\right)^{+}}f(b)+J^{\alpha}_{\left(\frac{a+b}{2}\right)^{-}}f(a)\right)\right| \quad (8)$$

$$\leq \frac{(b-a)^2}{2}\begin{cases}\left(\dfrac{1}{2^{\alpha+2}(\alpha+2)}-\dfrac{\lambda}{8}+\dfrac{\alpha\lambda^{1+\frac{2}{\alpha}}}{\alpha+2}\right)\left[|f''(a)|+|f''(b)|\right], & 0\leq\lambda\leq\frac{1}{2}\\ \left(\dfrac{\lambda}{8}-\dfrac{1}{2^{\alpha+2}(\alpha+2)}\right)\left[|f''(a)|+|f''(b)|\right], & \frac{1}{2}\leq\lambda\leq 1.\end{cases}$$

Proof. From Lemma 4 and by defination of $k(t)$, we get

$$\left|\left(\lambda-\frac{\alpha+1}{2^{\alpha}}\right)f\left(\frac{a+b}{2}\right)-\lambda\left(\frac{f(a)+f(b)}{2}\right)+\frac{\Gamma(\alpha+2)}{2(b-a)^{\alpha}}\left(J^{\alpha}_{\left(\frac{a+b}{2}\right)^{+}}f(b)+J^{\alpha}_{\left(\frac{a+b}{2}\right)^{-}}f(a)\right)\right| \quad (9)$$

$$\begin{aligned}
&\leq \frac{(b-a)^2}{2}\int_0^1 |k(t)|\left|f''(ta+(1-t)b)\right|dt\\
&= \frac{(b-a)^2}{2}\left\{\int_0^{\frac{1}{2}}|t(t^{\alpha}-\lambda)|\left|f''(ta+(1-t)b)\right|dt\right.\\
&\quad\left.+\int_{\frac{1}{2}}^{1}|(1-t)((1-t)^{\alpha}-\lambda)|\left|f''(ta+(1-t)b)\right|dt\right\}\\
&= \frac{(b-a)^2}{2}\{J_1+J_2\}.
\end{aligned}$$

We assume that $0\leq\lambda\leq\frac{1}{2}$, then using the convexity of $|f''|$,we get

$$\begin{aligned}
J_1 &\leq \int_0^{\frac{1}{2}}|t(t^{\alpha}-\lambda)|\left[t\left|f''(a)\right|+(1-t)\left|f''(b)\right|\right]dt \qquad (10)\\
&= \int_0^{\lambda^{\frac{1}{\alpha}}} t(\lambda-t^{\alpha})\left[t\left|f''(a)\right|+(1-t)\left|f''(b)\right|\right]dt\\
&\quad+\int_{\lambda^{\frac{1}{\alpha}}}^{\frac{1}{2}} t(t^{\alpha}-\lambda)\left[t\left|f''(a)\right|+(1-t)\left|f''(b)\right|\right]dt\\
&= \left|f''(a)\right|\left[\frac{2\alpha\lambda^{1+\frac{3}{\alpha}}}{3(\alpha+3)}+\frac{1}{2^{\alpha+3}(\alpha+3)}-\frac{\lambda}{24}\right]\\
&\quad+\left|f''(b)\right|\left[\frac{\alpha\lambda^{1+\frac{2}{\alpha}}}{\alpha+2}-\frac{2\alpha\lambda^{1+\frac{3}{\alpha}}}{3(\alpha+3)}+\frac{\alpha+4}{2^{\alpha+3}(\alpha+2)(\alpha+3)}-\frac{\lambda}{12}\right]
\end{aligned}$$

and similarly, we have

$$\begin{aligned} J_2 &\leq \int_{\frac{1}{2}}^{1-\lambda^{\frac{1}{\alpha}}} (1-t)\left((1-t)^{\alpha}-\lambda\right)\left[t\left|f''(a)\right|+(1-t)\left|f''(b)\right|\right]dt \qquad (11)\\ &\quad+\int_{1-\lambda^{\frac{1}{\alpha}}}^{1} (1-t)\left(\lambda-(1-t)^{\alpha}\right)\left[t\left|f''(a)\right|+(1-t)\left|f''(b)\right|\right]dt \\ &= \left|f''(a)\right|\left[\frac{\alpha\lambda^{1+\frac{2}{\alpha}}}{\alpha+2}-\frac{2\alpha\lambda^{1+\frac{3}{\alpha}}}{3(\alpha+3)}+\frac{\alpha+4}{2^{\alpha+3}(\alpha+2)(\alpha+3)}-\frac{\lambda}{12}\right] \\ &\quad+\left|f''(b)\right|\left[\frac{2\alpha\lambda^{1+\frac{3}{\alpha}}}{3(\alpha+3)}+\frac{1}{2^{\alpha+3}(\alpha+3)}-\frac{\lambda}{24}\right]. \end{aligned}$$

Using (10) and (11) in (9),we see thatthe first inequality of (8) holds. On the other hand, let $\frac{1}{2}\leq\lambda\leq 1$, then, using the convexity of $|f''|$ and by simple computation we have

$$\begin{aligned} J_1' &\leq \int_0^{\frac{1}{2}} \left|t\left(t^{\alpha}-\lambda\right)\right|\left[t\left|f''(a)\right|+(1-t)\left|f''(b)\right|\right]dt \qquad (12)\\ &= \int_0^{\frac{1}{2}} t\left(\lambda-t^{\alpha}\right)\left[t\left|f''(a)\right|+(1-t)\left|f''(b)\right|\right]dt \\ &= \left(\frac{\lambda}{24}-\frac{1}{2^{\alpha+3}(\alpha+3)}\right)\left|f''(a)\right|+\left(\frac{\lambda}{12}-\frac{\alpha+4}{2^{\alpha+3}(\alpha+2)(\alpha+3)}\right)\left|f''(b)\right| \end{aligned}$$

and similarly

$$\begin{aligned} J_2' &\leq \int_{\frac{1}{2}}^{1} \left|(1-t)\left((1-t)^{\alpha}-\lambda\right)\right|\left|f''(ta+(1-t)b)\right|dt \qquad (13)\\ &= \int_{\frac{1}{2}}^{1} (1-t)\left(\lambda-(1-t)^{\alpha}\right)\left[t\left|f''(a)\right|+(1-t)\left|f''(b)\right|\right]dt \\ &= \left(\frac{\lambda}{12}-\frac{\alpha+4}{2^{\alpha+3}(\alpha+2)(\alpha+3)}\right)\left|f''(a)\right|+\left(\frac{\lambda}{24}-\frac{1}{2^{\alpha+3}(\alpha+3)}\right)\left|f''(b)\right|. \end{aligned}$$

Thus if we (12) and (13) in (9), we obtain the second inequality of (8). This completes the proof. ■

Corollary 6 *Under the assumptions of Theorem 5 with $\lambda=0$, then we get the following inequality*

$$\begin{aligned} &\left|\frac{2^{\alpha-1}\Gamma(\alpha+1)}{(b-a)^{\alpha}}\left(J^{\alpha}_{\left(\frac{a+b}{2}\right)^+}f(b)+J^{\alpha}_{\left(\frac{a+b}{2}\right)^-}f(a)\right)-f\left(\frac{a+b}{2}\right)\right| \\ \leq\;& \frac{(b-a)^2}{(\alpha+1)(\alpha+2)}\left[\frac{|f''(a)|+|f''(b)|}{8}\right] \end{aligned}$$

which is proved by Noor and Awan in [16, Theorem 2 (for s=1)].

Remark 7 *If we take $\alpha = 1$ in Corollary 6, then we get the following inequality*

$$\left|\frac{1}{b-a}\int\limits_a^b f(t)dt - f\left(\frac{a+b}{2}\right)\right| \leq \frac{(b-a)^2}{24}\left[\frac{|f''(a)|+|f''(b)|}{2}\right]$$

which is given by Sarikaya et al. in [28].

Corollary 8 *Under the assumptions of Theorem 5 with $\lambda = \frac{\alpha+1}{2^\alpha}$, then we get the following inequality*

$$\begin{aligned}&\left|\frac{f(a)+f(b)}{2} - \frac{2^{\alpha-1}\Gamma(\alpha+1)}{(b-a)^\alpha}\left(J^\alpha_{\left(\frac{a+b}{2}\right)^+} f(b) + J^\alpha_{\left(\frac{a+b}{2}\right)^-} f(a)\right)\right| \\ \leq\ & \frac{(b-a)^2}{8(\alpha+1)(\alpha+2)}\left(\alpha(\alpha+1)^{1+\frac{2}{\alpha}} + 1 - \frac{(\alpha+1)(\alpha+2)}{2}\right)\left[\left|f''(a)\right| + \left|f''(b)\right|\right]\end{aligned}$$

for $\alpha \geq 3$ and

$$\begin{aligned}&\left|\frac{f(a)+f(b)}{2} - \frac{2^{\alpha-1}\Gamma(\alpha+1)}{(b-a)^\alpha}\left(J^\alpha_{\left(\frac{a+b}{2}\right)^+} f(b) + J^\alpha_{\left(\frac{a+b}{2}\right)^-} f(a)\right)\right| \\ \leq\ & \frac{(b-a)^2}{8(\alpha+1)(\alpha+2)}\left(\frac{(\alpha+1)(\alpha+2)}{2} - 1\right)\left[\left|f''(a)\right| + \left|f''(b)\right|\right]\end{aligned}$$

for $1 \leq \alpha \leq 3$.

Remark 9 *If we take $\alpha = 1$ in Corollary 8, then we get the following inequality*

$$\left|\frac{f(a)+f(b)}{2} - \frac{1}{b-a}\int\limits_a^b f(t)dt\right| \leq \frac{(b-a)^2}{12}\left[\frac{|f''(a)|+|f''(b)|}{2}\right]$$

which is given by Sarikaya and Aktan in [24].

Remark 10 *Under the assumptions of Theorem 5 with $\lambda = \frac{1}{3}$ and $\alpha = 1$, then we get the following inequality*

$$\left|\frac{1}{6}\left[f(a) + 4f\left(\frac{a+b}{2}\right) + f(b)\right] - \frac{1}{b-a}\int\limits_a^b f(t)dt\right| \leq \frac{(b-a)^2}{81}\left[\frac{|f''(a)|+|f''(b)|}{2}\right]$$

which is given by Sarikaya and Aktan in [24].

Remark 11 *Under the assumptions of Theorem 5 with $\lambda = \frac{1}{2}$ and $\alpha = 1$, then we get the following inequality*

$$\left|\frac{1}{b-a}\int\limits_a^b f(t)dt - \frac{1}{2}\left[\frac{f(a)+f(b)}{2} + f\left(\frac{a+b}{2}\right)\right]\right| \leq \frac{(b-a)^2}{48}\left[\frac{|f''(a)|+|f''(b)|}{2}\right]$$

which is given by Sarikaya and Aktan in [24].

Theorem 12 *Let $I \subset \mathbb{R}$ be an open intervial, $a, b \in I$ with $a < b$ and $f : I \to \mathbb{R}$ be a twice differentiable mapping such that f'' is integrable and $0 \leq \lambda \leq 1,\ \alpha \geq 1$. If $|f''|^q$ is a convex on $[a,b]$, $q \geq 1$ then the following inequalities hold:*

$$\left|\left[\left(\lambda - \frac{\alpha+1}{2^\alpha}\right) f\left(\frac{a+b}{2}\right) - \lambda\left(\frac{f(a)+f(b)}{2}\right) + \frac{\Gamma(\alpha+2)}{2(b-a)^\alpha}\left(J^\alpha_{\left(\frac{a+b}{2}\right)^+} f(b) + J^\alpha_{\left(\frac{a+b}{2}\right)^-} f(a)\right)\right]\right| \tag{14}$$
$$\leq \frac{(b-a)^2}{2}\left(\frac{\alpha\lambda^{1+\frac{2}{\alpha}}}{\alpha+2} + \frac{1}{2^{\alpha+2}(\alpha+2)} - \frac{\lambda}{8}\right)^{1-\frac{1}{q}}$$
$$\times\left\{\left[C_1\left|f''(a)\right|^q + C_2\left|f''(b)\right|^q\right]^{\frac{1}{q}} + \left[C_2\left|f''(a)\right|^q + C_1\left|f''(b)\right|^q\right]^{\frac{1}{q}}\right\}$$

for $0 \leq \lambda \leq \frac{1}{2}$ and

$$\left|\left(\lambda - \frac{\alpha+1}{2^\alpha}\right) f\left(\frac{a+b}{2}\right) - \lambda\left(\frac{f(a)+f(b)}{2}\right) + \frac{\Gamma(\alpha+2)}{2(b-a)^\alpha}\left(J^\alpha_{\left(\frac{a+b}{2}\right)^+} f(b) + J^\alpha_{\left(\frac{a+b}{2}\right)^-} f(a)\right)\right| \tag{15}$$
$$\leq \frac{(b-a)^2}{2}\left(\frac{\lambda}{8} - \frac{1}{2^{\alpha+2}(\alpha+2)}\right)^{1-\frac{1}{q}}$$
$$\times\left\{\left[C_3\left|f''(a)\right|^q + C_4\left|f''(b)\right|^q\right]^{\frac{1}{q}} + \left[C_4\left|f''(a)\right|^q + C_3\left|f''(b)\right|^q\right]^{\frac{1}{q}}\right\},$$

for $\frac{1}{2} \leq \lambda \leq 1$ where $\frac{1}{p} + \frac{1}{q} = 1$,

$$\begin{aligned}
C_1 &= \left(\frac{2\alpha\lambda^{1+\frac{3}{\alpha}}}{3(\alpha+3)} + \frac{1}{2^{\alpha+3}(\alpha+3)} - \frac{\lambda}{24}\right)\\
C_2 &= \left(\frac{\alpha\lambda^{1+\frac{2}{\alpha}}}{\alpha+2} - \frac{2\alpha\lambda^{1+\frac{3}{\alpha}}}{3(\alpha+3)} + \frac{\alpha+4}{2^{\alpha+3}(\alpha+2)(\alpha+3)} - \frac{\lambda}{12}\right)\\
C_3 &= \left(\frac{\lambda}{24} - \frac{1}{2^{\alpha+3}(\alpha+3)}\right)\\
C_4 &= \left(\frac{\lambda}{12} - \frac{\alpha+4}{2^{\alpha+3}(\alpha+2)(\alpha+3)}\right).
\end{aligned}$$

Proof. Suppose that $q \geq 1$. From Lemma 4 and using the well known power mean inequality, we have

$$\begin{aligned}
&\left|\left(\lambda-\frac{\alpha+1}{2^{\alpha}}\right)f\left(\frac{a+b}{2}\right)-\lambda\left(\frac{f(a)+f(b)}{2}\right)+\frac{\Gamma(\alpha+2)}{2(b-a)^{\alpha}}\left(J^{\alpha}_{\left(\frac{a+b}{2}\right)^{+}}f(b)+J^{\alpha}_{\left(\frac{a+b}{2}\right)^{-}}f(a)\right)\right| \quad (16)\\
\leq\ & \frac{(b-a)^2}{2}\int_0^1 |k(t)|\left|f''(ta+(1-t)b)\right|dt\\
=\ & \frac{(b-a)^2}{2}\left\{\int_0^{\frac{1}{2}}|t(t^{\alpha}-\lambda)|\left|f''(ta+(1-t)b)\right|dt\right.\\
&\left.+\int_{\frac{1}{2}}^{1}|(1-t)((1-t)^{\alpha}-\lambda)|\left|f''(ta+(1-t)b)\right|dt\right\}\\
\leq\ & \frac{(b-a)^2}{2}\left\{\left(\int_0^{\frac{1}{2}}|t(t^{\alpha}-\lambda)|dt\right)^{1-\frac{1}{q}}\left(\int_0^{\frac{1}{2}}|t(t^{\alpha}-\lambda)|\left|f''(ta+(1-t)b)\right|^{q}dt\right)^{\frac{1}{q}}\right.\\
&\left.+\left(\int_{\frac{1}{2}}^{1}|(1-t)((1-t)^{\alpha}-\lambda)|dt\right)^{1-\frac{1}{q}}\left(\int_{\frac{1}{2}}^{1}|(1-t)((1-t)^{\alpha}-\lambda)|\left|f''(ta+(1-t)b)\right|^{q}dt\right)^{\frac{1}{q}}\right\}
\end{aligned}$$

Let $0\leq\lambda\leq\frac{1}{2}$. Then since $|f'|^q$ is convex on $[a,b]$,we know that for $t\in[0,1]$

$$\left|f'(ta+(1-t)b)\right|^{q}\leq t\left|f'(a)\right|^{q}+(1-t)\left|f'(b)\right|^{q}$$

hence, by simple computation

$$\begin{aligned}
&\int_0^{\frac{1}{2}}|t(t^{\alpha}-\lambda)|\left|f''(ta+(1-t)b)\right|^{q}dt \quad (17)\\
\leq\ & \int_0^{\lambda^{\frac{1}{\alpha}}} t(\lambda-t^{\alpha})\left[t\left|f''(a)\right|^{q}+(1-t)\left|f''(b)\right|^{q}\right]dt\\
&+\int_{\lambda^{\frac{1}{\alpha}}}^{\frac{1}{2}} t(t^{\alpha}-\lambda)\left[t\left|f''(a)\right|^{q}+(1-t)\left|f''(b)\right|^{q}\right]dt\\
=\ & \left|f''(a)\right|^{q}\left[\frac{2\alpha\lambda^{1+\frac{3}{\alpha}}}{3(\alpha+3)}+\frac{1}{2^{\alpha+3}(\alpha+3)}-\frac{\lambda}{24}\right]\\
&+\left|f''(b)\right|^{q}\left[\frac{\alpha\lambda^{1+\frac{2}{\alpha}}}{\alpha+2}-\frac{2\alpha\lambda^{1+\frac{3}{\alpha}}}{3(\alpha+3)}+\frac{\alpha+4}{2^{\alpha+3}(\alpha+2)(\alpha+3)}-\frac{\lambda}{12}\right],
\end{aligned}$$

$$\begin{aligned}
&\int_{\frac{1}{2}}^{1}\left|(1-t)\left((1-t)^{\alpha}-\lambda\right)\right|\left|f''\left(ta+(1-t)b\right)\right|^{q}dt \qquad (18)\\
\leq &\int_{\frac{1}{2}}^{1-\lambda^{\frac{1}{\alpha}}}(1-t)\left((1-t)^{\alpha}-\lambda\right)\left[t\left|f''(a)\right|^{q}+(1-t)\left|f''(b)\right|^{q}\right]dt\\
&+\int_{1-\lambda^{\frac{1}{\alpha}}}^{1}(1-t)\left(\lambda-(1-t)^{\alpha}\right)\left[t\left|f''(a)\right|^{q}+(1-t)\left|f''(b)\right|^{q}\right]dt\\
= &\left|f''(a)\right|^{q}\left[\frac{\alpha\lambda^{1+\frac{2}{\alpha}}}{\alpha+2}-\frac{2\alpha\lambda^{1+\frac{3}{\alpha}}}{3(\alpha+3)}+\frac{\alpha+4}{2^{\alpha+3}(\alpha+2)(\alpha+3)}-\frac{\lambda}{12}\right]\\
&+\left|f''(b)\right|^{q}\left[\frac{2\alpha\lambda^{1+\frac{3}{\alpha}}}{3(\alpha+3)}+\frac{1}{2^{\alpha+3}(\alpha+3)}-\frac{\lambda}{24}\right],
\end{aligned}$$

$$\int_{0}^{\frac{1}{2}}\left|t\left(t^{\alpha}-\lambda\right)\right|dt=\int_{0}^{\lambda^{\frac{1}{\alpha}}}t\left(\lambda-t^{\alpha}\right)dt+\int_{\lambda^{\frac{1}{\alpha}}}^{\frac{1}{2}}t\left(t^{\alpha}-\lambda\right)dt=\frac{\alpha\lambda^{1+\frac{2}{\alpha}}}{\alpha+2}+\frac{1}{2^{\alpha+2}(\alpha+2)}-\frac{\lambda}{8} \qquad (19)$$

and

$$\begin{aligned}
&\int_{\frac{1}{2}}^{1}\left|(1-t)\left((1-t)^{\alpha}-\lambda\right)\right|dt \qquad (20)\\
= &\int_{\frac{1}{2}}^{1-\lambda^{\frac{1}{\alpha}}}(1-t)\left((1-t)^{\alpha}-\lambda\right)dt+\int_{1-\lambda^{\frac{1}{\alpha}}}^{1}(1-t)\left(\lambda-(1-t)^{\alpha}\right)dt\\
= &\frac{\alpha\lambda^{1+\frac{2}{\alpha}}}{\alpha+2}+\frac{1}{2^{\alpha+2}(\alpha+2)}-\frac{\lambda}{8}.
\end{aligned}$$

Substituting the equalities (17)-(20) in (16), the we obtain the inequality (14). One can prove the inequality (15) similar to (14). It is omited to readers. ■

Remark 13 *Under the assumptions Theorem 12 with $\alpha = 1$, then Theorem 12 reduces to Theorem 4 in [24].*

Remark 14 *Under the assumptions of Theorem 12 with $\lambda = \frac{1}{3}$ and $\alpha = 1$, then we get the following inequality*

$$\begin{aligned}
&\left|\frac{1}{6}\left[f(a)+4f\left(\frac{a+b}{2}\right)+f(b)\right]-\frac{1}{b-a}\int_{a}^{b}f(t)dt\right|\\
\leq &\frac{(b-a)^{2}}{162}\left[\left(\frac{59\left|f''(a)\right|^{q}+133\left|f''(b)\right|^{q}}{2^{6}\times 3}\right)^{\frac{1}{q}}+\left(\frac{133\left|f''(a)\right|^{q}+59\left|f''(b)\right|^{q}}{2^{6}\times 3}\right)^{\frac{1}{q}}\right]
\end{aligned}$$

which is given by Sarikaya and Aktan in [24].

Corollary 15 *Under the assumptions Theorem 12 with $\lambda = 0$, then we get the following* *inequality*

$$\begin{aligned}
&\left|\frac{2^{\alpha-1}\Gamma(\alpha+1)}{(b-a)^{\alpha}}\left(J^{\alpha}_{\left(\frac{a+b}{2}\right)^{+}}f(b)+J^{\alpha}_{\left(\frac{a+b}{2}\right)^{-}}f(a)\right)-f\left(\frac{a+b}{2}\right)\right| \qquad (21)\\
\leq\ &\frac{(b-a)^{2}2^{\alpha-1}}{\alpha+1}\left\{\left(\frac{1}{2^{\alpha+2}(\alpha+2)}\right)^{1-\frac{1}{q}}\right.\\
&\times\left[\left|f''(a)\right|^{q}\frac{1}{2^{\alpha+3}(\alpha+3)}+\left|f''(b)\right|^{q}\frac{\alpha+4}{2^{\alpha+3}(\alpha+2)(\alpha+3)}\right]^{\frac{1}{q}}\\
&\left.+\left[\left|f''(a)\right|^{q}\frac{\alpha+4}{2^{\alpha+3}(\alpha+2)(\alpha+3)}+\left|f''(b)\right|^{q}\frac{1}{2^{\alpha+3}(\alpha+3)}\right]^{\frac{1}{q}}\right\}.
\end{aligned}$$

References

[1] M. Alomari, M. Darus, U. S. Kirmaci, *Refinements of Hadamard-type inequalities for quasi-convex functions with applications to trapezoidal formula and to special means*, Comput. Math. Appl., 59 (2010), 225–232.

[2] G. A. Anastassiou, *General Fractional Hermite–Hadamard Inequalities Using m-Convexity and (s,m)-Convexity*, Frontiers in Time Scales and Inequalities. 2016. 237-255.

[3] A.G. Azpeitia, *Convex functions and the Hadamard inequality*, Rev. Colombiana Math., 28 (1994), 7-12.

[4] J. de la Cal, J. Carcamob, L. Escauriaza, *A general multidimensional Hermite-Hadamard type inequality*, J. Math. Anal. Appl., 356 (2009), 659–663.

[5] H. Chen and U.N. Katugampola, *Hermite–Hadamard and Hermite–Hadamard–Fejér type inequalities for generalized fractional integrals*, J. Math. Anal. Appl. 446 (2017) 1274–1291

[6] S.S. Dragomir and C.E.M. Pearce, Selected Topics on Hermite-Hadamard Inequalities and Applications, RGMIA Monographs, Victoria University, 2000. Online:[http://rgmia.org/papers/monographs/Master2.pdf].

[7] S.S. Dragomir, R.P. Agarwal, *Two inequalities for differentiable mappings and applications to special means of real numbers and to trapezoidal formula*, Appl. Math. lett. 11 (5) (1998) 91–95.

[8] R. Gorenflo, F. Mainardi, *Fractional calculus: integral and differential equations of fractional order*, Springer Verlag, Wien (1997), 223-276.

[9] J. Hadamard, *Etude sur les proprietes des fonctions entieres en particulier d'une fonction consideree par Riemann*, J. Math. Pures Appl. 58 (1893), 171-215.

[10] S. Hussain, M. I. Bhatti and M. Iqbal, *Hadamard-type inequalities for s-convex functions* I, Punjab Univ. Jour. of Math., Vol.41, pp:51-60, (2009).

[11] M. Iqbal, S. Qaisar and M. Muddassar, *A short note on integral inequality of type Hermite-Hadamard through convexity*, J. Computational analaysis and applications, 21(5), 2016, pp.946-953.

[12] H. Kavurmaci, M. Avci and M E. Ozdemir, *New inequalities of hermite-hadamard type for convex functions with applications*, Journal of Inequalities and Applications 2011, Art No. 86, Vol 2011.

[13] A. A. Kilbas, H. M. Srivastava and J. J. Trujillo, *Theory and Applications of Fractional Differential Equations*, North-Holland Mathematics Studies, 204, Elsevier Sci. B.V., Amsterdam, 2006.

[14] U. S. Kirmaci, *Inequalities for differentiable mappings and applications to special means of real numbers to midpoint formula*, Appl. Math. Comput., vol. 147, no. 5, pp. 137–146, 2004, doi: 10.1016/S0096-3003(02)00657-4.

[15] S. Miller and B. Ross, *An introduction to the Fractional Calculus and Fractional Differential Equations*, John Wiley & Sons, USA, 1993, p.2.

[16] M. A. Noor and M. U. Awan, Some integral inequalities for two kinds of convexities via fractional integrals, TJMM, 5(2), 2013, pp. 129-136.

[17] M. E. Özdemir, M. Avcı-Ardıç and H. Kavurmacı-Önalan, *Hermite-Hadamard type inequalities for s-convex and s-concave functions via fractional integrals,* Turkish J.Science,1(1), 28-40, 2016.

[18] M. E. Ödemir, M. Avci, and E. Set, *On some inequalities of Hermite–Hadamard-type via m-convexity*, Appl. Math. Lett. 23 (2010), pp. 1065–1070.

[19] M. E. Ödemir, M. Avci, and H. Kavurmaci, *Hermite–Hadamard-type inequalities via (α, m)-convexity*, Comput. Math. Appl. 61 (2011), pp. 2614–2620.

[20] J.E. Pečarić, F. Proschan and Y.L. Tong, *Convex Functions, Partial Orderings and Statistical Applications*, Academic Press, Boston, 1992.

[21] I. Podlubni, *Fractional Differential Equations*, Academic Press, San Diego, 1999.

[22] A. Saglam, M. Z. Sarikaya ve H. Yildirim, *Some new inequalities of Hermite-Hadamard's type*, Kyungpook Mathematical Journal, 50(2010), 399-410.

[23] M.Z. Sarikaya and H. Yildirim, *On Hermite-Hadamard type inequalities for Riemann-Liouville fractional integrals*, Miskolc Mathematical Notes, 7(2) (2016), pp. 1049–1059.

[24] M. Z. Sarikaya and N. Aktan, *On the generalization some integral inequalities and their applications* Mathematical and Computer Modelling, 54, Issues 9-10, pp. 2175-2182.

[25] M.Z. Sarikaya and H. Ogunmez, *On new inequalities via Riemann-Liouville fractional integration*, Abstract and Applied Analysis, Volume 2012 (2012), Article ID 428983, 10 pages.

[26] M.Z. Sarikaya, E. Set, H. Yaldiz and N., Basak, *Hermite -Hadamard's inequalities for fractional integrals and related fractional inequalities*, Mathematical and Computer Modelling, DOI:10.1016/j.mcm.2011.12.048, 57 (2013) 2403–2407.

[27] M.Z. Sarikaya and H. Budak, *Generalized Hermite-Hadamard type integral inequalities for fractional integrals*, Filomat 30:5 (2016), 1315–1326.

[28] M. Z. Sarikaya, A. Saglam, and H. Yildirim, *New inequalities of Hermite-Hadamard type for functions whose second derivatives absolute values are convex and quasi-convex*, International Journal of Open Problems in Computer Science and Mathematics (IJOPCM), 5(3), 2012, pp:1-14.

[29] E. Set, M. E. Ozdemir and M. Z. Sarikaya, *New inequalities of Ostrowski's type for s-convex functions in the second sense with applications*, Facta Universitatis, Ser. Math. Inform. Vol. 27, No 1 (2012), 67-82.

[30] J. Wang, X. Li, M. Feckan and Y. Zhou, *Hermite-Hadamard-type inequalities for Riemann-Liouville fractional integrals via two kinds of convexity*, Appl. Anal. (2012). doi:10.1080/00036811.2012.727986.

[31] J.Wang, X. Lia and Y. Zhou, *Hermite-Hadamard Inequalities Involving Riemann-Liouville Fractional Integrals via s-convex functions and applications to special means,* Filomat 30:5 (2016), 1143–1150.

[32] B-Y, Xi and F. Qi, *Some Hermite-Hadamard type inequalities for differentiable convex functions and applications,* Hacet. J. Math. Stat.. 42(3), 243–257 (2013).

[33] B-Y, Xi and F. Qi, *Hermite-Hadamard type inequalities for functions whose derivatives are of convexities,* Nonlinear Funct. Anal. Appl.. 18(2), 163–176 (2013)

[34] Y. Zhang and J-R. Wang, *On some new Hermite-Hadamard inequalities involving Riemann-Liouville fractional integrals,* Journal of Inequalities and Applications 2013, 2013:220.

A Fast and Simple Soft Decision-Making Algorithm: EMA18an

Serdar ENGİNOĞLU*
Çanakkale Onsekiz Mart University,
Department of Mathematics,
17100, Çanakkale, Turkey

Samet MEMİŞ
Çanakkale Onsekiz Mart University,
Department of Mathematics,
17100, Çanakkale, Turkey

Burak ARSLAN
Çanakkale Onsekiz Mart University,
Department of Mathematics,
17100, Çanakkale, Turkey

Abstract

The uni-int soft decision-making method [N. Çağman, S. Enginoğlu, Soft set theory and uni-int decision making, Eur. J. Oper. Res. 207 (2010) 848-855] is an efficient method to deal with some uncertainties. To be able to use in computer science such as machine learning and image enhancement, in this paper, we configure this method constructed by andnot-product/ornot-product via fuzzy parameterized fuzzy soft matrices ($fpfs$-matrices), faithfully to the original. However, the configured method, denoted by CE10n, has a drawback in terms of time and complexity in the problems containing a large amount of data. To overcome this problem, we propose a new algorithm, i.e. EMA18an, and prove that CE10n constructed by andnot-product (CE10an), is a special case of EMA18an in the event that first rows of the $fpfs$-matrices are binary. We then compare the running times of these two algorithms. The results show that EMA18an outperforms CE10an in any number of data. Finally, we discuss the need for further research.

Keywords: Fuzzy sets, Soft sets, Soft decision-making, Soft matrices, $fpfs$-matrices.

1 Introduction

To deal with uncertainties, the concept of soft sets was produced by Molodtsov [1] and has been applied to many studies from algebra to decision-making problems [2–25]. Lately, the uni-int soft decision-making algorithm [15] constructed by and-product/or-product has been configured via fuzzy parameterized fuzzy soft matrices ($fpfs$-matrices) by Enginoğlu and Memiş [26]. Furthermore, the authors note that it is worthwhile to study different configurations of this algorithm, denoted by CE10, for other products.

In Section 2 of the present study, we introduce the concept of $fpfs$-matrices [19]. In Section 3, we configure the uni-int decision-making method constructed by andnot-product/ornot-product via $fpfs$-matrices and denote it by CE10n. In Section 4, we propose a fast and simple algorithm, namely EMA18an, equivalent to CE10n constructed by andnot-product (CE10an) under the condition that first rows of the $fpfs$-matrices are binary. In Section 5, we compare the running times of these algorithms. Finally, we discuss the need for further research.

*Corresponding author. *E-mail address:* serdarenginoglu@gmail.com

2 Preliminaries

In this section, the concept of $fpfs$-matrices [19] and some of its basic definitions have been presented. Throughout this paper, let E be a parameter set, $F(E)$ be the set of all fuzzy sets over E, and $\mu \in F(E)$. Here, $\mu := \{^{\mu(x)}x : x \in E\}$.

Definition 2.1. [12, 19] *Let U be a universal set, $\mu \in F(E)$, and α be a function from μ to $F(U)$. Then the graphic of α, denoted by α, defined by*

$$\alpha := \{(^{\mu(x)}x, \alpha(^{\mu(x)}x)) : x \in E\}$$

that is called fuzzy parameterized fuzzy soft set ($fpfs$-set) parameterized via E over U (or briefly over U).

In the present paper, the set of all $fpfs$-sets over U is denoted by $FPFS_E(U)$.

Example 2.1. *Let $E = \{x_1, x_2, x_3, x_4\}$ and $U = \{u_1, u_2, u_3, u_4, u_5\}$. Then*

$$\alpha = \{(^{0.4}x_1, \{^{0.7}u_1, ^{0.3}u_2, ^{1}u_5\}), (^{1}x_2, \{^{0.6}u_3, ^{0.2}u_5\}), (^{0.3}x_3, \{^{0.6}u_1, ^{0.3}u_4, ^{0.2}u_5\}), (^{0}x_4, \{^{0.1}u_2, ^{0.4}u_3\})\}$$

is a $fpfs$-set over U.

Definition 2.2. [19] *Let $\alpha \in FPFS_E(U)$. Then $[a_{ij}]$ is called the matrix representation of α (or briefly $fpfs$-matrix of α) and defined by*

$$[a_{ij}] = \begin{bmatrix} a_{01} & a_{02} & a_{03} & \cdots & a_{0n} & \cdots \\ a_{11} & a_{12} & a_{13} & \cdots & a_{1n} & \cdots \\ \vdots & \vdots & \vdots & \ddots & \vdots & \vdots \\ a_{m1} & a_{m2} & a_{m3} & \cdots & a_{mn} & \cdots \\ \vdots & \vdots & \vdots & \ddots & \vdots & \vdots \end{bmatrix} \text{ for } i = \{0, 1, 2, \cdots\} \text{ and } j = \{1, 2, \cdots\}$$

such that

$$a_{ij} := \begin{cases} \mu(x_j), & i = 0 \\ \alpha(^{\mu(x_j)}x_j)(u_i), & i \neq 0 \end{cases}$$

Here, if $|U| = m - 1$ and $|E| = n$ then $[a_{ij}]$ has order $m \times n$.

From now on, the set of all $fpfs$-matrices parameterized via E over U is denoted by $FPFS_E[U]$.

Example 2.2. *Let's consider the $fpfs$-set α provided in Example 2.1. Then the $fpfs$-matrix of α is as follows:*

$$[a_{ij}] = \begin{bmatrix} 0.4 & 1 & 0.3 & 0 \\ 0.7 & 0 & 0.6 & 0 \\ 0.3 & 0 & 0 & 0.1 \\ 0 & 0.6 & 0 & 0.4 \\ 0 & 0 & 0.3 & 0 \\ 1 & 0.2 & 0.2 & 0 \end{bmatrix}$$

Definition 2.3. [19] *Let $[a_{ij}], [b_{ik}] \in FPFS_E[U]$ and $[c_{ip}] \in FPFS_{E^2}[U]$ such that $p = n(j-1)+k$. For all i and p,*

If $c_{ip} = \min\{a_{ij}, b_{ik}\}$, then $[c_{ip}]$ is called and-product of $[a_{ij}]$ and $[b_{ik}]$, denoted by $[a_{ij}] \wedge [b_{ik}]$.

If $c_{ip} = \max\{a_{ij}, b_{ik}\}$, then $[c_{ip}]$ is called or-product of $[a_{ij}]$ and $[b_{ik}]$, denoted by $[a_{ij}] \vee [b_{ik}]$.

If $c_{ip} = \min\{a_{ij}, 1 - b_{ik}\}$, then $[c_{ip}]$ is called andnot-product of $[a_{ij}]$ and $[b_{ik}]$, denoted by $[a_{ij}] \overline{\wedge} [b_{ik}]$.

If $c_{ip} = \max\{a_{ij}, 1 - b_{ik}\}$, then $[c_{ip}]$ is called ornot-product of $[a_{ij}]$ and $[b_{ik}]$, denoted by $[a_{ij}] \underline{\vee} [b_{ik}]$.

3 The Soft Decision-Making Method CE10n

In this section, we configure the uni-int decision-making method constructed by andnot-product/ornot-product via $fpfs$-matrices and denoted it by CE10n.

Step 1. Construct two $fpfs$-matrices $[a_{ij}]$ and $[b_{ik}]$

Step 2. Find andnot-product/ornot-product $fpfs$-matrix $[c_{ip}]$ of $[a_{ij}]$ and $[b_{ik}]$

Step 3. Find andnot-product/ornot-product $fpfs$-matrix $[d_{it}]$ of $[b_{ik}]$ and $[a_{ij}]$

Step 4. Obtain $[s_{i1}]$ denoted by $\max\text{-}\min(c_{ip}, d_{it})$ defined by

$$s_{i1} := \max\{\max_j \min_k(c_{ip}), \max_k \min_j(d_{it})\}$$

such that $i \in \{1, 2, \dots, m-1\}$, $I_a := \{j \,|\, a_{0j} \neq 0\}$, $I_b := \{k \,|\, b_{0k} \neq 0\}$, $I_a^* := \{j \,|\, 1 - a_{0j} \neq 0\}$, $I_b^* := \{k \,|\, 1 - b_{0k} \neq 0\}$, $p = n(j-1)+k$, $t = n(k-1)+j$, and

$$\max_j \min_k(c_{ip}) := \begin{cases} \max\limits_{j \in I_a} \left\{ \min\limits_{k \in I_b^*} c_{0p} c_{ip} \right\}, & I_a \neq \emptyset \text{ and } I_b^* \neq \emptyset \\ 0, & \text{Otherwise} \end{cases}$$

$$\max_k \min_j(d_{it}) := \begin{cases} \max\limits_{k \in I_b} \left\{ \min\limits_{j \in I_a^*} d_{0t} d_{it} \right\}, & I_a^* \neq \emptyset \text{ and } I_b \neq \emptyset \\ 0, & \text{Otherwise} \end{cases}$$

Step 5. Obtain the set $\{u_k \in U \,|\, s_{k1} = \max\limits_i s_{i1}\}$

Preferably, the set $\{^{s_{i1}}u_i \,|\, u_i \in U\}$ or $\{^{\frac{s_{k1}}{\max s_{i1}}}u_k | u_k \in U\}$ can be attained.

Note 3.1. *Let CE10an and CE10on denote CE10n constructed by andnot-product and ornot-product, respectively. It must be noted that the scores of CE10an and CE10on can be found without writing any product matrices. When the algorithm is written in this format, it offers time advantage, little though, over CE10n in most cases. Let's illustrate this for CE10an;*

Step 1. Construct two $fpfs$-matrices $[a_{ij}]$ and $[b_{ik}]$

Step 2. Obtain $[s_{i1}]$ defined by

$$s_{i1} := \begin{cases} \max\{\max\limits_{j \in I_a}\{\min\limits_{k \in I_b^*}\{\min\{a_{0j}, 1-b_{0k}\}, \min\{a_{ij}, 1-b_{ik}\}\}\}, \max\limits_{k \in I_b}\{\min\limits_{j \in I_a^*}\{\min\{b_{0k}, 1-a_{0j}\}, \min\{b_{ik}, 1-a_{ij}\}\}\}\}, & I_a, I_b, I_a^*, I_b^* \neq \emptyset \\ 0, & \text{Otherwise} \end{cases}$$

such that $i \in \{1, 2, \dots, m-1\}$, $I_a := \{j \,|\, a_{0j} \neq 0\}$, $I_b := \{k \,|\, b_{0k} \neq 0\}$, $I_a^* := \{j \,|\, 1 - a_{0j} \neq 0\}$, and $I_b^* := \{k \,|\, 1 - b_{0k} \neq 0\}$.

Step 3. Obtain the set $\{u_k \in U \,|\, s_{k1} = \max\limits_i s_{i1}\}$

Preferably, the set $\{^{s_{i1}}u_i \,|\, u_i \in U\}$ or $\{^{\frac{s_{k1}}{\max s_{i1}}}u_k | u_k \in U\}$ can be attained.

4 A Soft Decision-Making Method: EMA18an

In this section, we propose a fast and simple algorithm denoted by EMA18an.

Step 1. Construct two $fpfs$-matrices $[a_{ij}]$ and $[b_{ik}]$

Step 2. Obtain $[s_{i1}]$ denoted by $\max\text{-}\min(a_{ij}, b_{ik})$ defined by

$$s_{i1} := \max\{\max_j\min_k(a_{ij}, b_{ik}), \max_k\min_j(b_{ik}, a_{ij})\}$$

such that $i \in \{1, 2, \ldots, m-1\}$, $I_a := \{j \mid a_{0j} \neq 0\}$, $I_b := \{k \mid b_{0k} \neq 0\}$, $I_a^* := \{j \mid 1 - a_{0j} \neq 0\}$, $I_b^* := \{k \mid 1 - b_{0k} \neq 0\}$, and

$$\max_j\min_k(a_{ij}, b_{ik}) := \begin{cases} \min\left\{\max\limits_{j\in I_a}\{a_{0j}a_{ij}\}, \min\limits_{k\in I_b^*}\{(1-b_{0k})(1-b_{ik})\}\right\}, & I_a \neq \emptyset \text{ and } I_b^* \neq \emptyset \\ 0, & \text{otherwise} \end{cases}$$

$$\max_k\min_j(b_{ik}, a_{ij}) := \begin{cases} \min\left\{\max\limits_{k\in I_b}\{b_{0k}b_{ik}\}, \min\limits_{j\in I_a^*}\{(1-a_{0j})(1-a_{ij})\}\right\}, & I_a^* \neq \emptyset \text{ and } I_b \neq \emptyset \\ 0, & \text{otherwise} \end{cases}$$

Step 3. Obtain the set $\{u_k \in U \mid s_{k1} = \max\limits_i s_{i1}\}$

Preferably, the set $\{^{s_{i1}}u_i \mid u_i \in U\}$ or $\{^{\frac{s_{k1}}{\max s_{i1}}}u_k | u_k \in U\}$ can be attained.

Theorem 4.1. *EMA18an is equivalent to CE10an under the condition that first rows of the $fpfs$-matrices are binary.*

Proof. Suppose that first rows of the $fpfs$-matrices are binary. The functions s_{i1} provided in CE10an and EMA18an are equal in the event that $I_a = \emptyset$ or $I_b^* = \emptyset$. Assume that $I_a \neq \emptyset$ and $I_b^* \neq \emptyset$. Since $a_{0j} = 1$ and $b_{0k} = 0$, for all $j \in I_a := \{a_1, a_2, ..., a_s\}$ and $k \in I_b^* := \{b_1, b_2, ..., b_t\}$,

$$\begin{aligned}
\max_j\min_k(c_{ip}) &= \max_{j\in I_a}\left\{\min_{k\in I_b^*} c_{0p}c_{ip}\right\} \\
&= \max_{j\in I_a}\left\{\min_{k\in I_b^*}\{\min\{a_{0j}, 1-b_{0k}\}.\min\{a_{ij}, 1-b_{ik}\}\}\right\} \\
&= \max_{j\in I_a}\left\{\min_{k\in I_b^*}\{\min\{a_{ij}, 1-b_{ik}\}\}\right\} \\
&= \max\{\min\{\min\{a_{ia_1}, 1-b_{ib_1}\}, \min\{a_{ia_1}, 1-b_{ib_2}\}, \ldots, \min\{a_{ia_1}, 1-b_{ib_t}\}\}, \\
&\qquad \min\{\min\{a_{ia_2}, 1-b_{ib_1}\}, \min\{a_{ia_2}, 1-b_{ib_2}\}, \ldots, \min\{a_{ia_2}, 1-b_{ib_t}\}\}, \ldots, \\
&\qquad \min\{\min\{a_{ia_s}, 1-b_{ib_1}\}, \min\{a_{ia_s}, 1-b_{ib_2}\}, \ldots, \min\{a_{ia_s}, 1-b_{ib_t}\}\}\} \\
&= \max\{\min\{a_{ia_1}, \min\{1-b_{ib_1}, 1-b_{ib_2}, \ldots, 1-b_{ib_t}\}\}, \\
&\qquad \min\{a_{ia_2}, \min\{1-b_{ib_1}, 1-b_{ib_2}, \ldots, 1-b_{ib_t}\}\}, \ldots, \\
&\qquad \min\{a_{ia_s}, \min\{1-b_{ib_1}, 1-b_{ib_2}, \ldots, 1-b_{ib_t}\}\}\} \\
&= \min\{\max\{a_{ia_1}, a_{ia_2}, \ldots, a_{ia_s}\}, \min\{1-b_{ib_1}, 1-b_{ib_2}, \ldots, 1-b_{ib_t}\}\} \\
&= \min\left\{\max_{j\in I_a}\{a_{ij}\}, \min_{k\in I_b^*}\{1-b_{ik}\}\right\} \\
&= \min\left\{\max_{j\in I_a}\{a_{0j}a_{ij}\}, \min_{k\in I_b^*}\{(1-b_{0k})(1-b_{ik})\}\right\} \\
&= \max_j\min_k(a_{ij}, b_{ik})
\end{aligned}$$

In a similar way, $\max_k\min_j(d_{it}) = \max_k\min_j(b_{ik}, a_{ij})$. Consequently,

$$\max\text{-}\min(a_{ij}, b_{ik}) = \max\text{-}\min(c_{ip}, d_{it})$$

∎

5 Simulation Results

In this section, we compare the running times of CE10an and EMA18an by using MATLAB R2018b and a workstation with I(R) Xeon(R) CPU E5-1620 v4 @ 3.5 GHz and 64 GB RAM in this study.

We present the running times of CE10an and EMA18an in Table 1 and Fig. 1 for 10 objects and the parameters ranging from 1000 to 10000. We then give their running times in Table 2 and Fig. 2 for 10 parameters and the objects ranging from 1000 to 10000, in Table 3 and Fig. 3 for the parameters and the objects ranging from 10 to 100 and in Table 4 and Fig. 4 for the parameters and the objects ranging from 100 to 1000. The results show that EMA18an outperforms than CE10an in any number of data under the specified condition.

Table 1. The results for 10 objects and the parameters ranging from 1000 to 10000 (In Seconds)

	1000	**2000**	**3000**	**4000**	**5000**	**6000**	**7000**	**8000**	**9000**	**10000**
CE10an	1.7290	6.0002	12.4614	22.0133	34.2460	47.1654	67.6639	89.3932	112.0984	147.1362
EMA18an	0.0010	0.0015	0.0019	0.0022	0.0029	0.0031	0.0036	0.0040	0.0046	0.0048
Difference	1.7280	5.9987	12.4595	22.0111	34.2431	47.1623	67.6603	89.3892	112.0938	147.1314
Advantage (%)	99.9395	99.9755	99.9850	99.9901	99.9916	99.9934	99.9947	99.9956	99.9959	99.9967

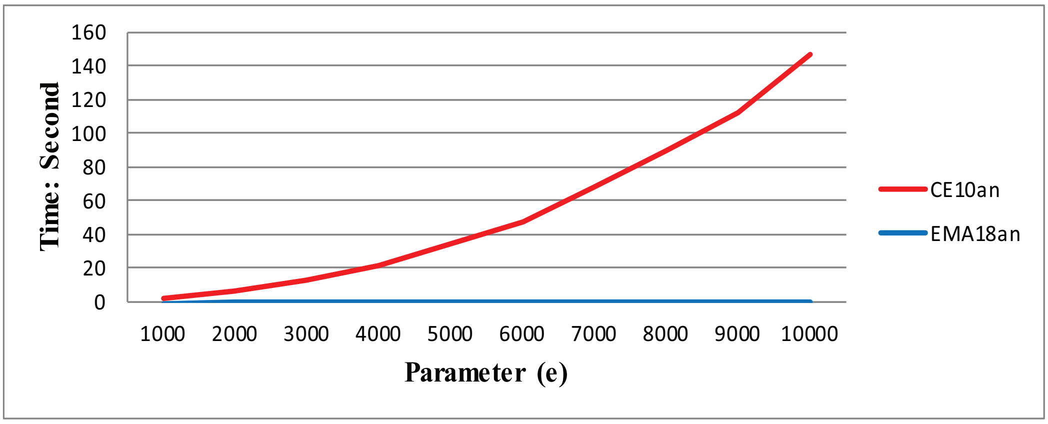

Fig. 1. The figure for Table 1

Table 2. The results for 10 parameters and the objects ranging from 1000 to 10000 (In Seconds)

	1000	**2000**	**3000**	**4000**	**5000**	**6000**	**7000**	**8000**	**9000**	**10000**
CE10an	0.0671	0.2553	0.4513	0.7131	1.0672	1.5062	1.9701	2.5841	3.2344	3.9714
EMA18an	0.0099	0.0193	0.0284	0.0387	0.0505	0.0626	0.0753	0.0891	0.1031	0.1204
Difference	0.0572	0.2360	0.4229	0.6744	1.0166	1.4436	1.8948	2.4950	3.1312	3.8509
Advantage (%)	85.2543	92.4443	93.7129	94.5697	95.2658	95.8456	96.1784	96.5534	96.8110	96.9675

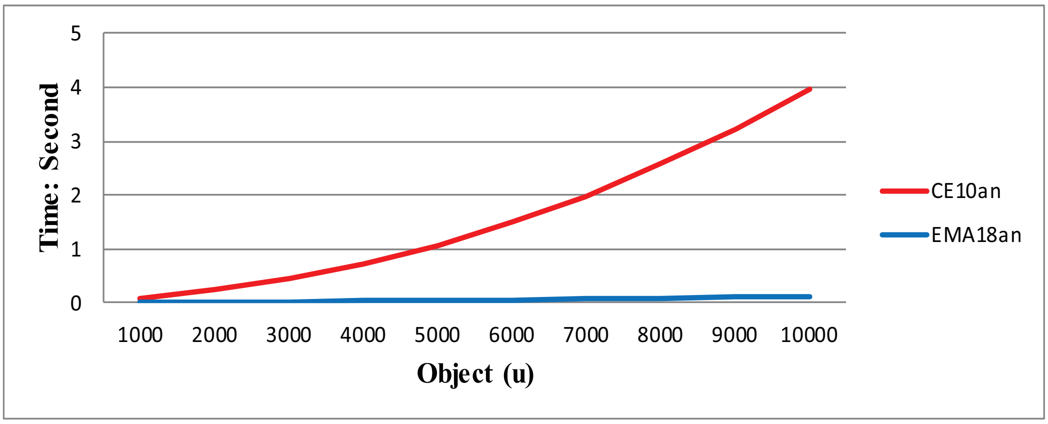

Fig. 2. The figure for Table 2

Table 3. The results for the parameters and the objects ranging from 10 to 100 (In Seconds)

	10	20	30	40	50	60	70	80	90	100
CE10an	0.0012	0.0024	0.0059	0.0133	0.0257	0.0459	0.0764	0.1078	0.1649	0.2358
EMA18an	0.0006	0.0003	0.0004	0.0005	0.0008	0.0007	0.0009	0.0010	0.0012	0.0013
Difference	0.0006	0.0021	0.0055	0.0128	0.0248	0.0452	0.0755	0.1069	0.1637	0.2346
Advantage (%)	50.9100	88.7774	93.4698	96.1678	96.7905	98.4441	98.7975	99.1153	99.2688	99.4640

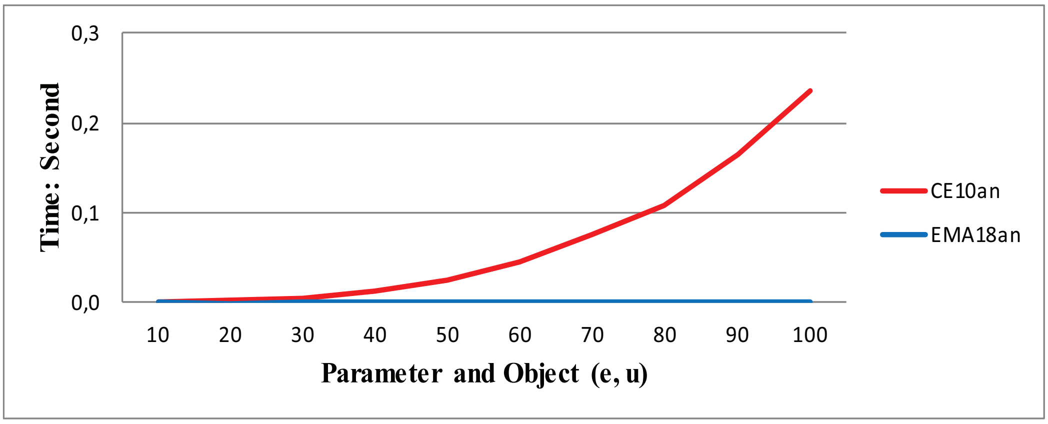

Fig. 3. The figure for Table 3

Table 4. The results for the parameters and the objects ranging from 100 to 1000 (In Seconds)

	100	200	300	40	500	600	700	800	900	1000
CE10an	0.2340	3.3294	14.1333	40.4840	94.0603	183.5776	324.8095	544.0888	868.8858	1327.7415
EMA18an	0.0026	0.0031	0.0057	0.0085	0.0121	0.0174	0.0223	0.0290	0.0369	0.0442
Difference	0.2314	3.3263	14.1276	40.4756	94.0482	183.5602	324.7872	544.0598	868.8488	1327.6973
Advantage (%)	98.8717	99.9072	99.9596	99.9791	99.9871	99.9905	99.9931	99.9947	99.9957	99.9967

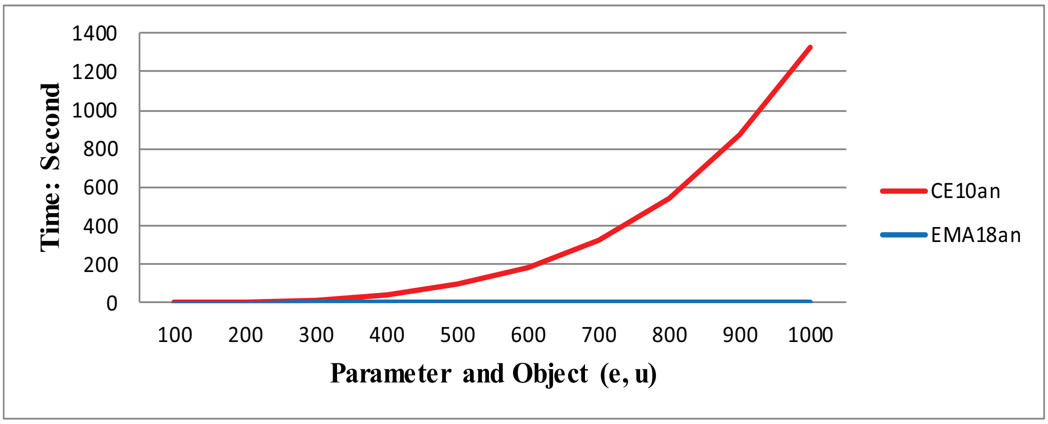

Fig. 4. The figure for Table 4

6 Conclusion

The uni-int decision-making method defined by Çağman and Enginoğlu [15] has been configured [26] via $fpfs$-matrices [19] because more general forms are needed for the method in the event that the parameters or objects have uncertainties. Moreover, the authors stated that different configurations of this method can be constructed for other products such as andnot-product/ornot-product. To this end, we have configured this method for andnot-product/ornot-product.

On the other hand, the method suffers from a drawback, i.e. its incapability of processing a large number of data on a standard computer, e.g. with 2.6 GHz i5 Dual Core CPU and 4GB RAM. Since the simplification of such methods is necessary for a wide range of scientific and industrial processes, we have proposed the method EMA18an, which is faster than CE10an. We also have shown that EMA18an is equivalent to CE10an under the condition that first rows of the $fpfs$-matrices are binary. Of course, it is possible to investigate other simplifications for the different products. We then have compared the running times of these algorithms, in Section 5. In addition to the results in Section 5, the results in Table 5 too show that EMA18an outperforms CE10an in any number of data under the specified condition.

Table 5. The mean advantage, max advantage, and max difference values of EMA18an over CE10an

Location	Objects	Parameters	Mean Advantage%	Max Advantage%	Max Difference
Table 1	10	$1000 - 10000$	99.9858	99.9967	147.1314
Table 2	$1000 - 10000$	10	94.3603	96.9675	3.8509
Table 3	$10 - 100$	$10 - 100$	92.1205	99.4640	0.2346
Table 4	$100 - 1000$	$100 - 1000$	99.8676	99.9967	1327.6973

In addition, other decision-making methods constructed by a different decision function such as minimum-maximum (min-max), max-max, and min-min can also be studied by the similar way.

Acknowledgements

The authors thank to Dr. Uğur Erkan for technical support. This work was supported by the Office of Scientific Research Projects Coordination at Çanakkale Onsekiz Mart University, Grant number: FBA-2018-1367.

References

[1] D. Molodtsov, Soft set theory-first results, Computers and Mathematics with Applications 37 (1999) 19–31.

[2] E. Muştuoğlu, A. Sezgin, Z. K. Türk, Some characterizations on soft uni-groups and normal soft uni-groups, International Journal of Computer Applications 155 (10) (2016) 8 pages.

[3] A. Sezgin, A new approach to semigroup theory I: Soft union semigroups, ideals and bi-ideals, Algebra Letters 2016 (3).

[4] A. Sezgin, N. Çağman, F. Çıtak, α-inclusions applied to group theory via soft set and logic, Communications Faculty of Sciences University of Ankara Series A1 Mathematics and Statistics 68 (1) (2019) 334–352.

[5] M. Tunçay, A. Sezgin, Soft union ring and its applications to ring theory, International Journal of Computer Applications 151 (9) (2016) 7–13.

[6] A. Ullah, F. Karaaslan, I. Ahmad, Soft uni-abel-grassmann's groups, European Journal of Pure and Applied Mathematics 11 (2) (2018) 517–536.

[7] İ. Zorlutuna, S. Atmaca, Fuzzy parametrized fuzzy soft topology, New Trends in Mathematical Sciences 4 (1) (2016) 142–152.

[8] S. Atmaca, Relationship between fuzzy soft topological spaces and (X, τ_e) parameter spaces, Cumhuriyet Science Journal 38 (2017) 77–85.

[9] S. Atmaca, İ. Zorlutuna, On topological structures of fuzzy parametrized soft sets, The Scientific World Journal 2014 (2014) Article ID 164176, 8 pages.

[10] S. Bera, S. K. Roy, F. Karaaslan, N. Çağman, Soft congruence relation over lattice, Hacettepe Journal of Mathematics and Statistics 46 (6) (2017) 1035–1042.

[11] N. Çağman, S. Enginoğlu, Soft matrix theory and its decision making, Computers and Mathematics with Applications 59 (2010) 3308–3314.

[12] N. Çağman, F. Çıtak, S. Enginoğlu, Fuzzy parameterized fuzzy soft set theory and its applications, Turkish Journal of Fuzzy Systems 1 (1) (2010) 21–35.

[13] N. Çağman, F. Çıtak, S. Enginoğlu, FP-soft set theory and its applications, Annals of Fuzzy Mathematics Information 2 (2) (2011) 219–226.

[14] N. Çağman, S. Enginoğlu, Fuzzy soft matrix theory and its application in decision making, Iranian Journal of Fuzzy Systems 9 (1) (2012) 109–119.

[15] N. Çağman, S. Enginoğlu, Soft set theory and uni-int decision making, European Journal of Operational Research 207 (2010) 848–855.

[16] N. Çağman, S. Enginoğlu, F. Çıtak, Fuzzy soft set theory and its applications, Iranian Journal of Fuzzy Systems 8 (3) (2011) 137–147.

[17] F. Çıtak, N. Çağman, Soft int-rings and its algebraic applications, Journal of Intelligent and Fuzzy Systems 28 (2015) 1225–1233.

[18] F. Çıtak, N. Çağman, Soft k-int-ideals of semirings and its algebraic structures, Annals of Fuzzy Mathematics and Informatics 13 (4) (2017) 531–538.

[19] S. Enginoğlu, Soft matrices, PhD dissertation, Gaziosmanpaşa University (2012).

[20] S. Enginoğlu, N. Çağman, S. Karataş, T. Aydın, On soft topology, El-Cezerî Journal of Science and Engineering 2 (3) (2015) 23–38.

[21] F. Karaaslan, Soft classes and soft rough classes with applications in decision making, Mathematical Problems in Engineering 2016 (2016) Article ID 1584528, 11 pages.

[22] P. K. Maji, R. Biswas, A. Roy, Soft set theory, Computers and Mathematics with Applications 45 (2003) 555–562.

[23] P. K. Maji, A. Roy, R. Biswas, An application of soft sets in a decision making problem, Computers and Mathematics with Applications 44 (2002) 1077–1083.

[24] P. K. Maji, R. Biswas, A. Roy, Fuzzy soft sets, The Journal of Fuzzy Mathematics 9 (3) (2001) 589–602.

[25] S. Enginoğlu, S. Memiş, Comment on Fuzzy soft sets [The Journal of Fuzzy Mathematics, 9(3), 2001, 589–602], International Journal of Latest Engineering Research and Applications 3 (9) (2018) 1–9.

[26] S. Enginoğlu, S. Memiş, A configuration of some soft decision-making algorithms via $fpfs$-matrices, Cumhuriyet Science Journal 39 (4) (2018) 871–881.

A Review on Some Soft Decision-Making Methods

Serdar ENGİNOĞLU*
Çanakkale Onsekiz Mart University,
Department of Mathematics,
17100, Çanakkale, Turkey

Samet MEMİŞ
Çanakkale Onsekiz Mart University,
Department of Mathematics,
17100, Çanakkale, Turkey

Abstract

The soft decision-making methods are used efficiently to cope with some problems containing uncertainty. Recently, some of them have been configured by Enginoğlu and Memiş via fuzzy parameterized fuzzy soft matrices ($fpfs$-matrices), faithfully to the original, because a more general form is needed for the methods in the event that the parameters or objects have uncertainty. In this study, we consider three configured methods therein, denoted by MRB02, CCE10 and CCE11. We then apply these methods to a decision-making problem in image denoising. Finally, we discuss the need for further research.

Keywords: Fuzzy sets, Soft sets, Soft decision-making, Soft matrices, $fpfs$-matrices.

1 Introduction

Lately, the concept of soft sets propounded by Molodtsov [1] has become a greatly preferred mathematical tool and many theoretical and applied studies have been conducted on this concept [2–27]. The configuring some of the known soft decision-making methods by Enginoğlu and Memiş [28] via fuzzy parameterized fuzzy soft matrices ($fpfs$-matrices) [14] has enabled to use these methods in computer science. However, though these configured methods define in different structures, some of these are equivalent in terms of sorting. This equivalence is clearly seen in the configured forms of these methods.

In Section 2 of this study, we present the concept of $fpfs$-matrices [14], MRB02, CCE10, and CCE11 [3, 7, 9, 28]. We then configure a similar method given in [29] via $fpfs$-matrices. In Section 3, we apply this method to a performance-based value assignment to the methods used in image denoising. Finally, we discuss the need for further research.

2 Preliminaries

In this section, firstly, we present the concept of $fpfs$-matrices [14]. Throughout this paper, let E be a parameter set, $F(E)$ be the set of all fuzzy sets over E, and $\mu \in F(E)$. Here, $\mu := \{^{\mu(x)}x : x \in E\}$.

Definition 2.1. [7, 14] *Let U be a universal set, $\mu \in F(E)$, and α be a function from μ to $F(U)$. Then the graphic of α, denoted by α, defined by*

$$\alpha := \{(^{\mu(x)}x, \alpha(^{\mu(x)}x)) : x \in E\}$$

that is called fuzzy parameterized fuzzy soft set ($fpfs$-set) parameterized via E over U (or briefly over U).

*Corresponding author. *E-mail address:* serdarenginoglu@gmail.com

In the present paper, the set of all $fpfs$-sets over U is denoted by $FPFS_E(U)$.

Example 2.1. *Let $E = \{x_1, x_2, x_3, x_4\}$ and $U = \{u_1, u_2, u_3, u_4, u_5\}$. Then*

$$\alpha = \{({}^{0.8}x_1, \{{}^{0.9}u_1, {}^{0.5}u_4\}), ({}^{0}x_2, \{{}^{0.3}u_2, {}^{0.5}u_3\}), ({}^{0.1}x_3, \{{}^{0.7}u_1, {}^{0.8}u_3, {}^{0.6}u_4\}), ({}^{1}x_4, \{{}^{0.1}u_3, {}^{0.9}u_5\})\}$$

is a $fpfs$-set over U.

Definition 2.2. [14] *Let $\alpha \in FPFS_E(U)$. Then $[a_{ij}]$ is called the matrix representation of α (or briefly $fpfs$-matrix of α) and defined by*

$$[a_{ij}] = \begin{bmatrix} a_{01} & a_{02} & a_{03} & \dots & a_{0n} & \dots \\ a_{11} & a_{12} & a_{13} & \dots & a_{1n} & \dots \\ \vdots & \vdots & \vdots & \ddots & \vdots & \vdots \\ a_{m1} & a_{m2} & a_{m3} & \dots & a_{mn} & \dots \\ \vdots & \vdots & \vdots & \ddots & \vdots & \vdots \end{bmatrix} \text{ for } i = \{0, 1, 2, \cdots\} \text{ and } j = \{1, 2, \cdots\}$$

such that

$$a_{ij} := \begin{cases} \mu(x_j), & i = 0 \\ \alpha({}^{\mu(x_j)}x_j)(u_i), & i \neq 0 \end{cases}$$

Here, if $|U| = m - 1$ and $|E| = n$ then $[a_{ij}]$ has order $m \times n$.

From now on, the set of all $fpfs$-matrices parameterized via E over U is denoted by $FPFS_E[U]$.

Example 2.2. *Let's consider the $fpfs$-set α provided in Example 2.1. Then the $fpfs$-matrix of α is as follows:*

$$[a_{ij}] = \begin{bmatrix} 0.8 & 0 & 0.1 & 1 \\ 0.9 & 0 & 0.7 & 0 \\ 0 & 0.3 & 0 & 0 \\ 0 & 0.5 & 0.8 & 1 \\ 0.5 & 0 & 0.6 & 0 \\ 0 & 0 & 0 & 0.9 \end{bmatrix}$$

Secondly, we present the algorithm MRB02 [3, 28].

Step 1. Construct an $fpfs$-matrix $[a_{ij}]$

Step 2. Obtain $[s_{i1}]$ defined by

$$s_{i1} := \sum_{j=1}^{n} a_{0j}a_{ij}, \quad i \in \{1, 2, \dots, m-1\}$$

Step 3. Obtain the set $\{u_k \mid s_{k1} = \max_i (s_{i1})\}$

Preferably, the set $\{{}^{\mu(u_k)}u_k | u_k \in U\}$ can be attained such that $\mu(u_k) = \frac{s_{k1}}{\max_i s_{i1}}$.

Note 2.1. *The reduction steps in the original algorithm haven't been considered because they lead to some errors* [30, 31].

Thirdly, we present the algorithm CCE10 [7, 28].

Step 1. Construct an $fpfs$-matrix $[a_{ij}]$

Step 2. Obtain $[s_{i1}]$ defined by

$$s_{i1} := \frac{1}{n} \sum_{j=1}^{n} a_{0j}a_{ij}, \qquad i \in \{1, 2, \dots, m-1\}$$

Step 3. Obtain the set $\{u_k \,|\, s_{k1} = \max\limits_i (s_{i1})\}$

Preferably, the set $\{^{s_{i1}}u_i|u_i \in U\}$ or $\{^{\mu(u_k)}u_k|u_k \in U\}$ can be attained such that $\mu(u_k) = \frac{s_{k1}}{\max\limits_i s_{i1}}$.

Fourthly, we present the algorithm CCE11 [9, 28].

Step 1. Construct an $fpfs$-matrix $[a_{ij}]$

Step 2. Obtain $[s_{i1}]$ defined by

$$s_{i1} := \frac{1}{\sum_{j=1}^{n} \operatorname{sgn}(a_{0j})} \sum_{j=1}^{n} a_{0j}a_{ij}, \qquad i \in \{1, 2, \ldots, m-1\}$$

Step 3. The set $\{u_k \,|\, s_{k1} = \max\limits_i (s_{i1})\}$ is attained

Preferably, the set $\{^{s_{i1}}u_i|u_i \in U\}$ or $\{^{\mu(u_k)}u_k|u_k \in U\}$ can be attained such that $\mu(u_k) = \frac{s_{k1}}{\max\limits_i s_{i1}}$.

Note 2.2. *It must be noted that the sorting of alternatives in a problem applied MRB02, CCE10 and CCE11 is same. Here, CCE10 and CCE11 generate fuzzy values as different from MRB02. Moreover, the values generated by CCE11 are closer to "1" comparing with those of generated by CCE10. Here, it can be seen easily that the values of s_{i1} are to become closer to "1" than those of the other methods in the event that they are obtained by using Riesz mean (see [29]). To avail of this advantage, in addition to the above-mentioned methods, we configure the method provided in [29] and denote it by YE12 as follows:*

Step 1. Construct an $fpfs$-matrix $[a_{ij}]$

Step 2. Obtain $[s_{i1}]$ defined by

$$s_{i1} := \frac{1}{\sum_{j=1}^{n} a_{0j}} \sum_{j=1}^{n} a_{0j}a_{ij}, \qquad i \in \{1, 2, \ldots, m-1\}$$

Step 3. The set $\{u_k \,|\, s_{k1} = \max\limits_i (s_{i1})\}$ is attained

Preferably, the set $\{^{s_{i1}}u_i|u_i \in U\}$ or $\{^{\mu(u_k)}u_k|u_k \in U\}$ can be attained such that $\mu(u_k) = \frac{s_{k1}}{\max\limits_i s_{i1}}$.

3 An Application of MRB02, CCE10, CCE11, and YE12

In this section, we consider some of the well-known methods used for salt-and-pepper noise removal. By using MATLAB R2018b, we evaluate the performance of Progressive Switching Median Filter (PSMF) [32], Decision Based Algorithm (DBA) [33], Modified Decision Based Unsymmetrical Trimmed Median Filter (MDBUTMF) [34], Noise Adaptive Fuzzy Switching Median Filter (NAFSMF) [35], and Different Applied Median Filter (DAMF) [36] by using 15 traditional images (Cameraman, Lena, Peppers, Baboon, Plane, Bridge, Pirate, Elaine, Boat, Lake, Flintstones, Living Room, House, Parrot, and Hill) with 512×512 pixels, ranging in noise densities from 10% to 90%, and an image quality metrics Structural Similarity (SSIM) [37]. The results in Table 1 show that DAMF outperforms in any noise density than the others.

Table 1. The mean SSIM results for the 15 traditional images

Algorithm	**10%**	**20%**	**30%**	**40%**	**50%**	**60%**	**70%**	**80%**	**90%**
PSMF	0.9605	0.9211	0.8439	0.7326	0.5097	0.1956	0.0666	0.0335	0.0147
DBA	0.9655	0.9212	0.8608	0.7841	0.6914	0.5890	0.4847	0.3855	0.3103
MDBUTMF	0.9425	0.7949	0.8381	0.8391	0.7839	0.6336	0.3224	0.0974	0.0217
NAFSM	0.9753	0.9506	0.9246	0.8966	0.8659	0.8309	0.7884	0.7309	0.6068
DAMF	**0.9865**	**0.9714**	**0.9538**	**0.9328**	**0.9085**	**0.8785**	**0.8409**	**0.7890**	**0.6959**

Let's suppose that the success in high noise densities is more important than in the others. In that case, the values given in Table 1 can be represented with a $fpfs$-matrix as follows:

$$[a_{ij}] := \begin{bmatrix} 0 & 0 & 0.1 & 0.3 & 0.5 & 0.7 & 0.9 & 1 & 1 \\ 0.9605 & 0.9211 & 0.8439 & 0.7326 & 0.5097 & 0.1956 & 0.0666 & 0.0335 & 0.0147 \\ 0.9655 & 0.9212 & 0.8608 & 0.7841 & 0.6914 & 0.5890 & 0.4847 & 0.3855 & 0.3103 \\ 0.9425 & 0.7949 & 0.8381 & 0.8391 & 0.7839 & 0.6336 & 0.3224 & 0.0974 & 0.0217 \\ 0.9753 & 0.9506 & 0.9246 & 0.8966 & 0.8659 & 0.8309 & 0.7884 & 0.7309 & 0.6068 \\ 0.9865 & 0.9714 & 0.9538 & 0.9328 & 0.9085 & 0.8785 & 0.8409 & 0.7890 & 0.6959 \end{bmatrix}$$

If we apply MRB02, CCE10, CCE11, and YE12 to the $fpfs$-matrix $[a_{ij}]$, then the score matrices and the decision set are as follows, respectively:

$$[s_{i1}] = [0.8041 \ 2.2113 \ 1.5803 \ \ 3.4233 \ \ 3.6861]^T$$

$$[s_{i1}] = [0.0893 \ 0.2457 \ 0.1756 \ \ 0.3804 \ \ 0.4096]^T$$

$$[s_{i1}] = [0.1149 \ 0.3159 \ 0.2258 \ \ 0.4590 \ \ 0.5266]^T$$

$$[s_{i1}] = [0.1787 \ 0.4914 \ 0.3512 \ \ 0.7607 \ \ 0.8191]^T$$

and

$$\{{}^{0.2181}\text{PSMF}, \ {}^{0.5999}\text{DBA}, \ {}^{0.4287}\text{MDBUTMF}, \ {}^{0.9287}\text{NAFSM}, \ {}^{1}\text{DAMF}\}$$

The scores show that DAMF is better than the other methods and the order DAMF, NAFSM, DBA, MDBUTMF, and PSMF is valid. It must be noted that the decision sets generated by these methods are the same.

4 Conclusion

In this study, we have reviewed the methods MRB02, CCE10, CCE11, and YE12 and illustrated their sorting abilities. Although these methods have defined different structures, their configured versions have same abilities in terms of sorting. Afterwards, we have applied the methods to order the filters, used in noise removal, in terms of performance. Moreover, these soft decision-making methods have a potential to different applications.

Acknowledgements

This work was supported by the Office of Scientific Research Projects Coordination at Çanakkale Onsekiz Mart University, Grant number: FBA-2018-1367.

References

[1] D. Molodtsov, Soft set theory-first results, Computers and Mathematics with Applications 37 (1999) 19–31.

[2] P. K. Maji, R. Biswas, A. Roy, Fuzzy soft sets, The Journal of Fuzzy Mathematics 9 (3) (2001) 589–602.

[3] P. K. Maji, A. Roy, R. Biswas, An application of soft sets in a decision making problem, Computers and Mathematics with Applications 44 (2002) 1077–1083.

[4] P. K. Maji, R. Biswas, A. Roy, Soft set theory, Computers and Mathematics with Applications 45 (2003) 555–562.

[5] N. Çağman, S. Enginoğlu, Soft set theory and uni-int decision making, European Journal of Operational Research 207 (2010) 848–855.

[6] N. Çağman, S. Enginoğlu, Soft matrix theory and its decision making, Computers and Mathematics with Applications 59 (2010) 3308–3314.

[7] N. Çağman, F. Çıtak, S. Enginoğlu, Fuzzy parameterized fuzzy soft set theory and its applications, Turkish Journal of Fuzzy Systems 1 (1) (2010) 21–35.

[8] N. Çağman, S. Enginoğlu, F. Çıtak, Fuzzy soft set theory and its applications, Iranian Journal of Fuzzy Systems 8 (3) (2011) 137–147.

[9] N. Çağman, F. Çıtak, S. Enginoğlu, FP-soft set theory and its applications, Annals of Fuzzy Mathematics Information 2 (2) (2011) 219–226.

[10] N. Çağman, S. Enginoğlu, Fuzzy soft matrix theory and its application in decision making, Iranian Journal of Fuzzy Systems 9 (1) (2012) 109–119.

[11] N. Çağman, İ. Deli, Means of FP-soft sets and their applications, Hacettepe Journal of Mathematics and Statistics 41 (5) (2012) 615–625.

[12] N. Çağman, İ. Deli, Products of FP-soft sets and their applications, Hacettepe Journal of Mathematics and Statistics 41 (3) (2012) 365–374.

[13] İ. Deli, N. Çağman, Relations on FP-soft sets applied to decision making problems, Journal of New Theory 3 (2015) 98–107.

[14] S. Enginoğlu, Soft matrices, PhD dissertation, Gaziosmanpaşa University (2012).

[15] S. Atmaca, İ. Zorlutuna, On topological structures of fuzzy parametrized soft sets, The Scientific World Journal 2014 (2014) Article ID 164176, 8 pages.

[16] F. Çıtak, N. Çağman, Soft int-rings and its algebraic applications, Journal of Intelligent and Fuzzy Systems 28 (2015) 1225–1233.

[17] S. Enginoğlu, N. Çağman, S. Karataş, T. Aydın, On soft topology, El-Cezerî Journal of Science and Engineering 2 (3) (2015) 23–38.

[18] M. Tunçay, A. Sezgin, Soft union ring and its applications to ring theory, International Journal of Computer Applications 151 (9) (2016) 7–13.

[19] F. Karaaslan, Soft classes and soft rough classes with applications in decision making, Mathematical Problems in Engineering 2016 (2016) Article ID 1584528, 11 pages.

[20] İ. Zorlutuna, S. Atmaca, Fuzzy parametrized fuzzy soft topology, New Trends in Mathematical Sciences 4 (1) (2016) 142–152.

[21] A. Sezgin, A new approach to semigroup theory I: Soft union semigroups, ideals and bi-ideals, Algebra Letters 2016 (3).

[22] E. Muştuoğlu, A. Sezgin, Z. K. Türk, Some characterizations on soft uni-groups and normal soft uni-groups, International Journal of Computer Applications 155 (10) (2016) 8 pages.

[23] S. Atmaca, Relationship between fuzzy soft topological spaces and (X, τ_e) parameter spaces, Cumhuriyet Science Journal 38 (2017) 77–85.

[24] S. Bera, S. K. Roy, F. Karaaslan, N. Çağman, Soft congruence relation over lattice, Hacettepe Journal of Mathematics and Statistics 46 (6) (2017) 1035–1042.

[25] F. Çıtak, N. Çağman, Soft k-int-ideals of semirings and its algebraic structures, Annals of Fuzzy Mathematics and Informatics 13 (4) (2017) 531–538.

[26] A. Ullah, F. Karaaslan, I. Ahmad, Soft uni-abel-grassmann's groups, European Journal of Pure and Applied Mathematics 11 (2) (2018) 517–536.

[27] A. Sezgin, N. Çağman, F. Çıtak, α-inclusions applied to group theory via soft set and logic, Communications Faculty of Sciences University of Ankara Series A1 Mathematics and Statistics 68 (1) (2019) 334–352.

[28] S. Enginoğlu, S. Memiş, A configuration of some soft decision-making algorithms via $fpfs$-matrices, Cumhuriyet Science Journal 39 (4) (2018) 871–881.

[29] Ş. Yılmaz, S. Eraslan, Fuzzy parameterized soft set and riesz summability appliying to a decision making problem, Gaziosmanpaşa Journal of Scientific Research 1 (2012) 27–34.

[30] D. Chen, E. C. C. Tsang, D. S. Yeung, X. Wang, The parameterization reduction of soft sets and its applications, Computers and Mathematics with Applications 49 (2005) 757–763.

[31] Z. Kong, L. Gao, L. Wang, S. Li, The normal parameter reduction of soft sets and its algorithm, Computers and Mathematics with Applications 56 (2008) 3029–3037.

[32] Z. Wang, D. Zhang, Progressive switching median filter for the removal of impulse noise from highly corrupted images, IEEE Transactions on Circuits and Systems II: Analog and Digital Signal Processing 46 (1) (1999) 78–80.

[33] A. Pattnaik, S. Agarwal, S. Chand, A new and efficient method for removal of high density salt and pepper noise through cascade decision based filtering algorithm, Procedia Technology 6 (2012) 108–117.

[34] S. Esakkirajan, T. Veerakumar, A. Subramanyam, C. PremChand, Removal of high density salt and pepper noise through modified decision based unsymmetric trimmed median filter, IEEE Signal Processing Letters 18 (5) (2011) 287–290.

[35] K. K. V. Toh, N. A. M. Isa, Noise adaptive fuzzy switching median filter for salt-and-pepper noise reduction, IEEE Signal Processing Letters 17 (3) (2010) 281–284.

[36] U. Erkan, L. Gökrem, S. Enginoğlu, Different applied median filter in salt and pepper noise, Computers and Electrical Engineering 70 (2018) 789–798.

[37] Z. Wang, A. Bovik, H. Sheikh, E. Simoncelli, Image quality assessment: From error visibility to structural similarity, IEEE Transactions on Image Processing 13 (4) (2004) 600–612.

An Integral Transform Solution for Fractional Advection-Diffusion Problem

Mehmet YAVUZ*
Department of Mathematics-Computer Sciences,
Necmettin Erbakan University,
Konya / TURKEY

Necati ÖZDEMİR
Department of Mathematics,
Balıkesir University,
Balıkesir / TURKEY

Abstract

In this paper, time-fractional advection-diffusion problem in terms of a new fractional derivative operator involving the normalized sinc function (NSF) is considered. This derivative operator is defined with nonsingular kernel. Therefore, it removes the computational complexities arising from the singular kernel functions inherit in the conventional fractional derivatives. In the present paper, we investigate the fundamental solution for heat-diffusion equation by using Sumudu transform (ST) with respect to the time and Fourier transform (FT) with respect to spatial coordinate. The mentioned fractional advection-diffusion problem is considered in a half space.

Keywords: Advection-diffusion equation, normalized sinc function, fractional derivative, Sumudu transform, Fourier transform.

1 Introduction

Modelling real-life problems with fractional partial differential equations (FPDEs) has a meaningful role in recent decades. Some important solution methods of the problems have been examined by using fractional operators. These operators can be classified as that include the power-law function [1], exponential function [2], Mittag-Leffler function [3, 4], stretched exponential function [5], stretched Mittag-Leffler function [6], and the normalized sinc function [7]. Recent studies made have shown that many problems are modeled and solved using these operators by some scientists [8, 9, 10, 11, 12, 13, 14, 15, 16, 17, 18].
In 2017, Yang et al. developed a new fractional derivative operator involving the normalized sinc function without singular kernel. They also defined some integral transforms and properties of the mentioned operator such as, Laplace, Fourier, Sumudu transforms. In this study, we consider the Dirichlet problem for the time-fractional advection-diffusion equation [19] and we get its fundamental solution by using Sumudu-Fourier transforms.

2 New Derivative Operator in the Normalized Sinc Function Sense

In this section, we explain the mentioned derivative operator and its some integral transforms.
Definition 1. The normalized sinc function is defined as [20]:

$$sinc\,(t) = \frac{\sin(\pi t)}{\pi t}, \qquad t \in R. \tag{1}$$

*Corresponding author. *E-mail address:* mehmetyavuz@konya.edu.tr

Definition 2. Let $u(\tau)$ be in $H^1(a,b)$, $b > a$. A new fractional derivative operator which is defined with the normalized sinc function (FDNSF) of the function $u(\tau)$ of order μ is defined by [7]:

$$ {}_{a}^{NSF}D_{\tau}^{\mu}u(\tau) = \frac{\mu\psi(\mu)}{1-\mu}\int_{a}^{\tau} sinc\left(-\frac{\mu(\tau-\varepsilon)}{1-\mu}\right)u'(\varepsilon)\,d\varepsilon, \quad a \in (-\infty,\tau), \tag{2} $$

where $\psi(\mu)$ is a normalization function such that $\psi(0) = \psi(1) = 1$.

Definition 3. The Sumudu transform of the FDNSF is defined as [7]

$$ \begin{aligned} \Psi\left\{{}_{0}^{NSF}D_{\tau}^{\mu}u(\tau)\right\} &= \Psi\left\{\tfrac{\mu\psi(\mu)}{1-\mu}\int_{0}^{\tau} sinc\left(-\tfrac{\mu(\tau-\varepsilon)}{1-\mu}\right)u'(\varepsilon)\,d\varepsilon\right\} \\ &= \tfrac{\mu\psi(\mu)}{\pi}\Psi\left\{ sinc\left(-\tfrac{\mu\tau}{1-\mu}\right)\right\}\Psi\left\{u'(\varepsilon)\right\} \\ &= \tfrac{\psi(\mu)}{\pi\vartheta^2}\left[u^*(\vartheta) - u(0)\right]\arctan\left(\tfrac{\mu\pi\vartheta}{1-\mu}\right), \end{aligned} \tag{3} $$

where $\Psi\{u(\tau)\} = u^*(\vartheta)$.

Definition 4. The Fourier transform of the FDNSF is defined by [7]

$$ \begin{aligned} \mathcal{F}\left\{{}_{0}^{NSF}D_{x}^{\mu}u(x)\right\} &= \mathcal{F}\left\{\tfrac{\mu\psi(\mu)}{1-\mu}\int_{0}^{x} sinc\left(-\tfrac{\mu(x-\varepsilon)}{1-\mu}\right)u'(\varepsilon)\,d\varepsilon\right\} \\ &= i\omega\psi(\mu)\sqrt{\tfrac{1}{2\pi}}\mathrm{H}\left(\tfrac{\mu\pi}{1-\mu} + |\omega|\right)\hat{u}(\omega), \end{aligned} \tag{4} $$

where $\mathcal{F}\{u(x)\} = \hat{u}(\omega)$ and $\mathrm{H}(.)$ is the Heaviside function [21].

Moreover, the infinite sin-Fourier transform with respect to spatial coordinate is defined as [22]

$$ \mathcal{F}\{u(x,s)\} = \hat{u}(\omega,s) = \int_{0}^{\infty} u(x,s)\sin(\omega x)\,dx. \tag{5} $$

The sin-Fourier transform property of the second order derivative in a half space is given by

$$ \mathcal{F}\left\{\frac{d^2u(x)}{dx^2}\right\} = -\omega^2\hat{u}(\omega) + \omega u(x)\big|_{x=0}. \tag{6} $$

3 Solution of Time-Fractional Advection-Diffusion Equation with the FDNSF

Consider the following special-type fractional heat equation [23] in the sense of FDNSF operator

$$ \frac{\partial^{\alpha}\varphi(x,\tau)}{\partial\tau^{\alpha}} = \sigma\frac{\partial^2\varphi(x,\tau)}{\partial x^2} - \frac{\kappa^2\varphi(x,\tau)}{4\sigma}, \quad 0 < x < \infty, \quad \tau > 0, \quad \sigma > 0, \quad \kappa > 0, \tag{7} $$

with the initial condition

$$ \tau = 0 \quad : \quad \varphi(x,0) = 0, \tag{8} $$

and the boundary condition

$$ \begin{aligned} x = 0 \quad &: \quad \varphi(0,\tau) = \delta(\tau), \\ x \to \infty \quad &: \quad \lim_{x\to\infty}\varphi(x,\tau) = 0. \end{aligned} \tag{9} $$

Applying the Sumudu transform (3) with respect to time variable τ and the finite sin-Fourier transform (5) with respect to spatial coordinate x, we obtain the following equation

$$ \frac{\psi(\mu)}{\pi\vartheta^2}\left[\hat{\phi}^*(\omega,\vartheta)\right]\arctan\left(\frac{\mu\pi\vartheta}{1-\mu}\right) = \sigma\left(-\omega^2\hat{\phi}^*(\omega,\vartheta) + \omega\right) - \frac{\kappa^2\hat{\phi}^*(\omega,\vartheta)}{4\sigma}. \tag{10} $$

After some arrangements, we get

$$\hat{\phi}^{*}(\omega,\vartheta)=\frac{\sigma\omega}{\frac{\psi(\mu)}{\pi\vartheta^{2}}\arctan\left(\frac{\mu\pi\vartheta}{1-\mu}\right)+\sigma\omega^{2}+\frac{\kappa^{2}}{4\sigma}}. \tag{11}$$

Using the inverse Sumudu transform and inverse Fourier transform in the last equation, we get the fundamental solution of suggested problem as

$$\begin{aligned}\phi(x,\tau)&=\mathcal{F}^{-1}\left\{\Psi^{-1}\left\{\hat{\phi}^{*}(\omega,\vartheta)\right\}\right\}=\mathcal{F}^{-1}\left\{\Psi^{-1}\left\{\frac{\sigma\omega}{\frac{\psi(\mu)}{\pi\vartheta^{2}}\arctan\left(\frac{\mu\pi\vartheta}{1-\mu}\right)+\sigma\omega^{2}+\frac{\kappa^{2}}{4\sigma}}\right\}\right\}\\&=\frac{2\sigma\mu\tau^{\mu-1}}{\pi}\int_{0}^{\infty}\left(\frac{\omega\varepsilon^{2}}{\left(\varepsilon+\sigma\omega^{2}+\frac{\kappa^{2}}{4\sigma}\right)^{2}}\right)\sum_{m=0}^{\infty}\left[\frac{\left(\frac{-\tau^{\mu}\mu\varepsilon\left(\sigma\omega^{2}+\frac{\kappa^{2}}{4\sigma}\right)}{\varepsilon+\sigma\omega^{2}+\frac{\kappa^{2}}{4\sigma}}\right)^{m}}{\Gamma(\mu m+\mu)}\right]\sin(\omega x)\,d\omega,\end{aligned} \tag{12}$$

where $\varepsilon=\frac{1}{1-\mu}$. If we consider the special case of fractional operator as $\mu\to1$ and $\varepsilon\to\infty$ in Eq. (12), we get the standard exact solution of the mentioned advection-diffusion equation as:

$$\phi(x,\tau)=\frac{2\sigma}{\pi}\int_{0}^{\infty}\omega\exp\left(-\tau\left(\sigma\omega^{2}+\frac{\kappa^{2}}{4\sigma}\right)\right)\sin(\omega x)\,d\omega. \tag{13}$$

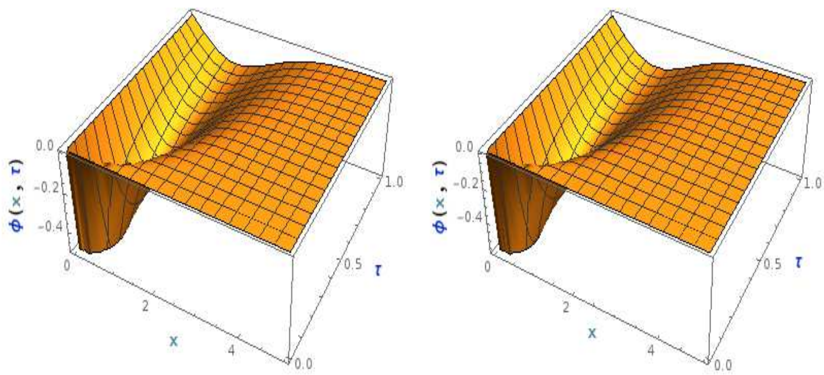

Figure 1: Solutions of Eq. (7) when $\mu\to1$ and $\kappa=0.5$ (left) and $\kappa=1$ (right).

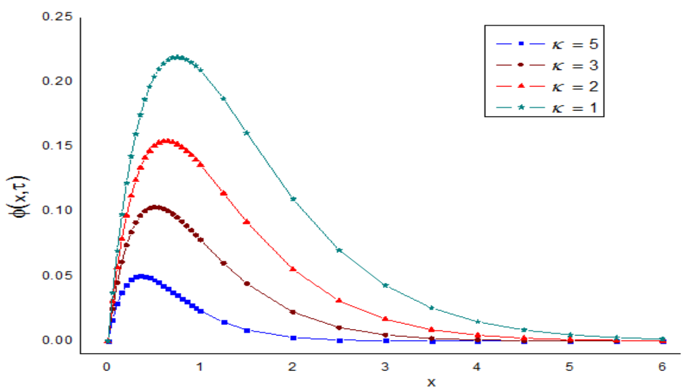

Figure 2: Solutions of Eq. (7) when $\mu=0.5$ and $\tau=0.1$ for various values of κ.

4 Concluding Remarks

In this paper, we consider a fractional advection-diffusion problem by using the newly defined fractional derivative operator. This operator is defined by normalized sinc function. We apply the integral transforms of the derivative operator to the advection-diffusion problem. This problem is considered in a half space $(0, \infty)$. We obtain the solution function of the problem and we present the results with figures. In Figure **??**, we get the solutions with respect to two different variables of the diffusion constant. In Figure **??**, we have the solutions include various variables of the diffusion constant when $\mu = 0.5$ and $\tau = 0.1$.

References

[1] M. Caputo, Linear Models of Dissipation Whose Q is Almost Frequency Independent–II, Geophysical Journal International, 13, 529-539 (1967).

[2] M. Caputo and M. Fabrizio, A New Definition of Fractional Derivative without Singular Kernel, Progress in Fractional Differentiation and Applications, 1, 1-13 (2015).

[3] Y. Xiao-Jun, Fractional Derivatives of Constant and Variable Orders Applied to Anomalous Relaxation Models in Heat Transfer Problems, Thermal Science, 21, 1161-1171 (2017).

[4] X.-J. Yang, J.T. Machado and D. Baleanu, Anomalous Diffusion Models with General Fractional Derivatives within the Kernels of the Extended Mittag-Leffler Type Functions, Romanian Reports in Physics, 69, 115 (2017).

[5] H. Sun, X. Hao, Y. Zhang and D. Baleanu, Relaxation and Diffusion Models with Non-Singular Kernels, Physica A: Statistical Mechanics and its Applications, 468, 590-596 (2017).

[6] A. Atangana and D. Baleanu, New Fractional Derivatives with Nonlocal and Non-Singular Kernel: Theory and Application to Heat Transfer Model, Thermal Science, 20, 763-769 (2016).

[7] X.J. Yang, F. Gao, J.A. Machado and D. Baleanu, A New Fractional Derivative Involving the Normalized Sinc Function without Singular Kernel, The European Physical Journal Special Topics, 226, 3567-3575 (2017).

[8] D. Avcı and A. Yetim, Analytical Solutions to the Advection-Diffusion Equation with the Atangana-Baleanu Derivative over a Finite Domain, Balıkesir Üniversitesi Fen Bilimleri Enstitüsü Dergisi, 20, 382-395 (2018).

[9] M. Yavuz, Novel Recursive Approximation for Fractional Nonlinear Equations within Caputo-Fabrizio Operator, Proceedings, ITM Web of Conferences: EDP Sciences, pp 01008, (2018).

[10] M. Yavuz, Characterizations of Two Different Fractional Operators without Singular Kernel, Mathematical Modelling of Natural Phenomena, 14, (2019).

[11] D. Baleanu, J.T. Machado, C. Cattani, M.C. Baleanu and X.-J. Yang, Local Fractional Variational Iteration and Decomposition Methods for Wave Equation on Cantor Sets within Local Fractional Operators, Abstract and Applied Analysis, 2014, (2014).

[12] F. Evirgen and M. Yavuz, An Alternative Approach for Nonlinear Optimization Problem with Caputo-Fabrizio Derivative, Proceedings, ITM Web of Conferences: EDP Sciences, pp 01009, (2018).

[13] V.F. Morales-Delgado, J.F. Gómez-Aguilar, H. Yépez-Martínez, D. Baleanu, R.F. Escobar-Jimenez and V.H. Olivares-Peregrino, Laplace Homotopy Analysis Method for Solving Linear Partial Differential Equations Using a Fractional Derivative with and without Kernel Singular, Advances in Difference Equations, 2016, 164 (2016).

[14] M. Yavuz and N. Özdemir, European Vanilla Option Pricing Model of Fractional Order without Singular Kernel, Fractal and Fractional, 2, 3 (2018).

[15] M. Yavuz, N. Ozdemir and H.M. Baskonus, Solutions of Partial Differential Equations Using the Fractional Operator Involving Mittag-Leffler Kernel, The European Physical Journal Plus, 133, 215 (2018).

[16] M. Yavuz and N. Ozdemir, Numerical Inverse Laplace Homotopy Technique for Fractional Heat Equations, Thermal Science, 22, 185-194 (2018).

[17] M. Yavuz and N. Özdemir, Comparing the New Fractional Derivative Operators Involving Exponential and Mittag-Leffler Kernel, Discrete and Continuous Dynamical Systems Series S, 13, 3 (2020).

[18] B.İ. Eroğlu, D. Avcı and N. Özdemir, Optimal Control Problem for a Conformable Fractional Heat Conduction Equation, Acta Physica Polonica A, 132, 658-662 (2017).

[19] Y.Z. Povstenko, Fractional Heat Conduction Equation and Associated Thermal Stress, Journal of Thermal Stresses, 28, 83-102 (2004).

[20] E.T. Whittaker, Xviii.—on the Functions Which Are Represented by the Expansions of the Interpolation-Theory, Proceedings of the Royal Society of Edinburgh, 35, 181-194 (1915).

[21] L. Debnath and D. Bhatta, Integral Transforms and Their Applications, Chapman and Hall/CRC, 2006.

[22] A. George, H.J. Weber and F. Harris, Mathematical Methods for Physicists. A Comprehensive Guide, Academic Press, Elsevier, 2013.

[23] Y. Povstenko and J. Klekot, Fundamental Solution to the Cauchy Problem for the Time-Fractional Advection-Diffusion Equation, Journal of Applied Mathematics and Computational Mechanics, 13, (2014).

Compressive Strength Estimation Of Glass Powder Added Concrete

Mehmet UZUN *
Department of Civil Engineering,
Karamanoglu Mehmetbey University,
Karaman/TURKEY

Sadik Alper YILDIZEL
Department of Civil Engineering,
Karamanoglu Mehmetbey University,
Karaman/TURKEY

Serdar ÇARBAŞ
Department of Civil Engineering,
Karamanoglu Mehmetbey University,
Karaman/TURKEY

Abstract

This study examined the effects of glass powder (GP), superplasticizer and spread diameter effect on the compressive strength estimation of GP added concrete mixes. GP was added into the mixes at the weight fractions of 10 %, 15 %, and 20 %. 80 compressive strength test results were recorded during the field studies. A Quasi-Newton method based artificial neural network system was proposed in order to predict compressive strength of the specimens. Analysis results showed that there is a strong correlation between the input parameters and the output compressive strength values. The mathematical expression of the proposed model was also presented within the scope of this study.

Keywords: Compressive strength, Quasi-Newton method, glass powder, prediction mathematical expression.

1 Introduction

Concrete is a building material that is widely used all over the world. Concrete is generally used in buildings, road construction, dams, and many other areas. Conventional concrete production is made by using water, cement, coarse and fine aggregate [1, 2]. There have various improvements in recent years to meet the needs of the building industry. These developments in concrete are generally classified as high durability, early high strength, long life, impermeability [2-6].

In conventional concrete, both linear and nonlinear regression models can be used to predict the concrete compressive strength. However, the relationship between the parametric inputs and the concrete compressive strength output becomes increasingly complicated due to the contributions of the admixtures used in the concrete. For this reason, prediction models in concrete that used additive materials can be developed using soft computing techniques such as artificial neural networks (ANNs) [2]. Also, data-driven models such as Adaptive Neuro-Fuzzy Inference System (ANFIS) and Multiple Linear Regression (MLR) are widely used in civil engineering data. With the predictions made by such models, the material becomes more understandable without the need for experimental data [7, 8].

Nowadays, prediction models are used to estimate concrete compressive strength for many parameters. By Shao et al. slump value of recyclable concrete is estimated [9]. By Bilgehan et

*Corresponding author. *E-mail address:* mehmetuzun@kmu.edu.tr

al. neural network model and concrete ultrasonic pulse velocity test is proposed for predicting concrete compressive strength [10]. By Sobhani et al. neural networks and the adaptive neuro-fuzzy inference systems are used together to develop a prediction model [11]. By Milicevic et al. artificial neural networks and regression techniques are used to estimate the relationship between concrete components and concrete properties [12, 13].

2 Material and method

2.1 Neural Network Development

The neural networks are used to reflect the predictive model. In Neural Designer neural networks allow deep architectures, which are a class of universal approximator. In this study, the conjugate gradient method was used. In the conjugate gradient, algorithm search is conducted along conjugate directions, which produces generally faster convergence than gradient descent directions. The training algorithm is given in Table 1.

Table 1: Training algorithm

Description		Value
Training direction method		FR
Training rate method		Brent Method
Training rate tolerance		0.0005
Min. parameters increment form	The norm of the parameters increment vector at which training stops.	1e-009
Min. loss increase	Minimum loss improvement between two successive iterations.	1e-012
Gradient norm goal		0.001
Max. iterations number		1000
Maximum time	Maximum training time.	3600

The ANN structure was proposed with three inputs for estimating concrete compressive strength. Three input parameters: spread diameter, plasticizer, glass powder (GP) content values were selected based on physical considerations and the experimental test results. The proposed ANN structure is presented in Figure 1.

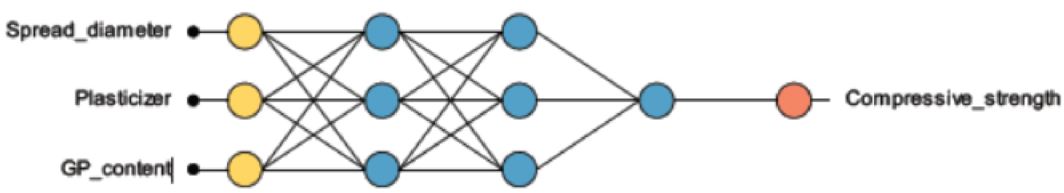

Figure 1: Proposed ANN structure

Necessary statistical information is precious when designing a prediction model. Because it allows fictive or error data to appear. It is a must to check for the correctness of the most important statistical measures of every single variable. Table 2 shows the minimums, maximums, means and standard deviations of all the variables in the data set.

Table 2: Dataset

	Minimum	Maximum	Mean	Deviation
Spread diameter	107	134	121.367	6.75805
Plasticizer	25	30	27.7848	1.91934
GP content	0	20	11.3924	7.37879
Compressive strength	24.03	36.76	29.8684	3.23252

All prediction studies have been performed with the aid of Neural Designer software. The size of the scaling layer is 3, the number of inputs. The scaling method for this layer is the Mean Standard Deviation. The neural network layer number is 3. Architecture of this neural network can be written as 3:3:3:1. The norm of the parameters gives a clue about the complexity of the predictive model. If the parameters norm is small, the model will be smooth.

On the other hand, if the parameters norm is very big, the model might become unstable. Also, note that the norm depends on the number of parameters. Proposed parameters norm was obtained as 3.17.

3 Discussions

Input values and their corresponding values are given in Table 3. The input variables are Spread diameter, Plasticizer, and GP content; and the output variable is a Compressive strength.

The proposed model produced the form of a function of the outputs concerning the inputs. The mathematical expression represented by the model can be used to embed it into another software, in the so-called production mode. The mathematical expression of the utilized neural network is written below (Figure 2). It takes the inputs Spread diameter, Plasticizer, GP content to produce the output Compressive strength.

Table 3: Inputs and corresponding output

Values	
Spread diameter	121.367
Plasticizer	27.7848
GP content	11.3924
Compressive strength	29.6360207

```
scaled_Spread_diameter=2*(Spread_diameter-107)/(134-107)-1;
scaled_Plasticizer=2*(Plasticizer-25)/(30-25)-1;
scaled_GP_content=2*(GP_content-0)/(20-0)-1;
y_1_1=tanh(-1.48288
-1.23639*scaled_Spread_diameter
-0.435604*scaled_Plasticizer
+1.46436*scaled_GP_content);
y_1_2=tanh(1.09902
+0.904411*scaled_Spread_diameter
-0.522549*scaled_Plasticizer
-1.90701*scaled_GP_content);
y_1_3=tanh(-0.706755
+1.17561*scaled_Spread_diameter
-0.174809*scaled_Plasticizer
+0.568513*scaled_GP_content);
y_2_1=tanh(1.69273
+3.10462*y_1_1
+1.20217*y_1_2
-0.845963*y_1_3);
y_2_2=tanh(0.508705
-0.683558*y_1_1
+0.742031*y_1_2
+0.0626998*y_1_3);
y_2_3=tanh(0.739577
-2.18643*y_1_1
-0.310819*y_1_2
-1.02106*y_1_3);
scaled_Compressive_strength=(-0.575387
-0.734912*y_2_1
-0.952582*y_2_2
+1.48156*y_2_3);
(Compressive_strength) = (0.5*(scaled_Compressive_strength+1.0)*(36.76-24.03)+24.03);
```

Figure 2: Mathematical expression

The proposed model performance was evaluated with Sum Squared Error (SSE), Mean Squared Error (MSE), Root Mean Squared Error (RMSE), Normalized Squared Error (NSE) and Minkowski Error (ME) operators. These errors are presented in Table 4. All error results of the ANN classification system were obtained as within the acceptable limits.

Table 4: Proposed network errors

	Training	Selection	Testing
	6.39178	4.51682	6.21518
Mean squared error	0.130444	0.301122	0.414345
Root mean squared error	0.361171	0.548745	0.643697
Normalized squared error	0.0146457	0.0285306	0.0302826
Minkowski error	8.54492	5.29992	6.63524

4 Conclusions

This research aims to develop an ANN-based Compressive strength estimation system in order to provide compressive strength effecting ingredients of the concrete mixes. For this purpose, the artificial neural network-based system was developed using a conjugate gradient algorithm. Conclusions of the research can be drawn as follows:

- The ANN model approves the strong correlation between the Pin puts parameters GP and plasticizer contents and spread diameter and the output parameter compressive strength.
- The outcomes of the study can be assessed by other artificial and mathematical systems for a better understanding of inputs effects on Compressive strength amounts.
- ANN models showed good fitting performances and this model could be applied to the compressive strength estimation studies.

References

[1] S. Kostic, D. Vasovic, Prediction Model for Compressive Strength of Basic Concrete Mixture Using Artificial Neural Networks, Neural Computing, and Applications 26(5) (2015) 1005-1024.

[2] Y. Yu, J. Li, T.N. Nguyen, A Novel Optimised Self-Learning Method for Compressive Strength Prediction of High-Performance Concrete, Construction and Building Materials 184(2018) (2018) 229-247.

[3] A. Behnood, J. Olek, M.A. Glinicki, Predicting Modulus Elasticity of Recycled Aggregate Concrete Using M5' Model Tree Algorithm, Construction and Building Materials 94(2015) (2015) 137-147.

[4] H.G. Russell, ACI Defines High-Performance Concrete, Concrete International 21(2) (1999) 56-57.

[5] M.J. Shannag, High Strength Concrete Containing Natural Pozzolan and Silica Fume, Cement and Concrete Composites 22(6) (2000) 399-406.

[6] I.-C. Yeh, Modeling of Strength of High Performance Concrete Using Articial Neural Networks, Cement and Concrete Research 28(12) (1998) 1797-1808.

[7] F. Khademi, S.M. Jamal, N. Deshpande, S. Londhe, Predicting Strength of Recycled Aggregate Concrete Using Artificial Neural Network, Adaptive Neuro-Fuzzy Inference System and Multiple Linear Regression, International Journal of Sustainable Built Environment 5(2) (2016) 355-369.

[8] B. Vakhshouri, S. Nejadi, Prediction of Compressive Strength of Self-Compacting Concrete by ANFIS Models, Neurocomputing 280(2018) (2018) 13-22.

[9] J. Shao, X. Ji, R. Li, Application on BP Neural Network Model in The Recycled Concrete Performance Prediction, International Conference on Advances in Energy, Environment and Chemical Engineering, Changsha, China, 2015, pp. 527-532.

[10] M. Bilgehan, P. Turgut, The Use of Neural Networks in Concrete Compressive Strength Estimation, Computers and Concrete 7(7) (2010) 271-283.

[11] J. Sobhani, M. Najimi, A.R. Pourkhorshidi, T. Parhizkar, Prediction of The COmpressive Strength of No-Slump Concrete: A Comparative Study of Regression, Neural Network and ANFIS Models, Construction and Building Materials 24(5) (2010) 709-718.

[12] F. Deng, Y. He, S. Zhou, Y. Yu, H. Cheng, X. Wu, Compressive Strength Prediction of Recycled Concrete Based on Deep Learning, Construction and Building Materials 175(2018) (2018) 562-569.

[13] I. Milicevic, T.K. Sipos, Prediction of Properties of Recycled Aggregate Concrete, Gradevinar 69(5) (2017) 347-357.

Complete Growth Series of Some Special Group Types

Esra KIRMIZI ÇETİNALP*
Karamanoglu Mehmetbey University,
Department of Mathematics,
70100, Karaman, TURKEY

Eylem GÜZEL KARPUZ
Karamanoglu Mehmetbey University,
Department of Mathematics,
70100, Karaman, TURKEY

Abstract

In the present paper, we study a generalization of the growth functions of finitely generated groups, namely the growth functions $\sum_{g\in G} gz^{|g|}$ with coefficients in the group ring $\mathbb{Z}[G]$. We compute complete growth series for finite number of amalgamated free products of some finite groups. Finally, we give a generalized formula for calculation of complete growth series of this kind of group product.

Keywords: Amalgamated free product, complete growth series, presentation.

1 Introduction and Preliminaries

There is a long history of studying combinatorial structures in the context of infinite groups. One example is complete growth series, where for a given set of generators, one writes the elements of length n. By calculating such series, it becomes possible to classify related groups. In [8], the authors studied complete growth functions on hyperbolic groups by languages determined by sets of forbidden words and rewriting system. Later, in [12], the author studied triangular Coxeter group and derived a formula for the complete growth series of that group by using complete rewriting system method. In [13], Mamaghani computed complete growth series of Coxeter groups with more than three generators as a continue work of [12]. Later, in [1], the authors showed that the property of having a rational complete growth series is preserved by direct and graph products, as well as certain free products with amalgamation. In literature, there are also some other important studies on growth series of groups. For example, some authors computed the growth series for some special groups, such as, for surface groups ([4]), for Fuchsian groups ([7]), for Heisenberg and Nil groups ([3, 15]) and for hyperbolic groups ([5]). Some other authors have also studied the growth series for special group (extensions) products. For example, in [14], Mann studied growth series on free products of groups. In [6], the authors calculated the growth series of amalgamated free products and HNN-extensions. Johnson ([10]) presented some results on the growth series of wreath products.

In this paper, we compute the complete growth series for finite number of amalgamated free products of some finite groups. Here, we use the formula given in [1] to compute the complete growth series of amalgamated free products of groups. In that paper, the authors have obtained that formula by using normal forms of elements of amalgamated free product.

Theorem 1 ([1]) *Let $G = A *_C B$ be a free product of groups A and B amalgamating C. Assume that $(C, S_C) \subset (A, S_A)$ and $(C, S_C) \subset (B, S_B)$ are both admissible. Then the complete growth*

*Corresponding author. *E-mail address:* esrakirmizi@kmu.edu.tr

series of G is given by

$$\frac{1}{F_G^c(z)} = \frac{1}{F_A^c(z)} + \frac{1}{F_B^c(z)} - \frac{1}{F_C^c(z)}.$$

Now we give group presentations of which complete growth series will be computed as follows. In the next section, the complete growth series of these groups will be given.

$$W_3 = < w_0,\ w_1,\ w_2;\ w_0^2 = w_1^2 = w_2^2 = (w_0w_1)^2 = (w_0w_2)^2 = (w_1w_2)^2 = 1 >, \quad (1)$$

$$W_4 = < w_0,\ w_1,\ w_2,\ w_3\ ;\ w_0^2 = w_1^2 = w_2^2 = w_3^2 = (w_0w_1)^2 = (w_0w_2)^2 = (w_0w_3)^2 = (w_1w_2)^2 = (w_1w_3)^2 = (w_2w_3)^2 = 1 > \quad (2)$$

and

$$W_n = < w_i\ (0 \le i \le n)\ ;\ w_i^2 = 1,\ (w_iw_j)^2 = 1\ \ (0 \le i < j \le n) > . \quad (3)$$

Let G be a finitely presented group with a semigroup generating set $S = \left\{s_1^{\mp1}, s_2^{\mp1}, \cdots, s_l^{\mp1}\right\}$. By the length $|g|$ of $g \in G$ with respect to S, we mean the quantity

$$|g| = \inf\{k : g = s_1 s_2 \cdots s_k,\ s_i \in S,\ 1 \le i \le k\}\ .$$

The function $f : \mathbb{N} \cup \{0\} \to \mathbb{N}$ defined by $f(0) = a_0 = 1$ and

$$f(n) = a_n = \#\{g \in G : |g| = n,\ n \ge 1\}$$

is called the *growth function* of G with respect to S, and the series $F(z) = \sum_{n=0}^{\infty} a_n z^n$ is called the *growth series* of G (see, for example, [2, 9]).

Let G be a finitely presented group with a semigroup generating set $S = \left\{s_1^{\mp1}, s_2^{\mp1}, \cdots, s_l^{\mp1}\right\}$ and $R[G]$ be the group ring on G. The function $f^c : \mathbb{N} \cup \{0\} \to R[G]$ defined by

$$f^c(0) = 1, \quad f^c(n) = \sum_{g \in G,\ |g| = n}^{\infty} g \in G$$

is called the *complete growth function* and the series $F^c(z) = \sum_{g \in G}^{\infty} g z^{|g|}$ is called the *complete growth series* of G with respect to S and R ([1, 12]).

2 Main Results

In this section, we compute the complete growth series for presentations given by (1) and (2). To do that, firstly, we will consider the presentations given by (1) and (2) as an amalgamated free product type. Then, with the help of formula given in Theorem 1 , we compute complete growth series for this kind of groups. Firstly, let us consider the presentation of W_3 given by (1). So we have the following result.

Theorem 2 *Let $F_{W_3}^c(z)$ be complete growth series of the group W_3. Then $F_{W_3}^c(z)$ is given as follows:*

$$\frac{1}{F_{W_3}^c(z)} = \frac{3 + Az}{(1 + w_0 z)(1 + w_1 z)(1 + w_2 z)} - \frac{2 - Az + z^2}{1 - z^2},$$

where $A = w_0 + w_1 + w_2$.

Proof. We can consider the presentation of W_3 group given by (1) as an amalgamated free product of groups. For that, let K_1, K_2 and K_3 be subgroups of W_3 and they have the following presentations

$$K_1 =< w_0,\ w_1;\ w_0^2 = w_1^2 = (w_0w_1)^2 = 1 >,$$
$$K_2 =< w_1,\ w_2;\ w_1^2 = w_2^2 = (w_1w_2)^2 = 1 >$$
and
$$K_3 =< w_0,\ w_2;\ w_0^2 = w_2^2 = (w_0w_2)^2 = 1 >,$$

respectively. Firstly, let H_1 be a subgroup of K_1 and K_2 presented by $H_1 =< w_1;\ w_1^2 = 1 >$. That is, $H_1 \subset K_1$ and $H_1 \subset K_2$. Then, we have

$$L_3 = K_1 *_{H_1} K_2 =< w_0,\ w_1,\ w_2;\ w_0^2 = w_1^2 = w_2^2 = (w_0w_1)^2 = (w_1w_2)^2 = 1 > .$$

Secondly, let H_2 be a subgroup of K_3 and L_3 presented by

$$H_2 =< w_0, w_2;\ w_0^2 = w_2^2 = 1 > .$$

Now we can consider amalgamated free product of K_3 and L_3 by H_2. Thus we get the following presentation.

$$W_3 = K_3 *_{H_2} L_3 =< w_0,\ w_1,\ w_2;\ w_0^2 = w_1^2 = w_2^2 = (w_0w_1)^2 = (w_0w_2)^2 = (w_1w_2)^2 = 1 > .$$

Then, by formula given in Theorem 1 we obtain

$$\begin{aligned}
\frac{1}{F^c_{W_3}(z)} &= \left(\frac{1}{F^c_{K_3}(z)} + \frac{1}{F^c_{L_3}(z)} - \frac{1}{F^c_{H_2}(z)}\right) \\
&= \left(\frac{1}{F^c_{K_3}(z)} + \left(\frac{1}{F^c_{K_1}(z)} + \frac{1}{F^c_{K_2}(z)} - \frac{1}{F^c_{H_1}(z)}\right) - \frac{1}{F^c_{H_2}(z)}\right) \\
&= \frac{1}{F^c_{K_1}(z)} + \frac{1}{F^c_{K_2}(z)} + \frac{1}{F^c_{K_3}(z)} - \frac{1}{F^c_{H_1}(z)} - \frac{1}{F^c_{H_2}(z)} \\
&= \frac{1}{1+(w_0+w_1)z+(w_0w_1)z^2} + \frac{1}{1+(w_1+w_2)z+(w_1w_2)z^2} \\
&+ \frac{1}{1+(w_0+w_2)z+(w_0w_2)z^2} - \frac{1-w_1z}{1-z^2} - \frac{1-(w_0+w_2)z+z^2}{1-z^2} \\
&= \frac{1}{(1+w_0z)(1+w_1z)} + \frac{1}{(1+w_1z)(1+w_2z)} + \frac{1}{(1+w_0z)(1+w_2z)} \\
&- \frac{2-(w_0+w_1+w_2)z+z^2}{1-z^2} \\
&= \frac{3+(w_0+w_1+w_2)z}{(1+w_0z)(1+w_1z)(1+w_2z)} - \frac{2-Az+z^2}{1-z^2},
\end{aligned}$$

where $A = w_0 + w_1 + w_2$. ■

For another result of this work, let us consider the presentation of W_4 group given by (2). Thus we have the following result.

Theorem 3 *Let $F^c_{W_4}(z)$ be complete growth series of the group W_4. Then complete growth series of W_4 is given as follows:*

$$\frac{1}{F^c_{W_4}(z)} = \frac{3+2(w_0+w_3)z+Az^2}{(1+w_0z)(1+w_1z)(1+w_2z)(1+w_3z)} - \frac{5-2Bz+2z^2}{1-z^2},$$

where $A = 2w_0w_3 + w_1w_3 + w_2w_3 - w_1w_2$ and $B = w_0 + w_1 + w_2 + w_3$.

Proof. We take the presentation of W_4 group given by (2) and consider it as an amalgamated free product type. To do that, let K_1, K_2 and K_3 be subgroups of W_4 and they have the following presentations

$$K_1 =< w_0,\, w_1,\, w_2;\;\; w_0^2 = w_1^2 = w_2^2 = (w_0w_1)^2 = (w_0w_2)^2 = (w_1w_2)^2 = 1 >,$$
$$K_2 =< w_1,\, w_2,\, w_3;\;\; w_1^2 = w_2^2 = w_3^2 = (w_1w_2)^2 = (w_1w_3)^2 = (w_2w_3)^2 = 1 >$$

and

$$K_3 =< w_0,\, w_3;\;\; w_0^2 = w_3^2 = (w_0w_3)^2 = 1 >,$$

respectively. Firstly, let H_1 be a subgroup of K_1 and K_2 and it is presented by $H_1 =< w_1, w_2;\;\; w_1^2 = w_2^2 = (w_1w_2)^2 = 1 >$. That is, $H_1 \subset K_1$ and $H_1 \subset K_2$. Let $L_3 = K_1 *_{H_1} K_2$.

Next, let H_2 be a subgroup of K_3 and L_3 and it is presented by $H_2 =< w_0, w_3;\;\; w_0^2 = w_3^2 = 1 >$. That is, $H_2 \subset K_3$ and $H_2 \subset L_3$. Now we can consider amalgamated free product of K_3 and L_3 by the subgroup H_2 as W_4. It is seen that W_4 has the following presentation

$$\begin{aligned} W_4 = K_3 *_{H_2} L_3 =< w_0,\, w_1,\, w_2,\, w_3;\;\; w_0^2 &= w_1^2 = w_2^2 = w_3^2 = (w_0w_1)^2 = (w_0w_2)^2 = (w_0w_3)^2 \\ &= (w_1w_2)^2 = (w_1w_3)^2 = (w_2w_3)^2 = 1 > . \end{aligned}$$

Hence, by formula given in Theorem 1 we obtain

$$\begin{aligned} \frac{1}{F^c_{W_3}(z)} &= \left(\frac{1}{F^c_{K_3}(z)} + \frac{1}{F^c_{L_3}(z)} - \frac{1}{F^c_{H_2}(z)}\right) \\ &= \left(\frac{1}{F^c_{K_3}(z)} + \left(\frac{1}{F^c_{K_1}(z)} + \frac{1}{F^c_{K_2}(z)} - \frac{1}{F^c_{H_1}(z)}\right) - \frac{1}{F^c_{H_2}(z)}\right) \\ &= \frac{1}{F^c_{K_1}(z)} + \frac{1}{F^c_{K_2}(z)} + \frac{1}{F^c_{K_3}(z)} - \frac{1}{F^c_{H_1}(z)} - \frac{1}{F^c_{H_2}(z)} \\ &= \frac{3 + (w_0 + w_1 + w_2)z}{(1 + w_0z)(1 + w_1z)(1 + w_2z)} - \frac{2 - (w_0 + w_1 + w_2)z + z^2}{1 - z^2} \\ &+ \frac{3 + (w_1 + w_2 + w_3)z}{(1 + w_1z)(1 + w_2z)(1 + w_3z)} - \frac{2 - (w_1 + w_2 + w_3)z + z^2}{1 - z^2} \\ &+ \frac{1}{1 + (w_0 + w_3)z + (w_0w_3)z^2} - \frac{1}{1 + (w_1 + w_2)z + (w_1w_2)z^2} - \frac{1 - (w_0 + w_3)z + z^2}{1 - z^2} \\ &= \frac{3 + 2(w_0 + w_3)z + (2w_0w_3 + w_1w_3 + w_2w_3 - w_1w_2)z^2}{(1 + w_0z)(1 + w_1z)(1 + w_2z)(1 + w_3z)} \\ &- \frac{5 - 2(w_0 + w_1 + w_2 + w_3)z + 2z^2}{1 - z^2} \\ &= \frac{3 + 2(w_0 + w_3)z + Az^2}{(1 + w_0z)(1 + w_1z)(1 + w_2z)(1 + w_3z)} - \frac{5 - 2Bz + 2z^2}{1 - z^2}, \end{aligned}$$

where $A = 2w_0w_3 + w_1w_3 + w_2w_3 - w_1w_2$ and $B = w_0 + w_1 + w_2 + w_3$. ■

Finally, let us consider the presentation of W_n group given by (3). Then we have

$$W_n = (W_2 *_{H_2} (W^{'}_{n-1} *_{H_{n-2}} W^{''}_{n-1})),$$

where W_2 is a commutator group with two generators of orders 2, $W^{'}_{n-1}$ and $W^{''}_{n-1}$ are commutator groups with $n-1$ generators of orders 2. Also, let $H_2 \subset (W^{'}_{n-1} *_{H_{n-2}} W^{''}_{n-1})$, $H_2 \subset W_2$, $H_{n-2} \subset W^{'}_{n-1}$ and $H_{n-2} \subset W^{''}_{n-1}$. Now we can present the last result of this work as follows.

Corollary 4 *Let $F^c_{W_n}(z)$ be complete growth series of the group $W_n = (W_2 *_{H_2} (W'_{n-1} *_{H_{n-2}} W''_{n-1}))$. Then $F^c_{W_n}(z)$ is given as follows:*

$$\frac{1}{F^c_{W_n}(z)} = \frac{1}{F^c_{W_2}(z)} + \frac{1}{F^c_{W'_{n-1}}(z)} + \frac{1}{F^c_{W''_{n-1}}(z)} - \frac{1}{F^c_{H_2}(z)} - \frac{1}{F^c_{H_{n-2}}(z)}.$$

We note that if we apply some operations on relators given the presentations in (1), (2) and (3), we the obtain some known important group types, namely elliptic Weyl groups of types $A_1^{(1,1)*}$, $A_1^{(1,1)}$ and n-extended affine Weyl group of type A_1, respectively.

Finally, we note that in [11], the authors obtained complete rewriting system and thus normal form of elements of W_3, W_4 and W_n groups by using their presentations given by (1), (2) and (3). Therefore they showed the solvability of the word problem for these groups. So this study can be considered as a continuation work of [11].

References

[1] D. Allen, M. Cream, K. Finlay, J. Meier, R. Rohatgi, Complete growth series and products of groups, *New York J. Math.*, **17** (2011) 321-329.

[2] J. M. Alonso, Growth functions of amalgams, *in Arboreal Group Theory*, Proceedings of a Workshop Held September 13-16, 1988, editors in Roger C. Alperin, Springer.

[3] M. Benson, On the rational growth of virtually nilpotent groups, in: Combinatorial Group Theory and Topology, *Princeton University Press*, (1987) 185-196.

[4] J. Cannon, The growth of the closed surface groups and the compact hyperbolic Coxeter groups, preprint (1980).

[5] J. Cannon, The combinatorial structure of compact discrete hyperbolic groups, *Geometriae Dedicata*, **16** (1984) 123-148.

[6] M. Edjvet, D. L. Johnson, The growth of certain amalgamated free products and HNN-extensions, *J. Austral. Math. Soc.(Series A)* **52** (1992) 285-298.

[7] W. Floyd, S. Plotnik, Growth functions on Fuchsian groups and the Euler characteristic, *Invent. Math.*, **88** (1987) 1-29.

[8] R. I. Grigorchuk, T. Nagnibeda, Complete growth functions of hyperbolic groups, *Inv. Math.*, **130** (1997) 159-188.

[9] P. de la Harpe, *Topics in Geometric Group Theory*, Chicago Lectures in Mathematics, (2000).

[10] D. L. Johnson, Rational growth of wreath products, *Cambridge University Press*, **160** (1991) 309-315.

[11] E. K. Çetinalp, E. G. Karpuz, Complete Rewriting Systems of Some Types of Amalgamated Free Product of Groups, ICOM2018, 3-6 July 2018 Conference Proceedings Book, pp 46-51.

[12] M. Mamaghani, Rewriting systems and the complete growth series for triangular Coxeter groups, *Mathematical Notes*, **71**(3) (2002) 392-399.

[13] M. J. Mamaghani, Complete growth series of Coxeter groups with more than three generators, *Math.Socienty* , **29**(1) (2003) 65-76.

[14] A. Mann, The growth of free products, *Journal of Algebra*, **326** (2011) 208-217.

[15] M. Shapiro, A geometric approach to growth and almost convexity in some nilpotent groups, *Mathematische Annalen*, **285** (1989) 601-624.

Optimum Design Of Spatial Steel Frames Using Water Cycle Algorithm With Evaporation Rate

Serdar ÇARBAŞ *
Department of Civil Engineering,
Karamanoglu Mehmetbey University,
Karaman/TURKEY

İbrahim AYDOĞDU
Department of Civil Engineering,
Akdeniz University,
Antalya/TURKEY

Abstract

In this paper, an algorithm is presented for the optimum design of the spatial steel frames. The optimum design problem is formulated according to specifications of LRFD-AISC. Design constraints include the displacement limitations, inter-story and top-story drift restrictions of multi-story frames, strength requirements for beams and beam-columns and geometric constraints. Water Cycle Algorithm (WCA), inspired by the observation of water cycle process and how rivers and streams flow to the sea. For improving the global search ability of WCA, a new concept of evaporation rate for different rivers and streams is defined that is so-called WCA with Evaporation Rate (WCA-ER). The design algorithm developed selects optimum W sections for beams and columns of spatial steel frames so that aforesaid constraints are satisfied and the frame has the minimum weight. A spatial steel frame has been designed by WCA-ER to test performance of the developed algorithm.

Keywords: Design optimization, water cycle algorithm, spatial steel frame.

1 Introduction

Mostly, spatial steel frames are opted for residential and commercial building construction since they have eminent strength and ductility characterization. Over than two decades, the natural resources have been melted away rapidly. One of the primary reasons to this danger of extinction is that the increment the utilized raw materials at the construction sites. If the designer meets required criteria and performance of buildings, and also considers how to design steel buildings most economically, usage of world's resources markedly reducible. That is to say, the designer has to pay regard to optimum design of steel buildings. Therewithal, design optimization of steel buildings is not a simple effort for designers since most design problems are highly nonlinear. Furthermore, they contain discrete design variables and consist of complex design restrictions on highest strength capacities of structural members, displacements, stability and geometric compatibilities [1]. Stochastic search optimization methods are significant instruments for optimum design of steel frame skeletal building problems. These techniques, which are so-called metaheuristics, take their basis from inspiring natural phenomena [2-4]. The Water Cycle Algorithm (WCA) is one of the recent additions to metaheuristics that is inspired from the based on the observation of water cycle and how rivers and streams flow downhill towards the sea in the real world [5]. WCA is a powerful technique used in engineering optimization and it has been used in engineering optimization studies [6].

*Corresponding author. *E-mail address:* scarbas@kmu.edu.tr

2 Mathematical Modeling Of Optimum Design Of Spatial Steel Frames

Optimum design of spatial steel frames problems are specified as the chosen of steel sections for its frame group members from available steel section profile lists in the standards such that serviceability, strength and geometric restrictions defined by the code of practice. The objective function of optimum design problem is depicted as the weight minimization of the steel frame which is expressed as [1]:

$$\mathrm{W(x)} = \sum_{\mathrm{r=1}}^{\mathrm{NG}} \mathrm{m_r} \sum_{\mathrm{s=1}}^{\mathrm{t_r}} \mathrm{l_s} \tag{1}$$

where; W is the weight of the steel frame, x is the vector of steel sections in the steel frame which are described as design variables, m_r is the unit weight of the steel section adopted for member group r, t_r is the total number of members in group r and NG is the total number of member groups, l_s is the length of member which belongs to group r. These optimization problems are subjected to design constraints functions which are described in a formula as follows:

$$[\mathrm{g_i(x)}]_{\mathrm{i=1}}^{\mathrm{NC}} = \sum \mathrm{g_s(x)},\ \sum \mathrm{g_d(x)},\ \sum \mathrm{g_{td}(x)},\ \sum \mathrm{g_{id}(x)},\ \sum \mathrm{g_{cc}(x)},\ \sum \mathrm{g_{bc}(x)} \tag{2}$$

where; g_s, g_d, g_{td}, g_{id}, g_{cc} and g_{bc} are the constraints functions for strength, deflection, inter-story drift, top story drift, column-to-column geometric and beam-to-column geometric constraints functions according to design code LRFD respectively. Strength constraint function is defined from inequalities given in Chapter H of LRFD-AISC as:

$$g_s(x) = \left(\frac{\mathrm{P_u}}{\phi_\mathrm{c}\mathrm{P_n}}\right) + \left(\frac{8}{9}\frac{\mathrm{M_{ux}}}{\phi_\mathrm{b}\mathrm{M_{nx}}}\right) \leq 1.0 \quad \text{for } \frac{\mathrm{P_u}}{\phi_\mathrm{c}\mathrm{P_n}} \geq 0.2 \tag{3}$$

$$g_s(x) = \left(\frac{\mathrm{P_u}}{2\phi_\mathrm{c}\mathrm{P_n}}\right) + \left(\frac{\mathrm{M_{ux}}}{\phi_\mathrm{b}\mathrm{M_{nx}}}\right) \leq 1.0 \quad \text{for } \frac{\mathrm{P_u}}{\phi_\mathrm{c}\mathrm{P_n}} \leq 0.2$$

where, M_{nx} is the nominal flexural strength at strong axis (x axis), M_{ny} is the nominal flexural strength at weak axis (y axis), M_{ux} is the required flexural strength at strong axis (x axis), M_{uy} is the required flexural strength at weak axis (y axis), P_n is the nominal axial strength (Tension or compression) and $P_u$is the required axial strength (Tension or compression) for member i. Deflection constraints are calculated by using

$$g_d(x) = \frac{\delta_{jl}}{L/Ratio} - 1.0 \leq 0.0 \qquad (\mathrm{j} = 1, 2, ..., \mathrm{n}_{sm},\ \mathrm{l} = 1, 2, ..., \mathrm{n}_{lc}) \tag{4}$$

where ,δ_{jl} is the maximum deflection of j^{th} member under the lth load case, L is the length of member, n_{sm} is the total number of members where deflections limitations are to be imposed, n_{lc} is the number of load cases. Top story drift constraint function is given as:

$$\mathrm{g_{td}(x)} = \frac{\Delta_{\mathrm{jl}}^{\mathrm{top}}}{\mathrm{H/Ratio}} - 1.0 \leq 0.0 \qquad (\mathrm{j} = 1, 2, ..., \mathrm{n_{jtop}},\ \mathrm{l} = 1, 2, ..., \mathrm{n_{lc}}) \tag{5}$$

Inter story drift constraint function is given as:

$$\mathrm{g_{id}(x)} = \frac{\Delta_{\mathrm{jl}}^{\mathrm{oh}}}{\mathrm{h}_{sx}/\mathrm{Ratio}} - 1.0 \leq 0.0 \qquad (\mathrm{j} = 1, 2, ..., \mathrm{n}_{st},\ \mathrm{l} = 1, 2, ..., \mathrm{n_{lc}}) \tag{6}$$

In these equations, H is the height of the frame, n_{jtop} is the number of joints on the top story, ${\Delta_{jl}}^{top}$ is the top story displacement of the j^{th} joint under lth load case, n_{st} is the number of story, n_{lc} is the number of load cases ,${\Delta_{jl}}^{oh}$ is the story drift of the j^{th} story under l^{th} load case, h_{sx} is the story height and Ratio is the limitation ratio for lateral displacements. Range of drift limits by first-order analysis is 1/750 to 1/250 times the building height H with a recommended value of H/400. Two types of geometric limitations, called column to column geometric constraints and beam to column geometric constraints are included in the design problem and defines as shown in Equations (7) and (8), respectively.

$$g_{cc}(x) = \sum_{i=1}^{n_{ccj}} \left(\frac{D_i^a}{D_i^b} - 1.0 \right) \text{ and } \sum_{i=1}^{n_{ccj}} \left(\frac{m_i^a}{m_i^b} - 1.0 \right) \leq 0.0 \tag{7}$$

$$g_{bc}(x) = \sum_{i=1}^{n_{j1}} \left(\frac{B_f^{bi}}{D^{ci} - 2t_b^{ci}} - 1.0 \right) \text{ or } \sum_{i=1}^{n_{j2}} \left(\frac{B_f^{bi}}{B_f^{ci}} - 1.0 \right) \leq 0.0 \tag{8}$$

In these equations; n_{ccj} is the number of column to column geometric constraints defined in the problem, m_i^a is the unit weight of W section selected for above story, m_i^b is the unit weight of W section selected for below story, D_i^a is the depth of W section selected for above story, D_i^b is the depth of W section selected for below story, n_{j1} is the number of joints where beams are connected to the web of a column, n_{j2} is the number of joints where beams connected to the flange of a column, D^{ci} is the depth of W section selected for the column at joint i, t_b^{ci} is the flange thickness of W section selected for the column at joint i, B_f^{ci} is the flange width of W section selected for the column at joint i and B_f^{bi} is the flange width of W section selected for the beam at joint i.

3 Water Cycle Algorithm With Evaporation Rate

The idea of the WCA is inspired by nature and based on the observation of water cycle process and how rivers and streams flow downhill toward the sea in nature [5]. To further clarify, some basics of how rivers are created and water travels down to the sea are provided as follows. A river, or a stream, is formed whenever water moves downhill from one place to another. This means that most rivers are formed high up in the mountains, where snow from the winter or ancient glaciers is melting. Water in rivers is evaporated, while plants discharge (transpire) water through photosynthesis process as shown in Figure 1.

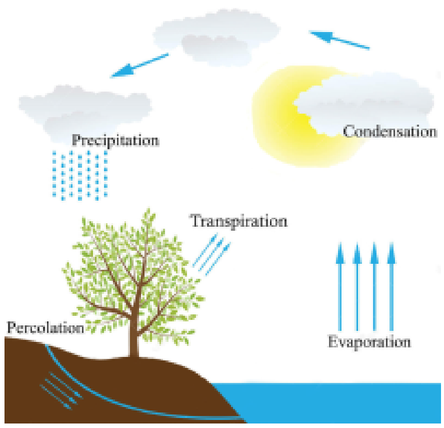

Figure 1: Hydrologic cycle (water cycle process

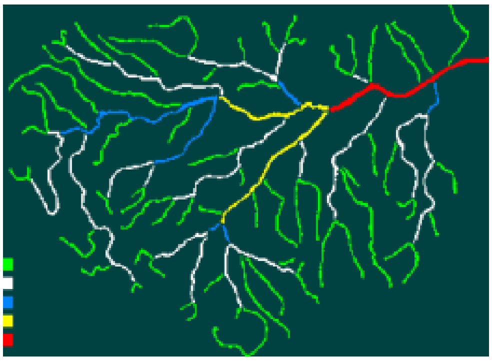

Figure 2: Diagram of streams having different orders flowing to a river

The evaporated water is carried into the air to produce clouds which then condenses in the colder weather. Afterwards, the water returns to earth in the form of rain. This natural procedure is known as the hydrologic cycle [7].Figure 2 is a schematic diagram of how streams having deferent orders flow to the river. The smallest river branches are the small streams where the rivers begin to form. These tiny streams are called first-order streams as shown in Figure 2 in green colors. A second-order stream shown in Fig. 2 in white colors is produced when two first-order streams are joined. A third-order stream is formed where two second-order streams join, which is shown in Figure 2 in blue colors, and such process continues until the river flows out into the sea [8]. Finally, all of the rivers flow to the sea (i.e., the most downhill place). WCA with Evaporation Rate (WCA-ER) was proposed in order to improve the performance of standard WCA [9]. In WCA-ER, available evaporation rate is de?ned to amend the evaporation of the water adaptively. In addition, WCA-ER forces new generated streams to search near sea using the concept of variance. In WCA-ER, the occurrence of evaporation condition decreases as the iteration continues. In evaporation based WCA (WCA-ER), similar to WCA, the surface run-off phase considered as updating equations (movement equations) does not altering WCA-ER. However, to increase the chance of escaping from the local optima, the evaporation condition is introduced in WCA by de?ning a speci?c criterion, which is called the Evaporation Rate (ER). In other words, in WCA-ER, the evaporation process is considered by adding the concept of ER based on the assigned number of streams to rivers [10]. The detail and more complex mathematical formulations are given and explained in Refs. [6, 9, 10] and which are not repeated here.

4 Design Example

A two-story, two-bay irregular spatial steel frame [11] having 21 members that are collected in two beam and three column design groups, is used as design example of this study. The dimensions and member groupings in the frame are shown in the Figure 3. The frame is subjected to wind loading of 50kN along Z axis in addition to 20kN/m gravity load which is applied to all beams. The drift ratio limits are defined as 1 cm for inter story drift 4 cm for top story drift where H is the height of frame. Maximum deflection of beam members is restricted as 1.39 cm. The initial optimization parameters used for the WCA-ER for the considered problem design are taken as N_{pop}, N_{sr}, d_{max}, max_iter (maximum number of iteration) whose values are assigned as 20, 4, 10^{-3} and 10000, respectively.

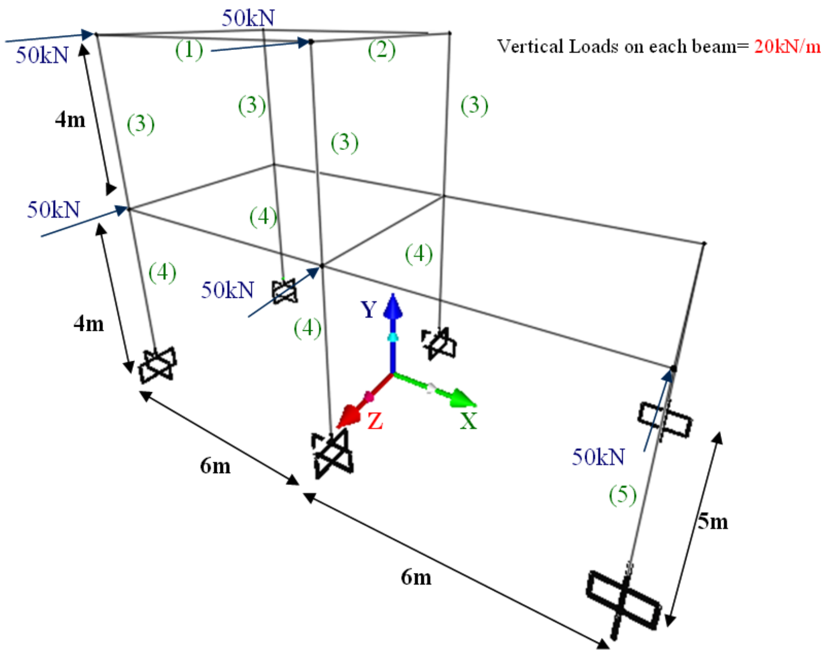

Figure 3: Two-story, two bay irregular spatial steel frame.

Table 1: Design results of two-story, two bay irregular spatial steelframe

Group number	Group type	Water Cycle Algorithm with Evaporation Rate
1	Beam	W460x60
2	Column	W360x32.9
3	Column	W410x60
4	Column	W410x67
5	Column	W310x38.7
Minimum weight-kN (kg)		49.13 (5009.88)
Maximum top story drift (cm)		1.85
Maximum inter- story drift (cm)		0.95
Maximum strength constraint ratio		0.852
Maximum number of Iterations		10000

The minimum weight, maximum constraints values and designated steel sections to the member groups of optimum designs obtained from WCA-ER are illustrated in Table 1. It is apparent from tables that the minimum weight is obtained as 49.13 kN (5009.88 kg). Moreover, the top-story drift, the inter-story drift and maximum strength constraint ratio are obtained as 1.85 cm, 0.95 cm, and 0.852, respectively. The inter-story drift is relatively very close to its upper bound of 1.0 if it is compared to the other constraints. So, these results shows that the inter-story drift constraint is dominate in this example and govern the optimization process.

5 Conclusions

In this study, an optimum design algorithm which is based on WCA-ER algorithm is developed for optimum design of spatial steel frame problems. A spatial steel frame is designed in order to test efficiency of WCA-ER for optimum design of spatial steel frame problems. Optimum design obtained from the WCA-ER indicates that the performance of the proposed algorithm is promising. Therefore it can be concluded that, WCA-ER is a robust and efficient approach that can be effectively used to determine the optimum designs of spatial steel frames.

References

[1] I. Aydogdu and A. Akin, Teaching and Learning Based Optimization Algorithm for Optimum Design of Steel Buildings, Comput. Civ. Build. Eng., ASCE, (2014) 20167-20175.

[2] M. P. Saka, Optimum Design of Skeletal Structures: A Review. Chapter 10 of Progress in Civil and Structural Engineering Computing, Saxe-Coburg Publications (2003) 237-284.

[3] M. P. Saka, Optimum Design of Steel Frames Using Stochastic Search Techniques Based on Natural Phenomena: A Review. Chapter 6 of Civil Engineering Computations: Tools and Techniques, Saxe-Coburgh Publications (2007) 105-147.

[4] M. P. Saka, I. Aydoğdu, O. Hasaçebi, and Z. W. Geem, Harmony Search Algorithms in Structural Engineering. Computational Optimization and Applications in Engineering and Industry, Studies in Computational Intelligence, Springer, (2011) 145-182.

[5] H. Eskandar, S. Sadollah, A. Bahreininejad, and M. Hamdi, Water cycle algorithm-A novel metaheuristic optimization method for solving constrained engineering optimization problems. Computs. Structs 110-111 (2012) 151-166.

[6] A. Sadollah, H. Eskandar, A. Bahreininejad, and J-H. Kim, Water cycle algorithm with evaporation rate for solving constrained and unconstrained optimization problems. Appl. Soft Comput., 30 (2015) 58-71.

[7] S. David, The Water Cycle (John Yates, Illus), Thomson Learning, New York,1993.

[8] A.N. Strahler, Dynamic basis of geomorphology, Geol. Soc. Am. Bull. 63 (1952) 923–938.

[9] A. Sadollah, H. Eskandar, and J. H. Kim, Water cycle algorithm for solving constrained multi-objective optimization problems, Appl. Soft Comput., 27 (2015) 279–298.

[10] S. M. Abedi Pahnehkolaei, A. Alfia, A. Sadollah, and J-H. Kim, Gradient-based Water Cycle Algorithm with evaporation rate applied to chaos suppression, Appl. Soft Comput., 53 (2017) 420–440.

[11] I. Aydogdu, Optimum Design of 3-D Irregular Steel Frames Using Ant Colony Optimization Method, Ph.D. Thesis, Middle East Technical University, Ankara, Turkey, 2010.

New Improvements of Hadamard Type Inequalities for $P-$ Functions via Katugampola Fractional Integral Operators

Ahmet OCAK AKDEMİR*
Department of Mathematics,
Faculty of Science and Letters,
Ağrı İbrahim Çeçen University,
Ağrı, Turkey

Erhan SET
Department of Mathematics,
Faculty of Science and Arts,
Ordu University,
Ordu, Turkey

Abstract

In this paper, some new improvements of Hadamard-type inequalities for $P-$functions by using Katugampola fractional integral operators have been proved.

1 Introduction

In this section, we will recall some definitions, inequalities and concepts. Firstly, we will start with the definition of convexity that has an important place in the inequality theory.

Definition 1 *Let I be an interval in $\mathbb{R}$ and $f : I \to \mathbb{R}$ is a function. We say that f is convex if the inequality;*

$$f(\alpha x + (1-\alpha)y) \leq \alpha f(x) + (1-\alpha)f(y)$$

holds for all $x, y \in I$ and $\alpha \in [0,1]$.

This famous function class has been used to obtain the celebrated Hermite-Hadamard inequality that give us upper and lower bounds for the mean value of functions. Let $a, b \in I$, $a < b$ and $f : I \subset \mathbb{R} \to \mathbb{R}$ be a convex function that is defined on a subset of real numbers. The following inequality is well known in the literature as the Hermite-Hadamard integral inequality (see [7, 8]):

$$f\left(\frac{a+b}{2}\right) \leq \frac{1}{b-a}\int_a^b f(x)dx \leq \frac{f(a)+f(b)}{2}.$$

The beginning of fractional integral calculus accompanies the beginning of the integral calculus, developed by Riemann. It originates int the research of Liouville from 1832 related to practical technical problems. Now we point few stages in evaluation of the fractional calculus, as needed in developing the new results. More details on the fractional differentiation and integration are in (see [6, 11, 13]), for example. The Riemann-Liouville fractional integral is, from historic point of view, at the origin of the fractional calculus. It comes from the following Cauchy n times iterative integration process,

$$\int_a^x dt_1 \int_a^{t_1} dt_2 \ldots \int_a^{t_{n-1}} f(t_n)dt_n = \frac{1}{\Gamma(\alpha)}\int_a^x (x-1)^{\alpha-1} f(t)dt$$

for $n \in \mathbb{N}^*$.

*Corresponding author. *E-mail address:* aocakakdemir@gmail.com

Definition 2 *(See [1]) Let $f \subseteq \mathbb{R} \to \mathbb{R}$ be a non-negative function. f is said to be $P-$function if the inequality;*

$$f(\alpha x + (1-\alpha)y) \leq f(x) + f(y)$$

holds for all $x, y \in I$, $\alpha \in [0,1]$

Katugampola ([9] and [10]) considered the following iterative process in 2011:

$$\int_a^x t_1^\rho dt_1 \int_a^{t_1} t_2^\rho dt_2 \ldots \int_a^{t_{n-1}} t_n^\rho f(t_n) dt_n = \frac{(\rho+1)^{1-n}}{(n-1)!} \int_a^x (t^{\rho+1} - \tau^{\rho+1})^{n-1} \tau^\rho f(\tau) d\tau.$$

Definition 3 See [9] *Let $f \in [a,b]$.*

1. *The left-sided Katugampola fractional integral ${}^\rho\mathcal{I}_{a+}^\alpha f$ of order $\alpha \in \mathbb{C}$, $\Re(\alpha) > 0$ is defined by*
$$ {}^\rho\mathcal{I}_{a+}^\alpha f(x) = \frac{\rho^{1-\alpha}}{\Gamma(\alpha)} \int_a^x \frac{t^{\rho-1}}{(x^\rho - t^\rho)^{1-\alpha}} f(t) dt, \quad x > a,$$
2. *The right-sided Katugampola fractional integral ${}^\rho\mathcal{I}_{b-}^\alpha f$ of order $\alpha \in \mathbb{C}$, $\Re(\alpha) > 0$ is defined by*
$$ {}^\rho\mathcal{I}_{b-}^\alpha f(x) = \frac{\rho^{1-\alpha}}{\Gamma(\alpha)} \int_x^b \frac{t^{\rho-1}}{(t^\rho - x^\rho)^{1-\alpha}} f(t) dt, \quad x < b.$$

Katugampola's operators are generalizations of A. Erdélyi and H. Kober operators introduced in 1940 (see [5] and [12]), as well. Other similar approaches on moving iterative integrals and derivatives into fractional framework in connection with theoretic and practical applications are in the mathematical literature of the last decade. For example, the results of Cristescu [4] in 2016.

Remark 4 *If we set $\rho = 1$, then the Katugampola fractional integrals become Riemann-Liouville fractional integrals.*

The main aim of this paper is to establish new Hermite-Hadamard type integral inequalities by using generalized Katugampola fractional integral for $P-$convex functions and prove some results connected with them (see for example, [2, 3, 14]).

2 Main Results

The following theorem includes integral inequalities of Hadamard-type for P-functions.

Theorem 5 *Let $f : [a^\rho, b^\rho] \to \mathbb{R}$ be a function with $0 \leq a < b$, and $f \in X_c^p(a^\rho, b^\rho)$. If f is $P-$function on $[a,b]$, then the following inequalities hold;*

$$\begin{aligned} & \frac{1}{2} f\left(\frac{a^\rho + b\rho}{2}\right) \\ \leq \quad & \frac{2^{\alpha-1}\alpha\rho^\alpha\Gamma(\alpha+1)}{(b^\rho - a^\rho)^\alpha} \left[{}^\rho\mathcal{I}^\alpha_{\left(\frac{a^\rho+b^\rho}{2}\right)^+} f(b^\rho) + {}^\rho \mathcal{I}^\alpha_{\left(\frac{a^\rho+b^\rho}{2}\right)^-} f(a^\rho) \right] \leq [f(a^\rho) + f(b^\rho)] \end{aligned} \tag{1}$$

where

$$\left[\left(\Re\left(2^{\frac{1}{\rho}} \geq 1\right) \vee \Re\left(2^{\frac{1}{\rho}} \leq 0\right) \vee 2^{\frac{1}{\rho}} \notin \mathbb{R} \right) \wedge \Re(\rho) > 0 \wedge \Re(\alpha\rho) > 0 \right]$$

the fractional integrals are considered for the function $f(x^\rho)$ and evaluated at a and b, respectively.

Proof. Since the function f is P-function on $[a,b]$, we can write

$$f\left(\frac{x^\rho+y^\rho}{2}\right)\leq f(x^\rho)+f(y^\rho)$$

for $x,y\in[a,b]$.

For $x^\rho=\frac{t^\rho}{2}a^\rho+\frac{2-t^\rho}{2}b^\rho$ and $y^\rho=\frac{2-t^\rho}{2}a^\rho+\frac{t^\rho}{2}b^\rho$, we have

$$f\left(\frac{a^\rho+b^\rho}{2}\right)\leq f\left(\frac{t^\rho}{2}a^\rho+\frac{2-t^\rho}{2}b^\rho\right)+f\left(\frac{2-t^\rho}{2}a^\rho+\frac{t^\rho}{2}b^\rho\right). \tag{2}$$

By multiplying both sides of (2) by $t^{\alpha\rho-1}$ and integrating with respect to t on $[0,1]$, we get

$$\begin{aligned}
&\frac{1}{\alpha\rho}f\left(\frac{a^\rho+b\rho}{2}\right) \qquad (3)\\
\leq\;& \int_0^1 t^{\alpha\rho-1}f\left(\frac{t^\rho}{2}a^\rho+\frac{2-t^\rho}{2}b^\rho\right)dt+\int_0^1 t^{\alpha\rho-1}f\left(\frac{2-t^\rho}{2}a^\rho+\frac{t^\rho}{2}b^\rho\right)dt\\
=\;& 2^\alpha\left[\int_a^{\left(\frac{a^\rho+b^\rho}{2}\right)^{\frac{1}{\rho}}}\left(\frac{x^\rho-a^\rho}{b^\rho-a^\rho}\right)^{\alpha-1}\frac{x^{\rho-1}}{(b^\rho-a^\rho)}f(x^\rho)dx\right.\\
&\left.+\int_{\left(\frac{a^\rho+b^\rho}{2}\right)^{\frac{1}{\rho}}}^b\left(\frac{b^\rho-x^\rho}{b^\rho-a^\rho}\right)^{\alpha-1}\frac{x^{\rho-1}}{(b^\rho-a^\rho)}f(x^\rho)dx\right]\\
=\;& \frac{2^\alpha\rho^{\alpha-1}\Gamma(\alpha+1)}{(b^\rho-a^\rho)^\alpha}\left[{}^\rho\mathcal{I}^\alpha_{\left(\frac{a^\rho+b^\rho}{2}\right)^+}f(b^\rho)+{}^\rho\mathcal{I}^\alpha_{\left(\frac{a^\rho+b^\rho}{2}\right)^-}f(a^\rho)\right]
\end{aligned}$$

which completes the proof of first inequality. To prove the second inequality, if we consider the definition of P-function, we have

$$f\left(\frac{t^\rho}{2}a^\rho+\frac{2-t^\rho}{2}b^\rho\right)\leq f(a^\rho)+f(b^\rho)$$

and

$$f\left(\frac{2-t^\rho}{2}a^\rho+\frac{t^\rho}{2}b^\rho\right)\leq f(a^\rho)+f(b^\rho).$$

By addition, we get

$$f\left(\frac{t^\rho}{2}a^\rho+\frac{2-t^\rho}{2}b^\rho\right)+f\left(\frac{2-t^\rho}{2}a^\rho+\frac{t^\rho}{2}b^\rho\right)\leq 2[f(a^\rho)+f(b^\rho)]. \tag{4}$$

By multiplying both sides of (4) by $t^{\alpha\rho-1}$ and integrating with respect to t on $[0,1]$, we deduce

$$\frac{2^\alpha\rho^{\alpha-1}\Gamma(\alpha+1)}{(b^\rho-a^\rho)^\alpha}\left[{}^\rho\mathcal{I}^\alpha_{\left(\frac{a^\rho+b^\rho}{2}\right)^+}f(b^\rho)+{}^\rho\mathcal{I}^\alpha_{\left(\frac{a^\rho+b^\rho}{2}\right)^-}f(a^\rho)\right]\leq\frac{2[f(a^\rho)+f(b^\rho)]}{\alpha\rho}$$

$$\left[\left(\Re\left(2^{\frac{1}{\rho}}\geq 1\right)\vee\Re\left(2^{\frac{1}{\rho}}\leq 0\right)\vee 2^{\frac{1}{\rho}}\notin\mathbb{R}\right)\wedge\Re(\rho)>0\wedge\Re(\alpha\rho)>0\right].$$

So, the proof is completed. ■

Corollary 6 *If we choose $\rho=1$ in (**??**), we have*

$$f\left(\frac{a+b}{2}\right)\leq\frac{2^{\alpha-1}\alpha\Gamma(\alpha+1)}{(b-a)^\alpha}\left[\mathcal{I}^\alpha_{\left(\frac{a+b}{2}\right)^+}f(b)+\mathcal{I}^\alpha_{\left(\frac{a+b}{2}\right)^-}f(a)\right]\leq[f(a)+f(b)].$$

Lemma 7 *(See [15]) Let $f:[a^\rho,b^\rho]\to\mathbb{R}$ be a differentiable function on (a^ρ,b^ρ) and $0\le a<b$. Then the following equality holds:*

$$\begin{aligned}&\frac{2^\alpha\rho^\alpha\Gamma(\alpha+1)}{(b^\rho-a^\rho)^\alpha}\left[{}^\rho\mathcal{I}^\alpha_{\left(\frac{a^\rho+b^\rho}{2}\right)^+}f(b^\rho)+{}^\rho\mathcal{I}^\alpha_{\left(\frac{a^\rho+b^\rho}{2}\right)^-}f(a^\rho)\right]-f\left(\frac{a^\rho+b^\rho}{2}\right) \qquad (5)\\ =\ &\frac{(b^\rho-a^\rho)\rho}{4}\left[\int_0^1 t^{\alpha\rho}f'\left(\frac{t^\rho}{2}a^\rho+\frac{2-t^\rho}{2}b^\rho\right)dt-\int_0^1 t^{\alpha\rho}f'\left(\frac{2-t^\rho}{2}a^\rho+\frac{t^\rho}{2}b^\rho\right)dt\right].\end{aligned}$$

Theorem 8 *Suppose that $f:[a^\rho,b^\rho]\to\mathbb{R}$ a differentiable function on (a^ρ,b^ρ) and $0\le a<b$. If $|f'|$ is $P-$function on $[a^\rho,b^\rho]$, the one has the following inequality*

$$\begin{aligned}&\left|\frac{2^\alpha\rho^\alpha\Gamma(\alpha+1)}{(b^\rho-a^\rho)^\alpha}\left[{}^\rho\mathcal{I}^\alpha_{\left(\frac{a^\rho+b^\rho}{2}\right)^+}f(b^\rho)+{}^\rho\mathcal{I}^\alpha_{\left(\frac{a^\rho+b^\rho}{2}\right)^-}f(a^\rho)\right]-f\left(\frac{a^\rho+b^\rho}{2}\right)\right| \qquad (6)\\ \le\ &\frac{(b^\rho-a^\rho)\rho}{2(\alpha\rho+1)}[|f'(a^\rho)|+|f'(b^\rho)|].\end{aligned}$$

Proof. By using the equality (5) with modulus and since $|f'|$ is P-function, we can write

$$\begin{aligned}&\left|\frac{2^\alpha\rho^\alpha\Gamma(\alpha+1)}{(b^\rho-a^\rho)^\alpha}\left[{}^\rho\mathcal{I}^\alpha_{\left(\frac{a^\rho+b^\rho}{2}\right)^+}f(b^\rho)+{}^\rho\mathcal{I}^\alpha_{\left(\frac{a^\rho+b^\rho}{2}\right)^-}f(a^\rho)\right]-f\left(\frac{a^\rho+b^\rho}{2}\right)\right|\\ \le\ &\frac{(b^\rho-a^\rho)\rho}{4}\left[\int_0^1 t^{\alpha\rho}\left|f'\left(\frac{t^\rho}{2}a^\rho+\frac{2-t^\rho}{2}b^\rho\right)\right|dt+\int_0^1 t^{\alpha\rho}\left|f'\left(\frac{2-t^\rho}{2}a^\rho+\frac{t^\rho}{2}b^\rho\right)\right|dt\right]\\ \le\ &\frac{(b^\rho-a^\rho)\rho}{4}\left[\int_0^1 t^{\alpha\rho}[|f'(a^\rho)|+|f'(b^\rho)|]dt+\int_0^1 t^{\alpha\rho}[|f'(a^\rho)|+|f'(b^\rho)|]dt\right]\\ \le\ &\frac{(b^\rho-a^\rho)\rho}{2(\alpha\rho+1)}[|f'(a^\rho)|+|f'(b^\rho)|]\end{aligned}$$

which is the desired result. ■

Corollary 9 *If we choose $\rho=1$ in (6), we obtain the following inequality;*

$$\left|\frac{2^{\alpha-1}\Gamma(\alpha+1)}{(b-a)^\alpha}\left[\mathcal{I}^\alpha_{\left(\frac{a+b}{2}\right)^+}f(b)+\mathcal{I}^\alpha_{\left(\frac{a+b}{2}\right)^-}f(a)\right]-f\left(\frac{a+b}{2}\right)\right|\le\frac{(b-a)}{2(\alpha+1)}[|f'(a)|+|f'(b)|].$$

Theorem 10 *Suppose that $f:[a^\rho,b^\rho]\to\mathbb{R}$ a differentiable function on (a^ρ,b^ρ) and $0\le a<b$. If $|f'|^q$ is P-function on $[a^\rho,b^\rho]$, the one has the following inequality*

$$\begin{aligned}&\left|\frac{2^\alpha\rho^\alpha\Gamma(\alpha+1)}{(b^\rho-a^\rho)^\alpha}\left[{}^\rho\mathcal{I}^\alpha_{\left(\frac{a^\rho+b^\rho}{2}\right)^+}f(b^\rho)+{}^\rho\mathcal{I}^\alpha_{\left(\frac{a^\rho+b^\rho}{2}\right)^-}f(a^\rho)\right]-f\left(\frac{a^\rho+b^\rho}{2}\right)\right| \qquad (7)\\ \le\ &\frac{(b^\rho-a^\rho)\rho}{2}\left(\frac{1}{\alpha\rho p+1}\right)^{\frac{1}{p}}[(|f'(a^\rho)|^q+|f'(b^\rho)|^q)^{\frac{1}{q}}]\end{aligned}$$

for $q>1$, $q^{-1}+p^{-1}=1$.

Proof. By using the equality (5) with Hölder inequality and due to $|f'|$ is P-function, we have

$$\begin{aligned}&\left|\frac{2^\alpha\rho^\alpha\Gamma(\alpha+1)}{(b^\rho-a^\rho)^\alpha}\left[{}^\rho\mathcal{I}^\alpha_{\left(\frac{a^\rho+b^\rho}{2}\right)^+}f(b^\rho)+{}^\rho\mathcal{I}^\alpha_{\left(\frac{a^\rho+b^\rho}{2}\right)^-}f(a^\rho)\right]-f\left(\frac{a^\rho+b^\rho}{2}\right)\right| \qquad (8)\\ \le\ &\frac{(b^\rho-a^\rho)\rho}{4}\left[\int_0^1 t^{\alpha\rho}\left|f'\left(\frac{t^\rho}{2}a^\rho+\frac{2-t^\rho}{2}b^\rho\right)\right|dt+\int_0^1 t^{\alpha\rho}\left|f'\left(\frac{2-t^\rho}{2}a^\rho+\frac{t^\rho}{2}b^\rho\right)\right|dt\right]\\ \le\ &\frac{(b^\rho-a^\rho)\rho}{4}\left(\int_0^1 t^{\alpha\rho p}dt\right)^{\frac{1}{p}}\\ &\times\left[\left(\int_0^1\left|f'\left(\frac{t^\rho}{2}a^\rho+\frac{2-t^\rho}{2}b^\rho\right)\right|^q dt\right)^{\frac{1}{q}}+\left(\int_0^1\left|f'\left(\frac{2-t^\rho}{2}a^\rho+\frac{t^\rho}{2}b^\rho\right)\right|^q dt\right)^{\frac{1}{q}}\right].\end{aligned}$$

It is easy to see that,

$$\int_0^1 \left| f'\left(\frac{t^\rho}{2}a^\rho + \frac{2-t^\rho}{2}b^\rho\right)\right|^q dt \le \int_0^1 [|f'(a^\rho)|^q + |f'(b^\rho)|^q]dt = |f'(a^\rho)|^q + |f'(b^\rho)|^q \quad (9)$$

and similarly

$$\int_0^1 \left| f'\left(\frac{2-t^\rho}{2}a^\rho + \frac{t^\rho}{2}b^\rho\right)\right|^q dt \le |f'(a^\rho)|^q + |f'(b^\rho)|^q. \quad (10)$$

By using (9) and (10) in (8), we have desired result. This completes the proof. ■

Corollary 11 *If we choose $\rho = 1$ in (7), we obtain the following inequality;*

$$\begin{aligned} &\left| \frac{2^{\alpha-1}\Gamma(\alpha+1)}{(b-a)^\alpha}\left[\mathcal{I}^\alpha_{\left(\frac{a+b}{2}\right)^+} f(b) + \mathcal{I}^\alpha_{\left(\frac{a+b}{2}\right)^-} f(a)\right] - f\left(\frac{a+b}{2}\right)\right| \\ \le\ & \frac{(b-a)}{2}\left(\frac{1}{\alpha p+1}\right)^{\frac{1}{p}} [|f'(a)|^q + |f'(b)|^q]^{\frac{1}{q}}. \end{aligned}$$

References

[1] S.S. Dragomir, J. Pečarić and L.E. Persson, *Some inequalities of Hadamard type,* Soochow J. Math., 21(3) (1995), 335-341.

[2] F. Chen, *A note on the Hermite-Hadamard inequality for convex functions on the coordinates,* J. Math. Ineq., 8(4) (2014), 915-923.

[3] H. Chen, U.N. Katugampola, *Hermite-Hadamard and Hermite-Hadamard-Fejer type inequalities for generalized fractional integrals,* J. Math. Anal. Appl., 446 (2017), 1274-1291.

[4] G. Cristescua, *Boundaries of Katugampola fractional integrals within the class of (h_1; h_2)- convex functions,* https://www.researchgate.net/publication/313161140.

[5] A. Erdeyi, *On fractional integration and its application to the theory of Hankel transforms,* The Quarterly Journal of Mathematics, Oxford, Second Series, 11 (1940), 293-303.

[6] R. Gorenflo and F. Mainardi, *Fractional calculus: integral and differential equations of fractional order,* Springer Verlag, Wien (1997), 223-276.

[7] J. Hadamard, *Etude sur les proprietes des fonctions entieres et en particulier define fonction considree par, Riemann,* J. Math. Pures. et Appl. 58 (1893), 171-215.

[8] J. Pečarić, F. Proschan and Y.L. Tong, *Convex Functions, Partial Orderings and Statistical Applications,* Academic Press, Inc 1992.

[9] U.N. Katugampola, *New approach to a generalized fractional integrals,* Appl. Math. Comput., 218(4) (2011), 860-865.

[10] U.N. Katugampola, *New approach to generalized fractional derivatives,* Bull. Math. Anal. Appl., 6(4), (2014), 1-15.

[11] A. A. Kilbas, H. M. Srivastava and J. J. Trujillo, *Theory and applications of fractional differential equations,* North-Holland Mathematics Studies, 204, Elsevier Sci. B.V., Amsterdam, 2006.

[12] H. Kober, *On fractional integrals and derivatives,* The Quarterly J. Math. (Oxford Series), 11(1) (1940), 193-211.

[13] S. Miller and B. Ross, *An introduction to the fractional calculus and fractional differential equations,* John Wiley & Sons, USA, 1993, p.2.

[14] M. Z. Sarıkaya, E. Set, H. Yaldız, N. Başak, *Hermite-Hadamard's inequalities for fractional integrals and related fractional inequalities,* Math Comput Model., 57(9-10) (2013), 2403-2407.

Conformable Double Laplace Transform For Fractional Partial Diferential Equations Arising in Mathematical Physics

Ozan ÖZKAN*
Selçuk University,
Department of Mathematics,
Konya, TURKEY

Ali KURT
Mustafa Kemal University,
Department of Mathematics,
Hatay, TURKEY

Abstract

The main aim of this article is obtaining the analytical solutions of space-time fractional partial differential equations arising in mathematical physics by using newly defined conformable double Laplace transform method. All the used derivatives are in conformable sense which is applicable, simple and well behaved arbitrary order derivative.

Keywords: Conformable Laplace transform, conformable fractional derivative, fractional partial differential equation.

1 Introduction

Differential equations which can be considered as modeled version of the nature is an interesting and essential area. They are used in many different disciplines of science such as engineering, physics, chemistry, social sciences. Due to the huge application area of differential equations the solution procedure of these equations have a great importance. One of the efficient and reliable technique for solutions of differential equations is integral transforms. By using integral transforms, differential equations can be reduced into algebraic equation. So the solution procedure becomes simple and more understandable.

Fractional calculus, which means arbitrary order differentiation and integration have been attracting many researchers' interest in the last decades [1, 2, 3, 4]. They are used for modeling the nonlinear and complex events in real world problems. Although there are many different definitions of fractional derivative and integrals, there are no evident geometrical interpretation because of their nonlocal character [5]. In addition to this scientists determined many flaws of these definitions. For instance [6]

1. The Riemann-Liouville derivative does not satisfy $D_a^\alpha 1 = 0$(Caputo derivative satisfies), if α is not a natural number.
2. All fractional derivatives do not satisfy the known formula of the derivative of the product of two functions.
$$D_a^\alpha(fg) = gD_a^\alpha(f) + fD_a^\alpha(g).$$
3. All fractional derivatives do not satisfy the known formula of the derivative of the quotient of two functions.
$$D_a^\alpha\left(\frac{f}{g}\right) = \frac{fD_a^\alpha(f) - gD_a^\alpha(g)}{g^2}.$$

*Corresponding author. *E-mail address:* oozkan@selcuk.edu.tr

4. All fractional derivatives do not satisfy the chain rule.

$$D_a^\alpha (fog)(t) = f^\alpha (g(t)) g^\alpha (t).$$

5. All fractional derivatives do not satisfy $D^\alpha D^\beta = D^{\alpha+\beta}$ in general.
6. In the Caputo definition it is assumed that the function f is differentiable.

To overcome these flaws Khalil *et. al.* [6] expressed a new fractional derivative and integral definition called conformable fractional derivative and integral.

Definition 1. *Let $f : [0,\infty) \to \mathbb{R}$ be a function. The α^{th} order "conformable fractional derivative" of f is defined by,*

$$D_\alpha (f)(t) = \lim_{\varepsilon \to 0} \frac{f(t + \varepsilon t^{1-\alpha}) - f(t)}{\varepsilon}$$

for all $t > 0, \alpha \in (0,1)$.

Definition 2. *If f is α-differentiable in some $(0,a), a > 0$ and $\lim_{t\to 0^+} f^{(\alpha)}(t)$ exists then define $f^{(\alpha)}(0) = \lim_{t\to 0^+} f^{(\alpha)}(t)$. The "conformable fractional integral" of a function f starting from $a \geq 0$ is defined as:*

$$I_\alpha^a (f)(t) = \int_a^t f(x) d_\alpha x = \int_a^t \frac{f(x)}{x^{1-\alpha}} dx$$

where the integral is the usual Riemann improper integral, and $\alpha \in (0,1]$.

This new fractional derivative satisfies the following basic properties and theorems referred in [6, 7]

1. $D_\alpha (cf + dg) = cD_\alpha (f) + cD_\alpha (g)$ for all $a, b \in \mathbb{R}$.
2. $D_\alpha (t^p) = pt^{p-\alpha}$ for all $p \in \mathbb{R}$.
3. $D_\alpha (\lambda) = 0$ for all constant functions $f(t) = \lambda$.
4. $D_\alpha (fg) = fD_\alpha (g) + gD_\alpha (f)$.
5. $D_\alpha \left(\frac{f}{g}\right) = \frac{gD_\alpha (f) - fD_\alpha (g)}{g^2}$.
6. If in addition to f is differentiable, then $D_\alpha (f)(t) = t^{1-\alpha} \frac{df}{dt}$.

2 Conformable Double Laplace Transform

Definition 3. *Let $u(x,t)$ be an exponential order, continuous function on the interval $[0,\infty)$ and for some $a, b \in \mathbb{R}$ $sup_{x>0,t>0} \frac{|u(x,t)|}{e^{\frac{ax^\beta}{\beta} + \frac{bt^\alpha}{\alpha}}} < \infty$ satisfied. Under these conditions conformable double Laplace transform is expressed by [8]*

$$\mathscr{L}_t^\alpha \mathscr{L}_x^\beta [u(x,t)] = U(p,s) = \int_0^\infty \int_0^\infty e^{-p\frac{x^\beta}{\beta} - s\frac{t^\alpha}{\alpha}} u(x,t) d_\alpha t d_\beta x \tag{1}$$

where $p, s \in \mathbb{C}$, $0 < \alpha, \beta \leq 1$ and the integrals are in the sense of conformable fractional integral.

2.1 Some Properties of Conformable Double Laplace Transform

Now some properties of conformable double Laplace Transform can be given as follows.

Theorem 4. *[8] Let $u(x,t)$, $w(x,t)$ be two functions which have the conformable double Laplace transform. Thus,*

1. *[i.]*
2. $\mathscr{L}_t^{\alpha}\mathscr{L}_x^{\beta}[c_1u(x,t)+c_2w(x,t)] = c_1\mathscr{L}_t^{\alpha}\mathscr{L}_x^{\beta}[u(x,t)]+c_2\mathscr{L}_t^{\alpha}\mathscr{L}_x^{\beta}[w(x,t)]$ *where c_1 and c_2 are real constants.*
3. $\mathscr{L}_t^{\alpha}\mathscr{L}_x^{\beta}[e^{-d\frac{x^{\beta}}{\beta}-c\frac{t^{\alpha}}{\alpha}}u(x,t)] = U(p+d, s+c)$.
4. $\mathscr{L}_t^{\alpha}\mathscr{L}_x^{\beta}[f(\gamma x, \sigma t)] = \frac{1}{r}U\left(\frac{p}{\gamma^{\beta}}, \frac{s}{\sigma^{\alpha}}\right)$ *where $r = \gamma^{\beta}\sigma^{\alpha}$.*
5. $(-1)^{m+n}\mathscr{L}_t^{\alpha}\mathscr{L}_x^{\beta}\left[\frac{x^{m\beta}}{\beta^m}\frac{t^{n\alpha}}{\alpha^n}u(x,t)\right] = \frac{\partial^{m+n}U(p,s)}{\partial p^m \partial s^n}$.

Lemma 5. *[8] The conformable double Laplace transform of β-th and α-th order fractional partial derivatives are given respectively as follows.*

$$\mathscr{L}_t^{\alpha}\mathscr{L}_x^{\beta}[{}_xD_{\beta}u(x,t)] = pU(p,s) - U(0,s), \tag{2}$$

$$\mathscr{L}_t^{\alpha}\mathscr{L}_x^{\beta}[{}_tD_{\alpha}u(x,t)] = sU(p,s) - U(p,0) \tag{3}$$

where ${}_xD_{\beta}u(x,t)$, ${}_tD_{\alpha}u(x,t)$ means β-th and α-th order conformable fractional partial derivatives respectively.
In the same manner the conformable double Laplace transform of mixed fractional partial derivatives

$$\mathscr{L}_t^{\alpha}\mathscr{L}_x^{\beta}[{}_xD_{\beta t}D_{\alpha}(u(x,t))] = psU(p,s) - pU(p,0) - sU(0,s) + U(0,0). \tag{4}$$

Theorem 6. *[8] Let $0 < \alpha, \beta \leq 1$ and $m, n \in \mathbb{N}$ such that $u(x,t) \in C^l(\mathbb{R}^+ \times \mathbb{R}^+)$, $l = max(m,n)$. Also let the conformable Laplace transforms of the functions $u(x,t)$, ${}_xD_{\beta}^{(i)}u(x,t)$ and ${}_tD_{\alpha}^{(j)}u(x,t)$ $i = 1, ..., m$, $j = 1, ..., n$ exist. Then*

$$\mathscr{L}_t^{\alpha}\mathscr{L}_x^{\beta}[{}_xD_{\beta}^{(m)}u(x,t)] = p^mU(p,s) - p^{m-1}U(0,s) - \sum_{i=1}^{m-1}p^{m-1-i}\mathscr{L}_t^{\alpha}[{}_xD_{\beta}^{(i)}U(0,t)], \tag{5}$$

$$\mathscr{L}_t^{\alpha}\mathscr{L}_x^{\beta}[{}_tD_{\alpha}^{(n)}u(x,t)] = s^nU(p,s) - s^{n-1}U(p,0) - \sum_{j=1}^{n-1}s^{n-1-j}\mathscr{L}_x^{\beta}[{}_tD_{\alpha}^{(j)}U(x,0)]. \tag{6}$$

Functions $f(x,t)$	Conformable Double Laplace Transform $f(p,s)$
ab	$\frac{ab}{ps}$
xt	$\beta^{\frac{1}{\beta}}\alpha^{\frac{1}{\alpha}}\frac{\Gamma(1+\frac{1}{\beta})\Gamma(1+\frac{1}{\alpha})}{p^{\frac{\beta+1}{\beta}}s^{\frac{\alpha+1}{\alpha}}}$
$\frac{x^{\beta}}{\beta}\frac{t^{\alpha}}{\alpha}$	$\frac{1}{p^2s^2}$
$\frac{x^{m\beta}}{\beta}\frac{t^{n\alpha}}{\alpha}$, *m,n are natural numbers*	$\frac{m!n!}{p^{m+1}s^{n+1}}$
$e^{\frac{x^{\beta}}{\beta}+\frac{t^{\alpha}}{\alpha}}$	$\frac{1}{(s-1)(p-1)}$
$e^{\frac{x^{\beta}}{\beta}+\frac{t^{\alpha}}{\alpha}}\frac{x^{m\beta}}{\beta}\frac{t^{n\alpha}}{\alpha}$, *m,n are natural numbers*	$\frac{m!n!}{(p-1)^{m+1}(s-1)^{n+1}}$
$\cos\left(\omega\frac{x^{\beta}}{\beta}\right)\cos\left(\omega\frac{t^{\alpha}}{\alpha}\right)$	$\frac{ps}{(w^2+s^2)(w^2+p^2)}$
$\sin\left(\omega\frac{x^{\beta}}{\beta}\right)\sin\left(\omega\frac{t^{\alpha}}{\alpha}\right)$	$\frac{w^2}{(w^2+s^2)(w^2+p^2)}$
$e^{\frac{x^{\beta}}{\beta}+\frac{t^{\alpha}}{\alpha}}\sinh\left(\frac{x^{\beta}}{\beta}\right)\sinh\left(\frac{t^{\alpha}}{\alpha}\right)$	$\frac{1}{(p-2)p(s-2)s}$
$e^{\frac{x^{\alpha}}{\alpha}+\frac{t^{\beta}}{\beta}}\cosh\left(\frac{x^{\alpha}}{\alpha}\right)\cosh\left(\frac{t^{\beta}}{\beta}\right)$	$\frac{(p-1)(s-1)}{(p-2)p(s-2)s}$

Table 1: Conformable double Laplace transform of some basic functions.

In the same way conformable double Laplace transform of mixed partial derivative

$$\begin{aligned}\mathscr{L}_t^{\alpha}\mathscr{L}_x^{\beta}[{}_xD^{(m)\beta}{}_tD^{(n)\alpha}(u(x,t))] = {} & p^m s^n\big(U(p,s)-s^{-1}U(p,0)\\ & -p^{-1}U(0,s)-\sum_{j=1}^{n-1}s^{-j-1}\mathscr{L}_x^{\beta}[{}_tD^{(j)\alpha}U(x,0)]\\ & -\sum_{i=1}^{m-1}p^{-i-1}\mathscr{L}_t^{\alpha}[{}_xD^{(i)\beta}U(0,t)]\\ & +\sum_{j=1}^{n-1}s^{-j-1}p^{-1}{}_tD^{(j)\alpha}U(0,0)\\ & +\sum_{i=1}^{m-1}s^{-1}p^{-i-1}{}_xD^{(i)\beta}U(0,0)\\ & +\sum_{i=1}^{m-1}\sum_{j=1}^{n-1}s^{-j-1}p^{-i-1}{}_tD^{(j)\alpha}{}_xD^{(i)\beta}U(0,0)\\ & +p^{-1}s^{-1}U(0,0)\big)\end{aligned} \tag{7}$$

where ${}_xD_{\beta}^{(m)}u(x,t)$, ${}_tD_{\alpha}^{(n)}u(x,t)$ *denotes* m, n *times conformable fractional derivatives of function* $u(x,t)$ *with order* β *and* α *respectively.*

3 Illustrative examples

Example 7. *Regard the conformable time-space fractional advection-diffusion equation*

$$D_t^{\alpha}u(x,t) = D_x^{(2)\beta}u(x,t) - D_x^{\beta}u(x,t) \tag{8}$$

with the conditions

$$\begin{aligned} u(0,t) &= 1+\frac{t^\alpha}{\alpha}, \\ u(x,0) &= e^{\frac{x^\beta}{\beta}}-\frac{x^\beta}{\beta}, \\ D_x^\beta u(0,t) &= 0 \end{aligned} \tag{9}$$

where $0<\beta\leq 1$, $0<\alpha\leq 1$, $x>0$, $t>0$, D_t^α, D_x^β *indicate* α*-th and* β*-th order conformable fractional derivatives of function* $u(x,t)$*. Using the the double conformable Laplace transform for Eq. (8)*

$$sU(p,s)-U(p,0)-p^2U(p,s)+pU(0,s)+D_x^\beta U(0,s)+pU(p,s)-U(0,s)=0 \tag{10}$$

where $U(p,s)$ *symbolizes the double conformable Laplace transformed form of the function* $u(x,t)$*. When the conformable Laplace transform is applied to the conditions given in (9) leads*

$$\begin{aligned} \mathscr{L}_t^\alpha[u(0,t)] &= U(0,s)=\frac{1}{s}+\frac{1}{s^2}, \\ \mathscr{L}_x^\beta[u(x,0)] &= U(p,0)=\frac{1}{p-1}-\frac{1}{p^2}, \\ \mathscr{L}_t^\alpha[D_x^\beta u(0,t)] &= D_x^\beta U(0,s)=0. \end{aligned} \tag{11}$$

Utilizing the equations given in (11) along with Eqn. (10) we get

$$U(p,s)=\frac{-p+p^2+s-ps+sp^2}{(-1+p)p^2s^2}.$$

Thus the unknown function can be evaluated as

$$u(x,t)=e^{\frac{x^\beta}{\beta}}+\frac{t^\alpha}{\alpha}-\frac{x^\beta}{\beta}.$$

Example 8. *Taking account into time-space fractional non-homogenous telegraph equation*

$$3D_t^\alpha u(x,t)+D_t^{(2)\alpha}u(x,t)-D_x^{(2)\beta}u(x,t)-3\left(\frac{x^{2\beta}}{\beta^2}+\frac{t^{2\alpha}}{\alpha^2}+1\right)=0, \tag{12}$$

with the conditions

$$\begin{aligned} u(0,t) &= \frac{t^\alpha}{\alpha}+\frac{t^{3\alpha}}{\alpha^3}, D_t^\alpha u(x,0)=1+\frac{x^{2\beta}}{\beta^2}, \\ u(x,0) &= \frac{x^\beta}{\beta}, D_x^\beta u(0,t)=1 \end{aligned} \tag{13}$$

with $0<\beta\leq 1$, $0<\alpha\leq 1$, $x>0$, $t>0$, $D_t^{(2)\alpha}$, $D_x^{(2)\beta}$ *means two times* α *and* β *order conformable fractional derivatives of function* $u(x,t)$*. Applying the conformable double Laplace transform to Eq. (12) produces*

$$\begin{aligned} &3sU(p,s)-3U(p,0)+s^2U(p,s)-sU(p,0)-D_t^\alpha U(p,0) \\ &-(p^2U(p,s)-pU(0,s)-D_x^\beta U(0,s))-3\left(\frac{2}{p^3}+\frac{2}{s^3}+\frac{1}{ps}\right)=\frac{-2}{ps}. \end{aligned} \tag{14}$$

Then applying conformable Laplace transform for the conditions (13)

$$U(0,s)=\frac{1}{s^2}+\frac{2}{s^4}, D_t^{\alpha}U(p,0)=\frac{1}{p}+\frac{2}{p^3},$$
$$U(p,0)=\frac{1}{p^2}, D_x^{\beta}U(0,s)=\frac{1}{s}. \tag{15}$$

Gathering all the results (14),(15) and making some algebraic arrangement lead

$$U(p,s)=\frac{2p^2+2s^2+p^2s^2+ps^3}{p^3s^4}.$$

In this way we can calculate the function $u(x,t)$ as

$$u(x,t)=\frac{x^{\beta}}{\beta}+\frac{t^{\alpha}}{\alpha}+\frac{x^{2\beta}}{\beta^2}\frac{t^{\alpha}}{\alpha}+\frac{t^{3\alpha}}{\alpha^3}$$

4 Conclusions

The conformable double Laplace transform is an efficient, reliable, applicable method to investigate the solutions of conformable fractional partial differential equations.

References

[1] *K.S. Miller, B. Ross,* An Introduction to the Fractional Calculus and Fractional Differential Equations, (John Wiley &Sons, New York, 1993).

[2] *A.Kilbas, H.M. Srivastava, J.J. Trujillo,* Theory and Applications of Fractional Differential Equations, (Elsevier, San Diego, 2006).

[3] *I. Podlubny,* Fractional Differential Equations, (Academic Press,San Diego, 1999).

[4] *K. Oldham, J. Spanier*, The fractional calculus theory and applications of differentiation and integration to arbitrary order. Elsevier, 1974.

[5] *I. Podlubny*, Geometric and physical interpretation of fractional integration and fractional differentiation, Fract. Calculus. Appl. Anal, 5, 367-386 (2002).

[6] *R. Khalil, M. Al Horani, A. Yousef, M. Sababheh*, A new definition of fractional derivative, J. Comput. Appl. Math. 264, 65 (2014).

[7] *T. Abdeljawad*, On conformable fractional calculus, J. Comput. Appl. Math. 279, 57 (2015).

[8] O. Özkan, A. Kurt, On conformable double Laplace transform. Optical and Quantum Electronics, 50(2), 103, (2018).

Application Of Taguchi Method To Optimize The Copper Recovery Efficiency

Mehmet Ali TOPÇU *
Department of Metallurgy and Material Engineering,
Karamanoglu Mehmetbey University,
Karaman/TURKEY

Aydın RUŞEN
Department of Metallurgy and Material Engineering,
Karamanoglu Mehmetbey University,
Karaman/TURKEY

Abstract

This paper deals with the application of Taguchi method to optimize the copper recovery from anode slime in different ionic liquid systems as leaching agents. In this method, reaction temperature, reaction duration and solid/liquid ratio were selected as process parameters of the ionic liquid systems, which were performed to measure the copper recovery efficiency. Taguchi orthogonal arrays, signal-to-noise (S/N) ratio and analysis of variance (ANOVA) are used to find the optimal levels and the effects of the process parameters on copper recovery from anode slime. A confirmation test with the optimal conditions of process parameters was carried out to demonstrate the effectiveness of the Taguchi method. Results of the experiments indicate that Taguchi optimization method is very applicable way to optimize the copper recovery efficiency from anode slime in different ionic liquids media.

Keywords: Optimization, Taguchi Method, ANOVA, Copper.

1 Introduction

The Taguchi method is known as an important experimental design method in producing high quality and low cost products or services. It is possible to reach much lower number of empirical studies by using the Taguchi method, where there is a lot of experimental work to be done for all combinations involving each level of each parameter affecting the system [1]. Taguchi method differs from other statistical experimental design methods because the parameters affecting an experiment are examined in two groups and it allows examining a large number of parameters in more than two levels. The Taguchi method states that all products must be produced at the desired target value, and that the losses from target have started and that the removal of these losses can only be achieved by reducing the variability around a good design and target value. This adds concepts like fractional factorial experiments design, robust design and orthogonal arrays [2-3]. Orthogonal array express which parameter will be used in which experiments. Taguchi has created unique orthogonal arrays for a lot of experimentation. The most important feature of orthogonal arrays is that many parameters should be evaluated with the least number of experiments and, unlike the traditional method, to change the parameter steps one by one instead of changing them simultaneously [4].

*Corresponding author. *E-mail address:* topcumali@kmu.edu.tr

In Taguchi method, the results obtained from the experiments conducted following the orthogonal experiment are converted to Signal/Noise Ratio (S/N) by a series of formulation and evaluated as analysis variable or performance statics. Taguchi has defined the Signal/Noise Ratio values as a performance criterion in experimental design to minimize variability [5]. Numerous performance statistics have been developed depending on the problem being investigated. Frequently used performance statistics are '*'the larger is the better"*, *''the smallest is the better"* and '*'the nominal is the better"*.

Furthermore, performance statistics graphs are used to determine the optimum conditions of a process with Taguchi method. The most common use of Taguchi method to determine the optimum conditions is by taking the peaks points of the performance statistics graphs. The values corresponding to the levels of each parameter in these graphs do not show the user the effect of that parameter. Many research applied this method for variance analysis. One of the most important steps of the Taguchi optimization method is to estimate the result obtained in the optimum condition and to verify this result. The optimum condition determined as a result of the evaluations was not included in the monitored orthogonal test set up and could not be performed during the experiments. In summary, the following steps are used to optimize processes involving one or more multi-performance characteristics with Taguchi method [7-9]; a) performance characteristics and factors to be evaluated are determined, b) the levels of factors affecting the process are determined, c) according to the factors and levels, orthogonal experimental setup is selected, d) experiments are performed according to the selected orthogonal sequence, e) the performance statistics is calculated, f) experimental results are analyzed using variance analysis, g) optimum levels of factors are selected, h) confirmation tests are performed to check the selected optimum levels.

There are many parameters such as the solvent composition and concentration affecting metal extraction from ores or wastes such as solvent concentration, leaching temperature, leaching duration, solid/liquid ratio, the pH of the leach solution, particle size [8]. Many scientists have used the Taguchi method to support the results of leaching studies with statistical data and to reduce the number of experiments [9-12].

In this study, the most commonly used parameters in metal extraction process such as solvent concentration (%), temperature (^{o}C), duration (h) and solid/liquid ratio (g/ml) are chosen as variable for copper extraction from anode slime.

2 Material and Experimental Method

Anode slime which consider as valuable waste due to it high content of precious metals was used as copper source. $1-\text{ethyl}-3-\text{methyl}$ imidazolium hydrogen sulfate ($EmimHSO_4$) and $1-\text{butyl}-3-\text{methyl}$ imidazolium hydrogen sulfate ($BmimHSO_4$) ionic liquids (IL) used as due to their excellent physical and chemical properties such as low vapor pressure, non-flammability, thermal stability and high ionic conductivity. All leaching tests were performed in glass flasks placed on a hot plate with magnetic stirrer. The leaching tests were carried out at constant volume of ionic liquids which prepared by deionized water. Experimental parameters and their levels selected for leaching tests is shown Table 1.

Table 1: The parameters and levels studied in the recovery of precious metals from anode slime

Levels	Parameters			
	Ionic Liquid Concentration (%)	Temperature (^{o}C)	Duration (h)	Solid / Liquid Ratio (g/mL)
1	20	25	0,5	1/10
2	40	45	1	1/15
3	60	75	2	1/20
4	80	95	4	1/25

According to the Taguchi method, the orthogonal array experimental design L_{16} (4^4) which denotes four parameters, each with four levels, was chosen because it is most suitable for the condition being investigated. [4,8] The Taguchi experimental design L_{16} (4^4) which generated using the test parameters and four level of these parameters is shown Table 2 with recovery efficiencies results.
In this work, to optimize copper extraction *''larger is better"* has been evaluated by using following equation:

$$\left(\frac{S}{N}\right)_L = -10 \left(\frac{1}{n}\sum_{i=1}^{n}\frac{1}{x_i^2}\right) \tag{2}$$

where $(S/N)_L$ is performance statistics, n number of repetitions done for an experimental combination, and x_i performance value of i^{th} experiment. Then, the collected data analyzed with Minitab 17 software program to evaluate the effect of each parameter on optimization criteria. By using SN analysis, it is possible to determine optimum level of each parameter and optimum set of parameter producing the maximum leaching efficiency. After determining optimum experimental conditions, the performance value corresponding to optimum conditions can be predicted by the following equation [13]:

$$\left(\frac{S}{N}\right)_{Predicted} = \left(\frac{S}{N}\right)_m + \sum_{n=1}^{n}\left(\left[\frac{S}{N}\right]_i - \left[\frac{S}{N}\right]_m\right) \tag{3}$$

where $(S/N)_m$ is arithmetic mean of performance statistics $(S/N)_L$ for all experiments, $(S/N)_i$ is performance statistic value at optimum level of each investigated parameter. After, determining of optimum condition was controlled by confirmation experiments performed at the optimum conditions. Furthermore, analysis of variance (ANOVA) in accordance with Taguchi method was done to determine which investigated parameters are dominant on the leaching performance.

3 Results and Discussion

The copper recovery experiments from anode slime were carried out by using $BmimHSO_4$ and $EmimHSO_4$ in the previous studies [14,15]. To determine the optimum conditions of the experiments for copper extraction, these copper recovery rates and the performance statistic of *' 'larger is better"* results are shown in Table 2.

Table 2: L_{16} test setup and performance statistic values for each experiment [14,15]

Exp. No	Experimental Parameters and Levels				$BmimHSO_4$		$EmimHSO_4$	
					Copper Recovery (%)	SN_L	Copper Recovery (%)	SN_L
	Ionic Liquid Concentration (%)	Temperature (^{o}C)	Duration (h)	Solid/Liquid Ratio (g/L)				
1	1	1	1	1	36,73	31,30	24,37	27,74
2	1	2	2	2	60,58	35,65	51,89	34,30
3	1	3	3	3	83,61	38,45	51,85	34,29
4	1	4	4	4	71,34	37,07	45,56	33,17
5	2	1	2	3	44,58	32,98	41,45	32,35
6	2	2	1	4	82,01	38,28	25,67	28,19
7	2	3	4	1	53,93	34,64	51,64	34,26
8	2	4	3	2	69,46	36,83	49,64	33,92
9	3	1	3	4	55,73	34,92	35,61	31,03
10	3	2	4	3	73,53	37,33	45,12	33,09
11	3	3	1	2	60,15	35,58	39,40	31,91
12	3	4	2	1	73,18	37,29	52,05	34,33
13	4	1	4	2	56,37	35,02	33,12	30,40
14	4	2	3	1	54,25	34,69	42,60	32,59
15	4	3	2	4	62,41	35,90	30,57	29,71
16	4	4	1	3	38,10	31,62	38,43	31,69

After to the results obtained after the experiments, performance statistics graph for each parameter were plotted by using Minitab 17 software program. Performance statistics of the parameters for copper recoveries from anode slime by using $BmimHSO_4$ and $EmimHSO_4$ ionic liquids are shown Fig 1.a and Fig 1.b, respectively.

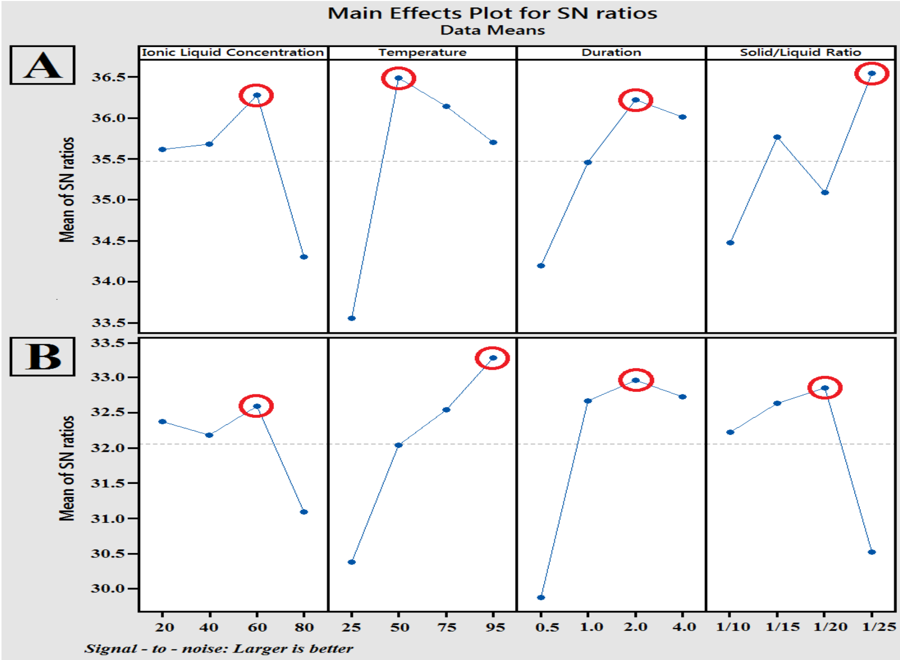

Figure 1: Performance statistics of the parameters investigated for copper recovery by using ionic liquids of a) $BmimHSO_4$ and b) $EmimHSO_4$

As seen in Fig 1, the top of the peak in each column of Fig.1.a and Fig. 1.b was marked to define the optimum condition for copper recovery by using $BmimHSO_4$ and $EmimHSO_4$, respectively. According to the Fig 1.a, the optimum copper condition for copper recovery from anode slime by using $BmimHSO_4$ was detected as; IL concentration: 60% (v/v), temperature: 50 ^oC, duration: 2 h, solid/liquid ratio: 1/25 g/L. Also, the optimum condition for copper recovery by $EmimHSO_4$ was determined as; IL concentration: 60% (v/v), temperature: 95 ^oC, duration: 2 h, solid/liquid ratio: 1/20 g/L. If the orthogonal array experimental design for copper recovery is analyzed carefully, it can be noticed that the determined optimum experimental conditions have not been performed during the experimental trials as a leaching experiment for both solvent. Therefore, the predicted recovery rate for $BmimHSO_4$ and $EmimHSO_4$ under optimum conditions calculated and confirmation experiment must be performed. Copper recoveries (%) confirmed experimentally and predicted theoretically with optimum conditions for each studied parameters are summarized in Table 3 [14,15].

Table 3: The optimum conditions for copper recoveries, predicted calculation and copper recovery rates obtained from the confirmation experiments

Parameter	Optimum Conditions			
	$BmimHSO_4$		$EmimHSO_4$	
	Value	Level	Value	Level
Ionic Liquid Concentration	% 60	3	%60	3
Temperature	50 ^oC	2	95	4
Duration	2 h	3	2	3
Solid/Liquid Ratio	1/25 g/ml	4	1/20	3
Predicted Copper Recovery	90.31%		55.13%	
Copper recovery obtained from confirmation test	87.52%		50.16%	

As seen in Table 3, under the optimum conditions with $BmimHSO_4$ and $EmimHSO_4$, the predicted percentages of copper recovery were 90.31% and 55.13%, respectively. Furthermore, copper recovery obtained from the confirmation experiments corresponds to 87.52% for $BmimHSO_4$ and 50.16% for $EmimHSO_4$. According to these results, it can be concluded that good agreement exist between the predicted and confirmed leaching efficiencies of copper.
In this study, Analysis of Variance (ANOVA) was used to specify which of the process parameters significantly affect the performance characteristics. The F-test was also used to determine the most effective parameter on the leaching efficiencies as previous studies [14,15]. The results of the ANOVA for copper recoveries by using $BmimHSO_4$ and $EmimHSO_4$ indicate that the temperature is the most effective parameter on copper recovery for $BmimHSO_4$ with 43.46% contribution rate and ionic liquid concentration is the most effective parameter for $EmimHSO_4$ with 37.16% contribution rate. According to these results, it can be concluded that $BmimHSO_4$ is more convenient leach agent than $EmimHSO_4$ for copper recovery from anode slime.

4 Conclusion

In this study, the Taguchi method was applied successfully to optimize the experimental conditions for copper recovery from anode slime in the ionic liquids. Reaction temperature, reaction duration, solid/liquid ratio and ionic liquid concentration were investigated with orthogonal experimental design of L_{16} (4^4). After experimental results, maximum copper recovery from anode slime by using $BmimHSO_4$ obtained at the conditions; IL concentration (60%), temperature (50 ^oC), duration (2h) and solid/liquid ratio (1/25) g/ml. With these conditions, copper recovery obtained from confirmation experiment and predicted values were detected as 87.53% and 90.31%, respectively. Also, the experimental conditions of copper recovery with $EmimHSO_4$ were optimized as IL concentration (60%), temperature (95 ^oC), duration (2 h), solid/liquid ratio (1/20 g/L). With the optimum conditions for $EmimHSO_4$, copper recovery was achieved as 50.16% and predicted copper recovery was calculated as 55.13%. These results indicate an excellent agreement between experimental conditions and copper recoveries. According to the ANOVA results, temperature and ionic liquid concentration were determined as the most effective leaching parameters for $BmimHSO_4$ and $EmimHSO_4$, respectively.

Acknowledgement

The authors would like to thank to Karamanoglu Mehmetbey University Scientific and Technological Researchers Application for analysis and Research Center Scientific Research Projects (BAP) Coordinating Office for support with grant number KMU-BAP-04-YL-15.

References

[1] G. Taguchi, S. Chowdhury, S., Y. Wu, Taguchi's quality engineering handbook (Vol. 1736) (2005). Hoboken, NJ: John Wiley Sons.

[2] H. Öktem, T. Erzurumlu, I. Uzman, Application of Taguchi optimization technique in determining plastic injection molding process parameters for a thin-shell part. Materials design, 28(4) (2007)1271-1278.

[3] C. Hamzaçebi, F. Kutay, Taguchi metodu: Bir uygulama. Teknoloji, 6(3-4) (2003) 7-17.

[4] N. Dhawan, M.S. Safarzadeh, M. Birinci, Kinetics of hydrochloric acid leaching of smithsonite. Russian Journal of Non-Ferrous Metals, 52(3) (2011) 209-216.

[5] M. S. Safarzadeh, D. Moradkhani, M. O. Ilkhchi, N. H. Golshan. Determination of the optimum conditions for the leaching of Cd–Ni residues from electrolytic zinc plant using statistical design of experiments. Separation and Purification Technology, 58(3), (2008) 367-376.

[6] C. Y. Nian, W. H. Yang, Y. S. Tarng, Optimization of turning operations with multiple performance characteristics. Journal of Materials Processing Technology, 95(1-3) (1999) 90-96.

[7] B. Bayrak, O. Laçin, H. Saraç, Ham manyezit cevherinin glukonik ssit çözeltilerinde çözündürülmesinin optimizasyonu. Anadolu Universıty Journal of Science and Technology–A Applied Sciences and Engineering, 16(2) (2015) 195-202.

[8] Z. H. Guo, F. K. Pan, X. Y. Xiao, L. Zhang, K. Q. Jiang,. Optimization of brine leaching of metals from hydrometallurgical residue. Transactions of Nonferrous Metals Society of China, 20(10) (2001) 2000-2005.

[9] A. V. Beşe, O. N. Ata, C. Celik, S. Colak, Determination of the optimum conditions of dissolution of copper in converter slag with chlorine gas in aqueous media. Chemical Engineering and Processing: Process Intensification, 42(4) (2003) 291-298.

[10] M. Yeşilyurt, Determination of the optimum conditions for the boric acid extraction from colemanite ore in HNO3 solutions. Chemical Engineering and Processing: Process Intensification, 43(10), (2004) 1189-1194.

[11] Z. Ekinci, E. Şayan, A.V. Beşe, O. N. Ata, Optimization and modeling of boric acid extraction from colemanite in water saturated with carbon dioxide and sulphur dioxide gases. International Journal of Mineral Processing, 82(4) (2007) 187-194

[12] F. Farahmand, D. Moradkhani, M. S. Safarzadeh, F. Raschi, Brine leaching of lead-bearing zinc plant residues: Process optimization using orthogonal array design methodology. Hydrometallurgy, 95(3-4) (2009) 316-324.

[13] S. M. Kim, K. S. Park, K. K. Do, S. D. Park, H. T. Kim, Optimization of Parameters for the synthesis of biomodal Ag Nanoparticles by Taguchi method. Journal of Industrial and Engineering Chemistry, 15(6) (2009) 894-897.

[14] A. Rüşen, M.A. Topçu, Investigation of an alternative chemical agent to recover valuable metals from anode slime. Chemical Papers, 72 (2018) 2879-2891.

[15] A. Rüşen, M.A. Topçu, The Effect of EmimHSO4 (1-Ethyl-3-Methyl-İmidazolium Hydrogen Sulfate) on Copper Recovery from Anode Slime, Afyon Kocatepe University Journal of Science and Engineering Journal, 17 (2017) 696-703.

Helicoidal Surface of Torus-Type in 3-Space

Erhan GÜLER*
Bartın University,
Department of Mathematics,
74100, Bartın, TURKEY

Ömer KİŞİ
BartınUniversity,
Department of Mathematics,
74100, Bartın, TURKEY

Abstract

We consider torus-type helicoidal surface in the three dimensional Euclidean space. We define torus-type helicoidal surface. We calculate its Gauss map, and then release its curvatures with some results.

Keywords: 3-space, torus-type helicoidal surface,curvatures.

1 Introduction

In [2], Chen posed the problem of classifying the finite type surfaces in the 3-dimensional Euclidean space $\mathbb{E}^3$. A Euclidean submanifold is said to be of Chen finite type if its coordinate functions are a finite sum of eigenfunctions of its Laplacian Δ. Further, the notion of finite type can be extended to any smooth function on a submanifold of a Euclidean space or a pseudo-Euclidean space. Then the theory of submanifolds of finite type has been studied by many geometers.

Takahashi [11] stated that minimal surfaces and spheres are the only surfaces in $\mathbb{E}^3$ satisfying the condition $\Delta r = \lambda r$, $\lambda \in \mathbb{R}$. Ferrandez, Garay and Lucas [6] proved that the surfaces of $\mathbb{E}^3$ satisfying $\Delta H = AH$, $A \in Mat(3,3)$ are either minimal, or an open piece of sphere or of a right circular cylinder. Choi and Kim [3] characterized the minimal helicoid in terms of pointwise 1-type Gauss map of the first kind. Dillen, Pas and Verstraelen [4] proved that the only surfaces in $\mathbb{E}^3$ satisfying $\Delta r = Ar + B$, $A \in Mat(3,3)$, $B \in Mat(3,1)$ are the minimal surfaces, the spheres and the circular cylinders.

Senoussi and Bekkar [10] studied helicoidal surfaces M^2 in $\mathbb{E}^3$ which are of finite type in the sense of Chen with respect to the fundamental forms I, II and III, i.e., their position vector field $r(u,v)$ satisfies the condition $\Delta^J r = Ar$, $J = I, II, III$, where $A = (a_{ij})$ is a constant 3×3 matrix and Δ^J denotes the Laplace operator with respect to the fundamental forms I, II and III.

When we focus on the ruled (helicoid) and rotational characters, we see Bour's theorem in the literature [1]. About helicoidal surfaces in Euclidean 3-space, do Carmo and Dajczer [7] proved that there exists a two-parameter family of helicoidal surfaces isometric to a given helicoidal surface using a result of Bour [1]. Kim et al [8] focused on Cheng-Yau operator and Gauss map of surfaces of revolution. Lawson [9] gave the general definition of the Laplace-Beltrami operator in his lecture notes. Some relations among the Laplace-Beltrami operator and curvatures of the helicoidal surfaces were shown by Güler, Yaylı and Hacısalihoğlu [7].

In this paper, we study the torus-type helicoidal surface in Euclidean 3-space $\mathbb{E}^3$. We give some basic notions of three dimensional Euclidean geometry in section 2. In section 3, we define helicoidal surface and torus surface. We obtain torus-type helicoidal surface, and calculate its curvatures in the last section.

*Corresponding author. *E-mail address:* eguler@bartin.edu.tr

2 Preliminaries

In the rest of this paper, we shall identify a vector (a,b,c) with its transpose $(a,b,c)^t$. We will introduce the first and second fundamental forms, matrix of the shape operator $\mathbf{S}$, Gaussian curvature K, and the mean curvature H of surface $\mathbf{M} = \mathbf{M}(u, v)$ in Euclidean 3-space $\mathbb{E}^3$.

Let $\mathbf{M}$ be an isometric immersion of surface M^2 in $\mathbb{E}^3$. The vector product of $\overrightarrow{x} = (x_1, x_2, x_3)$, $\overrightarrow{y} = (y_1, y_2, y_3)$ on $\mathbb{E}^3$ is defined as follows

$$\overrightarrow{x} \times \overrightarrow{y} = \det \begin{pmatrix} e_1 & e_2 & e_3 \\ x_1 & x_2 & x_3 \\ y_1 & y_2 & y_3 \end{pmatrix}.$$

For a surface $\mathbf{M}$ in $\mathbb{E}^3$ we have

$$\det I = \det \begin{pmatrix} E & F \\ F & G \end{pmatrix} = EG - F^2,$$

and

$$\det II = \det \begin{pmatrix} L & M \\ M & N \end{pmatrix} = LN - M^2,$$

where

$$\begin{array}{lll} E = \mathbf{M}_u \cdot \mathbf{M}_u, & F = \mathbf{M}_u \cdot \mathbf{M}_v, & G = \mathbf{M}_v \cdot \mathbf{M}_v, \\ L = \mathbf{M}_{uu} \cdot e, & M = \mathbf{M}_{uv} \cdot e, & N = \mathbf{M}_{vv} \cdot e, \end{array}$$

e is the Gauss map (i.e. the unit normal vector field). We compute

$$\begin{pmatrix} E & F \\ F & G \end{pmatrix}^{-1} \begin{pmatrix} L & M \\ M & N \end{pmatrix},$$

and it gives the matrix of the shape operator $\mathbf{S}$ as follows

$$\mathbf{S} = \frac{1}{\det I} \begin{pmatrix} GL - FM & GM - FN \\ EM - FL & EN - FM \end{pmatrix}. \tag{1}$$

So, we get the following formulas of the Gaussian and the mean curvatures:

$$K = \det(\mathbf{S}) = \frac{\det II}{\det I} = \frac{LN - M^2}{EG - F^2},$$

and

$$H = \frac{1}{2} tr\,(\mathbf{S}) = \frac{EN + GL - 2FM}{2\,(EG - F^2)}.$$

A surface $\mathbf{M}$ is minimal if $H = 0$ identically on $\mathbf{M}$.

3 Helicoidal and Torus Surfaces

For an open interval $I \subset \mathbb{R}$, let $\gamma : I \longrightarrow \Pi$ be a curve in a plane Π in $\mathbb{E}^3$, and let ℓ be a straight line in Π. A rotational surface in $\mathbb{E}^4$ is defined as a surface rotating a curve γ around a line ℓ (these are called the *profile curve* and the *axis*, respectively).

Suppose that when a profile curve γ rotates around the axis ℓ, it simultaneously displaces parallel lines orthogonal to the axis ℓ, so that the speed of displacement is proportional to the speed of rotation. Then the resulting surface is called the *helicoidal surface* with axis ℓ

and pitch $a \in \mathbb{R} \backslash \{0\}$. We may suppose that ℓ is the line spanned by the vector $(0,0,1)^t$. The orthogonal matrix which fixes the above vector is

$$Z(v) = \begin{pmatrix} \cos v & -\sin v & 0 \\ \sin v & \cos v & 0 \\ 0 & 0 & 1 \end{pmatrix}, \tag{2}$$

where $v \in \mathbb{R}$. The matrix Z can be found by solving the following equations simultaneously;

$$Z\ell = \ell, \quad Z^t Z = Z Z^t = I_3, \quad \det Z = 1.$$

When the axis of rotation is ℓ, there is an Euclidean transformation by which the axis is ℓ transformed to the x_3-axis of $\mathbb{E}^3$. Parametrization of the profile curve is given by

$$\gamma(u) = (f(u), 0, \varphi(u)),$$

where $f(u), \varphi(u) : I \subset \mathbb{R} \longrightarrow \mathbb{R}$ are differentiable functions for all $u \in I$. So, helicoidal surface which is spanned by the vector $(0,0,1)$ is as follows

$$\mathbf{H}(u,v) = Z(v)\gamma(u)^t + av\ell^t,$$

where $u \in I$, $v \in [0, 2\pi]$.

Clearly, we write helicoidal surface as follows

$$\mathbf{H}(u,v) = \begin{pmatrix} f(u)\cos v \\ f(u)\sin v \\ \varphi(u) + av \end{pmatrix}. \tag{3}$$

Now, taking profile curve as

$$\gamma(u) = (c + a\cos u, 0, a\sin u),$$

with the orthogonal matrix Z, then we get torus surface in $\mathbb{E}^3$ as follows

$$T(u,v) = \begin{pmatrix} (c + r\cos u)\cos v \\ (c + r\cos u)\sin v \\ r\sin u \end{pmatrix}, \tag{4}$$

where $a = 0, r, c, u \in \mathbb{R}\backslash\{0\}$ and $0 \leq v \leq 2\pi$.

4 Torus-Type Helicoidal Surface

We now define torus-type helicoidal surface as follows:

$$\mathfrak{T}(u,v) = \begin{pmatrix} (c + a\cos u)\cos v \\ (c + a\cos u)\sin v \\ a\sin u + bv \end{pmatrix}. \tag{5}$$

Using the first differentials of (5) with respect to u, v, we get the first quantities as follows

$$I = \begin{pmatrix} a^2 & ab\cos u \\ ab\cos u & \beta \end{pmatrix},$$

where $\beta = a^2\cos^2 u + 2ac\cos u + b^2 + c^2$, and we get

$$\begin{aligned} \det I &= a^2\beta - a^2b^2\cos^2 u \\ &= a^2\left(\left(a^2 - b^2\right)\cos^2 u + 2ac\cos u + b^2 + c^2\right). \end{aligned}$$

Using the second differentials with respect to u, v, we have the second quantities as follows

$$II = \begin{pmatrix} \frac{a(c+a\cos u)}{W} & -\frac{ab\sin^2 u}{W} \\ -\frac{ab\sin^2 u}{W} & \frac{\beta\cos u}{W} \end{pmatrix}$$

where $W = \sqrt{(a^2-b^2)\cos^2 u + 2ac\cos u + b^2 + c^2}$, and we have

$$\det II = \frac{1}{W^2}\left(-a^2b^2\sin^4 u + a^2\beta\cos^2 u + ac\beta\cos u\right).$$

The Gauss map of torus-type helicoidal surface is as follows

$$e_{\mathfrak{T}} = \frac{1}{W}\begin{pmatrix} -(c+a\cos u)\cos u\cos v - b\sin u\sin v \\ -(c+a\cos u)\cos u\sin v + b\sin u\cos v \\ -(c+a\cos u)\sin u \end{pmatrix}. \tag{6}$$

Finally, the Gaussian curvature of the torus hypersurface is as follows

$$K = \frac{-ab^2\sin^4 u + a\beta\cos^2 u + c\beta\cos u}{aW^4},$$

and the mean curvature is as follows

$$H = \frac{c\beta + 2a\beta\cos u + 2ab^2\cos u\sin^2 u}{2aW^3},$$

Corollary 1. *Let $\mathfrak{T} : M^2 \longrightarrow \mathbb{E}^3$ be an immersion given by (5). Then M^2 is minimal if and only if*

$$\left(a^2\cos^2 u + 2ac\cos u + b^2 + c^2\right)(c + 2a\cos u) + 2ab^2\cos u\sin^2 u = 0.$$

Proof. b solutions of the above eq. are as follows

$$b = \pm(c+a\cos u)\sqrt{\frac{-c-2a\cos u}{c - 2a\cos^3 u + 4a\cos u}}$$

where $c \neq 2a\left(\cos^2 u - 2\right)\cos u$.

Corollary 2. *Let $\mathfrak{T} : M^2 \longrightarrow \mathbb{E}^3$ be an immersion given by (5). Then M^2 is flat surface if and only if*

$$-ab^2\sin^4 u + \left(a^2\cos^2 u + 2ac\cos u + b^2 + c^2\right)(c + a\cos u)\cos u = 0.$$

Proof. b solutions of the above eq. are as follows

$$b = \pm\sqrt{\frac{(c+a\cos u)^3\cos u}{a + a\cos^4 u - 3a\cos^2 u - c\cos u}}$$

where $c \neq a\left(\cos^3 u - 3\cos u + \frac{1}{\cos u}\right)$.

Corollary 3. *Let $\mathfrak{T} : M^2 \longrightarrow \mathbb{E}^3$ be an immersion given by (5). Then M^2 has following relation*

$$2a\left(-ab^2\sin^4 u + \beta(c+a\cos u)\cos u\right)H - aW\left(\beta(c+2a\cos u) + 2ab^2\cos u\sin^2 u\right)K = 0.$$

Proof. b solutions of the above eq. are as follows

$$b = \pm(c+a\cos u)\sqrt{\frac{\left((2\cos u\,(c+a\cos u)H - W(c+2a\cos u)K)\right)}{\begin{pmatrix} 2\left(a + a\cos^4 u - 3a\cos^2 u - c\cos u\right)H \\ +W\left(c - 2a\cos^3 u + 4a\cos u\right)K \end{pmatrix}}},$$

where $a \neq 0$ and $2\left(a + a\cos^4 u - 3a\cos^2 u - c\cos u\right)H \neq -W\left(c - 2a\cos^3 u + 4a\cos u\right)K$.

References

[**1**] Bour E. Théorie de la déformation des surfaces. J. de l.École Imperiale Polytechnique 22-39 (1862) 1-148.

[**2**] Chen B.Y. Total mean curvature and submanifolds of finite type. World Scientific, Singapore, 1984.

[**3**] Choi M., Kim Y.H. Characterization of the helicoid as ruled surfaces with pointwise 1-type Gauss map. Bull. Korean Math. Soc. 38 (2001) 753-761.

[**4**] Dillen F., Pas J., Verstraelen L. On surfaces of finite type in Euclidean 3-space. Kodai Math. J. 13 (1990) 10-21.

[**5**] Do Carmo M., Dajczer M. Helicoidal surfaces with constant mean curvature. Tohoku Math. J. 34 (1982) 351-367.

[**6**] Ferrandez A., Garay O.J., Lucas P. On a certain class of conformally at Euclidean hypersurfaces. Proc. of the Conf. in Global Analysis and Global Differential Geometry, Berlin, 1990.

[**7**] Güler E., Yaylı Y., Hacısalihoğlu H.H. Bour's theorem on the Gauss map in 3-Euclidean space. Hacettepe J. Math. Stats. 39 (2010) 515-525.

[**8**] Kim D.S., Kim J.R., Kim Y.H. Cheng-Yau operator and Gauss map of surfaces of revolution. Bull. Malays. Math. Sci. Soc. 39 (2016) 1319-1327.

[**9**] Lawson H.B. Lectures on minimal submanifolds. 2nd ed.; Mathematics Lecture Series 9; Publish or Perish, Inc. Wilmington, Delaware (1980)

[**10**] Senoussi B., Bekkar M. Helicoidal surfaces with $\Delta^J r = Ar$ in 3-dimensional Euclidean space. Stud. Univ. Babeş-Bolyai Math. 60-3 (2015) 437-448.

[**11**] Takahashi T. Minimal immersions of Riemannian manifolds. J. Math. Soc. Japan 18 (1966) 380-385.

P-Functions on $\Delta = [a, b] \times [c, d]$ and Some Hadamard-Type Integral Inequalities on the Co-ordinates

Ahmet OCAK AKDEMİR *
Ağrı İbrahim Çeçen University,
Department of Mathematics,
04100, Ağrı, TURKEY

M. Emin ÖZDEMİR
Uludağ University,
Department of Mathematics Educations,
Bursa, TURKEY

Abstract

In this paper, we recall P- functions on $\Delta = [a, b] \times [c, d]$ and proved some inequalities of Hadamard-type for this class of functions on the co-ordinates.
Keywords: Hermite-Hadamard inequality, P-function.

1 Introduction

Dragomir has mentioned the concept of convexity on the co-ordinates as follows;

Definition 1 (See[7]) *A function $f : \Delta = [a, b] \times [c, d] \to \mathbb{R}$ is said to be convex on Δ if the following inequality:*

$$f(tx + (1-t)z, ty + (1-t)w) \leq tf(x, y) + (1-t)f(z, w)$$

holds for all $(x, y), (z, w) \in \Delta$ and $t \in [0, 1]$. A function $f : \Delta \to \mathbb{R}$ is said to be convex on the co-ordinates on Δ in the partial mappings $f_y : [a, b] \to \mathbb{R}$, $f_y(u) = f(u, y)$ and $f_x : [c, d] \to \mathbb{R}$, $f_x(v) = f(x, v)$ are convex where defined for all $x \in [a, b]$ and $y \in [c, d]$.

Özdemir et al. defined m-convex functions on the co-ordinates on Δ, as following;

Definition 2 (See[6]) *Consider the bidimensional interval $\Delta := [0, b] \times [0, d]$ in $[0, \infty)^2$. The mapping $f : \Delta \to \mathbb{R}$ is m-convex on Δ if*

$$f(tx + (1-t)z, ty + m(1-t)w) \leq tf(x, y) + m(1-t)f(z, w)$$

holds for all $(x, y), (z, w) \in \Delta$ with $t \in [0, 1]$ and for some fixed $m \in [0, 1]$ (Özdemir et al., 2010). A function $f : \Delta \to \mathbb{R}$ is m-convex on Δ is called co-ordinated m-convex on Δ if the partial mapping

$$f_y : [0, b] \to \mathbb{R}, f_y(u) = f(u, y)$$

and

$$f_x : [0, d] \to \mathbb{R}, f_x(v) = f(x, v)$$

are m-convex for all $x \in [0, b)$ and $y \in [0, d]$ with some fixed $m \in [0, 1]$.

*Corresponding author. *E-mail address:* aocakakdemir@gmail.com

Definition 3 (See [2]) *Suppose that $\Delta := [a,b] \times [c,d] \subset \mathbb{R}^2$ a bidimensional interval where $a < b$, $c < d$. $f : \Delta \to \mathbb{R}$ be non-negative function, we said that f is P-function on Δ, if the following inequality holds;*

$$f(\lambda x + (1-\lambda)z, \lambda y + m(1-\lambda)w) \leq f(x,y) + f(z,w)$$

for $\forall (x,y),(z,w) \in \Delta$ and $\lambda \in (0,1)$.

Lemma 4 (See [2]) *Every P-function that is defined as $f : \Delta \to \mathbb{R}$ is P-function on the coordinates.*

New class of convex functions on the co-ordinates, several new inequalities, generalizations, improvements and related results can be found in the papers [1]-[8].

The main purpose of this study is to prove some new Hadamard type integral inequalities on the co- ordinates on Δ for P-functions.

2 Main Results

Throughout the paper, the following notation will be used.

$$\begin{aligned} A &= \frac{(x-a)(y-c)f(a,c)+(x-a)(d-y)f(a,d)}{(b-a)(d-c)} \\ &+ \frac{(b-x)(y-c)f(b,c)+(b-x)(d-y)f(b,d)}{(b-a)(d-c)} \\ &- \frac{x-a}{(b-a)(d-c)}\int_c^d f(a,v)dv - \frac{b-x}{(b-a)(d-c)}\int_c^d f(b,v)dv \\ &- \frac{d-y}{(b-a)(d-c)}\int_a^b f(u,d)du - \frac{y-c}{(b-a)(d-c)}\int_a^b f(u,c)du. \end{aligned}$$

Lemma 5 *Let $a < b, c < d$ and $f : \Delta = [a,b] \times [c,d] \subseteq \mathbb{R}^2 \to \mathbb{R}$ be a twice differentiable function on Δ. If $\frac{\partial^2 f}{\partial t \partial s} \in L_1[\Delta]$, then the following identity holds;*

$$\begin{aligned} & A + \frac{1}{(b-a)(d-c)}\int_a^b\int_c^d f(u,v)dudv \\ = & \frac{(x-a)^2(y-c)^2}{(b-a)(d-c)}\int_0^1\int_0^1 (t-1)(s-1)\frac{\partial^2 f}{\partial t \partial s}(tx+(1-t)a, sy+(1-s)c)dsdt \\ + & \frac{(x-a)^2(d-y)^2}{(b-a)(d-c)}\int_0^1\int_0^1 (t-1)(1-s)\frac{\partial^2 f}{\partial t \partial s}(tx+(1-t)a, sy+(1-s)d)dsdt \\ + & \frac{(b-x)^2(y-c)^2}{(b-a)(d-c)}\int_0^1\int_0^1 (1-t)(s-1)\frac{\partial^2 f}{\partial t \partial s}(tx+(1-t)b, sy+(1-s)c)dsdt \\ + & \frac{(b-x)^2(d-y)^2}{(b-a)(d-c)}\int_0^1\int_0^1 (1-t)(1-s)\frac{\partial^2 f}{\partial t \partial s}(tx+(1-t)b, sy+(1-s)d)dsdt. \end{aligned}$$

Theorem 6 *Let $a < b, c < d$ and $f : \Delta = [a,b] \times [c,d] \subseteq \mathbb{R}^2 \to \mathbb{R}$ be a twice differentiable function on Δ. If $|\frac{\partial^2 f}{\partial t \partial s}|$, is P-function on Δ on the coordinates, then one has the following* *inequality;*

$$\begin{aligned}
&\left| A + \frac{1}{(b-a)(d-c)} \int_a^b \int_c^d f(u,v)dudv \right| \\
\leq\ & \frac{(x-a)^2(y-c)^2}{4(b-a)(d-c)} \left(\left| \frac{\partial^2 f}{\partial t \partial s}(x,y) \right| + \left| \frac{\partial^2 f}{\partial t \partial s}(x,c) \right| + \left| \frac{\partial^2 f}{\partial t \partial s}(a,y) \right| + \left| \frac{\partial^2 f}{\partial t \partial s}(a,c) \right| \right) \\
+\ & \frac{(x-a)^2(d-y)^2}{4(b-a)(d-c)} \left(\left| \frac{\partial^2 f}{\partial t \partial s}(x,y) \right| + \left| \frac{\partial^2 f}{\partial t \partial s}(x,d) \right| + \left| \frac{\partial^2 f}{\partial t \partial s}(a,y) \right| + \left| \frac{\partial^2 f}{\partial t \partial s}(a,d) \right| \right) \\
+\ & \frac{(b-x)^2(y-c)^2}{4(b-a)(d-c)} \left(\left| \frac{\partial^2 f}{\partial t \partial s}(x,y) \right| + \left| \frac{\partial^2 f}{\partial t \partial s}(x,c) \right| + \left| \frac{\partial^2 f}{\partial t \partial s}(b,y) \right| + \left| \frac{\partial^2 f}{\partial t \partial s}(b,c) \right| \right) \\
+\ & \frac{(b-x)^2(d-y)^2}{4(b-a)(d-c)} \left(\left| \frac{\partial^2 f}{\partial t \partial s}(x,y) \right| + \left| \frac{\partial^2 f}{\partial t \partial s}(x,d) \right| + \left| \frac{\partial^2 f}{\partial t \partial s}(b,y) \right| + \left| \frac{\partial^2 f}{\partial t \partial s}(b,d) \right| \right).
\end{aligned}$$

Proof. From Lemma 5, we can write;

$$\begin{aligned}
&\left| A + \frac{1}{(b-a)(d-c)} \int_a^b \int_c^d f(u,v)dudv \right| \\
\leq\ & \frac{(x-a)^2(y-c)^2}{(b-a)(d-c)} \int_0^1 \int_0^1 |(t-1)(s-1)| \left| \frac{\partial^2 f}{\partial t \partial s}(tx+(1-t)a, sy+(1-s)c) \right| dsdt \\
+\ & \frac{(x-a)^2(d-y)^2}{(b-a)(d-c)} \int_0^1 \int_0^1 |(t-1)(1-s)| \left| \frac{\partial^2 f}{\partial t \partial s}(tx+(1-t)a, sy+(1-s)d) \right| dsdt \\
+\ & \frac{(b-x)^2(y-c)^2}{(b-a)(d-c)} \int_0^1 \int_0^1 |(1-t)(s-1)| \left| \frac{\partial^2 f}{\partial t \partial s}(tx+(1-t)b, sy+(1-s)c) \right| dsdt \\
+\ & \frac{(b-x)^2(d-y)^2}{(b-a)(d-c)} \int_0^1 \int_0^1 |(1-t)(1-s)| \left| \frac{\partial^2 f}{\partial t \partial s}(tx+(1-t)b, sy+(1-s)d) \right| dsdt
\end{aligned}$$

Since $|\frac{\partial^2 f}{\partial t \partial s}|$ is P-function on Δ on the coordinates and by making use of necessary computations, we obtain;

$$\left| A + \frac{1}{(b-a)(d-c)} \int_a^b \int_c^d f(u,v)dudv \right|$$

$$\begin{aligned}
\leq\ & \frac{(x-a)^2(y-c)^2}{4(b-a)(d-c)} \left(\left| \frac{\partial^2 f}{\partial t \partial s}(x,y) \right| + \left| \frac{\partial^2 f}{\partial t \partial s}(x,c) \right| + \left| \frac{\partial^2 f}{\partial t \partial s}(a,y) \right| + \left| \frac{\partial^2 f}{\partial t \partial s}(a,c) \right| \right) \\
& + \frac{(x-a)^2(d-y)^2}{4(b-a)(d-c)} \left(\left| \frac{\partial^2 f}{\partial t \partial s}(x,y) \right| + \left| \frac{\partial^2 f}{\partial t \partial s}(x,d) \right| + \left| \frac{\partial^2 f}{\partial t \partial s}(a,y) \right| + \left| \frac{\partial^2 f}{\partial t \partial s}(a,d) \right| \right) \\
& + \frac{(b-x)^2(y-c)^2}{4(b-a)(d-c)} \left(\left| \frac{\partial^2 f}{\partial t \partial s}(x,y) \right| + \left| \frac{\partial^2 f}{\partial t \partial s}(x,c) \right| + \left| \frac{\partial^2 f}{\partial t \partial s}(b,y) \right| + \left| \frac{\partial^2 f}{\partial t \partial s}(b,c) \right| \right) \\
& + \frac{(b-x)^2(d-y)^2}{4(b-a)(d-c)} \left(\left| \frac{\partial^2 f}{\partial t \partial s}(x,y) \right| + \left| \frac{\partial^2 f}{\partial t \partial s}(x,d) \right| + \left| \frac{\partial^2 f}{\partial t \partial s}(b,y) \right| + \left| \frac{\partial^2 f}{\partial t \partial s}(b,d) \right| \right).
\end{aligned}$$

This completes the proof. ■

Corollary 7 *Under the assumptions of Theorem 6, if we choose $x = a, y = c$, then we have the following inequality;*

$$\begin{aligned}
&\left| f(b,d) - \frac{1}{(d-c)} \int_c^d f(b,v)dv - \frac{1}{(b-a)} \int_a^b f(u,d)du \right. \\
&\left. + \frac{1}{(b-a)(d-c)} \int_a^b \int_c^d f(u,v)dudv \right| \\
\leq\ & \frac{(b-a)(d-c)}{4} \left(\left| \frac{\partial^2 f}{\partial t \partial s}(a,c) \right| + \left| \frac{\partial^2 f}{\partial t \partial s}(a,d) \right| + \left| \frac{\partial^2 f}{\partial t \partial s}(b,c) \right| + \left| \frac{\partial^2 f}{\partial t \partial s}(b,d) \right| \right).
\end{aligned}$$

Corollary 8 *Under the assumptions of Theorem 6, if we choose $x=b, y=c$, then we have the following inequality;*

$$\begin{aligned}
&\left|f(a,d)-\frac{1}{(d-c)}\int_c^d f(a,v)dv-\frac{1}{(b-a)}\int_a^b f(u,d)du\right.\\
&\left.+\frac{1}{(b-a)(d-c)}\int_a^b\int_c^d f(u,v)dudv\right|\\
\leq\ & \frac{(b-a)(d-c)}{4}\left(\left|\frac{\partial^2 f}{\partial t\partial s}(a,c)\right|+\left|\frac{\partial^2 f}{\partial t\partial s}(a,d)\right|+\left|\frac{\partial^2 f}{\partial t\partial s}(b,c)\right|+\left|\frac{\partial^2 f}{\partial t\partial s}(b,d)\right|\right).
\end{aligned}$$

Corollary 9 *Under the assumptions of Theorem 6, if we choose $x=a, y=d$, then we have the following inequality;*

$$\begin{aligned}
&\left|f(b,c)-\frac{1}{(d-c)}\int_c^d f(b,v)dv-\frac{1}{(b-a)}\int_a^b f(u,c)du\right.\\
&\left.+\frac{1}{(b-a)(d-c)}\int_a^b\int_c^d f(u,v)dudv\right|\\
\leq\ & \frac{(b-a)(d-c)}{4}\left(\left|\frac{\partial^2 f}{\partial t\partial s}(a,c)\right|+\left|\frac{\partial^2 f}{\partial t\partial s}(a,d)\right|+\left|\frac{\partial^2 f}{\partial t\partial s}(b,c)\right|+\left|\frac{\partial^2 f}{\partial t\partial s}(b,d)\right|\right).
\end{aligned}$$

Corollary 10 *Under the assumptions of Theorem 6, if we choose $x=b, y=d$, then we have the following inequality;*

$$\begin{aligned}
&\left|f(a,c)-\frac{1}{(d-c)}\int_c^d f(a,v)dv-\frac{1}{(b-a)}\int_a^b f(u,c)du\right.\\
&\left.+\frac{1}{(b-a)(d-c)}\int_a^b\int_c^d f(u,v)dudv\right|\\
\leq\ & \frac{(b-a)(d-c)}{4}\left(\left|\frac{\partial^2 f}{\partial t\partial s}(a,c)\right|+\left|\frac{\partial^2 f}{\partial t\partial s}(a,d)\right|+\left|\frac{\partial^2 f}{\partial t\partial s}(b,c)\right|+\left|\frac{\partial^2 f}{\partial t\partial s}(b,d)\right|\right).
\end{aligned}$$

Theorem 11 *Let $a<b$, $c<d$ and $f:\Delta=[a,b]\times[c,d]\subseteq\mathbb{R}^2\to\mathbb{R}$ be a twice differentiable function on Δ. If $\left|\frac{\partial^2 f}{\partial t\partial s}\right|^{\frac{p}{p-1}}$ is $P-$function on Δ on the coordinates, then one has the following inequality;*

$$\begin{aligned}
&\left|A+\frac{1}{(b-a)(d-c)}\int_a^b\int_c^d f(u,v)dudv\right|\\
\leq\ & \frac{1}{(b-a)(d-c)(p+1)^{\frac{2}{p}}}\\
&\times\left[(x-a)^2(y-c)^2\left(\left|\frac{\partial^2 f}{\partial t\partial s}(x,y)\right|^q+\left|\frac{\partial^2 f}{\partial t\partial s}(x,c)\right|^q+\left|\frac{\partial^2 f}{\partial t\partial s}(a,y)\right|^q+\left|\frac{\partial^2 f}{\partial t\partial s}(a,c)\right|^q\right)^{\frac{1}{q}}\right.\\
&+(x-a)^2(d-y)^2\left(\left|\frac{\partial^2 f}{\partial t\partial s}(x,y)\right|^q+\left|\frac{\partial^2 f}{\partial t\partial s}(x,d)\right|^q+\left|\frac{\partial^2 f}{\partial t\partial s}(a,y)\right|^q+\left|\frac{\partial^2 f}{\partial t\partial s}(a,d)\right|^q\right)^{\frac{1}{q}}\\
&+(b-x)^2(y-c)^2\left(\left|\frac{\partial^2 f}{\partial t\partial s}(x,y)\right|^q+\left|\frac{\partial^2 f}{\partial t\partial s}(x,c)\right|^q+\left|\frac{\partial^2 f}{\partial t\partial s}(b,y)\right|^q+\left|\frac{\partial^2 f}{\partial t\partial s}(,c)\right|^q\right)^{\frac{1}{q}}\\
&\left.+(b-x)^2(d-y)^2\left(\left|\frac{\partial^2 f}{\partial t\partial s}(x,y)\right|^q+\left|\frac{\partial^2 f}{\partial t\partial s}(x,d)\right|^q+\left|\frac{\partial^2 f}{\partial t\partial s}(b,y)\right|^q+\left|\frac{\partial^2 f}{\partial t\partial s}(b,d)\right|^q\right)^{\frac{1}{q}}\right]
\end{aligned}$$

for $q>1$ and $\frac{1}{q}+\frac{1}{p}=1$.

Proof. From Lemma 2.1 and by using Hölder integral inequality for double integrals, we have

$$\left|A+\frac{1}{(b-a)(d-c)}\int_a^b\int_c^d f(u,v)dudv\right|$$

$$\begin{aligned}
\leq\ & \frac{(x-a)^2(y-c)^2}{(b-a)(d-c)}\left(\int_0^1\int_0^1 |(t-1)(s-1)|^p dsdt\right)^{\frac{1}{p}} \\
&\times\left(\int_0^1\int_0^1\left|\frac{\partial^2 f}{\partial t\partial s}(tx+(1-t)a,sy+(1-s)c)\right|^q dsdt\right)^{\frac{1}{q}} \\
&+\frac{(x-a)^2(d-y)^2}{(b-a)(d-c)}\left(\int_0^1\int_0^1 |(t-1)(s-1)|^p dsdt\right)^{\frac{1}{p}} \\
&\times\left(\int_0^1\int_0^1\left|\frac{\partial^2 f}{\partial t\partial s}(tx+(1-t)a,sy+(1-s)d)\right|^q dsdt\right)^{\frac{1}{q}} \\
&+\frac{(b-x)^2(y-c)^2}{(b-a)(d-c)}\left(\int_0^1\int_0^1 |(t-1)(s-1)|^p dsdt\right)^{\frac{1}{p}} \\
&\times\left(\int_0^1\int_0^1\left|\frac{\partial^2 f}{\partial t\partial s}(tx+(1-t)b,sy+(1-s)c)\right|^q dsdt\right)^{\frac{1}{q}} \\
&+\frac{(b-x)^2(d-y)^2}{(b-a)(d-c)}\left(\int_0^1\int_0^1 |(t-1)(s-1)|^p dsdt\right)^{\frac{1}{p}} \\
&\times\left(\int_0^1\int_0^1\left|\frac{\partial^2 f}{\partial t\partial s}(tx+(1-t)b,sy+(1-s)d)\right|^q dsdt\right)^{\frac{1}{q}}
\end{aligned}$$

Since $\left|\frac{\partial^2 f}{\partial t\partial s}\right|^q$ is P-function on Δ on the coordinates, we obtain;

$$\left|A+\frac{1}{(b-a)(d-c)}\int_a^b\int_c^d f(u,v)dudv\right|\leq\frac{1}{(b-a)(d-c)(p+1)^{\frac{2}{p}}}$$

$$\begin{aligned}
&\left[(x-a)^2(y-c)^2\left(\left|\frac{\partial^2 f}{\partial t\partial s}(x,y)\right|^q+\left|\frac{\partial^2 f}{\partial t\partial s}(x,c)\right|^q+\left|\frac{\partial^2 f}{\partial t\partial s}(a,y)\right|^q+\left|\frac{\partial^2 f}{\partial t\partial s}(a,c)\right|^q\right)^{\frac{1}{q}}\right. \\
&+(x-a)^2(d-y)^2\left(\left|\frac{\partial^2 f}{\partial t\partial s}(x,y)\right|^q+\left|\frac{\partial^2 f}{\partial t\partial s}(x,d)\right|^q+\left|\frac{\partial^2 f}{\partial t\partial s}(a,y)\right|^q+\left|\frac{\partial^2 f}{\partial t\partial s}(a,d)\right|^q\right)^{\frac{1}{q}} \\
&+(b-x)^2(y-c)^2\left(\left|\frac{\partial^2 f}{\partial t\partial s}(x,y)\right|^q+\left|\frac{\partial^2 f}{\partial t\partial s}(x,d)\right|^q+\left|\frac{\partial^2 f}{\partial t\partial s}(a,y)\right|^q+\left|\frac{\partial^2 f}{\partial t\partial s}(a,d)\right|^q\right)^{\frac{1}{q}} \\
&\left.+(b-x)^2(d-y)^2\left(\left|\frac{\partial^2 f}{\partial t\partial s}(x,y)\right|^q+\left|\frac{\partial^2 f}{\partial t\partial s}(x,d)\right|^q+\left|\frac{\partial^2 f}{\partial t\partial s}(b,y)\right|^q+\left|\frac{\partial^2 f}{\partial t\partial s}(b,d)\right|^q\right)^{\frac{1}{q}}\right].
\end{aligned}$$

Which completes the proof. ■

Theorem 12 *Let $a<b$, $c<d$ and $f:\Delta=[a,b]\times[c,d]\subseteq\mathbb{R}^2\to\mathbb{R}$ be a twice differentiable function on Δ. If $\left|\frac{\partial^2 f}{\partial t\partial s}\right|^q$ is $P-$function on Δ on the coordinates, then one has the following*

inequality;

$$
\begin{aligned}
& \left|A + \frac{1}{(b-a)(d-c)} \int_a^b \int_c^d f(u,v)dudv\right| \\
\leq & \frac{1}{4(b-a)(d-c)} \\
& \times\Bigg[(x-a)^2(y-c)^2\left(\left|\frac{\partial^2 f}{\partial t \partial s}(x,y)\right|^q + \left|\frac{\partial^2 f}{\partial t \partial s}(x,c)\right|^q + \left|\frac{\partial^2 f}{\partial t \partial s}(a,y)\right|^q + \left|\frac{\partial^2 f}{\partial t \partial s}(a,c)\right|^q\right)^{\frac{1}{q}} \\
& +(x-a)^2(d-y)^2\left(\left|\frac{\partial^2 f}{\partial t \partial s}(x,y)\right|^q + \left|\frac{\partial^2 f}{\partial t \partial s}(x,d)\right|^q + \left|\frac{\partial^2 f}{\partial t \partial s}(a,y)\right|^q + \left|\frac{\partial^2 f}{\partial t \partial s}(a,d)\right|^q\right)^{\frac{1}{q}} \\
& +(b-x)^2(y-c)^2\left(\left|\frac{\partial^2 f}{\partial t \partial s}(x,y)\right|^q + \left|\frac{\partial^2 f}{\partial t \partial s}(x,d)\right|^q + \left|\frac{\partial^2 f}{\partial t \partial s}(a,y)\right|^q + \left|\frac{\partial^2 f}{\partial t \partial s}(a,d,)\right|^q\right)^{\frac{1}{q}} \\
& +(b-x)^2(d-y)^2\left(\left|\frac{\partial^2 f}{\partial t \partial s}(x,y)\right|^q + \left|\frac{\partial^2 f}{\partial t \partial s}(x,d)\right|^q + \left|\frac{\partial^2 f}{\partial t \partial s}(b,y)\right|^q + \left|\frac{\partial^2 f}{\partial t \partial s}(b,d)\right|^q\right)^{\frac{1}{q}}\Bigg]
\end{aligned}
$$

for $q \geq 1$.

Proof. By a similar argument to the proof of Theorem 2.7, by using Lemma 2.1 and Power-mean inequality for double integrals, we obtain;

$$
\begin{aligned}
& \left|A + \frac{1}{(b-a)(d-c)} \int_a^b \int_c^d f(u,v)dudv\right| \\
\leq & \frac{(x-a)^2(y-c)^2}{(b-a)(d-c)}\left(\int_0^1\int_0^1 |(t-1)(s-1)|^p dsdt\right)^{1-\frac{1}{q}} \\
& \times\left(\int_0^1\int_0^1 \left|\frac{\partial^2 f}{\partial t \partial s}(tx+(1-t)a, sy+(1-s)c)\right|^q dsdt\right)^{\frac{1}{q}} \\
& +\frac{(x-a)^2(d-y)^2}{(b-a)(d-c)}\left(\int_0^1\int_0^1 |(t-1)(s-1)|^p dsdt\right)^{1-\frac{1}{q}} \\
& \times\left(\int_0^1\int_0^1 \left|\frac{\partial^2 f}{\partial t \partial s}(tx+(1-t)a, sy+(1-s)d)\right|^q dsdt\right)^{\frac{1}{q}} \\
& +\frac{(b-x)^2(y-c)^2}{(b-a)(d-c)}\left(\int_0^1\int_0^1 |(t-1)(s-1)|^p dsdt\right)^{1-\frac{1}{q}} \\
& \times\left(\int_0^1\int_0^1 \left|\frac{\partial^2 f}{\partial t \partial s}(tx+(1-t)b, sy+(1-s)c)\right|^q dsdt\right)^{\frac{1}{q}} \\
& +\frac{(b-x)^2(d-y)^2}{(b-a)(d-c)}\left(\int_0^1\int_0^1 |(t-1)(s-1)|^p dsdt\right)^{1-\frac{1}{q}} \\
& \times\left(\int_0^1\int_0^1 \left|\frac{\partial^2 f}{\partial t \partial s}(tx+(1-t)b, sy+(1-s)d)\right|^q dsdt\right)^{\frac{1}{q}}
\end{aligned}
$$

Since $\left|\frac{\partial^2 f}{\partial t \partial s}\right|^q$ is $P-$ function on Δ on the coordinates, we get;

$$\begin{aligned}
&\left|A + \frac{1}{(b-a)(d-c)}\int_a^b \int_c^d f(u,v)dudv\right| \\
\leq\ & \frac{1}{4(b-a)(d-c)} \\
&\times\Bigg[(x-a)^2(y-c)^2\left(\left|\frac{\partial^2 f}{\partial t\partial s}(x,y)\right|^q + \left|\frac{\partial^2 f}{\partial t\partial s}(x,c)\right|^q + \left|\frac{\partial^2 f}{\partial t\partial s}(a,y)\right|^q + \left|\frac{\partial^2 f}{\partial t\partial s}(a,c)\right|^q\right)^{\frac{1}{q}} \\
&+(x-a)^2(d-y)^2\left(\left|\frac{\partial^2 f}{\partial t\partial s}(x,y)\right|^q + \left|\frac{\partial^2 f}{\partial t\partial s}(x,d)\right|^q + \left|\frac{\partial^2 f}{\partial t\partial s}(a,y)\right|^q + \left|\frac{\partial^2 f}{\partial t\partial s}(a,d)\right|^q\right)^{\frac{1}{q}} \\
&+(b-x)^2(y-c)^2\left(\left|\frac{\partial^2 f}{\partial t\partial s}(x,y)\right|^q + \left|\frac{\partial^2 f}{\partial t\partial s}(x,d)\right|^q + \left|\frac{\partial^2 f}{\partial t\partial s}(a,y)\right|^q + \left|\frac{\partial^2 f}{\partial t\partial s}(a,d)\right|^q\right)^{\frac{1}{q}} \\
&+(b-x)^2(d-y)^2\left(\left|\frac{\partial^2 f}{\partial t\partial s}(x,y)\right|^q + \left|\frac{\partial^2 f}{\partial t\partial s}(x,d)\right|^q + \left|\frac{\partial^2 f}{\partial t\partial s}(b,y)\right|^q + \left|\frac{\partial^2 f}{\partial t\partial s}(b,d)\right|^q\right)^{\frac{1}{q}}\Bigg].
\end{aligned}$$

Which is the desired result. ■

References

[1] M.E. Özdemir, Ç. Yıldız and A. O. Akdemir, On The Co-ordinated Convex functions. Applied Mathematics and Information Sciences, 8 (3), 1085-1081 (2014).

[2] A.O. Akdemir and M.E. Özdemir, Some Hermite-type inequalities for co-ordinated $P-$convex functions and Godunova-Levin functions, American Institute of Phsyics (AIP) Conference Proceedings, 1309, 7-15.

[3] M.E. Özdemir, A.O. Akdemir, Ç. Yıldız, On Co-ordinated Quasi-Convex Functions, Czechoslovak Mathematical Joournal, 62 (137) (2012), 889-900.

[4] M.E. Özdemir, H.Kavurmacı, A.O. Akdemir, M.Avcı, Inequalities for convex and $s-$convex functions on $\Delta = [a,b] \times [c,d]$, Journal of Inequalities and Applications, 2012, 2012:20, doi:10.1186/1029-242X-2012-20, Published: 1 February 2012.

[5] M.E. Özdemir, Ç. Yıldız and A. O. Akdemir, On Some New Hadamard-type Inequalities for Co-ordinated Quasi-Convex Functions, Hacettepe Journal of Mathematics and Statistics, 41 (5) (2012), 697-707

[6] M.E.Özdemir, E.Set and M.Z. Sarıkaya, Sme new Hadamard's type inequalities for co-ordinated $m-$convex and α, m- convex functions, Hacettepe Journal of Mathematics and Statistic vol 40(2) (2012) 219-229.

[7] S.S. Dragomir, On the Hadamard's inequality for convex functions on the co-ordinates in rectangle from the plane, Taiwanese Journal of mathematics, 5(2001), no.4 775-788

[8] M.A. Latif and M. Alomari, On Hadamard-type inequalities for $h-$convex functions on the co-ordinates, Int. Journal of Math. Analysis, 3(33) (2009), 1645-1656.

On ∇_2-Statistical Convergence of Double Sequences in Random 2-Normed Space

Ömer KİŞİ*
Bartın University,
Department of Mathematics,
74100, Bartın, TURKEY

Erhan GÜLER
BartınUniversity,
Department of Mathematics,
74100, Bartın, TURKEY

Abstract

In this present paper, we introduce the notion of ∇_2-statistical convergence of double sequences, ∇_2-statistical Cauchy double sequences in random 2-normed spaces and obtain some results. We display examples which show that our method of convergence is more general in random 2-normed space.

Keywords: λ-convergence, 2-norm, 2-normed space.

1 Introduction

The idea of the statistical convergence was given by Zygmund [29] in the first edition of his monograph published in Warsaw in 1935. The concept of statistical convergence was introduced by Fast [6] and Steinhaus [27] and then reintroduced by Schoenberg [24] independently. Over the years, statistical convergence has been developed in ([2], [7], [8], [14], [18], [22], [28]) and turned out very useful to resolve many convergence problems arising in Analysis.

Definition 1 *([6]) A number sequence $x = (x_k)$ is said to be statistically convergent to the number l if for every $\varepsilon > 0$,*

$$\lim_{n\to\infty} \frac{1}{n} |\{k \leq n : |x_k - l| \geq \varepsilon\}| = 0.$$

In this case we write $st - \lim_{k\to\infty} x_k = l$. Statistical convergence is a natural generalization of ordinary convergence. If $\lim x_k = l$, then $st - \lim x_k = l$. The converse does not hold in general.

In literature, several interesting generalizations of statistical convergence have been appeared. One among these is -statistical convergence given by Mursaleen [16] with the help of a non-decreasing sequence $\lambda = (\lambda_n)$ be a nondecreasing sequence of positive real numbers tending to ∞ such that $\lambda_{n+1} \leq \lambda_n + 1$, $\lambda_1 = 1$.

The idea of λ-statistical convergence can be connected to the generalized de la Vallée-Poussin mean. It is defined by

$$t_n(x) = \frac{1}{\lambda_n} \sum_{k \in I_n} x_k$$

where $I_n = [n - \lambda_n + 1, n]$.

*Corresponding author. *E-mail address:* okisi@bartin.edu.tr

Definition 2 *([16]) A sequence $x = (x_k)$ of numbers is said to be λ-statistical convergent to a number l provided that for every $\varepsilon > 0$,*

$$\lim_{n\to\infty} \frac{1}{\lambda_n} |\{k \in I_n : |x_k - l| \geq \varepsilon\}| = 0.$$

In this case, the number l is called λ-statistical limit of the sequence $x = (x_k)$ and we write $S_\lambda - \lim_{k\to\infty} x_k = l$.

The concept of probabilistic normed spaces was initially introduced by A. N. Sherstnev [26] in 1962. Menger [15] introduced the notion of probabilistic metric spaces in 1942. The idea of Menger [15] was to use distribution function instead of non-negative real numbers as values of the metric. In last few years these spaces are grown up rapidly and many detereministic results of linear normed spaces are obtained for probabilistic normed spaces. For a detailed study on probabilistic functional analysis, we refer ([1], [11], [19], [25]). In 2005, Golet [10] used the concept of 2-norm of Gähler [9] and presented generalized probabilistic normed space which he called random 2-normed space. Gürdal and Pehlivan ([30], [31]) studied statistical convergence in 2-normed spaces and in 2-Banach spaces. Recently, Savaş [32] defined and studied generalized statistical convergence in random 2-normed space. Esi and Özdemir [5] introduced and studied the concept of generalized Δ^m-statistical convergence of sequences in probabilistic normed space. Esi [4], defined and studied the notion of ∇-statistical convergence and ∇-statistical Cauchy sequences using by λ-sequences in random 2-normed spaces, and proved some theorems.

The existing literature on statistical convergence and its generalizations appears to have been restricted to real or complex sequences, but in recent years these ideas have been also extended to the sequences in fuzzy normed [33] and intutionistic fuzzy normed spaces [12], [13], [20] and [21].

Let $\mathbb{R}$ denotes the set of reals and $\mathbb{R}_0^+ = [0, \infty)$. A function $f : \mathbb{R} \to \mathbb{R}_0^+$ is called a distribution function if it is non-decreasing and left-continuous with $\inf_{t\in\mathbb{R}} f(t) = 0$ and $\sup_{t\in\mathbb{R}} f(t) = 1$. We will denote the set of all distribution functions by $\mathcal{D}$. Also, a a distance distribution function is a non decreasing function $\mathcal{F}$ defined on $\mathbb{R}^+ = [0, \infty)$ that satisfies $\mathcal{F}(0) = 0$ and $\mathcal{F}(\infty) = 1$; and is left continuous on $(0, \infty)$. Let $\mathcal{D}^+$ denotes the set of all distance distribution functions.

A triangular norm, briefly t-norm, is a binary operation $*$ on $[0, 1]$ which is continuous, commutative, associative, non-decreasing and has 1 as neutral element, i.e., it is the continuous mapping $* : [0, 1] \times [0, 1] \to [0, 1]$ such that for all $a, b, c \in [0, 1]$:

(i) $a * 1 = a$,
(ii) $a * b = b * a$,
(iii) $c * d \geq a * b$ if $c \geq a$ and $d \geq b$,
(iv) $(a * b) * c = a * (b * c)$.

The $*$ operations $a * b = \max\{a + b - 1, 0\}$, $a * b = ab$, and $a * b = \min\{a, b\}$ on $[0, 1]$ are t-norms.

In following, we give some useful definitions.

Definition 3 *([9]) Let X be a real vector vector space of dimension $d > 1$ (d may be infinite). A real valued function $\|.,.\| : X^2 \to \mathbb{R}$ satisfying the following conditions:*

(i) $\|x_1, x_2\| = 0$, if and only if x_1, x_2 are linearly dependent.
(ii) $\|x_1, x_2\| = \|x_2, x_1\|$ for all $x_1, x_2 \in X$,
(iii) $\|\alpha x_1, x_2\| = |\alpha| \|x_1, x_2\|$, for any $\alpha \in \mathbb{R}$ and
(iv) $\|x_1 + x_2, x_3\| \leq \|x_1, x_3\| + \|x_2, x_3\|$

is called a 2-norm and the pair $(X, \|.,.\|)$ is called a 2-normed space.

Definition 4 *([10]) Let X be a real vector vector space of dimension $d > 1$ (d may be infinite),τ be a triangle function (a binary operation on $\mathcal{D}^+$ which is associative, commutative, nondecreasing and ε_0 as a unit) and $\mathcal{F} : X \times X \to \mathcal{D}^+$ (for $x, y \in X$, $\mathcal{F}(x, y; t)$ is the value of $\mathcal{F}(x, y)$ at $t \in \mathbb{R}$). Then $\mathcal{F}$ is called a probabilistic norm $(X, \mathcal{F}, \tau)$ a probabilistic 2-normed space if the following conditions are satisfied:*

(i) $\mathcal{F}(x, y; t) = H_0(t)$, if x, y are linearly dependent, where $H_0(t) = 0$ if $t \leq 0$ and $H_0(t) = 1$ if $t > 0$.
(ii) $\mathcal{F}(x, y; t) \neq H_0(t)$, if x, y are linearly dependent.
(iii) $\mathcal{F}(x, y; t) = \mathcal{F}(y, x; t)$, for all $x, y \in X$,
(iv) $\mathcal{F}(\alpha x, y; t) = \mathcal{F}\left(x, y; \frac{t}{|\alpha|}\right)$ for every $t > 0$, $\alpha \neq 0$ and $x, y \in X$,
(v) $\mathcal{F}(x + y, z; t) \geq \tau(\mathcal{F}(x, z; t), \mathcal{F}(y, z; t))$, where $x, y, z \in X$.

If (v) is replaced by $\mathcal{F}(x + y, z; t_1 + t_2) \geq \mathcal{F}(x, z; t_1) * \mathcal{F}(y, z; t_2)$ for all $x, y, z \in X$ and $t_1, t_2 \in \mathbb{R}_0^+$ then $(X, \mathcal{F}, *)$ is called a random 2-normed space.

Example 5 *Let $(X, \|.,.\|)$ be a 2-normed space with $\|x, z\| = |x_1 z_2 - x_2 z_1|$; $x = (x_1, x_2)$, $z = (z_1, z_2)$ and $a * b = ab$ for all $a, b \in [0, 1]$. For every $x, y \in X$ and $t > 0$ we define $\mathcal{F}(x, y; t) = \frac{t}{t + \|x, y\|}$, then $(X, \mathcal{F}, *)$ is a random 2-normed space.*

Definition 6 *([17]) Let $(X, \mathcal{F}, *)$ be a random 2-normed space. Then a sequence $x = (x_k)$ is said to be convergent to $x_0 \in X$ with respect to norm $\mathcal{F}$ if for every $\varepsilon > 0$, $t \in (0, 1)$ and non-zero $z \in X$, there exists a positive integer k_0 such that $\mathcal{F}(x_k - x_0, z; \varepsilon) > 1 - t$ whenever $k \geq k_0$. It is denoted by $\mathcal{F}\text{-}\lim x_k = x_0$.*

Definition 7 *([17]) Let $(X, \mathcal{F}, *)$ be a random 2-normed space. Then a sequence $x = (x_k)$ is said to be statistically convergent S^{R2N} convergent to $x_0 \in X$ with respect to norm $\mathcal{F}$ if for every $\varepsilon > 0$, $t \in (0, 1)$ and non-zero $z \in X$,*

$$\delta(\{k \in \mathbb{N} : \mathcal{F}(x_k - x_0, z; \varepsilon) \leq 1 - t\}) = 0.$$

In this case, we write $S^{R2N}\text{-}\lim x_k = x_0$.

Definition 8 *([3]) Let $(X, \mathcal{F}, *)$ be a random 2-normed space. Then a sequence $x = (x_k)$ is said to be statistically convergent to l with respect to $\mathcal{F}$ if for every $\varepsilon > 0$, $t \in (0, 1)$ and non-zero $z \in X$,*

$$\lim_{n \to \infty} \frac{1}{n} |(\{k \leq n : \mathcal{F}(x_k - l, z; \varepsilon) \leq 1 - t\})| = 0.$$

In this case, we write $S^{R2N}\text{-}\lim x_k = l$.

Throughout the paper, we consider $(X, \mathcal{F}, *)$ be an random 2-normed space and $\overline{\lambda}_{r,s} = \lambda_r \mu_s$ be the collection of such sequences $\overline{\lambda}$ will be denoted by Δ_2.

Let $\lambda = (\lambda_r)$ and $\mu = (\mu_s)$ be two non-decreasing sequences of positive real numbers, each tending to ∞ and such that $\lambda_{r+1} \leq \lambda_r + 1$, $\lambda_1 = 1$; $\mu_{s+1} \leq \mu_s + 1$, $\mu_1 = 1$. Let $I_r = [r - \lambda_r + 1, r]$, $I_s = [s - \mu_s + 1, s]$ and $I_{r,s} = I_r \times I_s$.

For any set $X \subseteq \mathbb{N} \times \mathbb{N}$, the number,

$$\delta_{\overline{\lambda}}(X) = P\text{-}\lim_{r,s \to \infty} \frac{1}{\overline{\lambda}_{r,s}} |\{(k, l) \in I_r \times I_s : (k, l) \in X\}|;$$

is said to be $\overline{\lambda}$-density of the set X, provided the limit exists, where $\overline{\lambda}_{r,s} = \lambda_r \mu_s$.

2 Main results

In this present study, we introduce the notion of ∇_2-statistical convergence of double sequences, ∇_2-statistical Cauchy double sequences in random 2-normed spaces and obtain some results. We display examples which show that our method of convergence is more general in random 2-normed space.

Definition 9 *A double sequence $x = (x_{kl})$ in random 2-normed space $(X, \mathcal{F}, *)$ is said to be ∇_2-convergent to $l \in X$ with respect to $\mathcal{F}$ if for each $\varepsilon > 0$, $t \in (0,1)$ and for non-zero $z \in X$, there exists an positive integer n_0 such that $\mathcal{F}\left(\frac{1}{\overline{\lambda}_{r,s}} \sum_{(k,l)\in I_{r,s}} x_{kl} - l, z; \varepsilon\right) > 1 - t$ whenewer $k, l \geq n_0$. In this case we write $\mathcal{F}_{\nabla_2} - \lim_{k,l\to\infty} x_{kl} = l$, and l is called the $\mathcal{F}_{\nabla_2}-$limit of $x = (x_{kl})$.*

Definition 10 *A double sequence $x = (x_{kl})$ in a random 2-normed space $(X, \mathcal{F}, *)$ is said to be ∇_2-Cauchy with respect to $\mathcal{F}$ if for every $\varepsilon > 0$, $t \in (0,1)$ and for non-zero $z \in X$, there exists positive integers p, q such that*

$$\mathcal{F}\left(\frac{1}{\overline{\lambda}_{r,s}} \sum_{(k,l)\in I_{r,s}} (x_{kl} - x_{mn}), z; \varepsilon\right) < 1 - t,$$

whenever $k, m > p$, $l, n > q$.

Definition 11 *A double sequence $x = (x_{kl})$ in a random 2-normed space $(X, \mathcal{F}, *)$ is said to be ∇_2-statistical convergent or S_{∇_2}-convergent to l with respect to $\mathcal{F}$ if for every $\varepsilon > 0$, $t \in (0,1)$ andfor non-zero $z \in X$ such that*

$$\delta_{\nabla_2}\left(\left\{(k,l) \in I_{r,s} : \mathcal{F}\left(\frac{1}{\overline{\lambda}^{\alpha}_{r,s}} \sum_{(k,l)\in I_{r,s}} x_{kl} - l, z; \varepsilon\right) \leq 1 - t\right\}\right) = 0.$$

In other ways we can write

$$\left|\left\{(k,l) \in I_{r,s} : \mathcal{F}\left(\lim_{r,s\to\infty} \frac{1}{\overline{\lambda}^{\alpha}_{r,s}} \sum_{(k,l)\in I_{r,s}} x_{kl} - l, z; \varepsilon\right) \leq 1 - t\right\}\right| = 0,$$

or, equivalently,

$$\delta_{\nabla_2}\left(\left\{(k,l) \in I_{r,s} : \mathcal{F}\left(\frac{1}{\overline{\lambda}_{r,s}} \sum_{(k,l)\in I_{r,s}} x_{kl} - l, z; \varepsilon\right) > 1 - t\right\}\right) =1,$$

i.e.,

$$S_{\nabla_2} - \lim_{r,s\to\infty} \mathcal{F}\left(\frac{1}{\overline{\lambda}_{r,s}} \sum_{(k,l)\in I_{r,s}} x_{kl} - l, z; \varepsilon\right) =1.$$

In this case, we write $S_{\nabla_2}(R2N) - \lim_{k,l} x_{kl} = l$ or $x_{kl} \to l\,(S_{\nabla_2}(R2N))$ and

$$S_{\nabla_2}(R2N)(X) = \left\{x = (x_{kl}) : \exists l \in \mathbb{R}, S_{\nabla_2}(R2N) - \lim_{k,l} x_{kl} = l\right\}.$$

The collection of all ∇_2-statistically convergent double sequences in random 2-normed space is symbolized as $S^{\alpha}_{\nabla_2}(R2N)(X)$.

Definition 12 *A double sequence $x=(x_{kl})$ in a random 2-normed space $(X,\mathcal{F},*)$ is said to be ∇_2-statistically Cauchy with respect to $\mathcal{F}$ if for every $\varepsilon>0$, $t\in(0,1)$ and for non-zero $z\in X$, there exists positive integers p,q such that for all $k,m>p$, $l,n>q$*

$$\delta_{\nabla_2}\left(\left\{(k,l)\in I_{r,s}:\mathcal{F}\left(\frac{1}{\overline{\lambda}_{r,s}}\sum_{(k,l)\in I_{r,s}}(x_{kl}-x_{mn}),z;\varepsilon\right)\leq 1-t\right\}\right)=0,$$

or, equivalently,

$$\delta_{\nabla_2}\left(\left\{(k,l)\in I_{r,s}:\mathcal{F}\left(\frac{1}{\overline{\lambda}_{r,s}}\sum_{(k,l)\in I_{r,s}}(x_{kl}-x_{mn}),z;\varepsilon\right)> 1-t\right\}\right)=1.$$

This definition, immediately implies the following Lemma.

Lemma 13 *Let $(X,\mathcal{F},*)$ be a random 2-normed space. If $x=(x_{kl})$ is a double sequence in X, then for every $\varepsilon>0$, $t\in(0,1)$ and for non-zero $z\in X$, then the following statetements are equivalent.*

(i) $S_{\nabla_2}-\lim_{k,l}x_{kl}=l$.

(ii) $\delta_{\nabla_2}\left(\left\{(k,l)\in I_{r,s}:\mathcal{F}\left(\frac{1}{\overline{\lambda}_{r,s}}\sum_{(k,l)\in I_{r,s}}x_{kl}-l,z;\varepsilon\right)\leq 1-t\right\}\right)=0$.

(iii) $\delta_{\nabla_2}\left(\left\{(k,l)\in I_{r,s}:\mathcal{F}\left(\frac{1}{\overline{\lambda}_{r,s}}\sum_{(k,l)\in I_{r,s}}x_{kl}-l,z;\varepsilon\right)> 1-t\right\}\right)=1$.

(iv) $S_{\nabla_2}-\lim_{k,l\to\infty}\mathcal{F}\left(\frac{1}{\overline{\lambda}_{r,s}}\sum_{(k,l)\in I_{r,s}}x_{kl}-l,z;\varepsilon\right)=1$.

Theorem 14 *Let $(X,\mathcal{F},*)$ be a random 2-normed space. If $x=(x_{kl})$ is a double sequence in X such that $S_{\nabla_2}(R2N)-\lim_{k,l}x_{kl}=l$ exists, then it is unique.*

Proof. Suppose that $S_{\nabla_2}(R2N)-\lim_{k,l}x_{kl}=l'$, where $l\neq l'$. Let $\varepsilon>0$ be given. Choose $\nu>0$ such that

$$(1-\nu)*(1-\nu)>1-\varepsilon. \tag{1}$$

Then, for any $t>0$ and for non-zero $z\in X$, we define

$$K_1(\upsilon,t)=\left\{(k,l)\in I_{r,s}:\mathcal{F}\left(\frac{1}{\overline{\lambda}_{r,s}}\sum_{(k,l)\in I_{r,s}}(x_{kl}-l),z;\frac{t}{2}\right)\leq 1-\nu\right\};$$

$$K_2(\upsilon,t)=\left\{(k,l)\in I_{r,s}:\mathcal{F}\left(\frac{1}{\overline{\lambda}_{r,s}}\sum_{(k,l)\in I_{r,s}}(x_{kl}-l'),z;\frac{t}{2}\right)\leq 1-\nu\right\}.$$

Since

$$S_{\nabla_2}(R2N)-\lim_{k,l}x_{kl}=l \text{ and } S_{\nabla_2}(R2N)-\lim_{k,l}x_{kl}=l',$$

we have

$$\delta_{\nabla_2}(K_1(\upsilon,t))=0 \text{ and } \delta_{\nabla_2}(K_2(\upsilon,t))=0 \text{ for all } t>0.$$

Let $K(\upsilon,t)=K_1(\upsilon,t)\cup K_2(\upsilon,t)$, then it is easy to observe that $\delta_{\nabla_2}(K(\upsilon,t))=0$ which immediately implies $\delta_{\nabla_2}(K^c(\upsilon,t))=1$. Let $k\in K^c(\upsilon,t)=K_1^c(\upsilon,t)\cap K_2^c(\upsilon,t)$. Now one can write,

$$\begin{aligned}\mathcal{F}\left(l-l',z;t\right) &\geq \mathcal{F}\left(\frac{1}{\overline{\lambda}_{r,s}}\sum_{(k,l)\in I_{r,s}}x_{kl}-l,z;\frac{t}{2}\right)*\mathcal{F}\left(\frac{1}{\overline{\lambda}_{r,s}}\sum_{(k,l)\in I_{r,s}}x_{kl}-l',z;\frac{t}{2}\right)\\ &> (1-\nu)*(1-\nu).\end{aligned}$$

It follows by (1) that

$$\mathcal{F}\left(l-l',z;t\right)>(1-\varepsilon).$$

Since ε is arbitrary, it follows that $\mathcal{F}(l-l',z;t)=1$, for all $t>0$ and non-zero $z\in X$. This shows that $l=l'$. ■

Theorem 15 *Let $(X,\mathcal{F},*)$ be a random 2-normed space. Let $x=(x_{kl})$ and $y=(y_{kl})$ be two double sequences in X.*

(i) If $S_{\nabla_2}(R2N)-\lim_{k,l}x_{kl}=l$ and $0\neq c\in\mathbb{R}$, then $S_{\nabla_2}(R2N)-\lim_{k,l}cx_{kl}=cl$.
(ii) If $S_{\nabla_2}(R2N)-\lim_{k,l}x_{kl}=l$ and $S_{\nabla_2}(R2N)-\lim_{k,l}y_{kl}=l'$, then $S_{\nabla_2}(R2N)-\lim_{k,l}(x_{kl}+y_{kl})=l+l'$.
Proof. The proof of the theorem is not so hard so is omitted here. ■

Theorem 16 *Let $(X,\mathcal{F},*)$ be a random 2-normed space. If $x=(x_{kl})$ be a double sequence in X such that $\mathcal{F}_{\nabla_2}-\lim_{k,l\to\infty}x_{kl}=l$, then $S_{\nabla_2}(R2N)-\lim_{k,l}x_{kl}=l$. Hovewer the converse need not be true in general.*

Proof. Since $\mathcal{F}_{\nabla_2}-\lim_{k,l\to\infty}x_{kl}=l$, for every $\varepsilon>0$, $t>0$ and for non-zero $z\in X$ there is a positive integer n_0 such that

$$\mathcal{F}\left(\frac{1}{\overline{\lambda}_{r,s}}\sum_{(k,l)\in I_{r,s}}x_{kl}-l,z;t\right)>1-\varepsilon,\ \forall k,l>n_0.$$

Since the set

$$K(\varepsilon,t)=\left\{(k,l)\in I_{r,s}:\mathcal{F}\left(\frac{1}{\overline{\lambda}_{r,s}}\sum_{(k,l)\in I_{r,s}}x_{kl}-l,z;t\right)\leq 1-\varepsilon\right\}$$

has at most finitely many terms. Also, since every finite subset of $\mathbb{N}$ has δ_{∇_2}-density zero, consequently we have $S_{\nabla_2}(K(\varepsilon,t))=0$. This shows that $S_{\nabla_2}(R2N)-\lim_{k,l}x_{kl}=l$. We next give the following example which shows that the converse need not be true. ■

Example 17 *Let $X=\mathbb{R}^2$ with the 2-norm $\|x,z\|=\|x_1z_2-x_2z_1\|$ where $x=(x_1,x_2)$, $z=(z_1,z_2)$ and $a*b=ab$ for all $a,b\in[0,1]$. Let $\mathcal{F}(x_{kl},z,t)=\frac{t}{t+\|x,z\|}$, where each $t>0$, non-zero $z\in X$, $z_2>0$. We define a sequence $x=(x_{kl})$ as follows:*

$$\frac{1}{\overline{\lambda}_{r,s}}\sum_{(k,l)\in I_{r,s}}x_{kl}=\begin{cases}(k,l), & \text{if } n-\sqrt{\lambda_n}+1\leq k\leq n,\ \ m-\sqrt{\mu_m}+1\leq l\leq m,\\ (0,0), & \text{otherwise.}\end{cases}$$

Now for $\varepsilon>0$, $t\in(0,1)$, write

$$K(\varepsilon,t)=\left\{(k,l)\in I_{r,s}:\mathcal{F}\left(\frac{1}{\overline{\lambda}_{r,s}}\sum_{(k,l)\in I_{r,s}}x_{kl}-l,z;t\right)\leq 1-\varepsilon\right\},$$

where $l = (0,0)$. *Then*

$$K(\varepsilon,t) = \left\{ (k,l) \in I_{r,s} : \frac{t}{t + \left| \frac{1}{\bar{\lambda}_{r,s}} \sum\limits_{(k,l)\in I_{r,s}} x_{kl} \right|} \leq 1-\varepsilon \right\}, \theta = (0,0)$$

$$= \left\{ (k,l) \in I_{r,s} : \left| \frac{1}{\bar{\lambda}_{r,s}} \sum_{(k,l)\in I_{r,s}} x_{kl} \right| \geq \frac{t\varepsilon}{1-\varepsilon} > 0 \right\}$$

$$= \{(k,l) \in I_{r,s} : x_{kl} = (k,l)\}$$

$$= \left\{ (k,l) \in I_{r,s} : n - \sqrt{\lambda_n} + 1 \leq k \leq n, \ \ m - \sqrt{\mu_m} + 1 \leq l \leq m \right\},$$

so we get

$$\frac{1}{\bar{\lambda}_{r,s}} |K(\varepsilon,t)| \leq \frac{1}{\bar{\lambda}_{r,s}} \left| \left\{ (k,l) \in I_{r,s} : r - \sqrt{\lambda_r} + 1 \leq k \leq r, \ \ s - \sqrt{\mu_s} + 1 \leq l \leq s \right\} \right| \leq \frac{\sqrt{\lambda_{rs}}}{\bar{\lambda}_{r,s}}$$

Takin limit n *approaches to* ∞, *we get*

$$\delta_{\nabla_2}(K(\varepsilon,t)) = \lim_{r,s\to\infty} \frac{1}{\bar{\lambda}_{r,s}} |K(\varepsilon,t)| \leq \lim_{r,s\to\infty} \frac{\sqrt{\lambda_{rs}}}{\bar{\lambda}_{r,s}} = 0.$$

This shows that $x_{kl} \to 0\,(S_{\nabla_2}(R2N)(X))$.

On the other hand the sequence is not $\mathcal{F}_{\nabla_2}-$convergent to zero as

$$\mathcal{F}\left(\frac{1}{\bar{\lambda}_{r,s}} \sum_{(k,l)\in I_{r,s}} x_{kl} - l, z; t \right) = \frac{t}{t + \left| \frac{1}{\bar{\lambda}_{r,s}} \sum\limits_{(k,l)\in I_{r,s}} x_{kl} \right|}$$

$$= \begin{cases} \frac{t}{t+(k+l)z_2}, & \text{if } n - \sqrt{\lambda_n} + 1 \leq k \leq n, \\ & m - \sqrt{\mu_m} + 1 \leq l \leq m, \\ 1, & \text{otherwise.} \end{cases}$$

$$\leq 1.$$

Example 18 *Let* $X = \mathbb{R}^2$ *with the 2-norm* $\|x,z\| = \|x_1 z_2 - x_2 z_1\|$ *where* $x = (x_1,x_2)$, $z = (z_1,z_2)$ *and* $a * b = ab$ *for all* $a,b \in [0,1]$. *Let* $\mathcal{F}(x_{kl},z,t) = \frac{t}{t+\|x,z\|}$, *where each* $t > 0$, *non-zero* $z \in X$, $z_2 > 0$. *We define a sequence* $x = (x_{kl})$ *as follows:*

$$\sum_{(k,l)\in I_{r,s}} x_{kl} = \begin{cases} (1,0), & \textit{if } k+l \textit{ is even,} \\ (0,0), & \textit{if } k+l \textit{ is odd.} \end{cases}$$

For $\varepsilon > 0$, $t \in (0,1)$, *if we define*

$$K(\varepsilon,t) = \left\{(k,l) \in I_{r,s} : \mathcal{F}\left(\tfrac{1}{\overline{\lambda}_{r,s}} \sum_{(k,l)\in I_{r,s}} x_{kl} - \theta, z; t\right) \leq 1-\varepsilon\right\}, \theta = (0,0)$$

$$= \left\{(k,l) \in I_{r,s} : \frac{t}{t+\left\|\frac{1}{\overline{\lambda}_{r,s}} \sum_{(k,l)\in I_{r,s}} x_{kl}-\theta, z\right\|} \leq 1-\varepsilon\right\}$$

$$= \left\{(k,l) \in I_{r,s} : \left\|\tfrac{1}{\overline{\lambda}_{r,s}} \sum_{(k,l)\in I_{r,s}} x_{kl} - \theta, z\right\| \geq \tfrac{\varepsilon t}{1-\varepsilon} > 0\right\}$$

$$= \{(k,l) \in I_{r,s} : (x_{kl}) = (1,0)\} = \{(k,l) \in I_{r,s} : k+l \textit{ is even}\};$$

then,

$$\lim_{r,s\to\infty} \frac{1}{\overline{\lambda}_{r,s}} |K(\varepsilon,t)| = \lim_{r,s\to\infty} \frac{1}{\overline{\lambda}_{r,s}} |\{(k,l) \in I_{r,s} : k+l \textit{ is even}\}| \leq \lim_{r,s\to\infty} \frac{\sqrt{\overline{\lambda}_{r,s}}+1}{2\overline{\lambda}_{r,s}} = 0$$

Similarly, for $\varepsilon > 0$, $t \in (0,1)$, *if we define*

$$B(\varepsilon,t) = \left\{(k,l) \in I_{r,s} : \mathcal{F}\left(\frac{1}{\overline{\lambda}_{r,s}} \sum_{(k,l)\in I_{r,s}} x_{kl} - x_0, z; t\right) \leq 1-\varepsilon\right\}, \ x_0 = (1,0)$$

then

$$\lim_{r,s\to\infty} \frac{1}{\overline{\lambda}_{r,s}} |B(\varepsilon,t)| = \lim_{r,s\to\infty} \frac{1}{\overline{\lambda}_{r,s}} |\{(k,l) \in I_{r,s} : k+l \textit{ is odd}\}| \leq \lim_{r,s\to\infty} \frac{\sqrt{\overline{\lambda}_{r,s}}+1}{2\overline{\lambda}_{r,s}} = 0$$

This shows that $S_{\nabla_2} - \lim_{k,l} x_{kl}$ *is not unique and we obtain a contradiction to theorem 1.*

Theorem 19 *Let* $(X, \mathcal{F}, *)$ *be a random 2-normed space. If* $x = (x_{kl})$ *be a sequence in* X, *then* $S_{\nabla_2} - \lim_{k,l} x_{kl} = l$ *if and only if there exists a subset* $K = \{k_m : k_1 < k_2 < ...\}$ *of* $\mathbb{N}$ *such that* $\lim_{r,s\to\infty} \frac{1}{\overline{\lambda}_{r,s}} |K| = 1$ *and* $\mathcal{F}_{\nabla_2} - \lim_{k,l\to\infty} x_{kl} = l$.

Proof. First suppose that $S_{\nabla_2} - \lim_{k,l} x_{kl} = l$. For $t > 0$ and non-zero $z \in X$ and $s \in \mathbb{N}$, if we define

$$A(s,t) = \left\{(k,l) \in I_{r,s} : \mathcal{F}\left(\frac{1}{\overline{\lambda}_{r,s}} \sum_{(k,l)\in I_{r,s}} x_{kl} - l, z; t\right) > 1 - \frac{1}{s}\right\}$$

$$K(s,t) = \left\{(k,l) \in I_{r,s} : \mathcal{F}\left(\frac{1}{\overline{\lambda}_{r,s}} \sum_{(k,l)\in I_{r,s}} x_{kl} - l, z; t\right) \leq 1 - \frac{1}{s}\right\}$$

Since $S_{\nabla_2} - \lim_{k,l} x_{kl} = l$ it follows that

$$\delta_{\nabla_2}(K(s,t)) = 0$$

Also, for $s = 1, 2, 3, ...$ and for $t > 0$, we observe that

$$A(s,t) \supset A(s+1,t)$$

and

$$\lim_{r,s\to\infty} \frac{1}{\lambda_{r,s}} |A(s,t)| = 1; \text{ i.e., } \delta_{\nabla_2}(A(s,t)) = 1. \tag{2}$$

Now, to prove the result in one way, it is sufficient to prove that $\mathcal{F}_{\nabla_2}-\lim_{k,l\to\infty} x_{kl} = l$. Suppose that for $k \in A(s,t)$, $x = (x_{kl})$ not convergent yo l with respect to $\mathcal{F}_{\nabla_2}$. Then, there exists some $u > 0$ such that

$$\left\{(k,l) \in I_{r,s} : \mathcal{F}\left(\frac{1}{\lambda_{r,s}} \sum_{(k,l)\in I_{r,s}} x_{kl} - l, z; t\right) \leq 1 - u\right\}$$

for infinitely many terms (x_{kl}). Let

$$A(u,t) = \left\{(k,l) \in I_{r,s} : \mathcal{F}\left(\frac{1}{\lambda_{r,s}} \sum_{(k,l)\in I_{r,s}} x_{kl} - l, z; t\right) > 1 - u\right\}$$

and $u > \frac{1}{s}$ for $s = 1, 2, 3....$ This implies that $\delta_{\nabla_2}(A(s,t)) = 0$, which contradicts (2) as $\delta_{\nabla_2}(A(s,t)) = 1$. Hence $\mathcal{F}_{\nabla_2}-\lim_{k,l\to\infty} x_{kl} = l$.

Conversely, suppose that there exists a subset

$$K = \{k_m : k_1 < k_2 < ...\}$$

of $\mathbb{N}$ such that $\lim_{r,s\to\infty} \frac{1}{\lambda_{r,s}} |K| = 1$ and $\mathcal{F}_{\nabla_2}-\lim_{k,l\to\infty} x_{kl} = l$. Then for every $\varepsilon > 0$ and $t > 0$ and non-zero $z \in X$, there exists a positive integer n_0 such that

$$\left\{(k,l) \in I_{r,s} : \mathcal{F}\left(\frac{1}{\lambda_{r,s}} \sum_{(k,l)\in I_{r,s}} x_{kl} - l, z; t\right) > 1 - \varepsilon\right\}$$

for all $k, l > n_0$. If we take

$$K(\varepsilon,t) = \left\{(k,l) \in I_{r,s} : \mathcal{F}\left(\frac{1}{\lambda_{r,s}} \sum_{(k,l)\in I_{r,s}} x_{kl} - l, z; t\right) \leq 1 - \varepsilon\right\}$$

then it is easy to see that

$$K(\varepsilon,t) \subset \mathbb{N} \times \mathbb{N} - \{n_0+1, n_0+2, ...\}$$

and consequently

$$\delta_{\nabla_2}(K(\varepsilon,t)) \leq 1 - 1 = 0.$$

Hence, $S_{\nabla_2} - \lim_{k,l} x_{kl} = l$. ■

Finally, we establish the Cauchy convergence criteria of double sequences of order α in random 2-normed spaces.

Theorem 20 *Let $(X, \mathcal{F}, *)$ be a random 2-normed space. A double sequence $x = (x_{kl})$ is said to be ∇_2-statistical convergent if and only if it is ∇_2-statistical Cauchy.*

Proof. Let $x = (x_{kl})$ be ∇_2-statistical convergent sequence. Suppose that $S_{\nabla_2}-\lim_{k,l} x_{kl} = l$. For $\varepsilon > 0$, $t > 0$ and non-zero $z \in X$ choose $s > 0$ such that $(1-s) * (1-s) > 1 - \varepsilon$. We define

$$A(s,t) = \left\{(k,l) \in I_{r,s} : \mathcal{F}\left(\frac{1}{\lambda_{r,s}} \sum_{(k,l)\in I_{r,s}} x_{kl} - l, z; \frac{t}{2}\right) \leq (1-s)\right\};$$

then

$$A^c(s,t)=\left\{(k,l)\in I_{r,s}:\mathcal{F}\left(\frac{1}{\overline{\lambda}_{r,s}}\sum_{(k,l)\in I_{r,s}}x_{kl}-l,z;\frac{t}{2}\right)>(1-s)\right\}.$$

Since $S_{\nabla_2}-\lim_{k,l}x_{kl}=l$ it follows that $\delta_{\nabla_2}(A(s,t))=0$ and consequently $\delta_{\nabla_2}(A^c(s,t))=1$. Let $(u,\gamma)\in A^c(s,t)$, then

$$\mathcal{F}\left(\frac{1}{\overline{\lambda}_{r,s}}\sum_{(k,l)\in I_{r,s}}x_{u\gamma}-l,z;\frac{t}{2}\right)>(1-s).$$

If we take

$$B(\varepsilon,t)=\left\{(k,l)\in I_{r,s}:\mathcal{F}\left(\frac{1}{\overline{\lambda}_{r,s}}\sum_{(k,l)\in I_{r,s}}x_{kl}-x_{u\gamma},z;t\right)\leq(1-\varepsilon)\right\},$$

then to prove the first part it is sufficient to prove that $B(\varepsilon,t)\subset A(s,t)$. Let $(k,l)\in B(\varepsilon,t)$, which gives

$$\mathcal{F}\left(\frac{1}{\overline{\lambda}_{r,s}}\sum_{(k,l)\in I_{r,s}}x_{kl}-x_{u\gamma},z;t\right)\leq(1-\varepsilon).$$

Suppose $(k,l)\notin A(s,t)$, then

$$\mathcal{F}\left(\frac{1}{\overline{\lambda}^{\alpha}_{r,s}}\sum_{(k,l)\in I_{r,s}}x_{kl}-l,z;t\right)>(1-s),$$

Also it can be easily seen that

$$\begin{aligned}1-\varepsilon&\geq\mathcal{F}\left(\frac{1}{\overline{\lambda}_{r,s}}\sum_{(k,l)\in I_{r,s}}x_{kl}-x_{u\gamma},z;t\right)\\&\geq\mathcal{F}\left(\frac{1}{\overline{\lambda}_{r,s}}\sum_{(k,l)\in I_{r,s}}x_{kl}-l,z;\frac{t}{2}\right)*\mathcal{F}\left(\frac{1}{\overline{\lambda}_{r,s}}\sum_{(k,l)\in I_{r,s}}x_{u\gamma}-l,z;\frac{t}{2}\right)\\&\geq(1-s)*(1-s)>1-\varepsilon.\end{aligned}$$

This contradiction shows that $B(\varepsilon,t)\subset A(s,t)$ and therefore, one way of the theorem is proved.

Conversely, let $x=(x_{kl})$ is ∇_2-statistical Cauchy double sequence of order α but not double ∇_2-statistical convergent with respect to $\mathcal{F}$. Now

$$\begin{aligned}&\mathcal{F}\left(\frac{1}{\overline{\lambda}_{r,s}}\sum_{(k,l)\in I_{r,s}}x_{kl}-x_{u\gamma},z;t\right)\\\geq&\ \mathcal{F}\left(\frac{1}{\overline{\lambda}_{r,s}}\sum_{(k,l)\in I_{r,s}}x_{kl}-l,z;\frac{t}{2}\right)*\mathcal{F}\left(\frac{1}{\overline{\lambda}_{r,s}}\sum_{(k,l)\in I_{r,s}}x_{u\gamma}-l,z;\frac{t}{2}\right)\\\geq&\ (1-s)*(1-s)>1-\varepsilon.\end{aligned}$$

since x is not double ∇_2-statistical convergent. Therefore $\delta_{\nabla_2}(B^c(t,\varepsilon))=0$, where

$$B(\varepsilon,t)=\left\{(k,l)\in I_{r,s}:\mathcal{F}\left(\frac{1}{\overline{\lambda}_{r,s}}\sum_{(k,l)\in I_{r,s}}x_{kl}-x_{u\gamma},z;t\right)\leq1-\varepsilon\right\}.$$

and so $\delta_{\nabla_2}(B(t,\varepsilon)) = 1$, which is contradiction, since x is ∇_2-statistical Cauchy double sequence. Hence x must be ∇_2-statistical Cauchy. This completes the proof. ■

References

[1] A. Aghajani and K. Nourouzi, Convex sets in probabilistic normed spaces, Chaos, Solitons and Fractals, vol. 36, no. 2, pp. 322–328, 2008, doi: 10.1016/j.chaos.2006.06.051.

[2] J. Connor, The statistical and strong p-Cesáro convergence of sequences, Analysis, vol. 8, pp. 47–63, 1988, doi: 10.1524/anly.1988.8.12.47.

[3] A. Esi and N. L. Braha, On λ-statistical convergence in random 2-normed space, Mathematical Sciences, vol. 6, p. 62, 2012, doi: 10.1186/2251-7456-6-62.

[4] A. Esi, On ∇-statistical convergence in random 2-normed space, Rev. Anal. Numér. Théor. Approx., Vol. 43 (2014) no. 2, 175-186.

[5] A. Esi and M. K. Ozdemir, Generalized Δ^m-Statistical convergence in probabilistic normed space, J. Comput. Anal. Appl., 13(5) (2011), pp. 923-932.

[6] H. Fast, Surla convergence statistique, Colloquium Mathematicum, vol. 2, pp. 241–244, 1951.

[7] J. A. Fridy, On statistical convergence, Analysis, vol. 5, pp. 301–313, 1985, doi:10.1524/anly.1985.5.4.301.

[8] J. A. Fridy, Statistical limit points, Proceeding of American Mathematical Society, vol. 118, pp.1187–1192, 1993, doi: 10.1090/S0002-9939-1993-1181163-6.

[9] S. Gähler, 2-metrische raume and ihre topologische struktur, Math. Nachr., vol. 26, pp. 115–148, 1963, doi: 10.1002/mana.19630260109.

[10] I. Golet, On probabilistic 2-normed spaces, Novi Sad J. Math., vol. 35, pp. 95–102, 2006.

[11] S. Karakus, Statistical convergence on probabilistic normed spaces, Math. Commun., vol. 12, pp. 11–23, 2007.

[12] S. Karakus, K. Demirci and O. Duman, Statistical convergence on intuitionistic fuzzy normed spaces, Chaos, Solitons and Fractals, 35 (2008), pp. 763-769.

[13] V. Kumar and M. Mursaleen, On (λ; μ)-statistical convergence of double sequences on intuitionistic fuzzy normed spaces, Filomat, 25(2) (2011), pp. 109-120.

[14] I. J. Maddox, Statistical convergence in a locally convex space, Math. Proc. Cambridge Philos. Soc., vol. 104, no. 1, pp. 141–145, 1988, doi: 10.1017/S0305004100065312.

[15] K. Menger, Statistical metrics, Proc. Nat. Acad. Sci., USA,, vol. 28, pp. 535–537, 1942, doi:10.1073/pnas.28.12.535.

[16] M. Mursaleen, λ-statistical convergence, Math. Slovaca, vol. 50, pp. 111–115, 2000.

[17] M. Mursaleen, On statistical convergence in random 2-normed spaces, Acta Sci. Math.(Szeged), vol. 76, no. 1-2, pp. 101–109, 2010.

[18] M. Mursaleen, C. Çakan, S. A. Mohiuddine, and E. Savaş, Generalised statistical convergence and statistical core of double sequences, Acta Math.Sinica Eng. Series, vol. 26, no. 11, pp. 2131–2144, 2010, doi: 10.1007/s10114-010-9050-2.

[19] M. Mursaleen and S. A. Mohiuddine, On ideal convergence in probabilistic normed spaces, Math. Slovaca, vol. 62, pp. 49–62, 2012, doi: 10.2478/s12175-011-0071-9.

[20] S. A. Mohiuddine and Q.M. Danish Lohani, On generalized statistical convergence in intuitionistic fuzzy normed space, Chaos, Solitons and Fractals, 42 (2009), pp. 1731-1737.

[21] M. Mursaleen and S.A. Mohiuddine, On lacunary statistical convergence with respect to the intuitionistic fuzzy normed space, J. Comput. Appl. Math., 233(2) (2009), pp. 142-149.

[22] M. Mursaleen and O. H. H. Edely, Statistical convergence of double sequences, J. Math. Anal. Appl., vol. 288, pp. 223–231, 2003, doi: 10.1016/j.jmaa.2003.08.004.

[23] M. Mursaleen and A. K. Noman, On the spaces of λ-convergent and bounded sequences, Thai J. Math., vol. 8, no. 2, pp. 311–329, 2010.

[24] I. J. Schoenberg, The integrability of certain functions and related summability methods, Amer. Math. Monthly, vol. 66, pp. 361–375, 1959, doi: 10.2307/2308747.

[25] B. Schweizer and A. Sklar, Statistical metric spaces, Pacific J. Math., vol. 10, pp. 314–344,1960, doi: 10.2140/pjm.1960.10.313.

[26] A. N. Sherstnev, Random normed spaces, problems of completeness, Kazan Gos. Univ. Ucen. Zap., vol. 122, pp. 3–20, 1962.

[27] H. Steinhaus, Sur la convergence ordinaire et la convergence asymptotique, Colloq Math, vol. 2, pp. 73–74, 1951.

[28] T. Śalát, On statistically convergent sequences of real numbers, Mathematica Slovaca, vol. 30, no. 2, pp. 139–150, 1980.

[29] A. Zygmund, Trigonometric series. Cambridge, UK: Cambridge University Press, 1979.

[30] M. Gurdal and S. Pehlivan, Statistical convergence in 2-normed spaces, South. Asian Bull. Math., 33 (2009), pp. 257-264.

[31] M. Gurdal and S. Pehlivan, The statistical convergence in 2-Banach spaces, Thai J. Math., 2(1) (2004), pp. 107-113.

[32] E.Savas, On generalized statistical convergence in random 2-normed space, Iranian Journal of Science & Technology, (2012) A4: 417-423.

[33] C. Sencimen and S. Pehlivan, Statistical convergence in fuzzy normed linear spaces in fuzzy normed linear spaces, Fuzzy Sets and Systems, 159 (2008), pp. 361-370.

The Applied Mathematical Model For The Multi-Level Dc To Dc Converter

Erol CAN *
Department of air craft Air frame, power plant,
Erzincan University,
Erzincam/TURKEY

Abstract

The need for increased energy on the world has made it necessary to work on energy production and transformation. There are many studies to produce electric energy from solar energy, wind energy and petroleum type fuels. These electrical energies need to be transformed and regulated after they are produced. For regulating on the electric energy, circuits such as inverters and converters are usually used. This study focuses on the applied mathematical model of the dc-dc converter, which converts direct current electrical energy from a lower level to a higher level. In this study, a mathematical model of a multi-level and multi-switch converter circuit is created, which is different from other similar works [3-5]. The converters known in the literature can have the mathematical differential equations of the inductor current and the capacitor voltage for a single time slot and the single phase while the mathematical differential equations of the different inductor currents and capacitor voltages for the various levels are formed in the proposed circuit. For each level, the number of switches and circuit elements to be operated varies. This leads to a different number of elements for each level and a changing mathematical pattern. According to this, the mathematical equations generated reveal the superiority and the difference of the circuit arrangement.

Keywords: the mathematical differential equations, changing mathematical pattern, the need for increased energy.

1 Introduction

The need for increased energy on the world has made it necessary to work on energy production and transformation. There are many studies to produce electric energy from solar energy, wind energy and petroleum type fuels [1, 2]. For different needs and uses, electrical energy must be converted and regulated. In order to regulate electrical energy, circuits such as inverters and converters are usually used. This study focuses on the applied mathematical model of the dc-dc converter, which converts direct current electrical energy from a lower level to a higher level. In this study, a mathematical model of a multi-level and multi-switch converter circuit, which is different from other similar studies, has been formed [3-5]. In this study, multi-level DA-DA converter circuit and mathematical equations are described. The results obtained with several converter circuits with different management centers can be obtained with a circuit topology which can be obtained with a single microcontroller in the proposed circuit.

*Corresponding author. *E-mail address:* cn_e@hotmail.com

2 Converter Circuit Structure

The three-level DA-DA circuit model is given in figure 1.

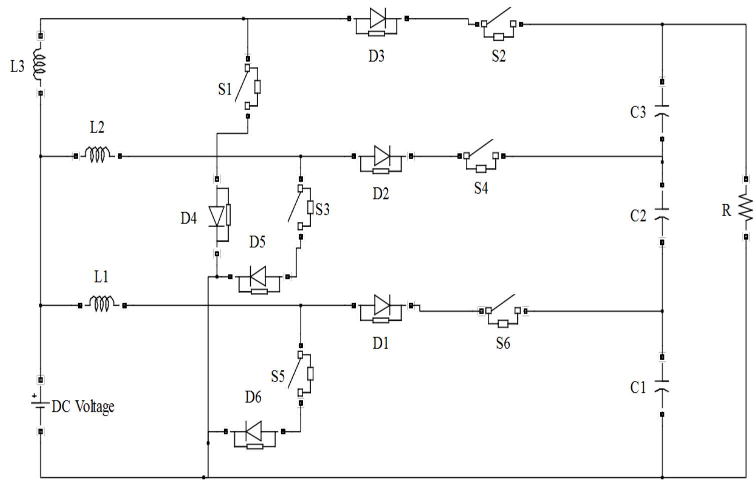

Figure 1: Three-level DC-DC circuit model

There are 6-switches, 3-inductors, 3-capacitors, 6-diodes and 1-DC source in this circuit. Pulse Width Modulation (DGM), which forms three different time periods for each floor of this circuit, is given in Figure 2.

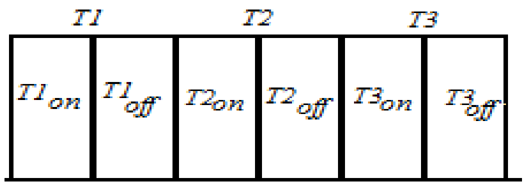

Figure 2: PWMs for the operation of switches

The equal-sized PWMs is providing an operating arrangement of circuit components as in table

Table 1: The working order of the circuit elements

	$T1_{on}$	$T1_{off}$	$T2_{\ on}$	$T2_{off}$	$T3_{\ on}$	$T3_{\ off}$
L1	1	1	0	0	0	
L2	0	0	1	1	0	0
L3	0	0	0.	0	1	1
C1	0	1	0	0	0	0
C2	0	0	0	1	0	0
C3	0	0	0	0	0	1
D1	0	1	0.	0	0	0
D2	.0	0	0.	1	0	0
D3	0	0	0	0	0	1
D4	0	0	0	0	1	0
D5	0	0	1	0	0	0
D6	1	0	0	0	0	0
S.1	0	0	0	0	1	0
S.2	0	0	0	0	0	1
S.3	0	0	1	0	0	0
S4	0	0	0	1	0	0
S5	1	0	0	0	0	0.
S6	0	1	0	0	0	0

For the three time zones, the current state on the coil at each level is given in figure 3.

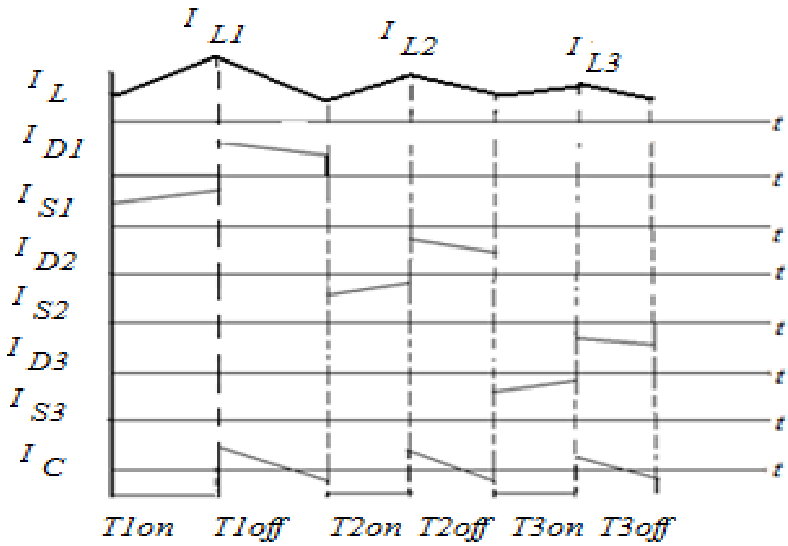

Figure 3: Current changes for each level of coil

T1 is the time set for the first level as one unit. For the time $T1_{on} = DT$, the circuit model in figure 4a is formed and the circuit model in figure 4b is formed for the time $T1_{off}$ $= (1\text{-}D)\ T$.

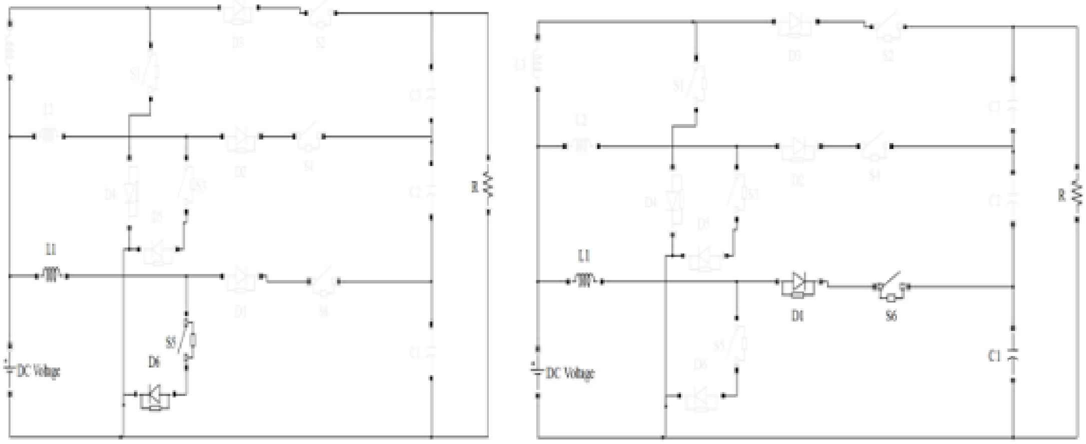

a) b)

Figure 4: Circuit models for the first level a) for $T1_{on}$ b) for $T1_{off}$

In the circuit in figure 4a, the first level coil $L1 = 2\ L$ will be active with the source voltage (E) for the time $T1_{on} = DT$. In this case, the current and voltage equality for first level will be in Eq.1 and Eq.2.di_1 is differential value of the current according to time.

$$E = \frac{di_1}{dt} 2L \tag{1}$$

$$\frac{E}{2L} = \frac{di_1}{dt} \tag{2}$$

In this case, the current will rise from the minimum level to the maximum level on the coil. For $T1_{on} = DT$, the current equation can be written as Eq. 3.

$$Imin - Imax = \frac{E}{L}\frac{DT}{2} \tag{3}$$

$T2$ is the time set for the second level as one unit. For the time $T2_{on} = DT$, the circuit model in figure 5a is formed and the circuit model in figure 5b is formed for the time $T2_{off}$ = *(1-D) T*.

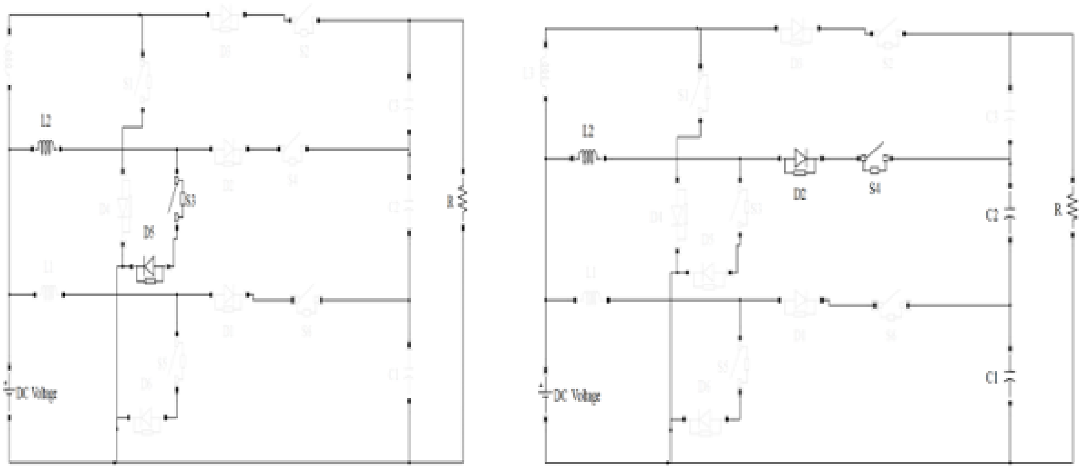

a) b)

Figure 5: Circuit models for the second level a) for $T2_{on}$ b) for $T2_{off}$

In the circuit in figure 5a, the second level coil $L2 = 4\ L$ will be active with the source voltage (E) for the time $T2_{on} = DT$. In this case, the current and voltage equality will be in Eq.4 and Eq.5 di_2 at the level-2 is differential value of the current according to time.

$$E = \frac{di_2}{dt} 4L \tag{4}$$

$$\frac{E}{4L} = \frac{di_2}{dt} \tag{5}$$

In the circuit in figure4b, the first level coil $L1 = 2L$ and the capacitor $C_1 = C$ will be active with the source voltage (E) for the time $T1_{off} = (1\text{-}D)T$. In this case, the current voltage will be as in Eq.6.

$$\left\{ \begin{array}{l} E = \frac{di_2}{dt} 2L + VC_1 \\ \frac{di_2}{dt} = \frac{E - VC_1}{2L} \\ Imax - Imin = \frac{E - VC_1}{L} \frac{(1-D)}{2} T \end{array} \right\} \tag{6}$$

In this case, the current will rise from the minimum level to the maximum level on the coil. For $T2_{on} = DT$, the current equation can be written as Eq. 7.

$$\left\{ \begin{array}{l} \frac{E}{4L} = \frac{di_2}{dt} \\ Imin - Imax = \frac{E}{L} \frac{DT}{4} \end{array} \right\} \tag{7}$$

The amount of charge accumulated in the capacitor at the first level can be expressed as a multiplication of the derivative of the current of I_1 with the transistor duty ratio (D) as in Eq.8.

$$Q1 = D \frac{di_1}{dt} \tag{8}$$

$$Q2 = D \frac{1}{2} \frac{di_1}{dt} \tag{9}$$

Eq.8 and Eq.9 can be found in Eq.10 and Eq.11.

$$Q2 = D \frac{1}{2} \frac{Q1}{D} \tag{10}$$

$$\frac{Q1}{2} = Q2 \tag{11}$$

Since two equal capacitors are connected in series for the second level, the capacitor unit value (C) is reduced by fifty percent for the second level. While the capacitor voltage VC_1 is written as the Eq. 11 for the first level, the capacitor voltage (VC_S) for the second level is written as the Eq.12.

$$VC_1 = \frac{Q_1}{C} \tag{12}$$

$$VC_S = \frac{Q_2}{C\frac{1}{2}} \tag{13}$$

Eq.10 and Eq.11 are used in Equation 12 to find a common capacitor voltage as VC_1 for the second level. So, Equations are calculated in Eq.13 and Eq.14.

$$\left(\begin{array}{l} VC_S = \frac{Q1\frac{1}{2}}{C\frac{1}{2}} \\ VC_S = \frac{VC_1 \frac{1}{2} C}{C\frac{1}{2}} \end{array} \right) \tag{14}$$

$$VCS = VC_1 \tag{15}$$

In $T2_{off}$ that is *(1-D) T*; current, voltage equality can be written from Eq. 15 and Eq. 16 as Eq.17.

$$E = \frac{di_2}{dt}4L + VC_1 \tag{16}$$

$$\frac{di_2}{dt} = \frac{E - VC_1}{4L} \tag{17}$$

$$Imax - Imin = \frac{E - VC_1}{L}\frac{(1-D)T}{4} \tag{18}$$

T3 is the time set for the third level as one unit. For the time $T3_{on} = DT$, the circuit model in figure 6a is formed and the circuit model in figure 6b is formed for the time $T3_{off}$ = *(1-D) T*.

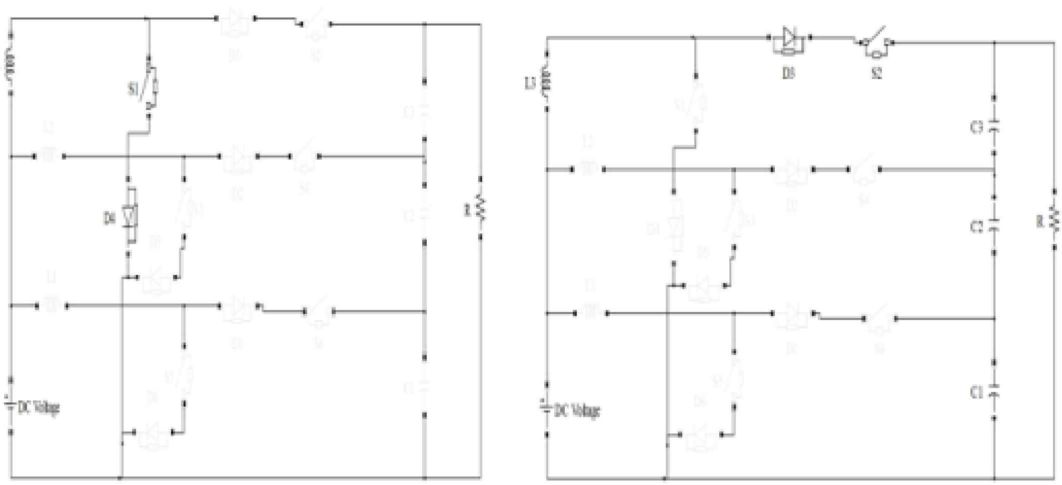

a) b)

Figure 6: Circuit models for the second level a) for $T3_{on}$ b) for $T3_{off}$

In the circuit in figure 6a, the second level coil *L3= 6 L* will be active with the source voltage (E) for the time $T3_{on} = DT$. In this case, the current and voltage equality will be in Eq.4 and Eq.5 di_3at the level-3 is differential value of the current according to time.

$$\left\{ \begin{array}{l} \frac{E}{6L} = \frac{di_3}{dt} \\ Imin - Imax = \frac{E}{6L}DT \end{array} \right\} \tag{19}$$

The inductor value increases to three times for the third level. Therefore, while the current is reduced by three times, the amount of the electric charge also decreases by three times in the capacitors as in Eq. 19. Q_3 is the amount of the electric charge for third level. D is constant of duty ratio for every level. D is time for charging capacitor. The current value is E / 2L for the first level and E / 6L is for current value of the third level. While the amount of current in the third level Eq.19 is one third of that in the first level, the amount of electric charge is as in Eq. 20.

$$Q_3 = D\frac{1}{3}\frac{di_1}{dt} \tag{20}$$

$$\left(\begin{array}{l} Q_3 = D\frac{1}{3}\frac{Q_1}{D} \\ \frac{Q_1}{3} = Q3 \end{array} \right) \tag{21}$$

Since three equal capacitors are connected in series for the third level, the capacitor unit value (C) is reduced by three times for the second level. While the capacitor voltage VC_1 is written as the Eq. 21 for the third level, the capacitor voltage (VC_T) for the third level is written as the Eq.22.

$$VC_1 = \frac{Q_1}{C} \tag{22}$$

$$VC_T = \frac{Q3}{\frac{C}{3}} \tag{23}$$

Eq. 20 and Eq. 21 are used in Equation 12 to find a common capacitor voltage as VC1 for the second level. So, Eq. is calculated Eq.23 and Eq. 24.

$$\left\{ \begin{array}{l} VCT = \frac{Q1\frac{1}{3}}{C\frac{1}{3}} \\ VCT = \frac{VC_1\frac{1}{3}C}{C\frac{1}{3}} \end{array} \right\} \tag{24}$$

$$VCT = VC1 \tag{25}$$

In $T3_{off}$ that is *(1-D)T*; current, voltage equality can be written from Eq. 25 and Eq. 26 as Eq.27.

$$E = \frac{di_3}{dt}6L + VC_1 \tag{26}$$

$$\frac{di_3}{dt} = \frac{E - VC_1}{6L} \tag{27}$$

$$Imax - Imin = \frac{E - VC_1}{L}\frac{(1-D)T}{6} \tag{28}$$

The converter output voltage can be found with a common solution for the three stages. The sum of the current values generated for the T_{on} durations and the sum of the current values occurring in the T_{off} is equalized as in Eq.(29) and Eq. (30).

$$-(\frac{E}{2L} + \frac{E}{4L} + \frac{E}{6L})\frac{DT}{1} = (\frac{E - VC_1}{2L} + \frac{E - VC_1}{4L} + \frac{E - VC_1}{6L})\frac{(1-D)T}{1} \tag{29}$$

$$-11EDT = (6E - 6VC_1 + 3E - 3VC_1 + 2E - 2VC_1)(1-D)T \tag{30}$$

Eq.30 and Eq. 31 are obtained from Eq. 29.

$$-11ED = (11E - 11VC1)(1-D) \tag{31}$$

$$\frac{E}{(1-D)} = VC1 \tag{32}$$

While each next level is running, the load stored at a capacitor of lower level at the lower level decreases as much as next level charging amount in capacitor of lower level. When $VC_1 + VC_2/2 + VC_3/3$ is named as VCa, the equation for the voltage on the total capacitor in the circuit is given by Eq.32, Eq.33.

$$\frac{E}{(1-D)} + \frac{E}{2(1-D)} + \frac{E}{3(1-D)} = VC_a \tag{33}$$

$$\frac{11E}{6(1-D)} = VCa \cong \frac{2E}{(1-D)} \tag{34}$$

3 Result

In this study, the working logic of a multi-level dc-dc converter is presented with mathematical equations.

References

[1] M. Bertsiou, E. Feloni, D. Karpouzos, & E. Baltas, management and electricity output of Hybrid Renewable Energy System (HRES) in FournoiIsland in Aegean Sea. Renewable Energy, 118(2), (2018).790-798

[2] A. K. Nag, & S. Sarkar, Modeling of hy bridenergy system for futuristic energy demand of an Indian rural area and their optimal and sensitivity analysis. Renewable Energy, 118(3), (2018) 477-488.

[3] H. Ardi, Ajami, M. Sabahi, A Novel HighStep-Up DC–DC Converter With Continuous Input Current Integrating Coupled Inductor for Renewable Energy Applications. IEE Transactions on Industrial Electronics, 65(2), (2018).1306-1315.

[4] S. Y. Kim, Y. J. Park, Ali, I., T. T. K. Nga, Ryu, H. C.,Khan, Design of a High Efficiency DC–DC Buck Converter With Two-Step Digital PWM and Low Power Self-Tracking Zero Current Detector for IoT Applications. IEEE Transactions on Power Electronics, 33(2), . (2018) 1428-1439.

[5] S. M., Chen, Liang, L. S. Yang, & J. F. Chen, A cascaded high step-up DC–DC converter with single switch for microsource applications. IEEE Transactions on Power Electronics, 26(4), (2011) 1146-1153.